NASA/CP—2001-211152



Proceedings of the Jet Noise Workshop

November 2001

The NASA STI Program Office . . . in Profile

Since its founding, NASA has been dedicated to the advancement of aeronautics and space science. The NASA Scientific and Technical Information (STI) Program Office plays a key part in helping NASA maintain this important role.

The NASA STI Program Office is operated by Langley Research Center, the Lead Center for NASA's scientific and technical information. The NASA STI Program Office provides access to the NASA STI Database, the largest collection of aeronautical and space science STI in the world. The Program Office is also NASA's institutional mechanism for disseminating the results of its research and development activities. These results are published by NASA in the NASA STI Report Series, which includes the following report types:

- TECHNICAL PUBLICATION. Reports of completed research or a major significant phase of research that present the results of NASA programs and include extensive data or theoretical analysis. Includes compilations of significant scientific and technical data and information deemed to be of continuing reference value. NASA's counterpart of peer-reviewed formal professional papers but has less stringent limitations on manuscript length and extent of graphic presentations.

- TECHNICAL MEMORANDUM. Scientific and technical findings that are preliminary or of specialized interest, e.g., quick release reports, working papers, and bibliographies that contain minimal annotation. Does not contain extensive analysis.

- CONTRACTOR REPORT. Scientific and technical findings by NASA-sponsored contractors and grantees.

- CONFERENCE PUBLICATION. Collected papers from scientific and technical conferences, symposia, seminars, or other meetings sponsored or cosponsored by NASA.

- SPECIAL PUBLICATION. Scientific, technical, or historical information from NASA programs, projects, and missions, often concerned with subjects having substantial public interest.

- TECHNICAL TRANSLATION. English-language translations of foreign scientific and technical material pertinent to NASA's mission.

Specialized services that complement the STI Program Office's diverse offerings include creating custom thesauri, building customized data bases, organizing and publishing research results . . . even providing videos.

For more information about the NASA STI Program Office, see the following:

- Access the NASA STI Program Home Page at ***http://www.sti.nasa.gov***

- E-mail your question via the Internet to help@sti.nasa.gov

- Fax your question to the NASA Access Help Desk at 301–621–0134

- Telephone the NASA Access Help Desk at 301–621–0390

- Write to:
  NASA Access Help Desk
  NASA Center for AeroSpace Information
  7121 Standard Drive
  Hanover, MD 21076

NASA/CP—2001-211152



Proceedings of the Jet Noise Workshop

Proceedings of a conference
sponsored by the AeroAcoustics Research Consortium
and hosted by NASA Glenn Research Center and the Ohio Aerospace Institute
November 7–9, 2000

National Aeronautics and
Space Administration

Glenn Research Center

November 2001

Acknowledgments

The AeroAcoustics Research Consortium is greatly appreciative of the efforts of all the people who helped make this event a success. Christopher Tam initially proposed the idea of having the workshop, helped contact many of the participants, and helped define the agenda. It was a great pleasure to have Geoffrey Lilley participate in the workshop and help write the proceedings; his early involvement in jet noise research provided a useful historical perspective. Thanks to Eugene Krejsa and Mary Jo Long-Davis for their help in writing portions of the proceedings. James Bridges helped define the agenda and identify potential participants. Special thanks to Christina Klamer and the Ohio Aerospace Institute for helping to organize the event and making sure each day was a success. Finally, thanks to all of the speakers and participants at the workshop. Everybody did a good job preparing their material and was willing to share not only their accomplishments, but also their failures. The hard work of everybody involved with the workshop made it a great success!

Contents were reproduced from the best available copy as provided by the authors.

Trade names or manufacturers' names are used in this report for identification only. This usage does not constitute an official endorsement, either expressed or implied, by the National Aeronautics and Space Administration.

Available from

NASA Center for Aerospace Information
7121 Standard Drive
Hanover, MD 21076

National Technical Information Service
5285 Port Royal Road
Springfield, VA 22100

Available electronically at http://gltrs.grc.nasa.gov/GLTRS

FOREWORD

Jet noise has been a major problem for aircraft for nearly 50 years. There has been considerable research performed around the world aimed at identifying ways to reduce jet noise. This work was first intended for turbojet aircraft and later extended to low bypass ratio turbofans. Many of the people who performed this pioneering research have retired or are no longer active in aeroacoustics. After so many years of work in jet noise, it is a challenge to piece together the history of its development through existing publications due to the large volume of documents. It is possible to forget important developments from the past as new researchers tackle similar problems. Therefore, a jet noise workshop was organized by the AeroAcoustics Research Consortium (AARC) with the intent of reviewing research that has been done by experts throughout the world. The forum provided a unique opportunity for current researchers to hear the diverse views from world experts on issues related to jet noise modeling and interpretation of experimental data.

Ninety-five workshop participants heard presentations and discussion based on answers to specific questions posed by the workshop organizers. The workshop was divided into four sessions: (1) jet mixing noise sources, (2) source identification techniques, (3) suppression methods, and (4) computational aeroacoustics for jet noise. Each session included invited speakers or panelists, and an opportunity for people from the audience to present prepared statements on the subject during an "open podium." There were specific questions posed for each session that the speakers and audience participants were asked to address.

It is hoped that these proceedings will serve as a focal point for references and viewpoints deemed to be important by jet noise experts. An attempt has been made to capture the important points from speakers, panelists, and discussion. It was never the intent of the workshop to reach consensus and draw conclusions from the presentation material. This is left for the reader and subsequent publications regarding jet noise research.

AeroAcoustics Research Consortium Peer Review Panel
David Reed, Boeing Commercial Airplane Group
Philip Gliebe, GE Aircraft Engines
David Ross, Honeywell International
Marvin Goldstein and Dennis Huff, NASA Glenn Research Center
Ann Heyward and Christina Klamer, Ohio Aerospace Institute

Workshop Organizing Committee
James Bridges
Dennis Huff
Christina Klamer
Christopher Tam

Summaries of Presentations and Discussion
Dennis Huff, Editor
Marvin Goldstein
Eugene Krejsa
Geoffrey Lilley
Mary Jo Long-Davis



Jet Noise Workshop Speakers.—Row 1: Tam, Ahuja, Kempton, Lilley, and Seiner; Row 2: Morris, Lele, Michel, Morfey, and Weir; Row 3: Huff, Bailey, Gliebe, and Glegg; Row 4: Lord, Mankbadi, Bhat, and Harper-Bourne.



Jet Noise Workshop Participants.

TABLE OF CONTENTS

Agenda xi

Opening Remarks 1

Session 1: Jet Noise Sources Summary
Invited Presentations 9
Acoustic Analogy—A Review
Geoffrey M. Lilley, University of Southampton 15

Noise From Large-Scale Turbulent Structures/Instability Waves
Philip J. Morris, Pennsylvania State University 65

Review of Noise Data and Recent Advances in Jet Noise Theory
Christopher Tam, Florida State University 121

Invited Panelist Presentations 273
Acoustic Analogy
Marvin Goldstein, NASA Glenn Research Center 277

Jet Noise Source Mechanisms—A Need for a Physics Based Modeling Procedure
John M. Seiner, University of Mississippi 293

Show Evidence if the Acoustic Analogy-Based Theory is Correct/Incorrect
Krish Ahuja, Georgia Institute of Technology 313

Is acoustic analogy really valid? Are large turbulent structures important?
Ulf Michel, DLR 353

Fundamental Problems in Aeroacoustics
Christopher L. Morfey, University of Southampton 381

Open Podium Presentations 399
Summary of A. Khavaran, NASA Glenn Research Center 399
Summary of V. Mengle, Boeing Company 400

Noise Sources—Use of Turbulence Space-Time Correlations in Lighthill's Equation Analyzed With Respect to a Fixed Frame of Reference
Marcus Harper-Bourne, DERA 401

Model Decomposition of Fluctuations in a Parallel Sheared Flow Based on the Displacement
Georges Elias, ONERA 427

Session 2: Source Identification and Location Techniques Summary
Invited Presentations 437
Jet Noise Source Location: A Review
Stewart A.L. Glegg, Florida Atlantic University 439

Source Identification and Location Techniques
Donald Weir, Honeywell; James Bridges and Femi Agboola, NASA Glenn Research Center; and Robert Dougherty, Boeing 479

Source Identification and Location Technique—Using a Phased Array
Thonse R.S. Bhat, Boeing Commercial Airplane Group 507

Open Podium Presentations 541
Source Identification and Location Technique
Marcus Harper-Bourne, DERA 543

Sound Source Identification Through Flow Density Measurement and Correlation With Far Field Noise
J. Panda, Ohio Aerospace Institute; and R.G. Seasholtz, NASA Glenn Research Center 561

Finding Internal Excess Jet Noise Source Characteristics by Varying Free-Jet Speed
Vinod G. Mengle, Rolls-Royce 571

Acoustic-Analogy-Based Jet Noise Prediction for Suppressor Nozzles
Krish Ahuja, Georgia Institute of Technology 595

Deficiencies of the Acoustic Analogy Approach
Christopher Tam, Florida State University 605

Session 3: Physics of Jet Noise Suppression Summary
Invited Presentations 613
Physics of Jet Noise Suppression: Industry Perspective on Prediction Methods, Future Direction/Needs
Wesley K. Lord, Pratt & Whitney 615

Physics of Jet Noise Suppression: The MGB Paradigm
Philip Gliebe, GE Aircraft Engines 631

Vorticity Dynamics and Its Relation to Jet Noise Reduction in Chevrons
Vinod G. Mengle, Rolls-Royce 653

Prediction of Jet Noise With Suppression Devices
Thonse R.S. Bhat, Boeing Commercial Airplane Group 667

Physics of Jet Noise Suppression:
Andrew Kempton, Rolls-Royce 685

Give Evidence Where Theory has Correctly Predicted Jet Noise
Krish Ahuja, Georgia Institute of Technology 699

Physics of Jet Noise Suppression
Marcus Harper-Bourne, DERA 701

Open Podium Presentations 719
Small-Scale Turbulence Noise
Abbas Khavaran, Dynacs Engineering, NASA Glenn Research Center 721

Mach Wave Suppression
Dimitri Papamoschou, University of California, Irvine 741

Anomalous Effect of Nozzle Length Reduction on Jet Noise of Forced Mixers
Vinod G. Mengle, Rolls-Royce 761

Session 4: Role of CAA for Jet Noise Physics Summary
Invited Presentations 781
CAA for Jet Noise Physics: Issues and Recent Progress
Sanjiva K. Lele, Stanford University 783

Jet Noise Computation: Direct and Hybrid Approaches
Christophe Bailly, Christophe Bogey, and Daniel Juve, Centre Acoustique Laboratoire de Mecanique des Fluides et d'Acoustique 833

CAA for Jet Noise Physics
Reda Mankbadi, Embry-Riddle Aeronautical University 891

Open Podium Presentations 939
DNS Vorticity Visualizations
Jonathan Freund, University of California, Los Angeles 941

Validation of a High-Order Compact Code for Nonlinear Flows About Complex Geometric
Ray Hixon, NASA Glenn Research Center 951

Integral Methods for Jet Aeroacoustics
Anastasios S. Lyrintzis, Purdue University 967

Assessment of Jet Noise Theory/Prediction Methods
K. Viswanathan, Boeing Company 979

Comparison of Lilley's Equation/Acoustic Analogy and Tam and Auriault's Model
Philip Morris, Pennsylvania State University 1011

Appendices
Appendix A—A Historical Perspective on Jet Noise Research 1017
Appendix B—Recent Particle Velocimetry Measurements from NASA Glenn Research Center 1021
Appendix C—Model Problem Proposed by Christopher Tam 1023
Appendix D—Jet Noise References Suggested by Workshop Participants 1029
Appendix E—Jet Noise Workshop Speakers Contact Information 1043
Appendix F—Jet Noise Workshop Attendees List and Contact Information 1047

JET NOISE WORKSHOP AGENDA

Tuesday, November 7, 2000

8:00 a.m.	Registration (OAI lobby)
8:30 a.m.	Welcome Address—Gerald Barna, NASA GRC Technical Address—Marvin Goldstein, NASA GRC AARC Introduction/Workshop Overview—Dennis Huff, NASA GRC
9:00 a.m.	Session 1: Jet Noise Sources *Invited presentations:* G.M. Lilley (University of Southampton)—Review of the Acoustic Analogies P. Morris (Pennsylvania State University)—Review Noise from Large Turbulence Structures/Instability Waves C. Tam (Florida State University)—Review Noise Data and Recent Advances
12:00–1:00 p.m.	Lunch (Sunroom)
1:00 p.m.	*Panel presentation:* Discuss mechanisms for jet mixing noise and give evidence (data and/or theory) to support specific mechanism(s). *Invited panelists*: M.E. Goldstein (NASA GRC) J.M. Seiner (University of Mississippi) K.K. Ahuja (Georgia Institute of Technology) U. Michel (DLR) C. Morfey (University of Southampton) *General discussion:* Is acoustic analogy really valid? Show evidence that the theory is correct/incorrect. Same discussion on large turbulence structure noise. What are some alternate approaches?
5:30 p.m.	Dinner

Wednesday, November 8, 2000

8:30 a.m.	Session 2: Source Identification and Location Techniques *Invited presentations:* S. Glegg (Florida Atlantic University) D. Weir (Honeywell) T. Bhat (Boeing)

General discussion:
Accuracy of technique and effect of nozzle geometry and jet operating conditions on source location.

12:00 p.m. Lunch (Sunroom)

12:45 p.m. Group photo in lobby

1:00 p.m. Session 3: Physics of Jet Noise Suppression
Panel presentation and discussion:
Give evidence where theory has correctly predicted jet noise trends with suppression devices.

Invited Panelists:
W. Lord (P&W)
P. Gliebe (GE)
T. Bhat (Boeing)
A. Kempton (Rolls-Royce)
K.K. Ahuja (GTRI)
M. Harper-Bourne (DERA)

Thursday, November 9, 2000

8:30 a.m. Session 4: Role for CAA for Jet Noise Physics
Invited presentations:
S. Lele (Stanford University)
C. Bailly (Ecole Centrale de Lyon)
R. Mankbadi (Embry-Riddle Aeronautical University)

General discussion:
Suppose the entire flow field is known both in space and time, what would we do with it to better understand jet noise sources?

11:15 a.m. *Summary of workshop*

OPENING REMARKS

The Jet Noise Workshop was opened by Gerald Barna, Acting Deputy Director, NASA Glenn Research Center. He welcomed all participants to this first Jet Noise Workshop sponsored by the AeroAcoustics Research Consortium (AARC). The NASA Glenn Research Center supports long-term research in both aeronautics and space. It is classified as a Center of Excellence for aircraft propulsion and is engaged in the new NASA "Quiet Aircraft Technology" Program.

Marvin Goldstein, Chief Scientist of the NASA Glenn Research Center, added his welcome to all participants and especially to his many friends and colleagues who were in attendance. He pointed out that this Jet Noise Workshop grew out of a suggestion by Chris Tam and the result is that we have here today nearly 100 participants from government research laboratories, industry, and universities to discuss the state of the art in understanding, prediction, and reduction of jet noise. He also noted that the demand to decrease jet noise continues to grow, in spite of the enormous effort that has been made to reduce it since Lighthill first introduced the Acoustic Analogy nearly 50 years ago. Progress continues to be hampered by the largely empirical nature of the prediction methods. Jet noise prediction, like the prediction of turbulence from which it is generated, remains an unsolved problem.

Dr. Goldstein noted that there is a need to further decrease the noise of civil commercial transport aircraft, and hence the noise of the current turbofan engine in spite of the overall reduction in fleet noise level resulting from the recent Stage 2 phaseout. This is primarily due to a greater awareness of noise in the community and to the greater annoyance resulting from the increased number of operations. The success of past noise-reduction efforts has led to an expectation that progress would continue if sufficient pressure could be exerted on the industry. It should therefore not be surprising that noise restrictions and curfews continue to grow at local airports.

Over the past 10 years, the emphasis has been on reducing fan noise but it is now realized that further reduction in fan noise will be ineffective unless the jet noise can be reduced as well. An additional reason for continuing jet noise research is to ensure that the necessary noise-reduction technology will be in place to meet the challenge of any future supersonic transport requirement. The recent High Speed Civil Transport (HSCT) program relied on a rather large and heavy mixer-ejector nozzle concept to achieve the required noise reduction. Future propulsion systems will have to be much lighter and still produce much lower noise levels in order to meet the required noise certification goals.

Dr. Goldstein reminded the audience that current jet noise prediction methods are largely empirical and are only completely satisfactory for round jets. They are incapable of predicting the changes in the sound field resulting from detailed changes in the flow and are therefore unable to account for the effects of complex nozzle geometry. He suggested that hybrid analytical/numerical approaches such as Large Eddy Simulation (LES) might play a major role in the development of improved prediction methods that capture the true physics of the source. He hoped the Jet Noise Workshop would contribute towards the development of such methods. He pointed out that the subject of aeroacoustics has been highly contentious over the years even though, from a fundamental point of view, the physics of the sound-generation process is quite simple: pressure fluctuations must occur in the flow in order to balance the fluctuations in momentum and as long as the medium is compressible, pressure will propagate away as sound. The controversy arises because only a small fraction of those energetic fluctuations actually radiate as sound, which makes the identification of the noise-generating structures very difficult. There is also considerable controversy about how these noise sources should be modeled. Can they be treated as acoustically compact convecting quadrupoles, as envisioned by Lighthill, or can they be better represented by an instability wave model for the large-scale structures? This workshop has been structured to address these issues in the presentations from the invited speakers and panelists.

Mr. Dennis Huff, Chief of the Acoustics Branch at the NASA Glenn Research Center, reported on the formation of the AARC with its current membership including Boeing, General Electric, Honeywell, NASA Glenn Research Center, and the Ohio Aerospace Institute. Mr. Huff believed the establishment of the AARC was timely for many engineers and scientists who had pioneered the research and development of jet noise and its impact on the design of modern turbofan aircraft propulsion engines and who are now

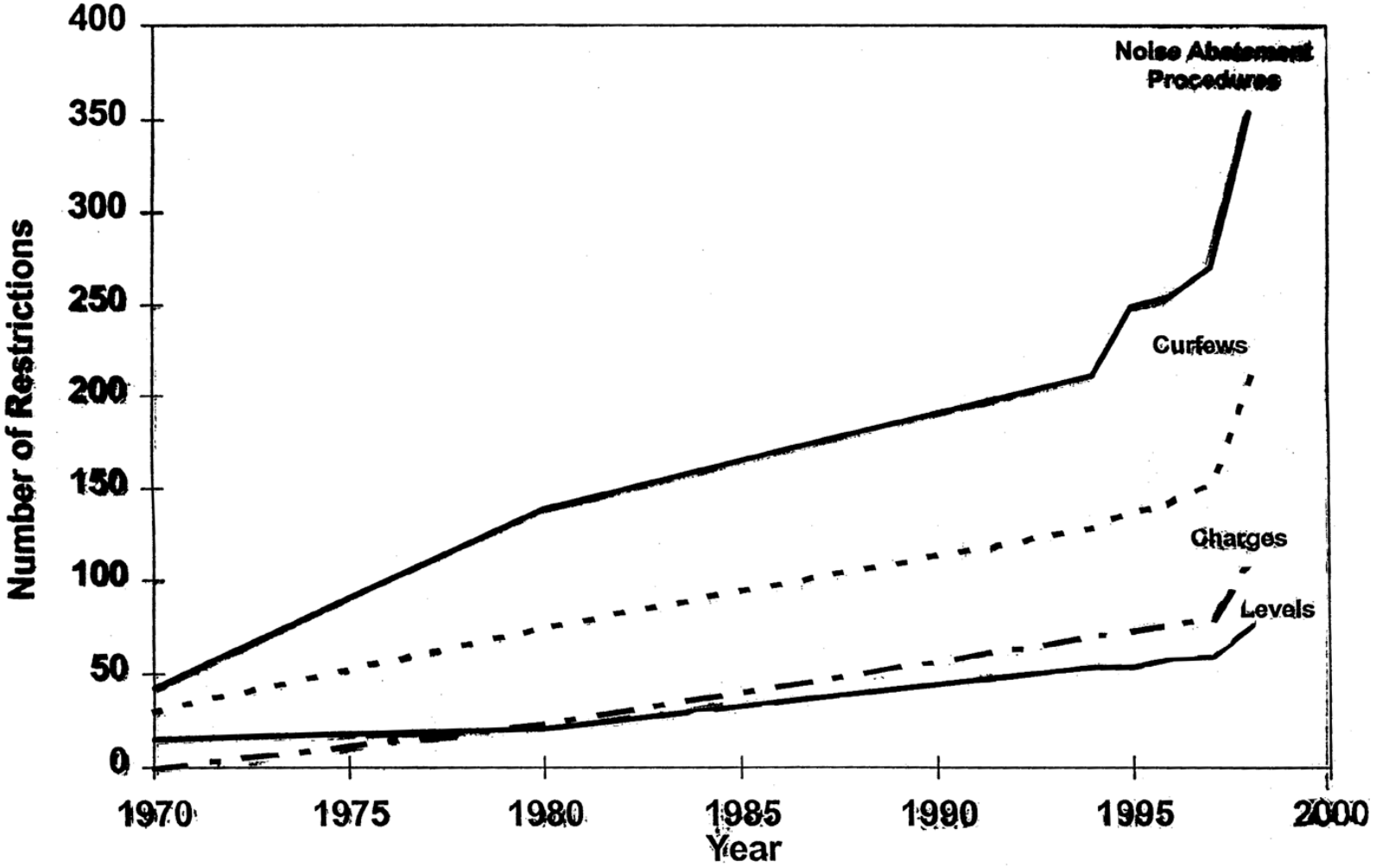
being lost through retirement. It was important that their contributions and expertise should not be lost, and the work of the AARC was devoted to ensure the new generation of workers in this field would be able to build on the achievements of the past. The aim of the AARC is to attract experts from all around the world and for them to discuss and advise on current and future research. Such interaction should assist in the generation of a better scientific understanding of fan, core, and jet noise problems, their noise prediction based on sound physical principles, and their noise reduction. Of these, jet noise remains an important research area and one deserving urgent attention.

The current membership of the AARC Peer Review Panel is Dave Reed (Boeing), Philip Gliebe (GE), David Ross (Honeywell), Marvin Goldstein and Dennis Huff (NASA Glenn), and Ann Heyward and Christina Klamer (OAI).

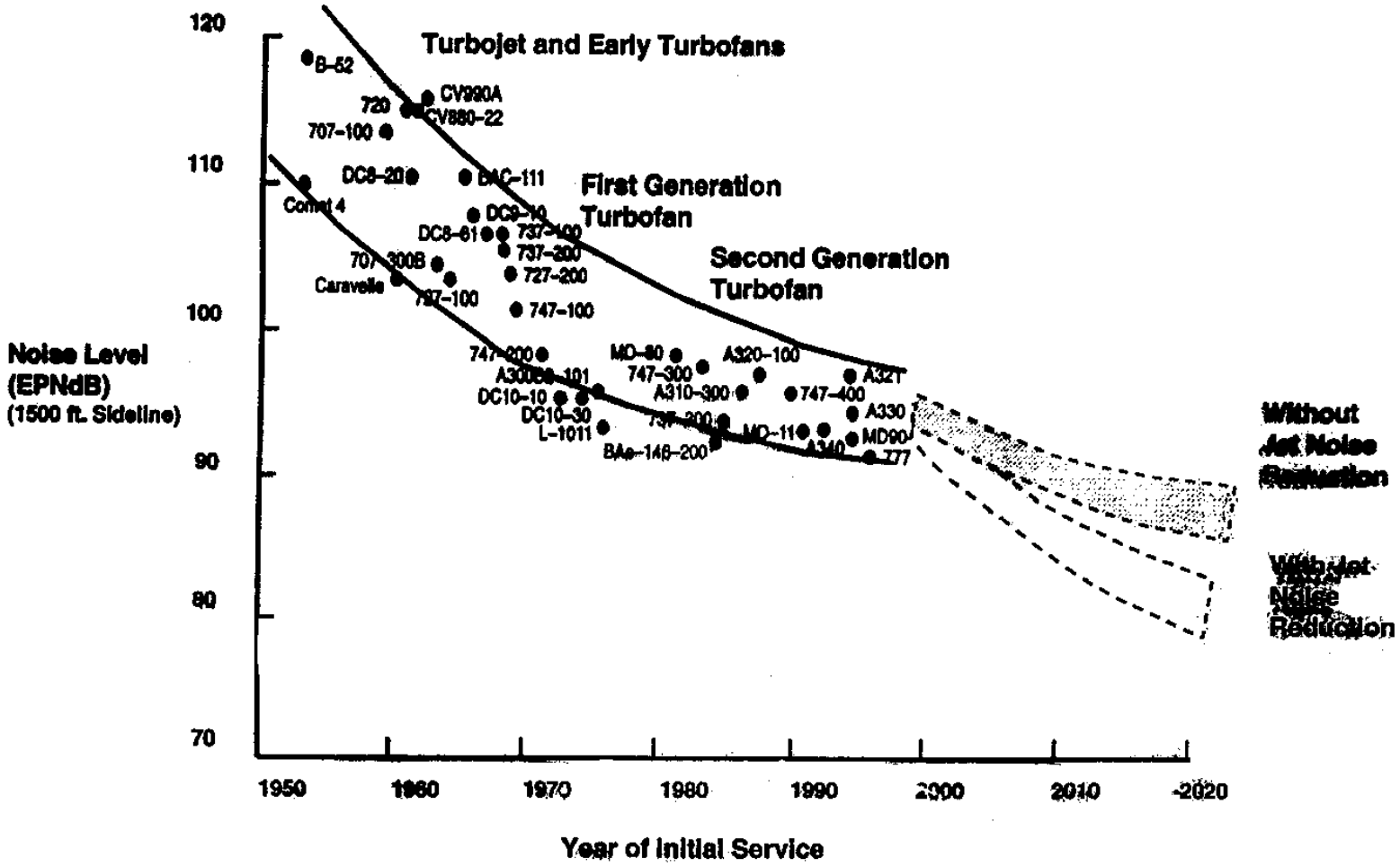
The aim of this Jet Noise Workshop is to review the approaches to modeling and defining jet noise sources and report on progress toward using jet noise prediction methods to properly guide noise-suppression methods.

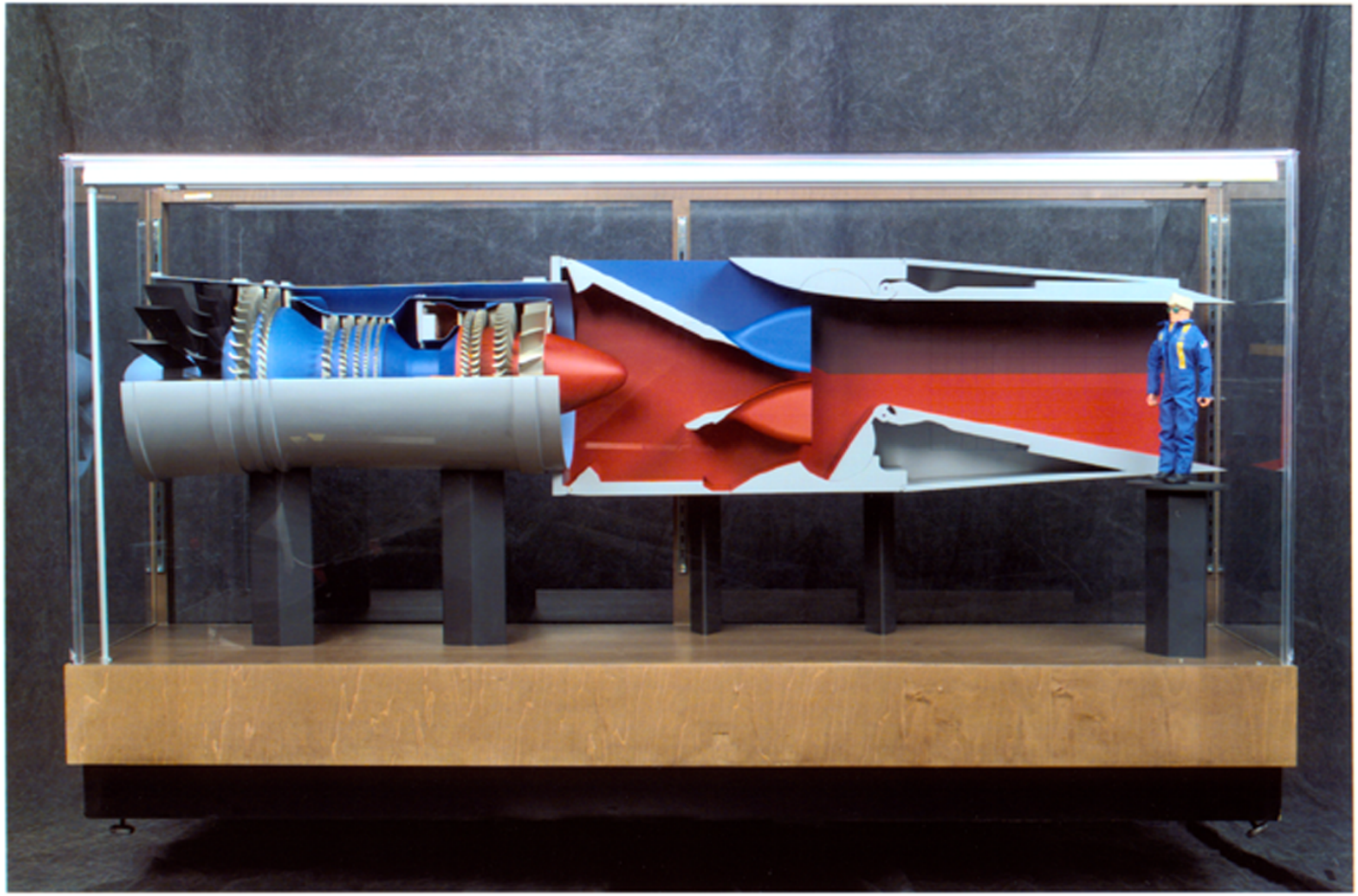
Noise Restrictions Continue to Grow

Number of Airports in Database: 591



Community Noise Trend During Takeoff





NASA
C-99-219

National Aeronautics and Space Administration
Lewis Research Center


DIRECT NUMERICAL SIMULATION IMPOSSIBLE AT HIGH REYNOLDS NUMBERS OF TECHNOLOGICAL INTEREST
High Reynolds number turbulent flow has large range of scales
Large scales radiate sound
YEH! THAT'S CALLED SUBGRID SCALE MODELING. IT'S A HIGHLY DEVELOPED SUBJECT.
THEN WHY NOT MODEL THE SMALL SCALES AND CALCULATE THE ACOUSTICALLY ACTIVE SCALES ?
CD-92 - 50253

NASA
C-91-10684



National Aeronautics and Space Administration
Lewis Research Center

SESSION 1: JET NOISE SOURCES

Summary by Geoffrey Lilley, University of Southampton

This session was devoted to three invited presentations, five invited panel presentations and open podium presentations. Discussion followed each presentation.

INVITED PRESENTATIONS

The Acoustic Analogy – A review by Geoffrey M. Lilley, University of Southampton

(a) The inclusion of external sources.

Professor Lilley noted that a major discussion point at this workshop was on the usefulness of acoustic analogies in the prediction of jet noise. It appeared that many of the participants were unfamiliar with the precise definition of an acoustic analogy. Lilley suggested that it would be helpful to refer all participants to the 'Dictionary of Acoustics' by C. L. Morfey recently published by the Academic Press (2000).

He indicated that a commonly used definition of *ACOUSTIC ANALOGIES* is:

'An acoustic analogy is an exact rearrangement of the Navier-Stokes or Euler equations which leads to an equation for the propagation of acoustic waves in a medium at rest or in a defined motion, with an equivalent source term wherein the sources of sound may move relative to the given mean motion of the medium.'

Lilley stressed that the medium is at rest in *Lighthill's Acoustic Analogy*. The strength and distribution of the equivalent acoustic sources must be determined from experiments**,** solutions of the exact Navier-Stokes equations or by some sort of modeling. Thus in *Lighthill's Acoustic Analogy* the Lighthill stress tensor, T_{ij}, should include all fluid fluctuations including the sound generated by the flow and its interaction with the flow. The propagation is along the straight line from source to observer. As stressed by Lighthill, in this acoustic analogy, there is no fluid flow, and the medium is everywhere at rest. The fluid flow is replaced by the equivalent acoustic sources and these may move but not the medium.

In *Lighthill's Acoustic Analogy* the equivalent acoustic sources are defined for the given flow field and their strength must fall sufficiently rapidly with increase in distance from what is defined as the boundaries of the unsteady flow. In such cases it can be shown that the far-field noise reaching an observer will be found from a weighted volume integration of the distribution of acoustic sources. This holds exactly for a compact source distribution, especially at low Mach numbers where the ratio of the characteristic length scale of the source region is negligible compared with the typical acoustic wavelength. At higher Mach numbers the

acoustic source becomes non-compact with the result that flow-acoustic interaction occurs within the flow.

If the observer is placed in a uniform flow it is appropriate to replace Lighthill's equation by the convected wave equation in which the operator, following the flow, refers to the given mean motion. The source terms given in terms of T_{ij} then include only the quadratic fluctuations. If the given mean motion is an arbitrary transverse shear flow the resulting acoustic analogy becomes Lilley's third-order convected wave equation where the equivalent acoustic sources are closely related to those given in Lighthill's acoustic analogy.

Lilley said that one criticism of Lighthill's acoustic analogy was that it was strictly an integro-differential equation since the density appeared both in the lefthand-side wave operator and in the acoustic source distribution on the righthand-side. However he did not believe this to be a major problem since he expected the effect of density fluctuations to be very small inside the flow.

Lilley said that in the Lighthill stress tensor only the quadratic fluctuating source terms are associated with noise generation and radiate to the far field. He argued that the linear fluctuating source terms do not radiate acoustic energy to the far field and referred to them as "the dominant part of the flow field fluctuations", since by comparison the fluctuations inside the flow due to the non-linear terms were very small. The Lilley convected wave equation for a given mean flow clearly shows the role played by acoustic – flow interaction, since its left hand-side becomes the Pridmore-Brown wave operator for the refraction of acoustic waves propagating in the presence of a mean shear. The right hand-side relates to the equivalent acoustic sources, which involve only quadratic flow fluctuations. A discussion of the properties of these sources and of the refraction of acoustic waves in the presence of a mean shear can be found in 'Aeroacoustics' by Goldstein (1976), in Goldstein (1984) and in the recent paper by Lele et al. (2000) presented at the AIAA Aeroacoustics Meeting at Hawaii.

Lilley noted that there are a number of other acoustic analogies details of which were not discussed in this presentation. He also described some of his work on the prediction of jet noise. He noted that in this analogy**,** the farfield noise intensity was related to the volume integral of the two-point space-retarded time covariance of the component of the Lighthill stress tensor in the direction from source to observer. Lilley referred to its local value, when non-dimensionalized with respect to the local kinetic energy, as the 'Lighthill filter function', or the acoustic efficiency, since this term, including its second time derivatives, expresses just that fraction of the flow's turbulent kinetic energy that is radiated to the farfield as noise. Lilley(1993,1996) used the DNS results for isotropic turbulence, obtained by Sarkar and Hussaini(1993), Dubois(1993) and Witowska and Juve(1993), to find an approximation for the space-retarded time properties of the 'Lighthill filter function', which could be assumed constant throughout a turbulent jet. The total acoustic power generated by a jet over a wide range of jet exit speeds and temperatures was therefore obtained approximately, from a knowledge of the mean

turbulent kinetic energy distribution over the entire jet, together with similar results for the mean of the stagnation enthalpy fluctuations. Both sets of fluctuations were found from RANS calculations and measurements. The comparison was shown to give agreement with a wide range of experimental data for the cold jet provided a correction was applied to allow for refraction. Similar agreement was found for the hot jet data. In the case of the hot jet it was shown that the noise generated was due to two source terms:

1. The source function for the cold jet, proportional to v^8, but with its convection speed along the divided streamline chosen to allow for changes in jet speed and temperature.
2. The additional source term derived from $\left(p - \rho c_\infty^2\right)$, which was dipole in character, and had a velocity dependence at low Mach numbers of v^6.

The hot jet results included the sum of the two source terms. When the results for the hot jet were plotted for a constant jet stagnation enthalpy ratio with respect to the ambient enthalpy, it was shown that the agreement with the experimental hot jet data was satisfactory. This confirmed that low Mach number hot jets of large stagnation enthalpy ratio, radiated as v^6, and were therefore noisier than cold jets, whereas at high Mach numbers the opposite occurred. In all cases a simple approximate allowance was made for the effects of refraction. An important result was found for all hot jets. For a given jet stagnation enthalpy there exists a maximum jet velocity associated with the isentropic expansion from the given stagnation enthalpy to a near vacuum. Thus the plotted results do not show the anticipated asymptotic approach to v^3, since the higher values of V_j/C_∞ are unattainable. (Typical plots of acoustic power in the literature show results for a wide range of jet exit temperatures all plotted on the same diagram with an averaged line drawn through all results. The result is that a v^3 law appears to be a good fit at high values of the 'acoustic Mach number', V_j/C_∞).

Prof. Lilley also provided a historical perspective on the development of the Acoustic Analogy (see Appendix A).

Comments by Farassat: Farassat noted that Lilley had not discussed the solution to Lighthill's equation for bounded and unbounded flows as given by Ffowcs Williams and Hawkings(1969), and which has been used extensively in the work of Farassat and Brentner on deriving the radiated noise from helicopters. This methodology clearly has applications to jet noise when hybrid methods are used to derive the farfield noise, and a compressible time-accurate flow field database is available from a flow solver using LES or URANS. The Ffowcs Williams-Hawkings surface must enclose all the dominant sources in the flow field, but unlike a Kirchhoff method the flow quantities do not have to be acoustic terms but may include weak vortical effects and the jet entrainment flow. There is reason to believe that this method will capture the far-field radiation and filter out the non-radiated components, performing a similar role to that of the 'Lighthill filter function'. It also captures effects, such as

refraction and reflection from surfaces exposed to the radiated sound, provided they lie within the Ffowcs Williams-Hawkings surface.

(b) Turbulence modeling for Unsteady Reynolds-Averaged Navier-Stokes (URANS)

Lilley discussed his current experience using URANS for obtaining the time accurate flow database for jets at high Reynolds numbers for incorporation into a hybrid scheme involving the Ffowcs Williams-Hawkings form of Lighthill's acoustic analogy for the calculation of the far-field noise. The method is currently being used for airframe noise calculations. He noted that the efficient calculation of the equivalent steady flow, corresponding to a given complex turbulent flow using RANS, has been the subject of an enormous scientific effort in the past 20 years and discussed the use of the Boussinesq type turbulence models in this approach. He gave arguments to show that the use of turbulence models in URANS is restricted to modeling the unresolved turbulent motion, just as in sub-grid scale models for LES and noted that**,** when the simple Boussinesq model is used as in steady RANS, it is found that the large damping provided by the eddy viscosity effectively dampens unsteady motion of the 'large scale structures'. This occurs before they can develop their full nonlinear distortion and stretching, and which the unsteady Euler equations could provide if this strong damping were excluded. He suggested that there are two important guidelines to be implemented when using URANS. Firstly the value of the dissipation rate must have a value in URANS almost equal to its value in RANS, since it is related to the viscous dissipation governed by the Kolmogoroff scales in the true high Reynolds number flow field. It is this value that governs the lossless transfer of energy up the frequency and wavenumber ranges including eddies of the size of the Taylor micro-scale. In URANS this range of eddy scales will form part of the unresolved motion. The second condition relates to introducing the unresolved turbulent motion into the unsteady Euler equations as equivalent body force terms, which only provide damping of the `large scale motion' through nonlinear interaction. They thus replace the strong damping introduced by the eddy viscosity model. This approach appears to be further justified by noting that eddy viscosity is a poor descriptor for describing the physical process due to the gradient of the fluctuation of the Reynolds stress. Eddy viscosity can be better described as large eddy circulation, which immediately reflects its role in establishing the turbulent vortex force and the dynamics of its interaction with the `large scale flow structures'.

In using the Lighthill acoustic analogy for the prediction of jet noise it is necessary to use a time accurate flow solver from which the T_{xx} space-retarded time covariance can be calculated in the direction from source to the selected observer. At low Reynolds number this can be obtained from DNS but at higher Reynolds number this information can be obtained from LES or URANS. Lilley argued that the T_{xx} covariance must depend on the anisotropic properties of the turbulence, which control the spectrum and the directivity of the radiated noise. The total acoustic power from a jet appears to be predicted satisfactorily assuming the 'Lighthill filter function' is based on a DNS isotropic turbulence simulation, but this

model as described above cannot be used for predicting the far-field sound spectrum and directivity.

The turbulent structure in the center of a jet-mixing region appears to contain long skewed cylindrical-like structures in which the integral scale in the radial direction is about 1/5 of its value in the axial direction. Thus the resolved turbulence intensities and turbulent length scales required for the amplitude and length scale of T_{xx} in the different directions of the far-field observer suggest the mixing-region turbulence radiates very differently in directions along the jet axis than, say, normal to the jet axis. In directions near 90° the small radial integral scale would be responsible for radiating noise of higher frequency than in other directions relative to the jet axis. This is in line with Tam et al.(1996) findings from their compilation of the large experimental databank of the radiated noise spectrum in different directions in the far-field. Townsend(1956, 1975) comments on this small radial integral scale in the jet and mixing region and suggests this arises from a compression of the energy containing eddies due to the transverse rate of strain between the opposing entrainment and radial diffusion of the jet core flow. (See Open Podium discussion by Khavaran.)

Lilley argued that the experimentally observed universality of the mean properties of the fully developed turbulent jet at all Reynolds numbers indicates that the characteristics of the large-scale structures and the energy containing eddies should be independent of Reynolds number. He also indicated that these eddies are likely to generate the largest contribution to the radiated jet noise. Thus a low Reynolds number DNS (in which all length scales are resolved according to the Reynolds number of the calculation) actually captures the same characteristics for the large and the energy containing eddies as found at much higher Reynolds numbers. He suggested that the problem is therefore one of establishing a fully developed turbulent flow and of avoiding the transition problem, from laminar to turbulent flow, say, downstream of the nozzle exit, as is frequently encountered in many experiments on jets. He noted that he referred to this problem in the Westley-Lilley jet noise studies and that Freund(1999) and Lele et al(2000) have discussed this problem in DNS and LES studies on the jet. He hoped that in the near future, he would see a comparison between the dominant energy containing structures they find in their DNS studies and those found in experiments at much higher Reynolds numbers. In all the available computational methods there remains the problem of computing the full high frequency spectrum up to the frequencies typical of those measured on the full-scale aircraft. *(A possible resolution of this problem is given in the following panel discussion by Goldstein.)*

Lilley drew attention to the prediction of the noise from complex multiple jet configurations as well as the interference effects on jets as installed on the aircraft. He stated that the problem of airframe-engine integration for optimum performance and low noise involves many flow features that are absent when the jet is considered in isolation. He described some of his recent work on airframe noise prediction and noise reduction which shows that the presence of potential scattering surfaces close to the convected turbulence can increase the radiated noise.

Finally Lilley reported that when questioned on whether a lower bound existed for the noise radiated from a 'clean' aircraft the answer was it depends on the engine. But it appeared that the airframe component of all airplanes flying in the 'clean' condition with flaps, slats, and undercarriage stowed, and including gliders and all birds, excluding the owl, generate noise in their far-field according to a universal law depending on their mass and speed. The exception is the owl, which not only is the quietest of all birds and flying objects above a mass of about 1kg, but also flies silently in the range of frequencies above 2kHz. All other flying objects, including aircraft, gliders, and birds (apart from the owl), have a broadband noise spectrum extending beyond 10kHz. It is by this silent flight above 2kHz that the owl has been able to survive for 20 million years, since this is the lower frequency of noise detection by its prey. It is well known that this frequency range between 2kHz and 10kHz, which is the human speech interference range, causes the greatest annoyance to people exposed continuously to aircraft noise. Now that 'owl's silent flight technology' is better understood, it appears that we should in jet noise research consider schemes for noise reduction in which an effort should be made to provide a large reduction in noise is this range of frequencies above 2kHz. In many current jet noise reduction schemes the noise is reduced in the low frequencies at the expense of an increase in the higher frequencies. Nature solved the problem by providing the owl with fine 'down' feathers on its wings and legs through which the pseudo-turbulent boundary layer flows and all noise greater than 2kHz is absorbed. Can we invent some device to add to the airplane and engine that can generate a quiet airplane above 2kHz?

In reply to a question regarding the effect of refraction on the total acoustic power of supersonic jets, Lilley agreed that the calculations included certain assumptions and possibly other (unknown) flow interference effects could have been present to explain the good agreement between the measured and calculated results.

Acoustic Analogy –

A Review

Geoffrey M. Lilley
University of Southampton

NASA/CP—2001-211152

ON THE ACOUSTIC ANALOGY - A REVIEW

Geoffrey M. Lilley
School of Engineering Sciences
Department of Aeronautics and Astronautics
University of Southampton. UK

NASA MS128
Langley Research Center
Hampton, VA. 23681-0001. USA

Visiting Professor
Penn State University
University Park. PA 16803. USA

Jet Noise Workshop, 7-9 November 2000
OAI, 22800 Cedar Point Road,
Cleveland, Ohio 44142. USA

Abstract

Ladies and gentlemen you do me a great honor in asking me to present the first paper at this 'Jet Noise Workshop'. I had been invited to NACA Lewis for the first time in 1955 following the Second Jet Noise Conference at NACA Langley Field which I had attended as an invited delegate from England. After the Langley Meeting I went first to Wright-Patterson Laboratories at Dayton. On my way to Cleveland the car, which was driving me to Columbus for the short flight to Cleveland, was hit by a truck and I finished up in hospital in Springfield, Ohio suffering from concussion, a fractured skull and my face smashed up. So I never saw NACA Lewis on that occaison and it was 2 long years before I was able to resume my researches into jet noise and Aircraft Noise Reduction. Dr. Marvin Goldstein invited me to NASA Lewis sometime after the publication of his textbook on Aeroacoustics. Marvin kindly included in that book much of the unpublished work I had written while a consultant in the early 1970's for Lockheed at Marietta, where the endeavour was to provide a sound database for hot jet noise at subsonic and supersonic speeds. An additional aim was to establish an improved prediction method for jet noise at subsonic and supersonic speeds. Some of this work is reported in the Harvey Hubbard volumes on Aircraft Noise.

During my slow recuperation after the 1955 motor accident I returned to my theoretical work on jet noise. By that time a good database had been established from model jet and engine measurements using improved instrumentation over what was available to Westley and myself, when we performed one of the first experimental attacks on the jet noise problem in 1949-1951. Our work was completed before Lighthill's theory was announced in 1951 and published in 1952. In 1957 I attempted a comprehensive modelling of the unsteady flow in a jet at subsonic and supersonic speeds. Independently Ribner at Toronto was attempting a similar model of the sources of jet noise.

In retrospect, after Lighthill had announced his theory of the Noise from Turbulent Flow, I argued that the more important problem was that of generation rather than the concentration on propagation as presented in Lighthill's theory. I spent long hours with my research student Peduzzi, studying the true convected wave equation for pressure in the flow in a bid to get closer to a model for the unsteady fluctuations of the Lighthill stress tensor which were undoubtedly the source of noise in a jet. Without the computational support we have today we reluctantly abandoned this effort since the complexity of the space-time turbulent correlation functions could neither be calculated or measured. At that time we had little confidence in model approximations.

In my later studies at Cranfield in 1956-7 I used the description of the turbulent structure of a jet introduced by Alan Townsend, in which all turbulent shear flows were described as having a large scale, of order the flow dimensions, and a smaller scale structure containing the bulk of the kinetic energy, but still very large at high Reynolds numbers compared with the eddies responsible for the dissipation of energy. It appeared from Lighthill's theory that the covariance based on the second retarded-time derivative of T_{ij} would, in the frequency domain, peak at a frequency slightly greater than that corresponding to the peak in the energy spectrum. Proudman's work on the noise from isotropic turbulence had arrived at the same conclusion. This had already been an observation in the experimental work of Westley and Lilley and Hubbard and Lassiter at Langley Field. When in turbulence we refer to small scale structures or eddies we refer to eddies slightly smaller than those containing most of the energy but much larger than the so-called Taylor microscale eddies which are close to the lower end of the inertial subrange which are also close to the start of the Kolmogorov dissipating range.

Thus the term fine-scale in the recent excellent work of Chris Tam is I believe a poor descriptor and one which will mislead many in the aeroacoustics world. To many 'fine' appears as very thin, or threadlike and may be confused with eddies in the Kolmogorov range. We need a simple descriptor, such as 'energy containing eddies'. In particular we are dealing with eddies of macroscopic scales not microscopic scales. There are many length scales of energy containing eddies in a turbulent jet associated with the growth of the mixing region from the nozzle exit, where the energy containing eddies are very small to far downstream where they are very large.

Returning to my earlier description of the dominant acoustic sources in a jet, it is now clear I made a very great error when I followed Lighthill in labelling the main sources of jet noise as associated with the mean-shear turbulent interaction, or the amplifying effect of mean shear, and the turbulent-turbulent interaction. The former relates to linear fluctuating terms while the latter concerns the quadratic fluctuating terms in T_{ij}. Independently Ribner had derived an almost similar model of jet noise based on Lighthill's Acoustic Analogy. Although my work had been accepted for publication, and Lighthill was one of the referees I realised whilst reading the proofs that although the dominant source of pressure fluctuations in the flow field was this mean shear-turbulent interaction this was not the only source of dominant noise radiation in the lower frequencies. This term in Lighthill's equation was equal to a non-linear acoustic source term multiplied by the mean shear plus a propagation term involving refraction. Without further careful investigation it appeared essential for it to be regarded as a propagation term, which when integrated over the entire acoustic field it would make zero contribution to the radiated noise. Later I was able to show that in the convected wave equation there were two major groups of acoustic source terms, which could be described as above, but now the contribution to the generation from the mean-shear interaction term would involve quadratic velocity fluctuations only.

Lighthill's inspired work on *The Theory of Aerodynamic Noise* in (1952), laid the foundation for all subsequent theoretical work in this field. It is a foundation on which we can all build. It concerns the noise generated from turbulent flows. But, even today, the theory of turbulence remains one of the most incomplete problems in the whole of mathematical physics. Many modeling techniques have been introduced to solve specific problems in turbulent flows, but in the theory of aerodynamic noise, where the radiated noise energy is miniscule compared with the energy of the turbulent flow, we have to admit our modeling remains incomplete. As Lighthill had pointed out the theory of Aerodynamic Noise requires a marrying together of Acoustics with Unsteady Aerodynamics, such as expressed in the field of Aeroacoustics. Without doubt I believe that few will disagree with the statement, '... that modeling the acoustic source terms in jet noise demands full mathematical and physical understanding of the time accurate nature of the unsteady fluid dynamics in the complex turbulent flow in a jet'. Once the complex fluid dynamics of a turbulent jet are known to a high degree of accuracy, the estimation of the characteristics of the radiated noise, including the sound intensity, directivity, and spectrum, which I will refer to as *the propagation problem*, will be possible using the reliable techniques we possess today. The major challenge then will be to improve the speed of computation of these complex unsteady and turbulent flow fields for a wide range of simple and complex nozzle geometries, so that we can not only explore the prediction of jet noise for a given geometry, but also have the ability to optimise that nozzle geometry to produce acceptable noise reductions for almost no loss in performance, such as the nozzle thrust.

In much of this work we will still have to rely on good experimental data, and indeed the inspiration for new ideas relating to jet noise reduction is more likely to come from the dedicated experimentalist rather than the theoretician. The theoretical modeling has an equally important role to play in helping to uncover the underlying physics of time accurate unsteady flow knowledge, providing a continuing updating of models and assessing what are the dominant parameters which determine the bulk of the noise, and providing a means to rapidly optimise possible break-throughs in jet noise reduction technology. The marriage between dedicated experimental jet noise groups and those concerned with the theory and computation of jet noise is important not only today but for many years to come. I cannot envisage a time in the future when we will with confidence, on theory alone, hand a nozzle design to an engine manufacturer with a guaranteed jet noise prediction for all operating conditions of the engine.

Before I close this introduction I wish to emphasize that the prediction of jet noise from a satisfactory knowledge of its time-accurate unsteady turbulent flow in the jet is not the only problem of interest to the engine and aircraft designer. One major problem concerns the effects of non-uniformity of the jet flow in respect of both velocity and temperature upstream of the nozzle exit, as well as the efficient mixing of the separate jet flows as in the core and bypass jet streams. Another major problem concerns installation effects on an aircraft. Now the concerns in Aircraft Noise Reduction relate not only to Engine Noise but also to Airframe Noise. In the latter case we find the possibility of enhanced noise from Installation Effects is very much related to the proximity of jets with the trailing edge of the wings and other potential scattering surfaces. Wind tunnel tests on model jet exhausts alone is clearly unacceptable and the need is to extend the tests to include all relevant surfaces of the aeroplane, including flaps at approach settings. Similar considerations concern the theoretical and computational work. I believe strongly that one of main goals of all theoretical and computational work on jet noise should be the establishment of the lower bounds of the far-field noise under ideal flow conditions. These goals provide the targets for work on noise reduction.

OUTLINE

- INTRODUCTION
- THE LIGHTHILL ACOUSTIC ANALOGY
- GENERATION AND PROPAGATION
- THE LIGHTHILL CONVECTED WAVE EQUATION
- CONVECTED WAVE AMPLIFICATION
- THE PRESSURE WAVE EQUATION
- THE EFFECT OF A UNIFORM MEAN SHEAR FLOW
- TURBULENCE MODELING
- DISCUSSION
- CONCLUSIONS

INTRODUCTION

- $$\frac{\partial^2 \rho}{\partial t^2} - c_\infty^2 \nabla^2 \rho = \frac{\partial^2 T_{ij}}{\partial x_i \partial x_j}(\boldsymbol{x}, t)$$

- $$T_{ij} = \rho v_i v_j - \tau_{ij} + \delta_{ij}(p - c_\infty^2 \rho)$$

- **T_{ij} is the Lighthill stress tensor, where $\boldsymbol{v}$, $\boldsymbol{\tau}$, p, and ρ are absolute values. T_{ij} must be known throughout the flow field and must include all interactions between the flow and the acoustic wave motion generated by the flow.**
- **In Lighthill's acoustic analogy, T_{ij}, which replaces the entire flow field, is the equivalent distribution of acoustic sources in a uniform medium at rest. Outside the flow $T_{ij} = 0$.**

INTRODUCTION-(cont)

- The fluctuating part of T_{ij} contains linear and quadratic velocity fluctuations as well as pressure, density and temperature fluctuations.
- In general we attach a mean convective Mach number to each point in the flow. T_{ij} includes effects of convective amplification and consequent *Doppler* changes in frequency between source and observer.
- At low flow Mach numbers the typical flow dimensions, $L \ll \lambda$, where, λ is the acoustic wavelength, and the source region is compact.
- At higher Mach numbers and higher frequencies much of the source region is non-compact. Acoustic disturbances suffer refraction and diffraction by mean velocity and temperature gradients, and scattering by turbulence within the flow. The Pridmore-Brown equation describes refraction of acoustic waves exposed to a uniform shear flow.

THE LIGHTHILL ACOUSTIC ANALOGY

- **Lighthill's fluctuating stress tensor** $\left(T'_{xx} = T_{xx} - \bar{T}_{xx}\right)$**, where** T_{xx} **is of the order** $2/3$ **times the local turbulent kinetic energy. It is anisotropic and its value differs along the different lines between the source and various far-field observers. It contains linear and quadratic velocity fluctuations. The linear velocity terms are associated with PROPAGATION effects, whereas quadratic velocity fluctuations provide GENERATION. Lighthill's solution provides, in effect, an energy efficiency, which we may call the 'Lighthill acoustic filter factor', between the fluctuating kinetic energy in the flow and the radiated acoustic energy. In low speed flows the small fraction of flow turbulent kinetic energy escaping as radiation is of order** 10^{-4}**.**

- $$(\rho - \rho\infty)(\boldsymbol{x}, t) \simeq \frac{1}{4\pi c_\infty^4} \int \frac{\partial^2}{\partial \tau^2} \left(\frac{T_{xx}(\boldsymbol{y}, \tau)}{\mid \boldsymbol{x} - \boldsymbol{y} \mid} \right) d\boldsymbol{y}^3$$

THE FAR-FIELD SOUND INTENSITY

- The farfield sound intensity, $I = < (\rho - \rho_\infty)^2 > c_\infty^3/\rho_\infty$, is given by

$$I(\boldsymbol{x}) = \frac{1}{16\pi^2 \rho_\infty c_\infty^5} \int (< (T'_{xx})^2 >)^2 (\boldsymbol{y}) \left(\int \frac{\partial^4}{\partial \tau^4} \left(R_{xx,xx}(\boldsymbol{y}, \boldsymbol{\delta}, \tau) \right) d\boldsymbol{\delta}^3 \right) d\boldsymbol{y}^3$$

  where $R_{xx,xx}(\boldsymbol{y}, \boldsymbol{\delta}, \tau)$ is the two-point, two-time retarded space-time correlation coefficient as a function of flow location, $\boldsymbol{y}$, and moving coordinate space and retarded-time separation, $\boldsymbol{\delta}$, and τ respectively. It is aligned in the direction between source and observer.

- The 'Lighthill acoustic filter factor' comprises the integral involving integration with respect to the two-point separation distance $\boldsymbol{\delta}$. A good working approximation is to assume in certain flows that its non-dimensional form is a constant throughout the flow.

- The sound intensity, and the total acoustic power, are found from the 'weighted' integral of the mean square of the fluctuations in T_{xx} taken over the entire flow field.

GENERATION AND PROPAGATION

- Lighthill derived the acoustic analogy for acoustic waves emerging from a flow into a medium at rest. Where there is FLOW-ACOUSTIC INTERACTION we need to consider a transformation of Lighthill's equation into a convected wave equation pertinent to the flow.
- To differentiate between PROPAGATION AND GENERATION effects we first consider the simple case where a bounded turbulent flow is embedded in a uniform mean flow, $\boldsymbol{V}_\infty = (V_\infty, 0, 0)$. The turbulent velocity is $\boldsymbol{v}$. We now define a new Lighthill stress tensor,

$$\boldsymbol{\mathcal{T}} = \rho \boldsymbol{v}\boldsymbol{v} - \boldsymbol{\tau} + (p - \rho c_\infty^2)\boldsymbol{I}$$

which retains only quadratic fluctuations in velocity. This is the dominant generation function in an unbounded turbulent flow. Propagation is governed by the linear velocity terms and transforms the wave equation at rest into a convected wave equation.

THE LIGHTHILL CONVECTED WAVE EQUATION

- The mean flow convective operator is

$$\frac{D_0}{Dt} \equiv \frac{\partial}{\partial t} + \boldsymbol{V}_c \cdot \nabla$$

  where $(\boldsymbol{V}_c = \boldsymbol{V}_\infty)$.

- The resulting convected wave equation is

$$\left(\frac{D_0^2}{Dt^2} - c_\infty^2 \nabla^2\right) \rho = \nabla^2 \boldsymbol{\mathcal{T}}$$

  where inside the turbulent flow both sides of the 'convected' wave equation are of equal order of magnitude. Solutions are required inside the flow in order to study FLOW-ACOUSTIC INTERACTION.

- The second order convected wave equation is exact and is used extensively in problems of aerocoustics. As was to be expected the source term contains only quadratic velocity fluctuations.

CONVECTED WAVE AMPLIFICATION

- **Lighthill obtained a simple solution to the problem of the convection of acoustic sources relative to a distant observer. Instead of using the convection equation Lighthill argued that the sound generated by a source travelling at constant velocity, $\boldsymbol{V}_c$, relative to an observer at rest could be obtained by using a Galilean transformation in the acoustic analogy integral.**
- **Thus defining the moving axis transformation ($\boldsymbol{M}_c = \boldsymbol{V}_c/c_\infty$)**

$$\boldsymbol{\eta} = \boldsymbol{y} - c_\infty \boldsymbol{M}_c \tau$$

$$\rho(\boldsymbol{x}, t) - \rho_\infty \sim \frac{1}{4\pi c_\infty^4 x \mid 1 - M_c \cos\theta \mid^3} \int \frac{\partial^2 \boldsymbol{T}_{xx}}{\partial \tau^2}(\boldsymbol{\eta}, \tau) d\boldsymbol{\eta}^3$$

- **This is the Lighthill-Ffowcs Williams convective amplification formula for $M_c \cos\theta < 1$.**

PRESSURE WAVE EQUATION

- **The convected wave equation for the pressure is**

$$\left(\frac{1}{c_\infty^2}\frac{D_0^2}{Dt^2} - \nabla^2\right) p = \nabla^2 \rho \boldsymbol{v}\boldsymbol{v} - \frac{(\gamma-1)}{2c_\infty^2}\frac{D_0^2}{Dt^2}v^2 - \frac{D_0}{Dt}\nabla\cdot\rho\boldsymbol{v}\frac{(h_s - h_\infty)}{h_\infty}$$

  where $\boldsymbol{v}$ is the turbulent velocity and we adopt a special form of the 'stagnation enthalpy', $h_s = h + v^2/2$, which includes only quadratic fluctuations in the velocity, and excludes the square of the mean velocity.

- **Morkovin(1964) and Bradshaw(1977) suggest**

$$\left|\frac{h'}{h_j}\right| \approx 1.6\frac{\sqrt{v^2}}{V_j}\frac{(h_j - h_\infty)}{(h_j + h_\infty)}$$

  showing that fluctuations in $(h_s - h_\infty)/h_\infty$ are of order h_j/h_∞, which is proportional to T_{st}/T_∞.

THE EFFECT OF NON-UNIFORM MEAN FLOW

- **The acoustic source terms in Lighthill's Acoustic Analogy are complicated by the presence of the density, ρ. This can be eliminated by using logarithmic thermodynamic quantities**

$$\pi = \ln p^{1/\gamma} : \chi = \ln \rho : \lambda = \ln h : \pi = \xi$$

- **When the thermodynamic processes in a turbulent flow are assumed to be isentropic we find $\pi = \chi$: $\lambda = (\gamma - 1)\pi$, since from the equation of state, $\gamma\pi = \chi + \lambda$.**
- **The conservation equations are**

$$\frac{D\pi}{Dt} + \nabla \cdot \boldsymbol{v} = 0 : \frac{D\boldsymbol{v}}{Dt} + c^2 \nabla \pi = 0$$

where $c = \sqrt{\gamma p/\rho} = \sqrt{(\gamma - 1)h}$ is the local speed of sound.

THE EFFECT OF NON-UNIFORM MEAN FLOW (cont)

- **The convected wave equation can be written is**

$$\frac{D^2\pi}{Dt^2} - \frac{\partial}{\partial x_j}\left(c^2\frac{\partial \pi}{\partial x_j}\right) = \frac{\partial v_i}{\partial x_j}\frac{\partial v_j}{\partial x_i}$$

  where, $\frac{D}{Dt} \equiv \frac{\partial}{\partial t} + v_j\frac{\partial}{\partial x_j}$**, and is the exact convected wave equation for** π**. It was originally due to Phillips(1960).**

- **It can also be written**

$$\frac{D^2\pi}{Dt^2} - c^2\nabla^2\pi = \nabla \boldsymbol{v} : \boldsymbol{v}\nabla + \frac{c^2}{(\gamma-1)}(\nabla\lambda)^2$$

LILLEY'S ACOUSTIC ANALOGY

- **The general THIRD-ORDER convected wave equation is exact but of little practical use. We require a convected wave equation for a known mean flow field, in which the mean enthalpy and mean velocity distibution are prescribed. Let us consider the simple case of a flow of constant mean pressure, p_0, and enthalpy, h_0. The mean velocity is $\boldsymbol{V} = (V_1(x_2), 0, 0)$. Thus, in this case, $\nabla \cdot \boldsymbol{V} = 0$. We assume the fluctuating flow is isentropic.**
- **The conservations equations reduce to**

$$\frac{D_0\pi'}{Dt} + \theta' = -\boldsymbol{v}' \cdot \nabla\pi' \; : \; \frac{D_0\boldsymbol{v}'}{Dt} + c_0^2\nabla\pi' + v_2'\frac{dV_0}{dx_2}\boldsymbol{i} = -\boldsymbol{v}' \cdot \nabla\boldsymbol{v}' - \frac{\gamma - 1}{2}c_\infty^2\nabla(\pi')^2$$

where the non-linear terms are arranged on the RHS.

- **We eliminate $D_0\theta'/Dt$ by D_0/Dt of the former minus $\nabla\cdot$ of the latter.**

LILLEY'S ACOUSTIC ANALOGY (cont.)

- **The THIRD-ORDER equation for a constant mean shear and enthalpy gradient leads to**

$$\mathcal{L}(\pi') = \mathcal{F}(\boldsymbol{x}, t)$$

where the operator

$$\mathcal{L} \equiv \frac{D_0}{Dt}\left(\frac{D_0^2}{Dt^2} - c_\infty^2 \nabla^2\right) + 2c_\infty^2 \frac{dV_1}{dx_2}\frac{\partial^2}{\partial x_1 \partial x_2}$$

- **The GENERATION source distribution equals**

$$\mathcal{F} = \frac{D_0}{Dt}\left(-\frac{D_0}{Dt}(\boldsymbol{v}' \cdot \nabla \pi') + \nabla \cdot \left(\boldsymbol{v}' \cdot \nabla \boldsymbol{v}' + \frac{\gamma - 1}{2} c_\infty^2 \nabla (\pi')^2\right)\right)$$

$$-\frac{d\lambda_0}{dx_2}\frac{D_0}{Dt}\left(\boldsymbol{v}' \cdot \nabla v_2' + \frac{\gamma - 1}{2} c_\infty^2 \frac{\partial (\pi')^2}{\partial x_2}\right)$$

$$-2\frac{dV_0}{dx_2}\left(\frac{\partial}{\partial x_1}(\boldsymbol{v}' \cdot \nabla v_2') + \frac{\gamma - 1}{2} c_\infty^2 \frac{\partial^2 (\pi')^2}{\partial x_1 \partial x_2}\right)$$

THE EFFECT OF UNIFORM MEAN SHEAR FLOW

- **The generalised convective wave equation for a uniform mean shear, dV_1/dx_2 is THIRD-ORDER, giving**
- $$\mathcal{L}(\rho) = \mathcal{F}(\boldsymbol{x}, t)$$
- **The LHS is the Pridmore-Brown operator.**

$$\mathcal{L} \equiv \frac{D_0}{Dt}\left(\frac{D_0^2}{Dt^2} - c_\infty^2 \nabla^2\right) + 2c_\infty^2 \frac{dV_1}{dx_2}\frac{\partial^2}{\partial x_1 \partial x_2}$$

- **The true generation terms, which are all quadratic in the fluctuations, are on the RHS.**

$$\mathcal{F} = \frac{D_0}{Dt}\frac{\partial^2 \mathcal{T}_{ij}}{\partial x_i \partial x_j} - 2\frac{dV_1}{dx_2}\frac{\partial^2 \mathcal{T}_{2j}}{\partial x_1 \partial x_j}$$

where $\mathcal{T}_{ij} = \rho v_i v_j + \delta_{ij}(p - c_\infty^2 \rho)$, when viscous effects are neglected.

THE PROPAGATION OF SOUND IN 1-D

- **The 1-D conservation equations for the propagation of isentropic disturbances in a compressible inviscid flow are**

$$\frac{\partial P}{\partial t} + u\frac{\partial P}{\partial x} + c\frac{\partial u}{\partial x} = 0$$

$$\frac{\partial u}{\partial t} + c\frac{\partial P}{\partial x} + u\frac{\partial u}{\partial x} = 0$$

where $dP = dp/\rho c = cd\rho/\rho$**. By adding and subtracting**

$$\frac{\partial}{\partial t}(P \pm u) + (c \pm u)\frac{\partial}{\partial x}(P \pm u) = 0$$

having the solutions $P + u = A$ **and** $P - u = B$**, where** A **and** B **are constants along the characteristics** $dx/dt = u + c$ **and** $dx/dt = u - c$ **respectively. It is from these equations that we develop Burgers equation for the nonlinear convective distortion of disturbances generated in a flow. These have been discussed by Lighthill(1994) in his theory of bunching and by Punekar et al.(1998).**

PROPAGATION OF SOUND WITH REFRACTION

- The wave equation in 1-D is given by the 1-D form of Lighthill's equation, namely

$$\frac{\partial^2 \rho}{\partial x^2} - c_\infty^2 \frac{\partial^2 \rho}{\partial x^2} = \frac{\partial^2}{\partial x^2}(\rho u^2 + (p - c_\infty^2 \rho))$$

- In recent work on modeling compressible turbulence Ristorcelli(1998) at turbulent Mach numbers, $M_T < 0.25$, has shown using a two-time analysis that there is a fast-time for the propagation of acoustic disturbances and a slow time for the convection of turbulence. The convective wave equation for the acoustic disturbances is third-order and is similar to Lilley's Acoustic Analogy. The acoustic mode develops on the fast scale and suffers refraction due to the mean shear.

THE REFRACTION PROBLEM

- Pridmore-Brown(1958), Goldstein(1976), Morfey et al. (1978), Lilley(1996), Lele et al.(2000) and others have investigated the effects of flow-acoustic interaction and thus refraction of the sound generated by the flow. It is an effect important at all jet Mach numbers.
- Outside a flow the acoustic equations are hyperbolic, but inside the flow the equations are mainly elliptic and only weakly hyperbolic.

TURBULENCE MODELING

- Turbulent jet flow at very large Reynolds numbers may be divided into a mean motion, V, a large scale turbulent motion, v', and a small scale turbulent motion, v'', which is almost independent of the large scale motion. The small scale turbulent motion at this large Reynolds number is in almost universal equilibrium. In a time dependent RANS calculation, v'', would be the unresolved motion.
- We write for all variables, such as $v = V + v' + v''$.
- A long time average, is denoted by an overbar, and a short time average of the large scale motion, but long compared with the characteristic time of the small scale motion, is denoted by tilde. We combine V and v' and write

$$\tilde{V} = V \widetilde{+} v' = V + \widetilde{v'}$$

noting $\widetilde{v''} = 0$, whereas the large scale fluctuation $\widetilde{v'}$ is non-zero.

TURBULENCE MODELING (cont.)

- We assume that the unresolved density fluctuations, $\rho'' \ll \tilde{\rho}$, and the unresolved fluctuations in the viscous shear stress, $\boldsymbol{\tau}'' \ll \tilde{\boldsymbol{\tau}}$.
- We introduce the stagnation pressure, h, and the vortex force, $\boldsymbol{f}$ given by

$$h = \int dp/\rho + \frac{v^2}{2} : \boldsymbol{f} = \rho\left(\boldsymbol{v} \times \boldsymbol{\omega}\right)$$

- Short-time average values are

$$\tilde{H} = \int \frac{d\tilde{P}}{\tilde{\rho}} + \frac{\tilde{\boldsymbol{V}}^2}{2} + \tilde{k} : \tilde{\boldsymbol{F}} = \tilde{\rho}\left(\tilde{\boldsymbol{V}} \times \tilde{\boldsymbol{\Omega}} + \boldsymbol{v}'' \,\widetilde{\times}\, \boldsymbol{\omega}''\right)$$

where the kinetic energy of the very small scale turbulent motion is written as $\tilde{k} = \widetilde{(v'')^2}/2$. In LES this equals the subgrid scale contribution to the turbulent kinetic energy.

TURBULENCE MODELING (cont.)

- We assume the small scale motion is uncorrelated with that of the larger scale motion, and there is 'adequate' separation between these scales. The short-time average of the total kinetic energy is $\tilde{\boldsymbol{V}}^2/2 + \tilde{k}$, noting $\tilde{\boldsymbol{V}}^2 = V^2 + 2\boldsymbol{V}\widetilde{\cdot}\,\boldsymbol{v}' + (\tilde{\boldsymbol{v}'})^2$. Clearly $\tilde{k} \ll \tilde{\boldsymbol{V}}^2/2$ even when $\tilde{k}$ may be a non-negligible fraction of $(\tilde{\boldsymbol{v}'})^2/2$.
- The rate of dissipation of the small scale motion is approximately $\tilde{\rho}\tilde{\epsilon} = \tilde{\rho}\nu(\widetilde{\omega''})^2$, where $(\widetilde{\omega''})^2$ is the enstrophy of the small-scale motion.
- $$h'' = \int \frac{dp''}{\tilde{\rho}} + \tilde{\boldsymbol{V}} \cdot \boldsymbol{v}'' + \left((v'')^2 - (\widetilde{v''})^2\right)/2$$

  and similarly

$$\boldsymbol{f}'' = \tilde{\rho}\left(\tilde{\boldsymbol{V}} \times \boldsymbol{\omega}'' + \boldsymbol{v}'' \times \tilde{\boldsymbol{\Omega}} + \left(\boldsymbol{v}'' \times \boldsymbol{\omega}'' - \boldsymbol{v}'' \,\widetilde{\times}\, \boldsymbol{\omega}''\right)\right)$$

TURBULENCE MODELING (cont.)

- Splitting turbulence into large(resolved) and small(unresolved) structures captures the time-accurate structure of the energy containing scales and the non-linear cascade development beyond the 'peak frequency'.
- This is the resolved turbulence structure that controls the $\mathcal{T}_{xx}$ space-retarded time covariance. A model for this fourth-order (two-point, two-time)covariance is available for isotropic turbulence. Currently a model has not been derived for shear flow turbulence.
- The estimation of the acoustic power from unheated isotropic turbulence per unit volume is, following Lighthill, $p_s = \alpha_P \frac{\rho_0^2}{\rho_\infty} \frac{v^8}{c_\infty^5 L}$.
- Assuming $\alpha_P = const$ in the flow, and given the distribution of k and L the total acoustic power was derived by simple quadrature. The paper in 1996 includes the contribution from heated turbulence. The agreement with experiments on cold and heated jets is satisfactory provided we include refraction at Mach numbers greater than unity.

TURBULENCE MODELING (cont.)

- Both h'' and $\boldsymbol{f}''$ represent the time dependent contributions with zero mean from the small scale turbulence. They both generate large fluctuations about the mean and such fluctuations arise from linear perturbations. The strongest interaction between the mean and turbulent motion(and that between the large and small eddy motion) is generated by linear fluctuations. Such fluctuations are missing entirely from the equivalent mean flow equations, such as steady RANS.

- The short time averaged flow equations of continuity and motion for the resolved large scale motion become

$$\frac{\partial \tilde{\rho}}{\partial t} + \nabla \cdot \tilde{\rho}\tilde{\boldsymbol{V}} = 0 : \tilde{\rho}\left(\frac{\partial \tilde{\boldsymbol{V}}}{\partial t} + \nabla \tilde{H}\right) - \tilde{\boldsymbol{F}} = \nabla \cdot \tilde{\boldsymbol{\tau}}$$

TURBULENCE MODELING (cont.)

- The divergence of the Reynolds stress tensor for the small scale motion, is a vector quantity, and is given by the identity, assuming $\nabla \cdot \boldsymbol{v}'' = 0$,

$$\nabla \cdot \widetilde{\boldsymbol{v}''\boldsymbol{v}''} = \left(\nabla \tilde{k} - \boldsymbol{v}'' \,\widetilde{\times}\, \boldsymbol{\omega}''\right)$$

- We note the influence of the small unresolved structures of the turbulent motion on the large eddy structure is through the divergence of the Reynolds stress tensor, where the latter has six independent components. But the divergence, being a force, has only three components. These are derived from the four independent quantities comprising $\tilde{k}$, and $\boldsymbol{v}'' \,\widetilde{\times}\, \boldsymbol{\omega}''$.
- Similarly the time accurate flow equations for the small scale motion are

$$\nabla \cdot \boldsymbol{v}'' = 0 : \tilde{\rho}\left(\frac{\partial \boldsymbol{v}''}{\partial t} + \nabla h''\right) - \boldsymbol{f}'' = \nabla \cdot \boldsymbol{\tau}''$$

TURBULENCE MODELING (cont.)

- The energy equation for the small scale turbulent motion is the short time average of the scalar product of $\boldsymbol{v}''$ with the equation of motion for the small scales,

$$\tilde{\rho}\left(\frac{\partial \tilde{k}}{\partial t} + \nabla \cdot \left(\widetilde{\boldsymbol{v}''h''} - \nu \cdot \boldsymbol{v}'' \mathbin{\widetilde{\times}} \boldsymbol{\omega}''\right)\right) + \tilde{\rho}\tilde{\boldsymbol{V}} \cdot \boldsymbol{v}'' \mathbin{\widetilde{\times}} \boldsymbol{\omega}'' = -\tilde{\rho}\tilde{\epsilon}$$

where we have used the approximation $\tilde{\epsilon} = \nu(\widetilde{\omega''})^2$.

- $$\nabla \cdot \widetilde{\boldsymbol{v}''\boldsymbol{v}''} = \left(\nabla \tilde{k} - \boldsymbol{v}'' \mathbin{\widetilde{\times}} \boldsymbol{\omega}''\right) = \tilde{\boldsymbol{R}}$$

where $\tilde{\boldsymbol{R}}$ has three components $\tilde{R}_1, \tilde{R}_2, \tilde{R}_3$, and $\tilde{R}^2 = (\tilde{R}_i)^2$.

- If $\Phi = \widetilde{\boldsymbol{v}''\boldsymbol{v}''}$, the self-conjugate dyadic, representing the small scale turbulent Reynolds stress, then

$$\nabla \cdot \left(\Phi \cdot \tilde{\boldsymbol{R}}\right) - \Phi : \nabla \tilde{\boldsymbol{R}} = \tilde{R}^2$$

showing the relationship between $\tilde{\boldsymbol{R}}$ and the Reynolds stress tensor.

TURBULENCE MODELING (cont.)

- The fundamental property of the turbulent flow, relating to the production of small scale turbulent energy from the large scale motion is,

$$\nabla \cdot \left(\Phi \cdot \tilde{\boldsymbol{V}} \right) - \Phi : \nabla \tilde{\boldsymbol{V}} = \tilde{\boldsymbol{V}} \cdot \tilde{\boldsymbol{R}}$$

- This important identity is between (i) the redistribution of energy, $\nabla \cdot \left(\Phi \cdot \tilde{\boldsymbol{V}} \right)$, (ii) the turbulent energy production, $-\Phi : \nabla \tilde{\boldsymbol{V}}$, and (iii) the work done against the turbulent force, $\tilde{\boldsymbol{V}} \cdot \tilde{\boldsymbol{R}}$.
- For the large scale motion

$$-\widetilde{\boldsymbol{v}''\boldsymbol{v}''} : \nabla \tilde{\boldsymbol{V}} \equiv \nabla \cdot \left(\tilde{\boldsymbol{V}} \cdot \left(\tilde{\boldsymbol{I}} \tilde{k} - \widetilde{\boldsymbol{v}''\boldsymbol{v}''} \right) \right) - \tilde{\boldsymbol{V}} \cdot \boldsymbol{v}'' \mathbin{\widetilde{\times}} \boldsymbol{\omega}''$$

where $\tilde{\boldsymbol{I}}$ is the idemfactor. Thus the integrated turbulent energy production equals the integrated work done against the vortex force.

DYNAMIC EFFECTS OF THE VORTEX FORCE

- The dynamic effects of the vortex force may be contrasted with the 'passive' role played by the components of the Reynolds stress tensor. In the case of the jet mixing region the Reynolds stress at a distance, y, from the nozzle lip line is obtained either from an integral across $y = -\infty$ to y, of the vortex force in the outer low speed mixing layer or from the corresponding integral from y to $y = \infty$, across the inner high speed mixing layer. These two integrals are equal even though the vortex force components in the two regions are highly variable and fluctuate temporally with extremely high amplitudes at very different frequencies in the two distinct regions and irrespective of the exact location of the observation position, y.

USE OF EDDY VISCOSITY IN URANS

- In steady RANS the 'linear' k - ϵ turbulence model replaces the Reynolds stress tensor by an eddy viscosity model thus replacing the 'dynamics' of the turbulence on average as a 'passive' diffusion effect. In unbounded shear layers such as the outer region of the boundary layer and the mixing region of a jet it has long been known that the mean velocity distribution in incompressible and compressible flow can be obtained by replacing the Reynolds stress tensor by an eddy viscosity, ν_T proportional to k^2/ϵ. Physically eddy viscosity has the same dimensions as circulation and thus it is more appropriate to refer to 'LARGE EDDY CIRCULATION' than 'eddy viscosity. For the properties of the time averaged flow the words 'dynamic' or 'passive' have no meaning since we are solving for an equivalent mean or averaged flow.

USE OF EDDY VISCOSITY IN URANS (cont.)

- A 'good' approximation to the mean flow field is found for streamwise growing shear layers is to assume the eddy viscosity is a function of downstream distance only. Using such approximate methods one can find the mean velocity and temperature profiles in a mixing region and jet as a function of Mach number. Such flows may be assumed self-preserving and their properties remain similar over all Mach numbers. However some solutions are singular near the origin of the shear layer and the correct solution can only be found using DNS locally and matching it with the self-preserving solution downstream.
- But when we require a time accurate flow solver it is important that each term in the conservation equations retains its full physical properties. Thus to include the effects of turbulence on the large scale structures in the flow-field by modeling the Reynolds stresses as diffusion effects provides an un-natural damping on the entire flow. Moreover since one of the objectives of URANS is to pro-

vide information regarding the properties of the nonlinear acoustic source terms for use in Lighthill Acoustic Analogy, with frequencies in the range beyond the energy containing range, any excess damping will prevent the proper evolution of these important structures. At high Reynolds most of the turbulent structures in the inertial range develop as near-inviscid structures.

- All RANS and URANS solutions are very sensitive to initial and boundary conditions. The large eddy structures need to be 'kicked' into shape to enable them to quickly develop their local self-generating turbulent role.

DISCUSSION

- The second-order convected wave equation for a uniform flow and the third-order equation for a uniform shear flow are exact and involve extensions to Lighthill's acoustic analogy. The acoustic sources are derived from Lighthill's stress tensor but include only quadratic velocity fluctuations.
- The solutions to the third-order equation are greatly simplified when Fourier transforms are taken with respect to time and in the plane perpendicular to the mean shear.
- The problem of acoustic propagation across a shear layer in aeroacoustics has many similarities with the work of Brekhovskih in underwater acoustics in wave propagation in non-uniform layered media.
- The refraction of sound propagating through velocity and temperature shear layers shows the complexity of the combined generation and propagation problem in aeroacoustics. It is a field of continuing research.

CONCLUSIONS

- This lecture prepared in honour of Sir James Lighthill pays tribute to his pioneering work on Aerodynamic Noise begun nearly half a century ago. His impact on the World of Science in his lifetime was immense but the work he started will continue to blossom and to branch out into directions even Sir James had never contemplated. But on reflection he would not have been surprised. Our debt to him is in recognition of how beautiful was the mathematics he taught us and the depth of understanding that we learnt from him to further our work in Acoustics and Waves in Fluids.

WHAT IS KNOWN ABOUT JET NOISE?

- 1. A fully turbulent jet into ambient fluid has a mean axial velocity distribution almost independent of Reynolds number. The transverse velocity component is small in comparison. It is associated with the entrainment. The width of the jet is a linear function of x. The mean velocity distribution is clearly a function of external velocity/jet velocity ratio.
- 2. The width is a function of the mean temperature ratio, (inverse of density ratio) and jet Mach number. Mixing region growth is an important function in jet noise prediction. It is also an important function varying with temperature ratio and Mach number.
- 3. Boundary layer effects in the nozzle, such as transition upstream or downstream of the nozzle exit can be a function of model Reynolds number, but are not normally an issue with full scale measurements.

WHAT IS KNOWN ABOUT JET NOISE? (cont.)

- 4. Pressure fluctuations measured in jet flows include effects of turbulence and sound waves and their interference with the flow. In the flow there is flow-acoustic interaction. This is an important phenomenon.
- 5. Convective amplification is important in its contribution to directivity and intensity at both subsonic and supersonic Mach numbers.
- 6. The turbulent Mach number, v_T/c_∞, is subsonic in most of the work referred to in this workshop. This covers subsonic and supersonic jet speeds.
- 7. Far-field noise measurements show proportionality with V_j^6 and V_j^8 for the hot jet and cold jet respectively. The hot jet is noisier than the cold jet at low Mach numbers. The cold jet is noisier at high Mach numbers.

WHAT IS KNOWN ABOUT JET NOISE? (cont.)

- 8. The exact equations for turbulent flow are the Navier-Stokes equations, and exact solutions can be obtained from DNS. Even low Reynolds number calculations for subsonic and supersonic jets for hot and cold fully turbulent flow provide important information on flow structure its physics and development. $V_x/V_j(x, y, z)$ is an almost universal function. The mean properties change little with Reynolds number if we can avoid all problems associated with transition. Even though DNS misses the large separation of scales between energy containing and Kolmogoroff scales. This does not affect the low frequency development of the turbulence and in much of the inertial range, provided there is reasonable separation between energy containing and cut-off, dependent on grid size, scales. Measurements show only small scale effect on turbulent intensity and length scale in jets.

WHAT IS KNOWN ABOUT JET NOISE?(cont.)

- **9. I label energy containing eddies of scale, ℓ_0, and amplitude, u_0, with the Reynolds number of these eddies equal to, $R_0 = u_0\ell_0/\nu$. If the Kolmogorov range is labelled, ℓ_s and u_s, then $R_s = u_s\ell_s/\nu = 1$. We find**

$$\frac{u_0}{u_s} = R_0^{1/4} : \frac{\ell_0}{\ell_s} = R_0^{3/4}$$

- **10. In growing shear layers the energy containing eddies are physically small near the origin of the shear layer. The dissipating eddies, in the same region are smaller. Further downstream the energy containing eddies are larger. The noise generated by these 'small' energy containing eddies will be of high frequency, while the 'large' eddies downstream will be of lower frequency. I prefer to discuss the scales of turbulence generating the greatest contribution to the radiated noise as 'scales slightly smaller than the energy-containing range'. The characteristic frequency, $\omega_0 \approx u_0/\ell_0$.**

WHAT IS KNOWN ABOUT JET NOISE?(cont.)

- **11. The noise radiation from a jet is made up of a 'peak' to 'low' frequency contribution from downstream of the potential core, and a 'peak' to 'high' frequency contribution from the nozzle exit to the end of the potential core. To obtain the radiated spectrum of the noise we do not have to resolve, in any flow calculation, frequencies approaching the Kolmogorov range.**
- **12. The rate of dissipation**

$$\epsilon = \frac{u_0^3}{\ell_0} = \frac{u_s^3}{\ell_s} = \frac{u_c^3}{\ell_c}$$

where u_c and ℓ_c are the characteristic scales at 'cut-off.

WHAT IS KNOWN ABOUT JET NOISE? (cont.)

- **13. The noise radiated from turbulence is a small percentage of the turbulent kinetic energy. The largest contribution comes from the central region of the mixing region. I call this quantity the 'Lighthill filter function'. In Lighthill's acoustic analogy it is the non-dimensional two-point, two-time T_{ij} space-retarded time covariance. Some measurements of this quantity have been attempted but the most complete evidence has come from DNS calculations in isotropic turbulence.**
- **14. The existing results gave the characteristics of this function but clearly results are needed at higher Reynolds numbers such as 512^3 and 1024^3 for forced stationary turbulence. We then need to explore if this function changes significantly across say a mixing region.**

WHAT IS KNOWN ABOUT JET NOISE? (cont.)

- 15. Lilley(1996) assumed a constant value for this function over fully expanding jet plumes at subsonic and supersonic, hot and cold jets. I selected the available kinetic energy and length scale distribution throughout a jet. The acoustic power plots show the fit is satisfactory and much better than would have been anticipated from such a crude model.
- 16. The overall characteristics of turbulent flow are highly non-linear. The large eddies are generated randomly from a background of smaller scale turbulent motion. These eddies have characteristics pertaining to the most unstable eigen-values and eigen functions of the local flow. Stability theory plays a large part in uncovering the large eddy structure in the jet. The growth-saturation-decay cycle, with the modes increasing in scale downstream, is part of the overall local self-generation cycle of the turbulence. The 'history' of the turbulence plays a relatively unimportant role in the jet.

WHAT IS KNOWN ABOUT JET NOISE? (cont.)

- 17. However linear stability theory can at best only provide an amplitude ratio and cannot predict an absolute magnitude for the eddies containing most of the energy. Hence a calibration is needed whch relies on experimental data. This applies also to the noise calculated from linear instability models. The noise generated arises from the non-linear distortion with the peak in the noise spectrum at a frequency greater than that of the energy containing eddies.
- 18. The instability models provide the physical structure of the turbulent flow and provide clues as to what is needed to reduce noise.

WHAT IS KNOWN ABOUT JET NOISE? (cont.)

- 19. A simple approach to noise reduction comes from the simple modeling discussed above. The most important dimension in the structure of the subsonic jet is the length of the potential core. If this can be reduced without changing the jet thrust a large reduction is noise is achieved. The 'peak' in the noise spectrum is lowered as well as the frequency at the peak. The mechanisms to produce this normally use some form of vortex generator and these have the disadvantage of increasing the noise at higher frequencies.

- 20. In airframe noise the spectrum is nominally broadband covering frequencies from about $20Hz$ to $10kHz$, and this includes all aircraft, gliders and birds. The exception is the 'owl' that has special feathers which cancel the noise at all frequencies greater than $2kHz$. Interest is being shown into the possibility of introducing 'owl technology' to effectively reduce the noise of aircraft in this critical frequency range above $2kHz$.

G. M. Lilley References

1. Bebber, van. (2000) "Numerical investigation concerning the non-stationary Kutta condition." *DLR Rep. No.,* **2000-23**.

2. Brekhovskikh, L.M. (1969) "Waves in layered Media" Academic Press. New York.

3. Brown, G.L. and Roshko, A. (1974) "On density effects and large structures in turbulent mixing layers." *J. Fluid. Mech,* **64**,pp.775-8l6.

4. Doak, P.E. (1971) "The generation and radiation of supersonic jet noise: vol. 1V" ed. Plumblee, H.E. AFAPL TR-72.53 US Air Force (Available from DTIC as 749 139.)

5. Ffowcs Williams, J.E. (1963) "The noise from turbulence convected at high speed. " *Phil. Trans. Roy. Soc. (A)* **255**, pp.469-503.

6. Ffowcs Williams, J.E. and Hawkings, D.L. (1969) "Sound generated by turbulence and surfaces in arbitra Phil. Trans.Roy.Soc. (A) **264**, pp.321-342.

7. Goldstein, M. E. (1976) "Aeroacoustics" Mc Graw-Hill(New York).

8. Goldstein, M.E. (1984) The Aeroacoustics of Turbulent Shear Flows, Annual Review of Fluid Mechanics Vol. 16 pp. 236-286.

9. Howe, M.S. (1998) "Acoustics of fluid-structure interactions." C.U.P.

10. Howe, M.S. (1975) "Contributions to the theory of aerodynamic sound, with applications to excess jet theory of the flute." J. Fluid. Mech, **71**, pp.625-673.

11. Lassiter, L.W. and Hubbard, H.H. (1952) "Experimental studies of noise from subsonic jets in still air" NACA TN., **2757**.

12. Lighthill, M.J. (1952) "On sound generated aerodynamically: 1. General Theory." *Proc. Roy. Soc(A)* **211**, pp.564-587.

13. Lighthill, M.J. (1954) "On sound generated aerodynamically: 2. Turbulence as a source of sound." *Proc. Roy. Soc (A)* **214**, pp.1-32.

14. Lighthill, M.J. (1962) "Sound generated aerodynamically: the Bakerian Lecture." Proc.J-Roy.Soc ('A) **267**, pp.147-182.

15. Lighthill, M.J. (1993) "The Final Panel Discussion - Computational Aeroacoustics, ed. Hardin, J.C. and Springer- Verlag.

16. Lilley, G.M. (1971) "Sound generation in shear flow turbulence" Fluid Dyn, Trans. (Poland) 6.405-420.

17. Lilley, G.M. (1996) "The radiated noise from isotropic turbulence with applications to the theory of jet *Jour. Sound and Vibr* **190**, pp.463-476.

18. Lilley, G.M. (1973) " On the noise from air jets." (In Noise Mechanisms.) *AGARD CP* 131, pp.13.1-13.12.

19. Lilley, G.M. (1991) "Jet noise Classical theory and experiments." *Aeroacoustics of Flight Vehicles: Theory and practice. Vol.1 ed. Hubbard, H.H.,* pp.211-289.

20. Morfey, C. (1973) "Amplification of aerodynamic noise by convected homogeneities." J. Sound and Vibration. 31. pp. 391-397.

21. Morfey, C.L. and Tester, B.J. (1978) "Noise measurements in a free jet flight simulation facility; Shear layer refraction and facility to flight correction." J. Sound and Vibration, **54,** pp. 83-106.

22. Morkovin, M.V. (1964) "Effects of compressibility on turbulent flows - The mechanics of turbulence" *Gordon and Breach Scient. Pub. Inc* pp.367-380.

23. Morris, P.J., Giridharen, M.G. and Lilley, G.M. (1990) "On the turbulent mixing if free shear layers.' *Proc. Roy. Soc. (A),* **43l**,pp.2l9-2Ll3.

24. Phillips, O.M. (1960) "On the generation of sound by supersonic shear layers." *J. Fluid. Mech,* **9**,pp. 1-28.

25. Pridmore-Brown (1957) "Sound propagating in a fluid flowing through an attenuating duct." *J. Fluid. Mech.*

26. Punekar, Morfey, Ball and Lilley, G.M. (1998).

27. Rayleigh, Lord. (1896) "Theory of sound(2 vols)." *Macmillan.*

28. Suzuki, T. and Lele, S and (2001) "Refracted arrival waves in zone of silence from a finite thickness mixing layer." Jacoust. Soc. Am. (submitted).

29. Tam, C.K.W. and Auriault, L. (1999) "Jet mixing noise from fine-scale turbulence." Jour. AIAA, 37, pp.145-153.

30. Tam, C.K.W., Golebiowski, M. and Seiner, J.M. (1996) "On the two components of turbulent mixing noise from supersonic jets." AIAA, 96-1716.

31. Tam, C.K.W. (1991) "Jet noise generated by large scale coherent motion." *Aeroacoustics of Flight Vehicles: Theory and practice. Vol.1 ed. Hubbard, H.H.,* pp.311-390.

32. Tester, B.J., and Morfey (1976) "Developments in jet noise modeling: Theoretical predictions with measured data." J. Sound and Vibration. 46. pp. 79-103.

33. Westley, R. and Lilley, G.M. (1952) "An investigation of the noise from a small jet and methods for its re *College of Aeronautics, Report, Cranfield.* 53.

Noise From Large-Scale Turbulent Structures/Instability Waves

Philip J. Morris
Penn State University

***Noise From Large-Scale Turbulent Structures/Instability Waves* -**
Philip J. Morris, Penn State University as summarized by Geoffrey Lilley.

Professor Morris recounted that the experiments of Brown and Roshko(1974) at a moderate Reynolds number had exhibited large-eddy structures having the appearance of a quasi-periodic train of traveling wave-like structures. Previous to this work it had been assumed that the large eddy structures in turbulent shear flow were randomly produced and contained only a small fraction of the turbulent kinetic energy. Similar pictures were obtained by Lepicovsky et al.(1986), and Martens et al.(1994) at higher Mach numbers. It was concluded that large coherent structures exist in a wide variety of turbulent shear flows in high Reynolds number flows at varying Mach numbers. Normally such large structures in two-dimensional mean flows are coupled to streamwise vortices and in three-dimensional mean flows, such as the jet, to helical and axisymmetric structures. Morris suggested that their physical behavior could be modeled by using a linear wave model having a slowly varying wavelength in the streamwise direction. The work of Gaster et al.(1985) showed that the amplitude and phase for a weak disturbance in a flow could be followed downstream exactly as predicted by linear theory. One weakness of the linear theory was that it could not predict amplitude, but only amplitude ratio. Morris discussed finite amplitude effects and receptivity, and gave examples due to Tam and Morris(1985) relative to tone excited jets, all showing good agreement with theory.

Morris discussed the justification for using the linearized model to describe the dominant features of a turbulent shear flow. He showed, using the momentum equations that the velocity, vorticity, and pressure fluctuations in the flow were all controlled by the linear terms, and the influence of the non-linear terms was relatively small. Morris showed how the large-scale structures in a turbulent shear flow could be modeled as a collection of near-inviscid instability waves, by solving the Rayleigh equation for given mean velocity and density distributions across the shear layer. The results for the axial growth of the shear layer and the axial variation of the instability amplitude with velocity, temperature or density ratio and Mach number were shown to be in good agreement with experiment. A convincing demonstration of the validity of the linearized instability model to predict the large-scale structure of a two-dimensional mixing layer was shown by a comparison of the computed streak-line simulation with the measured schlieren pictures obtained by Brown and Roshko, and discussed previously. It should be noted that the computation does not include the effects of the non-linear cascade energy transfer in the inertial and sub-inertial ranges towards dissipation. Nevertheless it captures, in this two-dimensional mixing region simulation, the evolution of the large-scale eddy motion containing a very large fraction of the turbulent kinetic energy for all fully turbulent flows at high Reynolds number. Later experimental work, not discussed here by Morris, has shown that in corresponding three-dimensional flows similar ‘coherent’ structures are present, and dominate the large-scale motion in the shear flow turbulence. However, there is in addition to the transverse large-scale motion, a strong pattern of longitudinal, or streamwise, vortices. The conclusion is drawn that the large scale mixing in many

turbulent shear flows is governed by the large-scale, 'coherent', structures derived from linearized stability theory.

Morris then turned to the application of the linearized stability theory to the prediction of jet noise in both the near and far-fields of circular and non-circular jets at subsonic and supersonic speeds. In this presentation Morris concentrated on applications to single supersonic jets. He discussed the matching problem between the near field instability wave calculation for a supersonic phase speed and the far-field acoustic radiation. The results of Dahl (1994) for an unheated jet at $M_j = 2$ showed fair agreement with the experimental results of Seiner and Ponton(1985). Morris also showed the comparison between the linear stability calculations of Tam and Burton(1984) and the experimental results of Troutt and McLaughlin(1982).

Morris stressed the direct link between the large-scale structures as modeled by the linearized instability model for the unsteady turbulent flow and the radiated noise. The method provides data on the length and time scales in the turbulent flow. However the one weakness of this approach is that it does not provide information on the amplitude of the far-field noise, since in the flow field it is only the amplitude ratio that is predicted. The method is complex even for a single circular jet and becomes even more complex for non-circular nozzles. Morris showed some further details of the comparison between the results of Dahl and Morris (1997) for the unheated jet at $M_j = 2$, with the experimental results of Seiner and Ponton(1985) for the directivity of the radiated noise at peak amplitude. The theoretical calculations showed good agreement with experiment from the jet boundary to about 45° to the downstream jet axis. This comparison suggested that another noise source was responsible for the radiated noise at angles from 45° to 180° to the downstream jet axis.

A further example discussed by Morris was that related to shock associated broadband noise and jet screech. The comparison between the stability results of Tam(1987) and the experimental results of broadband shock associated noise were shown to be in good agreement especially for directivities greater than 90° to the downstream jet axis. Similarly the results of Tam and Tanna(1982) for a circular jet screech frequency were in good agreement with experimental data. This was also true of the calculated jet screech for a rectangular jet given by Morris et al.(1989). Morris also showed the comparison of the noise directivity associated with different azimuthal mode numbers as obtained by Seiner et al.(1994). Further results were discussed for non-circular jets involving multiple instability modes involving varicose, flapping and wagging. Morris noted that for the elliptic supersonic jets the predictions of Morris and Bhat (1991) could only suggest trends.

Finally Morris referred to work using Computational AeroAcoustics (CAA) which encompassed the earlier work using linearized instability theory. He discussed the resolution requirements and some comparisons of recent results with a range of experimental data, showing that the CAA results followed similar trends. He also noted the narrow band experimental data of Seiner et al (1994) showing the large changes in the far-field directivity for a given Strouhal number for a hot jet with

M_j = 2. This showed the peak in the spectrum at about a Strouhal number of 0.1 and a directivity of 45°. He compared this with the recent compilation of the experimental spectral data of Tam et al (1996), suggesting that the current version of CAA was giving acceptable results in the lower frequencies and close to the peak. However, the current results could not predict the high frequency part of the noise spectrum due to limits imposed on the resolution requirements.

In a short discussion following the paper Morris reported that his analysis had focused on supersonic jets since clearly these were the strong candidates for the noise arising from the mixing due to large-scale structures. Their contribution at subsonic speeds was far weaker, arising from the smaller region in frequency-wave-number space supporting supersonic phase speeds. Morris also stressed the linearized stability approach gave answers for amplitude ratio only. In all comparisons with experiment it was essential to calibrate against a selected experimental data point. He also agreed that the present work was closely related to that of Mankbadi and Liu (1984)

The principles, advantages, and restrictions of hybrid methods were summarized. Features of the hybrid method are:

- Separation of sound generation and propagation
- Three steps to obtain the acoustic field
- Determination of the aerodynamic field
- Calculation of source terms
- Calculation of acoustic field

Advantages of the hybrid method include the ability to use the most appropriate computation method at each step and the use of conventional CFD codes to study complex geometries. Restrictions on the use of hybrid methods include the loss of information about flow-acoustic interactions and ambiguity in the definition of acoustic source terms.

Noise From Large Scale Structures/ Instability Waves

Philip J. Morris
Boeing/A. D. Welliver Professor
Department of Aerospace Engineering
Penn State University

Jet Noise Workshop
Ohio Aerospace Institute
November 7-9, 2000

PENNSTATE

Outline

- Experimental observations
- Theoretical background
- Application to turbulence modeling
- Application to jet noise
- Relationship to CAA simulations

Collaborators

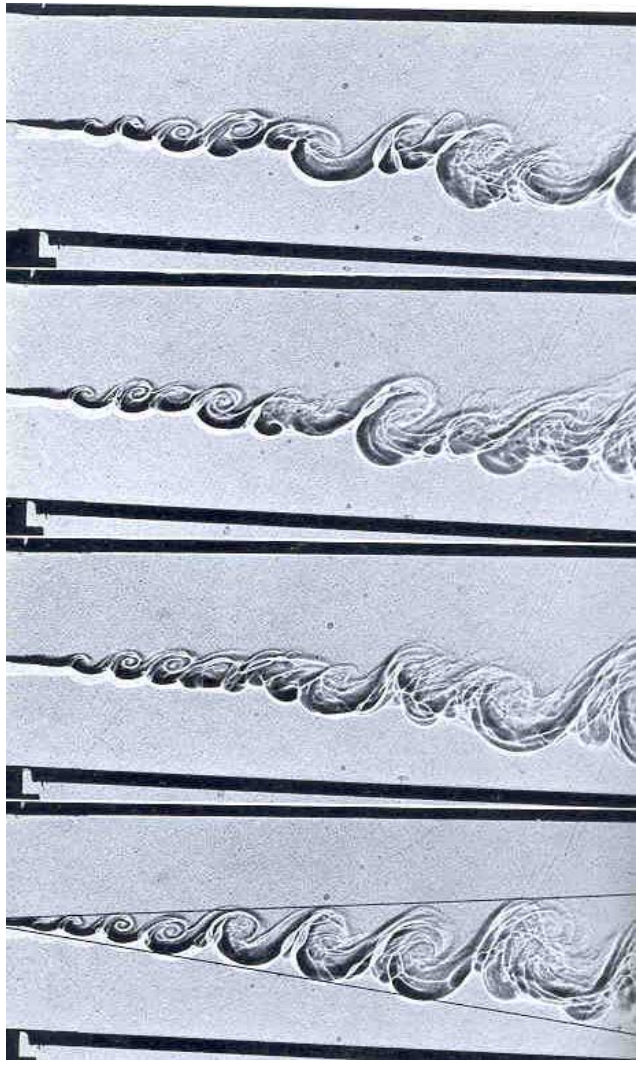
- G. M. Lilley, C. K. W. Tam, L. N. Long
- C. Baltas (Ph.D.), W.-S. Byon (Ph.D.), W.-W. Liou (Ph.D.), R. S. Baty (Ph.D.), T. R. S. Bhat (Ph.D.), M. G. Giridharan (Ph.D), K. Viswanathan (Ph.D), J. B. Augustin (MS), M. Dahl (Ph.D), L. S. Lee (Ph.D.), C. M. Shieh (Ph.D.)

Instability Wave Models

- Turbulent mixing controlled by large scale turbulent structures
- High speed convection in supersonic heated flows
- Direct link with acoustic field
- Reflects unsteady behavior of turbulence
  - applications to general geometries/conditions

Experimental Observations

Brown and Roshko
J. Fluid Mechanics,
Vol. 64, (1974)



Experimental Observations

Lepicovsky et al
J. Propulsion and Power, Vol. 2(4), pp. 323-330, 1986.



a .

M_j = 0.76
T_t = 291 K
St_j = 0.28
L_e = 143 dB



b .

M_j = 0.80
T_t = 295 K
St_j = 0.37
L_e = 142 dB



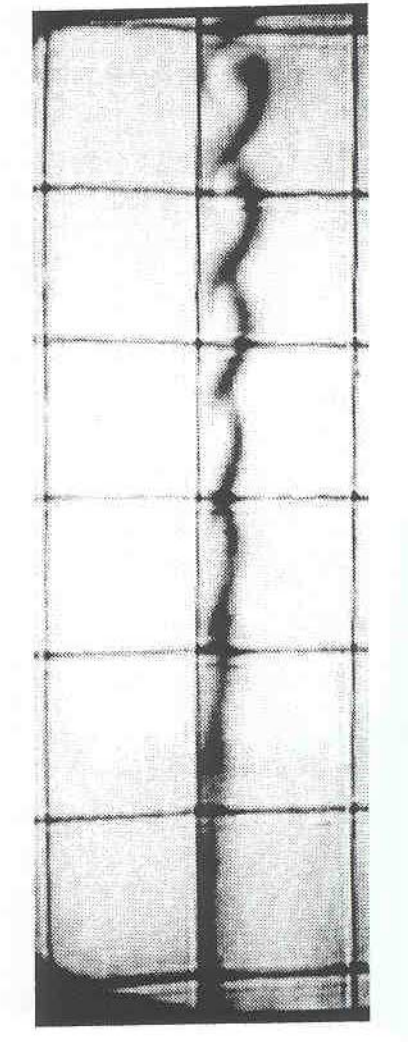
c .

M_j = 0.80
T_t = 293 K
St_j = 0.48
L_e = 138 dB

Experimental Observations

Martens, Kinzie and McLaughlin, *AIAA Journal* Vol. 32 (1994)

$M_1 = 4$, $M_2 = 1.2$

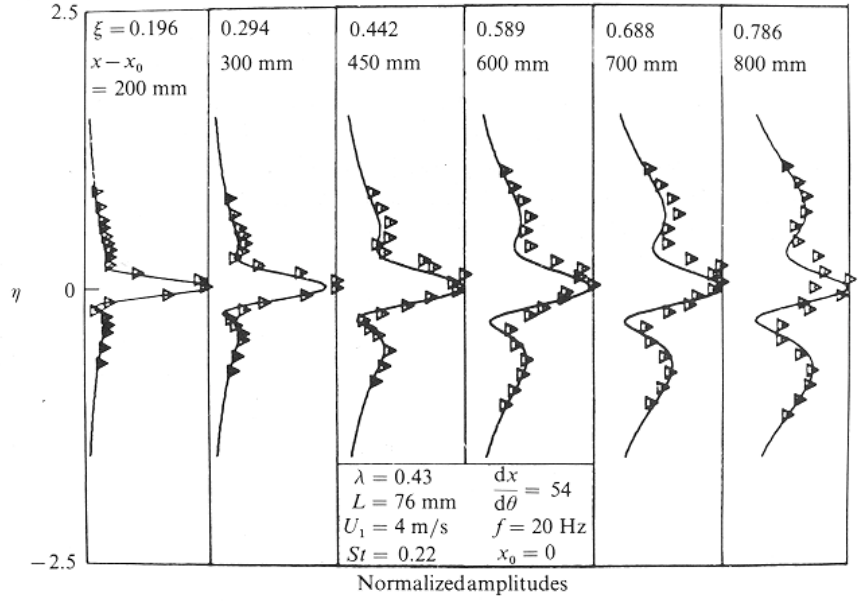


Theoretical Background

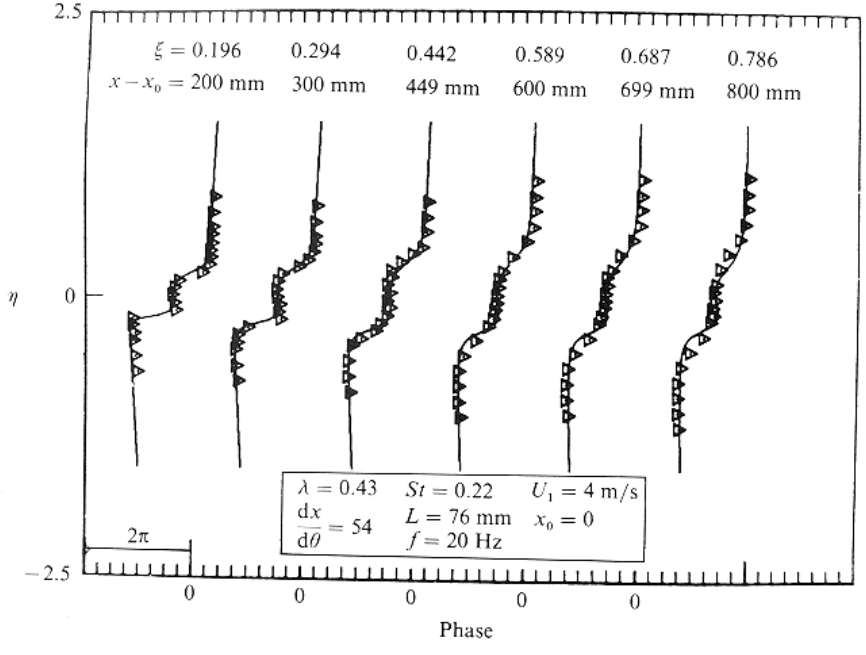
- Validity of Modeling
  - Linearization
  - Finite amplitude effects
  - Formal justification

Linear Models

Gaster, Kit and Wygnanski, J. Fluid Mechanics, Vol. 150 (1985)



Amplitude

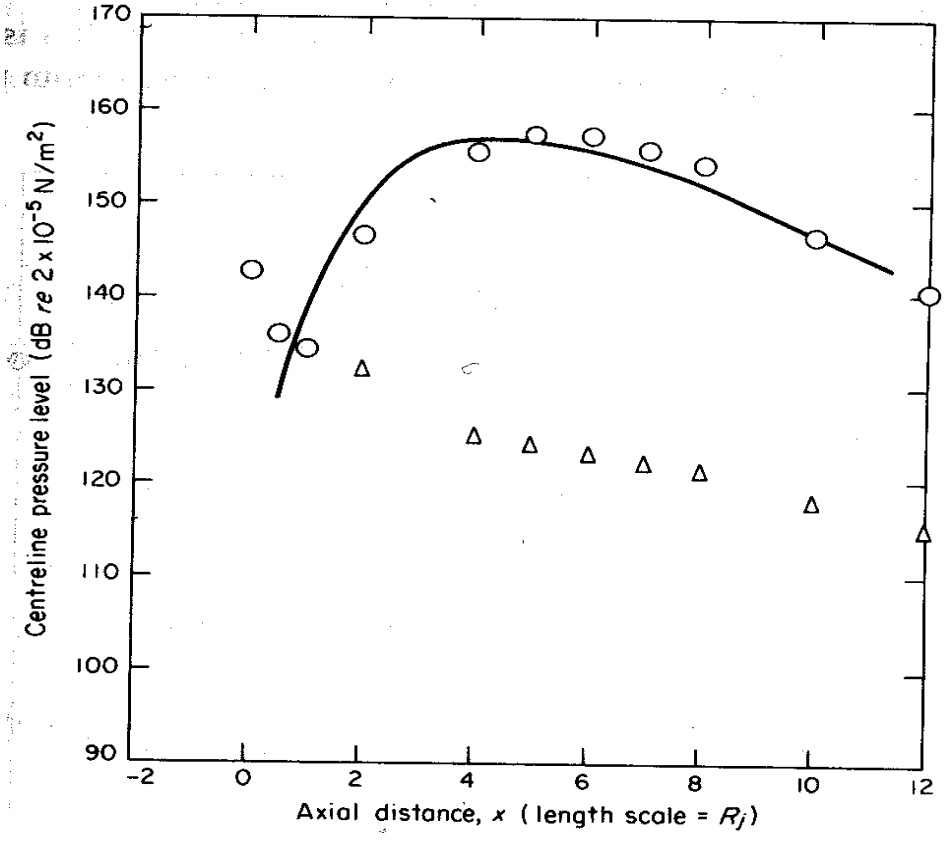


Phase

PENNSTATE

Finite Amplitude Effects

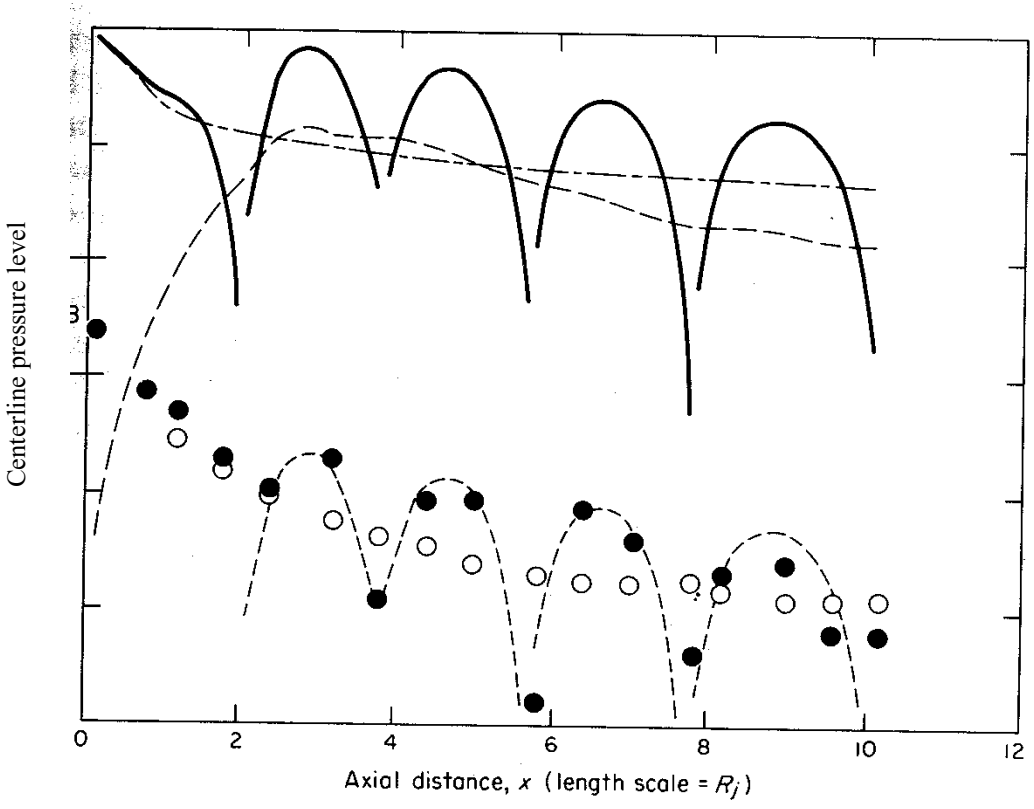
Tam and Morris, *J. Sound Vib*. Vol. 102, 1985
Tone Excited Jet



PENNSTATE

Finite Amplitude Effects

Tam and Morris, *J. Sound Vib*. Vol. 102, 1985
Tone Excited Jet



PENNSTATE

Linearized Analysis

Momentumequation

$$\frac{\partial \mathbf{q}}{\partial t} = \mathbf{f} - \nabla h - \nu \nabla \times \boldsymbol{\omega}$$

where

$$\mathbf{f} = \mathbf{q} \times \boldsymbol{\omega} \quad \text{and} \quad h = p + \frac{1}{2} q^2$$

The perturbation equationsare

$$\frac{\partial \mathbf{q}'}{\partial t} = \mathbf{f}' - \nabla h' - \nu \nabla \times \boldsymbol{\omega}'$$

with

$$\nabla^2 h' = \nabla \cdot \mathbf{f}'$$

$$\left(\partial / \partial t - \nu \nabla^2\right) \boldsymbol{\omega}' = \nabla \times \mathbf{f}'$$

PENNSTATE

Linearized Analysis

$$\mathbf{f}' = \mathbf{Q} \times \boldsymbol{\omega}' + \mathbf{q}' \times \boldsymbol{\Omega} + \mathbf{q}' \times \boldsymbol{\omega}' - \overline{\mathbf{q}' \times \boldsymbol{\omega}'}$$

Now, in the turbulent kinetic energy equation the source terms include

$$\overline{\mathbf{q}' \cdot \mathbf{f}'} = \overline{\mathbf{q}' \cdot \left(\mathbf{Q} \times \boldsymbol{\omega}' + \mathbf{q}' \times \boldsymbol{\Omega} + \mathbf{q}' \times \boldsymbol{\omega}' - \overline{\mathbf{q}' \times \boldsymbol{\omega}'} \right)}$$

So that

$$\overline{\mathbf{q}' \cdot \mathbf{f}'} = -\mathbf{Q} \cdot \overline{\mathbf{q}' \times \boldsymbol{\omega}'}$$

Since

$$\overline{\mathbf{q}' \cdot (\mathbf{q}' \times \boldsymbol{\Omega})} = \overline{\mathbf{q}' \cdot (\mathbf{q}' \times \boldsymbol{\omega}')} = 0$$

Application to Turbulence Modeling

- Instability Wave Model
- Integral Approach
  - Results
- Differential Approach

Instability Wave Model

- Large scale structures modeled as instability waves
- Satisfy Rayleigh equation locally
- Mean flow development
  - taken from experiments
  - predicted from energy exchange between large scale structures and mean flow

Instability Wave Model:
Integral Approach

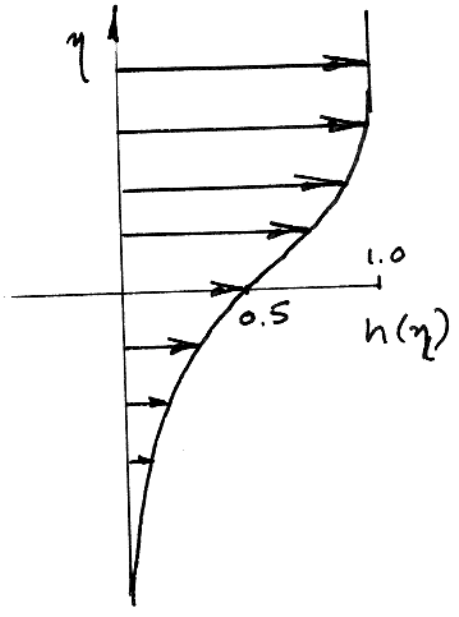
Assume shape functions for the mean flow

$$\bar{u} = f(\eta; R) = R + (1 - R)h(\eta)$$

$$\bar{\rho} = g(\eta; R, s)$$

$$\eta = \frac{y - y_o(x)}{\delta(x)}$$

$$R = \frac{\bar{u}_2}{\bar{u}_1} \quad \text{and} \quad s = \frac{\bar{\rho}_2}{\bar{\rho}_1}$$



PENNSTATE

Instability Wave Model

$$p'(x,y,t) = \frac{1}{2}\{A(x)\hat{p}(y)\exp[i(\alpha x - \omega t)] + \text{complex conjugate}\}$$

Rayleigh equation (two - dimensional, isothermal)

$$\frac{d^2\hat{p}}{dy^2} + \frac{2\alpha}{(\omega - \alpha U)}\frac{dU}{dy}\frac{d\hat{p}}{dy} - [\alpha^2 - (\omega - \alpha U)^2 M^2]\hat{p} = 0$$

Boundary conditions (two - dimensional)

$\hat{p}(y)$ decays or outgoing wave as $y \to \pm\infty$

Boundary conditions (axisymmetric case)

$\hat{p}(r)$ decays or outgoing wave as $r \to \infty$

$\hat{p}(r)$ finite as $r \to 0$

This is a boundary value problem with dispersion relationship

$$\alpha_r + i\alpha_i = \alpha(\omega)$$

Axial Evolution Equations

Axial variation of shear layer thickness

$$\frac{d\delta}{dx} = -\frac{4\delta|A|^2\alpha_I}{(1-R)^2[RI_3+(1-R)I_4]}$$

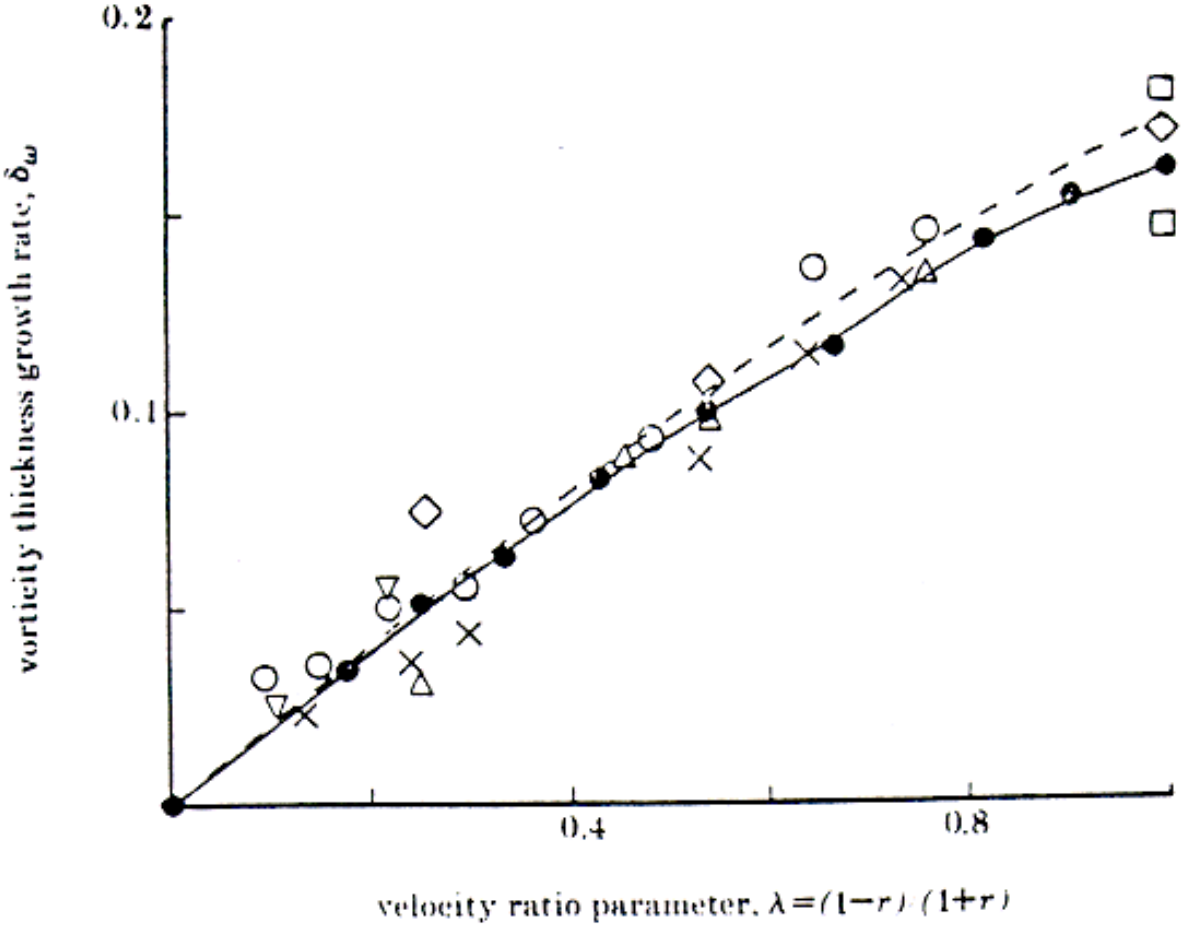
Axial variation of instability wave amplitude

$$\frac{d|A|^2}{dx} = -|A|^2\left\{2\frac{\alpha_I}{\delta}+\frac{1}{\delta}\frac{d\delta}{dx}\right\}$$

For "broadband model"

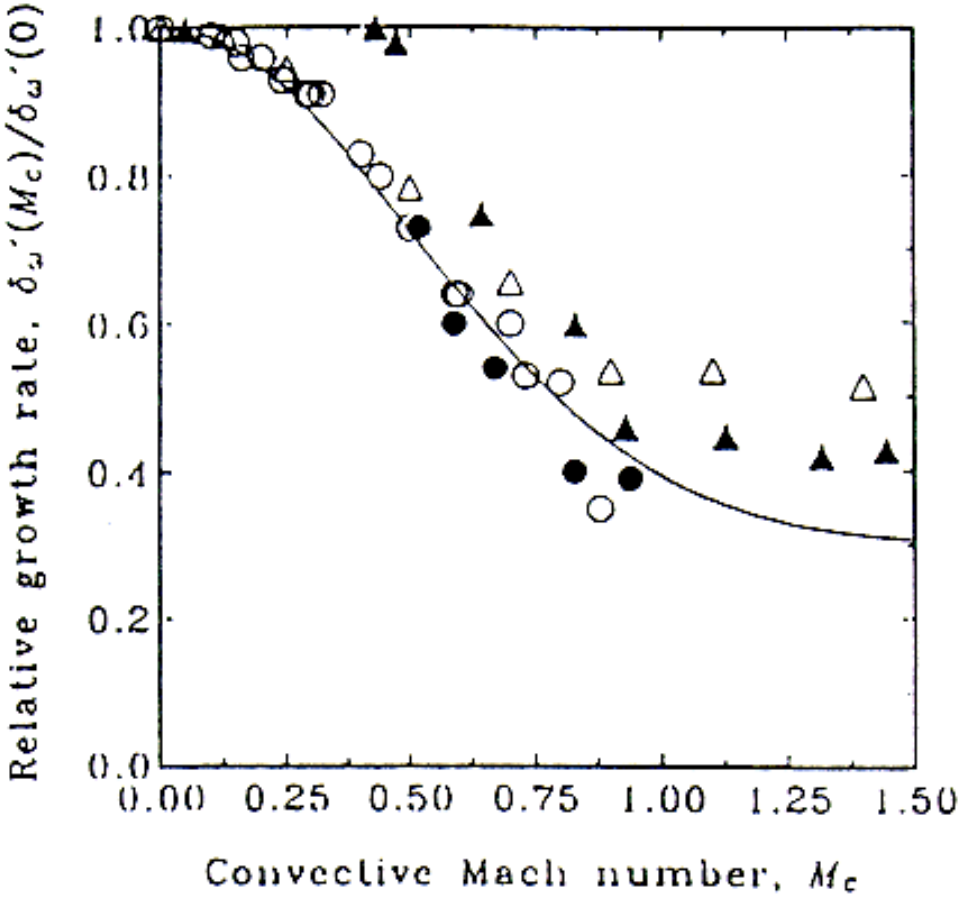
$$\frac{d\delta}{dx} = -\frac{4\delta}{(1-R)^2[RI_3+(1-R)I_4]}\int_0^\infty d\omega\int_{-\infty}^{\infty} d\beta\left\{\frac{\alpha_I(\omega,\beta)}{\delta}|A|^2(x;\omega,\beta)\right\}$$

Shear Layer Growth



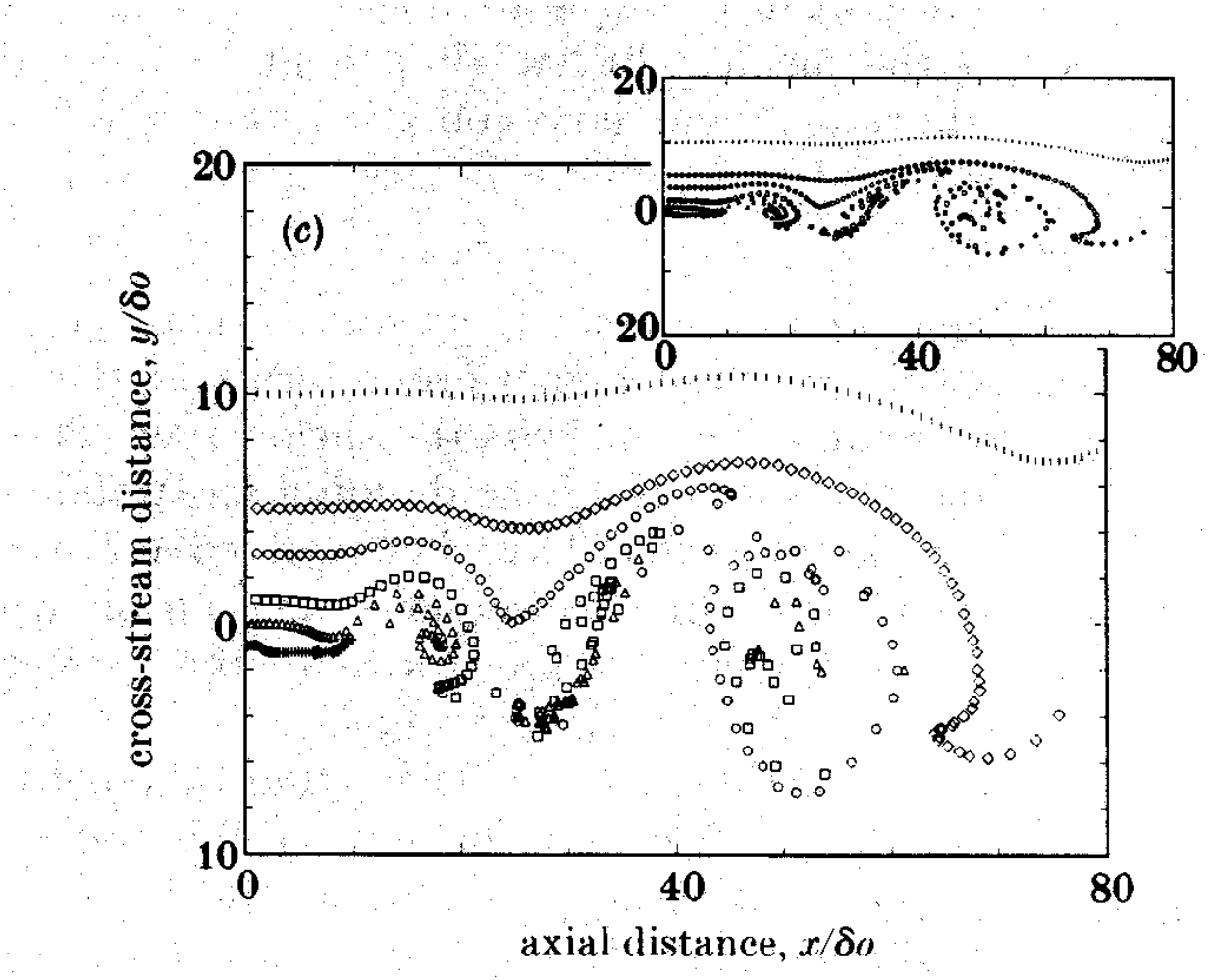
PENNSTATE

Effects of Mach Number



PENNSTATE

Streakline Simulation



PENNSTATE

Application to Jet Noise

- General procedure
- Near and far field predictions
- Non-circular jets
- Excited jets
- Shock-associated noise and screech

General Procedure

Instability wave growth

$$p'(x,y,t) = \hat{p}(y)\exp[i(\alpha x + n\theta - \omega t)]$$

Rayleigh equation (isothermal)

$$\frac{d^2\hat{p}}{dr^2} + \left\{\frac{1}{r} + \frac{2\alpha}{(\omega - \alpha U)}\frac{dU}{dr}\right\}\frac{d\hat{p}}{dr} + [(\omega - \alpha U)^2 M^2 - \frac{n^2}{r^2} - \alpha^2]\hat{p} = 0$$

Boundary conditions (axisymmetric case)

$\hat{p}(r)$ decays or outgoing wave as $r \to \infty$

$\hat{p}(r)$ finite as $r \to 0$

This is a boundary value problem with dispersion relationship

$\alpha_r + i\alpha_i = \alpha(\omega)$

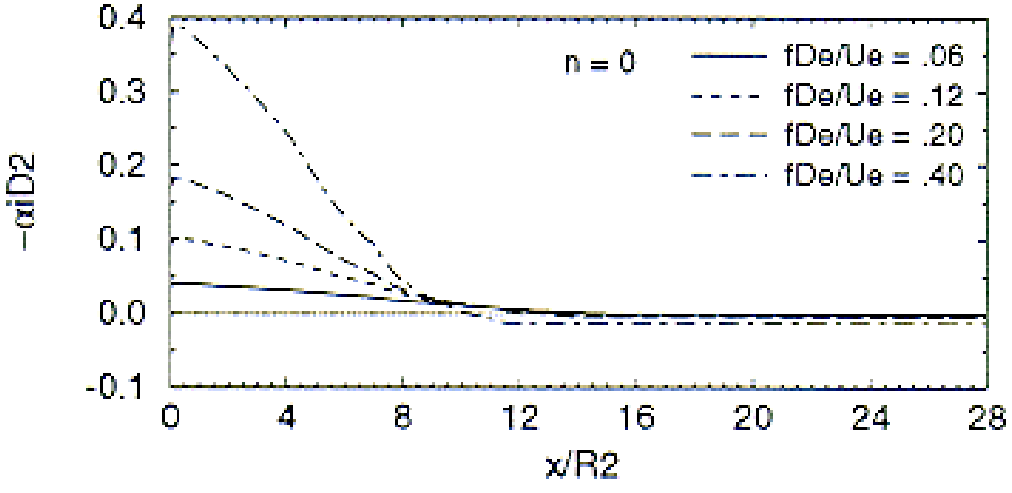
Growth rate $= -\alpha_I$

Phase velocity $= \omega / \alpha_R$

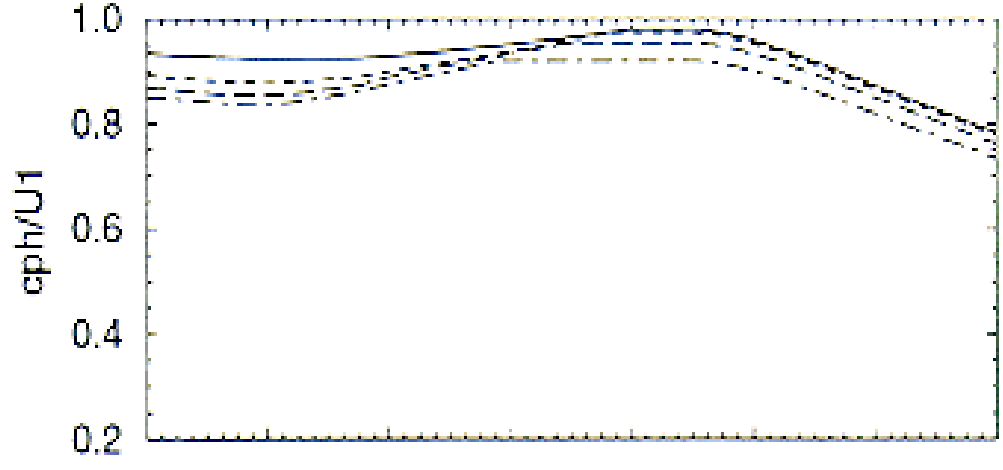
PENNSTATE

Wave Properties

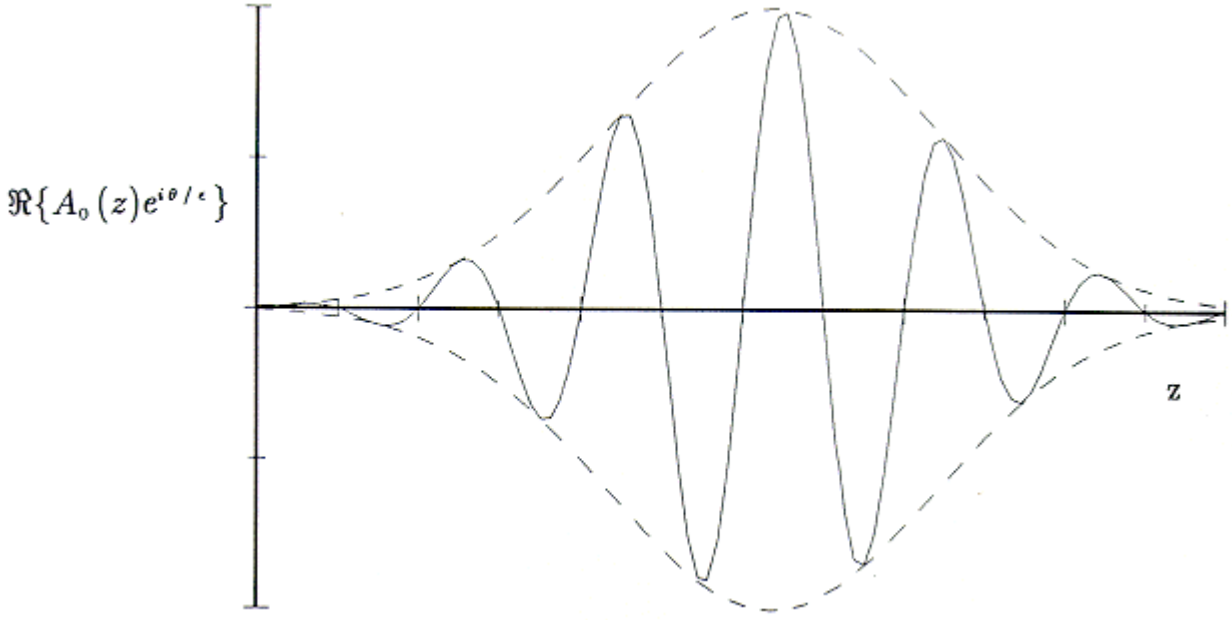
Growth rate



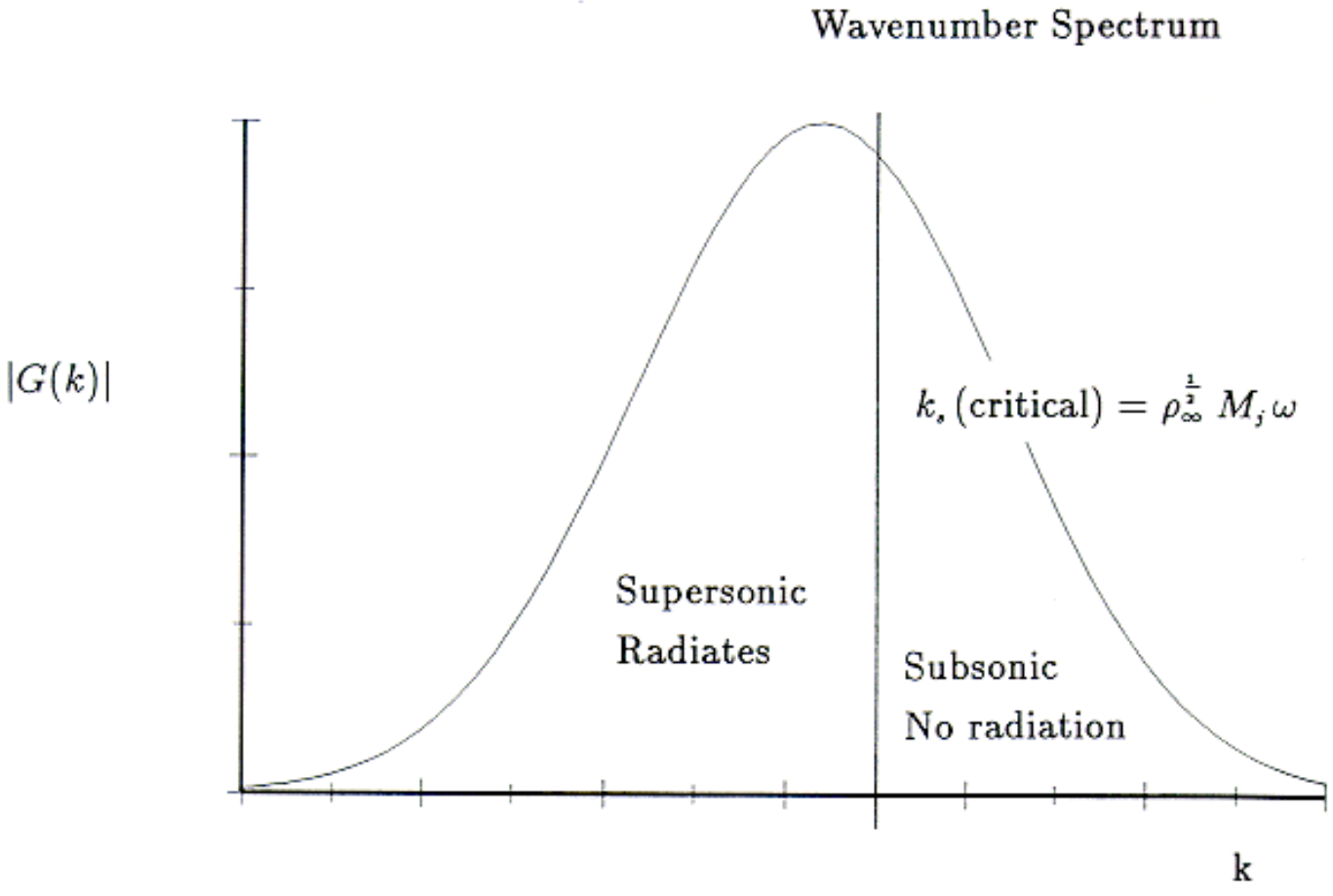
Phase velocity



Amplitude and Phase Evolution

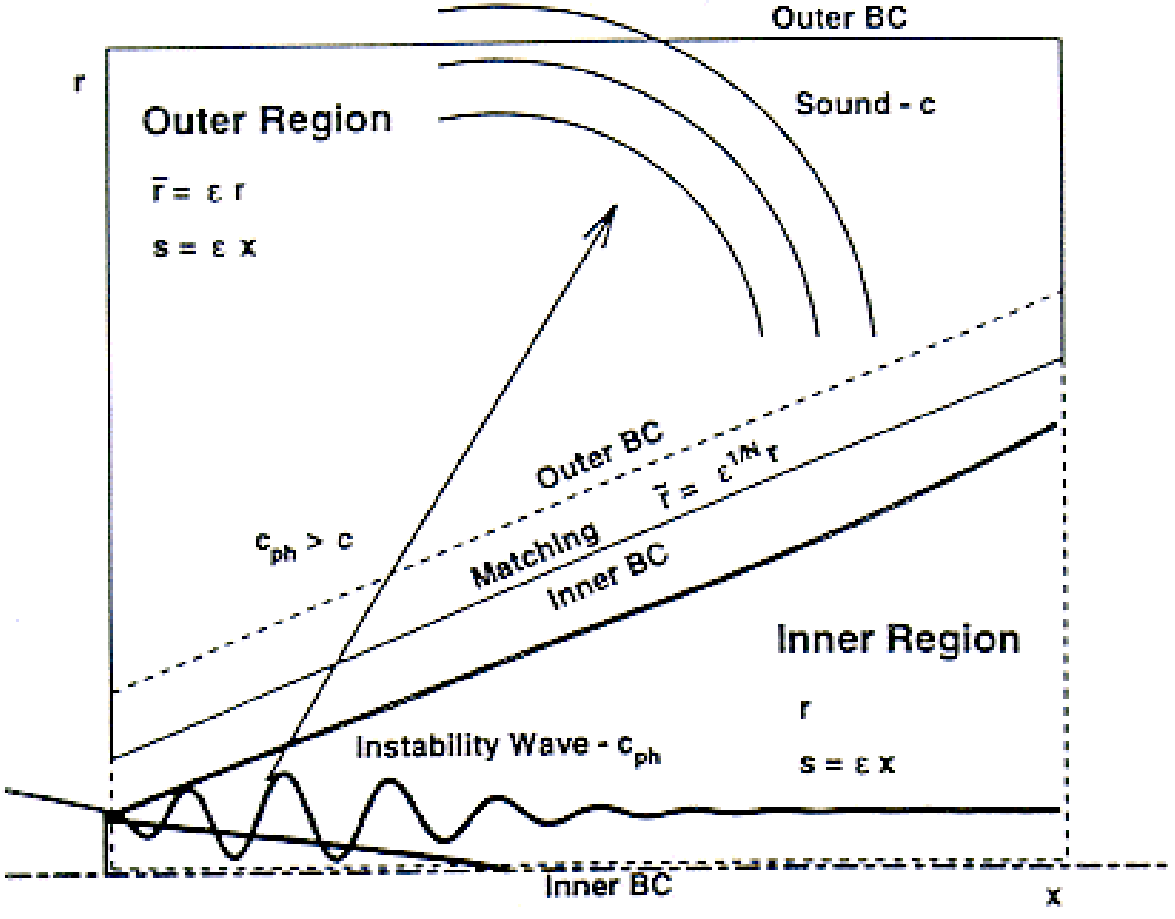


Wavenumber Spectrum



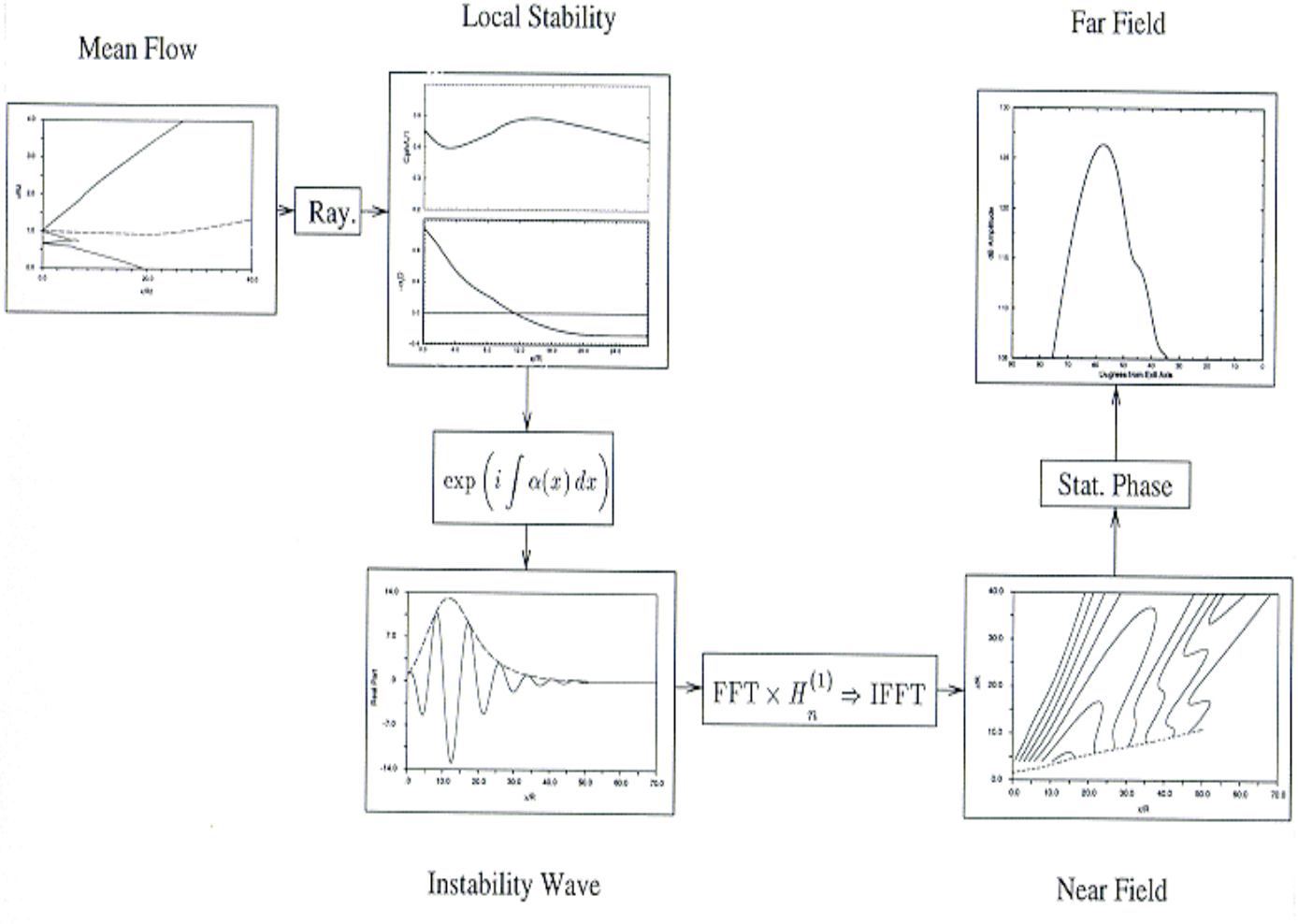
PENNSTATE

Matching to Acoustic Solution



PENNSTATE

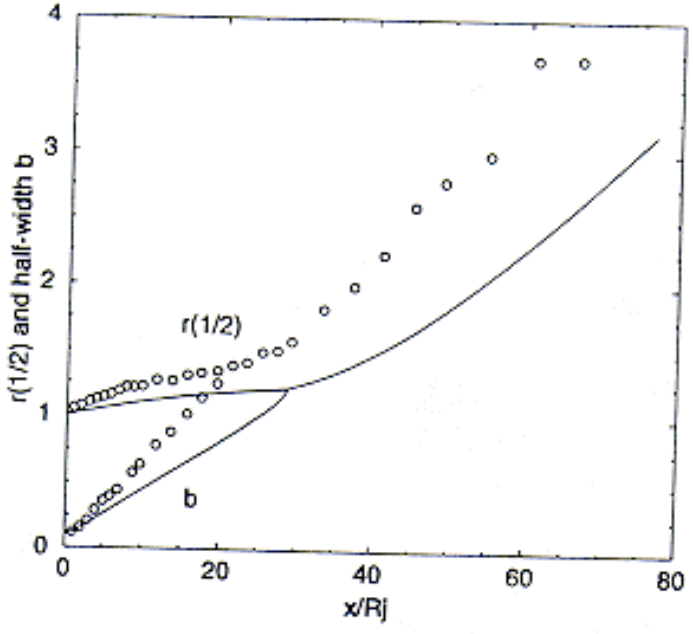
Computational Process

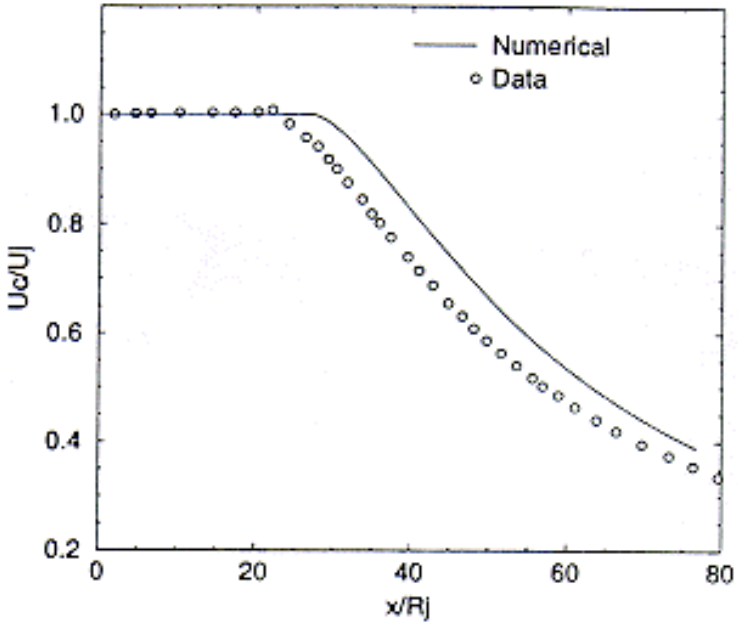


PENNSTATE

Example Solution: Single Jet

Experiment : $M_j = 2$, unheated, Seiner & Ponton (1985)



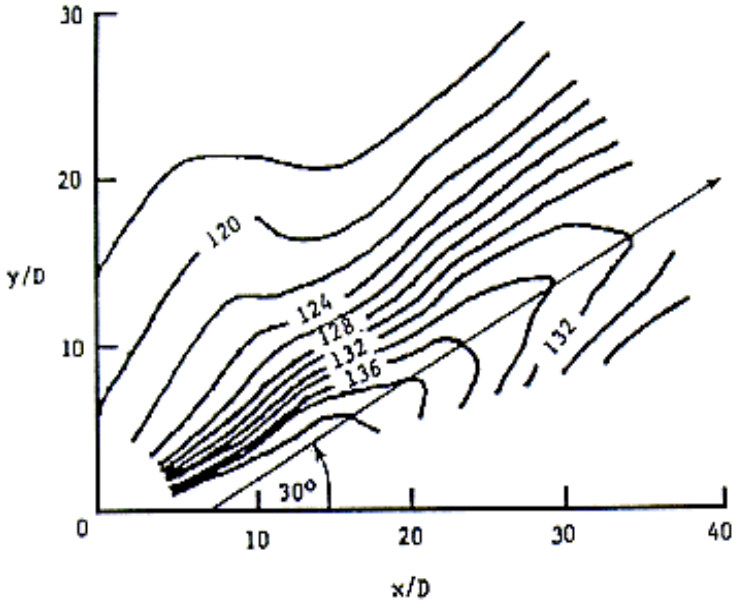


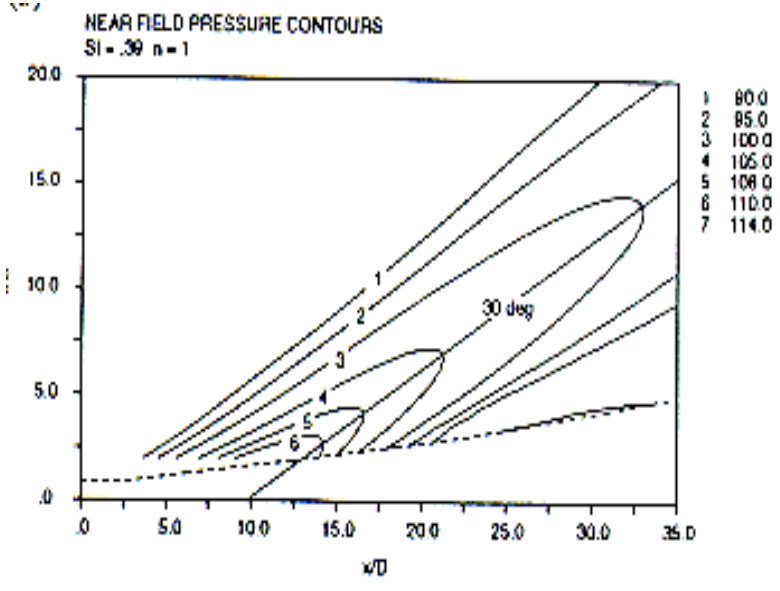
Analysis: Dahl and Morris, J. Sound Vib. Vol. 200 (1997)

PENNSTATE

Example Solution: Single Jet

$M_j = 2$, unheated, Seiner & Ponton (1985)





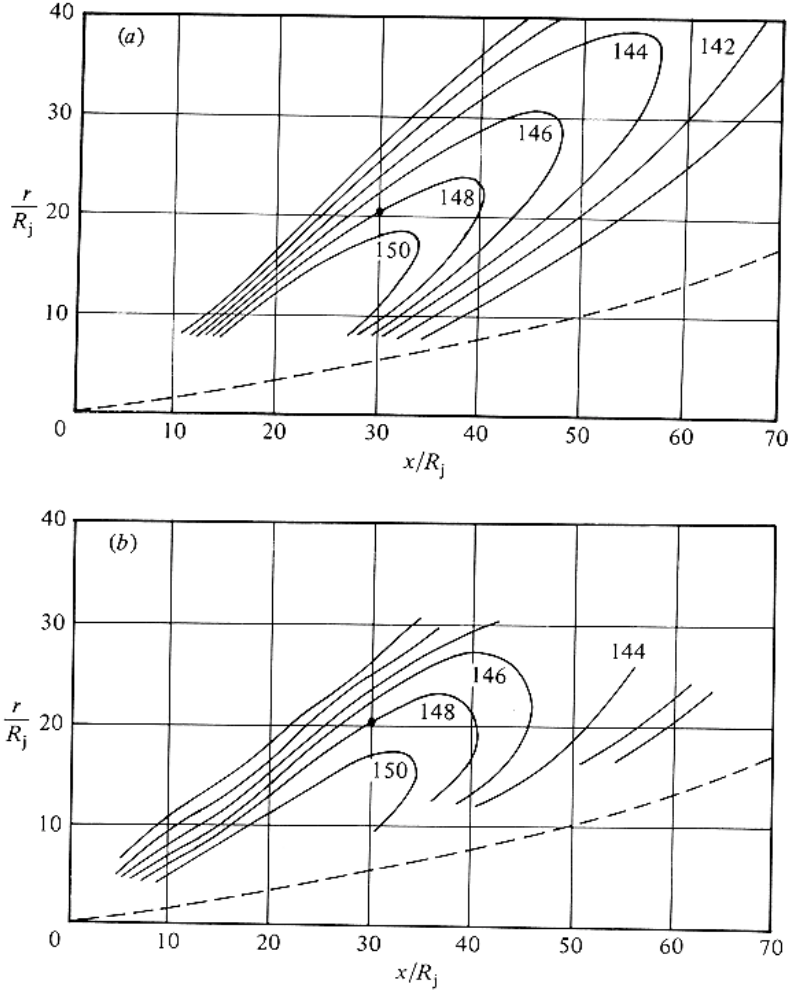
Analysis: Dahl and Morris, J. Sound Vib. Vol. 200 (1997)

PENNSTATE

Example Solution: Single Jet

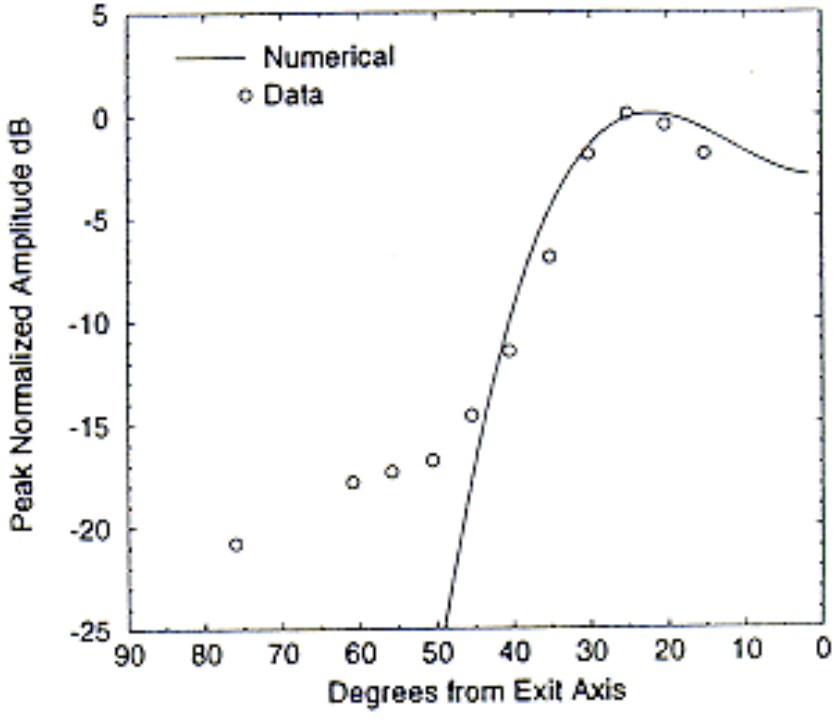
Experiment: Troutt and McLaughlin, *J. Fluid Mech.*, Vol. 162 (1982)

Analysis: Tam and Burton, *J. Fluid Mech.*, Vol. 138 (1984)



Example Solution: Single Jet

$M_j = 2$, unheated, Seiner & Ponton (1985)

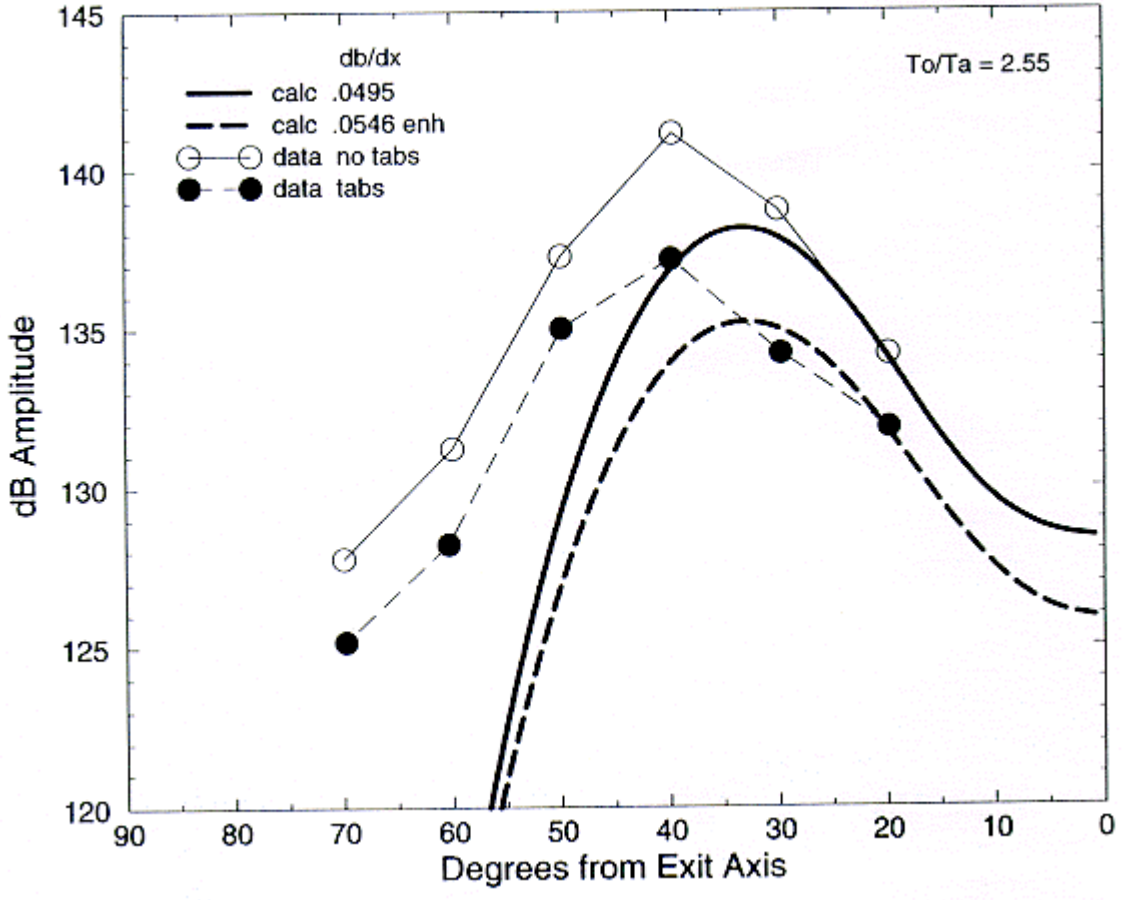


Analysis: Dahl and Morris, J. Sound Vib. Vol. 200 (1997)

PENNSTATE

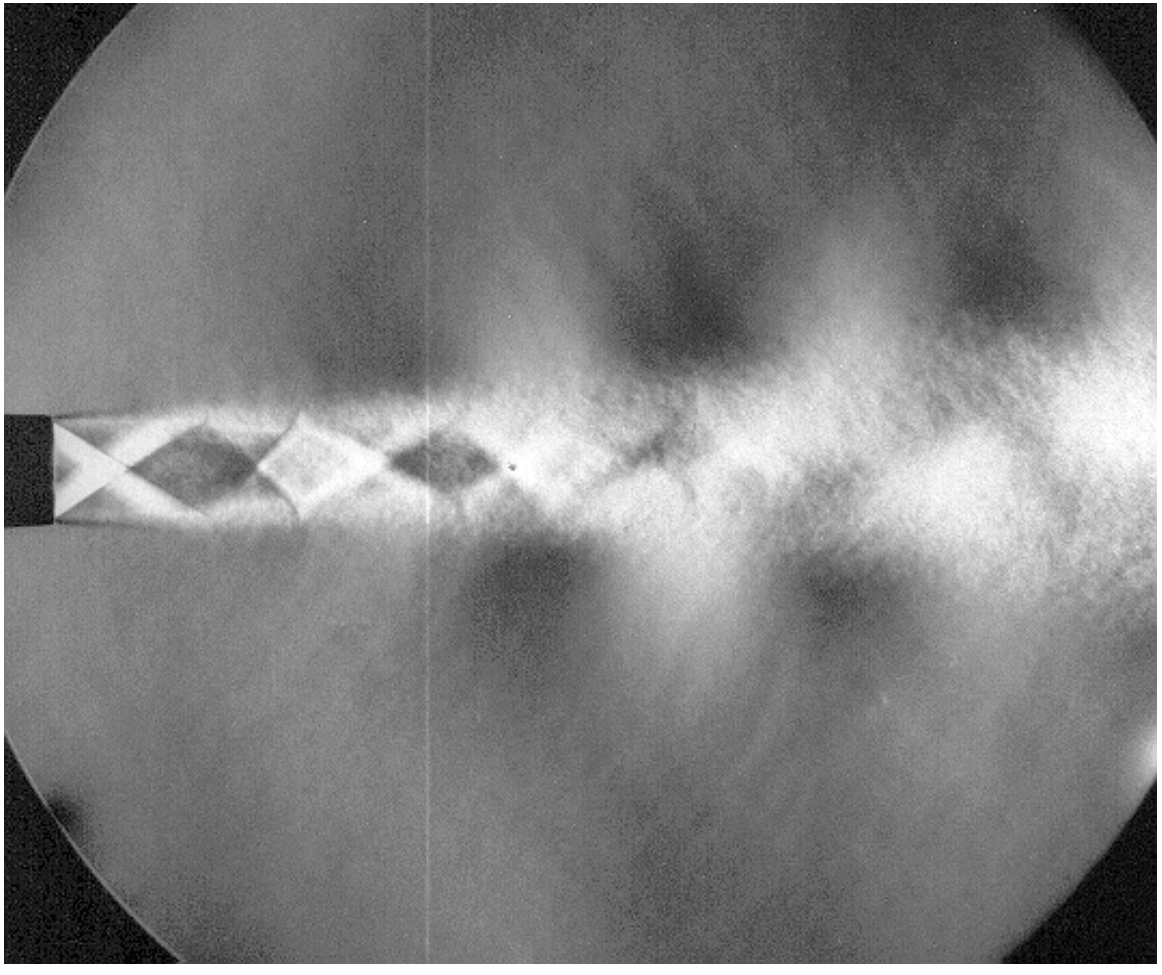
Effects of Enhanced Mixing

Dahl and Morris, *J. Fluids Engineering*, Vol. 120, 1998.



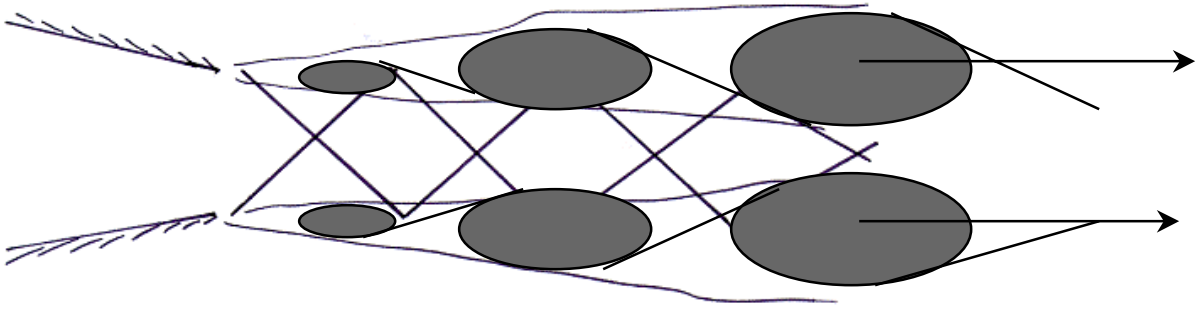
PENNSTATE

Shock-Associated Noise



PENNSTATE

Shock-Associated Noise



Shock cell structure

$$p_s = \sum_{n=0}^{\infty} a_n e^{\mathbf{i} k_n x} + \text{complex conjugate}$$

Instability waves

$$p_i = b_n e^{\mathbf{i}(\alpha x - \omega t)} + \text{complex conjugate}$$

Weak interaction gives pattern $p_c \sim p_s \times p_i$

$$p_c \sim a_n b_n \exp\{-i[(\alpha + k_n)x - \omega t]\} +$$
$$a_n b_n^* \exp\{-i[(\alpha - k_n)x - \omega t]\} + \textbf{c.c.}$$

Shock-Associated Noise

For broadband shock - associated noise

$$\frac{\omega \cos\theta}{\alpha - k_n} = c_o$$

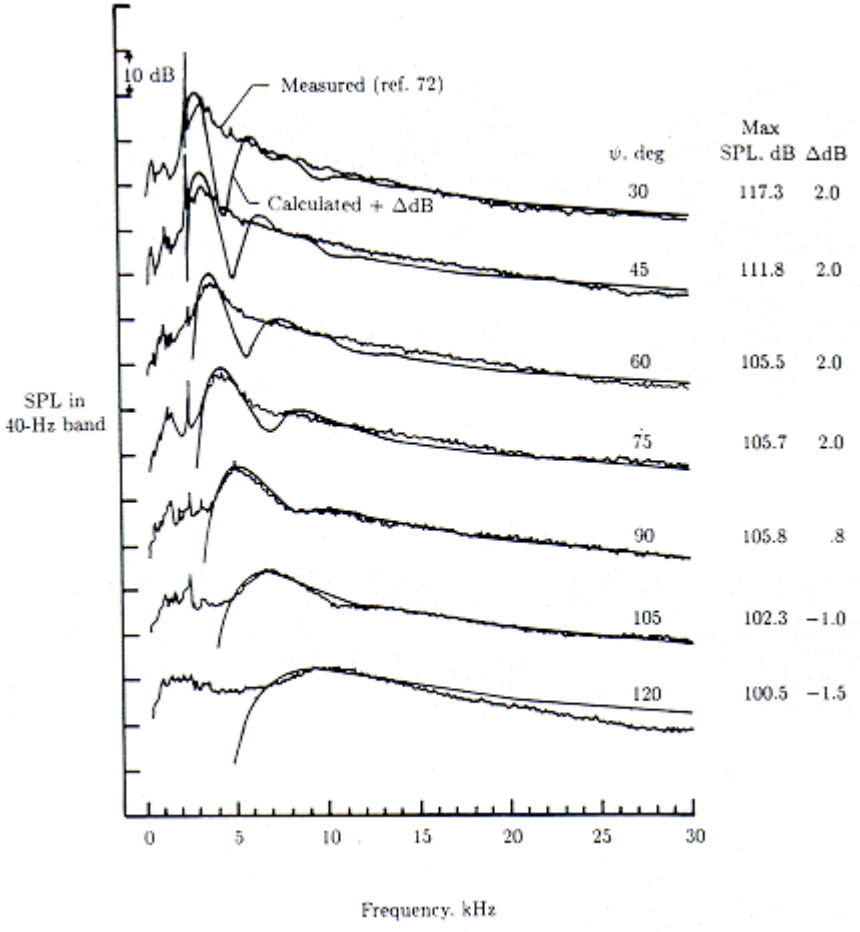
This gives a far field frequency variation

$$f = \frac{u_c}{L}\frac{1}{1 - M_c \cos\theta}$$

Shock-Associated Noise

Tam, *J. Sound Vib*. Vol. 116 1987

$M_j = 1.80, M_d = 2.0$



PENNSTATE

Screech: Circular Jet

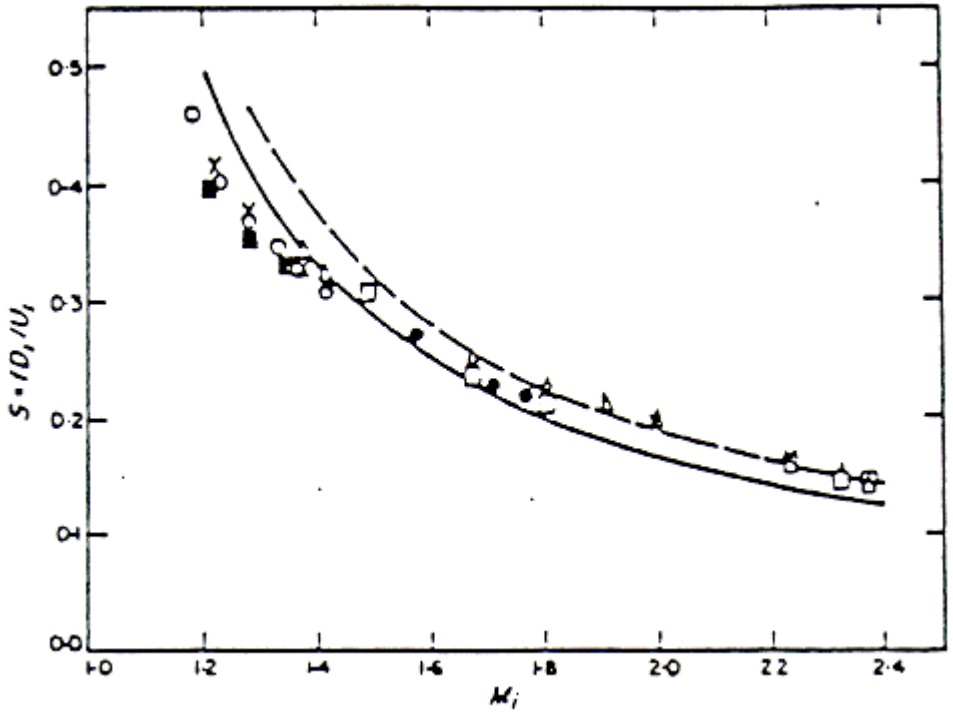
$$f = \frac{u_c}{L}\frac{1}{1 - M_c \cos\theta}$$

When $\theta = \pi$ a phase - locked loop can be initiated.

This gives a screech frequency

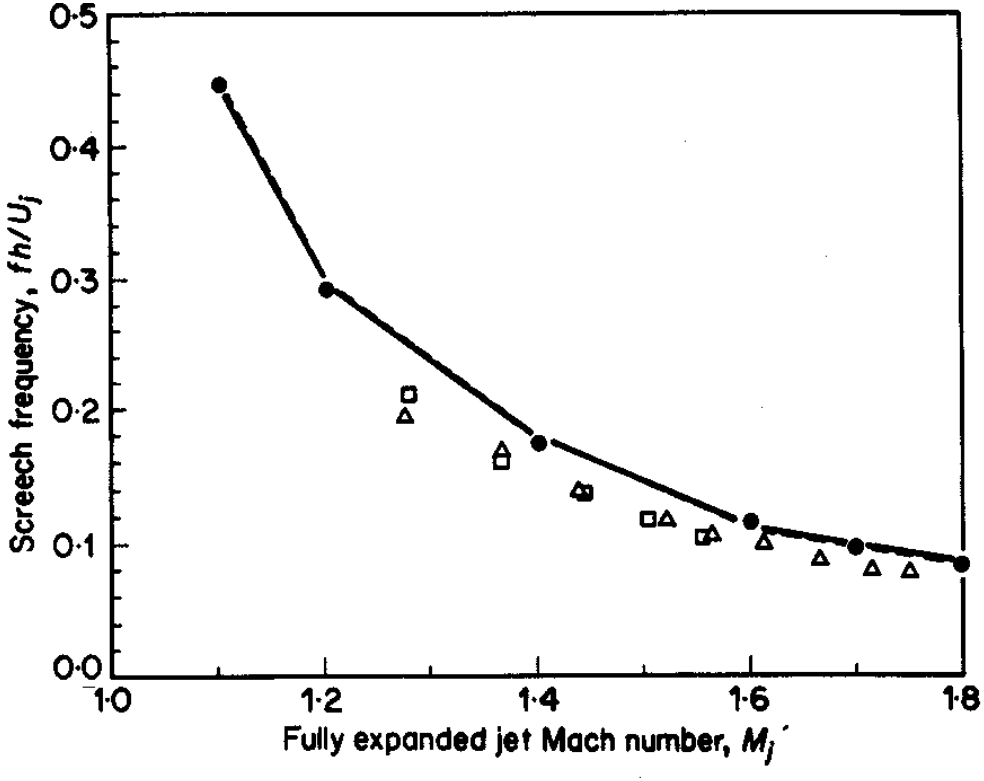
$$f_s = \frac{u_c}{L}\frac{1}{1 + M_c}$$

Tam, Seiner and Yu, *J. Sound Vib.*, Vol. 110 (1986)



Screech: Rectangular Jet

Morris, Bhat and Chen, *J. Sound Vib.* Vol. 132 (1989)



PENNSTATE

Effect of Mode Number

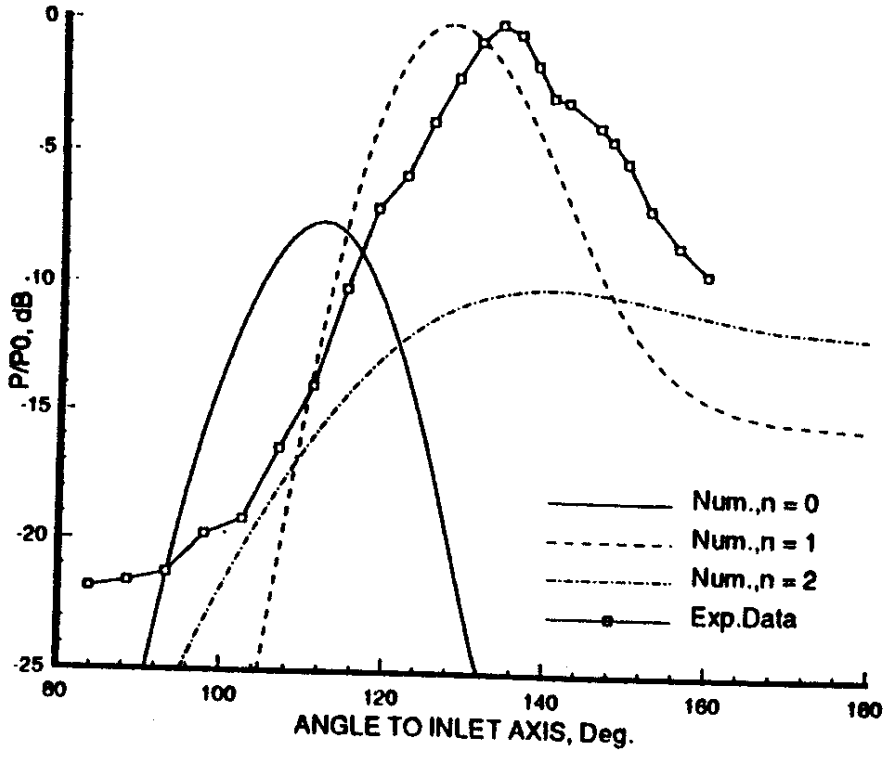


Figure 10. Far-field directivity, M_j = 2.0, T_o = 1370°K, S_t = 0.1.

Seiner, Bhat and Ponton, AIAA 93-0734

PENNSTATE

Instability Waves in Non-Circular Jets

- Multiple instability modes
  - Varicose, flapping and wagging
  - Have nearly equal growth rates (flapping mode is more dominant at high aspect ratios)
  - Calculations for elliptic supersonic jets have shown trends: but not good predictions (Morris & Bhat, AGARD CP-512 (1992)
- Role for CAA

Relation to CAA Simulations

- Computational Requirements
- Present Capabilities
- Future Directions

Frequency Spectrum

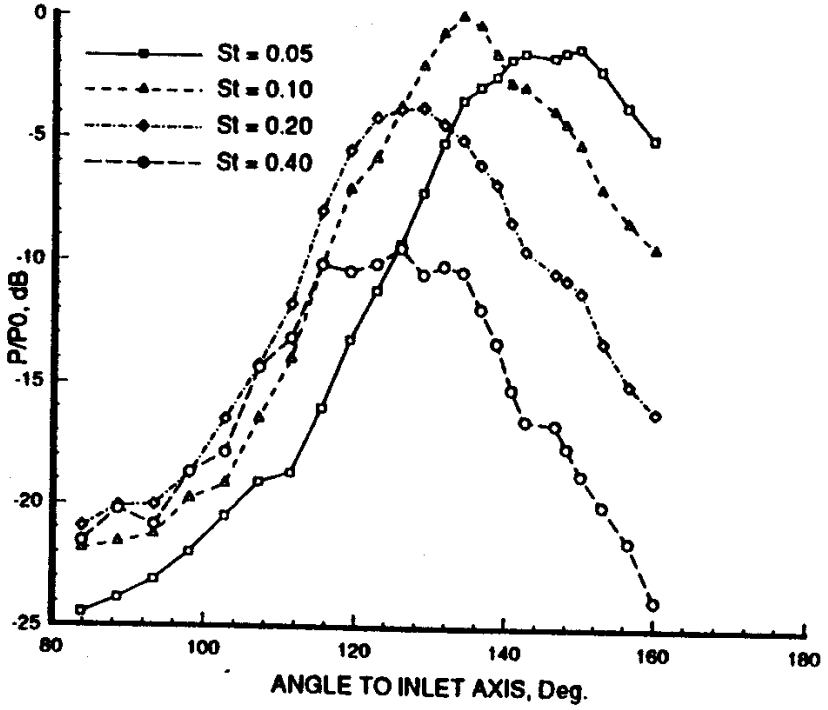


Figure 9. Far-field directivity, M_j = 2.0, T_o = 1370°K, (experimental data).

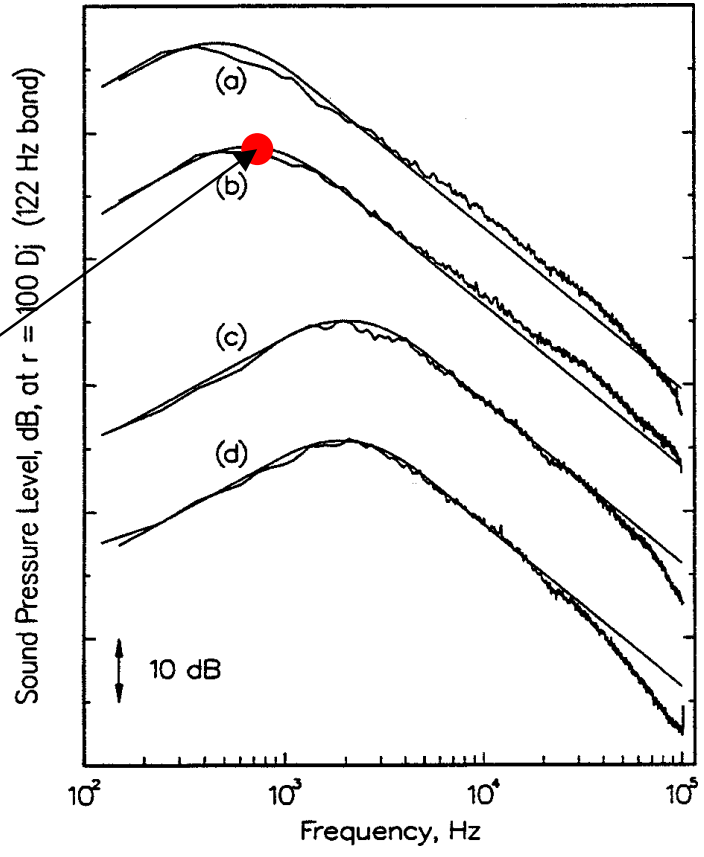
Seiner et al., DGLR/AIAA 92-02-046
24 Hz bandwidth

PENNSTATE

Noise From Large-Scale Turbulent Structures

Tam, Golebiowski & Seiner, AIAA 96-1716

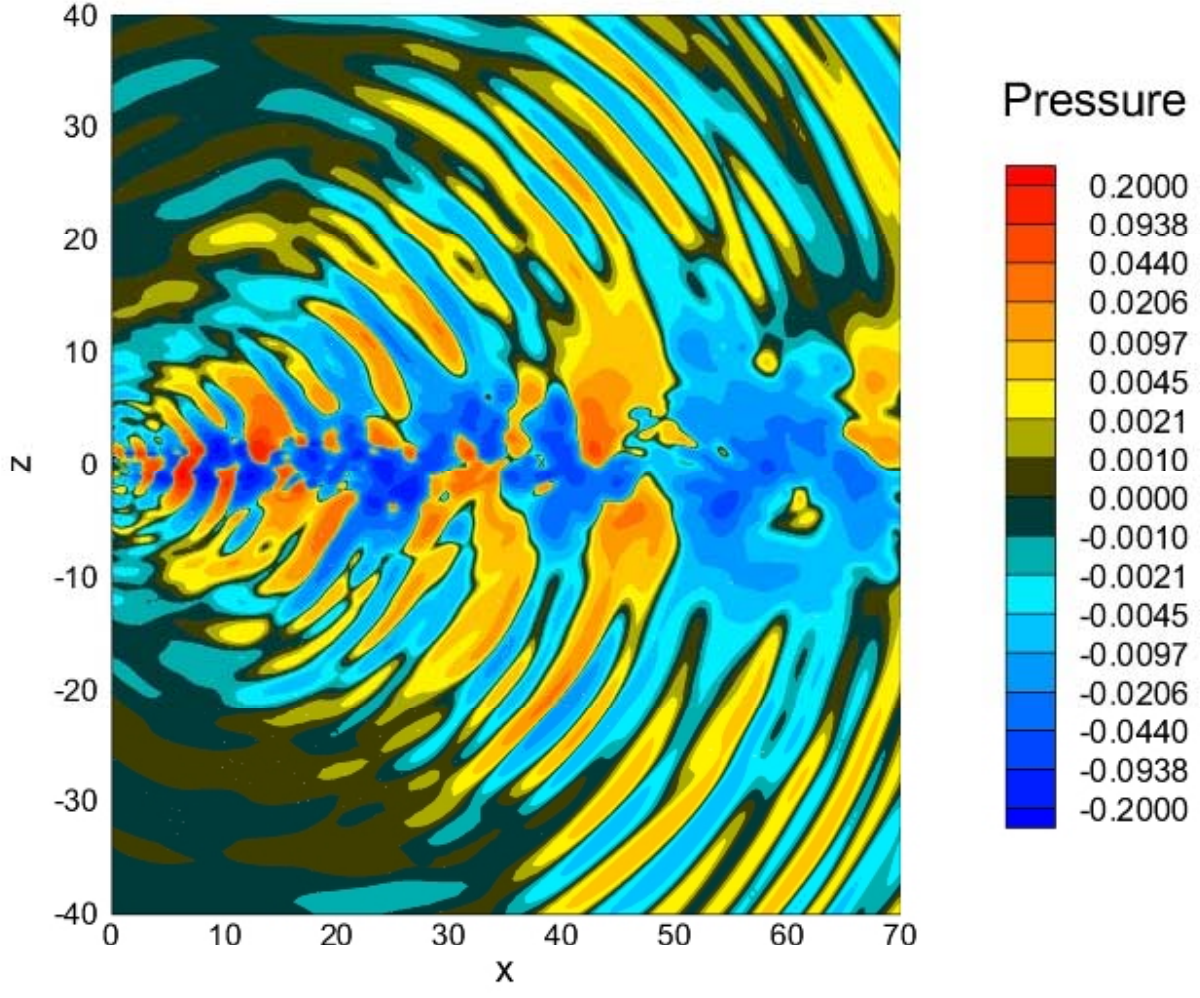
St =0.12



PENNSTATE

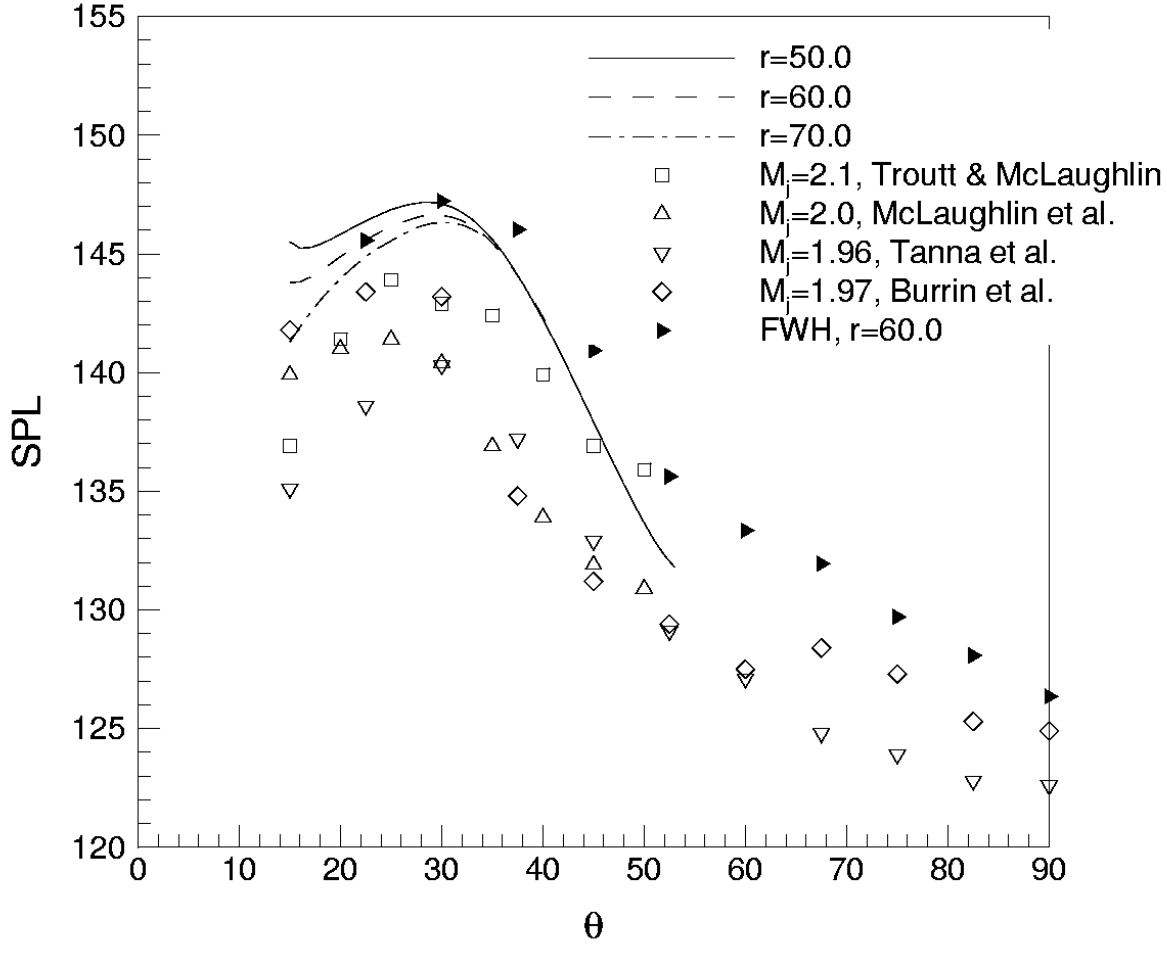
Instantaneous Pressure Contours
Circular Jet, M=2.1

PENNSTATE



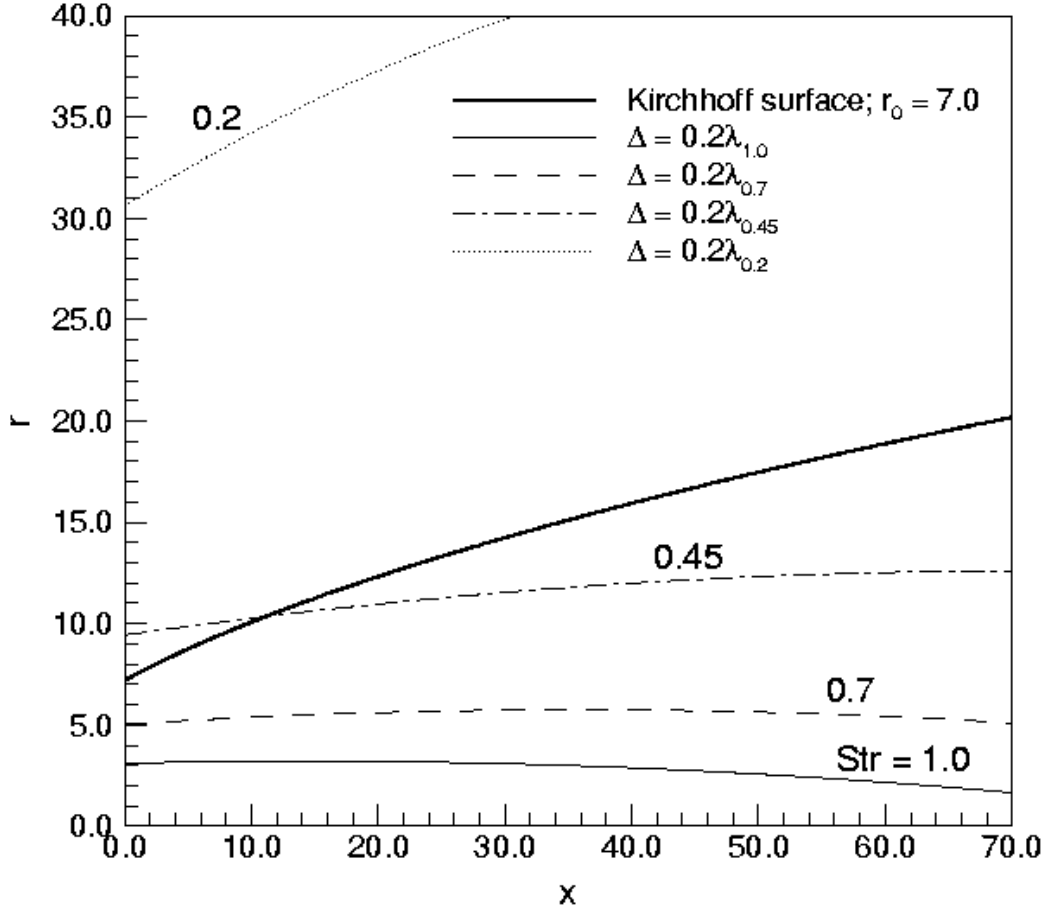
PENNSTATE

CAA Simulations



PENNSTATE

Resolution Requirements



PENNSTATE

Summary

- Large Scale Structures/Instability Wave Models Provide A Direct Link Between the Unsteady Turbulent Flow and The Radiated Noise
- Provide Information and Time and Length Scales of Turbulent Flow
- Does Not Predict Amplitude (Only Relative Levels)
- Increased Analytic Complexity for Non-Circular Jets
- Replacement by Direct Calculation Already Achieved

P. Morris References

1. Brown, G. L. and Roshko, A., (1974) “On density effects and large structure in mixing layers,” J. Fluid Mech., 64(4), pp. 775-816.

2. Lepicovsky, J., Ahuja, K. K., Brown, W. H. and Morris, P. J., (1986) "Acoustic Control of Free Jet Mixing," J. Propulsion and Power, 2(4), pp. 323-330.

3. Martens, S., Kinzie, K. W. and McLaughlin, D. K., (1994) “Measurements of Kelvin Helmholtz instabilities in a supersonic shear layer” AIAA J., 32(8), pp. 1633-1639.

4. Gaster, M., Kit, E. and Wygnanski, I., (1985) “Large scale structures in a forced turbulent mixing layer,” J. Fluid Mech. 150, pp. 23-39.

5. Tam, C. K. W. and Morris, P. J., (1985) "Tone Excited Jets, Part V: A Theoretical Model and Comparison with Experiment," Journal of Sound and Vibration, 102, pp. 119-151.

6. Dahl, M. (1994) “The aeroacoustics of supersonic coaxial jets,” Ph. D. thesis, Department of Aerospace Engineering, Penn State University.

7. Seiner, J. M. and Ponton, M. K., (1985) “Aeroacoustic data for high Reynolds number supersonic axisymmetric jets,” NASA TP-2072.

8. Tam, C. K. W. and Burton, D. E., (1984) “Sound generated by instability waves of supersonic flows. Part 2. Axisymmetric jets,” J. Fluid Mech., 138, pp. 273-295.

9. Troutt, T. R. and McLaughlin, D. K., (1982) “Experiments on the flow and acoustic properties of a moderate Reynolds number supersonic jet,” J. Fluid Mech., 116, pp. 233-256.

10. Dahl, M. and Morris, P. J., (1997) “Noise From Supersonic Coaxial Jets, Part II: Normal Velocity Profile Jets,” J. Sound and Vibration, 200(5), pp. 665-699.

11. Tam, C. K. W., (1987) “Stochastic model theory of broadband shock associated noise from supersonic jets,” J. Sound and Vibration, 116, pp. 265-302.

12. Tam, C. K. W. and Tanna, H. K., (1982) “Shock-associated noise of supersonic jets from convergent divergent nozzles,” J. Sound and Vibration, 81(3), pp. 337-358.

13. Morris, P. J., Chen, G. and Bhat, T. R. S., (1989) "A Linear Shock Cell Model for Jets of Arbitrary Exit Geometry," J. Sound and Vibration, 132(2), pp. 199-211.

14. Seiner, J. M., Bhat, T. R. S. and Ponton, M. K., (1994) “Mach Wave Emission from a High-Temperature Supersonic Jet,” AIAA Journal, 32(12), pp. 2345-2350.

15. Morris, P. J. and Bhat, T. R. S., (1991) "The Prediction of Noise Radiation from Supersonic Elliptic Jets," AGARD 78th B Specialists' Meeting on Combat Aircraft Noise, Conference Proceedings 512, Bonn, Germany.

16. Tam, C. K. W., Golebiowski, M. and Seiner, J. M., (1996) “On the two components of turbulent mixing noise from supersonic jets,” AIAA Paper No. 96-1716.

17. Mankbadi, R. and Liu, J. T. C., (1984) “Sound generated aerodynamically revisited: large scale structures in a turbulent jet as a source of sound,” Phil. Trans. Roy. Soc. Lond. A, 311, pp. 183-217.

Review of Noise Data and Recent Advances in Jet Noise Theory

Christopher Tam
Department of Mathematics
Florida State University

Review Of Noise Data and Recent Advances **- Christopher Tam, Florida State University as summarized by Geoffrey Lilley.**

In Part 1 of this presentation Professor Tam presented a number of examples from a wide range of experiments which suggest that turbulent shear flows, including jets, can be described in terms of a large-scale, coherent-like structure, and a small-scale motion, which he proposed should be labeled 'fine-scale'. He also showed Schlieren photographs where the sound radiation in the near field appeared to be generated by both sets of turbulent scales in motion along a jet. Tam also showed from the far-field radiated noise experimental databank of Seiner et al (1985), that the sound of greatest intensity for a Mach 2 jet at 500K was in the downstream arc between the jet boundary and 50 degrees to the jet axis. He then drew the conclusion that this radiation was the result of Mach wave radiation generated by the large-scale structures moving supersonically with respect to the medium at rest outside the jet, while the fine-scale motion was responsible for the dominant radiation in the sideline and upstream directions.

Tam also presented data to support the view that, for the relatively high Reynolds number of the fully developed turbulent jet experiments of Seiner et al (1985), the radiated acoustic spectra at fixed angles to the jet axis were all self-similar and thus independent of Reynolds number. From the examination of some 1900 data sets relating to the far-field jet noise narrow band spectra from circular convergent and convergent-divergent, rectangular and elliptic jets, all scaled to a distance of 100 nozzle diameters from the nozzle exit, and covering M_j = 1.37 to 2.24 and jet stagnation temperature to ambient temperature ratios of 1.0 to 4.9, Tam showed that the far-field spectra could be represented as a superposition of two universal spectra he associated one of these with the large-scale structures, and the other a with the fine-scale structures. These results were communicated in Tam et al (1996). The fit of each data set with these two universal curves were shown to be broadly in agreement around the peaks in the spectrum although some differences occurred especially at higher frequencies. Comparisons were also shown with other experimental data sets obtained by Norum and Brown(1993), Papamoschou(1990) for supersonic jets, and the subsonic data of Ahuja(1973), Lush(1971), Norum and Brown(1993) and Boeing(unpublished). Tam presented a mechanism, based on the growth and decay of the large turbulence structures, which allows subsonic jets to generate supersonic traveling wave components and hence noise radiation. However, as pointed out in the presentation by Morris, this mechanism appears to be very inefficient at subsonic speeds and the resulting sound field is therefore very weak. Tam also noted that there was no experimental evidence presented to confirm the existence of Mach waves in a subsonic jet.

Tam showed evidence that similar turbulent flow mechanisms were responsible for the generation of noise in subsonic and supersonic jets. Tam cited the classical acoustic Analogy results of Lighthill and Ffowcs Williams that the overall sound power is proportional to V_j^8 at subsonic jet speeds and proportional to V_j^3 at supersonic speeds. Although some old data have been presented in the past to support the validity of the theoretical results, if jet temperature variation is taken

into consideration, then both early as well as the more recent Seiner data show no indication of V_j^3 dependence even at relatively high supersonic Mach numbers.

Comments from Lilley: This information was taken from results presented by von Gierke(1960), and takes no account of the differences in jet stagnation temperature of the various data sets. In the presentation of Lilley similar experimental data sets were used and showed that cold jets followed a V_j^8 law at speeds less than $V_j / c_\infty < 2$ but hot jets showed that the velocity power law was a complex function of both V_j / c_∞ and T_{st} / T_∞ . Since V_j cannot increase without limit for a given stagnation temperature ratio it is impossible to draw the conclusion that all jets follow a V_j^3 law at supersonic speeds. However the overall conclusion that the source of noise in supersonic jets is similar to that in subsonic jets appears to be correct for cold jets. The view expressed by Lilley is that an additional source exists for all hot jets associated with the temperature fluctuations in the jet mixing region and this noise is additional to that associated with the velocity fluctuations alone as in a cold jet. Some of the differences in the spectra shown by Tam may relate to the changes imposed by the temperature fluctuations and their dependence on a velocity power law of V_j^6. The conclusion to Part 1, expressed by Tam, that the V_j^3 law is not supported by experiment for supersonic jets is also a conclusion from Lilley's work but for different reasons. The plots shown in Figs. 8 and 9 (of Tam's presentation), which show similar velocity power laws for hot and cold jets for the large-scale and fine-scale eddies respectively differs from the interpretation given by Lilley for the same sets of data.

The conclusion reached by Tam, from the compilation of the jet noise spectra and directivity from experimental data by Seiner and his colleagues at NASA Langley Research Center, is that there is evidence for two independent classes of sources responsible for the radiation from large-scale and fine-scale turbulence respectively, with different amplitudes and different directivities.

Comments from Lilley: Lilley noted that in an earlier period of jet noise research this same conclusion was drawn by both Lilley and Ribner, but the experimental data available at that time was insufficient to define universal spectra to the accuracy given by Tam.

Part 2 of the presentation by Tam related to the theory of jet noise from 'fine-scale' turbulence as published by Tam and Auriault(1999). Tam stated that this theory relates to the sources of noise in the jet that radiate in the direction normal to the jet and in the upstream arc relative to the jet axis. The theory includes the effects of refraction and convective amplification. The theory can be extended to include forward flight effects and to include nozzles of arbitrary geometry. Tam stated that this new theory is unrelated to the acoustic analogy. Tam describes it as a semi-empirical theory, which is based on turbulence information obtained by the k-ε turbulence model. The theory has three empirical constants which were determined by best fit to the noise data. Tam followed gas kinetic theory and derived**,** using a very simplified model of turbulent flow, a relationship between the average value of the local pressure fluctuations in the mixing region to the kinetic energy of the

turbulent velocity fluctuations. Tam then argued that the source of sound in a turbulent shear flow is Dq_s/Dt, where $q_s = (2/3)\ \rho\, k_s$, and this equals the turbulent pressure fluctuations. Tam then linearized the Reynolds Average Navier-Stokes (RANS) equations and retained only the derivatives of q_s as the noise source terms.

Comments from Lilley: Tam showed that q_s is related to an isotropic model of the turbulence so that $<\rho\ v^2> = (2/3)\ \rho\ k_s$, where v is local component of turbulence in any direction. Thus in the formulation of his model there is little difference between the Tam model and the acoustic analogy model in which the corresponding source term is T_{xx}, as derived from an isotropic turbulence model, and where the viscous terms are neglected. As stated Tam's linearized Euler equations are exact and include all flow-acoustic interaction effects such as refraction. Tam solves this set of equations rather than the equations of mass and momentum as previous investigators did using Lighthill's equations. Tam also omits the density fluctuations in the flow.

In a shear flow with $V = (V_1(x_2), 0, 0)$ *and writing* $D_0/Dt = \partial/\partial t + V\nabla$ *we find* $D_0\,\rho/Dt + \nabla \bullet \rho v = 0 : D_0\,\rho v/Dt + \nabla p = -\nabla\rho vv - i\,\rho v_2 dV_1/dx_2$.

The stagnation energy equation, for an isentropic flow, when combined with the equation of continuity gives,

$$(1/c_\infty^2)D_0\,(p - c_\infty^2\,\rho)/Dt = -(\gamma-1)/2c_\infty^2\ D_0\ \rho\, v^2/Dt - \nabla\cdot\rho\,\mathbf{v}(h_s - h_\infty)/h_\infty - ((\gamma-1)/c_\infty^2)\ \rho\, v_1 v_2\, dV_1/dx_2.$$

We see that the 'second' term in Lighthill's acoustic analogy is related to quadratic fluctuations in velocity and in the flux of stagnation enthalpy fluctuations. Note that the divergence of the mean velocity is zero, $\mathbf{v}$ *is the turbulent velocity fluctuation, h is the local enthalpy and* h_s *is the stagnation enthalpy, equal to* $h + v^2/2$. *These equations can easily be written in the form of an acoustic analogy, but are displayed here to show they are identical with Tam's linearized Euler equations, where the source terms replace the nonlinear terms. A major difference is that the nonlinear source terms in the acoustic analogy have to be obtained from a time accurate flow-field solution and must include both the large and the fine scale contribution to the turbulent pressure. Tam states that by splitting up the far-field noise into its separate large and fine scale components it is possible to split the corresponding contributions to the turbulent pressure. In the earlier work of Lilley and Ribner this split of the turbulent pressure in the turbulent flow formed a dominant component in their attempt to derive the* T_{xx} *covariance. As defined by Tam* q_s *is proportional to the kinetic energy of the fine scale turbulence, and is defined as a function of* (x_1, t). *In the Lighthill acoustic analogy the source term equal to the double divergence of* T_{ij} *in the moving frame contributes to the acoustic far-field radiation* $(1/c_\infty^2)\ \partial^2 T_{xx}/\partial t^2 = (1/c_\infty^2)\ D_0^2\ T_{xx}/Dt^2$. *The similarity with Tam's model is striking except that the second time derivative in Lighthill's model, is replaced by a single time-derivative.*

Tam explained that if the source function could be modeled, the solution to the inhomogeneous linearized Euler equations could be solved by quadrature once the Green's function had been calculated. The unique method used by Tam involved the calculation of the adjoint Green's function. Finally Tam described the determination of the pressure autocorrelation function for a point in the acoustic far-field. This involved introducing a model for the space-time correlation function in the nozzle fixed frame. Tam assumed this could be modeled similar to the measurements of Davies et al.(1963) for the two-point axial velocity covariance. The resulting spectral density contained terms arising from the turbulent kinetic energy, and the length and time scales of the turbulence in the nozzle fixed frame. Tam introduced empirical constants to allow the fine-scale components to be derived from the integral scales found by the k-ε turbulence model. Extensive comparisons with measured spectra at a number of angles between θ = 60 degrees to 120 degrees to the downstream jet axis were made. The comparisons extended to simulated forward flight and to non-axisymmetric jets.

Comments by Lilley: Overall, the details of the new method and the range of the comparisons with experiment, present an impressive effort in modeling that part of the turbulent fluctuations in the jet that the author claimed were responsible for the sound radiation, in directions around a normal to the jet and in the directions upstream of the nozzle exit. The claim made that the method introduced by the author is independent of Lighthill's acoustic analogy is correct, but the claim that it is unrelated to the Lighthill and other acoustic analogies is still being debated. The techniques used in solving the linearized RANS equations will certainly be used by future workers in this field. Tam's realization that the far-field noise spectrum is the sum of two universal spectra, each having different amplitudes and frequencies at their peaks is an important contribution to the development of any jet noise prediction scheme. However this enormous effort of Tam in no way reduces the further effort needed in seeking a greater physical understanding of the jet noise problem, its prediction and its reduction.

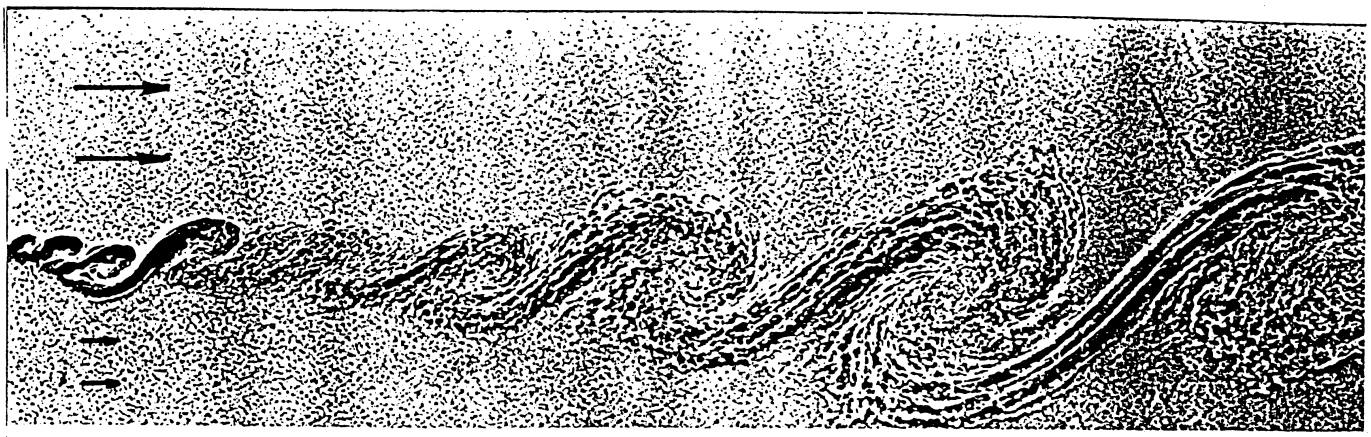
This presentation was followed by a brief discussion concerning Tam's assertion that the small angle spectra was primarily associated with the large scale coherent motion. Goldstein noted that the self-similarity of the spectra suggests that the sound generation mechanism is the same at subsonic speeds as it is at supersonic speeds. He also noted that the observed radiated sound levels at slightly subsonic Mach numbers were not much different from those at slightly supersonic Mach numbers. **In other words, the decrease in the spectral level was no more rapid in the vicinity of Mach numbers near unity than at any other Mach numbers.** Goldstein asked whether this was inconsistent with the instability wave theory of large scale structure noise, which predicts that there should be a rapid decrease in the sound radiated by the instability waves (and therefore the large structures) when the convection Mach number of the source decreases through unity.

Outline

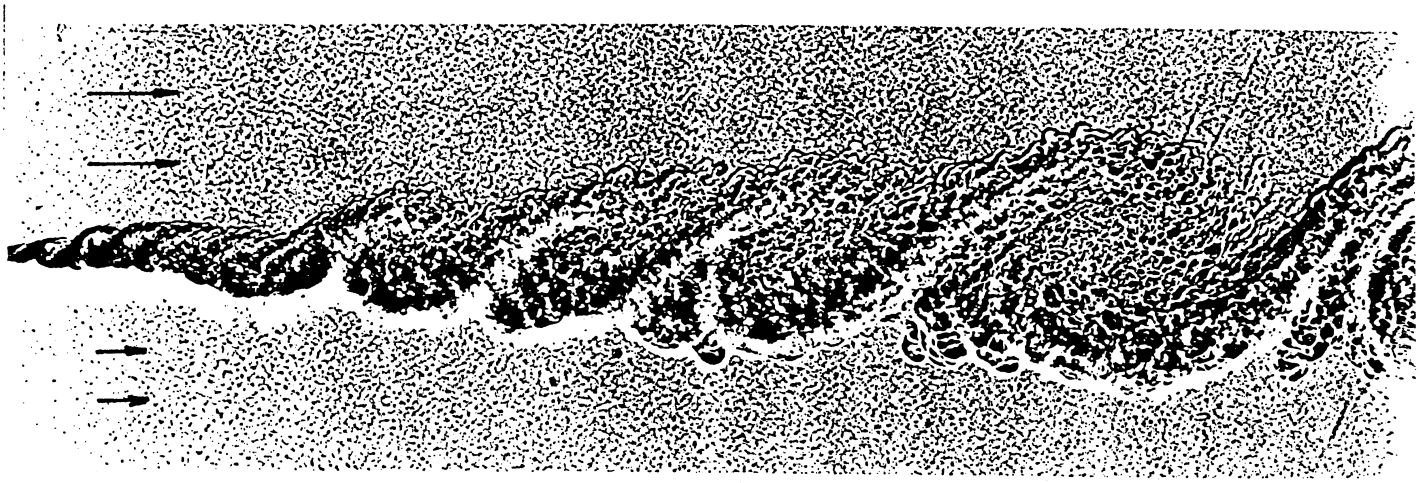
Part 1. Review of Jet Noise Data and Interpretations.

Part 2. New Theory and Comparisons with Experiments

Large Turbulence Structures and Fine Scale Turbulence



176. Large-scale structure in a turbulent mixing layer. Nitrogen above flowing at 1000 cm/s mixes with a helium-argon mixture below at the same density flowing at 380 cm/s under a pressure of 4 atmospheres. Spark shadow photography shows simultaneous edge and plan views, demonstrating the spanwise organization of the large eddies. The streamwise streaks in the plan view (of which half the span is shown) correspond to a system of secondary vortex pairs oriented in the streamwise direction. Their spacing at the downstream side of the layer is larger than near the beginning. *Photograph by J. H. Konrad, Ph.D. thesis, Calif. Inst. of Tech., 1976.*



177. Coherent structure at higher Reynolds number. This flow is as above but at twice the pressure. Doubling the Reynolds number has produced more small-scale structure without significantly altering the large-scale structure. *M. R. Rebollo, Ph.D. thesis, Calif. Inst. of Tech., 1976; Brown & Roshko 1974*

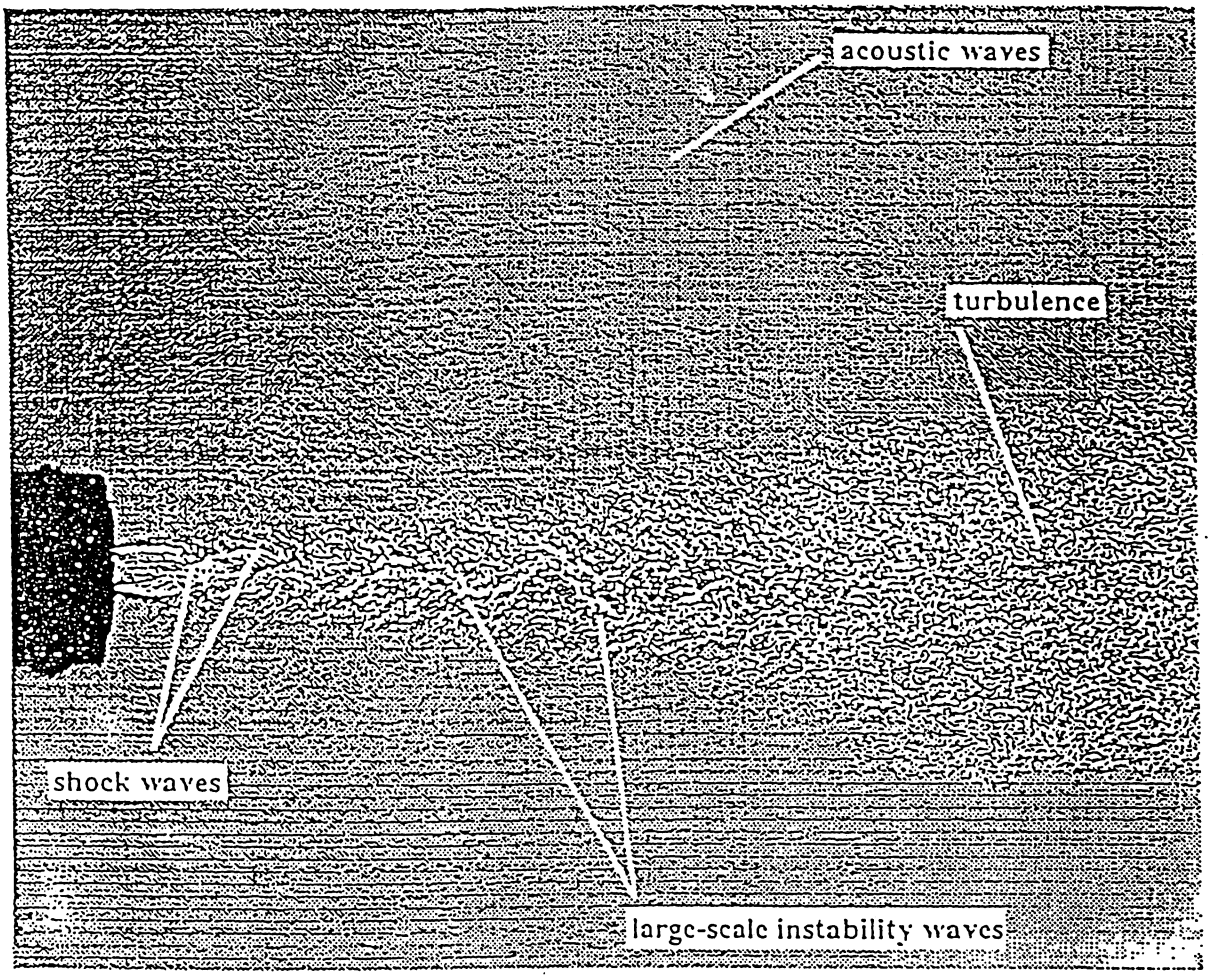
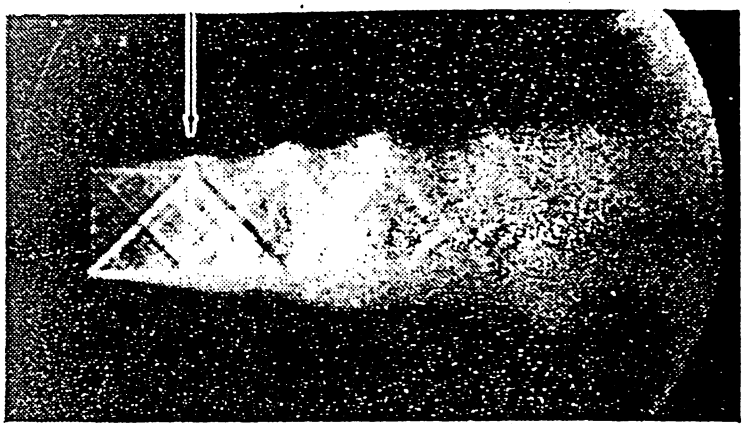
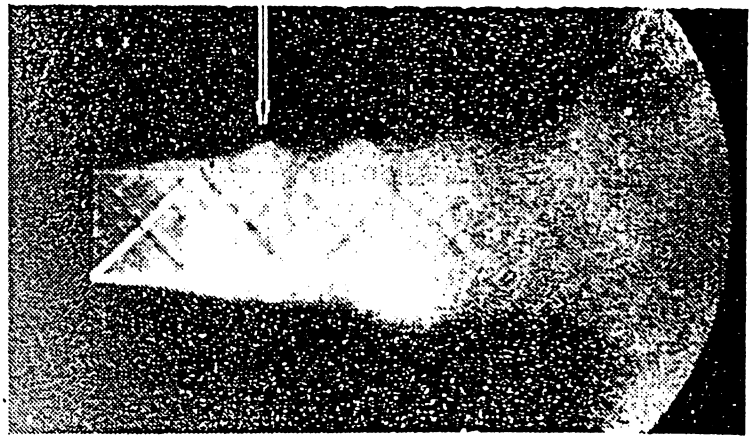


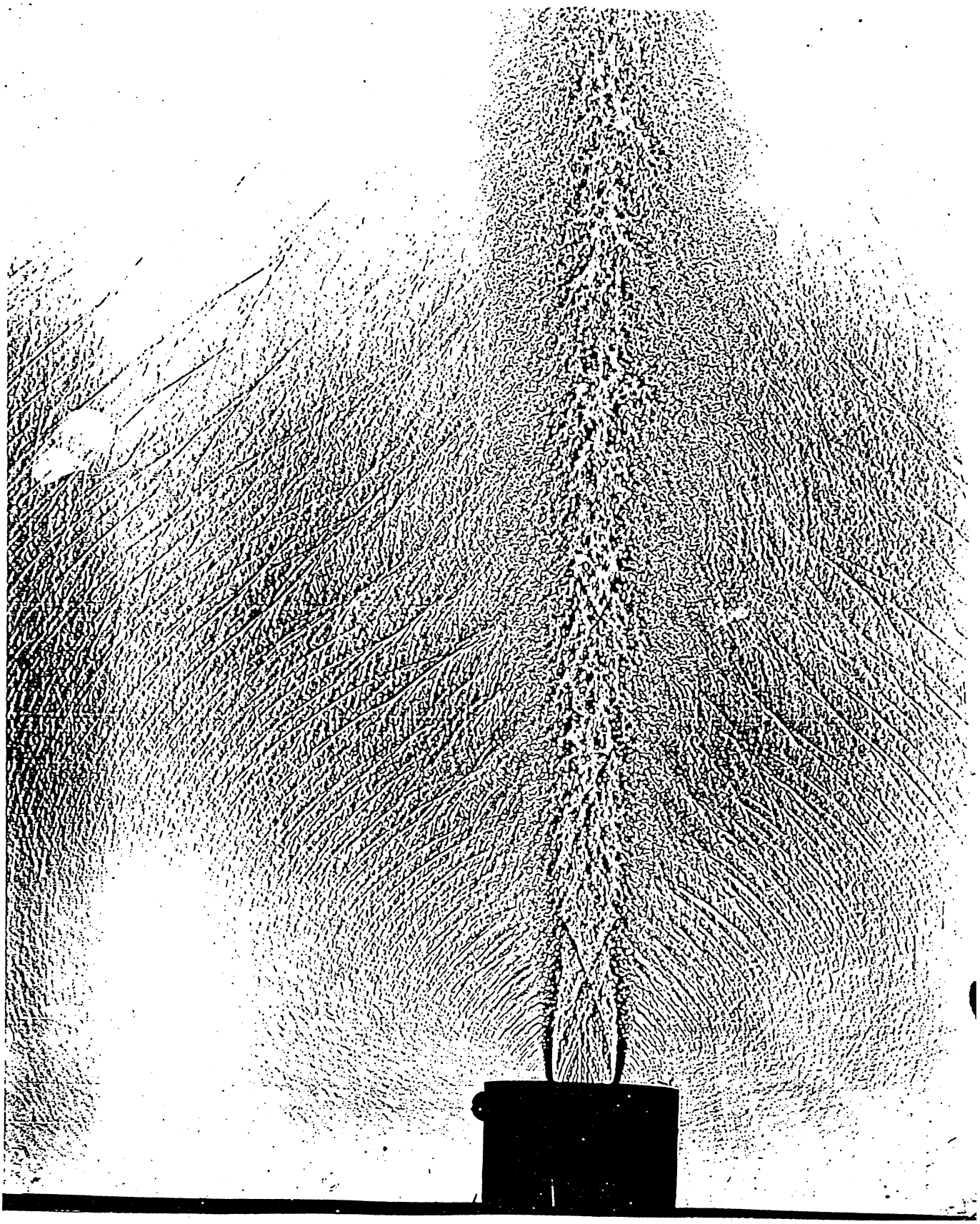
Figure 1: Visualization of a Mach 1.8 jet



(a) $\phi = 0°$.



(c) $\phi = 120°$.



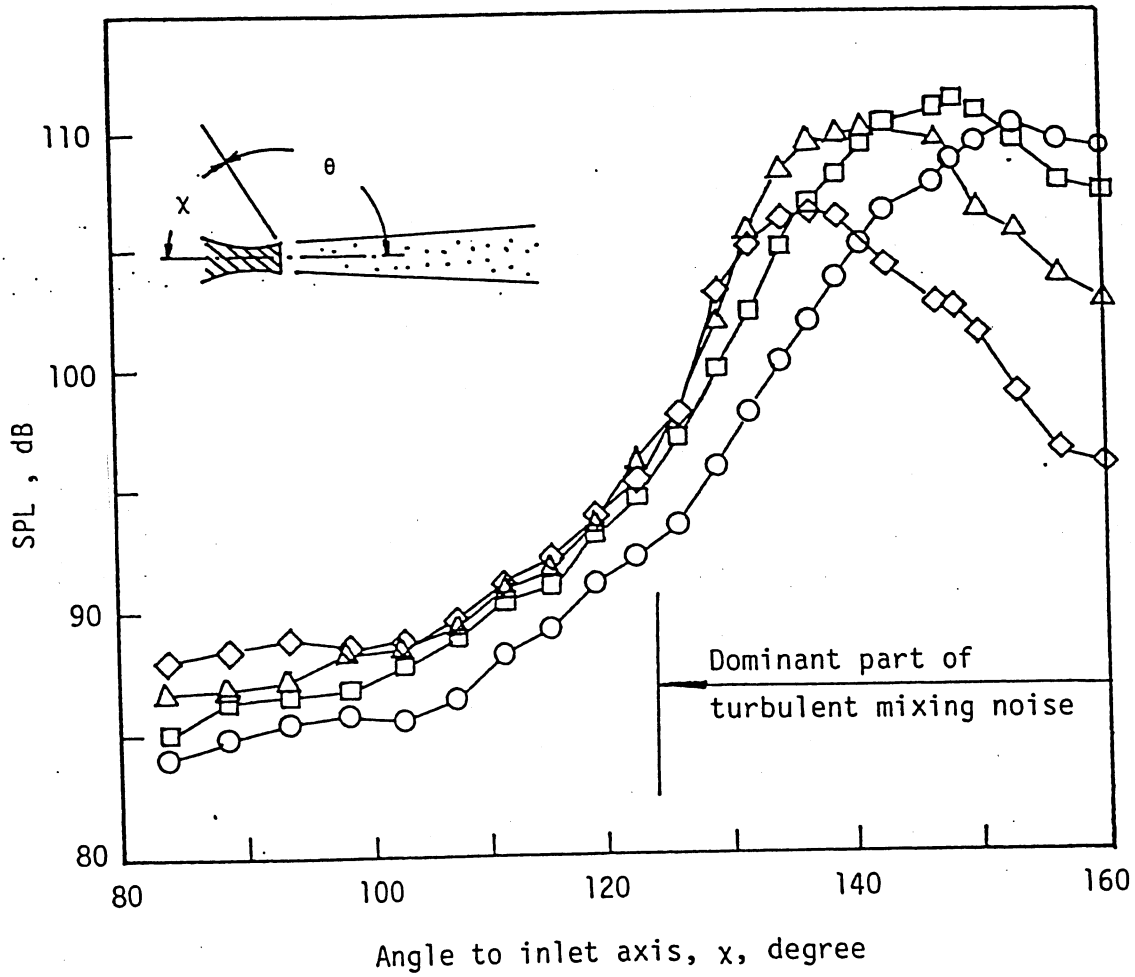
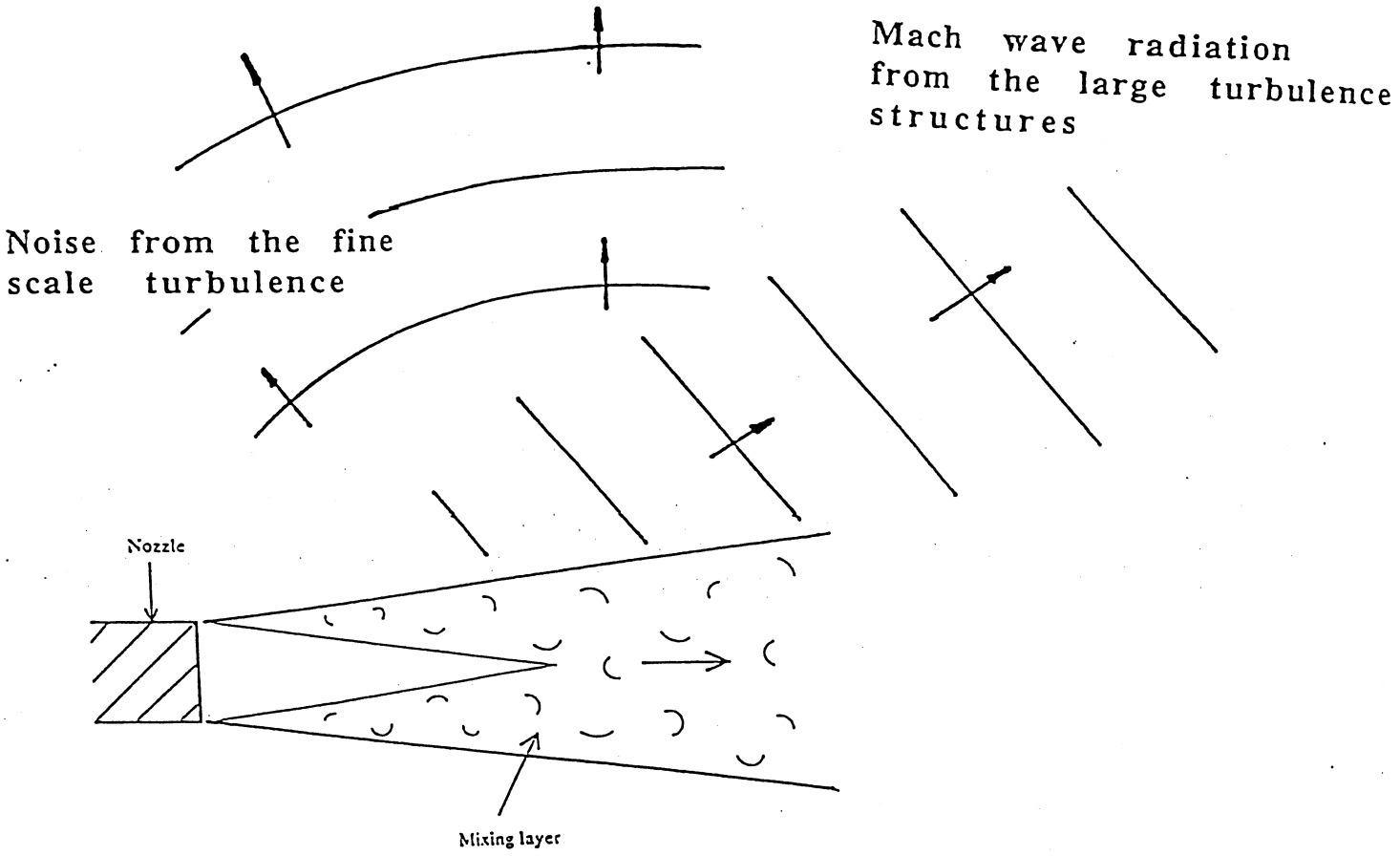


Figure 1. Measured[3] noise directivities at selected Strouhal numbers of a Mach 2 jet at a total temperature of 500°K. (Strouhal number=st). ○ st=0.067; □ st=0.12; △ st=0.20; ◇ st=0.40


Mach wave radiation from the large turbulence structures
Noise from the fine scale turbulence
Nozzle
Mixing layer

DATA BANK OF THE NASA LANGLEY RESERACH CENTER

1900 SPECTRA FROM AXISYMMETRIC JETS
SAMPLE SPECTRA FROM RECTANGULAR AND ELLIPTIC JETS

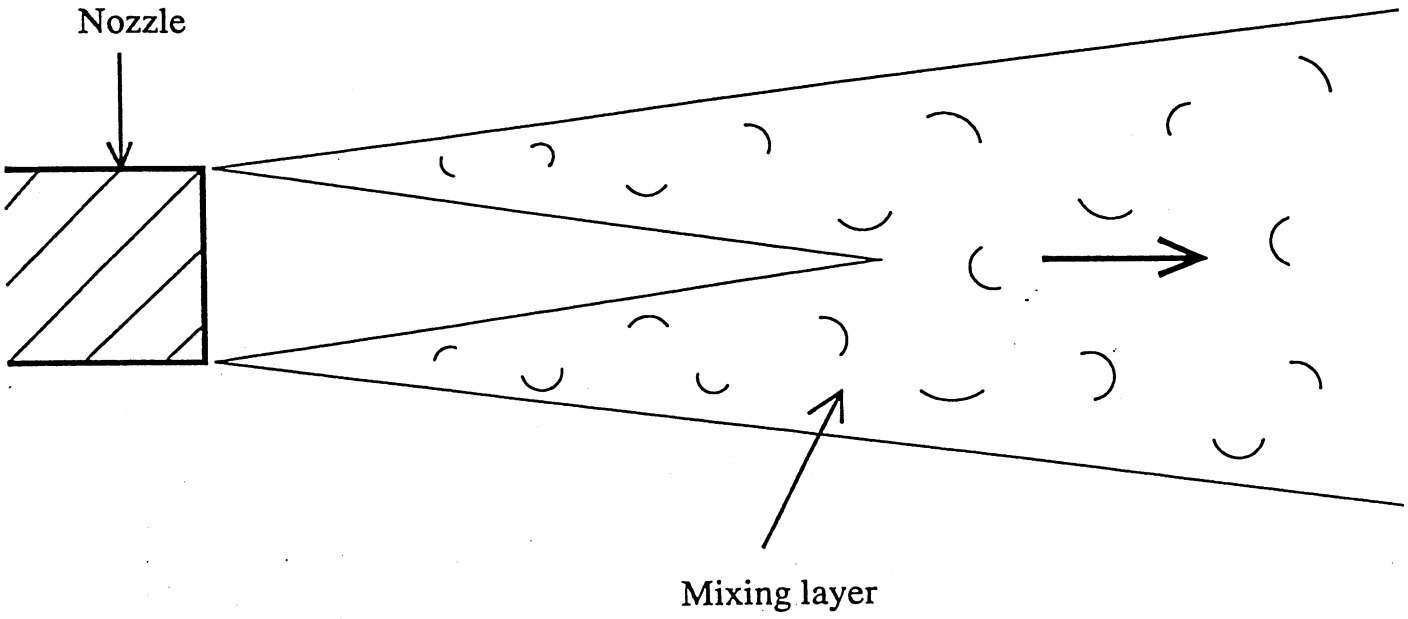
DATA USED IN 122 Hz BAND
SCALED TO R= 100 D_j

CHARACTERISTICS OF THE JET NOZZLES USED IN THE NASA LANGLEY EXPERIMENTS

M_d	D (cm)	Nozzle type	range of M_j	range of $\frac{T_r}{T_\infty}$
1.0	3.952	C†	1.37 to 1.8	1.0 to 2.24
1.5	4.267	CD*	1.37 to 1.8	1.0 to 2.35
2.0	4.989	CD	1.5 to 2.24	1.0 to 2.26
2.0	9.144	CD	2.0	1.12 to 4.9

† =convergent, * =convergent-divergent

SIMILARITY

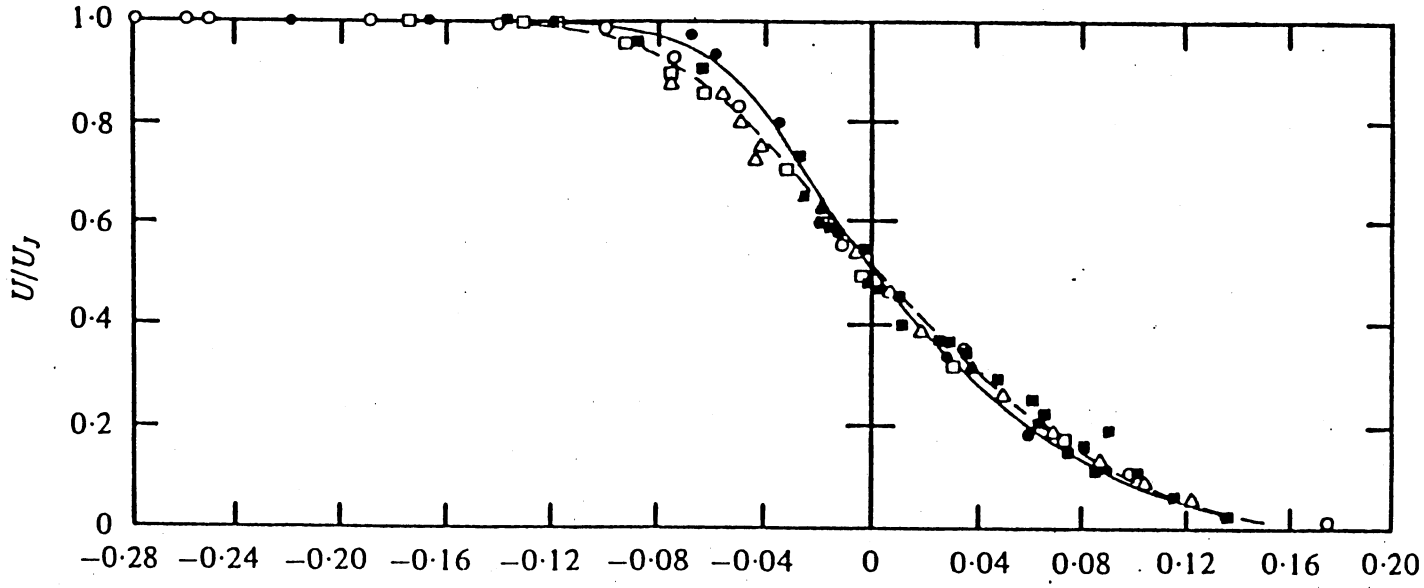


NO INTRINSIC LENGTH SCALE AT HIGH REYNOLDS NUMBER --> FLOW IS SELF-SIMILAR

SIMILARITY IN (a) MEAN FLOW PROFILE
(b) TURBULENCE STATISTICS

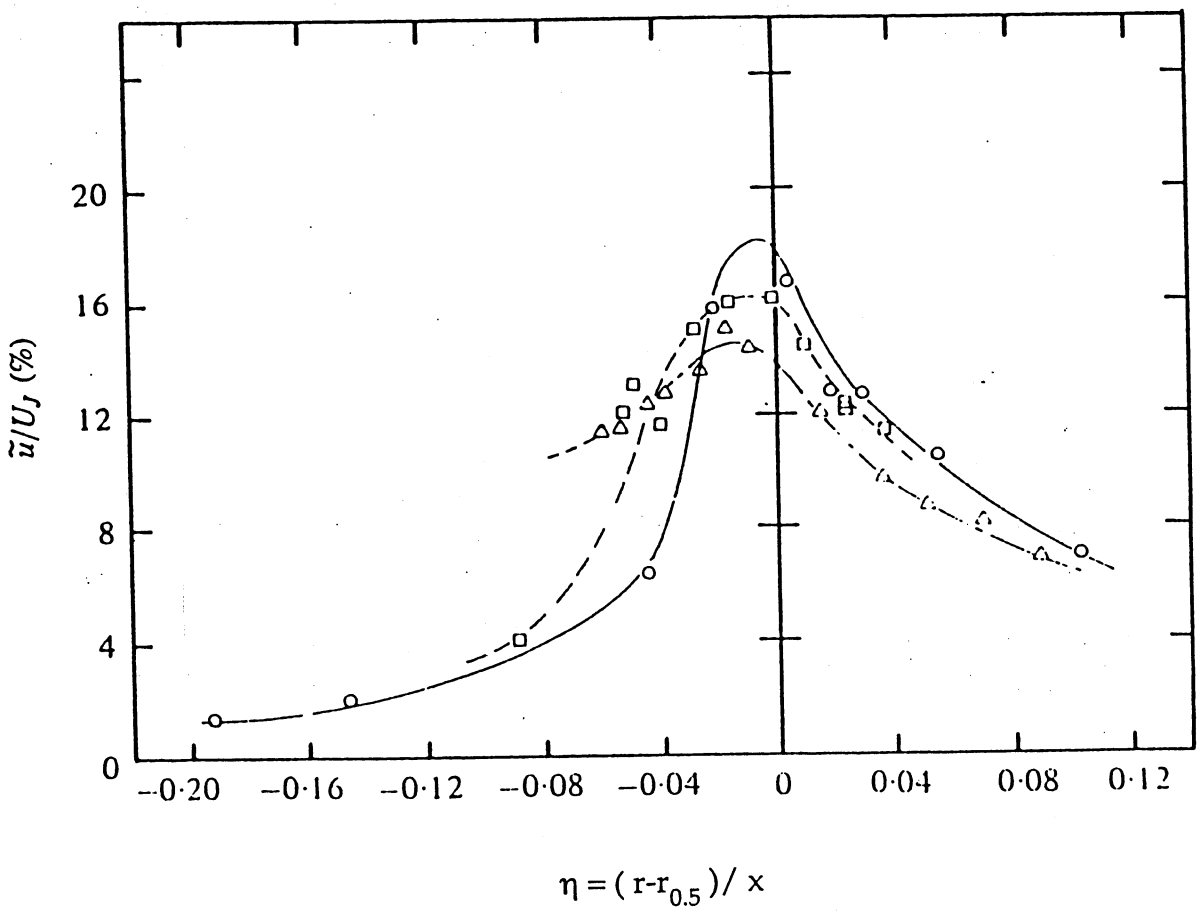
SIMILARITY ALSO APPLIED TO RADIATED NOISE

$$S\ (\ U_j, a_j, a_\infty, \chi, r,\ f\ )\ =\ A\ F(\ f/f_p\ )\ /\ r^2$$



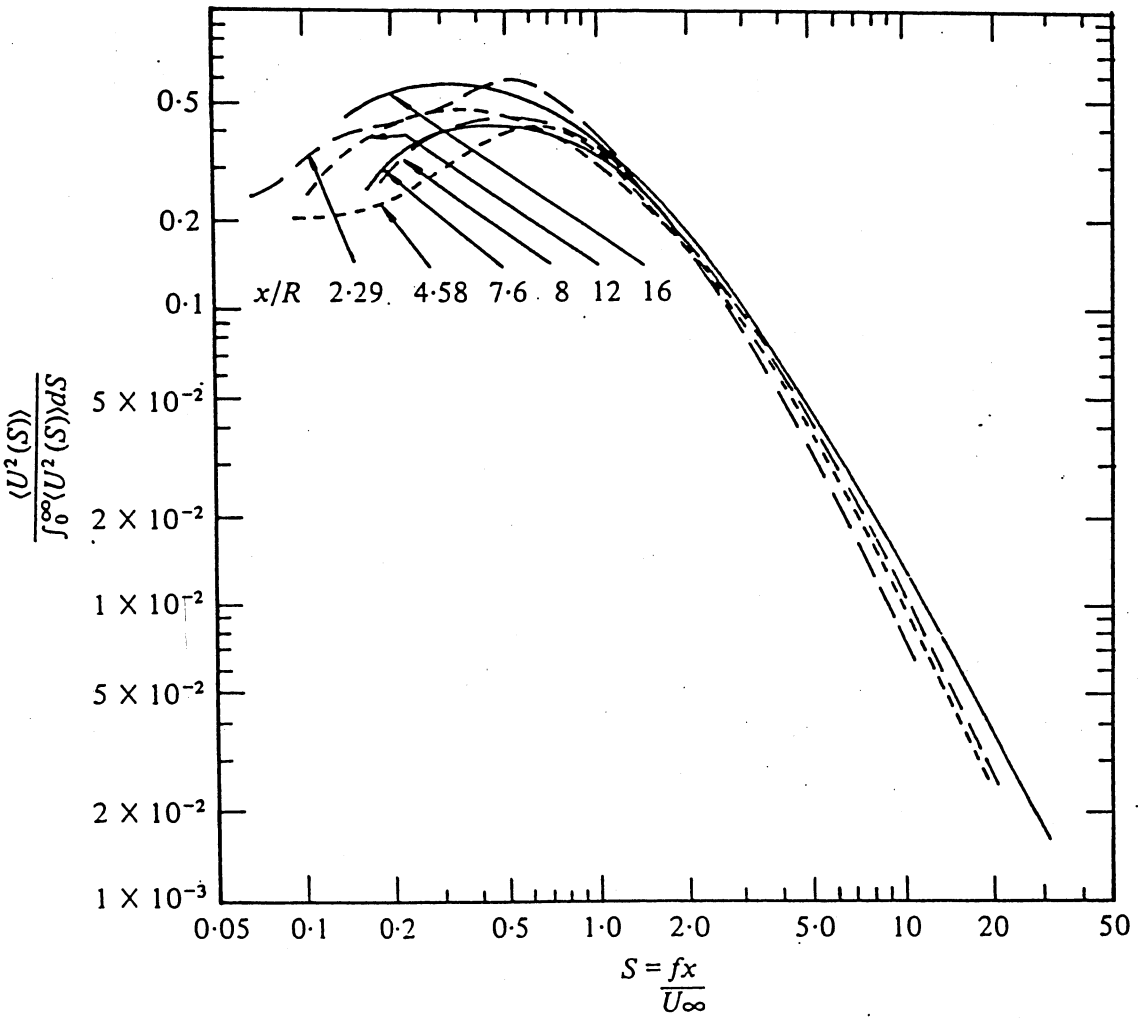
Radial distribution of the normalized axial mean velocity ($M_J = 0{\cdot}5$). $T_J/T_0 = 0{\cdot}95$ and 2·32 (solid symbols and full line). x/D: ○, 2; □, 4; △, 8.

J. C. Lau (JFM vol. 105, pp 193-218, 1981)



Radial distribution of the axial turbulence intensity ($\tilde{u}/U_J$). ($M_J = 0{\cdot}9$, $T_J/T_0 = 2{\cdot}32$). x/D: ○, 2; □, 4; △, 8.

J. C. Lau (JFM vol. 105, pp 193-218, 1981)



Normalized longitudinal turbulent spectra at various axial distances downstream of the nozzle exit of a 3·5 in. diameter jet at approximately one radius from the centre-line. Flow Mach number is 0·3. Data taken from Laurence (1956).

Laurence J. C. (NACA Report 1292, 1956)

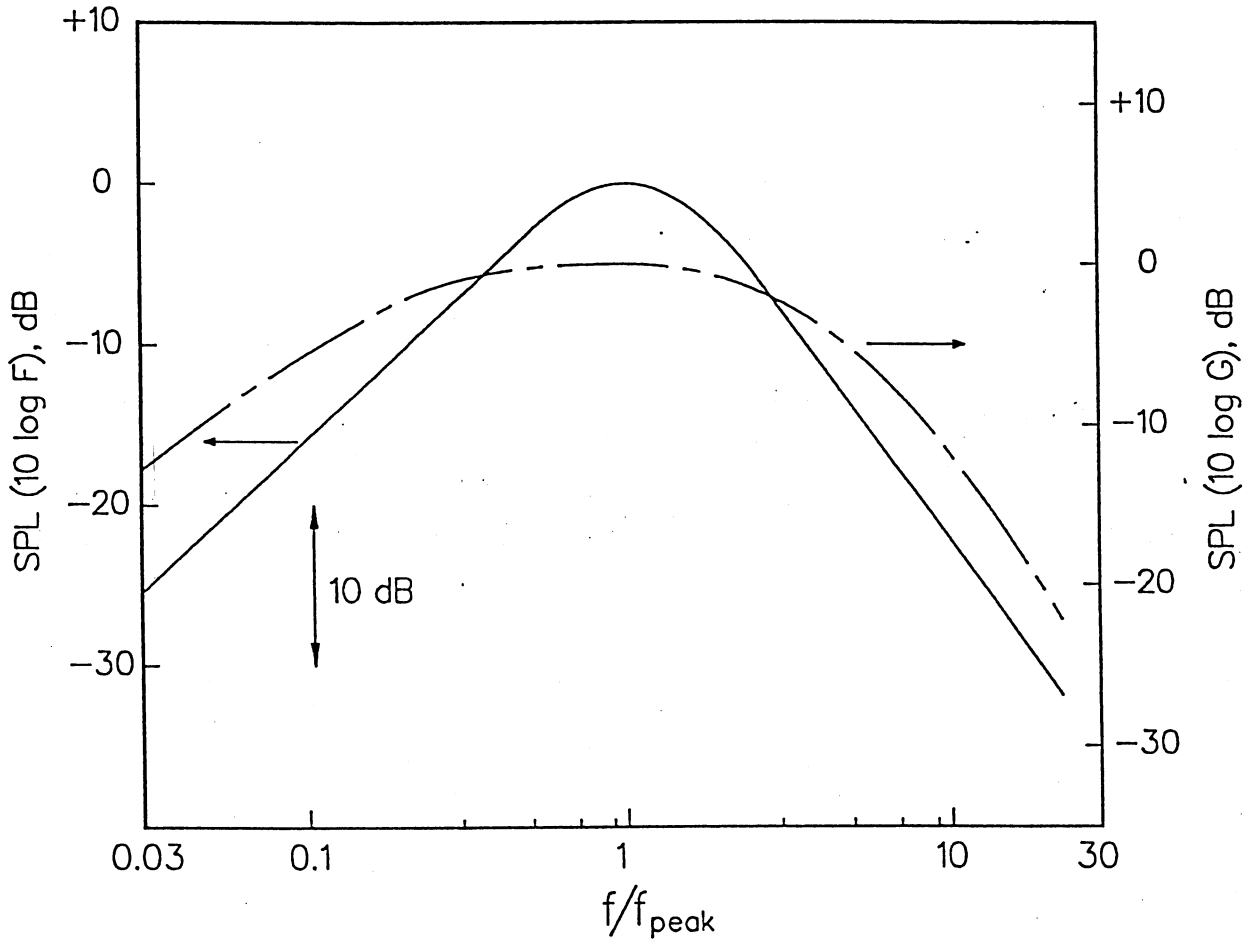


Figure 2. Similarity spectra for the two components of turbulent mixing noise.
——— large turbulence structures/ instability waves noise;
— - — fine scale turbulence noise.

independent of Mach number, jet temperature and direction of radiation

SIMILARITY SPECTRA

$$S = \left[AF\left(\frac{f}{f_L}\right) + BG\left(\frac{f}{f_F}\right) \right] \left(\frac{D_j}{r}\right)^2$$

A and B are the amplitudes

f_L and f_F are the peak frequencies

In Decibel scale

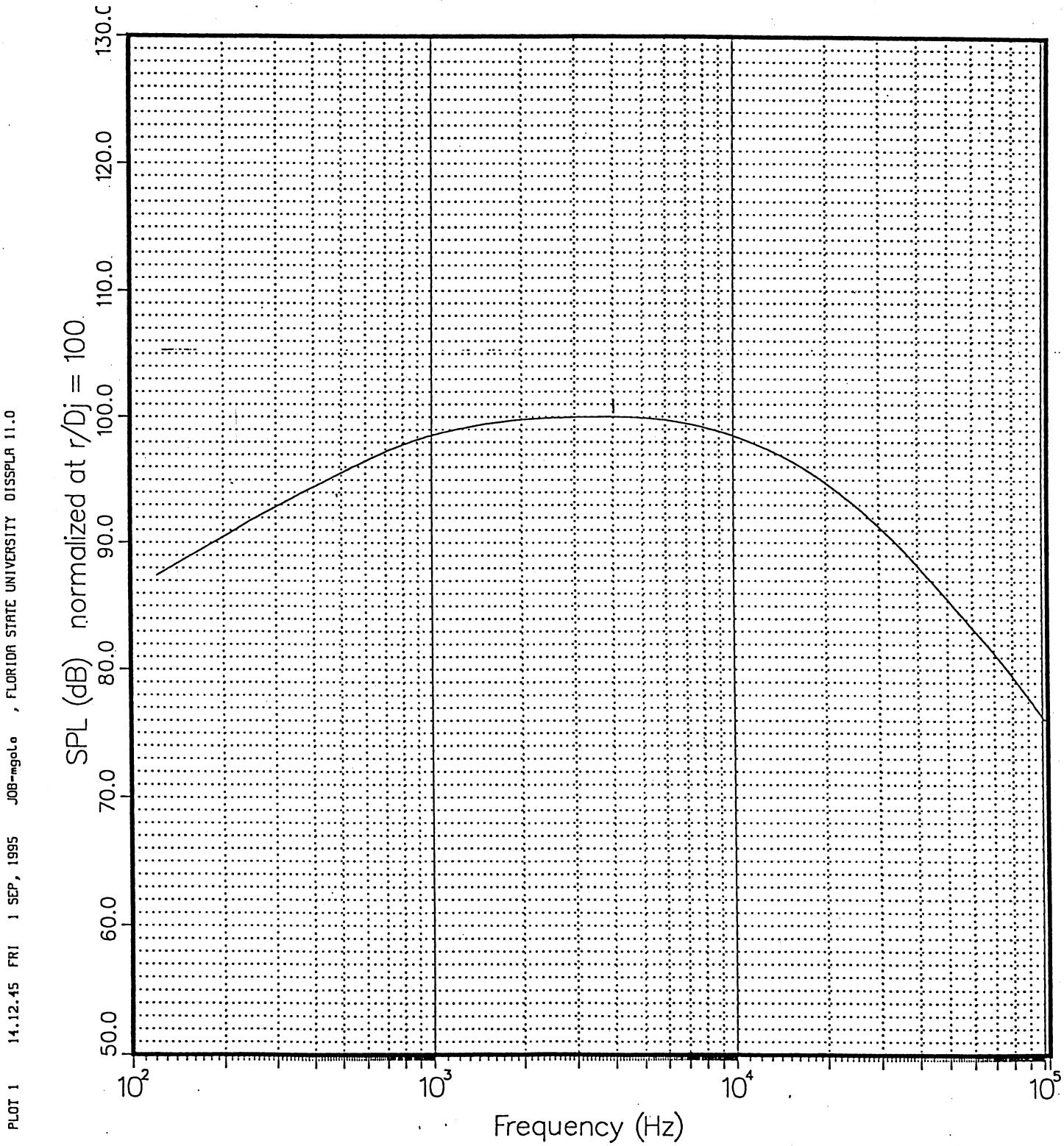
$$10\log\left(\frac{S}{p_{\text{ref}}^2}\right) = 10\log\left[\frac{A}{p_{\text{ref}}^2}F\left(\frac{f}{f_L}\right) + \frac{B}{p_{\text{ref}}^2}G\left(\frac{f}{f_F}\right)\right] - 20\log\left(\frac{r}{D_j}\right)$$

In the downstream direction

$$10\log\left(\frac{S}{p_{\text{ref}}^2}\right) = 10\log\left(\frac{A}{p_{\text{ref}}^2}\right) + 10\log F\left(\frac{f}{f_L}\right) - 20\log\left(\frac{r}{D_j}\right)$$

In the upstream direction

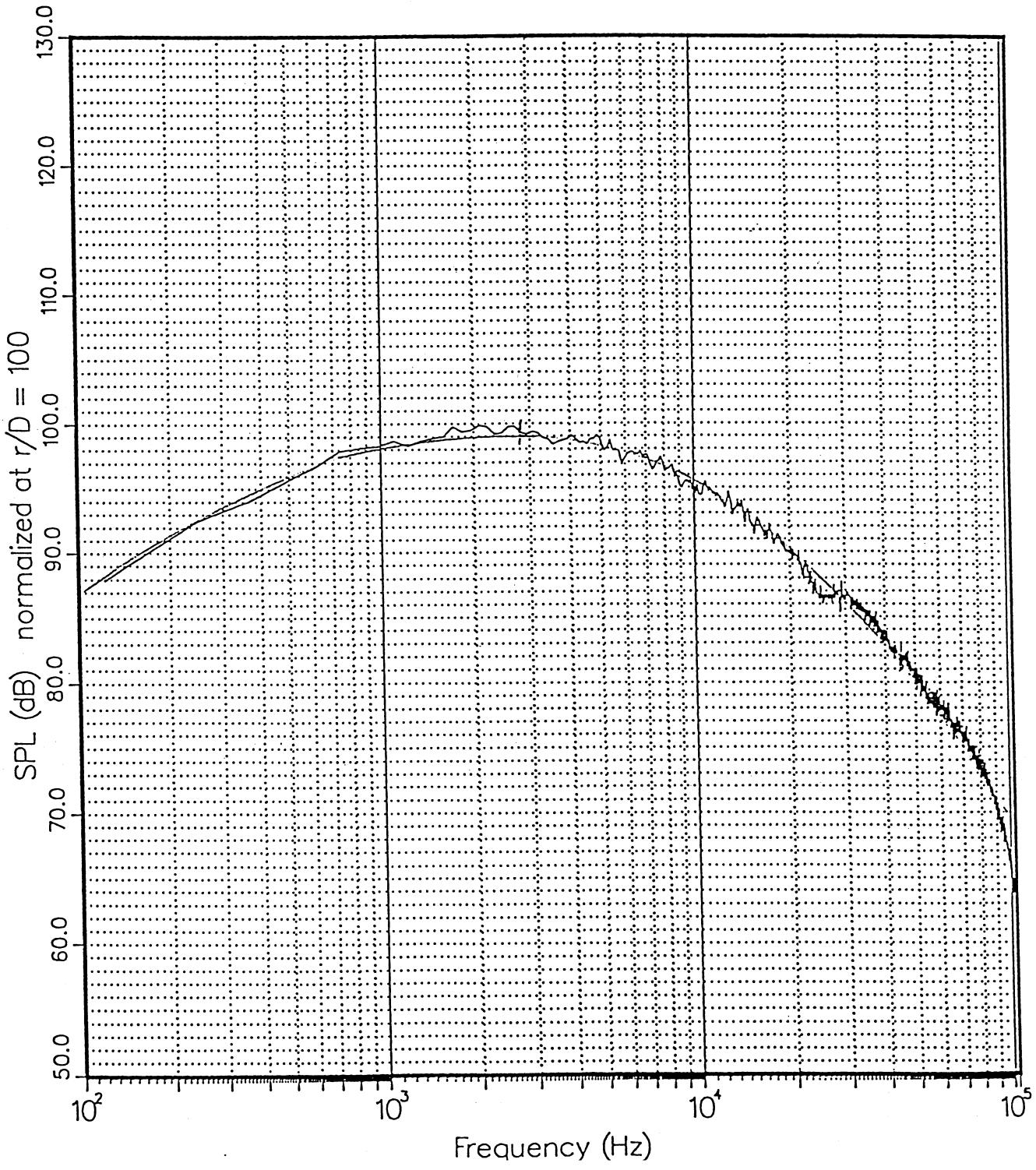
$$10\log\left(\frac{S}{p_{\text{ref}}^2}\right) = 10\log\left(\frac{B}{p_{\text{ref}}^2}\right) + 10\log G\left(\frac{f}{f_F}\right) - 20\log\left(\frac{r}{D_j}\right)$$


PLOT 1 14.12.45 FRI 1 SEP, 1995 JOB-mgole , FLORIDA STATE UNIVERSITY DISSPLA 11.0
SPL (dB) normalized at r/Dj = 100
130.0
120.0
110.0
100.0
90.0
80.0
70.0
60.0
50.0
10^2
10^3
10^4
10^5
Frequency (Hz)

DIRECTIONAL DEPENDENCE

Run 180 Jet Noise Spectrum

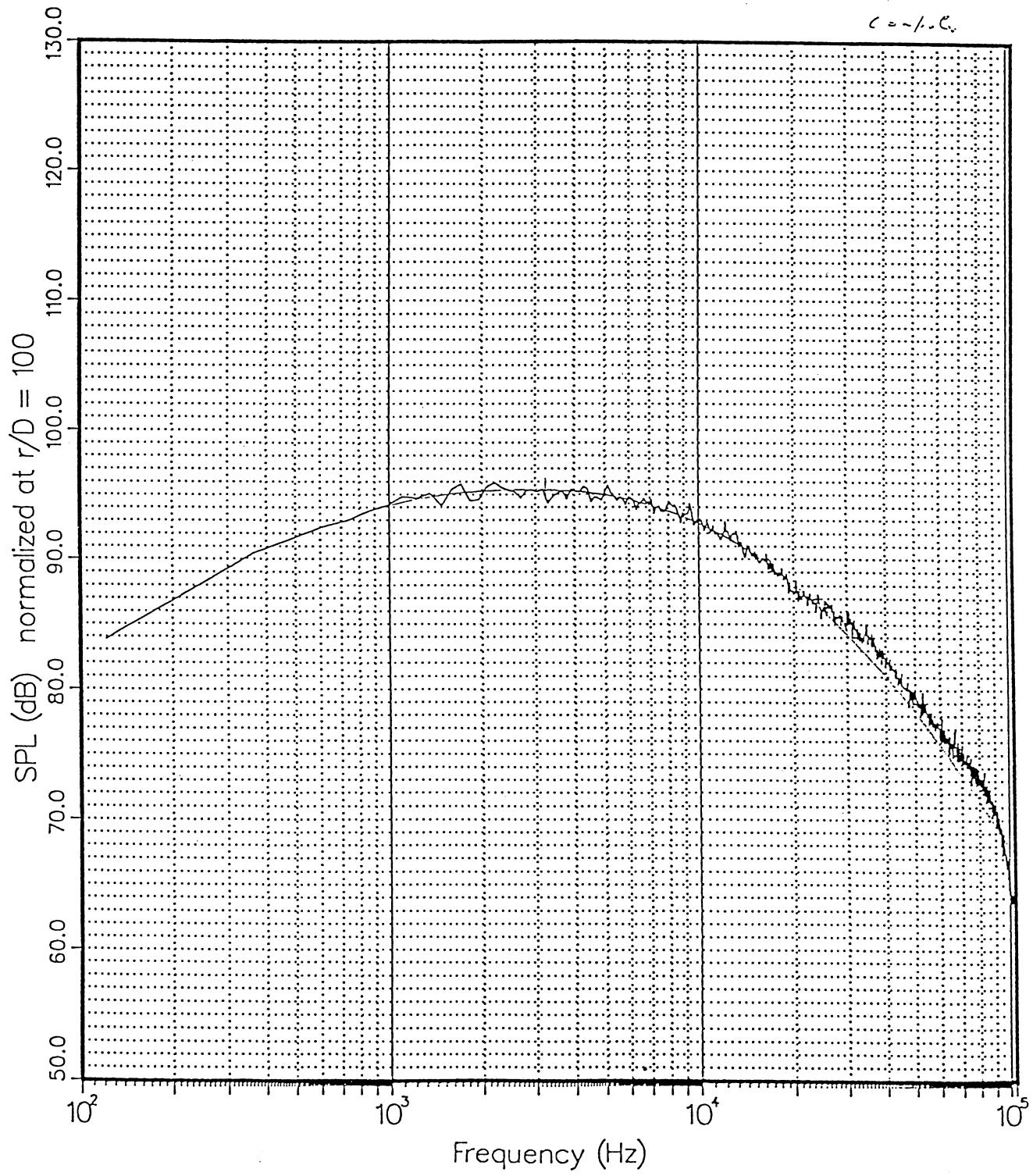
Nb micro	:	14		Mach exp.	:	1.96	
Nb nozzle	:	5		Temp. Ratio	:	.98	
P tot	:	109.26	PSIA	Angle	:	120.2	deg
T tot	:	286.3	K	P amb	:	14.76	PSIA
Diam	:	1.96	in	T amb	:	291.1	K
Rel Humidit	:	36.10	pourcent	R dist	:	4.23	m
OASPL volt	:	118.3	dB	R/D	:	84.82	
SPL Max	:	99.9	dB	OASPL integ	:	120.2	dB
				Freq(SPL Max)	:	2075.	Hz



PLOT 1 18.30.44 WED 11 JAN, 1995 JOB=ngole , FLORIDA STATE UNIVERSITY VISSIM 11.0

Run 180 Jet Noise Spectrum

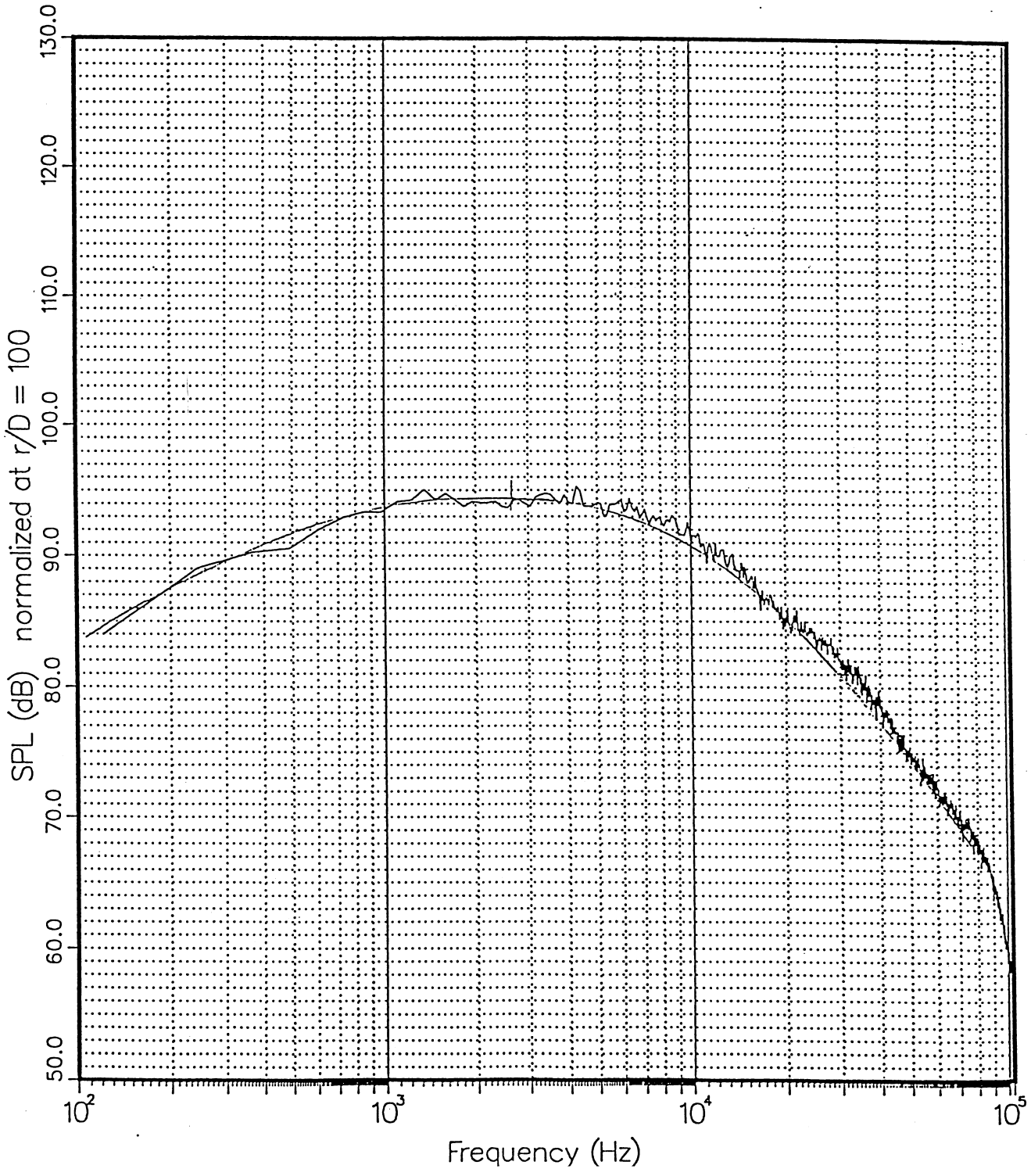
Mach exp.	:	1.96			
Nb micro	:	7	Temp. Ratio	:	.98
Nb nozzle	:	5	Angle	:	89.9 deg
P tot	:	109.26 PSIA	P amb	:	14.76 PSIA
T tot	:	286.3 K	T amb	:	291.1 K
Diam	:	1.96 in	R dist	:	3.66 m
Rel Humidit	:	36.10 pourcent	R/D	:	73.32
OASPL volt	:	116.7 dB	OASPL integ	:	118.7 dB
SPL Max	:	95.9 dB	Freq(SPL Max)	:	2197. Hz



PLOT 1 18.24.20 WED 11 JAN, 1995 JOB-ngale , FLORIDA STATE UNIVERSITY UISSPLH 11.0

Run 216 Jet Noise Spectrum

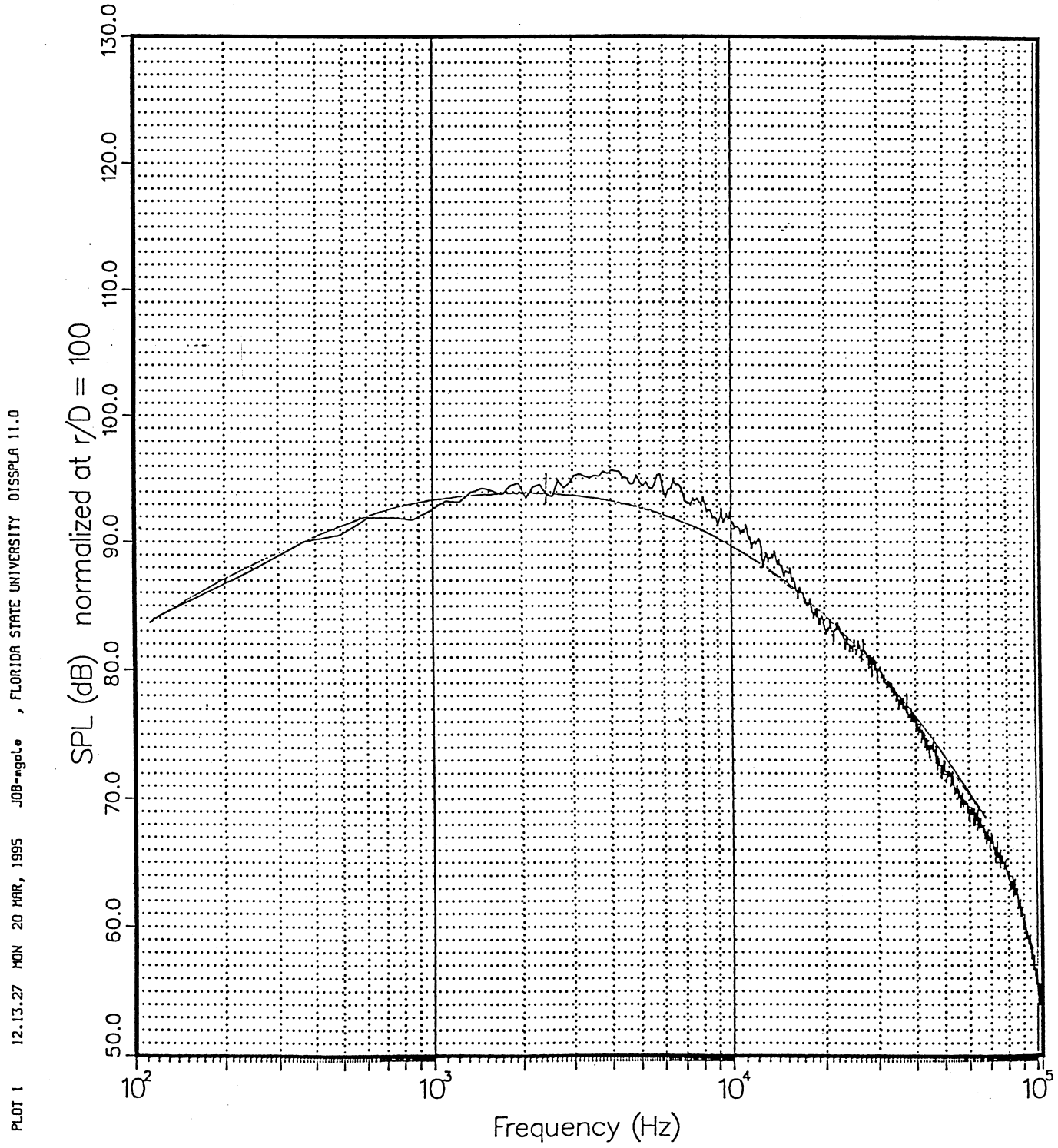
Nb micro	: 1		Mach exp.	: 1.96	
Nb nozzle	: 5		Temp. Ratio	: .99	
P tot	: 110.95	PSIA	Angle	: 83.3	deg
T tot	: 282.6	K	P amb	: 14.95	PSIA
Diam	: 1.96	in	T amb	: 285.2	K
Rel Humidit	: 67.11	pourcent	R dist	: 3.68	m
OASPL volt	: 115.2	dB	R/D	: 73.82	
SPL Max	: 95.3	dB	OASPL integ	: 117.1	dB
			Freq(SPL Max)	: 4272.	Hz



PLOT 1 13.35.24 MON 20 MAR, 1995 JOB=ngole , FLORIDA STATE UNIVERSITY DISSPLA 11.0

Run 181 Jet Noise Spectrum

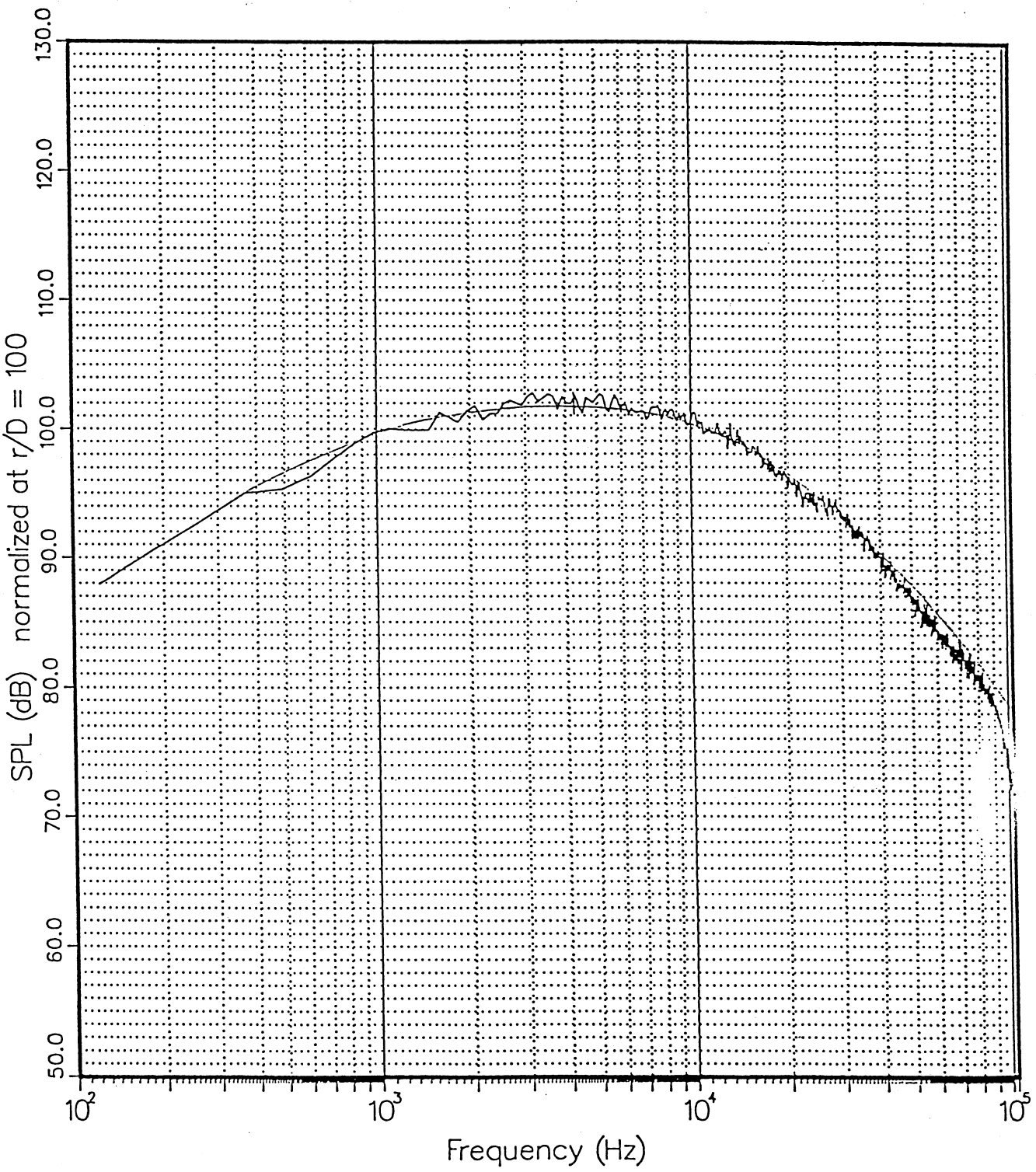
Nb micro	: 1		Mach exp.	: 1.96	
Nb nozzle	: 5		Temp. Ratio	: .98	
P tot	: 109.29	PSIA	Angle	: 63.4	deg
T tot	: 286.3	K	P amb	: 14.76	PSIA
Diam	: 1.96	in	T amb	: 291.0	K
Rel Humidit	: 36.11	pourcent	R dist	: 4.09	m
OASPL volt	: 114.1	dB	R/D	: 82.02	
SPL Max	: 95.7	dB	OASPL integ	: 116.1	dB
			Freq(SPL Max)	: 4028.	Hz



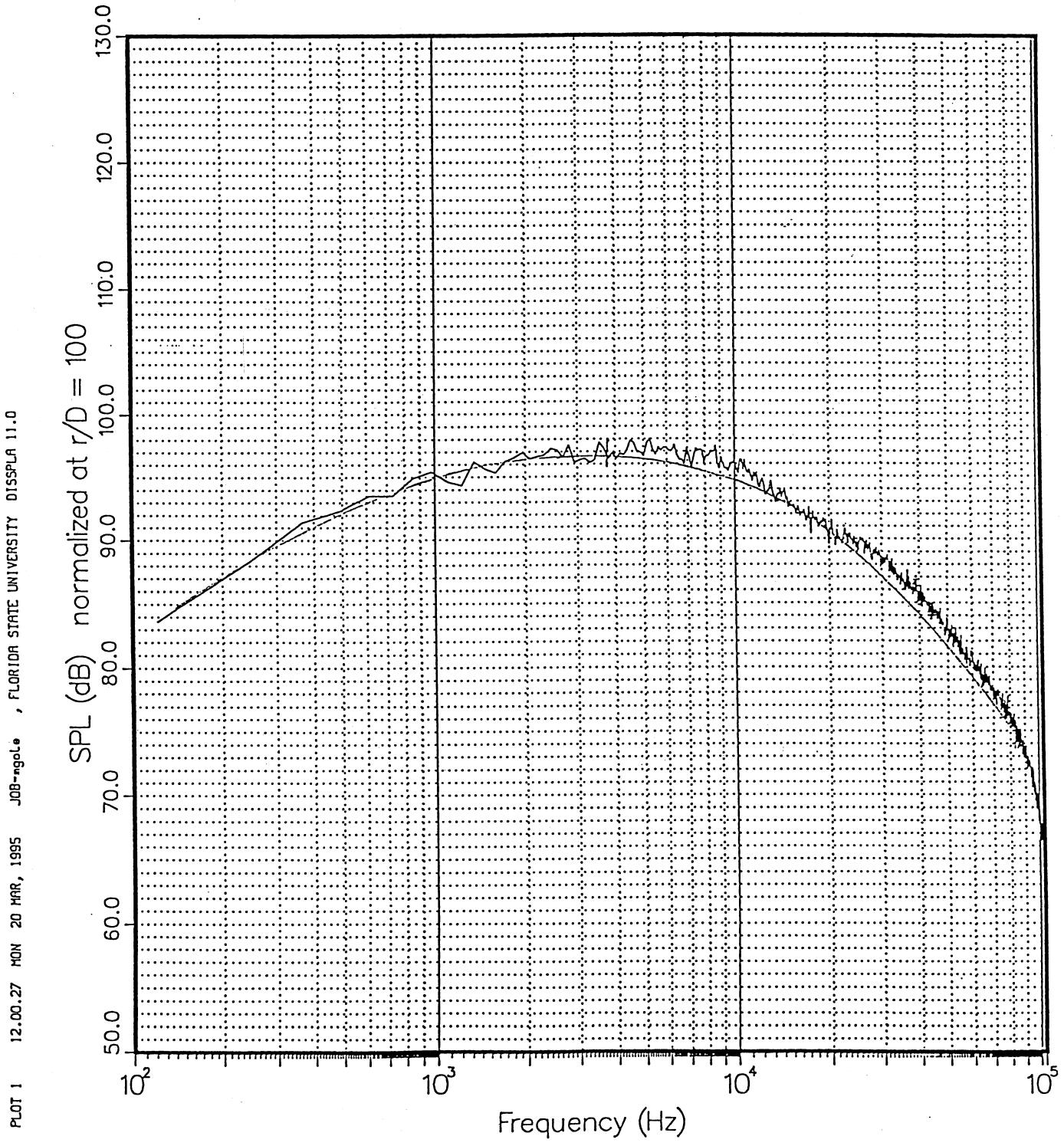
PLOT 1 12.13.27 MON 20 MAR, 1995 JOB-ngole , FLORIDA STATE UNIVERSITY DISSPLA 11.0

Run 219 Jet Noise Spectrum

Nb micro	: 7		Mach exp.	: 1.96	
Nb nozzle	: 5		Temp. Ratio	: 1.78	
P tot	: 110.54	PSIA	Angle	: 110.9	deg
T tot	: 513.4	K	P amb	: 14.94	PSIA
Diam	: 1.96	in	T amb	: 288.6	K
Rel Humidit	: 71.68	pourcent	R dist	: 3.92	m
OASPL volt	: 123.5	dB	R/D	: 78.50	
SPL Max	: 102.8	dB	OASPL integ	: 125.5	dB
			Freq(SPL Max)	: 3174.	Hz

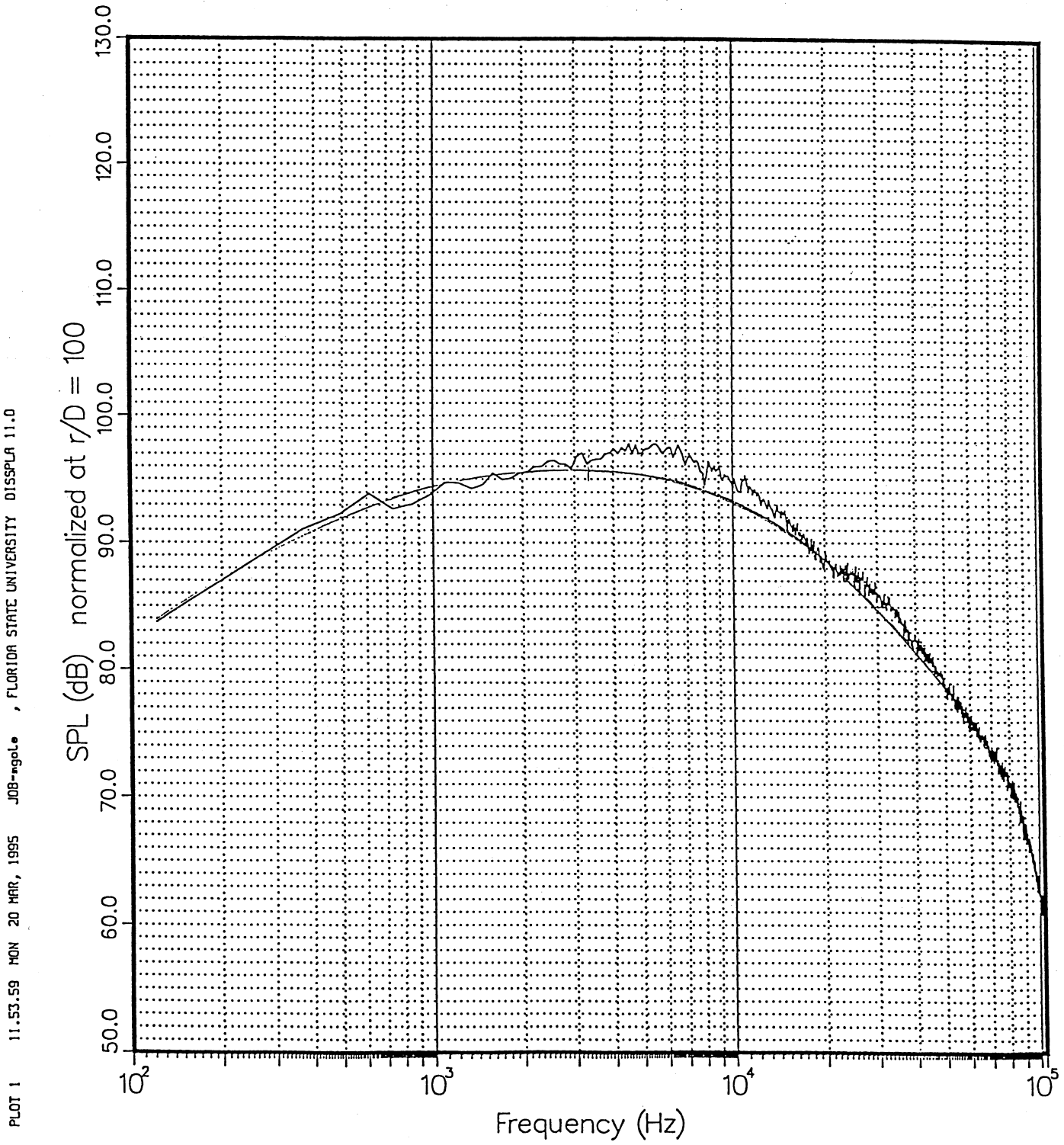


PLOT 1 19.54.31 MON 11 JUN, 1999


Run 194 Jet Noise Spectrum
Nb micro : 5
Nb nozzle : 5
P tot : 110.54 PSIA
T tot : 506.2 K
Diam : 1.96 in
Rel Humidit : 40.09 pourcent
OASPL volt : 119.1 dB
SPL Max : 98.0 dB
Mach exp. : 1.96
Temp. Ratio : 1.79
Angle : 80.4 deg
P amb : 14.93 PSIA
T amb : 283.0 K
R dist : 3.71 m
R/D : 74.35
OASPL integ : 121.0 dB
Freq(SPL Max) : 5249. Hz
SPL (dB) normalized at r/D = 100
130.0
120.0
110.0
100.0
90.0
80.0
70.0
60.0
50.0
10^2
10^3
10^4
10^5
Frequency (Hz)
PLOT 1 12.00.27 MON 20 MAR, 1995 JOB-ngole , FLORIDA STATE UNIVERSITY DISSPLA 11.0

Run 194 Jet Noise Spectrum

Nb micro	: 1		Mach exp.	: 1.96	
Nb nozzle	: 5		Temp. Ratio	: 1.79	
P tot	: 110.54	PSIA	Angle	: 63.4	deg
T tot	: 506.2	K	P amb	: 14.93	PSIA
Diam	: 1.96	in	T amb	: 283.0	K
Rel Humidit	: 40.09	pourcent	R dist	: 4.09	m
OASPL volt	: 117.3	dB	R/D	: 82.02	
SPL Max	: 97.8	dB	OASPL integ	: 119.2	dB
			Freq(SPL Max)	: 4517.	Hz



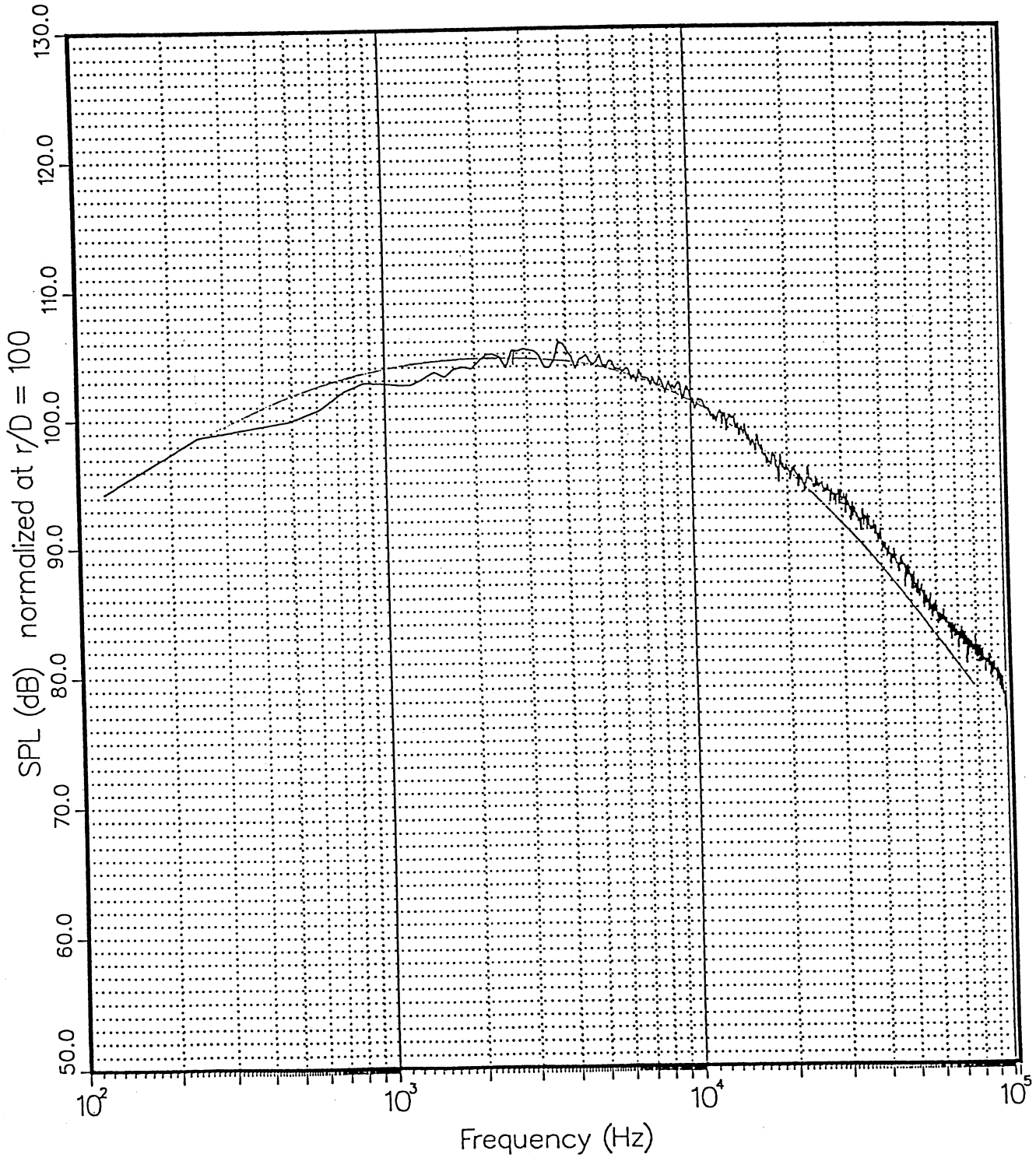
PLOT 1 11.53.59 MON 20 MAR, 1995 JOB-ngole , FLORIDA STATE UNIVERSITY DISSPLA 11.0

TEMPERATURE DEPENDENCE

Run 35 Jet Noise Spectrum

Nb micro	: 1	
Nb nozzle	: Hot Jet	
P tot	: 8008.75	hPa
T tot	: 1136.5	K
Diam	: 9.14	cm
Rel Humidit	: 72.50	pourcent
Tstatic jet	: 631.1	K
SPL Max	: 105.9	dB

Mach exp.	: 2.00	
Temp. Ratio	: 4.07	
Angle	: 83.8	deg
P amb	: 1028.01	hPa
T amb	: 278.9	K
R dist	: 3.68	m
R/D	: 40.24	
Jet Velocity	: 997.6	m/s
Freq(SPL Max)	: 3784.	Hz

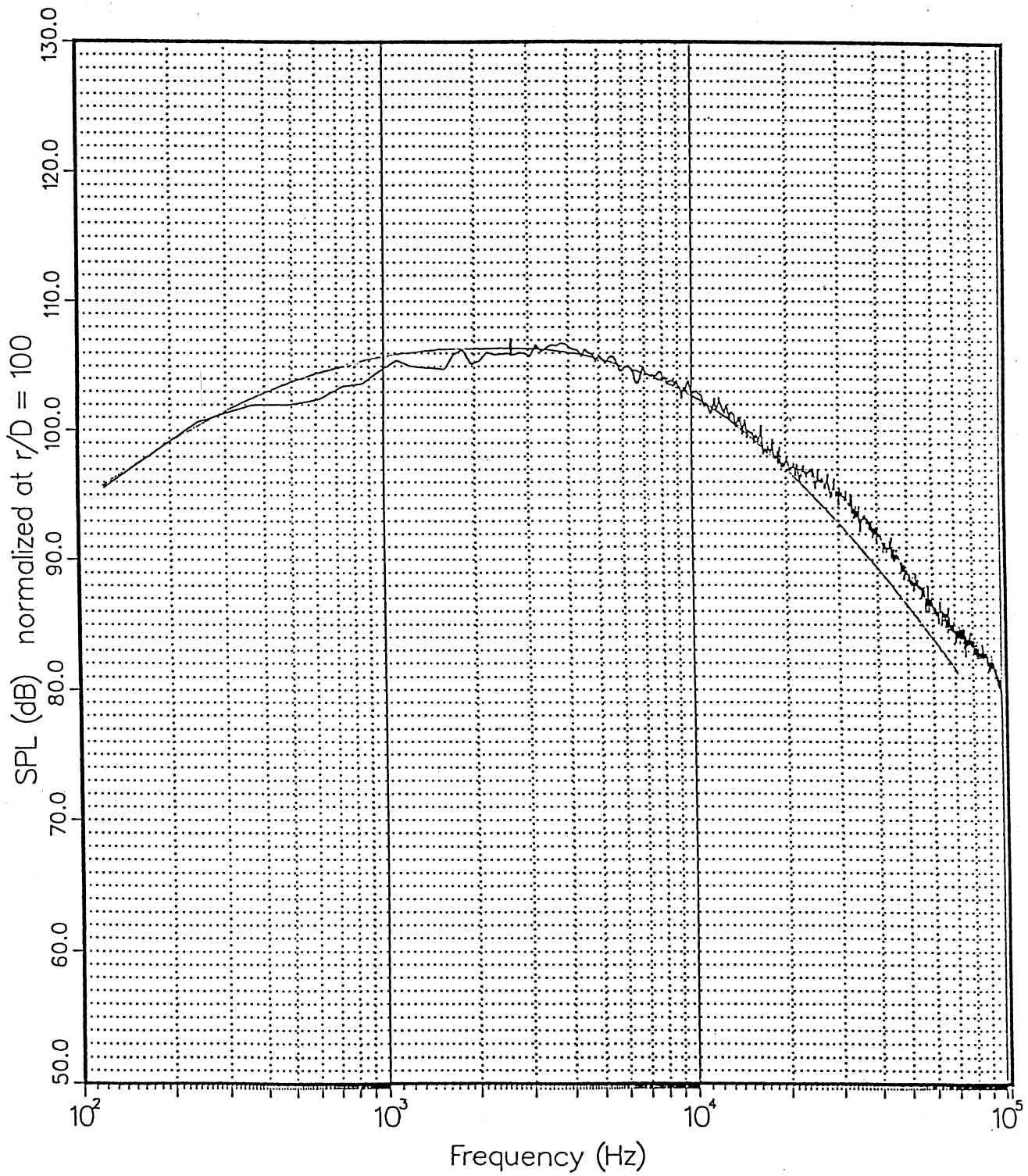


PLOT 1 19.54.45 WED 15 FEB, 1995 JOB=gol.e , FLORIDA STATE UNIVERSITY DISSPLA 11.0

Run 36 Jet Noise Spectrum

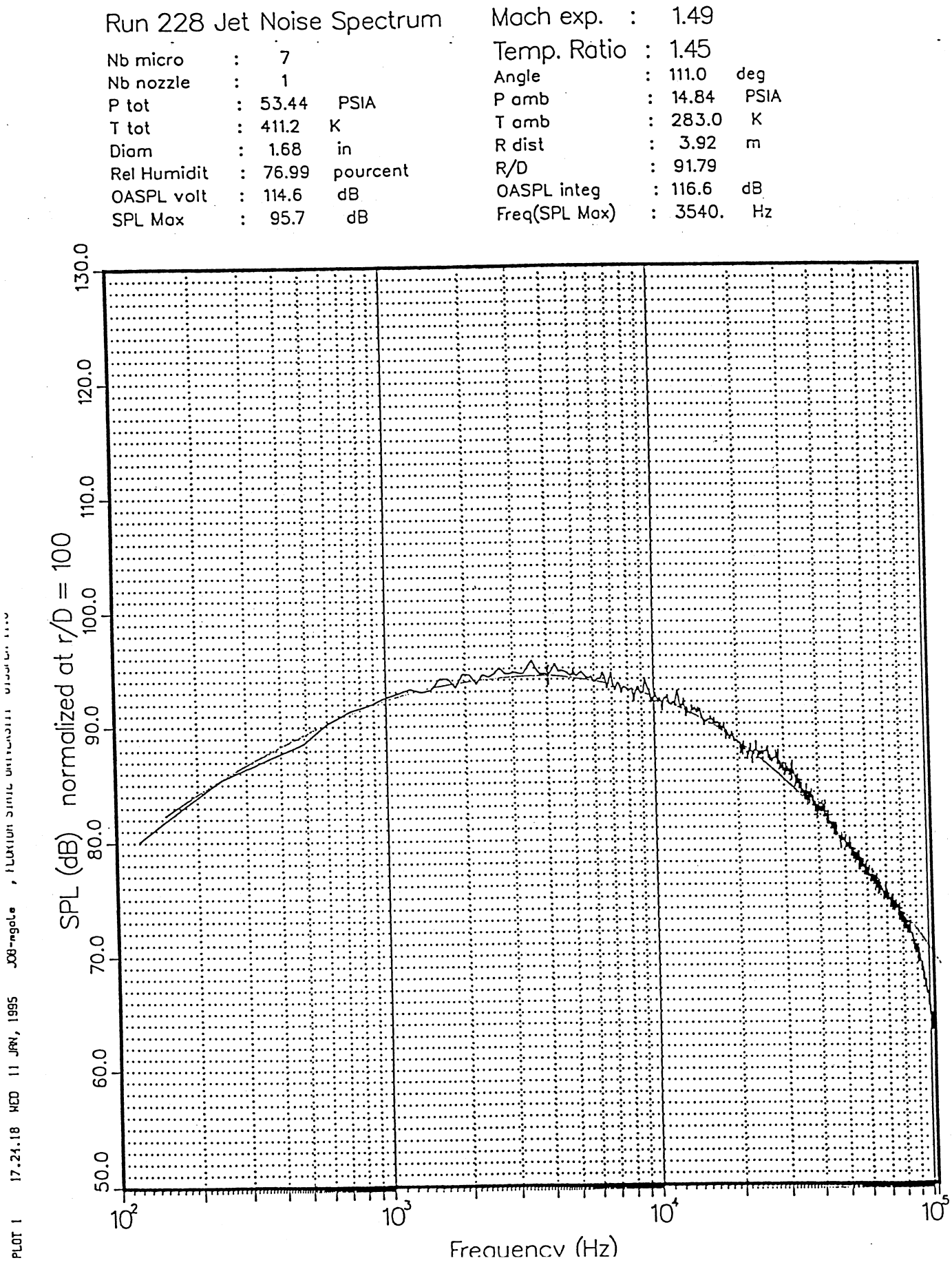
Nb micro	: 1		
Nb nozzle	: Hot Jet		
P tot	: 7997.00	hPa	
T tot	: 1370.4	K	
Diam	: 9.14	cm	
Rel Humidit	: 64.70	pourcent	
Tstatic jet	: 760.6	K	
SPL Max	: 106.8	dB	

Mach exp.	: 2.00	
Temp. Ratio	: 4.89	
Angle	: 83.8	deg
P amb	: 1028.01	hPa
T amb	: 280.5	K
R dist	: 3.68	m
R/D	: 40.24	
Jet Velocity	: 1089.9	m/s
Freq(SPL Max)	: 3784.	Hz



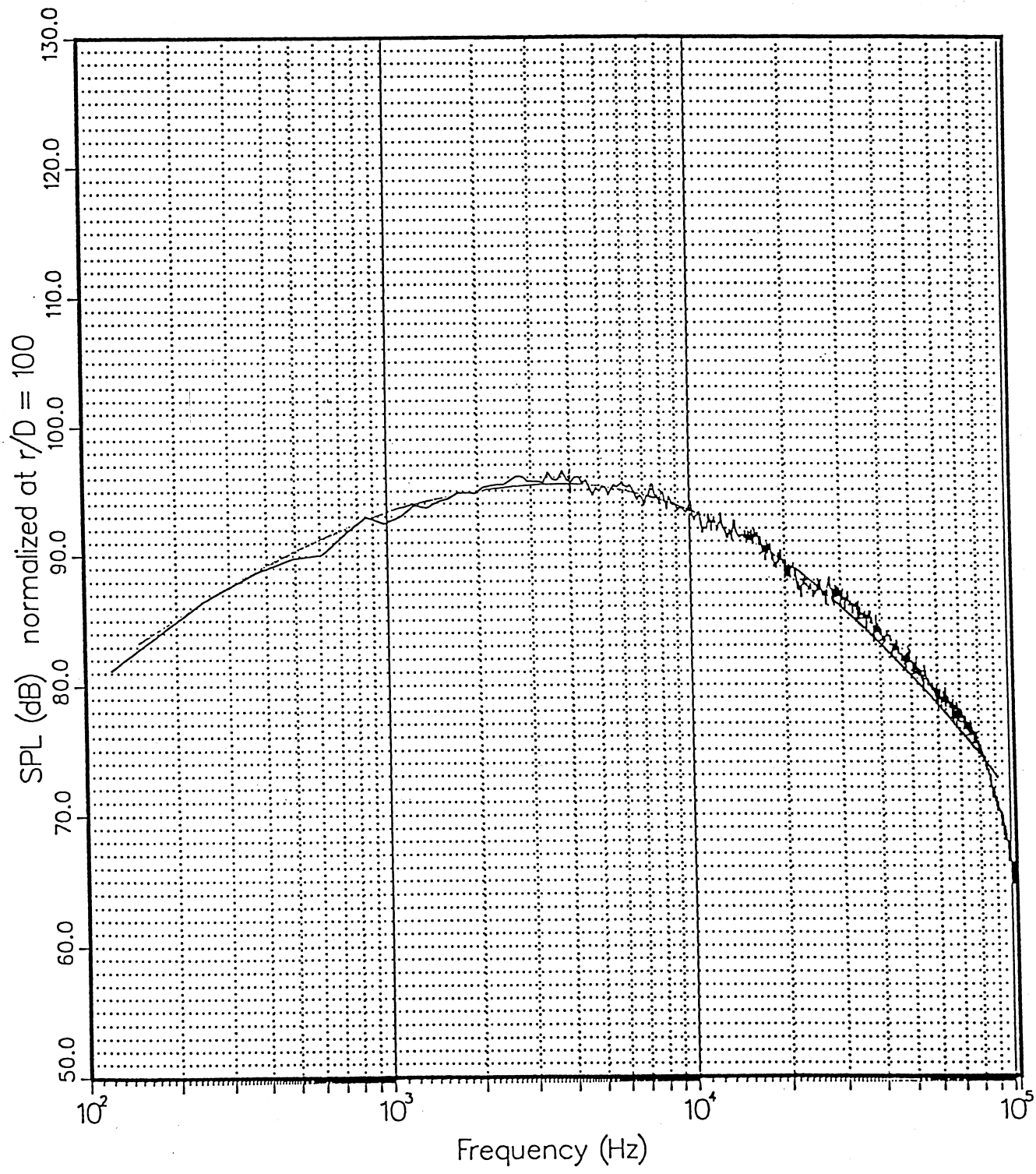
PLOT 1 22.07.08 WED 15 FEB, 1995 JOB=ngoLe , FLORIDA STATE UNIVERSITY DISSPLA 11.0

MACH NUMBER DEPENDENCE

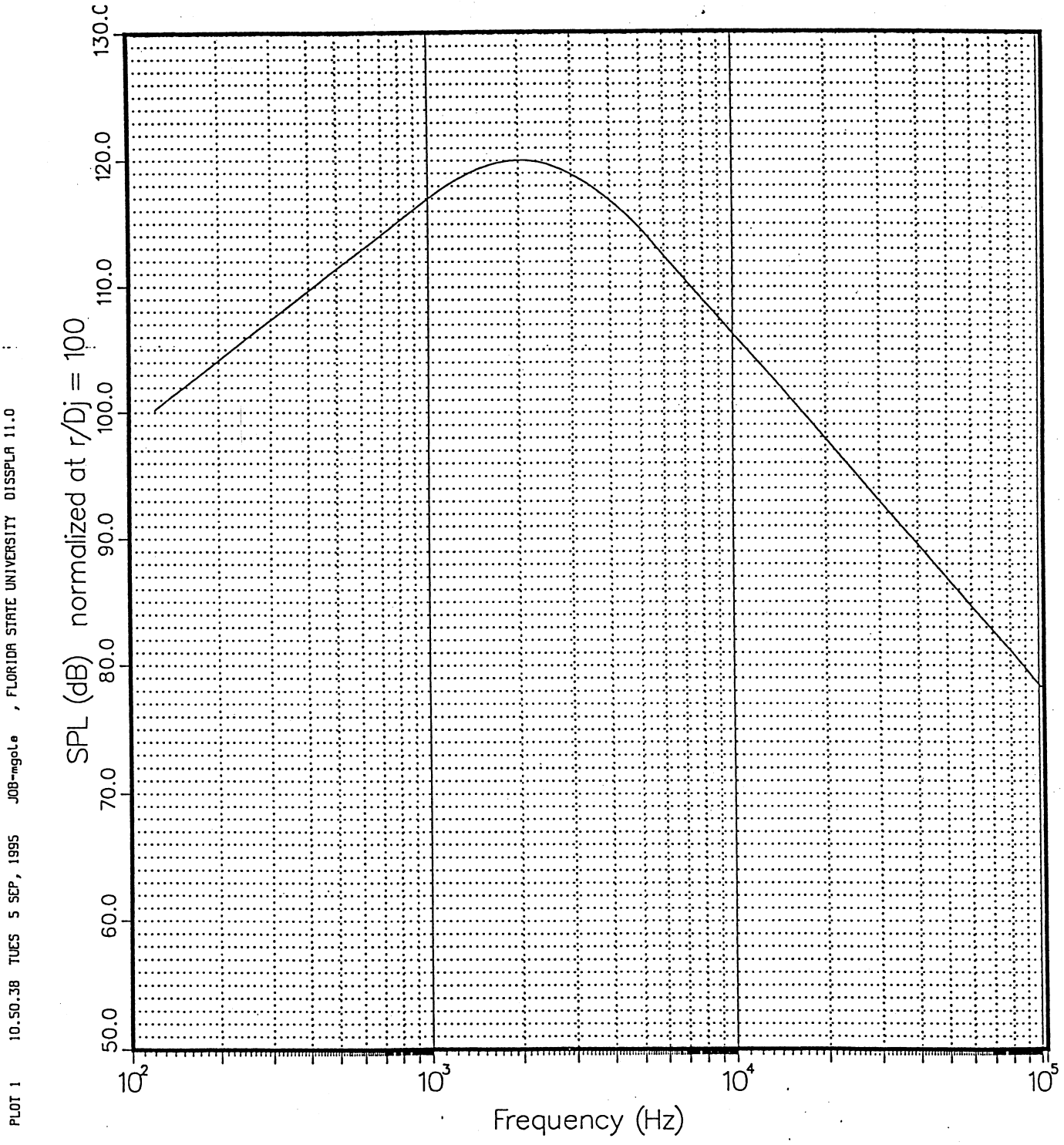

Run 228 Jet Noise Spectrum
Nb micro : 7
Nb nozzle : 1
P tot : 53.44 PSIA
T tot : 411.2 K
Diam : 1.68 in
Rel Humidit : 76.99 pourcent
OASPL volt : 114.6 dB
SPL Max : 95.7 dB
Mach exp. : 1.49
Temp. Ratio : 1.45
Angle : 111.0 deg
P amb : 14.84 PSIA
T amb : 283.0 K
R dist : 3.92 m
R/D : 91.79
OASPL integ : 116.6 dB
Freq(SPL Max) : 3540. Hz
SPL (dB) normalized at r/D = 100
130.0
120.0
110.0
100.0
90.0
80.0
70.0
60.0
50.0
10^2
10^3
10^4
10^5
Frequency (Hz)
PLOT 1 17.21.18 WED 11 JAN, 1995 JOB=mgole , FLUKUM SIMIL UNIVERSITY

Run 231 Jet Noise Spectrum

Nb micro	:	3		Mach exp.	:	1.49	
Nb nozzle	:	1		Temp. Ratio	:	2.35	
P tot	:	53.68	PSIA	Angle	:	92.9	deg
T tot	:	672.4	K	P amb	:	14.98	PSIA
Diam	:	1.68	in	T amb	:	286.7	K
Rel Humidit	:	69.74	pourcent	R dist	:	3.66	m
OASPL volt	:	116.1	dB	R/D	:	85.82	
SPL Max	:	96.5	dB	OASPL integ	:	118.0	dB
				Freq(SPL Max)	:	3784.	Hz



PLOT 1 17.47.45 WED 11 JAN, 1995 JOB-ngole , FLORIDA STATE UNIVERSITY DISSPLA 11.0


SPL (dB) normalized at r/Dj = 100
130.0
120.0
110.0
100.0
90.0
80.0
70.0
60.0
50.0
10^2
10^3
10^4
10^5
Frequency (Hz)
PLOT 1 10.50.38 TUES 5 SEP, 1995 JOB=mgole , FLORIDA STATE UNIVERSITY DISSPLA 11.0

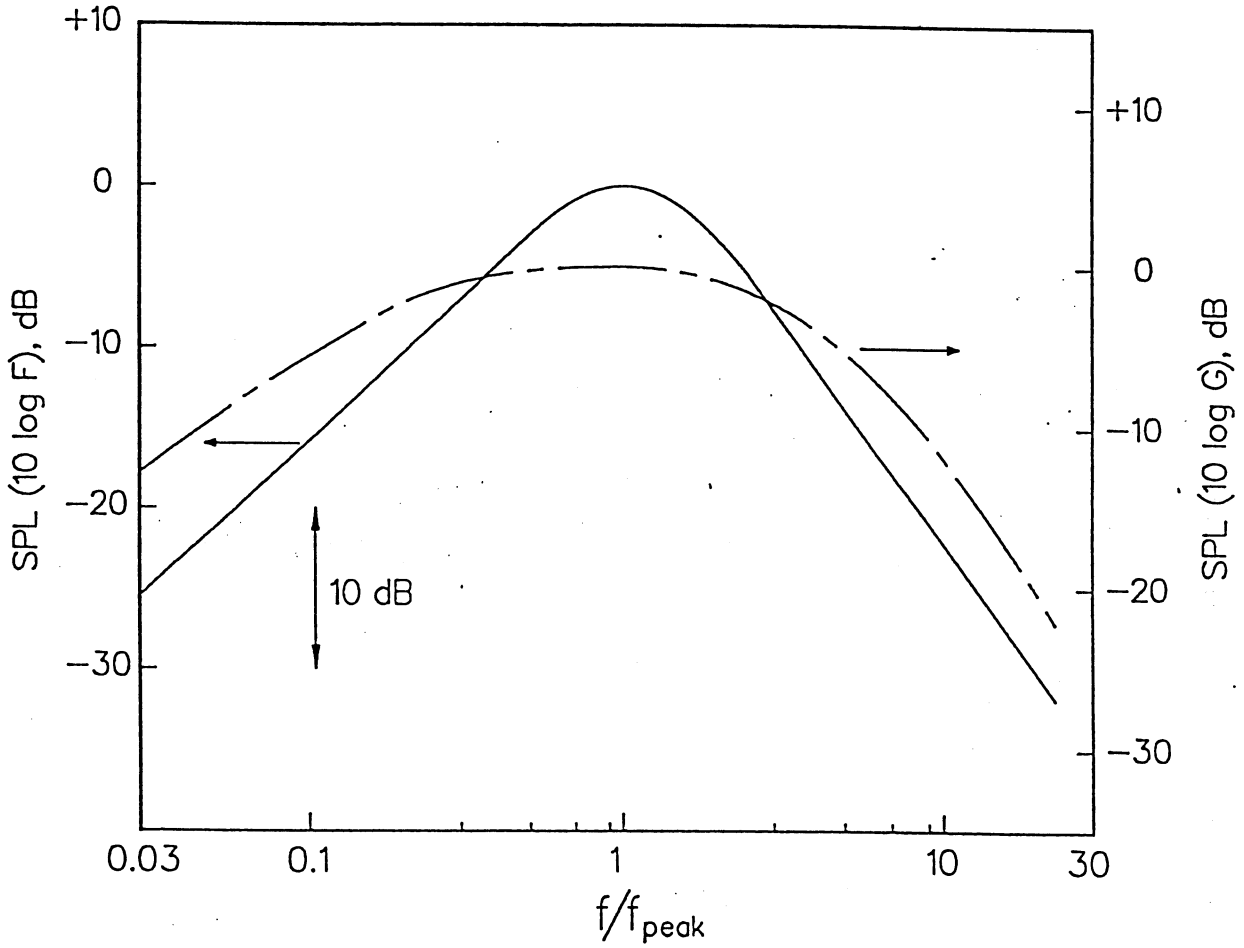
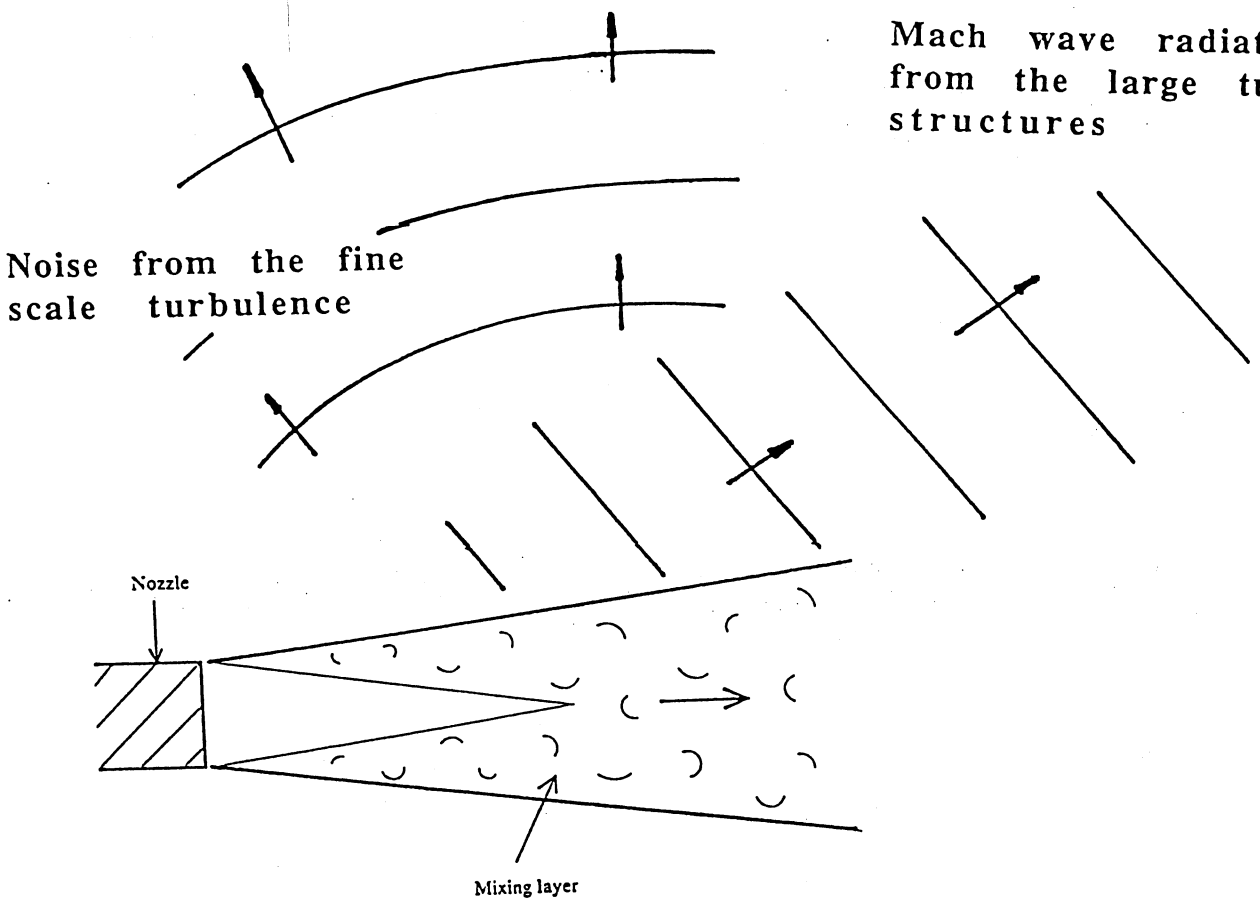


Figure 2. Similarity spectra for the two components of turbulent mixing noise.
——— large turbulence structures/ instability waves noise;
— - — fine scale turbulence noise.

independent of Mach number, jet temperature and direction of radiation

There are extensive experimental evidence that jet mixing noise consists of two independent components.

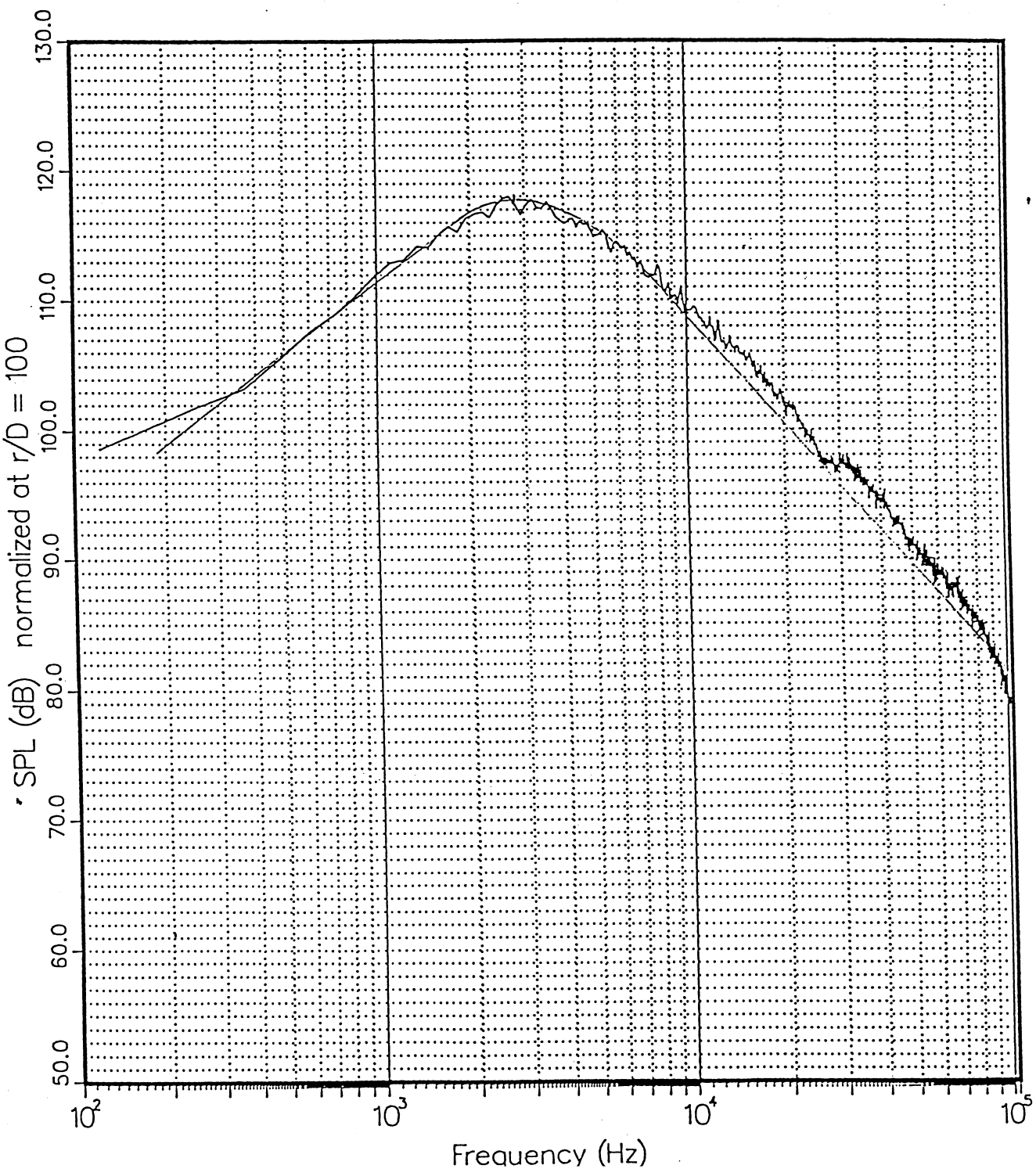
1. Noise from the large turbulence structures
2. Noise from the fine scale turbulence



DIRECTIONAL DEPENDENCE

Run 194 Jet Noise Spectrum

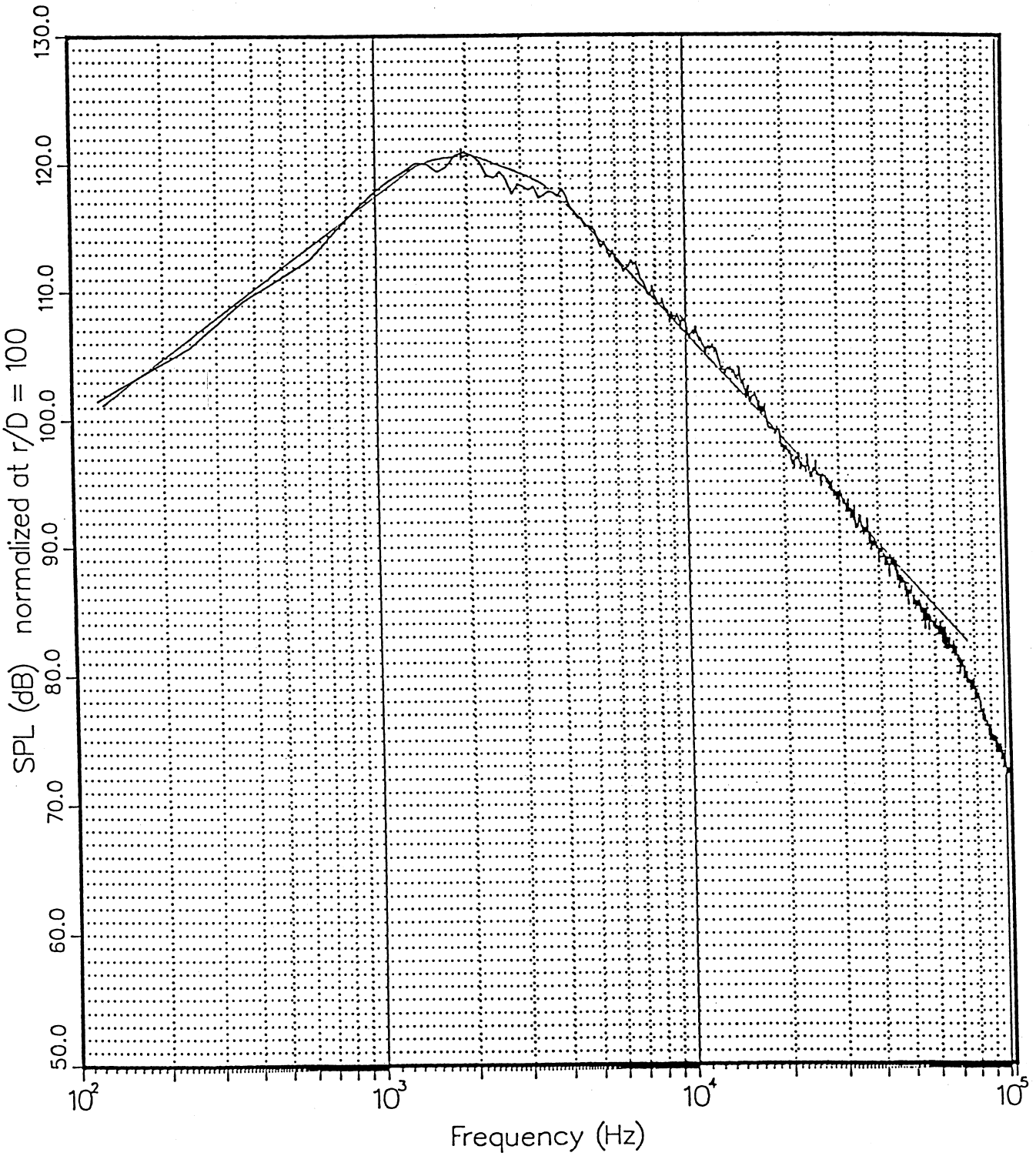
Nb micro	: 17		Mach exp.	: 1.96	
Nb nozzle	: 5		Temp. Ratio	: 1.79	
P tot	: 110.54	PSIA	Angle	: 129.7	deg
T tot	: 506.2	K	P amb	: 14.93	PSIA
Diam	: 1.96	in	T amb	: 283.0	K
Rel Humidit	: 40.09	pourcent	R dist	: 4.76	m
OASPL volt	: 132.7	dB	R/D	: 95.36	
SPL Max	: 118.0	dB	OASPL integ	: 134.7	dB
			Freq(SPL Max)	: 2686.	Hz



PLOT 1 18.51.17 WED 11 JAN, 1995 JOB=gal• , FLORIDA STATE UNIVERSITY DISSPLA 11.0

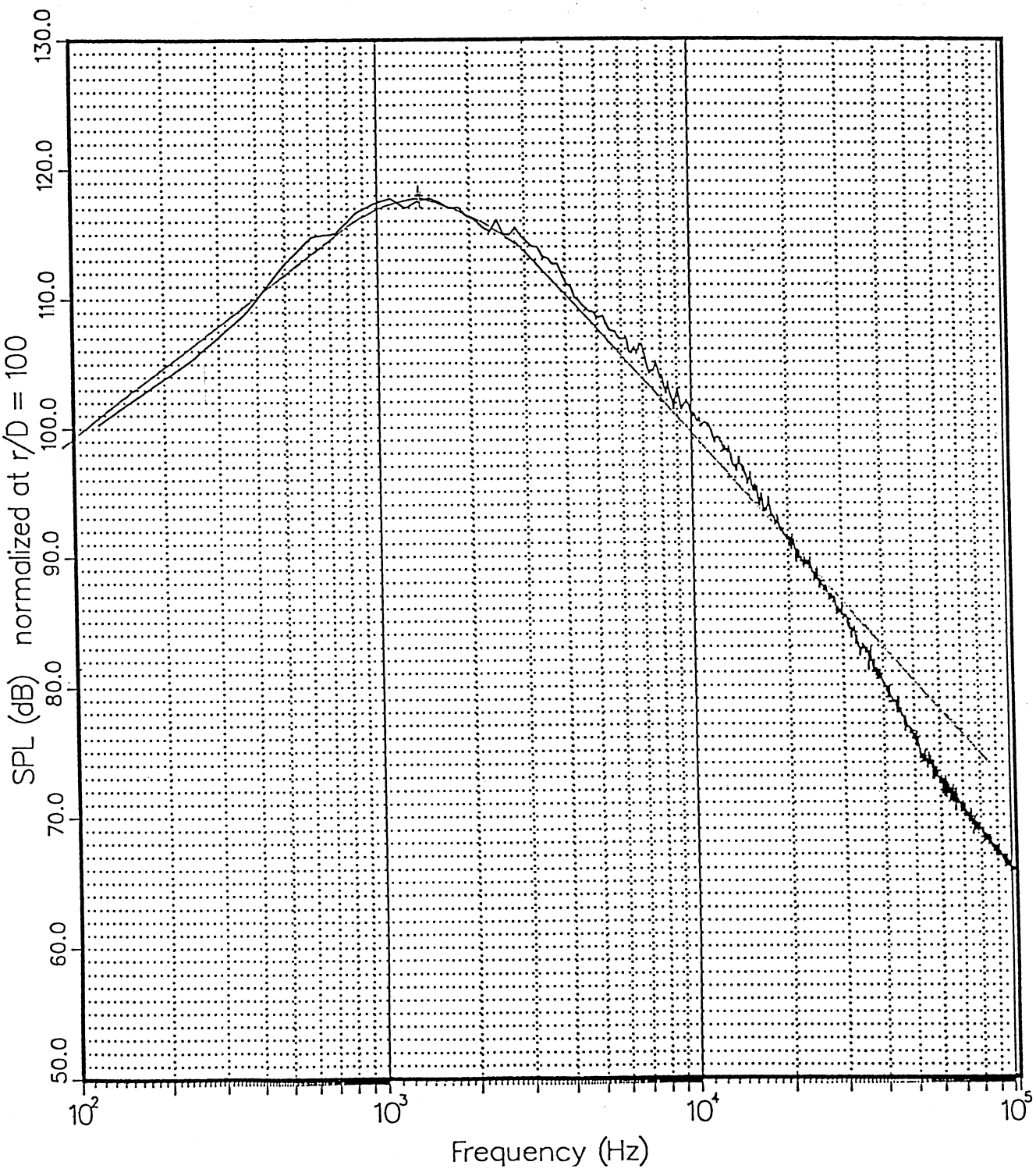
Run 219 Jet Noise Spectrum

Nb micro	:	16	Mach exp.	:	1.96
Nb nozzle	:	5	Temp. Ratio	:	1.78
P tot	:	110.54 PSIA	Angle	:	138.6 deg
T tot	:	513.4 K	P amb	:	14.94 PSIA
Diam	:	1.96 in	T amb	:	288.6 K
Rel Humidit	:	71.68 pourcent	R dist	:	5.53 m
OASPL volt	:	132.2 dB	R/D	:	110.77
SPL Max	:	120.9 dB	OASPL integ	:	134.2 dB
			Freq(SPL Max)	:	1953. Hz



Run 194 Jet Noise Spectrum

Nb micro	: 23		Mach exp.	: 1.96	
Nb nozzle	: 5		Temp. Ratio	: 1.79	
P tot	: 110.54	PSIA	Angle	: 145.7	deg
T tot	: 506.2	K	P amb	: 14.93	PSIA
Diam	: 1.96	in	T amb	: 283.0	K
Rel Humidit	: 40.09	pourcent	R dist	: 5.16	m
OASPL volt	: 129.1	dB	R/D	: 103.38	
SPL Max	: 117.8	dB	OASPL integ	: 131.0	dB
			Freq(SPL Max)	: 1099.	Hz

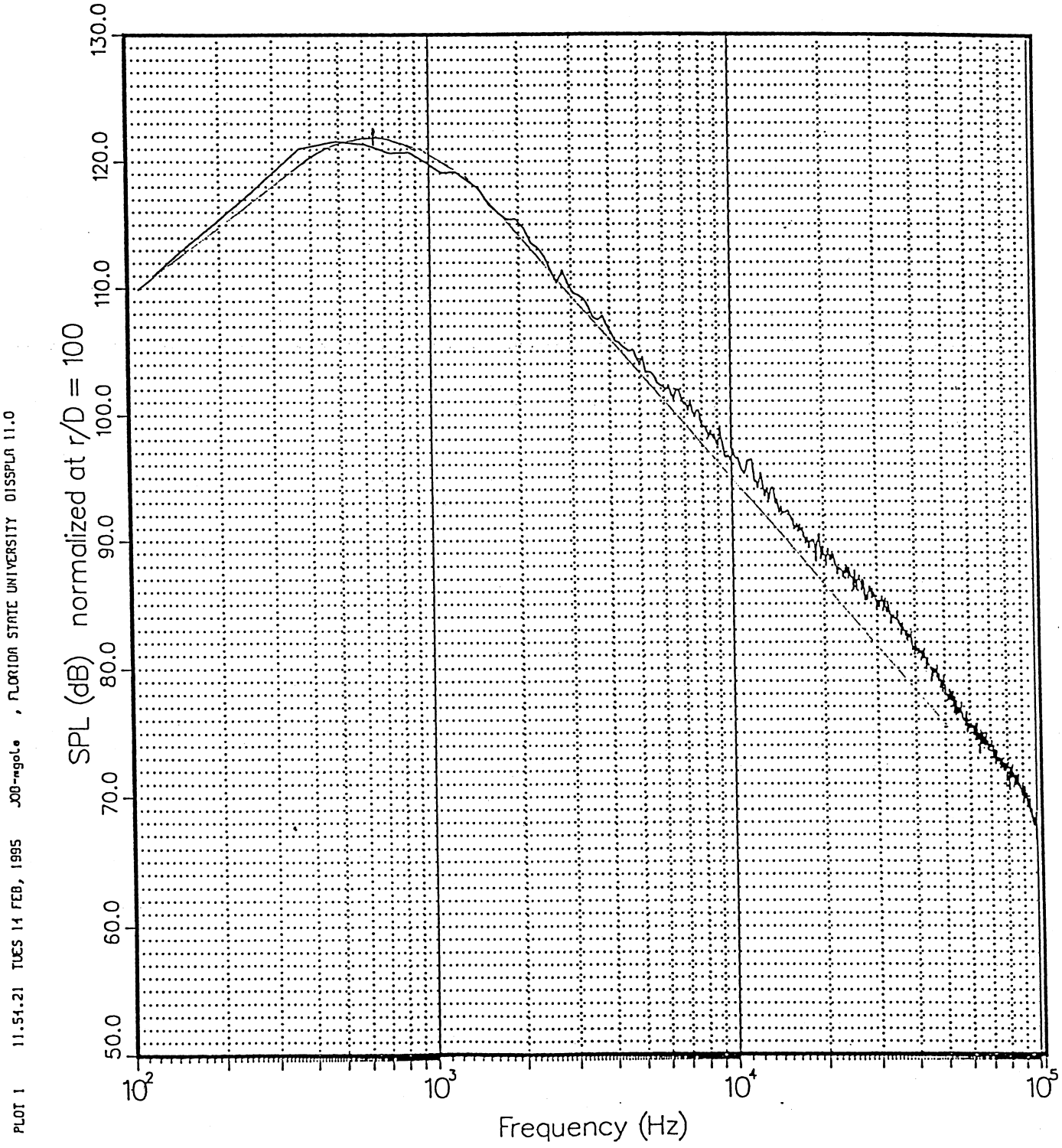


PLOT 1 18.56.33 WED 11 JAN, 1995

TEMPERATURE DEPENDENCE

Run 31 Jet Noise Spectrum

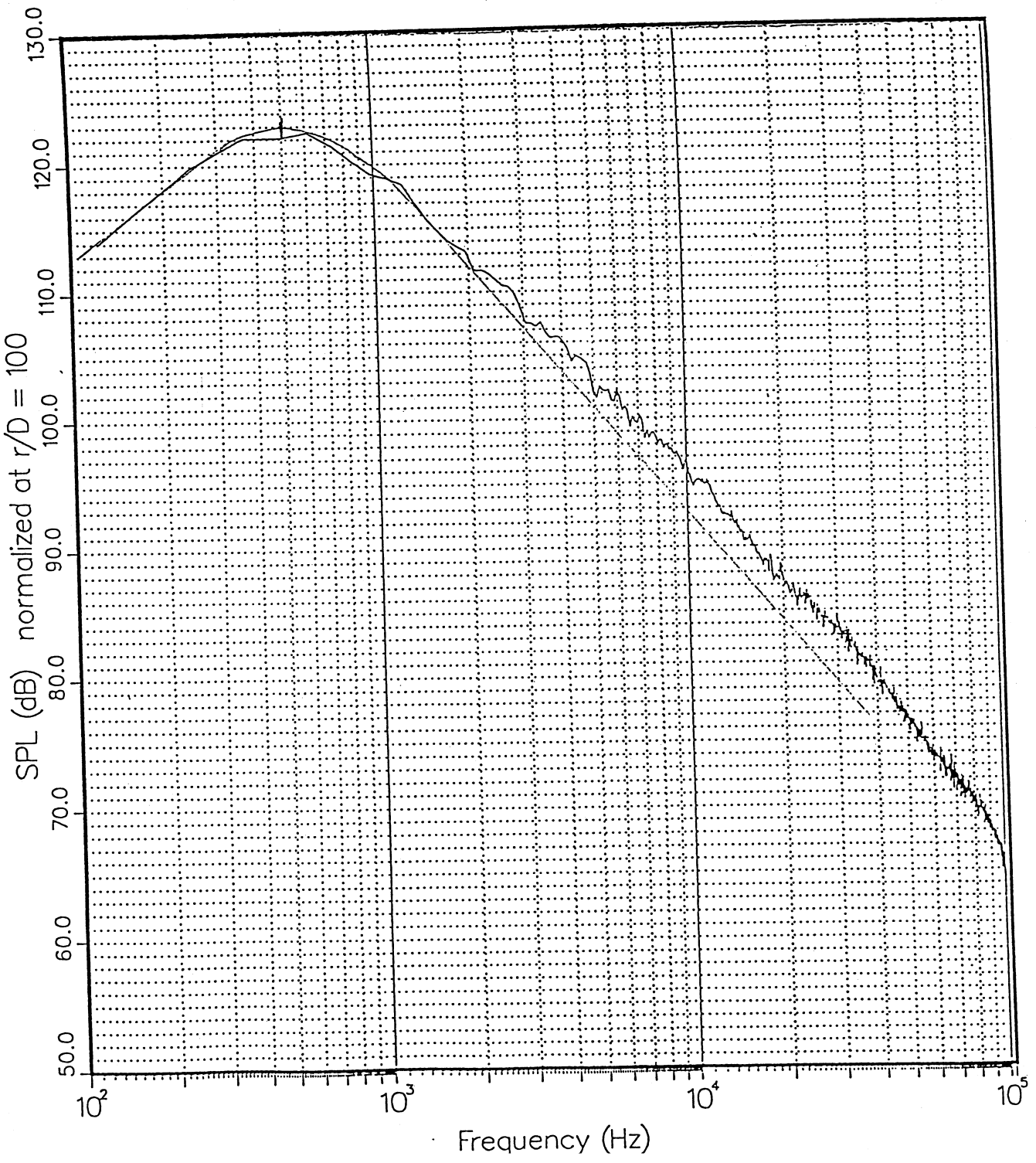
Nb micro	: 25		Mach exp.	: 2.00	
Nb nozzle	: Hot Jet		Temp. Ratio	: 1.12	
P tot	: 8038.25	hPa	Angle	: 160.1	deg
T tot	: 313.1	K	P amb	: 1027.33	hPa
Diam	: 9.14	cm	T amb	: 279.5	K
Rel Humidit	: 63.40	pourcent	R dist	: 6.06	m
Tstatic jet	: 174.0	K	R/D	: 66.30	
SPL Max	: 121.6	dB	Jet Velocity	: 528.8	m/s
			Freq(SPL Max)	: 488.	Hz



Run 40 Jet Noise Spectrum

Nb micro	: 25	
Nb nozzle	: Hot Jet	
P tot	: 8056.17	hPa
T tot	: 500.4	K
Diam	: 9.14	cm
Rel Humidit	: 79.30	pourcent
Tstatic jet	: 277.9	K
SPL Max	: 122.5	dB

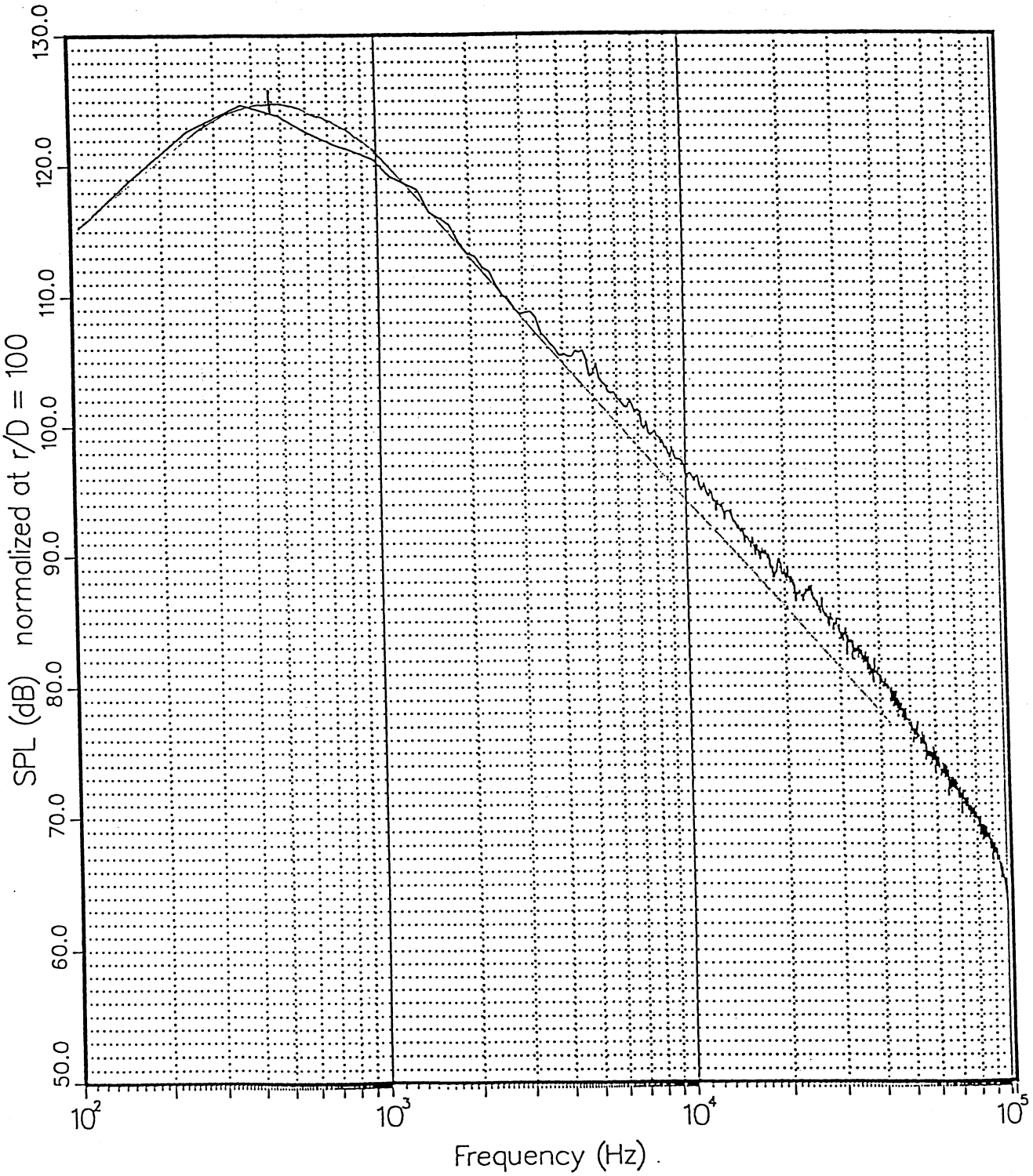
Mach exp.	: 2.00	
Temp. Ratio	: 1.80	
Angle	: 160.1	deg
P amb	: 1028.01	hPa
T amb	: 278.3	K
R dist	: 6.06	m
R/D	: 66.30	
Jet Velocity	: 668.6	m/s
Freq(SPL Max)	: 610.	Hz



PLOT 1 16.22.03 MER 15 FEB, 1995 JOB=mgole , Florida State University

Run 41 Jet Noise Spectrum

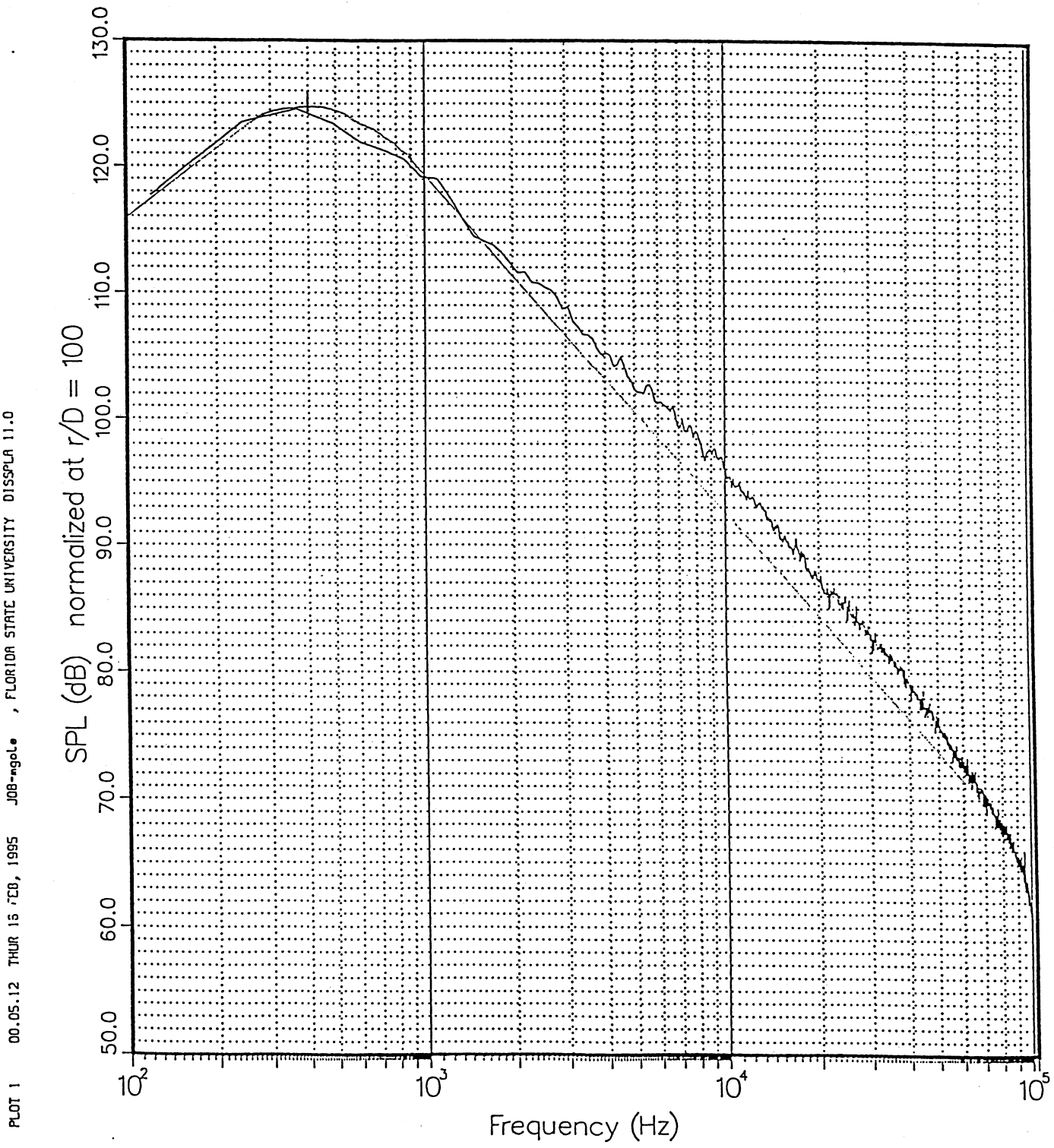
Nb micro	:	25	Mach exp.	:	2.00
Nb nozzle	:	Hot Jet	Temp. Ratio	:	3.28
P tot	:	8052.30 hPa	Angle	:	160.1 deg
T tot	:	913.2 K	P amb	:	1027.33 hPa
Diam	:	9.14 cm	T amb	:	278.6 K
Rel Humidit	:	78.80 pourcent	R dist	:	6.06 m
Tstatic jet	:	506.6 K	R/D	:	66.30
SPL Max	:	124.7 dB	Jet Velocity	:	899.3 m/s
			Freq(SPL Max)	:	366. Hz



PLOT 1 19.52.10 WED 15 FEB, 1995 JUB-ngole , Plotted with Unicos

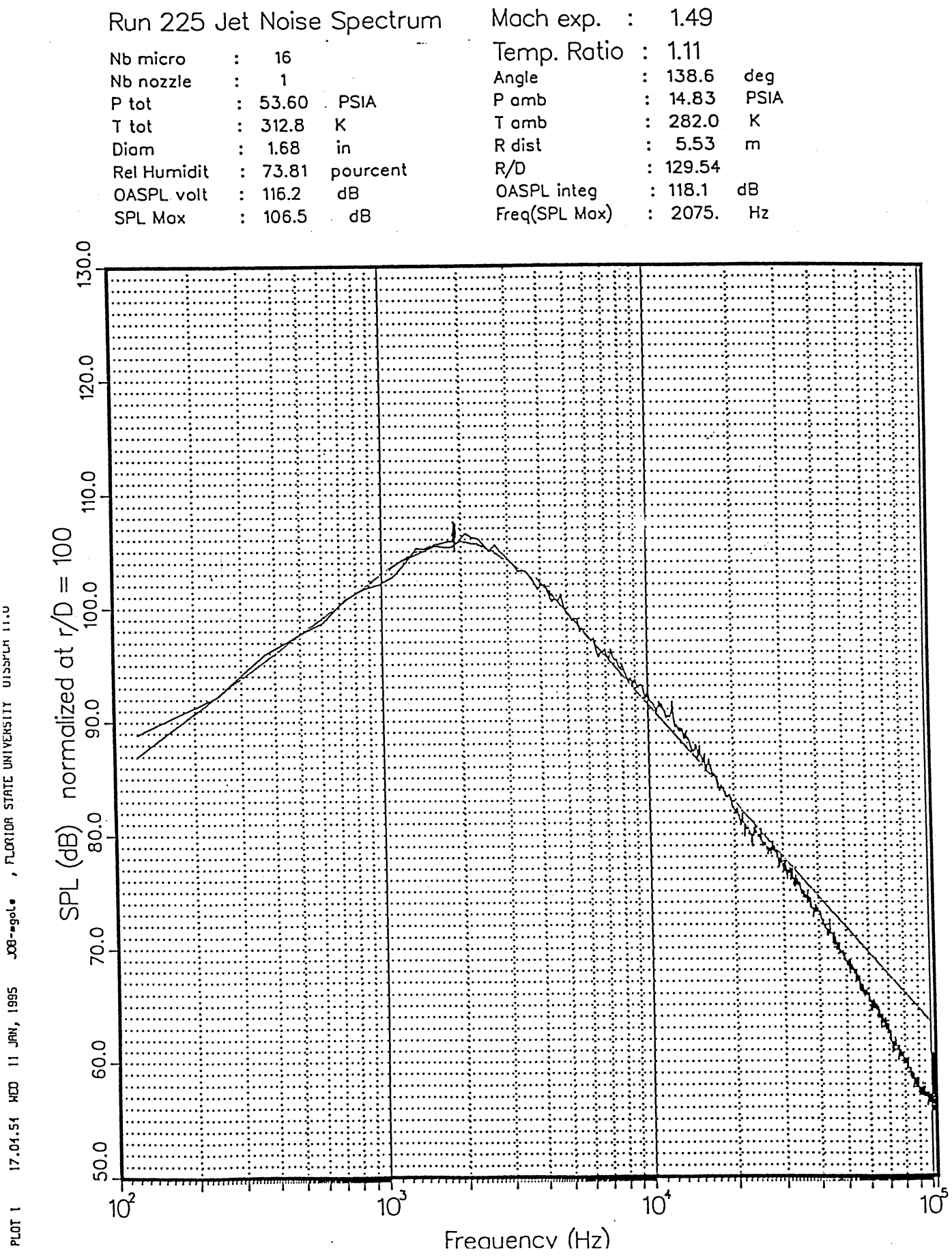
Run 36 Jet Noise Spectrum

Nb micro	: 25		Mach exp.	: 2.00	
Nb nozzle	: Hot Jet		Temp. Ratio	: 4.89	
P tot	: 7997.00	hPa	Angle	: 160.1	deg
T tot	: 1370.4	K	P amb	: 1028.01	hPa
Diam	: 9.14	cm	T amb	: 280.5	K
Rel Humidit	: 64.70	pourcent	R dist	: 6.06	m
Tstatic jet	: 760.6	K	R/D	: 66.30	
SPL Max	: 124.6	dB	Jet Velocity	: 1089.9	m/s
			Freq(SPL Max)	: 366.	Hz



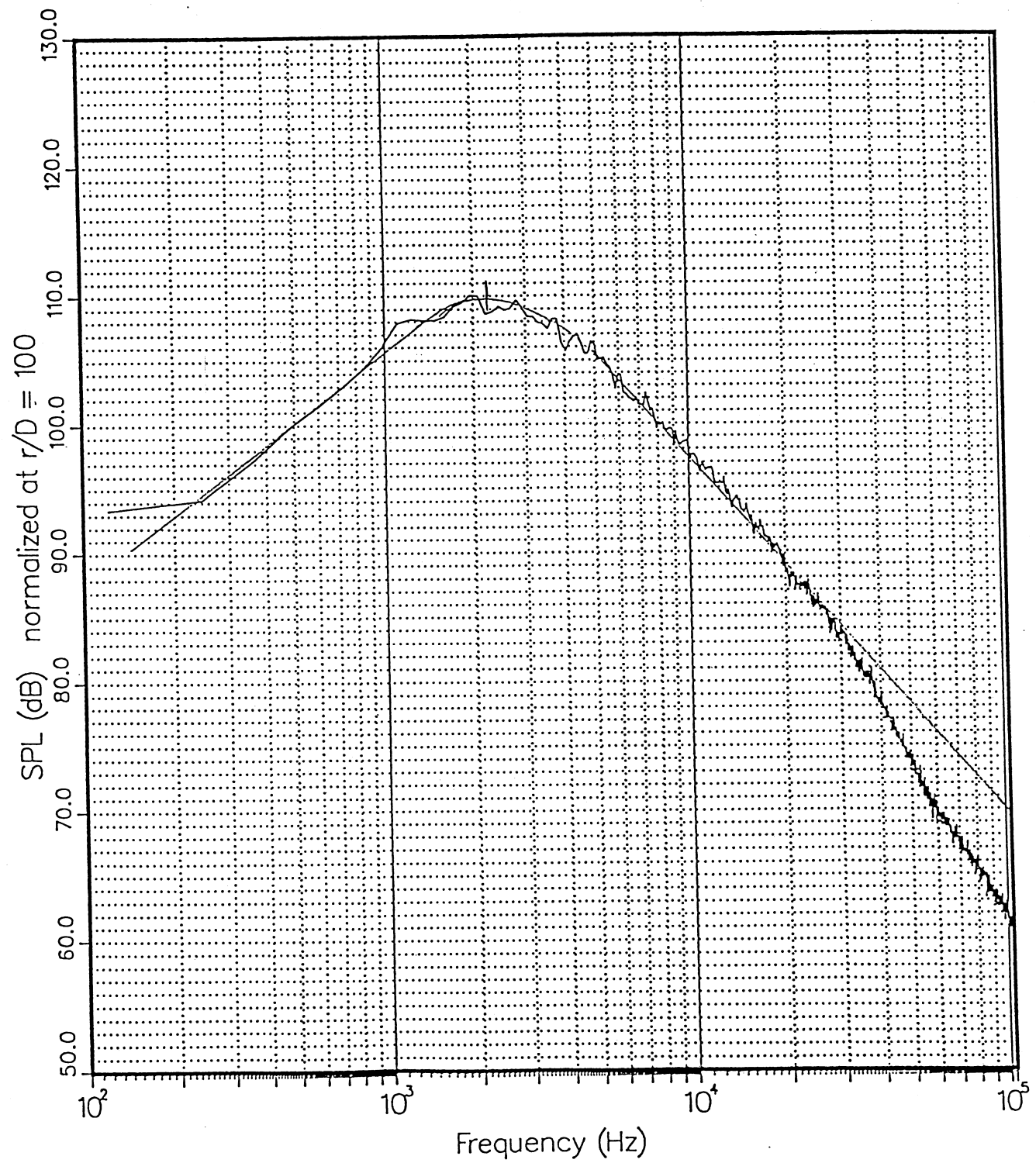
PLOT 1 00.05.12 THUR 16 FEB, 1995 JOB-ngole , FLORIDA STATE UNIVERSITY DISSPLA 11.0

MACH NUMBER DEPENDENCE

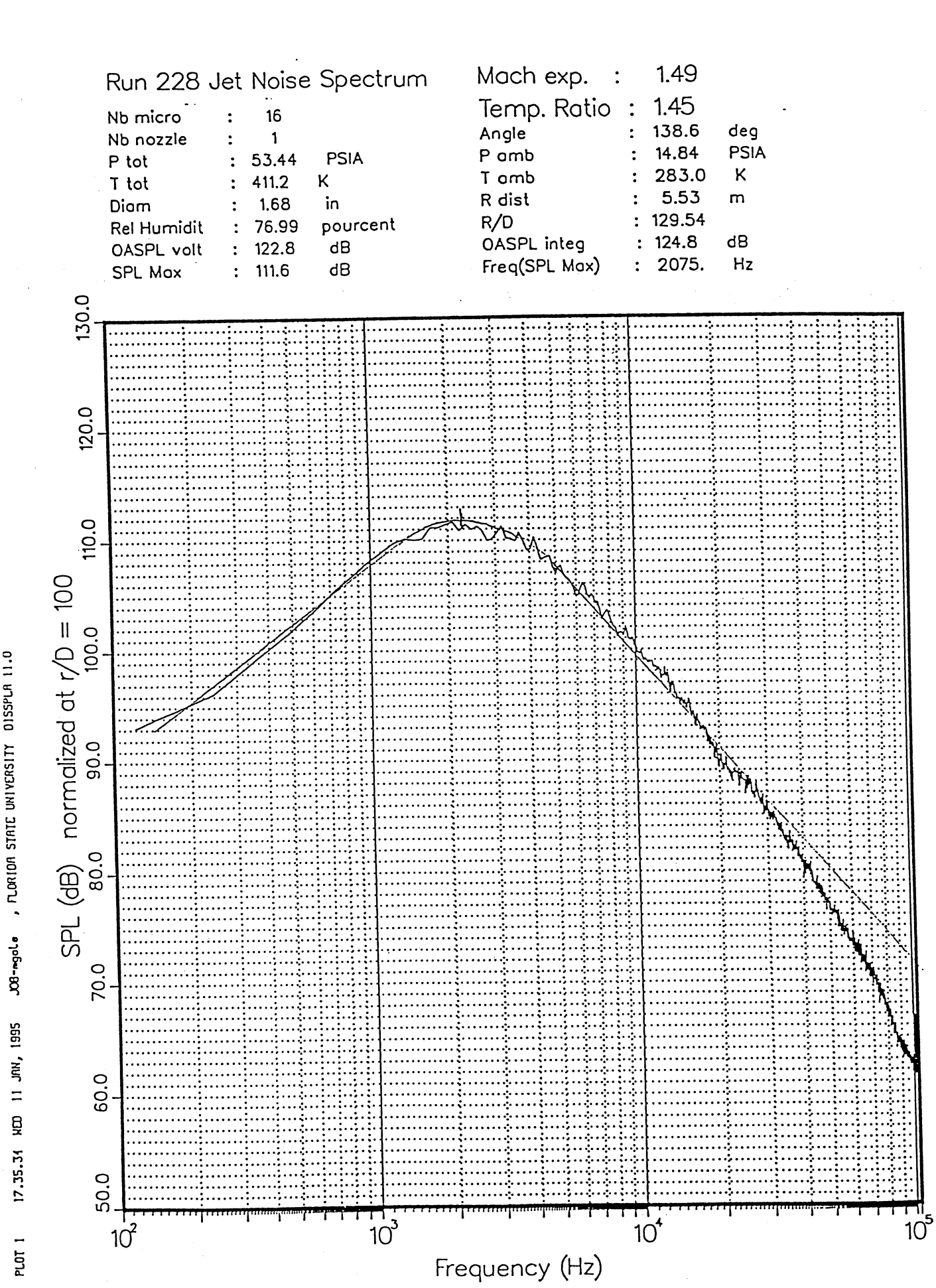

Run 225 Jet Noise Spectrum
Nb micro : 16
Nb nozzle : 1
P tot : 53.60 PSIA
T tot : 312.8 K
Diam : 1.68 in
Rel Humidit : 73.81 pourcent
OASPL volt : 116.2 dB
SPL Max : 106.5 dB
Mach exp. : 1.49
Temp. Ratio : 1.11
Angle : 138.6 deg
P amb : 14.83 PSIA
T amb : 282.0 K
R dist : 5.53 m
R/D : 129.54
OASPL integ : 118.1 dB
Freq(SPL Max) : 2075. Hz
SPL (dB) normalized at r/D = 100
130.0
120.0
110.0
100.0
90.0
80.0
70.0
60.0
50.0
10^2
10^3
10^4
10^5
Frequency (Hz)
PLOT 1 17.04.54 WED 11 JAN, 1995 JOB=gole , FLORIDA STATE UNIVERSITY DISSPLA 11.0

Run 5 Jet Noise Spectrum

Nb micro	:	21	Mach exp.	:	1.49
Nb nozzle	:	1	Temp. Ratio	:	1.33
P tot	:	52.55 PSIA	Angle	:	139.4 deg
T tot	:	393.4 K	P amb	:	14.63 PSIA
Diam	:	1.68 in	T amb	:	296.5 K
Rel Humidit	:	55.65 pourcent	R dist	:	5.62 m
OASPL volt	:	120.8 dB	R/D	:	131.70
SPL Max	:	110.1 dB	OASPL integ	:	122.5 dB
			Freq(SPL Max)	:	1953. Hz

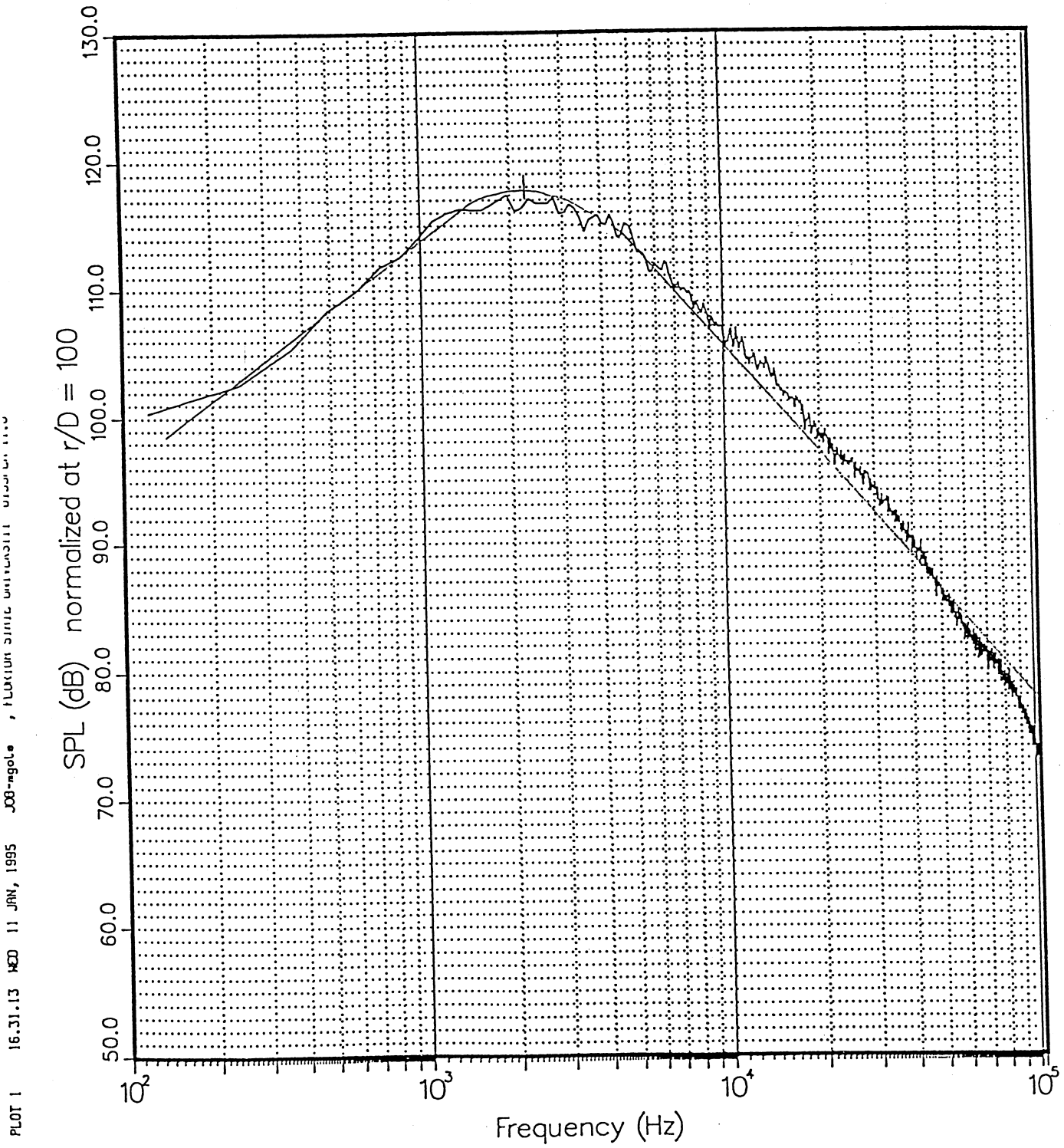


PLOT 1 15.41.28 WED 11 JAN, 1995 JOB-ngole , FLORIDA STATE UNIVERSITY DISPLAY 11.0


Run 228 Jet Noise Spectrum
Nb micro : 16
Nb nozzle : 1
P tot : 53.44 PSIA
T tot : 411.2 K
Diam : 1.68 in
Rel Humidit : 76.99 pourcent
OASPL volt : 122.8 dB
SPL Max : 111.6 dB
Mach exp. : 1.49
Temp. Ratio : 1.45
Angle : 138.6 deg
P amb : 14.84 PSIA
T amb : 283.0 K
R dist : 5.53 m
R/D : 129.54
OASPL integ : 124.8 dB
Freq(SPL Max) : 2075. Hz
SPL (dB) normalized at r/D = 100
130.0
120.0
110.0
100.0
90.0
80.0
70.0
60.0
50.0
10^2
10^3
10^4
10^5
Frequency (Hz)
PLOT 1 17.35.34 WED 11 JAN, 1995 JOB-mgale , FLORIDA STATE UNIVERSITY DISSPLA 11.0

Run 11 Jet Noise Spectrum

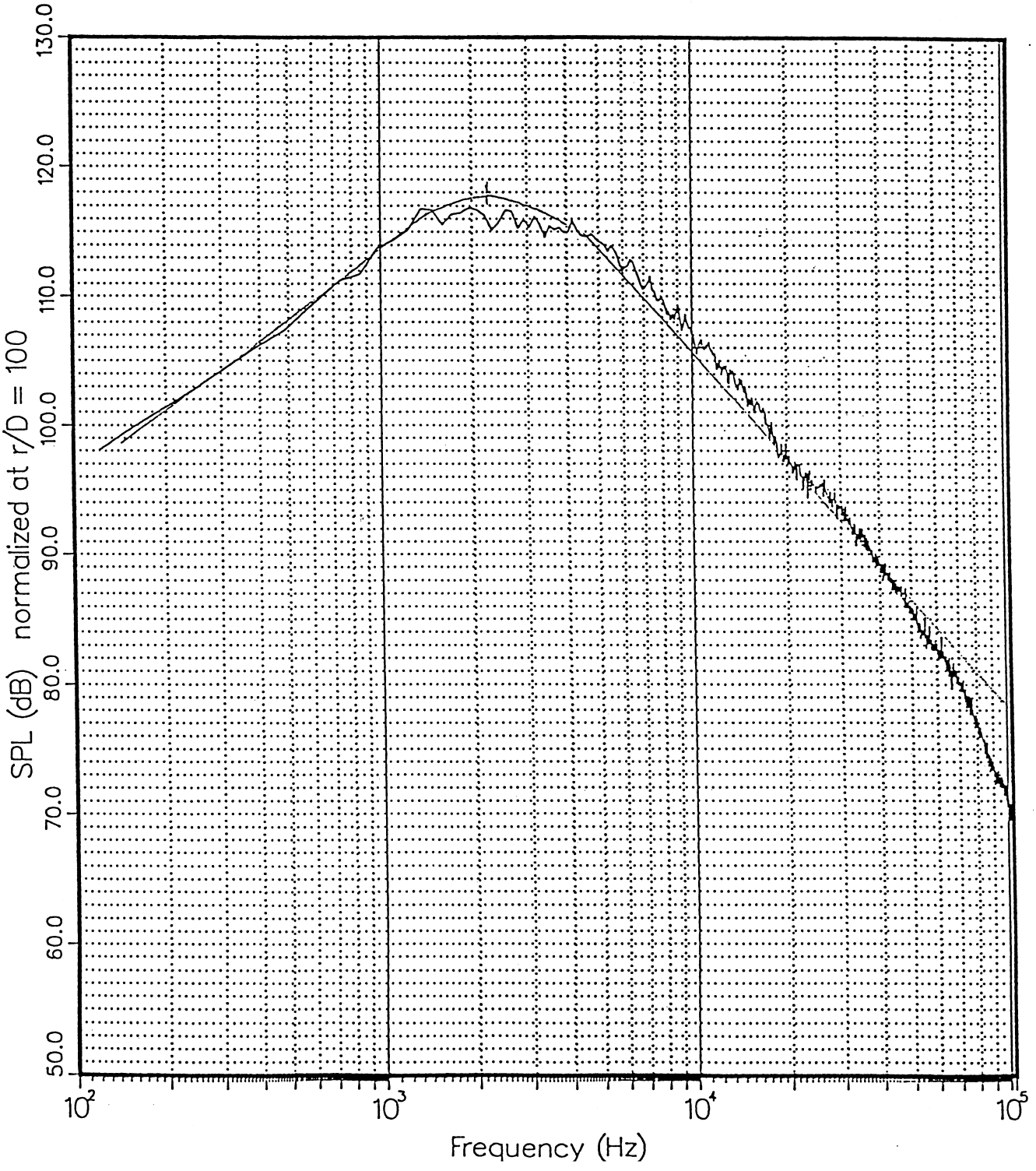
Nb micro	:	21	Mach exp.	:	1.49
Nb nozzle	:	1	Temp. Ratio	:	2.25
P tot	:	52.04 PSIA	Angle	:	139.4 deg
T tot	:	669.2 K	P amb	:	14.63 PSIA
Diam	:	1.68 in	T amb	:	297.8 K
Rel Humidit	:	57.90 pourcent	R dist	:	5.62 m
OASPL volt	:	128.9 dB	R/D	:	131.70
SPL Max	:	117.4 dB	OASPL integ	:	130.7 dB
			Freq(SPL Max)	:	1953. Hz



PLOT 1 16.31.13 MCD 11 JAN, 1995 JOB=gole , FLORIDA STATE UNIVERSITY DRAPER INC.

Run 231 Jet Noise Spectrum

Nb micro	:	16		Mach exp.	:	1.49	
Nb nozzle	:	1		Temp. Ratio	:	2.35	
P tot	:	53.68	PSIA	Angle	:	138.6	deg
T tot	:	672.4	K	P amb	:	14.98	PSIA
Diam	:	1.68	in	T amb	:	286.7	K
Rel Humidit	:	69.74	pourcent	R dist	:	5.53	m
OASPL volt	:	128.8	dB	R/D	:	129.54	
SPL Max	:	116.8	dB	OASPL integ	:	130.8	dB
				Freq(SPL Max)	:	1953.	Hz



PLOT 1 18.10.32 WED 11 JAN, 1995 JOB=ngole , FLORIDA STATE UNIVERSITY DISPLAY 11.0

Summary of Comparisons Between Empirical Noise Spectra and Experimental Measurements

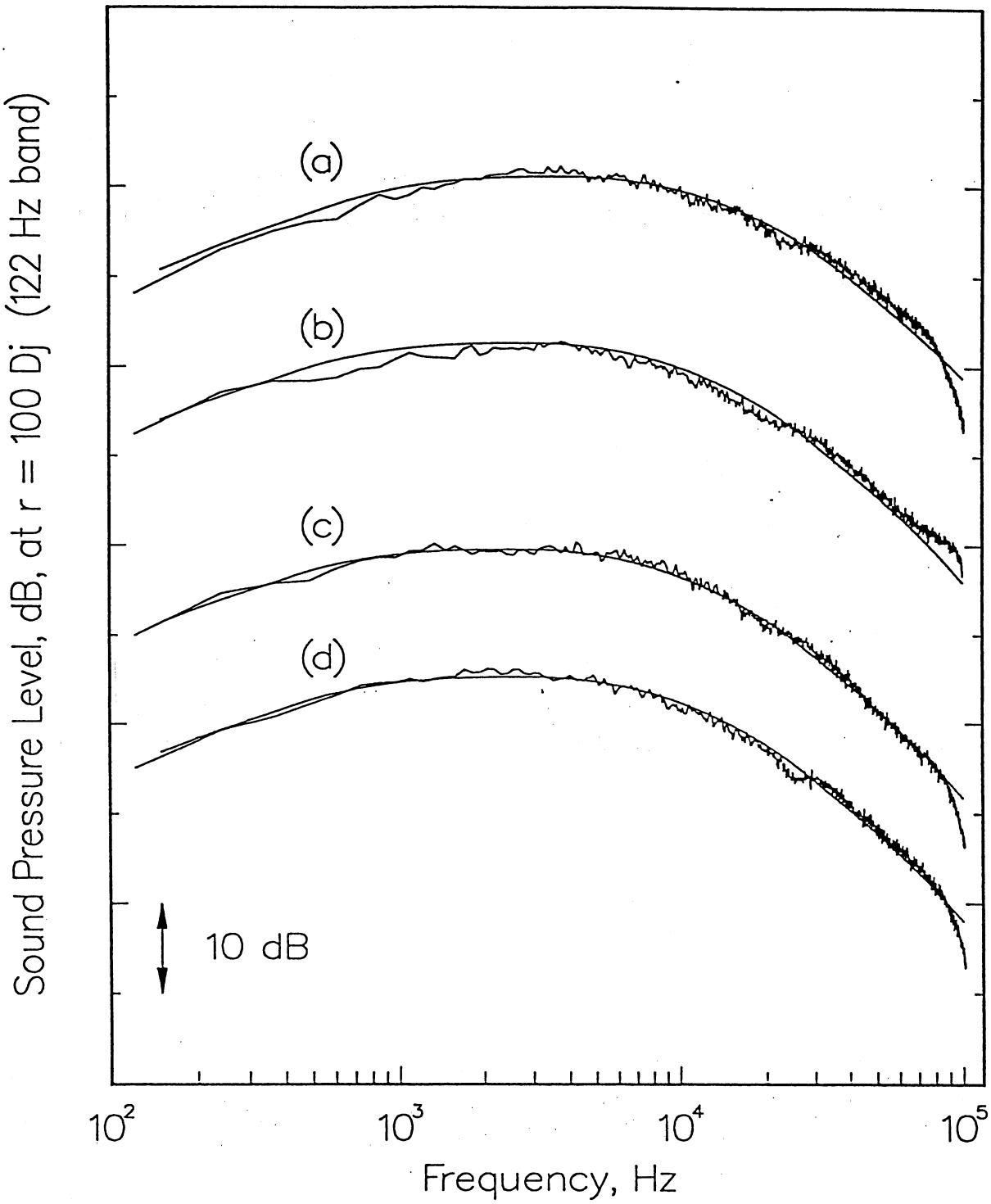


Figure 4. Comparison of the similarity spectrum of fine scale turbulence noise and measurements.
(a) $M_j = 1.49$, $T_r/T_\infty = 2.35$, $\chi = 92.9°$, $SPL_{\max} = 96$ dB,
(b) $M_j = 2.0$, $T_r/T_\infty = 4.89$, $\chi = 83.8°$, $SPL_{\max} = 107$ dB,
(c) $M_j = 1.96$, $T_r/T_\infty = 0.99$, $\chi = 83.3°$, $SPL_{\max} = 95$ dB,
(d) $M_j = 1.96$, $T_r/T_\infty = 0.98$, $\chi = 120.2°$, $SPL_{\max} = 100$ dB.

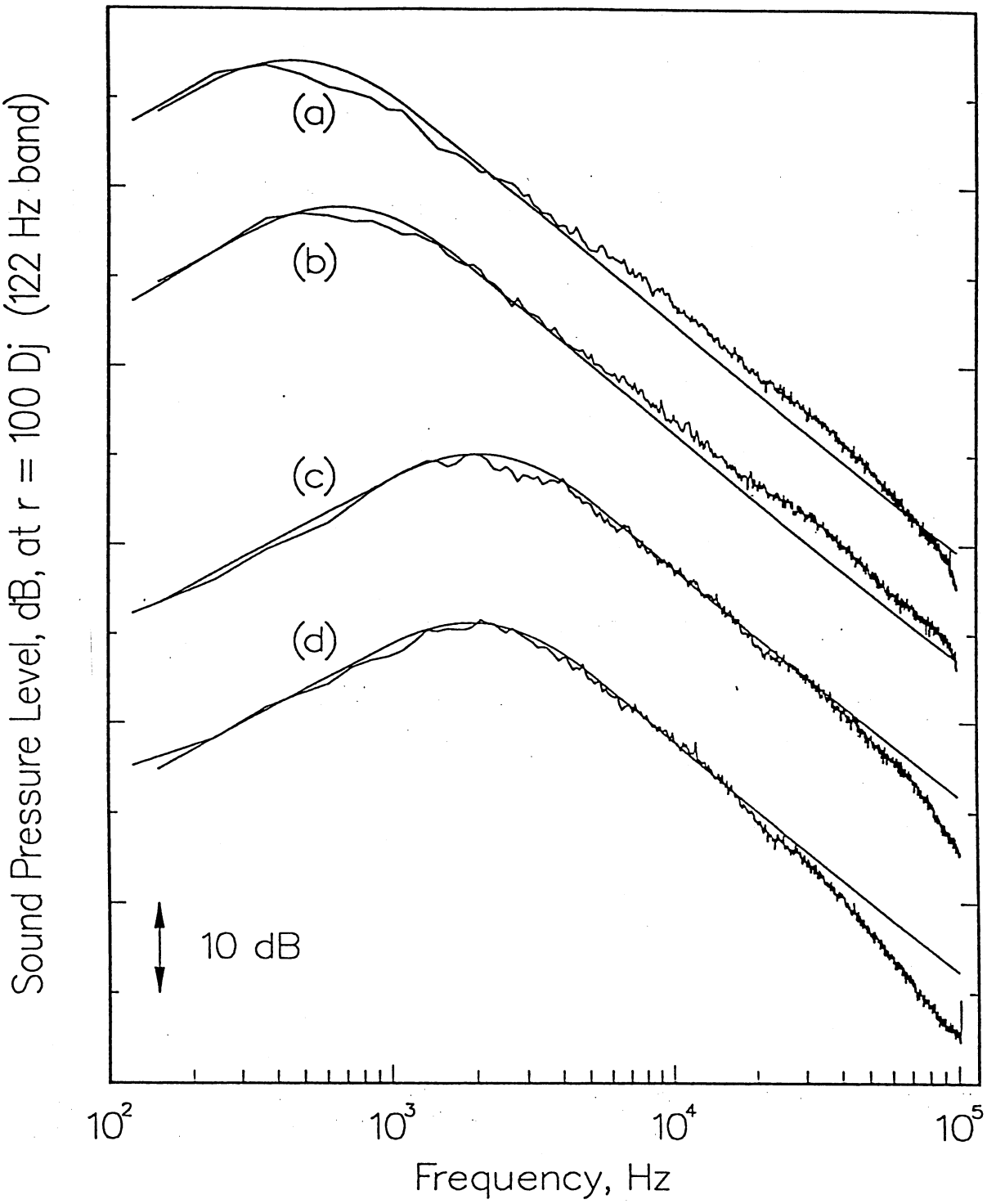


Figure 3. Comparison of the similarity spectrum of large turbulence structures/ instability waves noise and measurements.
(a) $M_j = 2.0$, $T_r/T_\infty = 4.89$, $\chi = 160.1°$, $SPL_{\max} = 124.7$ dB,
(b) $M_j = 2.0$, $T_r/T_\infty = 1.12$, $\chi = 160.1°$, $SPL_{\max} = 121.6$ dB,
(c) $M_j = 1.96$, $T_r/T_\infty = 1.78$, $\chi = 138.6°$, $SPL_{\max} = 121.0$ dB,
(d) $M_j = 1.49$, $T_r/T_\infty = 1.11$, $\chi = 138.6°$, $SPL_{\max} = 106.5$ dB.

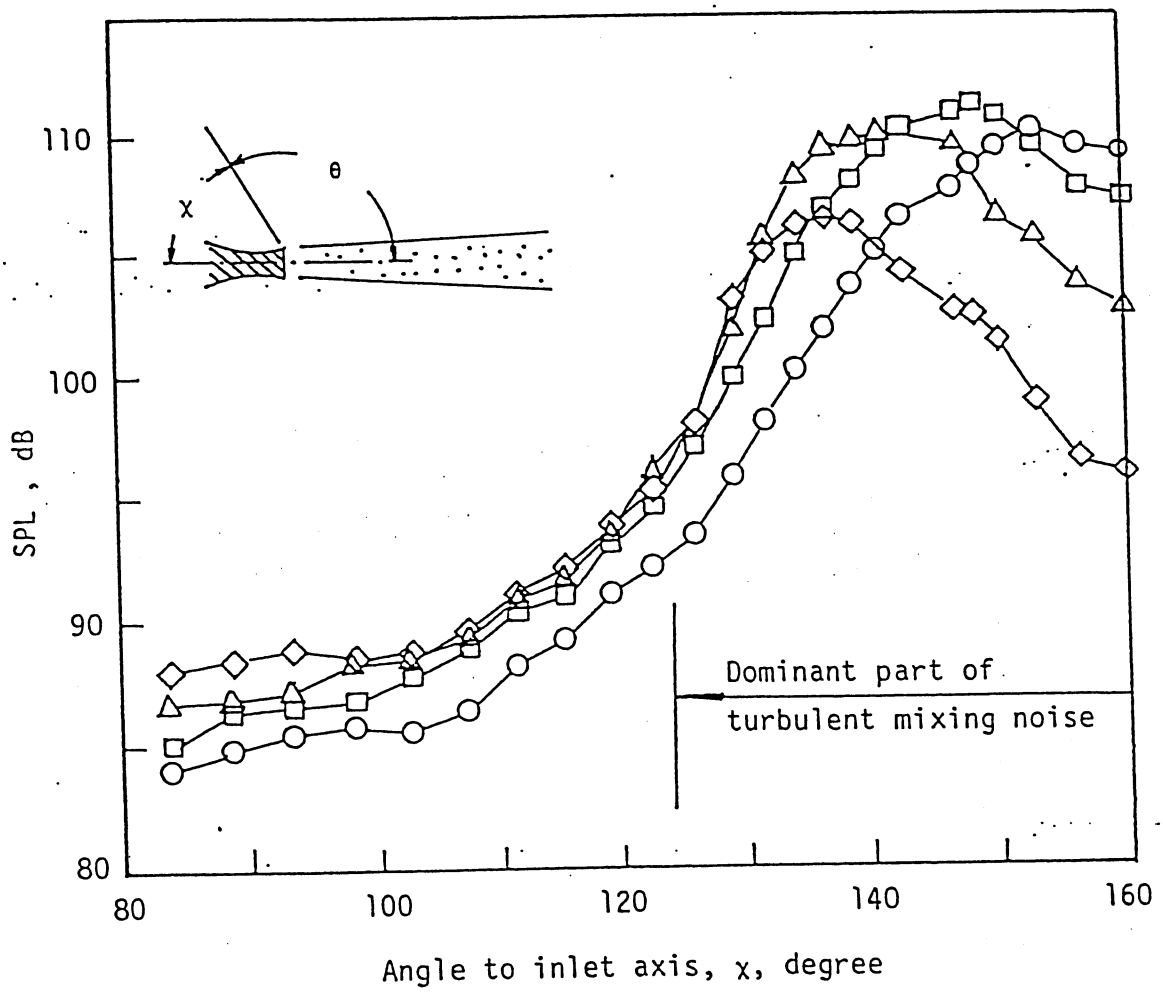


Figure 1. Measured[3] noise directivities at selected Strouhal numbers of a Mach 2 jet at a total temperature of 500°K. (Strouhal number=st). ○ st=0.067; □ st=0.12; △ st=0.20; ◇ st=0.40

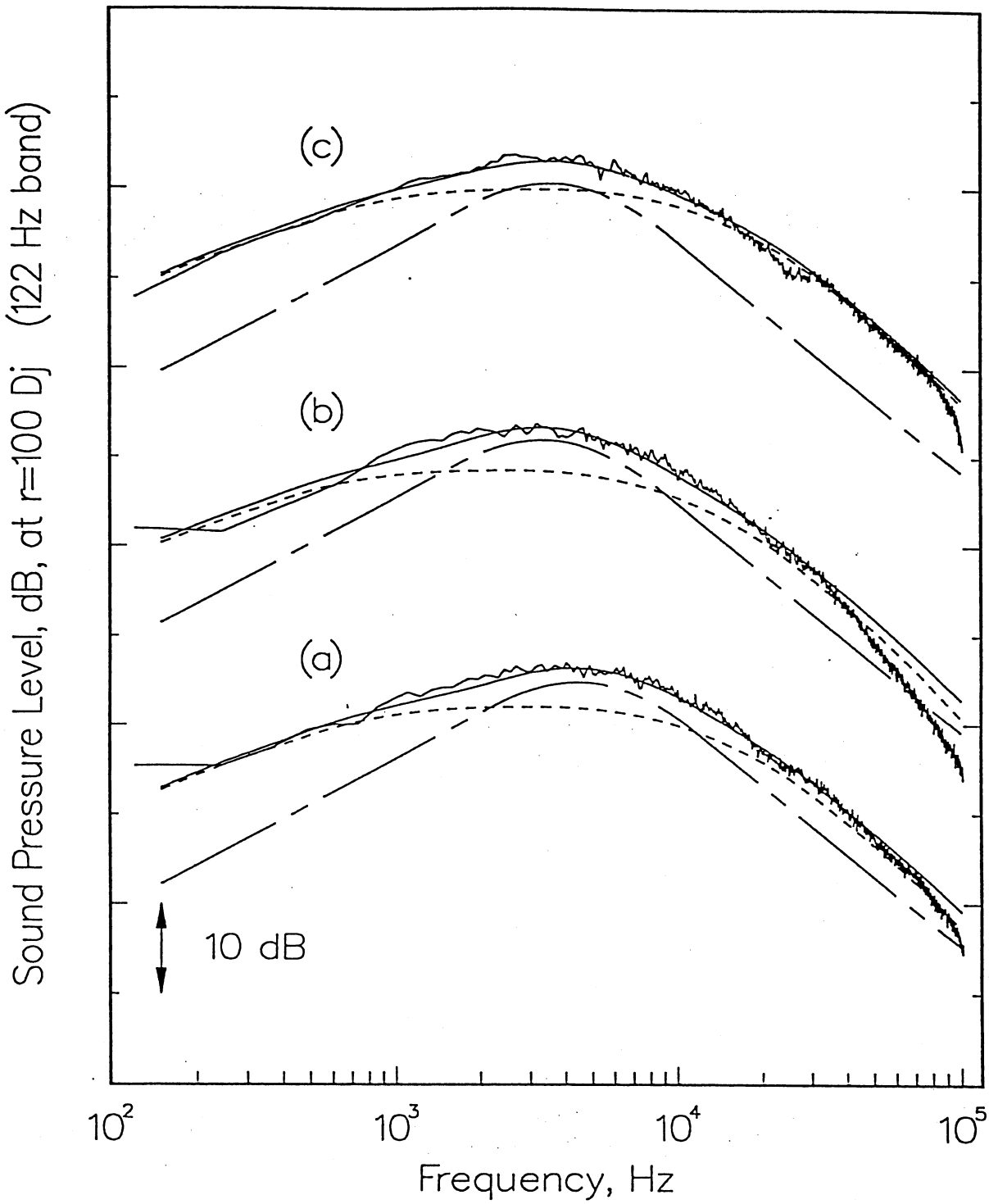


Figure 5. Comparison of the sum of the similarity spectra of both large and fine scale turbulence noise and measurements at intermediate direction of radiation. — - — large turbulence structures noise; - - - - - fine scale turbulence noise; ——— total.
(a) $M_j = 1.49$, $T_r/T_\infty = 2.25$, $\chi = 112.6°$, $SPL_{\max} = 101.5$ dB,
(b) $M_j = 1.49$, $T_r/T_\infty = 1.33$, $\chi = 126.9°$, $SPL_{\max} = 100.5$ dB,
(c) $M_j = 1.96$, $T_r/T_\infty = 1.79$, $\chi = 120.2°$, $SPL_{\max} = 107.0$ dB.

Summary

It appears that all the jet noise data from the NASA Langley Research Center Jet Noise Laboratory can be correlated by two empirical noise spectra regardless of the jet Mach number, jet temperature and direction of radiation.

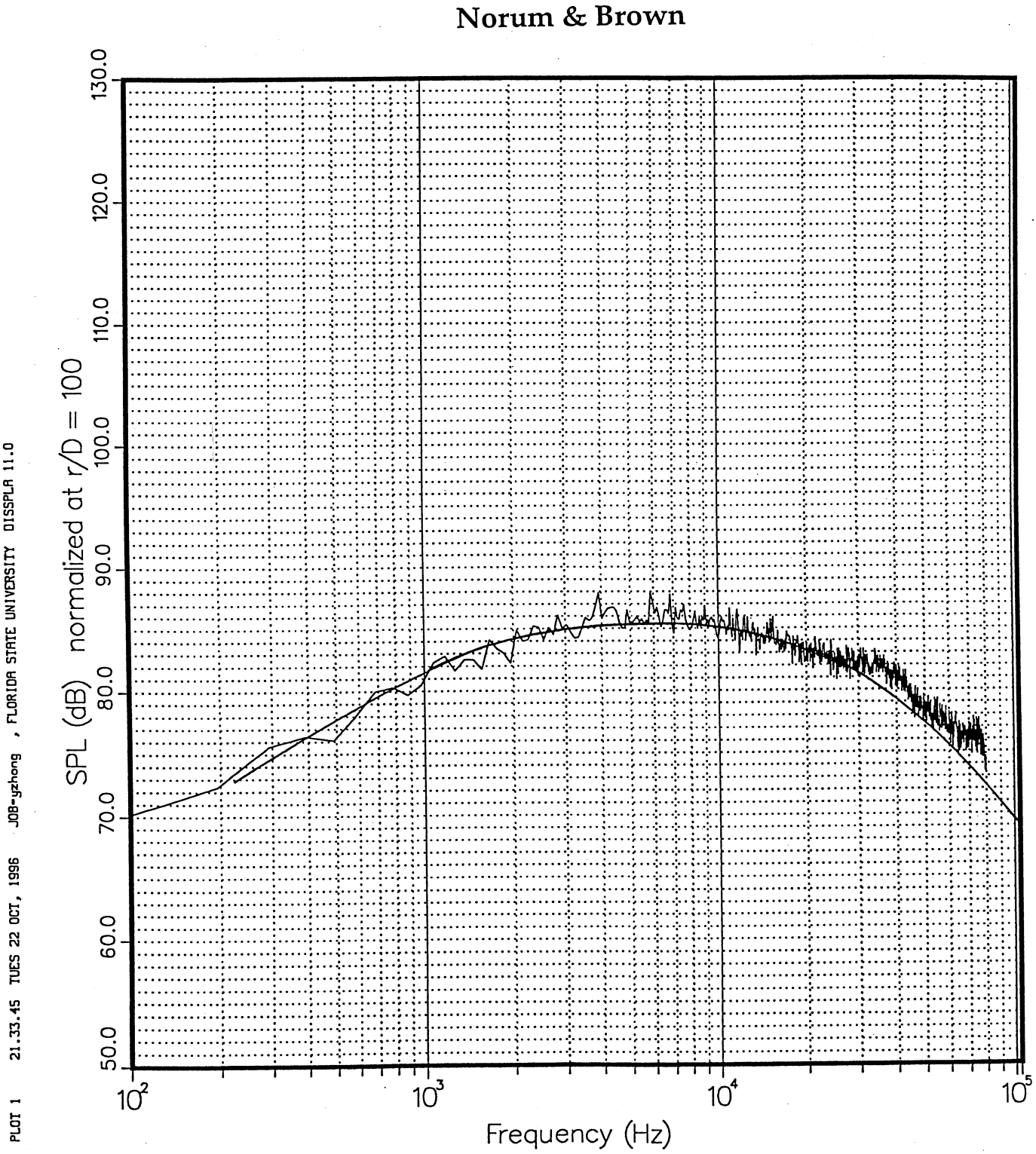
Other supersonic jet noise data

RUN NUMBER : 182

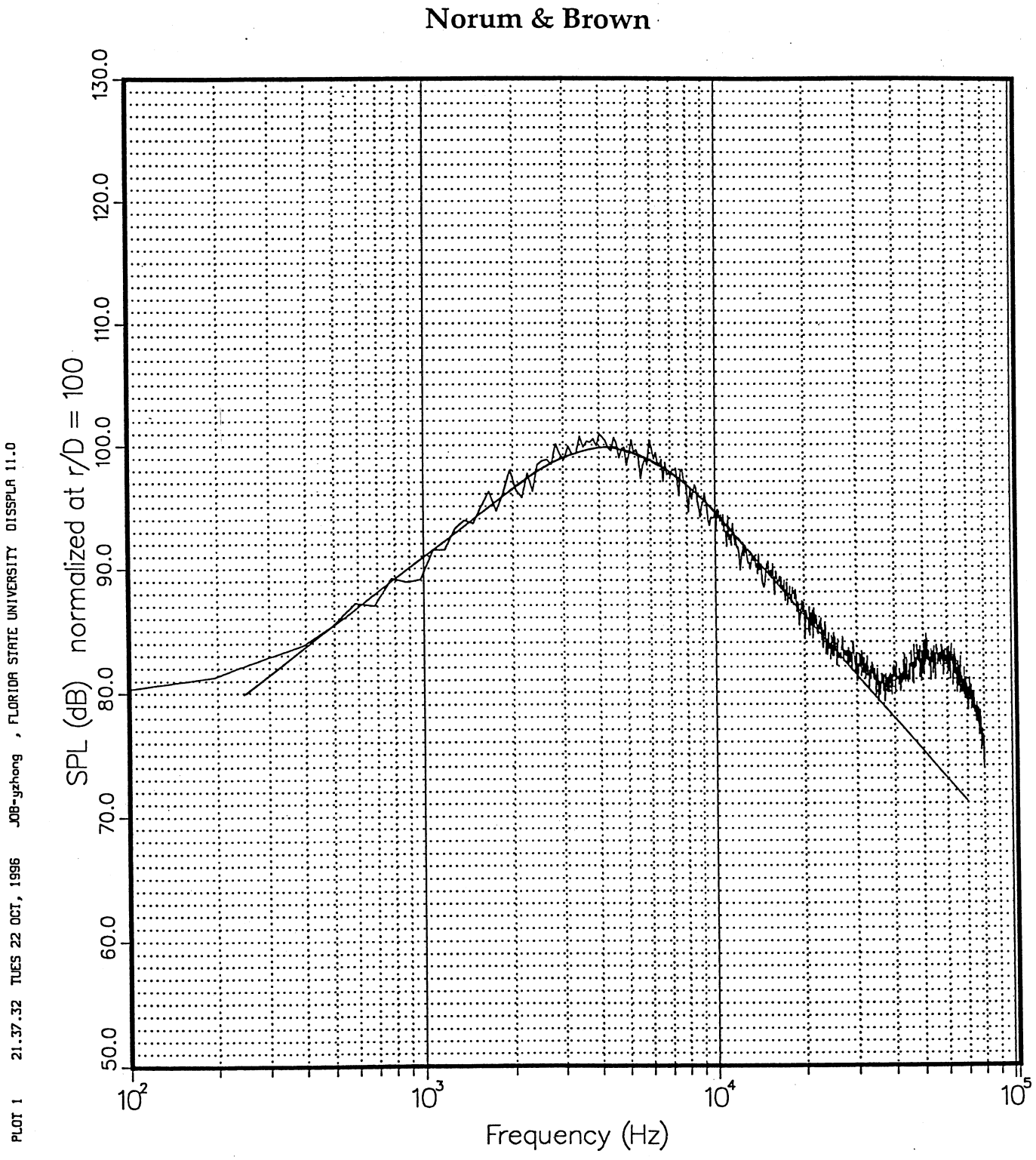
Fully Expanded Mach Number : 1.50
Num of Spectral Points : 819
Bandwidth : .097656 khz
Angel From Inlet Axis :110 deg

NOZZLE TYPE : 3

Free Jet Mach Number : .00
Maximum Frequency :79.980 khz
Channal Number : 9
Oaspl :111.2 dB

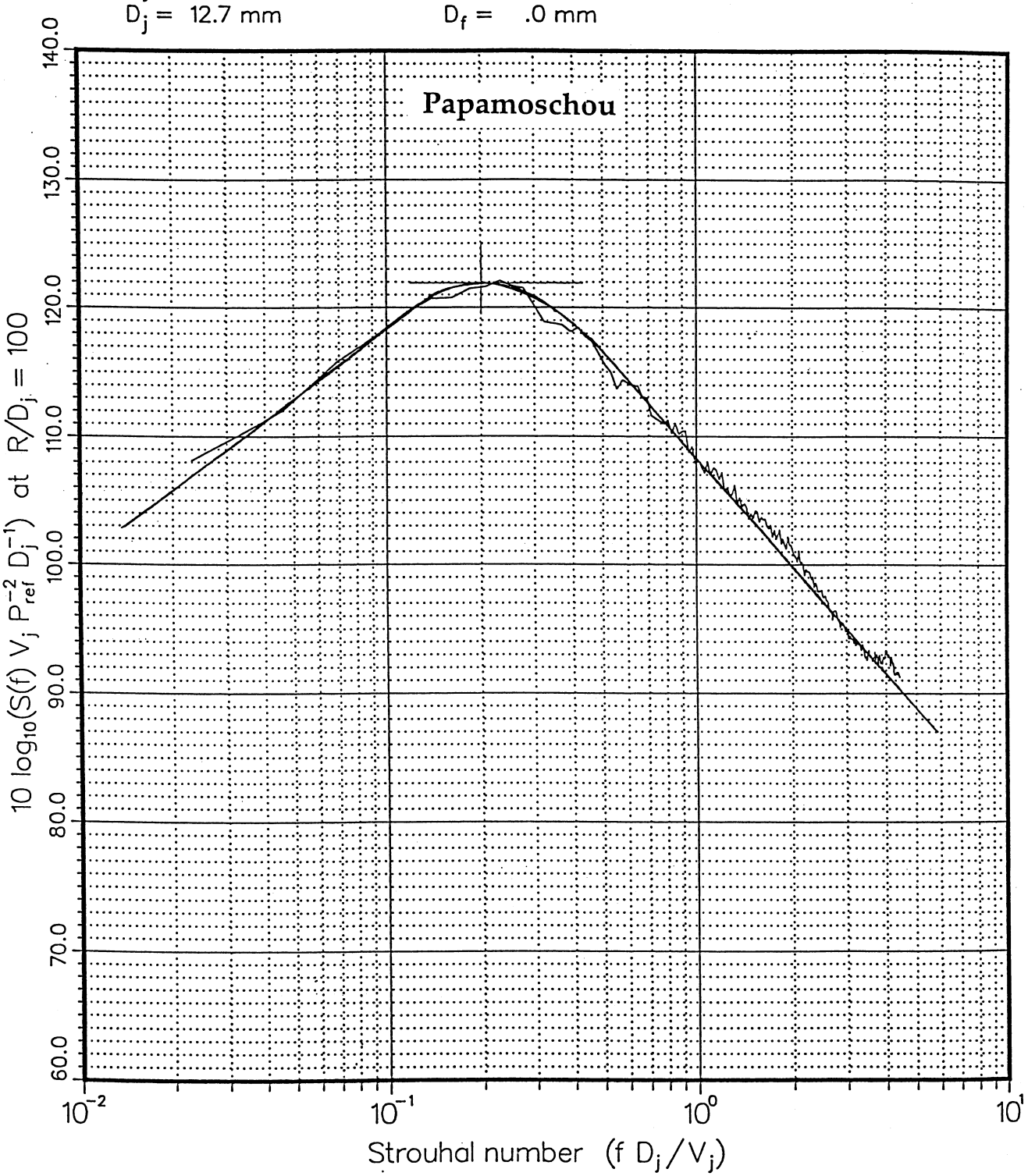


RUN NUMBER	: 182	NOZZLE TYPE	: 3
Fully Expanded Mach Number	: 1.50	Free Jet Mach Number	: .00
Num of Spectral Points	: 819	Maximum Frequency	:79.980 khz
Bandwidth	: .097656 khz	Channal Number	:12
Angel From Inlet Axis	:140 deg	Oaspl	:119.4 dB



AA0103

M_j (primary) = 1.50 M_f (coflow) = .00 Gas = Air
T_j (static) = 210K T_f (static) = 300K Θ = 40°
V_j = 430 m/s V_f = 0 m/s
D_j = 12.7 mm D_f = .0 mm

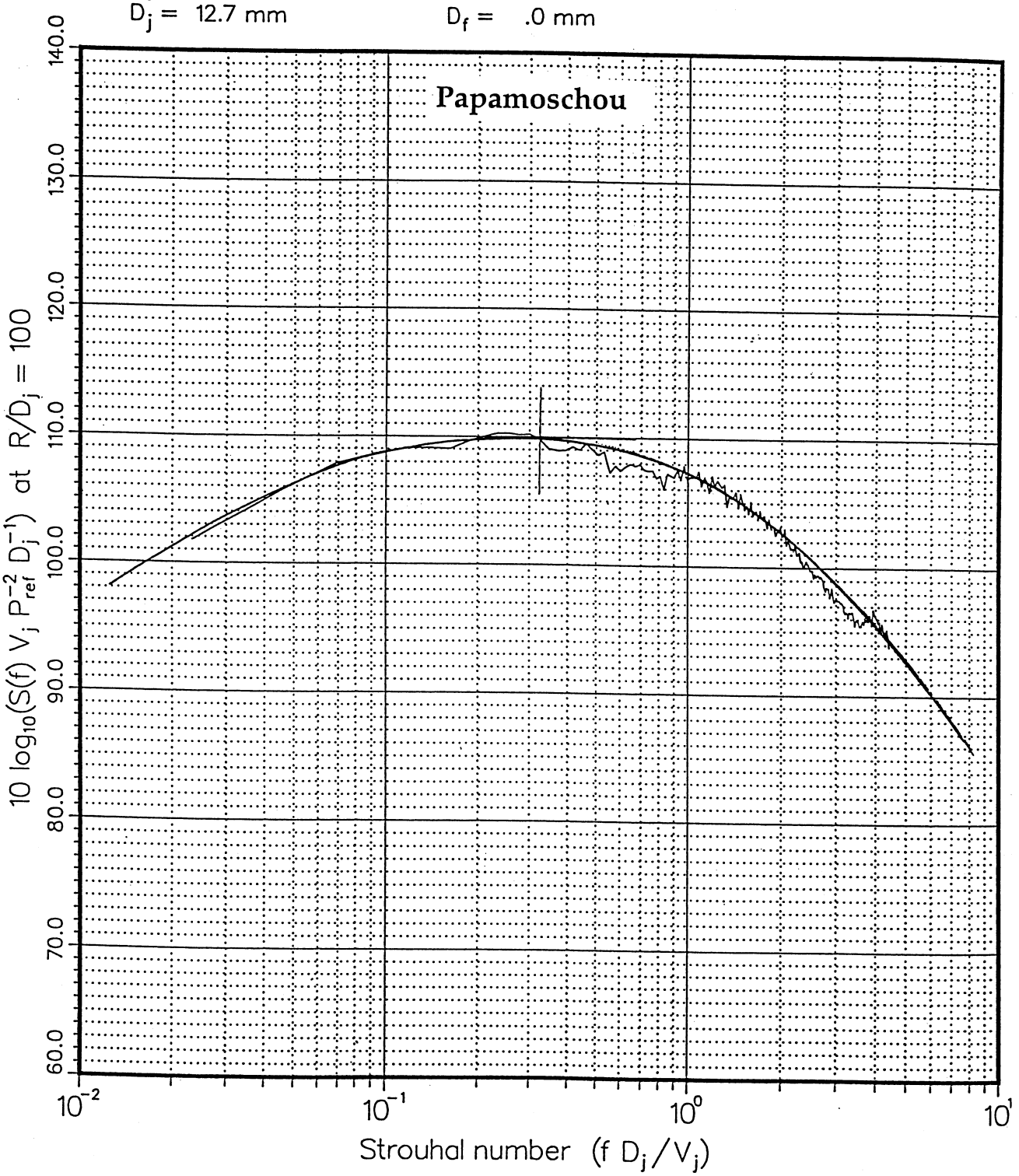


AA0106

M_j (primary) = 1.50
T_j (static) = 210K
V_j = 430 m/s
D_j = 12.7 mm

M_f (coflow) = .00
T_f (static) = 300K
V_f = 0 m/s
D_f = .0 mm

Gas = Air
Θ = 70°



Subsonic jet noise data

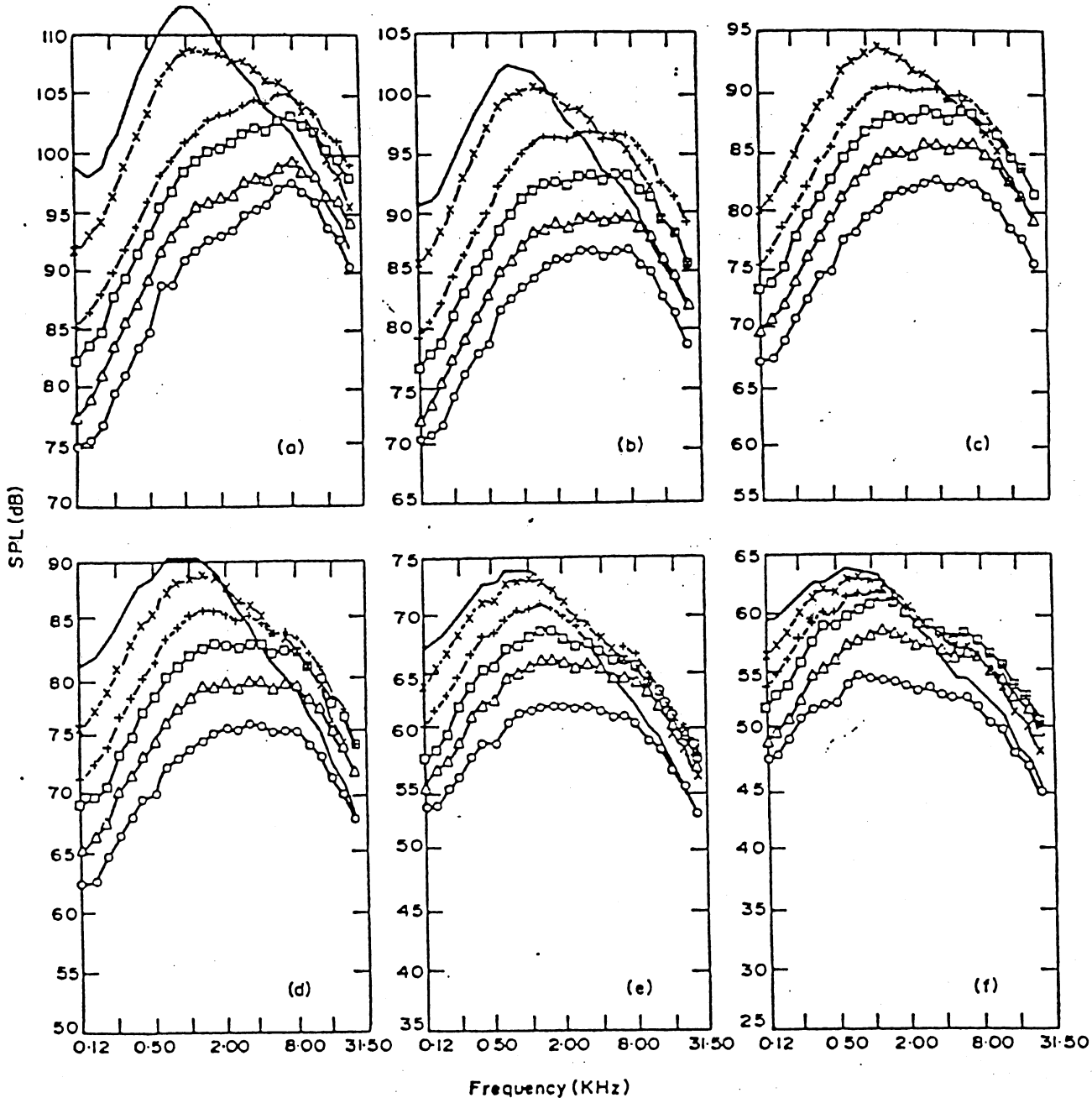


Figure 2. 1/3 octave spectra for nozzle diameter = 2·84 in. Jet velocity values: (a) 1000 ft/s; (b) 800 ft/s; (c) 700 ft/s; (d) 600 ft/s; (e) 400 ft/s; (f) 300 ft/s. Values for θ: —, 20°; ×, 30°; +, 45°; □, 60°; △, 90°; ○, 120°.

K. K. Ahuja J. Sound & Vib. ,29, 155-168, 1973

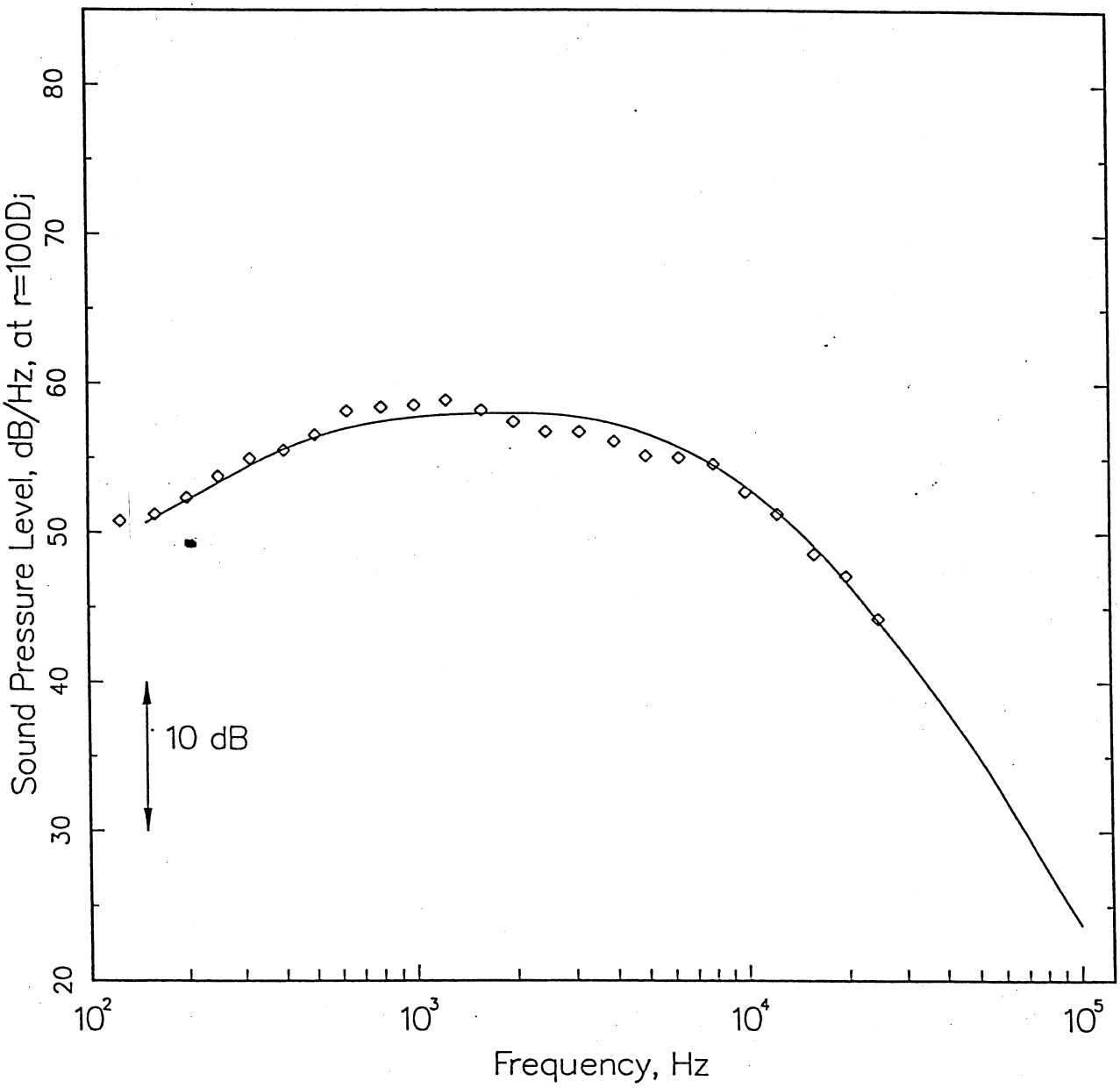


Figure 20. Comparison of the similarity spectrum of fine scale turbulence noise and subsonic jet noise measurement of Ahuja[18].
$M_j = 0.98$, $\chi = 90°$, $T_r/T_\infty = 1.0$.

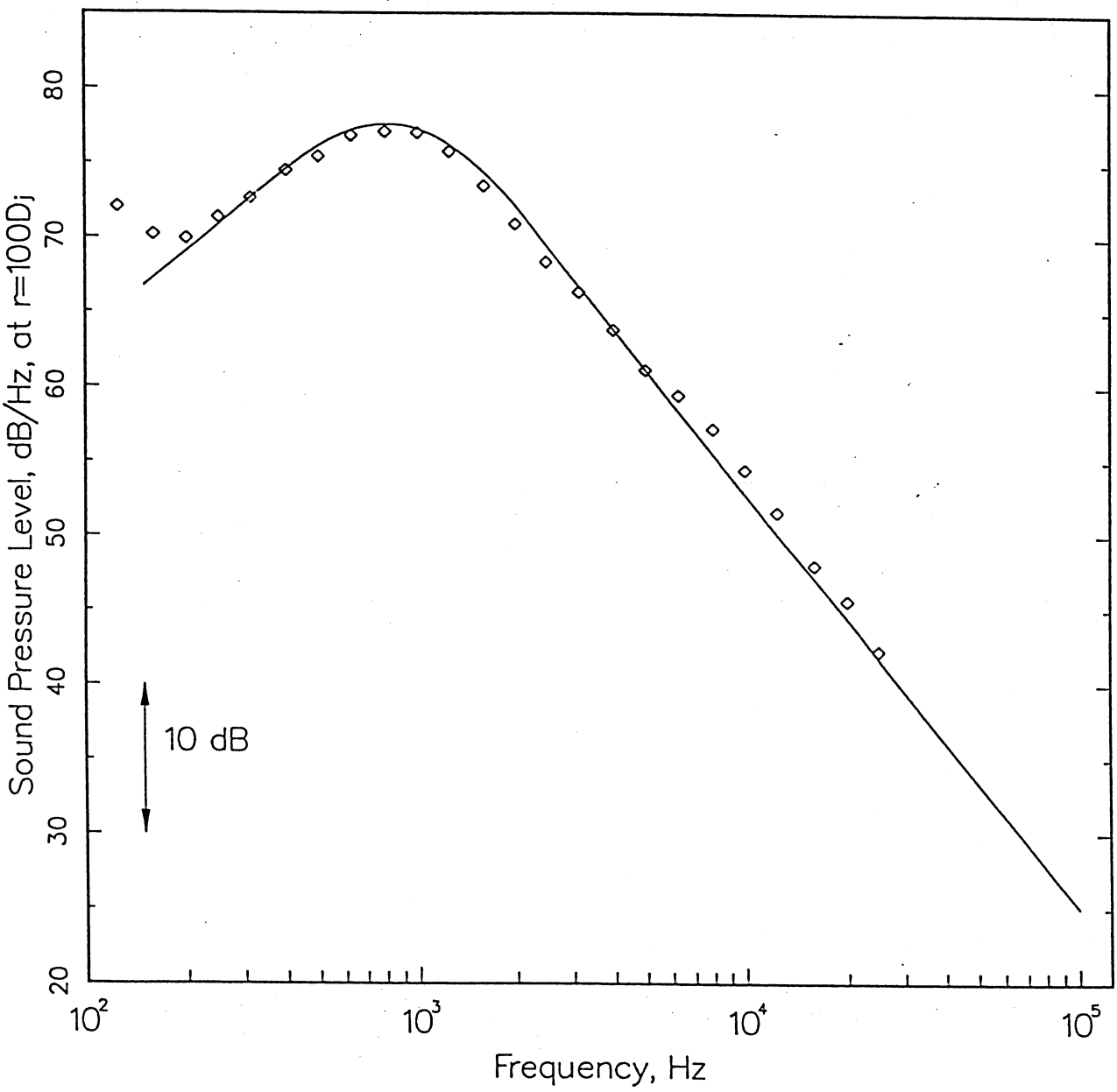
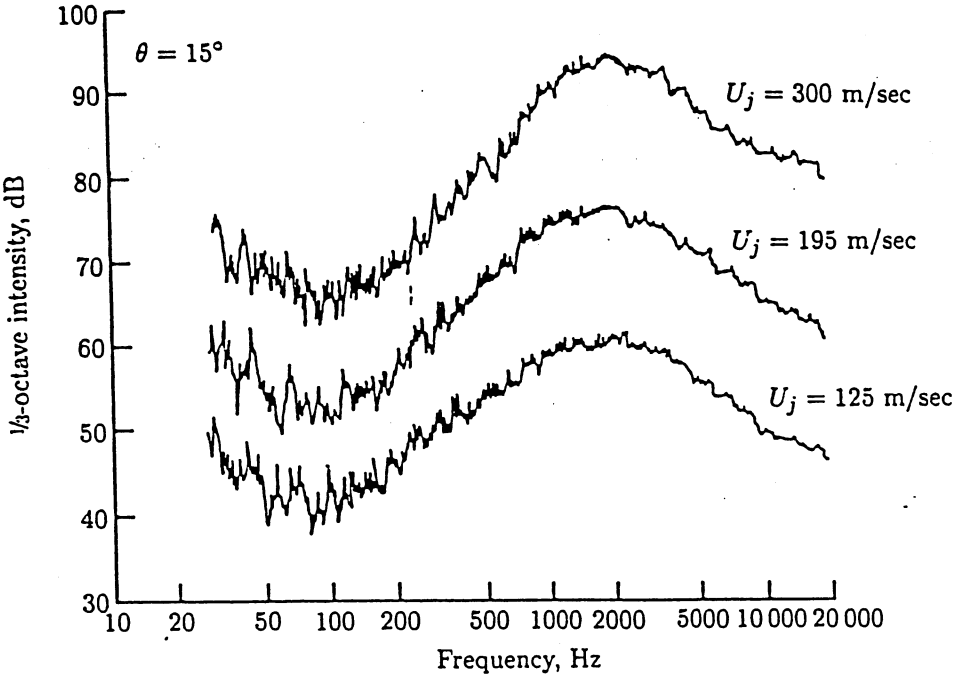
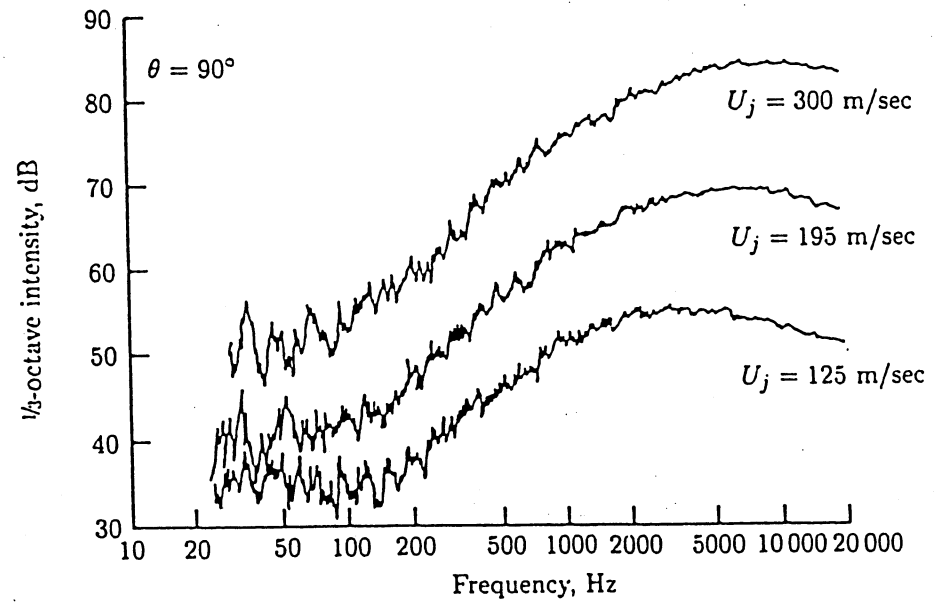


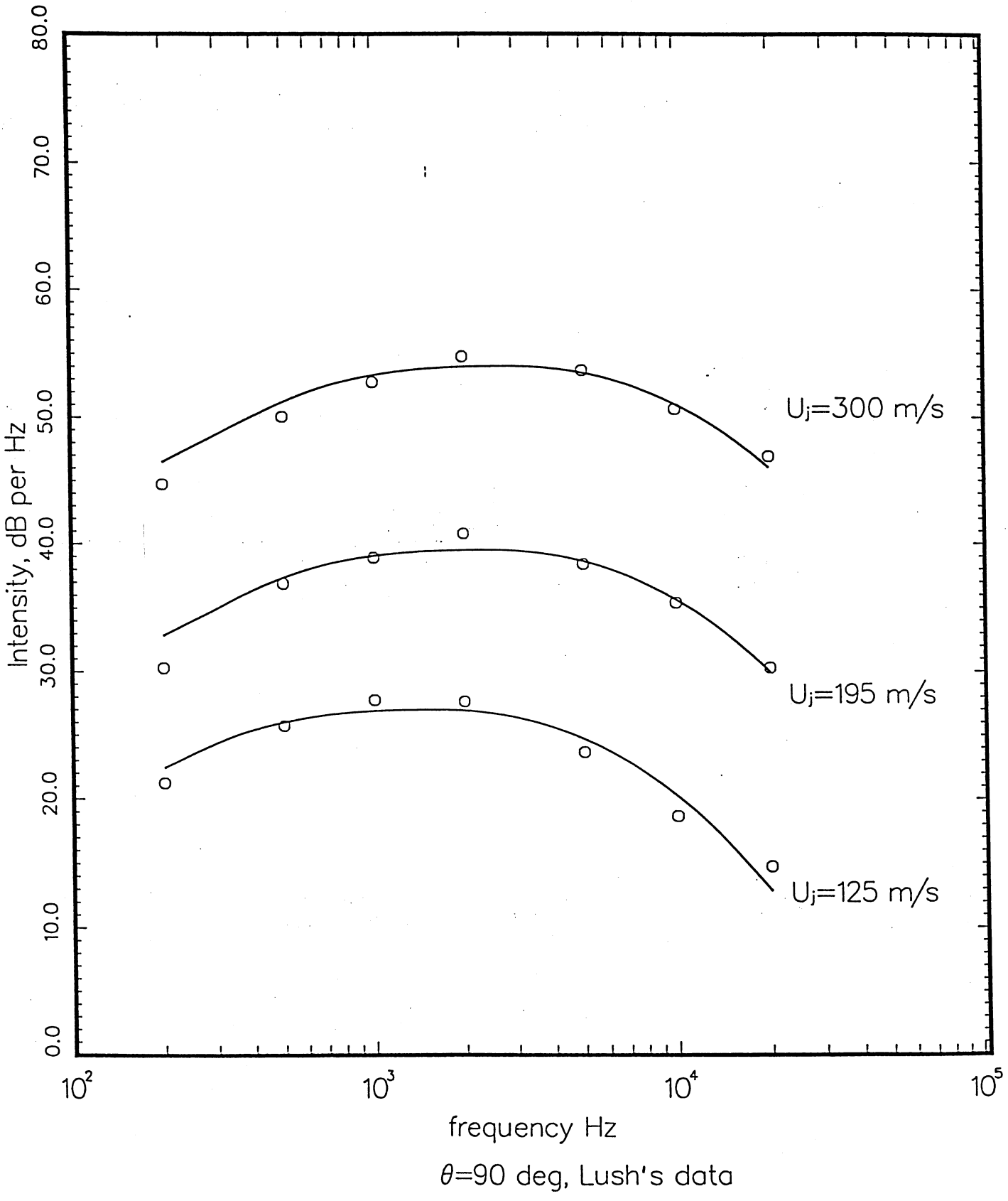
Figure 19. Comparison of the similarity spectrum of large turbulence structures/ instability waves noise and subsonic jet noise measurement of Ahuja[18]. $M_j = 0.98$, $\chi = 160°$, $T_r/T_\infty = 1.0$.

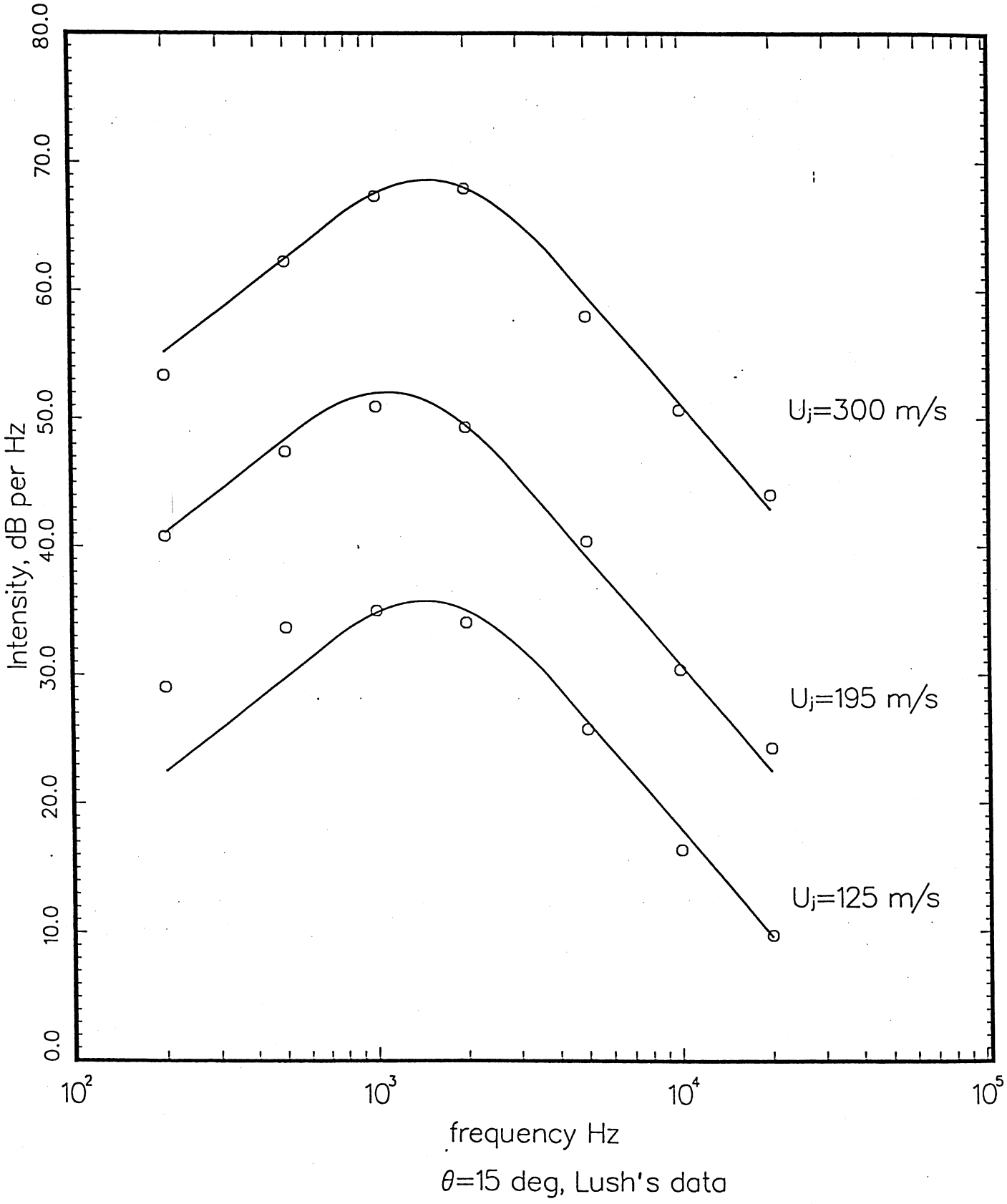


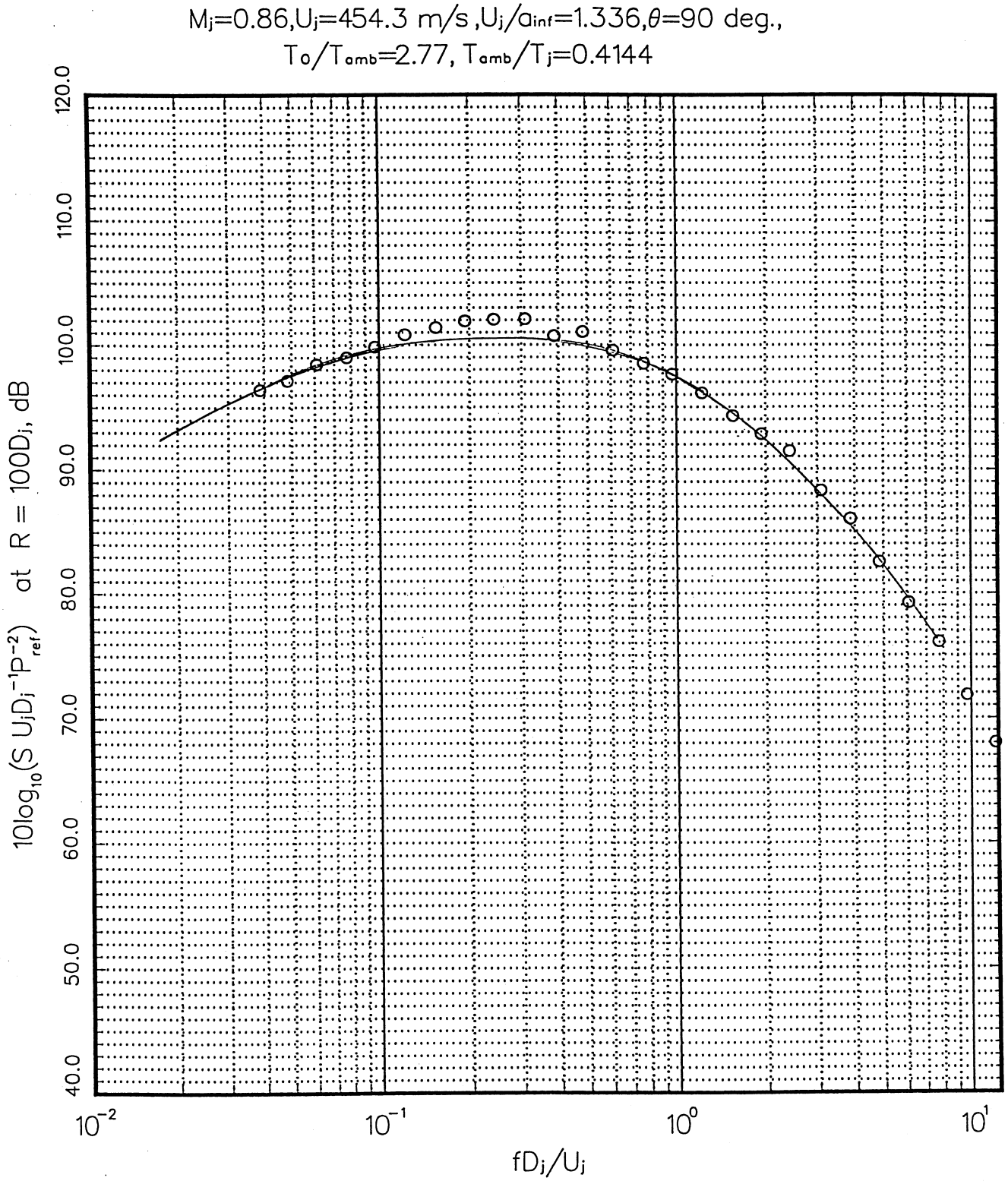


Jet noise spectra at $\theta = 15°$ and 90° for various jet velocities.

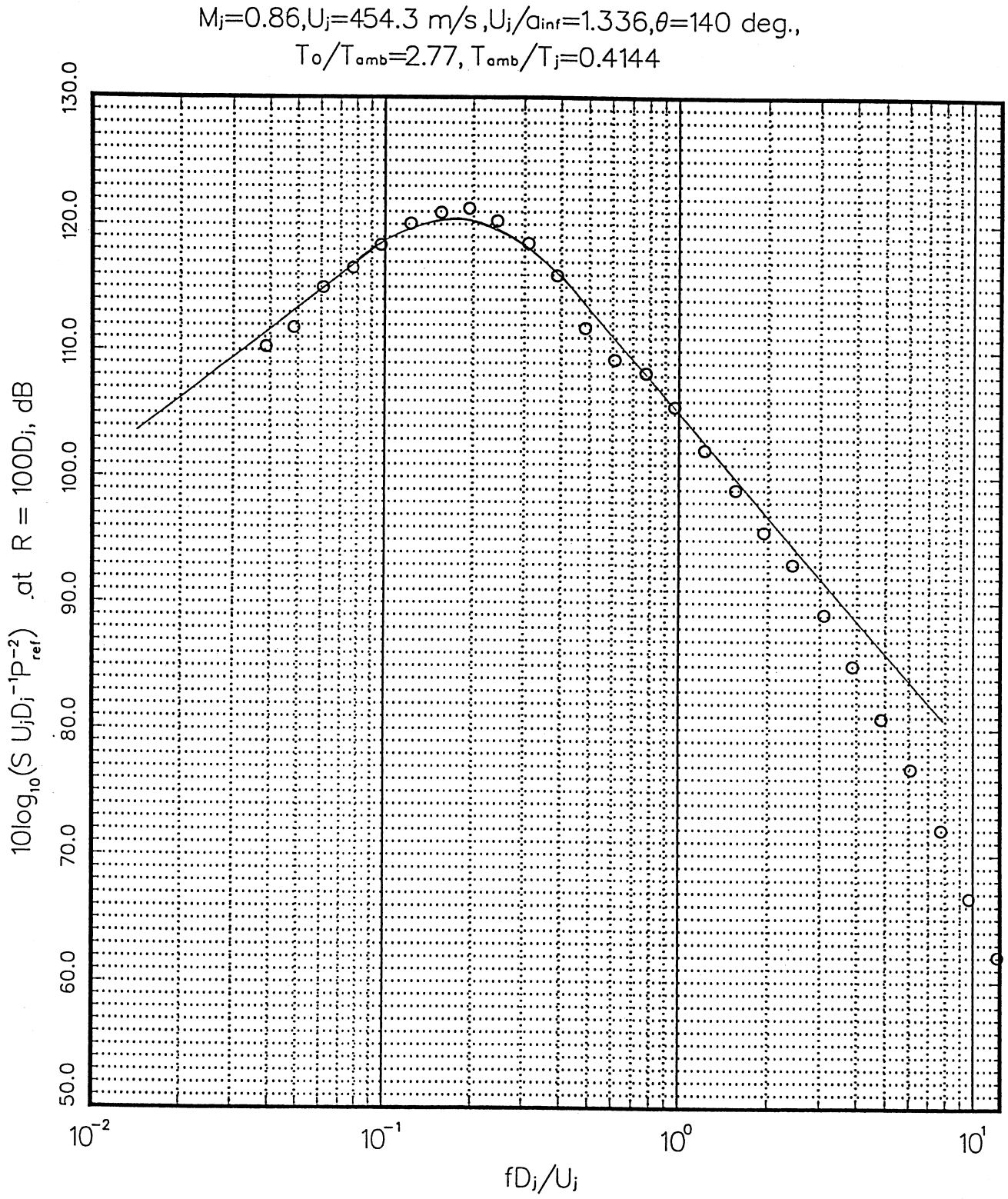
P. A. Lush (Journal of Fluid Mechanics, Vol. 46, 477-500, 1971)


80.0
70.0
60.0
50.0
40.0
30.0
20.0
10.0
0.0
Intensity, dB per Hz
U_j=300 m/s
U_j=195 m/s
U_j=125 m/s
10^2
10^3
10^4
10^5
frequency Hz
θ=90 deg, Lush's data


80.0
70.0
60.0
50.0
40.0
30.0
20.0
10.0
0.0
Intensity, dB per Hz
U_j=300 m/s
U_j=195 m/s
U_j=125 m/s
10^2
10^3
10^4
10^5
frequency Hz
θ=15 deg, Lush's data


Mj=0.86,Uj=454.3 m/s ,Uj/ainf=1.336,θ=90 deg.,
To/Tamb=2.77, Tamb/Tj=0.4144
120.0
110.0
100.0
90.0
80.0
70.0
60.0
50.0
40.0
10log10(S UjDj-1P-2ref) at R = 100Dj, dB
10-2
10-1
100
101
fDj/Uj

Boeing data


M_j=0.86,U_j=454.3 m/s ,U_j/a_{inf}=1.336,θ=140 deg.,
T_o/T_{amb}=2.77, T_{amb}/T_j=0.4144
$10\log_{10}(S\ U_j D_j^{-1} P_{ref}^{-2})$ .at R = 100D_j, dB
130.0
120.0
110.0
100.0
90.0
80.0
70.0
60.0
50.0
10^{-2}
10^{-1}
10^{0}
10^{1}
fD_j/U_j

Boeing data

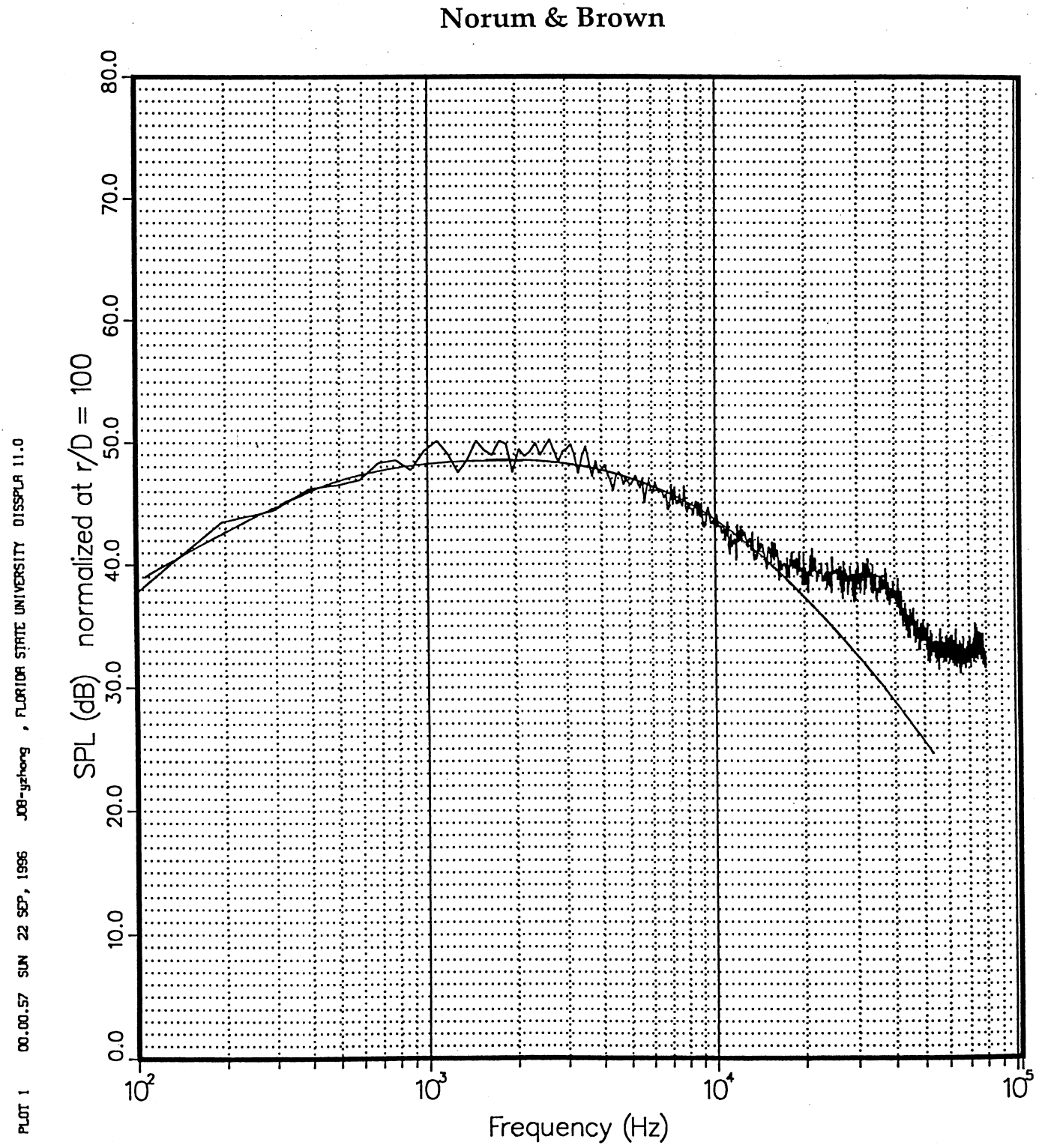
RUN NUMBER : 105 NOZZLE TYPE : 2

Fully Expanded Mach Number : .40 Free Jet Mach Number : .00

Num of Spectral Points : 819 Maximum Frequency :79.980

Bandwidth : .097656 khz Channal Number : 7

Angel From Inlet Axis : 90 deg Oaspl : 70.0



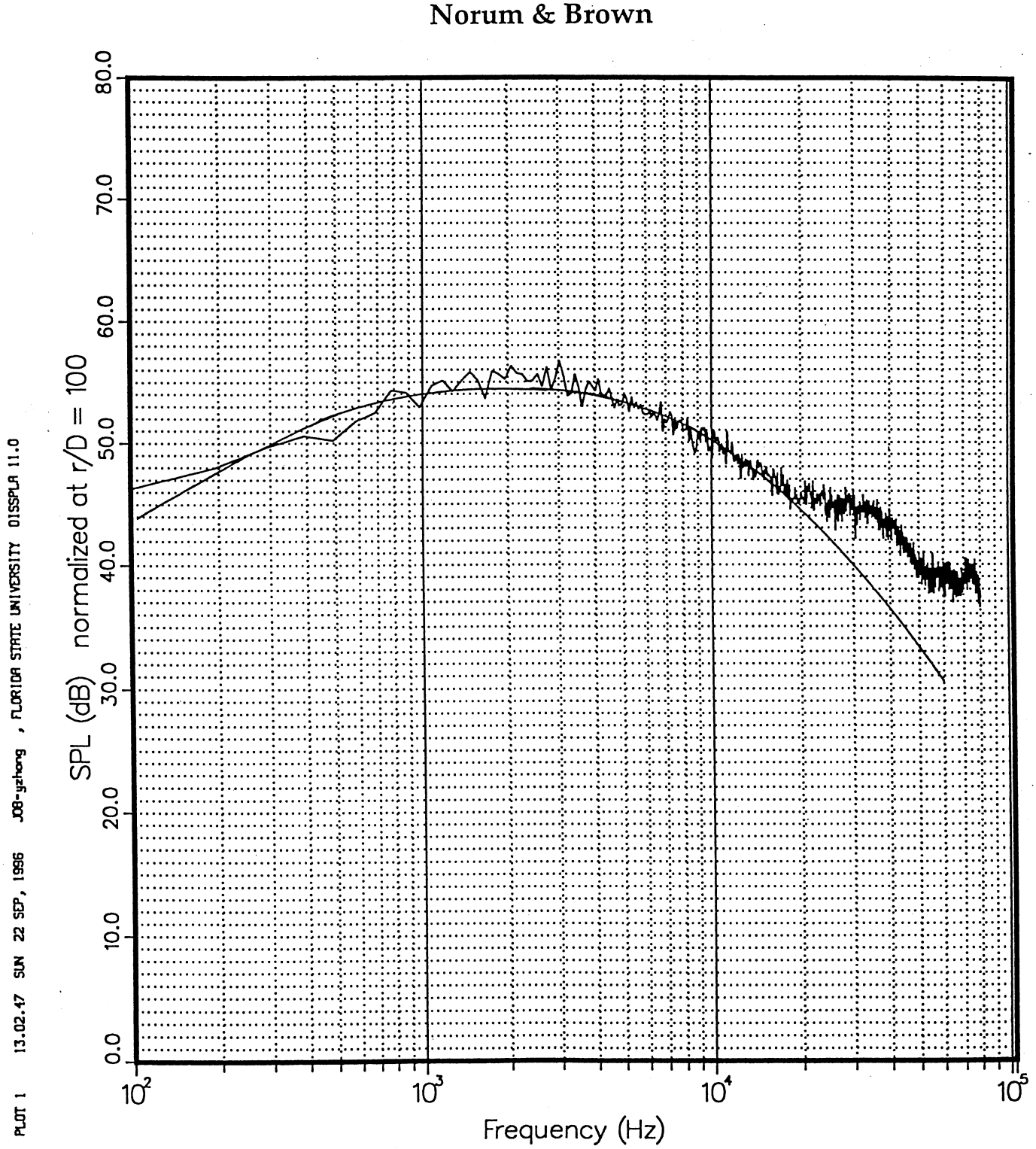
RUN NUMBER : 106 NOZZLE TYPE : 2

Fully Expanded Mach Number : .50 Free Jet Mach Number : .00

Num of Spectral Points : 819 Maximum Frequency :79.980

Bandwidth : .097656 khz Channal Number : 7

Angel From Inlet Axis : 90 deg Oaspl : 76.1



RUN NUMBER : 107 NOZZLE TYPE : 2

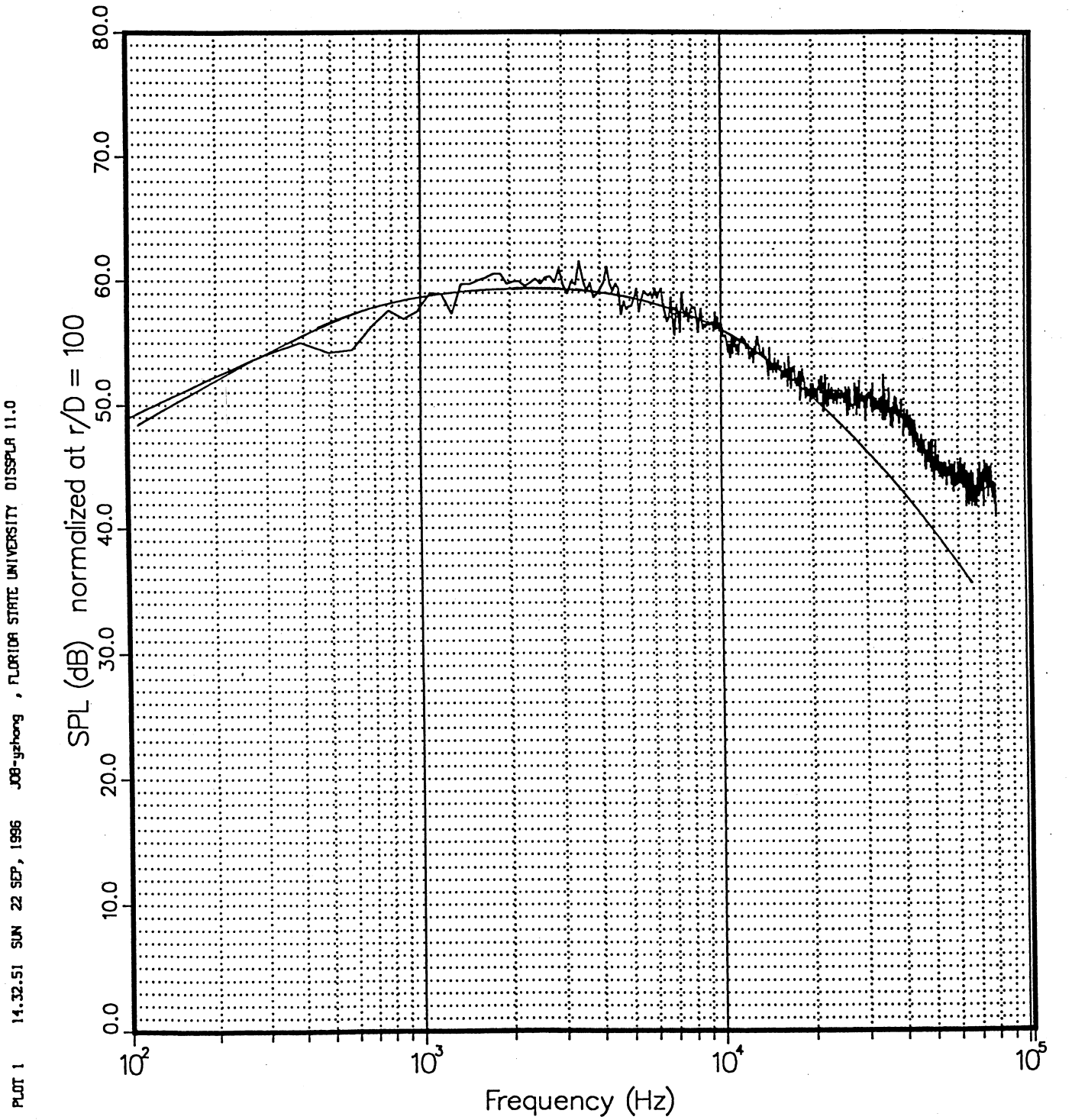
Fully Expanded Mach Number : .60 Free Jet Mach Number : .00

Num of Spectral Points : 819 Maximum Frequency :79.980 khz

Bandwidth : .097656 khz Channal Number : 7

Angel From Inlet Axis : 90 deg Oaspl : 81.4 dB

Norum & Brown



RUN NUMBER : 108 NOZZLE TYPE : 2

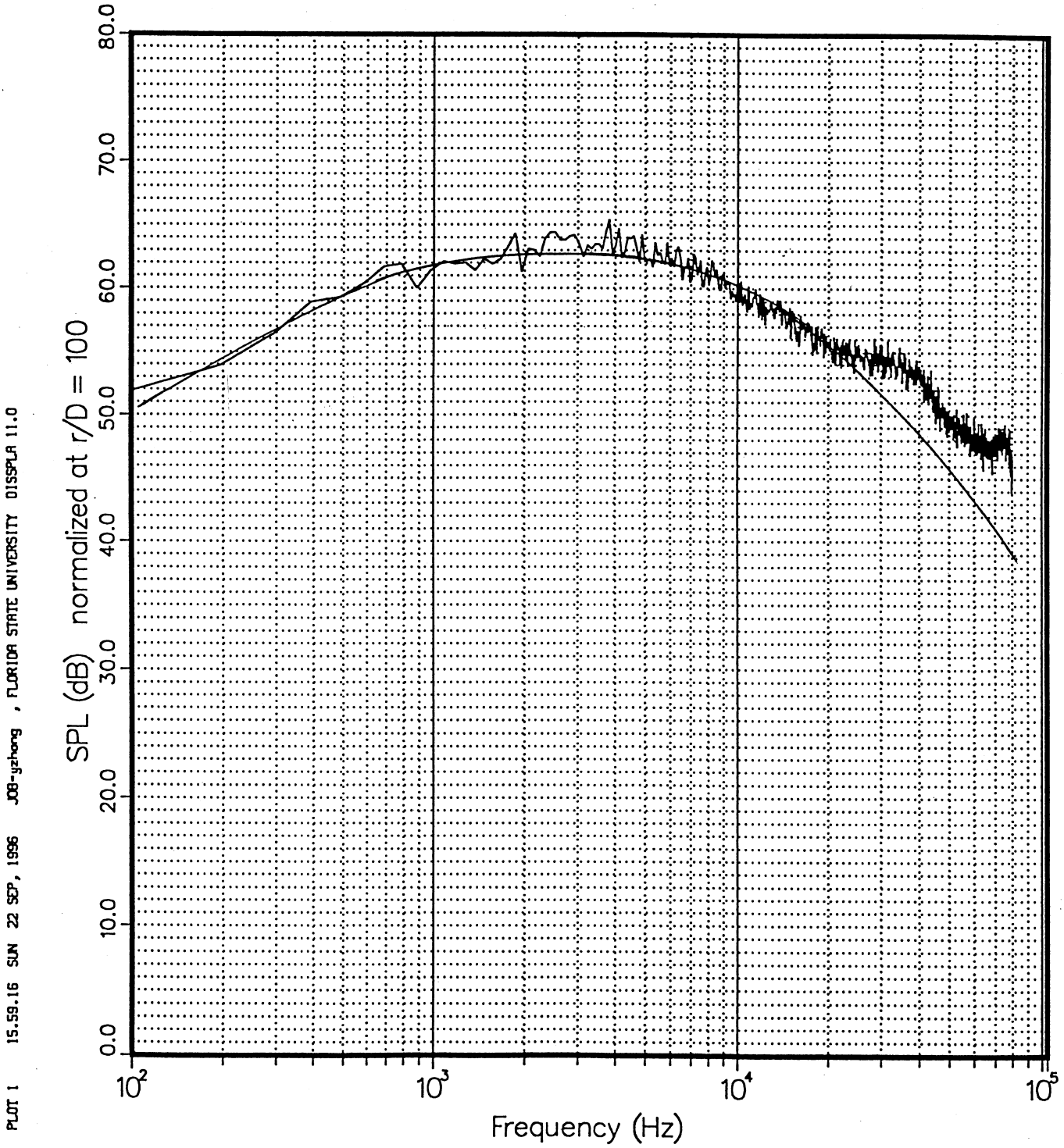
Fully Expanded Mach Number : .70 Free Jet Mach Number : .00

Num of Spectral Points : 819 Maximum Frequency :79.980 khz

Bandwidth : .097656 khz Channal Number : 7

Angel From Inlet Axis : 90 deg Oaspl : 85.4 dB

Norum & Brown



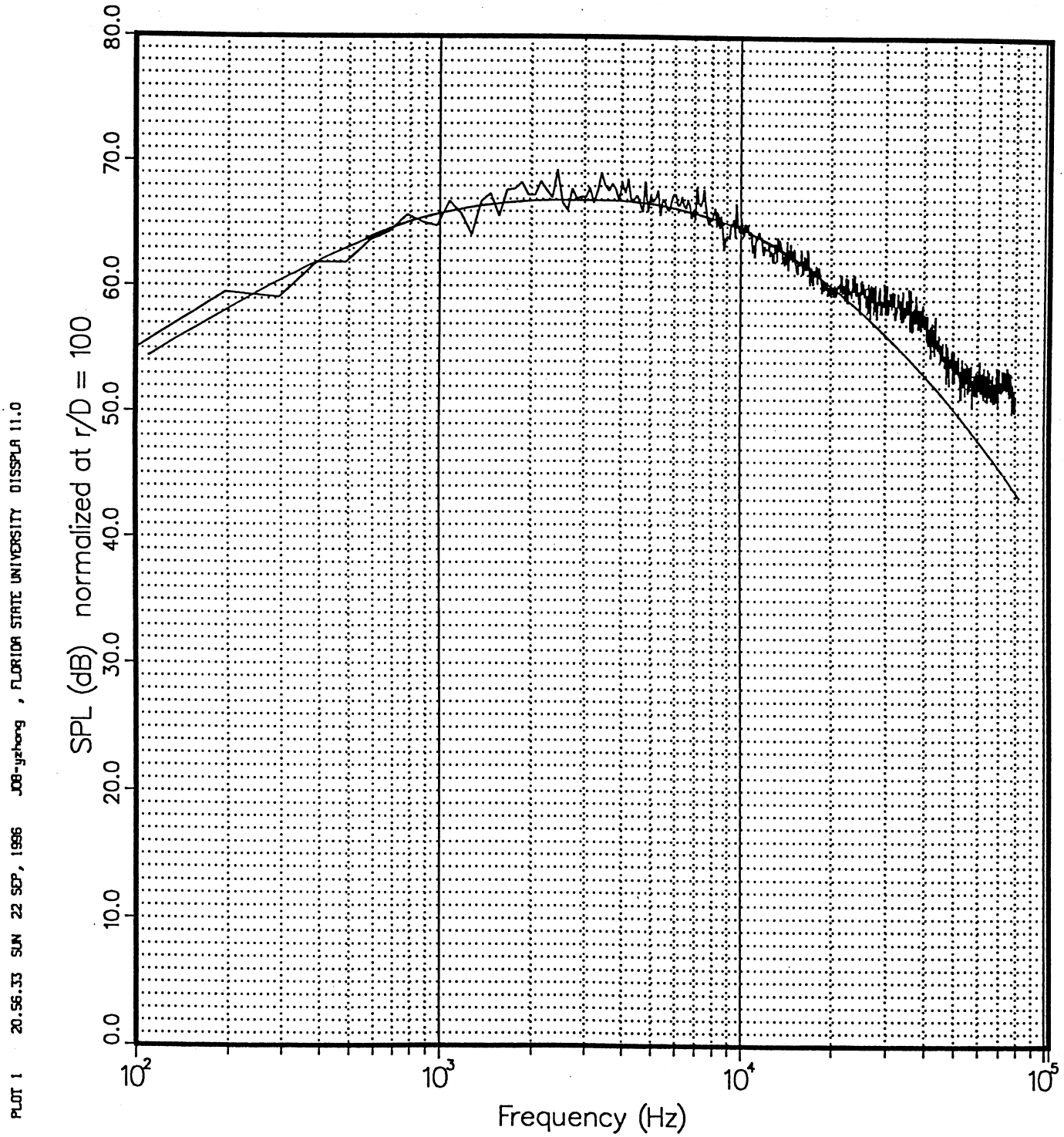
RUN NUMBER : 109

Fully Expanded Mach Number : .80
Num of Spectral Points : 819
Bandwidth : .097656 khz
Angel From Inlet Axis : 90 deg

NOZZLE TYPE : 2

Free Jet Mach Number : .00
Maximum Frequency :79.980 khz
Channal Number : 7
Oaspl : 89.8 dB

Norum & Brown



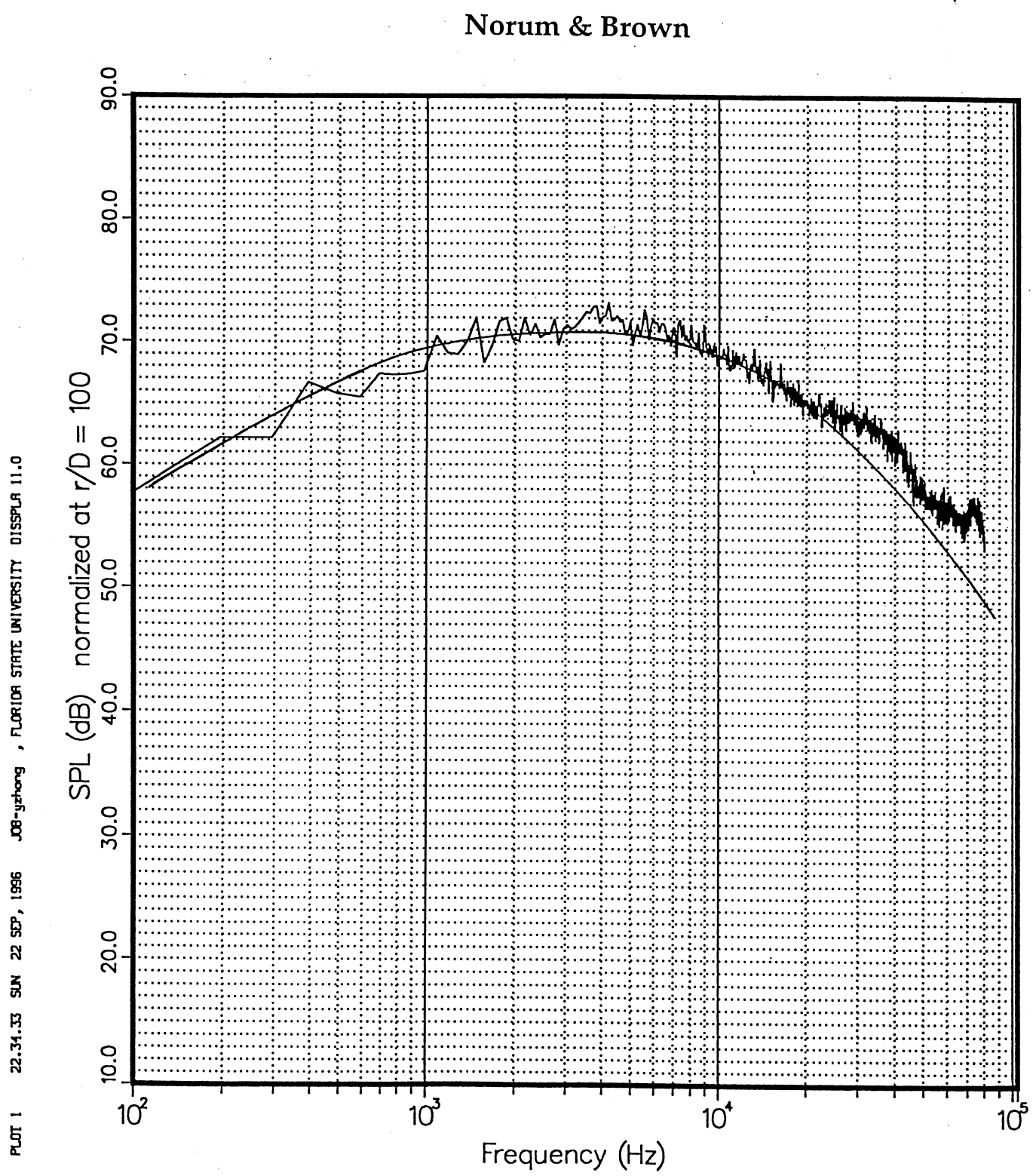
RUN NUMBER : 110 NOZZLE TYPE : 2

Fully Expanded Mach Number : .90 Free Jet Mach Number : .00

Num of Spectral Points : 819 Maximum Frequency :79.980 khz

Bandwidth : .097656 khz Channal Number : 7

Angel From Inlet Axis : 90 deg Oaspl : 94.3 dB



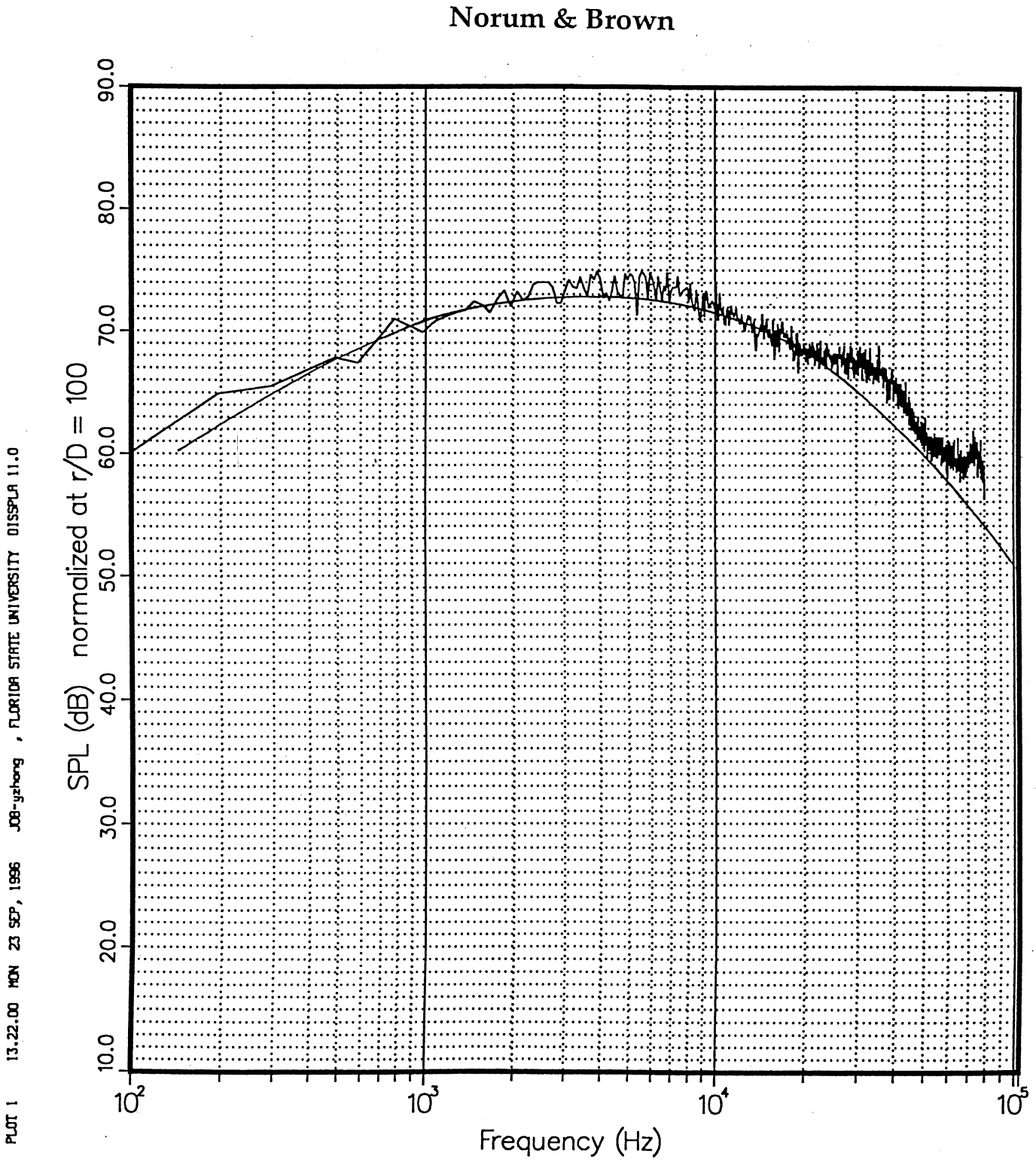
RUN NUMBER : 111 NOZZLE TYPE : 2

Fully Expanded Mach Number : 1.00 Free Jet Mach Number : .00

Num of Spectral Points : 819 Maximum Frequency :79.980 khz

Bandwidth : .097656 khz Channal Number : 7

Angel From Inlet Axis : 90 deg Oaspl : 97.2 dB



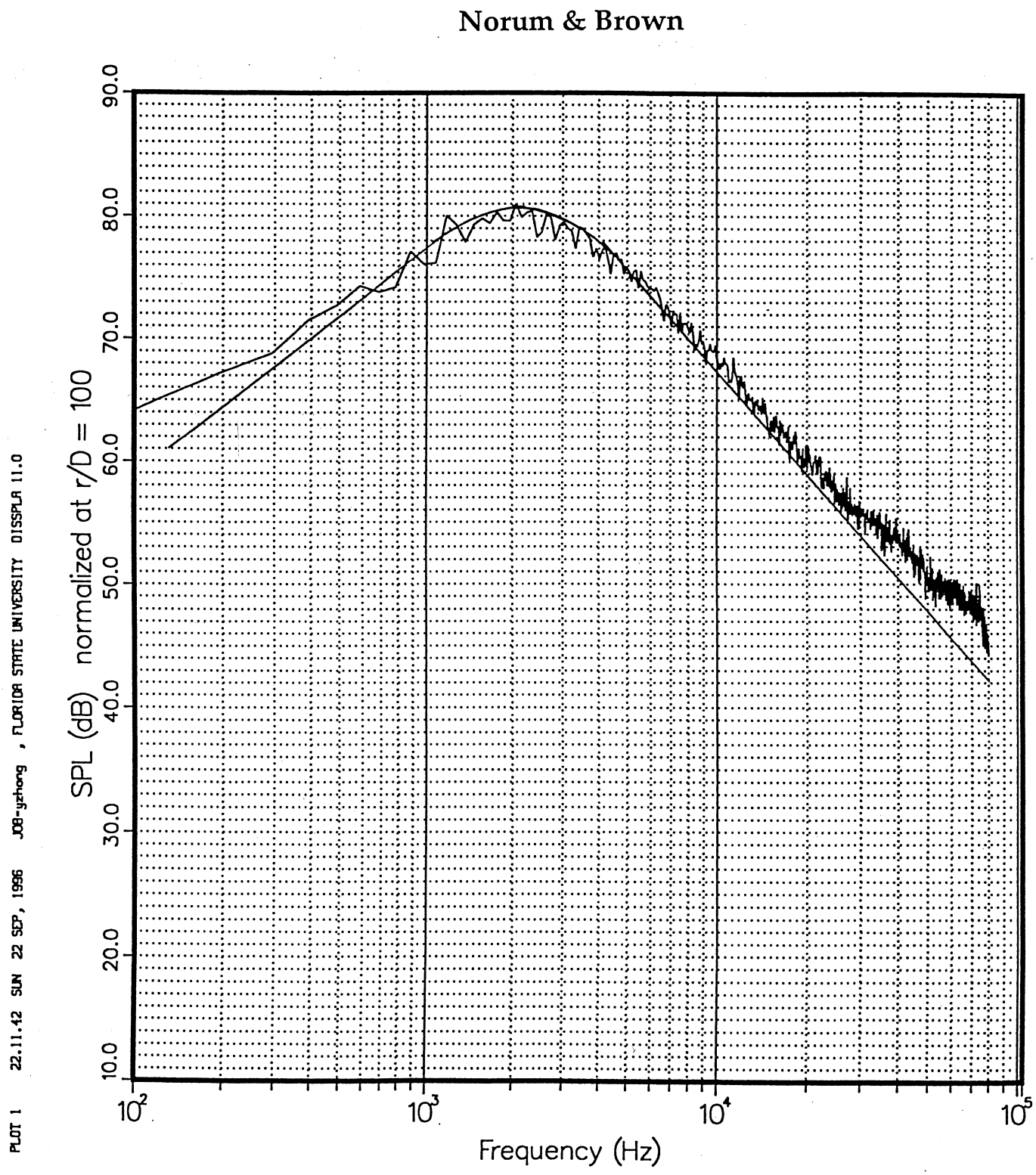
RUN NUMBER : 109 NOZZLE TYPE : 2

Fully Expanded Mach Number : .80 Free Jet Mach Number : .00

Num of Spectral Points : 819 Maximum Frequency :79.980 khz

Bandwidth : .097656 khz Channal Number :13

Angel From Inlet Axis :150 deg Oaspl : 96.9 dB



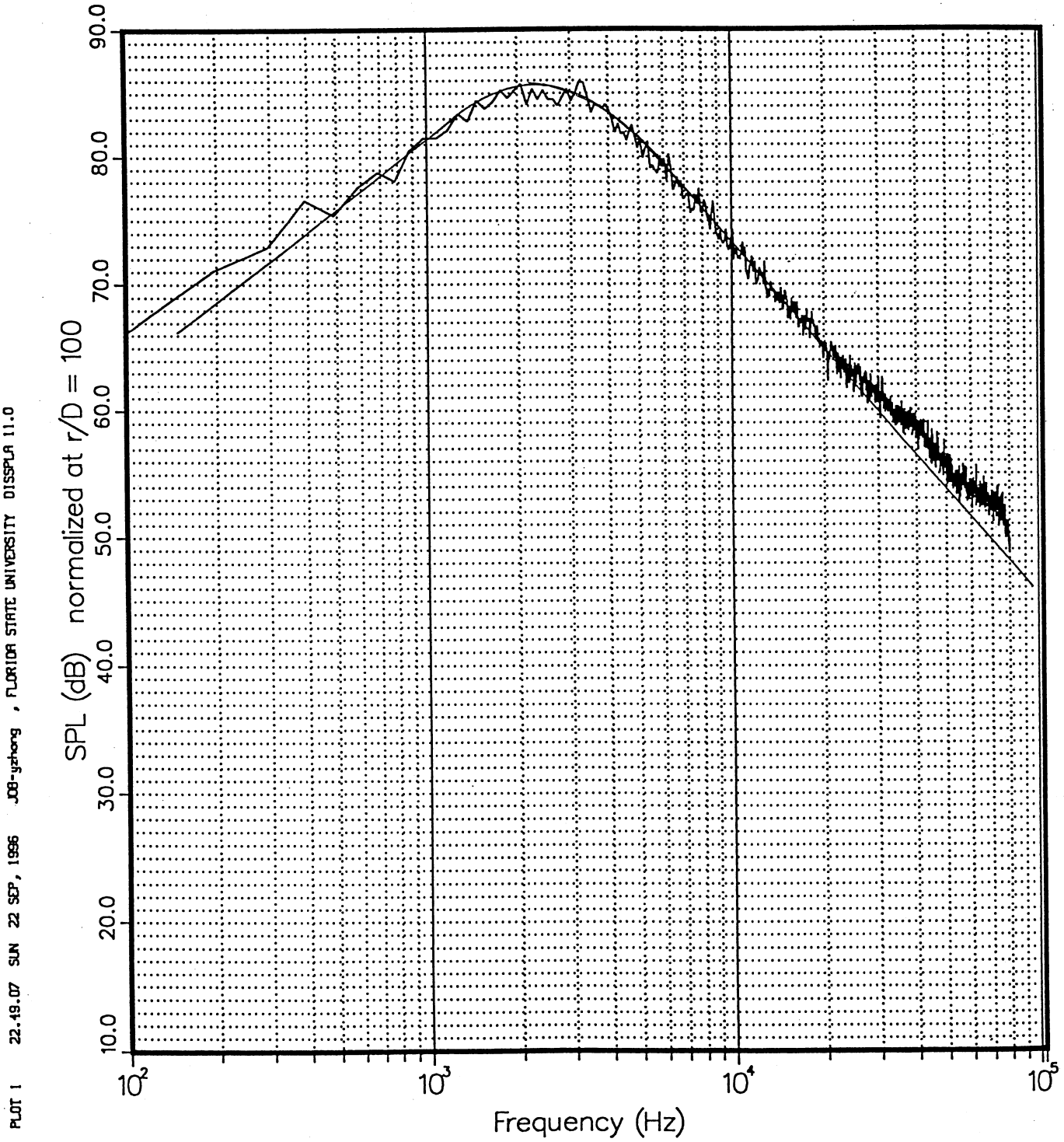
RUN NUMBER : 110

Fully Expanded Mach Number : .90
Num of Spectral Points : 819
Bandwidth : .097656 khz
Angel From Inlet Axis :150 deg

NOZZLE TYPE : 2

Free Jet Mach Number : .00
Maximum Frequency :79.980 khz
Channal Number :13
Oaspl :102.1 dB

Norum & Brown

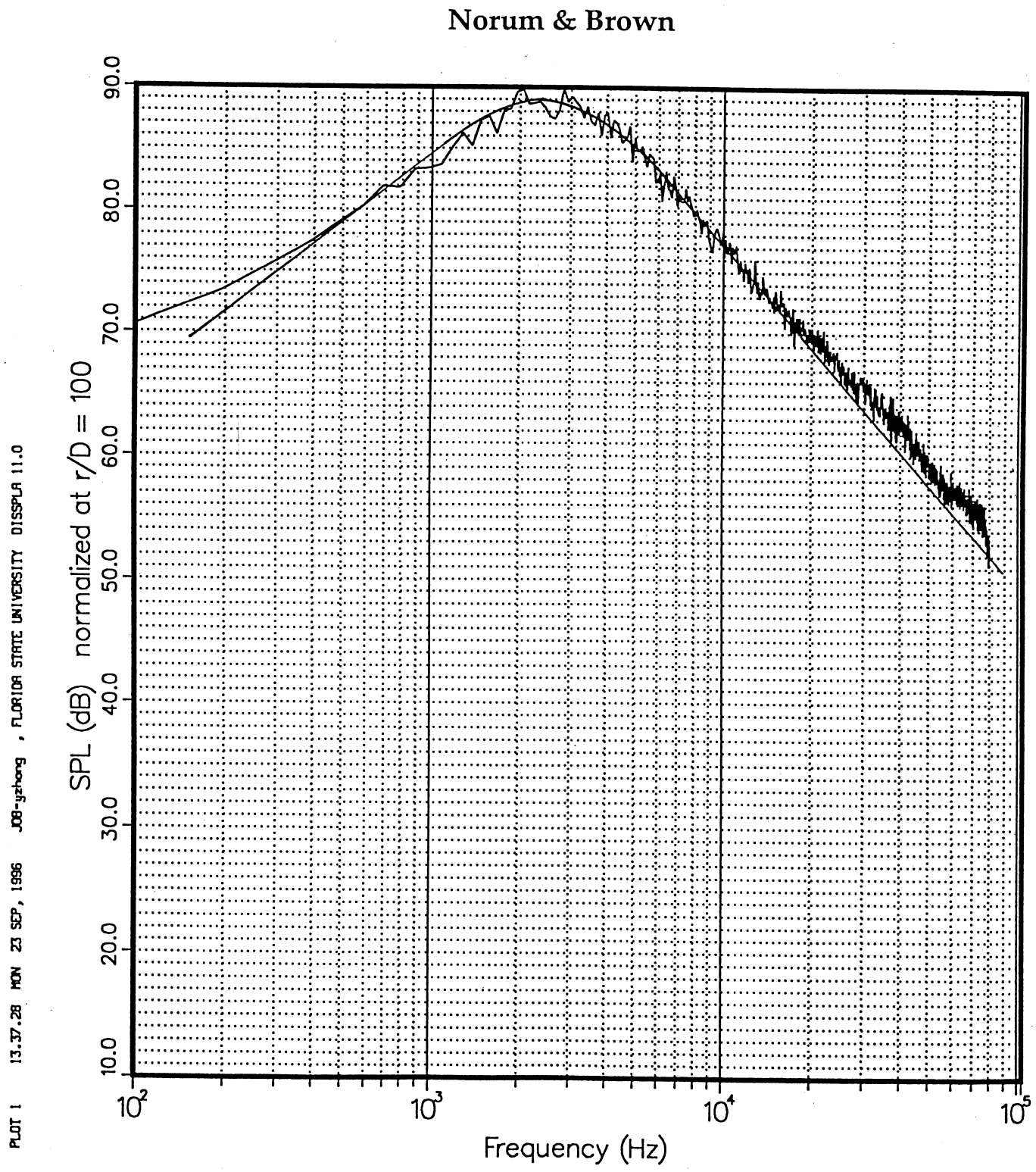


RUN NUMBER : 111

Fully Expanded Mach Number : 1.00
Num of Spectral Points : 819
Bandwidth : .097656 khz
Angel From Inlet Axis :150 deg

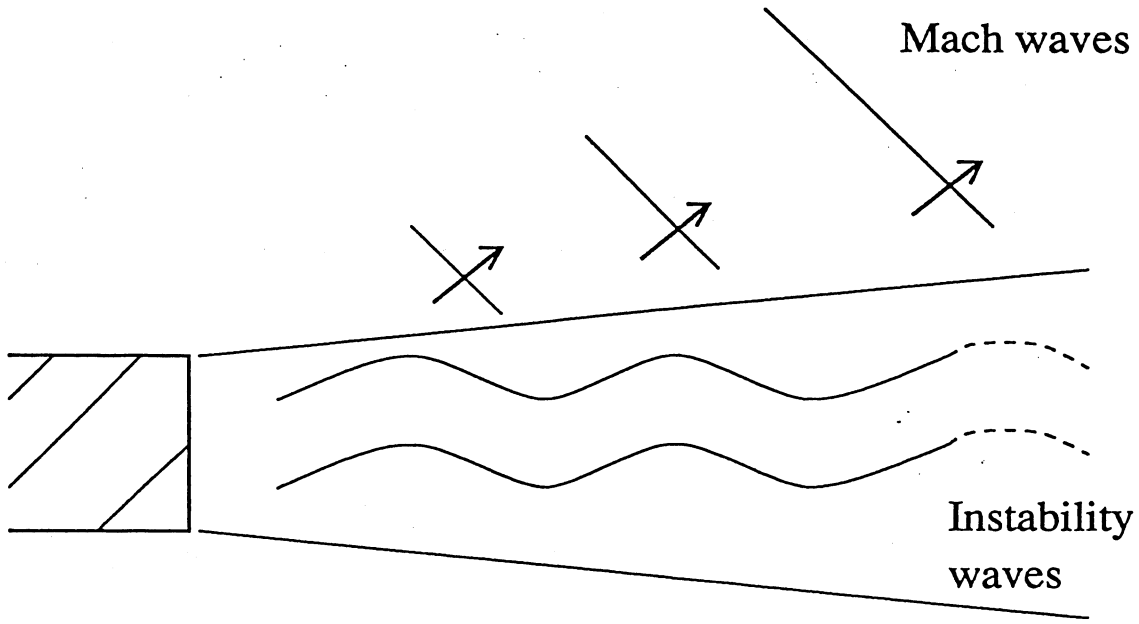
NOZZLE TYPE : 2

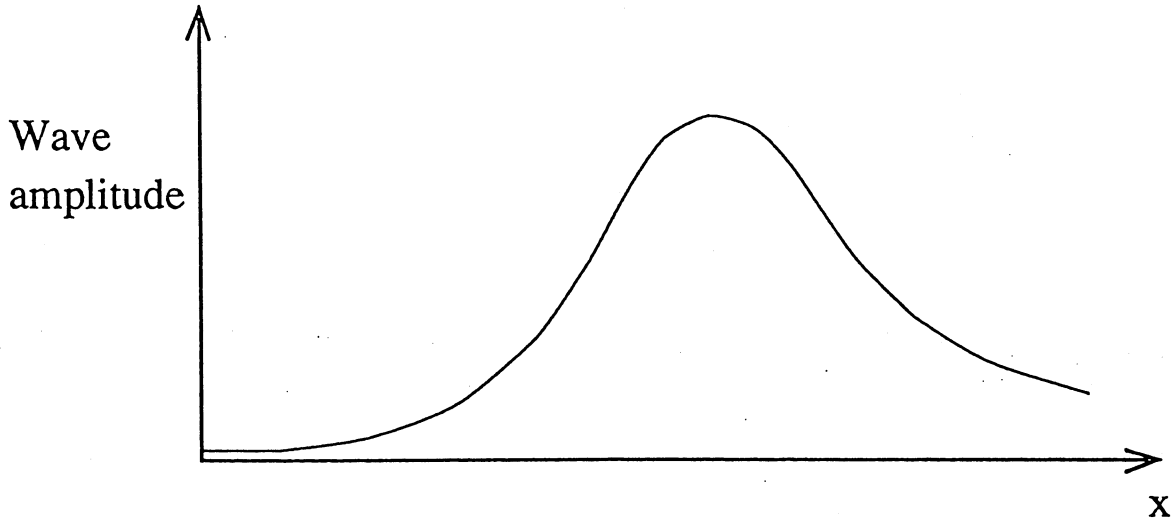
Free Jet Mach Number : .00
Maximum Frequency :79.980 khz
Channal Number :13
Oaspl :105.8 dB



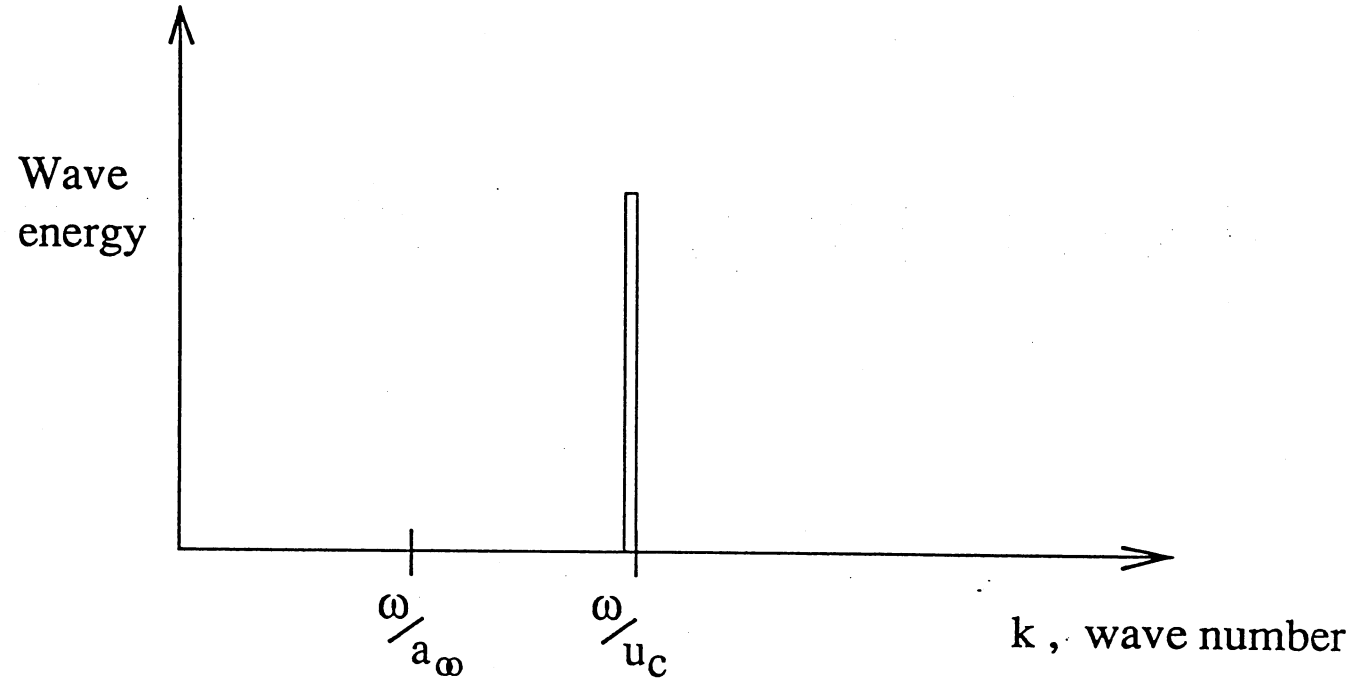
How can subsonic jets generate Mach wave radiation ?

GENERATION OF MACH WAVE RADIATION

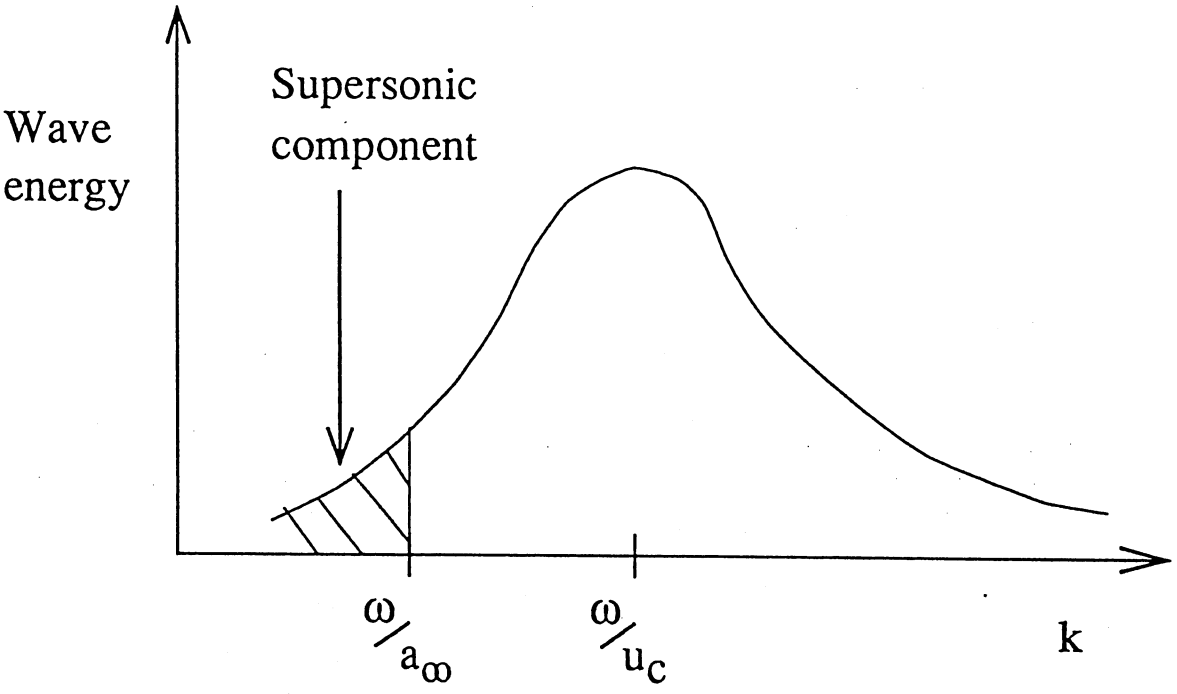




Spatial distribution of instability wave amplitude



Wave number spectrum of a constant amplitude wave



Wave number spectrum including amplitude variation

Are the turbulent mixing noise generation mechanisms the same for subsonic as well as for supersonic jets ?

SCALING LAWS FROM THE ACOUSTIC ANALOGY THEORY

SUBSONIC JETS

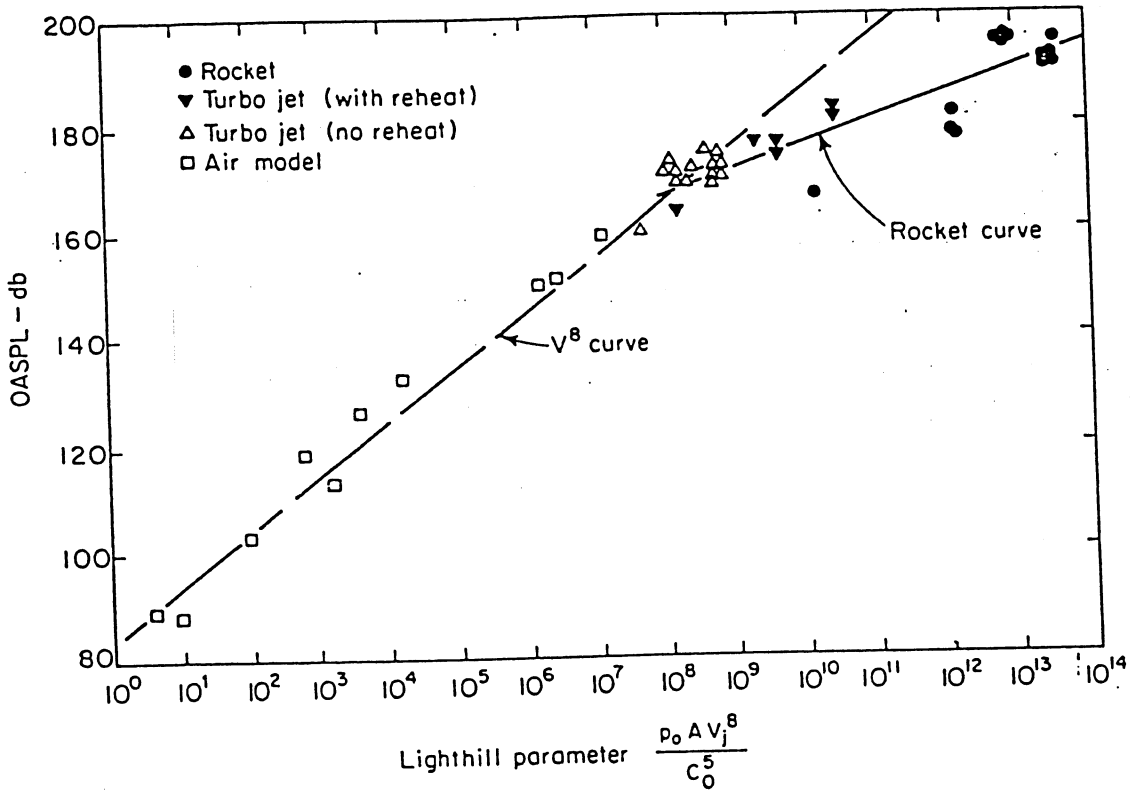
LIGHTHILL $I \alpha V^8$

SUPERSONIC JETS

FfOWCS WILLIAMS $I \alpha V^3$

Lighthill $I \alpha V^8 : M_j < 1.0$

Ffowcs-Williams $I \alpha V^3 : M_j > 1.0$



Overall sound pressure level from various jets as a function of the Lighthill jet velocity parameter (after von Gierke[4]).

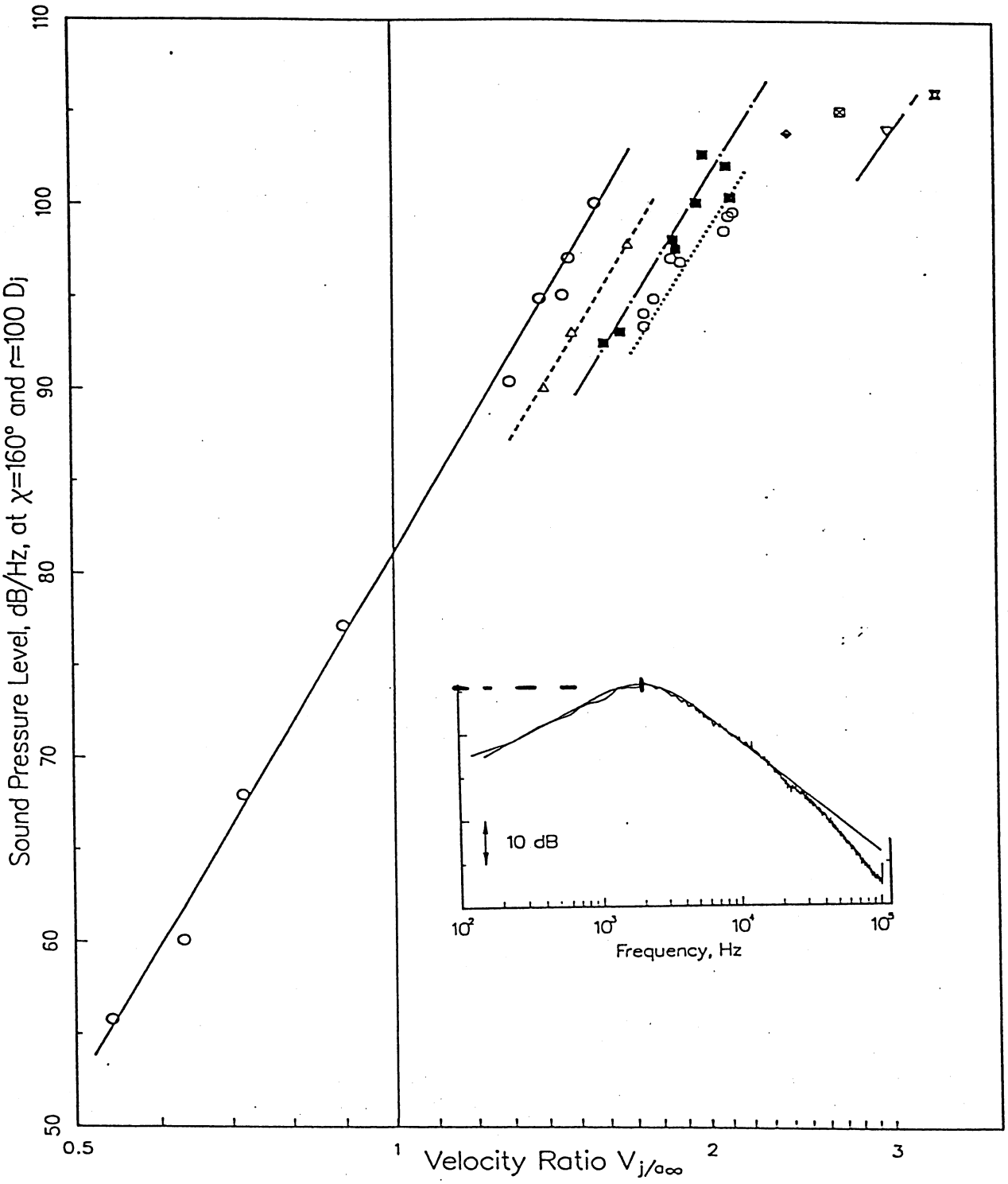


Figure 8. Variation of the peak amplitude of the noise spectrum of large turbulence structures/instability waves at $\chi = 160°$ with jet velocity and temperature ratios.

T_r/T_∞	1.0	1.4	1.8	2.2	2.7	3.3	4.1	4.9
measurements	o	△	■	o	◆	⊠	▽	⧓
Equation (7)	———	- - - - -	— · —	·····			— - —	

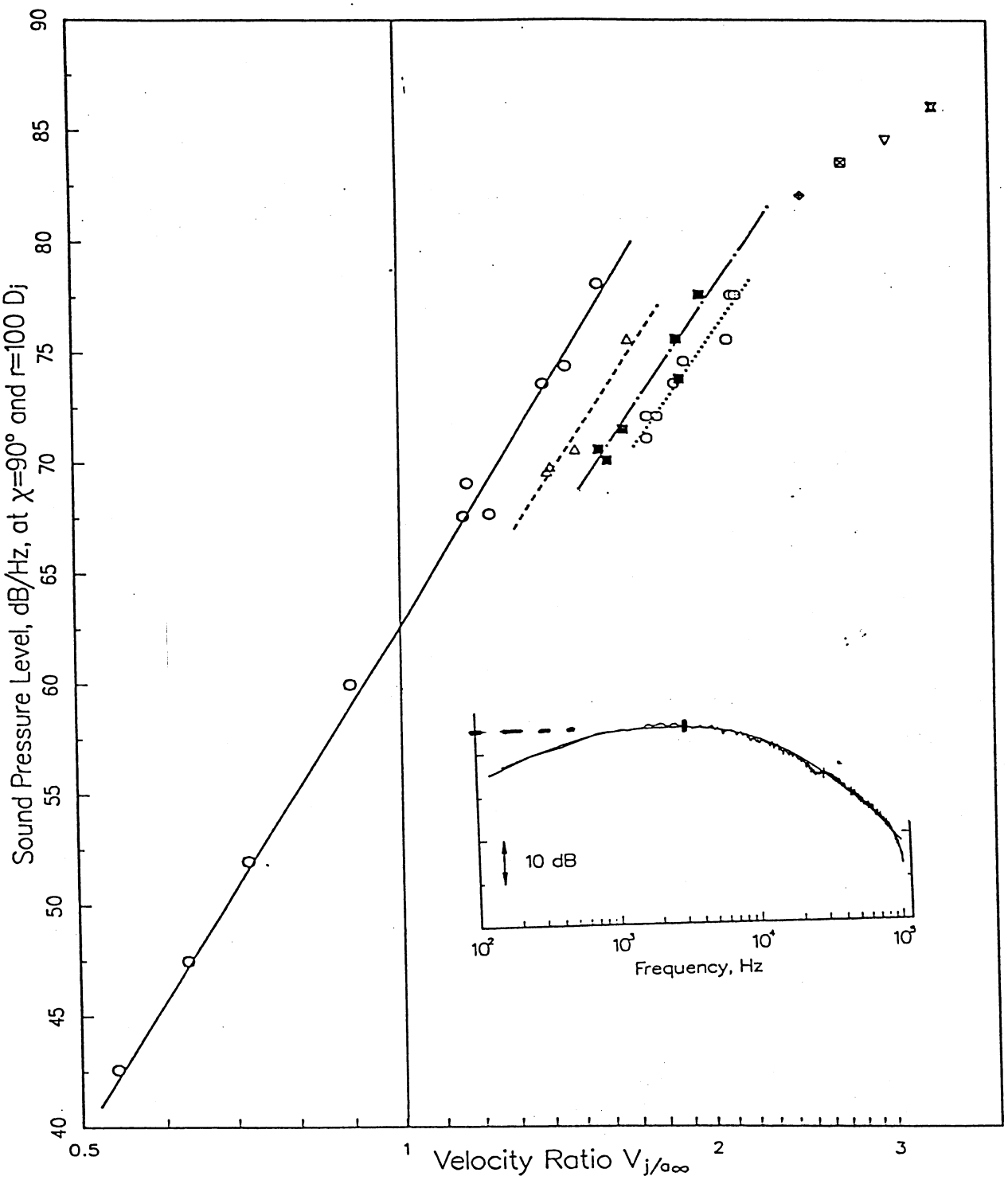


Figure 9. Variation of the peak amplitude of the noise spectrum of fine scale turbulence at $\chi = 90°$ with jet velocity and temperature ratios.

T_r/T_∞	1.0	1.4	1.8	2.2	2.7	3.3	4.1	4.9
measurements	o	△	■	○	◆	⊠	▽	⧓
Equation (9)	———	- - - - -	—·—	·····			—·—	

Conclusions

1. There are ample experimental evidence indicating that turbulent jet mixing noise is made up of two basic components. They are the large turbulence structures noise and the fine scale turbulence noise. The large turbulence structures noise dominates in the downstream directions. The fine scale turbulence noise dominates in the sideline and forward directions.

2. Jet noise appears to fit well by two seemingly universal empirical spectra regardless of jet Mach number, jet temperature, direction of radiation and to a great degree nozzle configuration.

Minor points :

- Noise generation mechanisms are the same for supersonic and subsonic jets.
- $I \alpha V^3$ scaling law is not supported by experiments

Part 2. New Theory and Comparisons with Experiments

JET NOISE PREDICTION THEORY

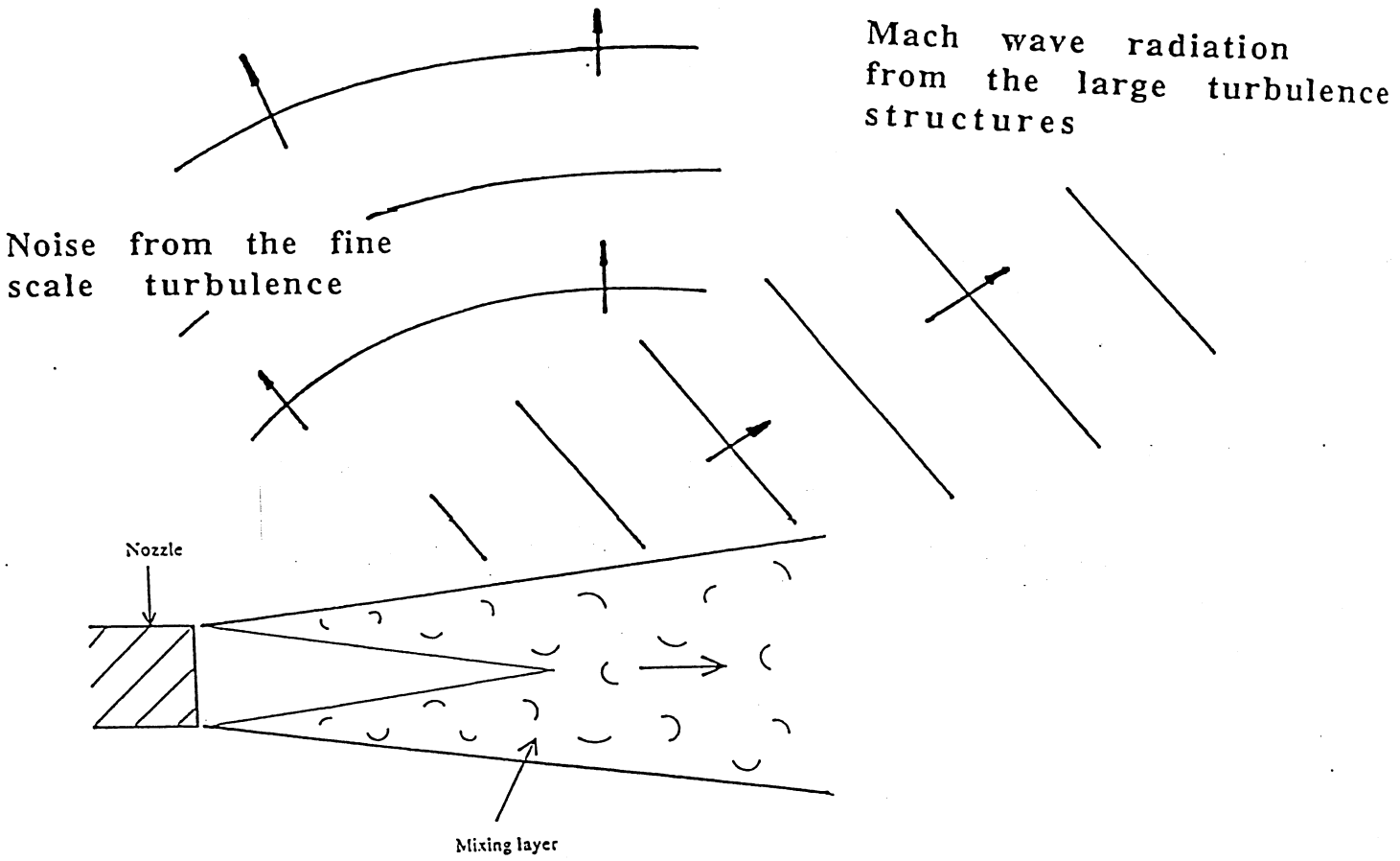
Tam & Auriault, " Jet mixing noise from fine-scale turbulence ", AIAA Journal, vol 37, p.145, 1999.

This theory is based on that the fine-scale turbulence of the jet flow is the source of noise (for the sideline and the forward directions).

Theory includes :

1. Mean flow refraction effect.
2. Convective amplification due to noise source in motion.

This theory can be extended to include forward flight effects and to jets with arbitrary plume geometry.


Mach wave radiation from the large turbulence structures
Noise from the fine scale turbulence
Nozzle
Mixing layer

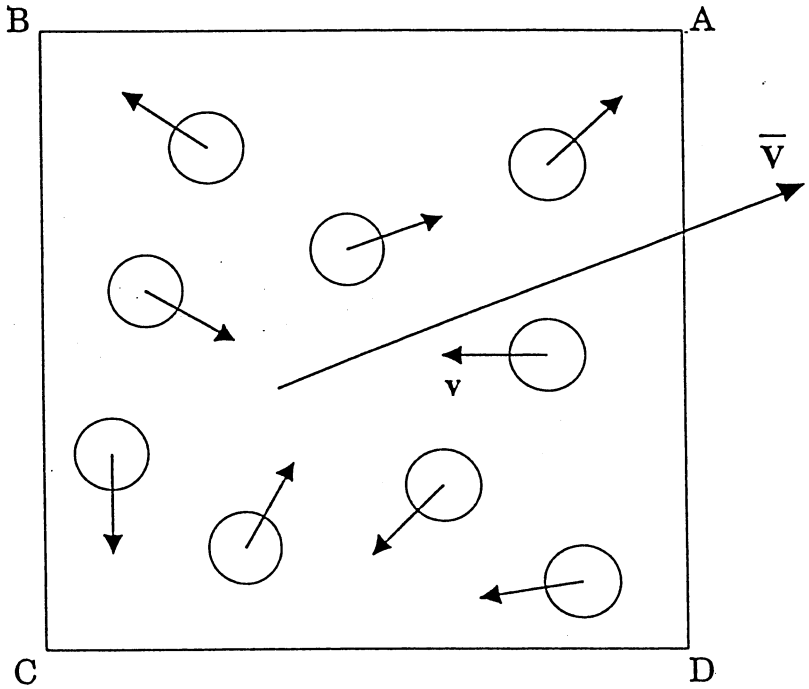
How does fine scale turbulence generate noise ?

Sound is pressure fluctuations.

How does fine scale turbulence produce pressure fluctuations in a jet ?

Pressure is a macroscopic variable.

Gas Kinetic Theory provides a physical description of pressure in macroscopic scale.

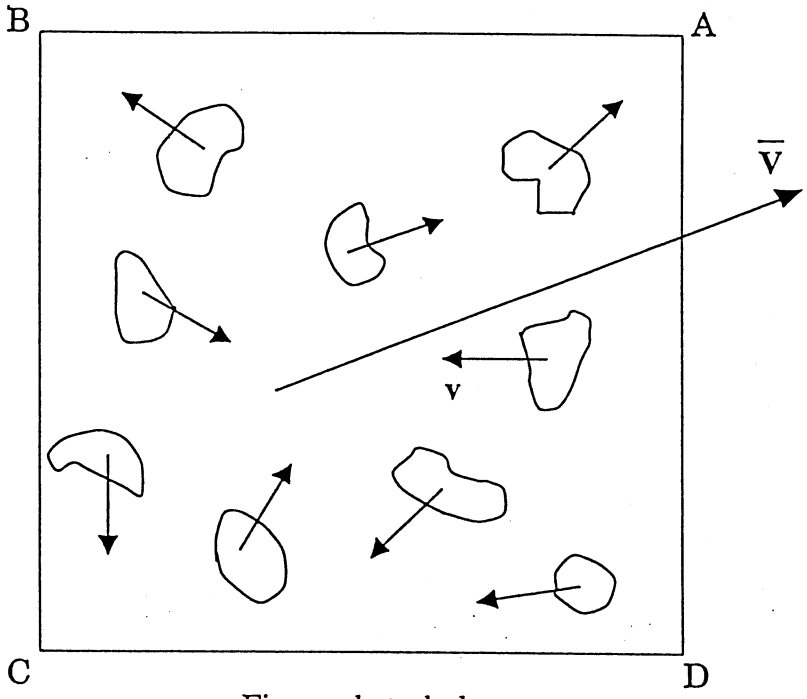


Gas molecules

$$p = \frac{1}{3} mn\langle \mathbf{v} \cdot \mathbf{v} \rangle = \frac{1}{3} \rho \langle v^2 \rangle$$

Fine scale turbulence consists of blobs of locally correlated fluid at random motion.

With respect to length scales larger than the blobs of fine scale turbulence but much less than that of the mean flow, the fine scale turbulence exerts a pressure on its surroundings.



Fine scale turbulence

$$p_{\text{turb}} = q_s \equiv \frac{1}{3}\rho\langle v^2\rangle = \frac{2}{3}\rho k_s$$

Changes in q_s or k_s will lead to unsteady pressure fluctuations and hence sound.

Expect the source of sound in turbulent flows to be

$$\frac{Dq_s}{Dt}$$

By ignoring the viscous and eddy viscous terms, and adopting the locally parallel flow approximation, the acoustic field equations are :

$$\overline{\rho}\left[\frac{\partial u_i}{\partial t}+\overline{u}_j\frac{\partial u_i}{\partial x_j}+u_i\frac{\partial \overline{u}_j}{\partial x_j}\right]+\frac{\partial p}{\partial x_i}=-\frac{\partial q_s}{\partial x_i}$$

$$q_s=\frac{2}{3}\overline{\rho}\,\widehat{k}_s$$

Formal Derivation

Reynolds Averaged Navier-Stokes Equation

$$\overline{\rho}\left(\frac{\partial \widetilde{u}_i}{\partial t}+\widetilde{u}_j\frac{\partial \widetilde{u}_i}{\partial x_j}\right)=-\frac{\partial \overline{p}}{\partial x_i}+\frac{\partial}{\partial x_j}\left(-\overline{\rho u_i'' u_j''}+\overline{\tau}_{ij}\right)$$

~ Favre Average ; $\overline{\ }$ Reynolds Average

Boussinesq eddy viscosity model

$$-\overline{\rho u_i'' u_j''}=2\mu_t\left(S_{ij}-\frac{1}{3}\Delta\delta_{ij}\right)-\frac{2}{3}\overline{\rho}\,k_s\delta_{ij}$$

$$S_{ij}=\frac{1}{2}\left(\frac{\partial \widetilde{u}_i}{\partial x_j}+\frac{\partial \widetilde{u}_j}{\partial x_i}\right),\quad \Delta=\frac{\partial \widetilde{u}_k}{\partial x_k}$$

$$\overline{\rho u_i'' u_i''}=2\overline{\rho}\,k_s$$

With respect to a cylindrical coordinate system (r, ϕ, x) centered at the nozzle exit the full set of governing equations are,

$$\overline{\rho}\left[\frac{\partial u}{\partial t} + \overline{u}\frac{\partial u}{\partial x} + v\frac{d\overline{u}}{dr}\right] + \frac{\partial p}{\partial x} = -\frac{\partial q_s}{\partial x} \qquad (10a)$$

$$\overline{\rho}\left[\frac{\partial v}{\partial t} + \overline{u}\frac{\partial v}{\partial x}\right] + \frac{\partial p}{\partial r} = -\frac{\partial q_s}{\partial r} \qquad (10b)$$

$$\overline{\rho}\left[\frac{\partial w}{\partial t} + \overline{u}\frac{\partial w}{\partial x}\right] + \frac{1}{r}\frac{\partial p}{\partial \phi} = -\frac{1}{r}\frac{\partial q_s}{\partial \phi} \qquad (10c)$$

$$\frac{\partial p}{\partial t} + \overline{u}\frac{\partial p}{\partial x} + \gamma\overline{p}\left[\frac{1}{r}\frac{\partial (vr)}{\partial r} + \frac{1}{r}\frac{\partial w}{\partial \phi} + \frac{\partial u}{\partial x}\right] = 0. \qquad (10d)$$

account for the mean flow refraction effect.

The pressure fields of the three original time harmonic Green's function are related to the adjoint Green's function by

$$\widehat{p}_1(\mathbf{x}, \mathbf{x}_1, \omega) = u_a(\mathbf{x}_1, \mathbf{x}, \omega)$$

$$\widehat{p}_2(\mathbf{x}, \mathbf{x}_1, \omega) = v_a(\mathbf{x}_1, \mathbf{x}, \omega)$$

$$\widehat{p}_3(\mathbf{x}, \mathbf{x}_1, \omega) = w_a(\mathbf{x}_1, \mathbf{x}, \omega).$$

the pressure field generated by the source terms on the right side of (10a) to (10d) is formally given by,

$$p(\mathbf{x}, t) = -\int_{-\infty}^{\infty}\int\int\int\int\int\int \left[u_a(\mathbf{x}_1, \mathbf{x}, \omega)\frac{\partial q_s(\mathbf{x}_1, t_1)}{\partial x_1} + v_a(\mathbf{x}_1, \mathbf{x}, \omega)\frac{\partial q_s(\mathbf{x}_1, t_1)}{\partial r_1}\right.$$

$$\left. + \frac{w_a(\mathbf{x}_1, \mathbf{x}, \omega)}{r}\frac{\partial q_s(\mathbf{x}_1, t_1)}{\partial \phi}\right] e^{-i\omega(t-t_1)} d\omega\, dt_1\, d\mathbf{x}_1 .$$

By integration by parts and the pressure equation of the adjoint Green's function, the pressure field produced by the time fluctuating fine scale turbulence intensity may be written in the form,

$$p(\mathbf{x},t) = -\int\int\int_{-\infty}^{\infty}\int\int\int q_s(\mathbf{x}_1,t_1)\left[\left(\frac{\partial}{\partial t_1}+\overline{u}\,\frac{\partial}{\partial x_1}\right)p_a e^{-i\omega(t-t_1)}d\omega\right]dt_1 d$$

Finally, by simple integration by parts, we find

$$p(\mathbf{x},t) = \int\int\int_{-\infty}^{\infty}\int\int\int\left[\int_{-\infty}^{\infty} p_a(\mathbf{x}_1,\mathbf{x},\omega)e^{-i\omega(t-t_1)}d\omega\right]\frac{Dq_s(\mathbf{x}_1,t_1)}{Dt_1}dt_1 d$$

x outside the jet

where $\frac{D}{Dt_1} = \frac{\partial}{\partial t_1} + \overline{u}\,\frac{\partial}{\partial x_1}$ is the convective derivative

noise from fine scale turbulence is generated by the time rate of change of the turbulence kinetic energy in the moving frame

The Spectral Density of the Radiated Sound

the autocorrelation function for a point in the acoustic far field

$$\langle p(\mathbf{x},t)p(\mathbf{x},t+\tau)\rangle =$$

$$\int_{-\infty}^{\infty}\cdots\iint p_a(\mathbf{x}_1,\mathbf{x},\omega_1)p_a(\mathbf{x}_2,\mathbf{x},\omega_2)\left\langle \frac{Dq_s(\mathbf{x}_1,t_1)}{Dt_1}\frac{Dq_s(\mathbf{x}_2,t_2)}{Dt_2}\right\rangle$$

$$\cdot\, e^{-i\omega_1(t-t_1)-i\omega_2(t-t_2)-i\omega_2\tau}d\omega_1 d\omega_2 dt_1 dt_2 d\mathbf{x}_1\, d\mathbf{x}_2\,.$$

$\langle\ \ \rangle$ is the ensemble average.

The spectral density of the radiated sound, $S(\mathbf{x},\omega)$ is the Fourie transform of the autocorrelation function

$$S(\mathbf{x},\omega)=\frac{1}{2\pi}\int_{-\infty}^{\infty}\langle p(\mathbf{x},t)p(\mathbf{x},t+\tau)\rangle e^{i\omega\tau}d\tau.$$

By using $\int_{-\infty}^{\infty} \exp[i(\omega-\omega_2)\tau]d\tau = 2\pi\delta(\omega-\omega_2)$,

it is straightforward to derive

$$S(\mathbf{x},\omega) = \int\!\!\int_{-\infty}^{\infty}\cdots\int\!\!\int p_a(\mathbf{x}_1,\mathbf{x},\omega_1)p_a(\mathbf{x}_2,\mathbf{x},\omega_2)\left\langle \frac{Dq_s(\mathbf{x}_1,t_1)}{Dt_1}\frac{Dq_s(\mathbf{x}_2,t_2)}{Dt_2}\right.$$

$$\left. \cdot\, e^{-i(\omega_1+\omega_2)t+i\omega_1 t_1+i\omega_2 t_2}\delta(\omega-\omega_2)d\omega_1 d\omega_2 dt_1 dt_2 d\mathbf{x}_1 d\mathbf{x}_2 \right.$$

To proceed further, we need a mathematical representation of th noise source space-time correlation function $\left\langle \frac{Dq_s(\mathbf{x}_1,t_1)}{Dt_1}\frac{Dq_s(\mathbf{x}_2,t_2)}{Dt_2}\right.$

This correlation function has never been measured before.

we propose to adopt a model space-time correlation function

similar to that of the measured two-point space-time correlatic function of the axial velocity by Davies, Fisher and Barrett[28]

Model Space-Time Noise Source Correlation Function

Let $\xi = x_1 - x_2$, $\eta = y_1 - y_2$, $\zeta = z_1 - z_2$, $\tau = t_1 - t_2$.

$$\left\langle \frac{Dq_s(\mathbf{x}_1, t_1)}{Dt_1} \frac{Dq_s(\mathbf{x}_2, t_2)}{Dt_2} \right\rangle = \frac{\widehat{q}_s^2}{c^2 \tau_s^2} e^{-\frac{|\xi|}{\overline{u}\,\tau_s} - \frac{\ln 2}{\ell_s^2}[(\xi - \overline{u}\,\tau)^2 + \eta^2 + \zeta^2]}$$

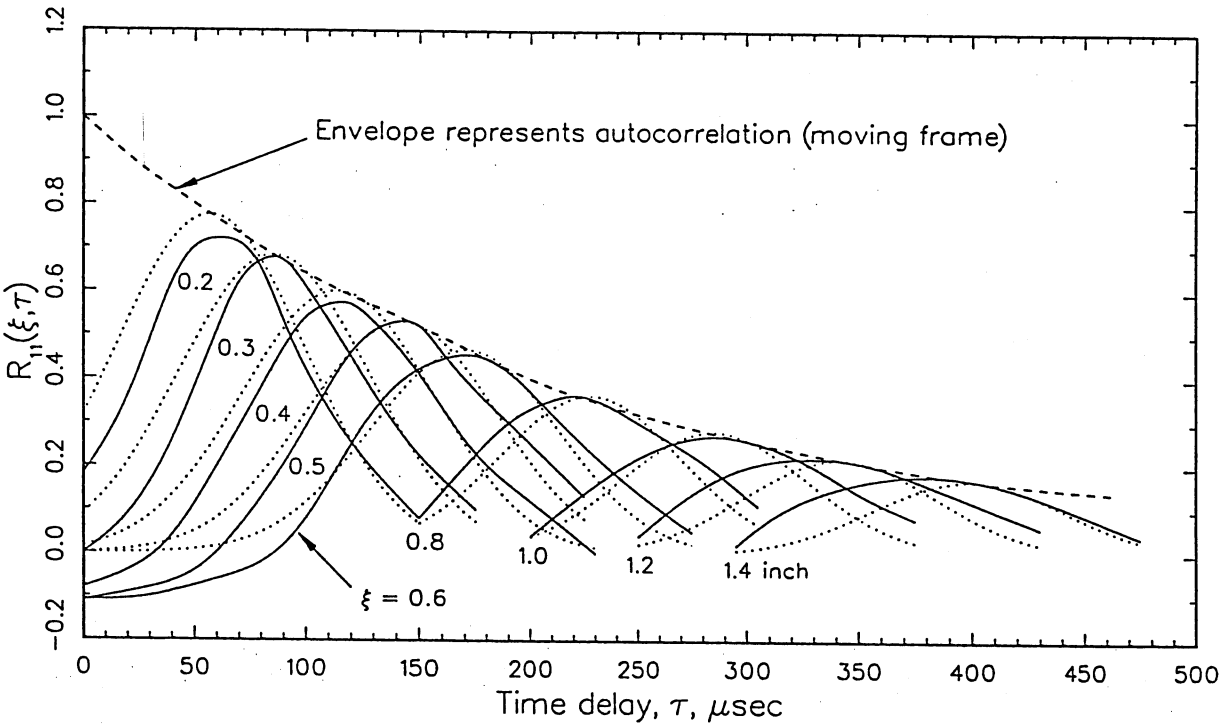


Figure 3. Two-point space-time correlation of the axial velocity component in a jet. ——— measured data, Davies et al. (1963), ····· model function.

Model Space-Time Correlation Function

$$\xi = x_1 - x_2,\ \eta = y_1 - y_2,\ \zeta = z_1 - z_2,\ \tau = t_1 - t_2.$$

$$\left\langle \frac{Dq_s(\mathbf{x}_1, t_1)}{Dt_1} \frac{Dq_s(\mathbf{x}_2, t_2)}{Dt_2} \right\rangle = \frac{\widehat{q}_s^2}{c^2 \tau_s^2} e^{-\frac{|\xi|}{\overline{u}\,\tau_s} - \frac{\ln 2}{\ell_s^2}[(\xi - \overline{u}\,\tau)^2 + \eta^2 + \zeta^2]}$$

The three parameters of the model are ℓ_s, τ_s and $\widehat{q}_s^2$.

ℓ_s is the characteristic size of the fine scale turbulence

τ_s is the characteristic decay time. $\overline{u}\,\tau_s$ is the decay distance.

In the limit $\xi, \eta, \zeta, \tau \to 0$,

$$\left\langle \left(\frac{Dq_s(\mathbf{x}, t)}{Dt} \right)^2 \right\rangle = \frac{\widehat{q}_s^2}{c^2 \tau_s^2}.$$

Thus $\widehat{q}_s$ is a measure of the RMS value of the fluctuating kinetic energy of the fine scale turbulence and $c\tau_s$ represents a typical time scale of the fluctuation.

The $k-\varepsilon$ model provides only two pieces of information about the turbulence of the jet flow. But with k and ε known, it is possible to form a length ℓ, and a decay time, τ, of the turbulence

$$\ell = \frac{k^{\frac{3}{2}}}{\varepsilon}, \quad \tau = \frac{k}{\varepsilon} \qquad \text{and} \quad \mathbf{k}$$

However, the $k-\varepsilon$ model includes contributions from the large turbulence structures whereas ℓ_s and τ_s are those of the fine scal turbulence alone. we propose to let,

$$\ell_s = c_\ell \ell = c_\ell \frac{k^{\frac{3}{2}}}{\varepsilon}, \quad \tau_s = c_\tau \tau = c_\tau \frac{k}{\varepsilon}$$

where c_ℓ and c_τ are constants to be determined empirically.

Also $$\frac{\widehat{q}_s^2}{c^2} = A^2 q^2$$

Empirical constants determined by best fit to noise data

$$c_\ell = 0.256, \quad c_\tau = 0.233 \quad \text{and} \quad A = 0.755.$$

Formula for the Noise Spectrum

On substituting the model two-point space-time noise source function into the noise spectrum formula, one obtains

$$S(\mathbf{x},\omega) = \int\!\!\int_{-\infty}^{\infty}\!\cdots\!\int\!\!\int p_a(\mathbf{x}_1,\mathbf{x},\omega_1)p_a(\mathbf{x}_2,\mathbf{x},\omega_2)\frac{\widehat{q}_s^2}{c^2\tau_s^2}$$

$$\cdot\, e^{-\frac{|x_1-x_2|}{\overline{u}\,\tau_s}-\frac{\ln 2}{\ell_s^2}[(x_1-x_2-\overline{u}(t_1-t_2))^2+(y_1-y_2)^2+(z_1-z_2)^2]}$$

$$\cdot\, e^{-i(\omega_1+\omega_2)t+i\omega_1 t_1+i\omega_2 t_2}\delta(\omega-\omega_2)\,dt_1\,dt_2\,d\omega_2\,d\omega_2\,d\,\mathbf{x}_1\,d\,\mathbf{x}_2$$

It turns out all the integrals except a final volume integral can be carried out step by step. This yields

$$S(\mathbf{x},\omega) = 4\pi\left(\frac{\pi}{\ln 2}\right)^{\frac{3}{2}}\int\!\!\int\!\!\int_{-\infty}^{\infty}\frac{\widehat{q}_s^2\,\ell_s^3}{c^2\tau_s}\frac{|p_a(\mathbf{x}_2,\mathbf{x},\omega)|^2 e^{-\frac{\omega^2\ell_s^2}{\overline{u}^2(4\ln 2)}}}{[1+\omega^2\tau_s^2(1-\frac{\overline{u}}{a_\infty}\cos\Theta)^2]}d\,\mathbf{x}_2\,.$$

Experimental Data for Comparisons with Theory

1. Seiner data (NASA Langley Research Center)

   M_j from 1.37 to 2.3

   T_r/T_a from 1.0 to 4.9

2. Norum and Brown data

   M_j 0.3 to 2.0

   $T_r/T_a = 1.0$

3. Lockheed (Tanna) data

   M_j 1.0 to 2.0

   T_r/T_a 1.0 to 2.2

4. Rolls Royce (Ahuja) data

   M_j 0.4 to 0.98

   T_r/T_a 1.0

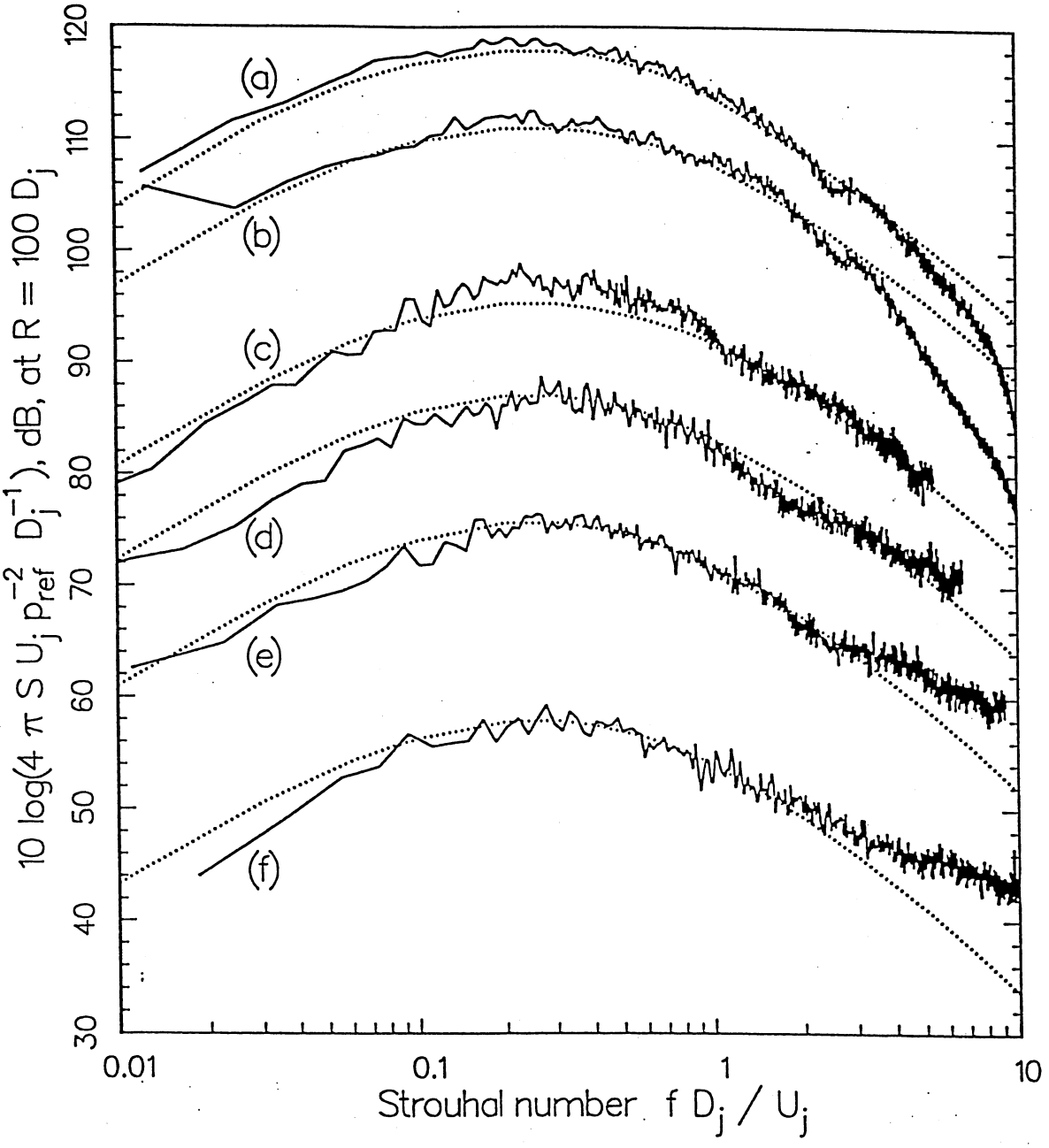


Figure 5a. Cold jet noise spectra at $\Theta = 60$ deg., $\frac{T_r}{T_\infty} = 1.0$. (a) $M_j = 2.0$, (b) $M_j = 1.49$, (c) $M_j = 0.9$, (d) $M_j = 0.7$, (e) $M_j = 0.5$, (f) $M_j = 0.3$. ——— experiments, Ref [10] , [32] ; ····· equation (36).

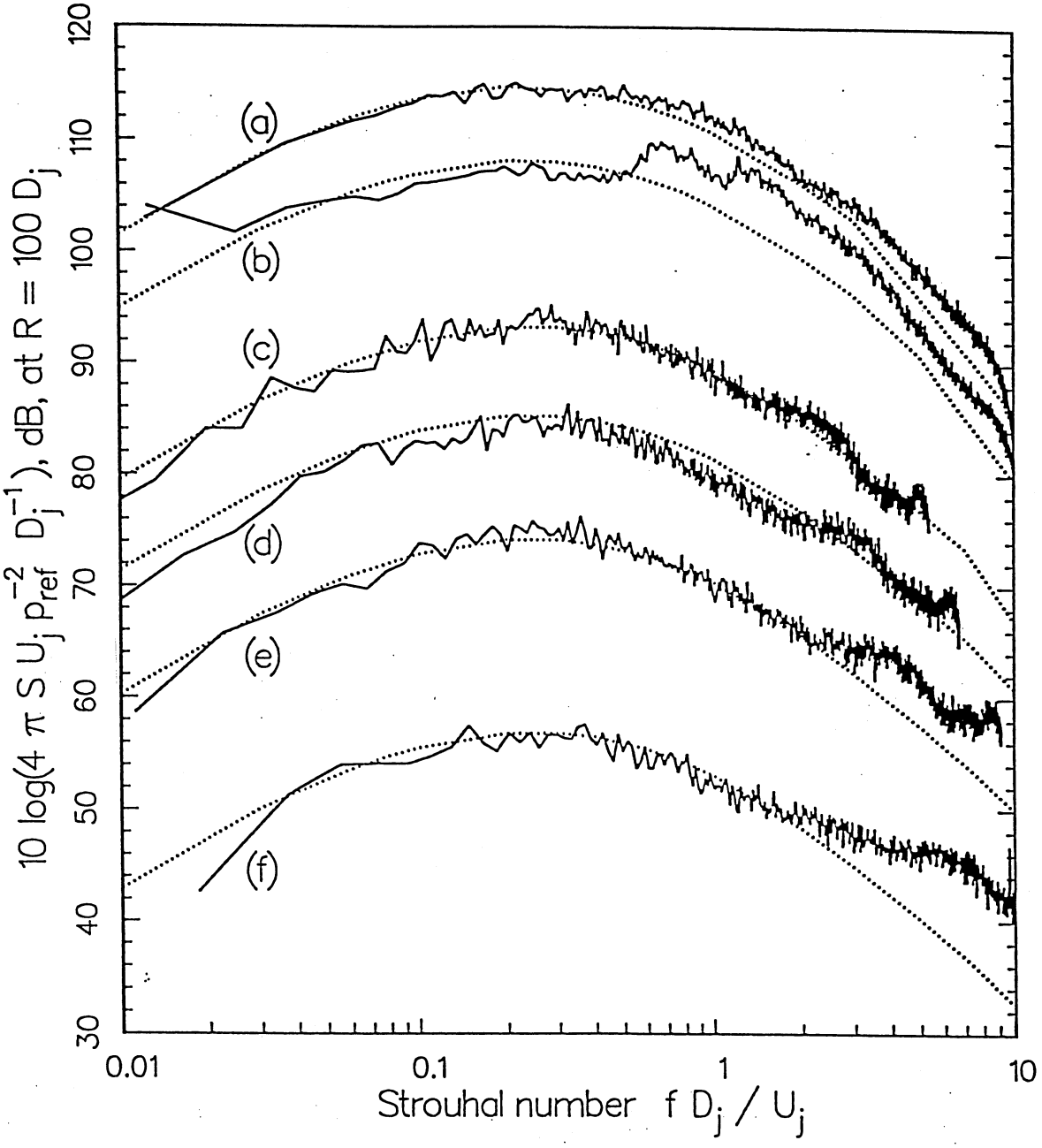


Figure 5b. Cold jet noise spectra at $\Theta = 90$ deg., $\frac{T_r}{T_\infty} = 1.0$.
——— experiments ; ····· equation (36).

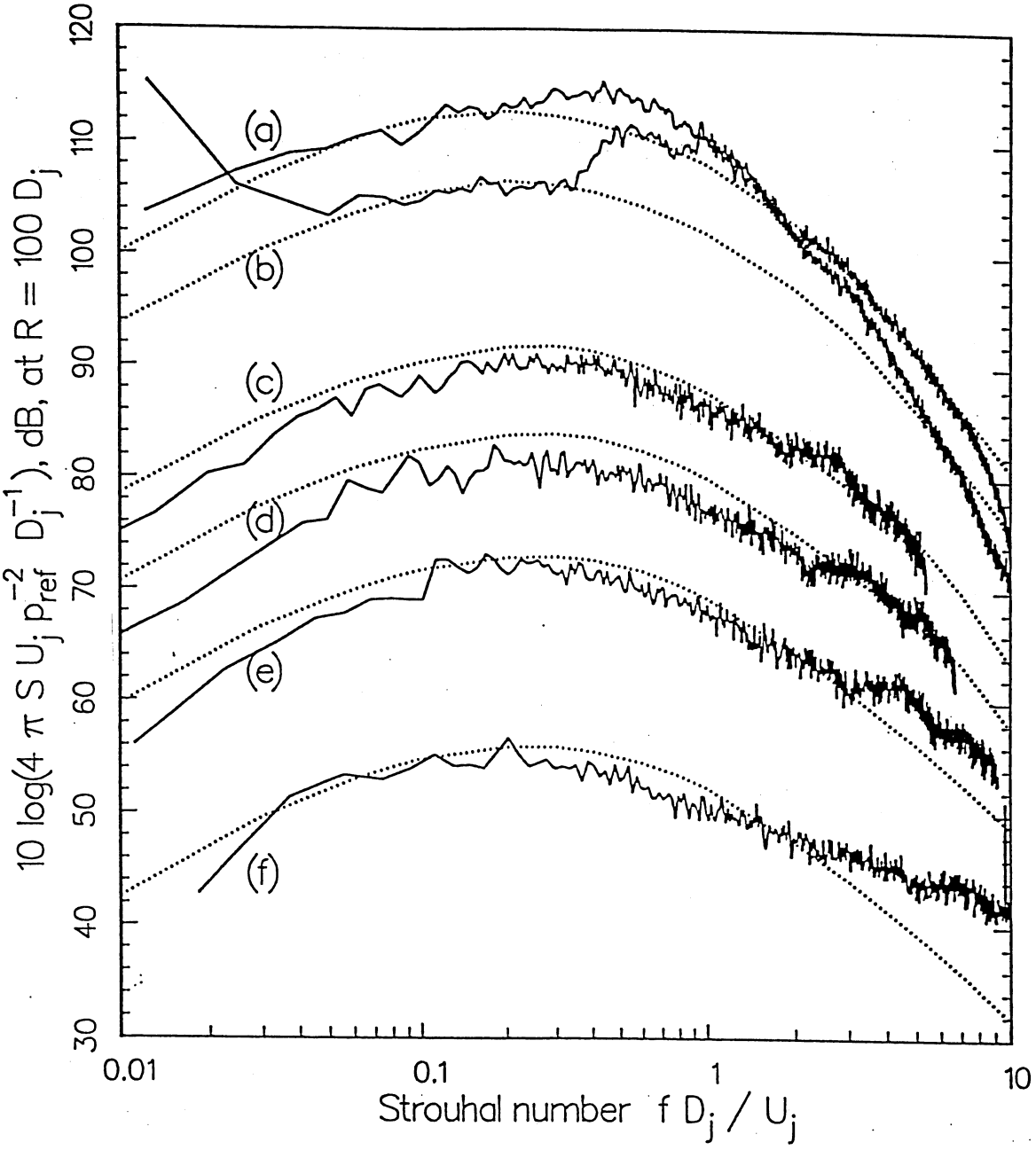


Figure 5c. Cold jet noise spectra at $\Theta = 120$ deg., $\frac{T_r}{T_\infty} = 1.0$.
——— experiments ; ····· equation (36).

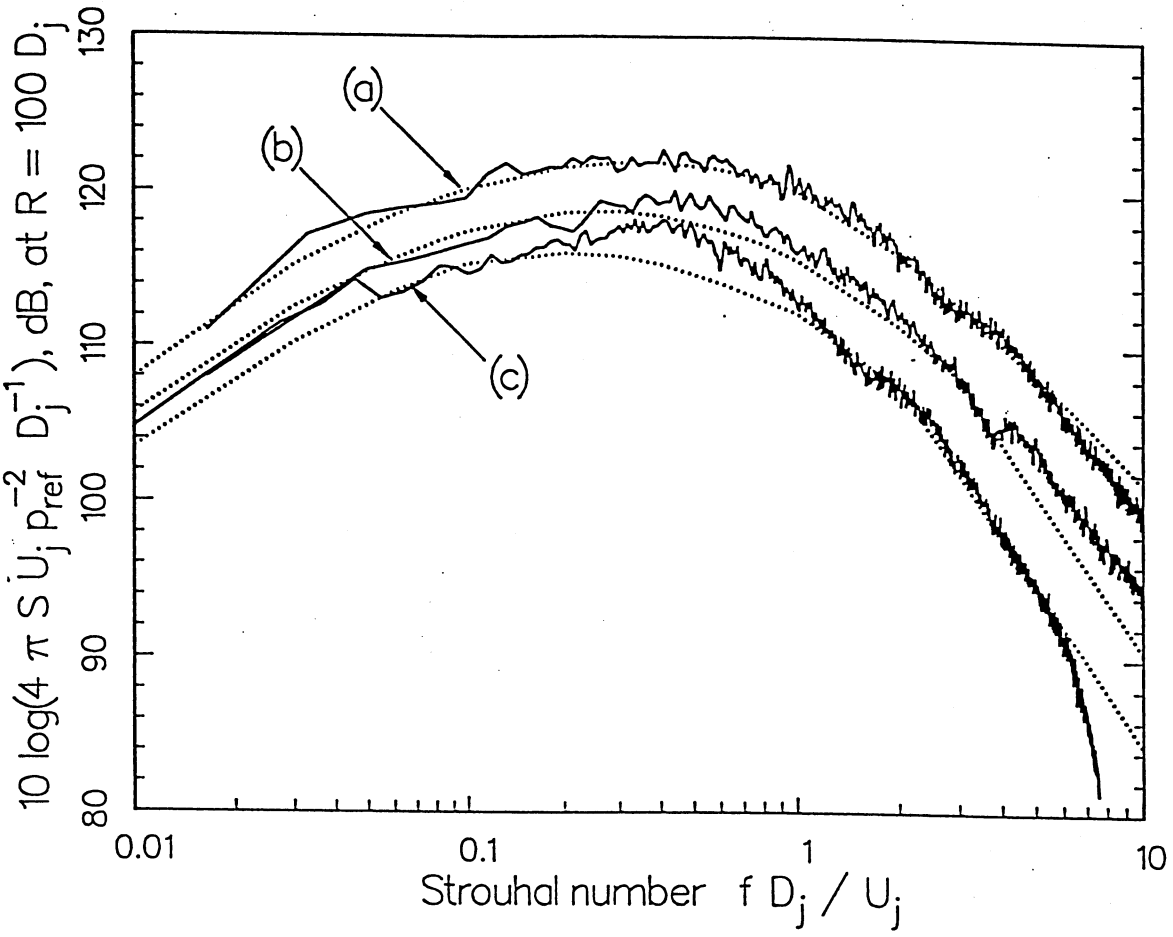


Figure 6. Hot jet noise spectra at $M_j = 2.0$, $\frac{T_r}{T_\infty} = 1.8$.
(a) $\Theta = 69$ deg., (b) $\Theta = 91$ deg., (c) $\Theta = 117$ deg.
——— experiments, Ref [10] ; ····· equation (36).

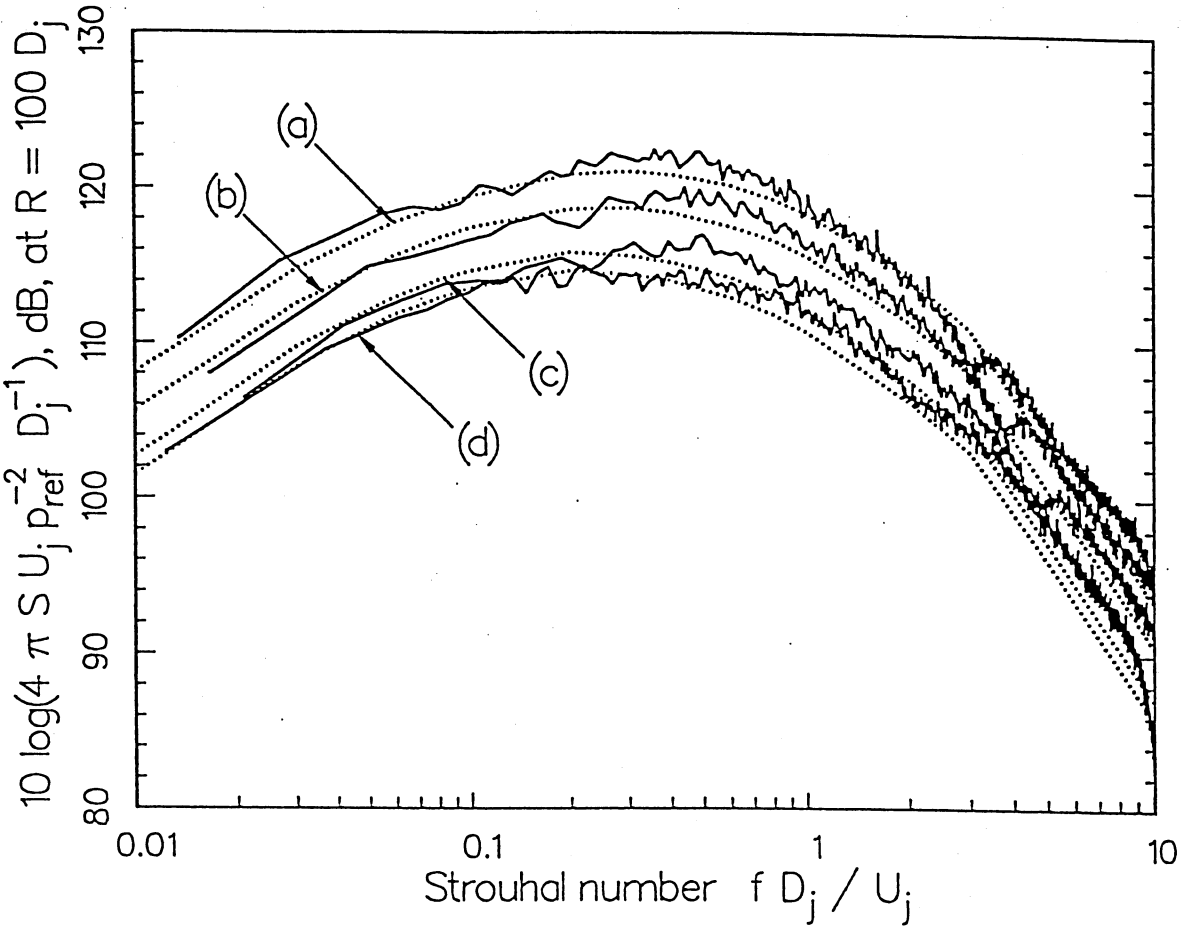


Figure 7. Effect of jet temperature on the noise spectrum at 90 degrees for a Mach 2.0 jet. (a) $\frac{T_r}{T_\infty} = 2.72$, (b) $\frac{T_r}{T_\infty} = 1.8$, (c) $\frac{T_r}{T_\infty} = 1.12$, (d) $\frac{T_r}{T_\infty} = 1.0$. ——— experiments ; ····· equation (36).

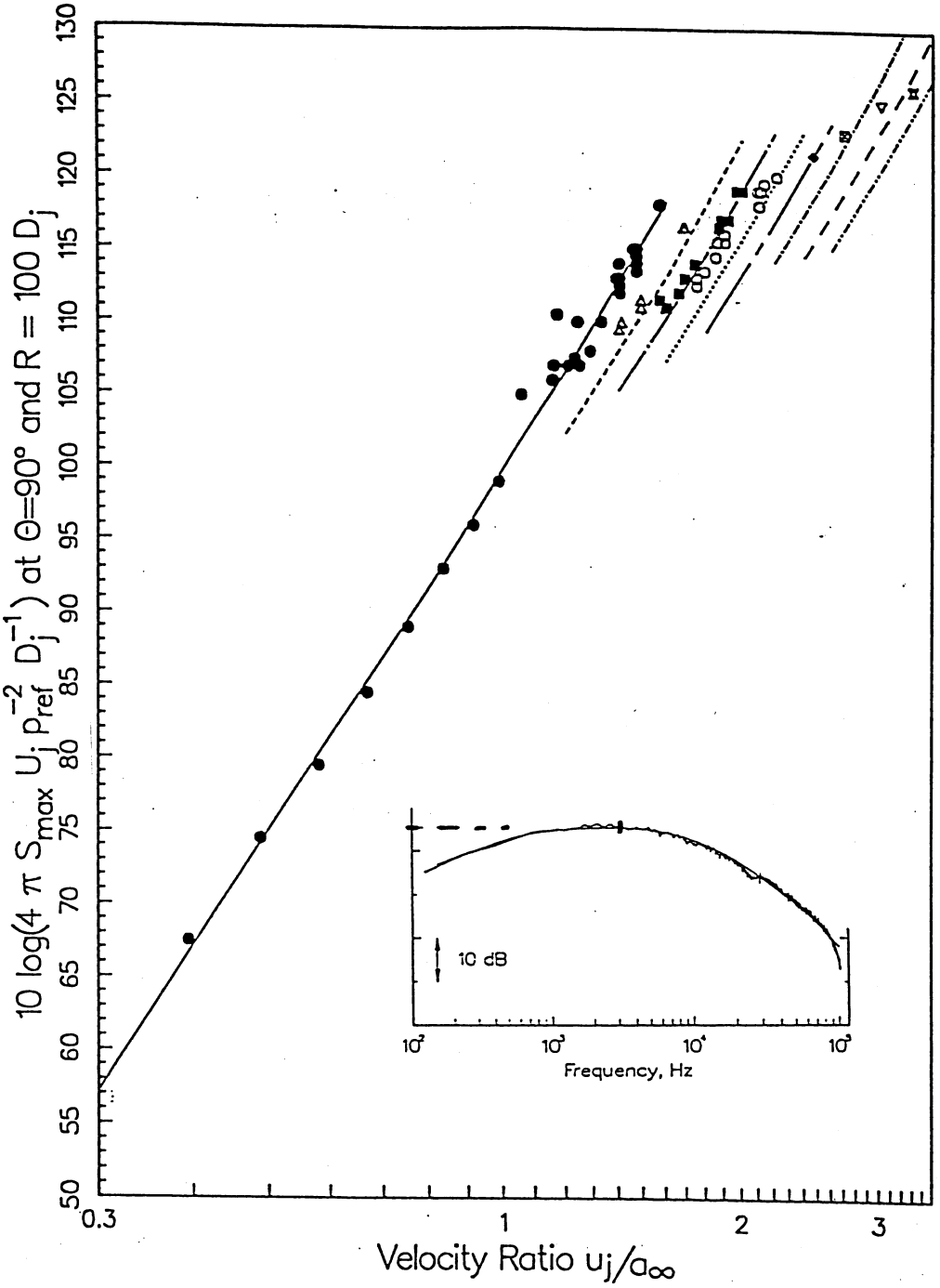


Figure 8a. Dependence of the peak level of the noise spectrum at $\Theta = 90°$ on velocity and temperature ratios.

T_r/T_∞	1.0	1.4	1.8	2.2	2.7	3.3	4.1	4.9
measurements	●	△	■	○	◈	⊠	▽	⧓
equation (36)	——	- - - -	— · —	·····	— — —	- · - ·	— —	— .. —

Data from Ref [10] and [32].

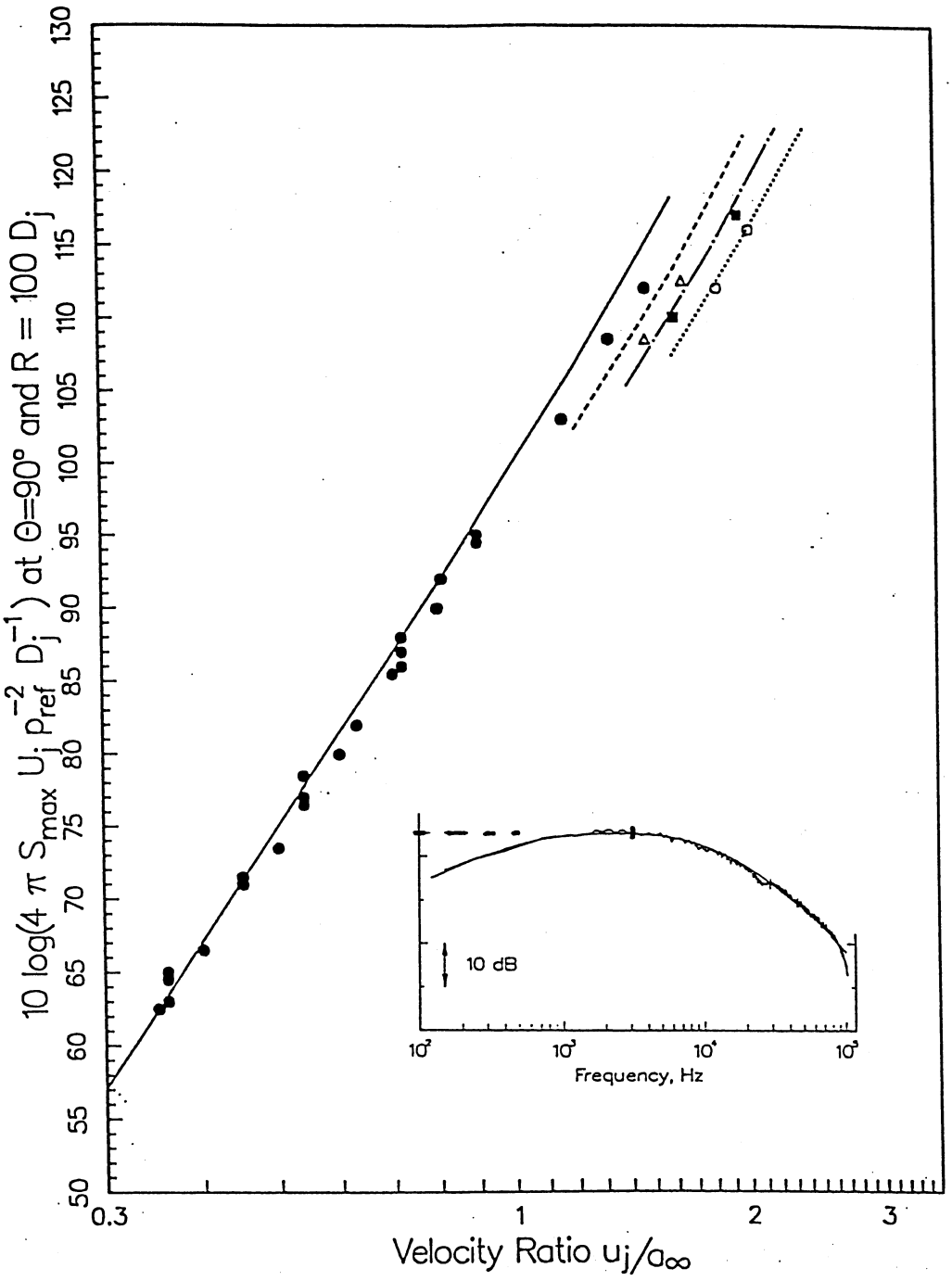
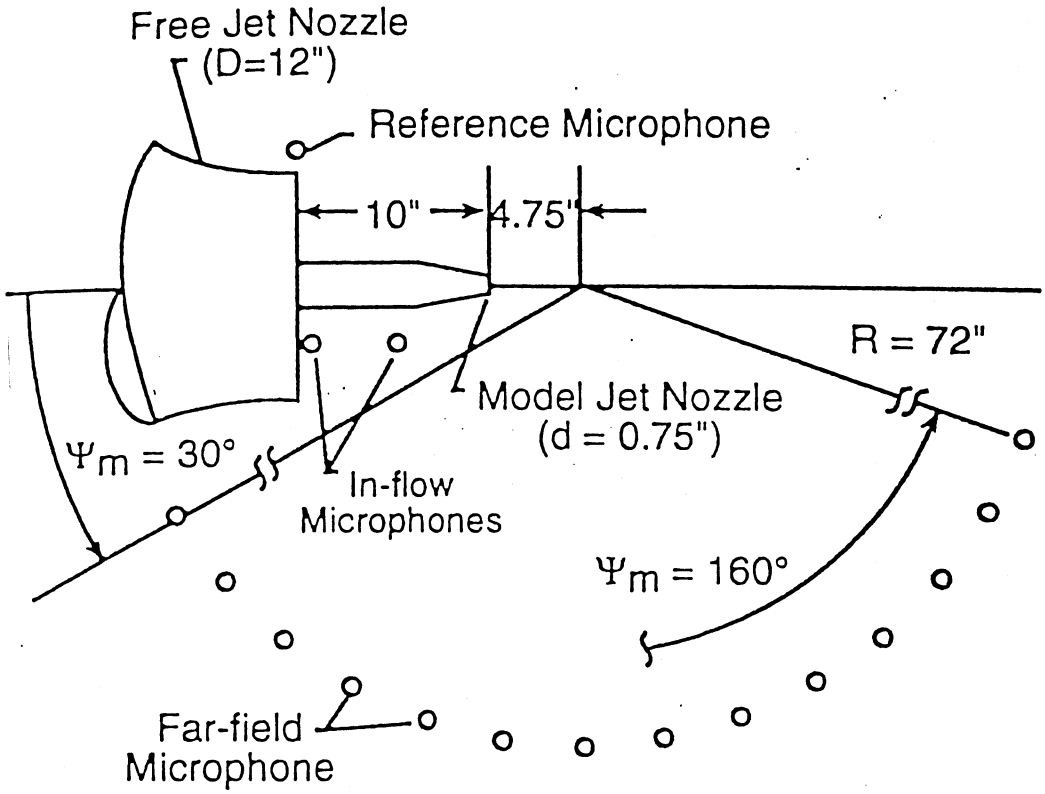


Figure 8b. Same as 8a. Data from Ref [33] and [34].

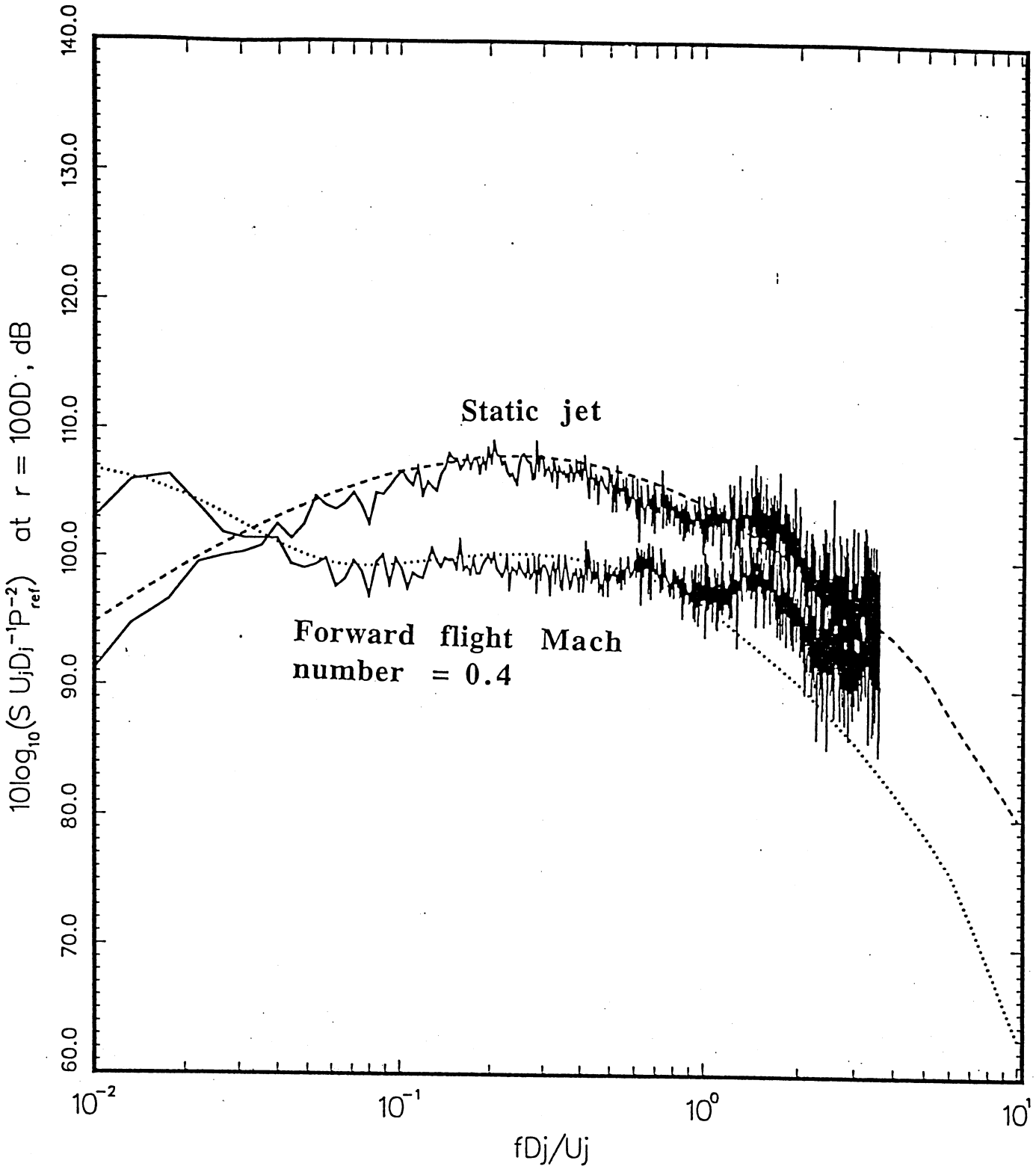
Prediction of Jet Noise with Simulated Forward Flight

Forward Flight Experiments

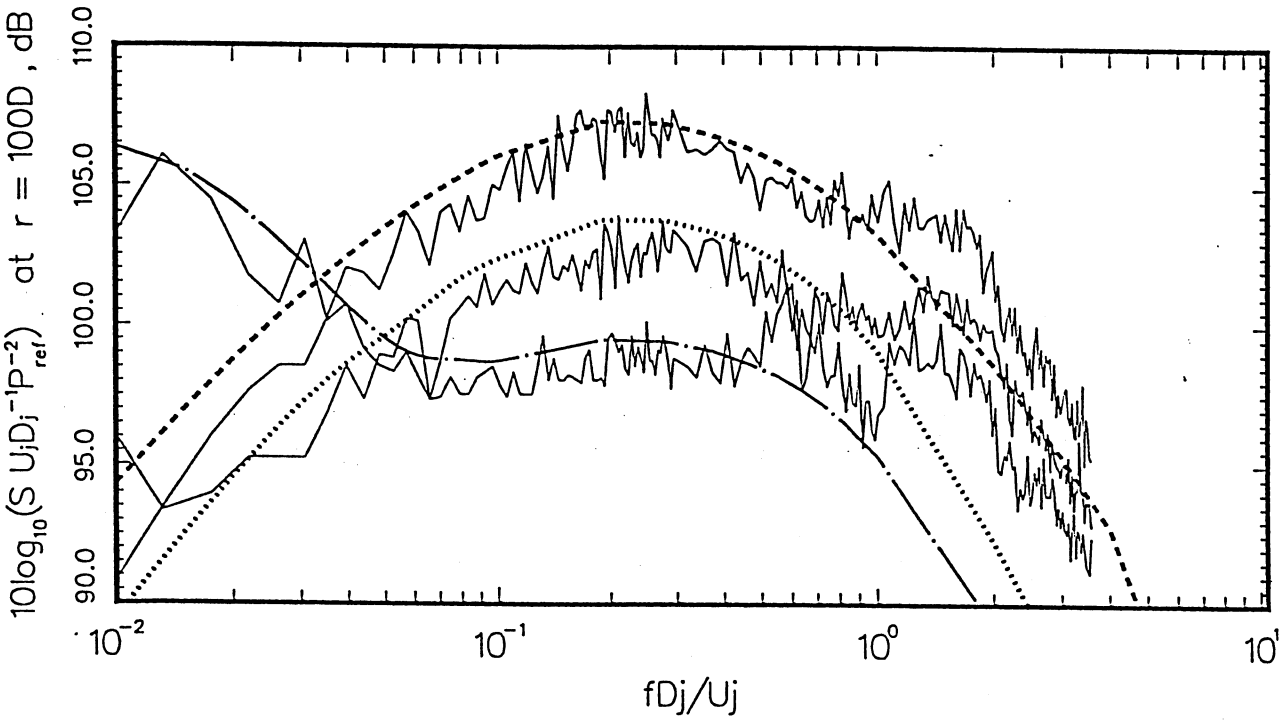


NASA Langley Research Center

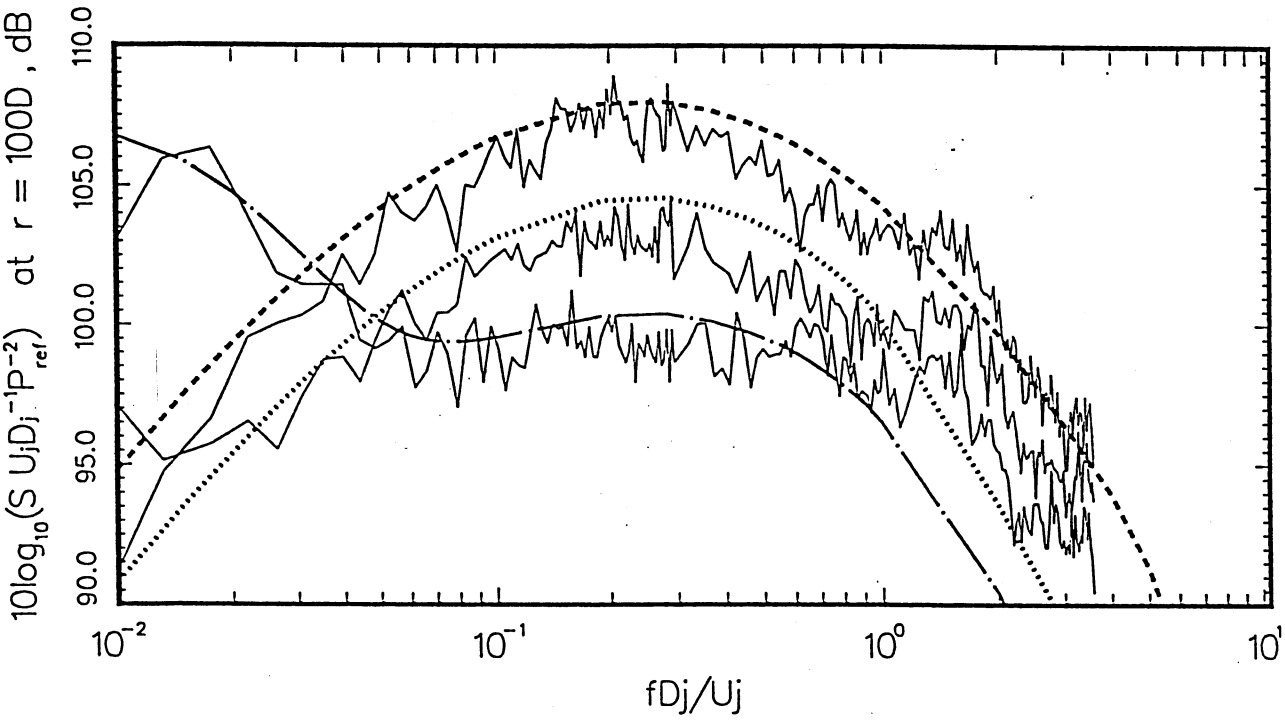
Norum & Brown



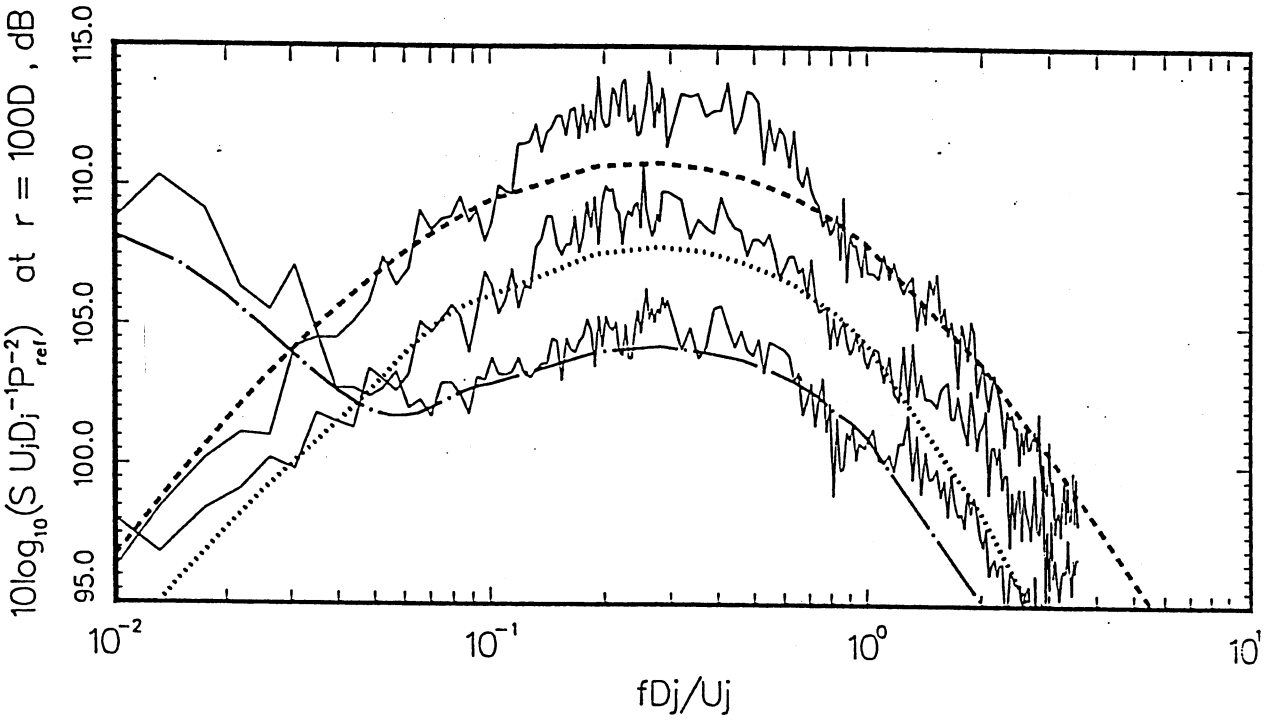
Mach 1.5 cold jet at Θ = 90°



Comparisons between measured and computed data for a Mach 1.5 cold jet at $\Theta = 80°$. ———— experimental data, - - - - - - - Free jet Mach number = 0.0, ... Free jet Mach number = 0.2, — · — · — · — Free jet Mach number = 0.4.



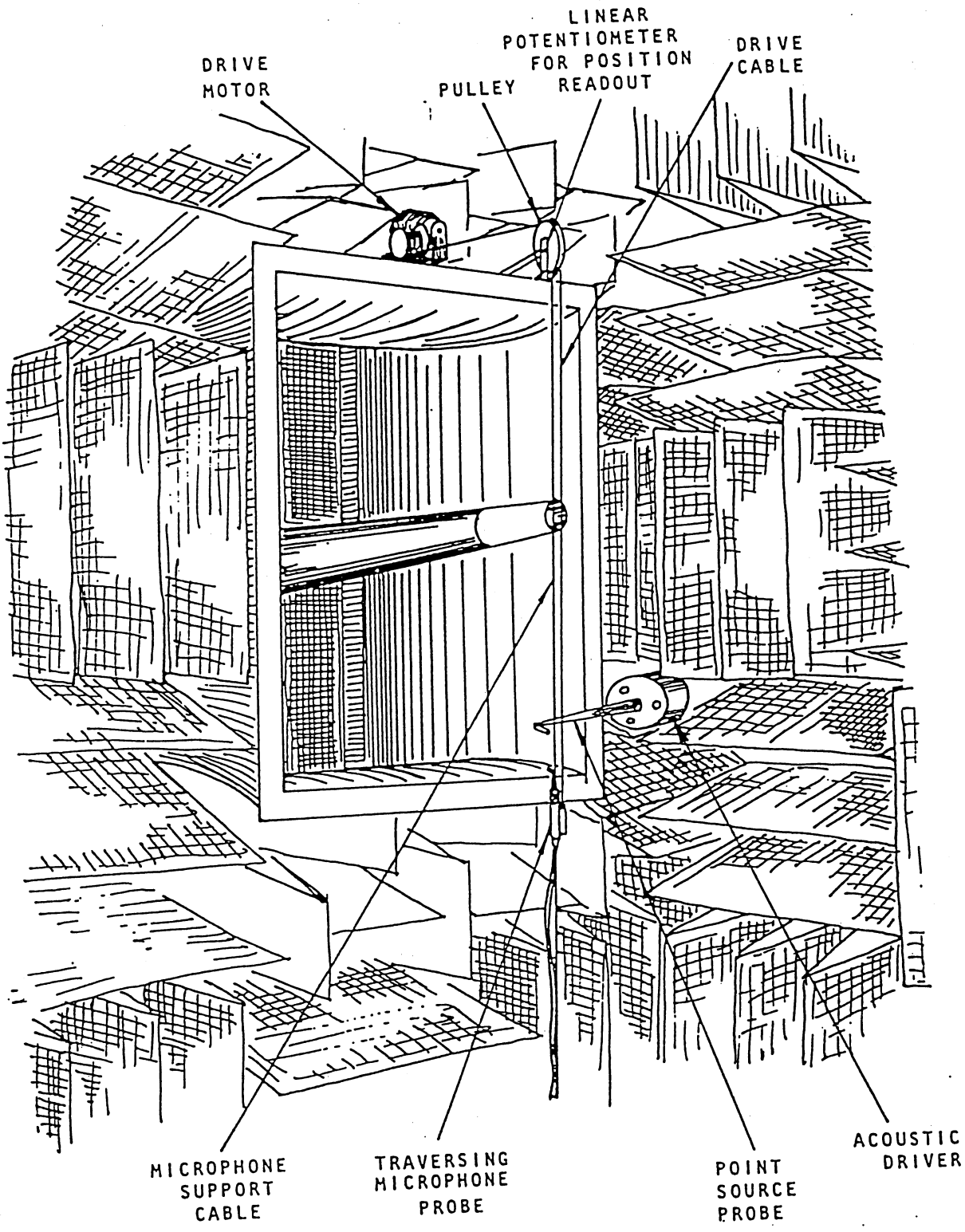
Comparisons between measured and computed data for a Mach 1.5 cold jet at $\Theta = 90°$. ——— experimental data, - - - - - - - Free jet Mach number = 0.0, ... Free jet Mach number = 0.2, — · — · — · — Free jet Mach number = 0.4.

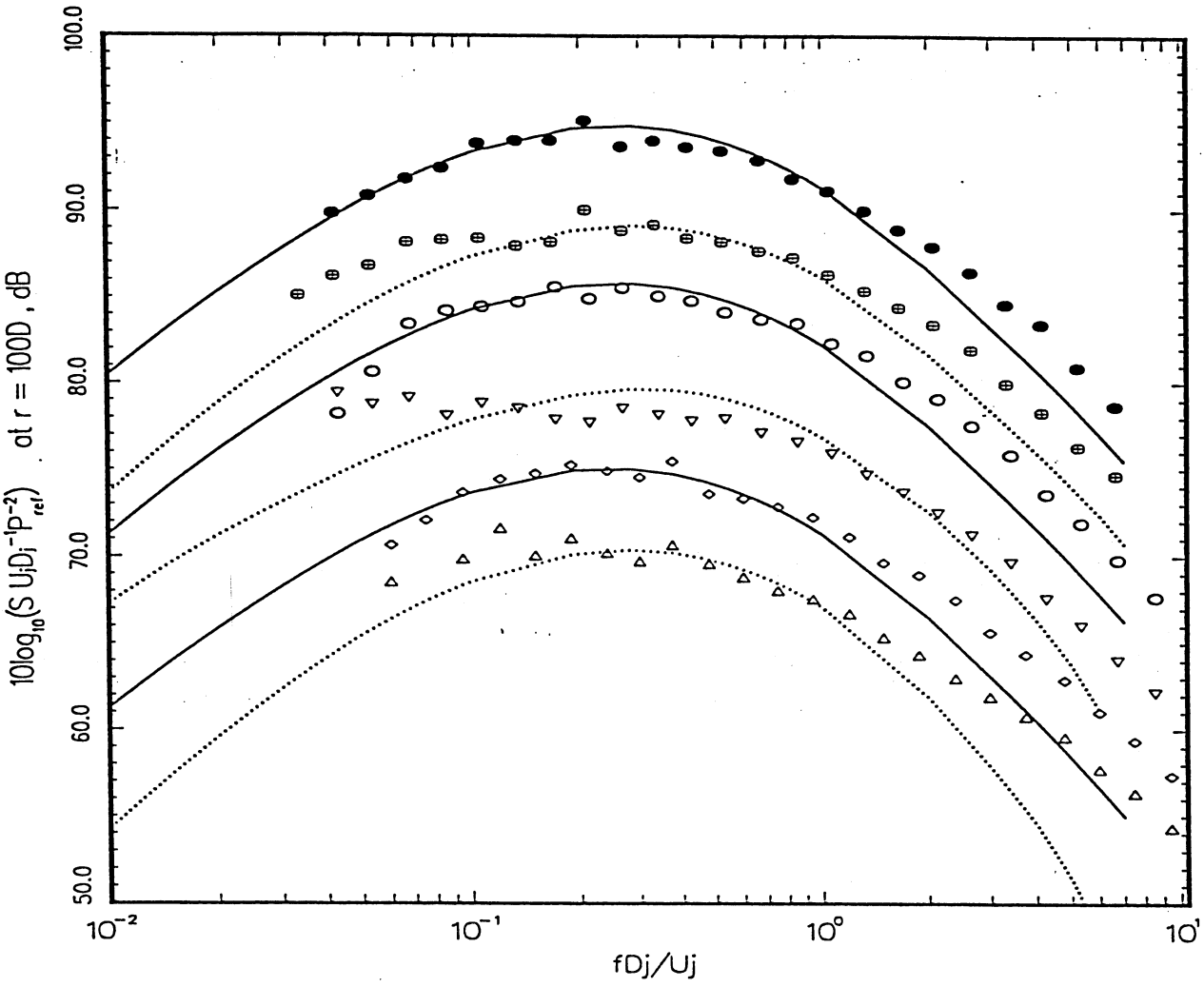


Comparisons between measured and computed data for a Mach 1.5 cold jet at $\Theta = 120°$. ———— experimental data, - - - - - - - Free jet Mach number = 0.0, ... Free jet Mach number = 0.2, — · — · — · — Free jet Mach number = 0.4.

Lockheed Forward Flight Experiments

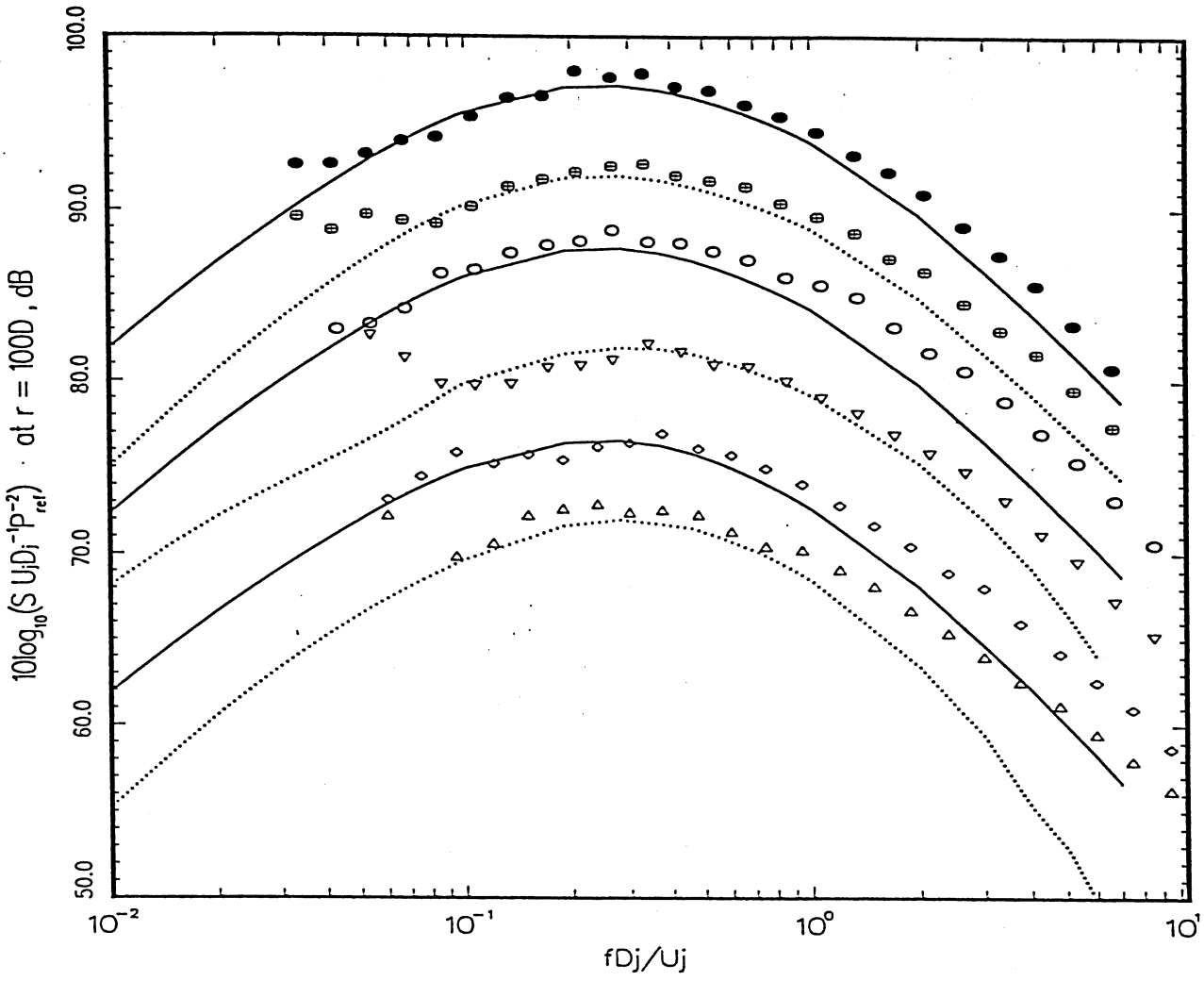
(Tanna)





Comparisons between measured and computed data for cold jets at $\Theta = 90°$.

- $\bullet$ $M_j = 0.98$ $M_f = 0.05$
- $\oplus$ $M_j = 0.98$ $M_f = 0.20$
- $\circ$ $M_j = 0.73$ $M_f = 0.04$
- $\triangledown$ $M_j = 0.74$ $M_f = 0.20$
- $\diamond$ $M_j = 0.51$ $M_f = 0.02$
- $\triangle$ $M_j = 0.51$ $M_f = 0.10$



Comparisons between measured and computed data for cold jets at $\Theta = 60°$.

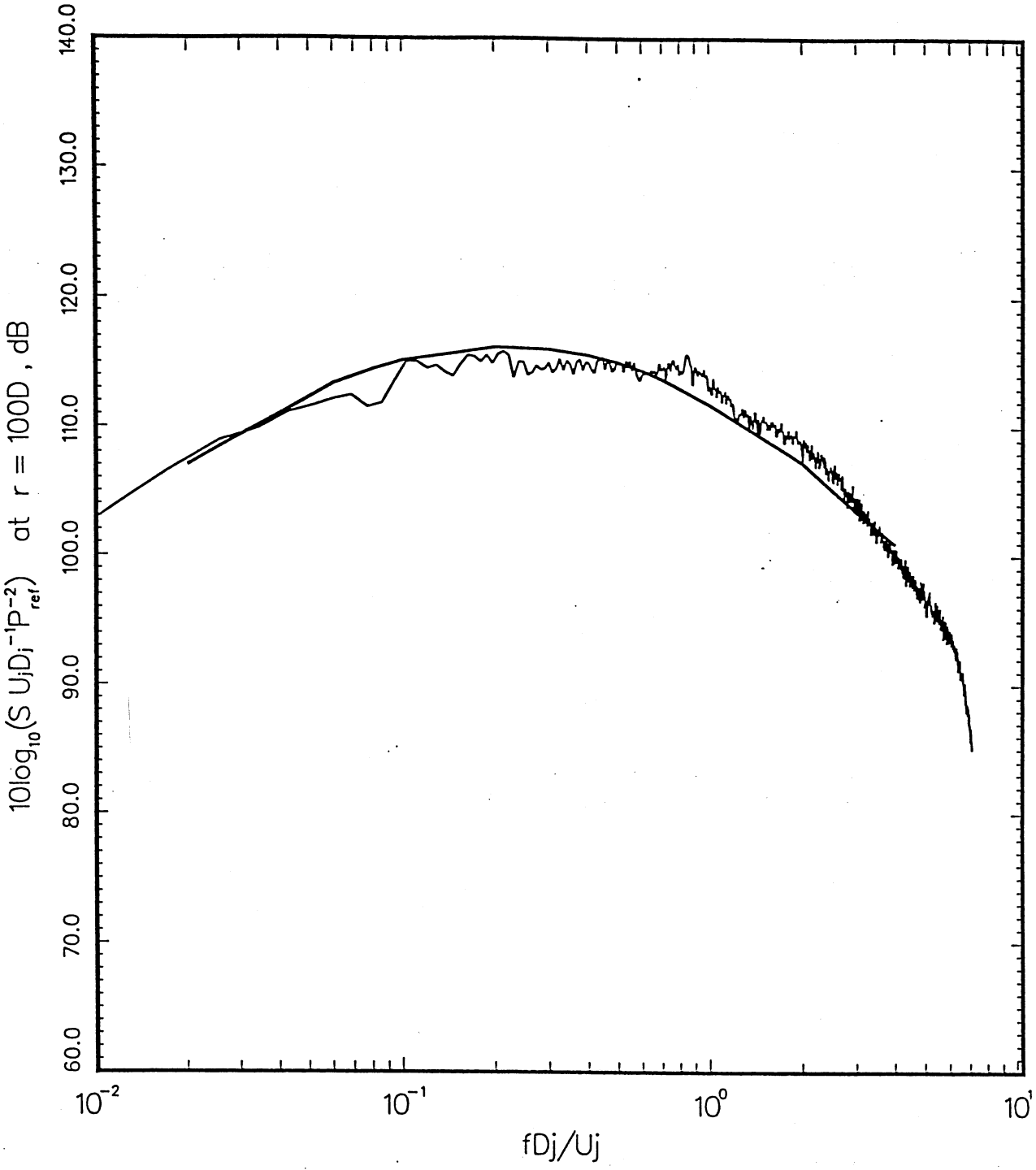
- $\bullet$ $M_j = 0.98$ $M_f = 0.05$
- $\oplus$ $M_j = 0.98$ $M_f = 0.20$
- $\circ$ $M_j = 0.73$ $M_f = 0.04$
- ∇ $M_j = 0.74$ $M_f = 0.20$
- $\diamond$ $M_j = 0.51$ $M_f = 0.02$
- $\triangle$ $M_j = 0.51$ $M_f = 0.10$

Prediction of Jet Noise from Non-axisymmetric Jets

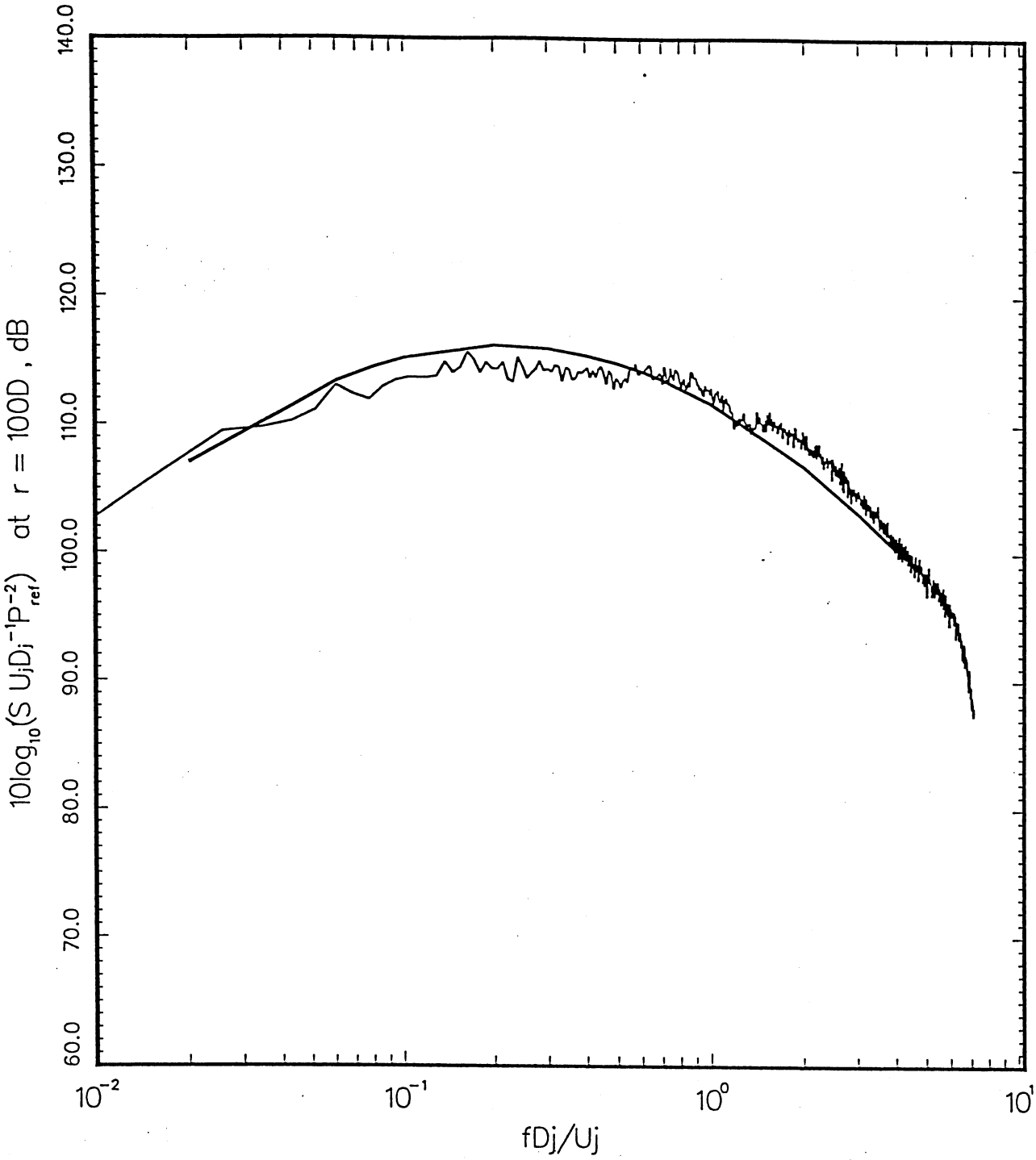
Comparisons with Seiner's Jet Noise Data

Elliptic Jet Aspect ratio 3 Mach 2.0

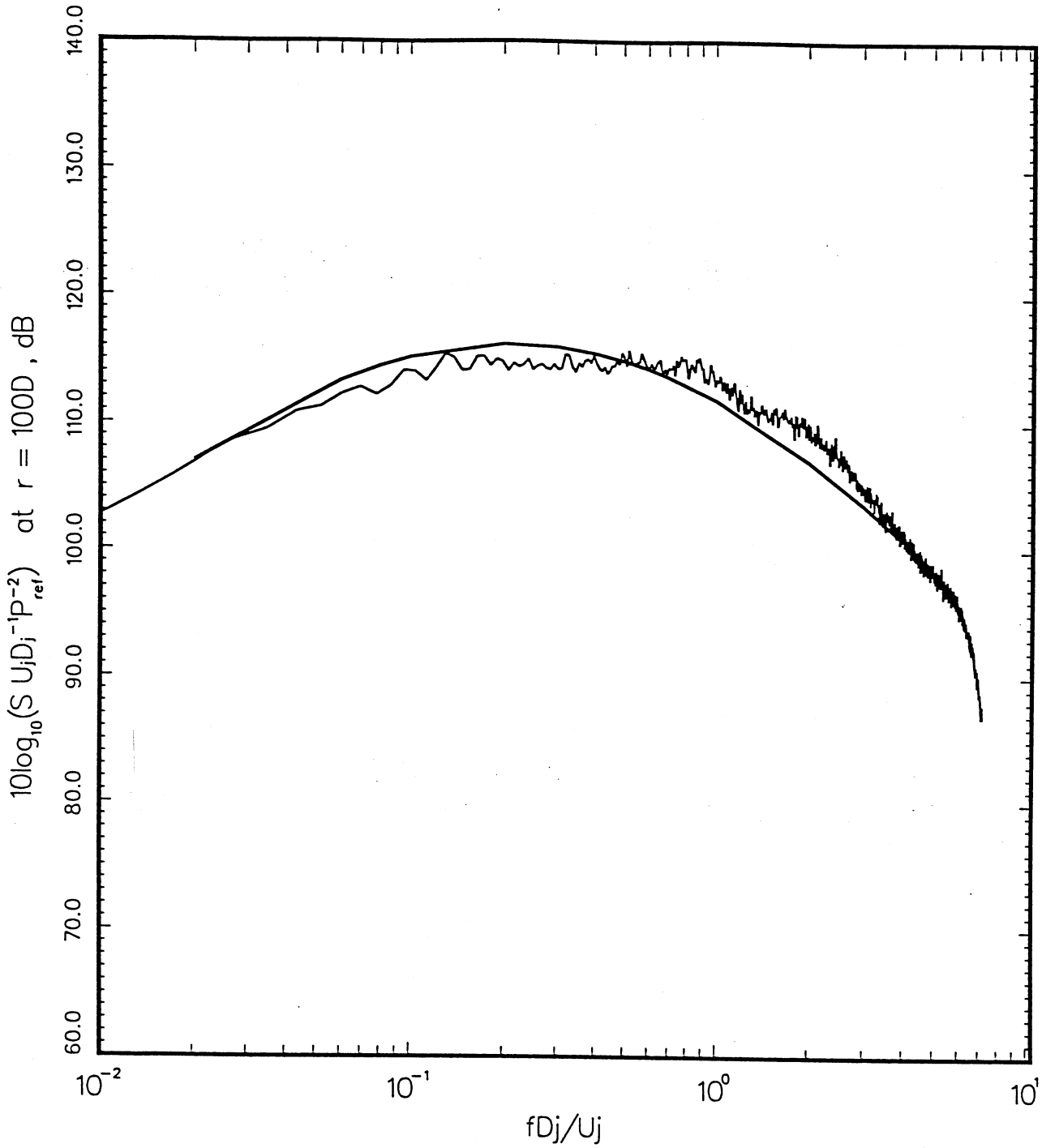
Rectangular Jet Aspect ratio 7.6 Mach 2.0



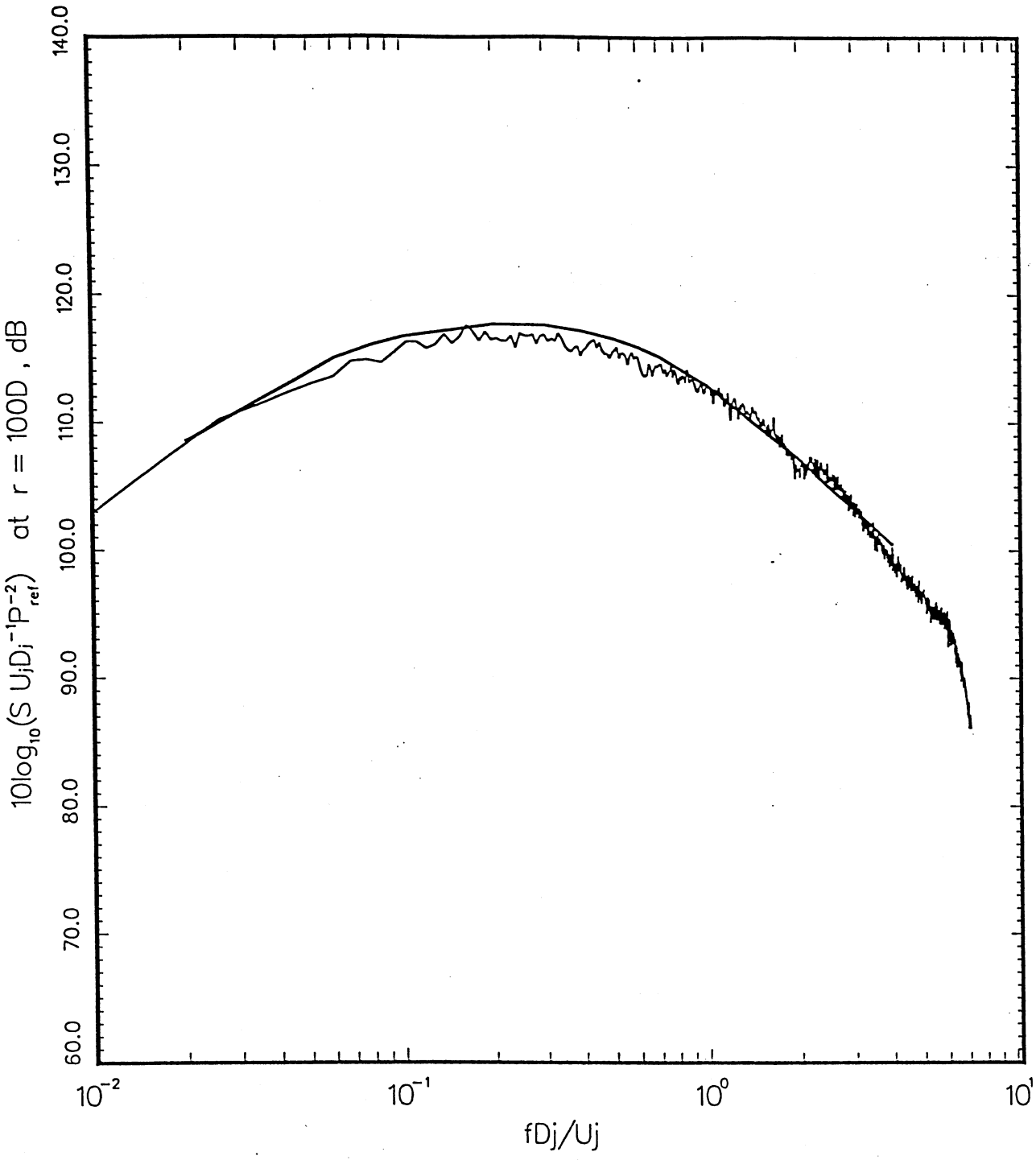
Elliptic, Ar = 3.0, Mach 2.0 jet, $T_r/T_\infty = 1.0$. Major axis plane, $\Theta = 90°$, $\tau_s = c_\tau \frac{k}{\epsilon+\epsilon_0}$, $l_s = c_l \frac{k^{3/2}}{\epsilon+\epsilon_0}$, $\epsilon_0 = 3.0 \cdot 10^{-5}$. Contribution only from turbulence with $k \leq 0.01 \cdot k_{max}$. The tolerance when computing Green's functions is 0.005



Elliptic, Ar = 3.0, Mach 2.0 jet, $T_r/T_\infty = 1.0$. Minor axis plane, $\Theta = 90°$, $\tau_s = c_\tau \frac{k}{\epsilon+\epsilon_0}$, $l_s = c_l \frac{k^{3/2}}{\epsilon+\epsilon_0}$, $\epsilon_0 = 3.0 \cdot 10^{-5}$. Contribution only from turbulence with $k \leq 0.01 \cdot k_{max}$. The tolerance when computing Green's functions is 0.005

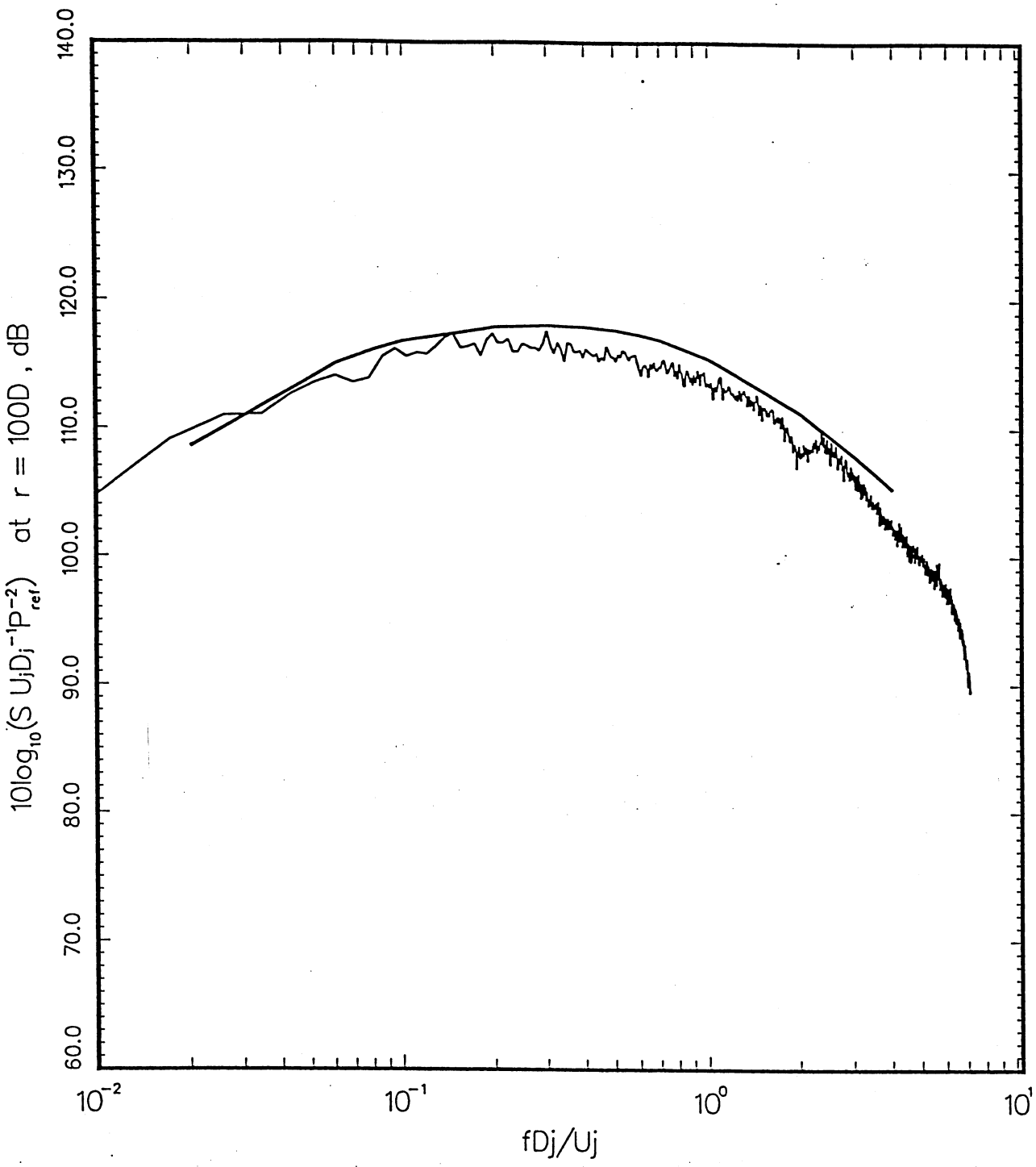


Elliptic, Ar = 3, nozzle, Mach 2.0 jet, $T_r/T_\infty = 1.0$. 58° axis plane, $\Theta = 90°$, $\tau_s = c_\tau \frac{k}{\epsilon+\epsilon_0}$, $l_s = c_l \frac{k^{3/2}}{\epsilon+\epsilon_0}$, $\epsilon_0 = 3.0 \cdot 10^{-5}$. Contribution only from turbulence with $k \leq 0.01 \cdot k_{max}$. The tolerance when computing Green's functions is 0.005.

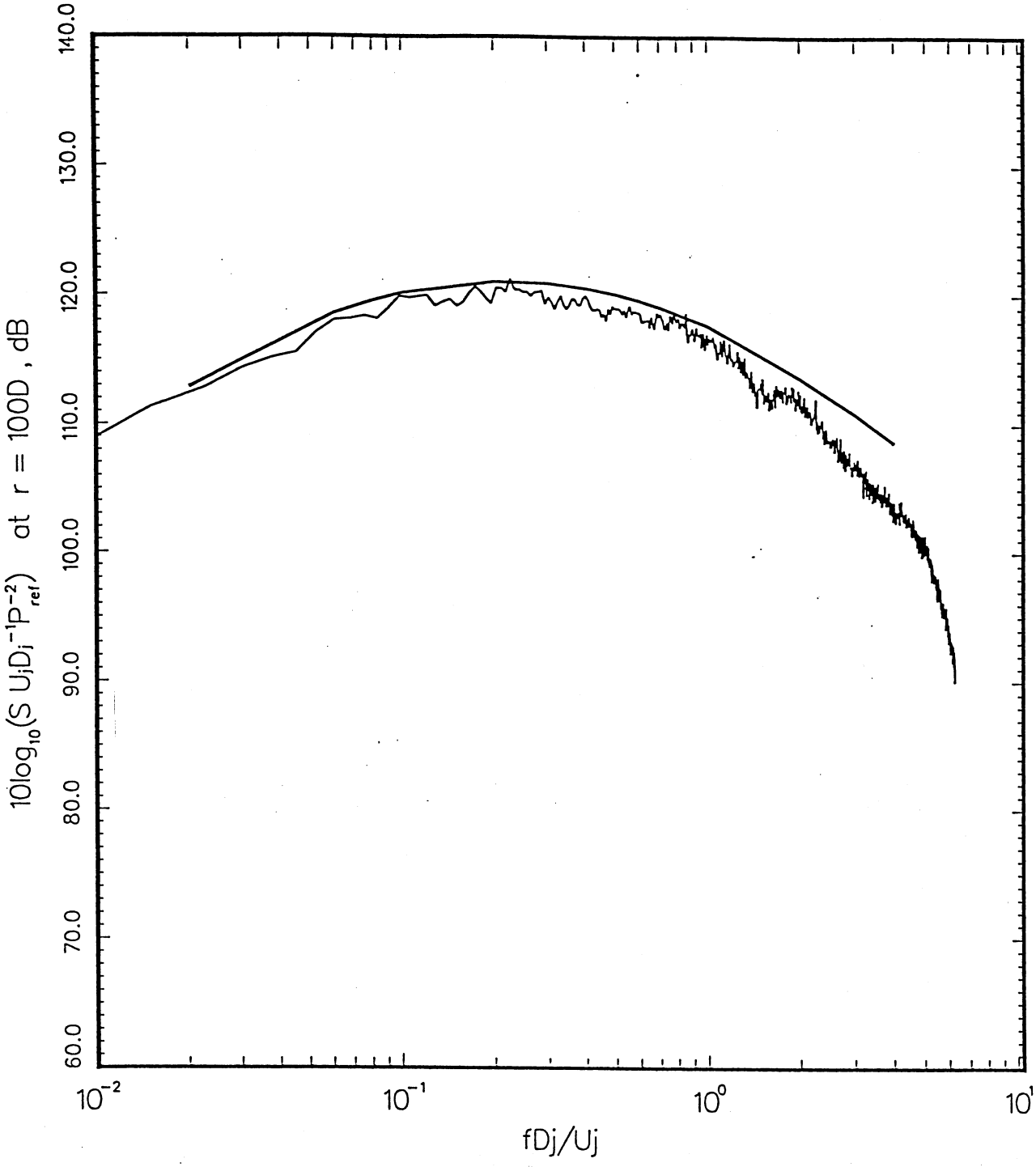


Elliptic, Ar = 3.0, Mach 2.0 jet, $T_r/T_\infty = 1.0$. Major axis plane, $\Theta = 72°$, $\tau_s = c_\tau \frac{k}{\epsilon+\epsilon_0}$, $l_s = c_l \frac{k^{3/2}}{\epsilon+\epsilon_0}$, $\epsilon_0 = 3.0 \cdot 10^{-5}$. Contribution only from turbulence with $k \leq 0.01 \cdot k_{max}$. The tolerance when computing Green's functions is 0.005

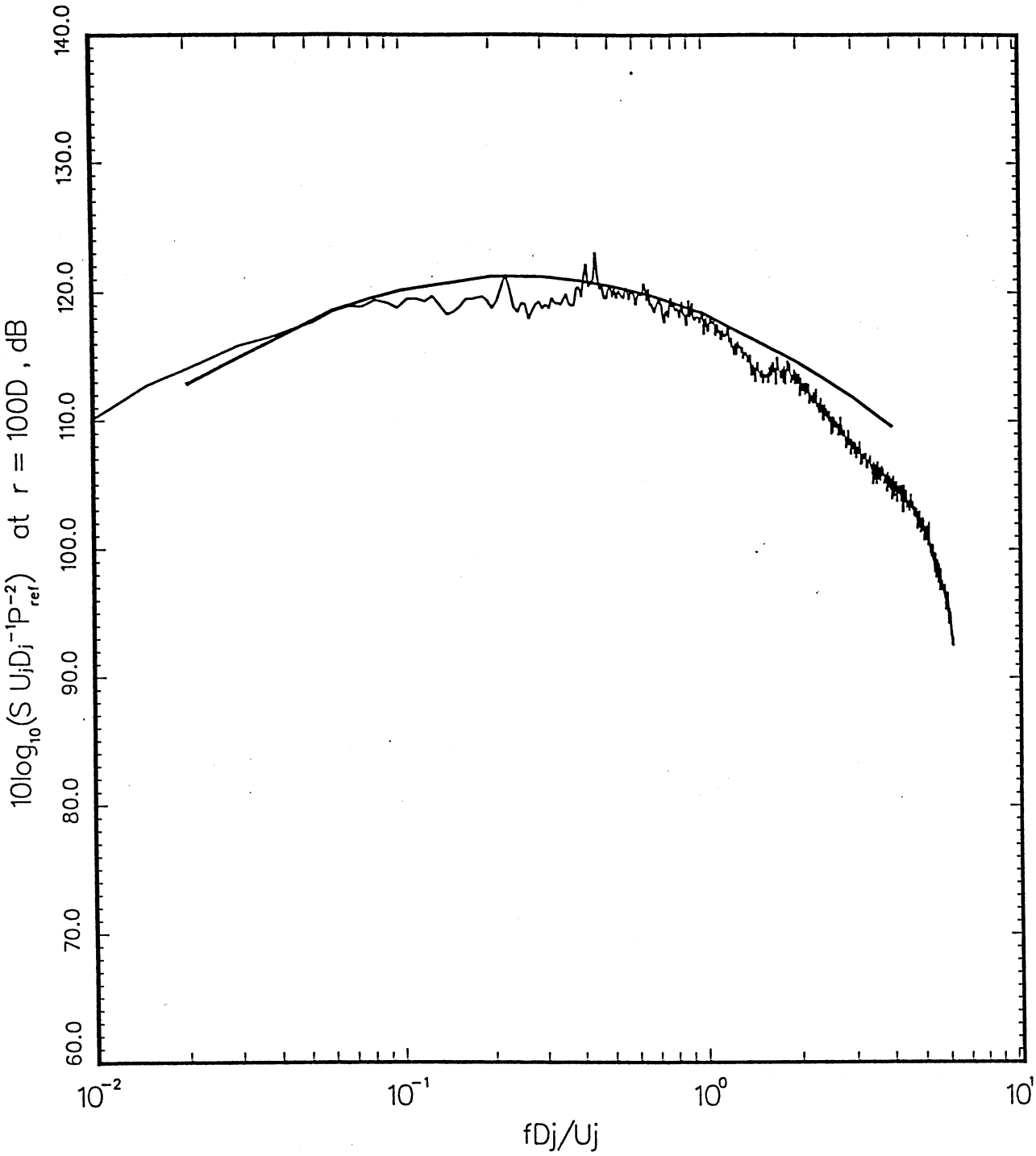
.



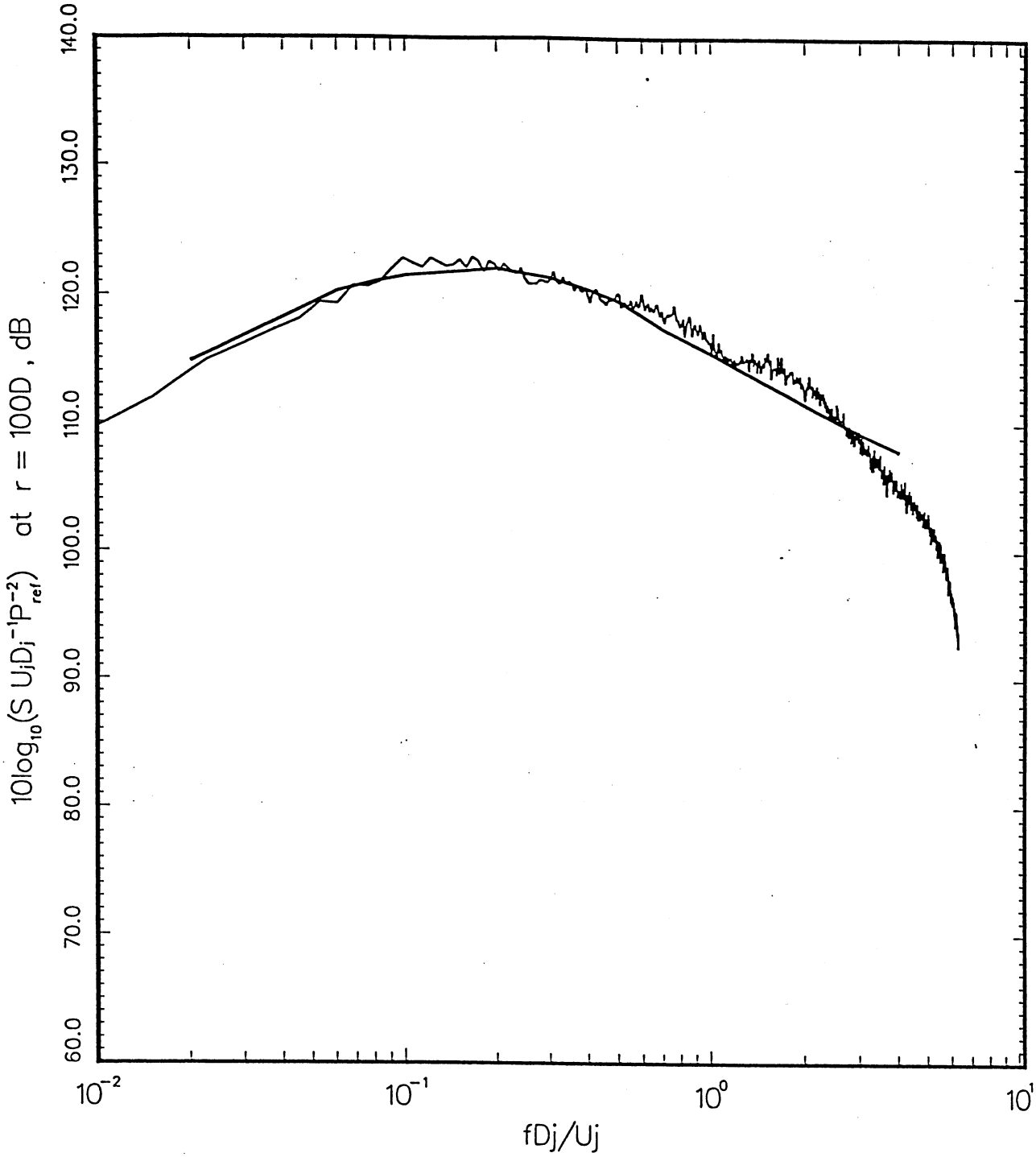
Elliptic, Ar = 3.0, Mach 2.0 jet, $T_r/T_\infty = 1.0$. Minor axis plane, $\Theta = 72°$, $\tau_s = c_\tau \frac{k}{\epsilon+\epsilon_0}$, $l_s = c_l \frac{k^{3/2}}{\epsilon+\epsilon_0}$, $\epsilon_0 = 3.0 \cdot 10^{-5}$. Contribution only from turbulence with $k \leq 0.01 \cdot k_{max}$. The tolerance when computing Green's functions is 0.005



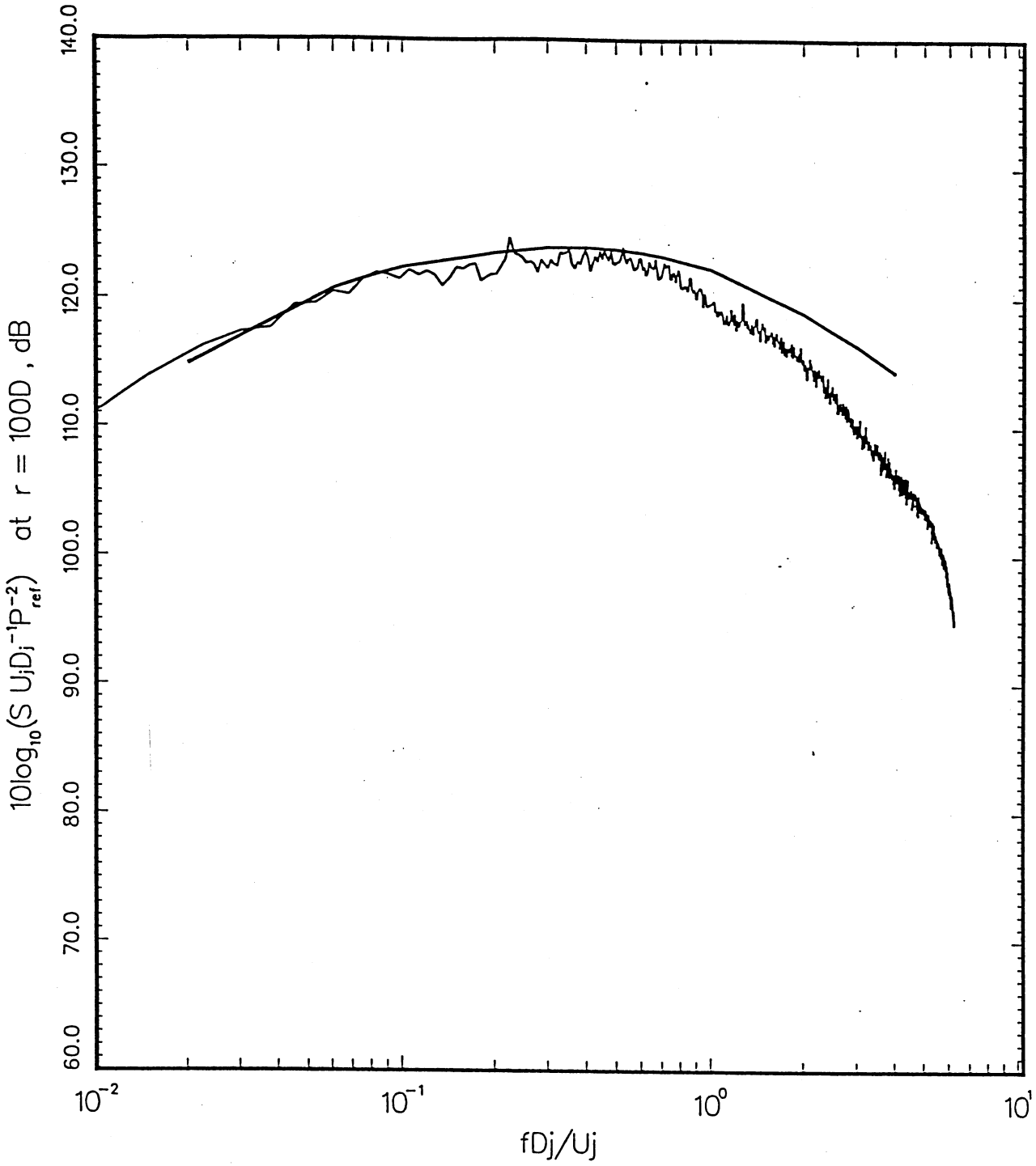
Rectangular, Ar = 7.6, Mach 2.0 jet, $T_r/T_\infty = 1.8$. Major axis plane, $\Theta = 90°$, $\tau_s = c_\tau \frac{k}{\epsilon+\epsilon_0}$, $l_s = c_l \frac{k^{3/2}}{\epsilon+\epsilon_0}$, $\epsilon_0 = 3.0 \cdot 10^{-5}$. Contribution only from turbulence with $k \leq 0.01 \cdot k_{max}$. The tolerance when computing Green's functions is 0.005 .



Rectangular, Ar = 7.6, Mach 2.0 jet, $T_r/T_\infty = 1.8$. Minor axis plane, $\Theta = 90°$, $\tau_s = c_\tau \frac{k}{\epsilon+\epsilon_0}$, $l_s = c_l \frac{k^{3/2}}{\epsilon+\epsilon_0}$, $\epsilon_0 = 3.0 \cdot 10^{-5}$. Contribution only from turbulence with $k \leq 0.01 \cdot k_{max}$. The tolerance when computing Green's functions is 0.005 .



Reactangular, Ar = 7.6, Mach 2.0 jet, $T_r/T_\infty = 1.8$. Major axis plane, $\Theta = 72°$, $\tau_s = c_\tau \frac{k}{\epsilon+\epsilon_0}$, $l_s = c_l \frac{k^{3/2}}{\epsilon+\epsilon_0}$, $\epsilon_0 = 3.0 \cdot 10^{-5}$. Contribution only from turbulence with $k \leq 0.01 \cdot k_{max}$. The tolerance when computing Green's functions is 0.005 .



Rectangular, Ar = 7.6, Mach 2.0 jet, $T_r/T_\infty = 1.8$. Minor axis plane, $\Theta = 72°$, $\tau_s = c_\tau \frac{k}{\epsilon+\epsilon_0}$, $l_s = c_l \frac{k^{3/2}}{\epsilon+\epsilon_0}$, $\epsilon_0 = 3.0 \cdot 10^{-5}$. Contribution only from turbulence with $k \leq 0.01 \cdot k_{max}$. The tolerance when computing Green's functions is 0.005 .

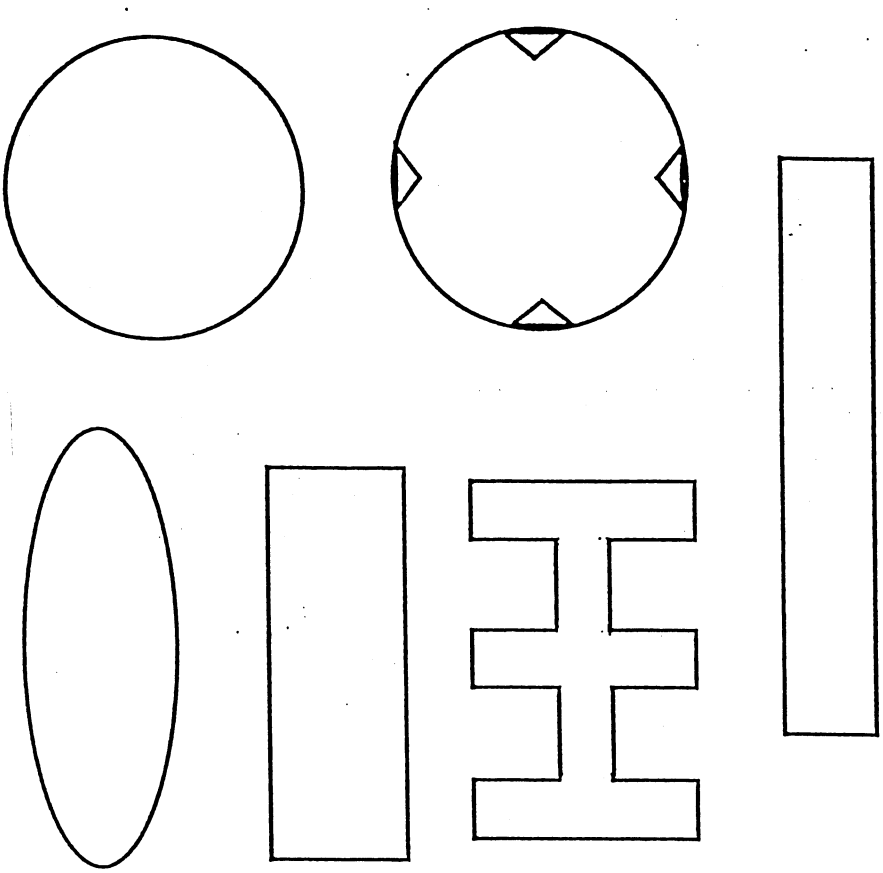
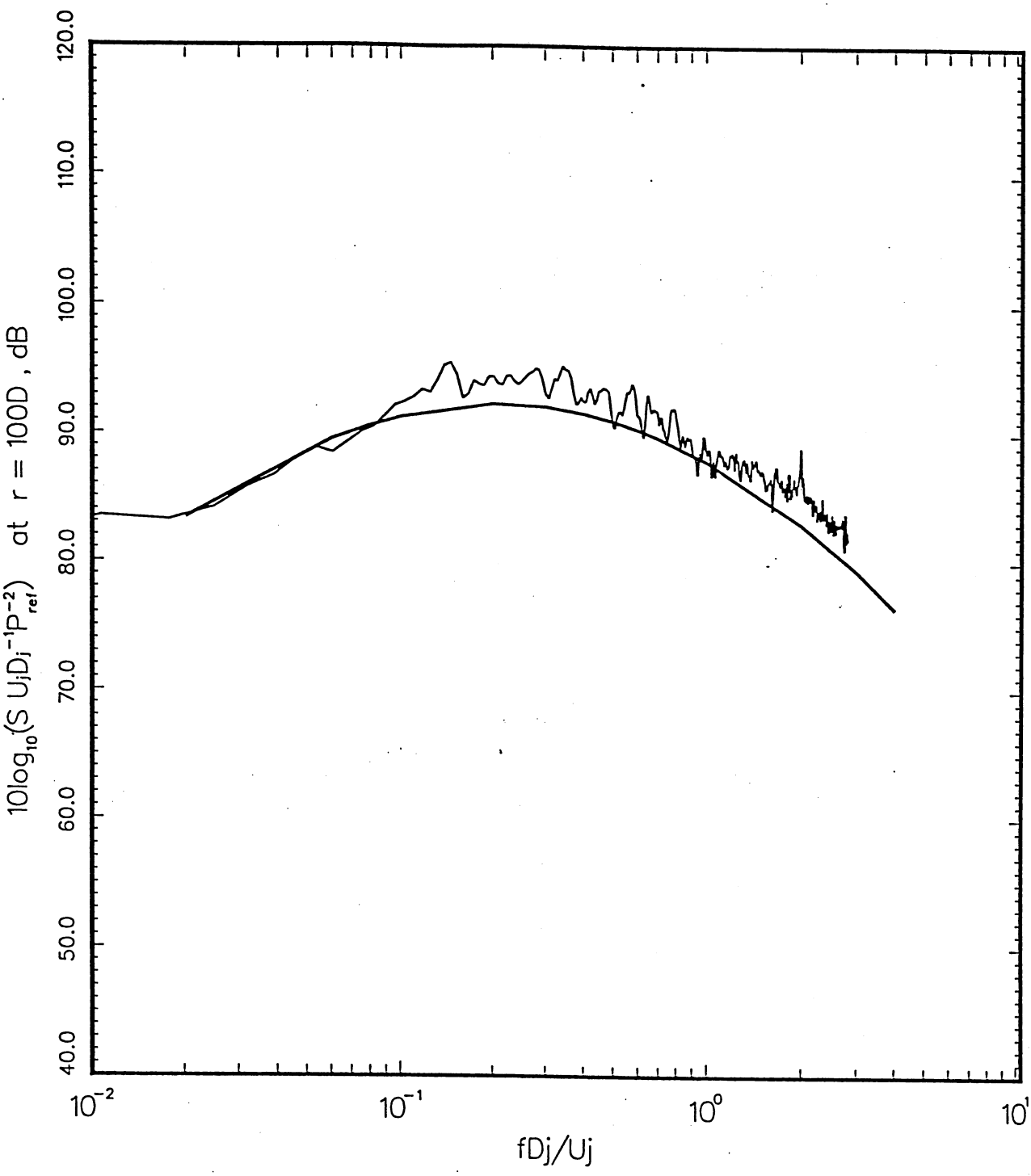
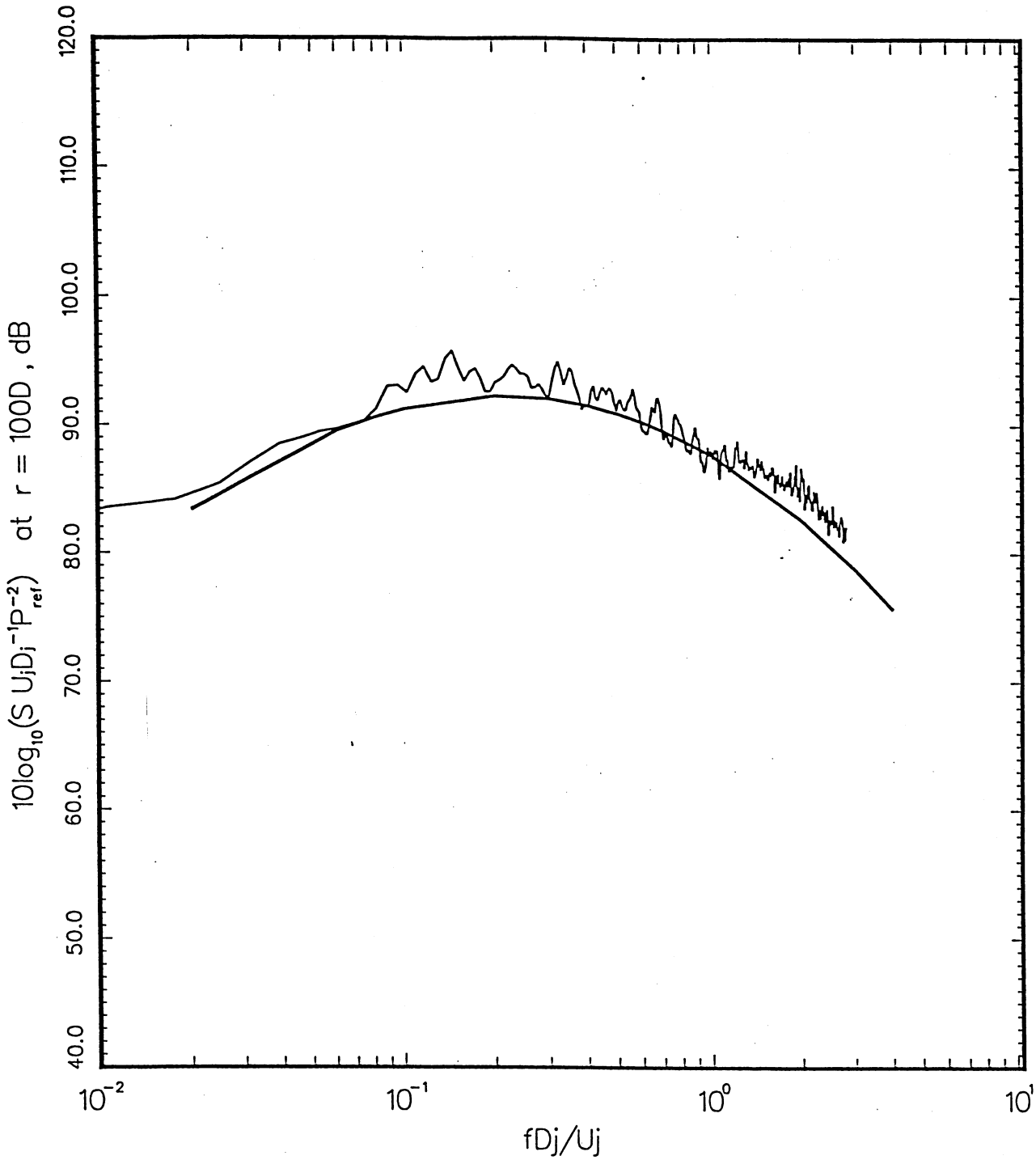


Figure 2 Schematic of the exit geometry of the nozzles. Clockwise from top left are: (1) circular, (2) circular with four tabs, (3) 8:1 rectangular, (4) six-lobed, (5) 3:1 rectangular and (6) 3:1 elliptic nozzles. Equivalent diameter (*D*) for all non-axisymmetric nozzles is 0.58 in, that of the circular nozzle is 0.5 in.



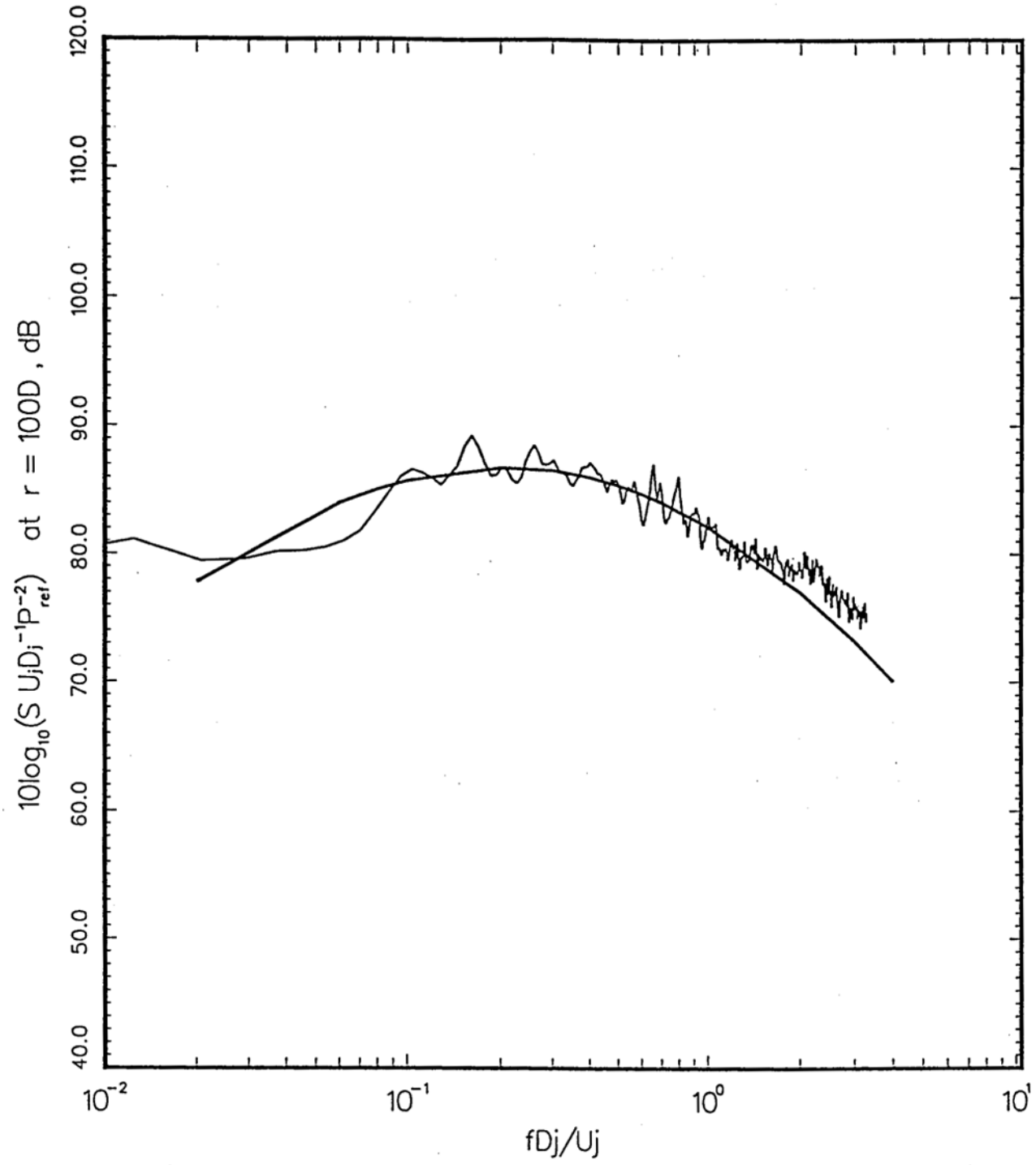
Elliptic, Ar = 3.0, Mach 0.82 jet, $T_r/T_\infty = 1.0$. Major axis plane, $\Theta = 90°$, $\tau_s = c_\tau \frac{k}{\epsilon+\epsilon_0}$, $l_s = c_l \frac{k^{3/2}}{\epsilon+\epsilon_0}$, $\epsilon_0 = 3.0 \cdot 10^{-5}$. Contribution only from turbulence with $k \leq 0.01 \cdot k_{max}$. The tolerance when computing Green's functions is 0.005

.

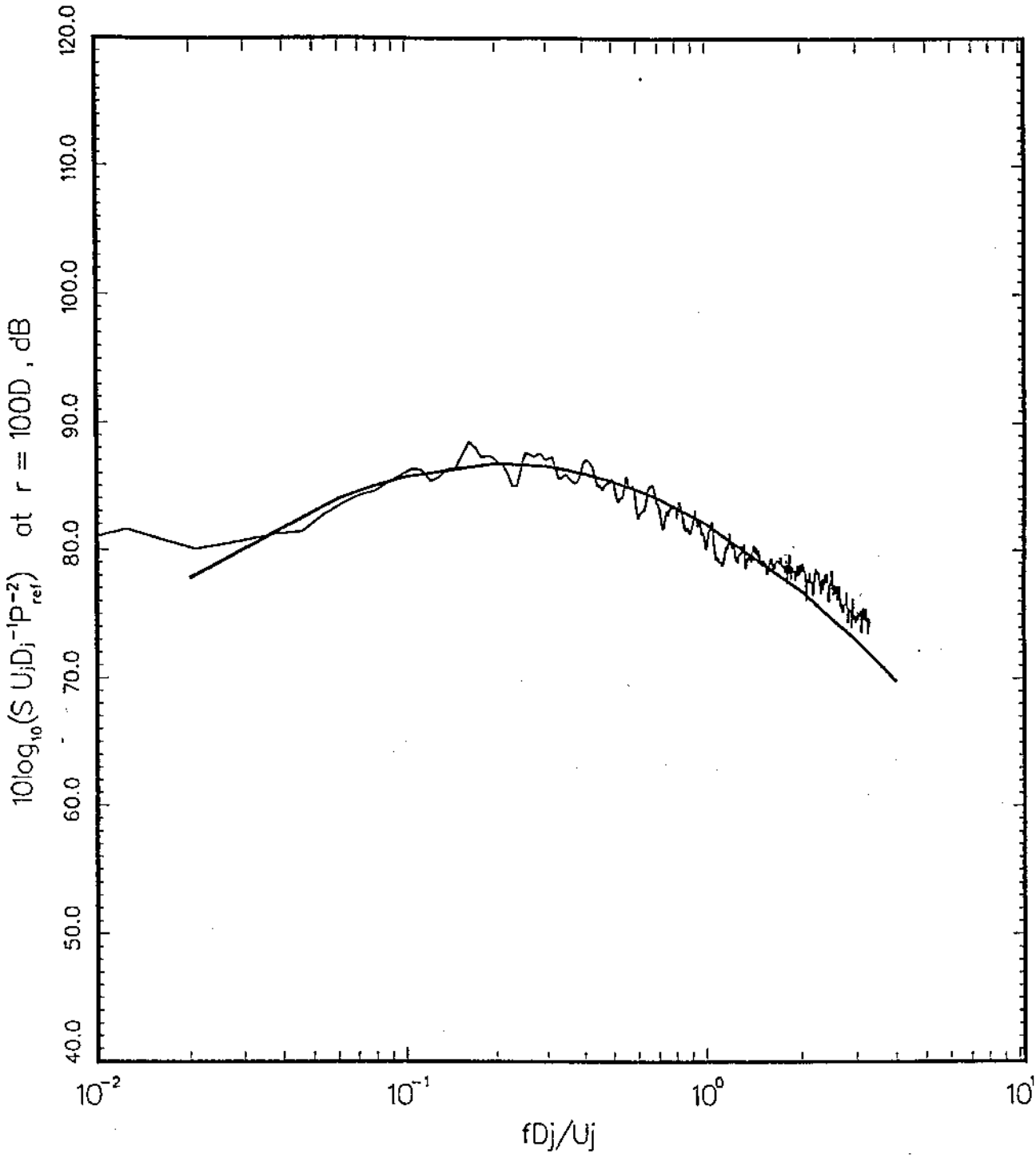


Elliptic, Ar = 3.0, Mach 0.82 jet, $T_r/T_\infty = 1.0$. Minor axis plane, $\Theta = 90°$, $\tau_s = c_\tau \frac{k}{\epsilon+\epsilon_0}$, $l_s = c_l \frac{k^{3/2}}{\epsilon+\epsilon_0}$, $\epsilon_0 = 3.0 \cdot 10^{-5}$. Contribution only from turbulence with $k \leq 0.01 \cdot k_{max}$. The tolerance when computing Green's functions is 0.005

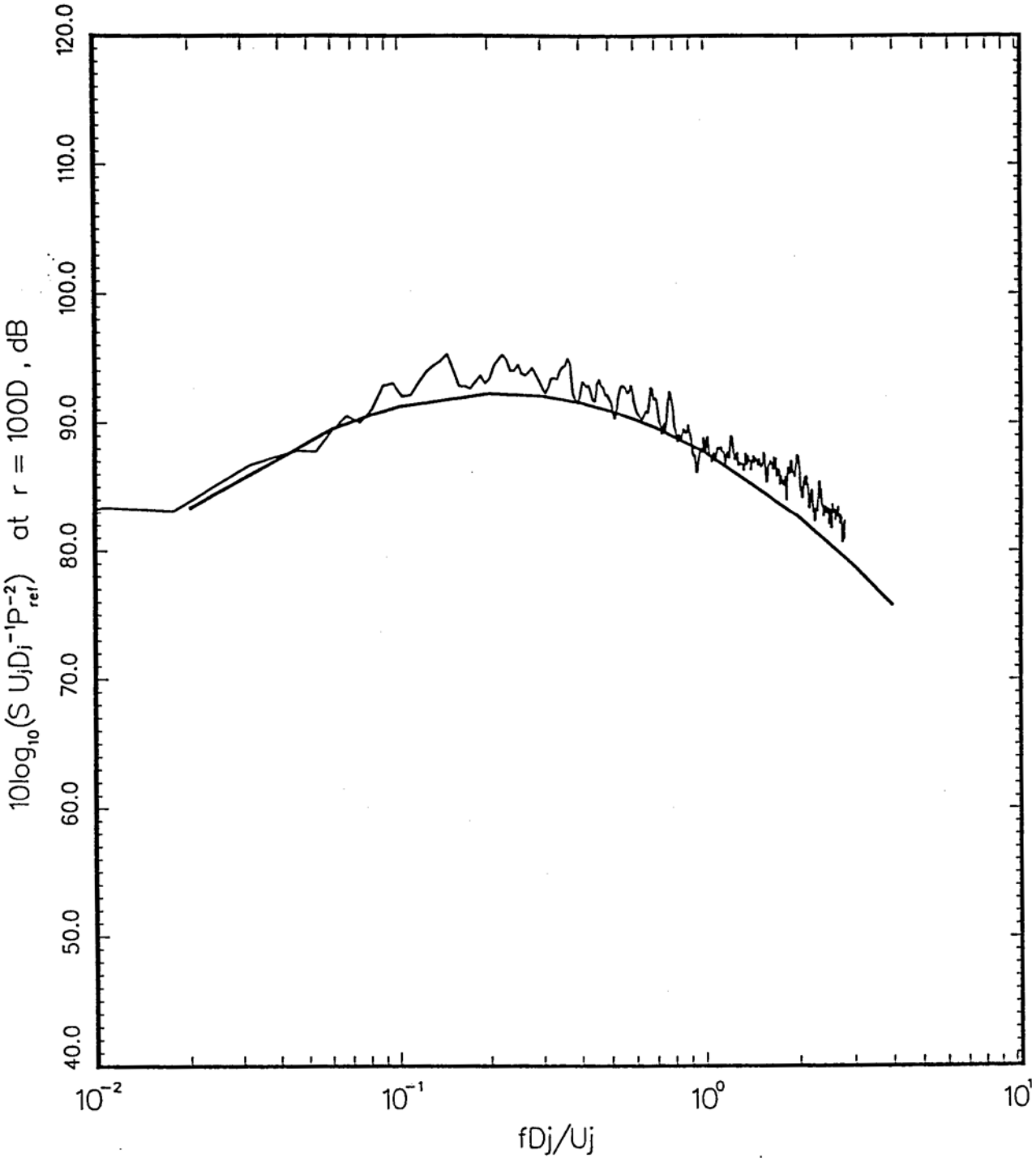
.



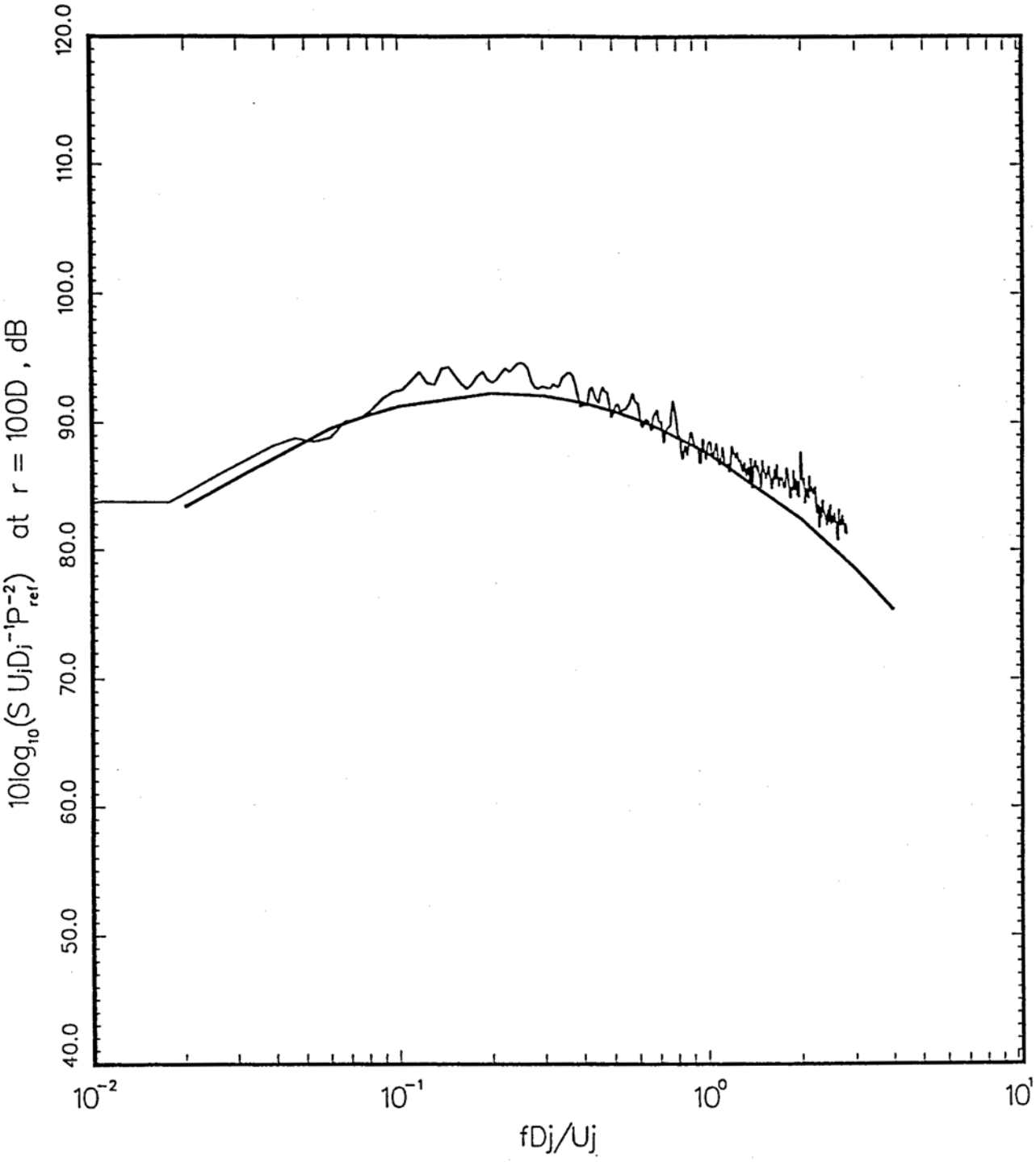
Rectangular, Ar = 3.0, Mach 0.7 jet, $T_r/T_\infty = 1.0$. Major axis plane, $\Theta = 90°$, $\tau_s = c_\tau \frac{k}{\epsilon+\epsilon_0}$, $l_s = c_l \frac{k^{3/2}}{\epsilon+\epsilon_0}$, $\epsilon_0 = 3.0 \cdot 10^{-5}$. Contribution only from turbulence with $k \leq 0.01 \cdot k_{max}$. The tolerance when computing Green's functions is 0.005 .



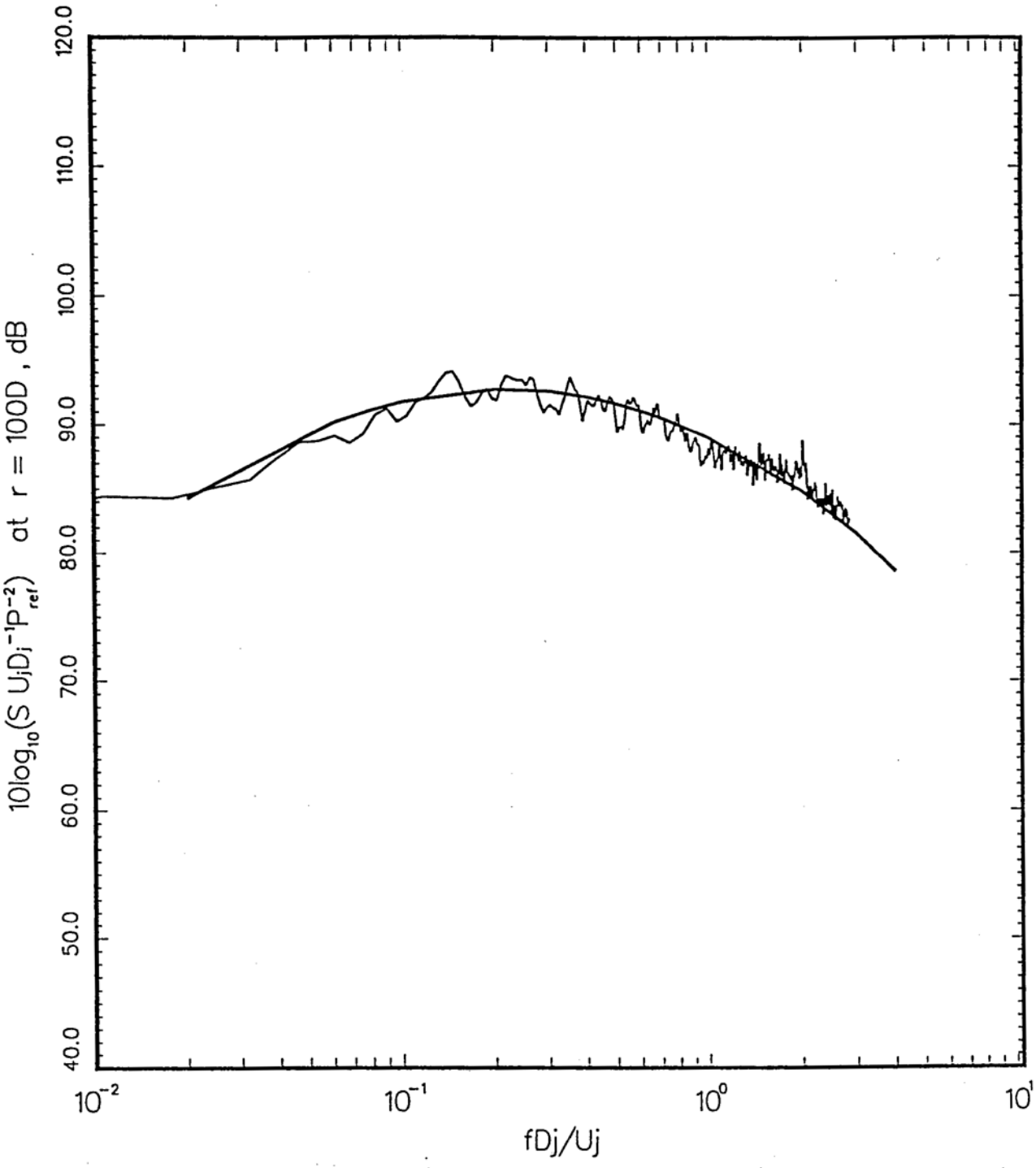
Rectangular, Ar = 3.0, Mach 0.7 jet, $T_r/T_\infty = 1.0$. Minor axis plane, $\Theta = 90°$, $\tau_s = c_\tau \frac{k}{\epsilon+\epsilon_0}$, $l_s = c_l \frac{k^{3/2}}{\epsilon+\epsilon_0}$, $\epsilon_0 = 3.0 \cdot 10^{-5}$. Contribution only from turbulence with $k \leq 0.01 \cdot k_{max}$. The tolerance when computing Green's functions is 0.005 .



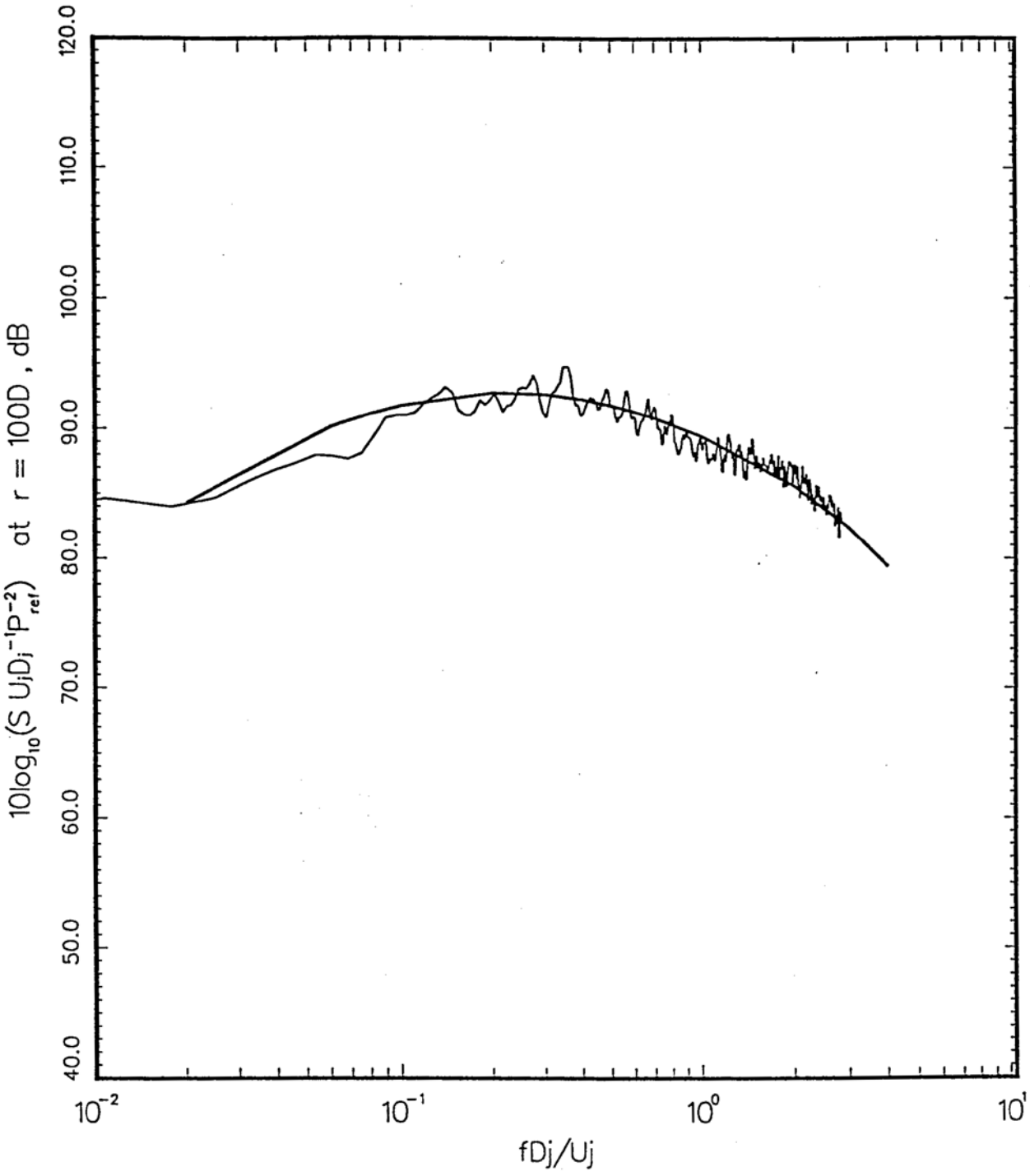
Rectangular, Ar = 3.0, Mach 0.82 jet, $T_r/T_\infty = 1.0$. Major axis plane, $\Theta = 90°$, $\tau_s = c_\tau \frac{k}{\epsilon+\epsilon_0}$, $l_s = c_l \frac{k^{3/2}}{\epsilon+\epsilon_0}$, $\epsilon_0 = 3.0 \cdot 10^{-5}$. Contribution only from turbulence with $k \leq 0.01 \cdot k_{max}$. The tolerance when computing Green's functions is 0.005 .



Rectangular, Ar = 3.0, Mach 0.82 jet, $T_r/T_\infty = 1.0$. Minor axis plane, $\Theta = 90°$, $\tau_s = c_\tau \frac{k}{\epsilon+\epsilon_0}$, $l_s = c_l \frac{k^{3/2}}{\epsilon+\epsilon_0}$, $\epsilon_0 = 3.0 \cdot 10^{-5}$. Contribution only from turbulence with $k \leq 0.01 \cdot k_{max}$. The tolerance when computing Green's functions is 0.005 .



Rectangular, Ar = 8.0, Mach 0.82 jet, $T_r/T_\infty = 1.0$. Minor axis plane, $\Theta = 90°$, $\tau_s = c_\tau \frac{k}{\epsilon+\epsilon_0}$, $l_s = c_l \frac{k^{3/2}}{\epsilon+\epsilon_0}$, $\epsilon_0 = 3.0 \cdot 10^{-5}$. Contribution only from turbulence with $k \leq 0.01 \cdot k_{max}$. The tolerance when computing Green's functions is 0.005 .



Reactangular, Ar = 8.0, Mach 0.82 jet, $T_r/T_\infty = 1.0$. Major axis plane, $\Theta = 90°$, $\tau_s = c_\tau \frac{k}{\epsilon+\epsilon_0}$, $l_s = c_l \frac{k^{3/2}}{\epsilon+\epsilon_0}$, $\epsilon_0 = 3.0 \cdot 10^{-5}$. Contribution only from turbulence with $k \leq 0.01 \cdot k_{max}$. The tolerance when computing Green's functions is 0.005 .

Conclusions

There is now, at least, one alternative jet noise Theory (from fine scale turbulence) that is not based on the Acoustic Analogy approach. This semi-empirical theory has 3 empirical constants.

The noise spectra predicted by the theory agree well with experiments for subsonic cold jets and for cold and hot supersonic jets. The predictions of the theory for jets in simulated forward flight and for non-axisymmetric jets are also in good agreement with experimental measurements.

C. Tam References

1. Tam, C.K.W. *Directional acoustic radiation from a supersonic jet generated by shear layer instability,* Journal of Fluid Mechanics, **46**, 757–768, 1971.

2. Tam, C.K.W. & Morris, P.J. *The radiation of sound by the instability waves of a compressible plane turbulent shear layer,* Journal of Fluid Mechanics, **98**, 349–381, 1980.

3. Tam, C.K.W. & Tanna, H.K. *Shock associated noise of supersonic jets from convergent-divergent nozzles* (with H.K. Tanna), Journal of Sound and Vibration, **81**, 337–358, 1982.

4. Ahuja, K. K., Lepicovsky, J., Tam, C.K.W. et al *Tone-excited jet — theory and experiments,* National Aeronautics and Space Administration CR–3538, 1982.

5. Tam, C.K.W. & Burton, D.E. *Sound generated by instability waves of supersonic flows: Part I.* Two Dimensional Mixing Layers , Journal of Fluid Mechanics, **138**, 249–271, 1984.

6. Tam, C.K.W. & Burton, D.E. *Sound generated by instability waves of supersonic flows: Part II.* Axisymmetric Jets, Journal of Fluid Mechanics, **138**, 273–295, 1984.

7. Tam, C.K.W., Jackson, J.A. & Seiner, J.M. *A multiple-scales model of the shock cell structure of imperfectly expanded supersonic jets,* Journal of Fluid Mechanics, **153**, 123–149, 1985.

8. Tam, C.K.W. *On broadband shock associated noise of supersonic jets,* Recent Advances in Aerodynamics and Aeroacoustics, 25–51, 1985.

9. Tanna, H.K., Brown, W.H. and Tam, C.K.W. *Shock associated noise of inverted-profile coannular jets: Part I. Experiments,* Journal of Sound and Vibration, **98**, 95–113, 1985.

10. Tam, C.K.W. & Tanna, H.K. *Shock associated noise of inverted-profile coannular jets: Part II. Condition for Minimum Noise,* Journal of Sound and Vibration, **98**, 115–125, 1985.

11. Tam, C.K.W. & Tanna, H.K. *Shock associated noise of inverted-profile coannual jets: Part III. Shock Structure and Noise Characteristics,* Journal of Sound and Vibration, **98**, 127–145, 1985.

12. Tam, C.K.W. and Morris, P.J. *Tone excited-jets — A theoretical model and comparison with experiment,* Journal of Sound and Vibration, **102**, 119–151, 1985.

13. Tam, C.K.W., Seiner, J.M. & Yu, J.C. *Proposed relationship between broadband shock associated noise and screech tones,* Journal of Sound and Vibration, **110**, 309–321, 1986.

14. Tam, C.K.W. *Stochastic model theory of broadband shock associated noise from supersonic jets,* Journal of Sound and Vibration, **116**, 265–302, 1987.

15. Tam, C.K.W. *The shock-cell structures and screech tone frequencies of rectangular and non-axisymmetric supersonic jets,* Journal of Sound and Vibration **121**, 135–147, 1988.

16. Tam, C.K.W. & Hu, F.Q. *On the three families of instability waves of high speed jets,* Journal of Fluid Mechanics, **201**, 447–483, 1989.

17. Tam, C.K.W. & Ahuja, K.K. *Theoretical model of discrete tone generation by impinging jets,* Journal of Fluid Mechanics, **214**, 67–87, 1990.

18. Tam, C.K.W. *Broadband shock associated noise of moderately imperfectly expanded supersonic jets,* Journal of Sound and Vibration, **140**, 55–71, 1990.

19. Tam, C.K.W. *Jet noise generated by large scale coherent motion,* Chapter 6 in Aeroacoustics of Flight Vehicles: Theory and Practice, volume 1, NASA RP–4258, 1991.

20. Tam, C.K.W. *Broadband shock associated noise from supersonic jets in flight.,* Journal of Sound and Vibration **151**, 131–147, 1991.

21. Tam, C.K.W. & Nofum, T. *Impingement tones of large aspect ratio supersonic rectangular jets,* American Institute of Aeronautics and Astronautics Journal, **30**, 304–311, 1992.

22. Tam, C.K.W. Chen, P. & Seiner, J.M. *Relationship between instability waves and noise of high-speed jets.* American Institute of Aeronautics and Astronautics Journal, **30**, 1747–1752, 1992.

23. Tam, C.K.W. *Broadband shock associated noise from supersonic jets measured by a ground observer,* AIAA Journal, **30**, 2395–2401, 1992.

24. Tam, C.K.W. & Thies, A.T. *Instability of rectangular jets,* Journal of Fluid Mechanics, **248**, 425–448, 1993.

25. Tam, C.K.W., Ahuja, K.K. & Jones, R.R. *Screech tones from free and ducted supersonic jets.* AIAA Journal, **32**, 917–922, 1994.

26. Tam, C.K.W. & Chen, P. *Turbulent mixing noise from supersonic jets,* AIAA Journal, **32**, 1774–1780, 1994.

27. Tam, C.K.W. *Supersonic jet noise*, Annual Review of Fluid Mech., **27**, 17–43, 1995.

28. Thies, A.T. & Tam, C.K.W. *Computation of turbulent axisymmetric and nonaxisymmetric jet flows using the k – ε model*, AIAA Journal, **34**, 309–316, 1996.

29. Tam, C.K.W. & Reddy, N.N. *A prediction method for broadband shock associated noise from supersonic rectangular jets*, Journal of Aircrafts, **33**, 298–303, 1996.

30. Tam, C.K.W., Shen, H. & Raman, G. *Screech tones of supersonic jets from beveled rectangular nozzles*, AIAA Journal, **35**. 1119–1125, 1997.

31. Tam, C.K.W. *Jet noise: Since 1952*, Theoretical and Computational Fluid Dynamics, **10**, 393–405, 1998.

32. Tam, C.K.W. *Influence of nozzle geometry on the noise of high-speed jets*, AIAA Journal, **36**, 1396–1400, 1998.

33. Tam, C.K.W. & Auriault, L. *Mean flow refraction effects on sound radiated from localized sources in a jet*, Journal of Fluid Mechanics, **370**, 149–174, 1998.

34. Shen, H. & Tam, C.K.W. *Numerical simulation of the generation of axisymmetric mode jet screech tones.* AIAA Journal, **36**, 1801-1807, 1998.

35. Tam, C.K.W. & Auriault, L. *Jet mixing noise from fine scale turbulence*, AIAA Journal, 37, 145–153, 1999.

36. Tam, C.K.W. & Zaman, K.B.M.Q. *Subsonic jet noise from non-axisymmetric and tabbed nozzles*, AIAA Journal, **38**, 592–599, 2000.

37. Shen, H. & Tam, C.K.W. *Effects of jet temperature and nozzle-lip thickness on screech tones*, AIAA Journal, **38**, 762–767, 2000.

38. Shen, H. & Tam, C.K.W. *Three Dimensional Numerical Simulation of the Jet Screech Phenomenon*, AIAA Paper 2001-0820, 2001.

39. Tam, C.K.W. & Pastouchenko, N. *Noise from the Fine Scale Turbulence of Nonaxisymmetric Jets*, AIAA Paper 2001-2187, 2001.

40. Tam, C.K.W., Golebiowski, M. & Seiner, J.M. *On the Two Components of Turbulent Jet Mixing Noise from Supersonic Jets*, AIAA Paper 96-1716, 1996.

Dr. Goldstein first commented on a question that was raised about the validity of Lighthill's acoustic analogy. He pointed out that the acoustic analogy had to be valid since it is based on an exact rearrangement of the Navier-Stokes equations. He indicated that a more appropriate question might be whether it could actually be used to calculate jet noise with sufficient accuracy and noted that it could- provided the flow field was known with sufficient accuracy, which, however, is usually not the case.

Goldstein also commented on the remarkable self-similarity of spectral shapes that was first discovered by Olsen (for the spectra at 80 degrees to the downstream jet axis) and, more recently, by Seiner and Tam for the spectra at small angles to the jet axis. He pointed out that Tam attributed the small angle spectra to the large scale coherent structures and the 80 degree spectra to the small scale mixing noise envisioned by Lighthill. He also pointed out that this assertion is currently generating considerable controversy.

Goldstein indicated that the most unambiguous way to resolve this as well as other contentious issues would be to carry out appropriate DNS simulations, but noted that the capabilities of currently available computers precluded doing this in a cost effective fashion -especially at the high Reynolds numbers of technological interest. He recommended using some sort of hybrid numerical / analytical (or modeling) method such as a Very Large Eddy Simulation (VLES) flow solver with the filtered Reynolds stresses modeled by using a Boussinesq or some other intermediate approximation. But he noted that the high frequency sound from full-scale aircraft engines is audibly very significant and that the Large Eddy Simulations (and especially the very large eddy simulations) performed to date seem to seriously under predict the high frequency component of the acoustic spectrum.

Goldstein attributed this to the fact that the current LES and VLES methods do not account for the sound radiated by the unresolved (or sub-grid) turbulence scales and proposed a new method for predicting the sound radiated by this component of the turbulence. In this approach, the sound from the unresolved scales is determined by an inhomogeneous linearized Euler equation with the linearization carried out about the (unsteady) large scale (i.e. filtered) velocity field and the source term primarily determined by fluctuating Reynolds stresses based on the unresolved scales. As in the usual acoustic analogy approach (in which the linearization is about the mean flow, see Goldstein 1999 Program and Abstracts of the 6 th International Congress on Sound and Vibration, Copenhagen "Some Recent Developments in Jet Noise Modeling "), this equation is an exact rearrangement of the Navier-Stokes equations, but the source term is unknown and has to be computed or modeled. Goldstein showed how this could be done by extending ideas developed for the Acoustic Analogy approach. He also pointed out that the total sound field could be calculated by simply adding the mean square pressures radiated by the resolved and unresolved components of the turbulence, provided an appropriate filter was used for the Large Eddy Simulation. Finally, Goldstein noted

that this approach reduces to the usual acoustic analogy approach (formulated in terms of the linearized Euler equations) in the limit as the filter width becomes infinite. This material was presented in more detail at the 38th AIAA Aerospace Sciences Meeting and Exhibit in Reno, Nevada, 2000.

Dr. Seiner quoted a remark of Lumley; 'The reason I would never work in the field of aeroacoustics is that its governing equation is not derived from first principles'. Seiner discussed the derivation of a finite amplitude non-linear wave equation including viscous damping, and argued that its solution applied to all acoustic waves propagating in free space, including the linearized solutions applicable for small amplitude waves. (Acoustic waves by definition are waves of infinitesimal amplitude. All finite amplitude waves are shock waves. The Lighthill acoustic analogy is concerned only with the generation and propagation of acoustic waves. If in a problem the amplitude of an outgoing acoustic wave is found to be large, its subsequent non-linear development along its ray tube, can be treated, using the non-linear wave propagation equations. Such a calculation will determine the shock strength and its attenuation with distance.) It was remarked that for many jet engines having supersonic jet speeds shock waves have been observed which propagate towards the far field. Seiner remarked that it was ironic that the theory based on the acoustic analogy predicted a zone of silence in just the region where the most sound was observed. Lilley pointed out that this had an easy explanation since the zone of silence referred to the high frequency noise, which was subjected to refraction. The low frequency noise was not subjected to refraction effects and hence propagated in this zone. Seiner also criticized the acoustic analogy in that it could only predict the total acoustic power from a circular jet. Lilley pointed out that this was untrue. The acoustic analogy can be used for any complex flow provided an accurate flow solver has been used to provide a time-accurate picture of the entire flow. Seiner also referred to the incorporation of flight effects, which can be modeled satisfactorily. He remarked that flight effects provide excellent sound suppression, since the turbulent intensity is reduced in proportion to the velocity difference between the jet and the external flow velocity. He commented on the reduced acoustic efficiency of rectangular nozzles as opposed to circular nozzles at subsonic and supersonic speeds. No explanation was offered for this observation.

Seiner noted that in turbulent jets having complex geometry the number of modes required, having supersonic phase speeds, was very large especially for hot jets. A requirement was to consider causality and the initial specification of wave amplitude. He reminded us that the sound generated by the turbulence is a low frequency phenomenon that occurs in the moving frame of the source. Current instrumentation, such as the UM/NCPA PIV system, was ideally suited to investigate the details of the noise generation process. The recent PIV measurements of Bridges shown at the meeting (Appendix B), was a good example of the resolution that can be obtained today. He showed detailed measurements of mean velocity distributions, turbulence intensities and two-point space-time correlations of T_{ij}, which could be used as data for comparison with DNS and LES calculations. Finally, Seiner showed a comparison of the change in source correlation when water was injected into a supersonic jet.

In the discussion that followed Lilley noted that the urgent need was the development of fast time-accurate flow solvers having adequate resolution to deal with complex nozzle geometries. The acoustic analogy was a robust tool for jet noise prediction, but its usefulness depended on the accuracy of the available flow solvers. The use of DNS, in spite of its low Reynolds number, remained a powerful computational tool that can assist in the provision of a physics based source description in jet noise prediction schemes and as a guide towards attacking jet noise reduction schemes.

Dr. Ahuja referred to a recent publication that was highly critical of the Lighthill acoustic analogy. (Some discussion ensued which suggested that until any new strategy was developed for jet noise prediction there was no reason to replace the acoustic analogy especially as it had a proven track record in predicting the noise of helicopters and in many aspects of aircraft noise technology.) He then presented various sets of experimental data that showed the departure from Strouhal scaling, and which could be explained as the result of flow-acoustic interaction. He also discussed a wide variety of data relating to the long slit nozzle, instability waves in excited jets, and the effects of forward flight. He also discussed the role of large eddies in subsonic flight. Ahuja gave details of work reported first in 1976 on the cross-correlation and coherence of jet noise as measured in the far-field. He finally presented work on noise measurements related to inverted velocity profiles and some simple ideas to explain the noise reductions achieved.

Dr. Michel agreed that the acoustic analogy was valid but this presupposed that time-accurate data was available for the turbulent flow in order to determine T_{xx}. He mentioned a number of features in which the simple application of the acoustic analogy agreed with experimental data and in other cases there was disagreement. These cases included the case of hot jets at low Mach numbers and problems associated with flow-acoustic interaction. Michel argued that the proper coordinate system to use for the description of acoustic sources was coordinates at rest rather than the moving axis system recommended by Lighthill. Michel described the complete description of the source model used by Michalke and Michel(1979). The cases of the static jet and the jet in flight were considered together with the effects of the large-scale motion, Mach wave radiation and screech. A very detailed description of the work of Michel is enclosed below.

Dr. Morfey introduced certain fundamental problems he had investigated in aeroacoustics. The first centered on the noise radiated from the rate of change of the dissipation with time. This was a monopole source which vanished when the ratio of the specific heats, $\gamma = 5/3$. The existence of this monopole source had been noted by Kambe(1984) but so far has not been observed, but there were cases where it would need to be investigated. Confidence in the Lighthill acoustic analogy could be established by the experimental results of Grosche et al. (1975) comparing the OASPL measurements from different gases at the same jet Mach numbers and the results of Hubbard and Lassiter(1952) comparing measurements using Freon-12 and air. Both sets of results confirmed that Lighthill's source function behaved as expected in terms of gas density and in terms of the velocity exponent with change

in jet Mach number. He noted that the cold jet radiated noise proportional to V_j^8 whereas at low Mach numbers the hot jet had an additional source proportional to V_j^6.

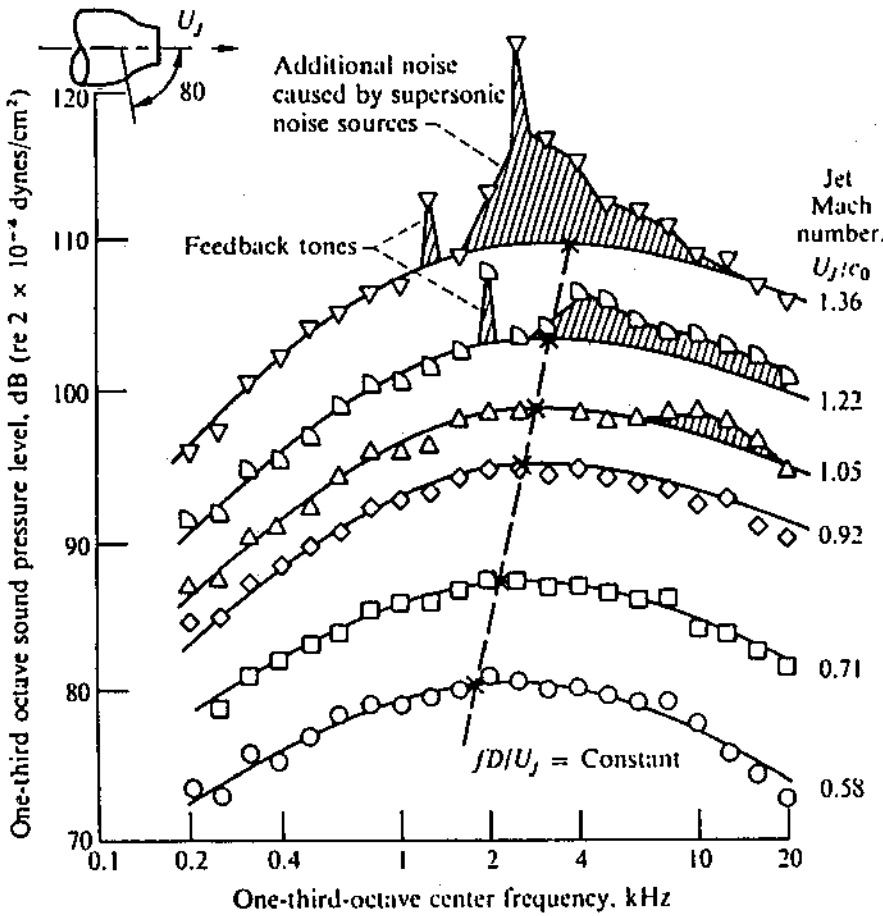
He noted the experiments of Brown and Roshko(1974) showed the importance of the two dominant structures in the mixing region, namely the large roller-like eddies and the much smaller structures which became more numerous as the Reynolds number was increased. Thus the major problem in using the Lighthill acoustic analogy is that it remains unclear as to the exact physical process which is taking place in the turbulence that is responsible for the creation of the radiated noise. The input of an exact value for T_{ij} into Lighthill's equation does not in itself describe the physical process in the mixing region where only a small fraction of the kinetic energy escapes as noise. But T_{ij} is rarely completely known and in almost all practical cases the important problem of flow-acoustic interaction needs to be considered separately. One of the advantages of the acoustic analogy in the form of the Lilley-Goldstein convected wave equation is that it deals directly with acoustic refraction due to a given mean velocity distribution across a shear layer. Morfey drew attention to the three source terms in this convected wave equation and the sensitivity of these terms. Errors can easily be introduced since there are strong cancellation effects, which can be missed if arbitrary approximations are introduced. The source terms must include the quadrupole term, otherwise it would suggest the dominant source was dipole and hence would be in conflict with Lighthill's acoustic analogy. Morfey stressed that arbitrary distributions of dipoles and quadrupoles in acoustic analogy models can give misleading results. (Farassat interposed with the comment that when a quadrupole is divided up into separate parts it is essential to retain all components.) The different types of sources were classified by Morfey and added in tabular form to his presentation.

Acoustic

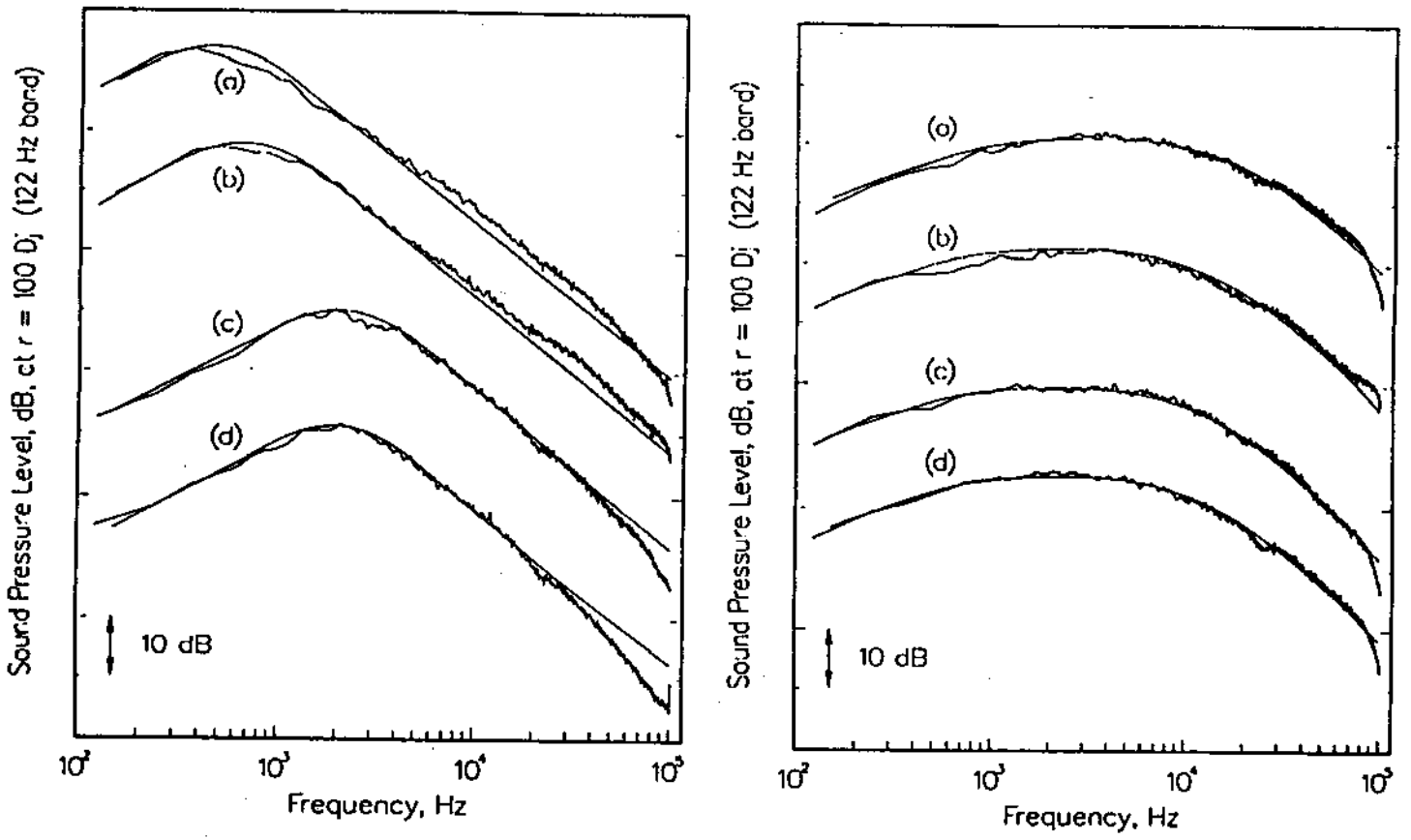
Analogy

Marvin Goldstein
NASA Glenn Research Center

One-Third Octave Jet Noise Spectra For A Convergent Nozzle At Subsonic And Supersonic Velocities; Angle from Downstream Jet Axis, 80°. Based On Data From Olsen



Narrow Band Jet Noise Spectra At 90° And Small Angles To Jet Axis From Tam, Golebiowski & Seiner (1996)



(a) $M_j = 2.0$, $T_t/T_\infty = 4.89$, $\chi = 160.1°$, $SPL_{max} = 124.7$ dB, $M_j = 1.49$, $T_t/T_\infty = 2.35$, $\chi = 92.9°$, $SPL_{max} = 96$ dB.
(b) $M_j = 2.0$, $T_t/T_\infty = 1.12$, $\chi = 160.1°$, $SPL_{max} = 121.6$ dB, $M_j = 2.0$, $T_t/T_\infty = 4.89$, $\chi = 83.8°$, $SPL_{max} = 107$ dB.
(c) $M_j = 1.96$, $T_t/T_\infty = 1.78$, $\chi = 138.6°$, $SPL_{max} = 121.0$ dB, $M_j = 1.96$, $T_t/T_\infty = 0.99$, $\chi = 83.3°$, $SPL_{max} = 95$ dB.
(d) $M_j = 1.49$, $T_t/T_\infty = 1.11$, $\chi = 138.6°$, $SPL_{max} = 106.5$ dB. $M_j = 1.96$, $T_t/T_\infty = 0.98$, $\chi = 120.2°$, $SPL_{max} = 100$ dB.

$$\chi \equiv 180^\circ - \theta$$

V-Large Eddy Simulation

Filtered N.S. Eqs. (Favre-averaged)

$$\frac{\partial}{\partial t}\begin{Bmatrix}\bar{\rho}\\ \bar{\rho}\tilde{v}_i\\ \bar{\rho}\tilde{s}\end{Bmatrix}+\frac{\partial}{\partial x_j}\begin{Bmatrix}\bar{\rho}\tilde{v}_j\\ \bar{\rho}\tilde{v}_i\tilde{v}_j+\delta_{ij}\bar{p}\\ \bar{\rho}\tilde{s}\tilde{v}_j\end{Bmatrix}-\text{viscous terms}=\frac{\partial}{\partial x_j}\begin{Bmatrix}0\\ \bar{\rho}\left(\widetilde{v_i v_j}-\tilde{v}_i\tilde{v}_j\right)\\ \bar{\rho}\left(\widetilde{sv}_j-\tilde{s}\tilde{v}_j\right)\end{Bmatrix}$$

unresolved Reynolds stress (to be modelled)

$$\tilde{f}\equiv\overline{\rho f}/\bar{\rho}$$

$$\bar{f}(\mathbf{x},t)=\int_{-\infty}^{\infty}\int_V F(\mathbf{x}-\xi,t-\tau)f(\xi,\tau)\,d\tau\,d\xi$$

CD-00-80849

Equation for Small Scale (Unresolved) Components

$$v_i = \tilde{v}_i + v_i', \quad \text{velocity} \qquad p = \bar{p} + p', \quad \text{pressure} \qquad s = \tilde{s} + s', \quad \text{entropy}$$

Inhomogenous Linearized Euler Equation

$$\underbrace{L_{ij} u_j}_{\substack{\text{Linear operator} \\ \text{(depends on filtered vel.)}}} \quad \underbrace{= S_i \equiv \frac{\partial}{\partial x_j}\left(T_{ij}' - \tilde{T}_{ij}\right) + \frac{\partial}{\partial t} T_i' + \text{visc. terms}}_{\text{source terms}}$$

$$ij = 1,2,\ldots 5$$

$$u_i = v_i', \; i = 1,2,3; \; u_4 = p', \; u_5 = s'$$

T'_{ij} is quadratic in unresolved quantities (unresolved Reynolds stress)

CD-00-80848

Formal Solution for Pressure

$$u_4 \equiv p' = L_{4j}^{-1} S_j \qquad \text{(sum on j)}$$

$$p' = \lim_{T\to\infty} \int_{-T}^{T}\int G_{4k}\left(\mathbf{x}|\mathbf{x}';t-t';\bar{t},\sigma\right) S_k(\mathbf{x}',t')\,d\mathbf{x}'dt'$$

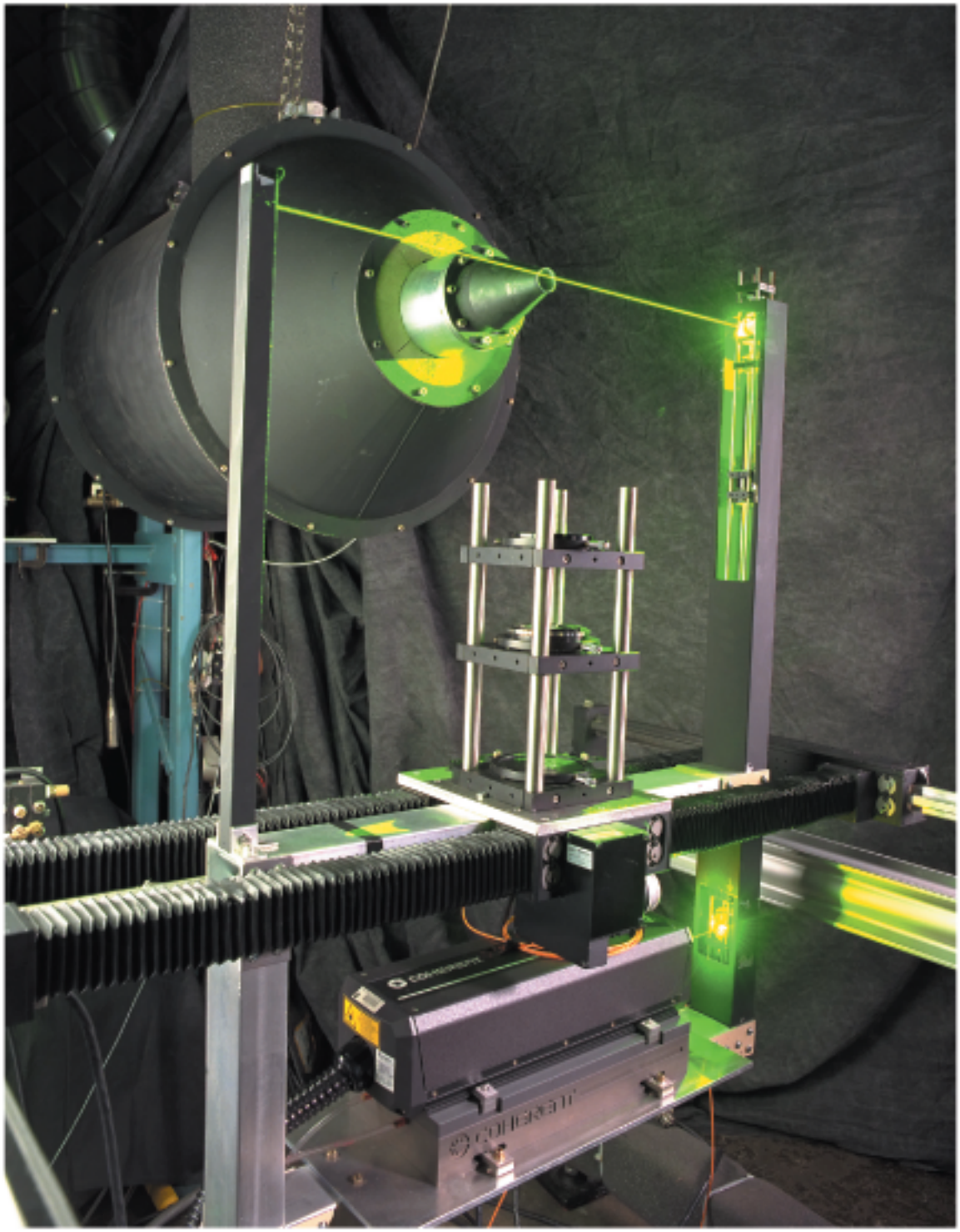
$$\left\langle p'(t+\tau,\mathbf{x})p'(\tau,\mathbf{x})\right\rangle = \text{pressure auto correlation function}$$

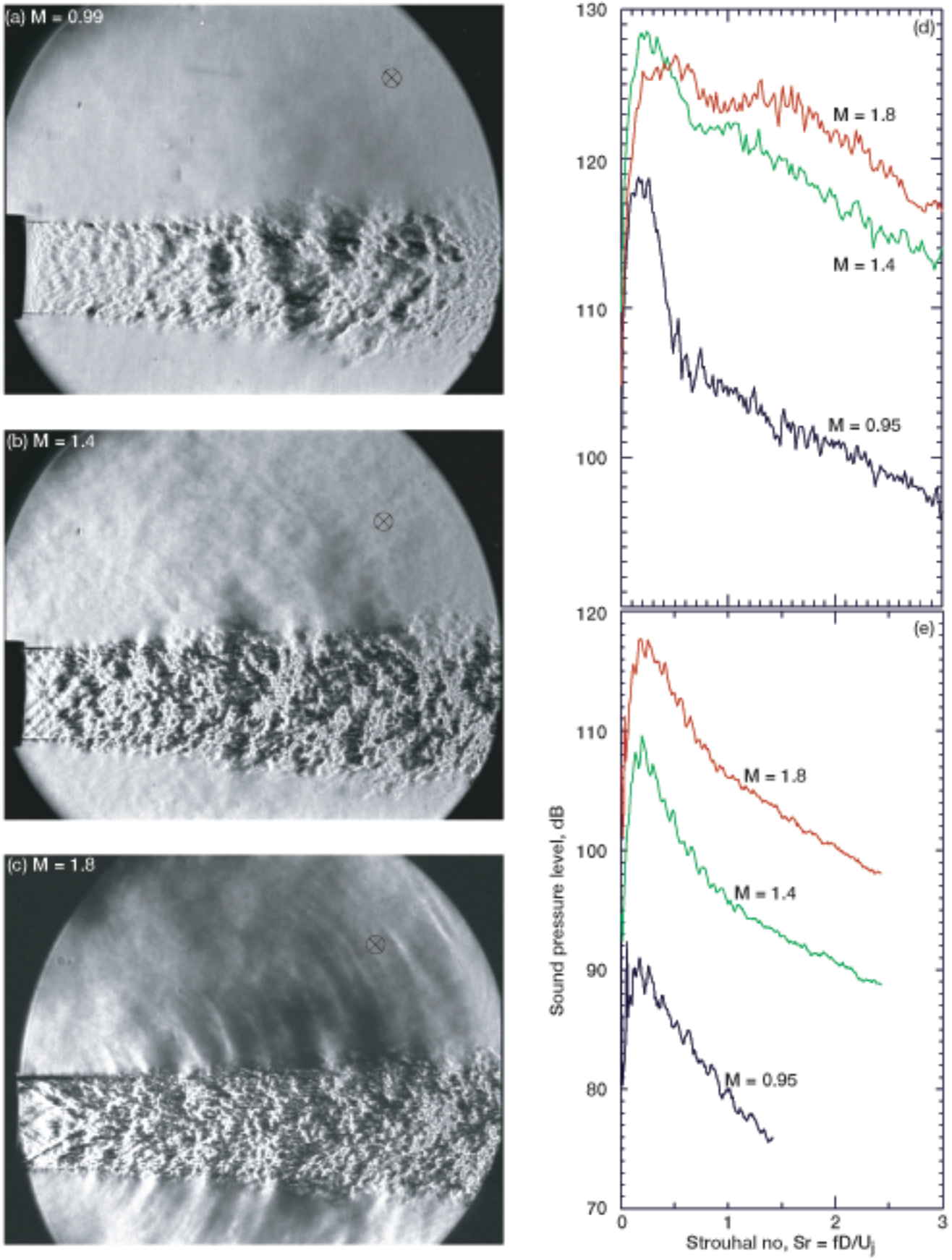
$$= \iiint \left[\Gamma_{k\ell}^{+}\left(\mathbf{x},t|\mathbf{x}',\mathbf{x}'',t'\right)\left\langle S_k(\mathbf{x}',t'+\tau)S_\ell(\mathbf{x}'',\tau)\right\rangle + \Gamma_{k\ell}^{-}\left(\mathbf{x},t|\mathbf{x}',\mathbf{x}'',t'\right)\left\langle\left|S_k(\mathbf{x}',t'+\tau)S_\ell(\mathbf{x}'',\tau)\right|\right\rangle\right] dt'd\mathbf{x}'d\mathbf{x}''$$

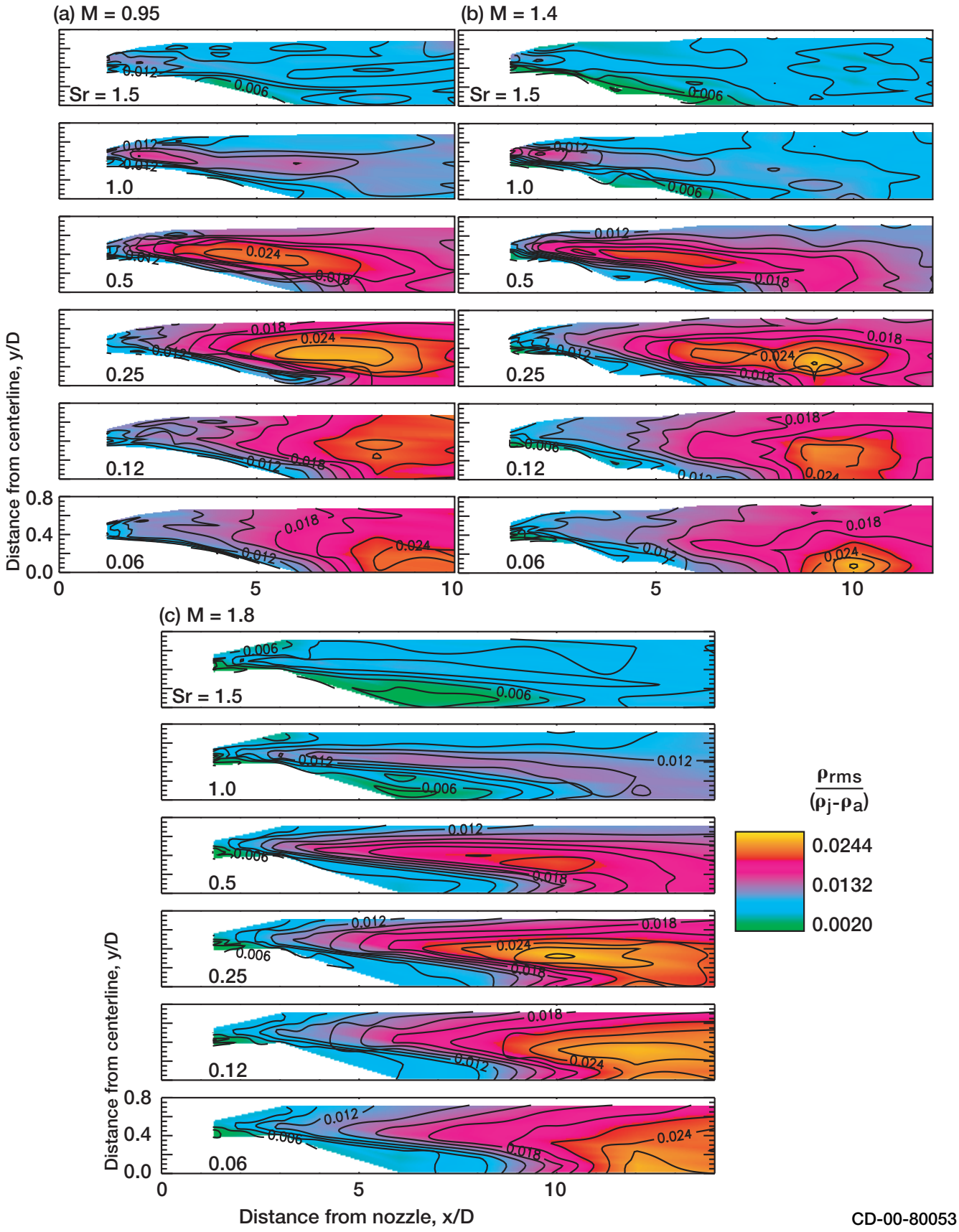
$$\left\langle \bullet \right\rangle \equiv \lim_{T\to\infty} \int_{-T}^{T} \bullet \; d\tau = \text{time average}$$

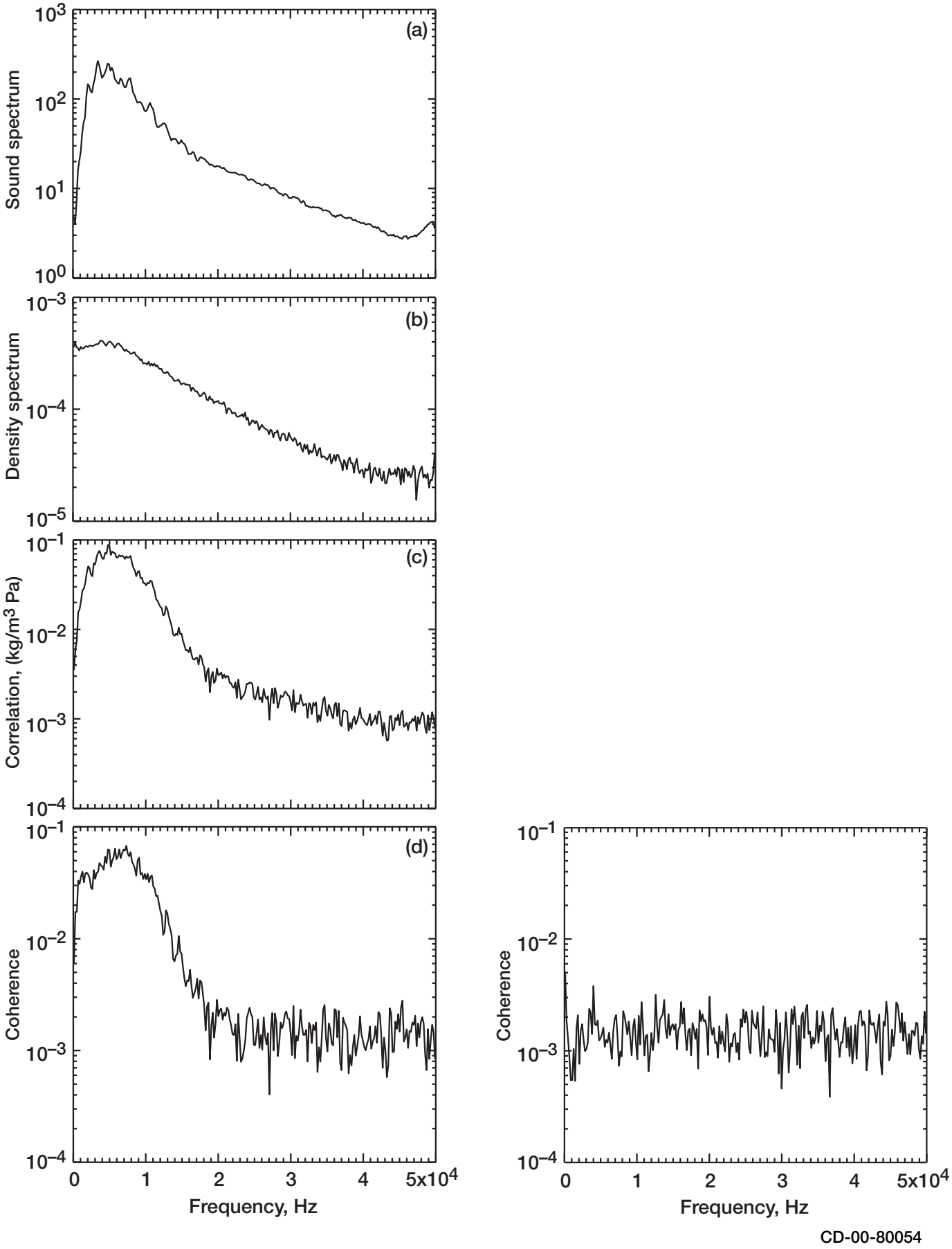
$$\left\langle \bar{f}(t+\tau)g'(\tau)\right\rangle = 0 \qquad \text{For tophat filter (in Fourier space)}$$

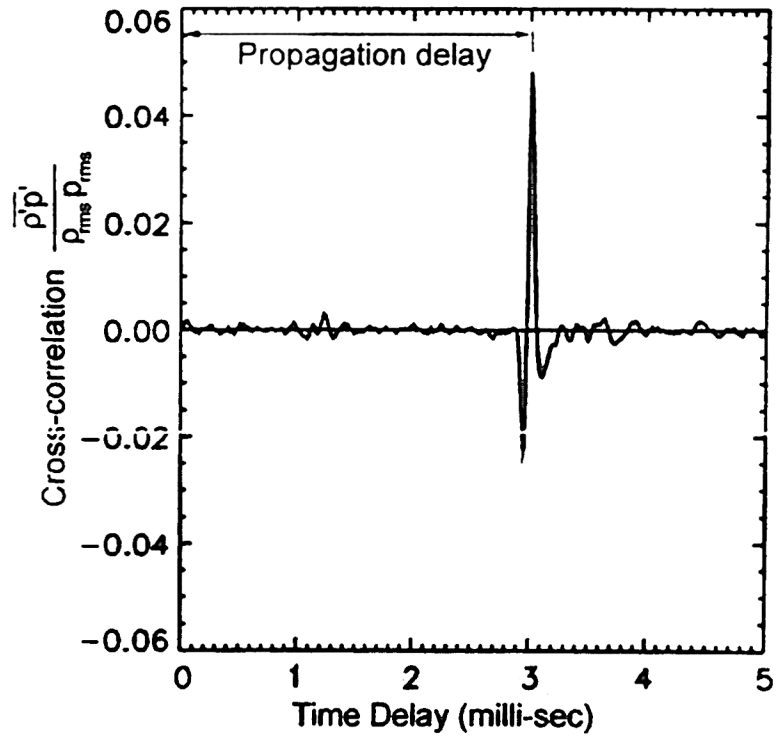
CD-00-80847

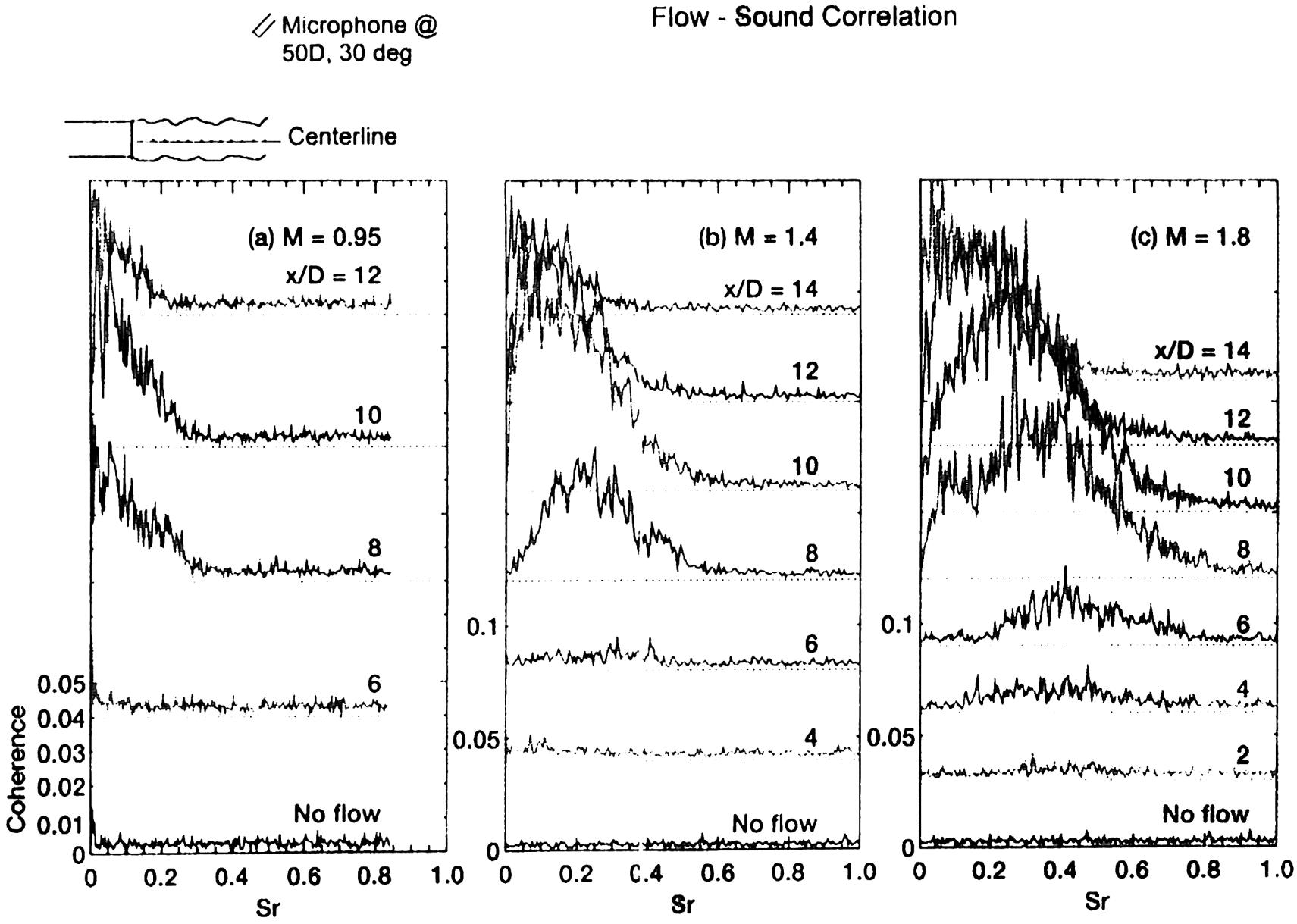


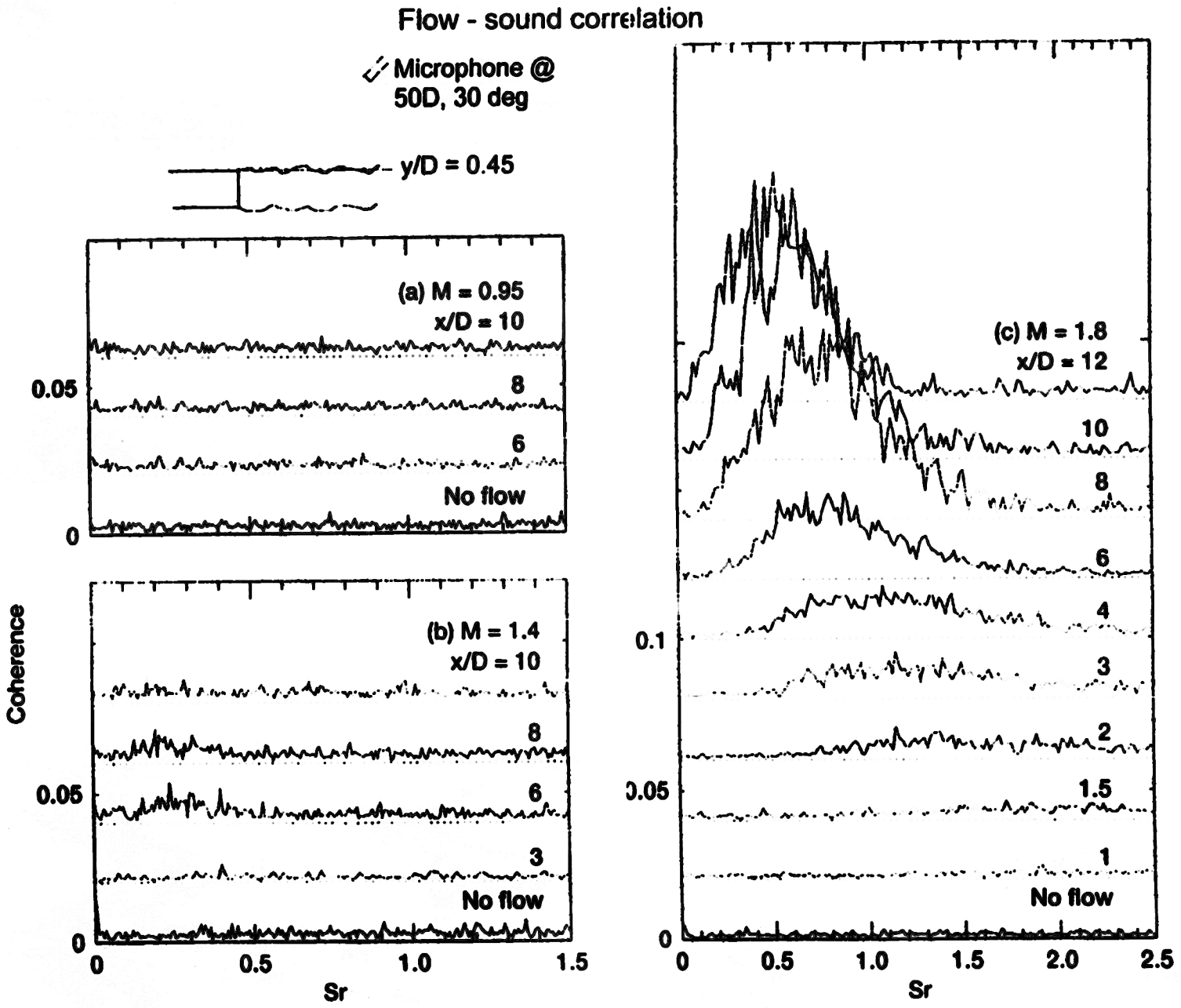

(a) M = 0.99
(b) M = 1.4
(c) M = 1.8
(d)
M = 1.8
M = 1.4
M = 0.95
(e)
M = 1.8
M = 1.4
M = 0.95
Sound pressure level, dB
Strouhal no, Sr = fD/U$_j$
130
120
110
100
90
80
70
0
1
2
3
CD-00-80046

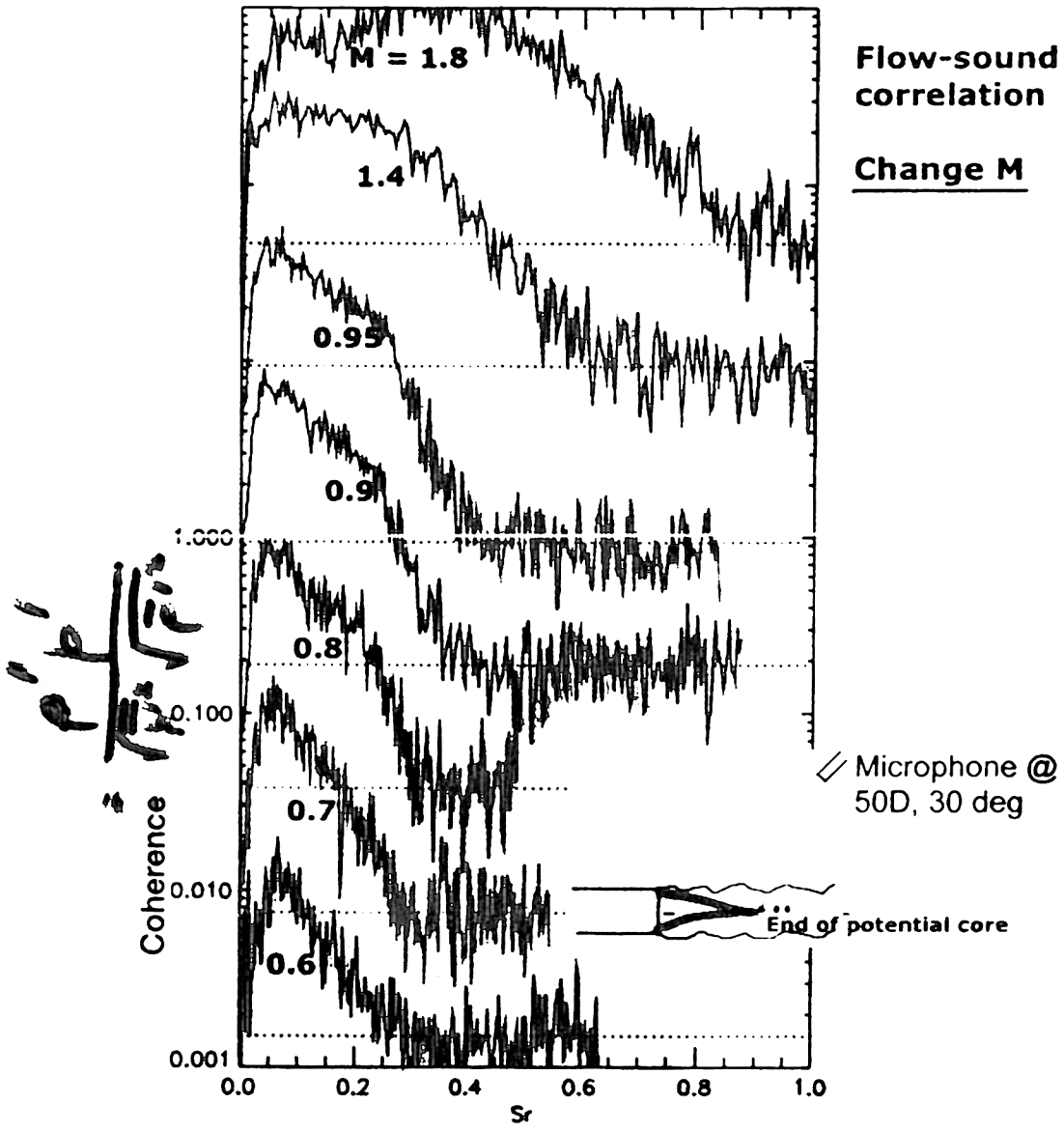

(a) M = 0.95
(b) M = 1.4
(c) M = 1.8
Sr = 1.5
1.0
0.5
0.25
0.12
0.06
Distance from centerline, y/D
Distance from nozzle, x/D
ρrms / (ρj-ρa)
0.0244
0.0132
0.0020
CD-00-80053


(a)
Sound spectrum
10^3
10^2
10^1
10^0
(b)
Density spectrum
10^{-3}
10^{-4}
10^{-5}
(c)
Correlation, (kg/m^3 Pa)
10^{-1}
10^{-2}
10^{-3}
10^{-4}
(d)
Coherence
10^{-1}
10^{-2}
10^{-3}
10^{-4}
0
1
2
3
4
5x10^4
Frequency, Hz
Coherence
10^{-1}
10^{-2}
10^{-3}
10^{-4}
0
1
2
3
4
5x10^4
Frequency, Hz
CD-00-80054


Propagation delay
0.06
0.04
0.02
0.00
−0.02
−0.04
−0.06
0
1
2
3
4
5
Time Delay (milli-sec)
Cross-correlation $\frac{\overline{p'p'}}{p_{rms}p_{rms}}$


Flow - Sound Correlation
Microphone @
50D, 30 deg
Centerline
(a) M = 0.95
x/D = 12
10
8
6
No flow
(b) M = 1.4
x/D = 14
12
10
8
6
4
No flow
(c) M = 1.8
x/D = 14
12
10
8
6
4
2
No flow
Coherence
0
0.01
0.02
0.03
0.04
0.05
0.1
0.2
0.4
0.6
0.8
1.0
Sr


Flow - sound correlation
Microphone @
50D, 30 deg
y/D = 0.45
(a) M = 0.95
x/D = 10
8
6
No flow
(b) M = 1.4
x/D = 10
8
6
3
No flow
(c) M = 1.8
x/D = 12
10
8
6
4
3
2
1.5
1
No flow
Coherence
0.05
0
0.1
0.05
0
0
0.5
1.0
1.5
2.0
2.5
Sr


Flow-sound correlation
Change M
M = 1.8
1.4
0.95
0.9
0.8
0.7
0.6
1.000
0.100
0.010
0.001
Coherence
0.0
0.2
0.4
0.6
0.8
1.0
Sr
Microphone @ 50D, 30 deg
End of potential core

M. Goldstein References

1. Goldstein, M. E. Aeroacoustics, McGraw-Hill 1976.

2. Olsin (Only published in Aeroacoustics Pg. 105).

3. Goldstein, M. E. (1984) Aeroacoustics of Turbulent Shear Flows, Annual Reviews of Fluid Mechanics Vol. 16, Pg. 263-286.

4. Goldstein, M. E. (1999) Program and Abstracts of the 6th International Congress on Sound and Vibration, Copenhagen "Some Recent Development in Jet Noise Modeling."

Jet Noise Source Mechanisms – A Need for a Physics Based Modeling Procedure

John M. Seiner
National Center for Physical Acoustics
The University of Mississippi

NASA/CP—2001-211152

Jet Noise Source Mechanisms – A Need for a Physics Based Modeling Procedure

John M. Seiner
National Center for Physical Acoustics
The University of Mississippi

Question 1

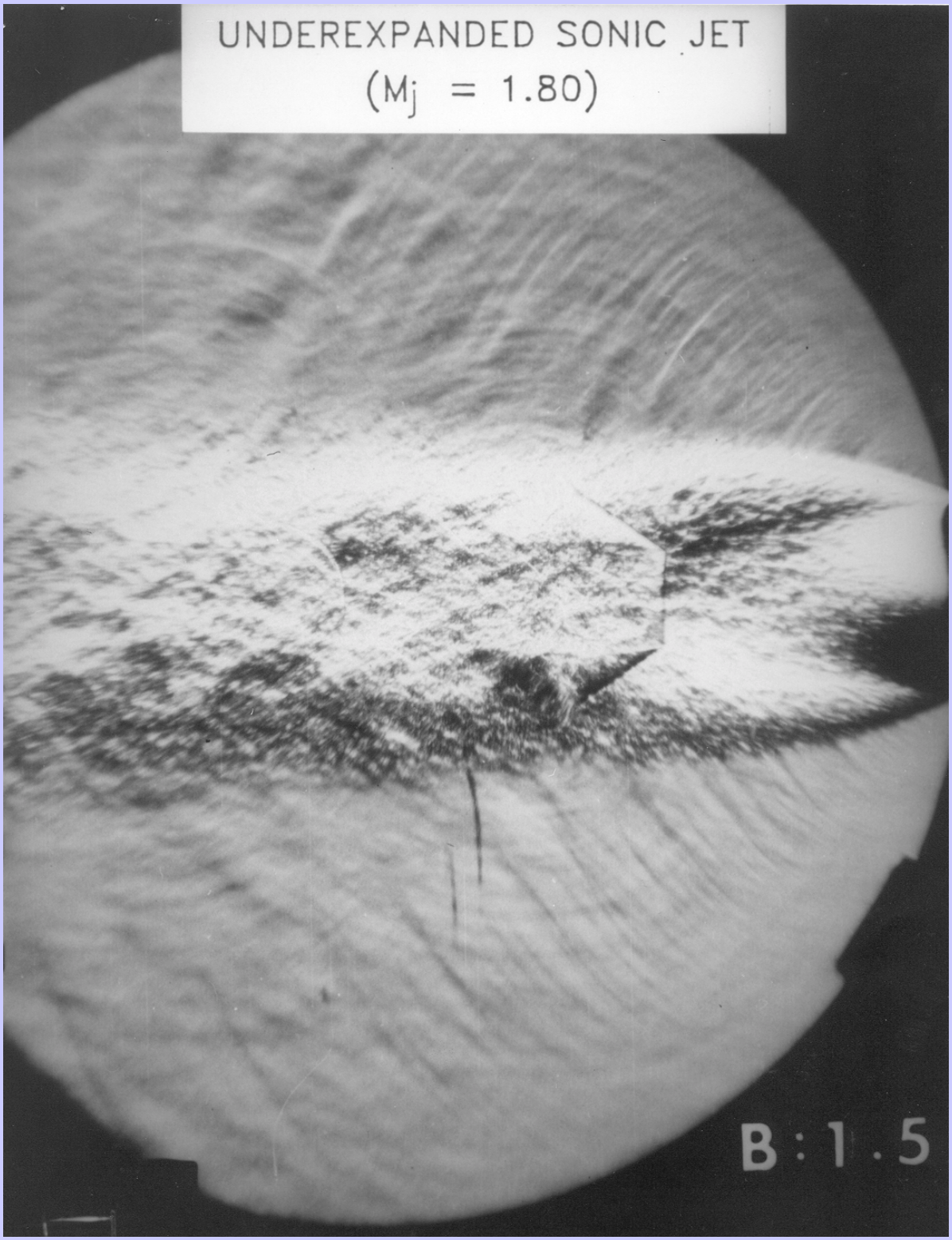
Is Acoustic Analogy Really Valid?

Jack:
The reason I would never work in the field of Aeroacoustics is that it's governing equation is not derived from first principles.

John L. Lumley, 1970

Question 1 Observations

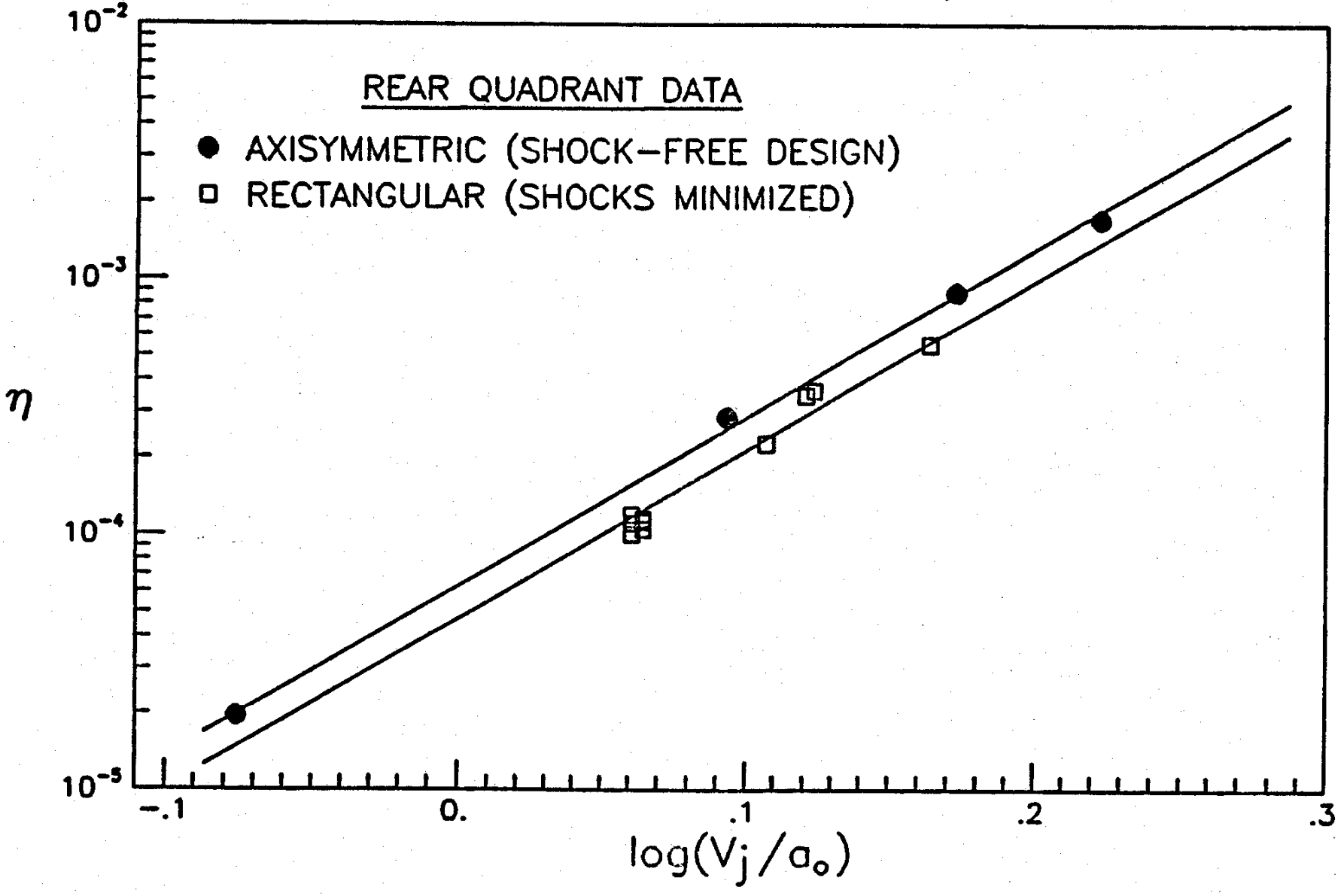
- First Principles Derivation of Free-Space Acoustic Wave Equation is Non-linear and Viscous. Works well when linearzed for small amplitude waves.
- Original Analogy Approach Only Cast for Small Amplitude Waves – Not Valid for Free-Space Propagation from Mach Wave Emission or Shock Noise.


UNDEREXPANDED SONIC JET
(Mj = 1.80)
B:1.5

Question 2 Comments

- Total Acoustic Power Predicted For Jets with Round Geometry Only.
- Theory Predicts Zone of Silence Where Most Sound is Observed.
- Flight Effects Well Represented. (Note flight effect is best sound suppression method ever seen)

ACOUSTIC BENEFIT OF RECTANGULAR NOZZLES (DECREASED ACOUSTIC EFFICIENCY)

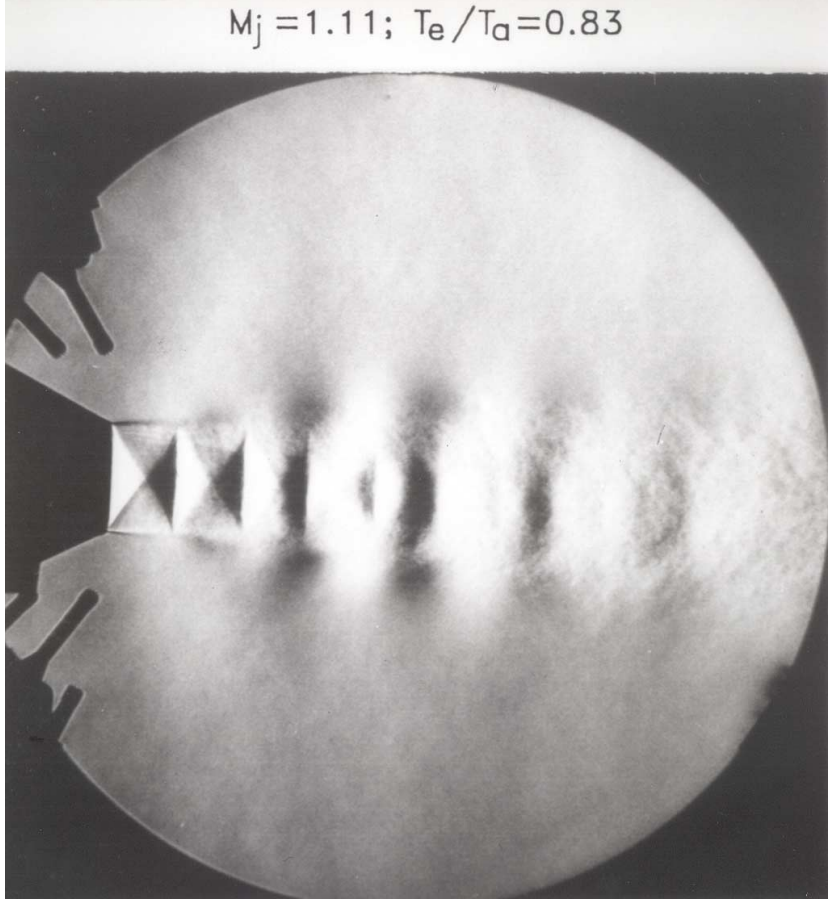


Question 3 Observations

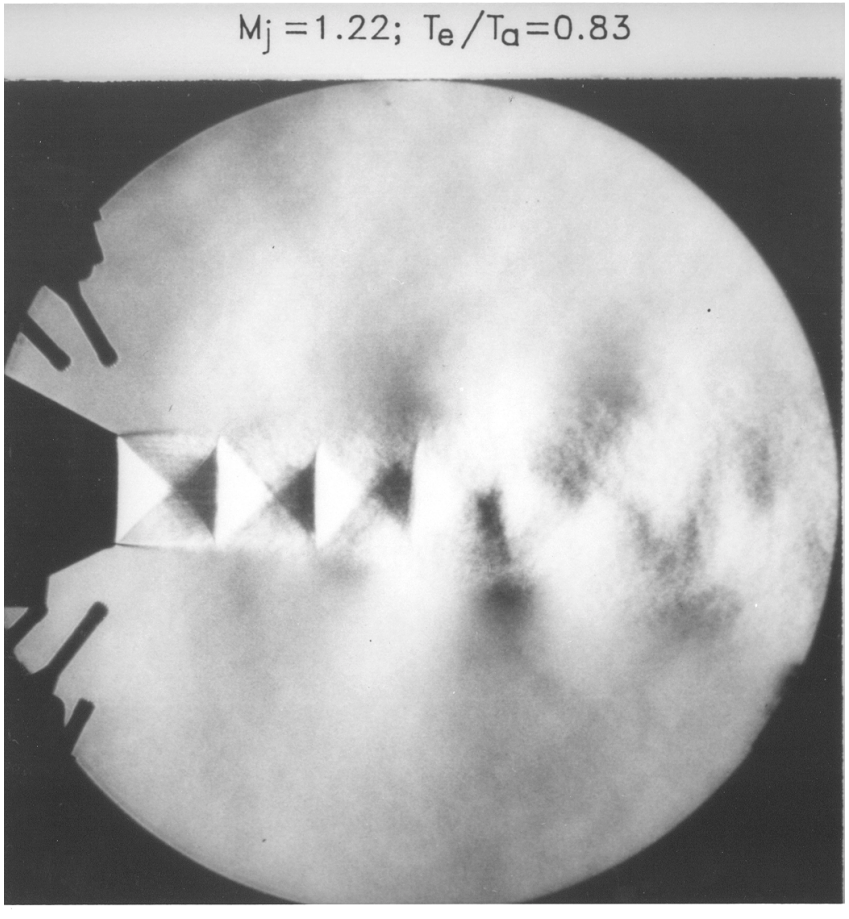
- Requires Waves with Supersonic Phase Speed Relative to Co-Flow Velocity & Sound Speed.
- Very Complex Application to Turbulent Flows With Extreme Geometry.
- Requires Initial Specification of Wave Amplitude.
- Large Number of Modes Required for Hot Flows.

Spatial Structure of Jet Screech

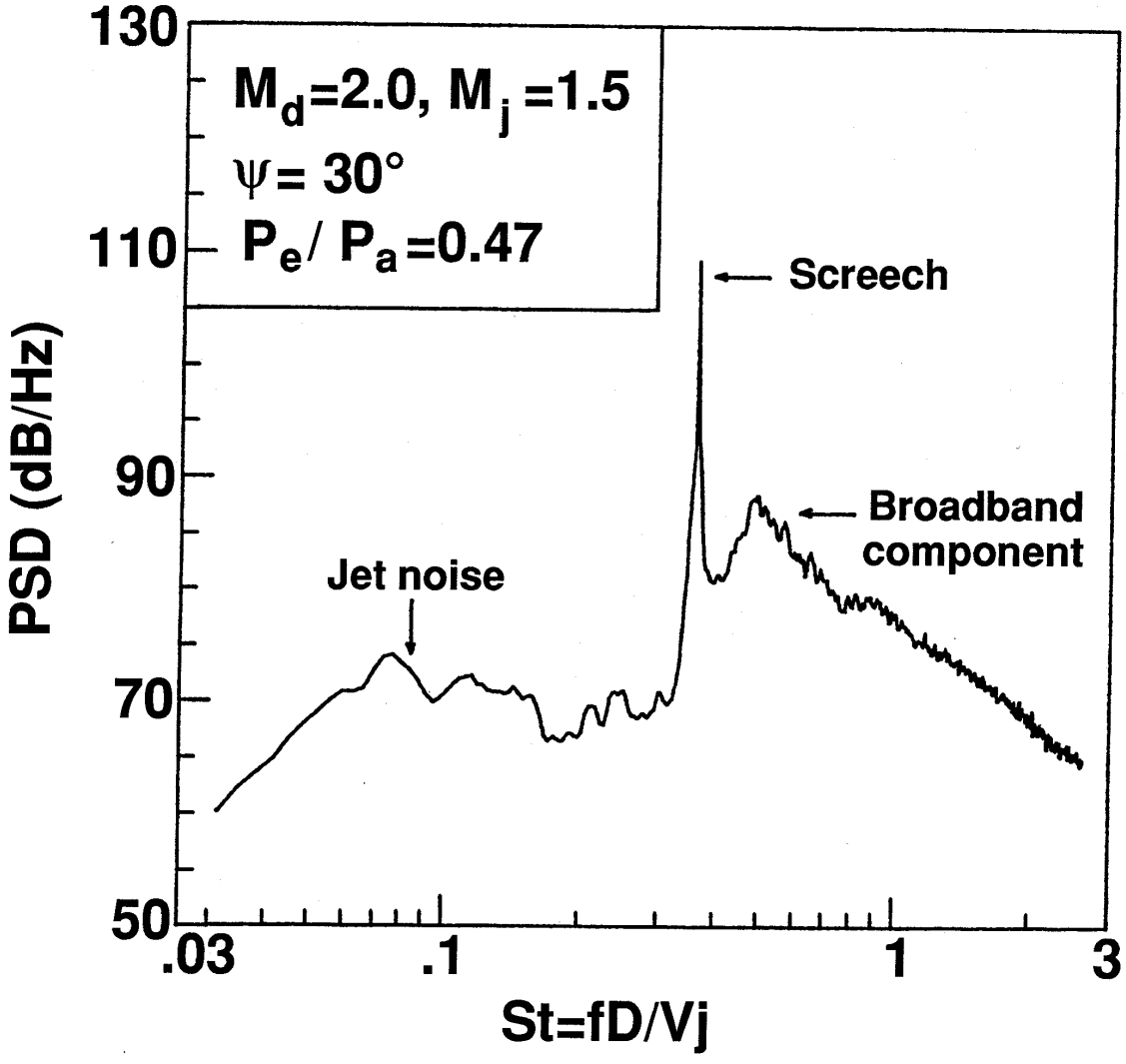
Axisymmetric Mode

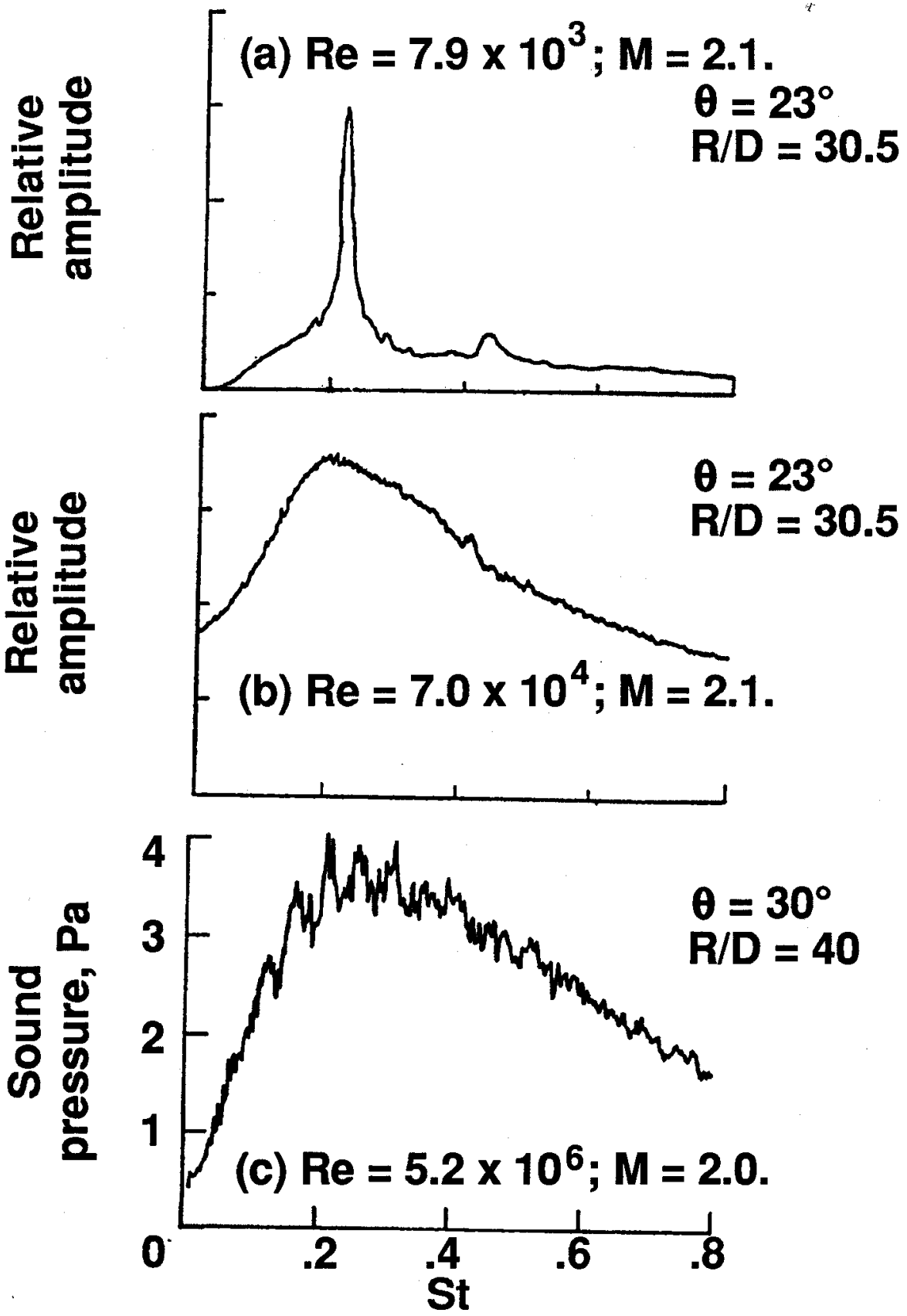


Helical Mode



Jet Noise Source Components

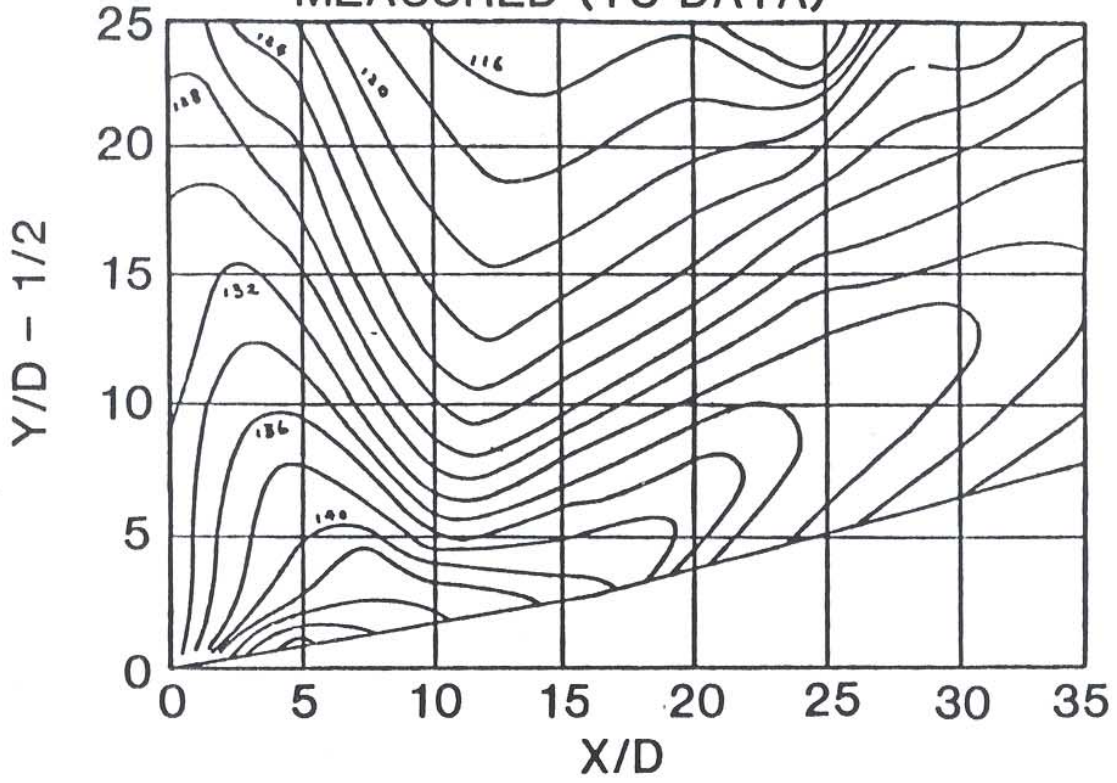



(a) Re = 7.9 x 10^3; M = 2.1.
θ = 23°
R/D = 30.5
Relative amplitude
θ = 23°
R/D = 30.5
(b) Re = 7.0 x 10^4; M = 2.1.
Relative amplitude
Sound pressure, Pa
θ = 30°
R/D = 40
(c) Re = 5.2 x 10^6; M = 2.0.
0
1
2
3
4
.2
.4
.6
.8
St

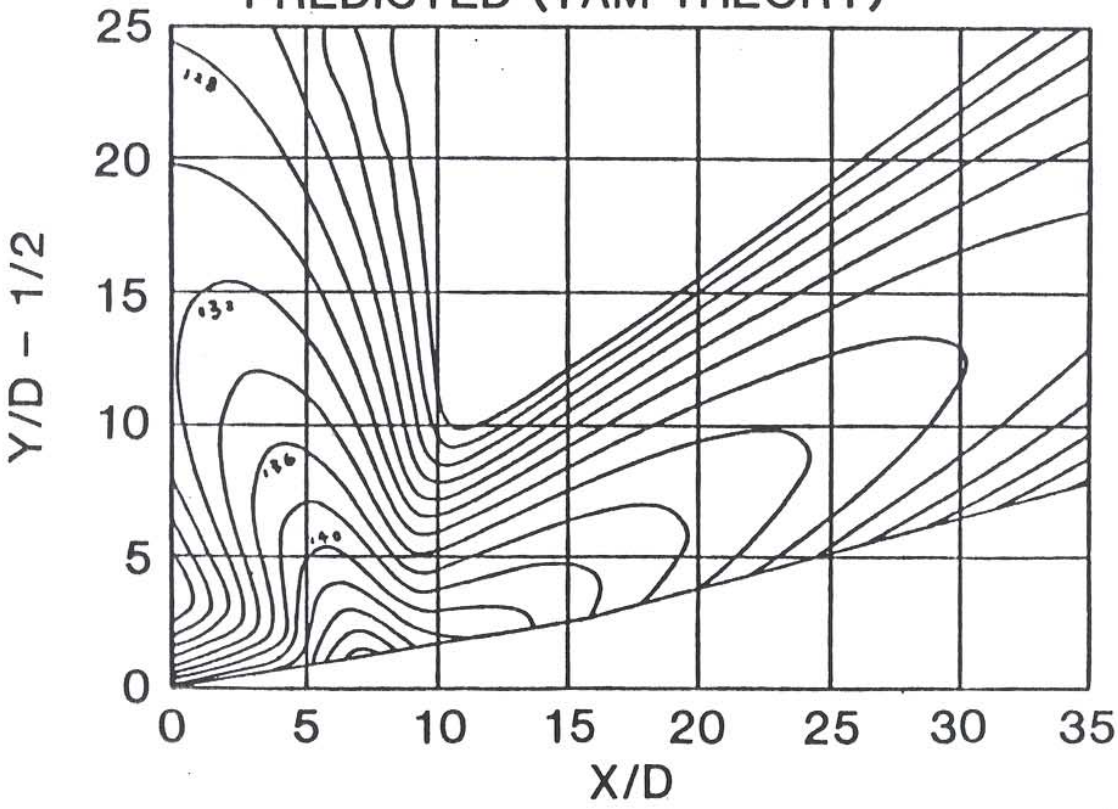
SUPERSONIC JET NOISE PREDICTION

(MACH 1.5 UNDEREXPANDED JET PLUME)

MEASURED (YU DATA)



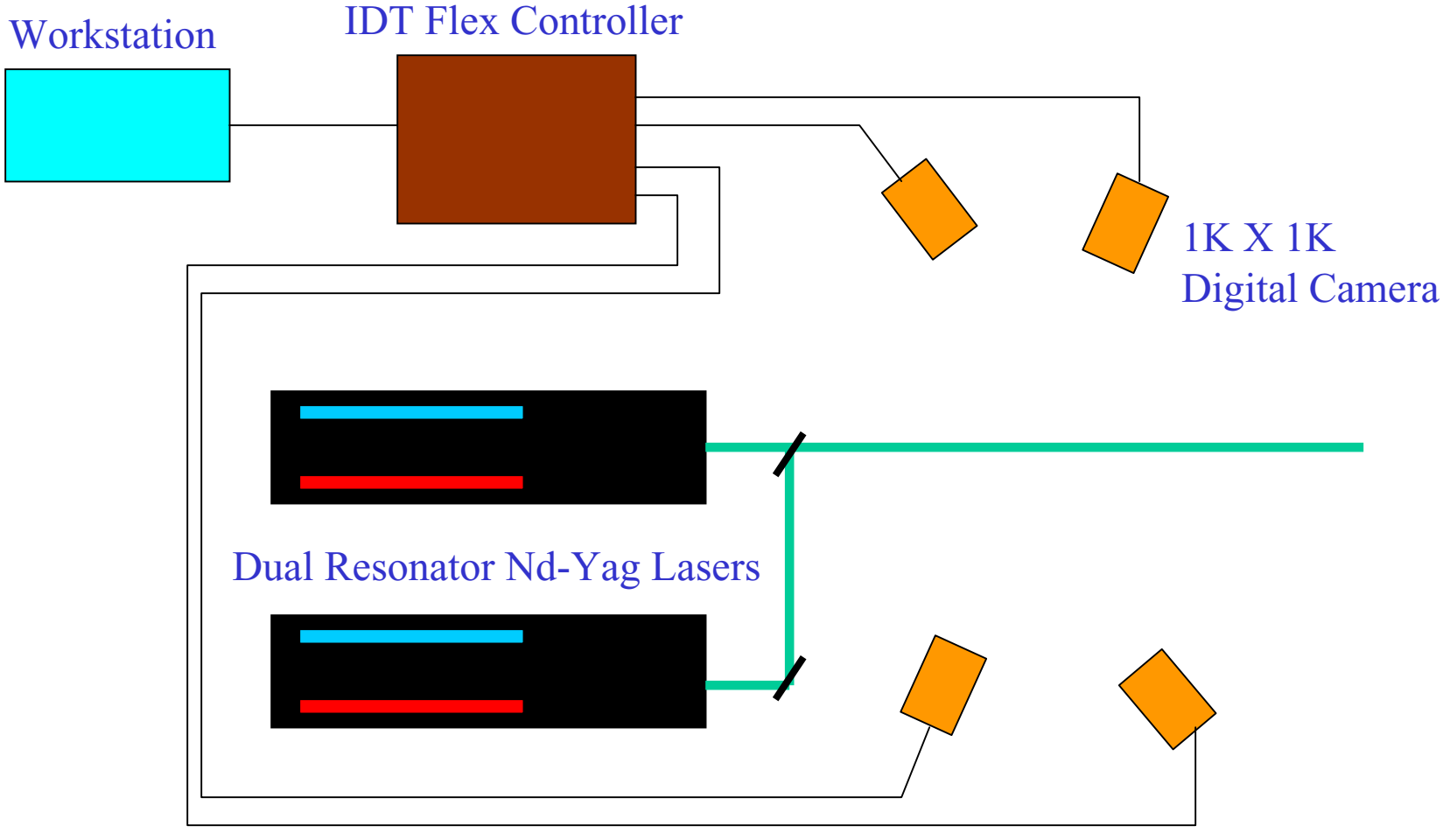
PREDICTED (TAM THEORY)



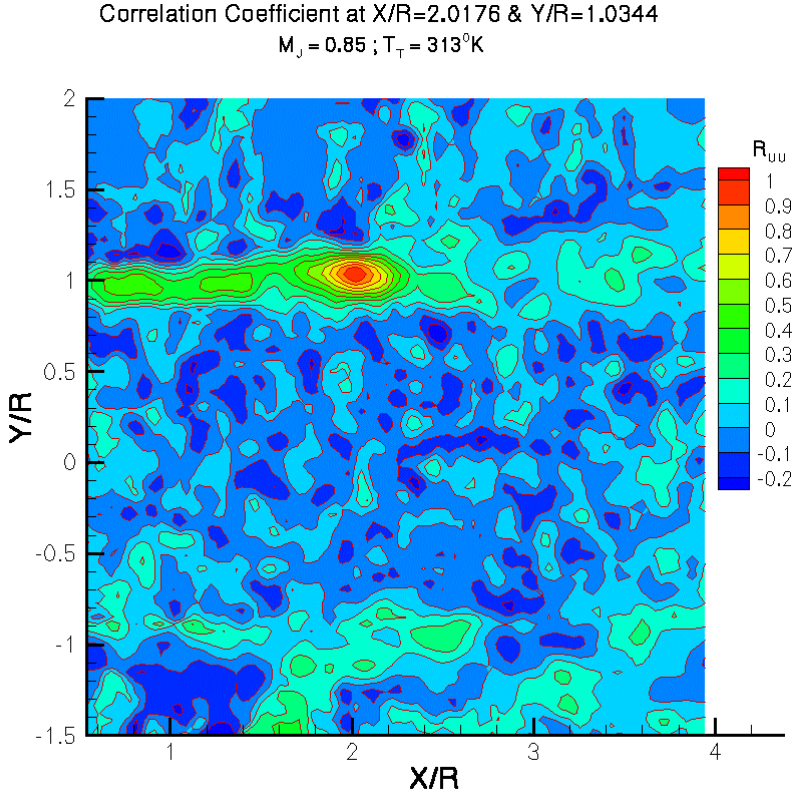
Question 4 Comment

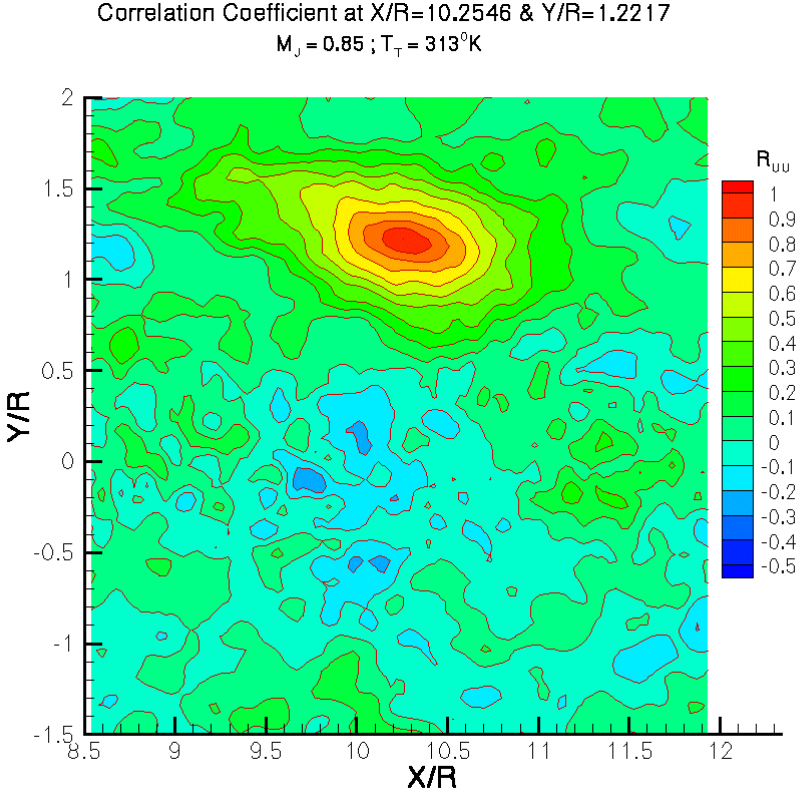
Requirement Exists to Address Issue of Causality – We need to know what drives those particular turbulent flow events that lead to the time dependent production of sound.

UM / NCPA PIV System Schematic



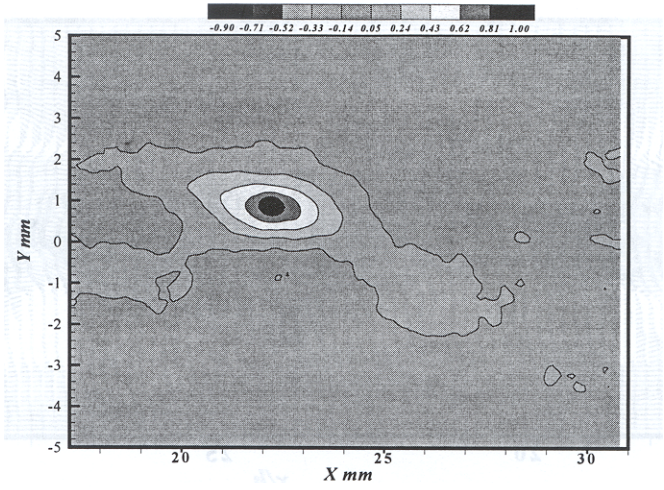
Turbulence Velocity Correlations Across Jet

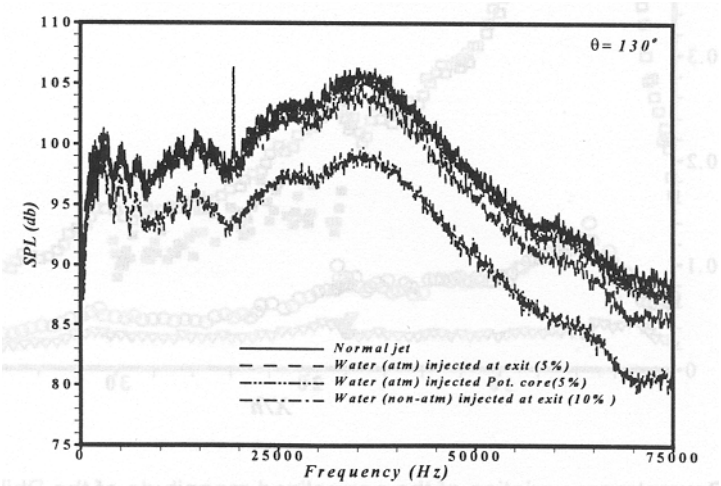




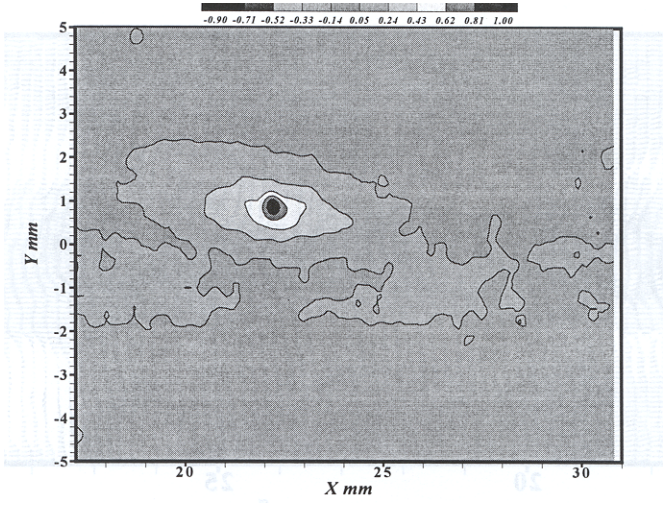
Effect of Water Injection On Source Correlations

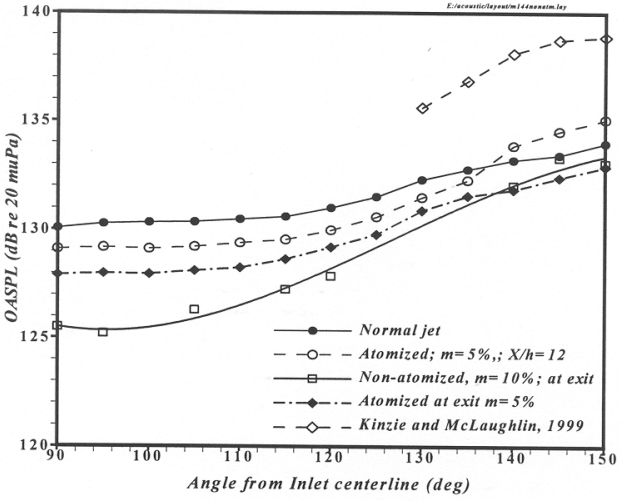
Baseline Jet





Jet With Water Injection





Krothpalli, Venkatatakrishnan, Elavarasan, & Lourenco, AIAA Paper 2000-2025

Optimization of Noise Reduction Concepts

- Development of Suitable Physics Based Algorithm Relating Noise Reduction to Turbulence Dynamics.
- Measure and Prediction of Two-Point Turbulence Statistics.
- Application of Data Compression Scheme: POD.
- Construction of Dynamics Systems Model For Operation With Non-Linear Closed Loop Controller.
- Development of Robust Actuators and Sensors.

J. Seiner References

1. Seiner, J.M., Ukeiley, L., and Ponton, M.K., 1999, Jet Noise Source Measurements Using PIV, AIAA Paper No. 99-1869.

2. Krothpalli, A., Venkatakrishnan, L., Elavarasan, R., and Lourenco, L., 2000, Supersonic Jet Noise Suppression by Water Injection, AIAA Paper No. 2000-2025.

Show Evidence if the Acoustic Analogy-Based Theory is Correct/Incorrect

Krish Ahuja
Georgia Institute Technology

NASA/CP—2001-211152

Show evidence if the Acoustic-Analogy-based theory is correct/incorrect

Krish Ahuja
Georgia Institute of Technology
Aerospace, Transportation and Advanced Systems Laboratory/GTRI
Atlanta, GA 30332
krishan.ahuja@gtri.gatech.edu

Jet Noise Scaling From Lighthill's Theory

(From Ahuja, K. K., JSV, Vol. 29(2) , 1973)

$$I \sim \frac{\rho_m^2}{\rho_0} \frac{V_j^8}{a_0^5} \frac{D^2}{R^2} (1 - M_c \cos\theta)^{-5},$$

where ρ_m is the density in the jet mixing region and ρ_0 is the density of the ambient air.

Jet Noise Correlation Guided by Lighthill's Theory

(From Ahuja, K. K., JSV, Vol. 29(2), 1973)

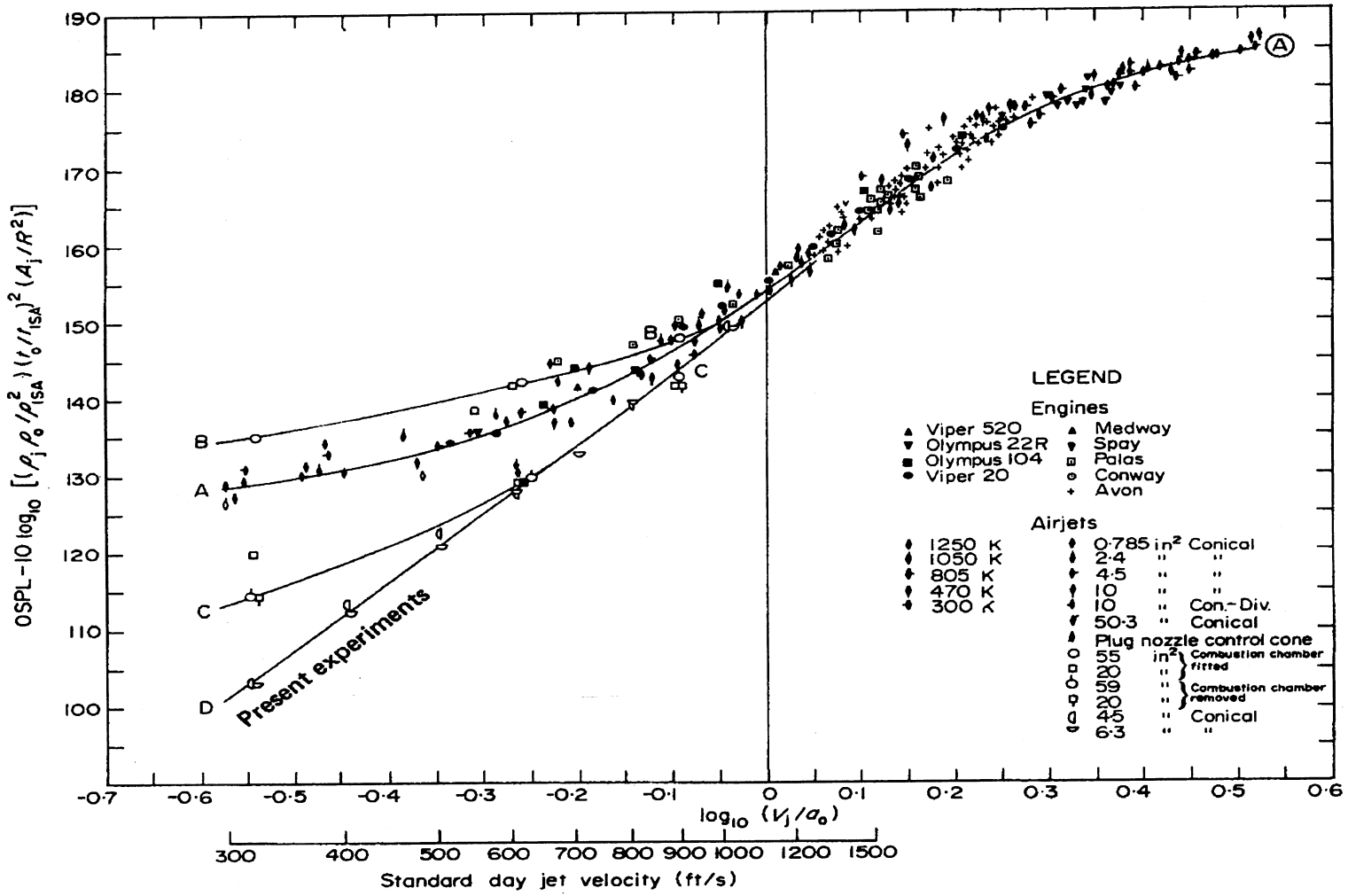
$$\text{OASPL} - 10\log_{10}\left[\frac{\rho_j \rho_0}{\rho_{ISA}^2}\left(\frac{t_0}{t_{ISA}}\right)^2 \frac{A_j}{R^2}\right] \quad \textit{versus} \quad \log_{10}\left(\frac{V_j}{a_0}\right)$$

at each angle, where

ρ_j = fully expanded jet density,
ρ_{ISA} = density of air at International Standard Atmospheric conditions,
t_0 = temperature of the ambient air,
t_{ISA} = temperature of the air at I.S.A. conditions,
A_j = nozzle exit area.

Jet Noise Correlation Guided by Lighthill's Theory

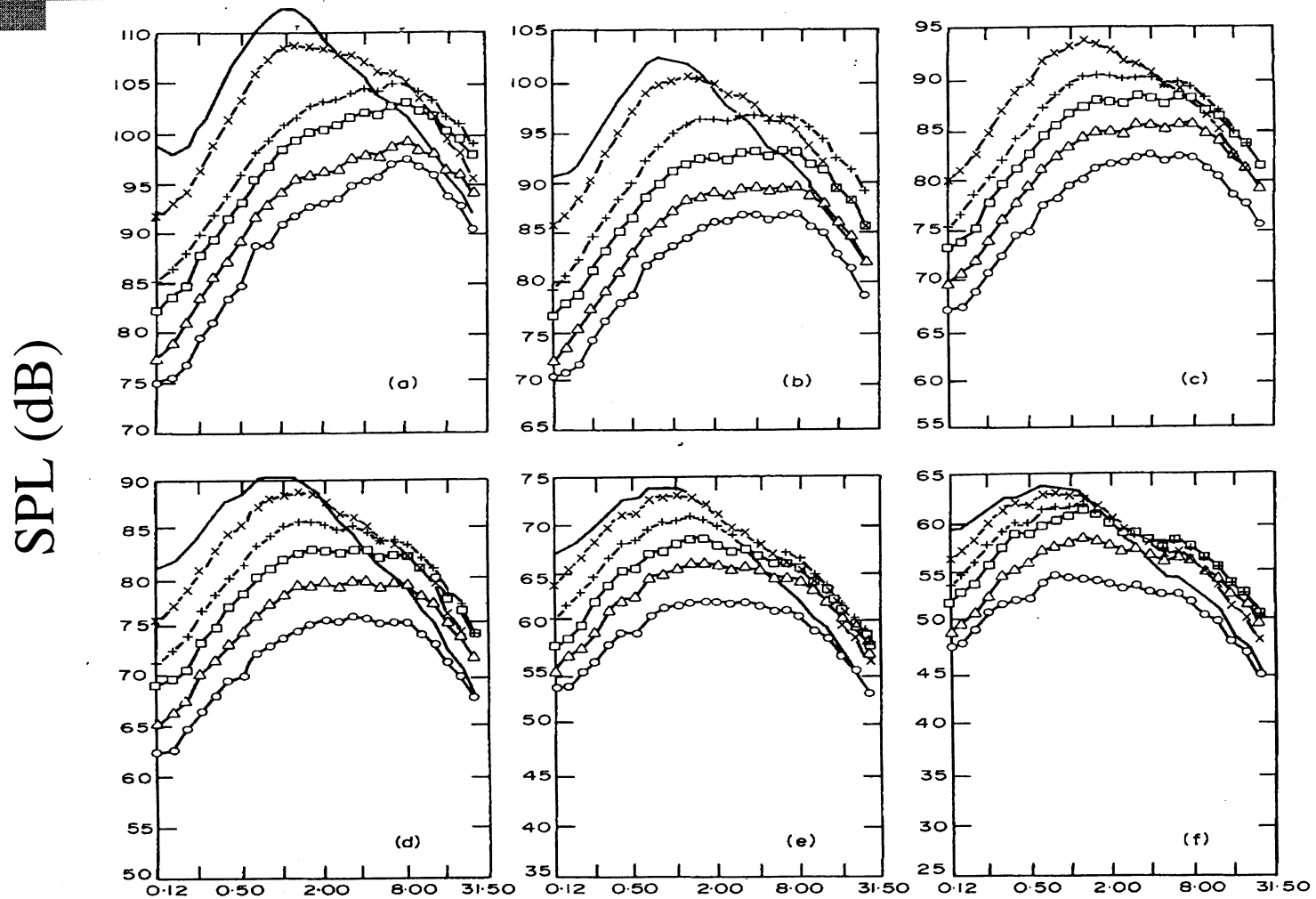
(From Ahuja, K. K., JSV, Vol. 29(2) , 1973)



Jet noise correlation, peak polar OASPL. From reference [2].

Typical 1/3-Octave Jet Noise Spectra

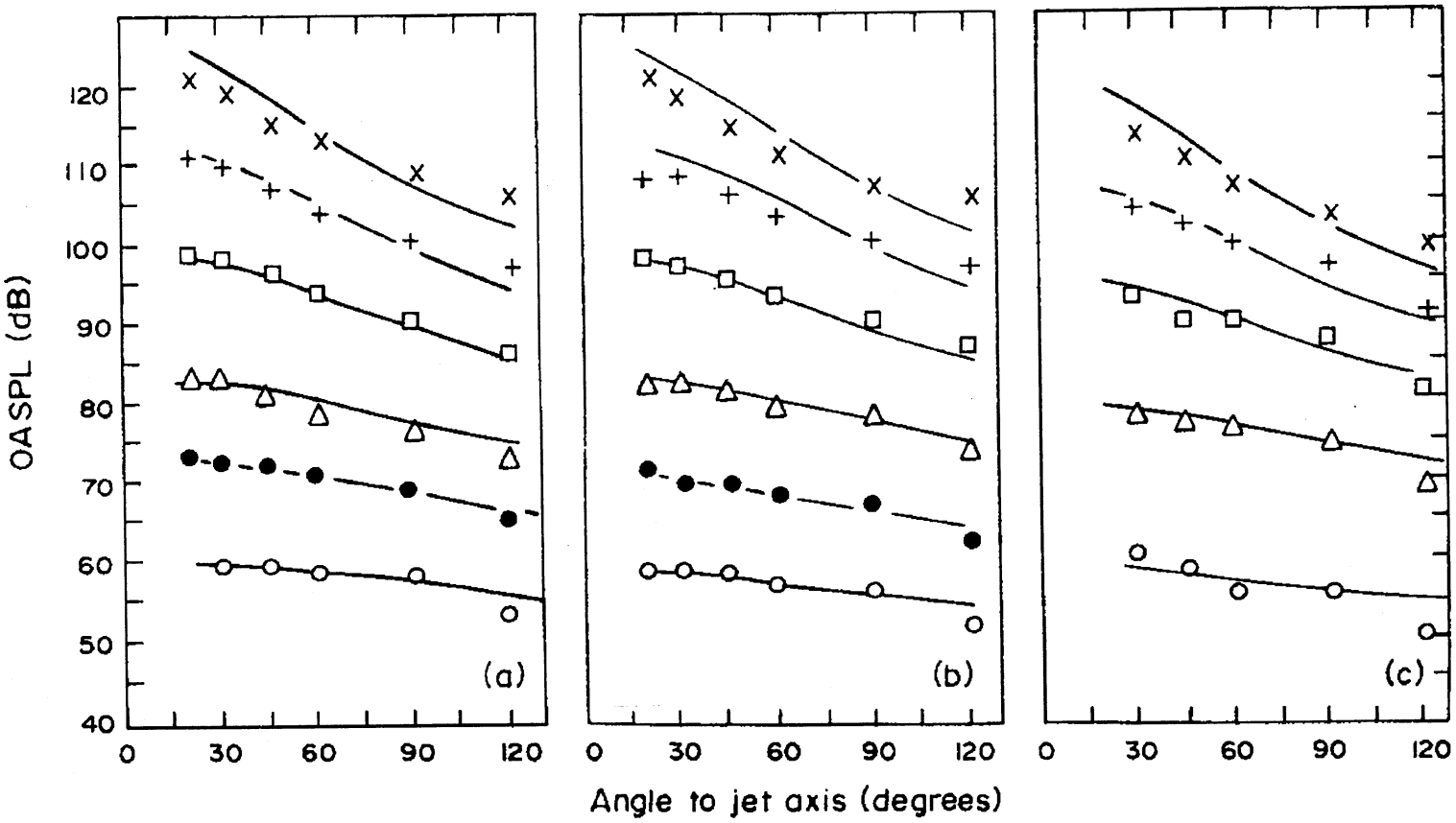
(From Ahuja, K. K., JSV, Vol. 29(2) , 1973)



1/3 octave spectra for nozzle diameter = 2·84 in. Jet velocity values: (a) 1000 ft/s; (b) 800 ft/s; (c) 700 ft/s; (d) 600 ft/s; (e) 400 ft/s; (f) 300 ft/s. Values for θ: —, 20°; ×, 30°; +, 45°; □, 60°; △, 90°; ○, 120°.

Overall Sound Pressure Levels And Lighthill's Scaling

(From Ahuja, K. K., JSV, Vol. 29(2), 1973)

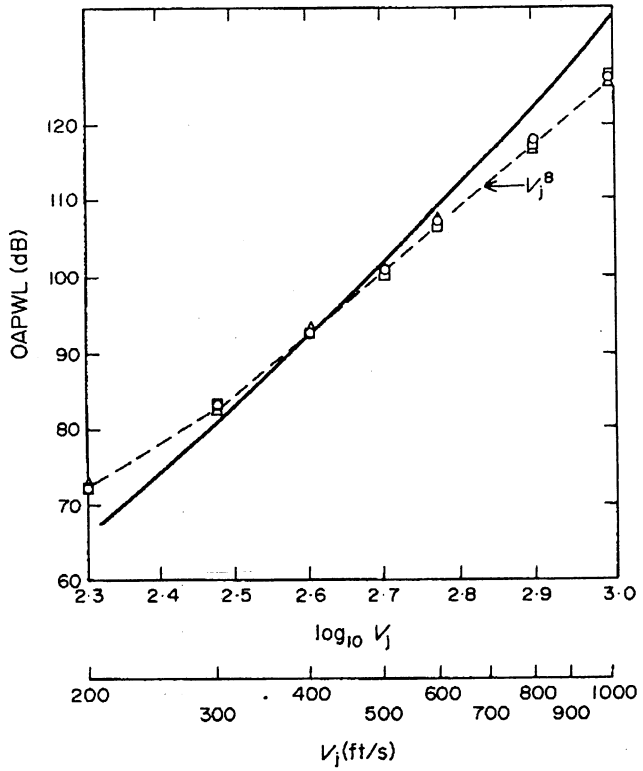


Directivities of OASPL's for "clean" jet noise. (a) $D = 2{\cdot}84$ in, (b) $D = 2{\cdot}40$ in, (c) $D = 1{\cdot}52$ in. Values for V_j: ×, 1000 ft/s; +, 800 ft/s; □, 600 ft/s; △, 400 ft/s; ●, 300 ft/s; ○, 200 ft/s. ——, Theory $V_j^8 (I - M_c \cos\theta)^{-5}$.

Overall Acoustic Power Levels and Lighthill's Theory

(From Ahuja, K. K., JSV, Vol. 29(2), 1973)

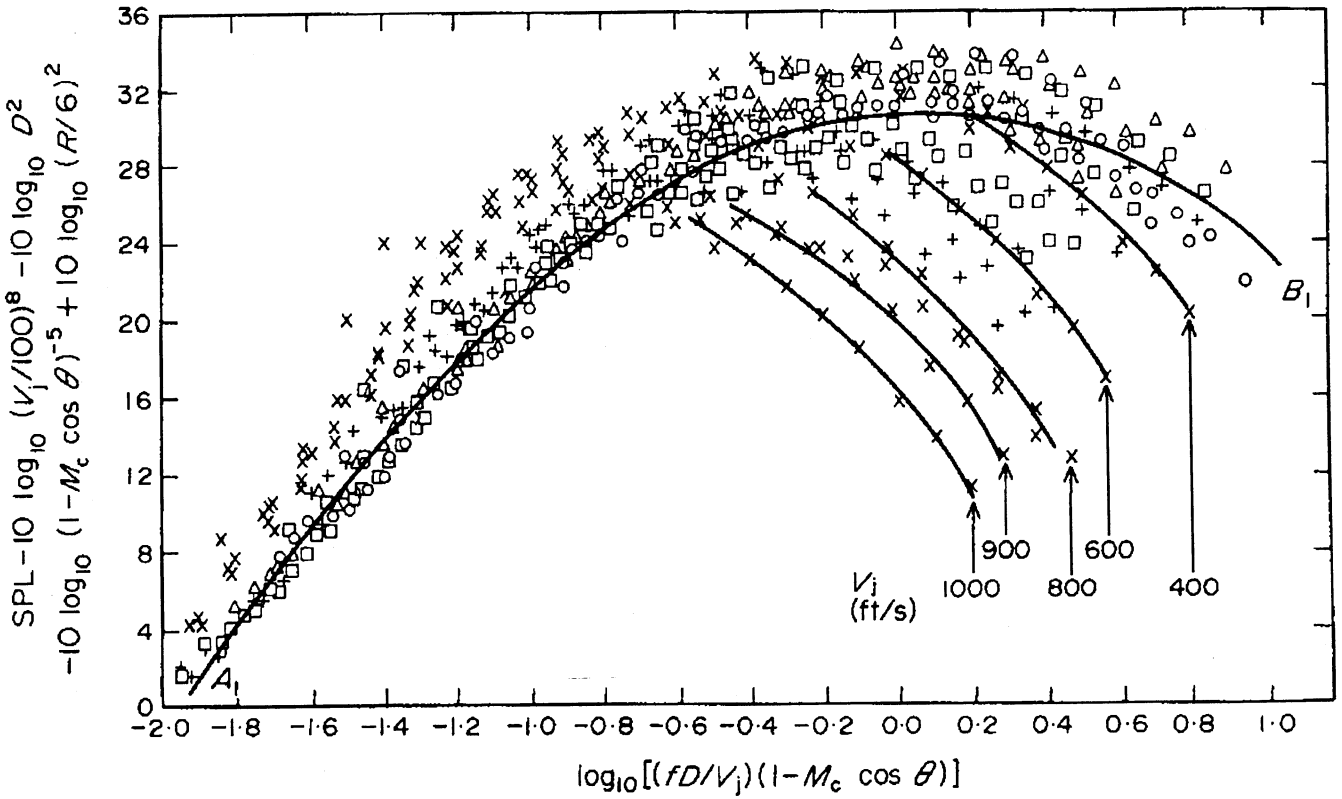
Theory $V_j^8[(1 + M_c^2)/(1 - M_c^2)^4]$



Velocity dependence of OAPWL's (normalized with respect to nozzle diameter = 2·4 in). △, D = 2·84 in; ○, D = 2·40 in; □, D = 1·52 in. ——, Theory $V_j^8[(1 + M_c^2)/(1 - M_c^2)^4]$.

Attempt at Verifying Lighthill's Scaling (D =1.52 in.)

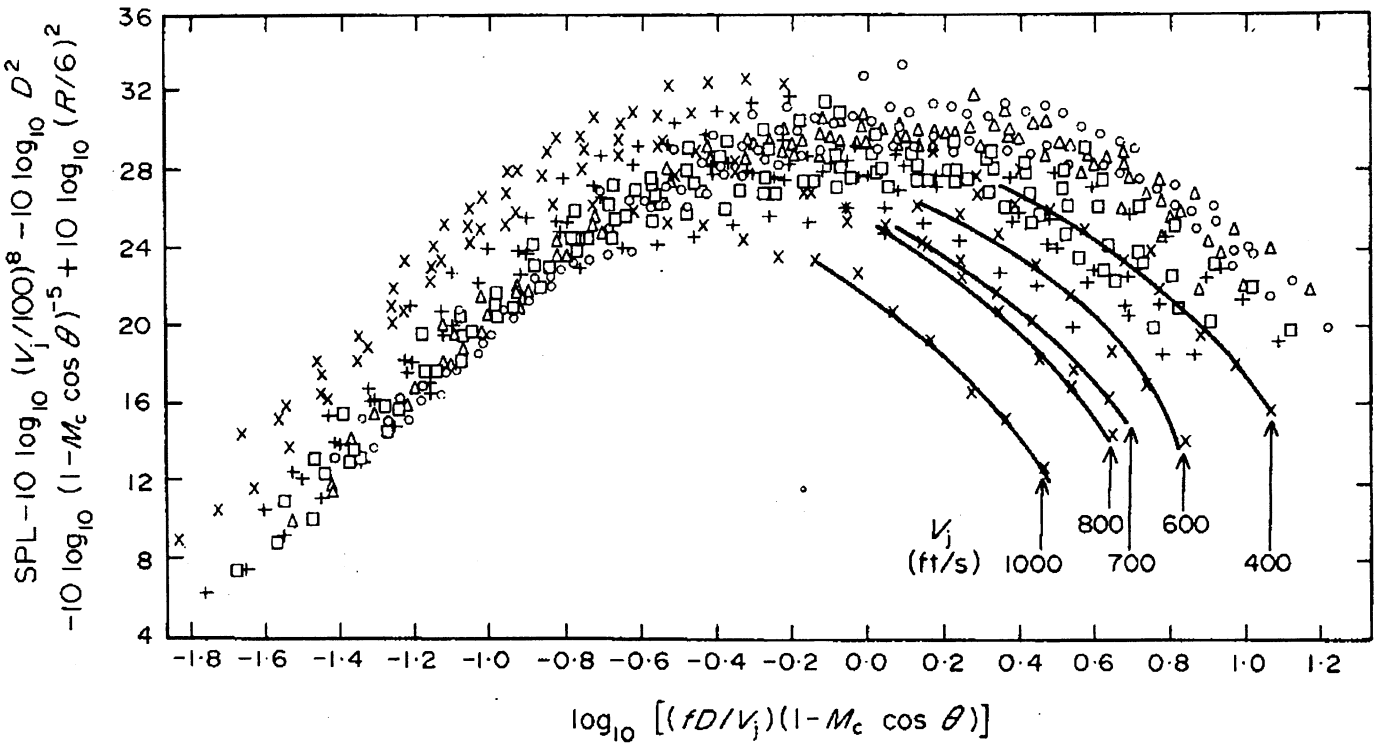
(From Ahuja, K. K., JSV, Vol. 29(2) , 1973)



Normalized 1/3 octave SPL's against Doppler corrected Strouhal number. $D = 1{\cdot}52$ in. Values for θ: ×, 30°; +, 45°; □, 60°; △, 90°; ○, 120°.

Attempt at Verifying Lighthill's Scaling (D =2.84 in.)

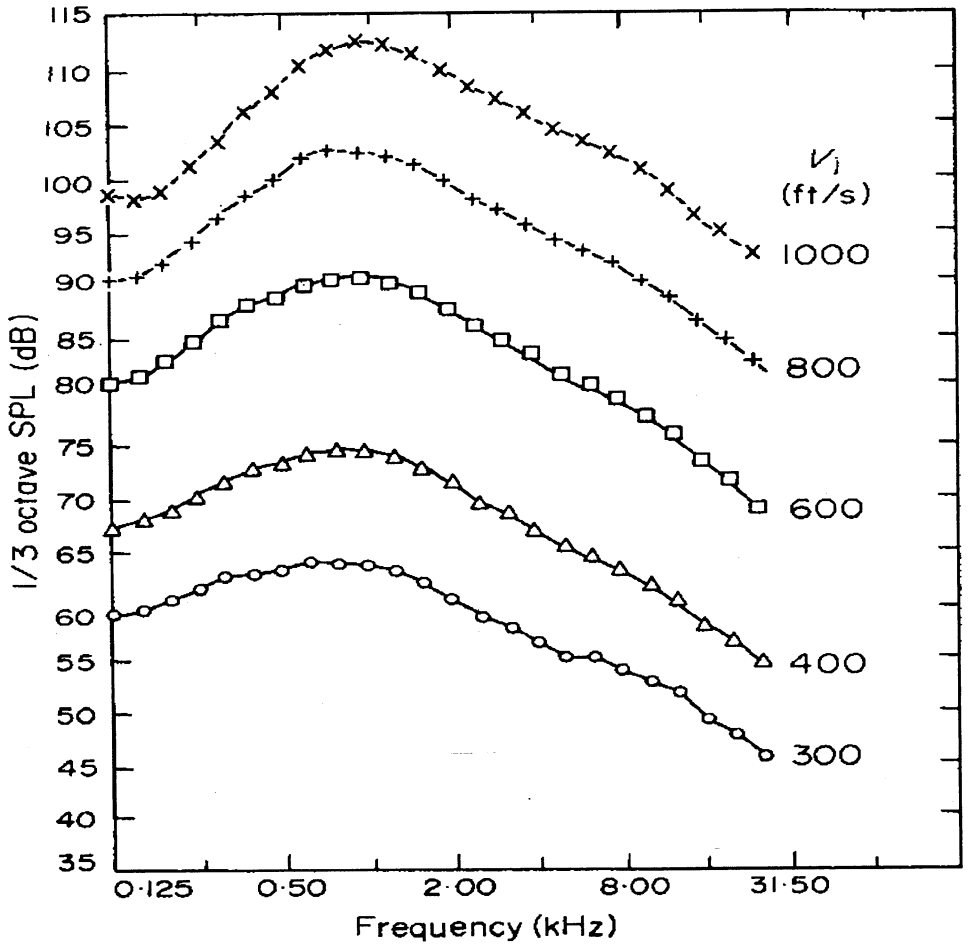
(From Ahuja, K. K., JSV, Vol. 29(2) , 1973)



Normalized 1/3 octave SPL's against Doppler corrected Strouhal number. $D = 2{\cdot}84$ in. Symbols as in Figure 3 legend.

Noise Spectra At Shallow Angles (20°) (D =2.84 in.)

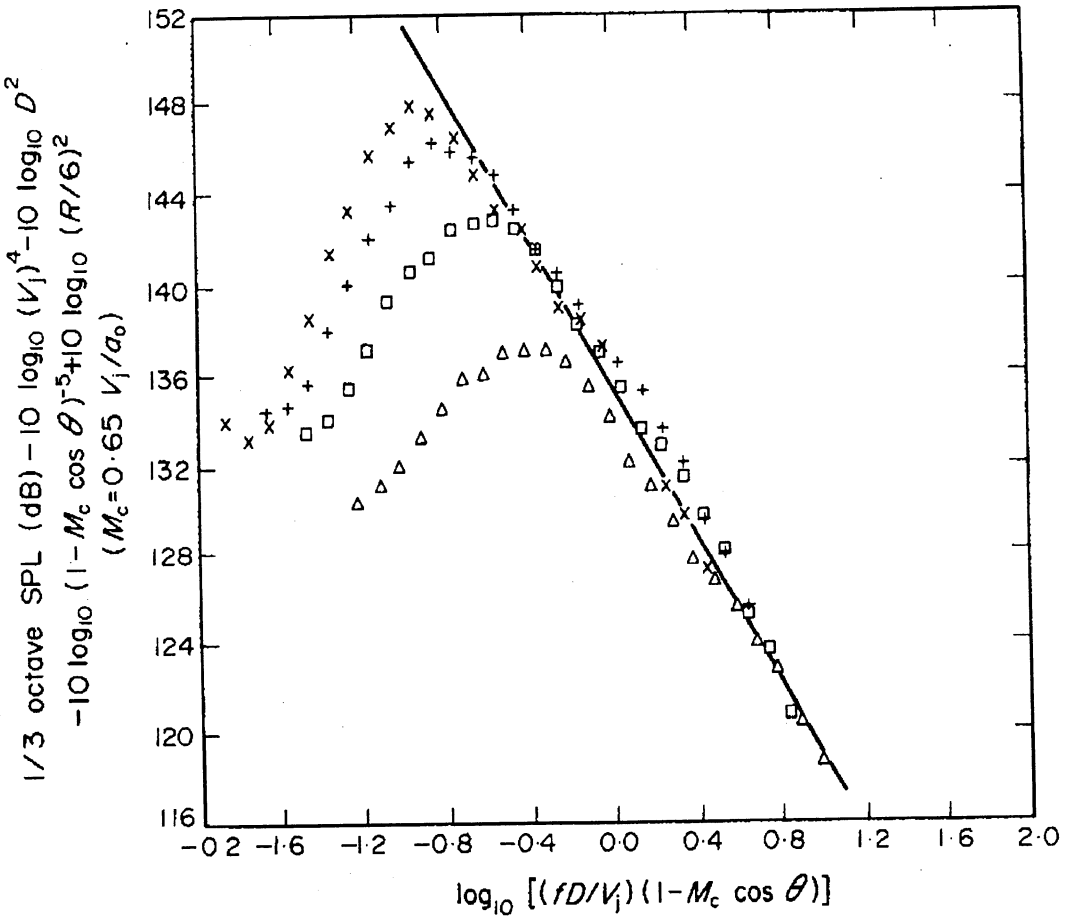
(From Ahuja, K. K., JSV, Vol. 29(2) , 1973)



Clean jet noise spectra at $\theta = 20°$ (to jet axis). Nozzle diameter = 2·84 inch.

V^4 Relationship At Shallow Angles (D =2.84 in.)

(From Ahuja, K. K., JSV, Vol. 29(2), 1973)

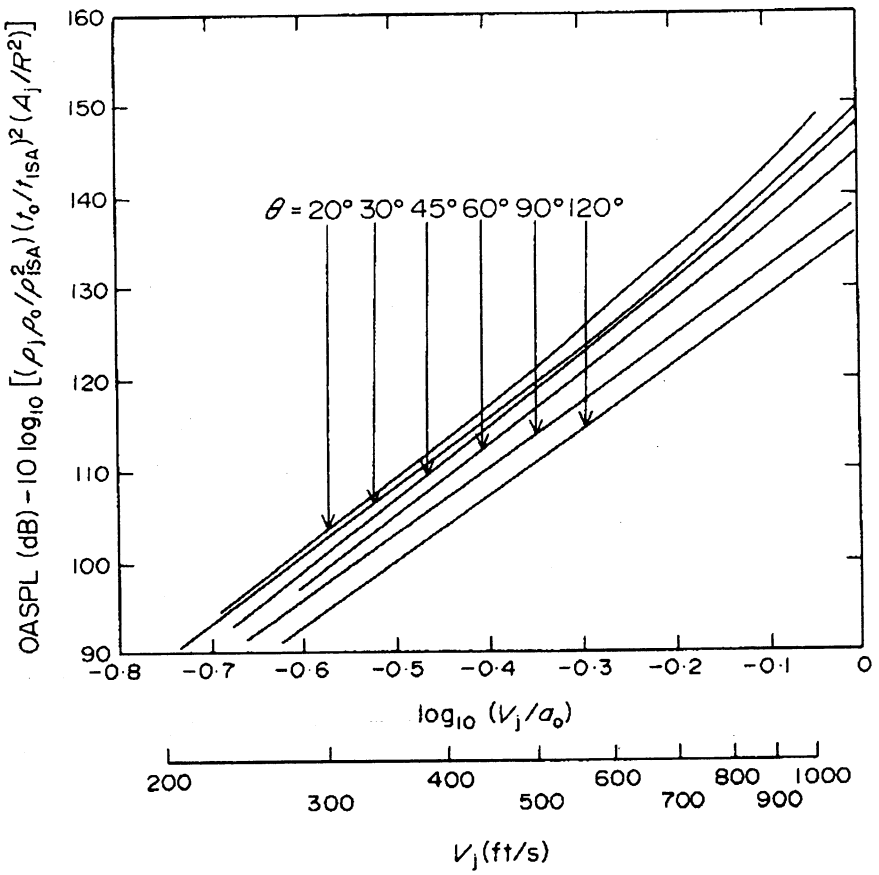


High frequency correlation of 1/3 octave SPL's for clean jets. $\theta = 20°$, $D = 2{\cdot}84$ in, $R = 6$ ft. Values for V_j: ×, 1000 ft/s; +, 800 ft/s; □, 600 ft/s; △, 400 ft/s.

Universality of the Eighth Power of Velocity for Cold Jets at 90°

Coles' and Bushell's Scaling Guided by Lighthill's Theory

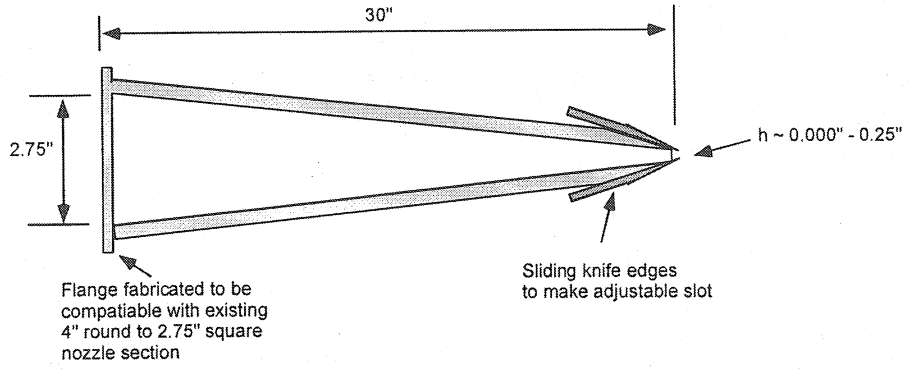
(From Ahuja, K. K., JSV, Vol. 29(2) , 1973)

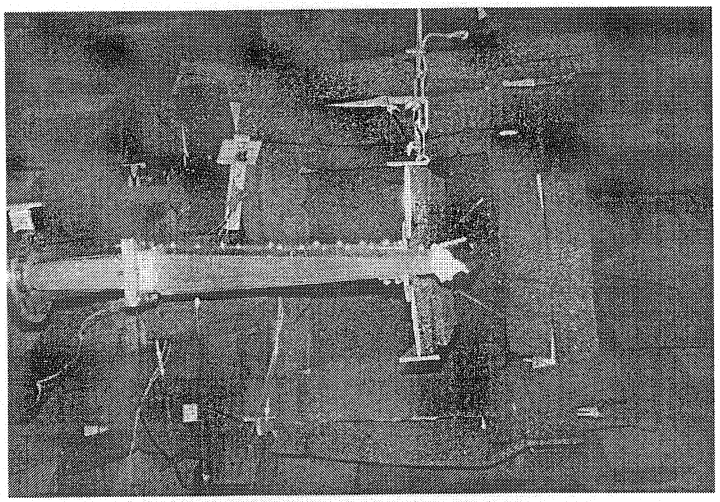


Jet noise correlation at different angles.

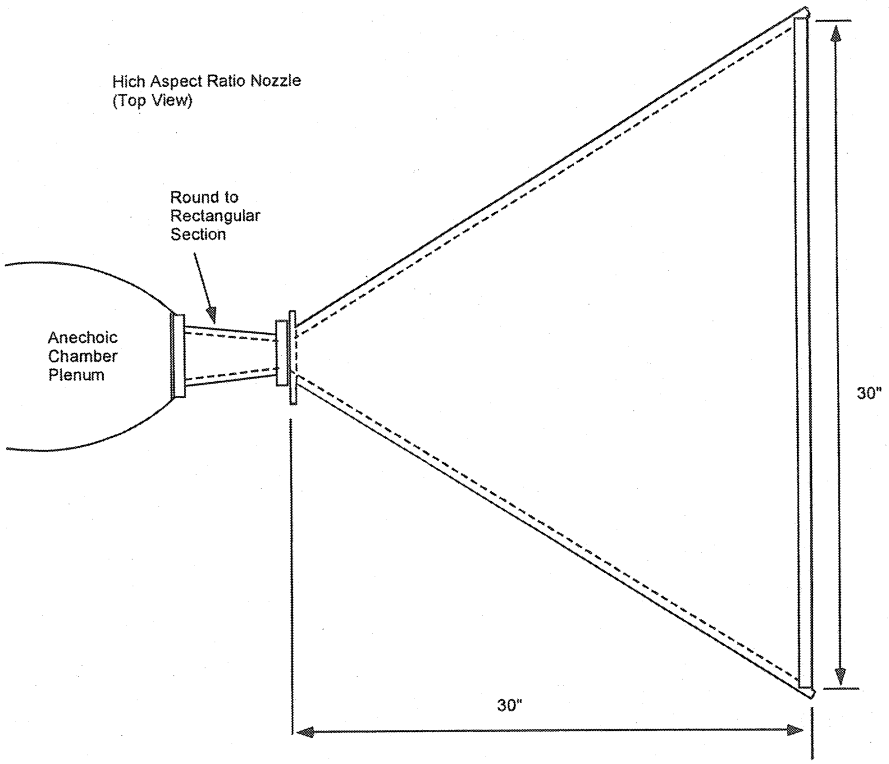
High Aspect Ratio Nozzle (HARN)

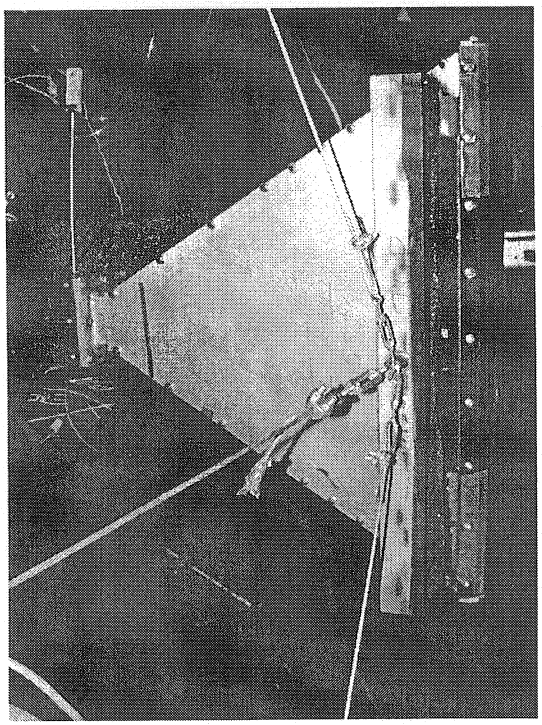
Side View



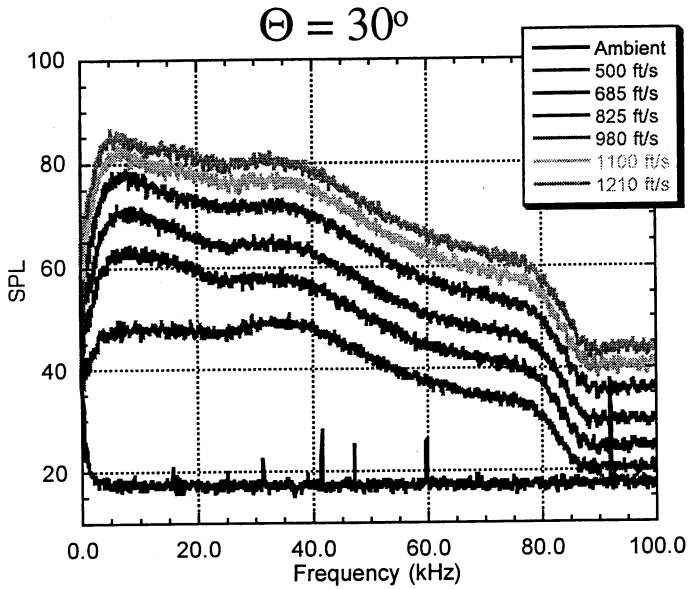


Hich Aspect Ratio Nozzle
(Top View)

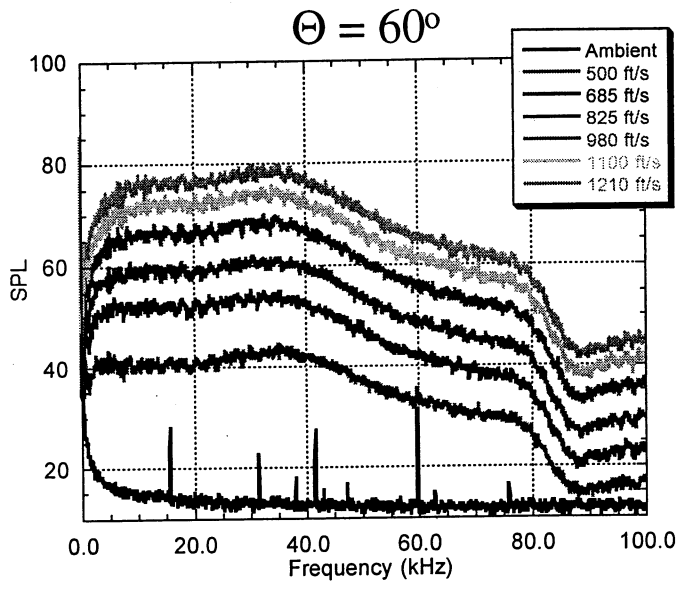




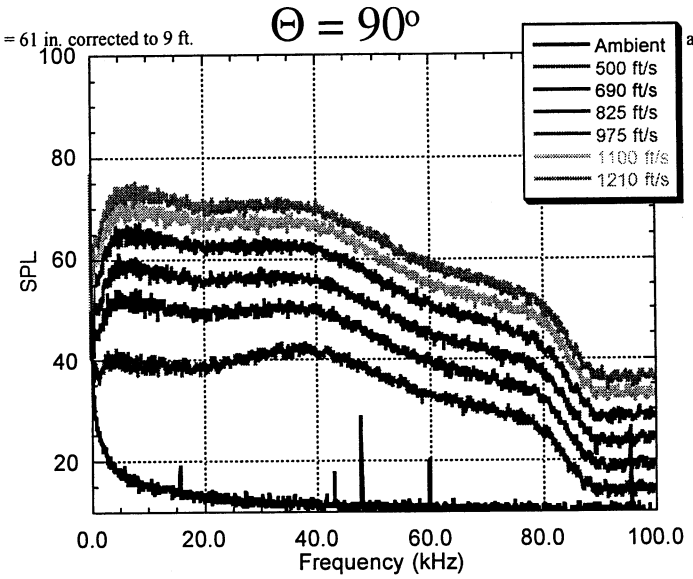
Typical HARN Spectra



HARN acoustic tests in the free flight facility. 30 ° microphone, r = 61 in. corrected to 9 ft.
h ~ 0.040, w = 14.75", test 092700_2



acoustic tests in the free flight facility. 60 ° microphone, r = 9 ft.
h ~ 0.040, w = 14.75", test 092700_2

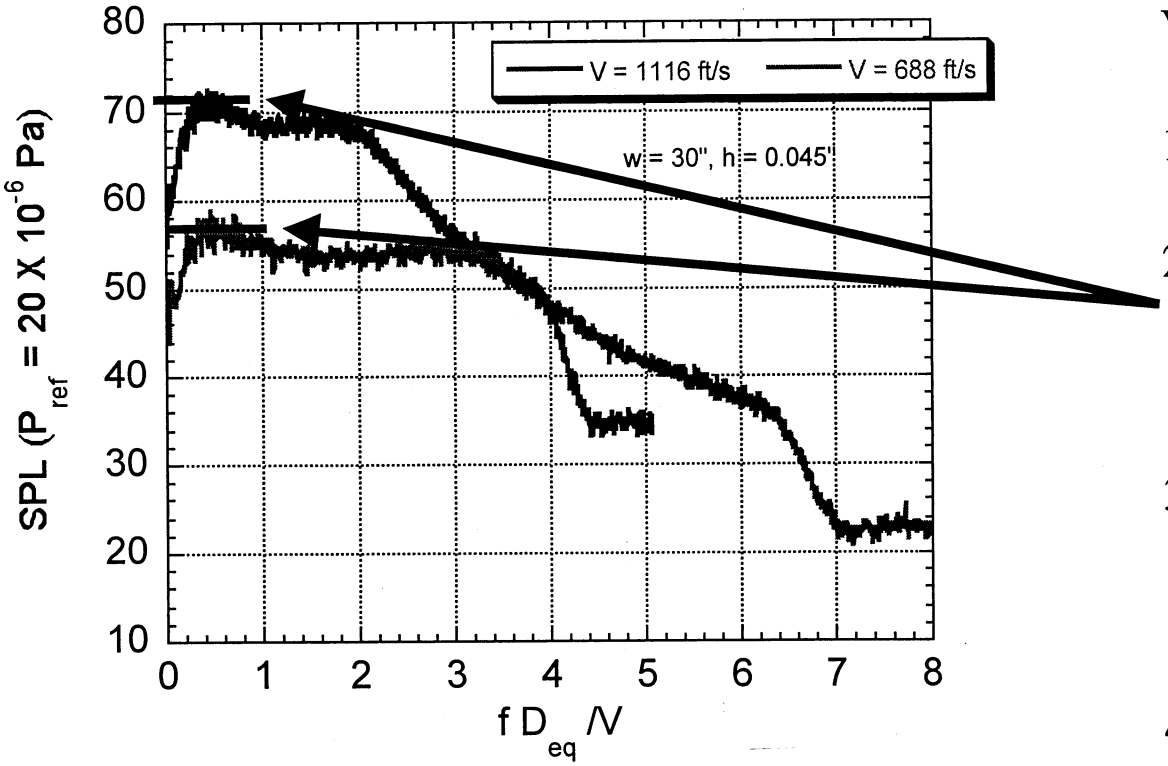


HARN acoustic tests in the free flight facility. 90 ° microphone, r = 9 ft.
h ~ 0.040, w = 14.75", test 092700_2

Establishing a Velocity Scaling

- Compare spectra for similar conditions
  - Same width (w)
  - Same height (h)
    - h varies with velocity
      - Plenum pressure pushes nozzle walls out slightly
      - Must carefully find two conditions with same h

Comparison of Spectra for Velocity Scaling



HARN acoustic tests in the free flight facility. $\Theta = 90^{\circ}$, r = 9ft.,
$\Delta f = 64$ Hz
harn 67, harn85

Note: $w_1 = w_2$, $h_1 = h_2$

To Generate a Point for Velocity Scaling plot :

1.) Identify peak for each curve

2.) Pick SPL value off curve

$SPL_1 = 72$ dB

$SPL_2 = 57$ dB

3.) Subtract to make

$\Delta SPL_{peak} = SPL_1 - SPL_2$

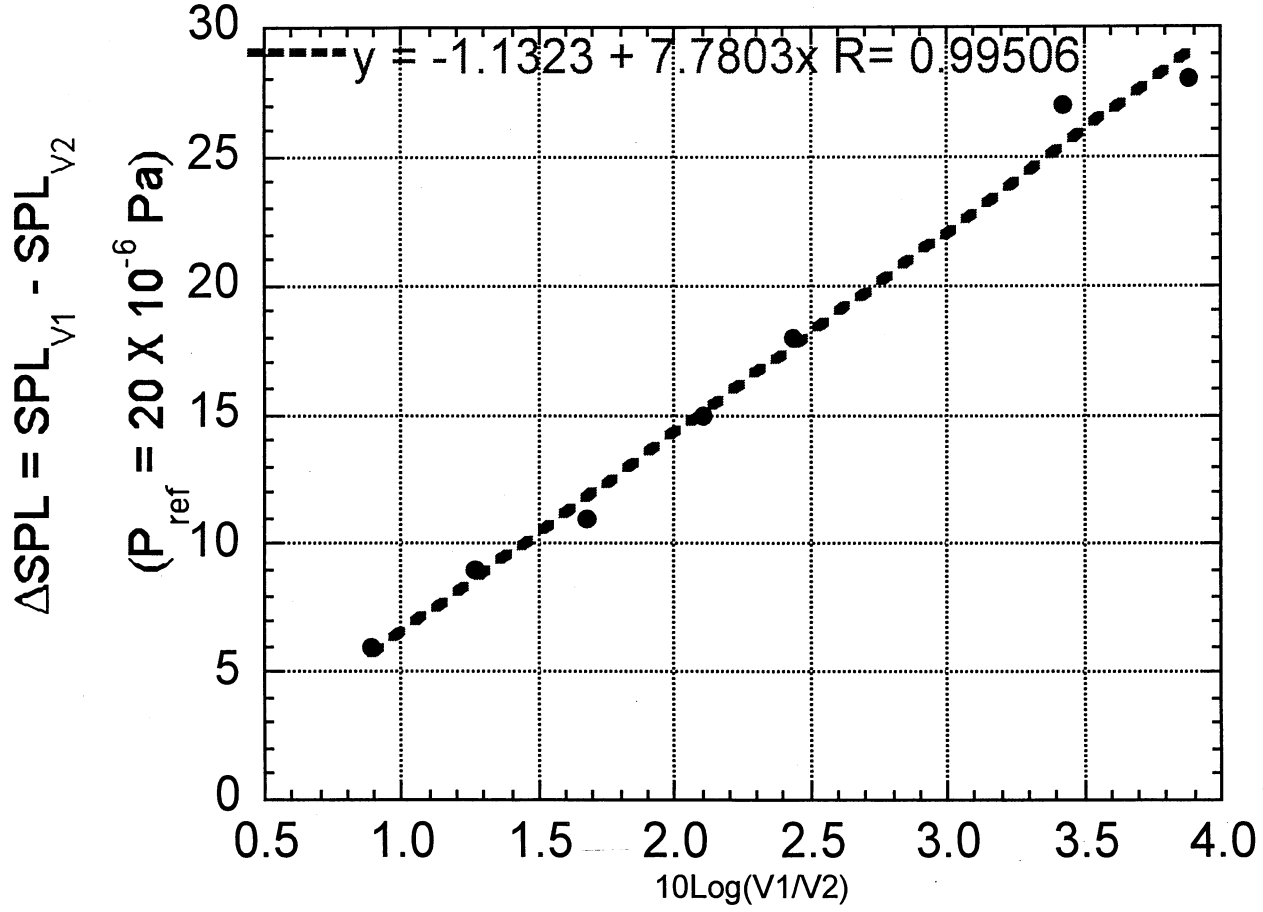
$\Delta SPL_{peak} = 15$ dB

4.) Take $10Log(V_1/V_2)$

$10Log(V_1/V_2) = 2.10$

This produces one point on the velocity scaling plot

Eighth-Power Velocity Scaling for a Slot Nozzle with Aspect Ratio in Excess of 350



HARN acoustic tests in the free flight facility. Velocity variation comparison.

$\Theta = 90^{\circ}$, r = 9ft.

Δf = 64 Hz

The V_j^8 Quadrupole Scaling Known Long before Lighthill's Derivation

Lighthill →

$$I \sim \frac{\rho_m^2}{\rho_0} \frac{V_j^8}{a_0^5} \frac{D^2}{R^2} (1 - M_c \cos\theta)^{-5},$$

Blokhinitsev →

The V_j^8 proportionality for quadrupole sources in diverse flows was revealed by Blokhinitsev long before Lighthill using simple dimensional analysis without recourse to any plausible theory of sound generation.

Fedorchenko →

"--one should **not** regard the rough approximation $I \approx kM^8$ that may be well obtained on the basis of dimensional analysis, as a triumph of Lighthill's Acoustic analogy."

NASA/CP—2001-211152

Large Scale Turbulence Structures

Role of Large-Scale Turbulence Structures in Jet Mixing and Noise

NASA Contractor Report 3538

Tone-Excited Jet
Theory and Experiments

K. K. Ahuja and J. Lepicovsky
Lockheed-Georgia Company
Marietta, Georgia

C. K. W. Tam
The Florida State University
Tallahassee, Florida

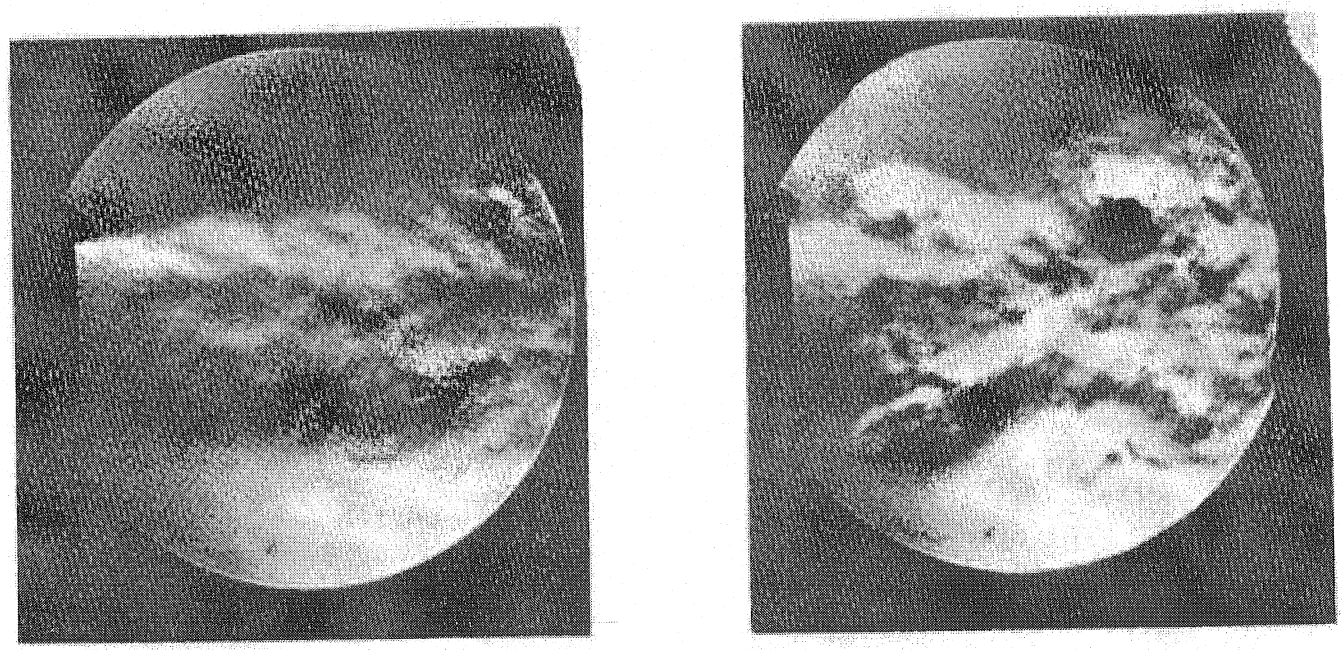
P. J. Morris
Pennsylvania State University
University Park, Pennsylvania

R. H. Burrin
Lockheed-Georgia Company
Marietta, Georgia

Prepared for
Lewis Research Center
under Contract NAS3-21987

NASA
National Aeronautics
and Space Administration
Scientific and Technical
Information Branch
1982

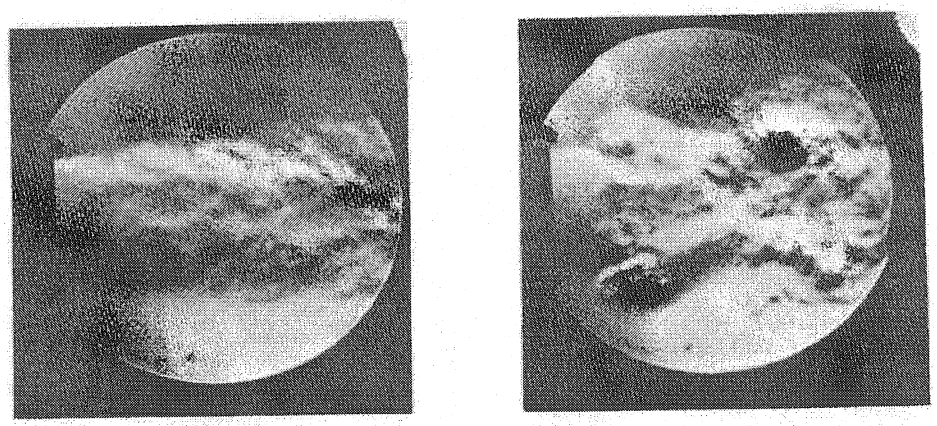
Unexcited versus Excited Jet



(a) (b)

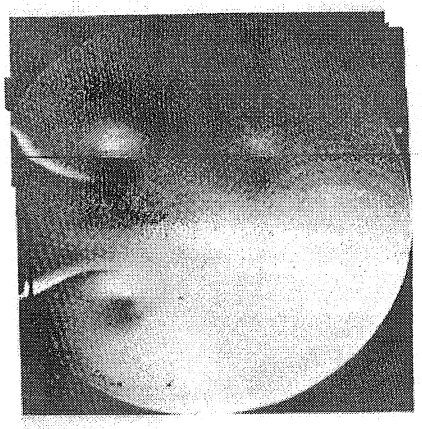
Schlieren photographs of (a) an unexcited and (b) an excited jet.

Instability Waves in Acoustically Excited Jets

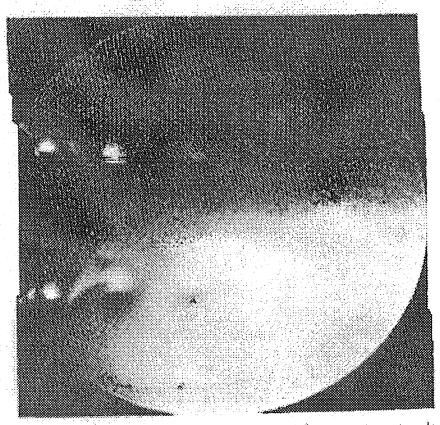


(a) (b)

Schlieren photographs of (a) an unexcited and (b) an excited jet.

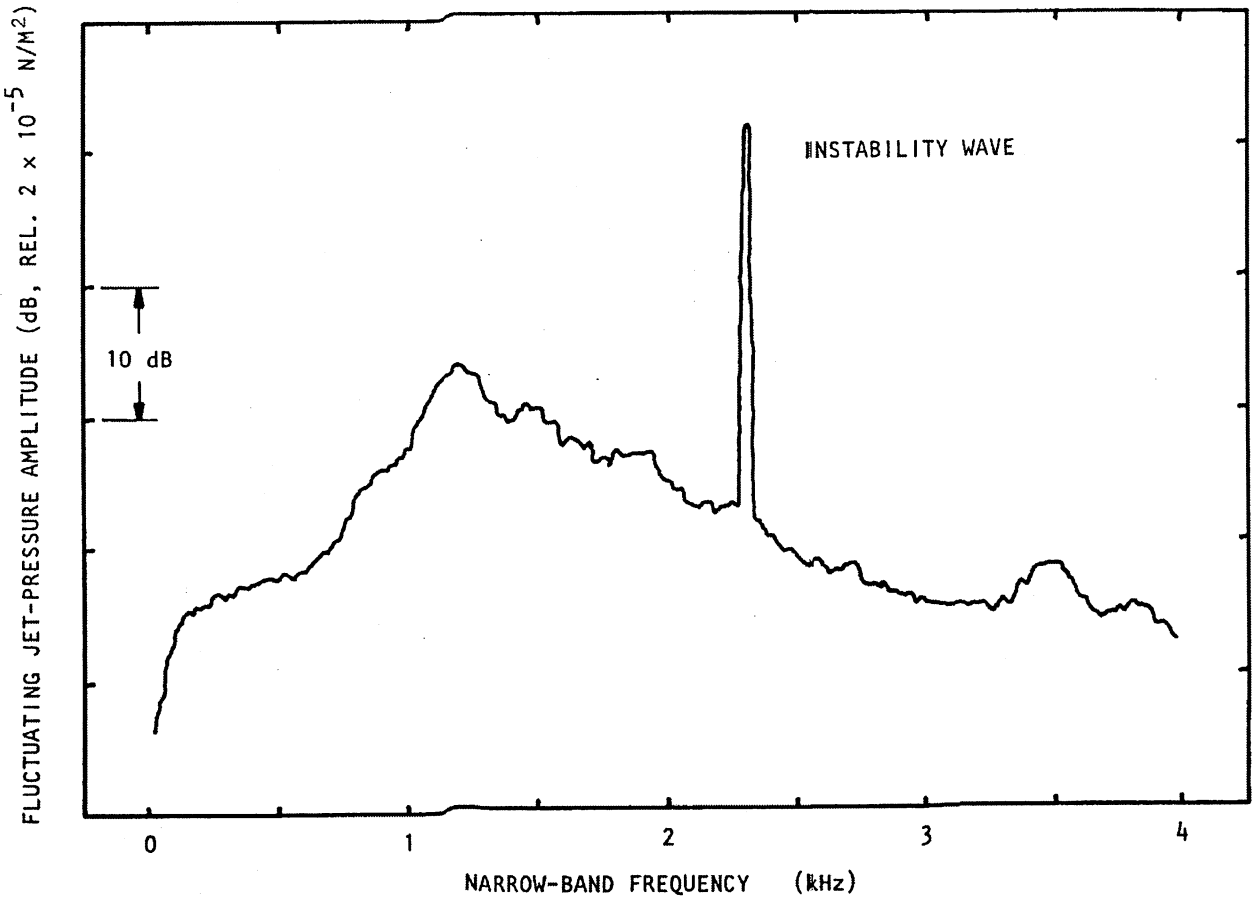


Photographic averaging of the excited jet shown in Figure 4.4(b).



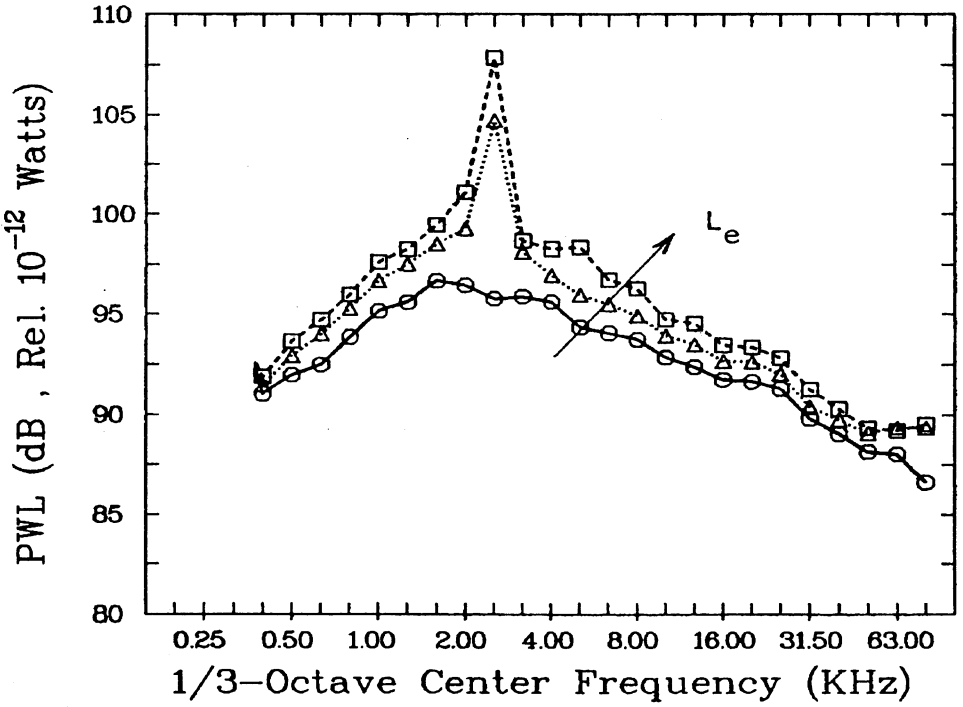
Photographically averaged schlieren photograph of a jet excited at twice the frequency of excitation used in Figure 4.5.

Instability Waves in the Pressure Spectrum Measured x = 3 D



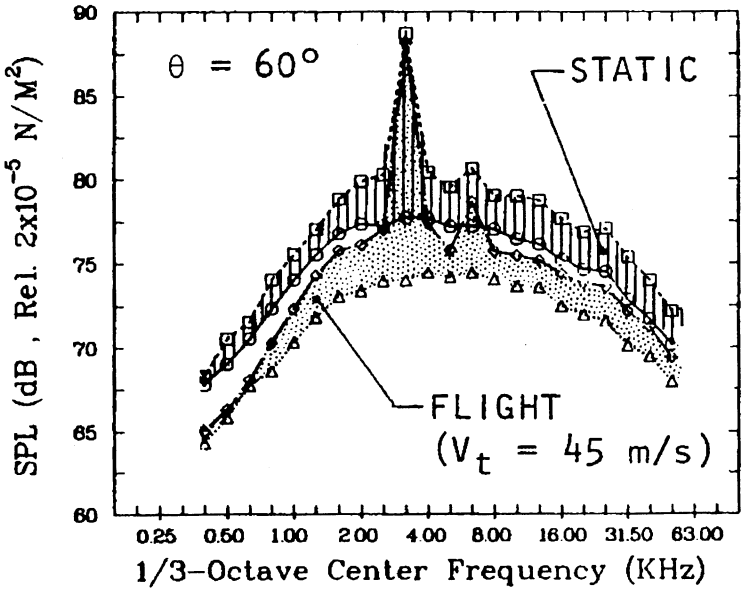
Typical spectrum of the jet-centerline pressure at $x/D_j = 3.0$. $M_j = 0.58$, Unheated, Static, $f_e = 2330$ Hz, $S_e = 0.6$, $L_e = 136$ dB, analysis bandwidth $\Delta f = 10$ Hz.

Broadband Sound Amplification by Acoustic Excitation



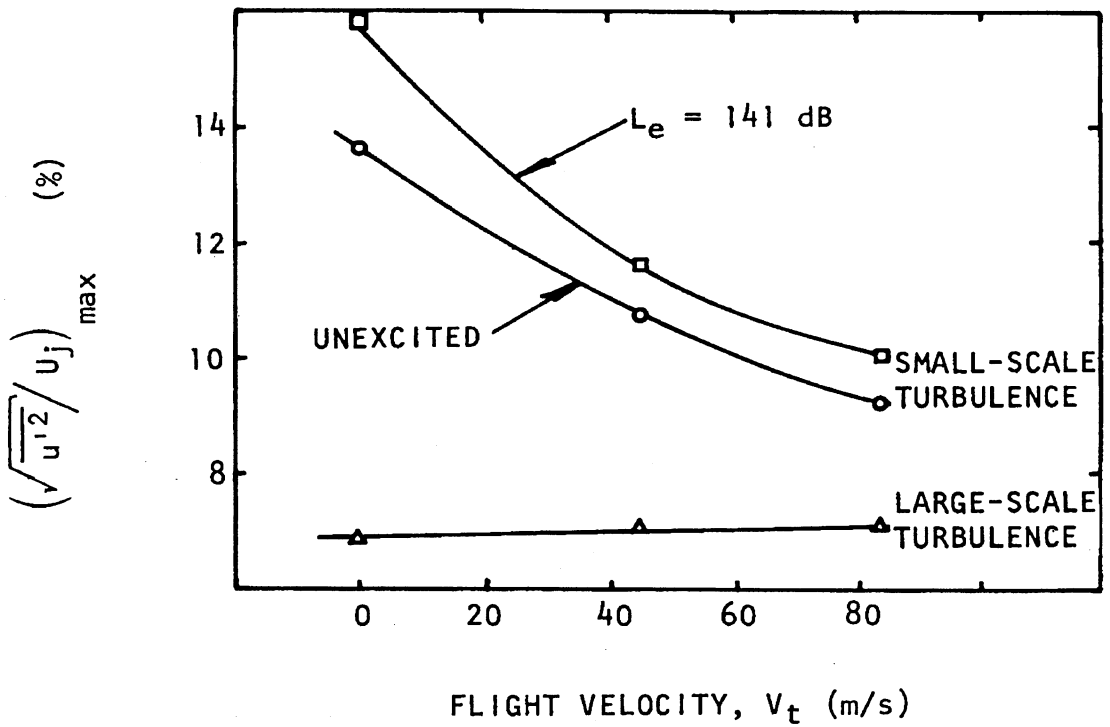
1/3-octave PWLs at various excitation levels:
○ , Unexcited; △ , 131 dB; □, 136 dB.
M_j = 0.58, U_j = 190 m/s, Unheated, Static, S_e = 0.63, (0,0) Mode.

Broadband Jet Noise Amplification for the Static and Flight Simulation Cases



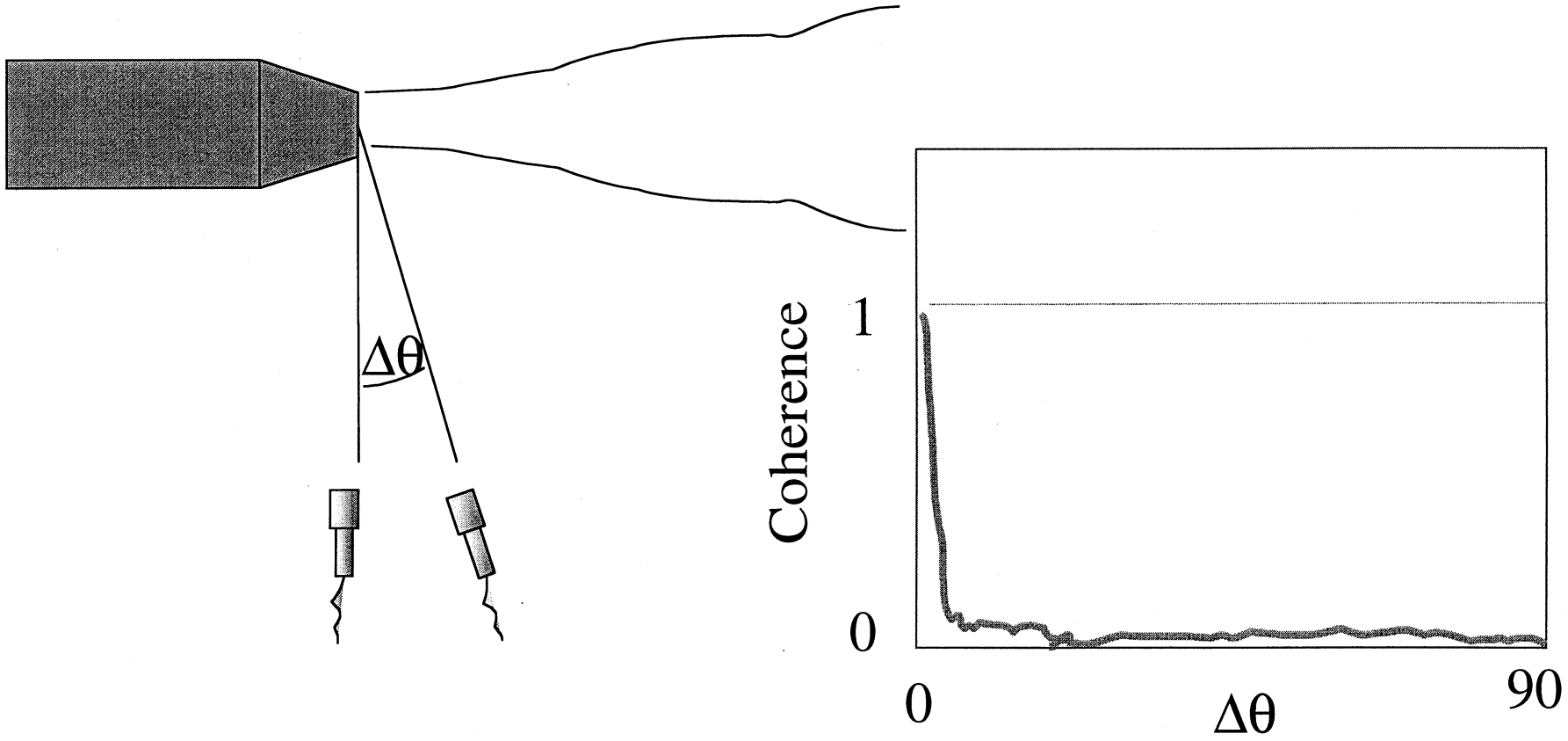
Comparison of broadband jet-noise amplification for the static ( ) and the flight-simulation ( ) case of $V_t = 45$ m/s. $M_j = 0.78$, $U_j = 251$ m/s, Unheated, $S_e = 0.63$, (0,0) mode.
L_e: ○,△, Unexcited; □,◇, 136 dB.

Reduction of Peak Centerline Turbulence Intensity with Flight Simulation



Variation of peak centerline turbulence intensities with forward velocity, V_t. M_j = 0.58, U_j = 190 m/s, Unheated, S_e = 0.5, (0,0) mode.

Any theory worth its salt should also be able to predict phase relationship at two farfield microphones



Jet Noise Beaming Concept

- See

1. Pao, S.P. and Maestrello, L. "Evidence of the Beam Pattern Concept on Subsonic Jet Noise Emission," NASA TN D-8104, 1976.

2. Maestrello, L "Two-Point Correlations of Sound Pressure in the Far-Field of a Jet: Experiment," NASA TM X-72835, 1976

3. Ribner, H.S.,"Theory of Two-Point Correlations of Jet Noise," NASA TN D-8330, 1976.

Definitions

Correlation Coefficient

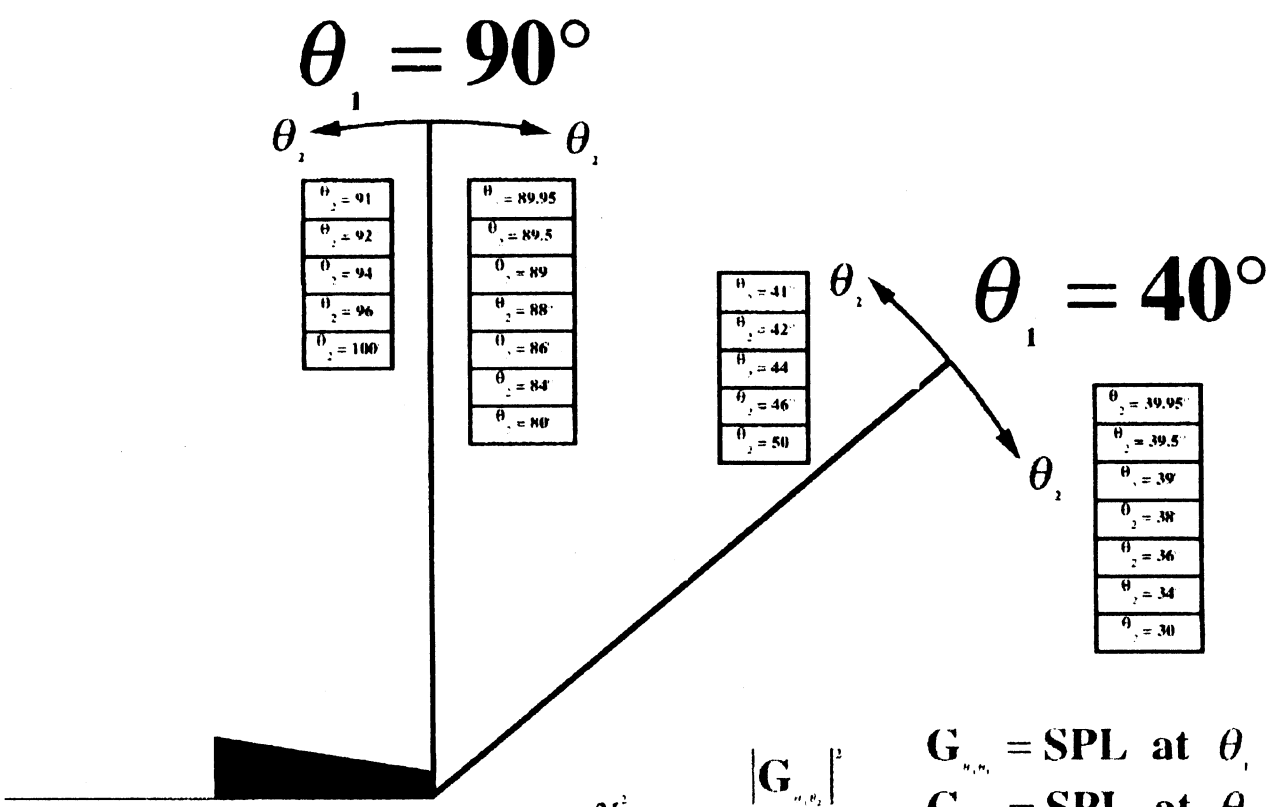
$$\rho_{xy}^2(\tau)=\frac{R_{xy}(\tau)^2}{R_{xx}(0)R_{yy}(0)}$$

Coherence

$$\gamma_{xy}^2(f)=\frac{\left|G_{xy}(f)\right|^2}{G_{xx}(f)G_{yy}(f)}$$

Coherence $\left(\gamma^2_{\theta_1\theta_2}\right)$

Coherence Measurements



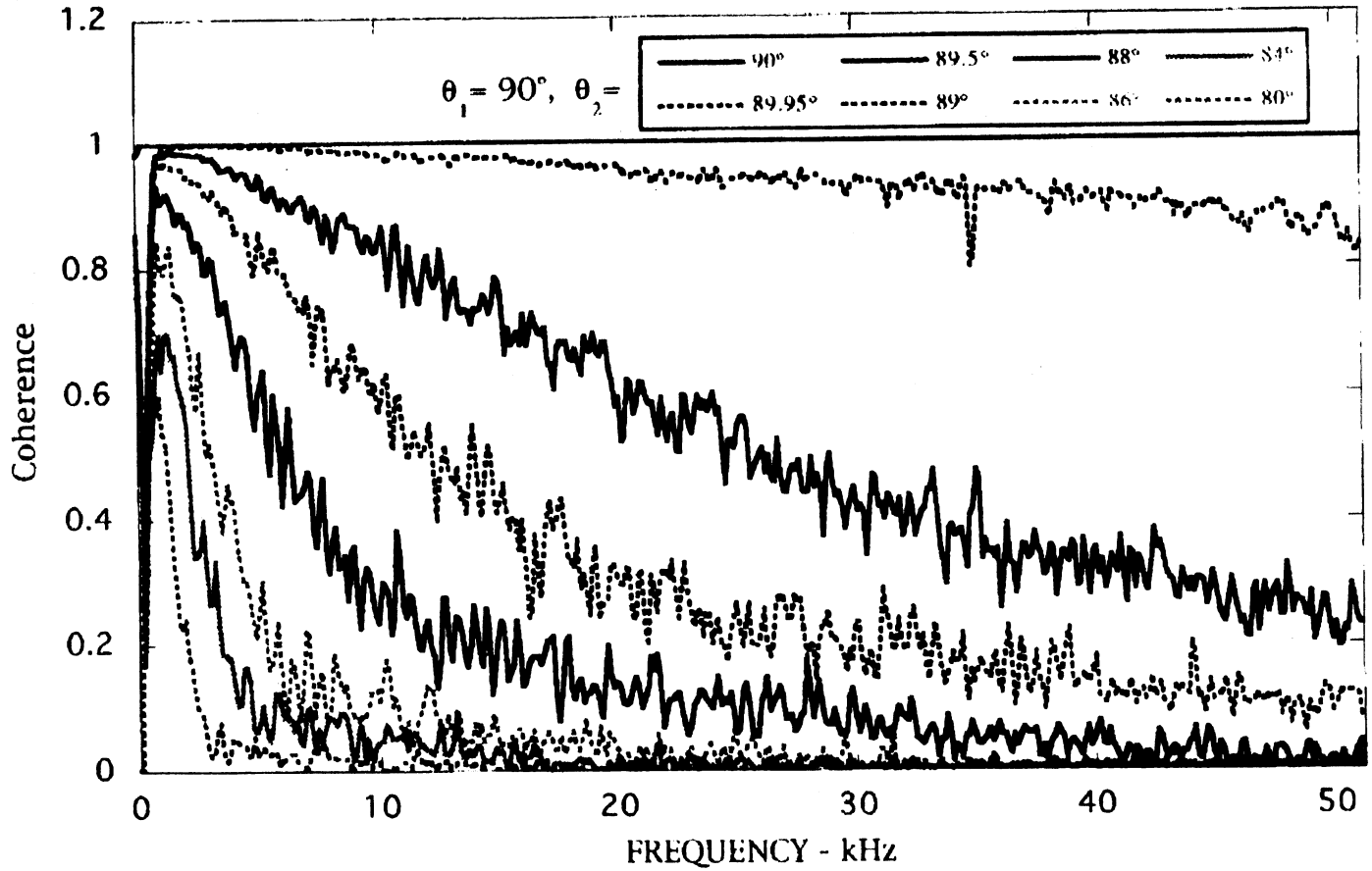
$$\gamma^2_{n_1 n_2}(f) = \frac{|G_{n_1 n_2}|^2}{G_{n_1 n_1} G_{n_2 n_2}}$$

$G_{n_1 n_1}$ = SPL at θ_1

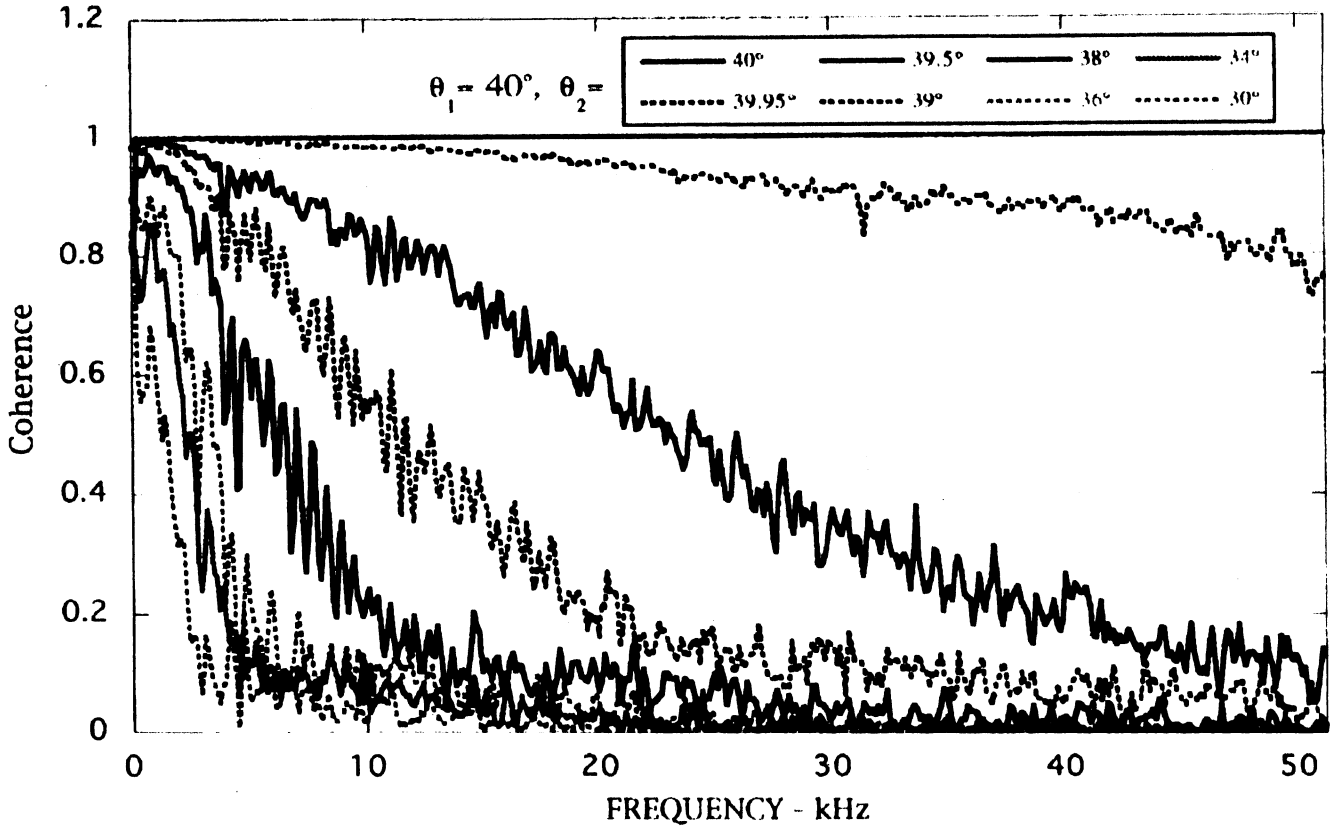
$G_{n_2 n_2}$ = SPL at θ_2

$G_{n_1 n_2}$ = Cross – Spectrum

Coherence As a Function of Microphone Separation θ_1=90°, M_j=0.8, Round Nozzle, D=2.44 inches

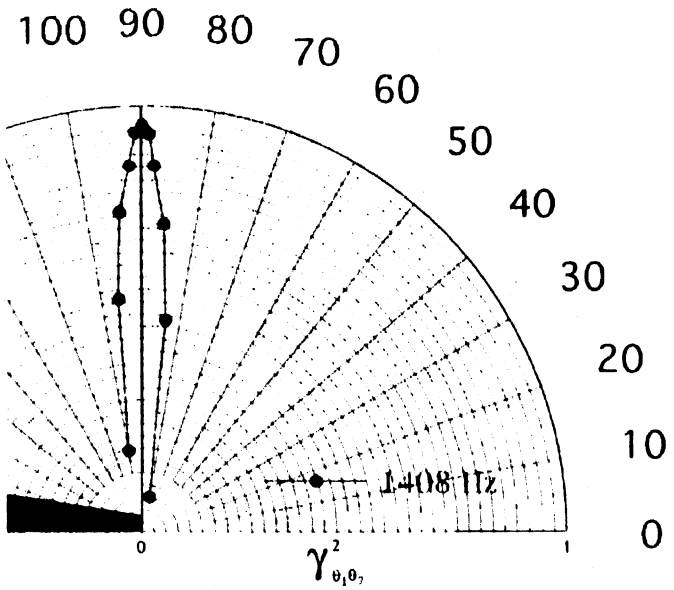


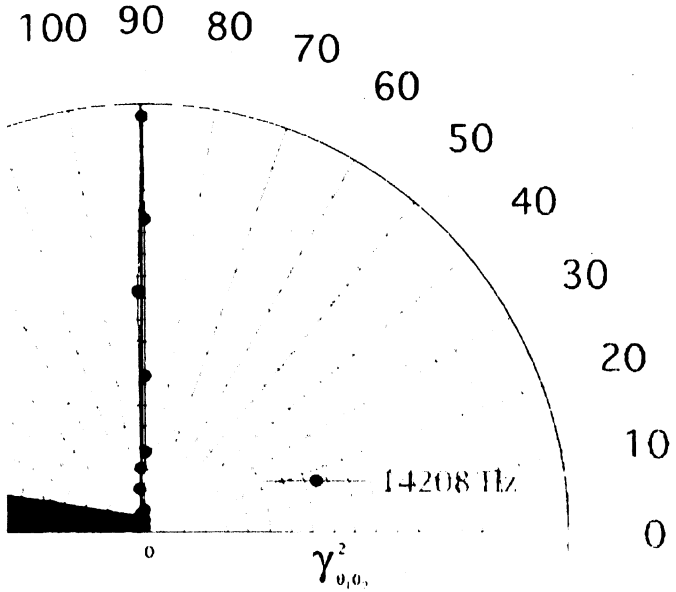
Coherence As a Function of Microphone Separation θ_i=40°, M_j=0.6, Round Nozzle, D =2.44 inches



JET

Coherence Beams of Jet Noise (D = 2.44in., M_j = 0.6)





K. Ahuja References

Published Journal Papers (Refereed)

1. Tam, C. K. W., Ahuja, K. K., and Jones, R. R. III, “Screech Tones From Free and Ducted Supersonic Jets,” AIAA Journal; Vol. 32, No. 5, pp.917 - 922, May, 1994.
2. Brown, W. H. and Ahuja, K. K., “Jet Mixing Enhancement by Hydrodynamic Excitation," AIAA Journal,, Vol. 31, No. 3, March 1993.
3. Tam, C. K. W. and Ahuja, K. K., “Theoretical Model of Discrete Tone Generation by Impinging Jets,” *Journal of Fluid Mechanics,* Vol. 214, pp. 67-87, 1990.
4. Lepicovsky, J., Ahuja, K. K., Brown, W. H., and Burrin, R. H., “Coherent Large-Scale Structures in High Reynolds Number Supersonic Jets,” *AIAA Journal,* Vol. 25, No. 11, pp. 1419-1425, 1988.
5. Ahuja, K. K., Tester, B. J., and Tanna, H. K., “Calculation of Far Field Jet Noise Spectra from Near Field Measurements with True Source Location,” *Journal of Sound and Vibration,* Vol. 116, No. 3, pp. 415-426, 1987.
6. Salikuddin, M., Brown, W. H., and Ahuja, K. K., “Noise from a Circulation Control Wing with Upper Surface Blowing,” *Journal of Aircraft,* Vol. 24, No. 1, pp 55-64, 1987.
7. Lepicovsky, J., Ahuja, K. K., Brown, W. H., and Morris, P. J., “Acoustic Control of Free Jet Mixing,” *Journal of Propulsion and Power,* Vol. 2, pp. 323-330, 1986.
8. Lepicovsky, J., Ahuja, K. K., Brown, W. H., and Burrin, R. H., “An Experimental Study of Tone-Excited Jets,” *Journal of Propulsion and Power,* Vol. 2, No. 2, pp. 149-154, 1986.
9. Ahuja, K. K., and Blakney, D. F., “Tone Excited Jets - Part IV: Acoustic Measurements,” *Journal of Sound and Vibration,* Vol. 102(1), pp. 93-117, 1985.
10. Lepicovsky, J., Ahuja, K. K., and Burrin, R. H., “Tone Excited Jets - Part III: Flow Measurements” *Journal of Sound and Vibration,* Vol. 102(1), pp. 71-91, 1985.
11. Ahuja, K. K., and Whiffen, M. C., “Tone Excited Jets - Part II: Flow Visualization” *Journal of Sound and Vibration,* Vol. 102(1), pp. 63-69, 1985.
12. Tanna, H. K., and Ahuja, K. K., “A Research Program at Lockheed on Tone Excited Jets - Part I: Introduction” *Journal of Sound and Vibration,* Vol. 102(1), pp. 57-61, 1985.

13. Lepicovsky, J., and Ahuja, K. K., "Experimental Results on Edge-Tone Oscillations in High-Speed Subsonic Jets," *AIAA Journal,* Vol. 23, No. 10, pp. 1463-1468, 1985.

14. Whiffen, M. C., and Ahuja, K. K., "An Improved Schlieren System and Some New Results on Acoustically Excited Jets," *Journal of Sound and Vibration,* Vol. 86, No. 1, pp. 99-105, 1983.

15. Ahuja, K. K., Lepicovsky, J., and Burrin, R. H., "Noise and Flow Structure of a Tone-Excited Jet," *AIAA Journal,* 20, 1982.

16. Ahuja, K. K., and Tam, C. K. W., "A Note on the Coupling Between Flow Instabilities and Incident Sound," *Journal of Sound and Vibration,* Vol. 83, No. 3, pp. 433-439, 1982.

17. Ahuja, K. K., Tanna, H. K., and Tester, B. J., "An Experimental Study of Transmission, Reflection, and Scattering of Sound in a Free Jet Flight Simulation Facility and Comparison with Theory," *Journal of Sound and Vibration,* Vol. 75, No. 1, pp. 51-85, 1981.

18. Dosanjh, D., Bhutiani, P. K., and Ahuja, K. K. "Supersonic Jet Noise Suppression by Coaxial Cold/Heated Jet Flows," *AIAA Journal,* Vol. 16, No. 3, pp. 268-270, 1978.

19. Ahuja, K. K., "An Experimental Study of the Effects of Upstream Obstruction on Subsonic Jet Noise," *Journal of Sound and Vibration,* Vol. 37, No. 2, pp. 205-234, 1974.

20. Ahuja, K. K., "Correlation and Prediction of Jet Noise," *Journal of Sound and Vibration,* Vol. 29, No. 2, pp. 155-168, 1973.

21. Ahuja, K. K., and Bushell, K. K., "An Experimental Study of Subsonic Jet Noise and Comparison with Theory," *Journal of Sound and Vibration,* Vol. 30, No. 3, pp. 317-341, 1973.

Conference Presentations with Proceedings (refereed)

1. Ahuja, K. K., and Spencer, D. A., "Aeroacoustics of Advanced STOVL Aircraft Plumes," Proceedings of the International Powered Lift Conference and Exposition: P-203, Santa Clara, CA, December 7-10, 1987, Published by SAE; pp. 531-542, February 1988.

Is Acoustic Analogy really valid? Are large turbulent structures important?

Ulf Michel
DLR, Institute of
Propulsion Technology

JET NOISE WORKSHOP

Ohio Aerospace Institute
Cleveland, Ohio
7-9 November 2000

U. Michel *

Is Acoustic Analogy really valid?

Are large turbulent structures important?

Evidence will be given in this presentation that

- the acoustic analogy is really valid and
- that large coherent structures in the jet turbulence are important for jet noise emission.

This will be demonstrated by comparing experimental data with scaling laws based on the acoustic analogy.
It will be shown that the following observations can be explained with the acoustic analogy:

1. U_j^8 and U_j^6 power laws for subsonic static jets,
2. limitation of the radiation efficiency for jets with very high jet speeds U_j,
3. independence of frequency on emission angle θ_0 over a wide angle range for static jets,
4. frequency of broadband shock noise and width of peak in frequency spectrum including the effect of flight speed,
5. screech frequency including the effect of flight speed.

Items 2, 4, and 5 require that the retarded time differences within the large coherent structures in the jet's turbulence are properly considered which demonstrates the importance of these structures.

Jet mixing noise was the first application of Lighthill's acoustic analogy (Lighthill [7, 8]). He introduced a source model based on acoustically compact moving sources (see Fig. 1).
A few of his results agree with experimental data:

- Sound power is proportional to the eighth power of the jet's speed (agreement only for jets with uniform density).
- Sound pressure level is larger in the rear arc (in the direction of the jet's mean velocity vector) than in the forward arc.
- Mach-wave radiation occurs for supersonic convection speeds.

*DLR, Institute of Propulsion Technology, Turbulence Research Section, Müller-Breslau-Str. 8, 10623 Berlin, Germany, Email: Ulf.Michel@dlr.de, Tel. +49 30 310006-26, Fax +49 30 310006-39

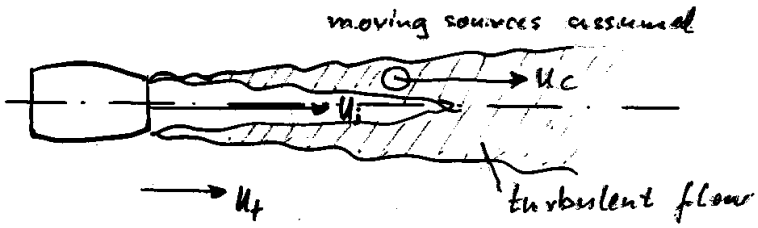


Figure 1: Moving sources (convected downstream within the shear layer with a convection speed of U_c) were assumed by Lighthill (1954) [8] and others.

However, there are many experimental results that cannot be explained with Lighthill's assumptions and this often leads to the conclusion that the acoustic analogy is not valid:

- Frequencies in the rear arc are not higher than in the forward arc (higher frequencies would be expected in the rear arc from moving sources). Experimental data for the forward arc are shown in Fig. 2 and for the rear arc in Fig. 3.
- Frequencies in flight are higher (Doppler shifted) in the forward arc which is incompatible with sources moving to the rear.
- Sound power of subsonic hot jets is only proportional to the sixth power of jet speed.
- Sound pressure levels in flight are unexpectedly high in forward arc.
- Sound power of supersonic jets increases much less than with the eighth or sixth power of jet speed (see Fig. 4).
- Supersonic jets exhibit broadband shock noise.
- Supersonic jets may generate screech.

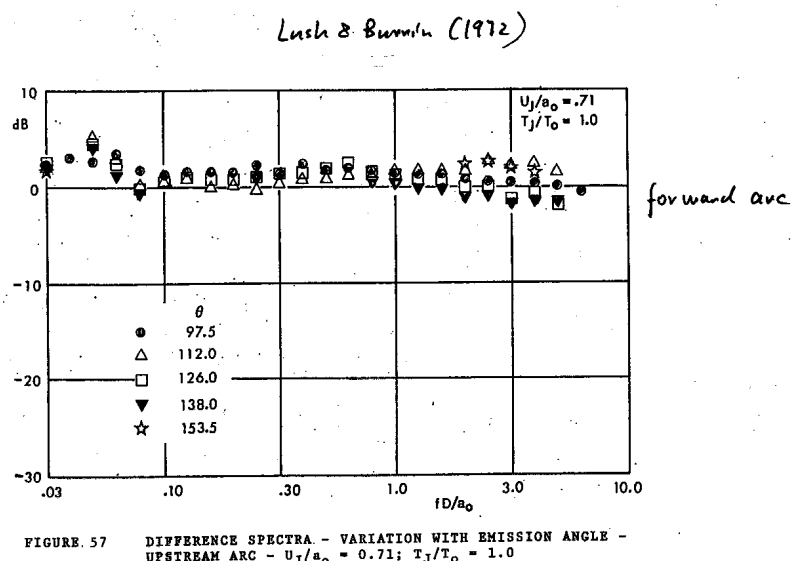


Figure 2: Normalized frequency spectra for various emission angles in the forward arc (angle is defined rel. to the downstream axis). The acoustic Mach number $U_j/a_0 = 0.71$ and temperature ratio $T_j/T_0 = 1.0$ (Lush and Burrin (1972) [9]). The frequency spectra are almost independent of emission angle.

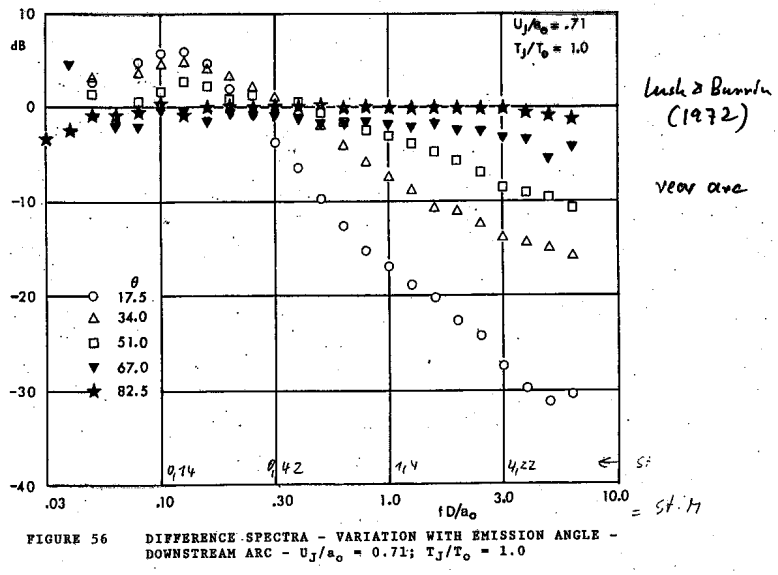


FIGURE 56 DIFFERENCE SPECTRA - VARIATION WITH EMISSION ANGLE - DOWNSTREAM ARC - U_J/a_o = 0.71; T_J/T_o = 1.0

Figure 3: Normalized frequency spectra for various emission angles in the rear arc (angle is defined rel. to the downstream axis). The frequency spectra change for small angles rel. to the jet axis. (Lush and Burrin (1972) [9]). The frequencies become lower for smaller angles rather than higher as would be expected from convected sources.

Figure 3.37. Jet mixing noise intensity versus jet velocity. (After Ref. 211, by permission)

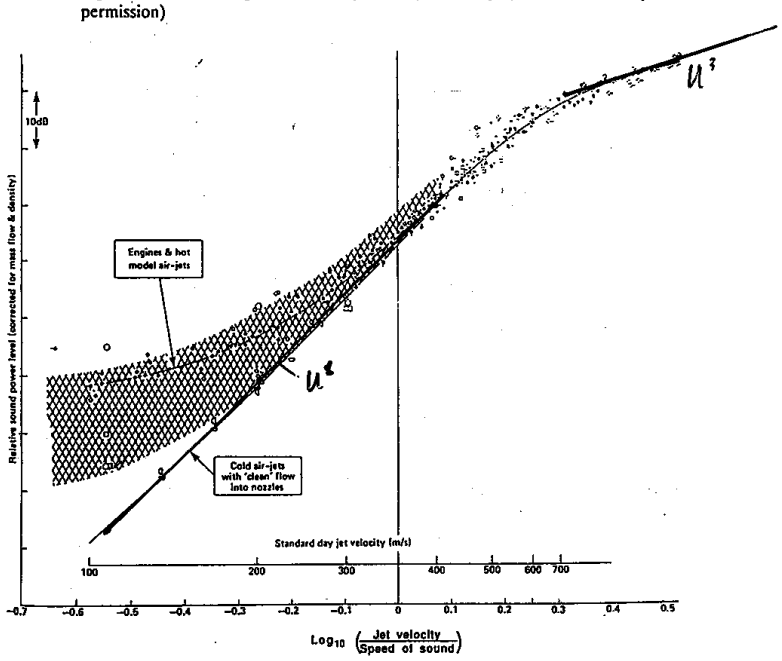


Figure 4: Sound power increases only with U_j^3 for very high jet speeds. (Figure taken from Smith (1989) [23])

SELECTION OF PROPER COORDINATE SYSTEM

All these experimental findings can be explained and described with the acoustic analogy provided the proper coordinate system and source model are chosen. The proper model is denoted WAVE MODEL in the following and is compared with the EDDY MODEL (see Fig. 5).

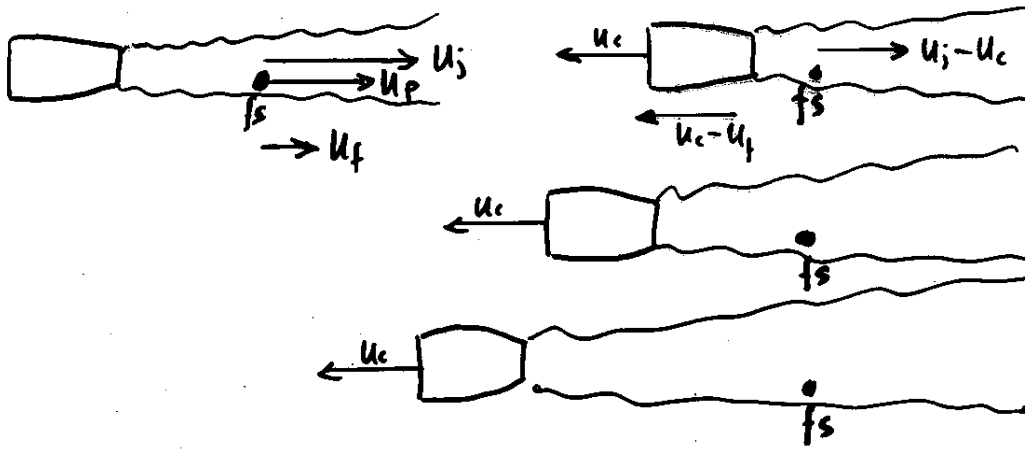


Figure 5: The coordinate system is fixed to the nozzle in the WAVE MODEL (left side) while it is fixed to the moving sources in the EDDY MODEL (right side). Consequently, the nozzle is moving in the EDDY MODEL. f_s is the frequency of the source in the frame of the chosen coordinate system, U_f, U_j, and U_c are flight speed, jet speed, and convection speed of the turbulence, respectively.

WAVE MODEL	EDDY MODEL
Coordinate system is fixed on the nozzle. (First proposed by Ribner (1959) [22], always used by Michalke (1970,1972) [11, 12].)	Coordinate system is fixed to the "moving sources". (Introduced by Lighthill (1954)[8] and used by Ffowcs Williams (1963) [3] and many others.)
Flow is stationary random and boundaries of turbulent flow field are stationary. Condition for validity of integral (e.g., Eq. (6)) over source volume is satisfied.	Flow field is not stationary random and boundaries are changing with time. Condition for validity of integral over source volume ("Lighthill integral") is **not** satisfied.
Turbulence length scales are not limited (Michalke (1972) [12]) and large scales can be considered, easily.	Sound sources are generally assumed to be compact.

CONVECTIVE WAVE EQUATION

The wave model requires use of the convective Lighthill equation which is given for the pressure (see Michalke and Michel (1979) [16]) by

$$\frac{1}{a_0^2}\left[\frac{\partial}{\partial t}+U_i\frac{\partial}{\partial x_i}\right]^2 p-\frac{\partial^2 p}{\partial x_i^2}=\frac{\partial^2 q_{ij}}{\partial x_i \partial x_j}+\frac{\partial q_i}{\partial x_i}, \tag{1}$$

where

$$\frac{\partial^2 q_{ij}}{\partial x_i \partial x_j} = \text{Quadrupole source function}, \tag{2}$$

$$\frac{\partial q_i}{\partial x_i} = \text{Dipole source function}. \tag{3}$$

Equation (1) describes the propagation of acoustic waves in a medium with sound speed a_0 and uniform flow velocity U_i if the right hand side of the equation is zero. This is approximately the case outside the

jet flow where the right hand side is quadratically small in the pressure fluctuations. The right hand side is nonzero within the flow region of a jet and is then causal for the sound field in the far field. Therefore, the two terms are denoted source terms although they also describe propagation effects.

SOURCE TERMS

The source terms, Eqs. (2) and (3), can be derived (see Michalke & Michel [16]) with the assumption that the entropy remains constant along particle pathlines (Morfey [20]) which means:

- The influence of the viscous stress on the sound sources is neglegted.
- The influence of heat conduction on the sound sources is neglected.

The additional assumption: $|p'|/(\kappa p_0) \ll 1$ (pressure fluctuation p' within the flow are small in comparison to the ambient pressure p_0) yields

$$q_{ij} = \rho_0 u_i u_j \left(1 + \frac{p'}{\kappa p_0}\right) - \left(1 - \frac{\rho_0}{\rho}\right) p' \delta_{ij}, \tag{4}$$

$$q_i = p' \frac{\partial}{\partial x_i} \left(\frac{\rho_0}{\rho}\right), \tag{5}$$

where κ is the ratio of the specific heat capacities. The derivation can be found in Michalke & Michel (1979).

FAR-FIELD SOLUTION

The big advantage of the acoustic analogy is that closed form solutions can be derived for the sound radiation of a turbulent flow. These solutions can be used to derive scaling laws.

The far-field solution for the power-spectral density of the sound pressure of a free jet can be written in form of a double integral as follows (Michel and Michalke (1981) [18], derivation can be found in Michel and Michalke (1981) [19])

$$W_{pp}(x_i, f) = \frac{1}{(4\pi r_0 a_0 D_f^2)^2} \underbrace{\int_V \underbrace{W_{ss1}}_{\text{strength}} \underbrace{\int_{V_c} \underbrace{\underbrace{\sqrt{W_{ss2}/W_{ss1}}}_{\text{rel. strength}} \underbrace{\gamma_{12}}_{\text{coherence}} \underbrace{\exp\{i(\psi_s + \psi_r)\}}_{\text{interference}}}_{\text{determines directivity}} dV_c(y_i + \eta_i)}_{\text{integral over coherence volume}} dV(y_i)}_{\text{integral over source volume}} . \tag{6}$$

W_{ss1} and W_{ss2} are the power-spectral densities of the source function $S(y_i, t)$ (Eq. (8)) in the two volume elements $dV(y_i)$ and $dV_c(y_i + \eta_i)$ which are separated by the separation vector η_i. W_{ss1} and W_{ss2} describe the (time averaged) strength of the sources. The randomness of the sources is considered by the coherence γ_{12} between the two source positions. The phase difference ψ_s describes the source motion and the phase difference ψ_r the retarded time difference between the two source positions.

The equation includes the influence of flight speed. Flight speed tends to increase the noise emission in the forward arc due to the presence of the Doppler factor D_f,

$$D_f = 1 - M_f \cos\theta_0, \tag{7}$$

where θ_0 is the (wave normal) emission angle relative to the flight direction and $M_f = U_f/a_0$ is the flight Mach number.

The source function $S(y_i, t)$ is given by

$$S(y_i, t) = \frac{1}{a_0 D_f} \frac{\partial^2 q_q(y_i, t)}{\partial t^2} + \frac{\partial q_d(y_i, t)}{\partial t}. \tag{8}$$

The quadrupole source term q_q and the dipole source term q_d are defined by

$$q_q = \rho_0 u_{r_0}^2 \left(1 + \frac{p'}{\kappa p_0}\right) - \left(1 - \frac{\rho_0}{\rho}\right) p', \tag{9}$$

$$q_d = p' \frac{\partial}{\partial y_{r_0}} \left(\frac{\rho_0}{\rho}\right), \tag{10}$$

where r_0 is the wave-normal distance, u_{r_0} the component of the relative velocity $u_i = c_i - U_i$ (U_i is introduced in Eq. (1) and c_i is the fluctuation velocity in the nozzle-fixed coordinate system) in the direction θ_0, $\partial/\partial y_{r_0}$ the gradient in the wave-normal direction θ_0.

It is interesting to note that the two source functions in Eq. (8) are differently affected by flight speed (expressed in terms of Doppler factor D_f). Therefore, the flight effects of a hot jet should be different from a cold jet.

WAVE-NORMAL COORDINATES

The wave-normal emission angle θ_0 and the wave-normal radiation distance r_0 are defined in Fig. 6. The choice of these emission coordinates (r_0, θ_0) rather than observer coordinates (r, θ) is causal for the compact form of equation (6). The observer coordinates can be transformed to emission coordinates by

$$r_0 = r \Big/ \left[\left(1 - M_f^2 \sin^2\theta\right)^{\frac{1}{2}} - M_f \cos\theta\right] \tag{11}$$

and

$$\cos\theta_0 = \cos\theta \left[\left(1 - M_f^2 \sin^2\theta\right)^{\frac{1}{2}} - M_f \cos\theta\right] + M_f. \tag{12}$$

POWER LAWS IN TERMS OF ACOUSTICAL JET MACH NUMBER

It was shown by Michalke and Michel (1979) [16] that the source term q_q yields a $(U_j/a_0)^8$ dependence of the sound intensity in the far field for an emission angle $\theta_0 = 90$ degrees while the term q_d yields a $(U_j/a_0)^6$ dependency. Engine jets show a $(U_j/a_0)^6$ dependence indicating that the density fluctuation source term q_d dominates.

DIRECTIVITY

- The directivity of jet mixing noise is determined by the integrand of the inner integral in Eq. (6), primarily by the product of coherence function and interference function $\gamma_{12} \exp\{i(\psi_s + \psi_r)\}$.
- No directivity of the sources (power-spectral density W_{ss} of source term S defined by Eq. (8) is required to explain the directivity of the sound emission into the far field.

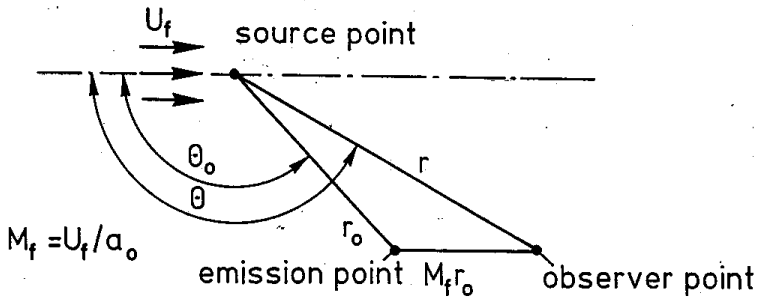


Figure 6: Relation between observer angle θ, observer distance r, emission (wave-normal) angle θ_0, and wave-normal distance r_0 for a source in a moving stream. While the sound propagates over the distance r_0 from the source point toward the emission point (r_0, θ_0) it is convected downstream by the flow over the distance $M_f r_0$ to reach the observer point (r, θ).

The coherence term $\gamma_{12}(f, y_i, \eta_i)$ describes the decay of the coherence between the two source volume elements dV and dV_c in the integral of Eq. (6) for a given position y_i of the volume element $dV(y_i)$ with increasing separation vector η_i.

The interference term $\exp\{i(\psi_s + \psi_r)\}$ describes the phase relationship between contributions from different source positions, where

ψ_s is the influence of the (source) propagation of the fluctuations within the flowR, and

ψ_r is the retarded time difference between the two source positions y_i and $y_i + \eta_i$.

INTERFERENCE WITH ONE-DIMENSIONAL JET MODEL

The interference term $\exp\{i(\psi_s + \psi_r)\}$ in Eq. (6) shall now be discussed with a one-dimensional simplification in which the jet is concentrated on its axis.

The fluctuations in the flow are governed by the equations of motion which result in **instability waves**, whose phase variation in the axial η_1-direction may be described by

$$\psi_s = 2\pi f \frac{\eta_1}{U_p}. \tag{13}$$

where η_1 is the axial component of the separation vector η_i between the two source positions, and U_p is the phase (convection) speed of the considered frequency component, $U_p \approx U_f + 0.7(U_j - U_f)$ where U_j is the jet speed and U_f is the flight speed.

The **retarded time difference** between the two volume elements yields a phase difference of

$$\psi_r = 2\pi f \frac{\eta_1 \cos\theta_0}{a_0 D_f}. \tag{14}$$

The sum of both phase differences is given by

$$\psi_s + \psi_r = \frac{2\pi f \eta_1}{a_0} \left(\frac{a_0}{U_p} + \frac{\cos\theta_0}{D_f} \right) \tag{15}$$

For a flight Mach number $M_f = 0$ and $U_p = 0.7\,U_j$, we obtain

$$\psi_s + \psi_r = \frac{2\pi f \eta_1}{a_0} \left(\frac{a_0}{0.7\,U_j} + \cos\theta_0 \right) \tag{16}$$

$\psi_s + \psi_r$ is largest for $\theta_0 \to 0$ (upstream direction) and smallest for $\theta_0 \to 180$ deg.

COHERENCE WITH ONE-DIMENSIONAL JET MODEL

The instability waves loose coherence during their propagation. If the radial extension of the jet is neglected, again, the coherence function γ_{12} may be modeled with an axial length scale L_{c1} yielding

$$\gamma_{12} = \exp\left[-\pi\left(\frac{\eta_1}{L_{c1}}\right)^2\right]. \tag{17}$$

This function decays rapidly with increasing η_1 if the coherence length scale L_{c1} is small.

SOURCE INTERFERENCE WITH ONE-DIMENSIONAL JET MODEL

By combining these two approximations and by neglecting the influence of $\sqrt{W_{ss2}/W_{ss1}}$, the integrand in Eq. (6) is determined by the following product of coherence and interference.

$$\gamma_{12}\,\exp\{i\,(\psi_s + \psi_r)\} = \underbrace{\exp\left[-\pi\left(\frac{\eta_1}{L_{c1}}\right)^2\right]}_{\text{coherence}}\ \underbrace{\exp\left[i2\pi\frac{f\eta_1}{a_0}\left(\frac{a_0}{U_p} + \frac{\cos\theta_0}{D_f}\right)\right]}_{\text{interference}}. \tag{18}$$

DIRECTIVITY FOR SMALL COHERENCE LENGTH SCALE

Eq. (18) is evaluated in Fig. 7 for a small normalized coherence length scale $L_c/\lambda = 0.1$. $\lambda = a_0/f$ is the wave length of the acoustic waves. The resulting function is plotted for three different emission angles for an acoustic convection speed defined by the convection Mach number $U_p/a_0 = 0.5$, and a flight Mach number $M_f = 0$.

The directivity is the integral of Eq. (18) over η_1/λ as a function of emission angle θ_0. It can be concluded from Fig. 7 that the influence of the emission angle on the integral (area under the curve) is minimal for a small coherence length scale within the turbulence. The consequence is an almost omnidirectional directivity of a jet for this case.

DIRECTIVITY FOR LARGE COHERENCE LENGTH SCALE

Fig. 8 shows the same evaluation for a large normalized coherence length scale $L_c/\lambda = 2$. The interference function is unchanged. The coherence function is shown as the envelope of all curves and extends over several wave lengths of the interference function. The resulting integral (not shown in the figure) becomes the smaller the more oscillations of the interference functions occur. The number of zero crossings increases in the forward arc (60 degrees) and decreases in the rear arc (120 degrees) resulting in smaller integrals in the forward arc than in the rear arc.

Directivity plots can be obtained by integrating the function plotted in Fig. 8. It has to be concluded that a considerable coherence length scale is required to explain the rear arc amplification found in the directivities of static jets. A large coherence length scale means that the turbulence structures do not change considerably while they are convected over a large distance. The structures itself need not to be large.

Fig. 9 shows an experimental result integrated over a wide frequency range. The difference between rear and forward arcs is of the order of 18 dB which requires a considerable length scale L_c/λ. It must be

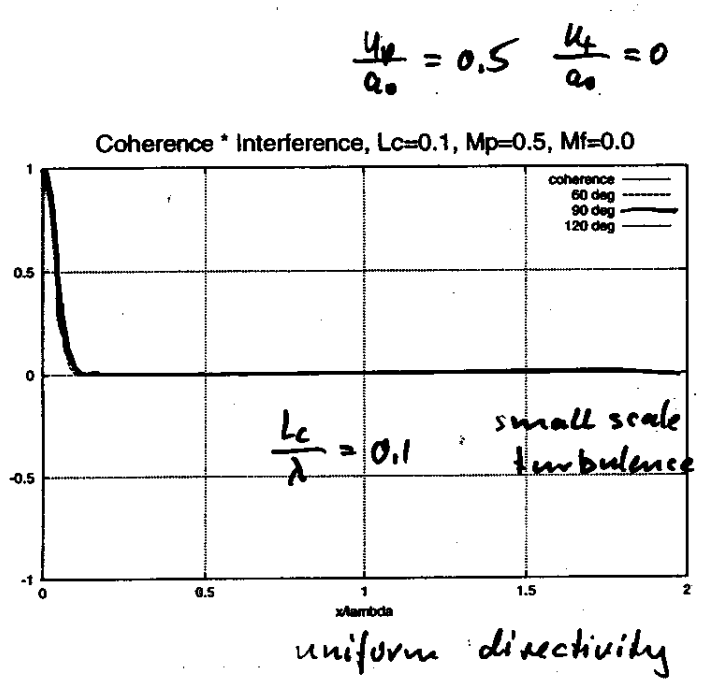


Figure 7: Evaluation of Eq. (18) as function of the normalized separation distance η_1/λ (denoted x/lambda in the figure) for a small coherence length scale with $L_c/\lambda = 0.1$, a convection Mach number $U_p/a_0 = 0.5$ of the turbulent fluctuations, and a flight Mach number $M_f = 0$. The result is seen to be almost independent of emission angle.

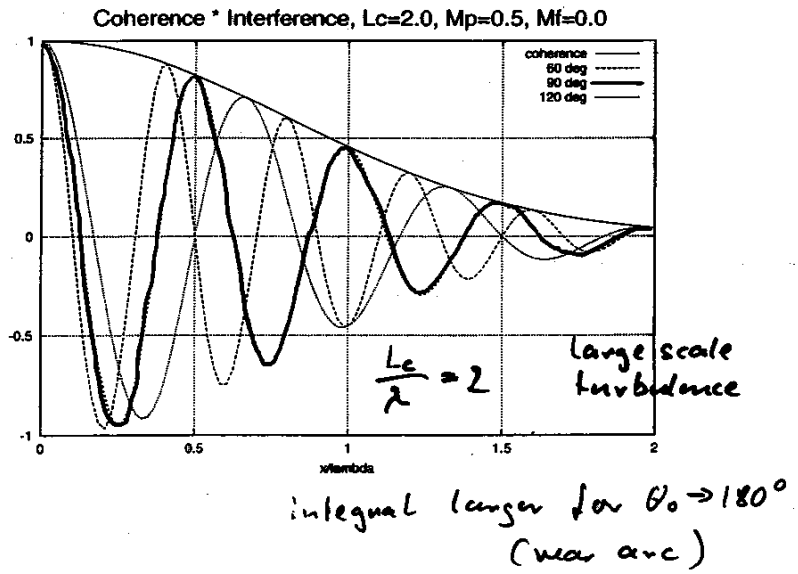


Figure 8: Evaluation of Eq. (18) as function of the normalized separation distance η_1/λ (denoted x/lambda in the figure) for a coherence length scale with $L_c/\lambda = 2.0$, a convection Mach number $U_p/a_0 = 0.5$ of the turbulent fluctuations, and a flight Mach number $M_f = 0$. The result is seen to be influenced considerably by the emission angle.

concluded that jet noise would not have a rear arc amplification without large coherent scales within the turbulent flow field. The dimple seen close to the jet axis is likely caused by refraction effects as was experimentally validated by Atvars et al. (1965) [1].

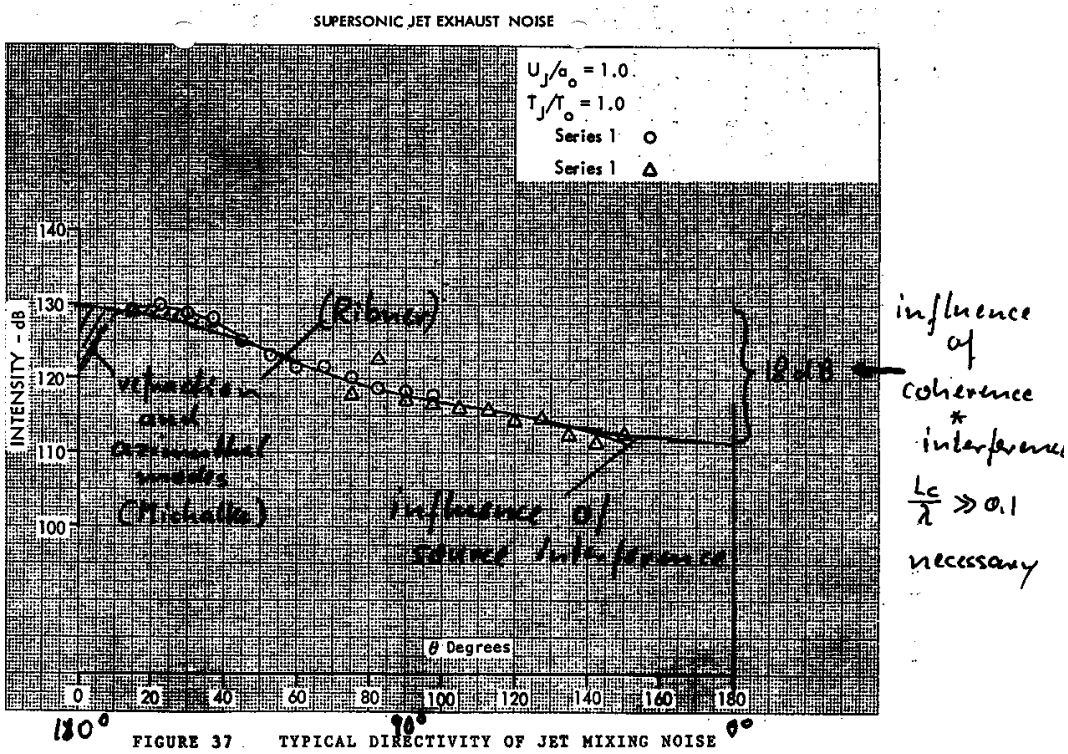


Figure 9: Directivity of a static jet with an acoustic jet Mach number $U_j/a_0 = 1.0$ and a temperature ration of $T_j/T_0 = 1.0$ as measured by Lush and Burrin (1972) [9].

DIRECTIVITY FOR SUPERSONIC PHASE SPEEDS

Eq. (18) shall now be studied for the supersonic convection Mach number $U_p/a_0 = 1.5$ and a flight Mach number $M_f = 0.3$ for four different normalized length scales $L_c/\lambda = 0.2$, 0.5, 1.0, and 2.0.

The result for the smallest length scale is plotted in Fig. 10. It can be seen that the function is almost independent of the emission angle which means that the radiation is almost independent of emission angle. This is known to be wrong.

The function of Eq. (18) is then plotted for the larger length scales $L_c/\lambda = 0.5$, 1.0, and 2.0 in the Figs. 11, 12, and 13, respectively. The increasing influence of interference can be noted and it can be concluded that coherence length scales $L_c/\lambda > 1.0$ are required for a significant directivity.

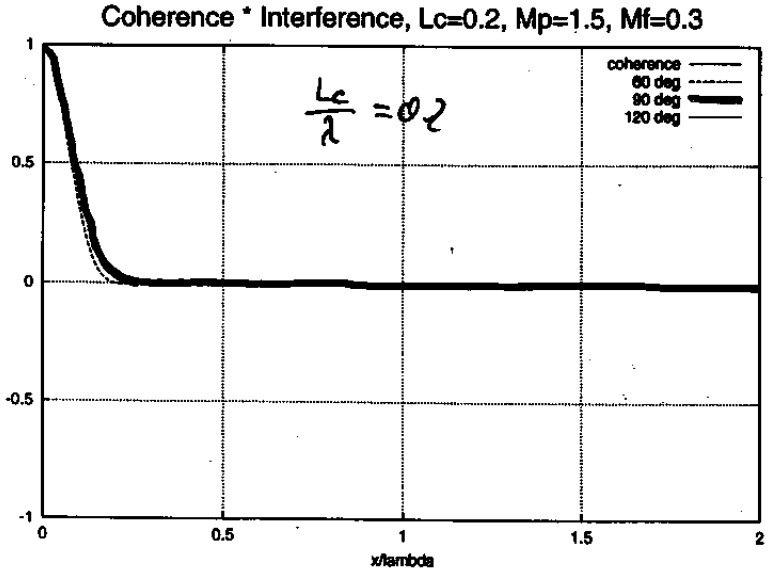


Figure 10: Evaluation of Eq. (18) as function of the normalized separation distance η_1/λ (denoted x/lambda in the figure) for a normalized coherence length scale $L_c/\lambda = 0.2$, a convection Mach number $U_p/a_0 = 1.5$ of the turbulent fluctuations, and a flight Mach number $M_f = 0.3$.

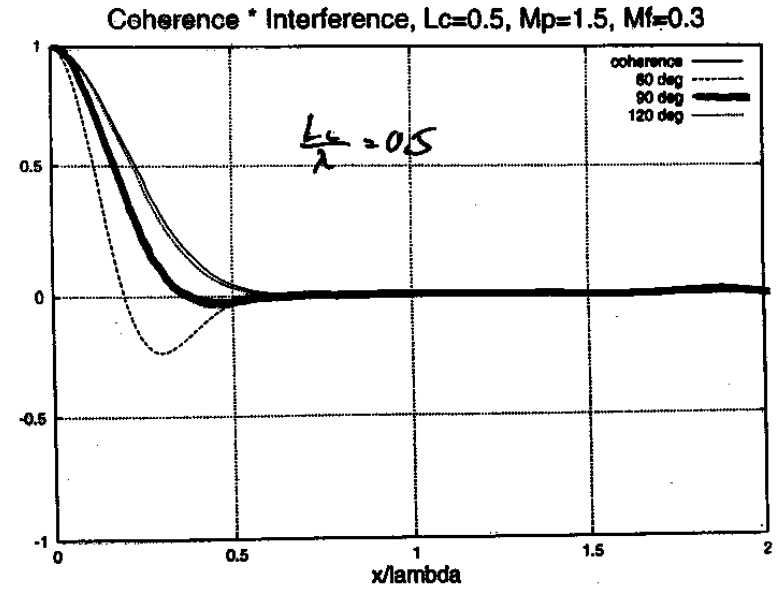


Figure 11: Evaluation of Eq. (18) as function of the normalized separation distance η_1/λ (denoted x/lambda in the figure) for a normalized coherence length scale $L_c/\lambda = 0.5$, a convection Mach number $U_p/a_0 = 1.5$ of the turbulent fluctuations, and a flight Mach number $M_f = 0.3$.

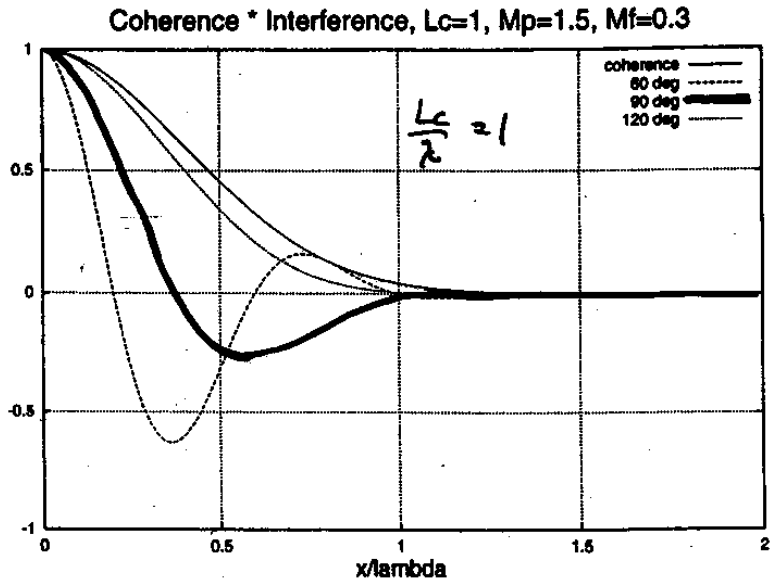


Figure 12: Evaluation of Eq. (18) as function of the normalized separation distance η_1/λ (denoted x/lambda in the figure) for a normalized coherence length scale $L_c/\lambda = 1.0$, a convection Mach number $U_p/a_0 = 1.5$ of the turbulent fluctuations, and a flight Mach number $M_f = 0.3$.

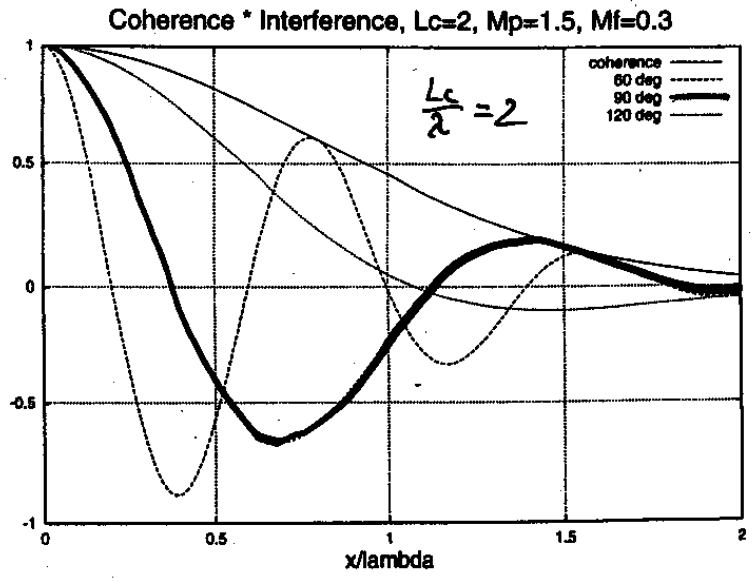


Figure 13: Evaluation of Eq. (18) as function of the normalized separation distance η_1/λ (denoted x/lambda in the figure) for a normalized coherence length scale $L_c/\lambda = 2.0$, a convection Mach number $U_p/a_0 = 1.5$ of the turbulent fluctuations, and a flight Mach number $M_f = 0.3$.

MACH-WAVE RADIATION, ONE-DIMENSIONAL JET MODEL

The sound emission is largest when the phase difference $\psi = \psi_s + \psi_r$ given by Eq. (15) for the one-dimensional model vanishes. This defines the situation of Mach-wave radiation and requires

$$\cos\theta_{0M} = -\frac{a_0}{0.7(U_j - U_f)}, \tag{19}$$

where a relative phase (convection) speed of the turbulent fluctuations of $(U_p - U_f)/(U_j - U_f) = 0.7$ is assumed.

Therefore, Mach-wave radiation is only possible for

$$\frac{U_j - U_f}{a_0} > \frac{1}{0.7}. \tag{20}$$

This factor reaches very high values for rocket jets,

$$\frac{U_j - U_f}{a_0} \approx 10, \tag{21}$$

yielding a Mach-wave radiation angle of

$$\theta_{0M} \approx 100 \text{ deg}. \tag{22}$$

It might be mentioned that the use of the wave model introduces no singularity in the case of Mach-wave radiation like it is the case for the eddy model. The width of the peak of the directivity at the Mach-wave radiation angle depends on the normalized turbulent coherent length scale L_c/λ. The length scale for a certain frequency could be determined from an experimental determination of the directivity for this frequency. However, it must be recalled that the one-dimensional model for jet turbulence is very crude.

The frequency at the Mach-wave radiation angle is equal to the source frequency in the wave model while it has the unphysical result of infinity in the case of the eddy model.

BROADBAND SHOCK NOISE, ONE-DIMENSIONAL JET MODEL

A supersonic jet, not perfectly expanded in a Laval nozzle, exhibits a cell structure shown in Fig. 14.

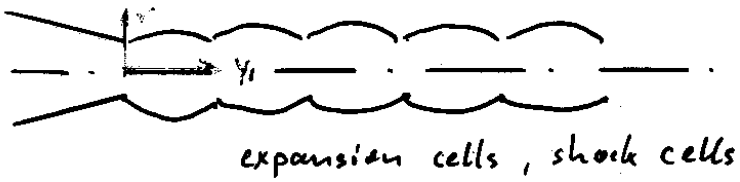


Figure 14: Cell structure of a supersonic jet.

This structure can be approximated by a Fourier series in the mean-flow direction y_1 with wave number α_n, e.g., for the mean pressure p. The following equation can be derived by simplifying Michalke's two-dimensional results (Michalke (1992) [14]) for the one-dimensional flow model (see Michel (1995) [17]).

$$p - p_0 = \sum_{n=1}^{\infty} P_n[\exp(i\alpha_n y_1) + \exp(-i\alpha_n y_1)]. \tag{23}$$

It is now assumed that the source function S given by Eq. (8) is modulated by the cells resulting in:

$$\hat{S} = \sum_{n=0}^{\infty} E_n S, \tag{24}$$

where $E_0 = 1$ is the undisturbed contribution. E_n is given by

$$E_n = a_n(r)\,\exp(i\alpha_n y_1) + b_n(r)\,\exp(-i\alpha_n y_1). \tag{25}$$

The cross-spectral density of the source function in Eq. (6) is then given by

$$\hat{W}_{ss} = \sum_{n=0}^{\infty}\sum_{m=0}^{\infty} E_n(y_i)\,E_m(y_i+\eta_i)W_{ss}. \tag{26}$$

The integrand of the double integral in Eq. (6) is then given by:

$$\begin{aligned}\hat{W}_{ss}\exp(i\psi_r) \;=\; & \sqrt{W_{ss1}\,W_{ss2}}\,\gamma_{12}\,\exp[i(\psi_s+\psi_r)] \\ & \{1 + a_1\exp(i\alpha_1 y_1) + b_1\exp(-i\alpha_1 y_1) \\ & \quad + \Big[a_1\exp(i\alpha_1 y_1) + a_1^2\exp(i2\alpha_1 y_1) + a_1 b_1\Big]\exp(i\alpha_1\eta_1) \\ & \quad + \Big[b_1\exp(-i\alpha_1 y_1) + b_1^2\exp(-i2\alpha_1 y_1) + a_1 b_1\Big]\exp(-i\alpha_1\eta_1) \\ & \quad + \cdots\}\end{aligned} \tag{27}$$

The first term in the braces ("1") describes the undisturbed solution. The second and third terms combine the exponential function of the axial separation η_1 with $\exp[i(\psi_s+\psi_r)]$ to a new interference function,

$$\exp(i\psi) = \exp[i(\psi_s + \psi_r \pm i\alpha_1\eta_1)]. \tag{28}$$

This new term yields a new "Mach-wave radiation" for the case when the argument of the exponential function in Eq. (28) is zero. While Mach-wave radiation occurred for a fixed angle in Eq. (19) it now appears for a number of frequencies which depend on the emission angle and the axial wave numbers α_n in Eq. (25),

$$f_n = \frac{\alpha_n \Delta U}{2\pi}\,\frac{(0.7 + \frac{U_f}{\Delta U})(1 - M_f\cos\theta_0)}{1 + 0.7\frac{\Delta U}{a_0}\cos\theta_0}, \tag{29}$$

where $\Delta U = U_j - U_f$.

This equation describes the frequency of broadband shock noise. For a flight Mach number $M_f = 0$ it simplifies to

$$f_n = \frac{\alpha_n U_j}{2\pi}\,\frac{0.7}{1 + 0.7\frac{U_j}{a_0}\cos\theta_0}, \tag{30}$$

which agrees with Harper Bourne & Fisher (1973) [6], Ffowcs Williams & Kempton (1978) [4], and Tam & Burton (1984) [27].

The influence of flight speed contained in Eq. (29) is quite surprising since the equation contains the Doppler factor in its numerator although this equation is only valid for the wind tunnel case.

The peak frequency of broadband shocknoise depends considerably on the emission angle θ. This dependence is plotted in Fig. 15 for different acoustic convection Mach numbers U_p/a_0.

The shae of the normalized power-spectral density of broadband shock noise can be calculated by evaluating Eq. (27) and is plotted in Figs. 16, 17, and 18 for the emission angles 90, 60, and 30 degrees, respectively. The spectra are plotted for three normalized coherence length scales $L_c/\lambda = 3.3$, 10, and 33 (the annotation reports the inverse of these values.) It can be seen that the width of the spectral peak depends very much on the normalized length scale and that very large coherence length scales result in a narrow peak. The width of the peak also depends on the emission angle and is rather small in the forward arc.

Experimental spectra are shown in Fig. 19. The peak frequencies are indicated in the figure with arrows. The frequencies scaled on Eq. (29) are indicated with circles ($U_p/a_0 = 1.6$) and triangle ($U_p/a_0 = 1.8$). The normalized turbulent length scale can be deduced from the experimental spectra and appears to be in the order of $L_c/\lambda = 2$.

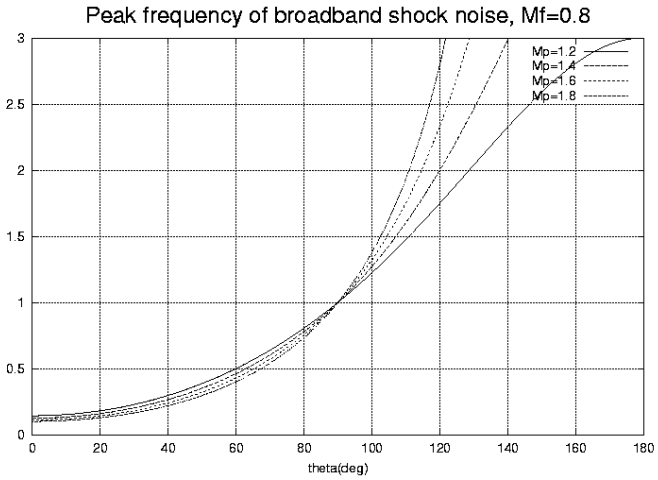


Figure 15: Normalized peak frequency of broadband shock noise as function of emission angle rel. to the flight direction for a flight Mach number of $M_f = 0.8$. The peak frequency is normalized with the frequency observed for an emission angle of 90 degrees. It can be seen that the acoustic convection Mach number U_p/a_0 has a large influence in the rear arc.

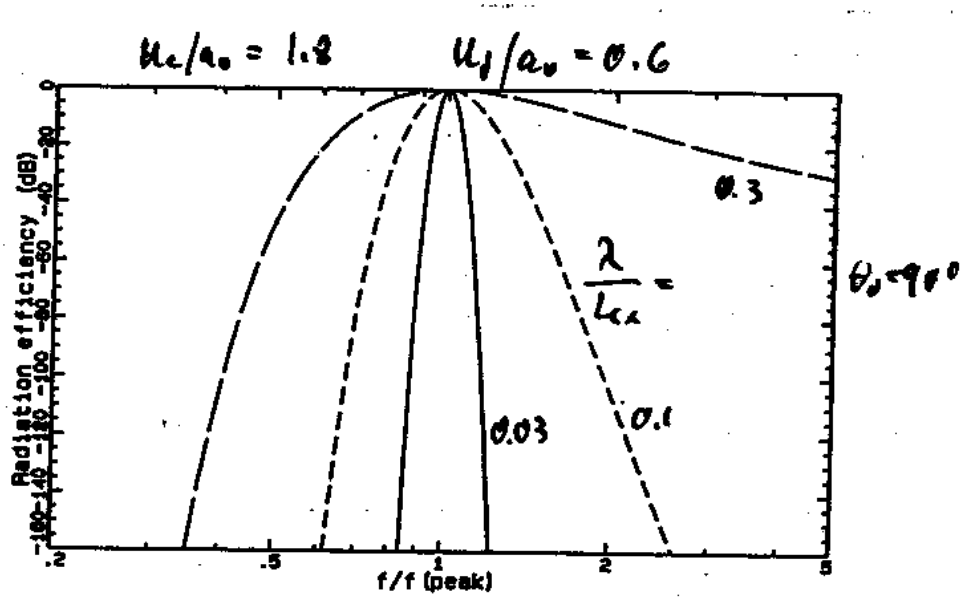


Figure 16: Normalized power-spectral density of broadband shock noise in flight for an emission angle of $\theta_0 = 90$ degrees. Flight Mach number $M_f = 0.6$, acoustic convection Mach number $U_p/a_0 = 1.8$. Curves are plotted for three normalized coherence length scales, $L_c/\lambda = 3.3$, 10, and 33. (The annotation reports the inverse of these values.)

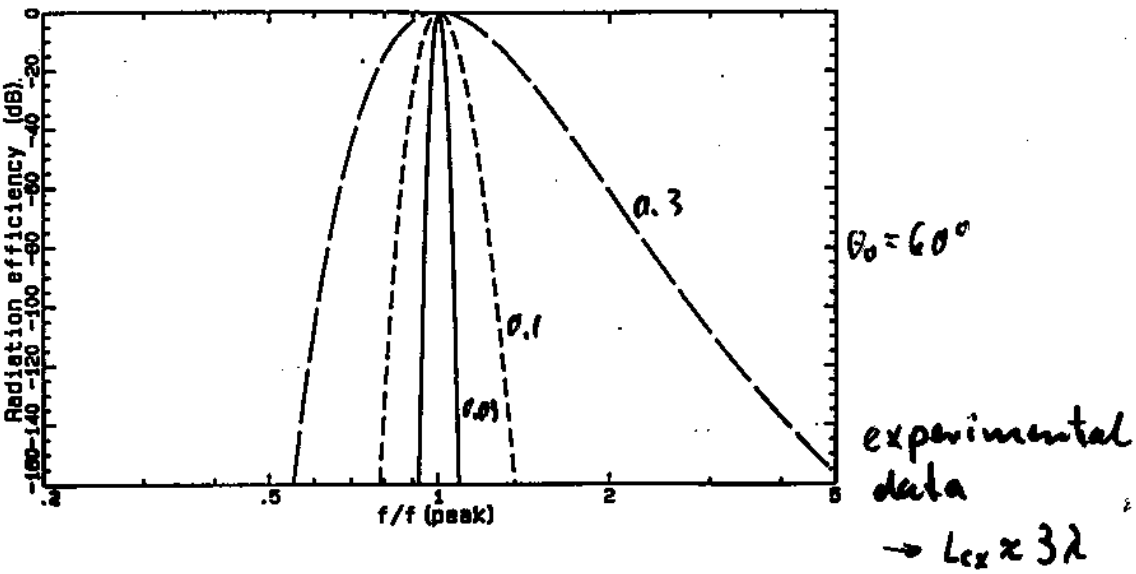


Figure 17: Normalized power-spectral density of broadband shock noise in flight for an emission angle of $\theta_0 = 60$ degrees. Flight Mach number $M_f = 0.6$, acoustic convection Mach number $U_p/a_0 = 1.8$. Curves are plotted for three normalized coherence length scales, $L_c/\lambda = 3.3$, 10, and 33. (The annotation reports the inverse of these values.)

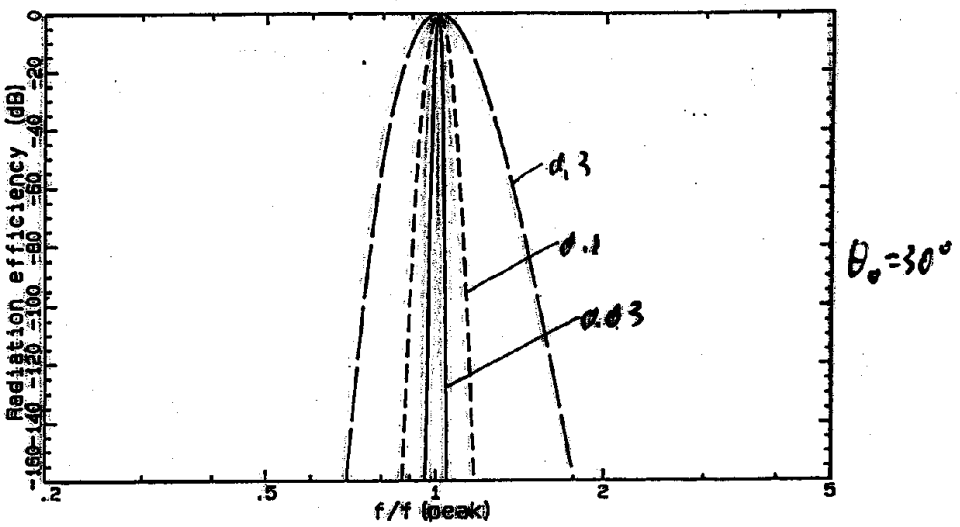


Figure 18: Normalized power-spectral density of broadband shock noise in flight for an emission angle of $\theta_0 = 30$ degrees. Flight Mach number $M_f = 0.6$, acoustic convection Mach number $U_p/a_0 = 1.8$. Curves are plotted for three normalized turbulent coherence length scales, $L_c/\lambda = 3.3$, 10, and 33. (The annotation reports the inverse of these values.)

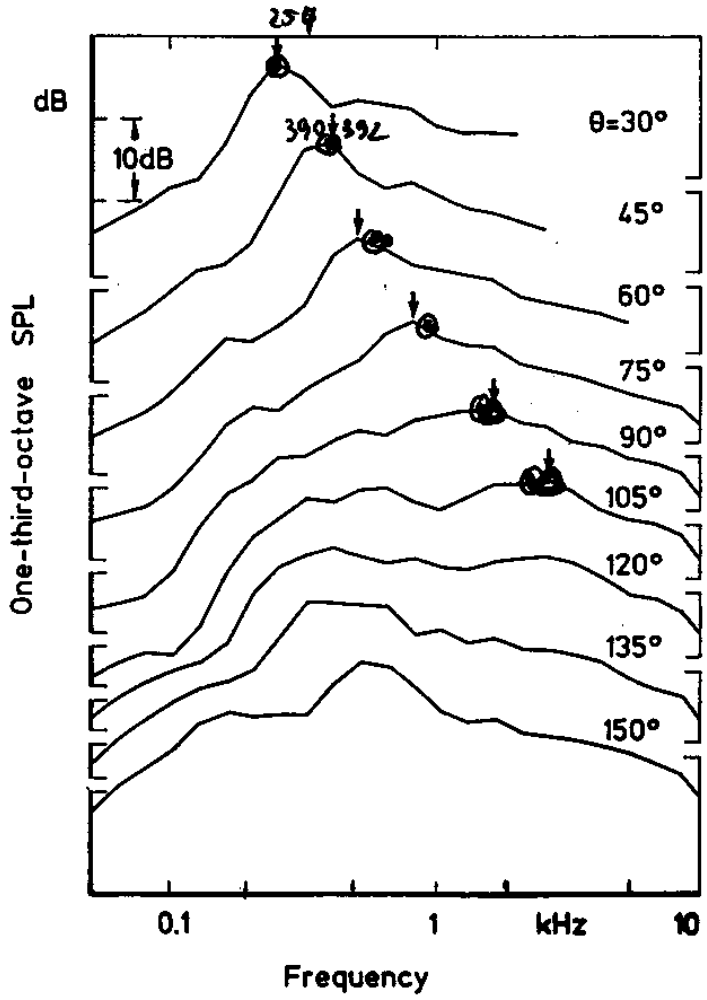


Figure 19: Frequency spectra containing broadband shock noise of a Tornado combat aircraft for a flight Mach number $M_f = 0.8$, a fully expanded jet Mach number of $M_j = 1.29$. The arrows indicate the peak frequencies in the spectra (from Böttcher and Michel (1994) [2].) The peak frequencies according to Eq. (29) for an acoustic convection Mach number $U_p/a_0 = 1.6$ are circled. Triangles indicate results for $U_p/a_0 = 1.8$.

CONCLUSIONS CONCERNING BROADBAND SHOCK NOISE

- Broadband shock noise can be derived by assuming a modulation of the source terms when they are convected through the shock cells.
- Broadband shock noise generation requires large normalized coherence length scales.
- Broadband shock noise is proportional to jet mixing noise.
- Broadband shock noise increases with the shock expansion cell strength.
- The width of the peak in the frequency spectrum is related to the axial coherence length scale.
- The passage of turbulence through shocks is not required for the appearance of broadband shock noise.

SCREECH, ONE-DIMENSIONAL JET MODEL

Screech noise is radiated when instability waves are generated at the nozzle lip in a phase locked loop through flow induced excitation.

If broadband shock noise is the source of excitation, the screech frequency is equal to the radiation frequency of broadband shock noise toward the nozzle. By assuming a normalized phase (convection) speed $(U_p - U_f)/(U_j - U_f) = 0.7$ (This may be valid for the one-dimensional flow model studied here. In the case of a radially extended jet, there are a number of possible spinning instability waves with different axial phase speeds.) we obtain

$$f_n = \frac{\alpha_n \Delta U}{2\pi} \frac{(0.7 + \frac{U_f}{\Delta U})(1 - M_f)}{1 + 0.7\frac{\Delta U}{a_0}}, \tag{31}$$

where $\Delta U = U_j - U_f$. For a flight Mach number $M_f = 0$ we obtain

$$f_{ns} = \frac{\alpha_n U_j}{2\pi} \frac{0.7}{1 + 0.7\frac{U_j}{a_0}}. \tag{32}$$

This equation is identical to the literature, e.g., Tam (1991) [26].

This screech frequency is plotted in Fig. 20 in comparison with experimental data of Tam, Seiner, and Yu (1986) [25]. The shock cell spacing (expressed in terms of α_n) was computed with the relation derived by Michalke (1992) [14].

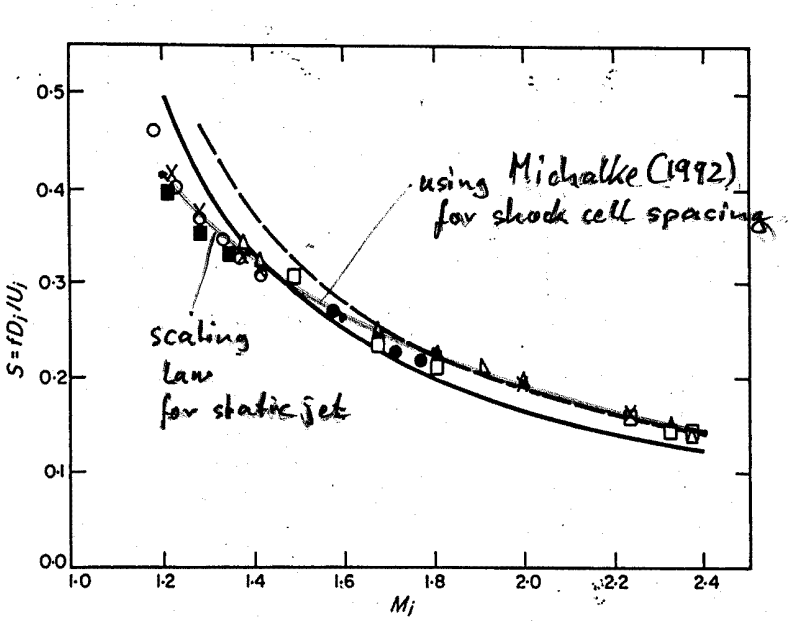


Figure 20: Normalized screech frequency as function of jet Mach number based on Eq. (32) and using the shock cell spacing of Michalke (1992) [14].

The screech frequency of Eq. (31) goes to zero when the flight Mach number approaches $M_f = 1$. This is shown in Fig. 21. The low frequencies at high subsonic Mach numbers can be of significance for the acoustic fatigue of structures in the nozzle region.

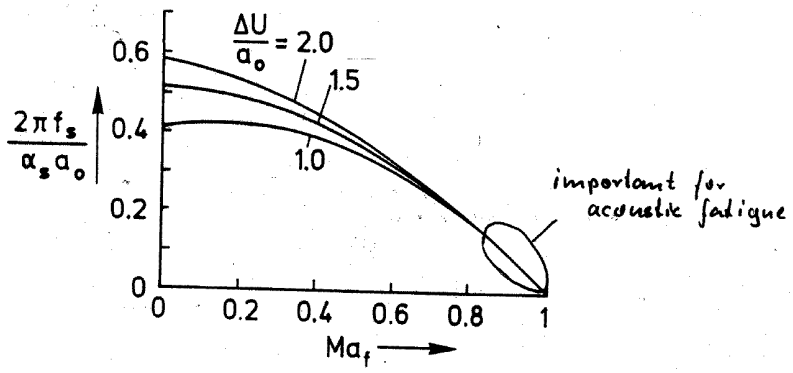


Figure 21: Normalized screech frequency as function of flight Mach number based on Eq. (31). Parameter is relative jet Mach number $(U_j - U_f)/a_0$.

FREQUENCY AS FUNCTION OF EMISSION ANGLE

The source frequency is considered in the nozzle fixed coordinate system in the wave model for the jet turbulence. Therefore, no Doppler frequency shift has to be applied for the far-field if the observer position is stationary rel. to the nozzle (static jet or wind-tunnel simulation). The observer frequency is Doppler shifted in a flyover situation which means that jet noise has a higher pitch in the forward arc.

The frequency spectra in the observer positions according to Eq. (6) would be similar to the source spectra W_{ss} if the interferences resulting from Eq. (18) were identical for all frequencies and all angles. This is not the case which explains that the frequency spectra change with emission angle. Part of the changes is due to refraction effects that are not included in the theory of this presentation.

RADIATION EFFICIENCY FOR HIGHLY SUPERSONIC JETS

Michalke (1977) [13] investigated the influence of spatial source coherence on the radiation of jet noise with the acoustic analogy. He included a model for the source intensity defined by a source length scale L_s. Fig. 22 is a result of this study and shows the acoustic power efficiency of a jet as function of the acoustic convection Mach number U_c/a_0. Parameter is the ratio of L_c/L_s between coherence and source length scales.

It can be seen that the power efficiency has a maximum near a convection Mach number slightly above $U_c/a_0 = 1.0$ and decreases for higher convection speeds. This may explain why the sound emission of a highly supersonic jet is proportional to $(U_j/a_0)^n$ with an exponent $n = 3$ rather than six or eight as seen for subsonic jets (compare Fig. 4).

That these results are true can be deduced from experimental data obtained with rocket jets. The sound radiation of a jet as function of axial position in a rocket jet is shown in Fig. 23. The position with peak radiation is located at about 20 nozzle diameters at the tip of the supersonic core where the jet speed is much lower than at the nozzle exit. The region with very high jet speeds directly behind the nozzle (10 times the ambient speed of sound) does not contribute significantly. The flow field is explained in Fig. 24.

The normalized frequency spectra of the sound radiated by rockets are shown in Fig. 25. The peak radiation frequency is independent of exhaust speed if it is normalized with the critical sound speed which should be very close to the jet speed in the peak radiation section of the jet and an effective jet diameter D_{eff} which is calculated from the sum of all fully expanded jet cross sections. It can be calculated from the specific thrust and the thrust (from Sutherland (1993) [24]). However, Fig. 25 is not a good example to support this proposed normalization because all spectra are from the same nozzle size.

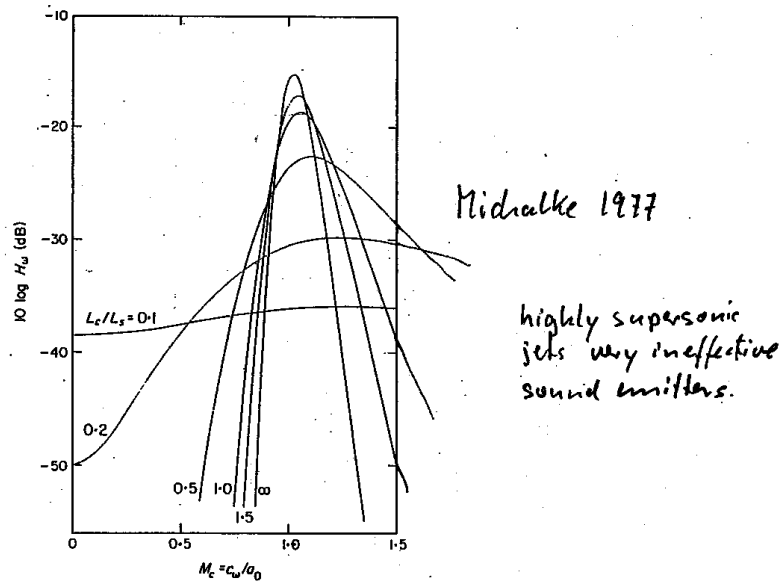


Figure 22: Power efficiency of the sound radiation of a jet as function of the acoustic convection Mach number U_c/a_0. (Michalke (1977) [13]).

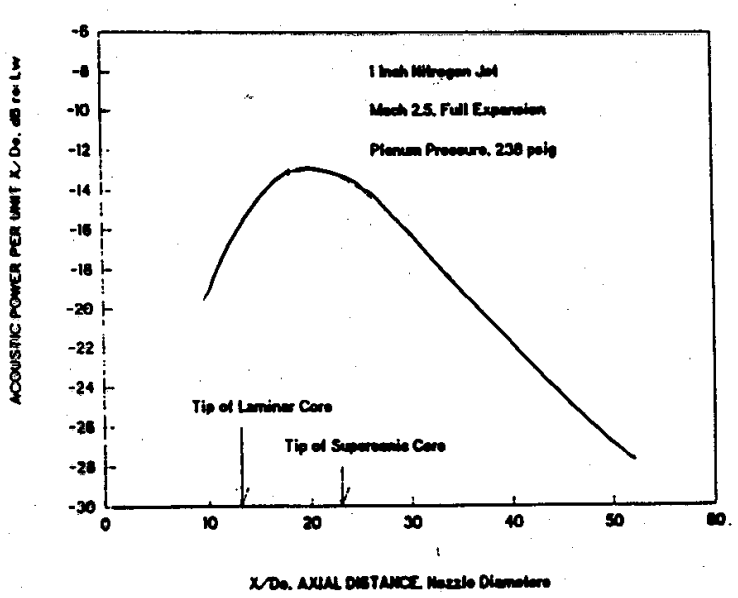


Figure 23: Sound power per unit jet length of a rocket jet as function of axial position (from Potter and Jones (1967) [21]).

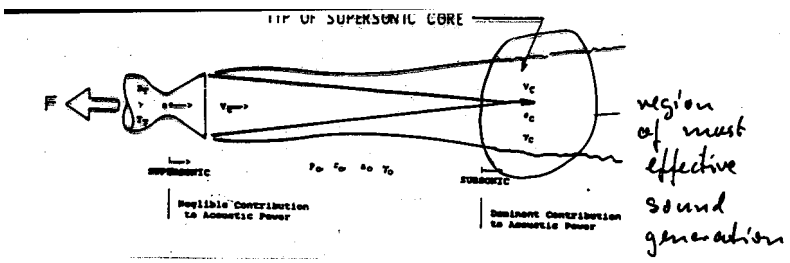


Figure 24: Illustration of sound generating region of a rocket jet (from Sutherland (1993) [24]).

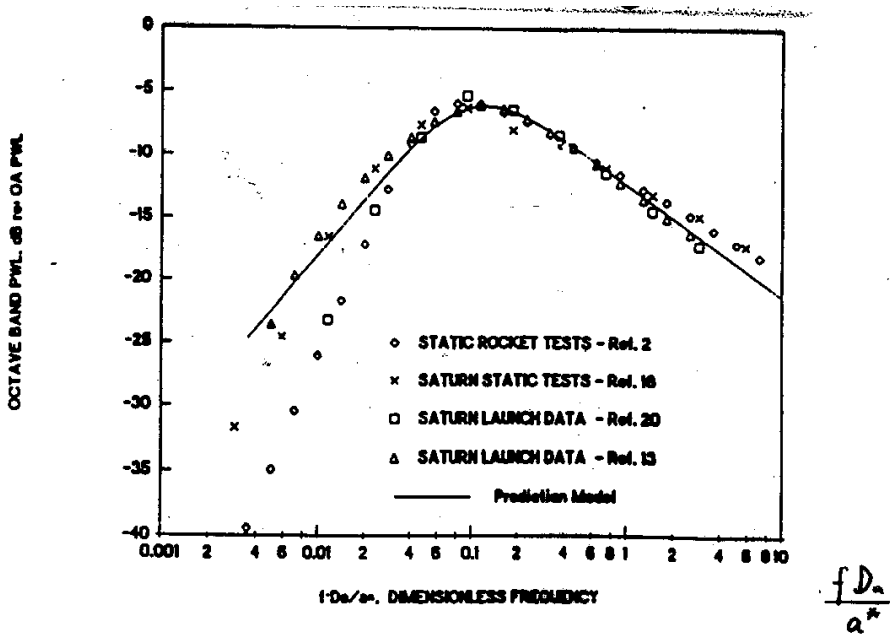


Figure 25: Relative octave band frequency spectra of the sound radiated by rockets (from Sutherland (1993) [24]).

AZIMUTHAL COMPONENTS OF JET NOISE

The assumption made so far was that the jet is concentrated on its jet axis. The consequence would be a completely axisymmetric sound field. In reality, the jet is radially extended, which gives rise to additional large scale structures in the form of helical motion.

It was shown by Michalke (1970,1972)[11, 12] how the flow field of a circular jet can be decomposed into azimuthal components and that the acoustic far field of the jet is likely be dominated by a few azimuthal components because the radiation efficiency of the higher order components decreases rapidly with increasing order.

This was experimentally demonstrated to be true in the far field for low frequencies by Maestrello (1977) [10]. Some results are shown for Strouhal numbers up to St= 0.375 in Fig. 26. The coherence between two microphones with identical emission angle of 90 degrees is plotted as a function of azimuthal separation angle $\Delta\phi$. The functions of $\Delta\phi$ can be decomposed into azimuthal components as shown in Fig. 27.

Similar measurements close to a model jet and an engine jet were reported by Fuchs and Michel (1977) [5]. These results are shown in Fig. 28. Although the measurements were performed much closer to the jet as the ones by Maestrello, the sound field in the near field is still dominated by a few azimuthal components.

It was shown by Michalke (1972) [12] that each azimuthal component in the near and far field is directly related to the corresponding component in the source region.

Measurements of the azimuthal coherence between two microphone signals and between two hot-wire signals in the source region are shown in Fig. 29. A decomposition of the pressure field into azimuthal components as a function of Strouhal number is shown in Fig. 30. It can be concluded that even inside the jet, the pressure field is composed of only a few azimuthal components.

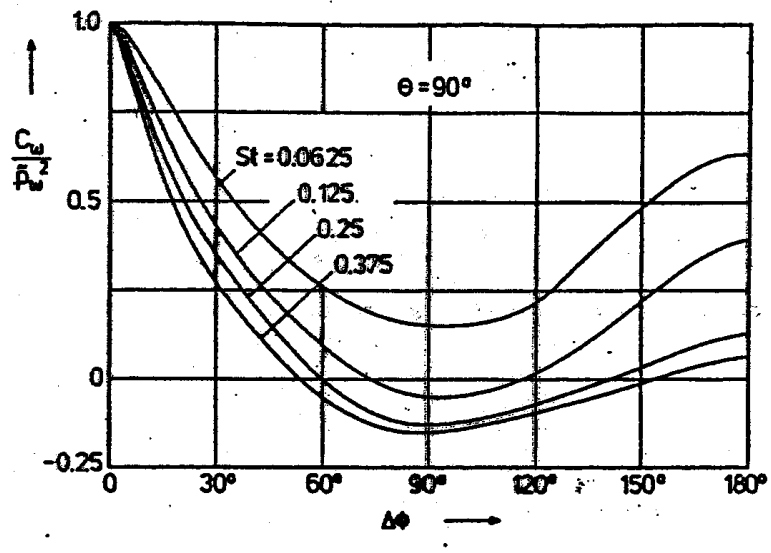


Figure 26: Coherence in azimuthal direction measured by Maestrello (1977) [10]

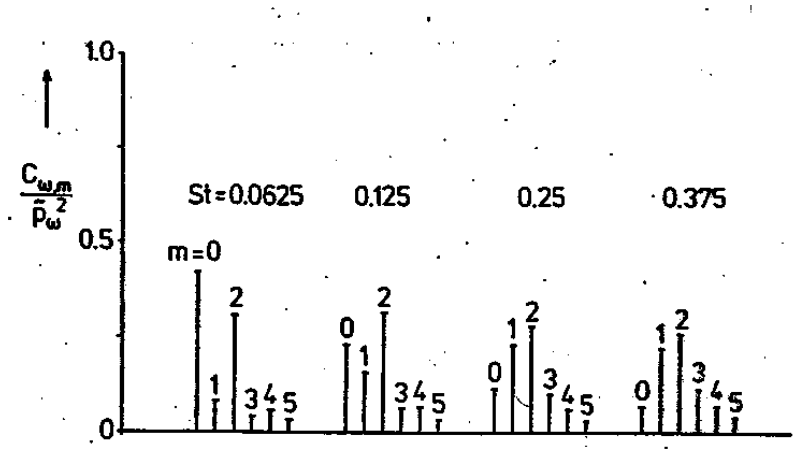


Figure 27: Decomposition of experimental data of Fig. 26 into azimuthal components. It can be seen that only a few azimuthal components dominate.

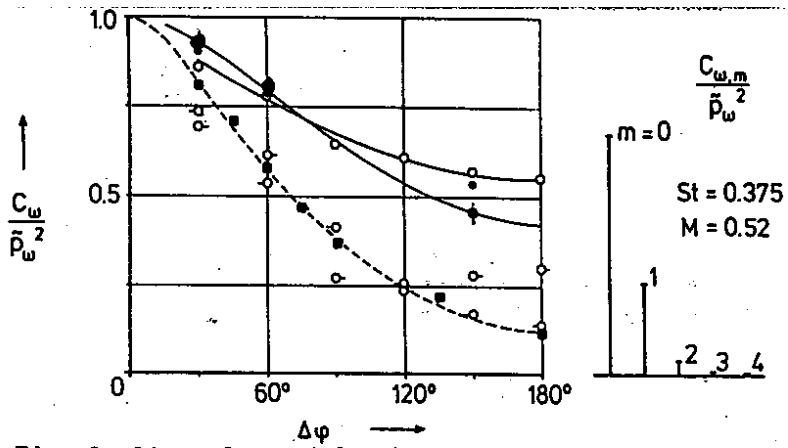


Fig. 8 Circumferential coherence and azimuthal constituents of near field pressure fluctuations.

Model jet: x = 3D, r = 1D, St = 0.375 --■-- M=0.30
Jet engine: x = 3D, r = 1.4D 0.375 —o— 0.35
0.375 —♦— 0.52
0.375 —●— 0.69
0.15 —o 0.35
0.7 o— 0.35

Figure 28: Coherence between circumferentially separated microphones located in an unheated model jet ($r = D$) and near a hot engine jet ($r = 1.4D$). The expansion into azimuthal components is shown for the engine data for a Strouhal number St= 0.375 and reveals a dominance of the axisymmetric ($m = 0$) and first helical ($m = 1$) components (from Fuchs and Michel (1977) [5]).

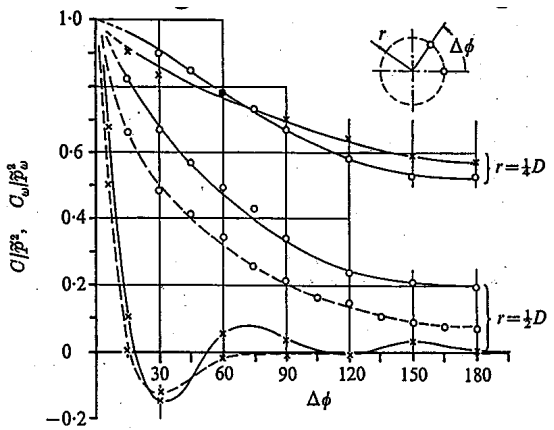


FIGURE 3. Azimuthal correlation coefficients in the plane $x = 3D$, at constant radii, for $St = 0{\cdot}45$, $\Delta f = 10$ Hz, $U_0 = 60\,\mathrm{m\,s^{-1}}$: ---, broad-band; ——, narrow-band analysis; ×, velocity correlation; ○, pressure correlation.

Figure 29: Coherence between two microphone signals and between two hot-wire signals in an unheated model jet as a function of azimuthal separation angle $\Delta\phi$ (from Michalke and Fuchs (1975) [15].

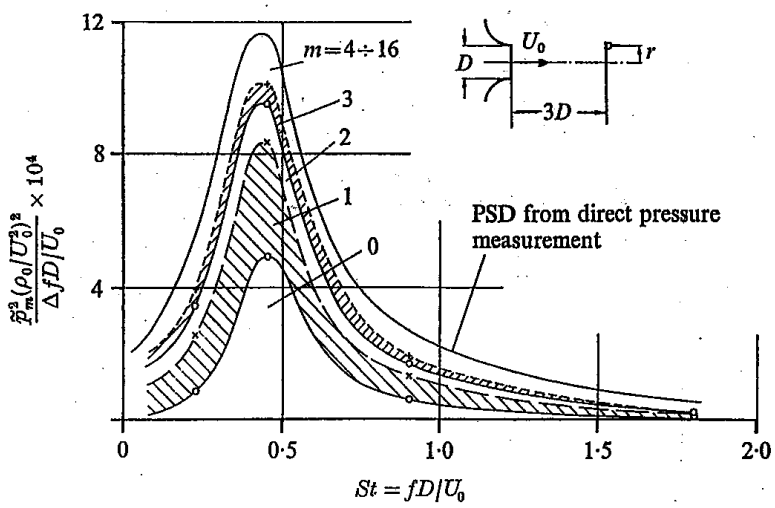


FIGURE 9. Synthesis of normalized PSD of jet pressure from $m = 16$ azimuthal constituents for $x = 3D$, $r = \frac{1}{2}D$.

Figure 30: Decomposition of the coherence as function of $\Delta\phi$ into azimuthal components. It can be seen that the first few azimuthal components suffice to describe the measured power-spectral density (from Michalke and Fuchs (1975) [15].

It may be concluded that

- helical modes in the source region of higher azimuthal order are inefficient sound radiators,
- small scale turbulence does not contribute substantially to the far-field noise.

AZIMUTHAL COMPONENTS AND DIRECTIVITY

Michalke (1972) [12] has shown that each azimuthal component has a unique directivity.

- Only the axisymmetric component radiates in the downstream and upstream directions.
- The higher order components radiate to the side.
- The "refraction dimple" of jet noise may partly be caused by the vanishing contribution of the higher order azimuthal components for emission angles θ_0 approaching 0 or 180 degrees.
- The radiation efficiency of the higher order components decreases rapidly with increasing order number.

CONCLUSIONS

1. The acoustic analogy is valid.
2. The acoustic analogy is a very powerful tool to derive scaling laws for jet mixing noise.
3. The use of a nozzle-fixed coordinate system is mandatory.
4. A wave model for the turbulent fluctuations must be used.
5. The far-field noise of a jet is dominated by its large-scale fluid motion.
6. Large coherence length scales are required to explain broadband shock noise and screech.
7. Large coherence length scales are also required for subsonic jets to explain the amplification of jet mixing noise in the rear arc.

References

[1] J. Atvars, L. K. Schubert, E. Grande, and H. S. Ribner. Refraction of sound by jet flow or jet temperature. TN 109 (1965); NASA CR-494 (1966), University of Toronto, Institute for Aerospace Studies, 1965.

[2] J. Böttcher and U. Michel. Noise characteristics of jet aircraft at high speed/low altitude flight. *Z. Flugwiss. Weltraumforsch.*, 18:303–310, 1994.

[3] J. E. Ffowcs Williams. The noise from turbulence convected at high speed. *Phil. Trans. Roy. Soc.*, A 225:469–503, 1963.

[4] J. E. Ffowcs Williams and A. J. Kempton. The noise from the large-scale structure of a jet. *J. Fluid Mech.*, 84:673–694, 1978.

[5] H. V. Fuchs and U. Michel. Experimental evidence of turbulent source coherence effecting jet noise. AIAA Paper 77-1348, 1977.

[6] M. Harper-Bourne and M. J. Fisher. The noise from shock waves in supersonic jets. In *Noise Mechanism*, 1973. AGARD-CP-131, Proceedings of an AGARD Conference.

[7] M. J. Lighthill. On sound generated aerodynamically. I. General theory. *Proc. Roy. Soc. London*, A 211:564–587, 1952.

[8] M. J. Lighthill. On sound generated aerodynamically. II. Turbulence as a source of sound. *Proc. Roy. Soc. London*, A 222:1–32, 1954.

[9] P. A. Lush and R. H. Burrin. The generation and radiation of supersonic jet noise, Volume V, An experimental investigation of jet noise variation with velocity and temperature. AFAPL-TR-72-53-Volume V, Air Force Aero Propulsion Laboratory, 1972.

[10] L. Maestrello. Statistical properties of the sound and source fields of an axisymmetric jet. AIAA Paper 77-1267, 1977. AIAA 4th Aeroacoustics Conference.

[11] A. Michalke. A wave model for sound generation in circular jets. Deutsche Luft- und Raumfahrt, DLR FB 70-57, 1970.

[12] A. Michalke. An expansion scheme for the noise from circular jets. *Z. Flugwiss.*, 20:229–237, 1972.

[13] A. Michalke. On the effect of spatial source coherence on the radiation of jet noise. *J. Sound Vib.*, 55:377–394, 1977.

[14] A. Michalke. On the effect of external flow and shear-layer thickness on the expansion cells of under-expanded supersonic circular jets. *European Journal of Mechanics, B/Fluids*, 11:363–382, 1992.

[15] A. Michalke and H. V. Fuchs. On turbulence and noise of an axisymmetric shear flow. *J. Fluid Mech.*, 70:179–205, 1975.

[16] A. Michalke and U. Michel. Prediction of jet-noise in flight from static tests. *J. Sound Vib.*, 67:341–367, 1979.

[17] U. Michel. Broadband shock noise: Theory vis-a-vis experimental results. In *First Joint CEAS/-AIAA Aeroacoustics Conference (16th AIAA Aeroacoustics Conference)*, pages 545 – 554, 1995. CEAS/AIAA Paper 95-071, DGLR-Bericht 95-01.

[18] U. Michel and A. Michalke. Prediction of flyover jet noise spectra. AIAA Paper 81-2025, 1981. AIAA 7th Aeroacoustics Conference.

[19] U. Michel and A. Michalke. Prediction of flyover jet noise spectra from static tests. NASA Technical Memorandum 83219, 1981.

[20] C. L. Morfey. Amplification of aerodynamic noise by convected flow inhomogeneities. *J. Sound Vib.*, 31:391–397, 1973.

[21] R. C. Potter and J. H. Jones. An experiment to locate the acoustic sources in a high speed jet exhaust stream. *J. Acoust. Soc. Am.*, 42:1214(A), 1967.

[22] H. S. Ribner. New theory of jet-noise generation, directionality, and spectra. *J. Acoust. Soc. Am.*, 31:245–246, 1959.

[23] M. J. T. Smith. *Aircraft Noise*. Cambridge Aerospace Series. Cambridge University Press, 1989.

[24] L. C. Sutherland. Progress and problems in rocket noise prediction for ground facilities. AIAA Paper 93-4383, 1993. AIAA 15th Aeroacoustics Conference.

[25] C. K. W. Tam. Proposed relationship between broadband shock associated noise and screech tones. *J. Sound Vib.*, 110:309–321, 1987.

[26] C. K. W. Tam. Jet noise generated by large-scale coherent motion. In *Aeroacoustics of Flight Vehicles: Theory and Practice, Volume 1: Noise Sources, NASA Reference Publication 1258, Vol. 1*, pages 311–490. NASA, 1991.

[27] C. K. W. Tam and D. E. Burton. Sound generated by instability waves of supersonic flows, Part 1: Two dimensional mixing layers. Part 2: Axisymmetric jets. *J. Fluid Mech.*, 138:249–271 and 273–295, 1984.

NASA/CP—2001-211152

Fundamental problems in aeroacoustics

Christopher L Morfey

Institute of Sound and Vibration Research
University of Southampton
Southampton SO17 1BJ, UK
clm@isvr.soton.ac.uk

University of Southampton

ISVR

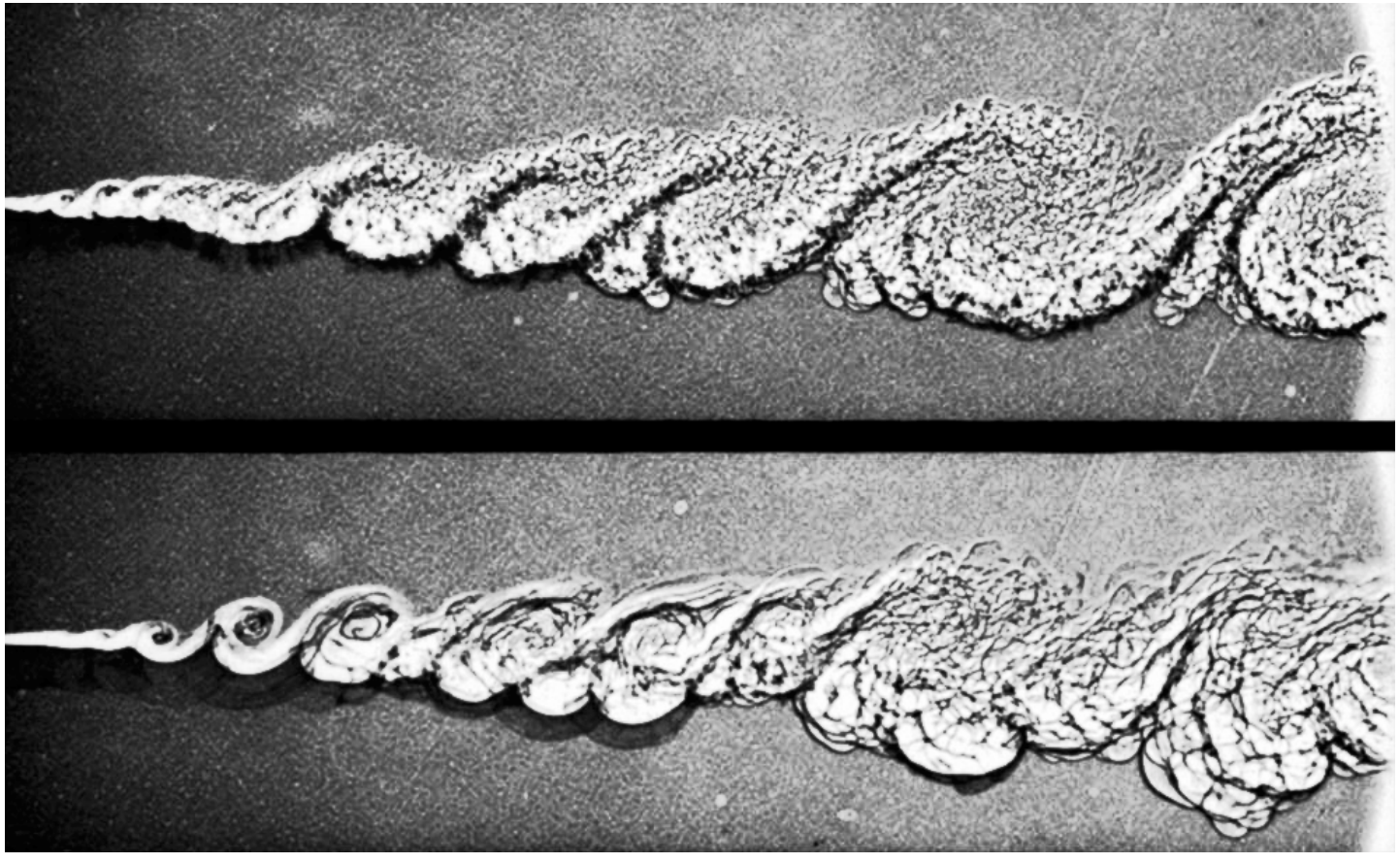
Dissipation noise from unbounded flows (Kambe 1984)

- Monopole component of radiated pressure:

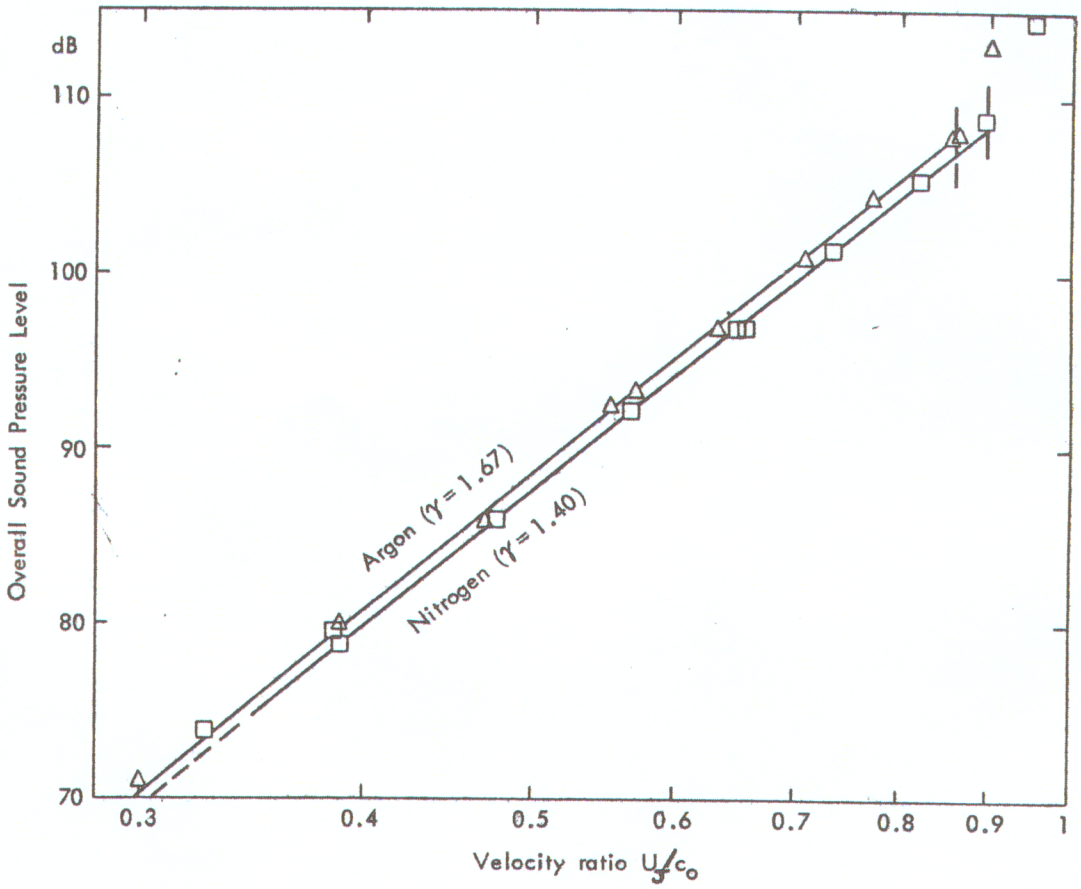
$$4\pi R p_{\mathrm{mono}} \approx \left(\gamma - \frac{5}{3}\right) c_0^{-2} \frac{\mathrm{d}}{\mathrm{d}t}\left(\dot{E}_{\mathrm{diss}}\right)$$

where $$\left(\gamma - \frac{5}{3}\right) = \underbrace{(\gamma - 1)}_{\text{entropy production}} + \underbrace{\left(-\tfrac{2}{3}\right)}_{\text{direct Reynolds stresses}}$$

Two-dimensional mixing layer (Brown & Roshko 1974)



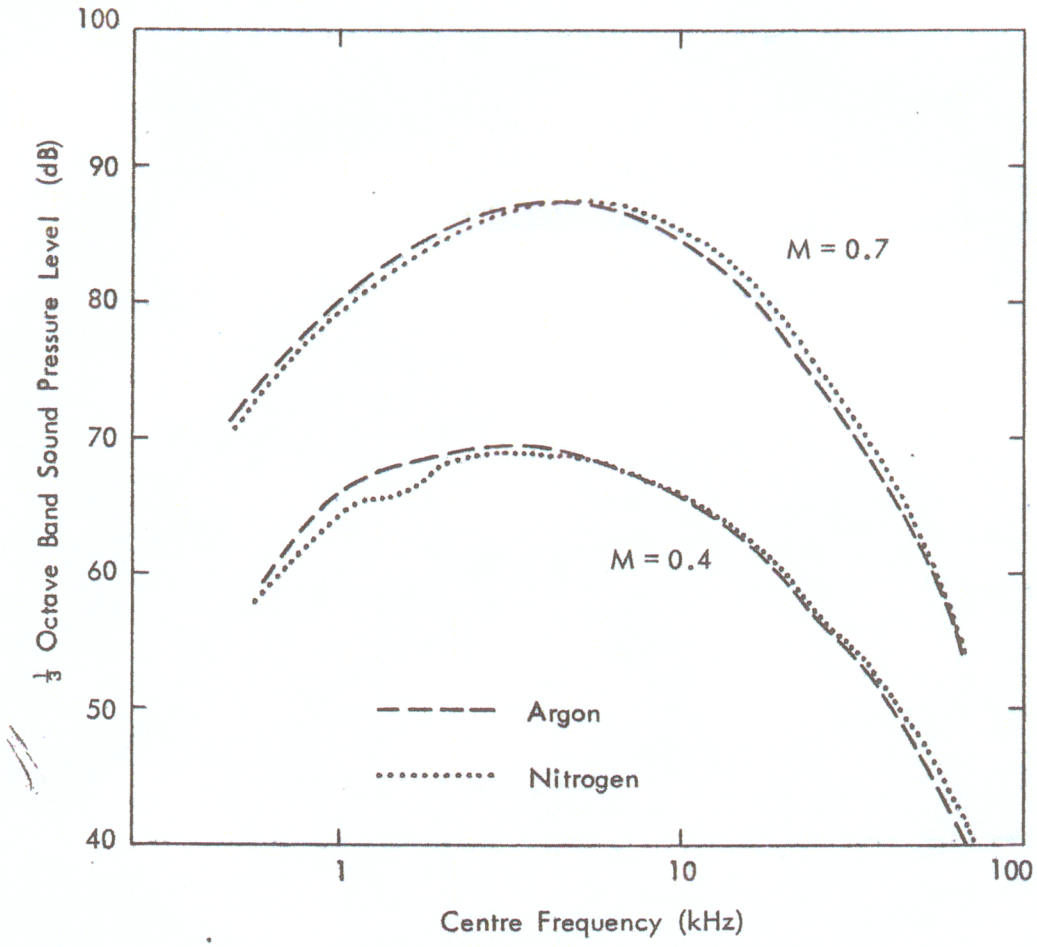
Jet noise measured in argon and nitrogen (Grosche *et al* 1975)



Reference:

F R Grosche, J Jones and G A Wilhold 1975 DFVLR-AVA Bericht No. 061-7217-31, DFVLR Göttingen

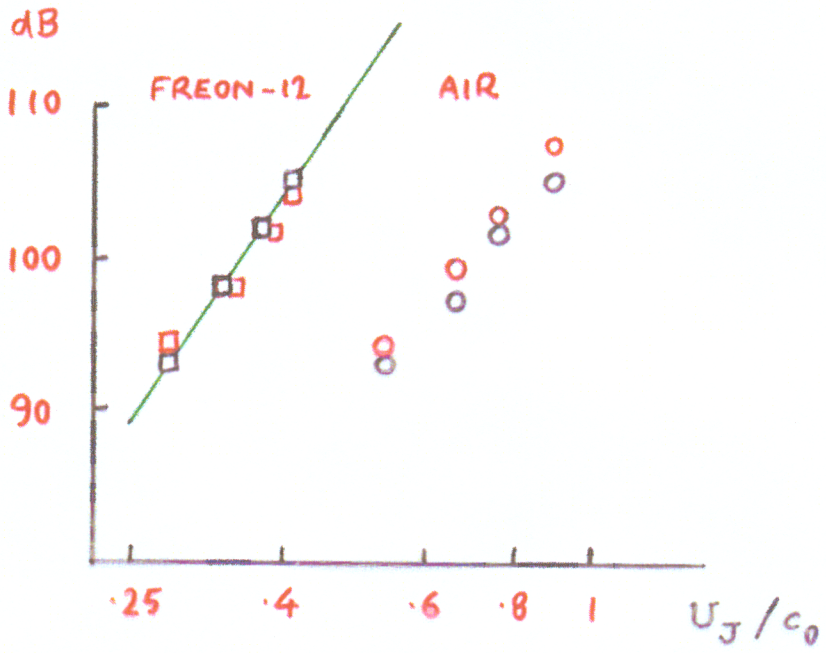
Comparison of jet noise spectra measured in two gases



Reference:
F R Grosche, J Jones and G A Wilhold 1975 DFVLR-AVA Bericht No. 061-7217-31, DFVLR Göttingen

Effect of jet density on mixing noise at low speed

Overall intensity at 90° to axis ($R = 16d$)



□ ○ Measurements by Lassiter and Hubbard (1952) *NACA TN* 2757

□ ○ Predicted levels based on hot air jet data

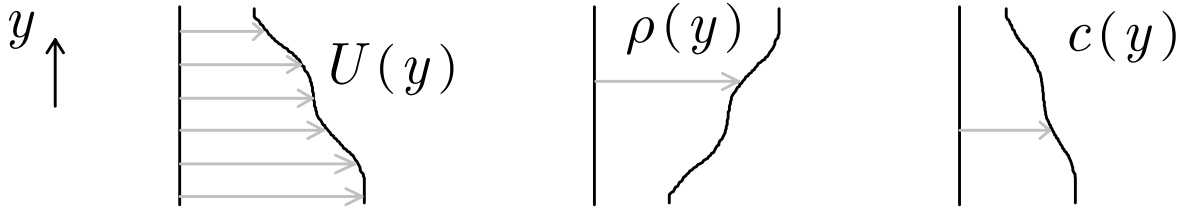
Equivalent sources in a high-speed shear flow (Lilley 1974; Goldstein 1976,1984)

- Euler equations for inviscid flow:

$$\nabla \cdot \mathbf{u} = q - \frac{1}{\rho}\frac{D\rho}{Dt}, \quad \frac{D\mathbf{u}}{Dt} = \mathbf{f} - \frac{1}{\rho}\nabla P, \quad \frac{Ds}{Dt} = 0.$$

- Linearised about a parallel shear flow, these provide a wave equation for sound propagation:

$$\mathrm{L}(p) = 0 \quad (\text{when } q = 0 \text{ and } \mathbf{f} = 0)$$



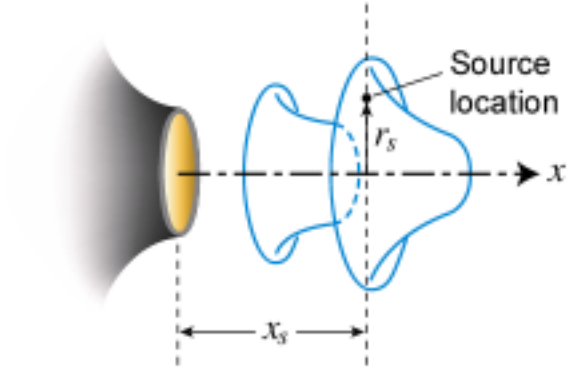
Source term in the Lilley–Goldstein analogy

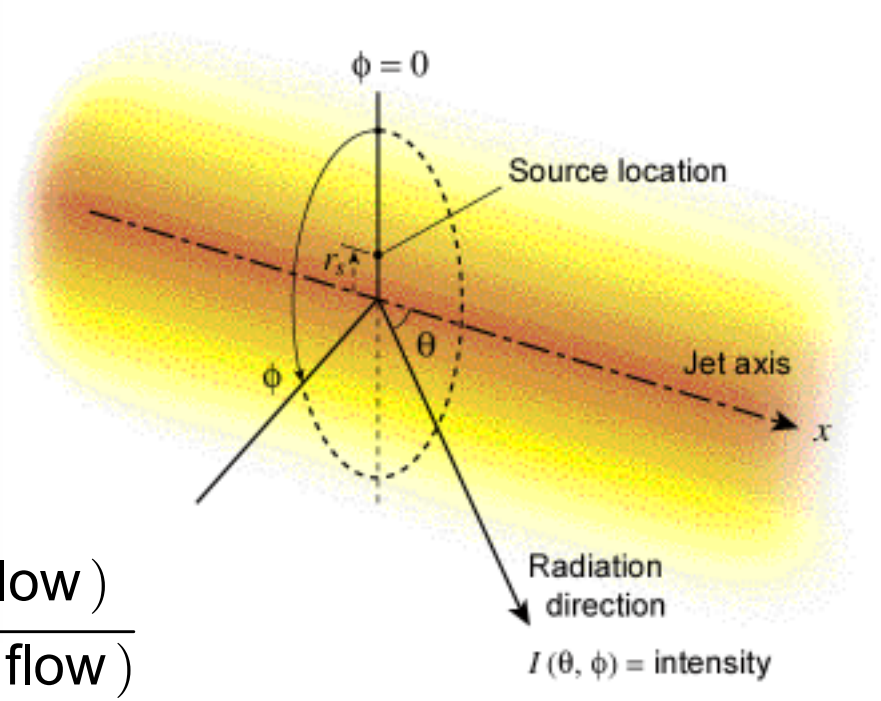
$$Q = \frac{\bar{\mathrm{D}}^2 q}{\mathrm{D}t^2} - \frac{\bar{\mathrm{D}}}{\mathrm{D}t}(\nabla \cdot \mathbf{f}) + 2\frac{\partial}{\partial x}(\mathbf{f} \cdot \nabla U)$$

- Nonlinear source term, due to second-order interactions, is equivalent to a force field per unit mass applied to the linearised equations:

$$f_j \approx -\frac{\partial}{\partial x_i}\left(u_i' u_j'\right) - \left(\frac{1}{\rho}\right)' \frac{\partial p}{\partial x_j}$$

Application of the Lilley–Goldstein analogy to sound radiation from a turbulent jet





$$F = \frac{\langle I(\theta,\ \phi)\rangle_\phi \quad (\text{with flow})}{\langle I(\theta,\ \phi)\rangle_\phi\,(\text{without flow})}$$

University of Southampton

ISVR

Flow factor trends in a hot jet: Monopole and dipole source models

Case	Source type	Physical interpretation	Source term $Q(\mathbf{x},t)$[a]	θ_0 dependence of flow factor	Asymptotic Ω, M dependence[b]	Coefficient[c]	Dominant mode
1A	Monopole	Point volume displacement	$\frac{\bar{D}^3}{Dt^3}[A(t)\delta(\mathbf{x}-\mathbf{x}_s)]$	–	–	1	$m=0$
2A	Dipole	Point volume displacement *r*-dipole (Tester & Morfey 1976)	$-\frac{\bar{D}^3}{Dt^3}[A_r(t)\delta_r(\mathbf{x}-\mathbf{x}_s)]$	–	–	$\left(\frac{\rho_s}{\rho_m}\right)^2 D_s^4$	$m=\pm1$
2B	Dipole	Point radial force (Goldstein 1976)	$-\frac{\bar{D}}{Dt}[B_r(t)\delta_r(\mathbf{x}-\mathbf{x}_s)]$ $+2\frac{\partial}{\partial x}\left[B_r(t)\frac{\mathrm{d}U}{\mathrm{d}r}\delta(\mathbf{x}-\mathbf{x}_s)\right]$	–	–	$\left(\frac{\rho_s}{\rho_m}\right)^2$	$m=\pm1$

a The radial-dipole singularity δ_r is defined by $\delta_r(\mathbf{x}) = \frac{1}{r}\frac{\partial}{\partial r}[r\delta(\mathbf{x})]$

b In the limits $M \to 0, \quad k_0 r_0 \to 0$

c In the plug flow limit $\delta / r_0 \to 0$

Flow factor trends in a hot jet: Volume displacement dipole and quadrupole

Case	Source type	Physical interpretation	Source term $Q(\mathbf{x},t)$[a]	θ_0 dependence of flow factor	Asymptotic Ω, M dependence	Coefficient	Dominant mode
2A	Dipole	Point volume displacement *r*-dipole	$-\frac{\bar{D}^3}{Dt^3}[A_r(t)\delta_r(\mathbf{x}-\mathbf{x}_s)]$	–	–	$\left(\frac{\rho_s}{\rho_m}\right)^2 D_s^4$	$m=\pm1$
3A	Quadrupole	Point volume displacement *rr*-quadrupole	$\frac{\bar{D}^3}{Dt^3}[A_{rr}(t)\delta_{rr}(\mathbf{x}-\mathbf{x}_s)]$	$\frac{1}{\sin^2\theta_0}$	$\frac{1}{M^2\Omega^2}$	$\frac{4}{3}\left[\frac{r_0}{\rho_m}\left(\frac{\mathrm{d}\bar{\rho}}{\mathrm{d}r}\right)_s\right]^2$	$m=\pm1$

a The radial-quadrupole singularity δ_{rr} is defined by $\delta_{rr}(\mathbf{x}) = \frac{1}{r}\frac{\partial^2}{\partial r^2}[r\delta(\mathbf{x})]$

Flow factor trends in a hot jet: Point force models (Goldstein 1976)

Case	Source Type	Physical interpretation	Source term $Q(\mathbf{x},t)$	θ_0 dependence of flow factor	Asymptotic Ω, M dependence	Coefficient	Dominant mode
2B	Dipole	Point radial force	$-\frac{\bar{D}}{Dt}\left[B_r(t)\delta_r(\mathbf{x}-\mathbf{x}_s)\right]$ $+2\frac{\partial}{\partial x}\left[B_r(t)\frac{\mathrm{d}U}{\mathrm{d}r}\delta(\mathbf{x}-\mathbf{x}_s)\right]$	–	–	$\left(\frac{\rho_s}{\rho_m}\right)^2$	$m=\pm 1$
3B	Quadrupole	Point radial force distribution of r-dipole type	$\frac{\bar{D}}{Dt}\left[Br_r(t)\delta_{rr}(\mathbf{x}-\mathbf{x}_s)\right]$ $-2\frac{\partial}{\partial x}\left[B_{rr}(t)\frac{\mathrm{d}U}{\mathrm{d}r}\delta_r(\mathbf{x}-\mathbf{x}_s)\right]$	$\frac{1}{\sin^2\theta_0}$	$\frac{1}{M^2\Omega^2}$	$\frac{4}{3}\left[\frac{r_0}{\rho_m}\left(\frac{\mathrm{d}\bar{\rho}}{\mathrm{d}r}\right)_s\right]^2 D_s^{-4}$	$m=\pm 1$

Flow factor trends in an isothermal jet: Dipole models

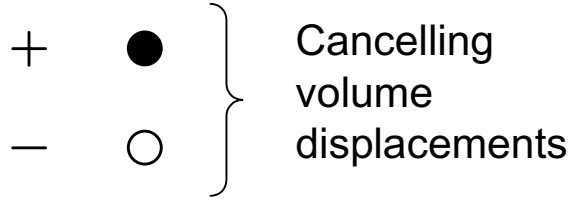
Case	Source type	Physical interpretation	Source term $Q(\mathbf{x},t)$	θ_0 dependence of flow factor	Asymptotic Ω, M dependence	Coefficient	Dominant mode
2A	Dipole	Point volume displacement *r*-dipole	$-\frac{\bar{D}^3}{Dt^3}[A_r(t)\delta_r(\mathbf{x}-\mathbf{x}_s)]$	–	–	D_s^4	$m=\pm1$
2B	Dipole	Point radial force	$-\frac{\bar{D}}{Dt}[B_r(t)\delta_r(\mathbf{x}-\mathbf{x}_s)]$ $+2\frac{\partial}{\partial x}\left[B_r(t)\frac{\mathrm{d}U}{\mathrm{d}r}\delta(\mathbf{x}-\mathbf{x}_s)\right]$	–	–	1	$m=\pm1$
2C	Dipole	Point *r*-dipole, temporal order $\nu\neq3$	$-\frac{\bar{D}^\nu}{Dt^\nu}[C_r(t)\delta_r(\mathbf{x}-\mathbf{x}_s)]$	$\frac{\cos^2\theta_0}{\sin^2\theta_0}$	$\frac{1}{\Omega^2}$	$(\nu-3)^2\left(\phi_s'\right)^2 D_s^{2\nu-8}$	$m=0$

Flow factor trends in an isothermal jet: Quadrupole models

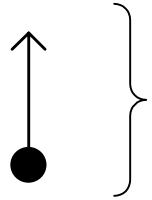
Case	Source type	Physical interpretation	Source term $Q(\mathbf{x},t)$	θ_0 dependence of flow factor	Asymptotic Ω, M dependence	Coefficient	Dominant mode
3A	Quadrupole	Point volume displacement *rr*-quadrupole	$\frac{\bar{D}^3}{Dt^3}[A_{rr}(t)\delta_{rr}(\mathbf{x}-\mathbf{x}_s)]$	$\frac{\cos^2\theta_0}{\sin^2\theta_0}$	$\frac{1}{\Omega^2}$	$\frac{16}{3}(\phi_s')^2 D_s^2$	$m=\pm1$
3B	Quadrupole	Point radial force distribution of *r*-dipole type	(as 3B earlier)	$\frac{\cos^2\theta_0}{\sin^2\theta_0}$	$\frac{1}{\Omega^2}$	$\frac{16}{3}\left(\frac{1-\phi_s}{\phi_s}\right)^2\left(\frac{\delta}{r_0}\right)^2 D_s^{-4}$ (no gradient term)	$m=\pm1$
3C	Quadrupole	Point *rr*-quadrupole, temporal order $\nu \neq 3$	$\frac{\bar{D}^\nu}{Dt^\nu}[C_{rr}(t)\delta_{rr}(\mathbf{x}-\mathbf{x}_s)]$	$\frac{\cos^2\theta_0}{\sin^4\theta_0}$	$\frac{1}{M^2\Omega^4}$	$\frac{8}{3}(\nu-3)^2(\phi_s'')^2 D_s^{2\nu-8}$	$m=0$

Conclusions from Lilley–Goldstein models for jet noise radiation

- The mean flow field can influence the radiation even in the low Mach number limit $(M \to 0)$
- The influence persists at low Strouhal numbers $(\Omega \to 0)$ and for thin shear layers $(\delta / \lambda \to 0)$
- Two alternative radial dipole models both predict $F \approx \left(\frac{\rho_{\mathrm{s}}}{\rho_{\mathrm{m}}} \right)^2$



Cancelling volume displacements



Point radial force

MODEL A

MODEL B

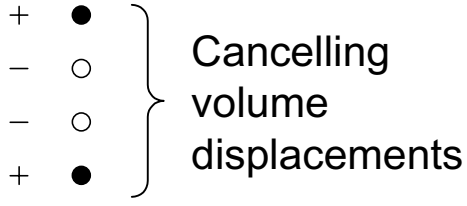
University of Southampton

Conclusions from Lilley–Goldstein models for jet noise radiation

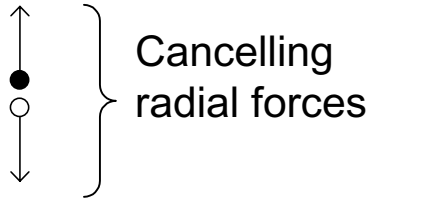
- Two alternative radial-radial quadrupole models both predict

$$F \sim \left(\frac{\mathrm{d}\overline{\rho}}{\mathrm{d}r}\right)^2 \cdot \frac{1}{M^2} \cdot \frac{1}{\Omega^2}$$

for sources in a mean density gradient



MODEL A (Tester/Morfey)



MODEL B (Goldstein/Balsa)

- The two models give **different** results for sources in a mean velocity gradient

Conclusions from Lilley–Goldstein models for jet noise radiation

- Model A for quadrupole sources corresponds to

$$Q = \frac{\bar{\mathrm{D}}^3}{\mathrm{D}t^3}\frac{\partial^2 q_{ij}}{\partial x_i \partial x_j} \qquad \left(\frac{\bar{\mathrm{D}}}{\mathrm{D}t} \equiv \frac{\partial}{\partial t} + U\frac{\partial}{\partial x}\right)$$

- Altering the temporal order from 3 leads to radically different predictions for sources in a mean velocity gradient:

$$F \sim \left(\frac{\mathrm{d}^2 U}{\mathrm{d}r^2}\right)^2 \frac{(\nu-3)^2}{M^2}\cdot\frac{1}{\Omega^4} \qquad \text{for } Q = \frac{\bar{\mathrm{D}}^\nu}{\mathrm{D}t^\nu}\frac{\partial^2 q_{ij}}{\partial x_i \partial x_j}$$

- This would lead to $I \sim U^6$ for an ambient-density turbulent jet

C. Morfey References

1. L W Lassiter and H H Hubbard 1952 NACA TN 2757 Experimental studies of noise from subsonic jets in still air.

2. G L Brown and A Roshko 1974 Journal of Fluid Mechanics 64, 775-816. On density effects and large structure in turbulent mixing layers.

3. F R Grosche, J Jones and G A Wilhold 1975 DFVLR-AVA Bericht Nr; 061-7217-31, DFVLR Göttingen.

4. T Kambe 1984 Journal of Sound and Vibration 95, 351-360. Influence of viscosity on aerodynamic sound emission in free space.

Mr. Harper-Bourne gave examples of hot wire measurements in the mixing region of a jet showing the peak in the turbulent intensity (spectral intensity for a Strouhal number of unity) in the center of the mixing region. He showed a comparison between the velocity covariance and that of the velocity squared, where the latter represented the contribution to noise generation. The characteristic longitudinal and lateral length scales for the velocity squared covariance varied greatly from that of the velocity alone, and also were a function of frequency. Harper-Bourne showed how the convective amplification, in Lighthill's acoustic analogy, can vary with the model used for the covariance. He showed the approximate self-similarity, except close to the jet boundary, in the directivity for a low Strouhal number over a range of subsonic Mach numbers, and a typical two-source model of a jet with axial distance over a range of frequencies. He concluded by showing a comparison between jet noise measurements on a convergent–divergent nozzle at $M_j = 1.5$ and $T_j = 875K$ with a line-source model in both the near and far fields. His conclusions were summarized as follows:

- Lighthill's classical theory provides a semi-empirical basis for jet near-field noise prediction for acoustic fatigue research.
- Rationale for the adoption of fixed frame analysis of jet noise successfully developed around relevant space-time turbulence measurements.
- Method treats Mach wave radiation as a limiting case of jet mixing noise.
- Line source model, utilizing polar correlation source location data, provides good agreement with measured near-field spectra for distances greater than one diameter from the nozzle exit.

Dr. Elias presented information on Galbrun's equation for wave propagation in the presence of an inhomogeneous flow. From the Lagrangian of the equation the acoustic intensity and the energy could be found. The equation had a structure related to that of the third-order convected wave equation.

Dr. Khavaran presented a computational methodology, based on Lilley's third-order wave equation, for the prediction of jet noise from a number of complex nozzle geometry's, and a comparison with experimental data. The model involved the calculation of the self-noise and shear-noise components and the values of the corresponding two-point space-retarded time covariances allowing for the Doppler effect corrections arising from the moving frame convection. The cases tested included a splitter plate nozzle, a twin core-fan stream nozzle, and nozzles with tabs and chevrons. This was a very challenging study and included the effects of flow-acoustic interaction at high frequencies.

Dr. Mengle presented experimental data concerning a mixer-nozzle with different nozzle lengths. The results showed that the low frequency noise was unaffected by mixer length. The source of low frequency was found to come from far downstream. It was a function of the total rate of mass flow. The lowest noise at higher frequencies was found from a nozzle of intermediate length. Similar results were obtained for both the static and flight experiments. The results were explained in terms of the changes in the axial and transverse components of the turbulent intensity observed for the different lengths of the mixer nozzle. The results were considered to be very geometry dependent.

In the discussion that followed the formal presentations there was further discussion on the usefulness of the Lighthill acoustic analogy. There appeared some confusion of the role played by each side of the equation. The left-hand-side is the propagation part of the equation with an observer placed outside the flow. In this case the density is the acoustic density fluctuation associated with sound waves propagating out from the flow. The right-hand-side is the distribution of the equivalent acoustic sources per unit volume in the domain occupied by the flow. The acoustic density at the observer is then given as the Green's function weighted retarded time integral taken over all the sources in the volume occupied by these equivalent sources. For an observer in the acoustic far field the source function reduces to $(1/c_\infty^2)$ times the second time derivative of T_{xx}, which is the component of T_{ij} in the direction from source to observer. When the field point is inside the domain of the sources both sides of the equation now combine to represent the generation problem. If we consider, by way of example, the case of a low flow Mach number, we find the terms T_{xx} are acoustically compact. We note that all variables are flow variables and not acoustic variables. The complete equation reduces to the elliptic, Poisson equation for the fluctuating pressure in the flow. We see its solution for any field point, either inside or outside the flow, is the same as for Lighthill's equation, with the only difference that the time in the elliptic solution must be changed to the retarded time to allow for the finite speed of sound. Thus Lighthill's equivalent distribution of acoustic sources are physically the contributions to the turbulent pressure fluctuations in the flow. Of course the larger part of the turbulent pressure fluctuations inside the flow is non-radiative, since only a small fraction escapes as sound. But the radiating acoustic efficiency is not an arbitrary constant in Lighthill's acoustic analogy since it is governed by the asymptotic expression for the far-field radiation described above.

The other major topic related to non-linear acoustic radiation. As discussed above this is a problem, which can first be treated as a linear acoustic problem in Lighthill's acoustic analogy. Once it is recognized that the acoustic amplitude external to the flow is outside the range of linear acoustics, then the non-linear distortion leading to the generation of shock waves, can be obtained by integrating the non-linear wave equations along each ray. The shocks will ultimately become N-waves.

Noise Sources

Use of Turbulence Space-Time Correlations in Lighthill's Equation Analyzed with Respect to a Fixed Frame of Reference

Marcus Harper-Bourne
DERA Pyestock, England

AeroAcoustics Research Consortium, Jet Noise Workshop
November 2000 / Ohio Aerospace Institute, Cleveland

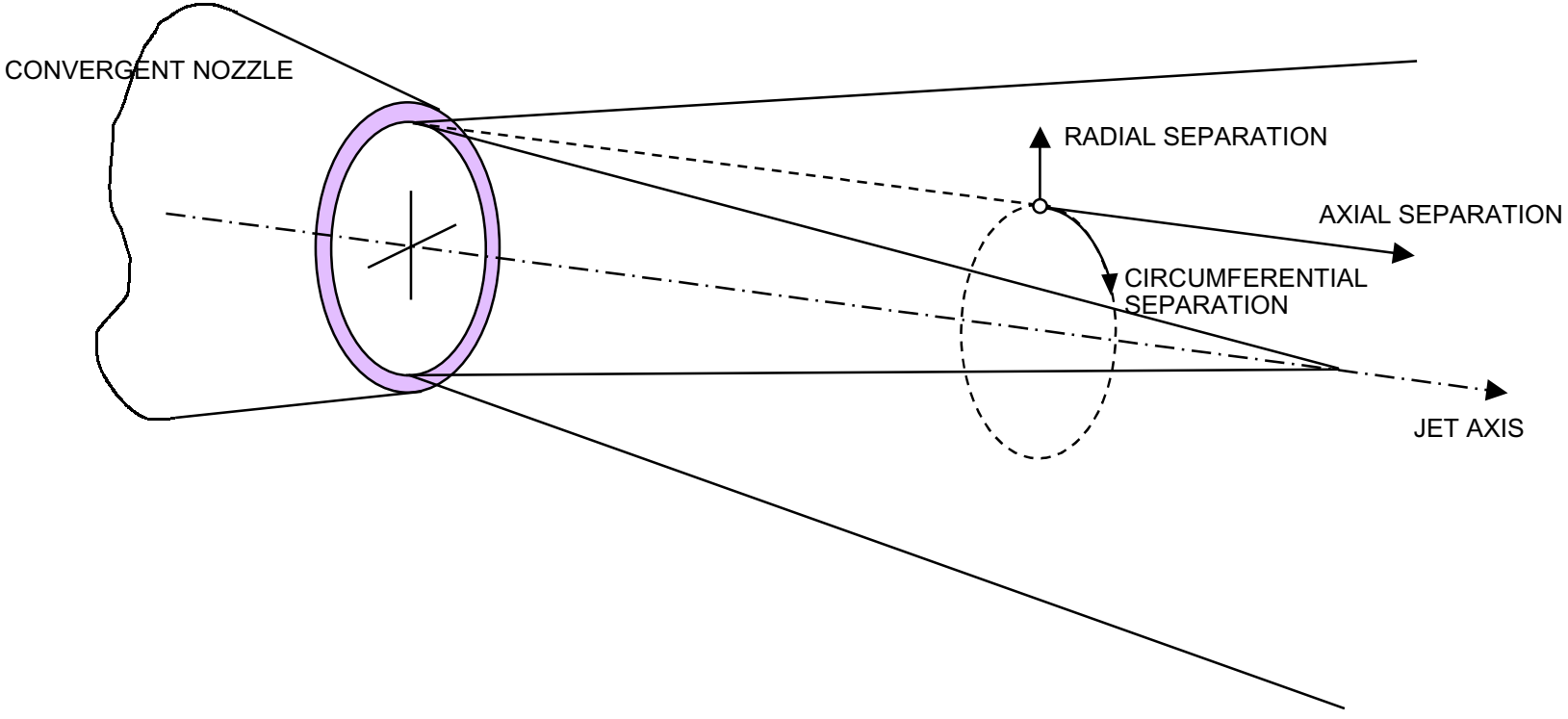
"NOISE SOURCES"

USE OF TURBULENCE SPACE-TIME CORRELATIONS IN LIGHTHILL'S EQUATION ANALYSED WITH RESPECT TO A FIXED FRAME OF REFERENCE
(AIAA 99-1838)

Marcus Harper-Bourne
DERA Pyestock, England

"Jet Mixing Noise"

M Harper-Bourne
OAI, 7 Nov 2000



STUDY OF TURBULENCE SPACE-TIME CORRELATIONS IN SHEAR LAYER OF A LOW SPEED AIR JET USING HOT-WIRE ANEMOMETRY

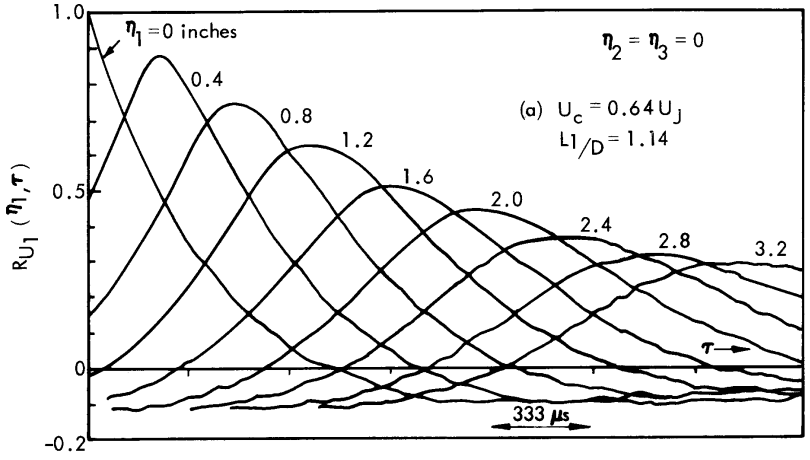
y_1=4D, y_2=0.5D

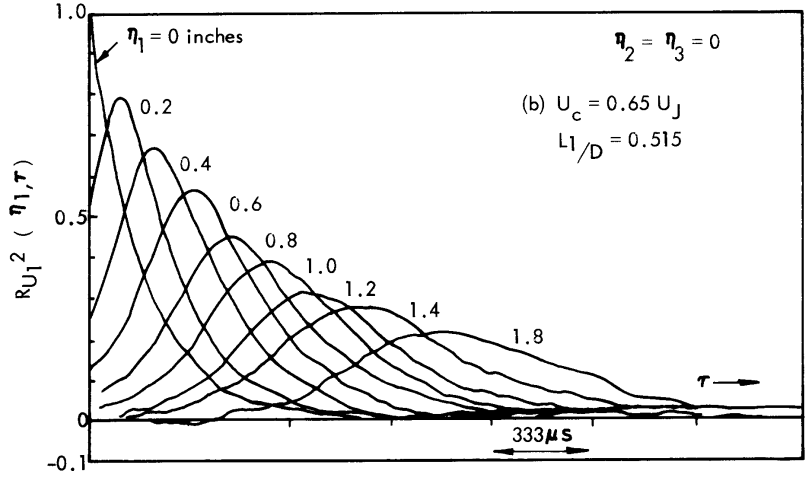
U_J=200 ft/s, D=2.0 in

DERA

"Jet Mixing Noise"

M Harper-Bourne
OAI, 7 Nov 2000

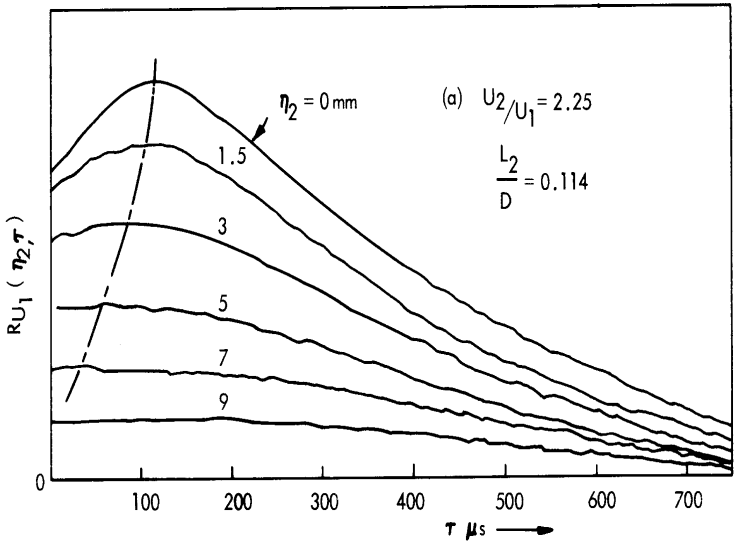


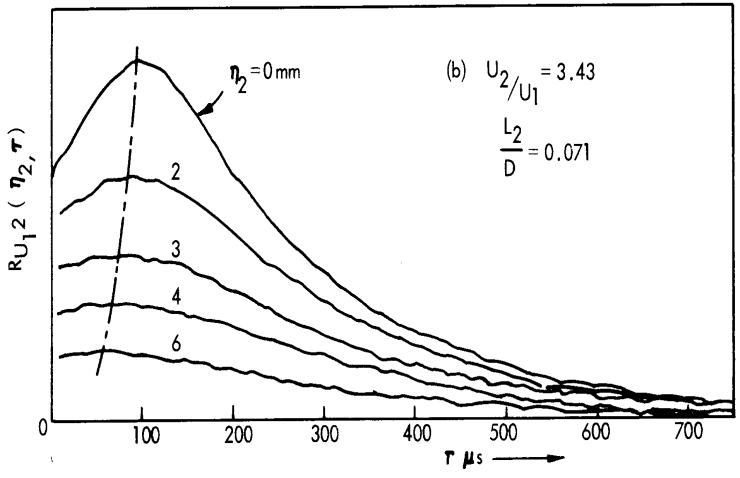


HOT-WIRE SPACE-TIME AXIAL CORRELATIONS FOR u_1 AND u_1^2 FLUCTUATIONS

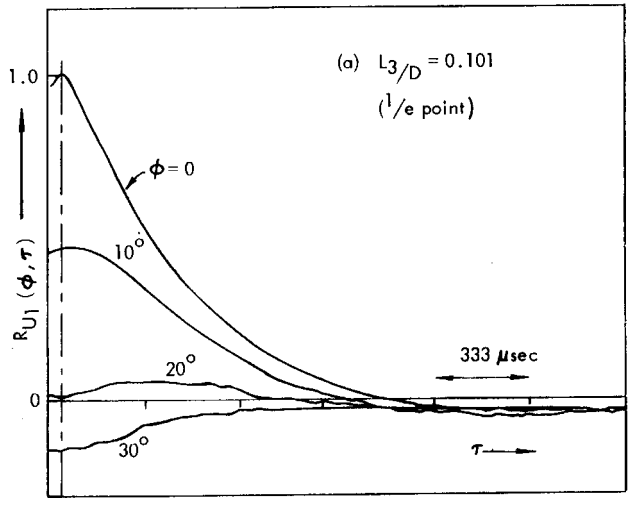
"Jet Mixing Noise"

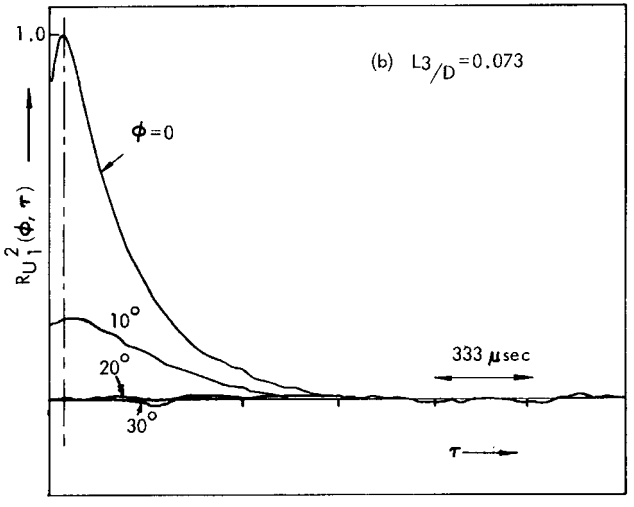
M Harper-Bourne
OAI, 7 Nov 2000





RADIAL CORRELATIONS

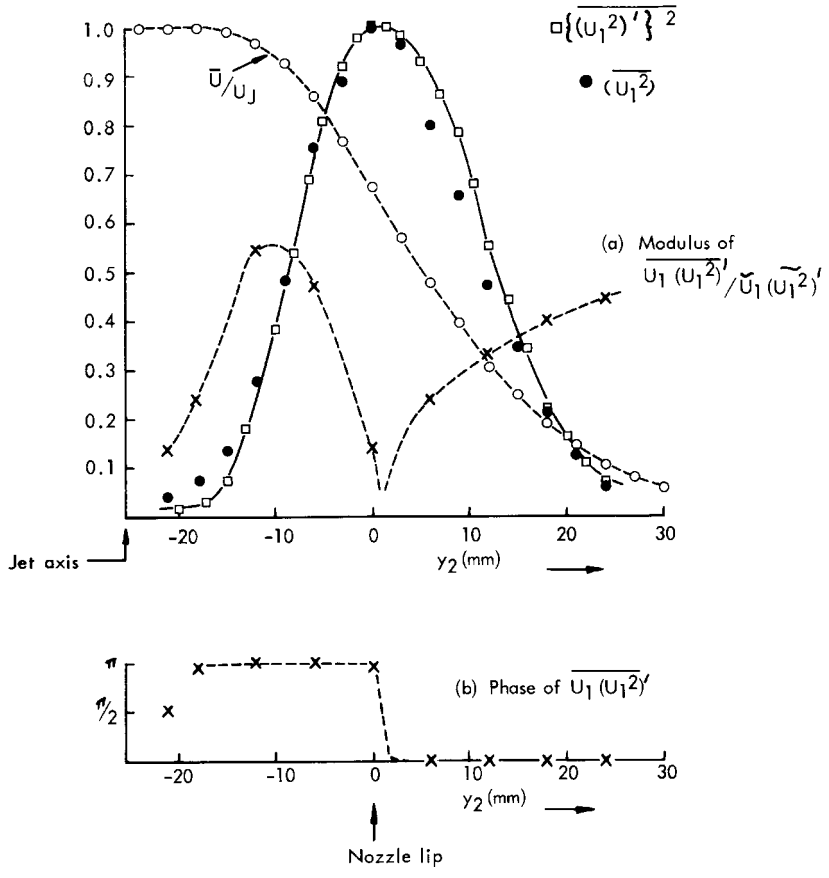




CIRCUMFERENTIAL CORRELATIONS

"Jet Mixing Noise"

M Harper-Bourne
OAI, 7 Nov 2000



MEAN VELOCITY AND TURBULENCE SPECTRAL INTENSITY (St=1) PROFILES ACROSS JET SHEAR LAYER AT y_1=4D

DERA

"Jet Mixing Noise"

M Harper-Bourne
OAI, 7 Nov 2000

ACOUSTIC ANALOGY
(AIAA 99-1838)

LIGHTHILL'S EQN: $$p(\hat{x},t)=\frac{1}{4\pi a_0^2}\int_{\hat{y}}\ddot{T}_{rr}(\hat{y},t-r/a_0)\frac{dV}{r}$$ (PROUDMAN FORM)

FIXED FRAME ANALYSIS

Power Spectral Density of p :

$$G_p(\hat{x},\omega)=\frac{\rho^2\omega^4}{\left(4\pi a_0^2\right)^2}\int_{\hat{y}}\int_{\hat{\eta}}\tilde{G}_{rr}(\hat{y},\hat{\eta},\omega).e^{jk\{r_1-r_2\}}\frac{dV_\eta}{r_2}\frac{dV_y}{r_1}=\frac{1}{\left(4\pi a_0^2\right)^2}\int\tilde{q}_r(\hat{y},\omega)\frac{dV_y}{r_1^{\,2}}$$

CPSD OF T_{rr}: $\tilde{G}_{rr}(\hat{y},\hat{\eta},\omega)=G_{rr}(\hat{y},\hat{\eta},\omega).e^{-j\omega\tau_p}$ PHASE: $\tau_p=\frac{\eta_1}{U_c}+\frac{\eta_2}{U_\sigma}$

LOCAL SOURCE STRENGTH DENSITY $$q_r(\hat{y},\omega)=\rho^2\omega^4.G_{rr}(\hat{y},0,\omega).V_{cor}(\hat{y},\omega).I(\hat{y},\omega)$$

RADIATION EFFICIENCY $$I(\hat{y},\omega)=\frac{1}{V_{cor}}\int_{\eta_3}\int_{\eta_2}\int_{\eta_1}R(\hat{y},\hat{\eta},\omega).\cos[k\{r_1-r_2\}-\omega\tau_p]d\eta_1 d\eta_2 d\eta_3$$

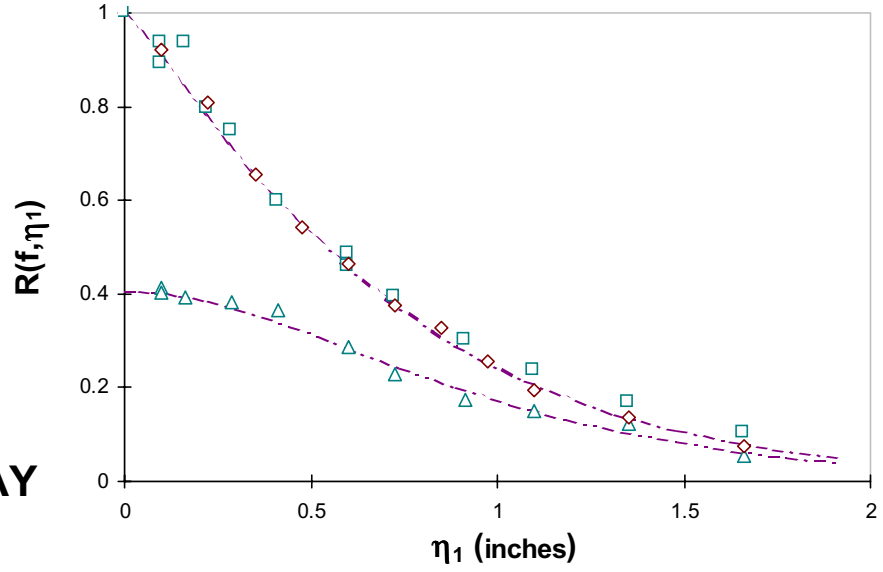
"Jet Mixing Noise"

M Harper-Bourne
OAI, 7 Nov 2000

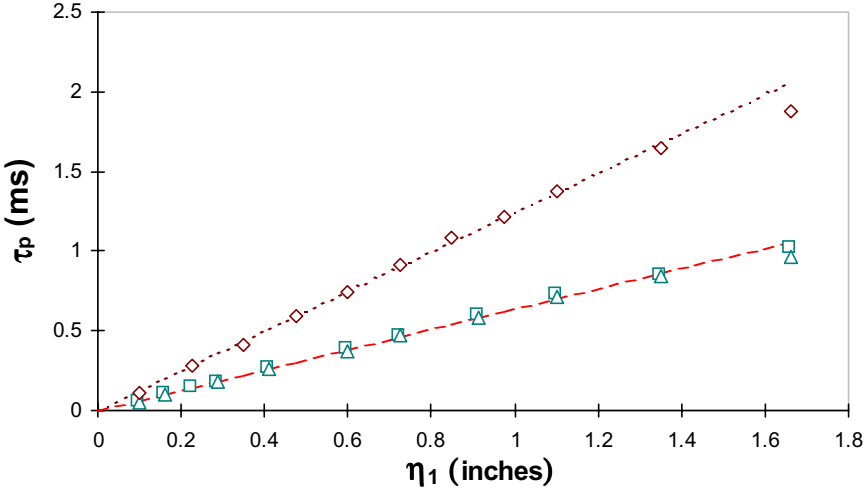
u_1^2 AXIAL DECAY AND CONVECTION

St=1

(a) Coherence



(b) Phase Delay

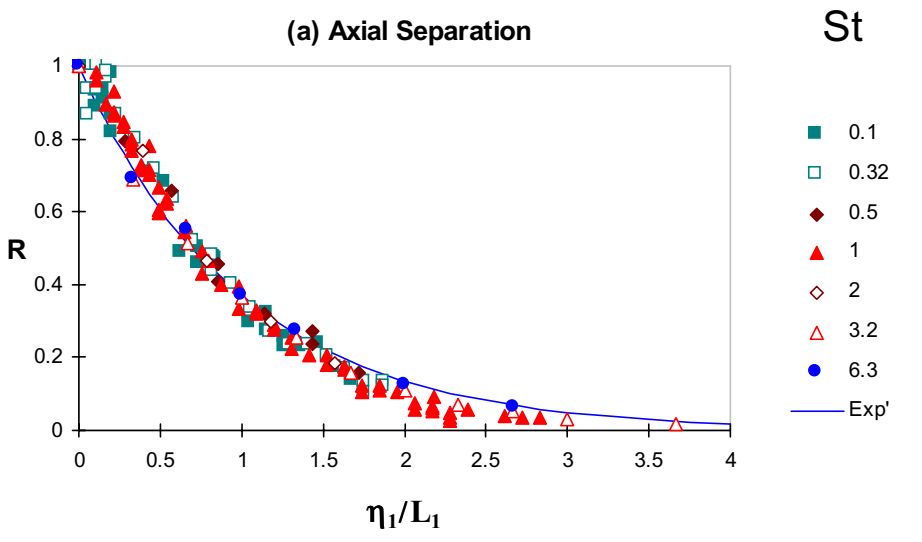


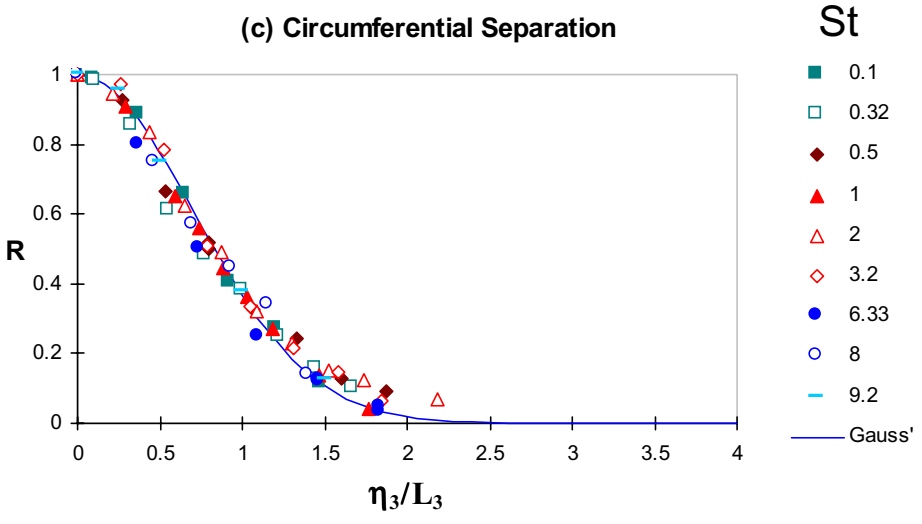
- phi=0 (200ft/s, 1200Hz)
- phi=6 (200ft/s, 1200Hz)
- phi=0 (100ft/s, 600Hz)
- Uj=100 ft/s, Uc/Uj=0.67
- Uj=200ft/s, Uc/Uj=0.65

DERA

"Jet Mixing Noise"

M Harper-Bourne
OAI, 7 Nov 2000

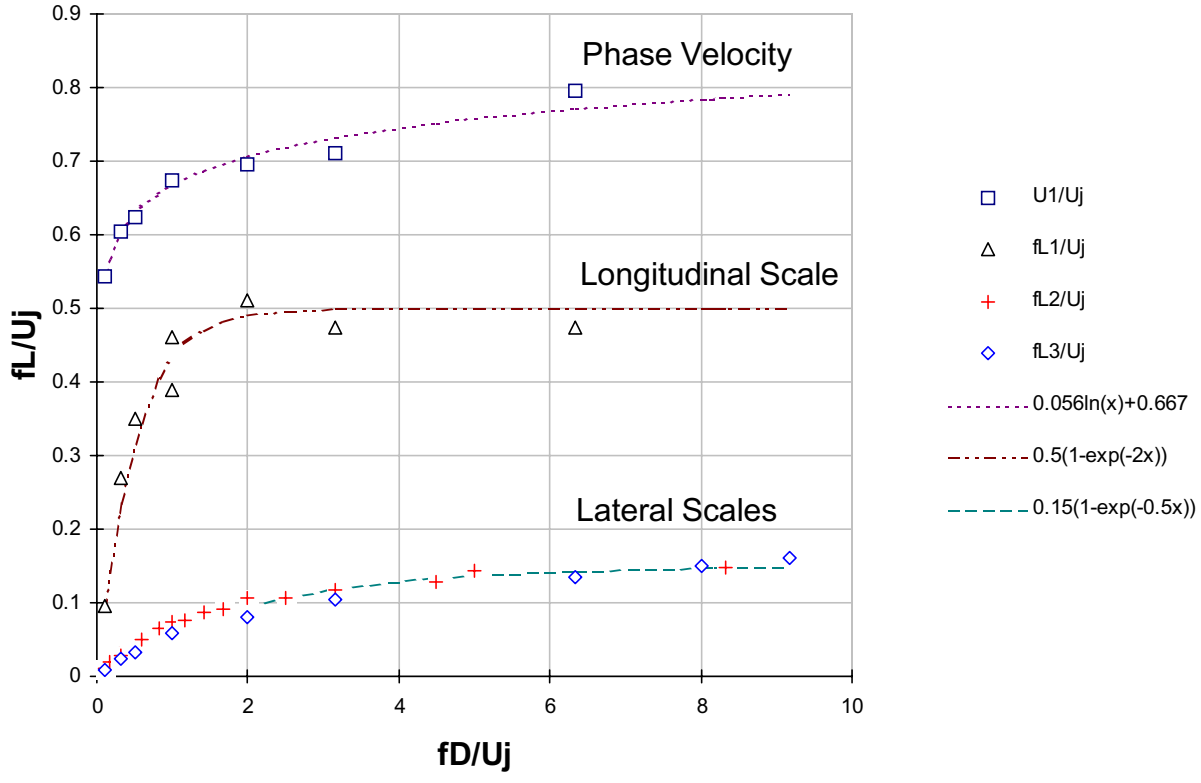




FILTERED u_1^2 CORRELATION MODULUS VERSUS NORMALISED SEPARATION FOR DIFFERENT STROUHAL NUMBER

"Jet Mixing Noise"

M Harper-Bourne
OAI, 7 Nov 2000

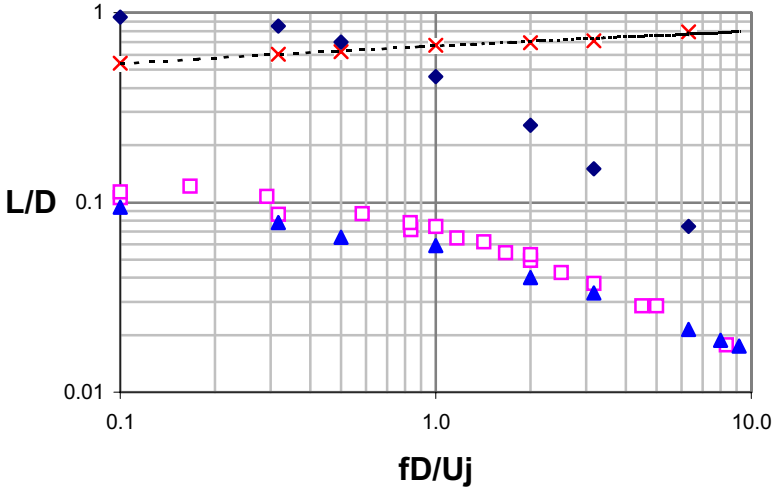


SPATIAL DECAY SCALES AND PHASE VELOCITY FOR u_1^2

y_1=4D, y_2=0.5D, U_j =200ft/s

"Jet Mixing Noise"

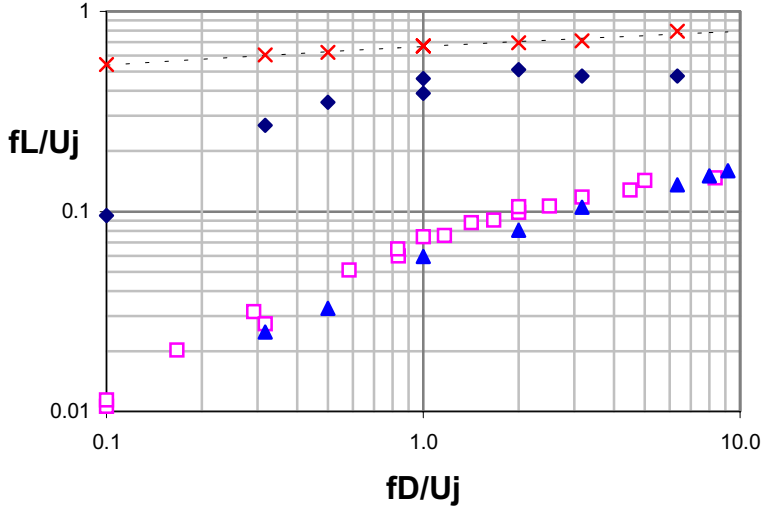
M Harper-Bourne
OAI, 7 Nov 2000



U_C/U_J

L_1

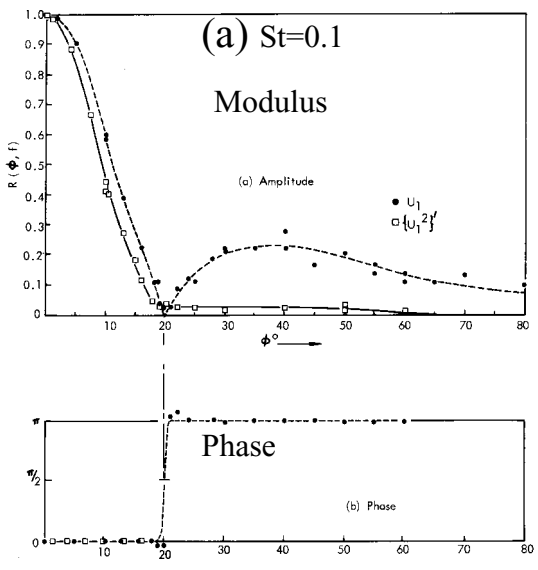
L_2 & L_3

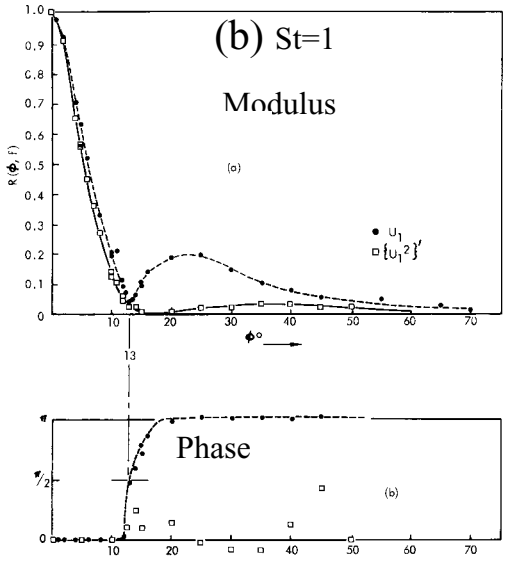


SPATIAL DECAY SCALES AND AXIAL PHASE VELOCITY VERSUS STROUHAL NUMBER FOR u_1^2

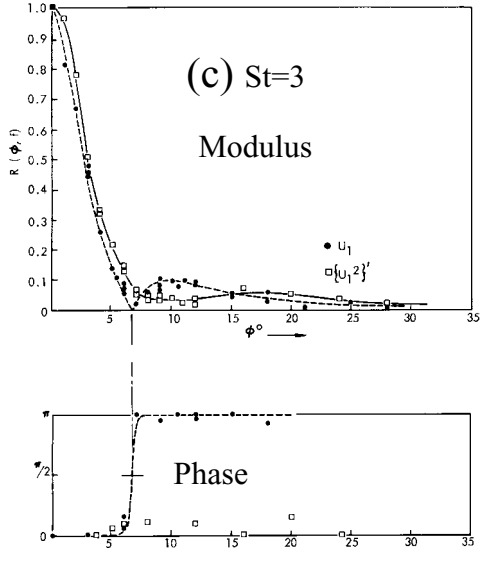
"Jet Mixing Noise"

M Harper-Bourne
OAI, 7 Nov 2000



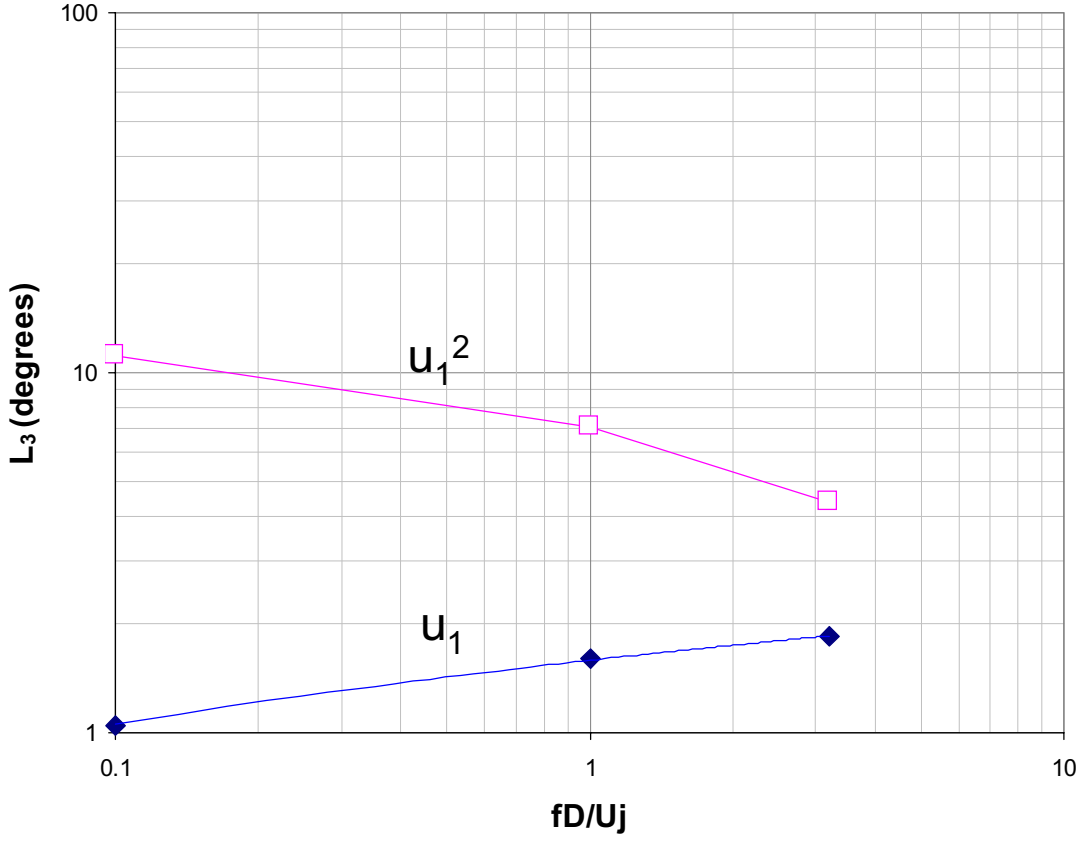


FILTERED CIRCUMFERENTIAL CORRELATIONS u_1 AND u_1^2



"Jet Mixing Noise"

M Harper-Bourne
OAI, 7 Nov 2000



AZIMUTH INTEGRAL SCALES

"Jet Mixing Noise"

M Harper-Bourne
OAI, 7 Nov 2000

TURBULENCE MODEL - CONVECTIVE AMPLFICATION

Normalised Separation $\overline{\eta}_i = \eta_i / L_i$

1-D $R(\overline{\eta}_1) = e^{-\overline{\eta}_1}$ $R(\overline{\eta}_2) = e^{-\overline{\eta}_2^2}$ $R(\overline{\eta}_3) = e^{-\overline{\eta}_3^2}$ Separation of Variables

3-D $R(\overline{\eta}) = e^{-\overline{\eta}}$ $\overline{\eta} = \sqrt{\overline{\eta}_1^2 + \overline{\eta}_2^2 + \overline{\eta}_3^2}$ Exponential Decay

$\overline{\eta} = \sqrt{\overline{\eta}_1^2 + (\overline{\eta}_2^2 + \overline{\eta}_3^2)^2}$ Exponential/Gaussian Decay

$$I(\hat{y}, \omega) = \frac{1}{\left[1 + \left(\frac{\omega L_1}{U_c}[1 - M_c \cos\theta]\right)^2\right]^{3/2}} \longrightarrow$$

1.0
1.5
2.0

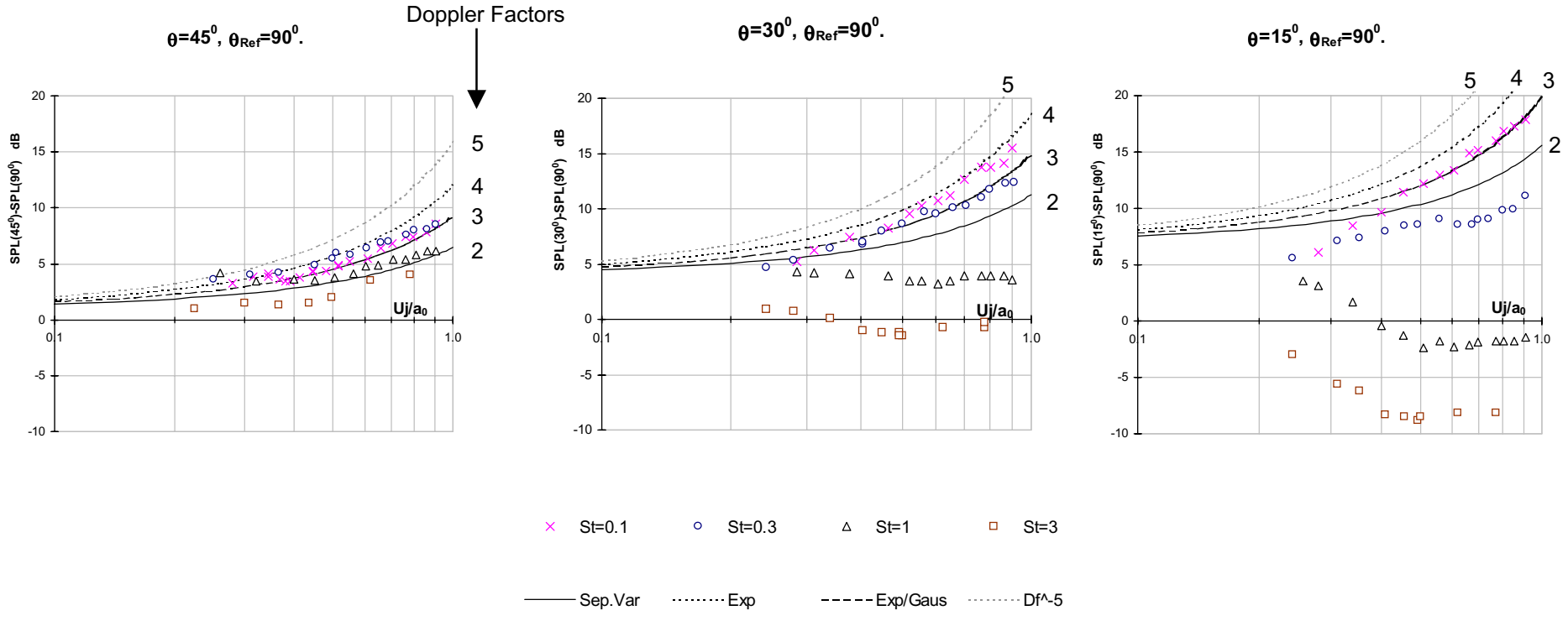
$$C_A(\hat{y}, \omega, D_f) = \frac{\left[1 + \left(\frac{\omega L_1}{U_c}\right)^2\right]^{m/2}}{\left[1 + \left(\frac{\omega L_1}{U_c}[1 - M_c \cos\theta]\right)^2\right]^{m/2}} \approx \frac{1}{[1 - M_c \cos\theta]^m} \longrightarrow$$

m	
2	Sep. Var.
3	Exp/Gaus
4	Exp
5	Moving Frame

AT MACH ANGLE, RADIATION EFFICIENCY I=1 (NO SINGULARITY)

"Jet Mixing Noise"

M Harper-Bourne
OAI, 7 Nov 2000

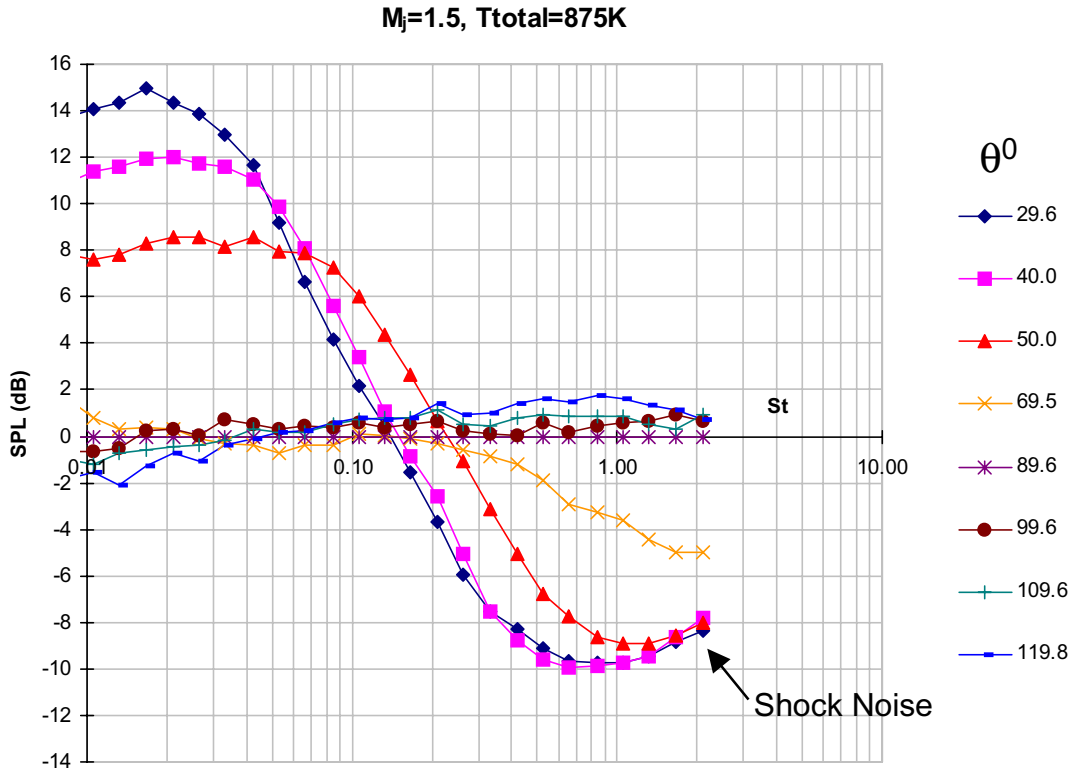


STUDY OF CONVECTIVE AMPLIFICATION

1 inch jet, Tj=295^{0}K

"Jet Mixing Noise"

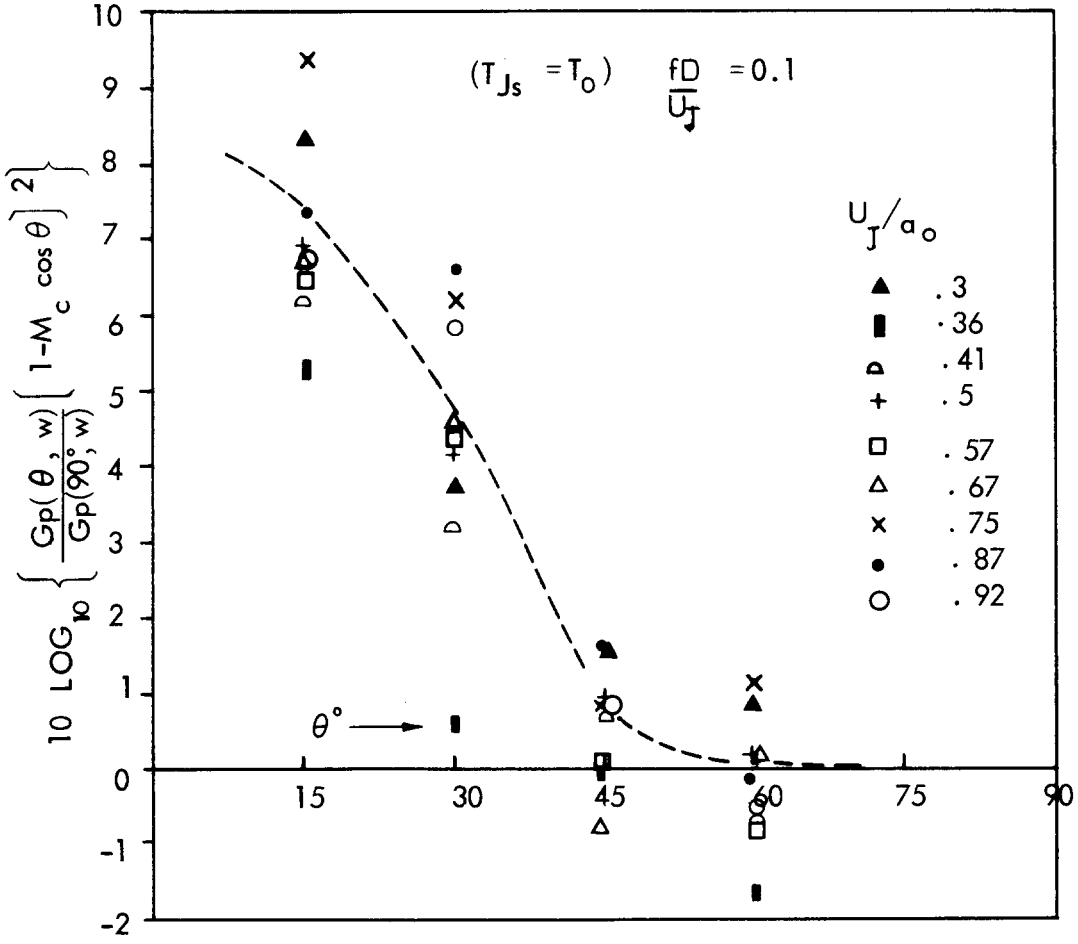
M Harper-Bourne
OAI, 7 Nov 2000



INHERENT DIRECTIVITY SPECTRUM, CON-DI Mj=1.5, 875K

"Jet Mixing Noise"

M Harper-Bourne
OAI, 7 Nov 2000



INHERENT DIRECTIVITY MEASURED AT LOW FREQUENCY
(SUBSONIC, UNHEATED)

"Jet Mixing Noise"

M Harper-Bourne
OAI, 7 Nov 2000

LINE SOURCE MODEL

$$S_r(y_1,\omega) = G_{90}(\omega).D_p(y_1,\theta,\omega).C_A(y_1,D_f,\omega).S(y_1,\omega).D^2$$

$$\int_0^\infty S(y_1,\omega)dy_1 = 1$$

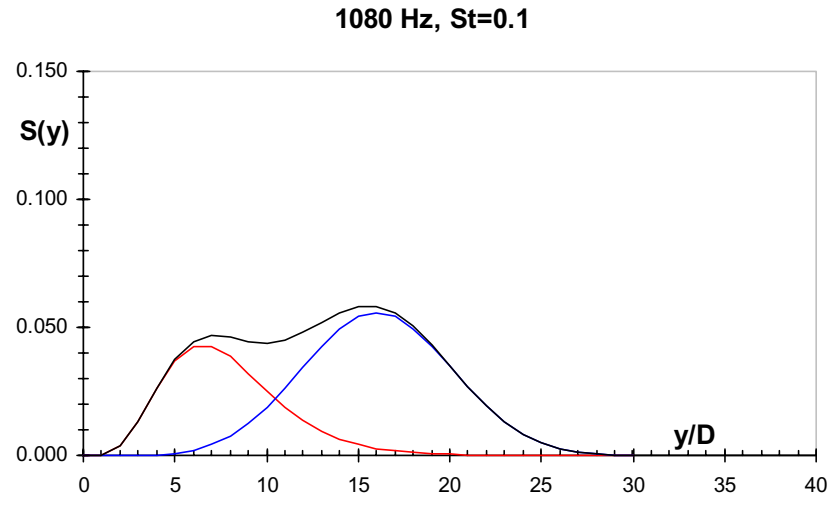
$$C_A = \frac{I(\theta,\omega)}{I(\pi/2,\omega)}$$

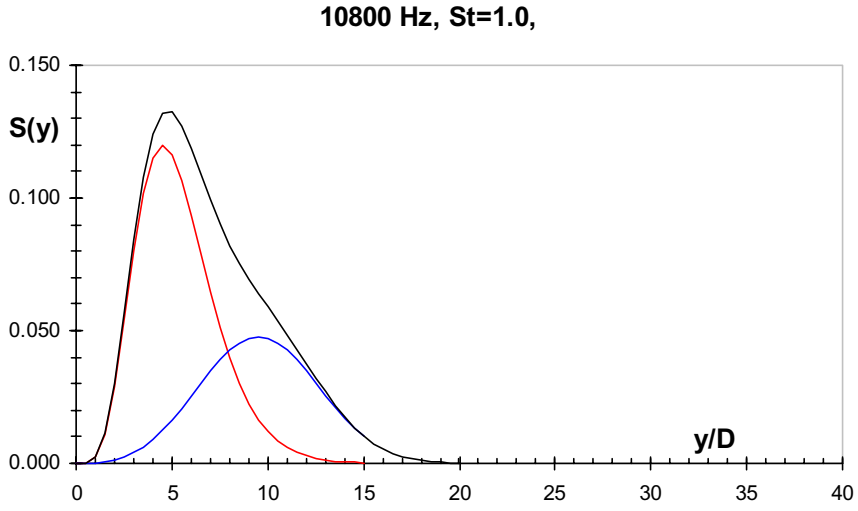
$$G_p(\hat{x},\omega) = \sum_i \frac{S_r(y_i,\omega)}{r_1^2}\Delta y_i \qquad \text{Single}$$

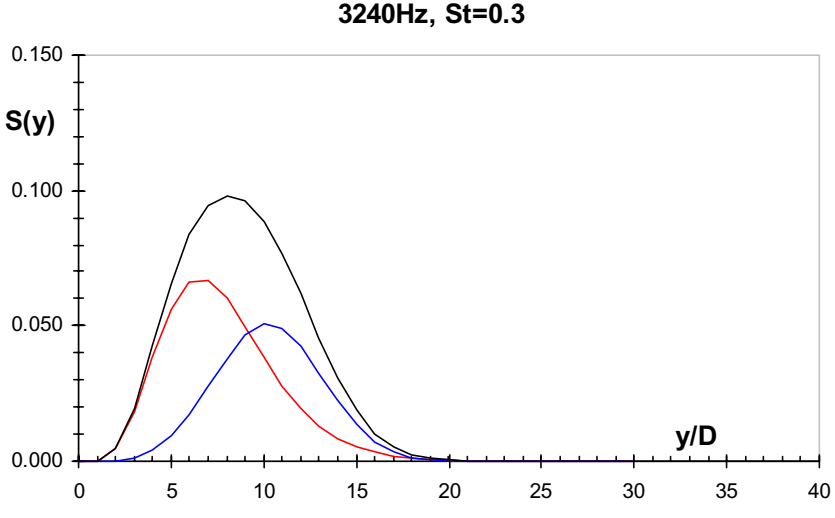
$$G_p(\hat{x},\omega) = \sum_i \frac{S_{r_1}(y_i,\omega)}{r_1^2}\Delta y_i + \sum_i \frac{S_{r_2}(y_i,\omega)}{r_2^2}\Delta y_i \qquad \text{Twin}$$

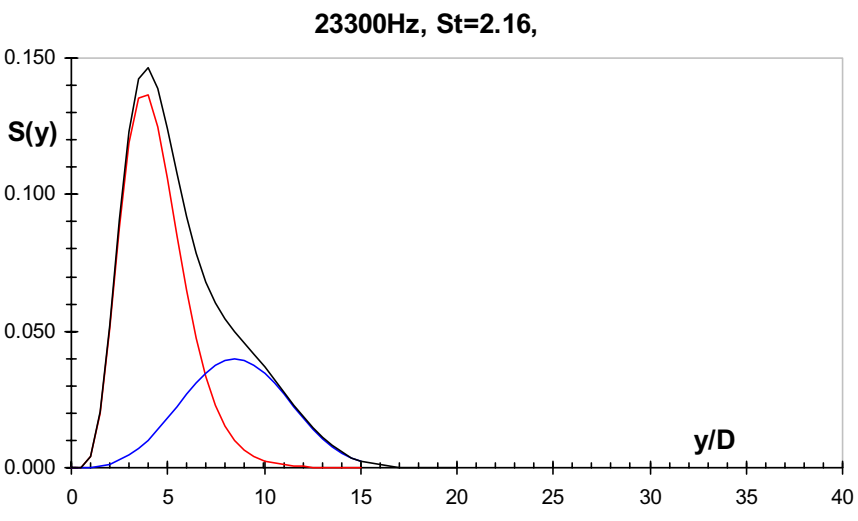
"Jet Mixing Noise"

M Harper-Bourne
OAI, 7 Nov 2000







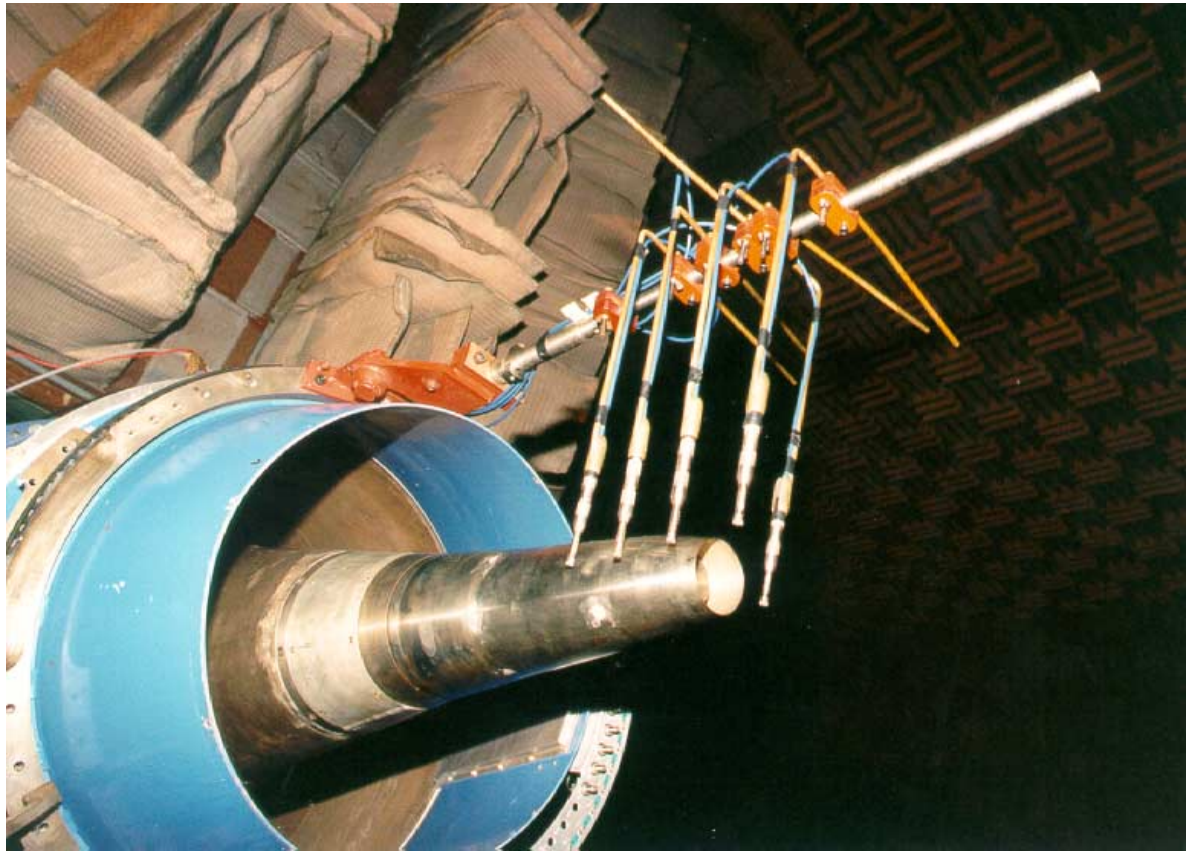


TWO-SOURCE BREAKDOWN OF JET MIXING NOISE

DERA

“Jet Mixing Noise”

M Harper-Bourne
OAI, 7 Nov 2000

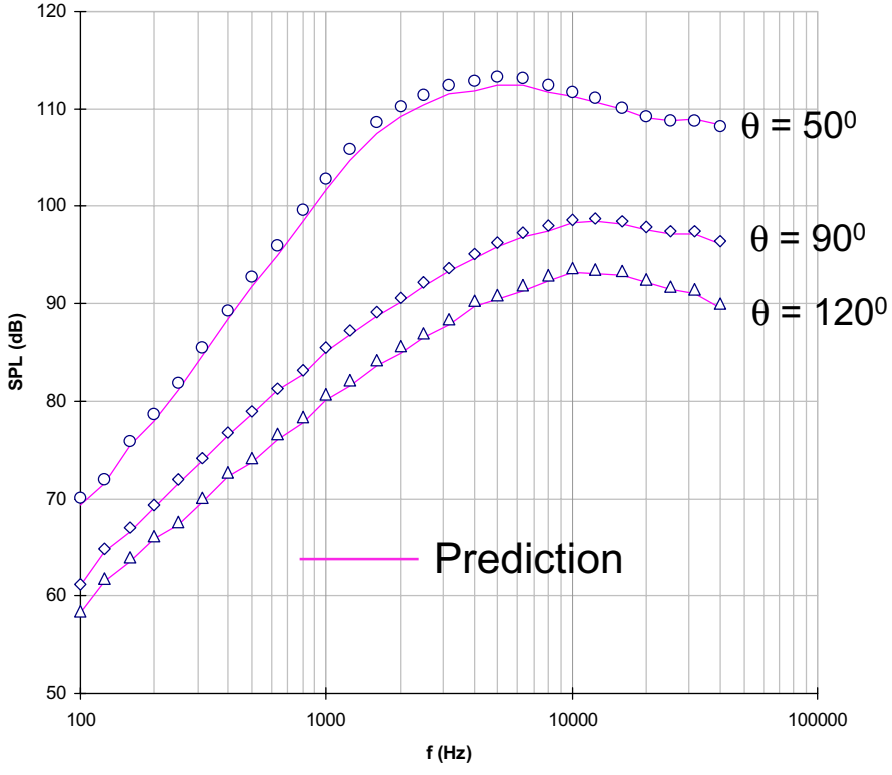


MEASUREMENT OF JET NEAR-FIELD NOISE IN THE DERA PYESTOCK LARGE ANECHOIC “NOISE TEST FACILITY”

DERA

"Jet Mixing Noise"

M Harper-Bourne
OAI, 7 Nov 2000



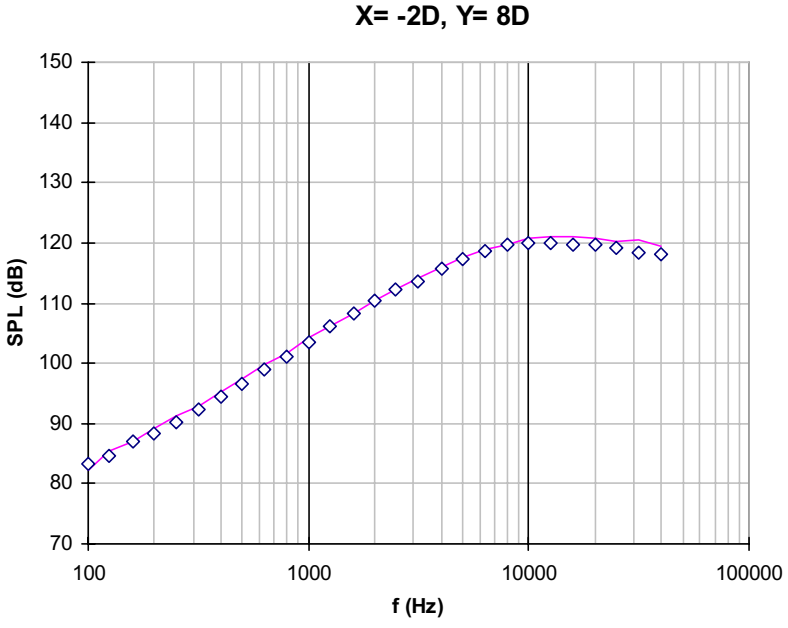
FAR-FIELD (R/D=307): COMPARISON OF MIXING NOISE PREDICTION WITH NTF MEASUREMENTS

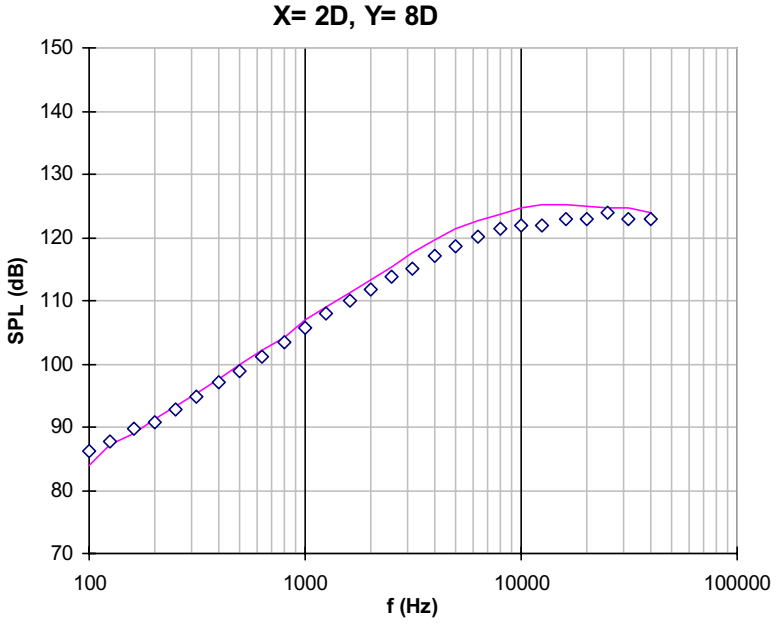
FULLY EXPANDED M1.5 CD NOZZLE

D=39mm, T_J=875^{0}K

"Jet Mixing Noise"

M Harper-Bourne
OAI, 7 Nov 2000



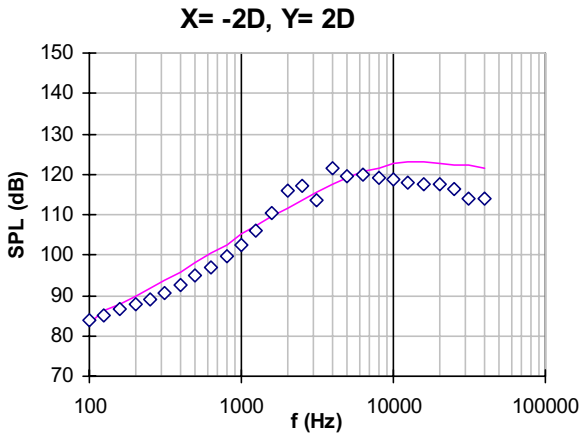


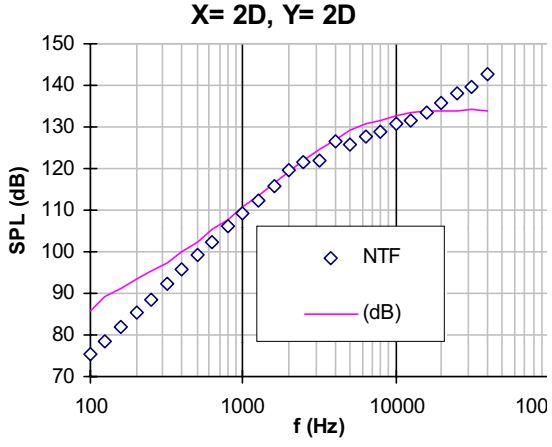
OUTER NEAR-FIELD: COMPARISON OF MIXING NOISE PREDICTION WITH NTF MEASUREMENTS

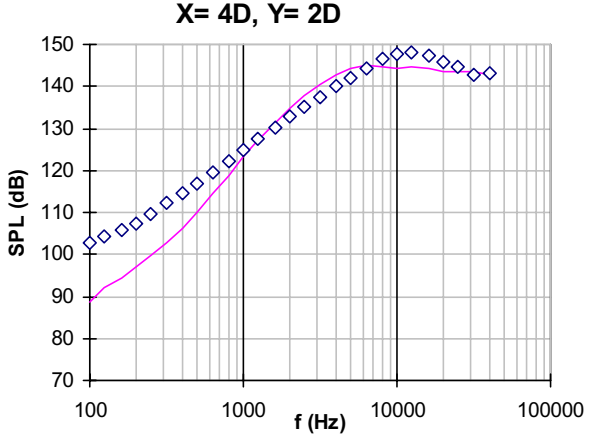
FULLY EXPANDED M1.5 CD NOZZLE, $T_J=875^0K$

"Jet Mixing Noise"

M Harper-Bourne
OAI, 7 Nov 2000







NEAR-FIELD: COMPARISON OF MIXING NOISE PREDICTION WITH NTF MEASUREMENTS

FULLY EXPANDED M1.5 CD NOZZLE, T_J=875^{0}K

M Harper-Bourne
OAI, 7 Nov 2000

CONCLUSIONS

- OVERALL AND FILTERED TWO-POINT SPACE-TIME CORRELATIONS OF u_1 AND u_1^2 IN THE MIXING REGION OF A ROUND LOW SPEED JET HAVE BEEN MEASURED USING HOT-WIRE PROBES

- FROM THE MEASUREMENTS, THE FIXED FRAME COHERENCE AND ASSOCIATED DECAY SCALES HAVE BEEN DETERMINED AS A FUNCTION OF STROUHAL NUMBER FOR THE LONGITUDINAL, RADIAL AND AZIMUTH SEPARATION CO-ORDINATES.

- USING LIGHTHILL'S ACOUSTIC ANALOGY THESE DATA ARE ANALYSED WITH RESPECT TO A FIXED FRAME OF REFERENCE AND SHOWN TO YIELD LEVELS OF CONVECTIVE AMPLIFICATION (~ THREE POWERS) IN KEEPING WITH JET NOISE MEASUREMENTS. AT THE MACH ANGLE, WHEN IT EXISTS, THE RADIATION REMAINS FINITE IN THIS MODEL.

- COMBINING THE FIXED FRAME MODEL OF MIXING NOISE WITH SOURCE LOCATION MEASUREMENTS, A METHODOLOGY FOR PREDICTING NEAR-FIELD NOISE IS DERIVED AND SHOWN TO GIVE GOOD AGREEMENT WITH MEASUREMENTS MADE ON A M1.5 CON-DI JET, FOR R/D>2

- IN THE FIXED FRAME MODEL MACH WAVE RADIATION IS ENCOMPASSED AS A LIMITING CASE OF JET MIXING NOISE WITH THE RADIATION EFFICIENCY BEING UNITY AT THE MACH ANGLE

M Harper-Bourne References

1. M Harper-Bourne, “Radial Distribution of Jet Noise Sources Using Far-Field Microphones”, AIAA Paper 98-237, 4th AIAA/CEAS Aeroacoustics Conference, Toulouse, France, June 1998.

2. M Harper-Bourne, “Jet Near-Field Noise Prediction”, AIAA Paper 99-1838, 5th AIAA/CEAS Aeroacoustics Conference, Seattle, May 1999.

3. M Harper-Bourne, “Twin-Jet Near-Field Noise Prediction”, AIAA Paper 2000-2084, 6th AIAA/CEAS Aeroacoustics Conference, Maui, June 2000.

Model Decomposition of Fluctuations in a Parallel Sheared Flow Based on the Displacement

Georges Elias
ONERA

NASA/CP—2001-211152

MODAL DECOMPOSITION OF FLUCTUATIONS IN A PARALLEL SHEARED FLOW BASED ON THE DISPLACEMENT

429

Georges ELIAS

ONERA

GALBRUN's EQUATION (1934)

Exact propagation equation in the presence of non homogeneous flow as function of the displacement

$$\rho_0 \frac{D^2\xi_i}{Dt^2} - \frac{\partial}{\partial x_i}\left(\rho_0 a_0^2 \vec{\nabla}.\vec{\xi}\right) + \left(\vec{\nabla}.\vec{\xi}\right)\frac{\partial p_0}{\partial x_i} - \frac{\partial \xi_j}{\partial x_i}\frac{\partial p_0}{\partial x_j} = 0$$

$$\begin{cases} \rho = -\rho_0 \vec{\nabla}.\vec{\xi} - \vec{\xi}.\vec{\nabla}\rho_0 \\ p = -\rho_0 a_0^2 \vec{\nabla}.\vec{\xi} - \vec{\xi}.\vec{\nabla}p_0 \\ \vec{v} = \dfrac{D\vec{\xi}}{Dt} - \left(\vec{\xi}.\vec{\nabla}\right)\vec{V}_0 \end{cases}$$

ONERA

LAGRANGIAN OF THE GALBRUN's EQUATION

$$L=\frac{1}{2}\rho_0\left(\frac{D\vec{\xi}}{Dt}\right)^2-\frac{1}{2}\rho_0 a_0^2\left(\vec{\nabla}.\vec{\xi}\right)^2-\left(\vec{\xi}.\vec{\nabla}p_0\right)\vec{\nabla}.\vec{\xi}-\frac{1}{2}\xi_i\frac{\partial^2 p_0}{\partial x_i\partial x_j}\xi_j$$

ENERGY AND INTENSITY DERIVED FROM THE LAGRANGIAN

$$\begin{cases} e=\dfrac{1}{2\rho_0}\left(\dfrac{d\vec{\xi}}{dt}\right)^2+\dfrac{1}{2\rho_0 a_0^2}\left((p^E)^2-(\vec{\xi}.\vec{\nabla}p_0)^2\right)-\rho_0\dfrac{d\vec{\xi}}{dt}.\left(\vec{V}_0.\vec{\nabla}\right)\vec{\xi}\right) \\ \vec{i}=p^E\dfrac{\partial\vec{\xi}}{\partial t}+\rho_0\left(\dfrac{\partial\vec{\xi}}{\partial t}.\dfrac{d\vec{\xi}}{dt}\right)\vec{V}_0 \\ \dfrac{\partial e}{\partial t}+\vec{\nabla}.\vec{i}=0 \end{cases}$$

ONERA

MODAL DECOMPOSITION FOR A STRATIFIED FLOW

$$\begin{cases} \dfrac{dR_1}{dt} + \gamma \vec{\nabla}.\vec{V}_1 = F \\ \gamma \dfrac{d\vec{V}_1}{dt} + a_1^2 \vec{\nabla} R_1 = \vec{G} \end{cases}$$

$$R_1 = R_0 + r^{(1)} + r^{(2)} + \ldots \qquad \vec{\xi} = \vec{\xi}^{(1)} + \vec{\xi}^{(2)} + \ldots$$

System at any order *n*:

$$\boxed{\begin{cases} r + \gamma \vec{\nabla}.\vec{\xi} = P \\ \gamma \dfrac{D^2\vec{\xi}}{Dt^2} + a_0^2 \vec{\nabla} r = \vec{R} \end{cases}}$$

$$\frac{D}{Dt}\left(\frac{D^2 r}{Dt^2} - \vec{\nabla}.\left(a_0^2 \vec{\nabla} r\right) \right) + 2a_0^2 \frac{dV_0}{dx} \frac{\partial^2 r}{\partial x \partial z} = \frac{D^3 P}{Dt^3} - \frac{D}{Dt} \vec{\nabla}.\vec{R} + 2 \frac{\partial V_0}{\partial x} \frac{\partial R_x}{\partial z} = S$$

$$\vec{R} = \frac{D^2 \vec{Q}}{Dt^2} \quad \Rightarrow \quad \frac{D}{Dt} \vec{\nabla}.\vec{R} - 2 \frac{\partial V_0}{\partial x} \frac{\partial R_x}{\partial z} = \frac{D^3}{Dt^3} \vec{\nabla}.\vec{Q}$$

$$\vec{Q} = \vec{\nabla}\psi + \vec{\nabla} \wedge \vec{K} \quad \Rightarrow \quad \boxed{\vec{R} = \frac{D^2}{Dt^2}\left(\vec{\nabla}\psi + \vec{\nabla} \wedge \vec{K}\right)} \quad S = \frac{D^3}{Dt^3}\left(P - \Delta\psi\right)$$

ONERA

Pressure mode:

$$\begin{cases} r_p = r = \dfrac{D^3\varphi}{Dt^3} \\ \vec{\xi}_p = \dfrac{1}{\gamma}\left(\vec{\nabla}\psi - a_0^2 \dfrac{D}{Dt}\vec{\nabla}\varphi - 3a_0^2 \dfrac{\partial V_0}{\partial x}\dfrac{\partial \varphi}{\partial z}\vec{u}_x \right) \\ \dfrac{D}{Dt}\left(\dfrac{D^2\varphi}{Dt^2} - \vec{\nabla}.\left(a_0^2\vec{\nabla}\varphi\right)\right) - a_0^2 \dfrac{\partial V_0}{\partial x}\dfrac{\partial^2 \varphi}{\partial z \partial x} - 3\dfrac{\partial}{\partial x}\left(a_0^2 \dfrac{\partial V_0}{\partial x}\dfrac{\partial \varphi}{\partial z}\right) = P - \Delta\psi \end{cases}$$

Vorticity mode:

$$\begin{cases} r_\Omega = 0 \\ \vec{\xi}_\Omega = \vec{\nabla} \wedge \vec{K} \end{cases}$$

$$\gamma \frac{D^2 \vec{\xi}}{Dt^2} + a_0^2 \vec{\nabla} r = \frac{D^2}{Dt^2} \left(\vec{\nabla} \psi + \vec{\nabla} \wedge \vec{K} \right)$$

$$a_0^2 \vec{\nabla} r = \frac{D^2 \vec{A}}{Dt^2} \qquad \vec{A} \quad ? \qquad \boxed{r = \frac{D^3 \varphi}{Dt^3}}$$

$$a_0^2 \vec{\nabla} \frac{D^3 \varphi}{Dt^3} = \frac{D^2}{Dt^2} \left(a_0^2 \frac{D}{Dt} \vec{\nabla} \varphi + 3 a_0^2 \frac{\partial V_0}{\partial x} \frac{\partial \varphi}{\partial z} \vec{u}_x \right)$$

$$\boxed{\vec{\xi} = \frac{1}{\gamma} \left(\vec{\nabla} \psi - a_0^2 \frac{D}{Dt} \vec{\nabla} \varphi - 3 a_0^2 \frac{\partial V_0}{\partial x} \frac{\partial \varphi}{\partial z} \vec{u}_x \right) + \vec{\nabla} \wedge \vec{K}}$$

G. Elias References

1. Peyret (C.). -A coustic propagation in presence of an arbitrary flow. Journal of the acoustical Society of America, vol. 103, n° 5, mai 1998, p. 2840.

2. Peyret (C.) et Elias (G.). -A finite element method to study harmonic aeroacoustics problems. Journal of the acoustical Society of America, revised in 2001.

SESSION 2: SOURCE IDENTIFICATION AND LOCATION TECHNIQUES

Summary by Eugene Krejsa, Consultant

The session consisted of three invited presentations and several presentations during the open podium portion of the session. Discussion followed each presentation.

INVITED PRESENTATIONS

Jet Noise Source Location: A Review - Stewart A. L. Glegg, Florida Atlantic University

Dr. Glegg presented a review of jet noise source location techniques. He pointed out that the only undisputed definition of source strength is defined on a Kirchhoff surface enclosing all the sources. However, the objective of jet noise source location techniques is to determine the source distribution inside the surface. The definition of this source distribution is not necessarily unique and may depend on the assumptions made in the implementation of the technique.

Dr. Glegg summarized techniques used prior to 1985. These included acoustic mirrors, microphone array techniques, two microphone methods, causality correlation and coherence techniques, and a method referred to as the automated source breakdown. The causality correlation and coherence techniques attempt to correlate measurements within the jet, usually velocity fluctuations, with the far field acoustic signature. Dr. Glegg pointed out that one of the major difficulties with this approach is the low value of correlation. However, the technique has been used by several researchers. The other techniques estimate the source distribution from the radiated acoustic signals.

Techniques using the acoustic field to estimate the source distribution require a description of the source characteristics, e.g. directivity, and a model for the propagation from the source to the microphone. Dr. Glegg asserted that the value of the estimated source strengths depends on the model chosen to represent the sources and the propagation and the accuracy of the process used to invert the source model. One issue that Dr. Glegg addressed was the assumption of uniform source directivity. Its significance is related to the array resolution, which is determined by the angles subtended, by the ends of the array and the acoustic wavelength. Increasing the angular range of the array to improve resolution increases the degree to which the source directivity will be nonuniform over the extent of the array. An example was provided which showed that the effect of nonuniform source directivity was not great.

Results from several tests were shown. These results showed that the source location was a function of Strouhal number, with high frequency sources being located close to the nozzle exit and low frequency sources being located further

downstream. This finding was consistent with that based on Lighthill's acoustic analogy. Results from a jet containing shocks showed multiple sources associated with the shock structure within the jet. Results using the automated source breakdown method were also shown. This method has been used to assess the noise components from turbofan engines. Application of this technique to a co-axial jets showed that a co-axial jet could have two source distributions, one related to the primary jet/ambient mixing and the second with the secondary/ambient mixing. A comparison of results from a heated jet and a cold jet indicated that the sources were closer to the nozzle for the heated jet.

More recent approaches to jet noise source location include the two microphone method of Ahuja, causality correlation and coherence techniques, and the use of microphone arrays. Results of tests conducted by Harper Bourne were summarized. A major finding presented was that the jet appeared to have two source regions, an upstream source associated with the initial mixing region, and a downstream source associated with the fully developed flow. Dr. Glegg summarized results from several phased array studies. Major findings were: Source distributions are of smaller axial extent then previously reported; Hot jet sources are located further downstream than those for cold jets (This is in conflict with previous findings.); and that the data conflicts with some of the turbulence modeling assumptions made in jet noise modeling. In Dr. Glegg's overview of modern signal processing techniques for acoustic arrays, he pointed out that the proper choice of the inversion scheme could improve the results. Alternative approaches for inverting the matrix and the use of modal decomposition of the source strength were discussed.

The following conclusions and recommendation were made by Dr. Glegg:

- The two source model for jet noise source distribution has been shown to be important for prediction.
- Parametric source breakdown approaches have given new insight.
- The effect of nozzle exit flow conditions has been identified as affecting the source distribution, but has not been measured in detail.
- More needs to be done with non-intrusive flow probes and far field arrays.
- Determining the details of the acoustic source correlation structure will give new insight into the mechanisms of sound generation.

The following is a brief summary of open discussion following Dr. Glegg's presentation:

- Variation in source distribution with observer location should be expected since the source is directional.
- Both non-uniform source directionality and phase can bias the results.
- Attempts have been made to account for jet refraction effects.
- The contradiction in results for heated jets has not been resolved. Need to use both the polar correlation technique and an acoustic array on the same heated jet to resolve this issue.

Jet Noise Source Location: A Review

Stewart A. L. Glegg
Center for Acoustics and Vibration
Florida Atlantic University

NASA/CP—2001-211152

Jet Noise Source Location: A Review

Stewart A.L. Glegg
Center for Acoustics and Vibration
Florida Atlantic University

Presented at the
Jet Noise Workshop
Ohio Aerospace Institute
November 2000

Objectives

- To review jet noise source location measurements : *What has been measured?*
- To identify new approaches to jet noise source location: *What should be measured?*

Outline of Talk

- Jet Noise Source Location prior to 1985
- Recent measurements
- Modern array processing methods
- Recommendations for the future

Jet Noise Source Location prior to 1985

- **Acoustics Mirrors**

  Laufer et al(1972), Grosche (1973), Glegg(1975)

- **Microphone Arrays**

  Harper Boune(1998) , Fisher et al(1976), Billingsley and Kinns(1976), Maestrello(1976)

- **Two Microphone Methods**

  Parthasarathy (1974), Kinns(1976)

- **Causality Correlation and Coherence Techniques**

  Siddon (1971), Lee and Ribner(1972), Shivashankara(1978)

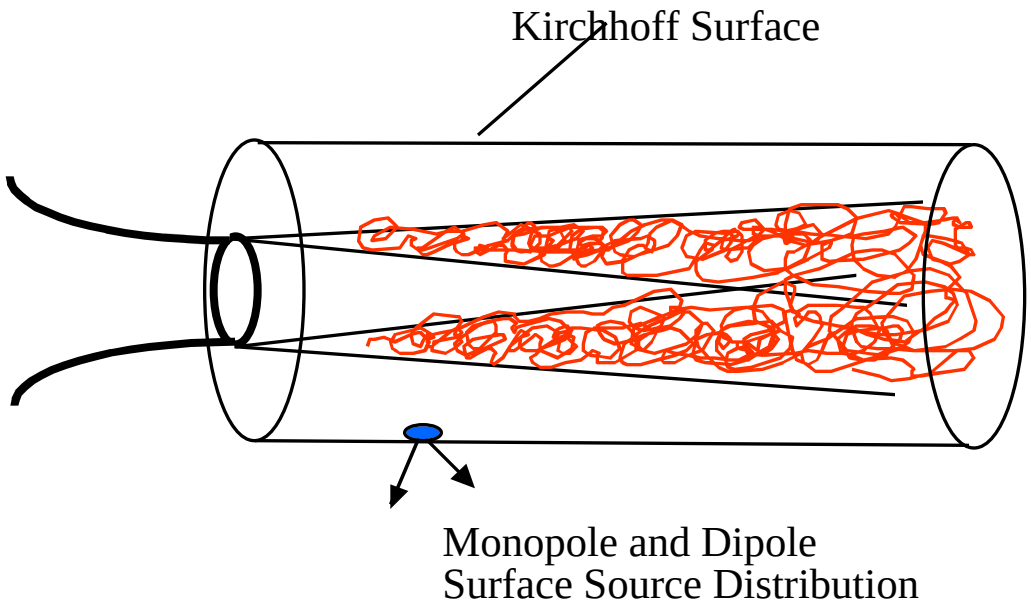
- **Automated Source Breakdown**

  Tester and Fisher (1981), Strange et al(1984)

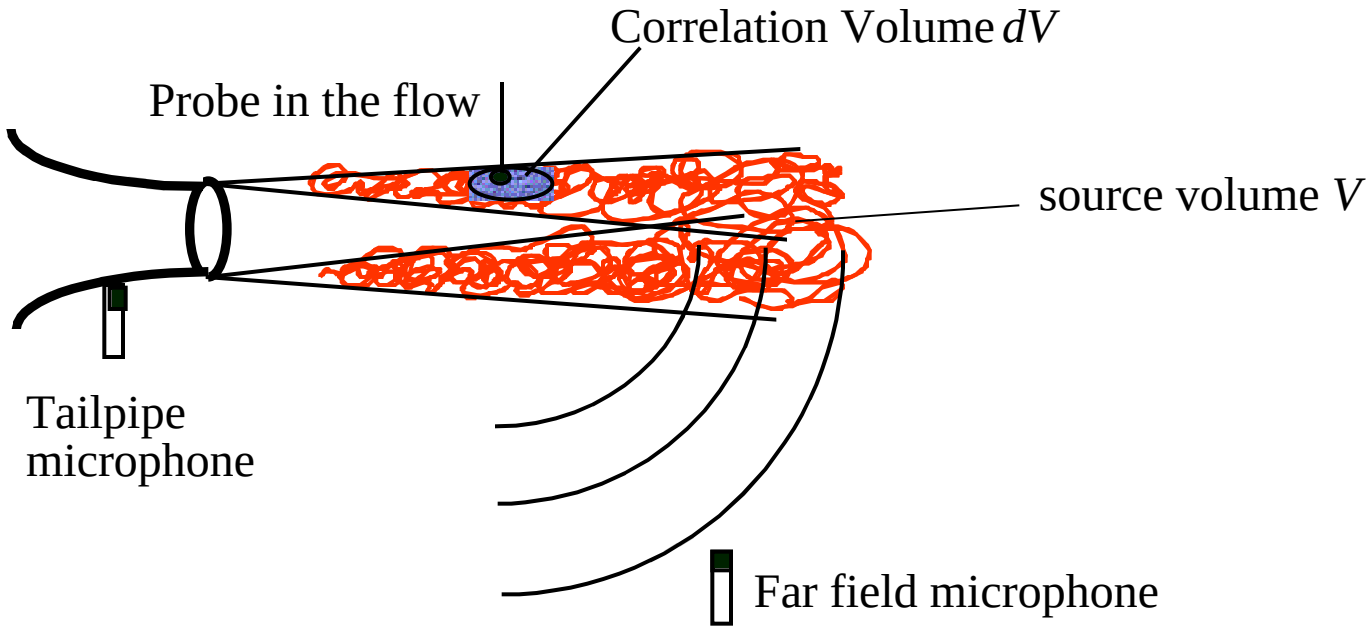
Source Strength

• The only *undisputed* definition of source strength is defined on a Kirchhoff surface enclosing all the sources.

• The issue is how to determine the source distribution inside the surface.



Causality Correlation (Siddon (1971))



- Attempts to correlate the velocity fluctuations in the jet with far field acoustic signature.
- Correlation tends to zero when *dV/V* is small
- Probe noise must be less than noise produced by *dV*
- Has been used successfully to extract tailpipe noise from far field spectra (Shivashankara (1981) Hsu and Ahuja (1998))

Source Location from the Acoustic Field

Non-acoustic inputs

Source Strengths *Source Model*Propagation = Acoustic Field

Estimated Source Strengths = [Source Model*Propagation]$^{-1}$ * Acoustic Measurements

Inverse of source model
(sensitivity to noise can be an issue)

• The value of the *estimated source strengths* depends on the the model chosen to represent the sources and accuracy of the inversion process.

Multipole Nature of Jet Noise

All acoustic source location measurements have simplified the multipole nature of jet noise by using the far field assumption $r>>\lambda$

$$\rho' c_o^2(\mathbf{x},\omega) = -k^2 \int_V T_{rr}(\mathbf{y},\omega)\frac{e^{ikr}}{4\pi r}dV$$

$$\rho' c_o^2(\mathbf{x},\omega) = \int_V q(\mathbf{y},\omega)\frac{e^{ikr}}{4\pi r}dV$$

- q is a model for T_{rr} if the inherent directionality of T_{rr} is constant over the measurement region.

Stochastic Nature of Jet Noise

Since source fluctuations are stochastic we define the far field cross spectrum

$$C_{pp}(\mathbf{x},\mathbf{x}',\omega) = \int_V \int_{V_1} \frac{\pi}{T} Ex[q(\mathbf{y},\omega)q^*(\mathbf{y}_1,\omega)] \frac{e^{ik(r-r_1')}}{(4\pi)^2 r r_1'} dV dV_1$$

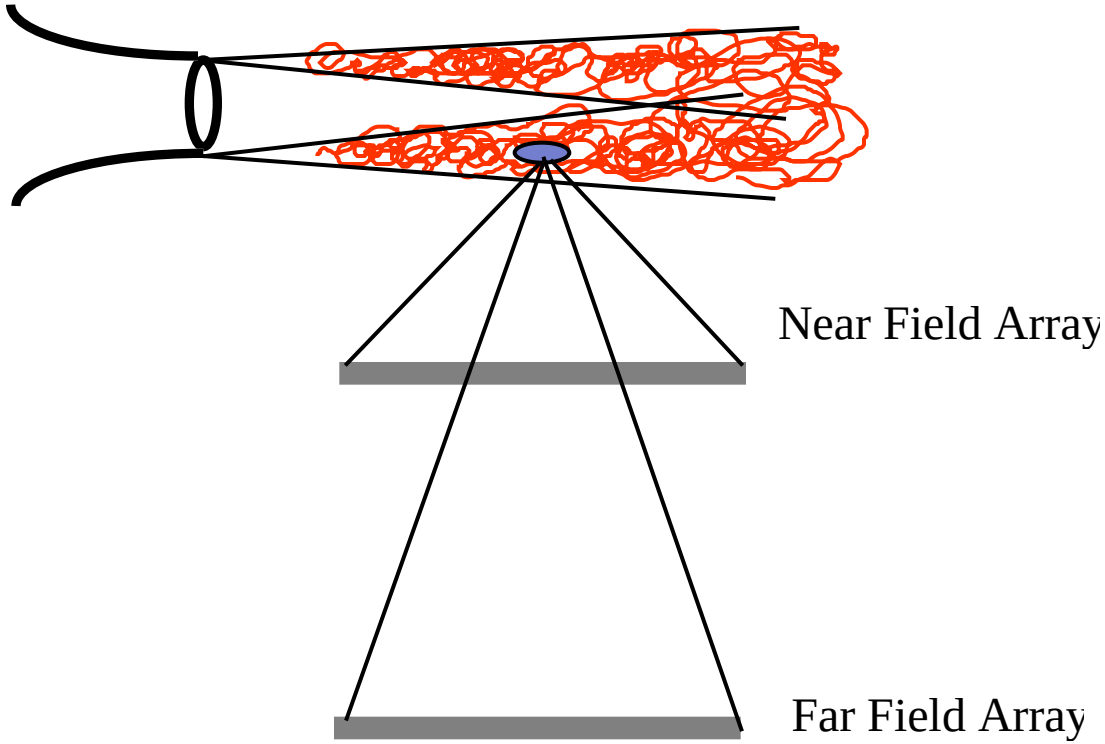
$$= \int_V Q(\mathbf{y},\omega,\mathbf{x}') \frac{e^{ik(r-r')}}{(4\pi)^2 r r'} dV$$

$$Q(\mathbf{y},\omega,\mathbf{x}') = \int_{V_1} \frac{\pi}{T} Ex[q(\mathbf{y},\omega)q^*(\mathbf{y}_1,\omega)] \frac{r' e^{ik(r'-r_1')}}{r_1'} dV_1$$

$$r = |\mathbf{x}-\mathbf{y}| \qquad r_1' = |\mathbf{x}'-\mathbf{y}_1| \qquad r' = |\mathbf{x}'-\mathbf{y}|$$

- Q is directional and depends on the coherence between source fluctuations

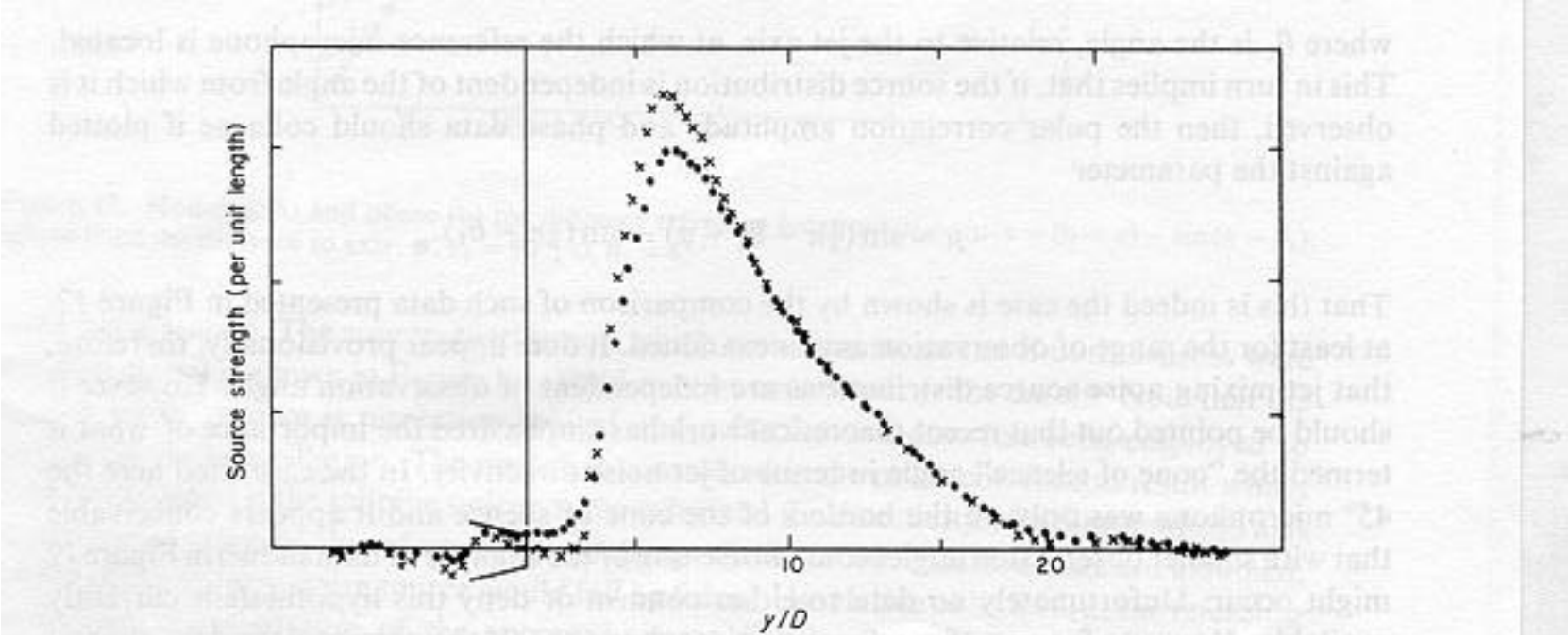
Source Directionality



- The source directionality can be specified as a *bias error* which tends to zero if the measurement aperture is small.
- The primary effect of source directionality is to modify the weightings which are applied to each array element.
- The effect of source directionality is more severe for near field arrays

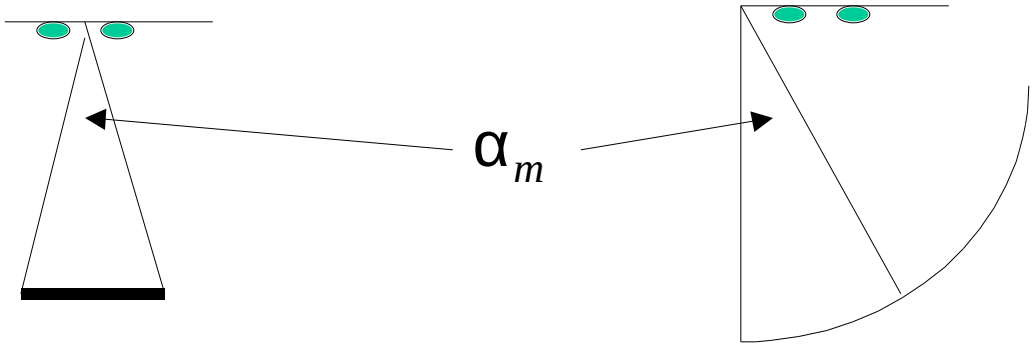
Estimating the Directionality Error

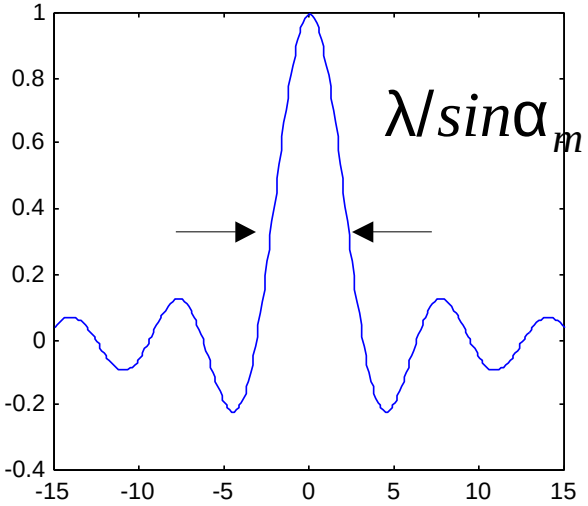
By normalizing the far field array measurements by the measured directionality Harper Bourne showed that the effects were small at 90˚ to the jet.



Array resolution

Array resolution is determined by the angles subtended by the ends of the array and the wavelength





*Jet noise source distributions(*Harper-Bourne*)*

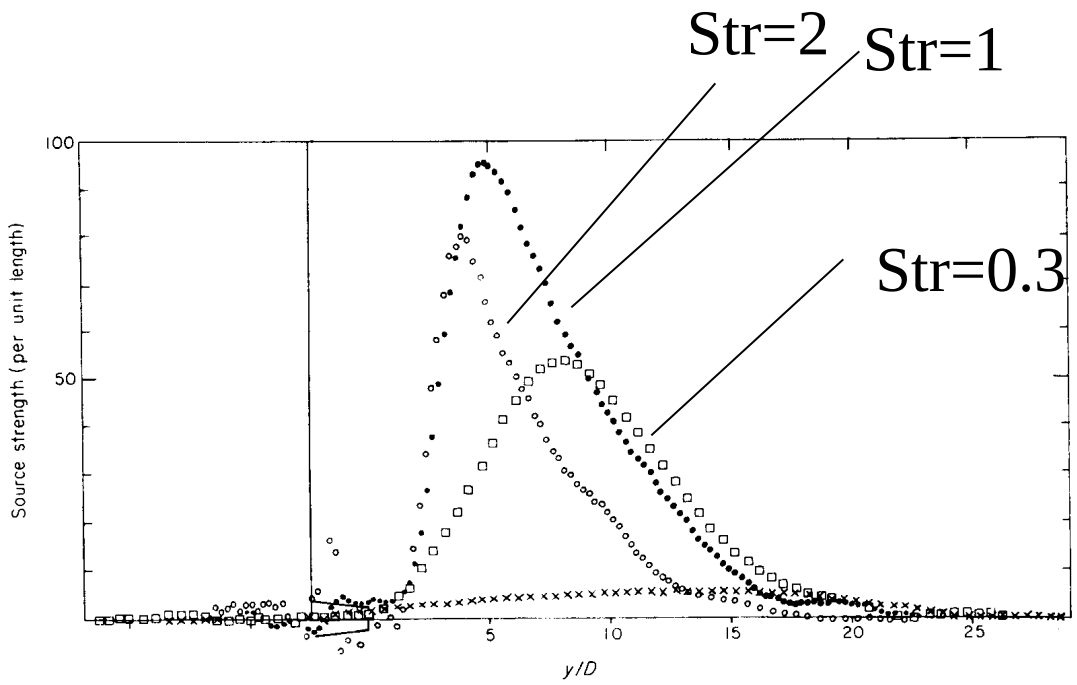
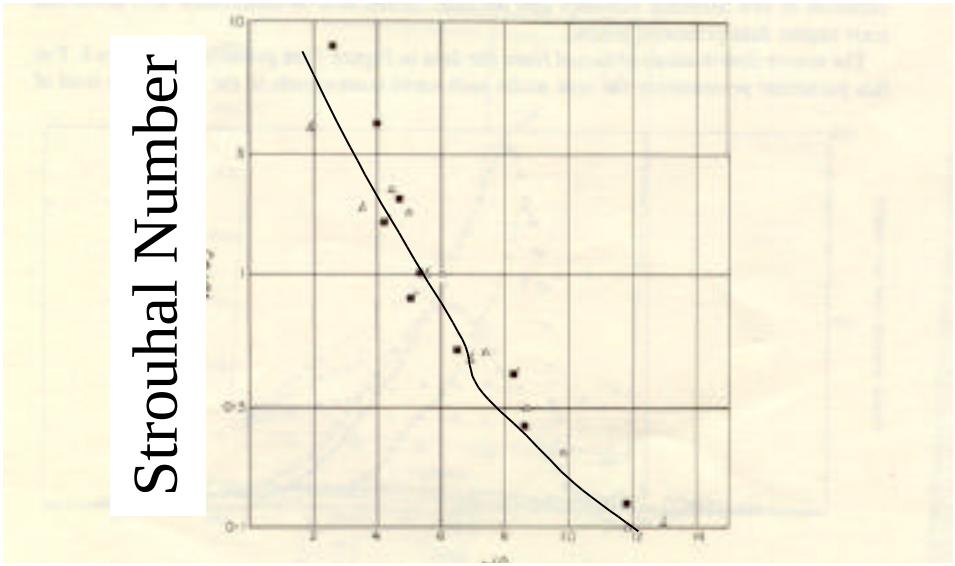


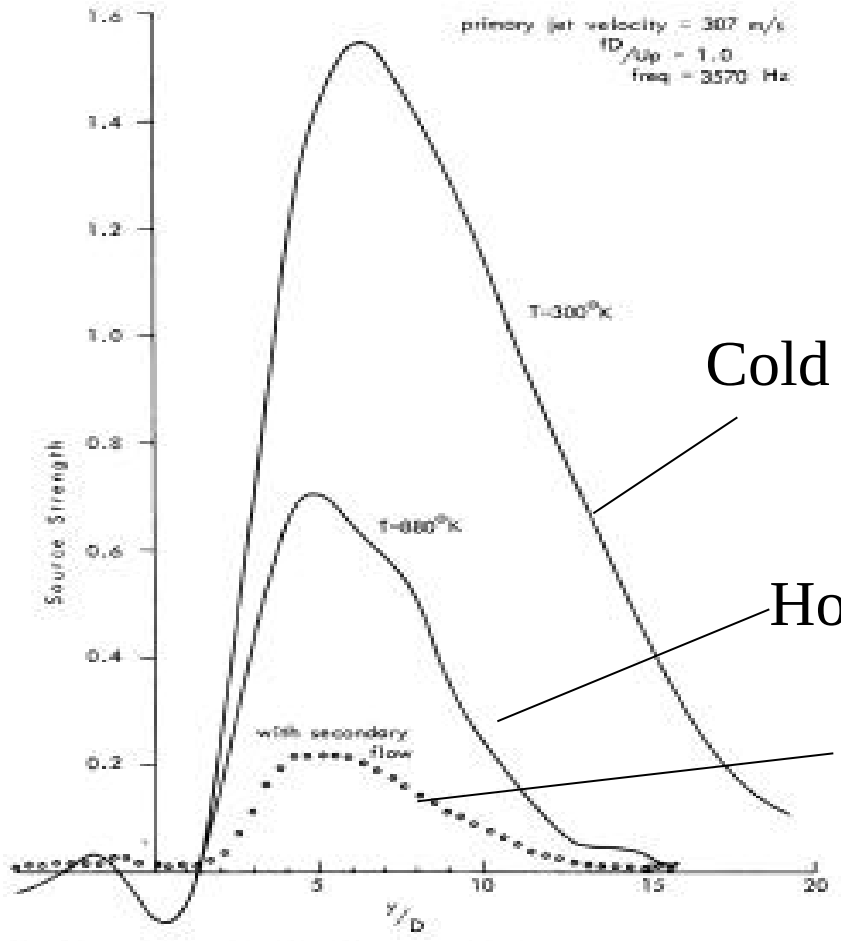
Figure 8. Acoustic source strength per unit slice of jet for various Strouhal numbers. Efflux velocity $U_J = 0{\cdot}8\ a_0$, $D = 25{\cdot}4$ mm, $T_{TOT} = 290°$ K. Values of fD/U_J and λ/D, respectively: ×, 0·1, 12·5; □, 0·3, 4·2; ●, 1, 1·25; ○, 2·16, 0·58.

Source Centroid as a Function of Frequency



• Lilley (1990) compared these measurements with a model based on Lighthills Analogy and found good agreement if corrections were included in his model for the initial thickness of the mixing layer at the nozzle exit.

The Effect of Jet Temperature and Secondary Flow



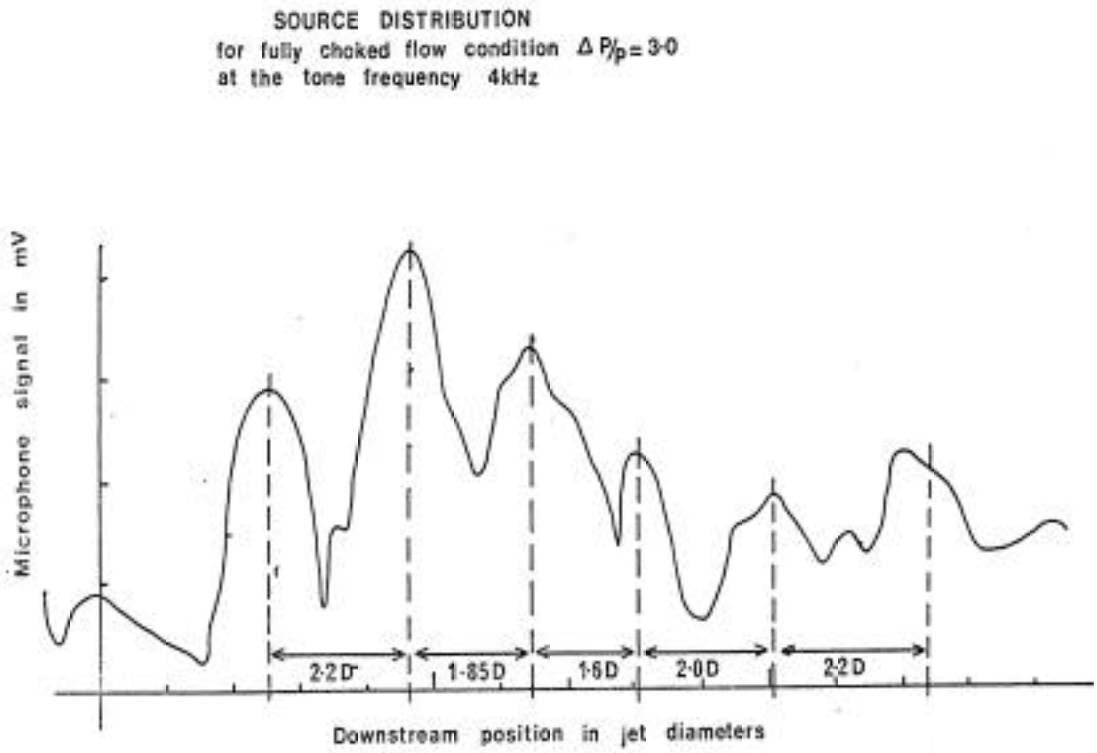
Cold jet

Hot Jet

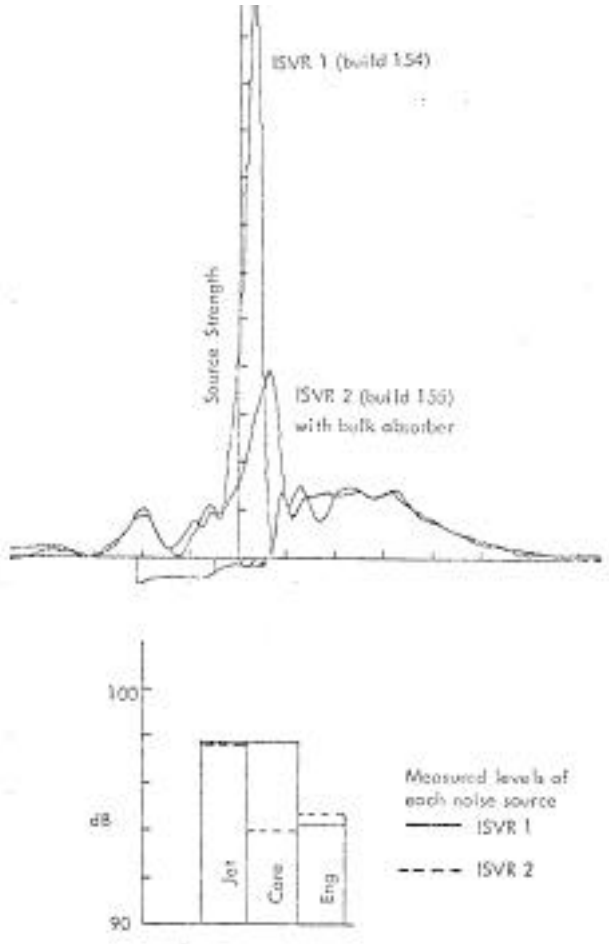
Effect of secondary flow

FIG. 4. RESULTS FROM NOISE TEST FACILITY AT N.G.T.E.

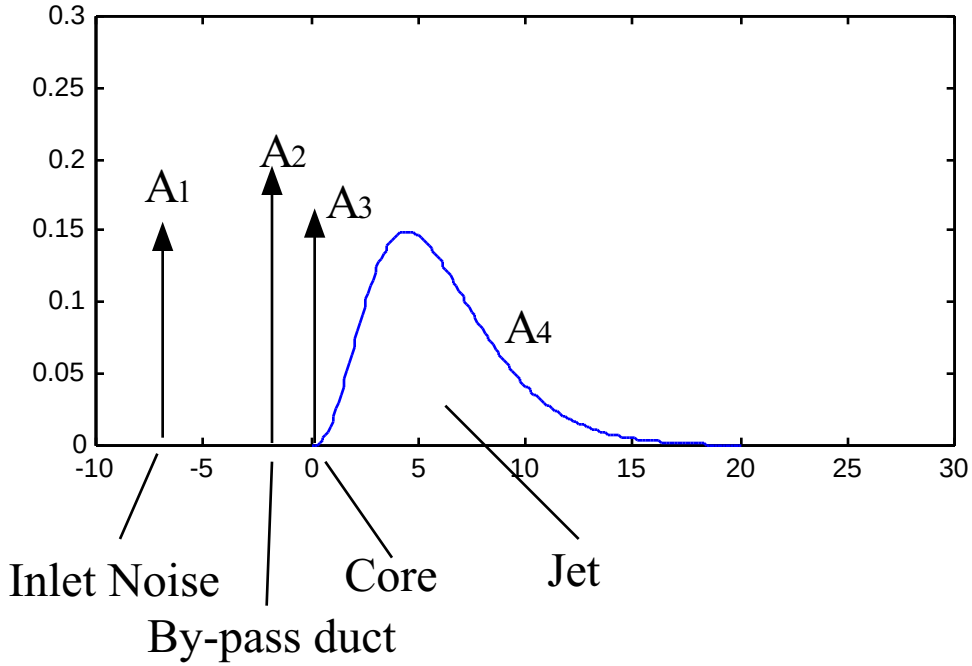
Shock associated noise



Engine Noise Sources



Automated Source Breakdown (Tester and Fisher (1981))

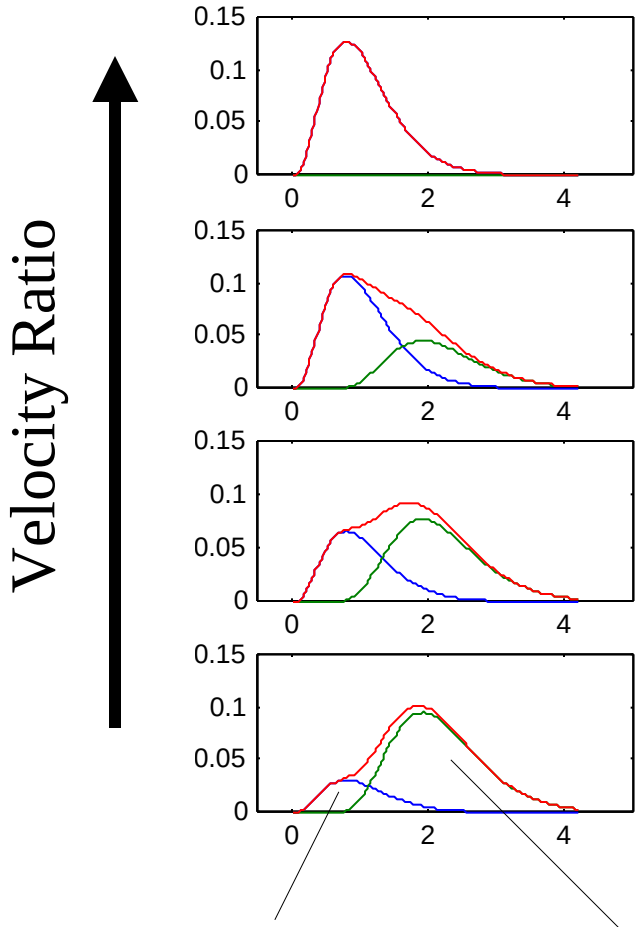


$$C(\mathbf{x},\mathbf{x}',\omega) = \sum_{i=1,2,3} A_i e^{iky_i \sin\alpha} + \frac{A_4}{(1+(iky_c \sin\alpha)/m)^m}$$

$$\sin\alpha = (x_1 - x_1')/|\mathbf{x}-\mathbf{x}'| \qquad |\mathbf{x}-\mathbf{x}'| = \text{constant}$$

- Tester and Fisher(1981) were able to invert this equation without instability problems and generate individual source spectra.

Coaxial Jet Noise (Strange et al (1984))



Strange,Podmore, Fisher and Tester showed that a co-axial jet could have two source distributions, one related to primary jet/ambient mixing and the second with secondary jet/ambient mixing. The importance of each flow, the source distributions and source spectra were presented for both model and full scale applications with flight effects.

Recent Developments

- **Microphone Arrays**

  Harper Boune(1998,1999,2000) , Narayanan(2000)

- **Two Microphone Methods**

  Ahuja et al(1998)

  Showed source centroid moved as expected with turbulence mixing enhancement.

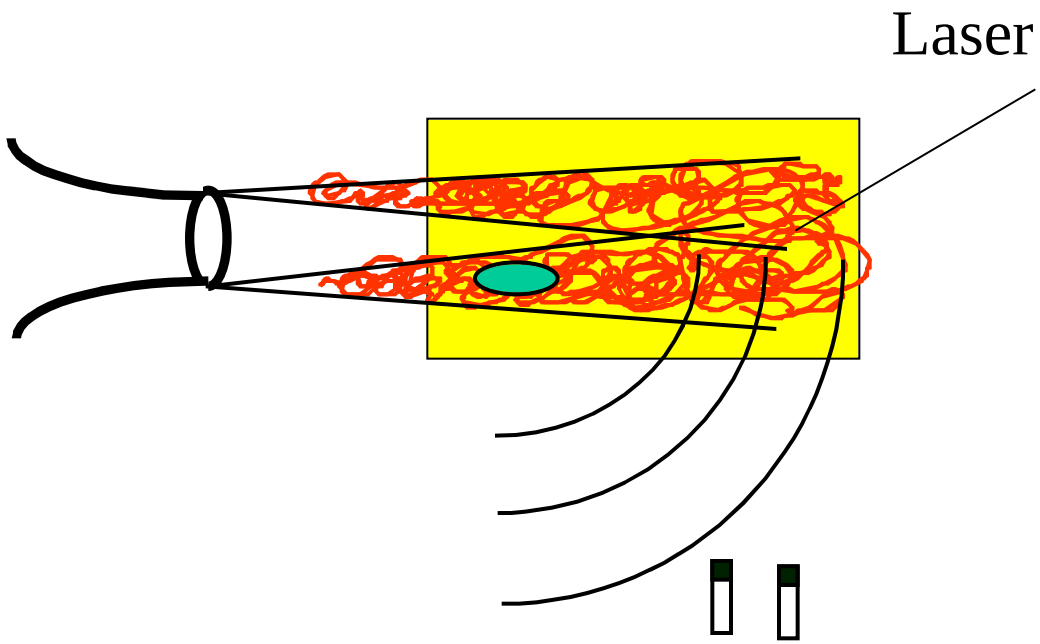
- **Causality Correlation and Coherence Techniques**

  Hsu and Ahuja(1998), *Extracted tailpipe noise source from spectra*

  Gui et al (1998), *Attempted to identify coherent structures by educing signals from probe in the flow based on far field acoustic measurements.*

  Hileman and Samimy(2000)

Hileman and Samimy(2000), *Used a laser light sheet to capture the flow and attempted to relate peaks in the far field signature with large eddies. Some interesting results reported, ongoing study.*

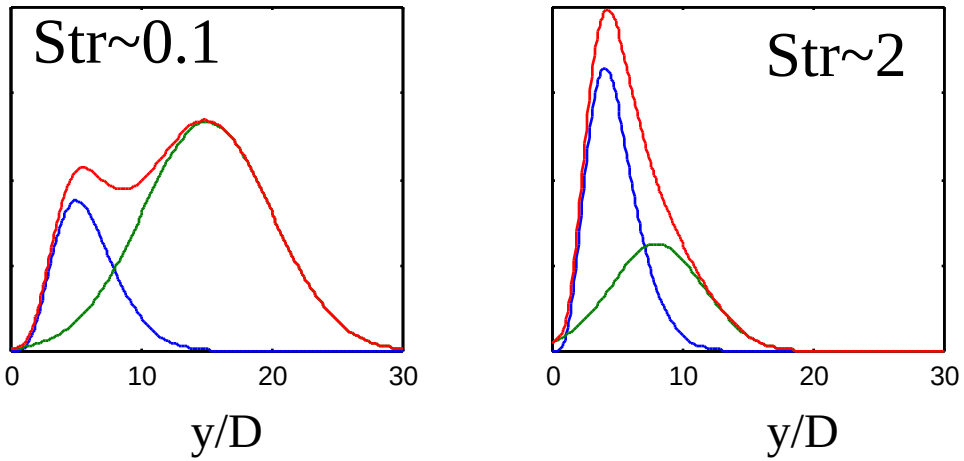


Using Source Distributions to Predict Near Field Jet Noise
Harper Bourne (1998,1999,2000)

•To predict near field jet noise it is necessary to know the spatial distribution of noise sources.

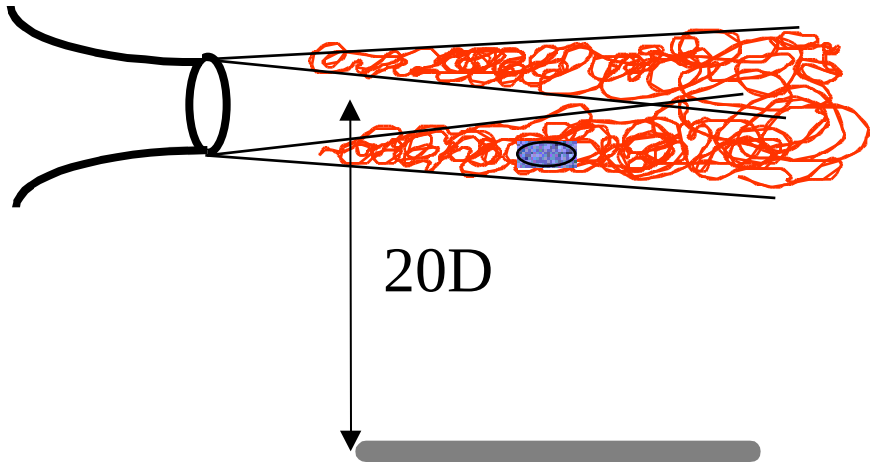
• Source distributions were determined to have two separate parts. The upstream source was associated with the mixing region and the downstream source with the fully developed flow.

•Nozzle exit flow was found to be an issue with the source distribution required for prediction



Phased Array Study:

Narayanan et al (2000), Venkatesh et al (2000), Simmonich et al (2000)



Phased Array

- Adaptive processor used to give resolution of 5D at all frequencies
- Compared source location results with flow measurements

Phased Array Study:

Narayanan et al (2000), Venkatesh et al (2000), Simmonich et al (2000)

- Source distributions were reported to be of a smaller axial extent than previous results.
- Hot jets had sources located further downstream than cold jets.
- The flow and source location measurements highlighted the differences between the source positions assumed in the MGB jets noise model based on RANS calculations ($4<y/D<12$) and the measured source distribution($y/D<6$ at high frequencies).
- MGB turbulence model only applies at $y/D>10$.

NASA/CP—2001-211152

Modern Array Processing Methods

Modern Signal Processing Techniques

$$p(\mathbf{x}_m) = \int q(\mathbf{y}) G(\mathbf{x}_m \mid \mathbf{y}) dV$$

$$p_m = \sum_n G_{mn} q_n$$

$$C_{mj} = \frac{\pi}{T} Ex[p_m p_j^*] = \sum_n \sum_k G_{mn} G_{jk}^* Q_{nk}$$

$$Q_{nk} = \frac{\pi}{T} Ex[q_n q_k^*]$$

$$\mathbf{C = G Q G^H}$$

$$\mathbf{Q_{meas} = G_{inv}\ C\ (G_{inv})^H} \qquad \mathbf{G_{inv} \sim G^{-1}}$$

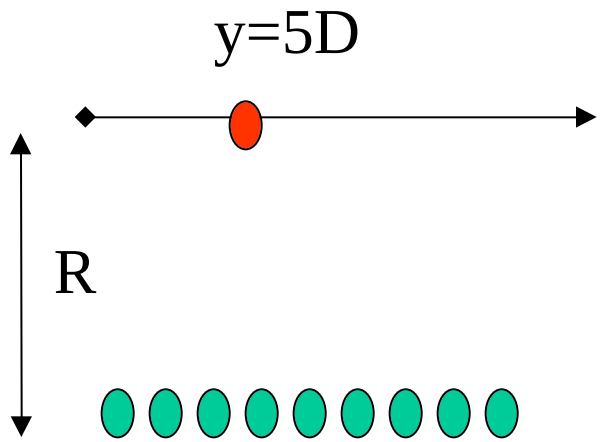
- Choosing the correct inversion scheme *can* improve results
- Geometry of the array defines G and is not necessarily constrained

Alternative Approaches

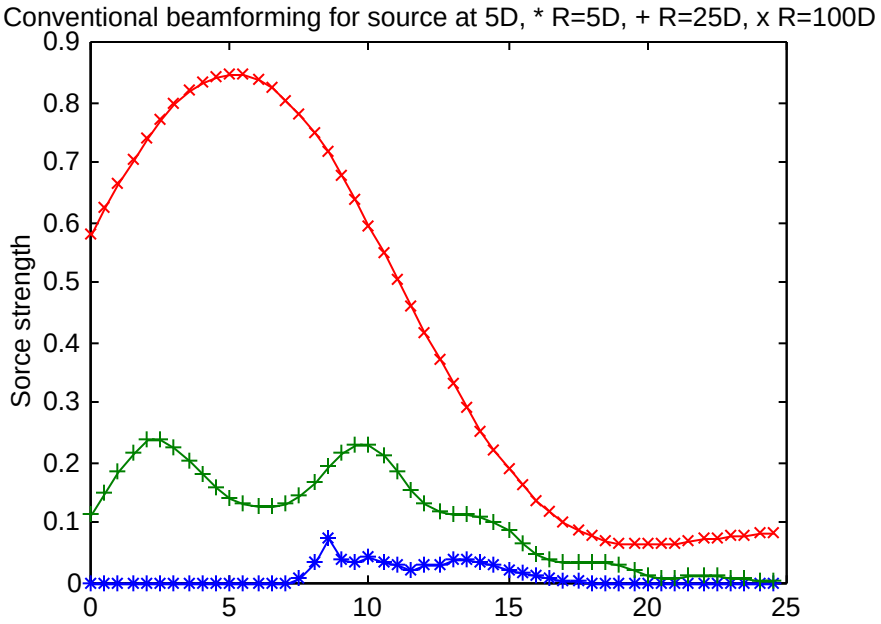
Method	*G_{inv}*
Polar Correlation ($(\mathbf{G}_{inv})^{H}$ sparse)	
Acoustic Telescope	Specified analytically
Conventional Beamforming	
Automated Source Breakdown	Found iteratively from a constrained parameter set
Minimum Variance	Determined from **C**
CLEAN	Iterates to eliminate loudest sources

Estimating the Source Distribution using Conventional Beamforming

$$\mathbf{G}_{inv} = exp(-ikyx_m / R)$$



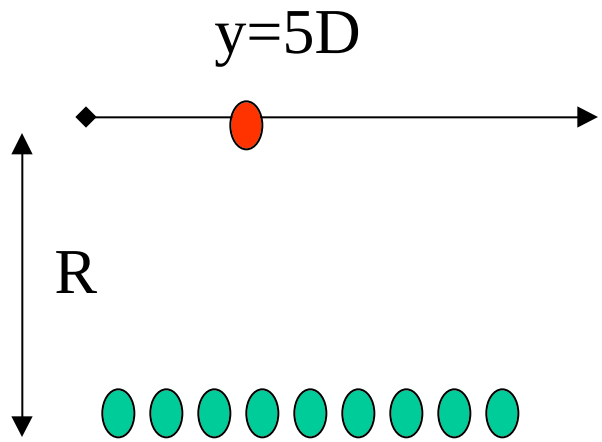
Str=0.3 M=0.9



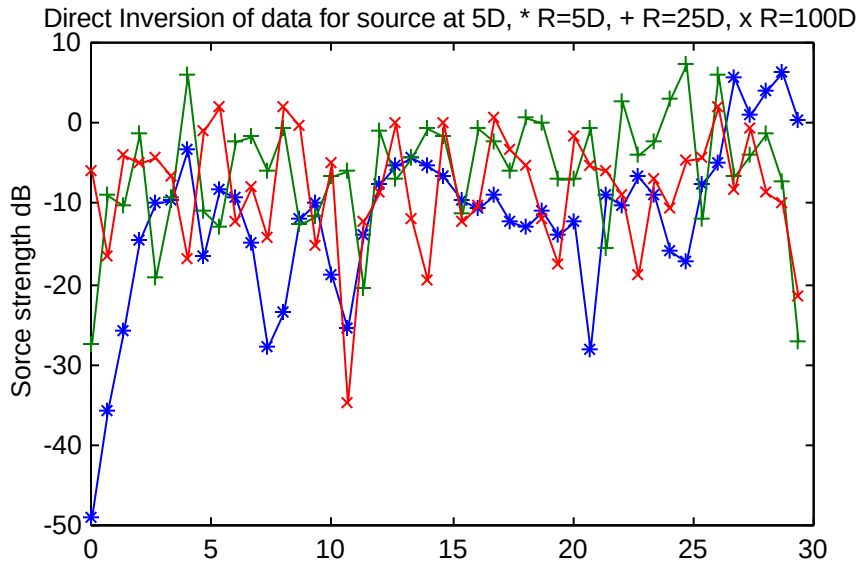
Conventional beamforming for a linear array at R=5,25,100D

Estimating the Source Distribution from Least Squares Inversion of Cross Spectrum Matrix

$$\mathbf{G}_{inv}=(\mathbf{G}^{H}\mathbf{G})^{-1}\mathbf{G}^{H}$$



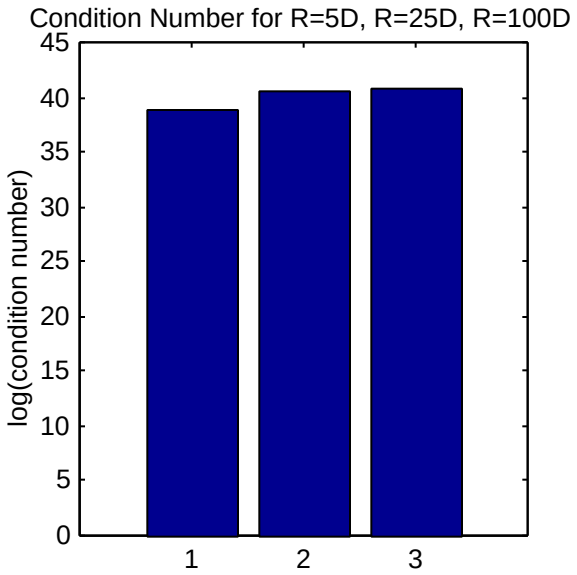
Str=0.3 M=0.9



Least Squares inversion for a linear array at R=5,25,100D

Condition Number κ

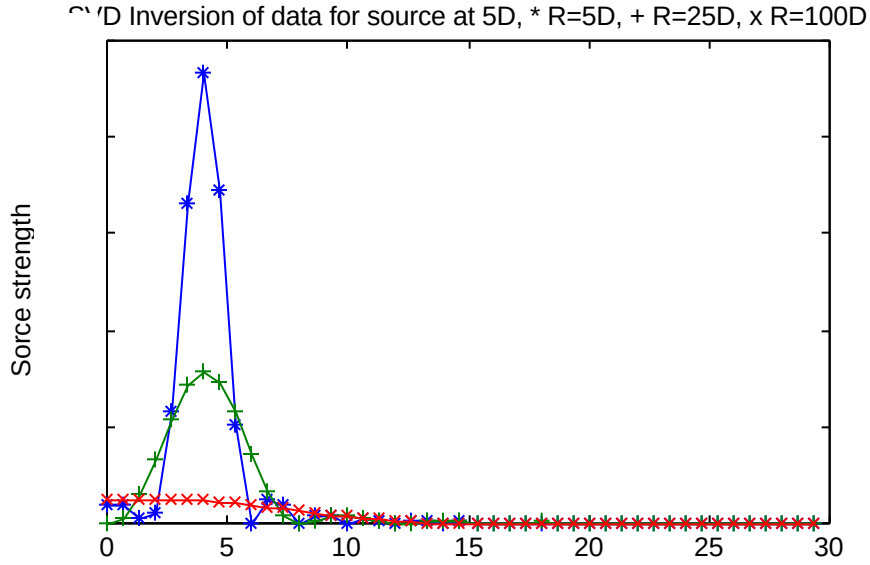
$$\frac{\|\delta \mathbf{Q}\|}{\|\mathbf{Q}\|} = \kappa \frac{\|\delta \mathbf{p}\|}{\|\mathbf{p}\|}$$



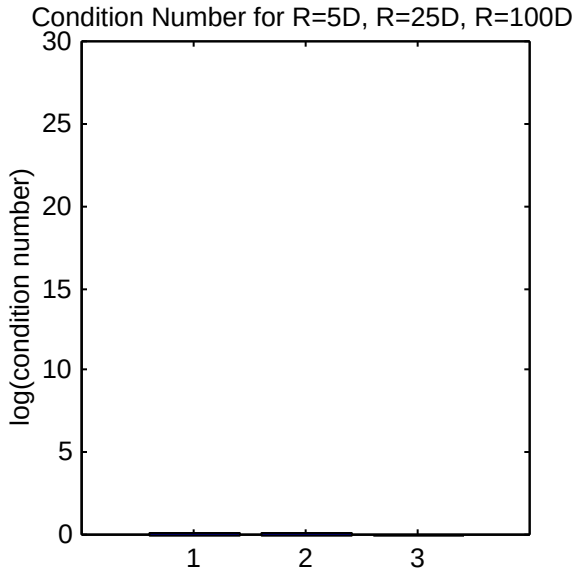
Estimating the Source Distribution using Singular value Decomposition and Tikonov Regularization(Nelson (1999))

The singular values of the inverted **G** *matrix are eliminated so that the matrix becomes well conditioned and noise is reduced using eigenvectors of cross spectral matrix* **C**

SVD inversion for a linear array
at R=5,25,100D (Stable estimate)

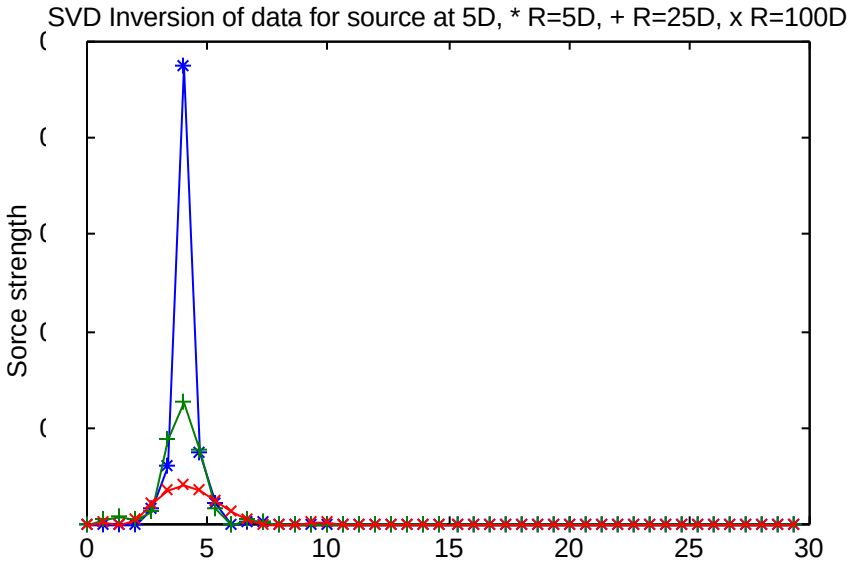


Condition Number κ~*1*
10dB of noise added

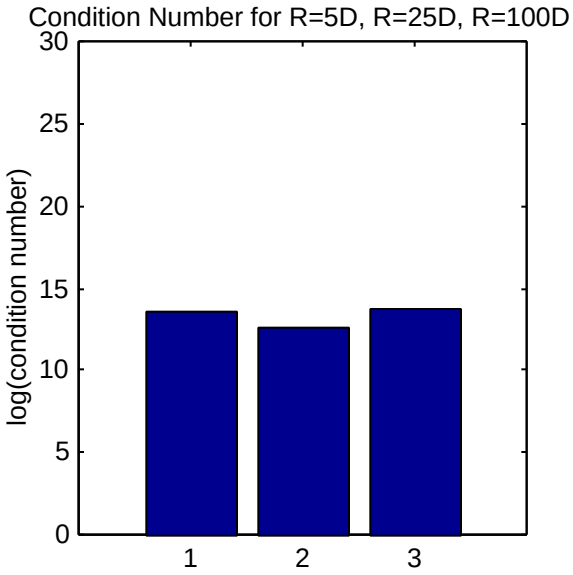


Condition number can be adjusted using Tikonov regularization

SVD inversion for a linear array
at R=5,25,100D (Less stable estimate)



Condition Number κ~10^6
10dB of noise added



Modal Decompositon of Source Strength

Glegg and Devenport (2000)

For any stochastic source distribution

$$q(\mathbf{y},\omega) = \sum_m a_m q^{(m)}(\mathbf{y},\omega)$$

$$\frac{\pi}{T} Ex[q(\mathbf{y}) q^*(\mathbf{y}_1)] = \sum_m \lambda_m q^{(m)}(\mathbf{y}) \left(q^{(m)}(\mathbf{y}_1)\right)^*$$

$$C_{pp}(\mathbf{x},\mathbf{x}',\omega) = \sum_m \lambda_m \left(\int_V q^{(m)}(\mathbf{y}) \frac{e^{ikr}}{4\pi r} dV \right) \left(\int_{V_1} q^{(m)}(\mathbf{y}_1) \frac{e^{ikr_1'}}{4\pi r_1'} dV_1 \right)^*$$

- $q^{(m)}(\mathbf{y})$ are the distributions of correlated sources
- Can we use advanced signal processing methods to determine the details of the correlation regions??

Conclusions and Recommendations

- The two source model for jet noise source distributions has been shown to be important for prediction.
- Parametric source breakdown approaches have given new insight.
- The effect of nozzle exit flow conditions has been identified as affecting the source distributions, but has not been measured in detail
- More needs to be done with non-intrusive flow probes and far field arrays.
- Determining the details of the acoustic source correlation structure will give new insight into the mechanisms of sound generation.

S. Glegg References

Array Processing methods

1. R.P. Dougherty and Robert W. Stoker, “Sidelobe suppression for phased array aeroacoustic measurements”, AIAA 98-2242, 4th AIAA/CEAS Aeroacoustics Conference, Toulouse, France, June 1998.

2. S. R. Venkatosh, D. R. Polak, and S. Narayanan “Phased array design, validation and application to jet noise source localization” AIAA 2000-1934.

3. S. Oerlemans and P. Sijtsma “Effects of wind tunnel side plates on airframe noise measurements with phased arrays” AIAA 2000-1938, AIAA/CEAS Aeroacoustic Conference, Lahainia, June 2000.

4. M. Mosher “Phased arrays for aeroacoustic testing – theoretical development” 2nd AIAA/CEAS Aeroacoustic conference, State College, PA, May 1996.

5. J. Hayes, W. Horne, S. Jaeger, and P. Soderman, “Measurement of Reynolds Number effect on airframe noise in the 12 ft pressure wind tunnel” AIAA 99-1959, AIAA/CEAS Aeroacoustics conference, Seattle, May 1999.

6. P. Sjitsma and H. Holthusen “Source location by phased array measurements in closed wind tunnel test sections” AIAA 99-1814, AIAA/CEAS Aeroacoustics conference, Seattle, May 1999.

7. J. Piet, G. Elias and P. Lebigot “Localization of acoustic source from a landing aircraft with a microphone array” AIAA 99-1811, 5th AIAA/CEAS Aeroacoustic conference, Seattle, May 1999.

8. T. Brooks, W. Humphrey, and W. Hunter, “Effect of directional array size on measurement of airframe noise components” AIAA 99-1958, AIAA/CEAS Aeroacoustic conference, Seattle, May 1999.

9. P.Nelson, "Some inverse problems in acoustics", 5th International Congress on Sound and Vibration, July 1999.

10. Mosher, M. AIAA 97-1678, Atlanta.

11. W. C. Horne, J. A. Hayes, S. M. Jaeger and S. Jovic “Effects of distributed source coherence on the response of phased acoustic arrays” AIAA 2000-1935.

Flow/acoustic correlations

1. T.E. Siddon, "Noise source diagnostics using causality correlation", AGARD CP 131, 1973.

2. H.K. Lee and H.S. Ribner, "Direct correlation of noise and flow of a jet", JASA, Vol 52(5), pt.1 1972, pp 1280-1290.

3. J.S. Hsu and K.K. Ahuja, “A coherence based technique to separate ejector internal mixing noise from far field measurements”, AIAA 98-2296, 4th AIAA/CEAS Aeroacoustics Conference, Toulouse, France, June 1998.

4. G. Gui, R. Camussi, M. Carley, A. Ragni, T.D. D’Alessio, and M. Bosi, “Pressure conditioning for coherent structure identification in a turbulent jet”, AIAA 98-2358, 4th AIAA/CEAS Aeroacoustics Conference, Toulouse, France, June 1998.

5. J. Hileman and M. Samimy “An attempt to identify noise generating structures in high speed axisymmetric jet” AIAA 2000-2020, AIAA/CEAS Aeroacoustic Conference, Lahainia, June 2000.

6. J.F. Piet and G. Elias, “Airframe noise source localization using a microphone array”, AIAA 97-1643, 3rd AIAA/CEAS Aeroacoustics Conference, June 1997.

7. R.A. Gramann and J. Mocio, “Aero-acoustic measurements in wind tunnels using conventional and adaptive beamforming methods”, “Sidelobe suppression for phased array aeroacoustic measurements”, AIAA 93-4341.

8. B.N. Shivashankara, “High by-pass ratio engine noise component separation by coherence technique”, AIAA 81-2054.

Two microphone methods

1. K. K. Ahuja, K. C. Massey, M. S. D’Agosino, “A simple technique of locating noise sources of a jet under simulated forward motion” AIAA 98-2359, 4th AIAA/CEAS Aeroacoustics conference, June 1998, Toulouse, France.

2. S.P. Parthasarathy, "Jet Noise Source Location by cross correlation of far filed microphone signals", AIAA paper no. 75-456, 1975.

3. R. Kinns, Jnl of Sound and Vibration, 44(2), 1976, p. 275.

Array measurements

1. M.J. Fisher, M. Harper-Bourne and S.A.L. Glegg, "Jet Noise source location: The polar correlation technique", Jnl of Sound and Vibration, 51, 1977.

2. S.A.L. Glegg, "Jet Noise Source Location", Ph.D. Thesis, University of Southampton, 1979.

3. S.A.L. Glegg, "The accuracy of source distributions measured by using polar correlation", Jnl of Sound and Vibration, 80(1), 1982, pp31-40.

4. M.J. Fisher and S.A.L. Glegg, Conference on Time Series Analysis, Southampton, September l977, "Source Location."

5. J. Billingsley and R. Kinns, "The acoustic telescope", Jnl of Sound and Vibration, 48,1976.

6. J. Billingsley, "A comparison of the source location techniques of the acoustic telescope and polar correlation", Jnl of Sound and Vibration, 61,1978.

7. L. Maestrello, "On the relationship between acoustic energy density flux near the jet and far filed acoustic intensity" AIAA paper no 73-988, Seattle, 1973.

8. P.J.R. Strange, G. Podmore, M.J. Fisher and B.J. Tester, “Co-axial jet noise source distributions””, AIAA 84-2361, AIAA Aeroacoustics Conference, 1984.

9. B.J. Tester and M.J. Fisher, “Engine noise source breakdown: theory, simulation and results”, AIAA 81-2040, AIAA Aeroacoustics Conference, 1981.

10. P.M.W. Pack and P.J.R. Strange, “Recent Developments in Source Location”, AIAA 87-2685, AIAA Aeroacoustics Conference, Palo Alto CA, 1987.

11. J. C. Simonich, S. Narayanan and T. J. Barber: High Subsonic Jet Experiments: Aeroacoustic characterization, noise reduction and dimensional scaling effects” AIAA, 2000-2022.

12. S. Narayanan, T. J. Barber, D. R. Polak “High Subsonic Jet Experiments Part II: Turbulence and noise generation studies” AIAA 2000-2023.

Acoustic Mirrors

1. F_R Grosche, "Distributions of sound source intensities in subsonic and supersonic jets" AGARD CP-131, 1973.

2. W.T. Chu J. Laufer and K. Kao, "Noise source distribution in subsonic jets", Proceedings of Inter-Noise 72, 1972.

3. J. Laufer, R. Schlinker and R.E. Kaplan, "Experiments on supersonic jet noise", AIAA Jnl. Vol 14. 1976, pp 489-497.

4. S.A.L. Glegg, "The location of Jet Noise Sources using an acoustic mirror", M.Sc. Thesis, University of Southampton, 1975.

Source Identification

and

Location Techniques

Donald Weir
Honeywell

James Bridges and Femi Agboola
NASA Glenn Research Center

Robert Dougherty
Boeing

***Source Identification and Location Techniques* - Donald Weir, Honeywell and James Bridges, Femi Agboola, NASA Glenn Research Center and Robert Dougherty, Boeing summarized by Eugene Krejsa as summarized by Eugene Krejsa.**

Mr. Weir presented source location results obtained from an engine test as part of the Engine Validation of Noise Reduction Concepts program. Two types of microphone arrays were used in this program to determine the jet noise source distribution for the exhaust from a 4.3 bypass ratio turbofan engine. One was a linear array of 16 microphones located on a 25 ft. sideline and the other was a 103 microphone 3-D "cage" array in the near field of the jet. Data were obtained from a baseline nozzle and from numerous nozzle configuration using chevrons and/or tabs to reduce the jet noise.

Mr. Weir presented data from two configurations: the baseline nozzle and a nozzle configuration with chevrons on both the core and bypass nozzles. This chevron configuration had achieved a jet noise reduction of 4 EPNdB in small scale tests conducted at the Glenn Research Center. IR imaging showed that the chevrons produced significant improvements in mixing and greatly reduced the length of the jet potential core.

Comparison of source location data from the 1-D phased array showed a shift of the noise sources towards the nozzle and clear reductions of the sources due to the noise reduction devices. Data from the 3-D array showed a single source at a frequency of 125 Hz. located several diameters downstream from the nozzle exit. At 250 and 400 Hz., multiple sources, periodically spaced, appeared to exist downstream of the nozzle. The trend of source location moving toward the nozzle exit with increasing frequency was also observed. The 3-D array data also showed a reduction in source strength with the addition of chevrons. The overall trend of source location with frequency was compared for the two arrays and with classical experience. Similar trends were observed. Although overall trends with frequency and addition of suppression devices were consistent between the data from the 1-D and the 3-D arrays, a comparison of the details of the inferred source locations did show differences. A flight test is planned to determine if the hardware tested statically will achieve similar reductions in flight.

The following conclusions were made by Mr. Weir:

- IR imaging is effective in confirming that chevrons produce increased core flow mixing.
- The improvement in core/fan mixing results in significant noise reduction.

- Both 1-D and 3-D array measurement techniques were successful in identifying noise source locations.
- Source location data from this test program confirms the classical semi-empirical location model.

In the discussion following the presentation, the observation was made that the microphones in the 3-D array are in the acoustic and geometric near fields. Thus the point source and far field assumptions used to derive the steering vectors are not appropriate for the 3-D array. The comment was made that acoustic holography does allow for the microphones to be in the near field.

Honeywell

Honeywell Engines and Systems
Engine Validation of Noise Reduction Concepts

AeroAcoustics Research Consortium
Jet Noise Workshop

Source Identification and Location Techniques

Donald Weir
(602) 231-1214
James Bridges and Femi Agbooli (NASA Glenn)
Robert Dougherty (Boeing)
November 8, 2000

Outline

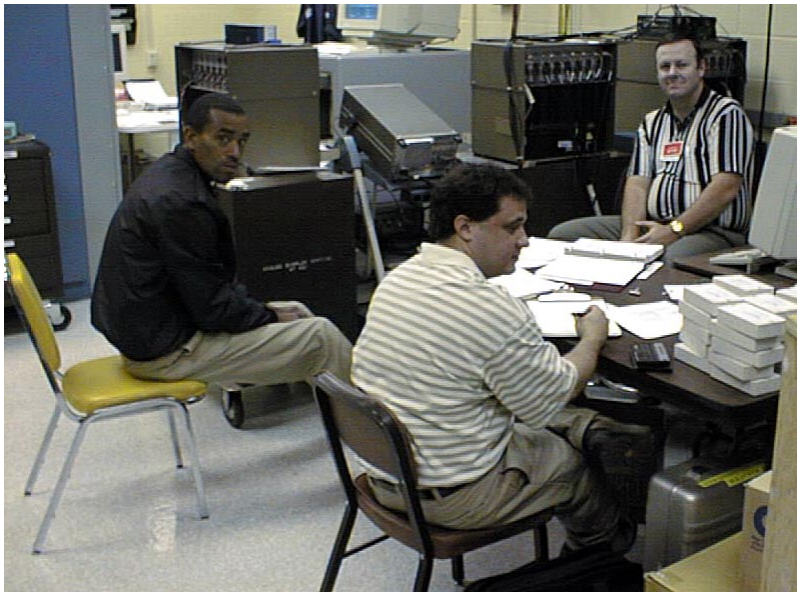
- Test Description
- Far Field Noise
- 1-D FF Array
- 3-D NF Array
- Comparisons
- Conclusions



Honeywell EVNRC - Some Statistics

- Engine Starts: 187
- Engine Hours: 136
- Far Field Test Points: 374
- Test Configurations: 157
- Digital Photographs: 683

- Organizations: 7
- Test Site Visitors: 24
- Microphones: 292
- 28-Channel Tapes: 25
- Far Field Spectra: 11,968

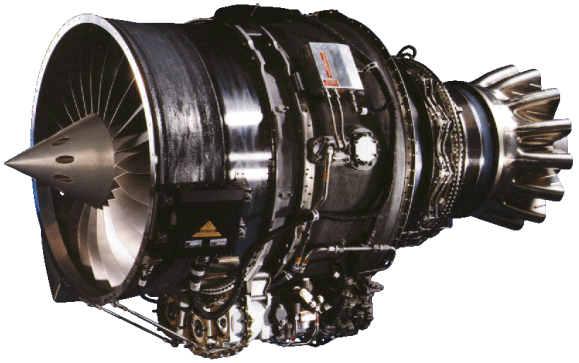




Engine Description

TFE731-60 Turbofan Engine

- Takeoff, Sea Level, Static Thrust = 5000 lb
- Takeoff Bypass Ratio = 4.3
- Cycle Pressure Ratio = 22
- Geared Fan Pressure Ratio = 1.70
- Fan Blades = 22
- Fan Exit Vanes = 52



- Engine is currently certified on the Dassault Falcon 900EX
- Part of the TFE731-20/40/60 engine family that also powers
  - Learjet 45
  - IAI Astra SPX
  - Dassault Falcon 50EX
  - Hawker 450



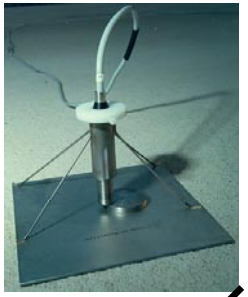
Honeywell

Honeywell Outdoor Acoustic Test Facility

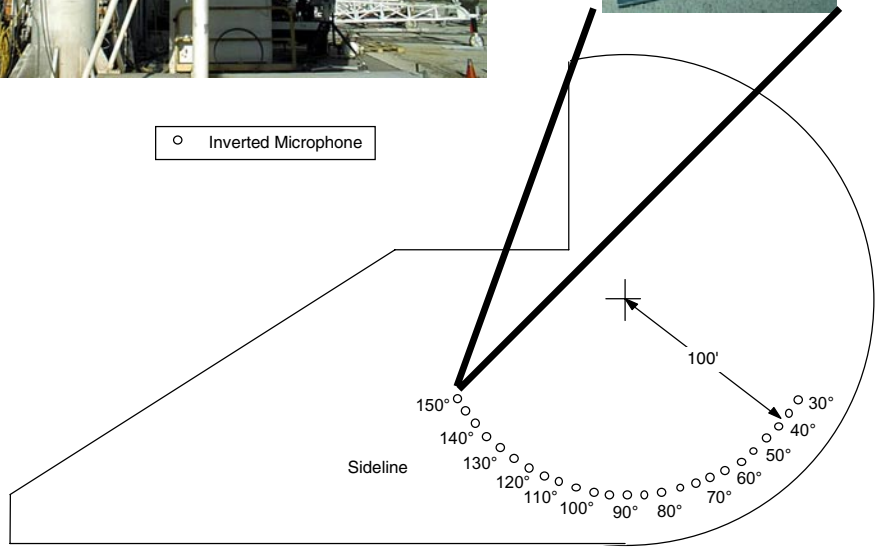
- SAE ARP 1846 Standard
- FAA Approved







- **Large acoustically reflecting surface**
- **Minimum interference test stand**
- **Instrumentation for weather measurements**
- **Engine inflow control device (ICD)**
- **Polar arc and sideline noise measurements**
- **Low ambient noise levels**



Honeywell

Various Core and Bypass Nozzle Configurations

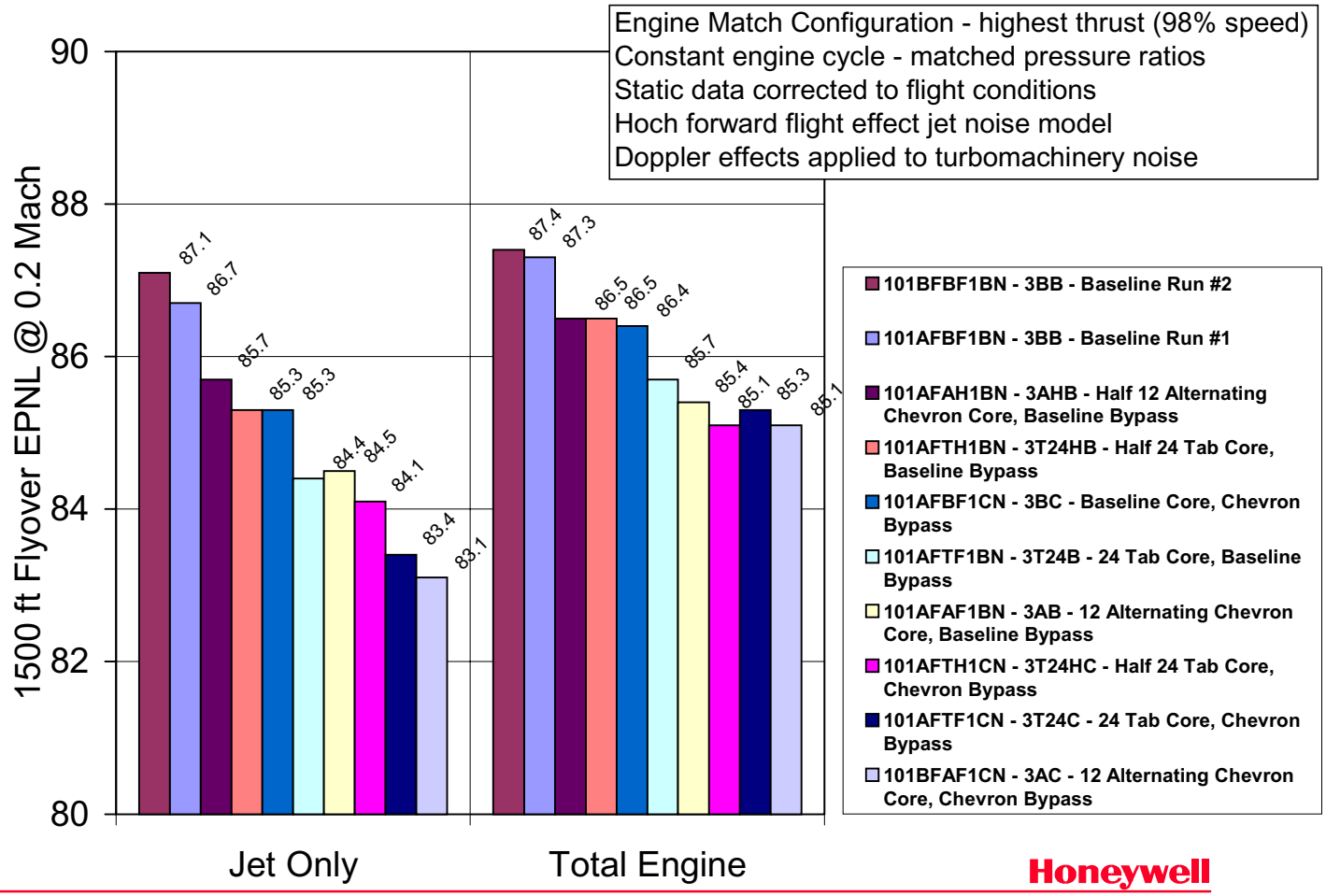
Core Nozzles



Bypass Nozzles

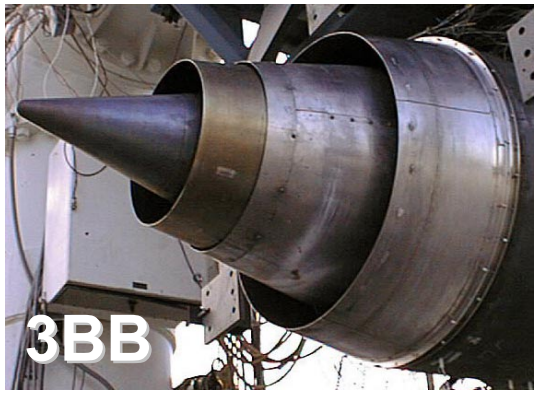


Significant EPNL benefit measured - confirmed results from NASA Glenn rig test

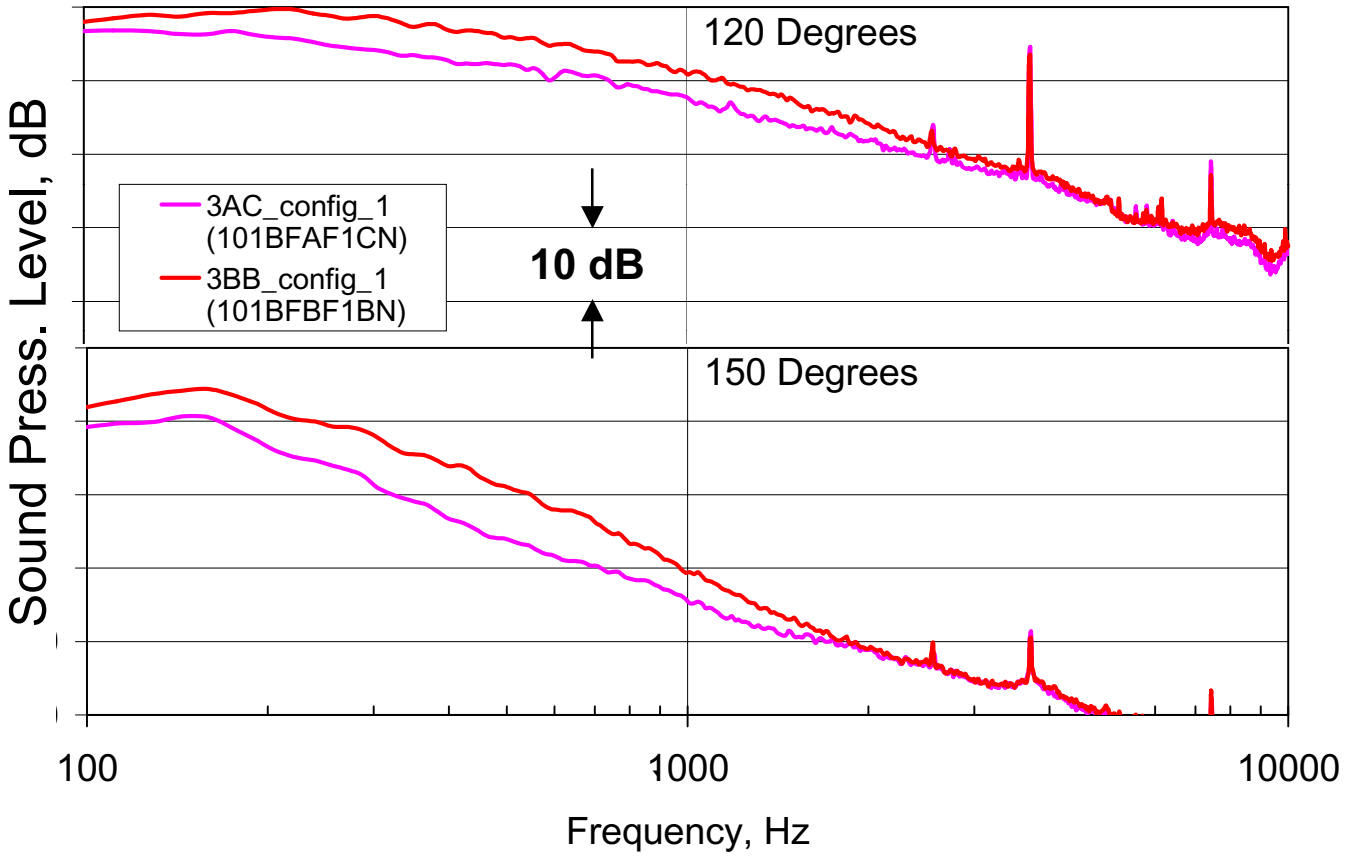


Focus on Two Nozzle Configurations...

...At the highest thrust setting (1070 fps mixed jet velocity)



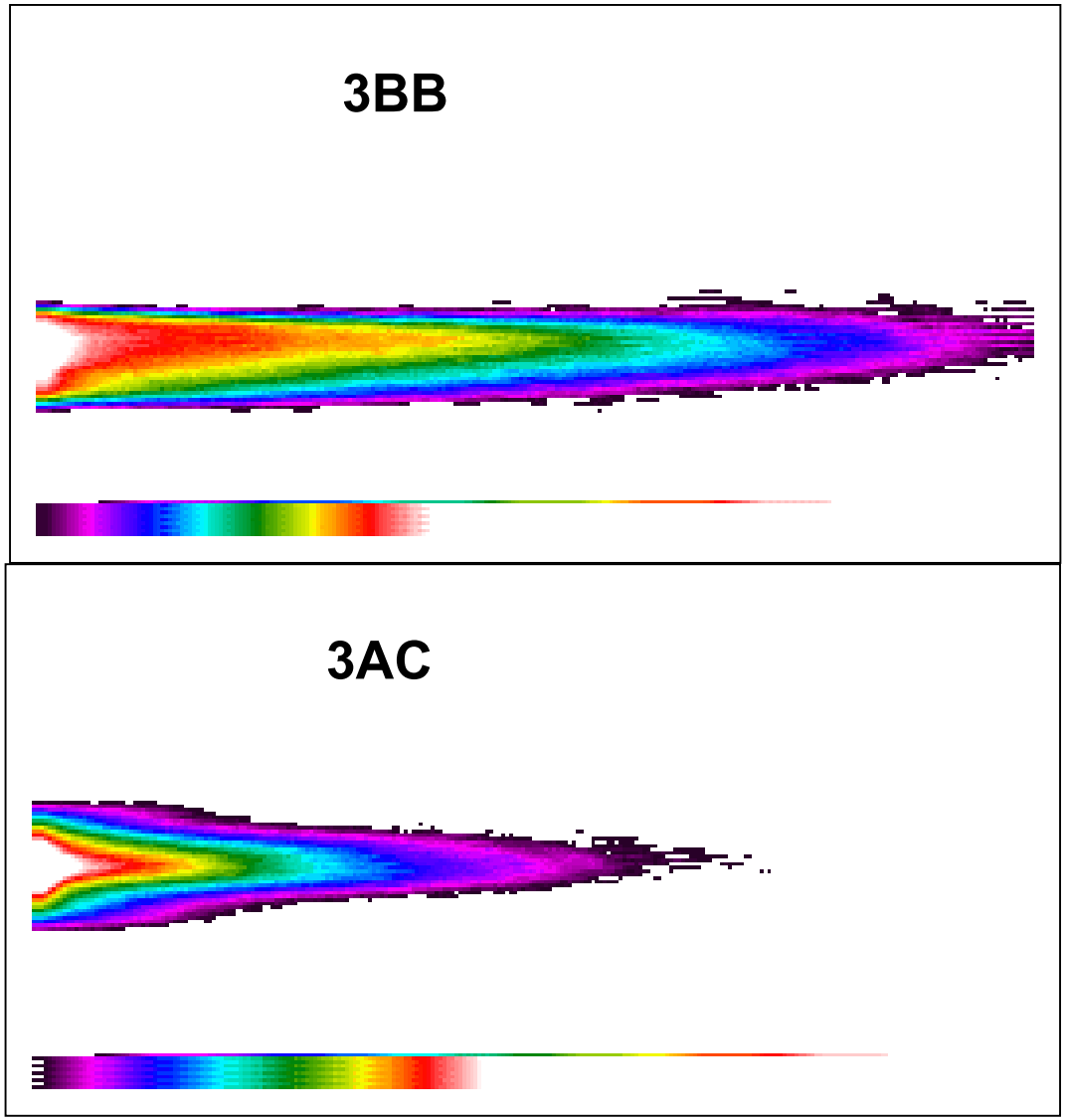




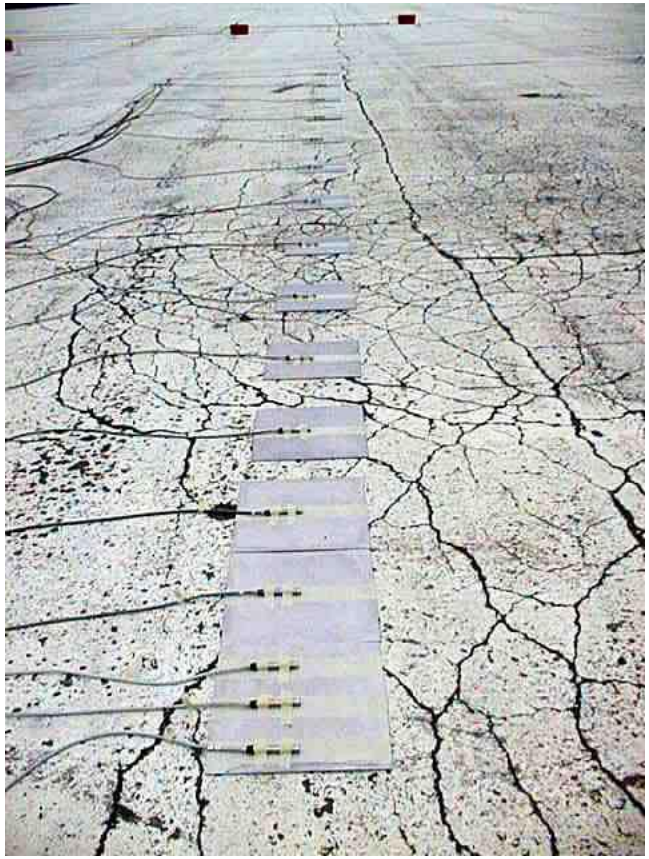
Infrared Images of Plume

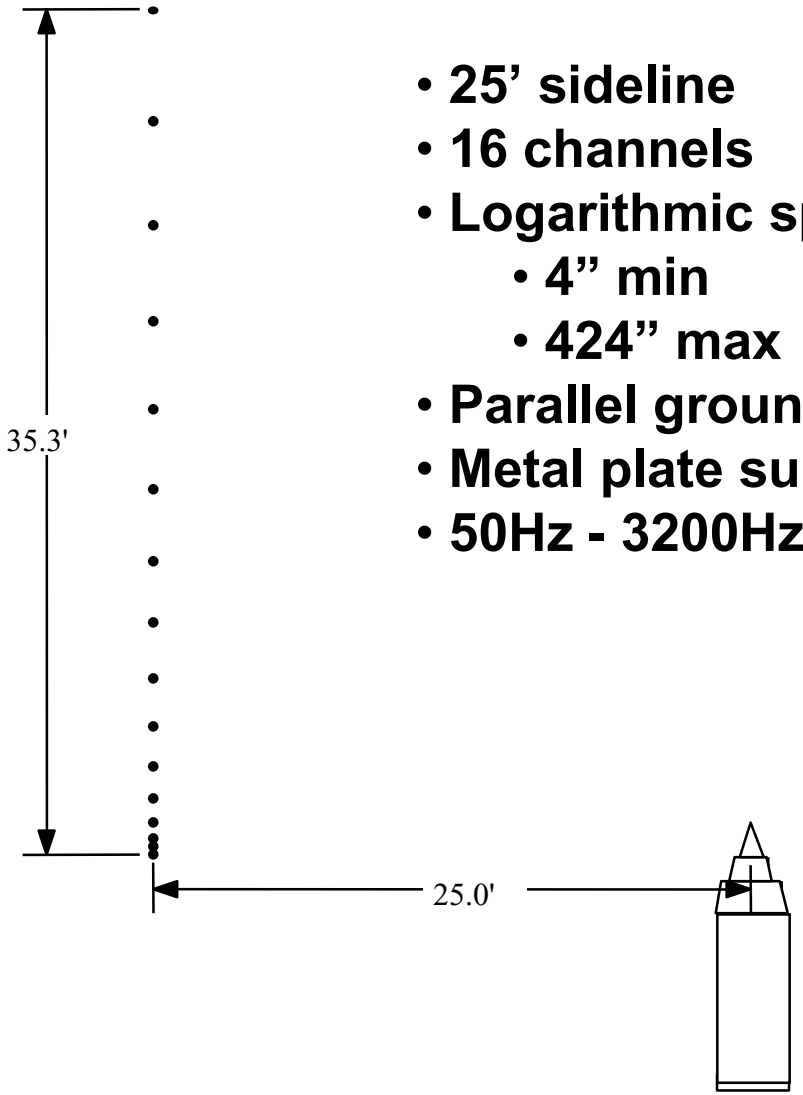
- **IR imaging is effective in confirming that chevrons produced radical improvements in core/fan mixing**

Infrared image data from Agboola and Bridges



NASA Glenn 1-D Phased Array at San Tan Facility



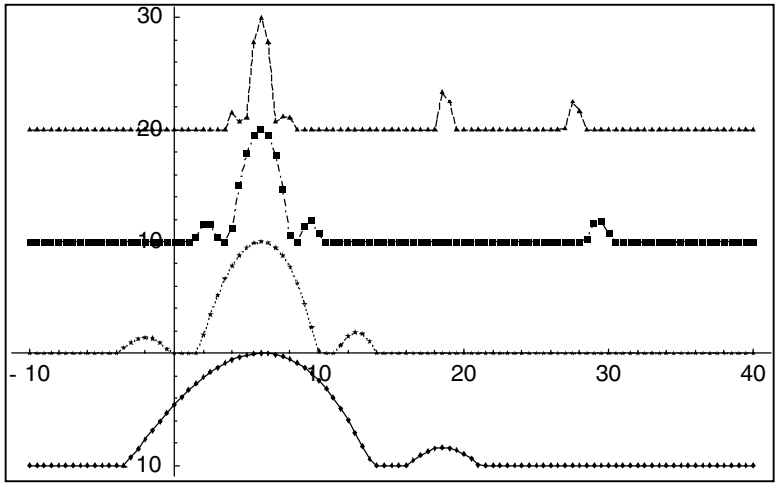


- 25’ sideline
- 16 channels
- Logarithmic spacing
  - 4” min
  - 424” max
- Parallel ground mics
- Metal plate surfaces
- 50Hz - 3200Hz

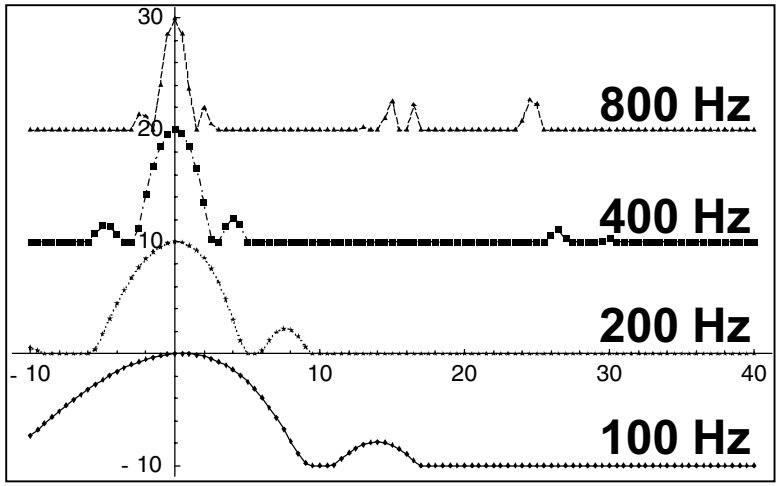
Honeywell

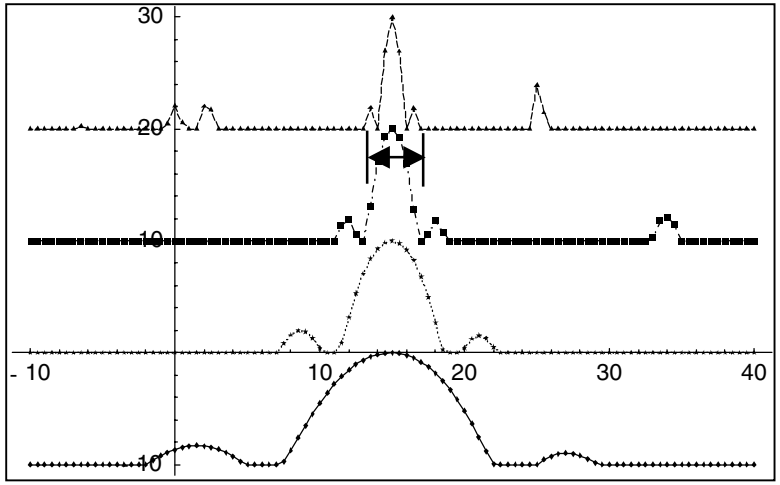
NASA Glenn 1-D Array Performance

- **Point Spread Function obtained by synthesizing signals at array microphones for a known source location, then beamforming for all possible locations.**
- **Here, source is at 0, 6, and 15 feet downstream of nozzle on jet axis.**
- **No spurious sidebands above 6dB.**



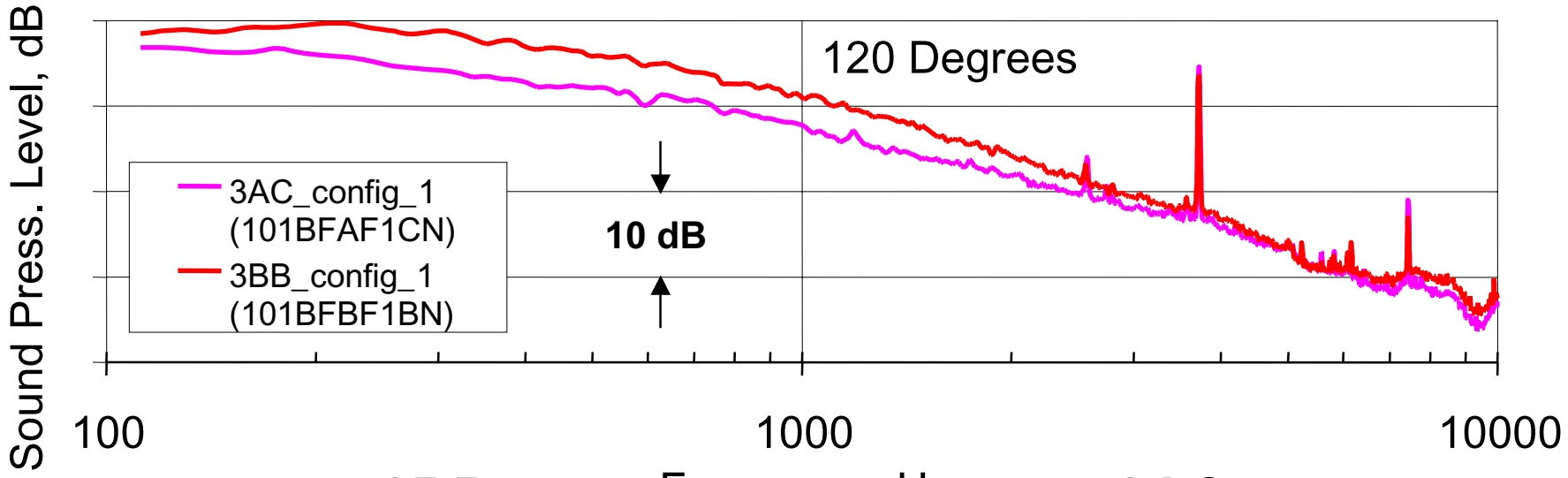
Linear phased array data from Agboola and Bridges

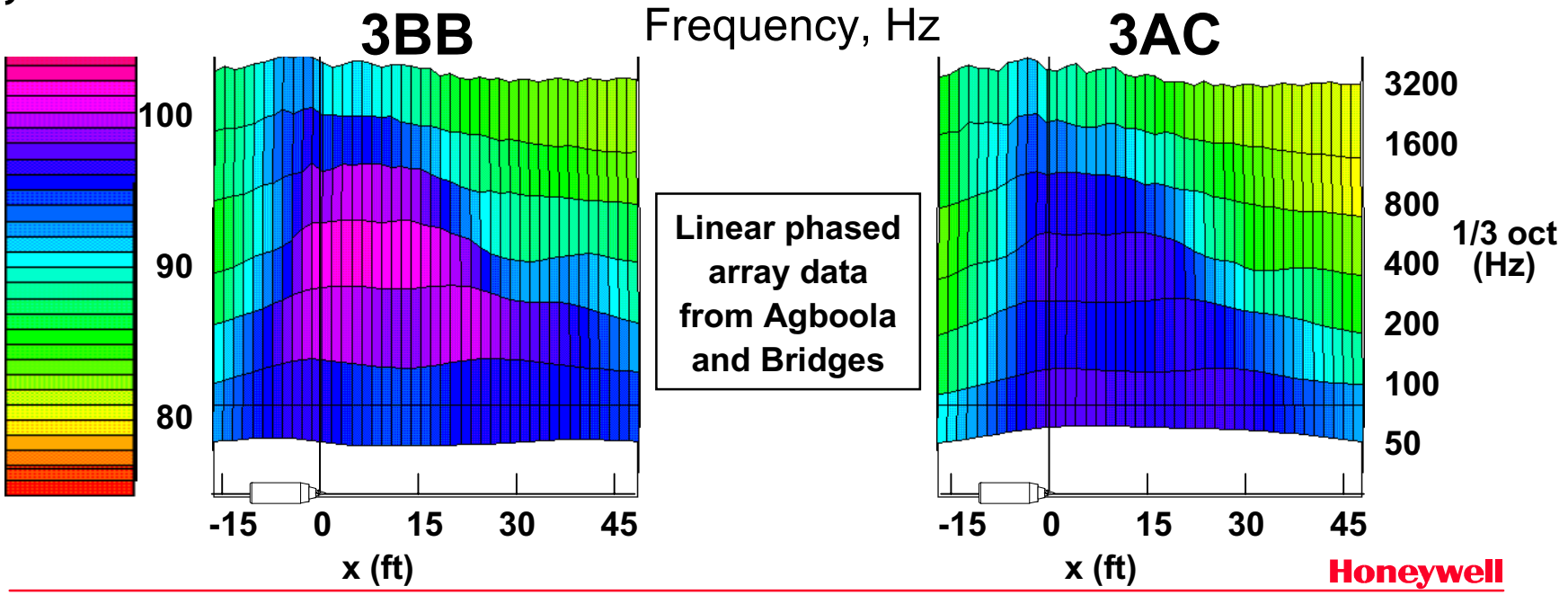




Honeywell

NASA Glenn 1-D Array Location Results

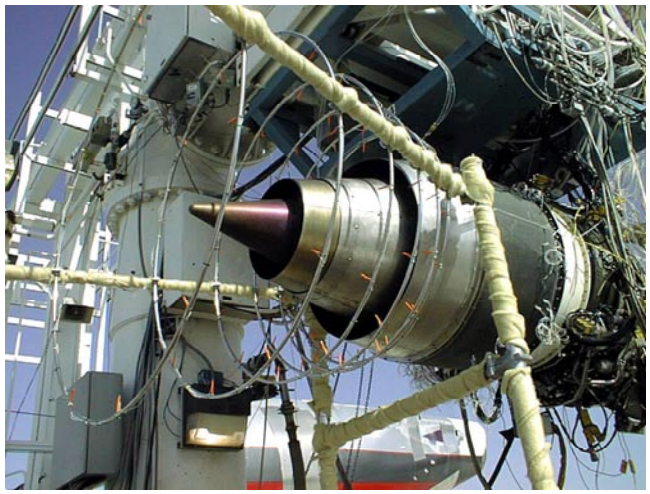


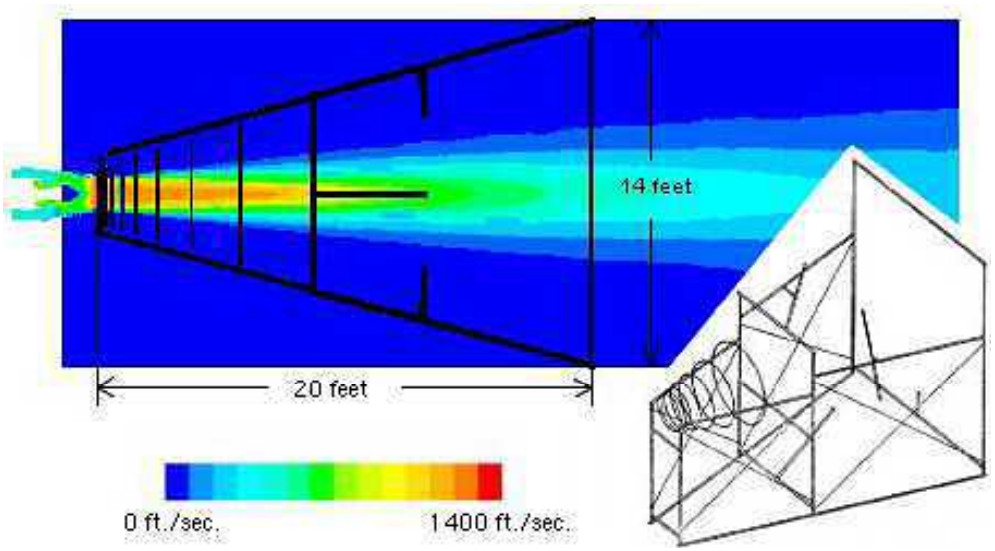


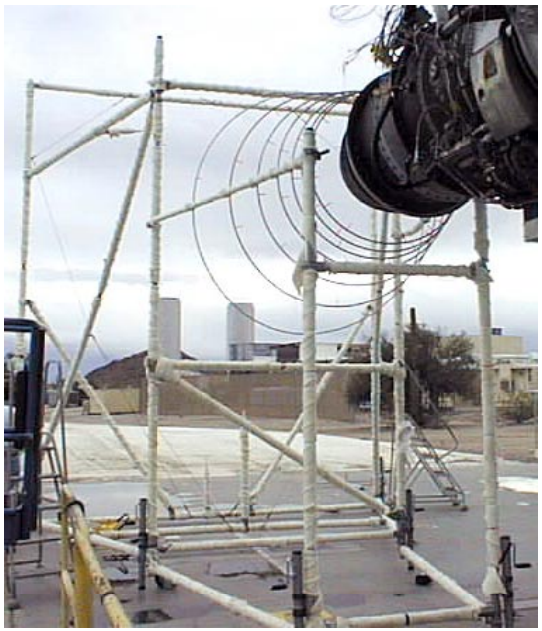
Honeywell

Boeing Near Field 3-D "Cage" Array

- 103 Kulite microphones in a sparse, logarithmic array
- Speakers used for calibrations
- Photogrammetry used for positions
- Coaxial shear layers modeled for ray tracing analysis



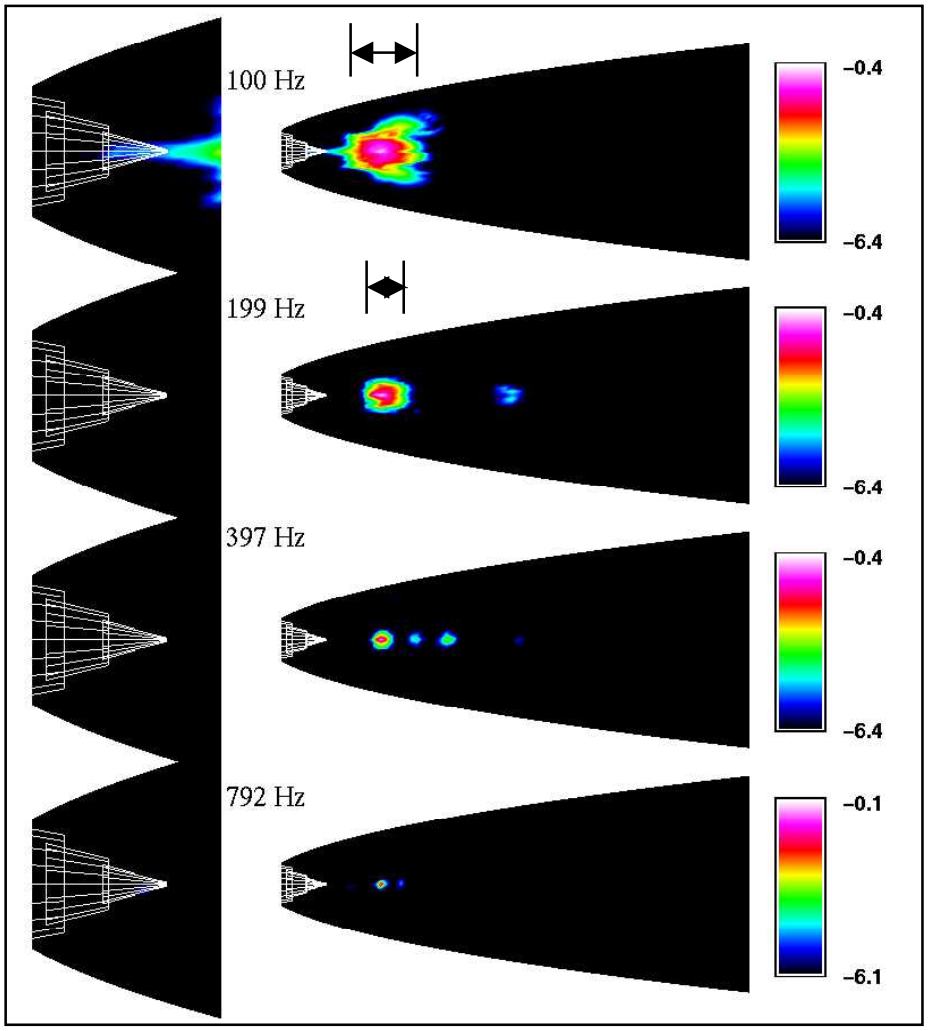




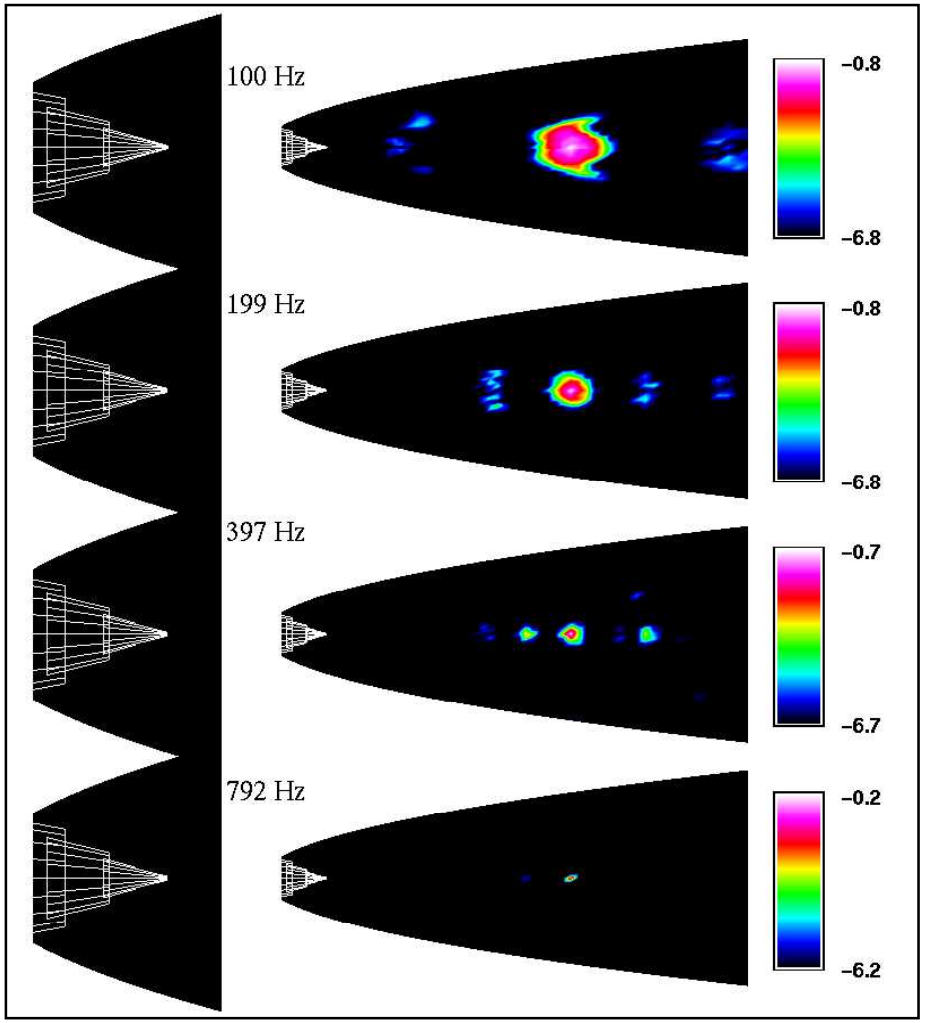
Honeywell

Cage Array Point Spread Functions

2.5 Fan nozzle dia. downstream



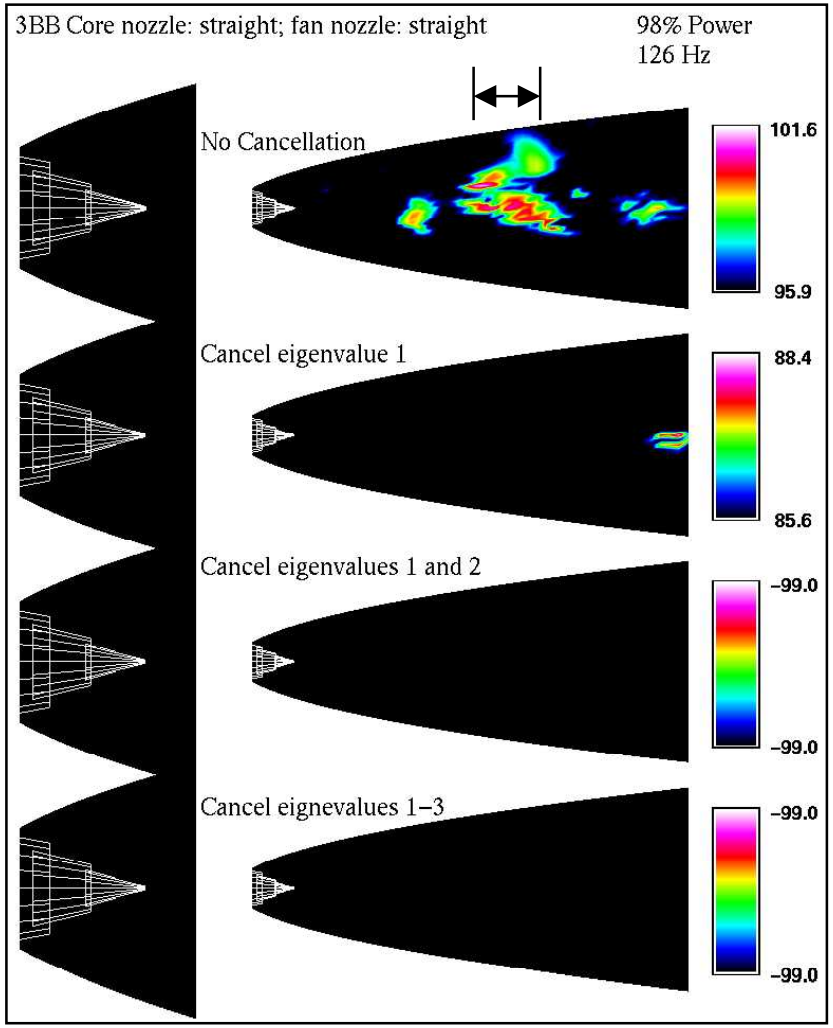
8.25 fan nozzle dia. downstream



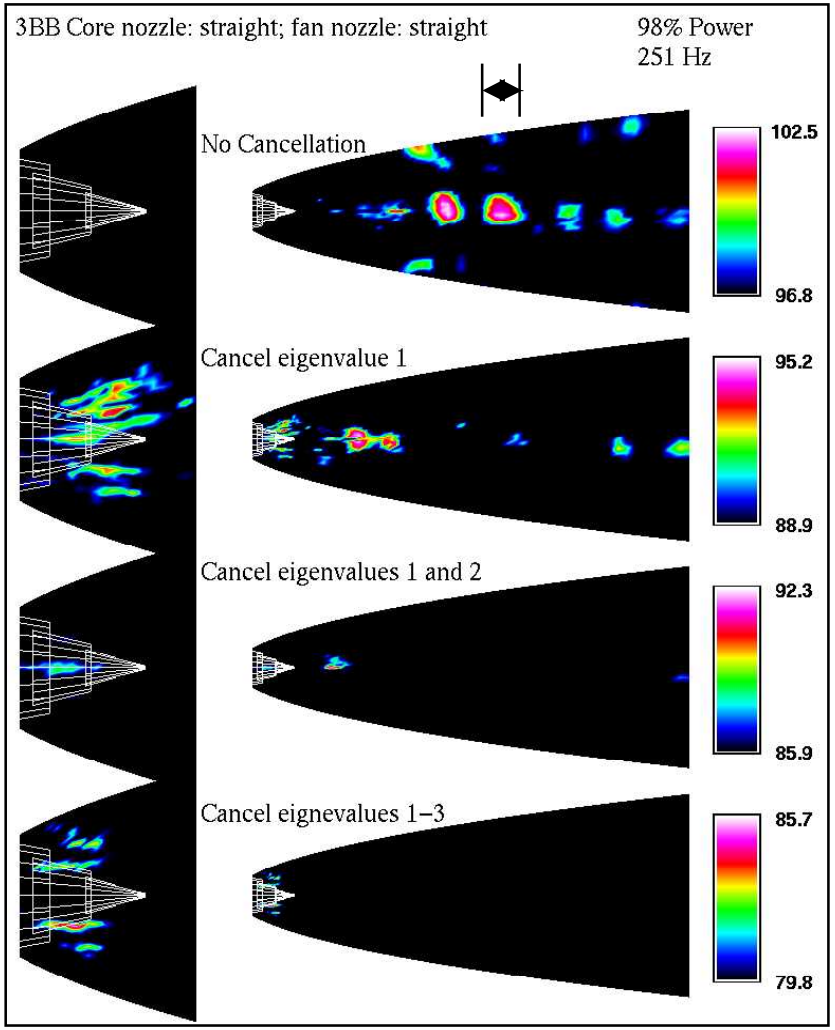
Cage array data from Dougherty

Cage Array Results - Baseline Nozzle (3BB)

125 Hz



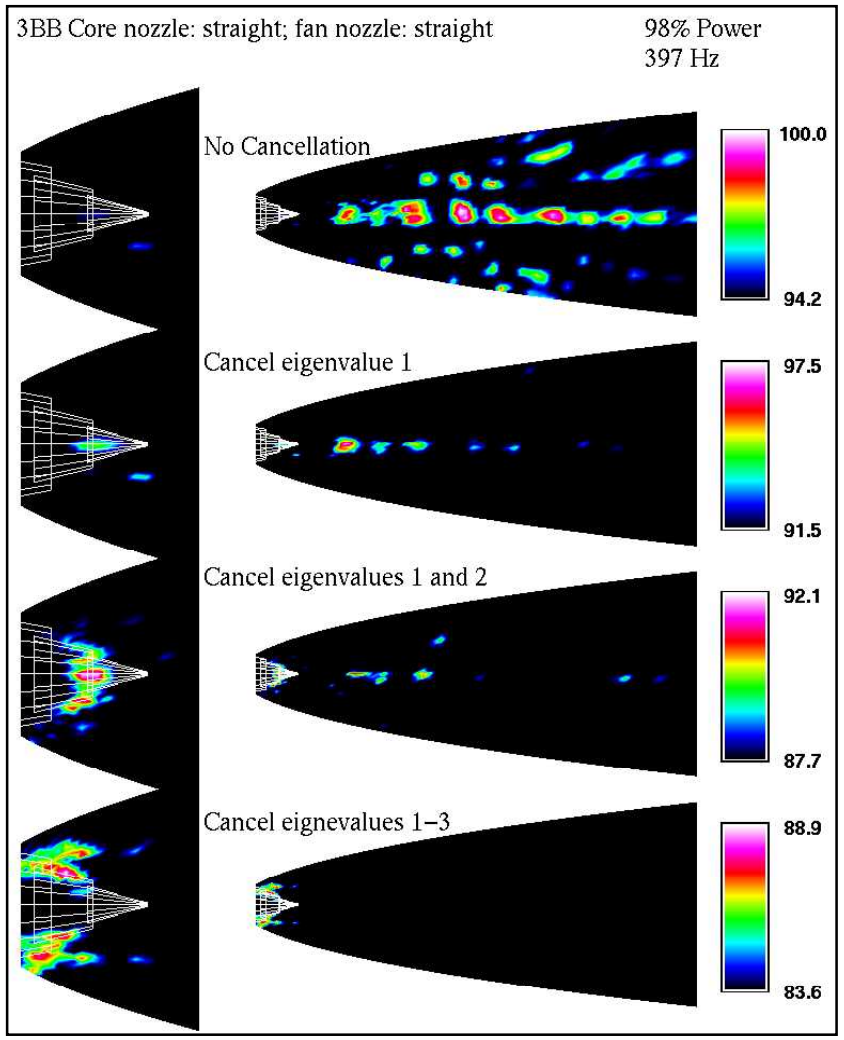
250 Hz



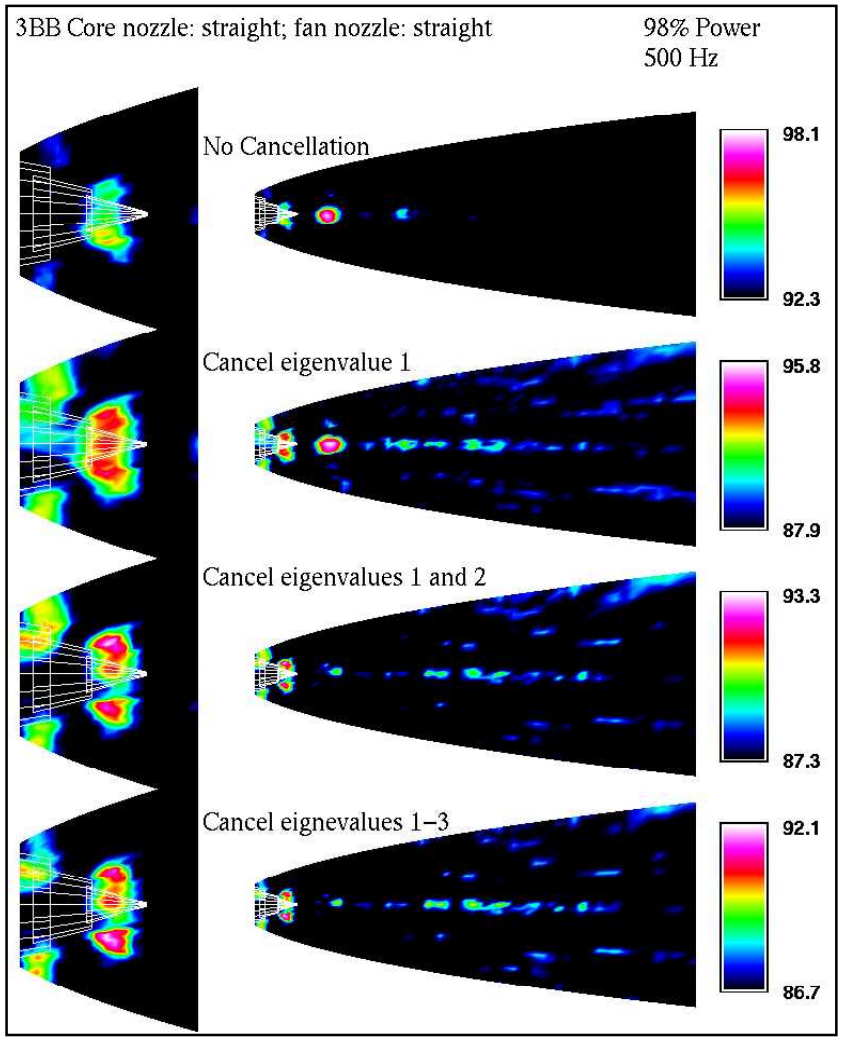
Cage array data from Dougherty

Cage Array Results - Baseline Nozzle (3BB)

400 Hz



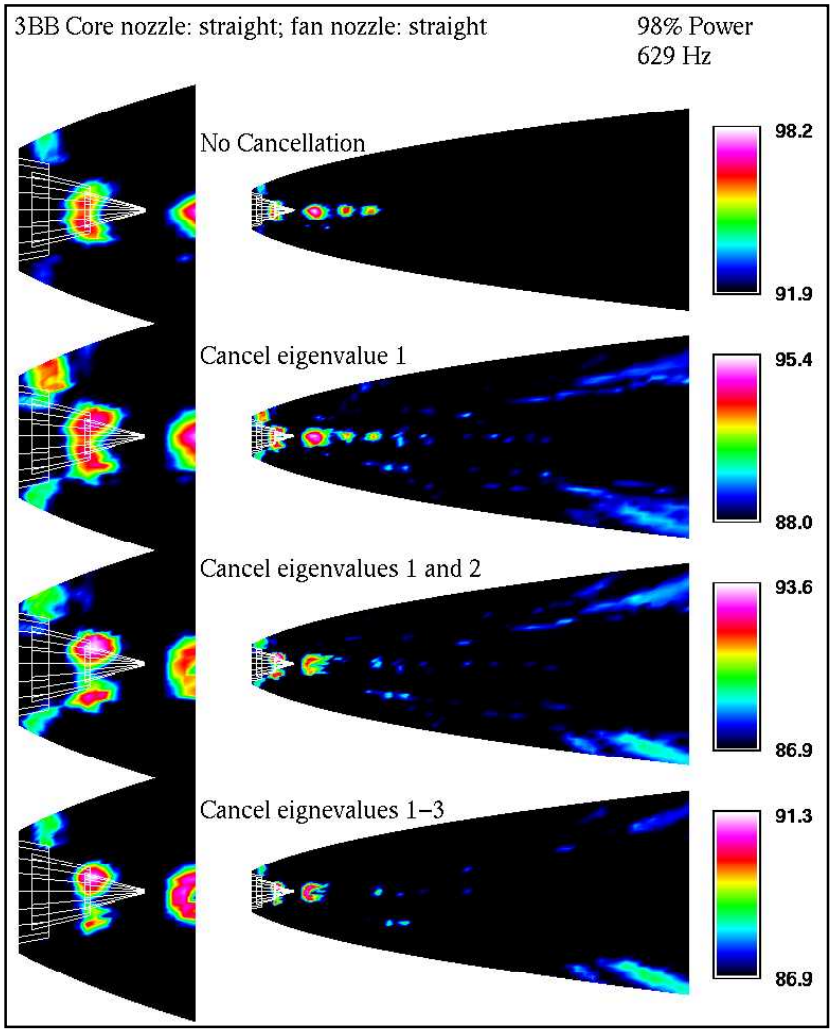
500 Hz



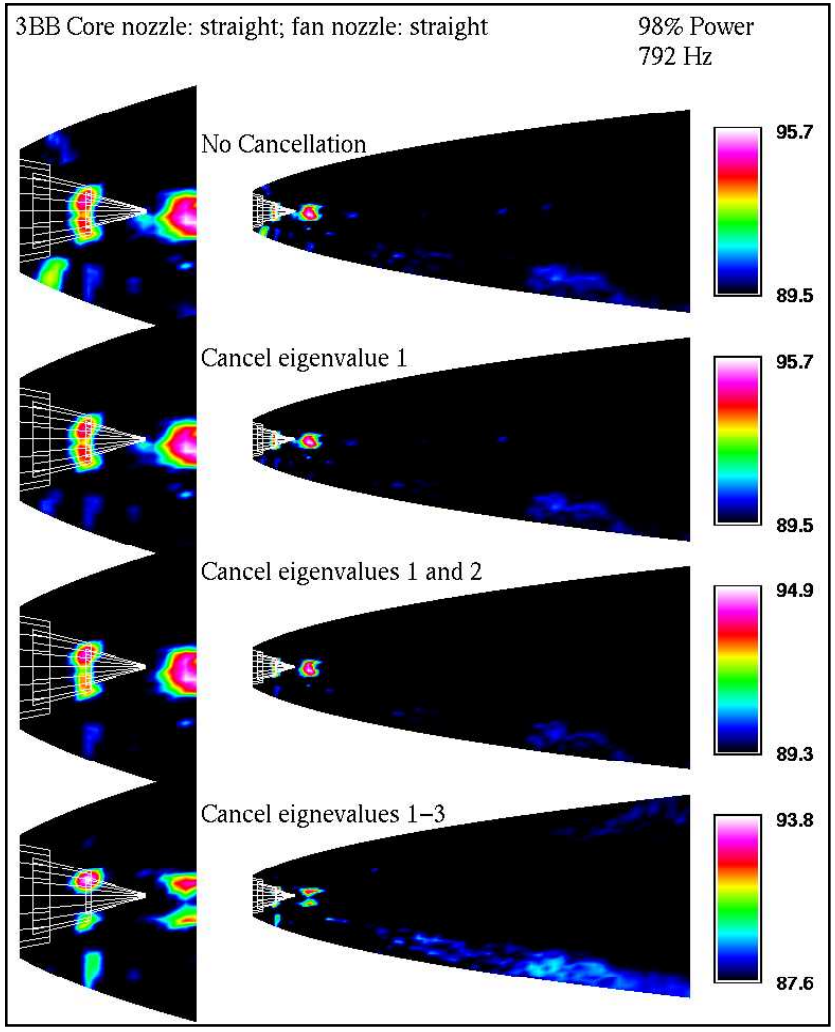
Cage array data from Dougherty

Cage Array Results - Baseline Nozzle (3BB)

630 Hz



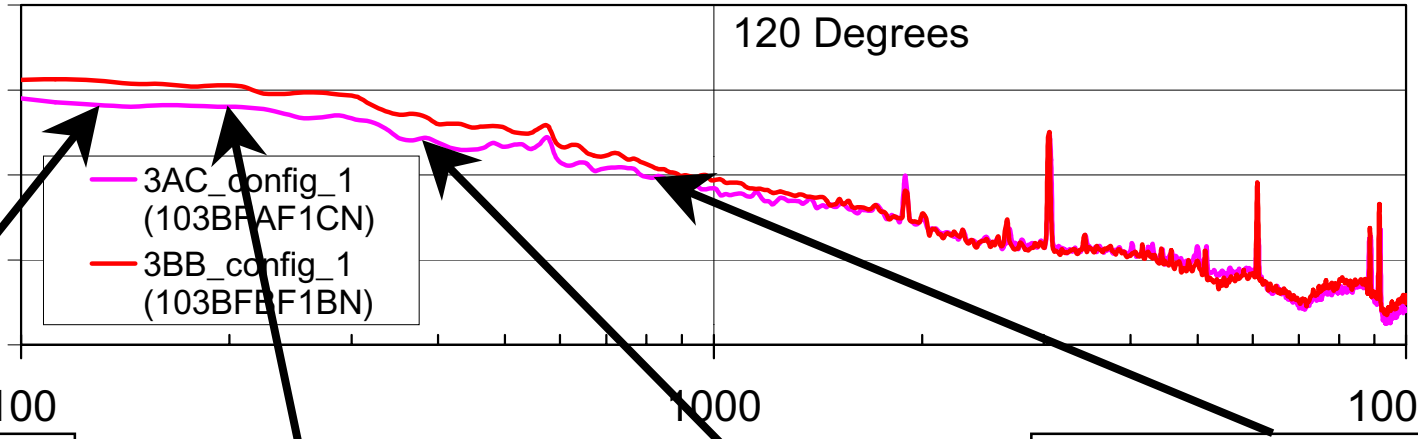
800 Hz

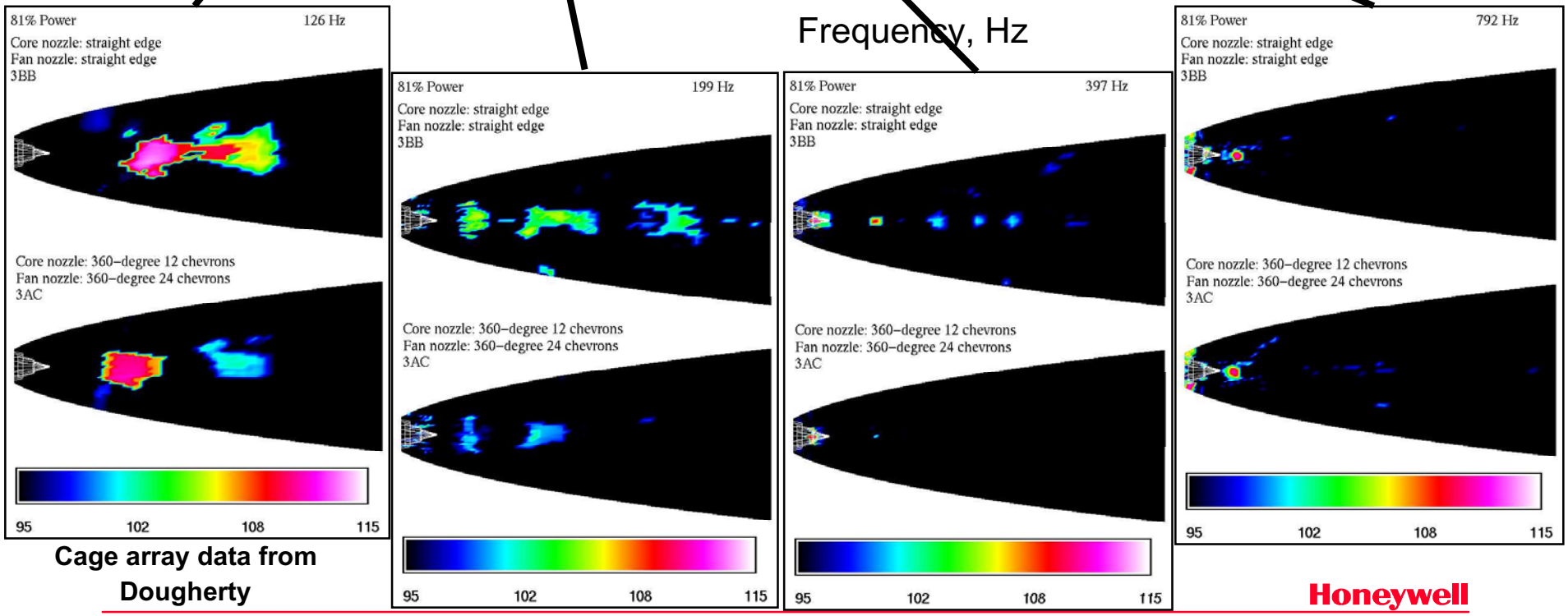


Cage array data from Dougherty

Cage Array Estimate of Noise Benefit of 3AC Nozzle

800 fps mixed jet velocity





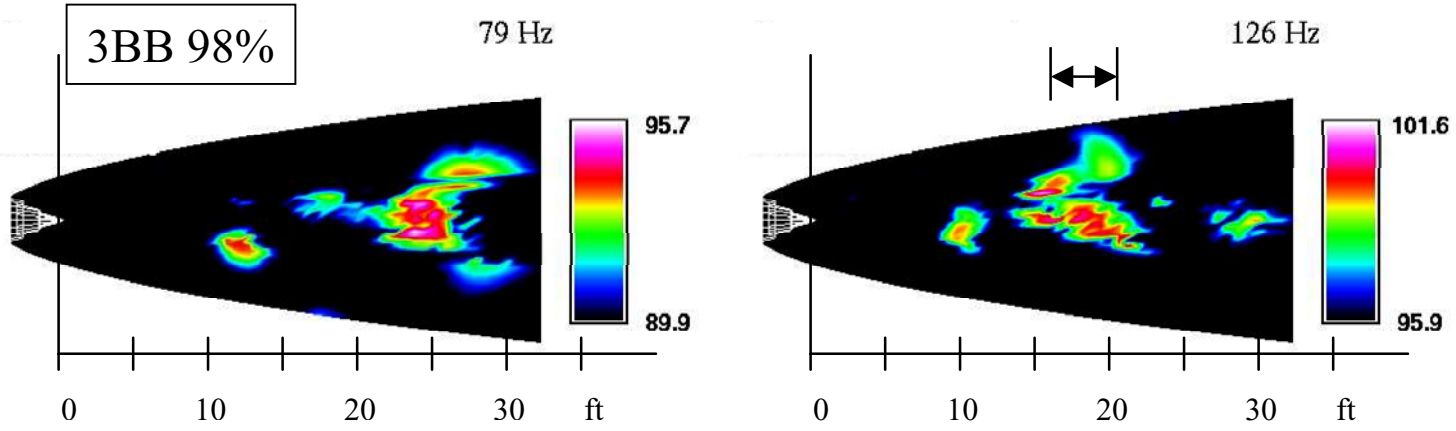
Cage array data from Dougherty

Honeywell

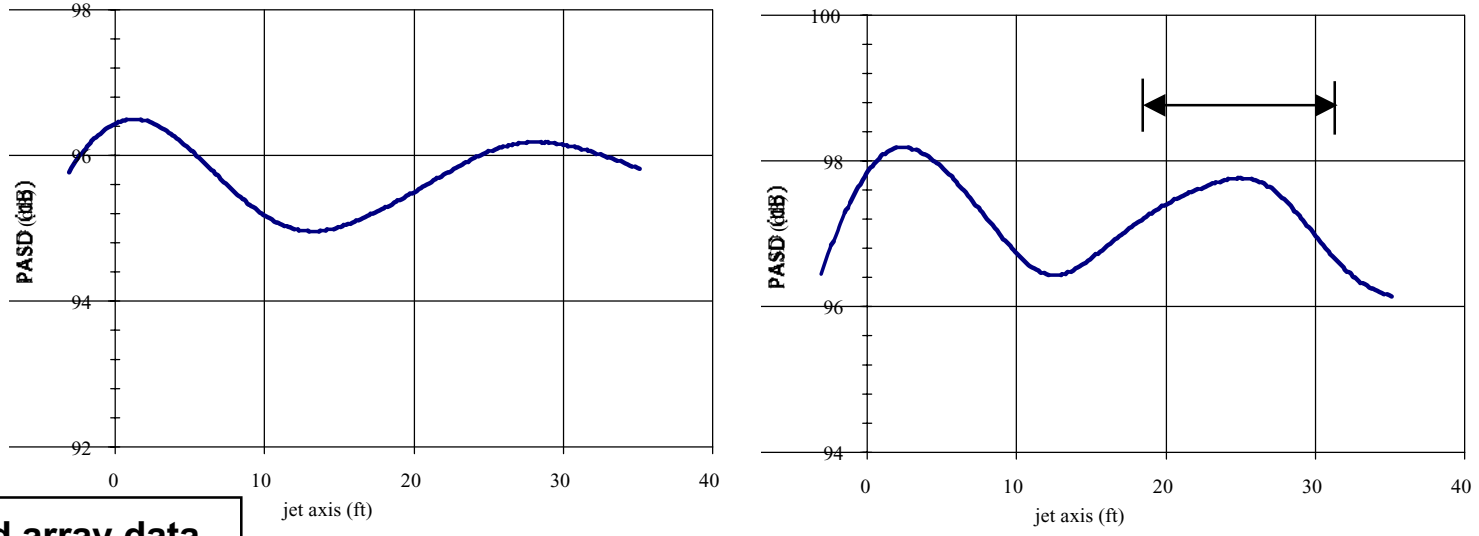
Comparison of Far Field 1-D & Near Field 3D Arrays

Cage array data from Dougherty

Boeing Cage Array



GRC Linear Array

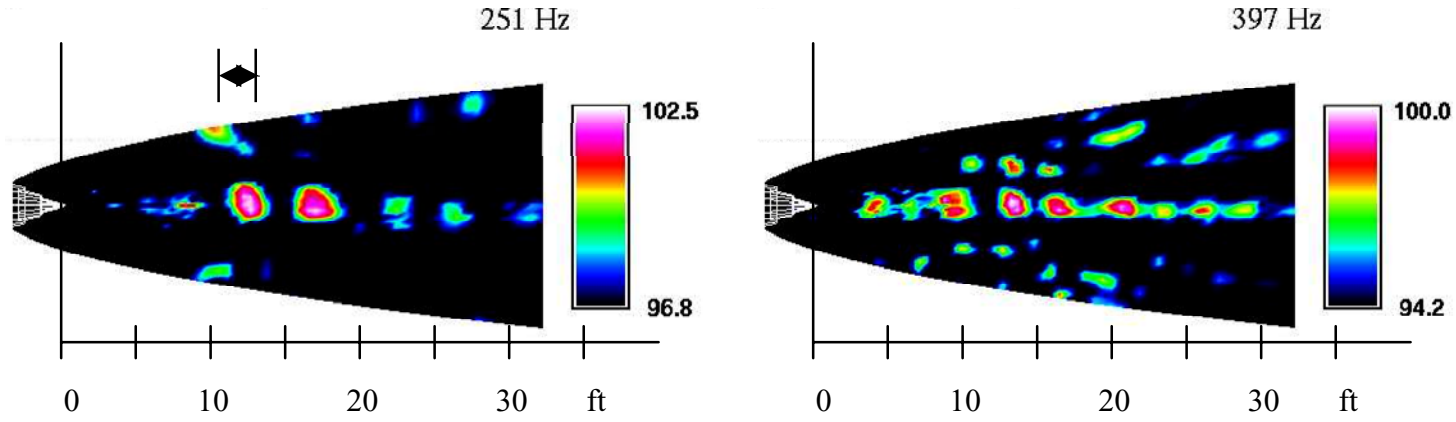


Linear phased array data from Agboola and Bridges

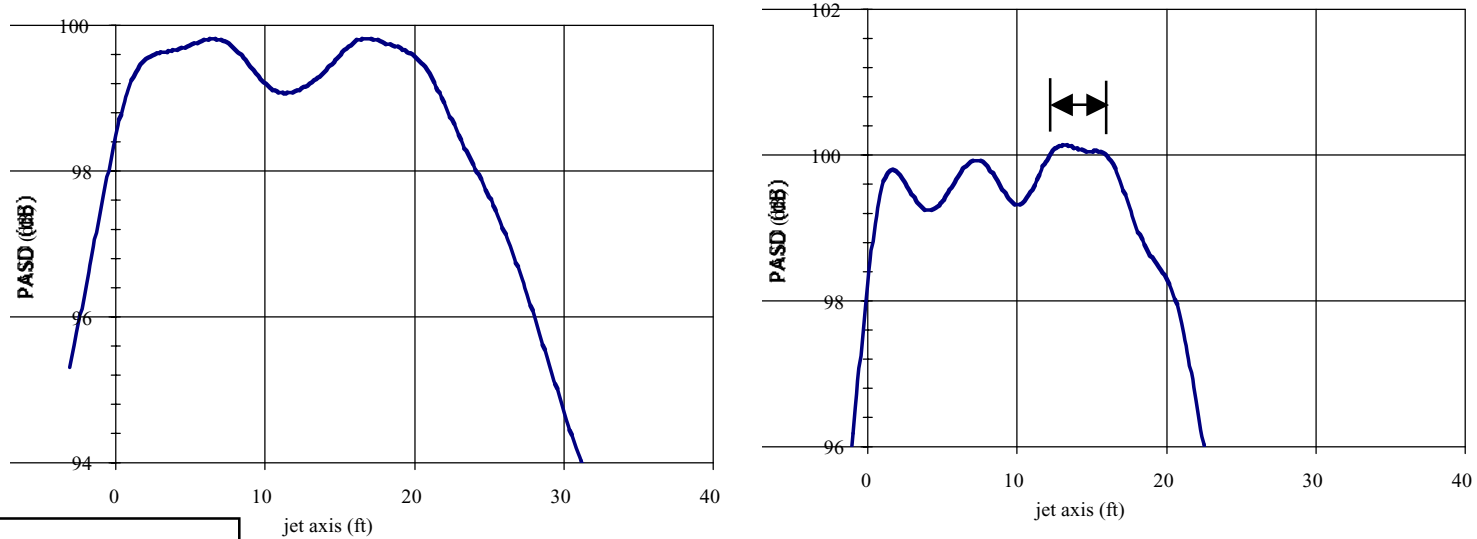
Comparison of Far Field 1-D & Near Field 3D Arrays

Cage array data from Dougherty

Boeing Cage Array



GRC Linear Array

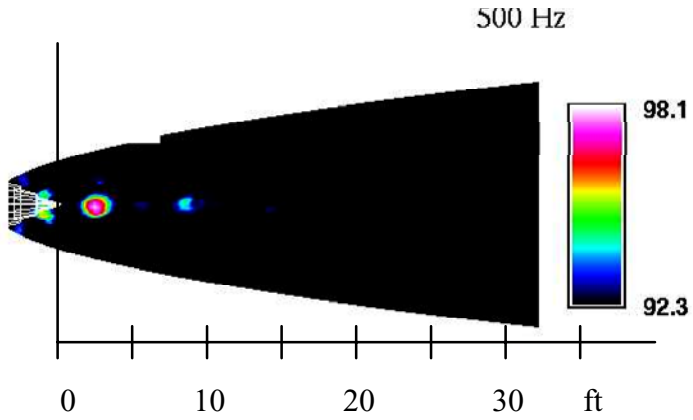


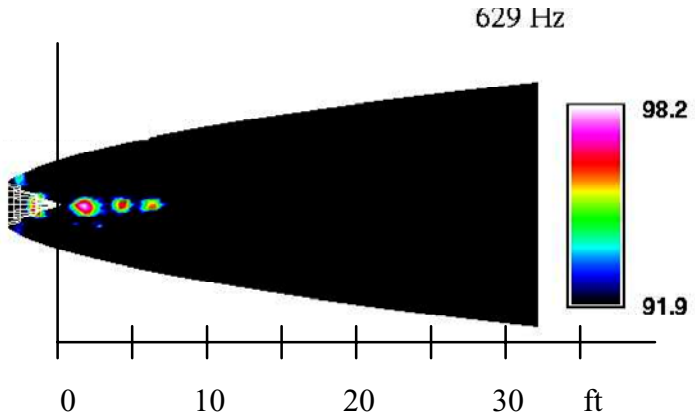
Linear phased array data from Agboola and Bridges

Comparison of Far Field 1-D & Near Field 3D Arrays

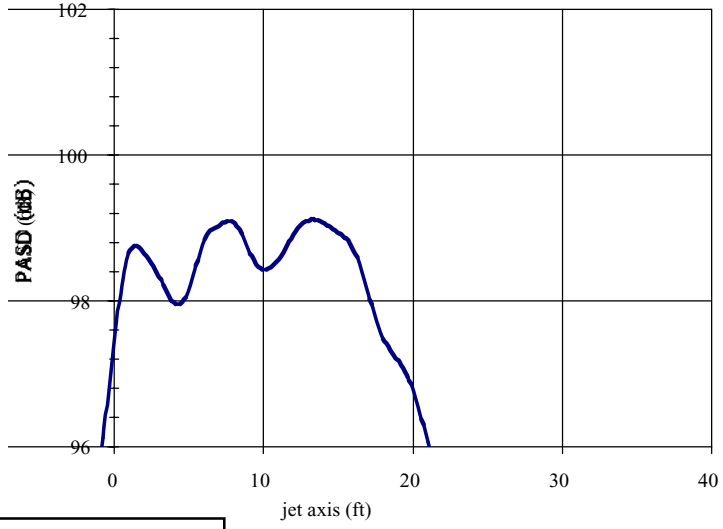
Cage array data from Dougherty

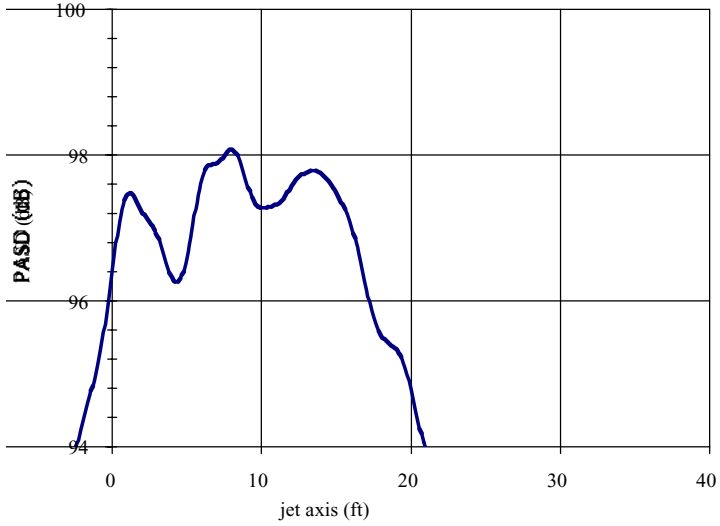
Boeing Cage Array





GRC Linear Array

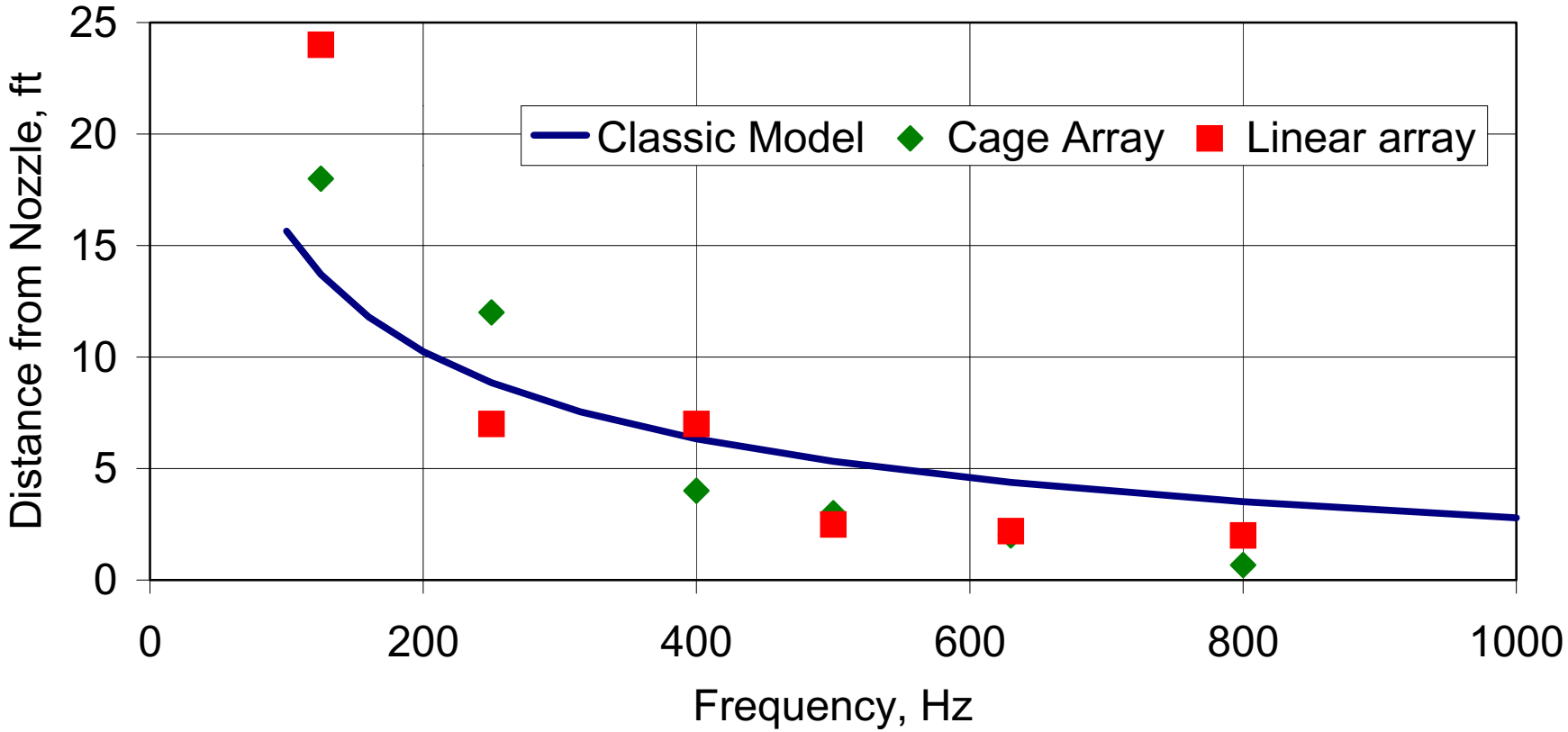




Linear phased array data from Agboola and Bridges

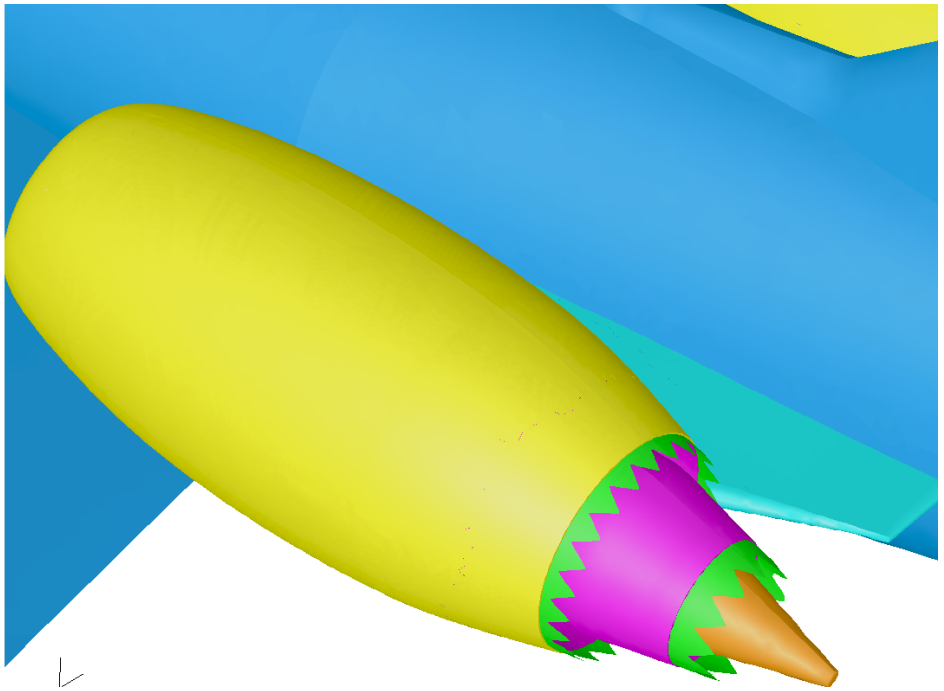
Source Location Comparison

- **Maximum SPL estimated from classical beam-forming**
- **Comparison made with "classic" source location empirical model,** $x/D = \left(0.057 \cdot S + 0.021 \cdot S^2\right)^{-1/2}$



Next Step - EVNRC Flight Test





- **Determine if the hardware tested statically will achieve similar noise reductions in flight**

Honeywell

Conclusions

- IR imaging is effective in confirming that chevrons produce increased core flow mixing
- The improvement in core/fan mixing results in significant noise reduction
- Both 1-D and 3-D array measurement techniques were successful in identifying noise source locations
- Source location data from this test program confirms the classical semi-empirical location model

D. Weir References

1. Dougherty, R.P., and R.W. Stoker, "Sidelobe suppression for phased array aeroacoustic measurements", AIAA/CEAS 98-2242.
2. Dougherty, R.P., "Source location with sparse acoustic arrays; interference cancellation" CEAS-ASC Workshop, "Wind Tunnel Testing in Aeroacoustics", DNW, Noordoostpolder, the Netherlands, November 5-6, 1997.

Source Identification and Location Technique – Using a Phased Array

Thonse R. S. Bhat
Boeing Commercial
Airplane Group

Source Identification & Location Technique – Using a Phased Array **Thonse R. S. Bhat, Boeing Commercial Airplane Group as summarized by Eugene Krejsa.**

Dr. Bhat presented results from the use of a phased array system. Sample results from the application of this system to the determination of airframe noise source locations. A detailed summary of beamforming theory was presented. The conclusion of this summary was that "if the array is well designed and the steering vectors are correctly computed, then the plot (the beamform map) will have peaks corresponding to the true sources, with the peak heights equal to the source strength (magnitude squared)."

Results from the application of phased arrays to scale model tests, at Glenn Research Center, of separate flow nozzles were presented. These small scale tests were for geometries and noise reduction concepts similar to those tested during the engine test described by Mr. Weir of Honeywell. Three array configurations were used during these small scale tests. Each of the arrays were purported to have their own advantages. A large 7 arm logarithmic spiral array was used to determine source density both axially and vertically. This array was described as working best between 1000 and 8000 Hz. A small 7 arm logarithmic spiral was used to determine source location in two dimensions over a frequency range of 8000 to 50000 Hz. A linear sideline array was also used. This array provided source location along the jet axis over a frequency range of 1000 to 50000 Hz.

Results from these tests indicated that, at low frequencies, a single source exists at several diameters downstream of the nozzle exit. The location of this did not seem to move with frequency. At higher frequencies a second source appeared near the nozzle exit. This source appeared to be less sensitive to power setting and flight Mach number then the downstream source.

The following conclusions were made by Dr. Bhat:

- Phased arrays can be used to qualitatively image jet noise sources.
- Two separate source regions exist, one upstream near the nozzle exit and one several nozzle diameters downstream.
- The upstream region is less affected by increases in power than the downstream.
- The upstream is less affected by increases in tunnel Mach number than the downstream.

- Jet mixing devices increase the upstream region and decrease the downstream region.
- Preliminary results of using phased array measurements to determine far-field spectra are promising.

In the open discussion following the presentation it was recommended that a good benchmark experiment be conducted to obtain validated results. It was also suggested that the results from the small scale tests be compared with those from the engine test.

Source Identification & Location Technique - Using a Phased Array

NOISE ENGINEERING TECHNOLOGY
Boeing Commercial Airplane Group

Thonse R. S. Bhat

Jet Noise Workshop
Ohio Aerospace Institute
Cleveland, OH

November 7-9, 2000

BOEING®

Outline

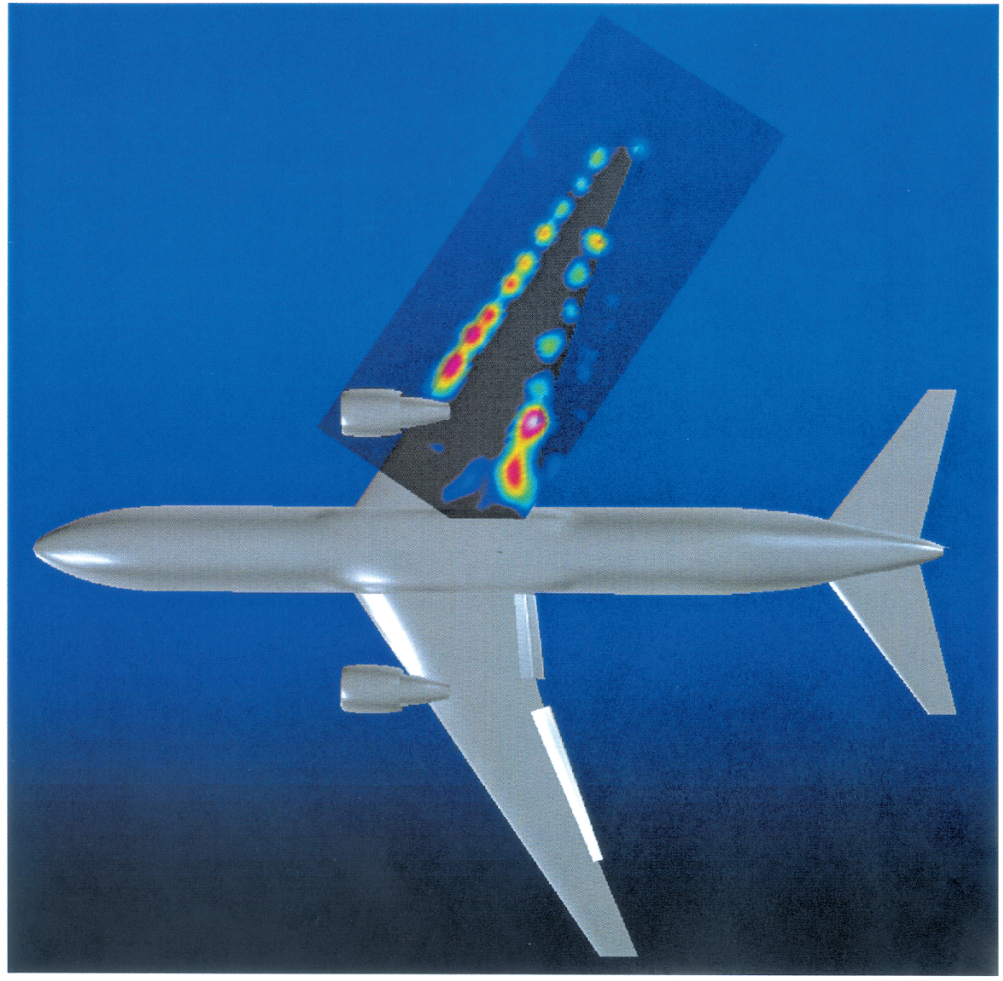
- Sample applications
- Theory
- Example
- Jet Noise Test Results

Sample Applications

- Airframe noise
  - Flap-edge noise
  - Slat noise
  - Landing gear noise
- Engine noise
  - Inlet fan noise
  - Aft fan noise
  - Jet noise

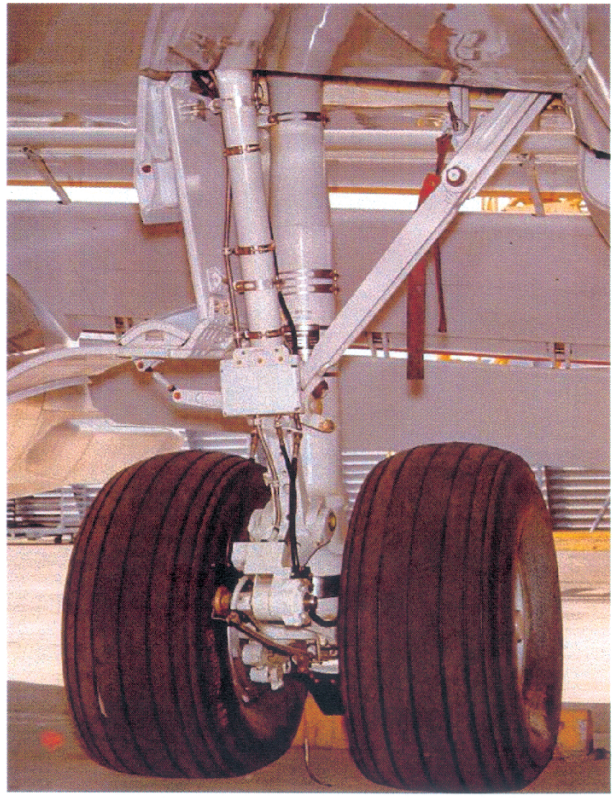
BOEING®

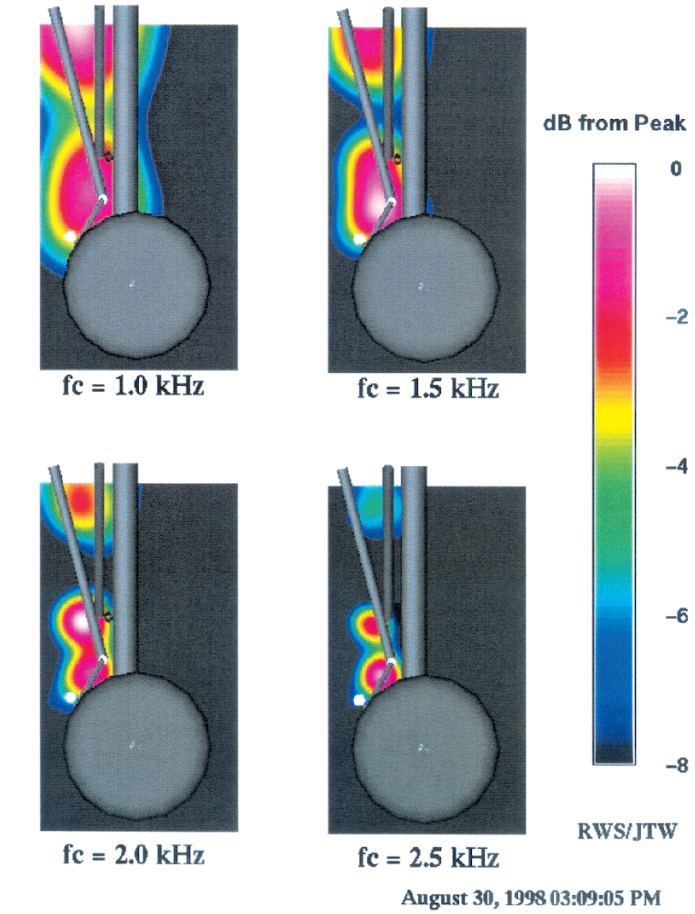
Sample applications: flap and slat noise



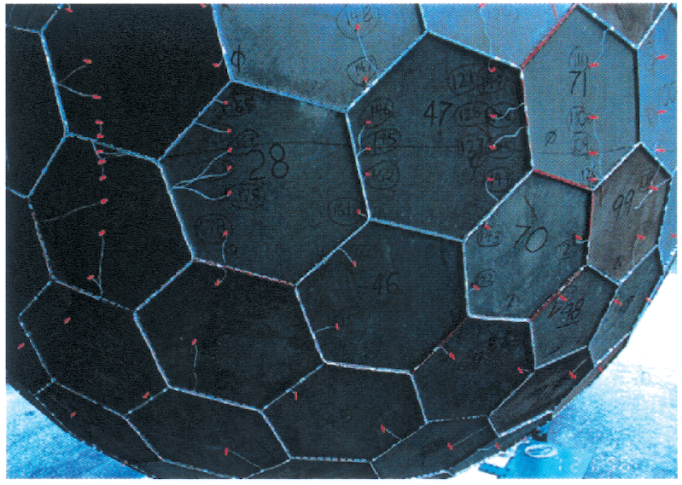
RWS

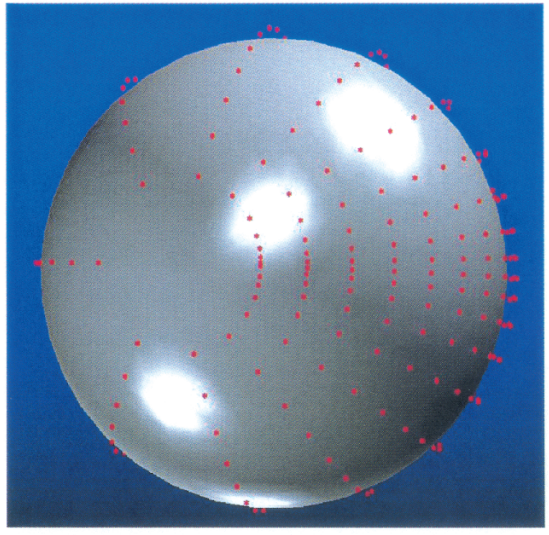
Sample applications: landing gear noise

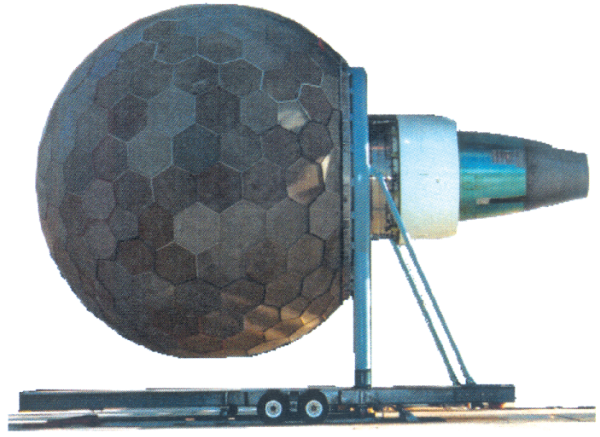




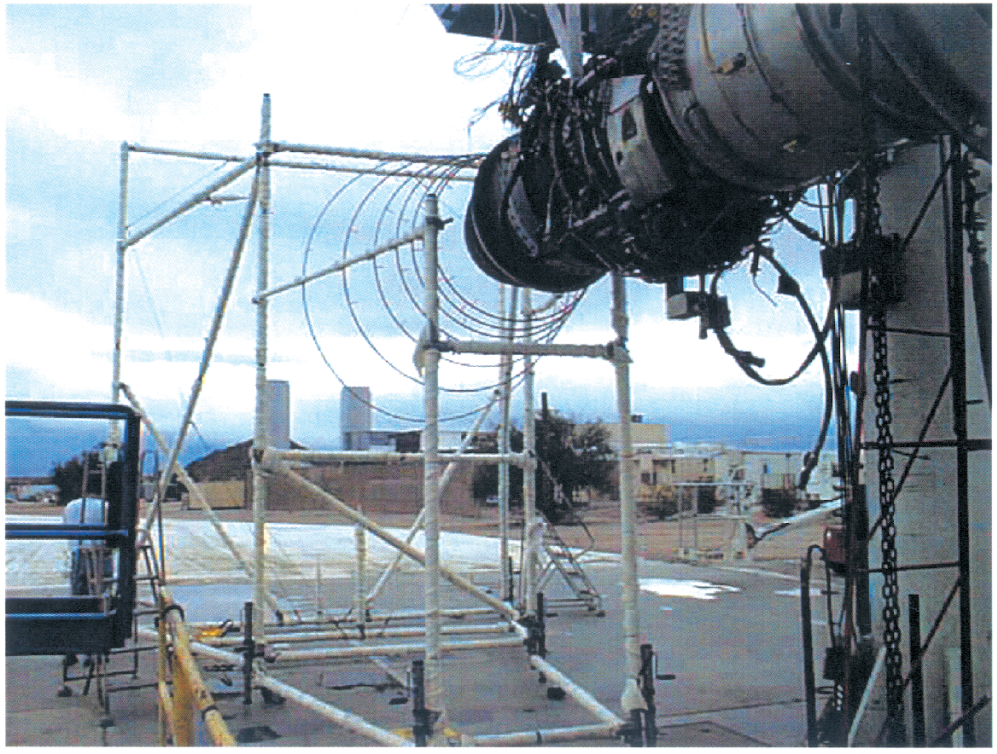
Sample applications: ICD array for inlet noise

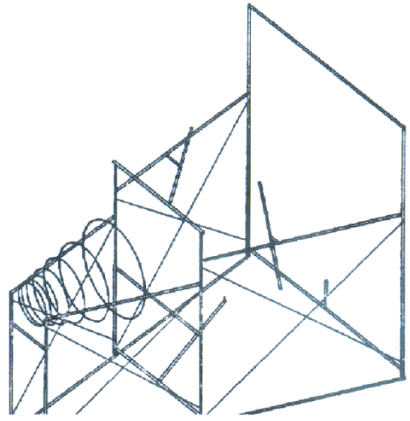


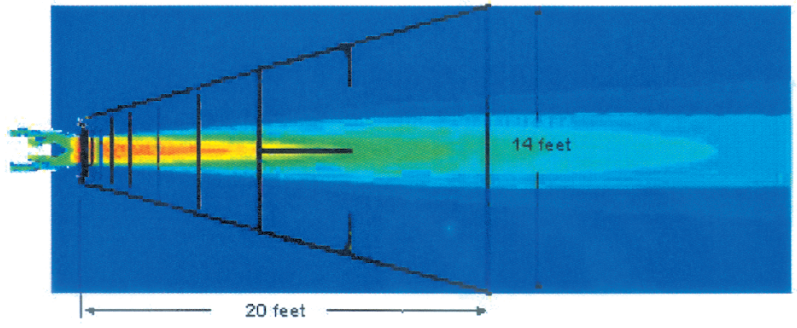




Sample applications: aft fan and jet noise







Beamforming theory: narrowband data



N microphones

$p_n(t)$ = time-domain pressure at microphone n, $n = 1,\ldots, N$. (real)

$$u_n(t) = \int_{-\tau/2}^{\tau/2} p_n(t+t')e^{j\omega t'}\,dt'$$

= narrowband pressure at microphone n (complex).

noise

narrowband data

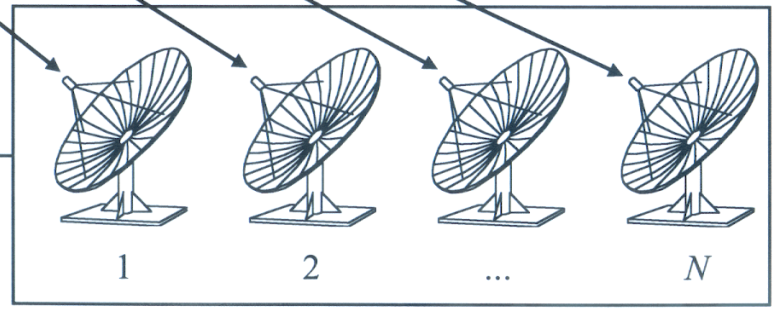
τ = block length ~ 1-100 ms $1/\tau$ = bandwidth

$$\vec{u}(t) = \begin{bmatrix} u_1(t) \\ u_2(t) \\ u_3(t) \\ \ldots \\ u_N(t) \end{bmatrix}$$

Note: A Hanning window is often used in practice to improve rejection of low frequency tunnel background noise.

Digital filter or window for narrowbanding

Data acquisition system (amplifiers, anti-alias filters, A/D converters, disk storage)



phased array of microphones

Beamforming theory: cross spectral matrix

$$\vec{u}(t) = \begin{bmatrix} u_1(t) \\ u_2(t) \\ u_3(t) \\ \cdots \\ u_N(t) \end{bmatrix} \qquad A = \langle \vec{u}\,\vec{u}^{\dagger} \rangle \qquad \text{time average} \quad \langle f(t) \rangle = \frac{1}{T}\int_0^T f(t)dt$$

T ~ 20 seconds (limited by disk storage)

The $N \times N$ cross spectral matrix, A, is the data for narrowband beamforming.

Facts about A:

- A is hermitian
- Element ik of A is given by $A_{ik} = \frac{1}{T}\int_0^T u_i(t)u_k^*(t)dt$
- The SPL at microphone i is given by $10 \log_{10} (A_{ii}/P_{ref}^2)$
- The coherence of microphones i and k is given by $|A_{ik}|/(A_{ii}\,A_{kk})^{1/2}$
- A has full rank, in general. For tones, it may be acceptable to use a single column of A.
- In the antenna literature, A is called the covariance matrix.

Beamforming theory: steering vectors

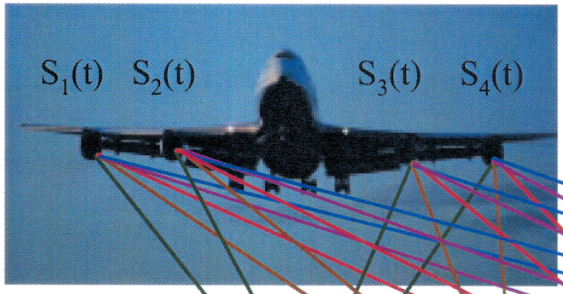
$\vec{C}_m$ = array steering vector for source m

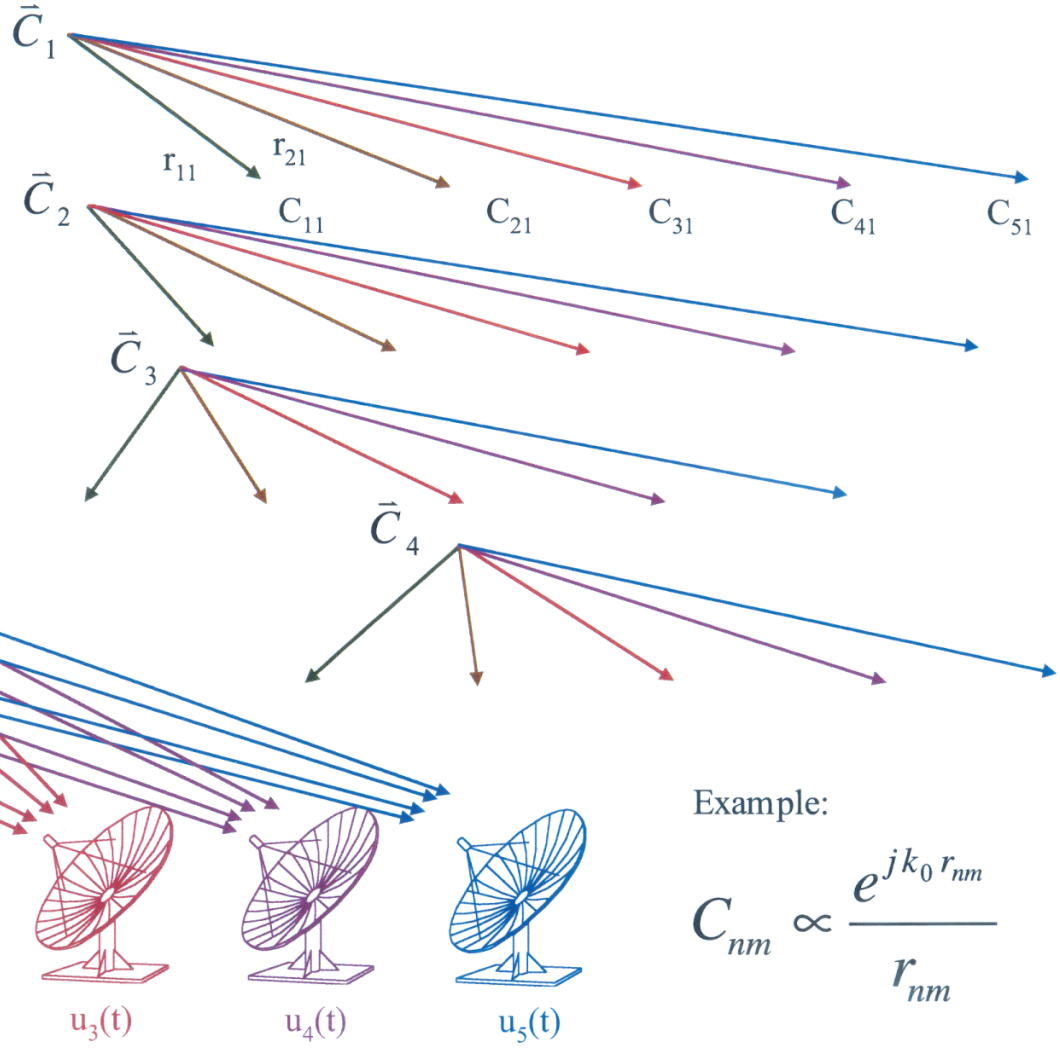
$$C = \left[\vec{C}_1 \quad \vec{C}_2 \quad \ldots \quad \vec{C}_M\right]$$

= $N \times M$ steering vector matrix

$S_m(t)$ = narrowband strength of source m

M sources (assumed stationary)



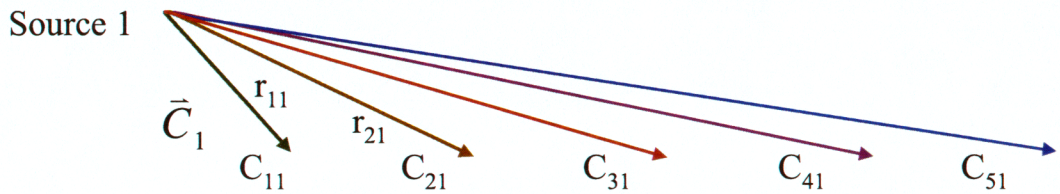


N microphones

Example:

$$C_{nm} \propto \frac{e^{jk_0 r_{nm}}}{r_{nm}}$$

Beamforming theory: steering vectors in more detail



For convenience, steering vectors should usually be normalized: $\vec{C}_m^{\dagger}\,\vec{C}_m = 1$

They need to be computed in great numbers for beamforming.

Simplest case:

- Monopole point source
- Free field propagation
- No flow

Then $C_{nm} = \alpha \dfrac{e^{jk_0 r_{nm}}}{r_{nm}}$ where $\alpha = \dfrac{1}{\sqrt{\sum_{n=1}^{N} r_{nm}^{2}}}$

r_{nm} = distance from source m to microphone n.

For uniform or nonuniform flow, r_{nm} can be replaced by the product of the speed of sound and the ray propagation time. More on this in the next lecture. For spinning modes, and other cases of ducts which not large compared with the wavelength, elaborate propagation codes are needed. In any case, the array should be designed so that the steering vectors are approximately orthogonal to each other. Array design is also treated in the next lecture.

Classical beamforming

The simplest and most robust beamforming method:

Consider a set of M' possible sources (perhaps point monopoles at distinct locations)

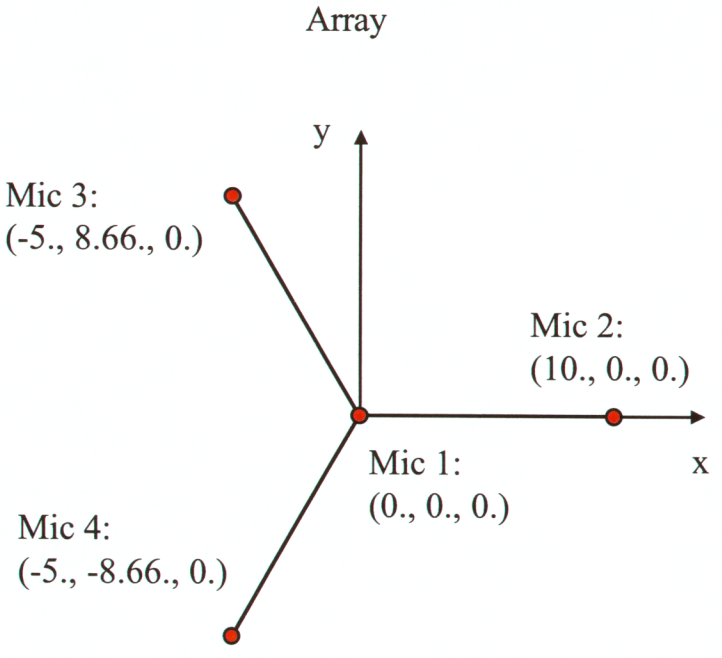
Compute the array steering vector for each for each candidate source: $\bar{C}_{m'}$

For each steering vector, compute and plot the beamforming expression

$$b(m') = \bar{C}_{m'}^{\dagger} A \bar{C}_{m'}$$

Claim: if the array is well designed and the steering vectors are correctly computed, then the plot (the beamform map) will have peaks corresponding to the true sources, with the peak heights equal to the source strengths (magnitude squared) .

Example 1: four microphone array



(dimensions in inches)

Frequency f = 1000 Hz

Temperature = 77° F

c = 12[1.4*1718*(459.7+ 77° F)]$^{1/2}$ = 13634 in/sec

$k_0 = 2\pi f / c$ = 0.4608 rad/sec

Source location: (0., 0., 20.) (out of the screen)

Source to microphone distances

r_n = 20., 22.36, 22.36, 22.36

$$C_n = \alpha \frac{e^{j k_0 r_n}}{r_n}$$

αC =

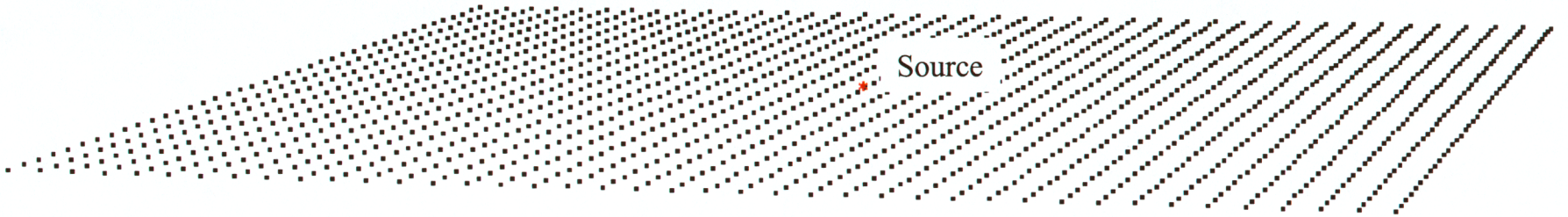
```
-0.0489 + 0.0104I
-0.0285 - 0.0344I
-0.0285 - 0.0344I
-0.0285 - 0.0344I
```

C =

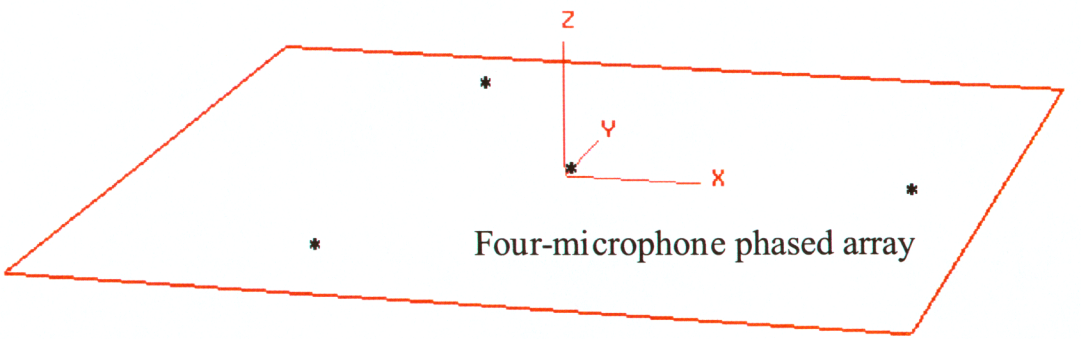
```
-0.5305 + 0.1124I
-0.3095 - 0.3735I
-0.3095 - 0.3735I
-0.3095 - 0.3735I
```

$C^{\dagger} C = 1$

Example 1: Beamforming



Beamforming grid (thinned by factors of 4 in both directions)



Example 1: Source time history and array data

Narrowband source time history

$S(t)$ =

```
1.0D+05 *
 0.4372 - 0.0053I   -0.0111 + 0.8899I   -0.1572 + 0.3954I   0.3577 - 0.1324I   -0.4097 - 0.4975I   -1.7068 + 0.6177I   0.0343 - 1.1219I   0.4321 + 0.2337I
-0.0577 + 1.2663I   -0.3771 + 0.4007I   -0.3940 - 0.0091I   -1.1874 - 0.2159I   -0.7086 - 0.4381I   -0.4231 + 1.0949I   0.1424 + 0.2979I   0.8497 + 0.1633I
-0.3958 + 0.1963I    0.0650 + 0.2073I    0.6556 + 0.1176I   -0.3999 - 0.2350I    1.2202 + 0.1319I    0.5218 + 0.7760I   0.0726 + 0.7083I   1.1537 - 0.1073I
 0.4891 + 0.5086I   -0.1536 - 0.7897I   -1.4279 + 1.0132I    0.7537 + 0.7622I    0.4733 + 0.2853I    1.0013 - 0.5930I   -0.1297 + 0.3158I   -0.6174 + 0.7710I
-0.9967 - 0.6554I    0.5588 - 0.0513I   -0.1496 + 0.6420I    1.1985 + 0.3786I    0.0140 - 0.4303I   -1.0613 + 0.7102I   -0.0912 + 0.3565I   -1.1507 + 0.3796I
 0.2652 - 0.4008I   -0.3612 - 0.4157I   -1.0290 + 0.3781I   -0.6148 - 0.8390I    0.4544 - 1.5932I    0.7114 - 0.5162I   0.5572 + 0.7951I    1.2494 - 0.5682I
-0.6857 - 0.0558I   -1.2259 - 0.1041I    0.8371 - 0.3124I   -0.3174 - 0.6586I    1.2806 - 0.1836I   -0.0328 - 0.4285I   -0.8204 - 0.1896I   -0.3042 - 0.1236I
-1.1532 - 0.1882I    1.4586 - 0.7353I   -0.5725 - 0.5543I   -0.5386 - 1.7208I    0.8148 - 0.3490I    0.1500 - 0.3746I   0.5601 - 0.9509I    0.5558 + 0.6187I
-0.1043 + 0.3196I   -0.5156 - 1.9243I   -1.0276 + 0.2411I   -0.0542 - 0.1193I    1.2722 - 0.9999I    0.8046 - 0.9468I   0.3592 - 0.8539I    -0.1072 + 1.3918I
 0.0426 - 0.7906I   -1.2598 + 0.0467I   -0.1181 + 0.0015I    0.1134 + 0.7755I    0.6373 + 0.3767I    0.5541 + 0.8653I   -0.4180 - 1.1655I    0.7532 - 0.7065I
-0.8913 + 0.2200I   -0.6066 - 0.7307I    0.8391 - 0.5260I    0.0104 + 0.5951I   -0.6113 - 0.2615I   -1.3231 + 0.4056I   -1.2092 + 1.2497I   -0.6496 + 0.7265I
 0.2656 - 0.9320I   -0.6406 - 0.2940I    0.0264 - 1.7844I   -1.0850 + 0.9833I    0.1247 + 0.2723I   -0.1021 - 0.3437I   -0.2462 - 0.3744I   -0.1857 + 0.3210I
 0.5138 + 0.7417I    0.4722 + 0.3091I   -1.3402 + 0.9874I    0.0901 + 0.9001I
```

(100 normally distributed complex numbers) $\left\langle S(t)S^*(t)\right\rangle = \dfrac{1}{100}\sum_{k=1}^{100} S_k S_k^* = 1.0E\ 10 = 100\,dB$

Narrowband array data $\vec{u}(t) = \bar{C}S(t)$ = 4×100 complex matrix

(σ was chosen for 100 dB)

Cross spectral matrix $A = \left\langle \vec{u}(t)\vec{u}'(t)\right\rangle$ $\quad A_{ij} = \dfrac{1}{100}\sum_{k=1}^{100} u_i(t_k)u_j^*(t_k)$

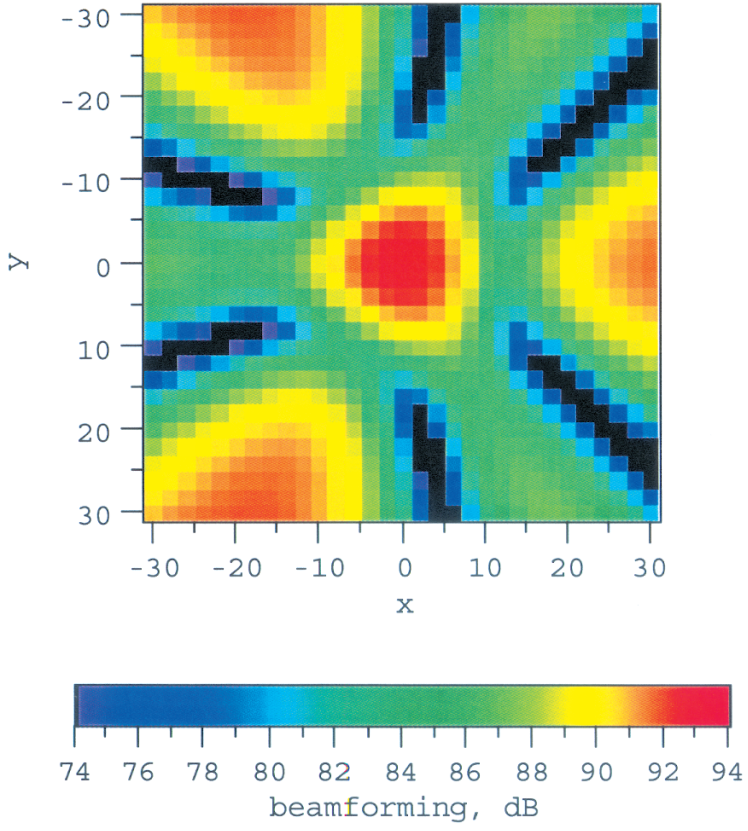
A =

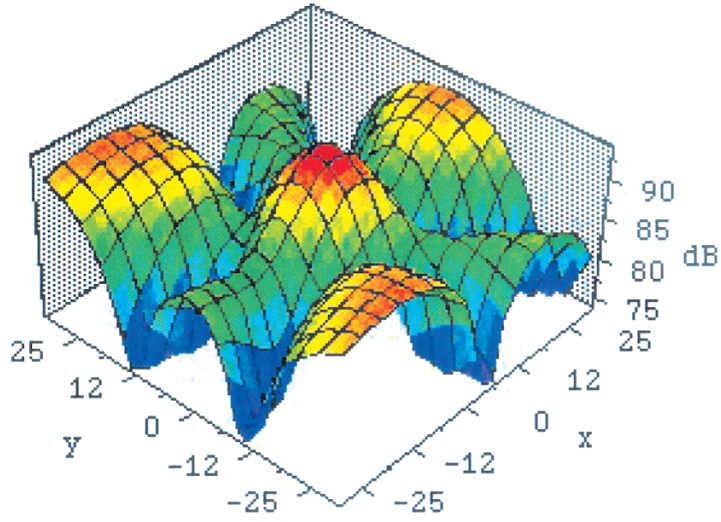
```
1.0D+09 *

2.9411 - 0.0000I   1.2225 - 2.3294I   1.2225 - 2.3294I   1.2225 - 2.3294I
1.2225 + 2.3294I   2.3530 - 0.0000I   2.3530 - 0.0000I   2.3530 - 0.0000I
1.2225 + 2.3294I   2.3530 - 0.0000I   2.3530 - 0.0000I   2.3530 - 0.0000I
1.2225 + 2.3294I   2.3530 - 0.0000I   2.3530 - 0.0000I   2.3530 - 0.0000I
```

Example 1: Beamforming

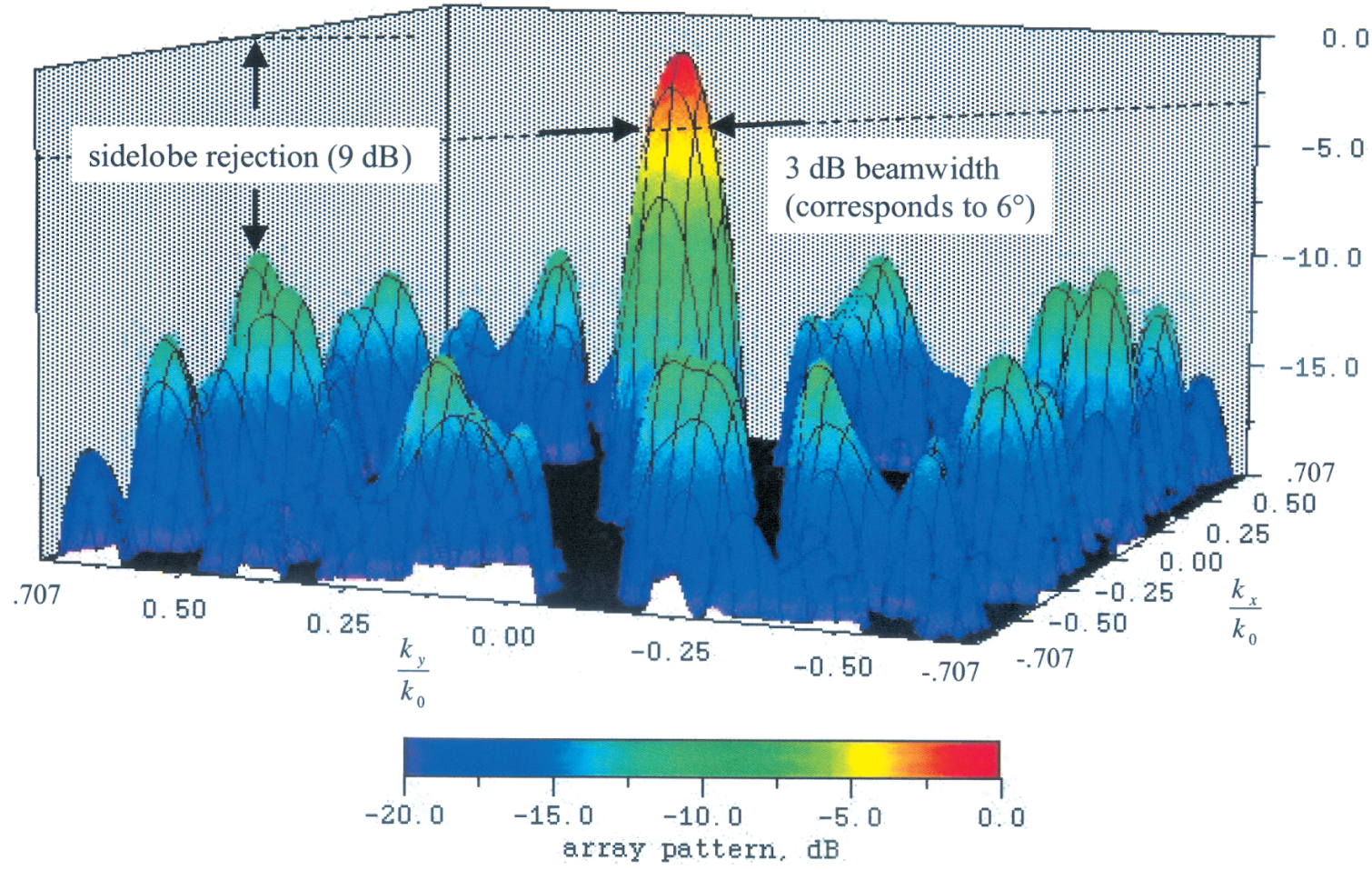
- The code make_grid.f was used to create a grid of points in the plane z = 20 (grid_20.fmt)
- The cross spectral matrix was translated into the input format for the code beamform99.f (A1a)
- The code make_time.f was used to to make a file of gird to microphone propagation times (g20.tim)
- beamform99.f was run using the above as inputs





Array design: beamwidth and sidelobes

Plane wave evaluation of 64 element spiral array at 8000 Hz



Setup for the SFJN test

Phased array measurements for the SFJN test at LeRC

Three arrays were used during testing.

- **Each array has its own advantages**

Array A: Large 7 arm logarithmic spiral

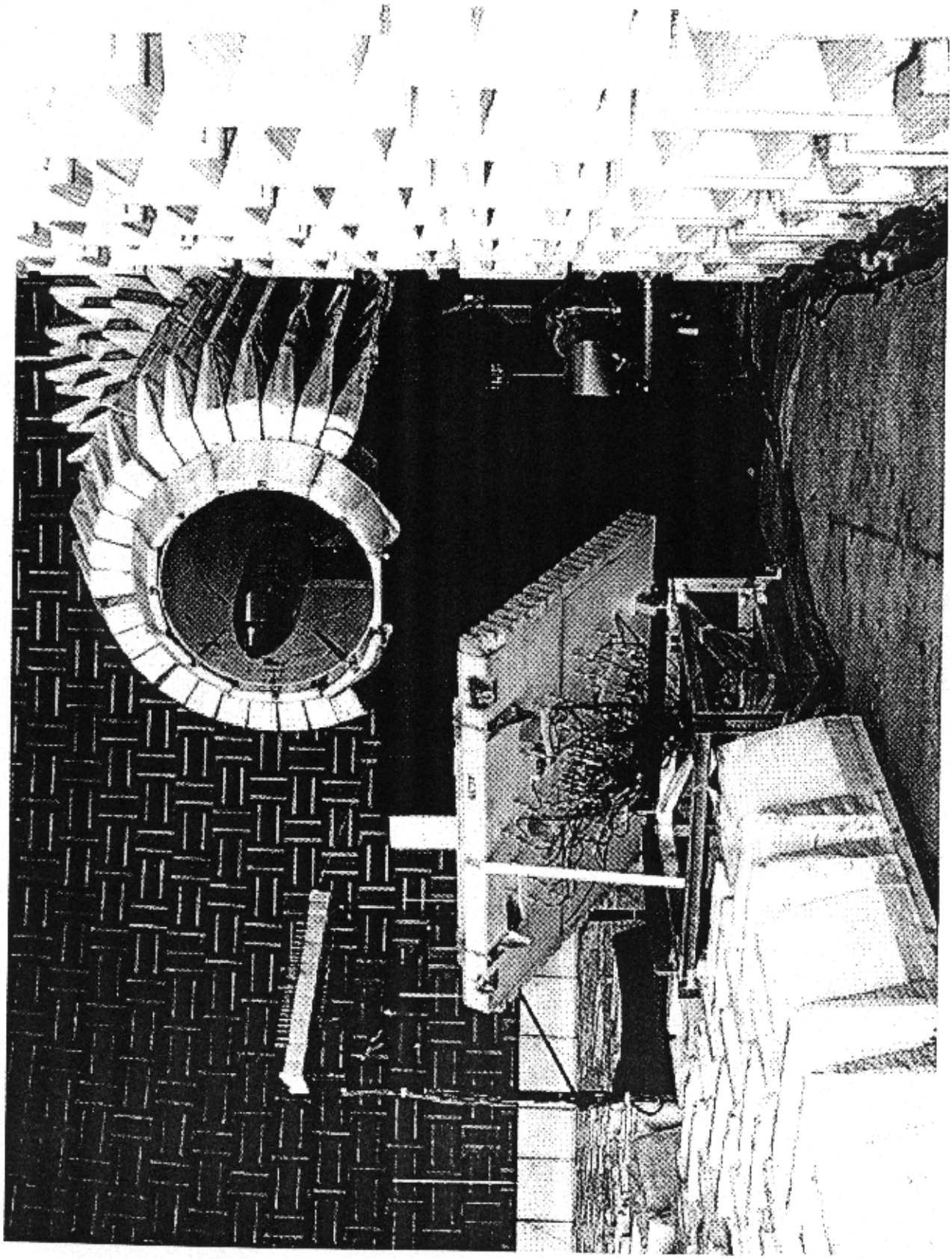
- **Determines source density in two dimensions**
- **Located below the jet at 90 and 120 degrees**
- **Works well from 1000 to 8000 Hertz**

Array B: Small 7 arm logarithmic spiral (contained within array A)

- **Determines source density in two dimensions**
- **Located below the jet at 90 and 120 degrees**
- **Works well from 8000 to 50000+ Hertz**

Array C: Sideline linear array

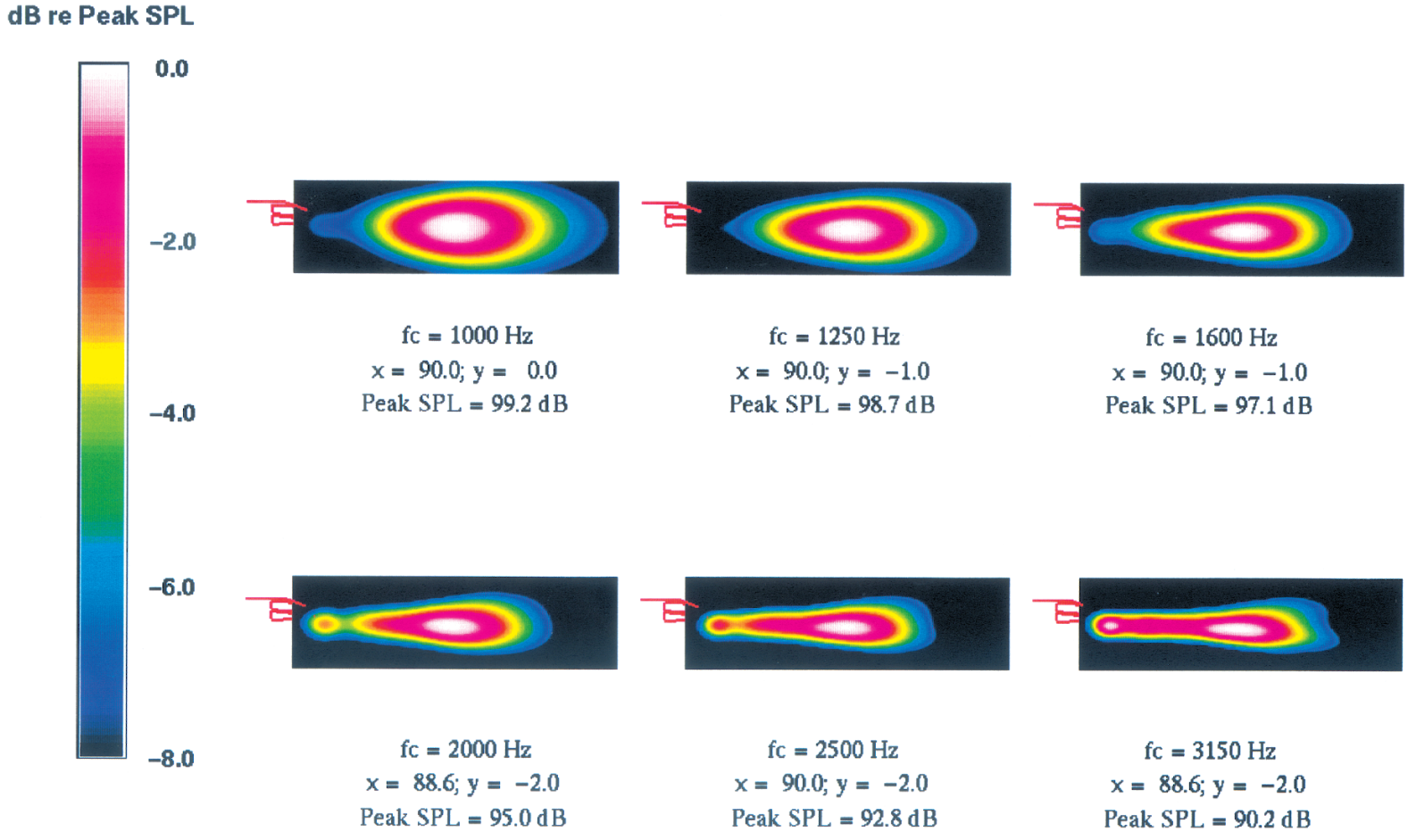
- **Image in one direction along axis of jet**
- **Works well from 1000 to 50000 Hertz**



Separate Flow Jet Noise Reduction Test

Model 3BB viewed with array A

Run: 1115 **Point: 21** **Mach: 0.28**

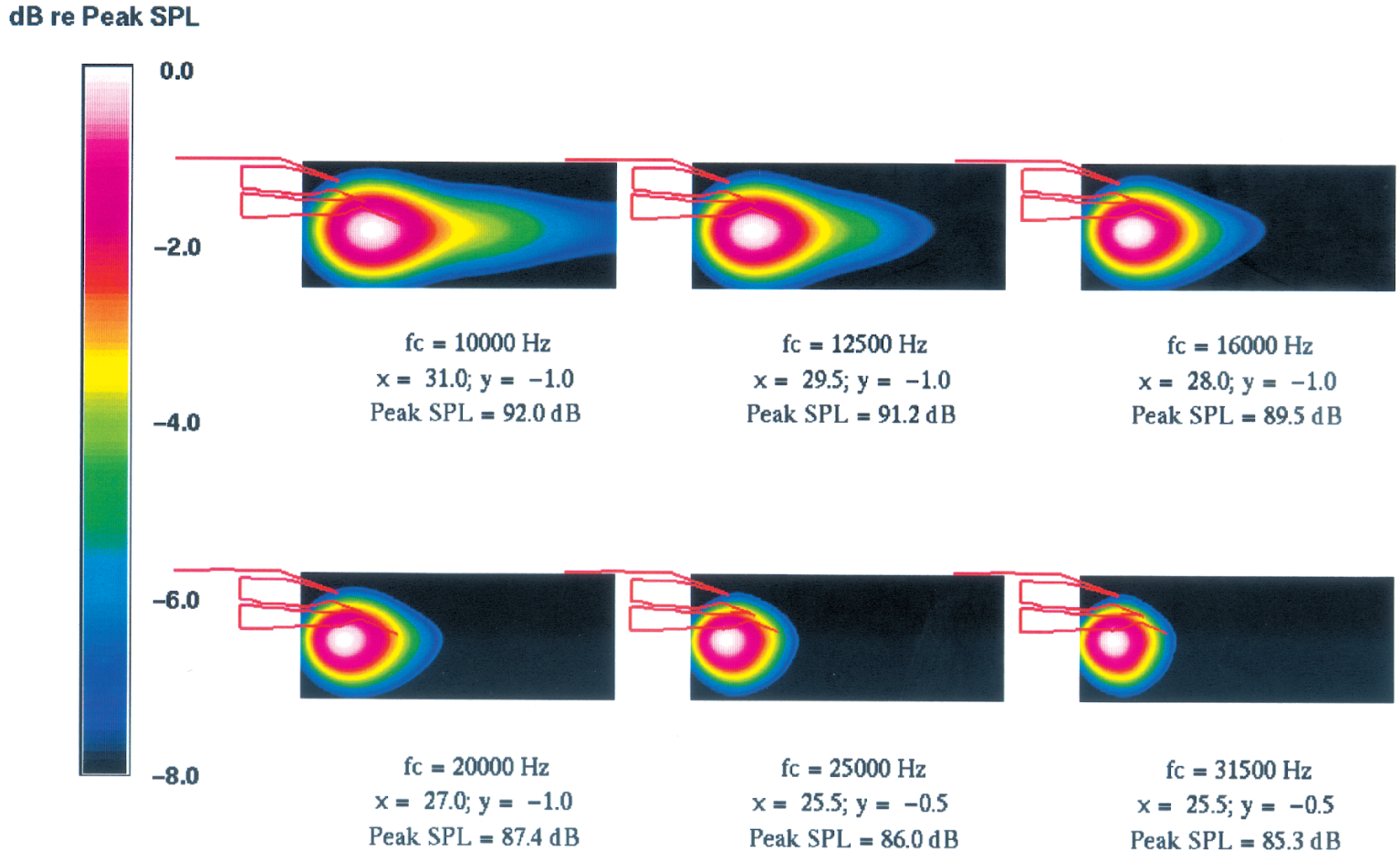


JWP June 05, 1997 09:36:09 AM

Separate Flow Jet Noise Reduction Test

Model 3BB viewed with array B

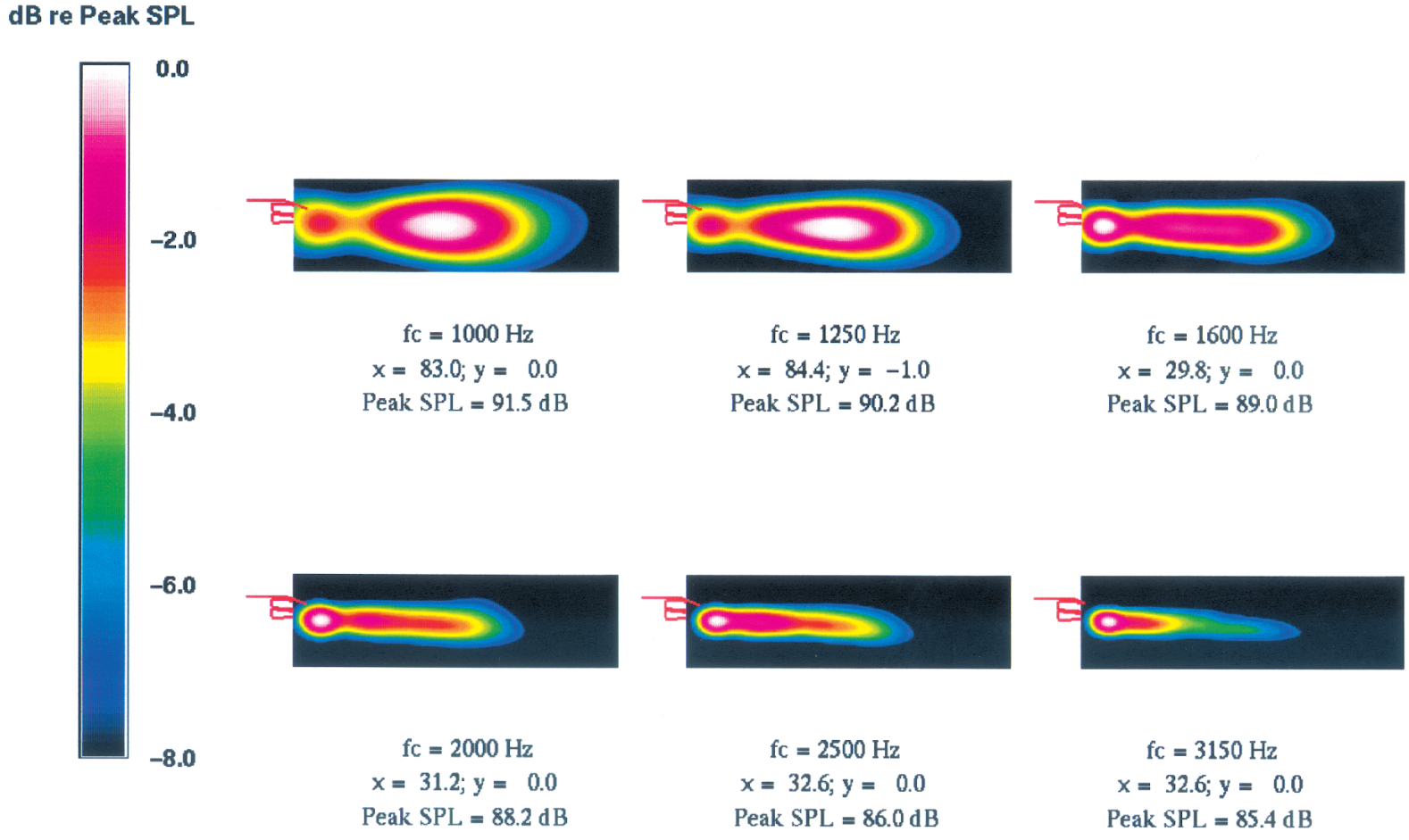
Run: 1115 **Point: 21** **Mach: 0.28**



Separate Flow Jet Noise Reduction Test

Model 3BB viewed with array A

Run: 1113 **Point: 23** **Mach: 0.28**

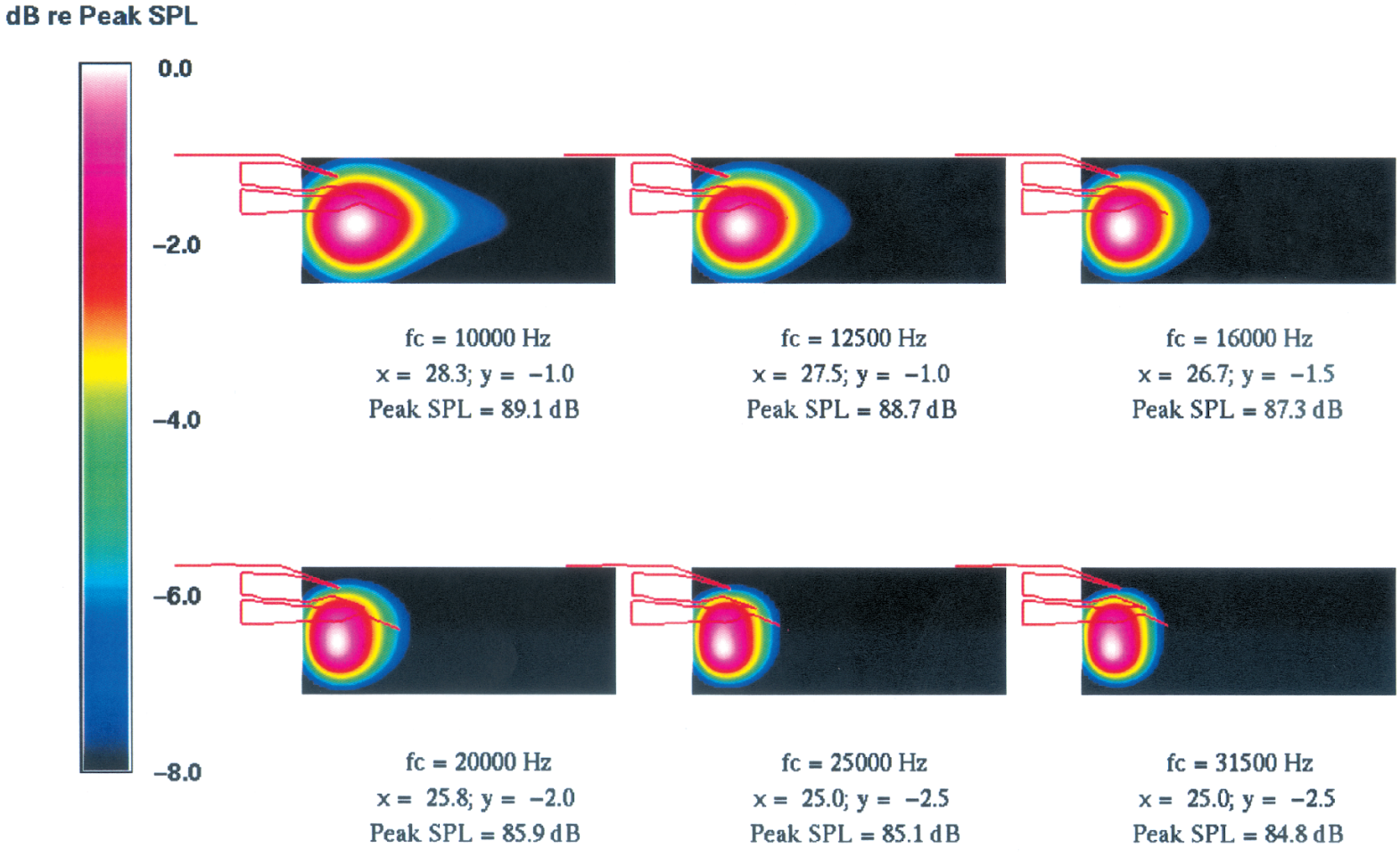


JWP June 05, 1997 09:33:19 AM

Separate Flow Jet Noise Reduction Test

Model 3BB viewed with array B

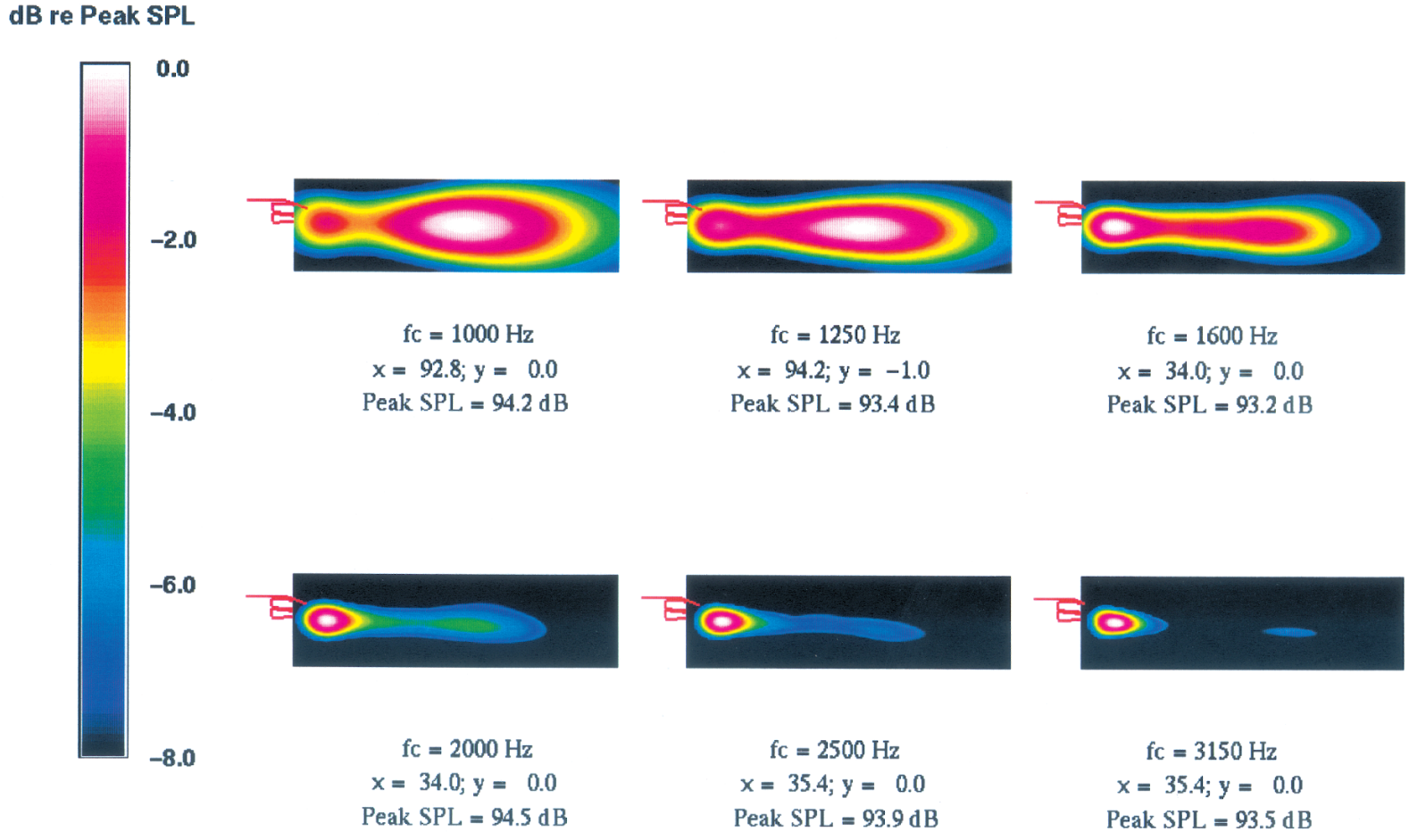
Run: 1113 **Point: 23** **Mach: 0.28**



Separate Flow Jet Noise Reduction Test

Model 3IC viewed with array A

Run: 1109 **Point: 21** **Mach: 0.28**

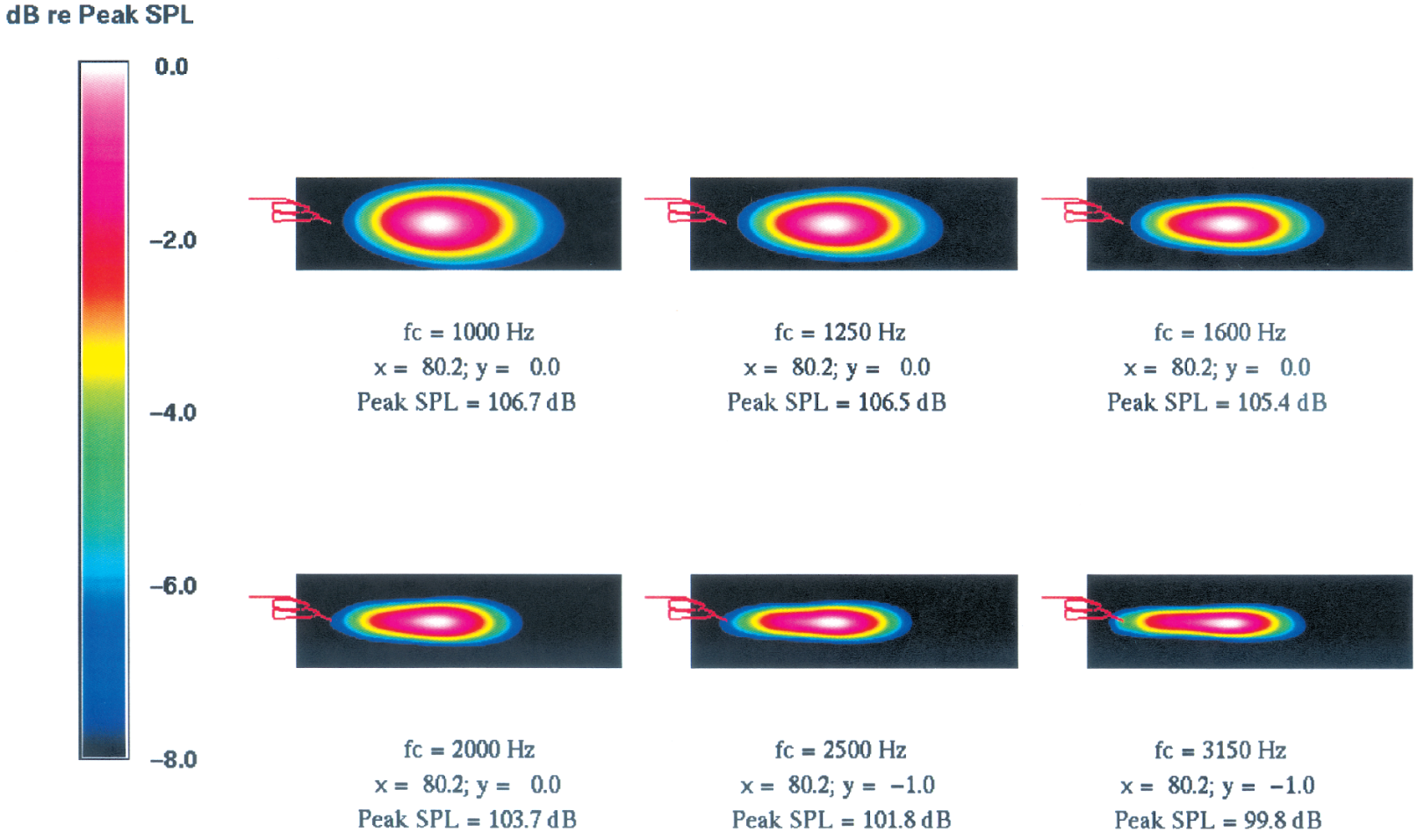


JWP June 05, 1997 09:25:49 AM

Separate Flow Jet Noise Reduction Test

Model 3BB viewed with array A

Run: 1118 **Point: 21** **Mach: 0.00**

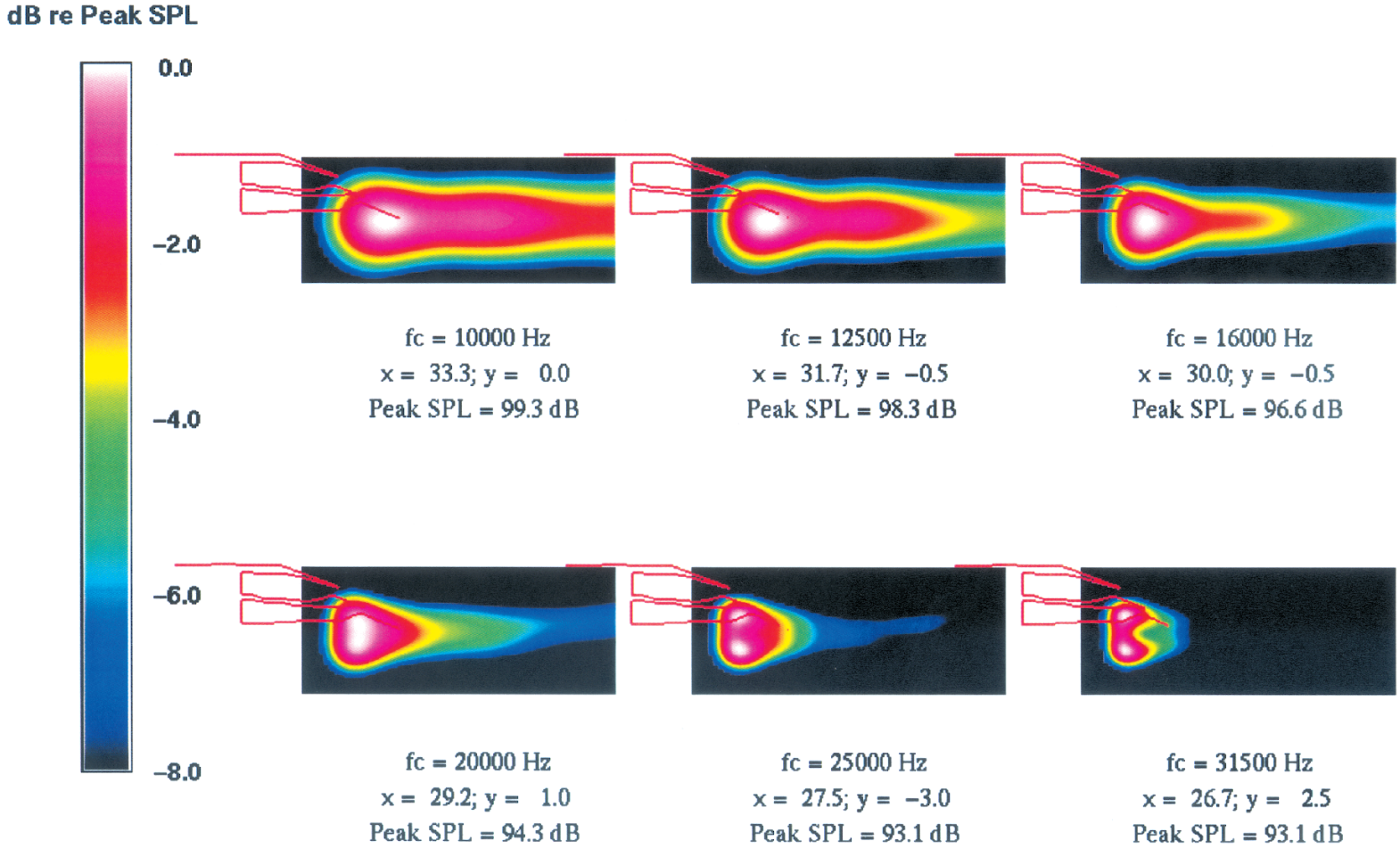


JWP November 02, 2000 07:45:35 PM

Separate Flow Jet Noise Reduction Test

Model 3BB viewed with array B

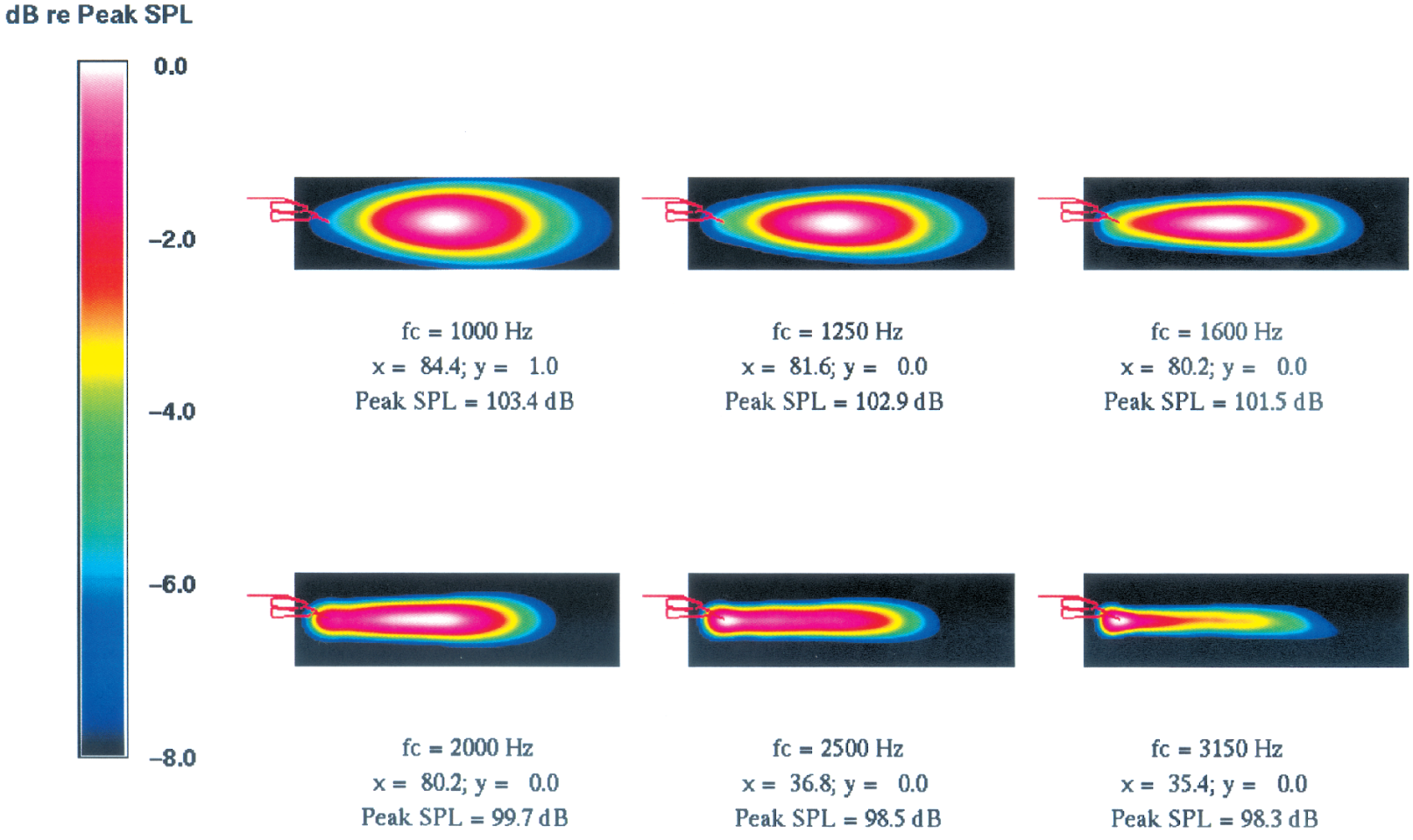
Run: 1118 **Point: 21** **Mach: 0.00**



Separate Flow Jet Noise Reduction Test

Model 3IC viewed with array A

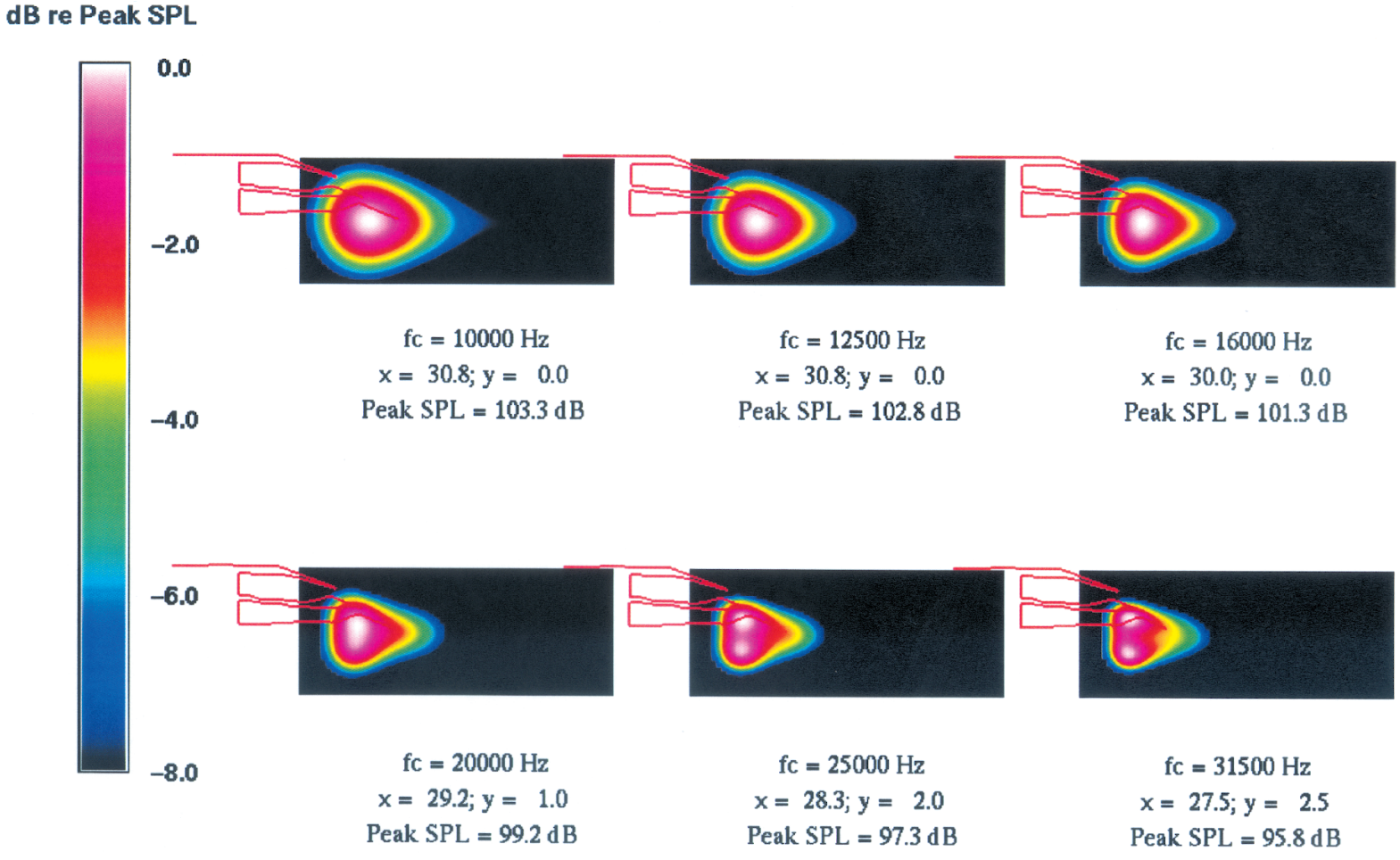
Run: 1110 Point: 21 Mach: 0.00



Separate Flow Jet Noise Reduction Test

Model 3IC viewed with array B

Run: 1110 Point: 21 Mach: 0.00



Conclusions

Phased array measurements for the SFJN test at LeRC

- Phased arrays can be used to qualitatively image jet noise sources
- Two separate source regions:
  - upstream near nozzle exit (Region 1)
  - downstream several nozzle diameters (Region 2)
- The upstream region is less affected by increases in power than the downstream
- The upstream region is less affected by increases in tunnel Mach number than the downstream
- Jet Mixing devices:
  - increase upstream sources (Region 1)
  - decrease downstream sources (Region 2)
- Preliminary results of using phased array measurements to determine far–field spectra are promising

T. Bhat References

1. Phased Array Beamforming for Aeroacoustics, Robert P. Dougherty, Boeing Commercial Airplane Group, AIAA Short Course, May 8-9,1999.

2. Advanced Subsonic Technology (AST) Separate-Flow High Bypass Ratio Nozzle Noise Reduction Program Test Report, John K. C. Low, Paul S. Schweiger and John W. Premo, NASA CR-2000-210040.

Mr. Marcus Harper-Bourne of DERA presented typical results from the application of the polar correlation technique and results from azimuthal correlation. Results indicated that there may be two source distributions within the jet at a given frequency. Results from azimuthal correlation indicated that the jet noise sources are located just outside of the jet lip line for a single flow jet. The method could be applied to coaxial jets.

Conclusions made by Mr. Harper-Bourne are:

- The acoustic analogy with microphone correlation continues to be useful as a source location and diagnostic tool at both model and full scale
- Extension of polar correlation to azimuthal correlation was demonstrated for lateral source measurement.
- A simplified method involving correlation of the sound at two microphones placed at diametrically opposite sides of a round jet was developed and analyzed.
- Used successfully on a model air jet in an anechoic chamber
- Potential use of the method on coaxial jets was illustrated

Dr. Jay Panda of NASA Glenn presented results obtained by cross-correlation of measured density fluctuation within a jet with far-field sound. The density fluctuations were measured using a Rayleigh scattering technique. For subsonic flow the correlations were very low, while for supersonic flow significant correlation was measured.

Dr. Venod Mengle of Rolls Royce presented an analytical approach to separate internally generated noise sources and those external sources within the core near the jet exit from and externally generated noise for internal mixer nozzles. The approach was based on the assumption that internal noise sources and those external sources within core near the jet exit do not change with free jet speed whereas the other external sources do. The method was applied to several mixer nozzle configurations. Internal noise dominated at high frequencies. Dr. Mengle found that internal sources are more dominant in unscalloped mixers than scalloped generally at higher speed over an angular range of 75 to 100 degrees from the jet inlet axis.

Dr. Krish Ahuja of Georgia Tech summarized a source location technique based on the polar directivity of the coherence of far field microphones as a function of microphone separation. The technique has been applied to identify jet source distributions.

Source Identification and Location Technique

The Use of Azimuthal Microphone Correlation to Determine the Lateral Distribution of Mixing Noise Sources in a Round Jet

Marcus Harper-Bourne
DERA Pyestock, England

M Harper-Bourne
OAI 7-11-2000

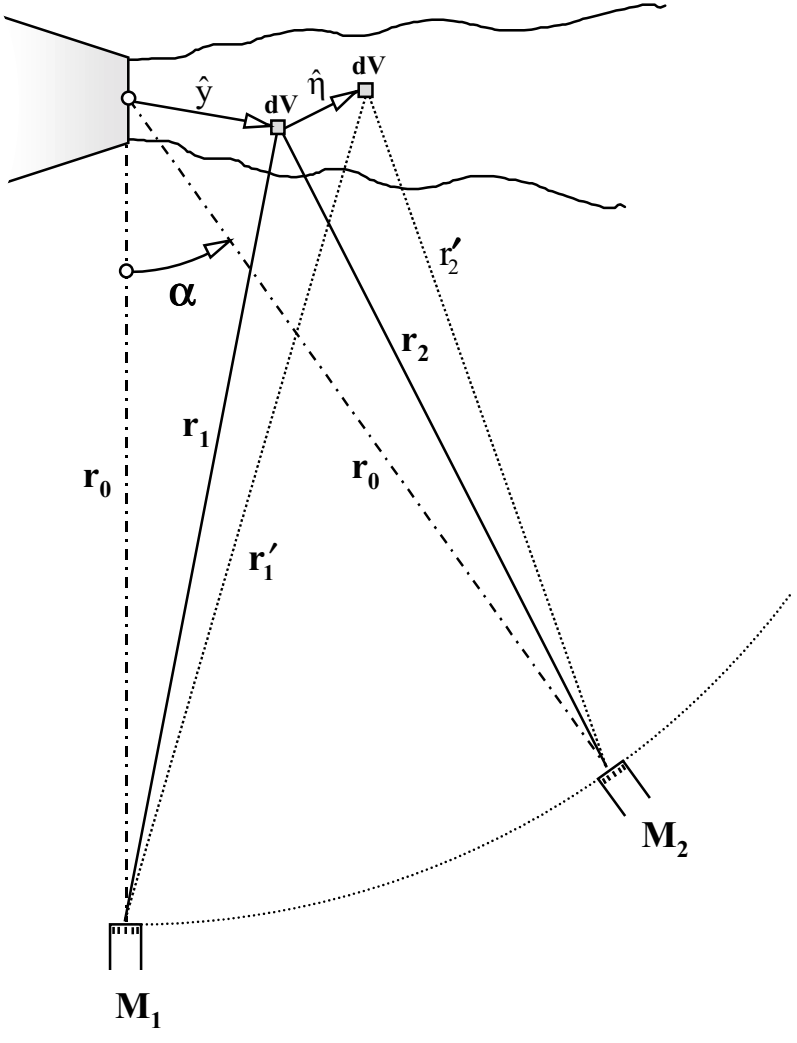
AeroAcoustics Research Consortium, Jet Noise Workshop
November 2000 / Ohio Aerospace Institute, Cleveland

"SOURCE IDENTIFICATION AND LOCATION TECHNIQUE"

THE USE OF AZIMUTHAL MICROPHONE CORRELATION TO DETERMINE THE LATERAL DISTRIBUTION OF MIXING NOISE SOURCES IN A ROUND JET
(AIAA 98-2357)

Marcus Harper-Bourne
DERA Pyestock, England

WAVE FIELD IMAGE SYNTHESIS USING MICROPHONES (AIAA 98-2357)



For α small, general equation for cross power spectral density (cpsd) or cross-spectrum between two field points for a 3D source is:

$$\tilde{C}_{12}(\omega) = \int_{\hat{y}} \tilde{q}_1(\hat{y},\omega) e^{-jK\{r_1 - r_2\}} \frac{dV}{r_1 r_2} \qquad \textbf{(1)}$$

Applying (1) to an axial line source S(y) yields the Polar Correlation eqn:

$$\tilde{R}(\alpha,\omega) = \int_{y_1} \tilde{S}(y_1,\omega).e^{-jKy_1 \sin\alpha} dy_1 \qquad \textbf{(2)}$$

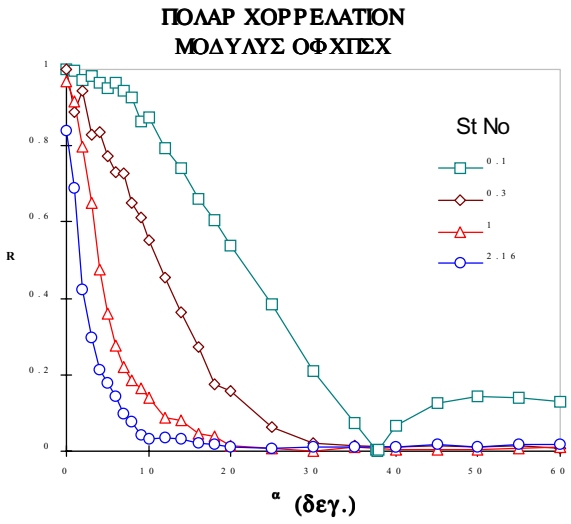
where S is the source strength per unit slice of jet and R and S are a Fourier Transform pair. Hence:

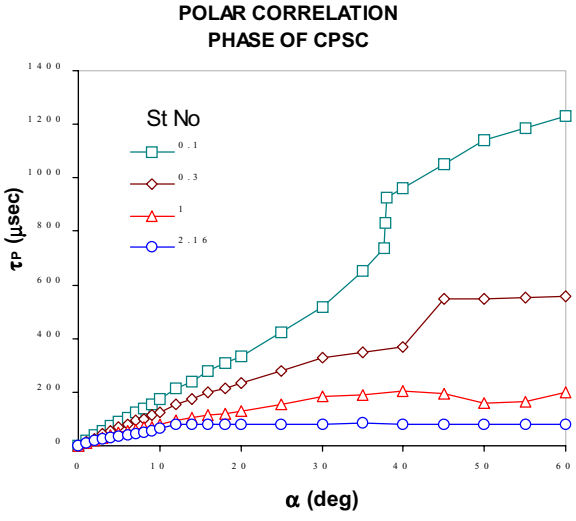
$$\tilde{S}'(y_1,\omega) = \frac{1}{2\pi} \int_{-k_m}^{k_m} \tilde{R}(\alpha,\omega).e^{jky_1} dk \qquad \textbf{(3)}$$

$$k_m = K \sin\alpha_m \text{ and } K = \omega / a_0$$

"Source Identification and Location Technique"

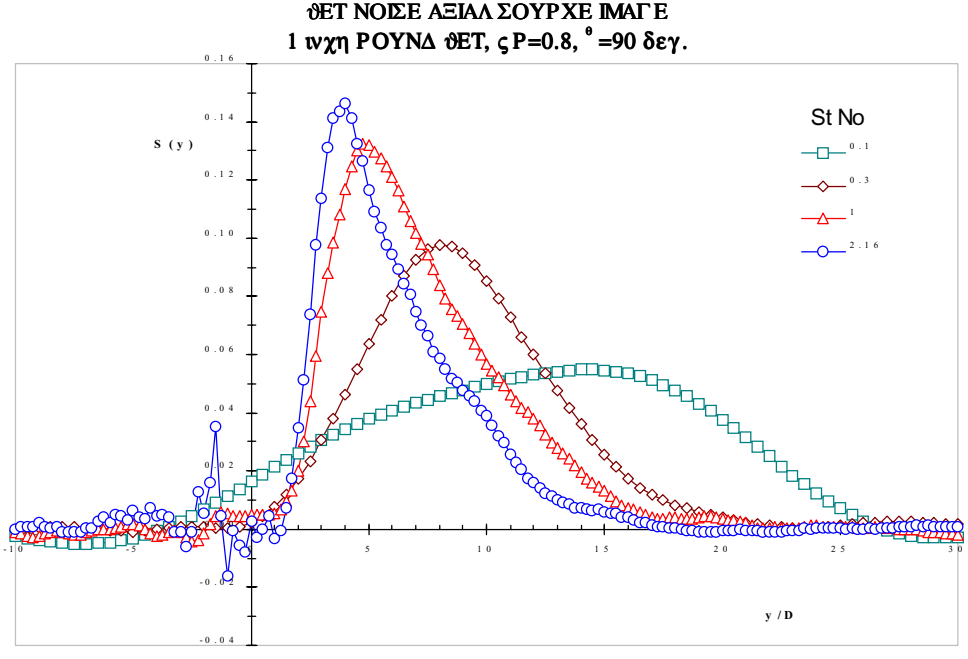
M Harper-Bourne
OAI 7-11-2000





(a) Measured polar CPSD in far-field of high subsonic round air jet

Polar Correlation applied to high subsonic round unheated air jet



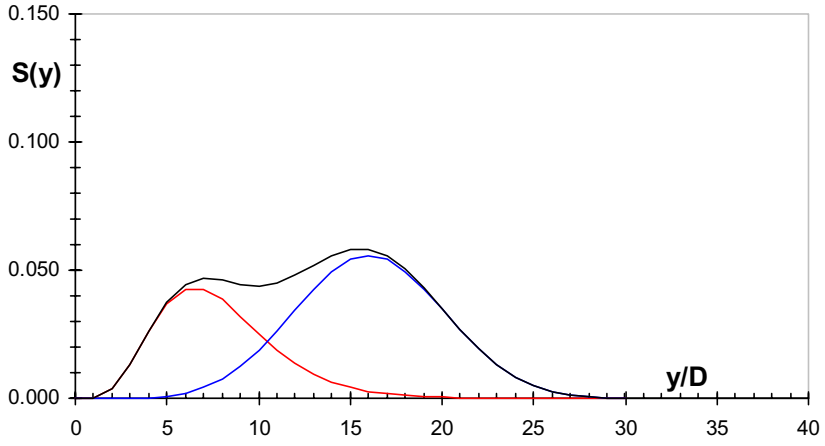
(b) Axial source distribution determined directly from FT of polar CPSD data (rectangular window)

DERA

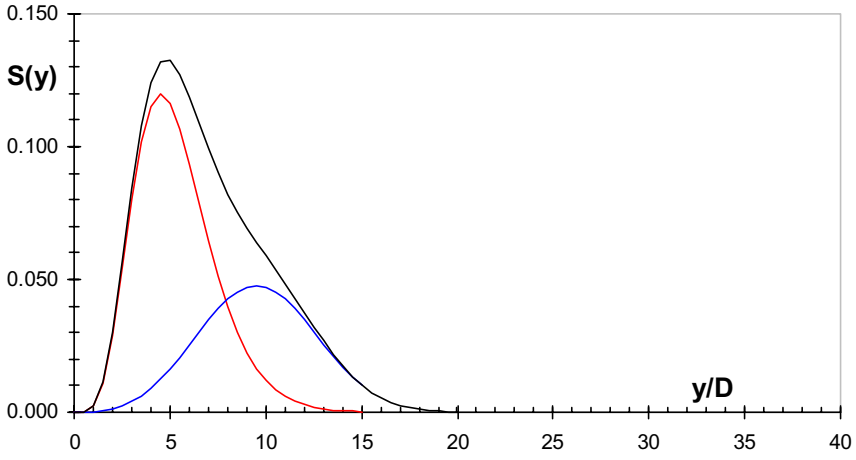
"Source Identification and Location Technique"

M Harper-Bourne
OAI 7-11-2000

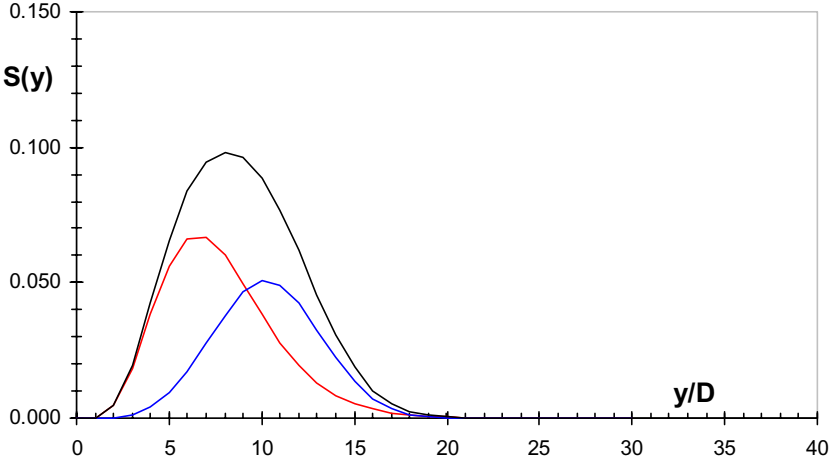
1080 Hz, St=0.1



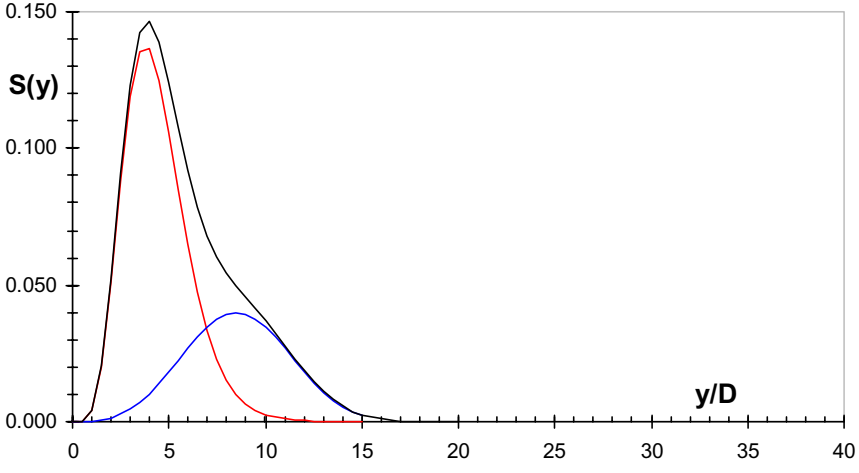
10800 Hz, St=1.0,



3240Hz, St=0.3



23300Hz, St=2.16,



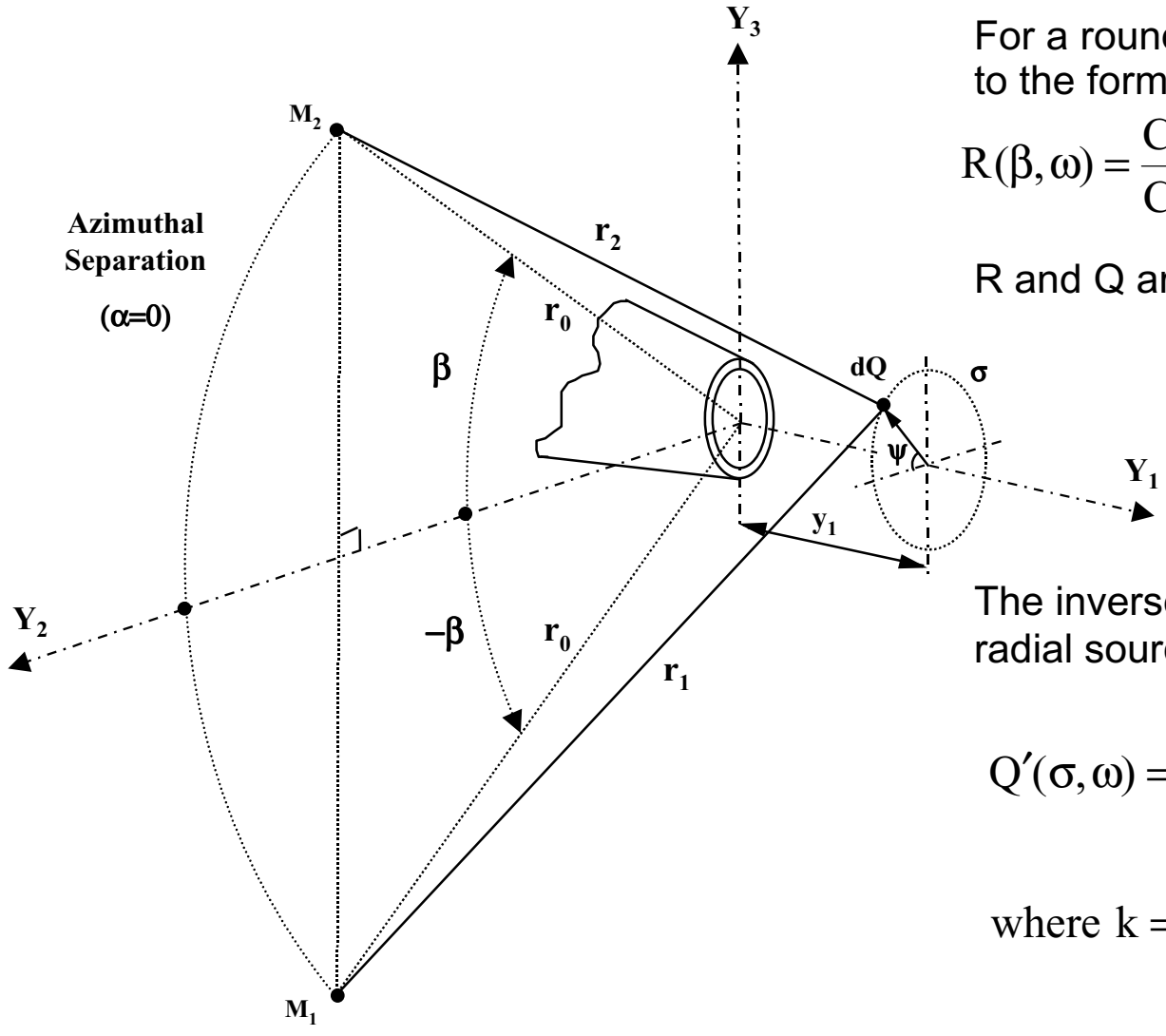
EDUCED TWO SOURCE BREAKDOWN FOR JET MIXING NOISE SOURCES AIAA 99-1838

DERA

M Harper-Bourne
OAI 7-11-2000

APPLICATION OF EQN (1) TO AZIMUTHAL CORRELATION

For azimuthal microphone separation:



$$r_1 - r_2 = 2y_1 \sin\alpha.\cos\beta + 2y_3 \sin\beta$$

For a round jet eqn. (1) can be reduced to the form

$$R(\beta,\omega) = \frac{C(\beta,\omega)}{C(0,\omega)} = \int_0^\infty \sigma Q(\sigma,\omega) J_0(2K\sigma\sin\beta)d\sigma$$

R and Q are Hankel Transform pair. **(4)**

The inverse transform of (4) yields average radial source image at frequency • :-

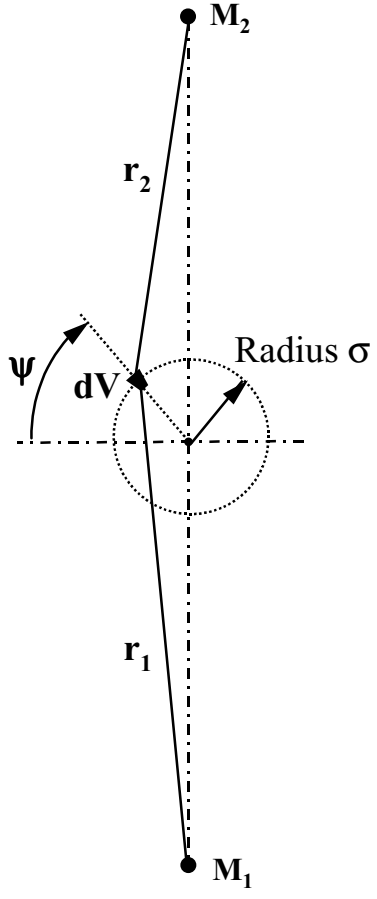
$$Q'(\sigma,\omega) = \int_0^{k_m} k\, R(k,\omega) J_0(k\sigma)dk \qquad \textbf{(5)}$$

where $k = 2K\sin\beta$ and $k_m = 2K\sin\beta_{max}$

DERA

M Harper-Bourne
OAI 7-11-2000

FREQUENCY AVERAGED RADIAL SOURCE IMAGE ($\beta=90^0$)



$\alpha=0$, $\beta=90^0$

With the microphones fixed on diametrically opposite sides of the jet and normal to it:

$$r_1 - r_2 = 2\sigma \sin\psi$$

$$R(\tfrac{\pi}{2},\omega) = \frac{C(\tfrac{\pi}{2},\omega)}{C(0,\omega)} = \int_0^\infty \sigma \overline{Q}(\sigma) J_0(2K\sigma) d\sigma \qquad \textbf{(6)}$$

i.e. a Hankel Transform pair

Radial Source Image is obtained from the inverse Hankel Transform, namely:-

$$\overline{Q'}(\sigma,\omega) = \int_0^{k_m} k\, R(\tfrac{\pi}{2},\omega) J_0(k\sigma) dk \qquad \textbf{(7)}$$

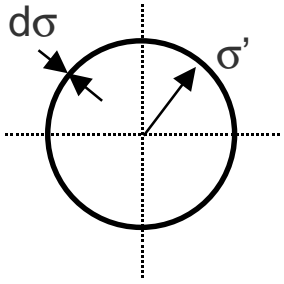
$$k = 2K \quad \text{and} \quad k_m = 2K_{max}$$

and $\overline{Q'}$ is the average radial source strength for the whole jet and all frequencies

M Harper-Bourne
OAI 7-11-2000

ANNULAR 'POINT' SOURCE FUNCTION

Derivation of an annular (point) source image for the radial source problem is outlined here:



Applicable cross-spectrum is $R(\omega) = J_0(2K\sigma')$

Applying the Hankel transform, eqn (7), yields for the image:

$$Q'(\sigma) = \frac{K_m}{\sigma'^2 - \sigma^2}[\sigma' J_0(2K_m\sigma) J_1(2K_m\sigma') - \sigma J_0(2K_m\sigma') J_1(2K_m\sigma)]$$

We can expand Q in a Bessel series to obtain:

$$H(\nu, x) = b_0 J_0(x) + [a_1 + xb_1]\frac{J_1(x)}{x} + [a_2 + xb_2]\frac{J_2(x)}{x} + [a_3 + xb_3]\frac{J_3(x)}{x} + \text{etc.....}$$

Where $H(\nu, x) = \frac{[\sigma + \sigma']}{2K_m} Q'(\sigma - \sigma')$ $\quad K_m = \frac{\omega_{max}}{a_0}$ $\quad x = 2K_m[\sigma - \sigma'] = \mu - \nu$

and $\nu = 2K_m\sigma'$

$$a_1 = \nu[b_1 + 2J_1^{\,2}(\nu)] \qquad b_0 = J_0(\nu)J_1(\nu)$$

$$a_2 = \nu[b_2 - 2J_1(\nu)J_2(\nu)] \qquad b_1 = J_0(\nu)[J_0(\nu) - J_2(\nu)]$$

$$a_3 = \nu[b_3 + 2J_1(\nu)J_3(\nu)] \qquad b_2 = -J_0(\nu)[J_1(\nu) - J_3(\nu)]$$

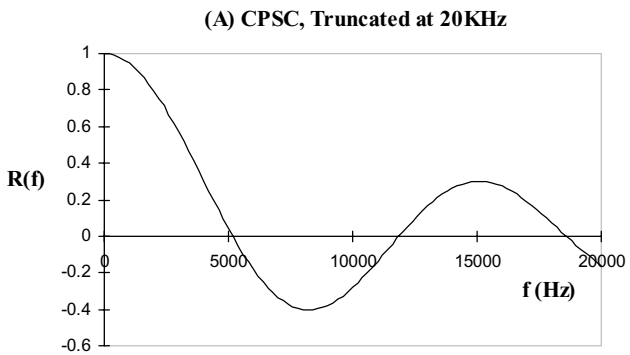
$$\ldots\ldots\ldots\text{etc} \qquad b_3 = J_0(\nu)[J_2(\nu) - J_4(\nu)]$$

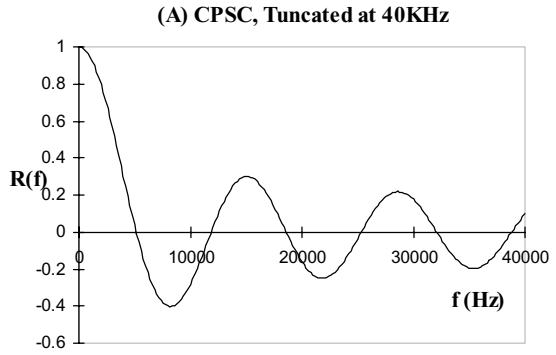
$$\ldots\ldots\ldots\ldots\text{etc}$$

DERA

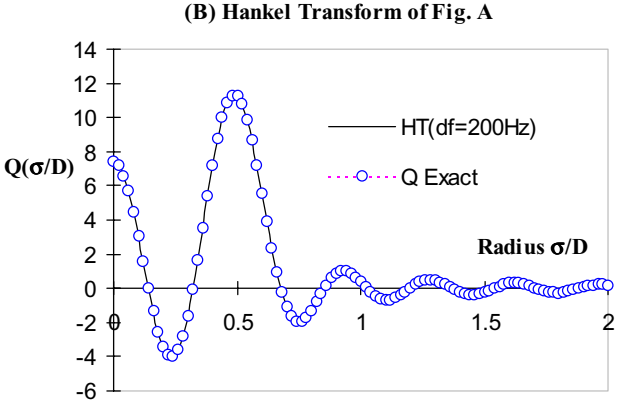
"Source Identification and Location Technique"

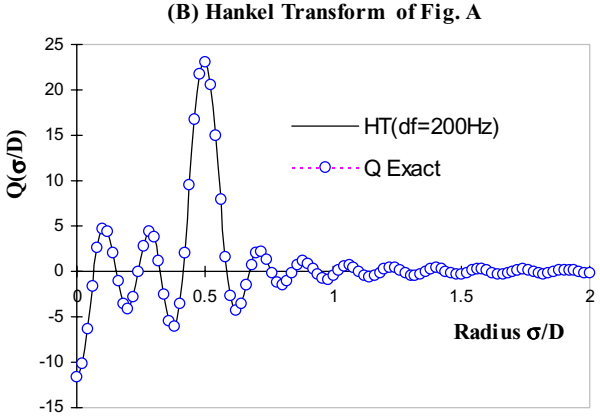
M Harper-Bourne
OAI 7-11-2000



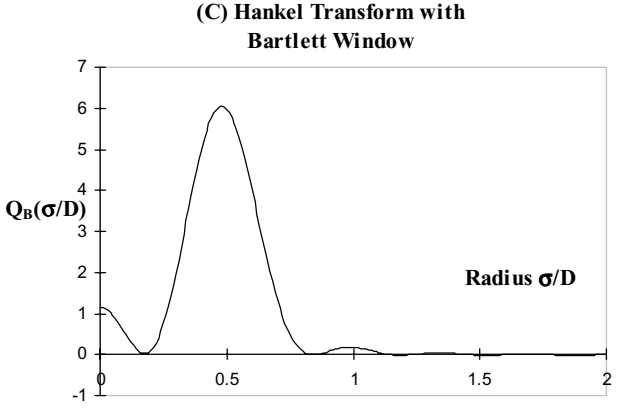


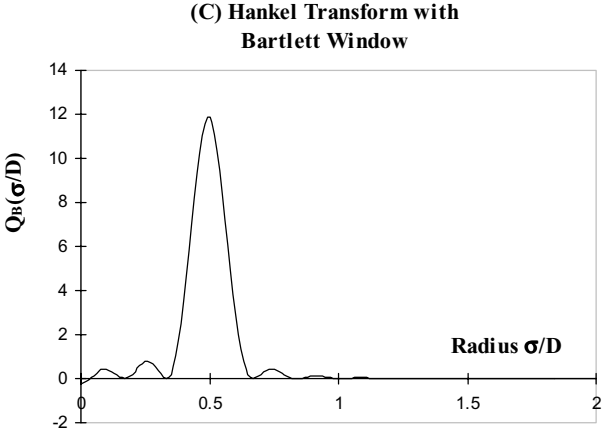
(a) CPSD for 'point' annular source for maximum frequencies of 20kHz and 40kHz





(b) 'Point' annular source image (Rectangular window)





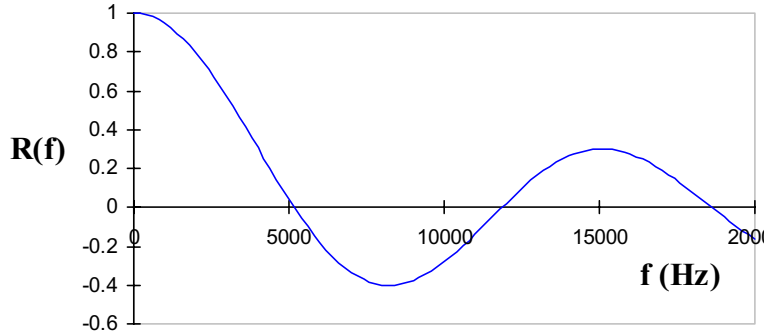
(c) 'Point' annular source image (Bartlett window)

DERA

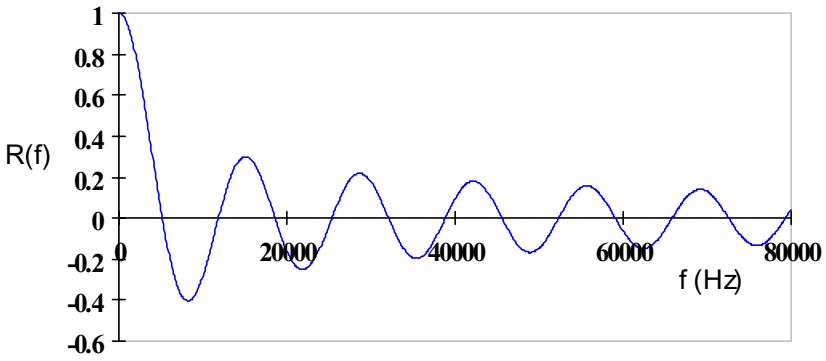
"Source Identification and Location Technique"

M Harper-Bourne
OAI 7-11-2000

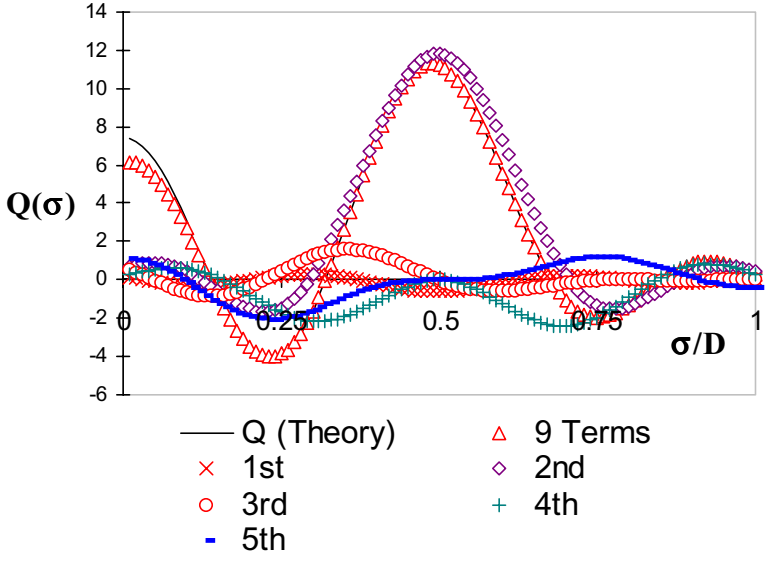
(A) CPSC for Ring Source of Radius 0.5D, Truncated at 20KHz



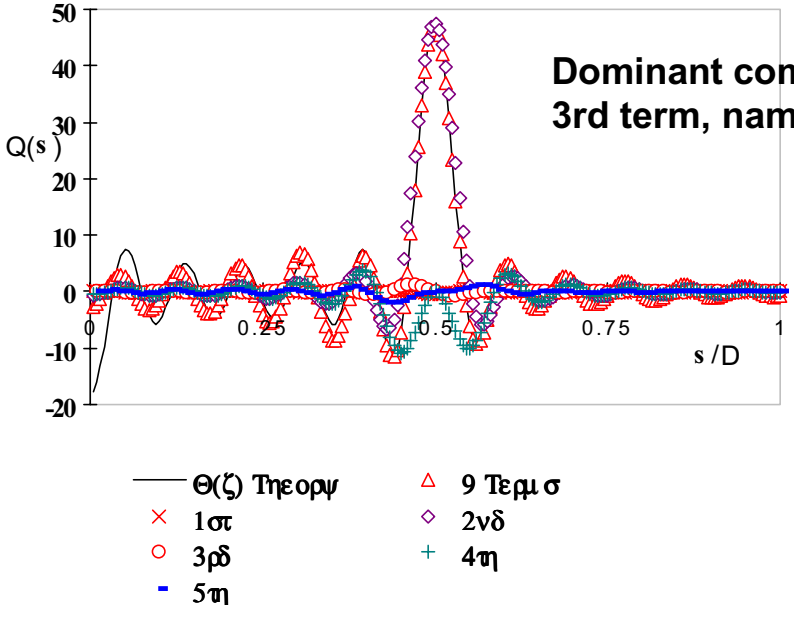
(A) CPSC for Ring Source of Radius 0.5D, Truncated at 80KHz



(B) Hankel Transform of Fig. A Showing Constituent Bessel Components



(B) Hankel Transform of Fig. A Showing Constituent Bessel Components

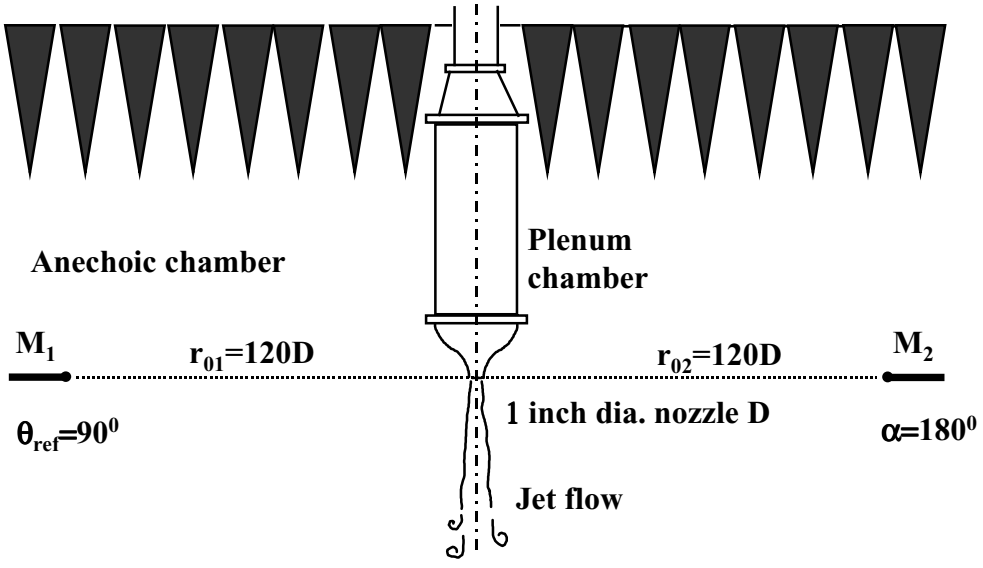


Dominant component is 3rd term, namely: $a_1 \frac{J_1(x)}{x}$

DERA

"Source Identification and Location Technique"

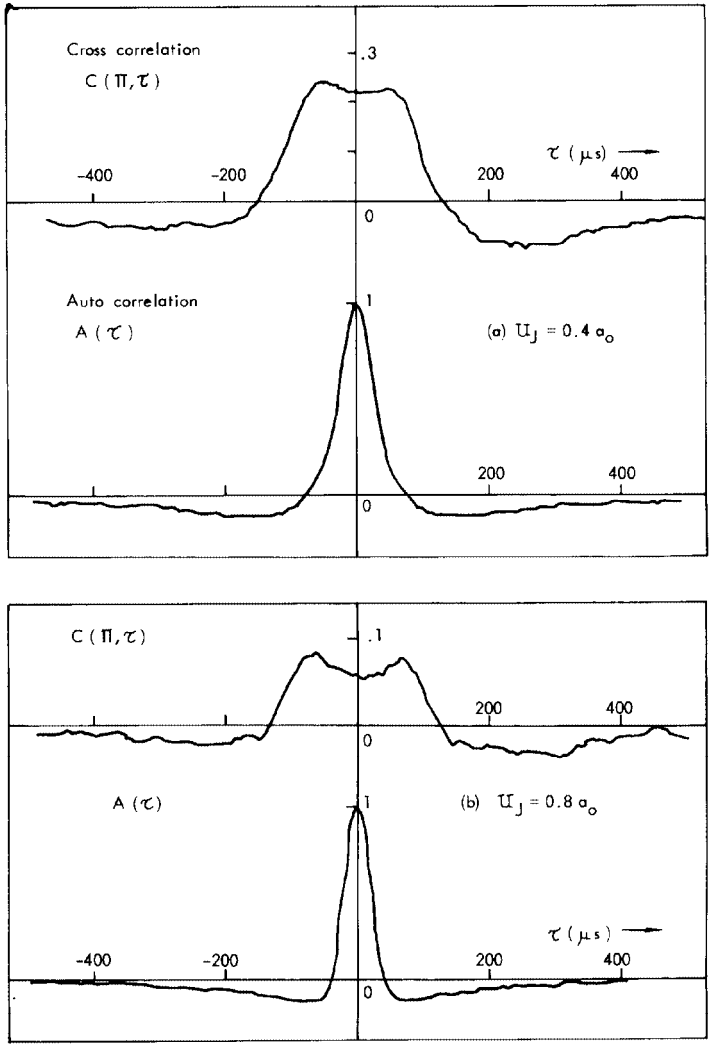
M Harper-Bourne
OAI 7-11-2000



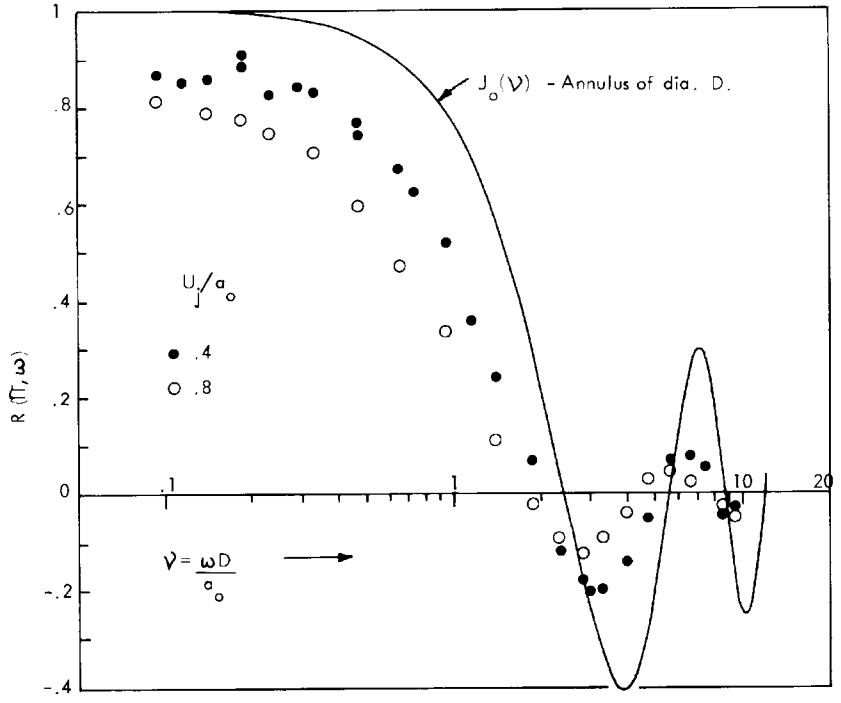
EXPERIMENTAL TEST SET-UP FOR LATERAL SOURCE MEASUREMENT ON SUBSONIC UNHEATED ROUND AIR JET IN AN ANECHOIC CHAMBER

"Source Identification and Location Technique"

M Harper-Bourne
OAI 7-11-2000



(a) Overall Correlations measured for two jet speeds

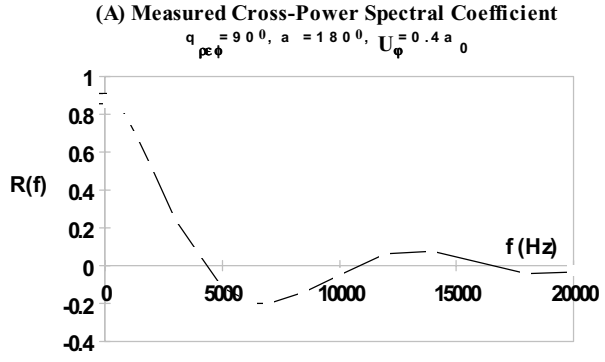


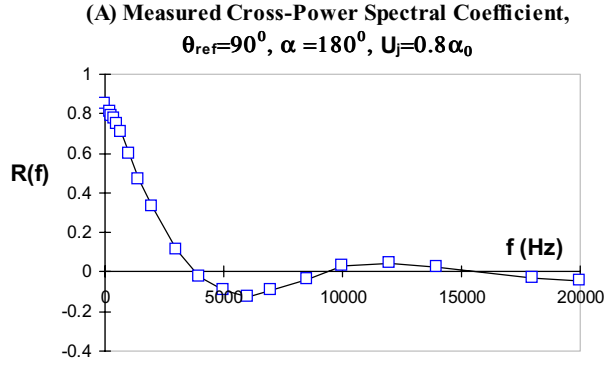
(b) Measured Cross-Power Spectral Density (CPSD) two jet speeds

DERA

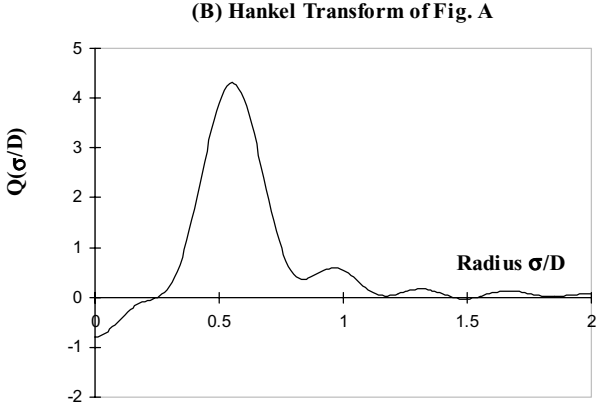
"Source Identification and Location Technique"

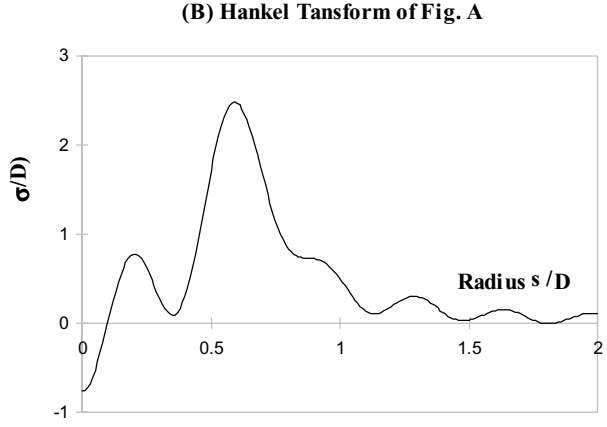
M Harper-Bourne
OAI 7-11-2000



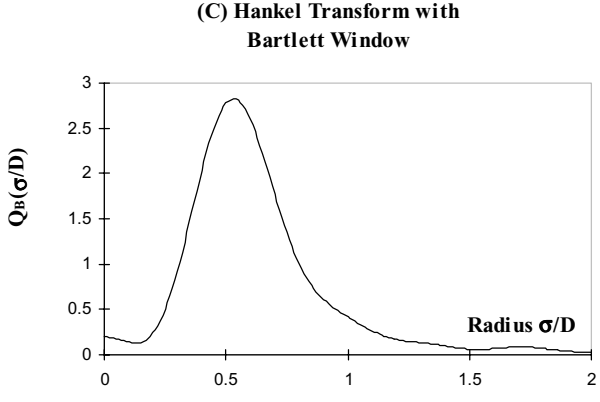


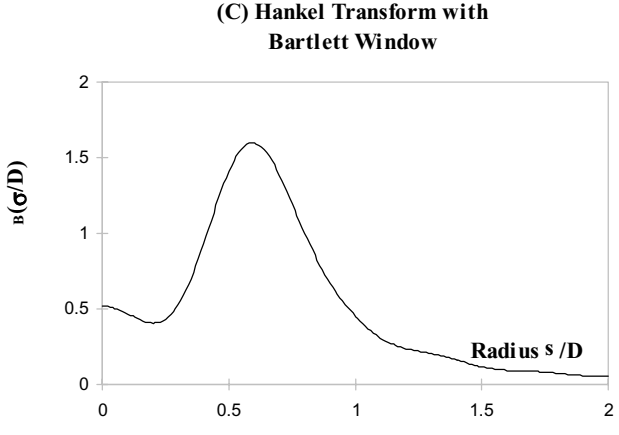
(a) Measured CPSD for Round Subsonic Jet (U_j/a_0=0.4 and 0.8)





(b) Radial Source Distributions (Rectangular window)



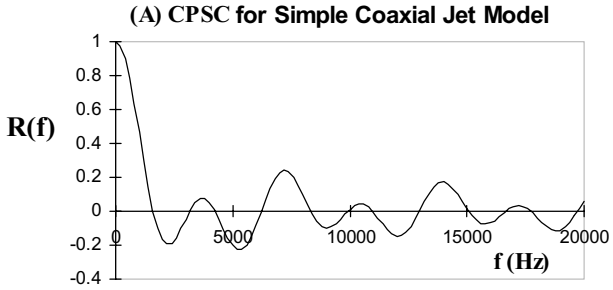


(c) Radial Source Distributions (Bartlett window)

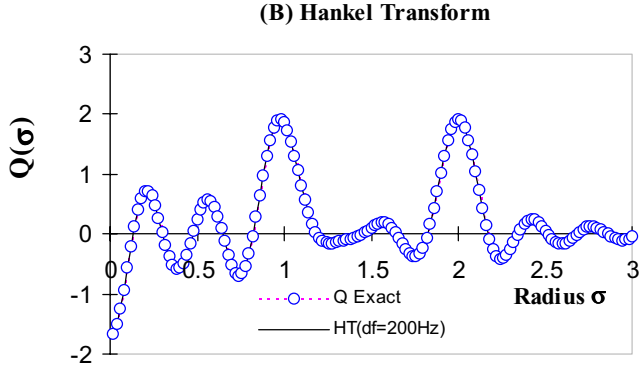
DERA

"Source Identification and Location Technique"

M Harper-Bourne
OAI 7-11-2000

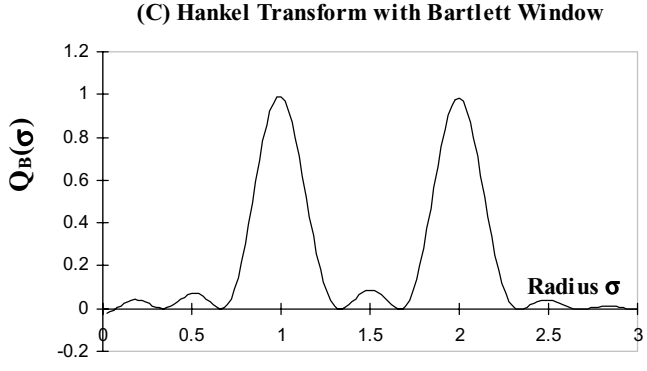


(a) CPSD for Coaxial Source Simulation ($S_s = S_p$; $R_s = 2R_p$)



(b) Radial Source Distribution (Rectangular Window)

Numerical example of Azimuthal Correlation applied to an idealised coaxial jet



(c) Radial Source Distribution (Bartlett Window)

DERA

M Harper-Bourne
OAI 7-11-2000

CONCLUSIONS

- THE LIGHTHILL ACOUSTIC ANALOGY APPLIED TO MICROPHONE CORRELATION CONTINUES TO BE USEFUL IN THE DEVELOPMENT OF SOURCE LOCATION / DIAGNOSTIC TOOLS AT BOTH MODEL AND FULL SCALE
- EXTENSION OF POLAR CORRELATION TO AZIMUTHAL CORRELATION HAS BEEN DEMONSTRATED FOR MEASUREMENT OF LATERAL (RADIAL) SOURCE DISTRIBUTIONS
- APPLICATION OF THE METHOD TO A ROUND SUBSONIC SMALL SCALE AIR JET IN AN ANECHOIC CHAMBER HAS SUCCESSFULLY IDENTIFIED THE MAIN NOISE PRODUCING REGION IN THE CENTRE OF THE SHEAR LAYER CONSISTENT WITH OUR CURRENT UNDERSTANDING OF JET MIXING NOISE.
- THIS RESULT ALSO SUPPORTS THE VALIDITY OF THE LIGHTHILL ANALOGY WHEN SMALL LATERAL SCALES AND ISOTROPY IN THE LATERAL PLAIN ARE ASSUMED
- POTENTIAL USE OF THE METHOD ON COAXIAL JETS HAS BEEN ILLUSTRATED

M. Harper-Bourne References

1. M Harper-Bourne, “Radial Distribution of Jet Noise Sources Using Far-Field Microphones”, AIAA Paper 98-237, 4th AIAA/CEAS Aeroacoustics Conference, Toulouse, France, June 1998.

2. M Harper-Bourne, “Jet Near-Field Noise Prediction”, AIAA Paper 99-1838, 5th AIAA/CEAS Aeroacoustics Conference, Seattle, May 1999.

3. M Harper-Bourne, “Twin-Jet Near-Field Noise Prediction”, AIAA Paper 2000-2084, 6th AIAA/CEAS Aeroacoustics Conference, Maui, June 2000.

Sound Source Identification through Flow Density Measurement and Correlation with Far Field Noise

J. Panda
Ohio Aerospace Institute

R. G. Seasholtz
NASA Glenn Research Center

Sound source identification through flow density measurement and correlation with far field noise

J. Panda, Ohio Aerospace Institute
R. G. Seasholtz, NASA Glenn Research Center

Sound sources in the plumes of unheated round jets, in the Mach number range 0.6 to 1.8, were investigated experimentally using "causality" approach, where air density fluctuations in the plumes were correlated with the far field noise. The air density was measured using a newly developed Molecular Rayleigh scattering based technique, which did not require any seeding. The reference at the end provides a detail description of the measurement technique.

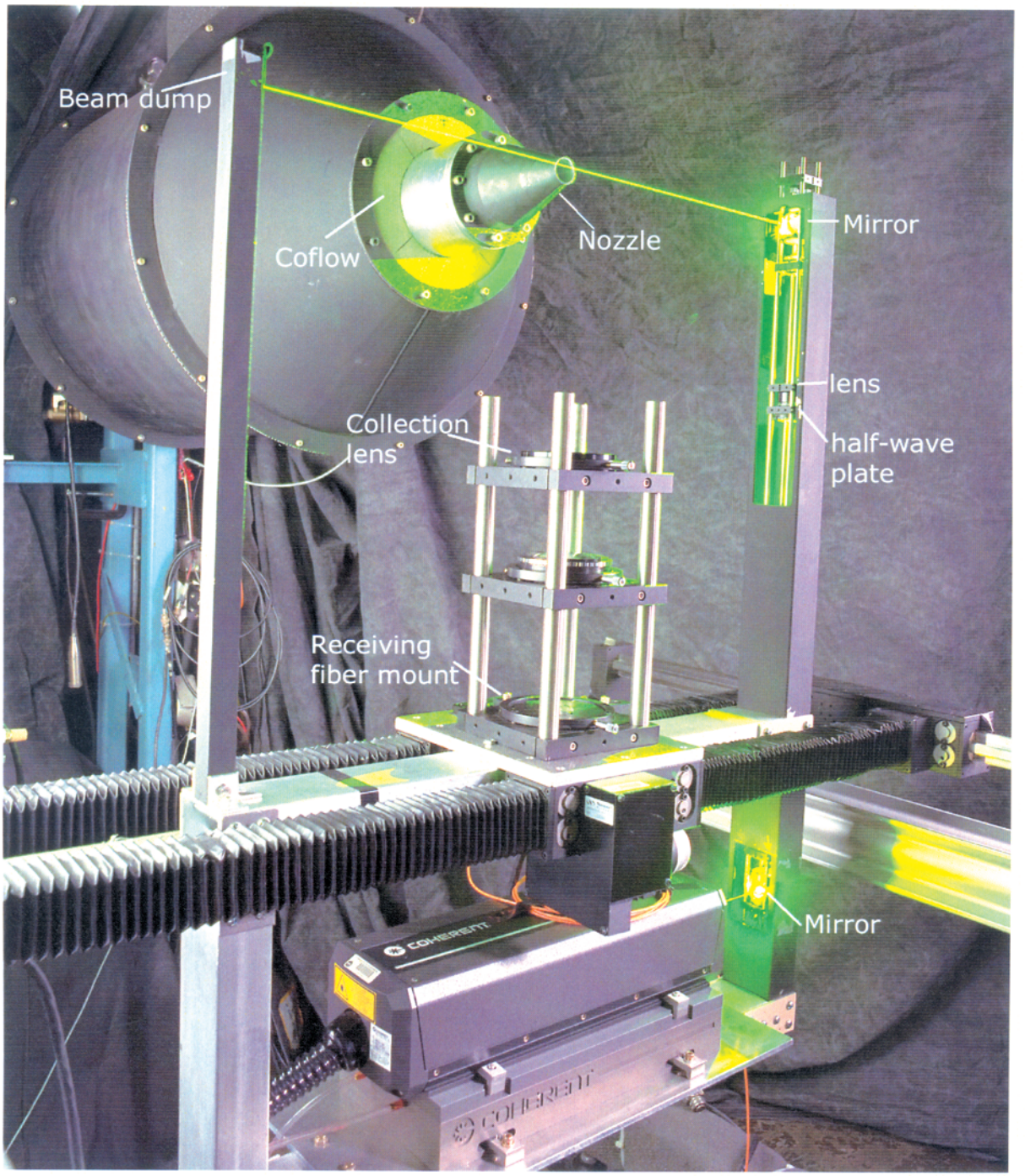


Fig. 1. A photograph of the nozzle facility and the optical arrangement.
Discussion: A narrow laser beam from a CW, Nd:VO_4 laser was passed perpendicular to the flow direction. The point measurement technique depends on collecting molecular scattered light from 1mm long probing region along the laser beam and focusing on the receiving fiber face. The optical arrangement was mounted on a X-Y traverse that allowed positioning the probe volume on a longitudinal plane. According to the Rayleigh scattering principle, intensity of the collected light is proportional to the local air density.

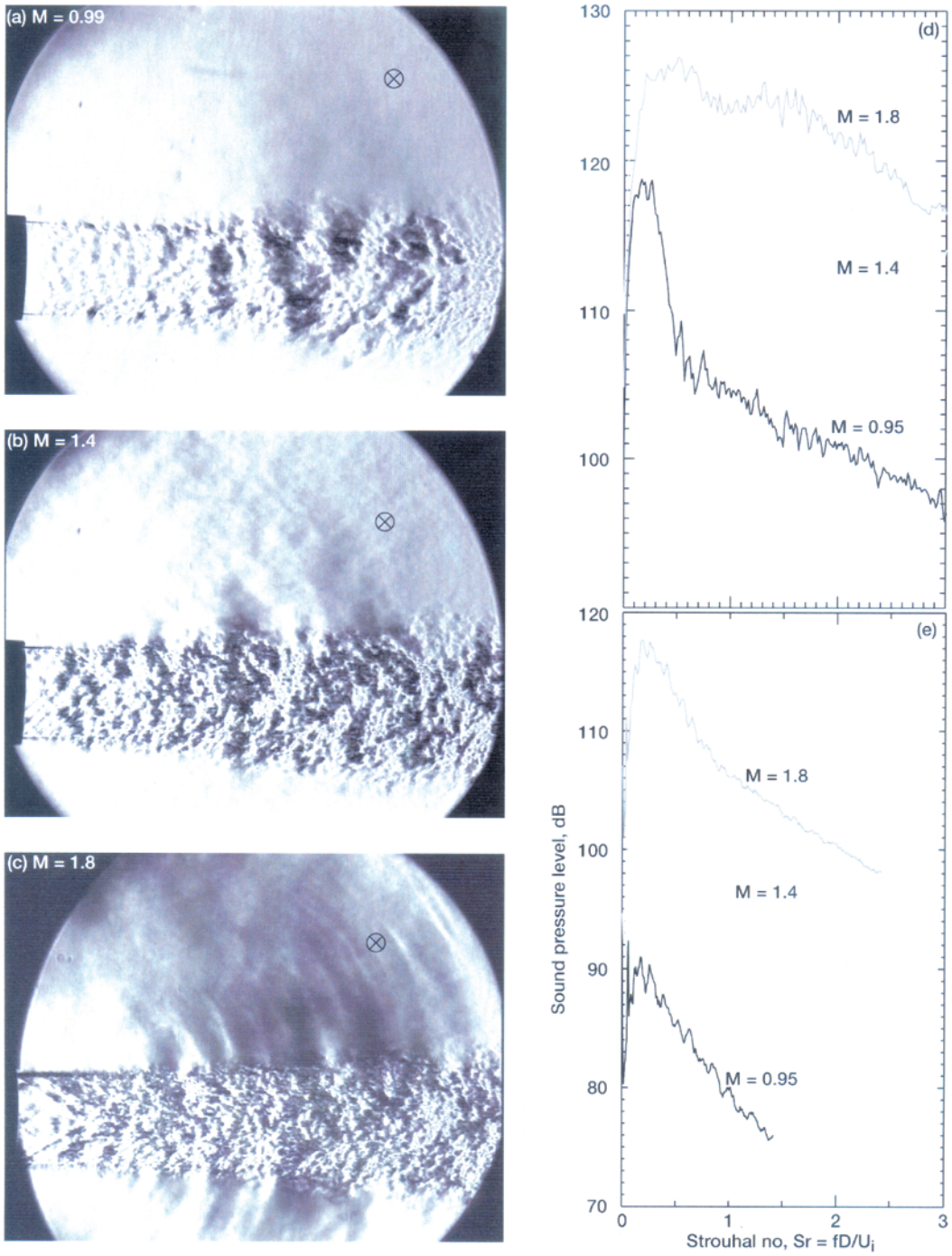


Fig. 2. (a), (b), (c) Spark schlieren photographs of fully expanded jets at indicated Mach number conditions.; (d) pressure fluctuation measured at x/D=4, y/D=2 (shown by ⊗ in schlieren photos); (e) sound pressure fluctuations at 50D & 30° to the flow direction)

Discussion: Three jets at Mach numbers 0.95, 1.4 & 1.8 were studied in details. The supersonic jets were produced from CD nozzles. Schlieren photographs show Mach wave emission in M=1.8 jet and its absence in M =0.99 jet. The M=1.4 jet is somewhat in between. An estimation of convective speed of turbulent eddies shows that it becomes supersonic with respect to the ambient sound speed in M=1.8 jet, while remaining

subsonic for M=0.99 jet. The near-field microphone data show a significant increase in high frequency pressure fluctuations with the onset of 'Mach wave' emission.

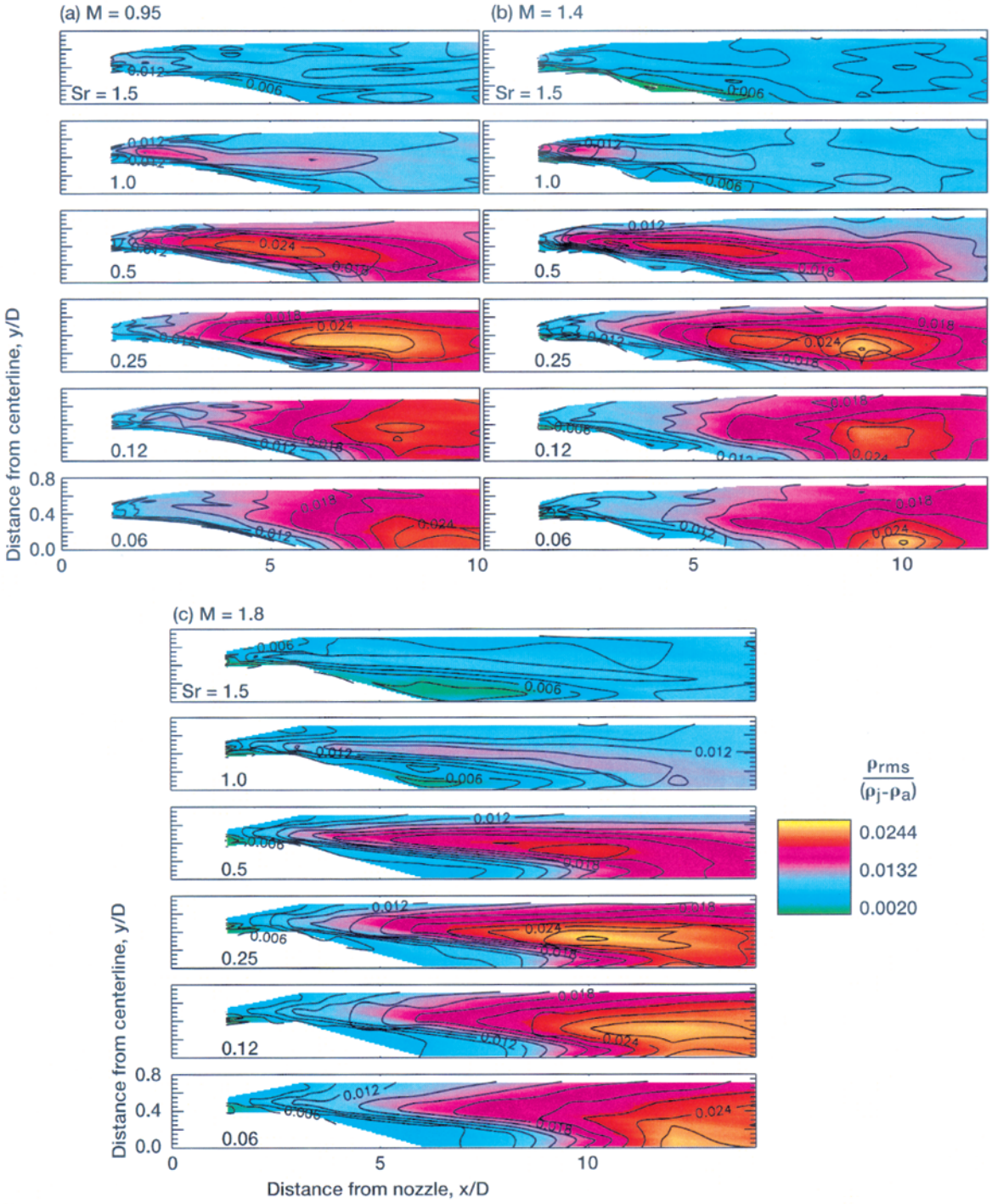


Fig. 3. The distribution of density fluctuation (normalized by ρ_{jet}-ρ_{amb}) at the indicated Strouhal frequencies (St = fD/U) for three different Mach numbers.
Discussion: These data were compiled from a large number of density fluctuation spectra measured in each jet flow. The fluctuation energy in the specified St values was isolated and plotted. As expected the high St fluctuations are concentrated in the lip shear layer

near the nozzle exit, while the low St fluctuation peaks beyond the potential core. The primary observation is a similarity in the flow fluctuations irrespective of the plume Mach number. The only difference is an increased downstream stretching with the increase in the jet Mach number. In sharp contrast to this similarity in flow fluctuation, the locations of the sound sources and their measured intensity is very different. This is discussed in the following.

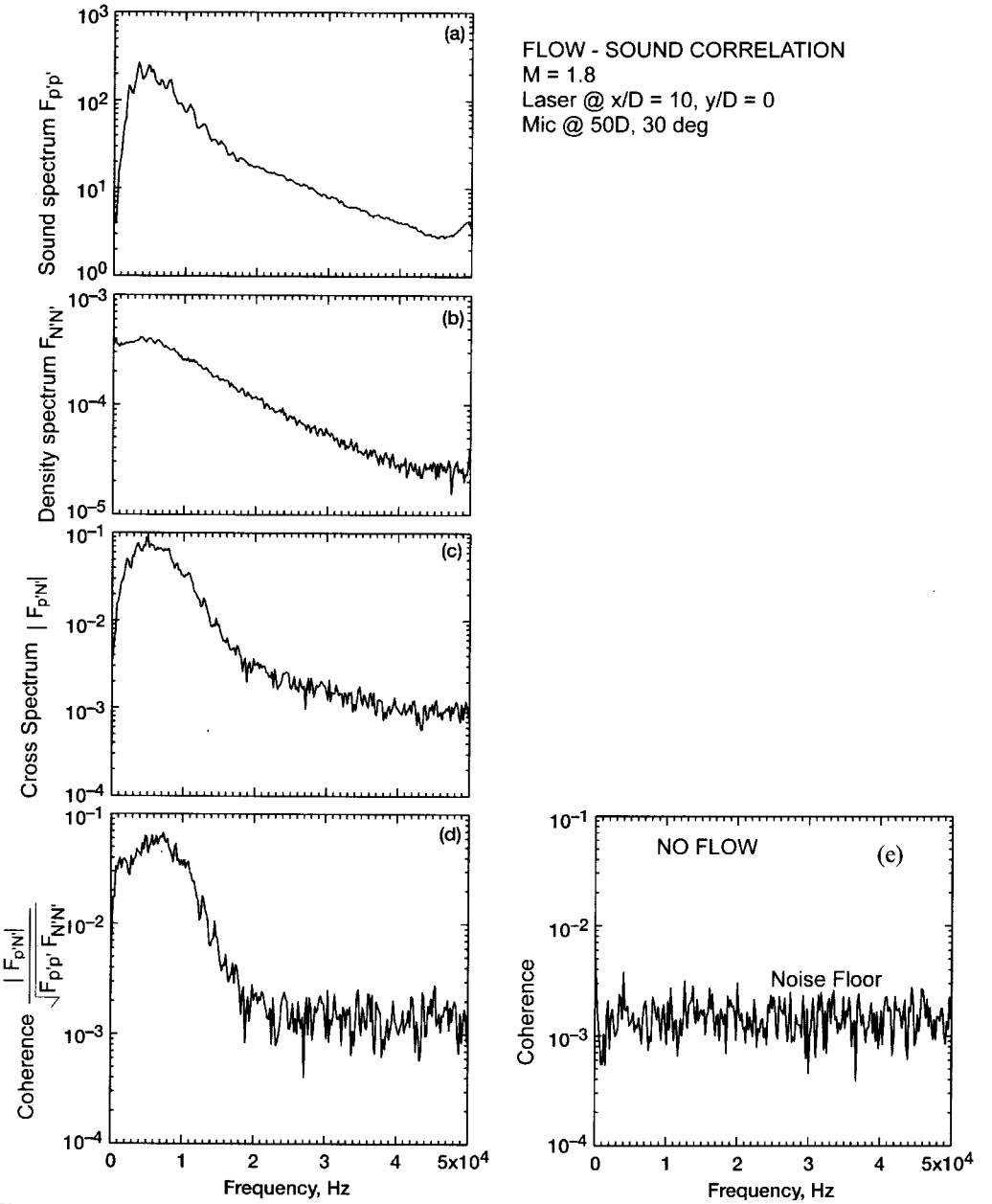


Fig. 4. Cross-correlation between flow density fluctuations and sound pressure fluctuations in M=1.8 jet, laser probe at centerline and x/D=10, microphone at farfield x/D=50, θ=30°. (a) sound pressure spectrum (b)density spectrum (c)cross-spectrum & (d)normalized cross-spectrum (coherence) (e) normalized cross-

spectrum at no-flow condition demonstrating the noise floor in cross-spectral measurement.

Discussion: The coherence (also called normalized cross-spectrum) effectively shows the correlation $\overline{\rho'}\,\overline{p'}/(\sqrt{\overline{\rho'^2}}\sqrt{\overline{p'^2}})$ and is used for the subsequent description of correlation data. The no flow correlation data is useful in finding out noise floor in such measurements. A comparison between parts (d) & (e) of this figure shows a measurable correlation below 2KHz frequency. Above this value, the measured data falls into noise floor.

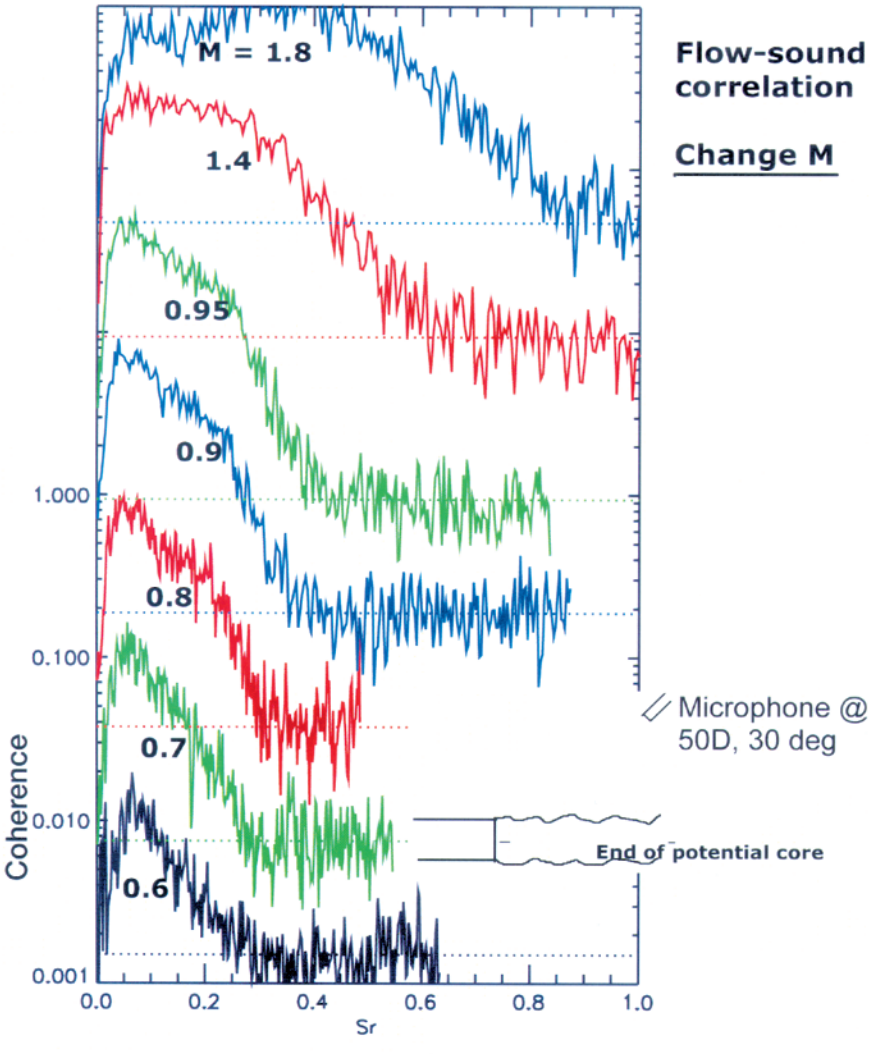


Fig. 6. Normalized cross-spectrum between flow density fluctuation and sound pressure fluctuations at different jet Mach number conditions. The probe volume was placed at the centerline & end of potential core (7D for M=0.6 jet, 9D for M=1.8 jet) & the microphone was placed at 50D & 30°.

Discussion: Some correlation in the low Strouhal number range is always measured at all Mach number conditions; indicating the end of the potential core is a low frequency noise source.

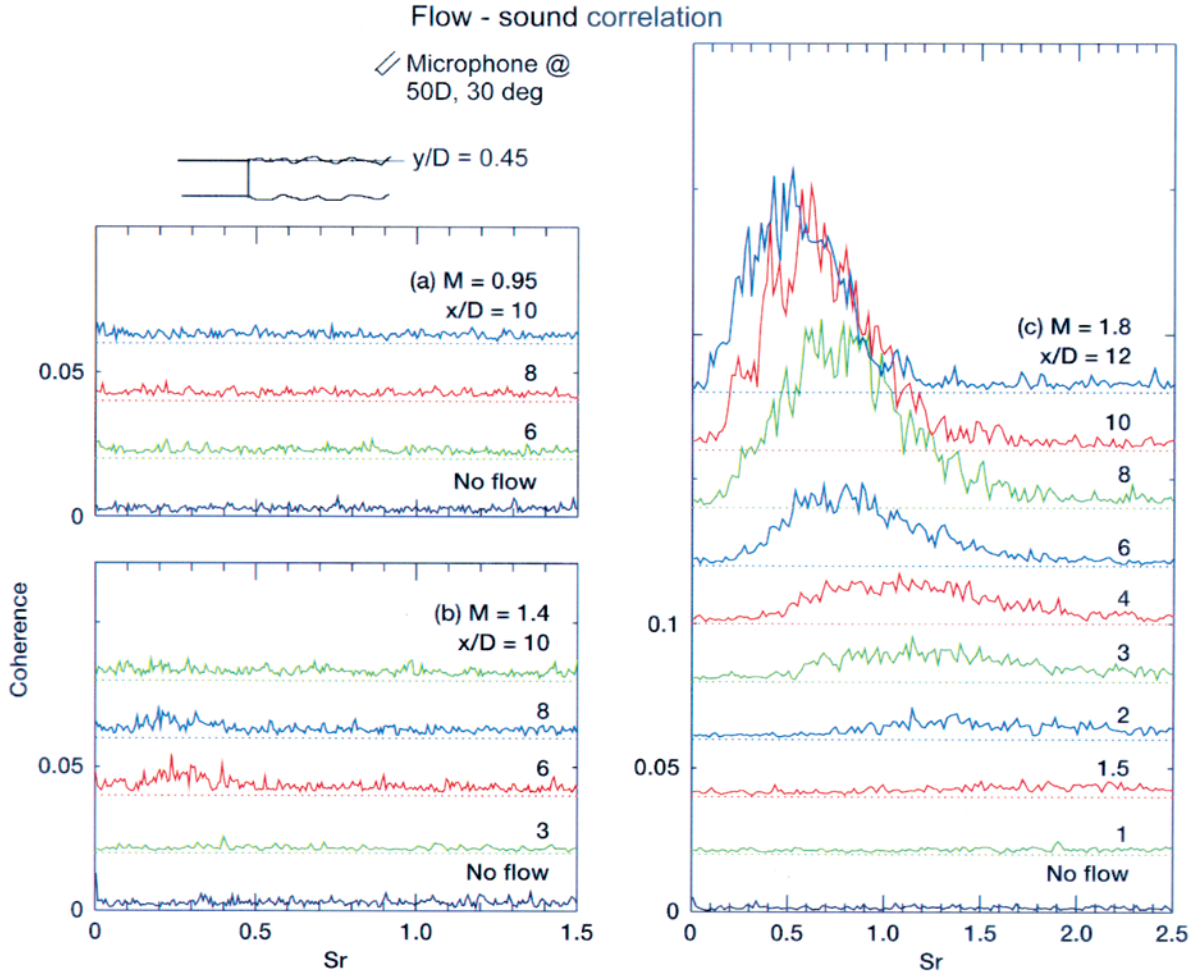


Fig. 7. Normalized cross-spectrum measured form the shear layer. The laser probe volume was moved from point to point along r/D=0.45 at the indicated x/D locations for the 3 Mach number jets and the correlation spectrum with a fixed far field microphone was measured.

Discussion: Very good correlation coefficients (up to 0.2) was measured in the supersonic M=1.8 jet while all data in subsonic M=0.95 jet falls in the noise floor (around 0.002). Small correlation values are measured for M=1.4 jet. Interestingly, the M=1.8 jet correlation data show the same trend of peak fluctuations moving to lower St frequency, with an increase in downstream distance, as expected from the Kelvin-Helmholtz instability waves. Also note that the instability waves are expected to be moving at supersonic speed in the M=1.8 jet and at subsonic speed in M=0.95 jet. All of these point out that the Kelvin-Helmholtz instability waves are directly responsible for sound generation when their speed becomes supersonic. This is also the reason for success of the instability wave based theories in predicting noise source of high supersonic jets. However, the same can not be said for subsonic jets.

J. Panda References

1. Panda, J.: "Shock oscillation in underexpanded screeching jets," *Journal of Fluid Mechanics*, vol. 363, pp. 173-198, 1998.

2. Panda, J., "An Experimental Investigation of Screech Noise Generation," *Journal of Fluid Mechanics,* vol. 378, pp.71-96, 1999.

3. Panda J., Raman, G. & Zaman, K. B. M. Q. "Underexpanded screeching jets from circular, rectangular and elliptic nozzles," AIAA paper no. 97-1623, 3rd AIAA/CEAS Aeroacoustics conference, May 1997.

4. Panda, J. & Seasholtz, R. G. "Shock structure and shock-vortex interaction in screeching jets measured using Rayleigh scattering," *Physics of Fluids,* vol. 11, no. 12, 3761-3777, Dec. 1999.

5. Panda, J. & Seasholtz, R. G. "Investigation of density fluctuations in supersonic free jets and correlation with generated noise," AIAA paper 2000-2099, 6th AIAA/CEAS Aeroacoustics conference, June 2000. Also submitted to the *Journal of Fluid Mechanics*.

6. Panda, J. & Seasholtz, R. G. "Velocity and Temperature Measurement in Supersonic Free Jets Using Spectrally Resolved Rayleigh Scattering," AIAA paper no. 99-0296, 37th AIAA Aerospace Sciences Meeting and Exhibit, 1999.

7. Panda, J. & Zaman, K. B. M. Q. "Density fluctuations in asymmetric nozzle plumes and correlation with far field noise," AIAA paper no 2001-0378, 39th AIAA Aerospace Sciences Meeting & Exhibit, 2001.

Finding Internal Excess Jet Noise Source Characteristics by Varying Free-Jet Speed

Vinod G. Mengle
Rolls-Royce, Indianapolis

NASA/CP—2001-211152

573

Finding Internal Excess Jet Noise Source Characteristics by Varying Free-Jet Speed

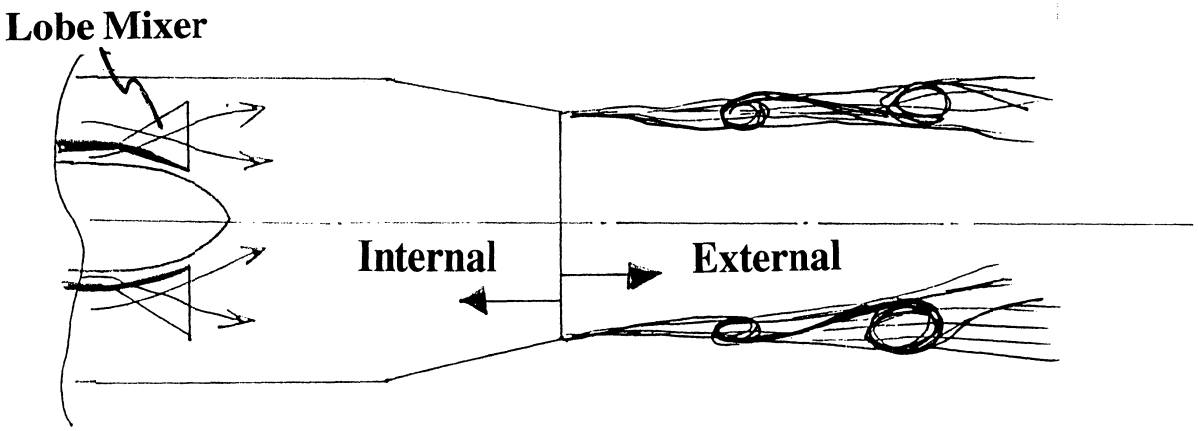
Vinod G. Mengle
Rolls-Royce, Indianapolis

Presented at
NASA/OAI Jet Noise Workshop, Cleveland, OH
Nov. 7-9, 2000



Rolls-Royce

Definition of "Excess" Noise



- Excess Noise = Total noise of Mixer-Nozzle Jet -
  Noise of "equivalent" single stream
  nozzle with uniform nozzle exit flow
- Excess Noise = Internal noise + External residual
  noise

Rolls-Royce

Background & Motivation

- Excess Noise ⇨ Wavelength = Order(Lobe width)
  ⇨ Intermediate-to-high frequency
  ⇨ "Annoying" frequency range
- Low Bypass Ratio Lobed Mixers
  - Saiyed, Bridges, Krejsa (1996) - Compared SPL of mixer with simple round nozzle at different free-jet Mach numbers but same observation angles & applied a 4th order Doppler factor correction
    - Wholly external residual mixing noise; no internal noise
- High Bypass Ratio Lobed Mixers
  - Mengle et al (1997) - Variation with free-jet speeds did not change SPL in certain frequency ranges in certain angles; close to peak PNL angles ⇨ led to this work

Objectives

- To develop a method to study the excess noise of forced mixers by using far-field SPL data with varying free-jet speeds

- To understand the spectral and directivity characteristics of excess noise of forced mixers

Examination of Excess Noise in Mixers

- 20 lobe, unscalloped mixer (20UH)
- 20-lobe deeply scalloped mixer (20DH)
- (Actually studied several other mixers with 12, 16 and 20 lobes, and different parameters but are not reported here for brevity)
- Model data extrapolated by scale factor of 1:4 at 150 ft in the reference frame of nozzle after usual free-jet/ambient shear-layer corrections are applied

- **Nominal Operating Conditions:**

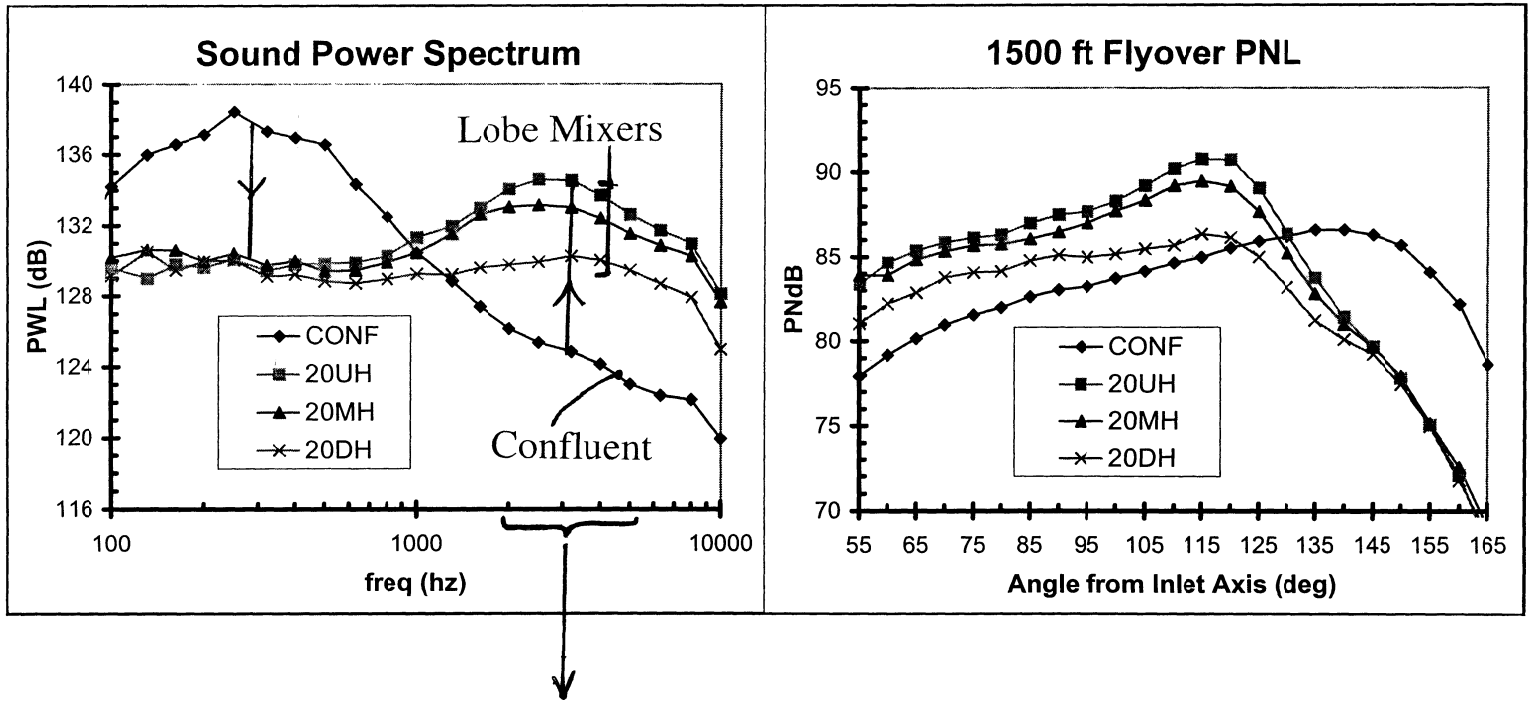
TO	NPR_{fan}	NPR_{core}	T_{tcore}/T_{tfan}
#1	1.44	1.39	2.34
#2	1.61	1.54	2.62
#3	1.82	1.74	2.79

- Free-Jet Mach numbers

  M_{fj} = 0.0, 0.2, 0.3

Rolls-Royce

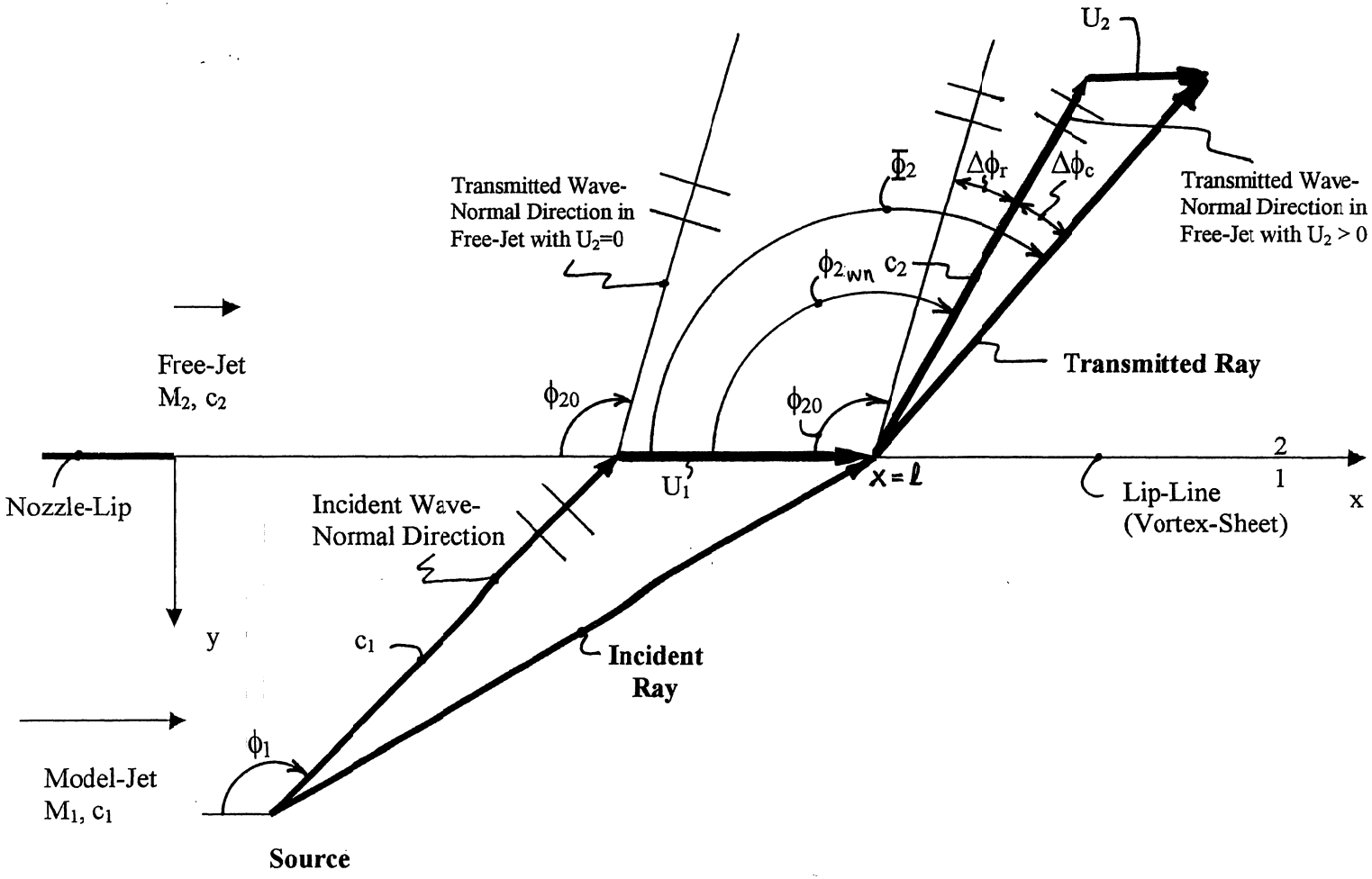
TO # 3 Results (V(mix) = 1060 ft/sec)



High Noy weighting for PNL at these frequencies
⇒ Important because close to peak PNL

Rolls-Royce

Development of the Method



Rolls-Royce

Angular Relations

- Equality of x-component of wave-number vectors in both flows gives:
- $\varphi_{2_{wn}}$ and $\Delta\varphi_c$ are completely known in terms of flow 2 properties (I.e. free-jet flow); model jet flow properties do not appear

$$\frac{(\omega/c_1)\cos\varphi_1}{1-M_1\cos\varphi_1} = \frac{(\omega/c_2)\cos\varphi_{2_{wn}}}{1-M_{2_{wn}}\cos\phi_{2_{wn}}}$$

$$\cos\phi_{2_{wn}} = \frac{\cos\varphi_{20}}{1+M_2\cos\varphi_{20}}$$

$$\tan(\Delta\varphi_c) = \frac{M_2\sin\varphi_{2_{wn}}}{1-M_2\cos\varphi_{2_{wn}}}$$

Rolls-Royce

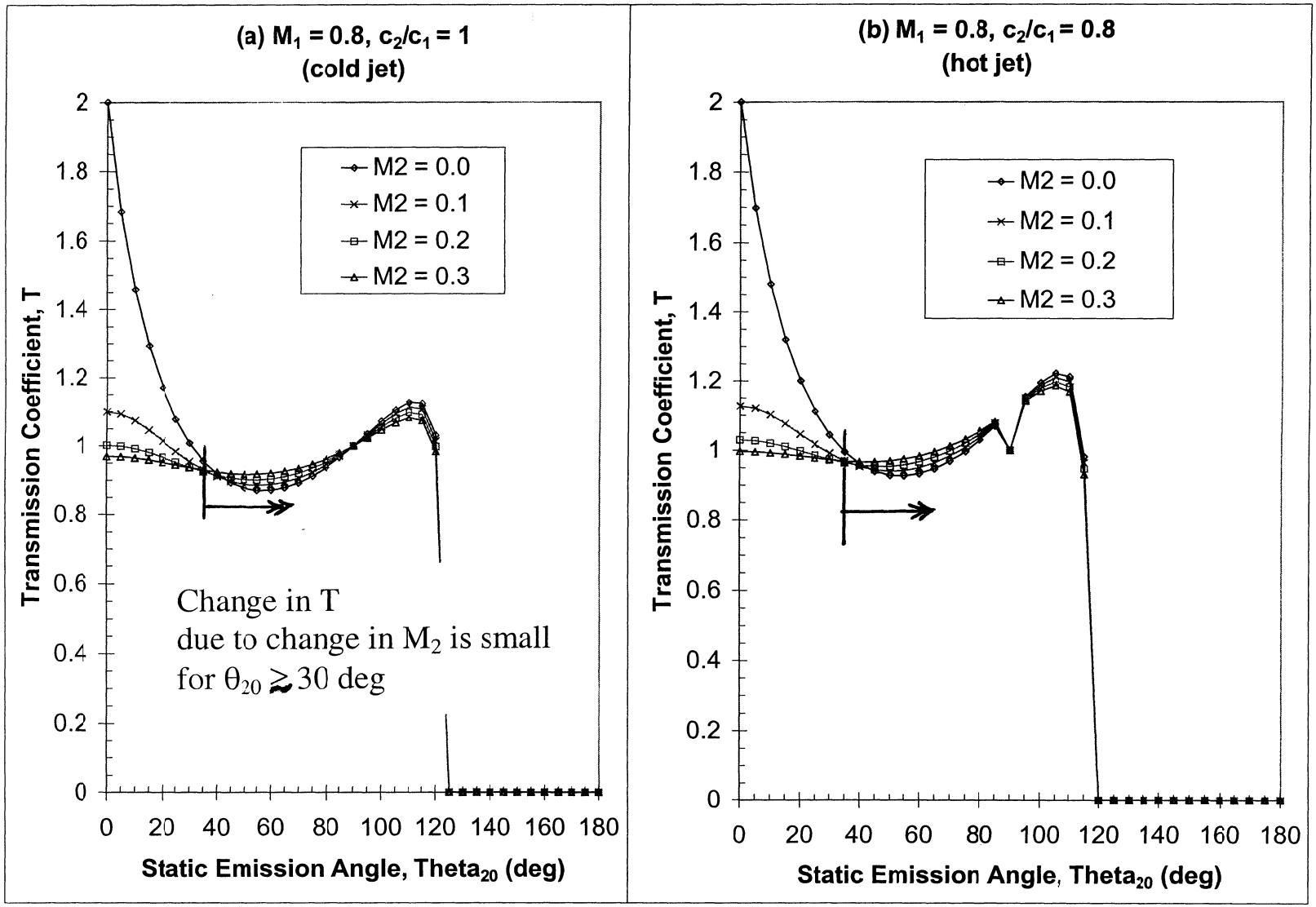
Shifted-Angle Table

$$SPL(M_{fj} = 0.0, \theta_{20}) \leftrightarrows SPL(M_{fj} > 0.0, \theta_{2wn})$$

$M_{fj} = 0$	$M_{fj} = 0.1$		$M_{fj} = 0.2$		$M_{fj} = 0.3$	
$Theta_{20}$	$Theta_{2wn}$	$THETA_2$	$Theta_{2wn}$	$THETA_2$	$Theta_{2wn}$	$THETA_2$
0	24.6	27.2	33.6	41.1	39.7	53.7
5	25.0	27.7	33.8	41.4	39.9	54.0
10	26.3	29.1	34.6	42.4	40.5	54.7
15	28.3	31.2	35.9	43.9	41.5	55.9
20	30.8	34.0	37.7	46.0	42.9	57.5
25	33.8	37.3	39.9	48.5	44.6	59.5
30	37.2	40.9	42.4	51.4	46.6	61.9
35	40.8	44.8	45.3	54.7	48.9	64.6
40	44.6	49.0	48.4	58.2	51.5	67.6
45	48.7	53.3	51.7	61.9	54.3	70.8
50	52.8	57.7	55.3	65.8	57.4	74.2
55	57.1	62.2	59.0	69.9	60.7	77.7
60	61.6	66.8	63.0	74.1	64.2	81.5
65	66.1	71.5	67.1	78.4	68.0	85.4
70	70.7	76.3	71.3	82.8	71.9	89.4
75	75.4	81.1	75.8	87.3	76.1	93.5
80	80.2	85.9	80.3	91.9	80.5	97.8
85	85.0	90.8	85.1	96.5	85.1	102.2
90	90.0	95.7	90.0	101.3	90.0	106.7
95	95.0	100.7	95.1	106.2	95.1	111.4
100	100.2	105.7	100.4	111.1	100.6	116.2
105	105.4	110.8	105.8	116.2	106.3	121.2
110	110.7	115.9	111.5	121.4	112.4	126.4
115	116.2	121.1	117.5	126.7	118.9	131.9
120	121.8	126.4	123.7	132.3	126.0	137.7
125	127.5	131.8	130.4	138.1	133.9	144.0
130	133.4	137.3	137.5	144.2	142.8	151.1
135	139.5	143.0	145.4	151.0	153.8	159.8
140	146.1	149.0	154.8	158.9	174.1	175.4
145	153.2	155.5	168.4	170.3	-	-
150	161.5	163.1	-	-	-	-
155	175.3	175.7	-	-	-	-
160	-	-	-	-	-	-
165	-	-	-	-	-	-
170	-	-	-	-	-	-
175	-	-	-	-	-	-
180		-	-	-	-	-

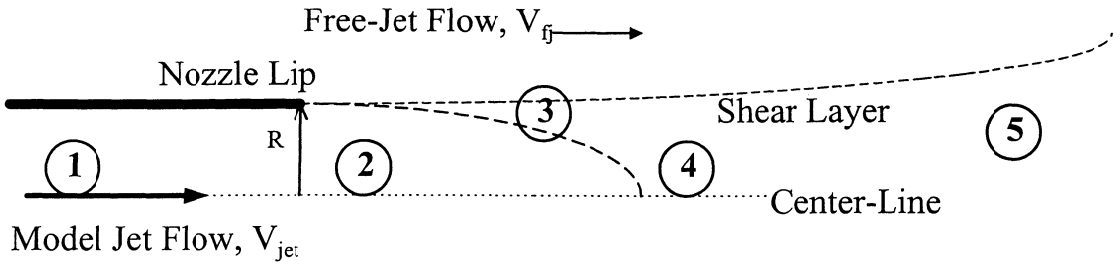
Rolls-Royce

Transmission Coefficient Results



Rolls-Royce

Shifted-Angle Diagnostic Method

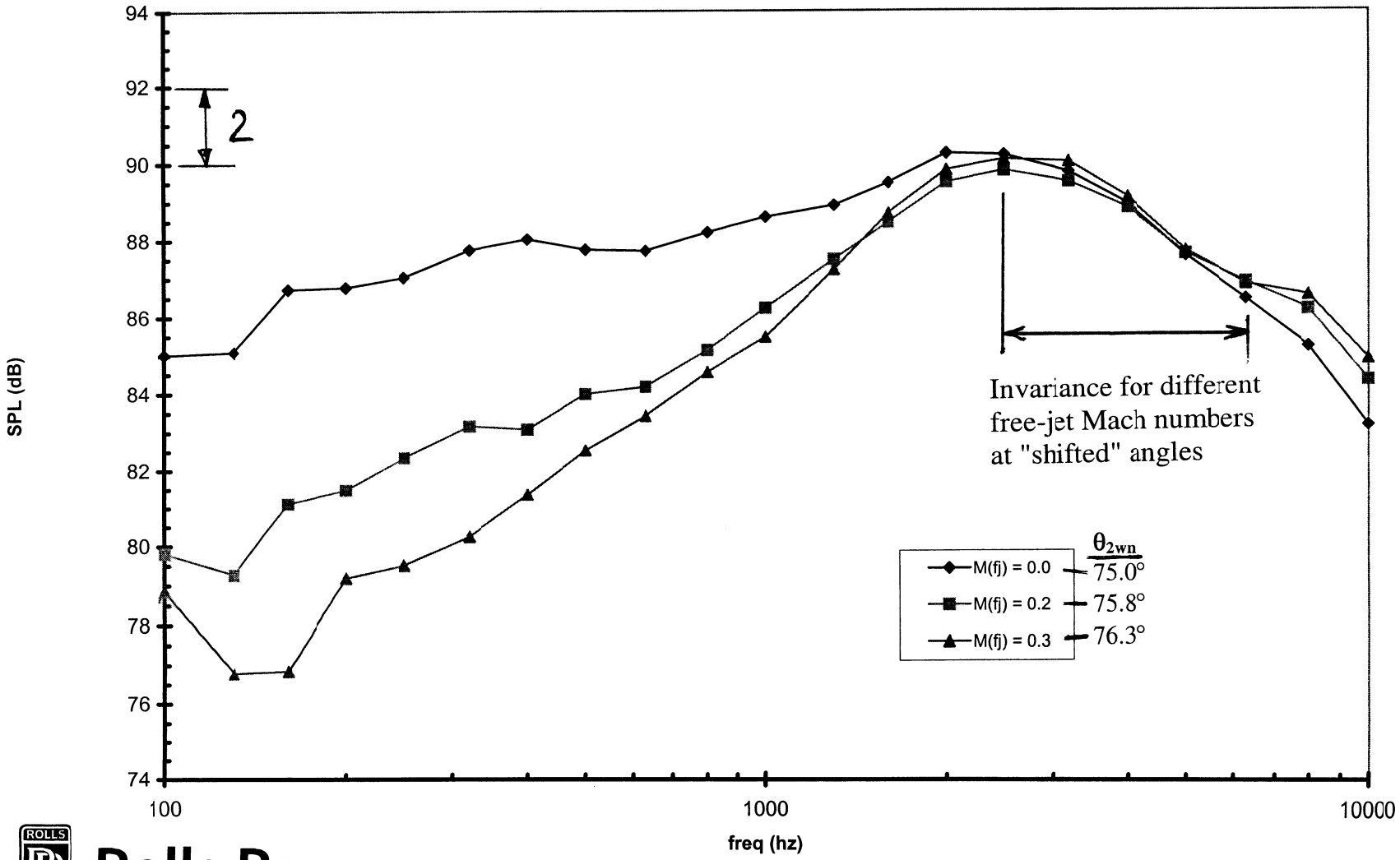


Jet noise sources that do *not* change with free-jet speed variations	1, 2
Jet noise sources that can change with free-jet speed variations	3, 4, 5

- SPL-invariance with M_{fj} at shifted angles
  - ⇨ Sources are at 1 or 2
    - ⇨ Further, if exit flow is uniform then only the internal sources at 1 are responsible
- SPL changes with M_{fj} at shifted angles
  - ⇨ Either sources near 1 or 2 are not dominant, or excess noise sources, if any, have merged with free-jet shear layer (method fails)

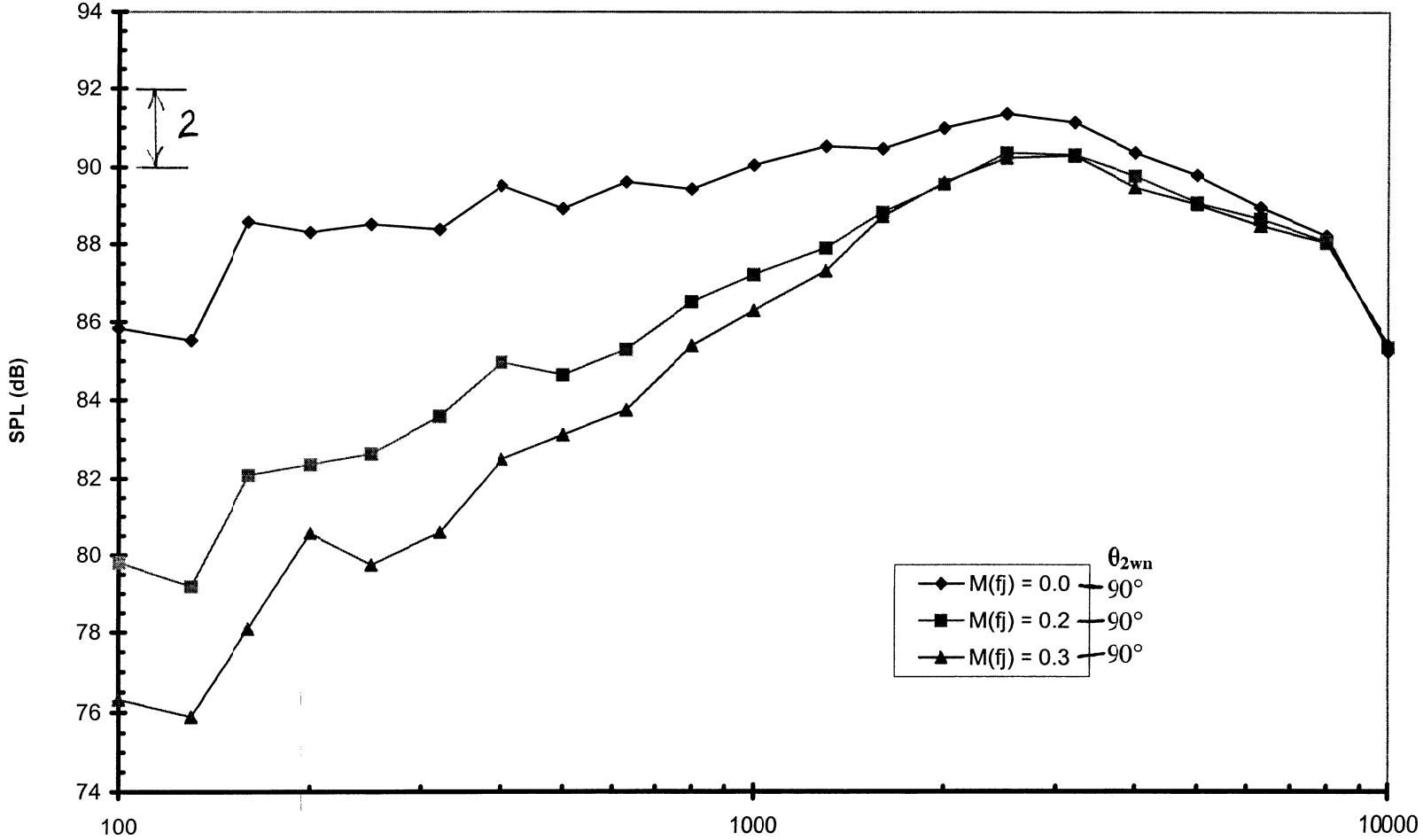
Rolls-Royce

20UH, TO #3, θ_{20} = 75 deg
SPL spectral comparison at shifted angles



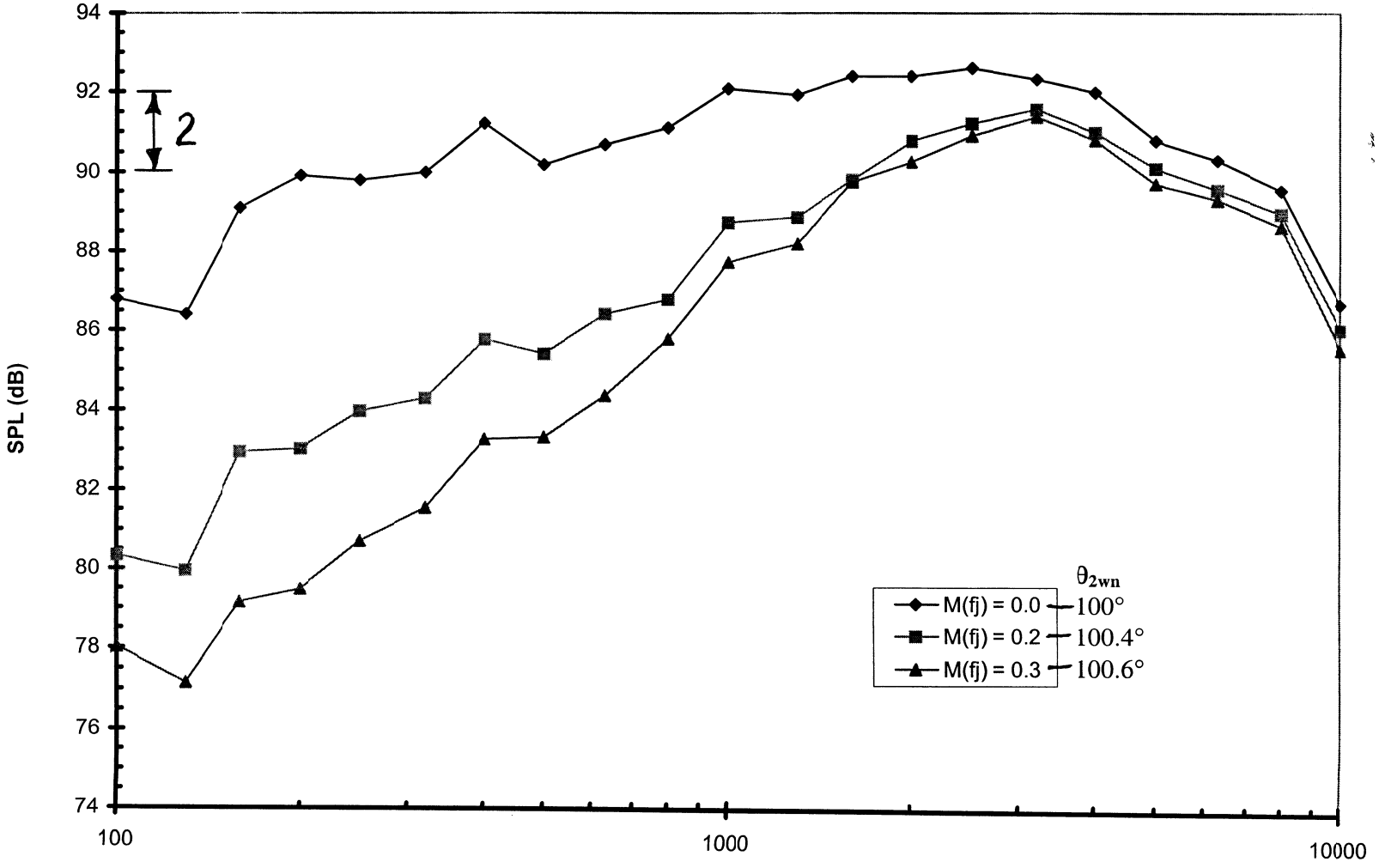
Rolls-Royce

20UH, TO #3, θ_{20} = 90 deg
SPL spectral comparison at shifted angles



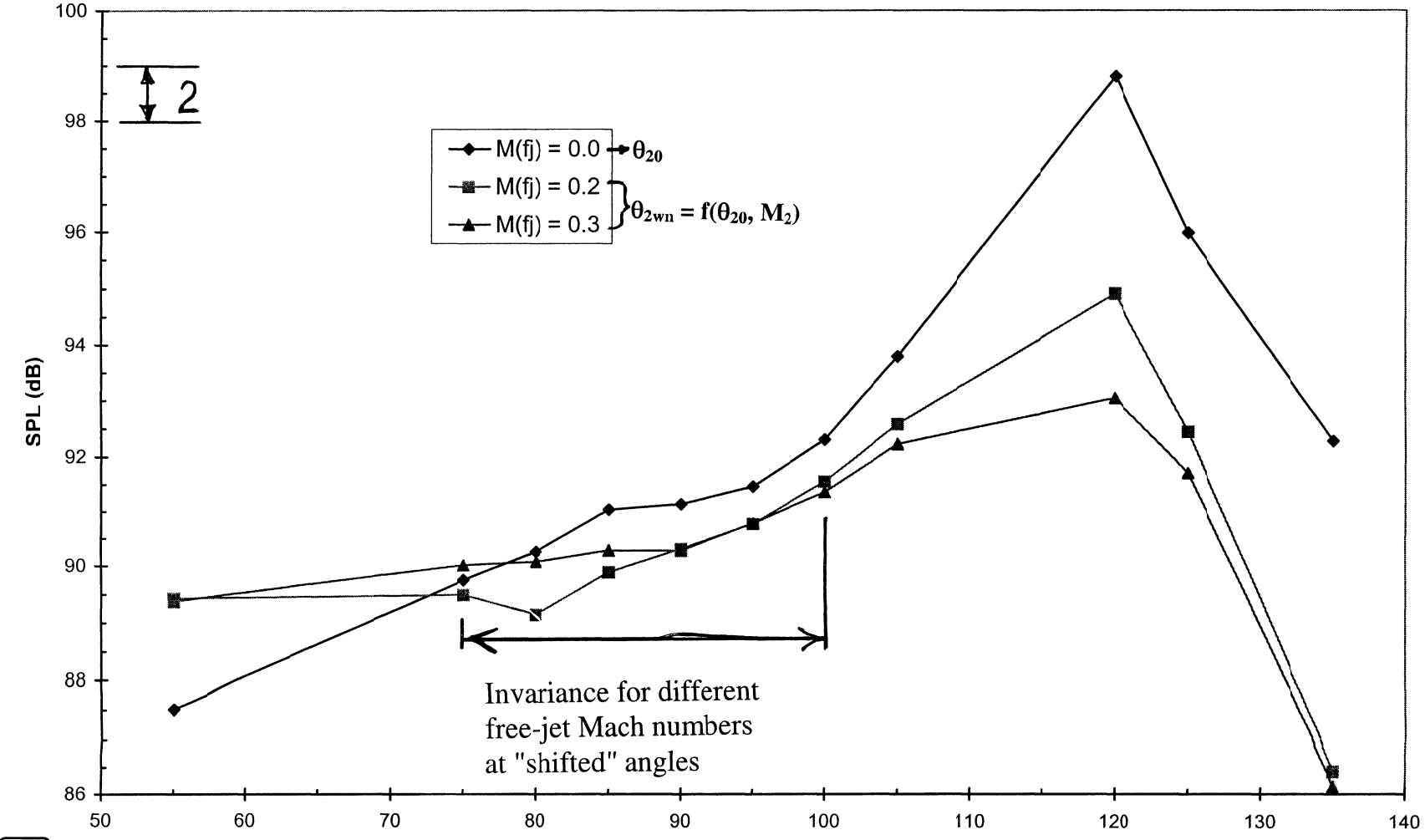
Rolls-Royce

20UH, TO #3, θ_{20} = 100 deg
SPL spectral comparison at shifted angles



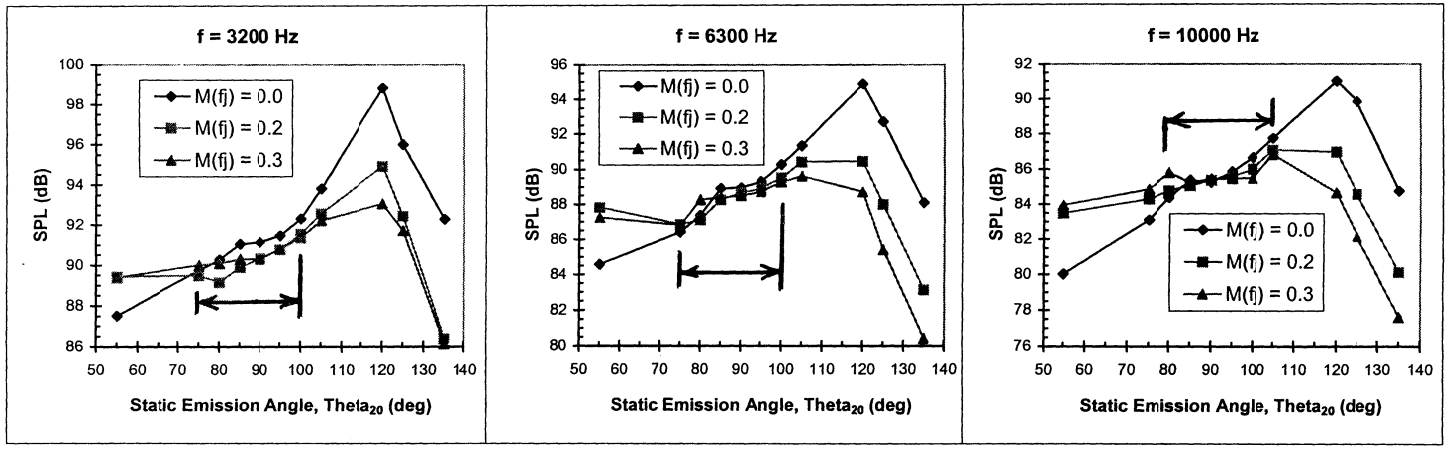
Rolls-Royce

20UH, TO #3, f = 3200 Hz
SPL directivity comparison at "shifted" angles



Rolls-Royce

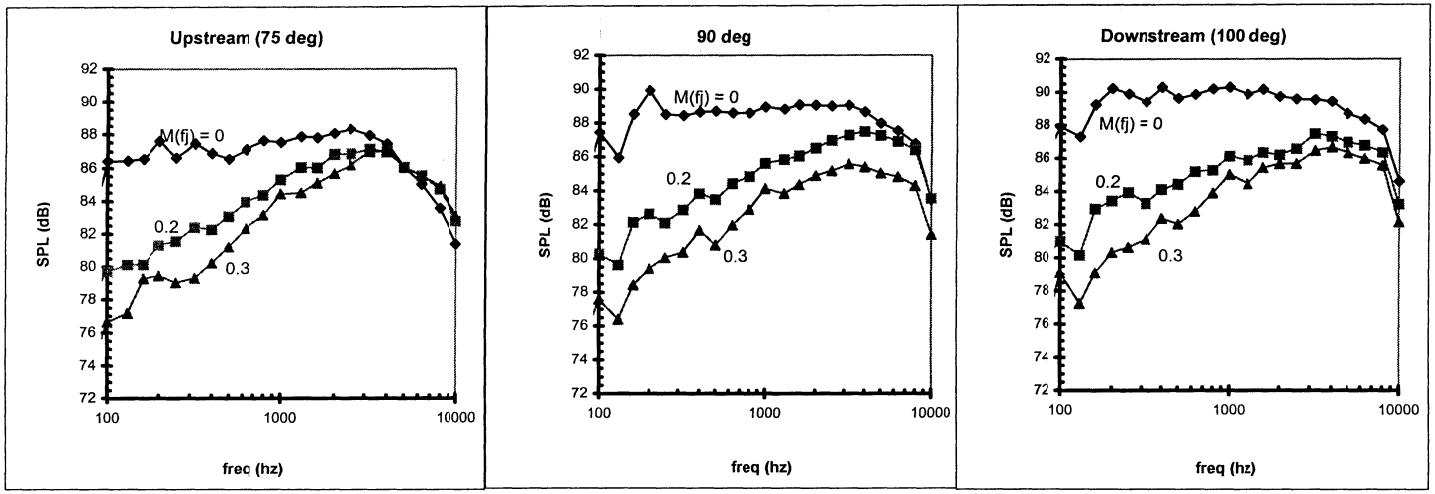
20UH, TO #3, High Frequencies
SPL directivity comparison at "shifted" angles



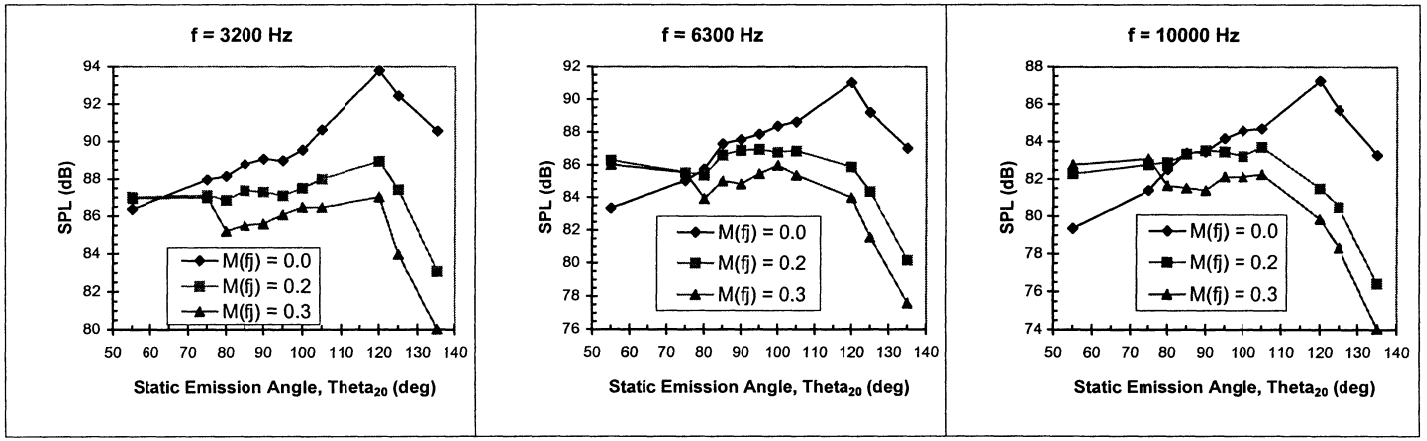
- High frequency SPL nearly invariant for $\theta \in (75°, 100°)$

Rolls-Royce

20DH, TO #3
SPL spectral & directivity comparison at "shifted" angles



(a) SPL spectra at different angles

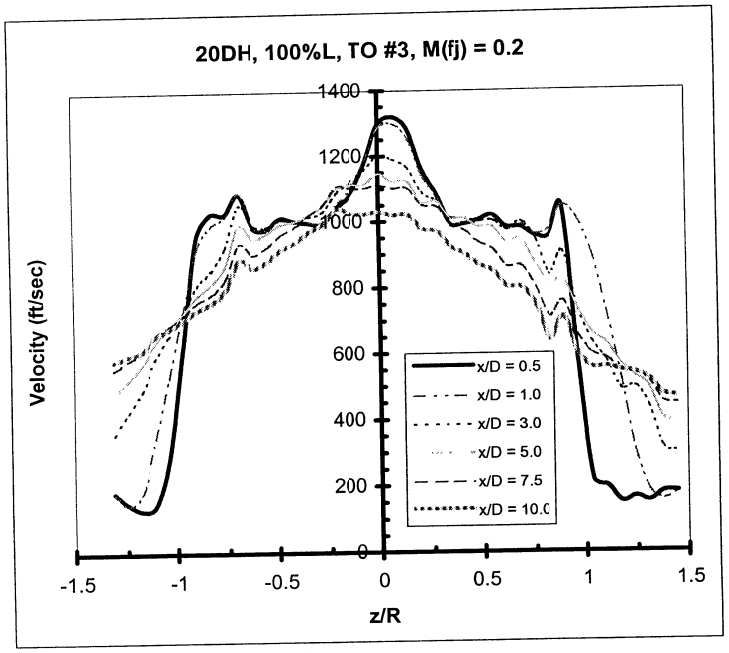


(b) SPL directivity at different frequencies

Figure 8. Shifted-angle results for the scalloped 20DH mixer at TO #3.

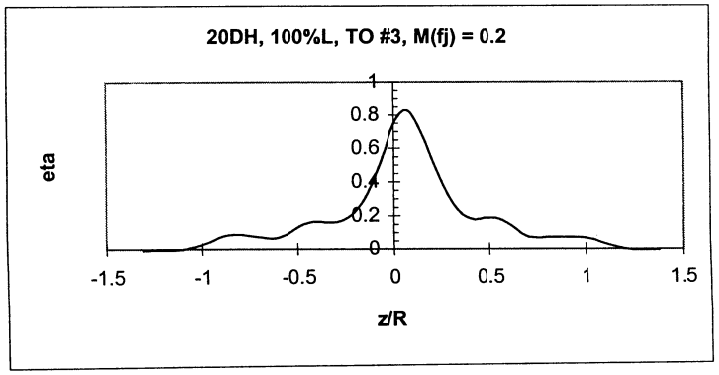
Rolls-Royce

Plume Flow, 20DH, TO #3, M_{fj} = 0.2



(a) Velocity profiles at several axial stations

- Apart from central hot core fairly uniform at exit
- Also velocity profiles decay like uniform exit flow
- Suggests that SPL-invariance, if any, is strongly possible due to internal noise sources



(b) Temperature profile at x/D = 0.5

Rolls-Royce

Conclusions

- Developed a method to find the spectral and directivity characteristics of some components of excess sources in internally mixed jets, wherever they are dominant

- Applied to several lobed mixer configurations at widely differing operating conditions (830 ft/sec to 1060 ft/sec)

- External residual and internal sources are more dominant in unscalloped mixers than scalloped generally at higher jet speeds over an angular range of 75 deg to 100 deg



Rolls-Royce

References

- Saiyed, N.H., Bridges, J.E., Krejsa, E.A. (1996): Core and fan stream's mixing noise outside the nozzle for subsonic jet engines with internal mixers. AIAA Paper 96-1667.
- Mengle, V.G., Dalton, W.N., Bridges, J.C., Boyd, K.C. (1997): Noise reduction with lobed mixers: Nozzle-length and free-jet speed effects. AIAA Paper 97-1682-CP.
- **Mengle, V.G. (1999): Finding excess noise in internally-mixed jets by varying free-jet speed. AIAA Paper 99-1967.** (The work presented here is based on this paper.)

V. G. Mengle References

1. Mengle, V. G., Shin, H-W., Askew, J., Whitfield, C.E. (1992): *Aero-Performance and Aero-Mixing Tests of 2D-CD Mixer/Ejector Nozzles. Part II. Sample of Aero-Mixing Test Data & Inferences.* Paper No. 1, 1st NASA/Industry High Speed Research Program Nozzle Symposium, NASA CP (to be numbered), pp. 3-23 to 3-35, Nov. 17-19, 1992.

2. Mengle, V. G., Shin, H-W., Whitfield, C. E., Wisler, S., Askew, J. (1992*): Acoustic and Aero-Mixing Tests of Fluid-Shield Nozzles. Part II - 2D Fluid-Shield Nozzle Aero-Mixing Tests.* Paper No. 2, 1st NASA/Industry High Speed Research Program Nozzle Symposium, NASA CP (to be numbered), pp. 4-21 to 4-28, Nov. 17-19, 1992.

3. Salikuddin, M., Brausch, J., Mengle, V. (1992): *Acoustic and Aero-Mixing Tests of Fluid-Shield Nozzles. Part I -Acoustics.* Paper No. 2, 1st NASA/Industry High Speed Research Program Nozzle Symposium, NASA CP (to be numbered), pp. 4-1 to 4-19, Nov. 17-19, 1992.

4. Mengle, V. G. (1995*): Acoustic Duct Waveguide Modes Excited by an Axially Convecting Noise Source in Sheared Flow*. 1st NASA Advanced Subsonic Technology Engine Noise Workshop Proceedings, Session 2: Jet Noise, pp. 269-284, Dec. 12-14, 1995.

5. Mengle, V. G., Dalton, W. N., Bridges, J., Boyd, K. (1997): *Noise Reduction with Lobed Mixers - Nozzle Length and Free-Jet Speed Effects.* AIAA Paper No. 97-1682. 18th AIAA Aeroacoustics Conference, May 10-14, 1997.

6. Mengle, V. G. (1997): *Certain Limitations and Extensions of MGB Jet Noise Computer Code.* NASA Advanced Subsonic Technology "MGB Jet Noise Prediction Workshop" Proceedings, Sept. 9, 1997.

7. Janardan, B.A., Hoff, G.E., Barter, J.W., Martens, Gliebe, P. R., Mengle, V. and Dalton, W.N. (1998*): Separate-Flow Exhaust System Noise Reduction Concept Evaluation.* Final Report, NASA Contract NAS3-27720, GE Report No. R98AEB152, May 1998. NASA CR (to be numbered).

8. Mengle, V. G., Dalton, W. N.(1998): *Lobed Mixer Design for Noise Suppression. Vol. 1 - Acoustic and Aerodynamic Test Data Analysis.* Final Report, NASA Contract NAS3-27394, Task Order No. 6, Rolls-Royce EDR No. 18580, July 1, 1998, NASA CR (to be numbered), 298 p.

9. Mengle, V. G., Baker, V. D., Dalton, W. N. (1998): *Lobed Mixer Design for Noise Suppression. Vol. 2 - Plume, Aerodynamic & Acoustic Data.* Final Report, NASA Contract NAS3-27394, Task Order No. 6, Rolls-Royce EDR No. 18581, July 1, 1998. NASA CR (to be numbered), 629 p.

10. Mengle, V. G. (1999): *Jet Noise Reduction by Lobed Mixers with Boomerang Scallops*. AIAA Paper No. 99-1923, 5th AIAA/CEAS Aeroacoustics Conf., May 10-12, 1999.

11. Mengle, V. G. (1999): *Anomalous Effect of Nozzle Length Reduction on Jet Noise of Forced Mixers*. AIAA Paper No. 99-1968, 5th AIAA/CEAS Aeroacoustics Conf., May 10-12, 1999.

12. Mengle, V. G. (1999): *Finding Excess Noise in Internally-Mixed Jets by Varying Free-Jet Speed*. AIAA Paper No. 99-1967, 5th AIAA/CEAS Aeroacoustics Conf., May 10-12, 1999.

13. Mengle, V. G. (2000): *Optimization of Lobe Mixer Geometry and Nozzle Length for Minimum Jet Noise*. AIAA Paper No. 2000-1963, 6th AIAA/CEAS Aeroacoustics Conf., June 12-14, 2000.

14. Mengle, V. G. (2000): *Finding Internal Excess Jet Noise Source Characteristics by Varying Free-Jet Speed*. NASA/OAI Jet Noise Workshop, November 7-9, 2000, NASA CP (to be numbered).

15. Mengle, V. G. (2000): *Vorticity Dynamics and Its Relation to Jet Noise Reduction in Chevrons*. NASA/OAI Jet Noise Workshop, November 7-9, 2000, NASA CP (to be numbered).

16. Mengle, V. G. (2000): *Anomalous Effect of Nozzle Length Reduction on Jet Noise of Forced Mixers*. NASA/OAI Jet Noise Workshop, November 7-9, 2000, NASA CP (to be numbered).

17. Mengle, V. G. (2001): *Tongue Mixer - A New Concept for Jet Noise Reduction*. (Submitted for presentation at the 7th AIAA/CEAS Aeroacoustics Conf., May 28-30, 2001).

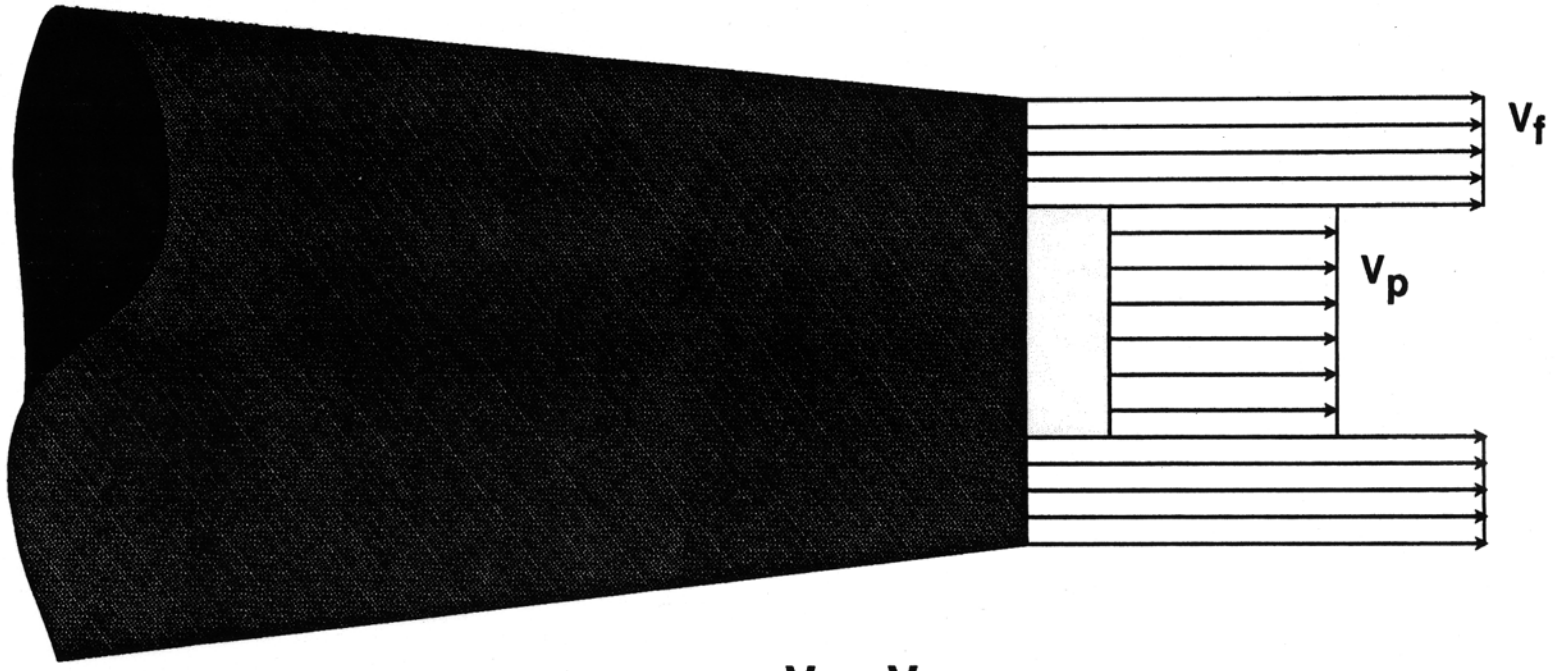
18. Mengle, V. G. (2001): *Duct Waveguide Mode Excitation by Sound Sources Convecting in Sheared Flows*. (Submitted for presentation at the 7th AIAA/CEAS Aeroacoustics Conf., May 28-30, 2001).

NASA/CP—2001-211152

Acoustic-Analogy-based Jet Noise prediction for Suppressor Nozzles

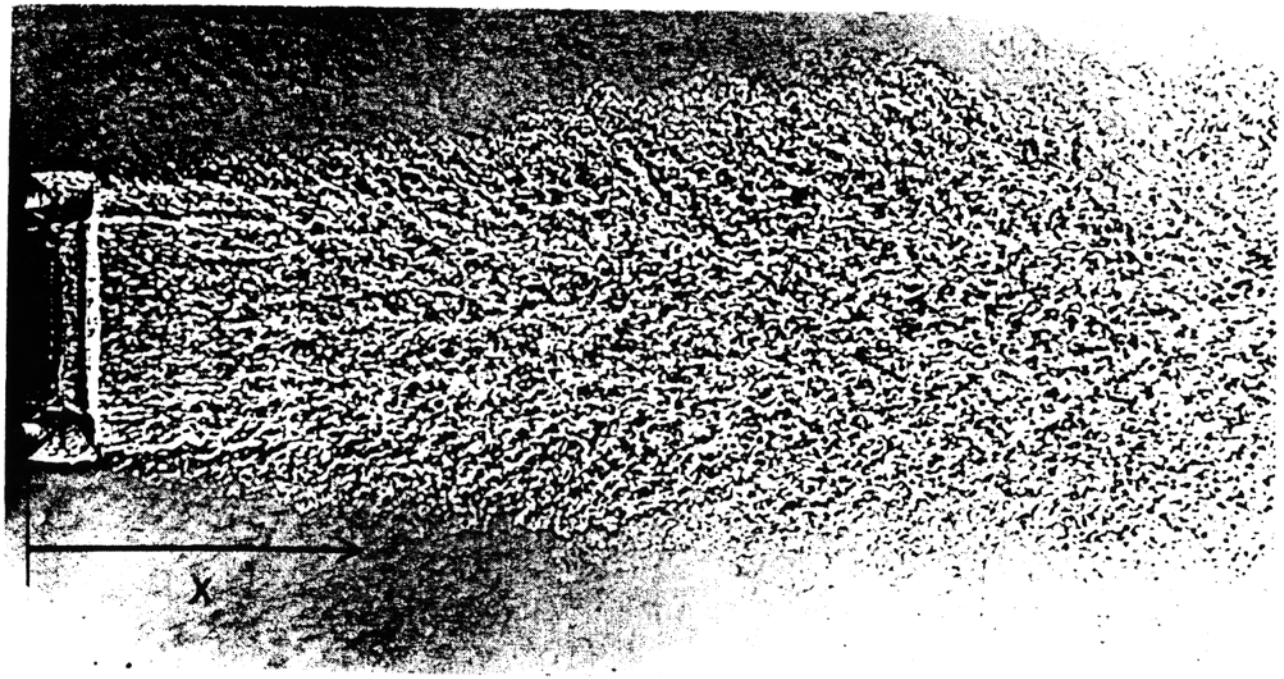
Krish Ahuja
Georgia Institute of Technology
Aerospace, Transportation and Advanced Systems Laboratory/GTRI
Atlanta, GA 30332
krishan.ahuja@gtri.gatech.edu

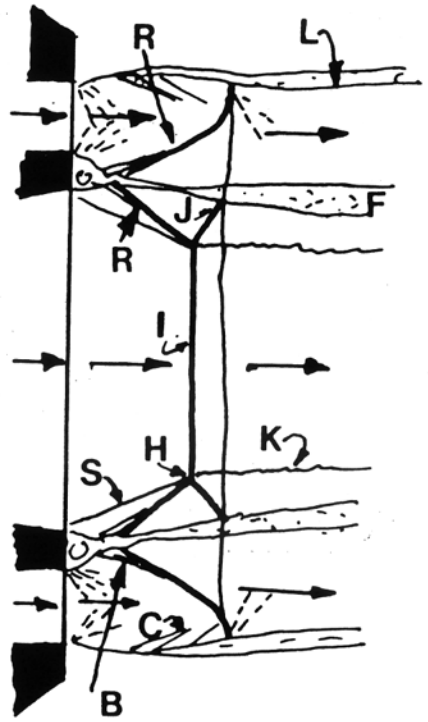
Inverted Velocity Profile (IVP)



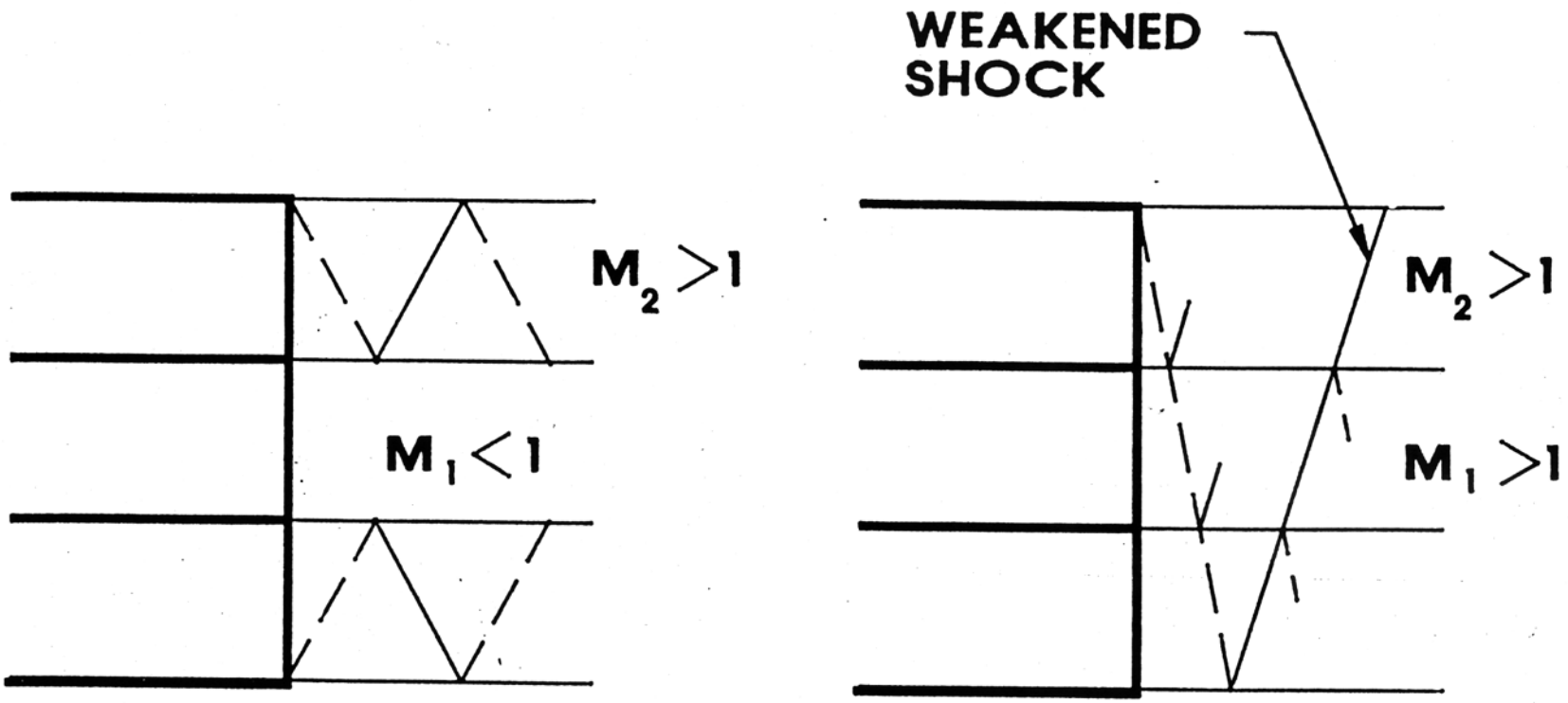
$V_f > V_p$

Explanation of the Mechanism by Dosanjh and Colleagues





SHOCK WEAKENING IN SUPERSONIC JETS



PRINCIPLE OF IVP NOISE REDUCTION

Low Frequency Prediction for an Inverted Velocity Profile Suppressor

$$U_{eff} = \frac{T_1 + T_2}{\dot{m}_1 + \dot{m}_2}$$

$$\rho_{eff} = \frac{\dot{m}_1 + \dot{m}_2}{(A_1 + A_2)U_{eff}}$$

$$St_{L.F.} = \frac{fD_{i2}}{U_{eff}}$$

High Frequency Prediction for an Inverted Velocity Profile Suppressor

$$U_{eff} = \frac{T_1 + T_2}{\dot{m}_1 + \dot{m}_2}$$

$$\rho_{eff} = \frac{\dot{m}_1 + \dot{m}_2}{(A_1 + A_2)U_{eff}}$$

$$\rho_m = (\rho_{j1}\rho_{j2}\rho_a)^{1/3}$$

Prediction of Mixing Noise of Inverted Velocity Profile Suppressor

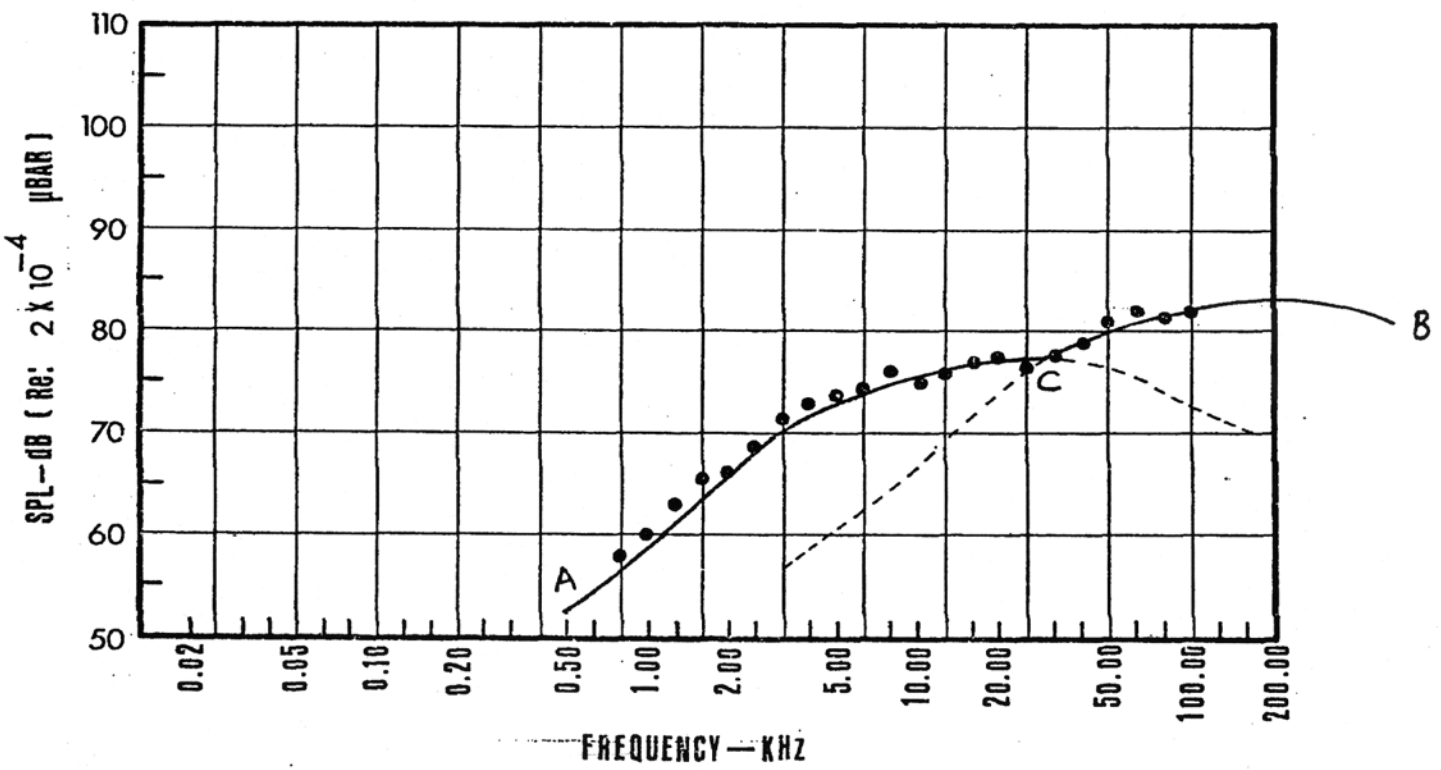


FIG. 7.37 LOW AND HIGH FREQUENCY PREDICTION SUPERIMPOSED

● NOISE LEVELS FROM SMALLER FACILITY BY BASSIOUNI [157] (APPROPRIATELY CORRECTED FOR FREQUENCY AND AMPLITUDE SHIFT)

—— PREDICTED LEVELS

K. Ahuja References

Published Journal Papers (Refereed)

1. Tam, C. K. W., Ahuja, K. K., and Jones, R. R. III, "Screech Tones From Free and Ducted Supersonic Jets," AIAA Journal; Vol. 32, No. 5, pp.917 - 922, May, 1994.
2. Brown, W. H. and Ahuja, K. K., "Jet Mixing Enhancement by Hydrodynamic Excitation," AIAA Journal,, Vol. 31, No. 3, March 1993.
3. Tam, C. K. W. and Ahuja, K. K., "Theoretical Model of Discrete Tone Generation by Impinging Jets," *Journal of Fluid Mechanics,* Vol. 214, pp. 67-87, 1990.
4. Lepicovsky, J., Ahuja, K. K., Brown, W. H., and Burrin, R. H., "Coherent Large-Scale Structures in High Reynolds Number Supersonic Jets," *AIAA Journal,* Vol. 25, No. 11, pp. 1419-1425, 1988.
5. Ahuja, K. K., Tester, B. J., and Tanna, H. K., "Calculation of Far Field Jet Noise Spectra from Near Field Measurements with True Source Location," *Journal of Sound and Vibration,* Vol. 116, No. 3, pp. 415-426, 1987.
6. Salikuddin, M., Brown, W. H., and Ahuja, K. K., "Noise from a Circulation Control Wing with Upper Surface Blowing," *Journal of Aircraft,* Vol. 24, No. 1, pp 55-64, 1987.
7. Lepicovsky, J., Ahuja, K. K., Brown, W. H., and Morris, P. J., "Acoustic Control of Free Jet Mixing," *Journal of Propulsion and Power,* Vol. 2, pp. 323-330, 1986.
8. Lepicovsky, J., Ahuja, K. K., Brown, W. H., and Burrin, R. H., "An Experimental Study of Tone-Excited Jets," *Journal of Propulsion and Power,* Vol. 2, No. 2, pp. 149-154, 1986.
9. Ahuja, K. K., and Blakney, D. F., "Tone Excited Jets - Part IV: Acoustic Measurements," *Journal of Sound and Vibration,* Vol. 102(1), pp. 93-117, 1985.
10. Lepicovsky, J., Ahuja, K. K., and Burrin, R. H., "Tone Excited Jets - Part III: Flow Measurements" *Journal of Sound and Vibration,* Vol. 102(1), pp. 71-91, 1985.
11. Ahuja, K. K., and Whiffen, M. C., "Tone Excited Jets - Part II: Flow Visualization" *Journal of Sound and Vibration,* Vol. 102(1), pp. 63-69, 1985.
12. Tanna, H. K., and Ahuja, K. K., "A Research Program at Lockheed on Tone Excited Jets - Part I: Introduction" *Journal of Sound and Vibration,* Vol. 102(1), pp. 57-61, 1985.

13. Lepicovsky, J., and Ahuja, K. K., "Experimental Results on Edge-Tone Oscillations in High-Speed Subsonic Jets," *AIAA Journal,* Vol. 23, No. 10, pp. 1463-1468, 1985.

14. Whiffen, M. C., and Ahuja, K. K., "An Improved Schlieren System and Some New Results on Acoustically Excited Jets," *Journal of Sound and Vibration,* Vol. 86, No. 1, pp. 99-105, 1983.

15. Ahuja, K. K., Lepicovsky, J., and Burrin, R. H., "Noise and Flow Structure of a Tone-Excited Jet," *AIAA Journal,* 20, 1982.

16. Ahuja, K. K., and Tam, C. K. W., "A Note on the Coupling Between Flow Instabilities and Incident Sound," *Journal of Sound and Vibration,* Vol. 83, No. 3, pp. 433-439, 1982.

17. Ahuja, K. K., Tanna, H. K., and Tester, B. J., "An Experimental Study of Transmission, Reflection, and Scattering of Sound in a Free Jet Flight Simulation Facility and Comparison with Theory," *Journal of Sound and Vibration,* Vol. 75, No. 1, pp. 51-85, 1981.

18. Dosanjh, D., Bhutiani, P. K., and Ahuja, K. K. "Supersonic Jet Noise Suppression by Coaxial Cold/Heated Jet Flows," *AIAA Journal,* Vol. 16, No. 3, pp. 268-270, 1978.

19. Ahuja, K. K., "An Experimental Study of the Effects of Upstream Obstruction on Subsonic Jet Noise," *Journal of Sound and Vibration,* Vol. 37, No. 2, pp. 205-234, 1974..

20. Ahuja, K. K., "Correlation and Prediction of Jet Noise," *Journal of Sound and Vibration,* Vol. 29, No. 2, pp. 155-168, 1973

21. Ahuja, K. K., and Bushell, K. K., "An Experimental Study of Subsonic Jet Noise and Comparison with Theory," *Journal of Sound and Vibration,* Vol. 30, No. 3, pp. 317-341, 1973.

Conference Presentations with Proceedings (refereed)

1. Ahuja, K. K., and Spencer, D. A., "Aeroacoustics of Advanced STOVL Aircraft Plumes," Proceedings of the International Powered Lift Conference and Exposition :P-203, Santa Clara, CA, December 7-10, 1987, Published by SAE; pp. 531-542, February 1988.

Deficiencies of the Acoustic Analogy Approach

Christopher Tam
Florida State University

At this point, the discussion returned to open items from the first day of the workshop. Prof. Tam made a short presentation on why he felt the Acoustic Analogy has shortcomings for jet noise. A summary of his presentation and the resulting discussion is included below:

Deficiencies of the Acoustic Analogy Approach **– Christopher Tam, Florida State University**

Lighthill's Acoustic Analogy has been the dominant theory of jet aeroacoustics for almost fifty years. Prof. Tam claimed that, except for the U^8 scaling formula (which was derived by dimensional analysis), the Acoustic Analogy approach has not been particularly successful in predicting jet noise and pointed to a number of its attributes that he considered to be deficiencies and weaknesses.

One of these is that the formulation possesses some degrees of built-in nonuniqueness. One nonuniqueness is the choice of variable to characterize sound. Lighthill chose density, ρ, as such a variable. Tam noted that other investigators, following Lighthill's idea, preferred to use pressure, p. While still others preferred some other quantities. He pointed out that one significant consequence of this arbitrariness is that the noise source terms, formulated according to the Acoustic Analogy, are different when a different choice of variable is made and that the true physical noise sources of a jet should not change because one decides to use a different variable to characterize sound.

Tam noted that another nonuniqueness of the Acoustic Analogy theories is the choice of the appropriate wave propagation operator. Lighthill cast the equations of motion into a nonhomogeneous simple wave equation. The left side of the equation represents the propagation of small amplitude acoustic waves in an otherwise static quiescent environment. He argued that since the left side represented acoustic wave propagation, by analogy to situations where small amplitude sound waves were generated by the addition of mass and momentum, the right side of the nonhomogeneous wave equation must be the source terms. These noise source terms behave like acoustic quadrupoles when the sources are compact. Lighthill noted that any source of lower multipole order would require that an externally applied force or mass source be applied to the flow. This is the basis by which quadrupoles are considered the sources of jet noise. Tam stated that no one, since Lighthill's original work, has offered a more physical or compelling reason that quadrupoles are, indeed, the noise sources.

In a jet or in the presence of a nonuniform mean flow, refraction effects on the propagation of sound due to velocity or density gradients cannot be neglected. Upon recognizing the importance of mean flow refraction, Lilley (1974) suggested to incorporate these effects into the wave propagation operator on the left side of the Acoustic Analogy equation. In Lilley's version of the Acoustic Analogy, some of the convective terms, which were put on the right side of the Lighthill nonhomogeneous wave equation and regarded as quadrupole noise source terms, were moved to the left side of the equation and became wave propagation terms to account for refraction effects. In this way, the famous Lilley equation was derived. It turns out,

what is the appropriate wave propagation operator that would include mean flow refraction effects is not at all self-evident. Earlier, Phillips (1960) chose a different convective wave propagation operator. The Phillip's equation, although not as popular as the Lilley's equation, had attracted a number of followers over the years. Tam stated that the noise source terms of the Phillip, Lilley and Lighthill equations are all different and that (from the point of view of developing noise suppression methods and technology) the nonunique noise sources of all these theories (all based on the same Acoustic Analogy framework) presents a grave problem. Tam believes that the noise sources should be unique and well defined.

Tam argued that nonlinear propagation effects cannot be dismissed and should be incorporated into the wave propagation operator in the Acoustic Analogy formulation in the near field of a jet where the sound pressure level can easily reach 160 dB and higher. (See Seiner's invited panel presentation.) Tam stated the correct wave propagation operator that included both refraction and nonlinear propagation effects would then be the full Euler equations. In which case the only terms left over for the source term would be the viscous stresses, which clearly are not the noise sources of a turbulent high-speed jet. He concluded from this that the validity of the Acoustic Analogy must be carefully re-examined.

To demonstrate the weakness of the Lighthill approach, Tam numerically solved the full Euler equations for an infinite domain in which the sound was generated by an initial pressure distribution in the form of a Gaussian. He then solved the Lighthill equation by the same numerical scheme using the quadrupole terms found as the nonhomogeneous source terms on the right side of the wave equation. Not surprisingly**,** this solution was found to be exactly the same (within numerical accuracy of the scheme) as the original solution of the full Euler equations. Tam stated that this implied that the quadrupoles were mere fictitious sources terms of the Lighthill equation for this problem where the acoustic disturbances were generated by the initial conditions. He said that the fact that the original exact solution is recovered does not prove the correctness of Lighthill's assertion as some past investigators tried to claim.

This generated a number of comments explaining why this example may not be applicable to the use of Lighthill's equation for calculating the time stationary sound field from a turbulent jet. For example, Lilley pointed out that Tam overlooked the fact that he had used a version of Lighthill's equation that excluded all external source terms such as mass sources, body force sources and energy sources. These must be added to the righthand-side of the wave equation, and in cases, such as a prescribed impulsive motion, the Lighthill stress tensor is absent. The typical solutions in these cases are given in 'Waves in fluids' by Lighthill(1975). The notes added to Lilley's presentation (from the first day of the workshop) show both the general form of Lighthill's equation when all external sources are added, together with the exact equivalent of the `second' component of the Lighthill stress tensor as derived from use of the energy and mass conservation equations. In this derivation all diffusive terms are absent, and the thermodynamic processes are assumed isentropic.

More information on the test problem proposed by Prof. Tam can be found in Appendix C.

C. Tam References

1. Tam, C.K.W. *Directional acoustic radiation from a supersonic jet generated by shear layer instability*, Journal of Fluid Mechanics, **46**, 757–768, 1971.

2. Tam, C.K.W. & Morris, P.J. *The radiation of sound by the instability waves of a compressible plane turbulent shear layer*, Journal of Fluid Mechanics, **98**, 349–381, 1980.

3. Tam, C.K.W. & Tanna, H.K. *Shock associated noise of supersonic jets from convergent-divergent nozzles* (with H.K. Tanna), Journal of Sound and Vibration, **81**, 337–358, 1982.

4. Ahuja, K.K., Lepicovsky, J., Tam, C.K.W. et al *Tone-excited jet — theory and experiments*, National Aeronautics and Space Administration, CR–3538, 1982.

5. Tam, C.K.W. & Burton, D.E. *Sound generated by instability waves of supersonic flows: Part I.* Two Dimensional Mixing Layers, Journal of Fluid Mechanics, **138**, 249–271, 1984.

6. Tam, C.K.W. & Burton, D.E. *Sound generated by instability waves of supersonic flows: Part II.* Axisymmetric Jets, Journal of Fluid Mechanics, **138**, 273–295, 1984.

7. Tam, C.K.W., Jackson, J.A. & Seiner, J.M. *A multiple-scales model of the shock cell structure of imperfectly expanded supersonic jets*, Journal of Fluid Mechanics, **153**, 123–149, 1985.

8. Tam, C.K.W. *On broadband shock associated noise of supersonic jets*, Recent Advances in Aerodynamics and Aeroacoustics, 25–51, 1985.

9. Tanna, H.K., Brown, W.H. and Tam, C.K.W. *Shock associated noise of inverted-profile coannular jets: Part I. Experiments*, Journal of Sound and Vibration, **98**, 95–113, 1985.

10. Tam, C.K.W. & Tanna, H.K. *Shock associated noise of inverted-profile coannular jets: Part II. Condition for Minimum Noise*, Journal of Sound and Vibration, **98**, 115–125, 1985.

11. Tam, C.K.W. & Tanna, H.K. *Shock associated noise of inverted-profile coannual jets: Part III. Shock Structure and Noise Characteristics*, Journal of Sound and Vibration, **98**, 127–145, 1985.

12. Tam, C.K.W. and Morris, P.J. *Tone excited-jets — A theoretical model and comparison with experiment,* Journal of Sound and Vibration, **102**, 119–151, 1985.

13. Tam, C.K.W., Seiner, J.M. & Yu, J.C. *Proposed relationship between broadband shock associated noise and screech tones,* Journal of Sound and Vibration, **110**, 309–321, 1986.

14. Tam, C.K.W. *Stochastic model theory of broadband shock associated noise from supersonic jets,* Journal of Sound and Vibration, **116**, 265–302, 1987.

15. Tam, C.K.W. *The shock-cell structures and screech tone frequencies of rectangular and non-axisymmetric supersonic jets,* Journal of Sound and Vibration **121**, 135–147, 1988.

16. Tam, C.K.W. & Hu, F.Q. *On the three families of instability waves of high speed jets* , Journal of Fluid Mechanics , **201**, 447–483, 1989.

17. Tam, C.K.W. & Ahuja, K.K. *Theoretical model of discrete tone generation by impinging jets* , Journal of Fluid Mechanics, **214**, 67–87, 1990.

18. Tam, C.K.W. *Broadband shock associated noise of moderately imperfectly expanded supersonic jets,* Journal of Sound and Vibration, **140**, 55–71, 1990.

19. Tam, C.K.W. *Jet noise generated by large scale coherent motion*, Chapter 6 in Aeroacoustics of Flight Vehicles: Theory and Practice, volume 1, NASA RP–4258, 1991.

20. Tam, C.K.W. *Broadband shock associated noise from supersonic jets in flight.,* Journal of Sound and Vibration **151**, 131–147, 1991.

21. Tam, C.K.W. & Nofum, T. *Impingement tones of large aspect ratio supersonic rectangular jets,* American Institute of Aeronautics and Astronautics Journal, **30**, 304–311, 1992.

22. Tam, C.K.W. Chen, P. & Seiner, J.M. *Relationship between instability waves and noise of high-speed jets.* American Institute of Aeronautics and Astronautics Journal, **30**, 1747–1752, 1992.

23. Tam, C.K.W. *Broadband shock associated noise from supersonic jets measured by a ground observer,* AIAA Journal, **30**, 2395–2401, 1992.

24. Tam, C.K.W. & Thies, A.T. *Instability of rectangular jets,* Journal of Fluid Mechanics, **248**, 425–448, 1993.

25. Tam, C.K.W., Ahuja, K.K. & Jones, R.R. *Screech tones from free and ducted supersonic jets.* AIAA Journal, **32**, 917–922, 1994.

26. Tam, C.K.W. & Chen, P. *Turbulent mixing noise from supersonic jets*, AIAA Journal, **32**, 1774–1780, 1994.

27. Tam, C.K.W. *Supersonic jet noise*, Annual Review of Fluid Mech., **27**, 17–43, 1995.

28. Thies, A.T. & Tam, C.K.W. *Computation of turbulent axisymmetric and nonaxisymmetric jet flows using the k – ε model*, AIAA Journal, **34**, 309–316, 1996.

29. Tam, C.K.W. & Reddy, N.N. *A prediction method for broadband shock associated noise from supersonic rectangular jets* , Journal of Aircrafts, **33**, 298–303, 1996.

30. Tam, C.K.W., Shen, H. & Raman, G. *Screech tones of supersonic jets from beveled rectangular nozzles*, AIAA Journal, **35**. 1119–1125, 1997.

31. Tam, C.K.W. *Jet noise: Since 1952*, Theoretical and Computational Fluid Dynamics, **10**, 393–405, 1998.

32. Tam, C.K.W. *Influence of nozzle geometry on the noise of high-speed jets*, AIAA Journal, **36**, 1396–1400, 1998.

33. Tam, C.K.W. & Auriault, L. *Mean flow refraction effects on sound radiated from localized sources in a jet*, Journal of Fluid Mechanics, **370**, 149–174, 1998.

34. Shen, H. & Tam, C.K.W. *Numerical simulation of the generation of axisymmetric mode jet screech tones.* AIAA Journal, **36**, 1801-1807, 1998.

35. Tam, C.K.W. & Auriault, L. *Jet mixing noise from fine scale turbulence*, AIAA Journal, 37, 145–153, 1999.

36. Tam, C.K.W. & Zaman, K.B.M.Q. *Subsonic jet noise from non-axisymmetric and tabbed nozzles*, AIAA Journal, **38**, 592–599, 2000.

37. Shen, H. & Tam, C.K.W. *Three Dimensional Numerical Simulation of the Jet Screech Phenomenon,* AIAA Paper 2001-0820, 2001.

38. Tam, C.K.W. & Pastouchenko, N. *Noise from the Fine Scale Turbulence of Nonaxisymmetric Jets*, AIAA Paper 2001-2187, 2001.

39. Tam, CK.W. , Golebiowski, M. & Seiner, J.M. *On the Two Components of Turbulent Jet Mixing Noise from Supersonic Jets,* AIAA Paper 96-1716, 1996.

SESSION 3: PHYSICS OF JET NOISE SUPPRESSION

Summary by Mary Jo Long-Davis, NASA Glenn Research Center

The session consisted of six presentations by invited panelists and several presentations during the open podium portion of the session. The panelists were requested to give evidence where theory has correctly predicted jet noise trends with suppression devices. Discussion followed each presentation.

INVITED PRESENTATIONS

Physics of Jet Noise Suppression: Industry Perspective on Prediction Methods, Future Direction/Needs - Wesley K. Lord, Pratt & Whitney

Dr. Lord presented an industry perspective on the physics of jet noise suppression, discussed prediction methods, and indicated P&W's future direction and needs. He discussed two broad categories of jet noise suppression devices: internal mixing devices and external mixing devices. Turbofan fan-core mixers and ejector nozzles are included in the first category of internal mixing devices. The intent of the internal mixing devices is to reduce the high velocity core flow. The mixing process creates mixing noise, but this mixing noise can be attenuated through the use of acoustic liners. Lord indicated that P&W has the ability to apply 3D Computational Fluid Dynamics (CFD) Reynolds Averaged Navier-Stokes (RANS) codes for modeling the internal mixing devices. Unfortunately, they've had no means of relating the flow field solutions obtained using the RANS codes to noise. The empirical noise prediction tools neglect internal noise sources. Lacking any better acoustic design philosophy, the paradigm has been to strive for better mixing at the nozzle exit.

Suppressor nozzles, serrations (e.g., tabs/chevrons), and flexible filaments are included in the category of external mixing devices. The intent of the external mixing devices is to modify the shear layer structure to reduce the peak amplitude. A good external mixing device is one that achieves large reductions in low frequency noise with very little increase in high frequency noise. Lord discussed the recent emergence of computationally-based noise prediction methods. P&W has adopted the jet noise modeling approach put forth by Tam, Golebiowski, and Seiner which proposes two noise source mechanisms: large-scale structure noise and fine-scale turbulence noise.

The computational models for fine-scale turbulence noise involve a two-step prediction process—aerodynamics and noise. Using RANS CFD for a given three-dimensional nozzle geometry, the mean flow and turbulence properties are calculated. This information is input to a noise model that predicts the spectra and directivity. P&W has been focused on Tam's computational model for fine-scale turbulence noise since mid-1999.

Lord presented results from a single-stream jet experiment to validate the aerodynamic and noise prediction methodology. Results for the single-stream hot jet indicated good agreement between the prediction and the data for angles from 80 to 110 degrees. At aft angles, however, over 10 dB difference was observed between the prediction and the data. This large difference between the prediction and the data could be attributed to large scale structure noise which dominates at the aft angles, and is not captured by the fine-scale turbulence noise model.

Noise models are needed for the large-scale structure noise. Several modeling approaches were highlighted. Lord emphasized that the method needs to be able to capture effects due to geometry differences in real-world complex nozzle designs. Large Eddy Simulation (LES) would be appropriate if the grid resolution required at the right Reynolds numbers can be achieved. Lord presented results from an LES calculation of a high Reynolds number single-stream jet. The LES calculation had reasonable agreement with the data at the low frequencies, but failed to accurately predict at the higher frequencies. The numerical issues associated with the LES method include accurate boundary conditions and grid resolution. It was projected that over 1 billion grid points would be required to obtain an accurate LES solution for a high Reynolds number jet.

The objective of this panel discussion was to give evidence where theory has correctly predicted jet noise trends with suppression devices. P&W is beginning to be able to do this using their aero/noise methodology based on Tam's computational model for fine-scale turbulence noise. Lord emphasized the need for a noise model with a direct connection to the actual 3D nozzle geometry and RANS CFD. Quality data for validation of both aero/turbulence and noise models in hot subsonic jets is needed. Models for large- scale structure noise are needed to improve the aero/noise prediction in the aft angles.

Question: What is the thrust loss due to these chevrons and tabs?

Answer: There is some thrust loss. You'll see there's a range of jet velocities and bypass ratios that these devices are well suited for. Thrust loss is relatively small (0.1-0.2% loss). The decision to use them is made on a case-by-case basis depends on the airplane application.

Question: Is anybody doing any work on coarser estimates using CFD solutions to determine noise reduction to replace current--more like crude engineering estimates?

Answer: P&W is attempting to get a more physics-based handle on the noise at this time.

Physics of Jet Noise Suppression: Industry Perspective on Prediction Methods, Future Direction/Needs

Wesley K. Lord
Pratt & Whitney

"Physics of Jet Noise Suppression"

- Industry Perspective
- Prediction Methods
- Future Direction/ Needs

AeroAcoustics Research Consortium
Jet Noise Workshop
OAI Cleveland, Ohio
November 8, 2000

Wesley K Lord
Jinzhang Feng
Pratt & Whitney

Jet Noise Suppression Devices
Two Broad Categories of Devices

Internal Mixing Devices

turbofan fan/core mixer
ejector nozzle

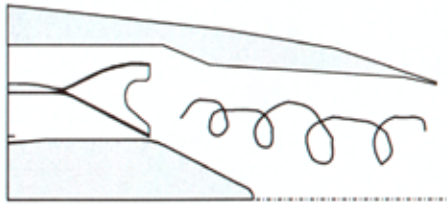
External Mixing Devices

suppressor nozzle
nozzle tabs/chevrons
flexible filaments

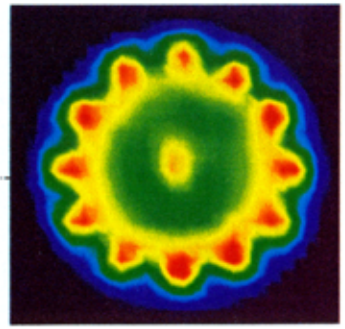
Internal Mixing Devices

Fan/Core Mixer

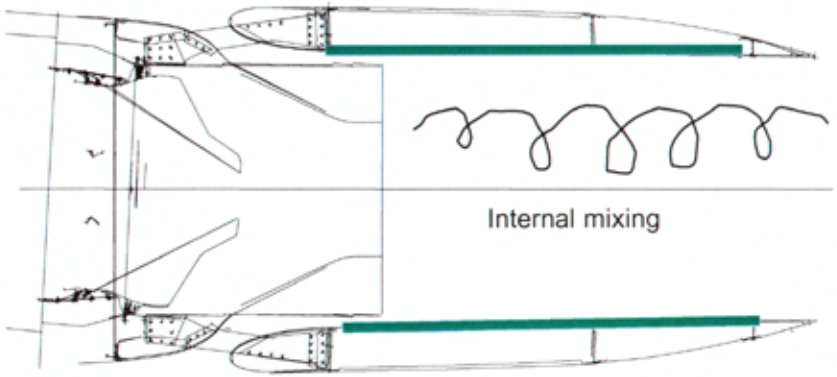




Nozzle exit temperature



Ejector Nozzle



Internal mixing devices → reduce jet velocity at nozzle exit, jet noise ~ V_{jet}^{N}
parasitic noise of internal mixing process → attenuate with liner

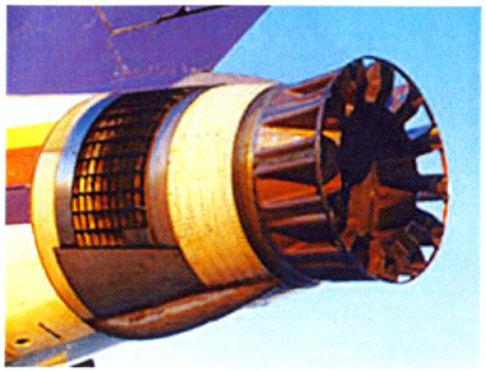
Prediction Methods?

1980's, 90's

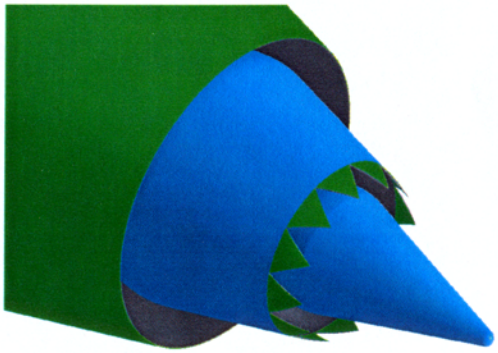
Mixing → CFD (RANS)
Noise → empirical, SAE or other, neglect internal noise
scale-model data
initial work on noise modeling

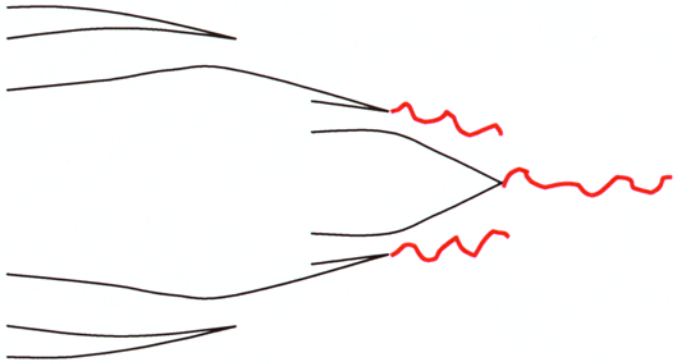
External Mixing Devices

Suppressor Nozzle



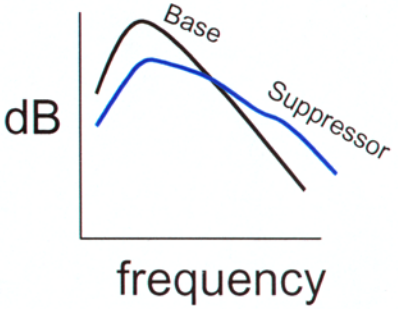
Tabs or Chevrons





Flexible Filaments

External Mixing Devices → modify external flow/ shear layer structure
→ generally reduce low-frequency noise
→ may increase small-scale turbulence/ high-frequency noise



Prediction Methods?
Late 1990's emergence of computationally-based jet noise models

Jet Noise Modeling

Two Noise Source Mechanisms

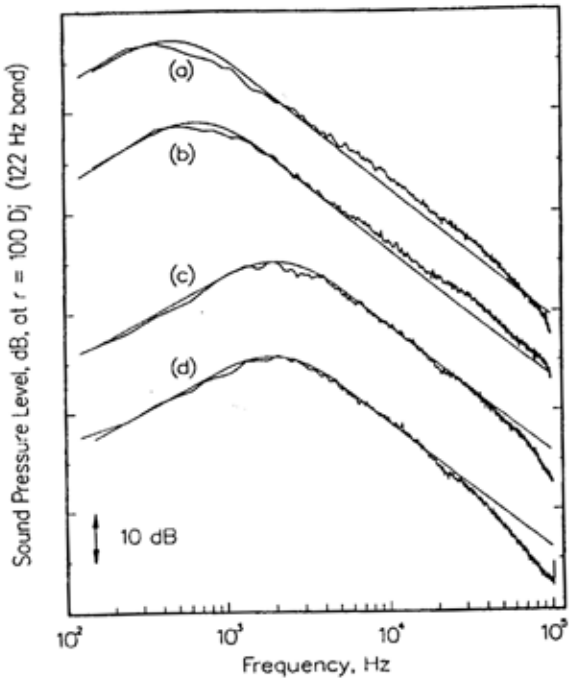


Figure 5. Comparison of the similarity spectrum of large turbulence structures/instability waves noise and measurements. (a) $M_j = 2.0$, $T_t/T_\infty = 4.89$, $\chi = 160.1°$, $SPL_{max} = 124.7$ dB, (b) $M_j = 2.0$, $T_t/T_\infty = 1.12$, $\chi = 160.1°$, $SPL_{max} = 121.6$ dB, (c) $M_j = 1.96$, $T_t/T_\infty = 1.78$, $\chi = 138.6°$, $SPL_{max} = 121.0$ dB, (d) $M_j = 1.49$, $T_t/T_\infty = 1.11$, $\chi = 138.6°$, $SPL_{max} = 106.5$ dB.

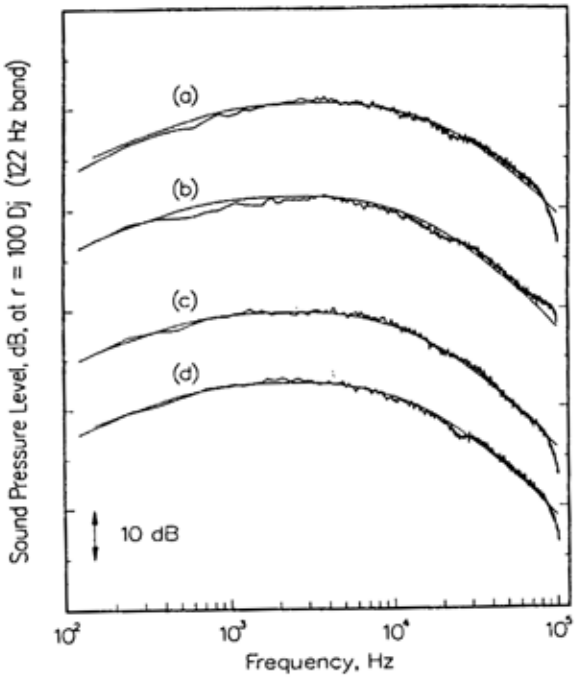


Figure 6. Comparison of the similarity spectrum of fine-scale turbulence noise and measurements. (a) $M_j = 1.49$, $T_t/T_\infty = 2.35$, $\chi = 92.9°$, $SPL_{max} = 96$ dB, (b) $M_j = 2.0$, $T_t/T_\infty = 4.89$, $\chi = 83.8°$, $SPL_{max} = 107$ dB, (c) $M_j = 1.96$, $T_t/T_\infty = 0.99$, $\chi = 83.3°$, $SPL_{max} = 95$ dB, (d) $M_j = 1.96$, $T_t/T_\infty = 0.98$, $\chi = 120.2°$, $SPL_{max} = 100$ dB.

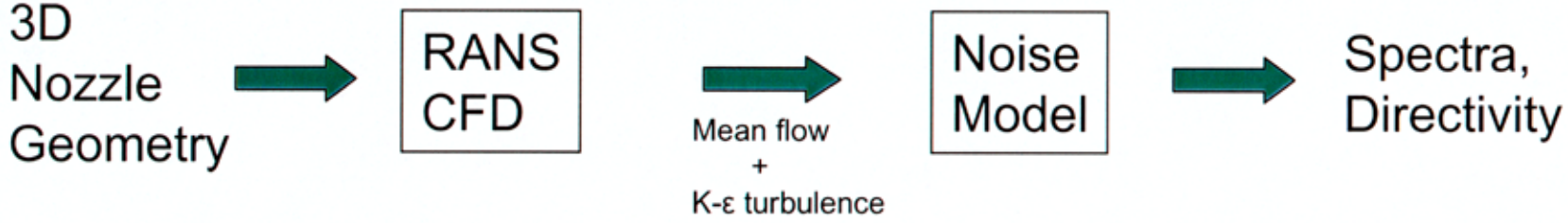
Large-scale structure noise

Fine-scale turbulence noise

Reference: C.K.W.Tam, M.Golebiowski, J.M.Seiner 1996

Computational Models for "Fine-Scale Turbulence" Noise

Two-Step Process: 1) Aero 2) Noise

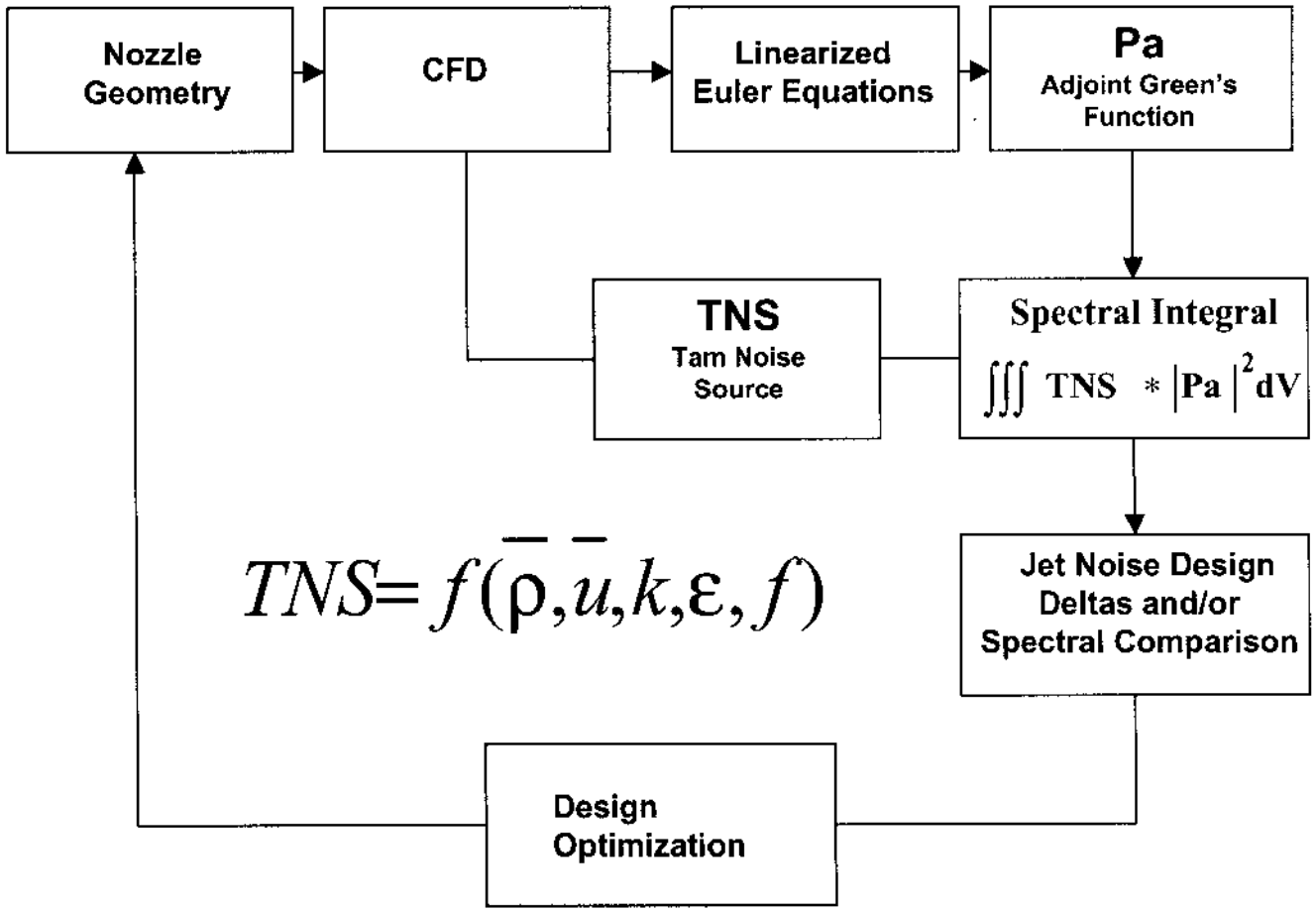


Computational jet noise models:

- MGBK
- Tam → PW focus since mid-'99
- ?
- ?
- ?

Tam Computational Model for Fine-Scale Turbulence Noise

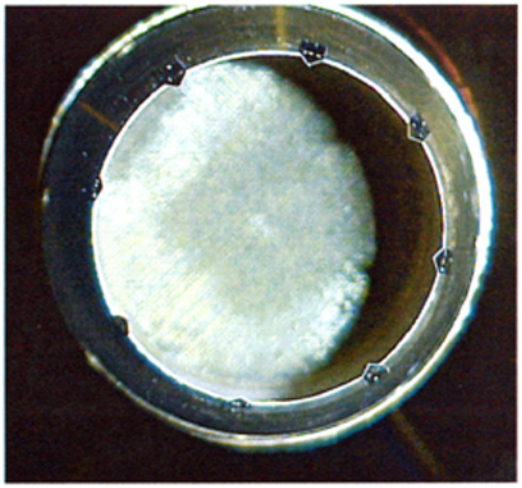
Reference: C.K.W.Tam, L.Auriault AIAA J 1999



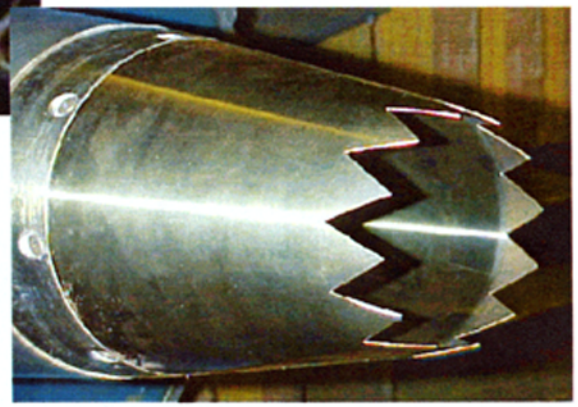
Aero/Noise Validation I: Single-Stream Nozzle



Single-stream conical nozzle
Acoustic Research Tunnel UTRC



Tab Nozzle



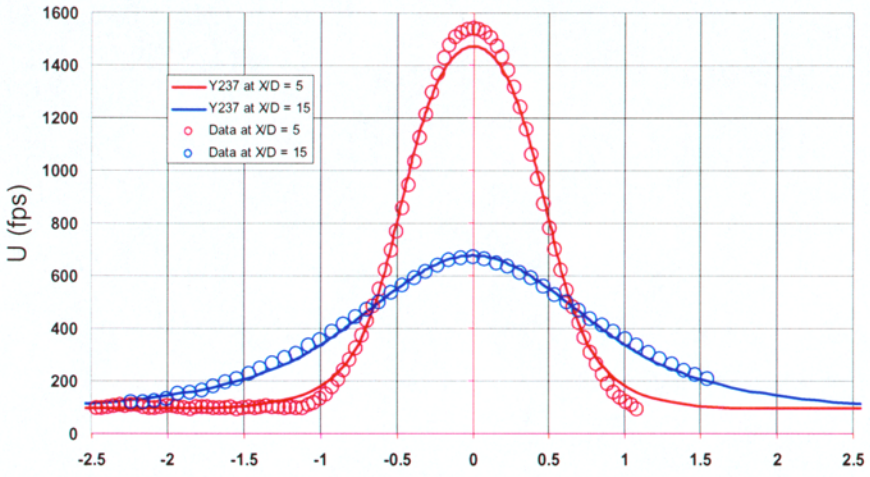
Single-stream nozzle with chevrons

Experiments: mean flow, turbulence (cold),
noise source diagnostics,
far-field noise

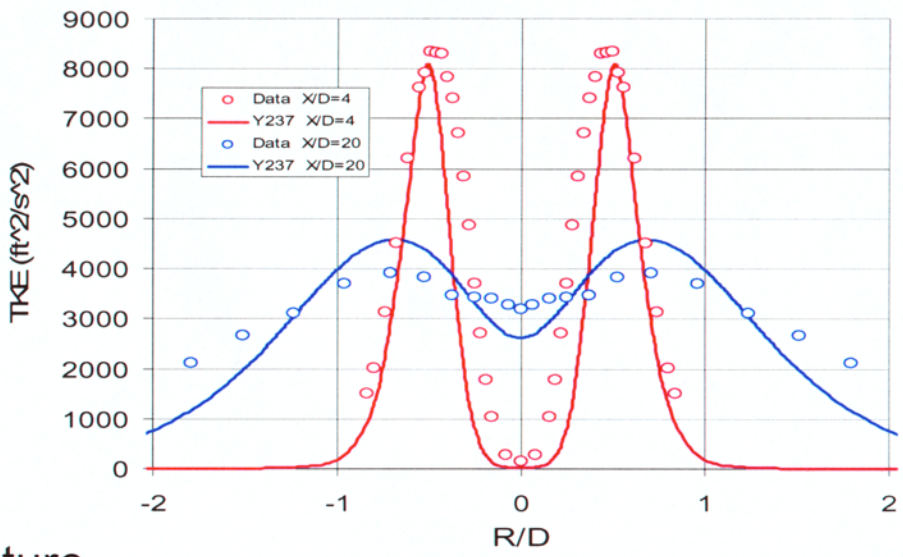
Reference: J.C.Simonich et al. AIAA/CEAS 2000

RANS CFD Validation for Single-Stream Hot & Cold Jets

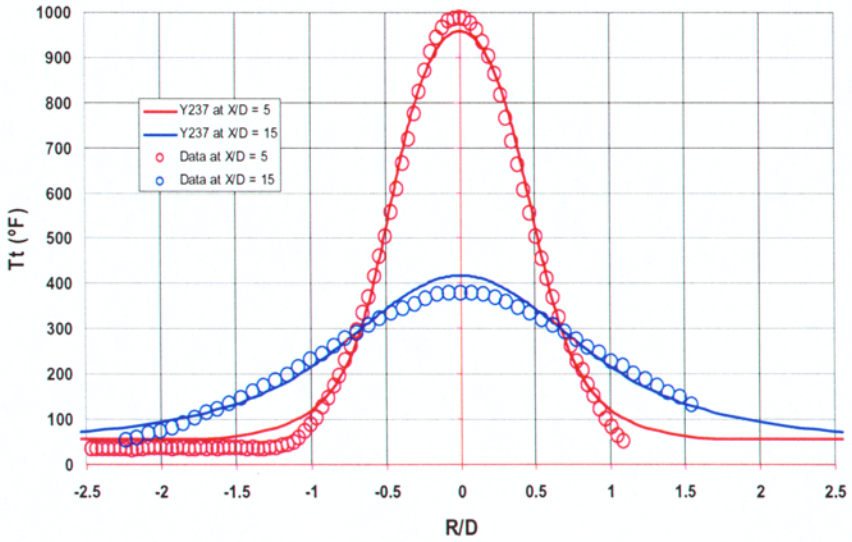
Velocity

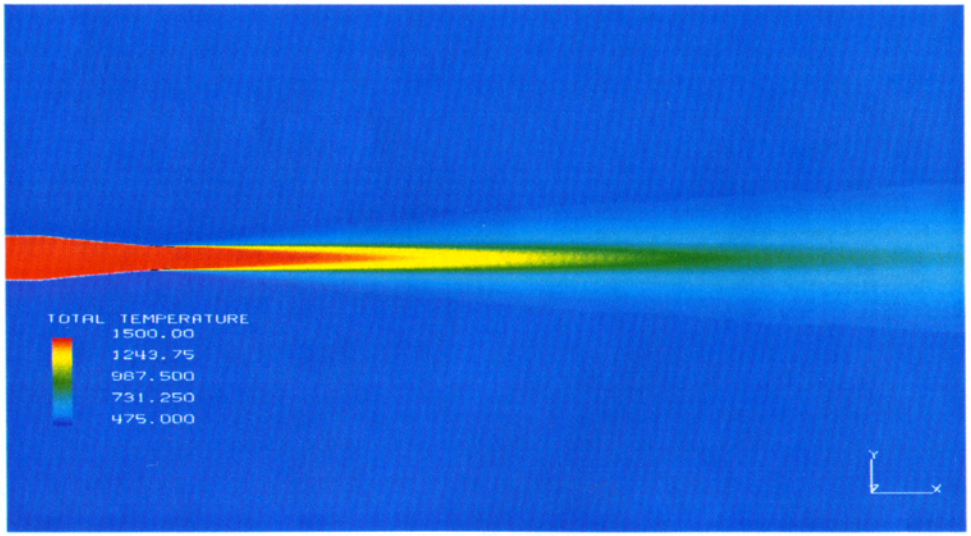


Turbulence (cold)

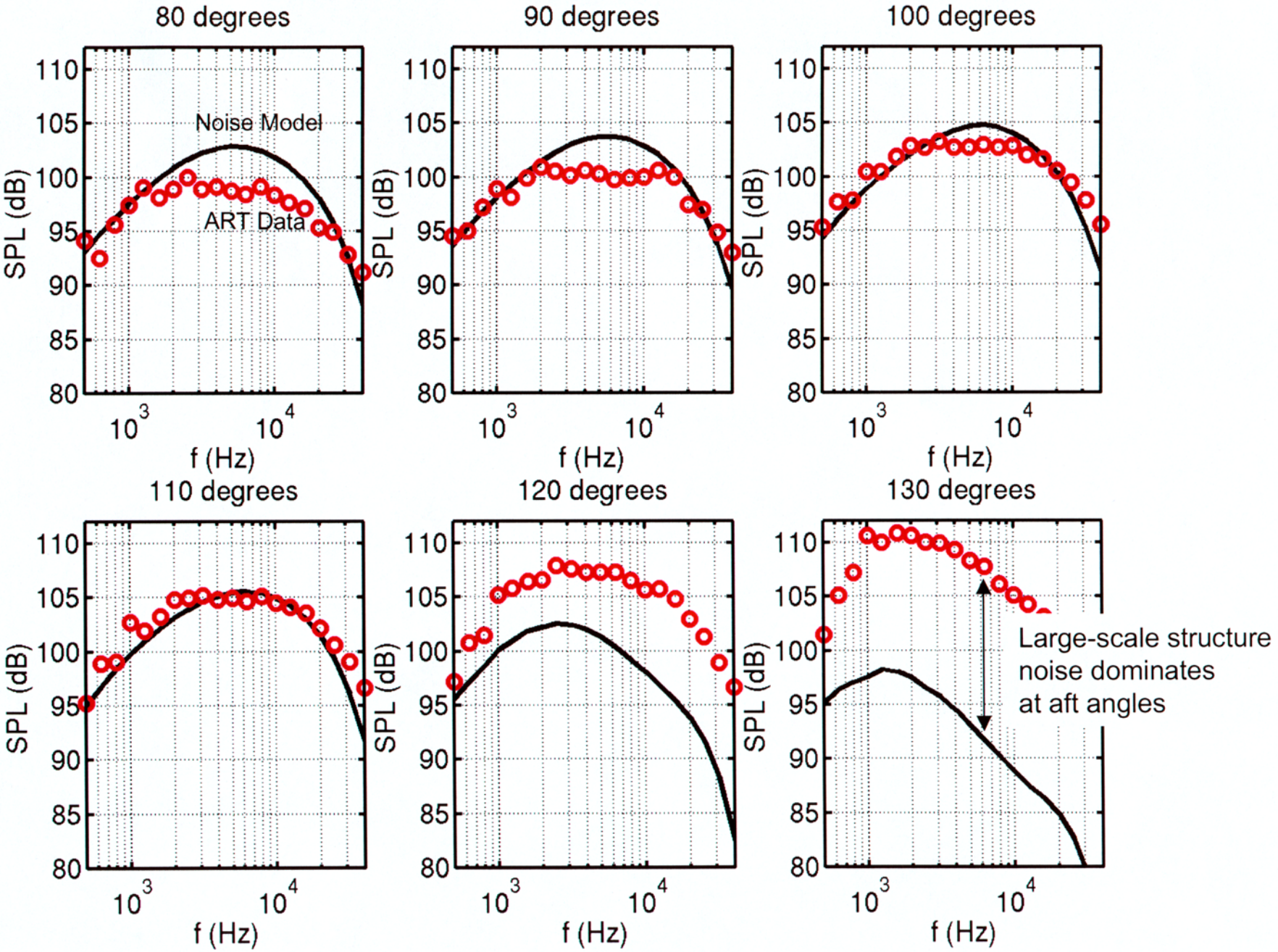


Temperature

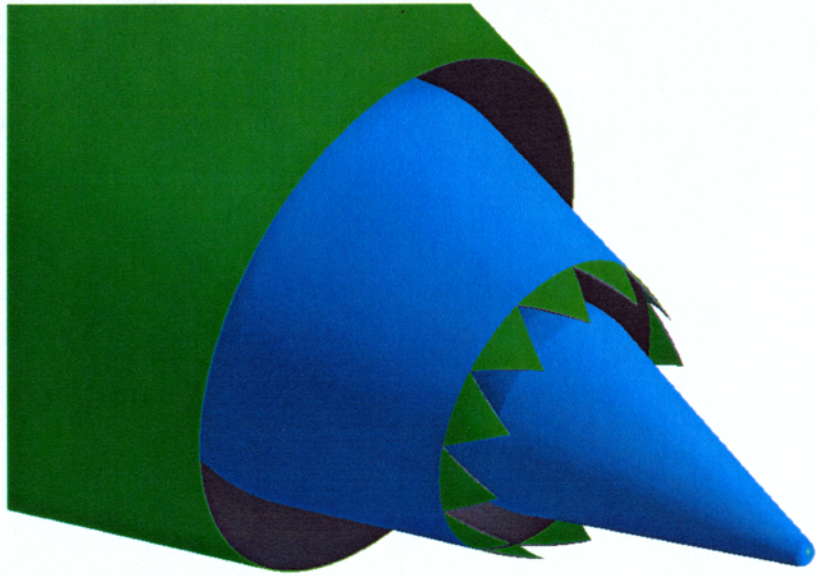


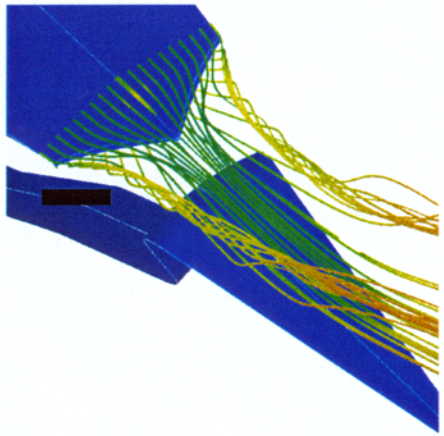


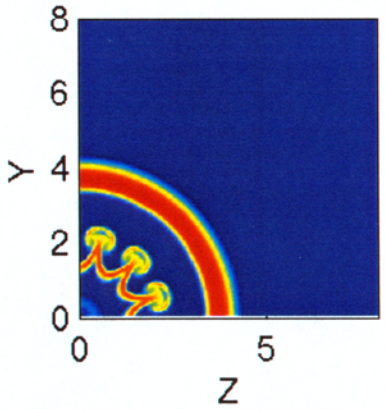
Noise Model Validation for Single-Stream Hot Jet



Aero/Noise Validation II: Turbofan Separate-Flow Nozzle







Aero/Noise Model Validation in progress….

Noise Model(s) Needed for Large-Scale Structure Noise

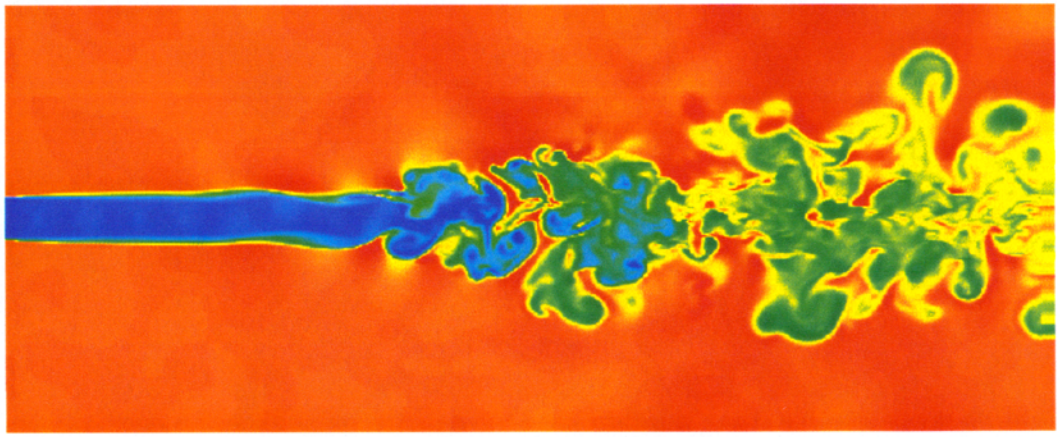
Modeling Approaches:
- LES?
- Hybrid RANS/LES techniques, DES?
- Unsteady RANS with "improved" turbulence model?
- Stability Methods, PSE?
- Modal Decomposition, POD?
- Vortex Methods?

Reminder: the method needs to be able to capture effects due to geometry differences in real-world complex nozzle designs

LES for High Reynolds Number Jet

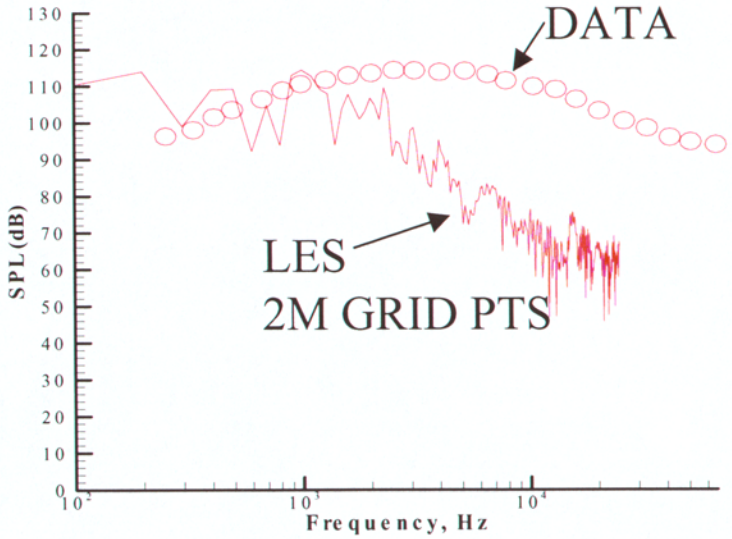
Reference: D.Choi, T.J.Barber, L.M.Chiappetta, M.Nishimura AIAA 1999

Single-Stream Axisymmetric Jet, RE_D ~ 1M



LES Numerical Issues

- ***Farfield Boundary Conditions***
- ***Inlet Unsteady B.C.***
- ***Grid Resolution***



Estimated Grid Requirement
> 1B grid pts

Summary

"Give evidence where theory has correctly predicted jet noise trends with suppression devices"
→ there is evidence that we are beginning to be able to do this

Industry Needs (PW Perspective)

Noise models with a direct connection to actual 3D geometry and RANS CFD

Quality data for validation of both aero/turbulence and noise models in hot subsonic jets

Models for large-scale structure noise

Physics of Jet Noise Suppression: The MGB Paradigm

Philip Gliebe
GE Aircraft Engines

***Physics of Jet Noise Suppression: The MGB Paradigm* - Philip Gliebe, GE Aircraft Engines as summarized by Mary Jo Long-Davis.**

Mr. Gliebe provided qualitative evidence that indicated jet noise suppression trends could be explained by the physics of jet noise in the MGB model. As evidence, results from the NASA Advanced Subsonic Technology (AST) Separate-Flow Exhaust System Noise Reduction Concept Evaluation program were examined. As part of this AST test program, a series of chevrons were added to the trailing edge of the fan and core nozzles. Flow field surveys were performed and acoustic measurements were made. Gliebe noted that the MGB noise prediction for the separate flow nozzle has not yet been performed, 3D CFD RANS solutions are still being computed. The intent of this presentation was to confirm that the 'ingredients' in the MGB model inherently capture the physics of the jet noise problem as evidenced by the test data and to provide an early indication of the expected prediction by the MGB model prediction based on its formulation.

Experimental results indicated chevrons typically reduced the low frequency noise, without a lot of change in the high frequency noise, relative to the baseline. Alternating inward/outward chevrons provided the best low frequency noise reduction but could create high frequency noise as well. Gliebe indicated that one has to be careful with these devices to ensure a balance between low frequency noise reduction and high frequency noise generation. Gliebe posed the question: do the fluid mechanics suggest that this is right? The alternating inward/outward chevron configuration, that increased the high frequency noise relative to the baseline, is shown in the velocity contour plot. Examination of the shear layer perimeter (in yellow on the contour plot) revealed that it is increased for this configuration relative to the baseline. The contention is that this very large shear layer perimeter may be the cause of the increase in high frequency noise with the alternating inward/outward chevrons.

The basic noise characteristics are dependent on three physical processes involved in jet mixing: 1) noise source generation, 2) noise source convective amplification, and 3) noise source jet shielding. The MGB model assumes far field noise is proportional to the source intensity spectrum, convective amplification factor, and the fluid shielding factor. Gliebe examined the formulation of each of these factors in relation to the observed trends in the data. He concluded that the fundamental mixing noise conceptual model in MGB is not inconsistent with experimental evidence for impact of chevrons on reducing jet mixing noise.

Question: Will there be Reynolds effects that will change the results gotten in model scale?

Answer: These configurations have been tested on a full-scale engine, and results comparable to the model test results were obtained.

Immediately following the presentation made by Gliebe, Vinod Mengle of Rolls-Royce posed an alternate explanation as to why alternating inward/outward chevrons have increased higher frequency noise than inwardly flipped chevrons. He proposed that since alternating inward/outward chevrons have half the number of vortex mushrooms as compared to the case of all inward chevrons, it cannot be concluded that the shear-perimeter for the alternating inward/outward chevrons is higher. Mengle continued this argument by looking at the vorticity dynamics to provide an explanation of the difference in the number of vortex mushrooms.

Gliebe response to Mengle explanation: It is agreed that the chevron concept does produce longitudinal vortex formations which promote entrainment of the core fluid into the fan flow and vice versa. In fact, it was this principle or hypothesis that guided the development of the chevron concept in the first place - see reference [5]. However, the alternating chevron does in fact increase the mixing layer perimeter substantially, even though it produces only half the number of vortices as does the inward-bent chevron. This is because the resulting vortices are larger, and they persist longer (further downstream) before merging with one-another because they are circumferentially farther apart. It is believed that the differences between the inward-bent and alternating chevron flow field and noise characteristics are still consistent with the MGB paradigm.

NASA/CP—2001-211152



NASA-OAI Jet Noise Workshop
Ohio Aerospace Institute
Cleveland, Ohio

Physics of Jet Noise Suppression: The MGB Paradigm ……

Philip Gliebe
GE Aircraft Engines
November 8, 2000



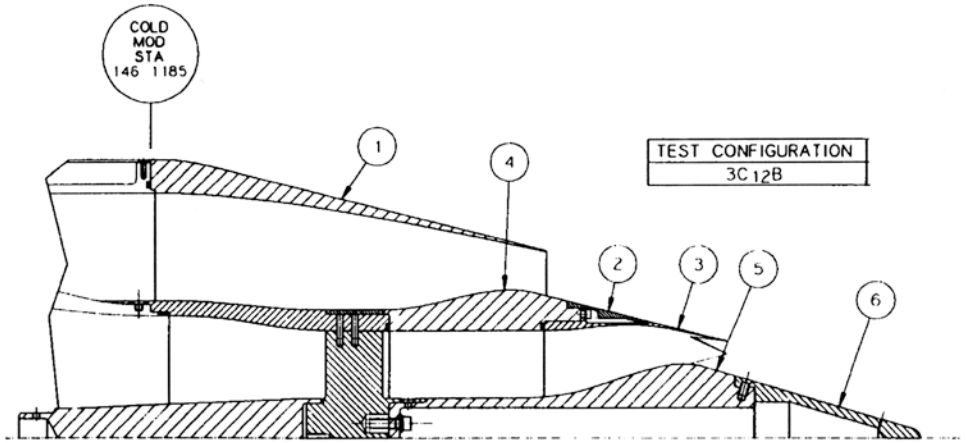
Qualitative Evidence that Observed Jet Noise Suppression Trends can be explained by the MGB Model

Data Source: NASA AST Separate Flow Exhaust System Noise Reduction Concept Evaluation Program

(NASA Contract NAS3-27720 - Area of Interest 14.3)

- Description of Noise Reduction Devices - Chevrons
- Sample Flow Field Survey Results
- Sample Acoustic Results
- MGB Noise Mechanisms
- Confirming Evidence of the MGB "Ingredients"

REVISIONS					
ZONE	REV	DESCRIPTION	DATE	APPROVED	MLSE
-	-	-	-		



TEST CONFIGURATION
3C12B

QTY	ITEM	PART NO	DESCRIPTION	SPECIFICATION
LIST OF MATERIALS				
1	6	2078-411	TAIL CONE	CONFIG #3
1	5	2078-402	TAIL CONE ADAPTER	CONFIG #3
1	4	2078-404	CORE NOZZLE FORWARD SECTION	CONFIG #2 & #3
1	3	2078-422	CORE NOZZLE 9a	CONFIG #3
1	2	2078-605	CORE NOZZLE COVER RING CONFIG	#2 & #3
1	1	2078-001	FAN NOZZLE CONFIG	#2 THRU #5

1 SEE DRAWING 2078 419 FOR ITEMS NOT SHOWN ON THIS DRAWING

NOTE:

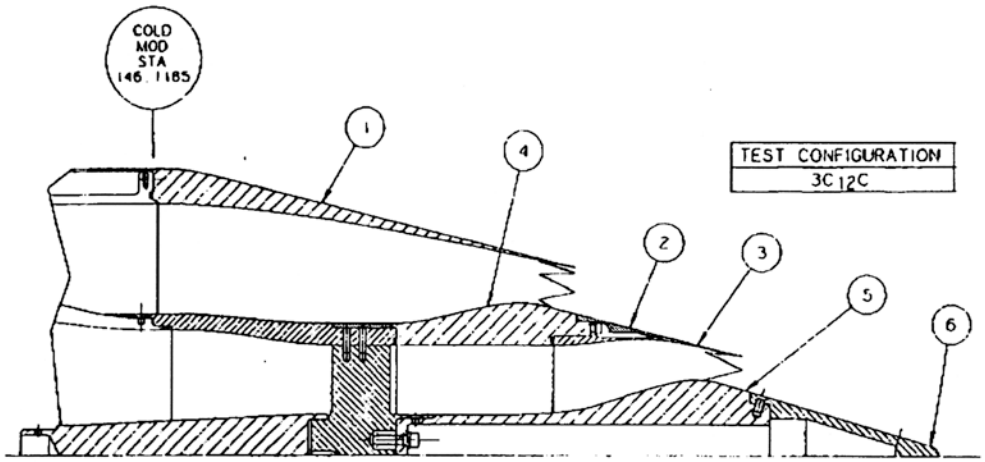
DRILLED HOLE TOLERANCE
0 - 125 DIA +.004 -.001
126 - 250 DIA +.005 -.001
251 - 500 DIA +.006 -.001
501 - 750 DIA +.008 -.001
751 - 1 000 DIA +.010 -.001

UNLESS OTHERWISE SPECIFIED DIMENSIONS ARE IN INCHES TOLERANCES ARE
DECIMALS XXX ±.005 XX ±.010 X ±.030
FRACTIONS ±1/16 MACHINED ANGLES ±1/2°
THREADS PER FED STD H28
MAIN DRAWING NO OR PART
MACHINED SURFACE ROUGHNESS 125
MATERIAL SEE L/M
FINISH -
NHA -
CAD NO -
XR NO LNG 2078 [illegible]

SIGNATURES		DAY MO YR
DRAWN	WMW	15JAN97
CHK	WMW	17JAN97
ENGR	WMW	28JAN97
RLSE		
MFR'G		
PART NO		
TYPE/TITLE		

ASE AERO SYSTEMS ENGINEERING, INC
356 EAST FILLMORE AVENUE ST PAUL MINNESOTA 55107 • USA

FLUIDYNE AEROTEST GROUP
13625 SCHMIDT LAKE RD PLYMOUTH MINNESOTA 55448 • USA



TEST CONFIGURATION
3C12C

REVISIONS					
ZONE	REV	DESCRIPTION	DATE	APPROVED	BLM
-	A	REVISED ITEM 3 PICTURE	14APR97	RLM	-

ITEM	QTY	PART NO	DESCRIPTION	SPECIFICATION
6	1	2078-411	TAIL CONE	CONFIG #3
5	1	2078-402	TAIL CONE ADAPTER	CONFIG #3
4	1	2078-404	CORE NOZZLE FORWARD SECTION - CONFIG. #2 & #3	
3	1	2078-422	CORE NOZZLE 9A	CONFIG #3
2	1	2078-805	CORE NOZZLE COVER RING CONFIG. #2 & #3	
1	1	2078-003	CONFIG. #7A	CHEVRON FAN NOZZLE

LIST OF MATERIALS

	SIGNATURE	DATE
DRAWN	WAW	14JAN97
CHK	WAW	16JAN97
ENGR	RLM	28JAN97
PROJ	-	-
SERV		
PART NO.	-	
TYPE/SIZE	-	

ASE AERO SYSTEMS ENGINEERING, INC.
330 EAST FULLMORE AVENUE, ST. PAUL, MINNESOTA 55107 • USA

FLUIDYNE AEROTEST GROUP
13123 20TH AVE. LANE NO. PLYMOUTH, MINNESOTA 55448 • USA

UNLESS OTHERWISE SPECIFIED DIMENSIONS ARE IN INCHES
TOLERANCES ARE
DECIMALS XXX ±.005 XX ±.010 X ±.030
FRACTIONS ±1/64
MACHINED ANGLES ±1/2°
THREADS PER FED STD H28
MACH. SURFACE ROUGHNESS 125

MATERIAL: SEE L/M
FINISH: -

CAGE NO -
JOB NO 696-2078-186932

CALLED SIZE TOLERANCE
0 - 125 DIA +.004 -.000
126 - 250 DIA +.005 -.000
251 - 500 DIA +.006 -.000
501 - 730 DIA +.008 -.000
731 - 1,000 DIA +.010 -.000

1. SEE DRAWING 2078-419 FOR ITEMS NOT CALLED OUT ON THIS DRAWING

NOTE:

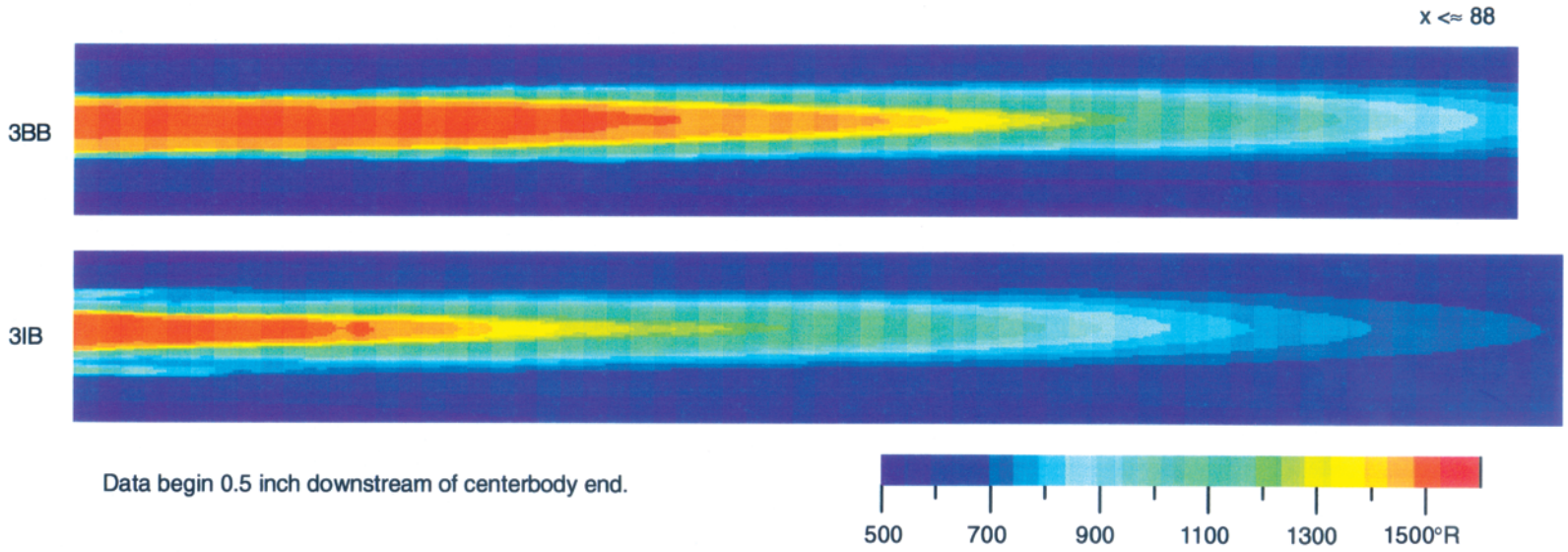


Figure 109. Total Temperature Profiles Along the Nozzle Centerline (3BB and 3IB)

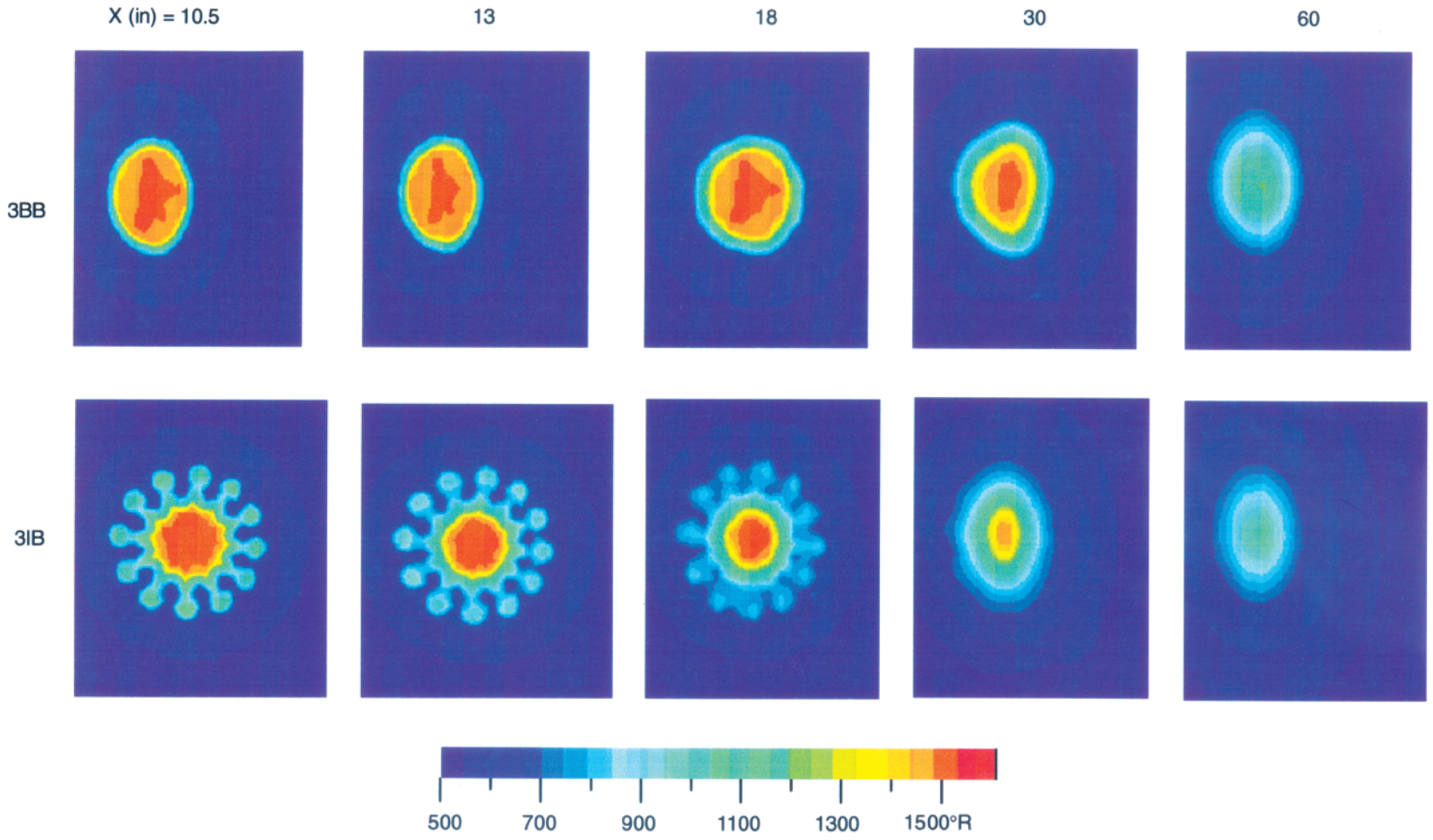


Figure 110. Total Temperature Plume Survey Axial Slices (3BB and 3IB)



Physics of Jet Noise in MGB Model:

Basic noise characteristics dependent on three physical processes involved in jet mixing:

- Noise Source Generation
- Noise Source Convective Amplification
- Noise Source Jet Shielding (refraction and shielding)

Far Field Noise ~ SI • CA • FS (per unit eddy volume)

where SI ~ Source Intensity Spectrum
CA ~ Convective Amplification Factor
FS ~ Fluid Shielding Factor

NASA/CP—2001-211152

Source Intensity Spectrum (SI):

$$dI(\omega) = \frac{\rho_0 \ell^3}{c_0^5 R^2} (u')^4 \omega^4 H(\mu) \cdot dV$$

where $\mu = \omega / \omega_0$ and $\omega_0 \approx \frac{dU}{dr}$

$\ell \approx u' / \omega_0$ and $u' = \sqrt{\tau / \rho}$

H(μ) = Fourier Transform of moving-frame, Space-Time Cross-correlation of u', involving various quadrupole types (x-x, x-y, y-y, etc.)

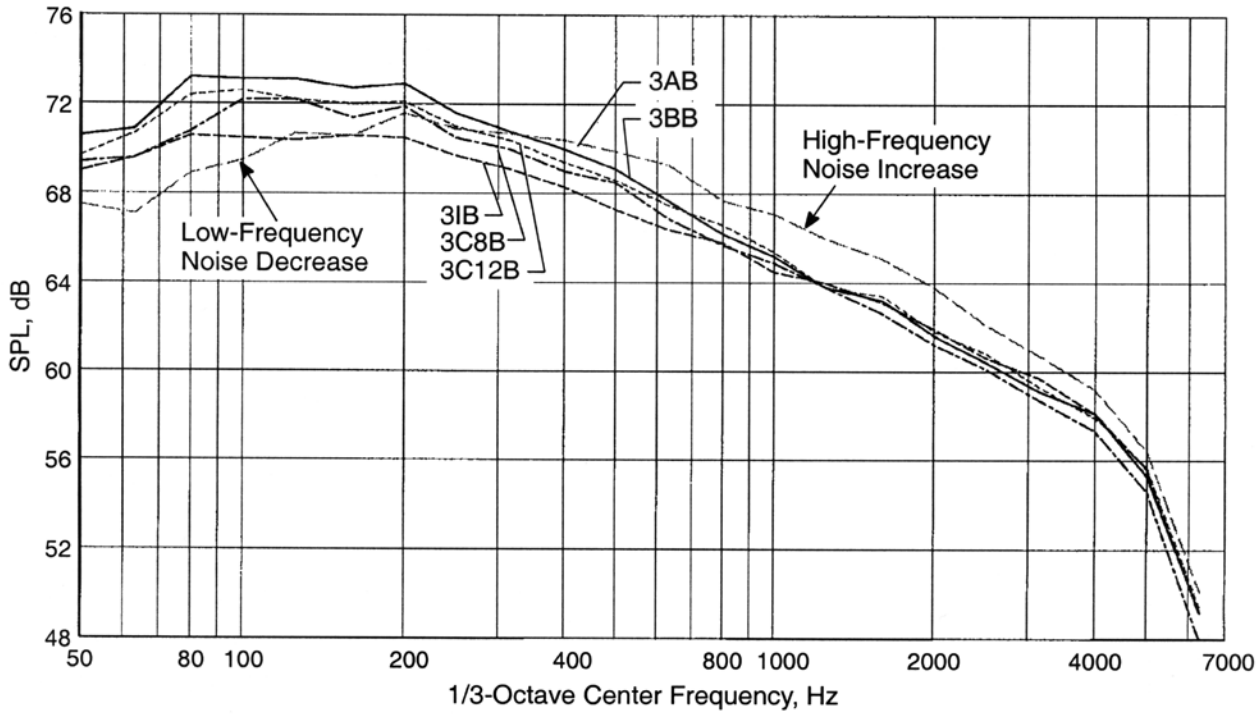


Figure 119. One-Third Octave Spectrum at 90° for Core Chevron Devices Without Fan Chevrons

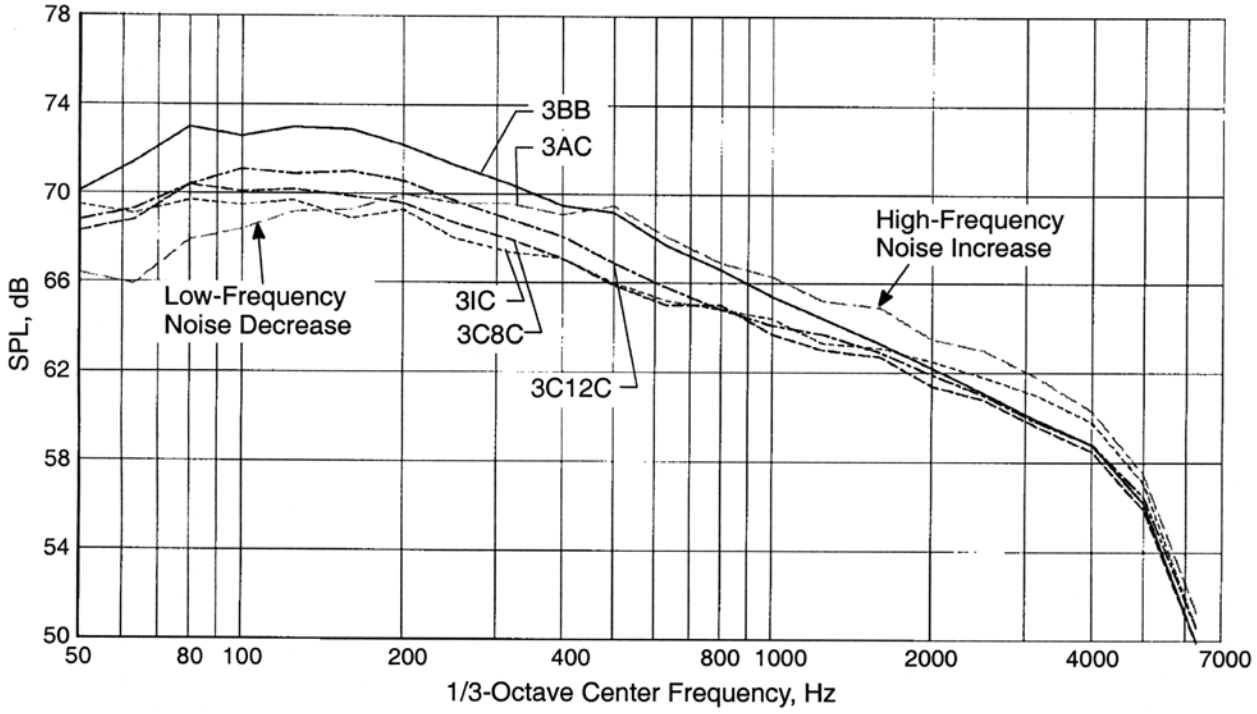


Figure 120. One-Third Octave Spectrum at 90° for Core Chevron Devices With Fan Chevrons

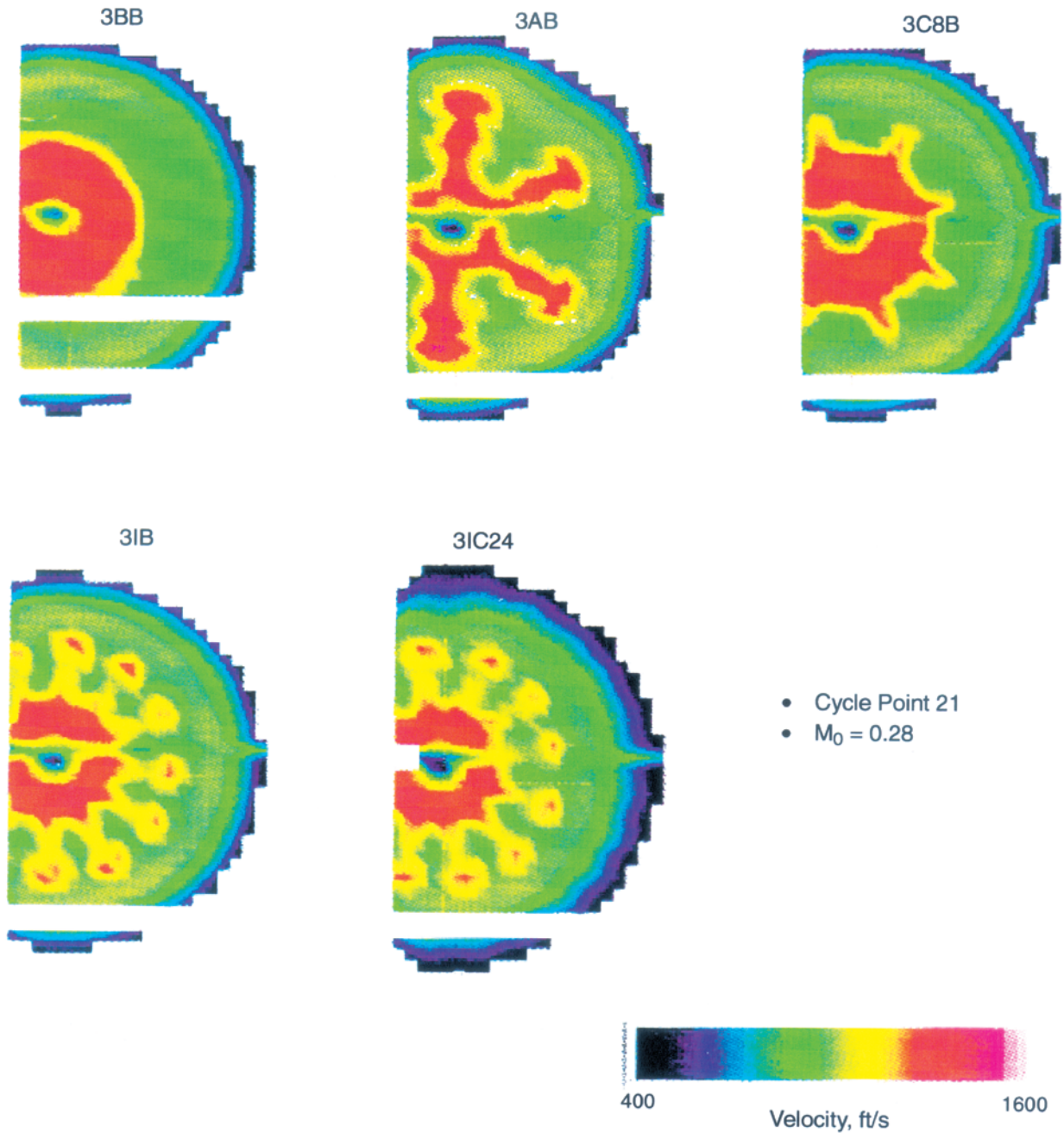


Figure 112. Mean Velocity Field Contours 10.5 Inches Downstream of Plug Tip

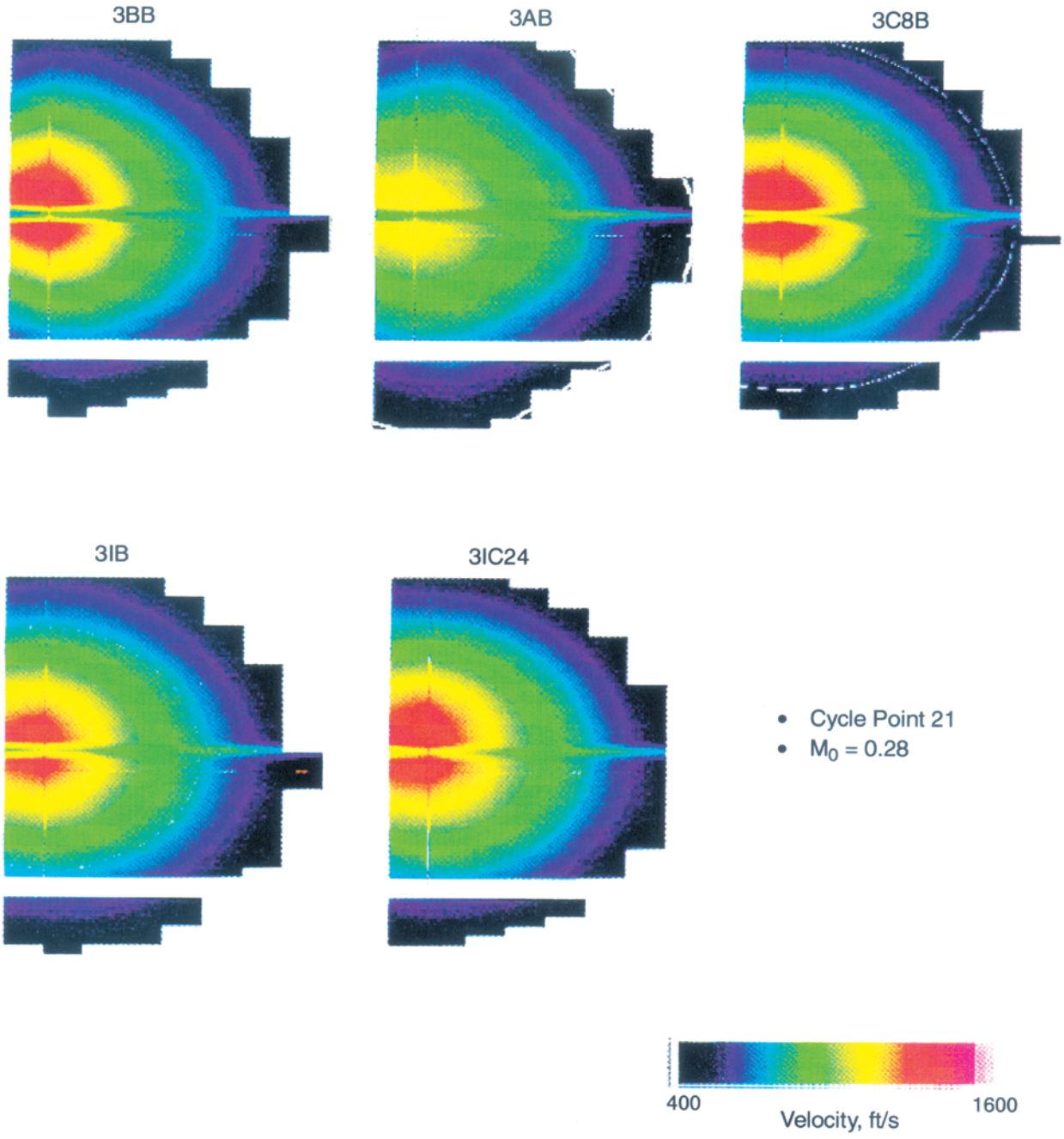


Figure 116. Mean Velocity Field Contours 60 Inches Downstream of Plug Tip

Convective Amplification Factor:

$$CA = \left[(1 - M_c \cos\theta)^2 + \alpha \cdot (u'/c_0)^2\right]^{n/2}$$

Where M_c = source eddy volume convection speed

For $M_c < 1$, *CA is approximated by*

$$CA \approx (\ 1 - M_c \cos\theta\ )^n$$

Exponent n depends on source Quadrupole type (x-x, x-y, y-y, etc.)

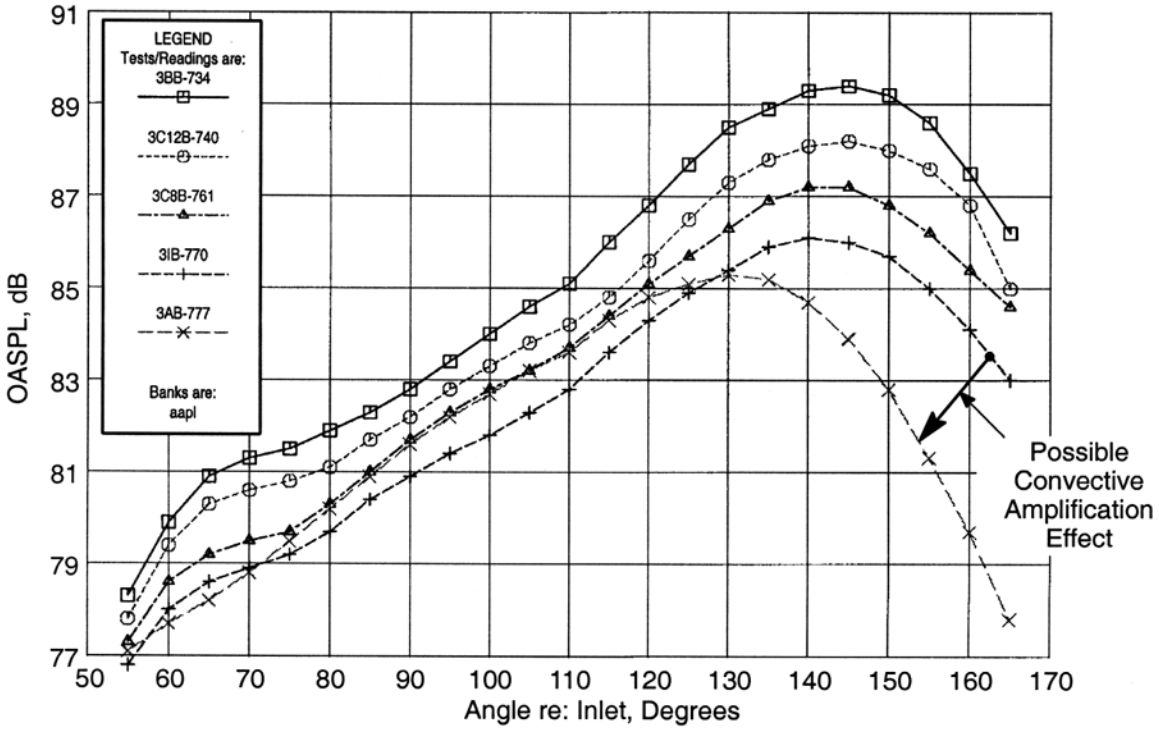


Figure 121. OASPL Directivity for Core Chevron Devices Without Fan Chevrons

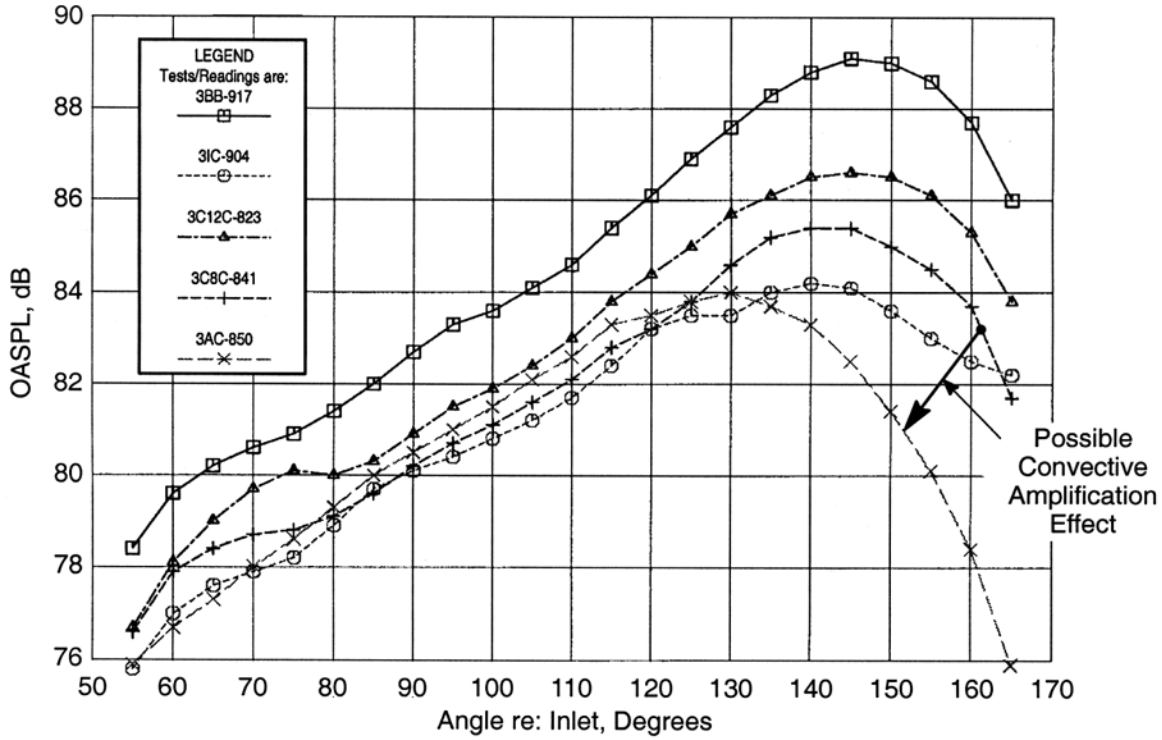


Figure 122. OASPL Directivity for Core Chevron Devices With Fan Chevrons

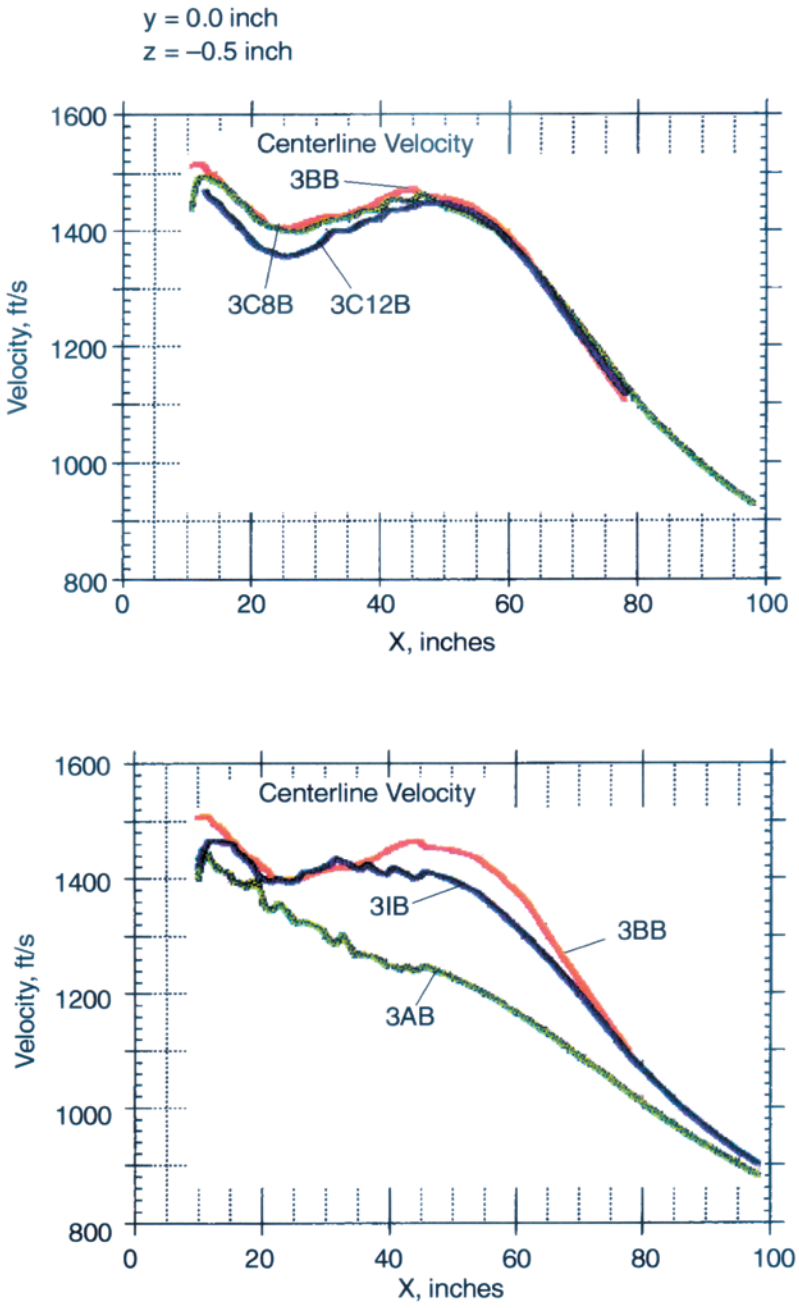
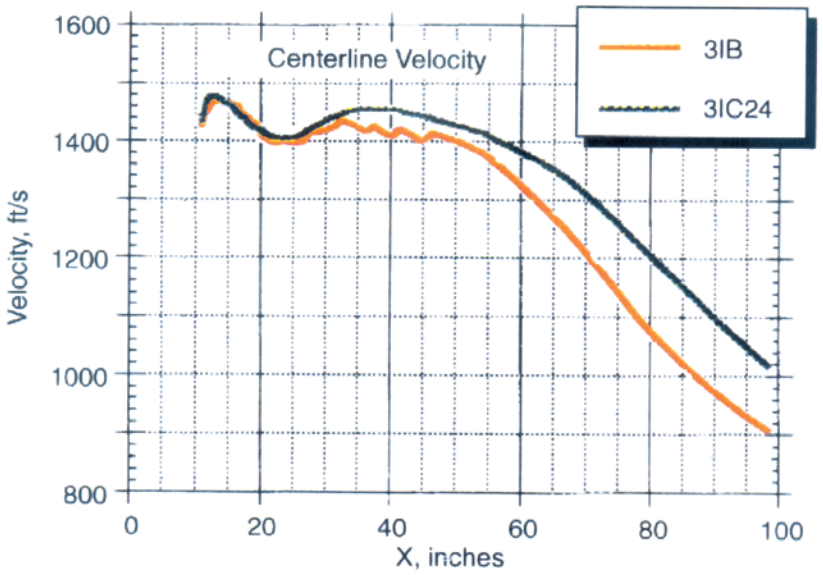


Figure 117. Velocity Profiles: Core Chevron Comparisons

y = 0.0 inch
z = –0.5 inch



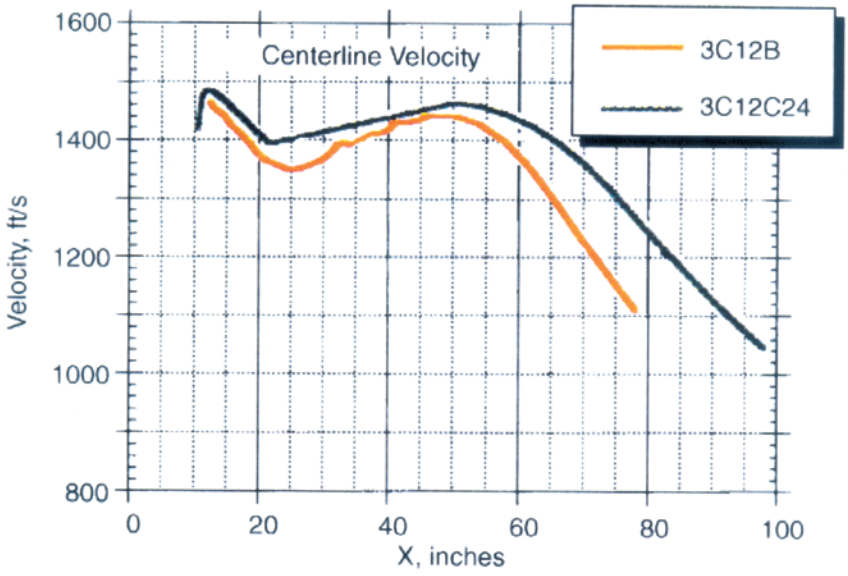


Figure 118. Velocity Profiles: Fan Chevron Comparisons



Fluid Shielding Factor:

- Refraction and shielding of imbedded sources by jet flow itself
- Increases with increasing frequency of source
- Increases with increasing emission angle toward jet axis
- Increases with increasing flow velocity gradients



Summary and Conclusions

- Fundamental mixing noise conceptual model in MGB is not inconsistent with experimental evidence for impact of chevrons on reducing jet mixing noise
- Notion of turbulent, convecting, quadrupole source distributions can qualitatively explain some observed effects
- Chevron nozzles reduce convective amplification through more rapid plume decay
- reduced far-downstream turbulence intensities produce reductions at low frequencies
- increased shear layer perimeter near nozzle exit causes increase in high-frequency noise
- No clear indication that fluid shielding is either increased or decreased

P. Gliebe Jet Noise References

1. Balsa, T.F., Gliebe, P.R., Kantola, R.A., Mani, R., Stringas, E.J., and Wang, J.C.F., "High Velocity Jet Noise Source Location and Reduction, Task 2 - Theoretical Development and Basic Experiments," FAA Report FAA-RD-76-79, II, 1978.

2. Gliebe, P.R., "High Velocity Jet Noise Source Location and Reduction, Task 2 Supplement - Computer Program for Calculating the Aeroacoustic Characteristics of Jets from Nozzles of Arbitrary Shape," FAA Report FAA-RD-76-79, IIa, 1977.

3. Balsa, T.F., and Gliebe, P.R., "Aerodynamics and Noise of Coaxial Jets," AIAA Journal, Vol. 15, 1977, pp. 1550-1558.

4. Gliebe, P.R., "Diagnostic Evaluation of Jet Noise Suppression Mechanisms," Journal of Aircraft, Vol. 17, 1980, pp. 837-842.

5. Janardan, B.A., Hoff, G.E., Barter, J.W., Martens, S., Gliebe, P.R., Mengle, V., and Dalton, W.N., "Separate-Flow Exhaust System Noise Reduction Concept Evaluation," NASA Contractor Final Report for NAS3-27720, Area of Interest 14.3, prepared for NASA Glenn Research Center, May 1998.

Vorticity Dynamics and its Relation to Jet Noise Reduction in Chevrons

Vinod G. Mengle
Rolls-Royce, Indianapolis

NASA/CP—2001-211152

655

A Note on

Vorticity Dynamics and its Relation to Jet Noise Reduction in Chevrons

Vinod G. Mengle

Rolls-Royce, Indianapolis

Presented at

NASA/OAI Jet Noise Workshop, Cleveland, OH

Nov. 7-9, 2000



Rolls-Royce

Motivation

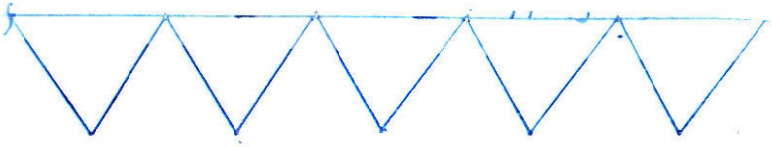
- Alternately flipped core chevrons (3AB) show distinctly different far-field noise signature than inwardly flipped core chevrons (3IB) (see Gliebe's presentation at this workshop or Janardan et al (1999)):
  - 3AB shows *increased* mid-to-high frequency sound than 3IB
  - 3AB shows *decreased* low frequency sound than 3IB
- What is the reason for this?
- Relationship of different flow patterns to sound?

Vorticity Dynamics ➔ Sound

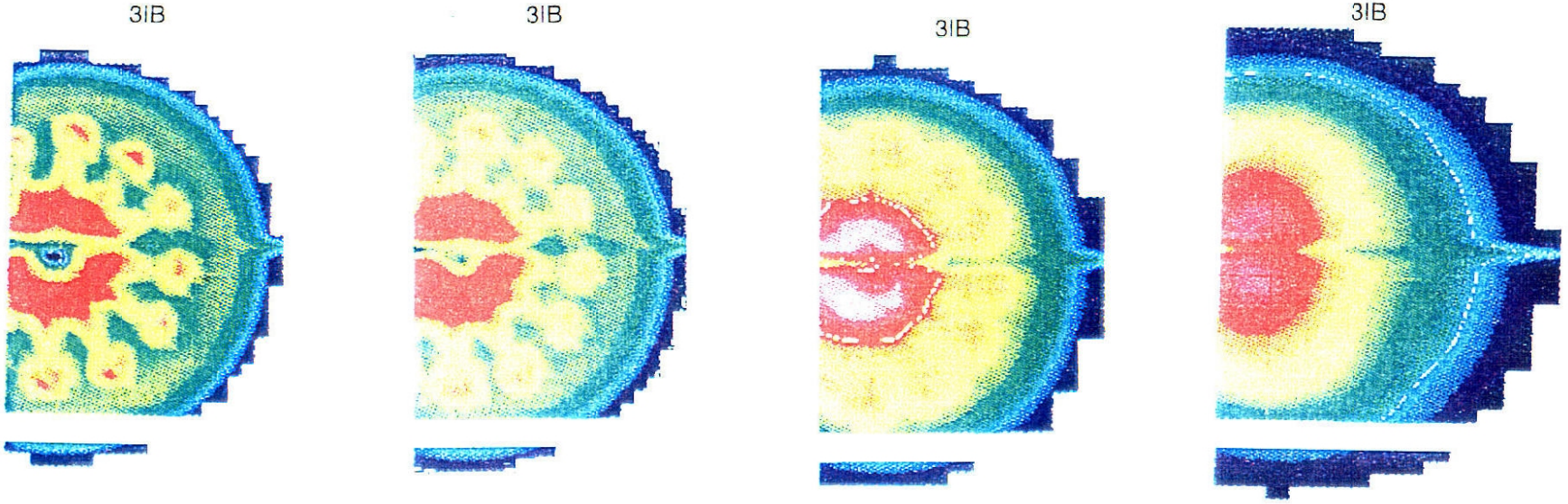
Rolls-Royce

12 Inwardly Flipping Core Chevrons

Bypass (b)
Core (c)



Mean Speed Contours (Red = 1600 ft/s (max); Violet = 400 ft/s (min))



X = 10.5 in.

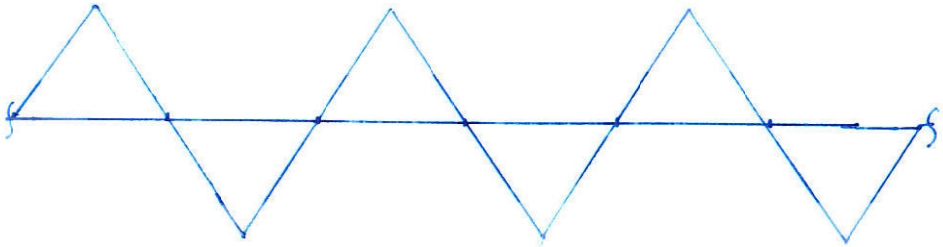
13.5 in.

18 in.

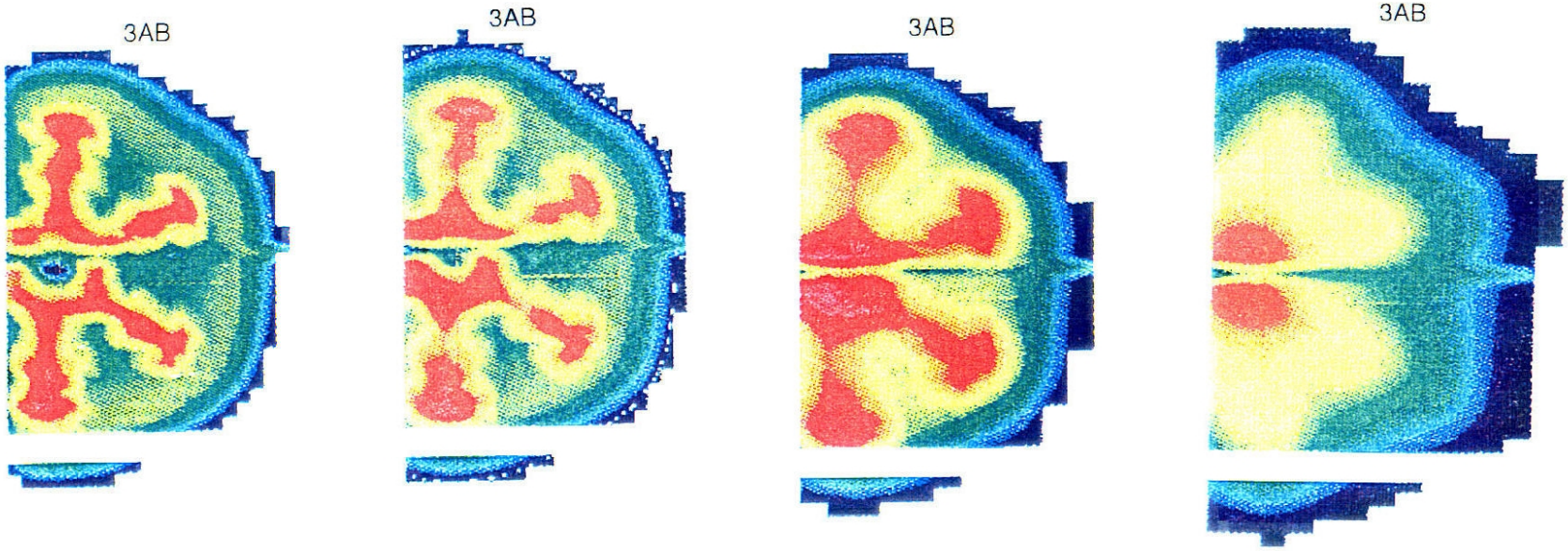
30 in.

Rolls-Royce

12 Alternately Flipping Core Chevrons



Mean Speed Contours (Red = 1600 ft/s (max); Violet = 400 ft/s (min))



X = 10.5 in. 13.5 in. 18 in. 30 in.

Rolls-Royce

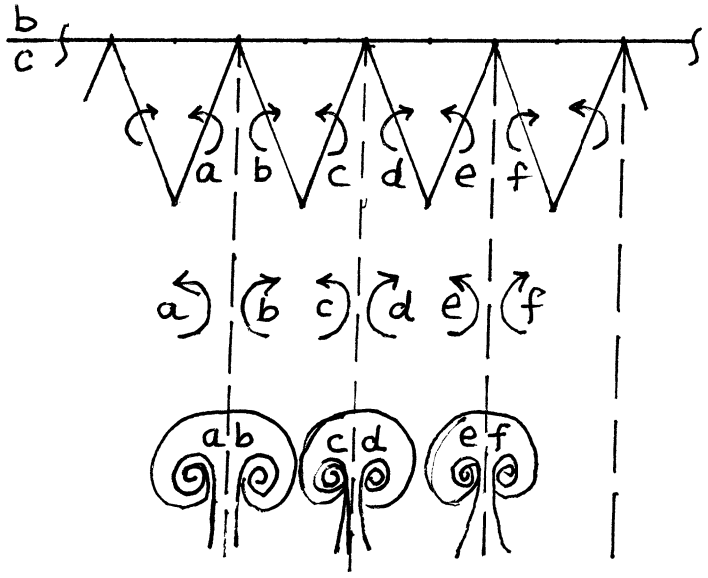
Observation from Plume Data

- Alternately flipped chevrons (3AB)
  - have half as many "vortex-mushrooms" as those for inwardly flipped chevrons (3IB) and which are also bigger
  - do not appear to mix azimuthally as well as 3IB in the region close to the nozzle exit (there are higher high-speed hot-spots in the outer periphery in 3AB)
  - has smaller high-speed hot-spot core region than 3IB
  - has faster near-field centerline velocity decay (not shown here but see Janardan et al, fig. 117)

- Due to the first observation, we cannot conclude that the shear perimeter between bypass and core flows in 3AB is higher than 3IB and hence it leads to the observed noise differences, as was done by Gliebe

  ➔ **Need to closely examine why 3AB has half as many vortex mushrooms as 3IB**

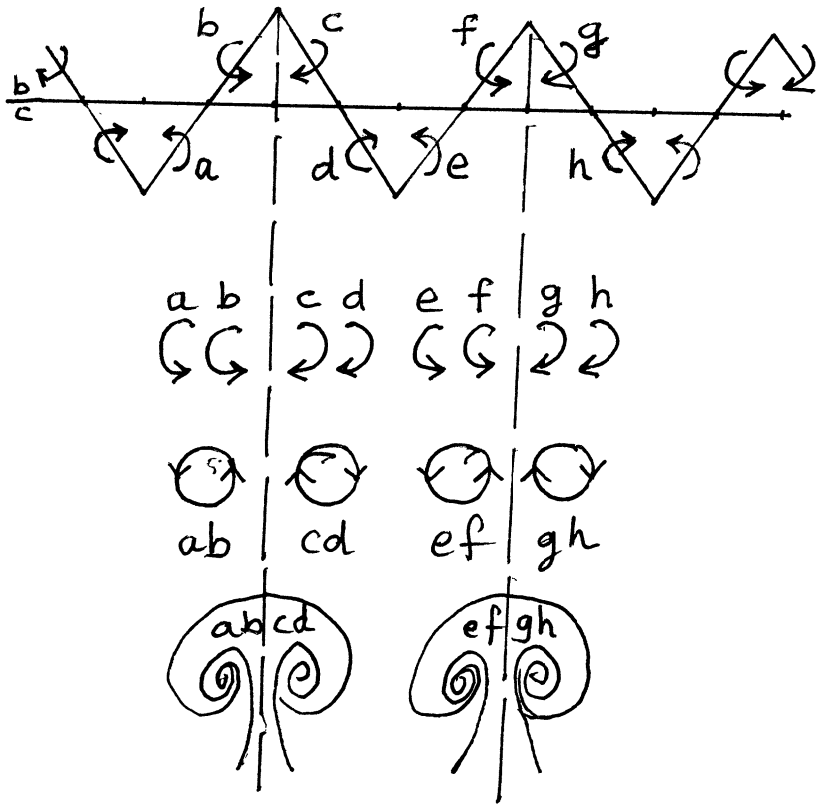
Inwardly Flipped Chevrons



- Trailing-edge vortex directions on each chevron are governed by the sense of flow from higher pressure region to lower pressure region as shown
- Vortices from adjacent edges of adjacent chevrons have *opposite* signs (e.g., *a* and *b*)
- When chevrons are placed very close to each other the vortices from adjacent edges of adjacent chevrons (*a* and *b*) influence each other more than those from the same chevron (*b* and *c*)
- Thus *a* and *b* form a vortex mushroom pair, and so do *c* and *d*
- **Hence, # Vortex Mushrooms = # Chevrons in 3IB**

Rolls-Royce

Alternately Flipped Chevrons



- Vortices from adjacent edges of adjacent chevrons have *same* signs (e.g., *a* and *b*)
- Vortices with same signs which are closer to each other at birth **merge** and become bigger and stronger

  $a + b \rightarrow ab;\ \ c + d \rightarrow cd$
- *ab* and *cd* have opposite signs and can form a vortex-mushroom as shown
- The reason why *ab* and *cd* form a pair, as observed, rather than *cd* and *ef* may have to do with the inherent unsymmetry in the flow (core is *faster* than bypass and *cylindrical* geometry)
- Thus **vortex merging** and unsymmetry imply:

  # Vortex-Mushrooms = 1/2 # Chevrons,

  bigger vortex-mushrooms
- Bigger and fewer vortices in 3AB dissipate slower than in 3IB delaying the axial decay in 3AB of (i) axial circulation (as observed by Yu et al) and (ii) hot-spots, which can possibly lead to increased high frequency sound
- This vortex structure in 3AB possibly also induces more flow out from the hot core flow region, reducing it in size and accelerating the decay of center-line velocity which leads to reduced low frequency

Rolls-Royce

Extensions

- The vorticity argument given before can also be extended to explain observed differences in noise due to ratio of number of fan chevrons to core chevrons (e.g., odd versus even ratio), as well as, extrapolation to relative “clocking” effect between fan and core chevrons

References

- Janardan, B.A., Hoff, G.E., Barter, J.W., Martens, S., Gliebe, P.R., Mengle, V., Dalton, W.N. (1998): Separate-Flow Exhaust System Noise Reduction Concept Evaluation. Final Report: NAS3-27720, Area of Interest 14.3. GE Report No. R98AEB152. NASA CR (to be numbered)
- Yu, S.C.M., Koh, P.K. (2001): An Experimental Investigation of Two-Stream Mixing Flow with Multiple Tabs. (to appear in AIAA J.)

V. G. Mengle References

1. Mengle, V. G., Shin, H-W., Askew, J., Whitfield, C.E. (1992): *Aero-Performance and Aero-Mixing Tests of 2D-CD Mixer/Ejector Nozzles. Part II. Sample of Aero-Mixing Test Data & Inferences.* Paper No. 1, 1st NASA/Industry High Speed Research Program Nozzle Symposium, NASA CP (to be numbered), pp. 3-23 to 3-35, Nov. 17-19, 1992.

2. Mengle, V. G., Shin, H-W., Whitfield, C. E., Wisler, S., Askew, J. (1992*): Acoustic and Aero-Mixing Tests of Fluid-Shield Nozzles. Part II - 2D Fluid-Shield Nozzle Aero-Mixing Tests.* Paper No. 2, 1st NASA/Industry High Speed Research Program Nozzle Symposium, NASA CP (to be numbered), pp. 4-21 to 4-28, Nov. 17-19, 1992.

3. Salikuddin, M., Brausch, J., Mengle, V. (1992): *Acoustic and Aero-Mixing Tests of Fluid-Shield Nozzles. Part I -Acoustics.* Paper No. 2, 1st NASA/Industry High Speed Research Program Nozzle Symposium, NASA CP (to be numbered), pp. 4-1 to 4-19, Nov. 17-19, 1992.

4. Mengle, V. G. (1995*): Acoustic Duct Waveguide Modes Excited by an Axially Convecting Noise Source in Sheared Flow*. 1st NASA Advanced Subsonic Technology Engine Noise Workshop Proceedings, Session 2: Jet Noise, pp. 269-284, Dec. 12-14, 1995.

5. Mengle, V. G., Dalton, W. N., Bridges, J., Boyd, K. (1997): *Noise Reduction with Lobed Mixers - Nozzle Length and Free-Jet Speed Effects.* AIAA Paper No. 97-1682. 18th AIAA Aeroacoustics Conference, May 10-14, 1997.

6. Mengle, V. G. (1997): *Certain Limitations and Extensions of MGB Jet Noise Computer Code.* NASA Advanced Subsonic Technology "MGB Jet Noise Prediction Workshop" Proceedings, Sept. 9, 1997.

7. Janardan, B.A., Hoff, G.E., Barter, J.W., Martens, Gliebe, P. R., Mengle, V. and Dalton, W.N. (1998*): Separate-Flow Exhaust System Noise Reduction Concept Evaluation.* Final Report, NASA Contract NAS3-27720, GE Report No. R98AEB152, May 1998. NASA CR (to be numbered).

8. Mengle, V. G., Dalton, W. N.(1998): *Lobed Mixer Design for Noise Suppression. Vol. 1 - Acoustic and Aerodynamic Test Data Analysis.* Final Report, NASA Contract NAS3-27394, Task Order No. 6, Rolls-Royce EDR No. 18580, July 1, 1998, NASA CR (to be numbered), 298 p.

9. Mengle, V. G., Baker, V. D., Dalton, W. N. (1998): *Lobed Mixer Design for Noise Suppression. Vol. 2 - Plume, Aerodynamic & Acoustic Data.* Final Report, NASA Contract NAS3-27394, Task Order No. 6, Rolls-Royce EDR No. 18581, July 1, 1998. NASA CR (to be numbered), 629 p.

10. Mengle, V. G. (1999): *Jet Noise Reduction by Lobed Mixers with Boomerang Scallops*. AIAA Paper No. 99-1923, 5th AIAA/CEAS Aeroacoustics Conf., May 10-12, 1999.

11. Mengle, V. G. (1999): *Anomalous Effect of Nozzle Length Reduction on Jet Noise of Forced Mixers*. AIAA Paper No. 99-1968, 5th AIAA/CEAS Aeroacoustics Conf., May 10-12, 1999.

12. Mengle, V. G. (1999): *Finding Excess Noise in Internally-Mixed Jets by Varying Free-Jet Speed*. AIAA Paper No. 99-1967, 5th AIAA/CEAS Aeroacoustics Conf., May 10-12, 1999.

13. Mengle, V. G. (2000): *Optimization of Lobe Mixer Geometry and Nozzle Length for Minimum Jet Noise*. AIAA Paper No. 2000-1963, 6th AIAA/CEAS Aeroacoustics Conf., June 12-14, 2000.

14. Mengle, V. G. (2000): *Finding Internal Excess Jet Noise Source Characteristics by Varying Free-Jet Speed*. NASA/OAI Jet Noise Workshop, November 7-9, 2000, NASA CP (to be numbered).

15. Mengle, V. G. (2000): *Vorticity Dynamics and Its Relation to Jet Noise Reduction in Chevrons*. NASA/OAI Jet Noise Workshop, November 7-9, 2000, NASA CP (to be numbered).

16. Mengle, V. G. (2000): *Anomalous Effect of Nozzle Length Reduction on Jet Noise of Forced Mixers*. NASA/OAI Jet Noise Workshop, November 7-9, 2000, NASA CP (to be numbered).

17. Mengle, V. G. (2001): *Tongue Mixer - A New Concept for Jet Noise Reduction*. (Submitted for presentation at the 7th AIAA/CEAS Aeroacoustics Conf., May 28-30, 2001).

18. Mengle, V. G. (2001): *Duct Waveguide Mode Excitation by Sound Sources Convecting in Sheared Flows*. (Submitted for presentation at the 7th AIAA/CEAS Aeroacoustics Conf., May 28-30, 2001).

Prediction of Jet Noise with Suppression Devices

Thonse R. S. Bhat
Boeing Commercial
Airplane Group

Prediction of Jet Noise with Suppression Devices **- Thonse R.S. Bhat, Boeing Commercial Airplane Group as summarized by Mary Jo Long-Davis**.

Dr. Bhat presented an overview of the various prediction models used by Boeing. Bhat explained that the current suite of prediction tools has issues and limitations. Boeing's in-house, semi-empirical model for subsonic problems assumes three different noise source regions: 1) primary-secondary shear layer, 2) secondary-ambient shear-layer, and 3) mixed-ambient shear-layer. The sound pressure level is a function of the source strength, Strouhal number, velocity, mass flow, frequency, emission angle, and area ratio. Boeing's in-house, semi-empirical model for supersonic problems (JN8C5 code) assumes four different noise sources: 1) primary internal, 2) primary external, 3) mixed, and 4) shock-associated. The comparison between the model prediction and the test data indicated good agreement.

In summary, the Boeing models are semi-empirical and are developed mainly from model-scale test databases. As such, the models' applicability is limited to the envelope defined by the test database—deviating too far from that envelope may lead to erroneous predictions. Dr. Bhat emphasized the need for a tool that can be used to predict noise from mixers for realistic geometries and flow conditions.

NASA/CP—2001-211152

Prediction of Jet Noise with Suppression Devices

NOISE ENGINEERING TECHNOLOGY
Boeing Commercial Airplane Group

Thonse R. S. Bhat

Jet Noise Workshop
Ohio Aerospace Institute
Cleveland, OH

November 7-9, 2000

BOEING®

Outline

- Different prediction models
- Description of in-house models
- Comparisons with data
- Concluding remarks

Prediction models

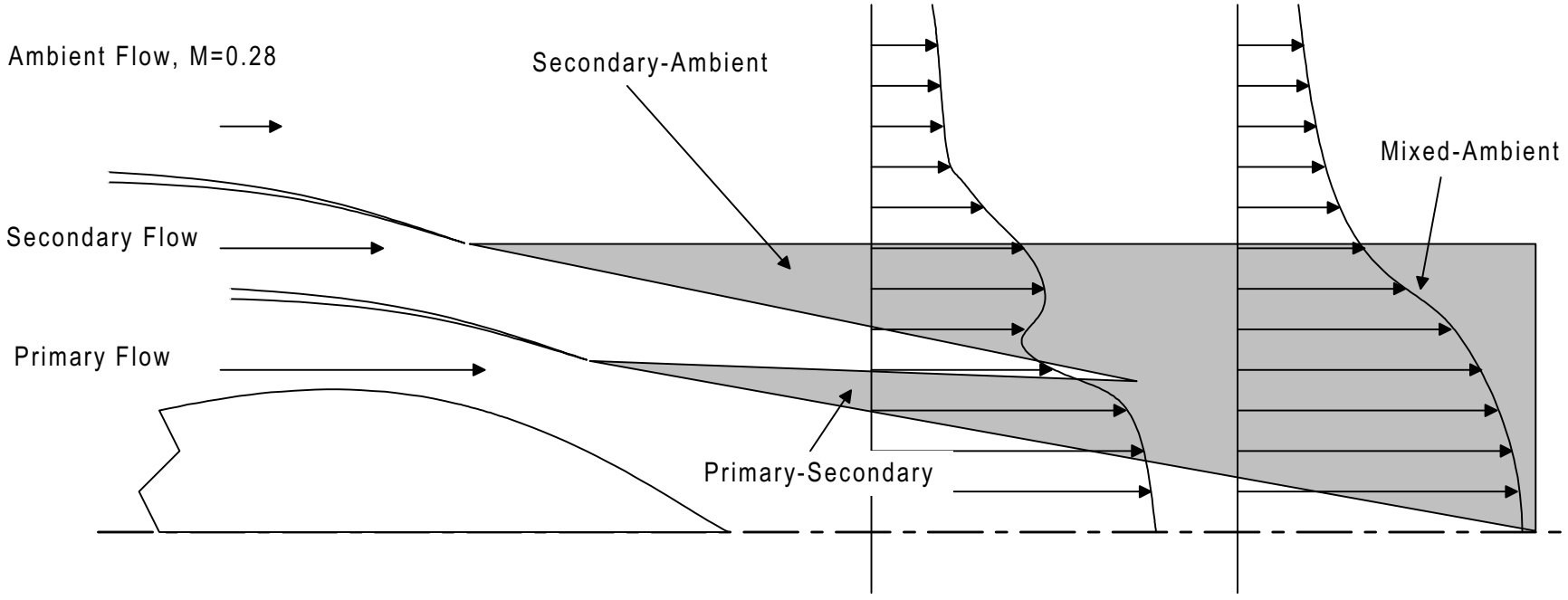
- DNS - not practical for problems of interest
- LES - may be feasible
- Tam's models - can be extended for mixers
- MGB model - can also be extended for mixers
- In-house models (Ref: An Empirical Model for Prediction of Coaxial Jet Noise in Ambient Flow, H. Y. Lu, AIAA Paper No. 86-1912)

Jet Noise Prediction Model

- Co-axial jet divided into three noise source regions
  - Primary-secondary shear layer
  - Secondary-ambient shear layer
  - Mixed-ambient shear layer
- Each region has its own noise characteristics and source distribution
- Model predicts the 1/3 octave band SPL for each component
- Total jet SPL = $10 \log (10^{0.1SPLp} + 10^{0.1SPLs} + 10^{0.1SPLm})$

BOEING®

Jet Noise Source Model

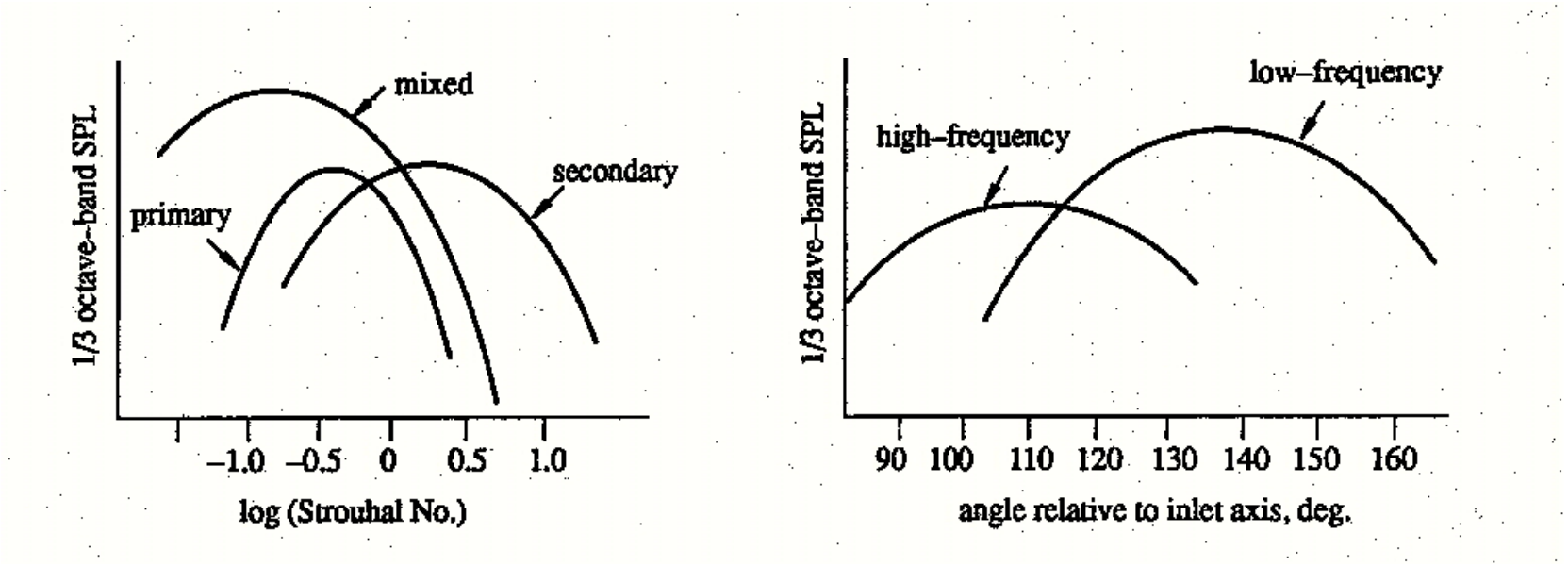


BOEING®

Jet Noise Prediction Model

- Empirical expressions for each component of jet noise are categorized into three parts:
  - SPL associated with the shear layer velocity difference, turbulent eddy convection velocity and ambient flow effects
  - normalization factors associated with pressure, density, spherical divergence, geometric and acoustic near-field effects
  - effects of internal acoustic excitation

Jet Noise Component Spectra



Jet Noise Component Formula

- $SPL = [Z1 \log (FV) + Z2][\log (S) - Z3 \log(FV) - Z4]^2 + Z5 \log(FV) + Z6$

  - FV -- Source strength function = f (vel. comp.)
  - S -- Strouhal number
  - Z1 to Z6 -- Coefficients = f (velocity, mass flow, frequency, emission angle and area ratio)

BOEING®

Inputs to the Prediction Model

- Primary flow: velocity, temperature, mass flow, area
- Secondary flow: velocity, temperature, mass flow, area
- Mixed (merged) flow: velocity, temperature, mass flow, area -- All computed
- No details of the mixers (lobe length, penetration, etc.) are taken into account

Mixer-Ejector Noise Prediction Model

- Empirical model predicts the 1/3 octave band levels of a jet from a rectangular mixer-ejector nozzle
- The SPLs for the following observer points are predicted:
  - in-flight jet noise on airplane-fixed or wind tunnel-fixed coordinates
  - flyby jet noise on ground-fixed coordinates
  - static jet noise (special case with ambient velocity zero)
  - jet noise on the fuselage including boundary layer effect

Mixer-Ejector Noise Prediction Model

- SPLs for the following components are predicted:
  - primary internal jet noise generated by the mixing of primary & entrained streams
  - primary external jet noise generated by the continued mixing of the streams and initial mixing with the freestream
  - mixed jet noise generated by the merged jet and its mixing with the ambient flow
  - shock-associated noise generated y
    - the supersonic primary jet
    - the supersonic mixed jet

Inputs to the Mixer-Ejector Noise Prediction Model

- Configuration input:
  - nozzle areas, number of lobes, lobe penetration, ejector equivalent diameter, ejector length, aspect ratio, installation angle, etc.
- Gas condition input:
  - Velocities, temperatures and mass flows for primary & secondary streams
  - Pressure, temperature, etc. for the ambient flow
- Formulate coefficients, normalization terms, source locations, etc. to calculate SPLs.

Concluding Remarks

- Models are semi-empirical and are developed, mainly, from model-scale test databases
- Models applicability limited to test database ranges
- Need a tool which can be used to predict noise from mixers of various types for realistic geometries and flow conditions

BOEING®

T. Bhat Reference

1. An Empirical Model for Prediction of Coaxial jet Noise in Ambient Flow, H. Y. Lu, Boeing Commercial Airplane Group, AIAA-86-1912, AIAA 10th Aeroacoustics Conference, July 9-11, 1986, Seattle, WA.

Physics of

Jet Noise

Suppression

Andrew Kempton
Rolls-Royce

Physics of Jet Noise Suppression **- Andrew Kempton, Rolls-Royce as summarized by Mary Jo Long-Davis.**

Dr. Kempton reviewed that successful suppression devices for high-bypass-ratio engines rely on reducing the peak jet velocity while avoiding additional high-frequency penalties. Methods of reducing peak jet velocity include increased fan diameter, internal mixing (lobed mixers), and external mixing (nozzle serrations, chevrons). Kempton's presentation concentrated on forced mixers to realize the potential jet noise benefit due to internal mixing. Although the enhanced mixing reduces low frequency noise, it could increase the high frequency noise (and the benefit is lost). Kempton indicated that, by careful design practice, Rolls-Royce is able eliminate any high frequency noise penalty.

Results were presented from model scale testing and flight testing of forced mixers and annular mixers. Kempton emphasized that model scale testing is crucial for 3 reasons:

1. Controlled environment (avoids weather problems)
2. Avoid other engine noise sources
3. Can simulate flight much better/more controlled

How theory helps in understanding jet noise was discussed. Rolls-Royce's in-house, semi empirical model assumes four noise source regions: 1) secondary-ambient shear layer, 2) primary-ambient shear layer, 3) mixed ambient shear layer, and 4) primary-secondary shear layer. Using this semi-empirical, single-stream source model with truncated spectra achieved reasonable agreement between the prediction and the data over the entire frequency range.

Physics of Jet Noise Suppression

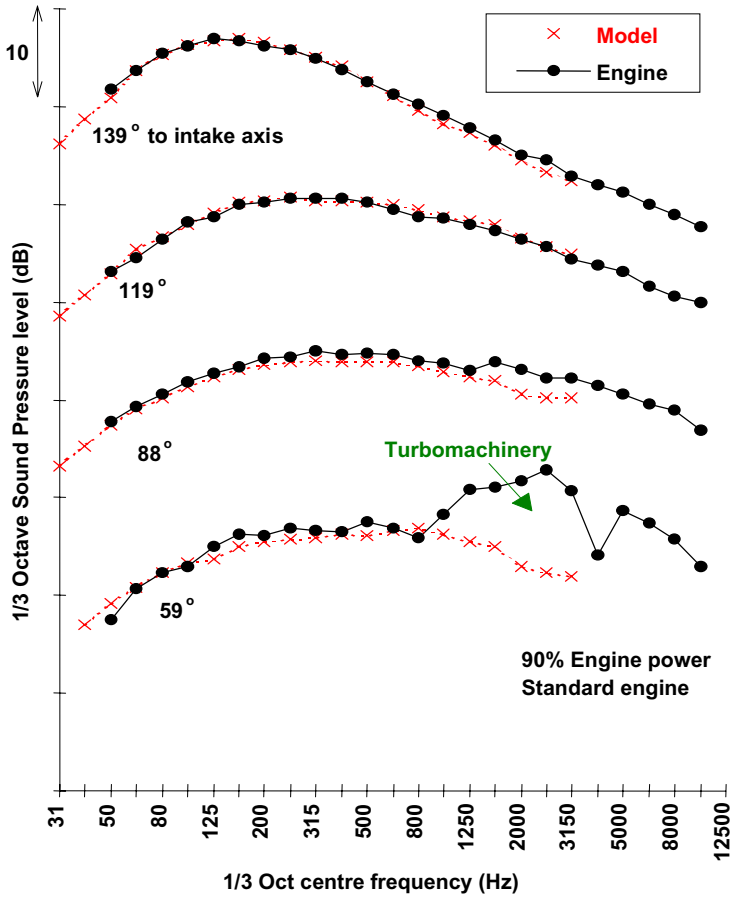
Introduction

Successful suppression devices for high-bypass-ratio engines rely on reducing peak jet velocity whilst avoiding additional high-frequency noise (which might not reduce in flight)

Methods of reducing peak jet velocity include:

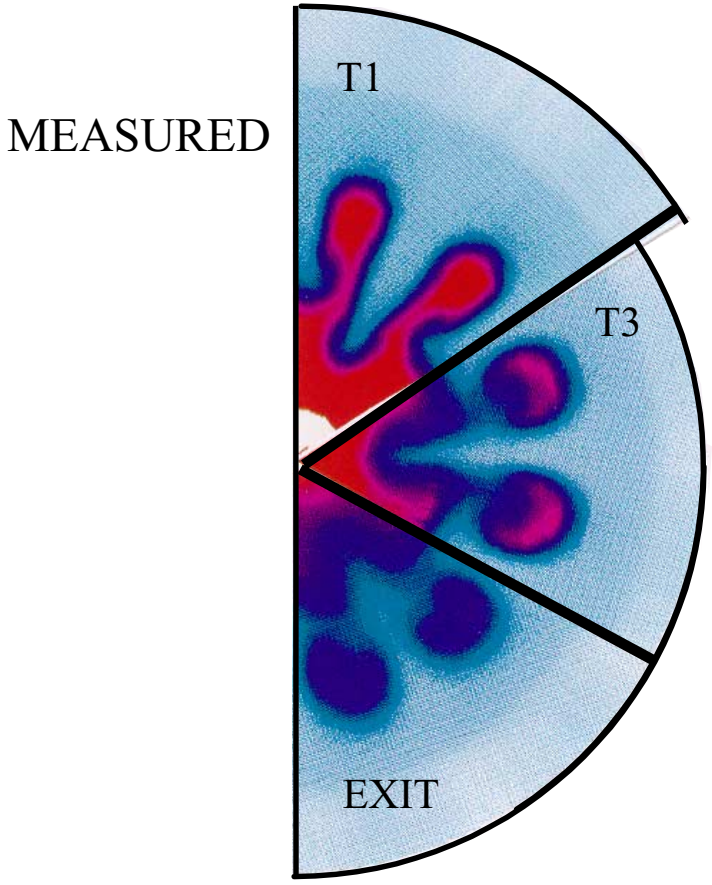
- Increased fan diameter
- Internal mixing (e.g. lobed mixer)
- External mixing (e.g. nozzle serrations)

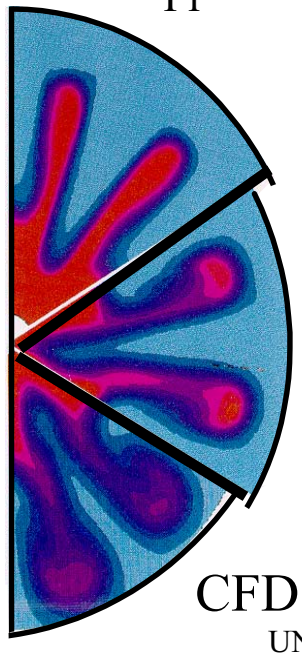
Model-scale Testing

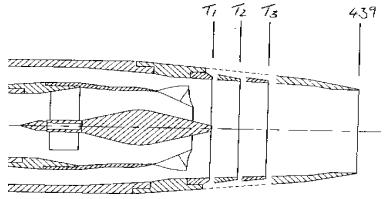


Physics of Jet Noise Suppression

Realising the Potential Jet Noise Benefit due to Internal Mixing



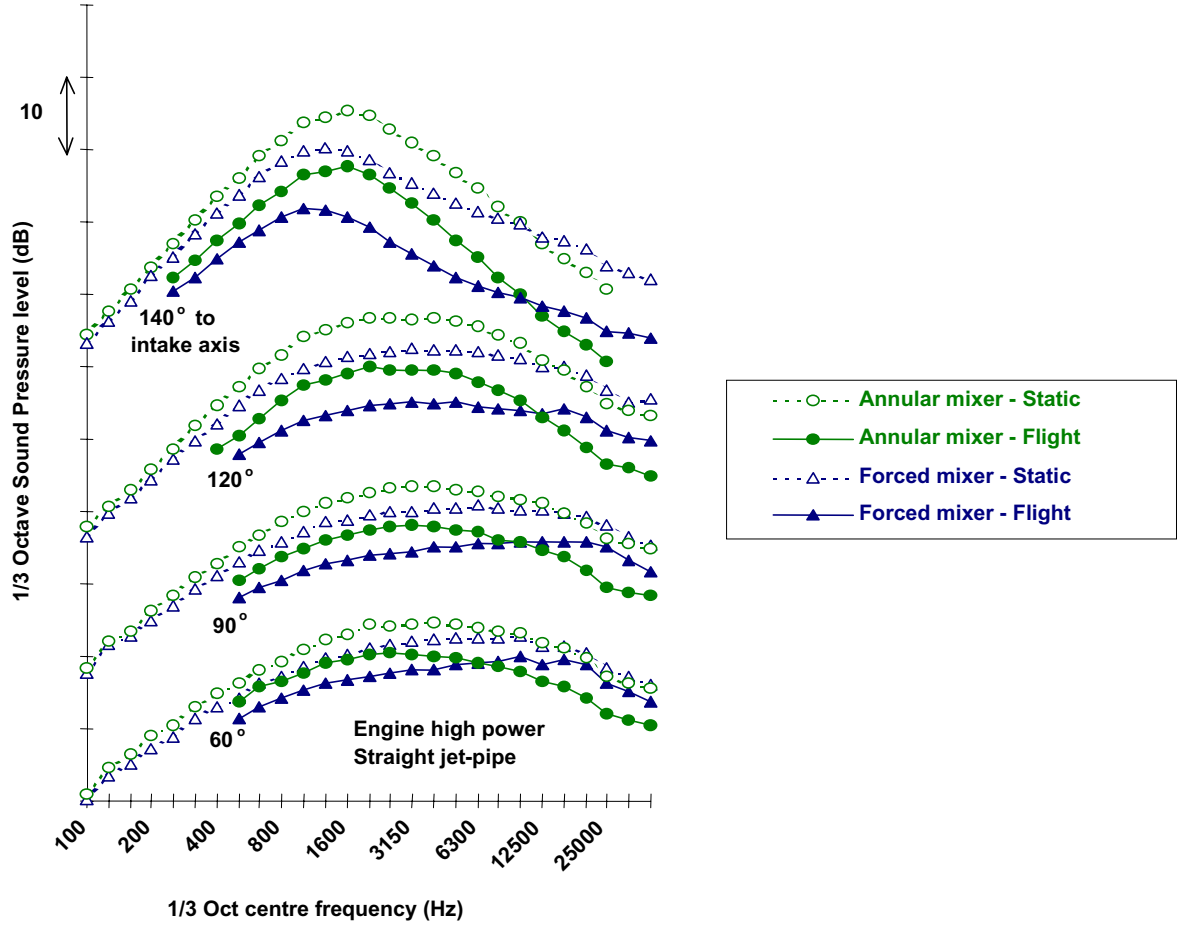




CFD PREDICTION
UNSTRUCTURED GRID

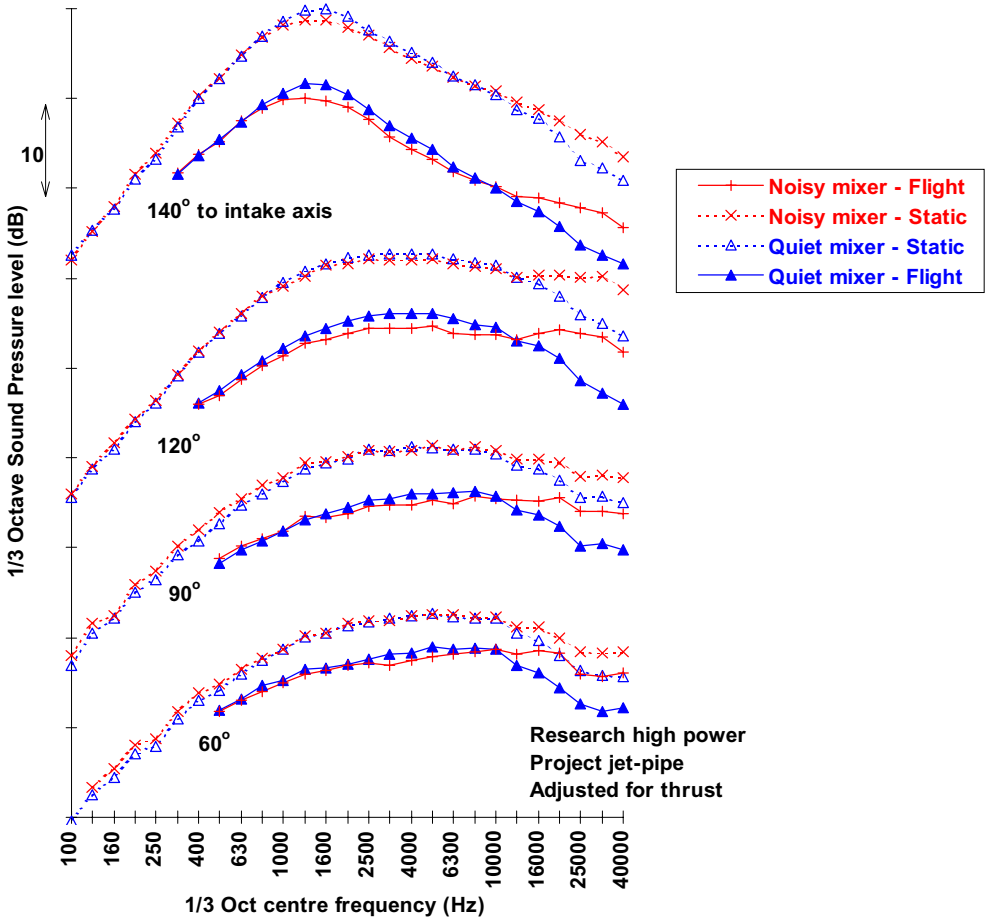
Physics of Jet Noise Suppression

Realising the Potential Jet Noise Benefit due to Internal Mixing



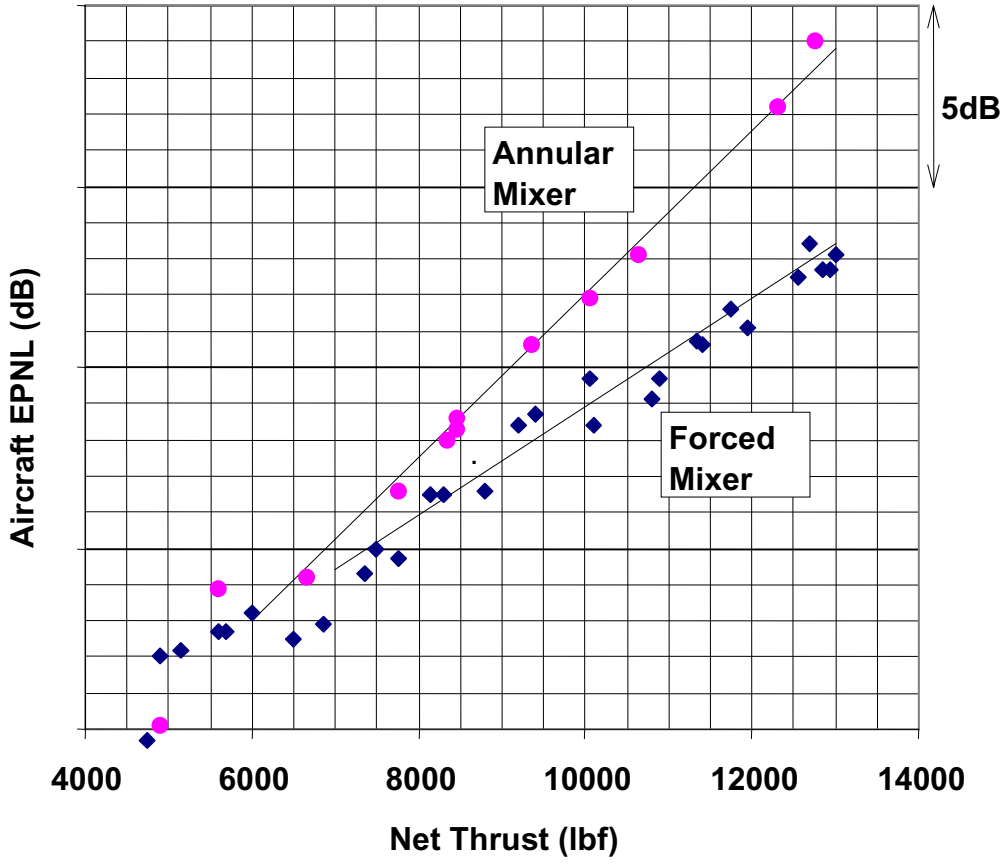
Physics of Jet Noise Suppression

Realising the Potential Jet Noise Benefit due to Internal Mixing



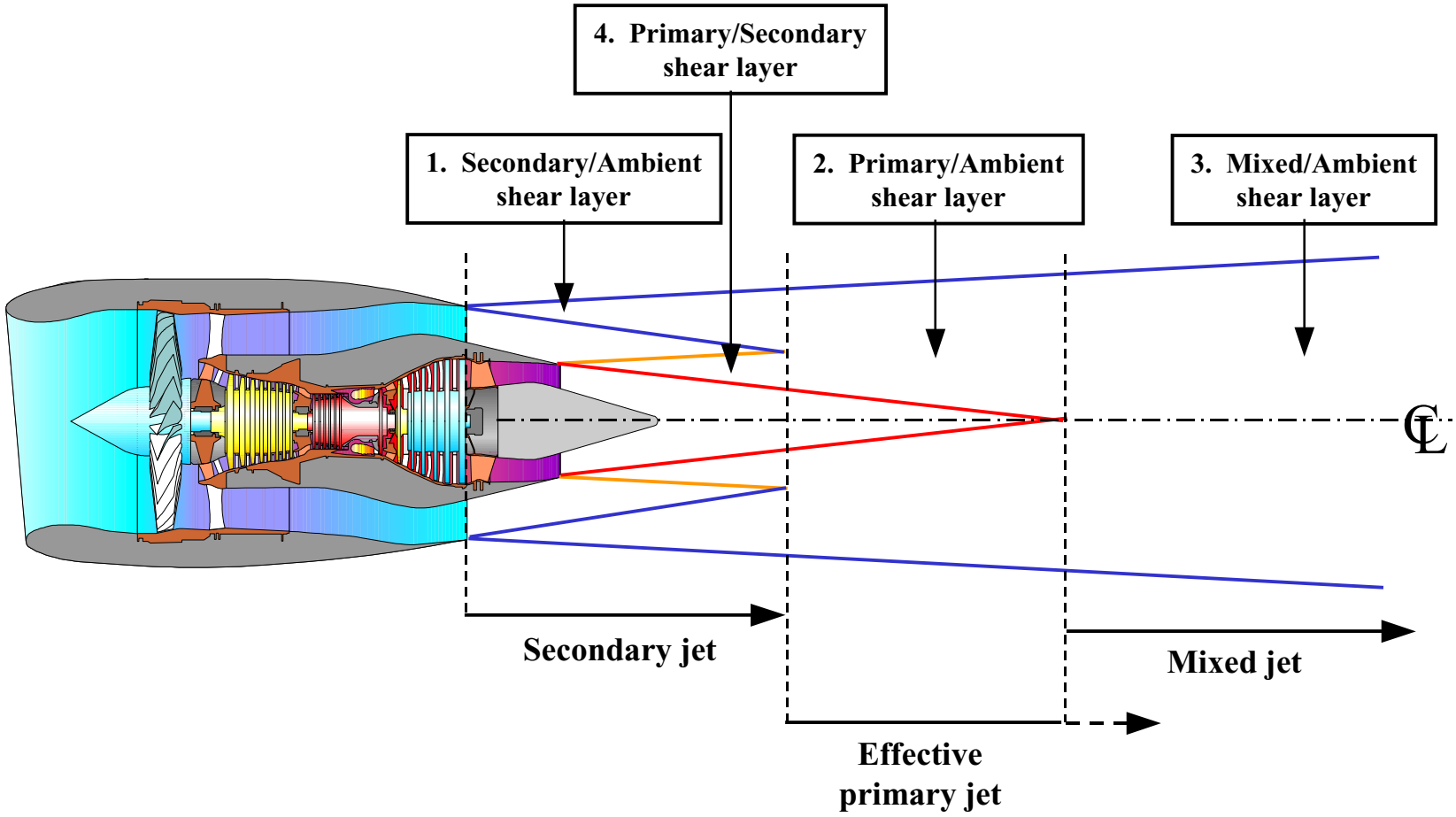
Physics of Jet Noise Suppression

Fokker F100/Tay 650 measurements from Granada



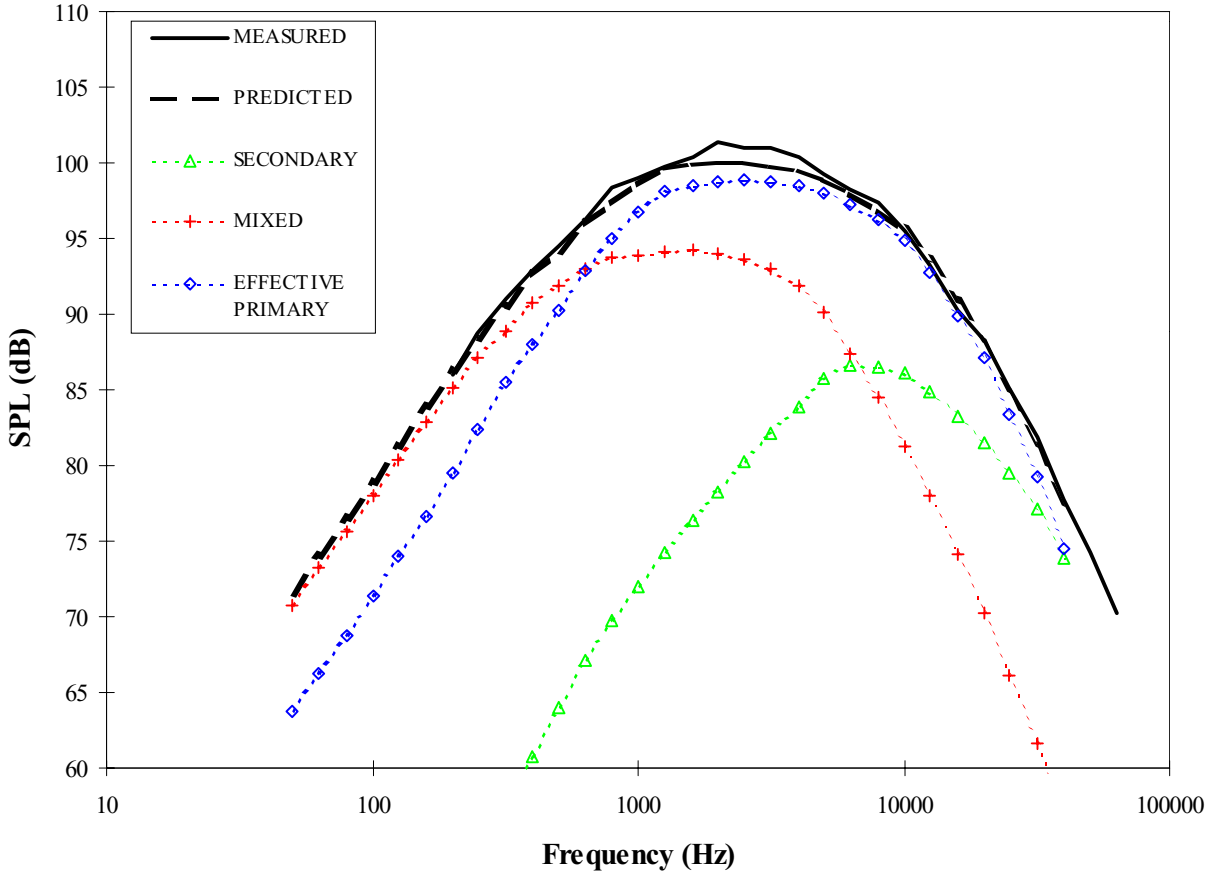
Physics of Jet Noise Suppression

Semi-empirical Prediction Methods



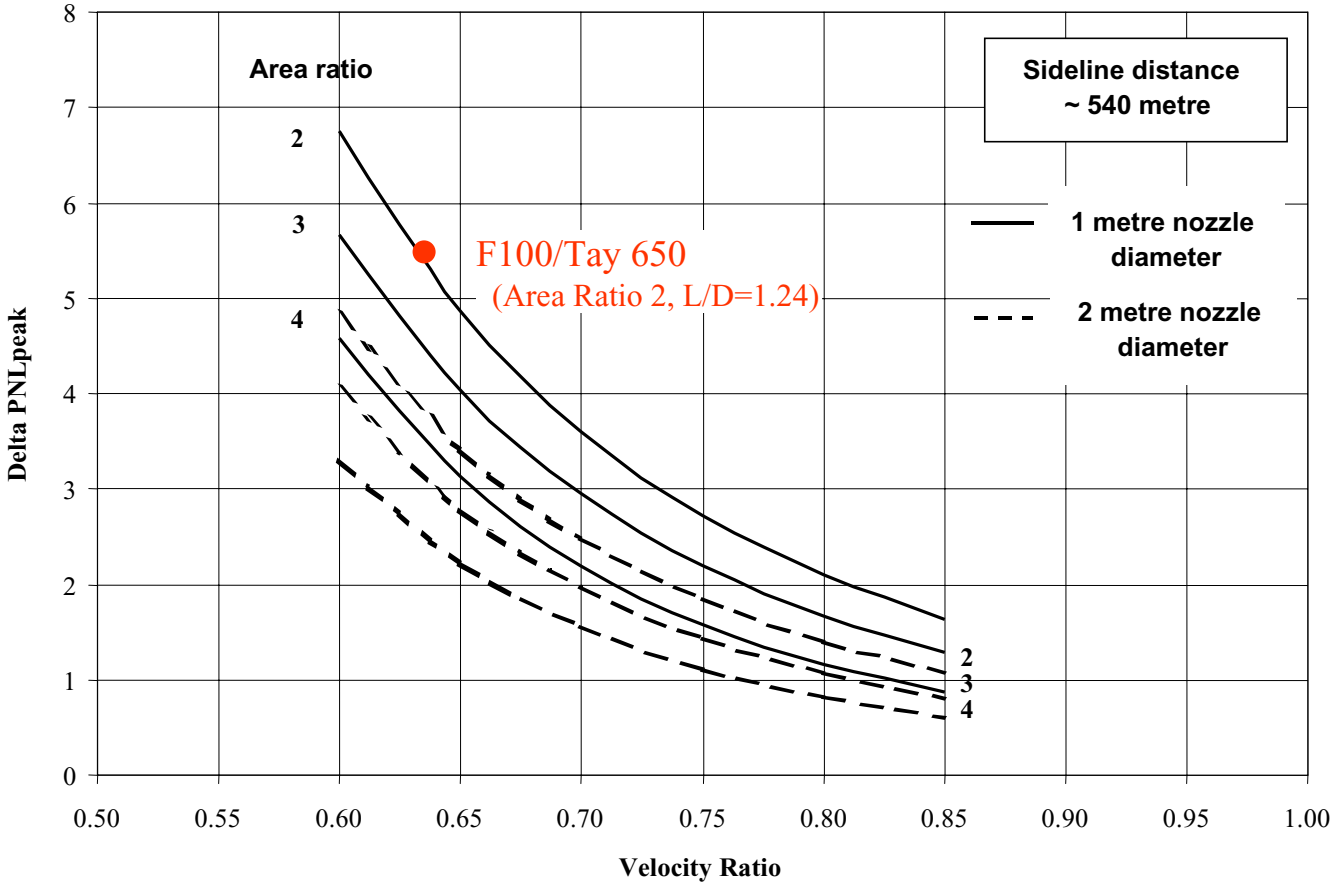
Physics of Jet Noise Suppression

Semi-empirical Prediction Methods



Physics of Jet Noise Suppression

Potential Jet Noise Benefit due to Internal Mixing



***Give evidence where theory has correctly predicted jet noise* - Krish Ahuja, Georgia Institute of Technology as summarized by Mary Jo Long-Davis.**

Dr. Ahuja presented historical data from his Ph.D. dissertation relative to shock weakening in supersonic jets. Specifically he discussed the principle of the Inverted Velocity Profile (IVP). His objective was to demonstrate that even for a complex suppressor nozzle it is possible to predict noise using simple scaling assumptions from Lighthill's theory. Ahuja computed a low frequency prediction for an IVP suppressor and performed the same calculation for the high frequency. The predictions matched the data very well. Ahuja postured that there are many different schemes, but they all revolve around the same line of thinking.

Physics of Jet Noise Suppression

Marcus Harper-Bourne
DERA

Physics of jet noise suppression **- Marcus Harper-Bourne, DERA as summarized by Mary Jo Long-Davis.**

Mr. Harper-Bourne presented results on passive (offset primary nozzle, coaxial elliptic nozzles) and active (harmonic acoustic forcing) approaches for jet noise suppression. Harper-Bourne's presentation utilized areas of DERA's jet exhaust noise R&D activity to give evidence where theory has correctly predicted jet noise.

Results from the offset primary nozzle indicated some noise reduction at various angles to the jet axis. These results also illustrated how noise propagation with coaxial jets can affect the results. Results from the coaxial elliptic nozzles showed effects of noise refraction. Harper-Bourne presented data from the harmonic forcing of twin jets at Mj = 0.9 and T_j = 850K. Acoustic predictions of the near-field of twin jets were made using a line source model based on the acoustic analogy and compared to the data with and without harmonic forcing. The results indicated that the measured increase in broadband noise observed with acoustic forcing was accompanied by approximately 50% shortening of the axial source distribution. Refraction effects not included in the analogy were significant in the near field 'shadow regions' of the twin jets studied.

Harper-Bourne concluded with the following:

- The reduction of jet noise at source remains a challenge. However, a 'hole' in the sound field can be created for coaxial jets by harnessing the effect of refraction through the introduction of engineered flow field asymmetry.
- An example of the acoustic forcing of a twin jet resulted in amplification of the broadband jet mixing noise.
- Analysis of twin jet near field noise, using a line source model based on the acoustic analogy, indicated axial shortening of the jet mixing region (by ~50%), in the presence of acoustic forcing.
- The use of the acoustic analogy also confirmed that refraction effects can be significant in the modelling of twin jet near field noise

AeroAcoustics Research Consortium, Jet Noise Workshop
November 2000 / Ohio Aerospace Institute, Cleveland

"PHYSICS OF JET NOISE SUPPRESSION"



Presented by Marcus Harper-Bourne

DERA Pyestock, England

DERA

SCOPE

- **PASSIVE: -**

EFFECT OF NOZZLE GEOMETRY ON (1) THE NOISE AT SOURCE AND (2) NOISE PROPAGATION

- **ACTIVE: -**

EXAMPLE OF HARMONIC ACOUSTIC FORCING AND EFFECT ON SOURCE STRENGTH AND DISTRIBUTION

"Physics of Jet Noise Suppression"

M Harper-Bourne
OAI, 8 Nov 2000

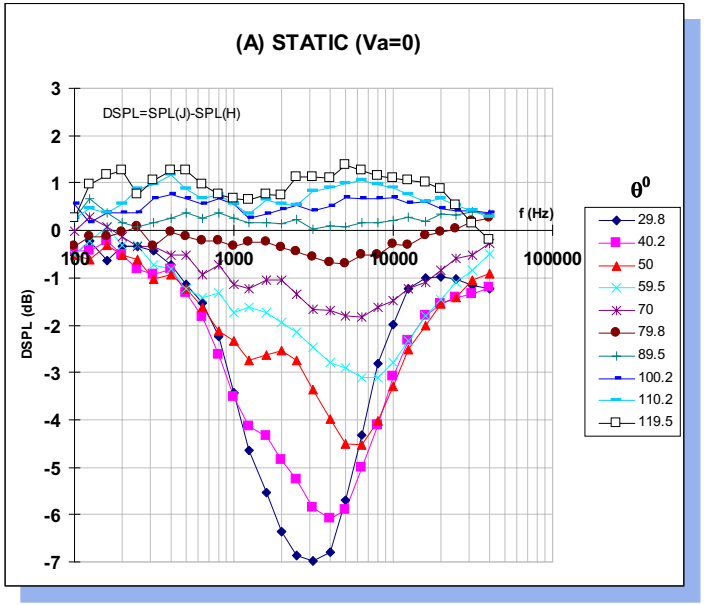
PRACTICAL EXAMPLES

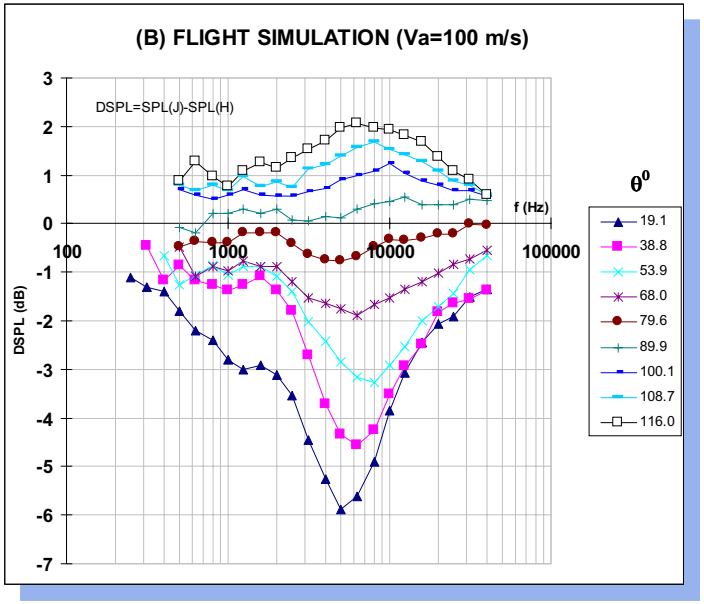
Example	AREAS OF DERA JET EXHAUST NOISE R/D ACTIVITY	Modelling	Exp.
(Ex.3)	NEAR AND FAR-FIELD JET EXHAUST NOISE	✓	✓
	CONCORDE NOZZLE		✓
	COAXIAL JETS:	✓	✓
	INTERNAL MIXERS (AIAA 98-2256	✓	✓
Ex.1	OFFSET NOZZLES		✓
Ex.2	ELLIPTIC NOZZLES		✓
	LIP TREATMENT		✓
	SHIELDING AND INSTALLATION (AIAA-98-2207)	✓	✓
(Ex.3)	TWIN-JETS (AIAA 2000-2084)	✓	✓
	SUPERSONIC (AIAA 99-1838)	✓	✓
	EJECTORS		✓
Ex.3	ACTIVE CONTROL		✓
	COMBUSTION NOISE		✓

"Physics of Jet Noise Suppression"

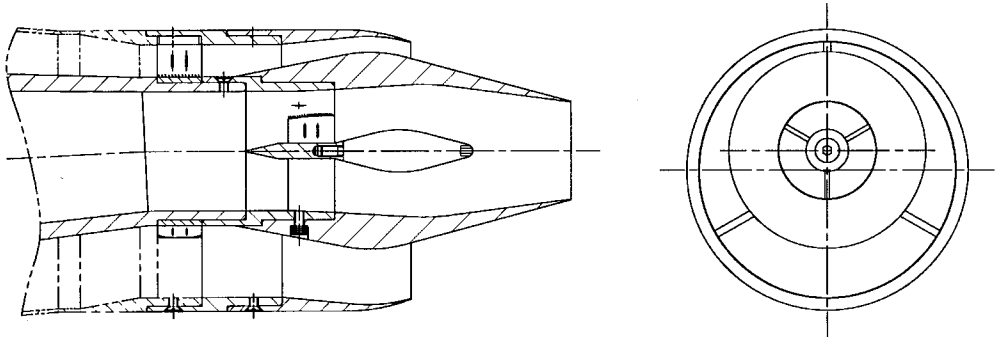
M Harper-Bourne
OAI, 8 Nov 2000

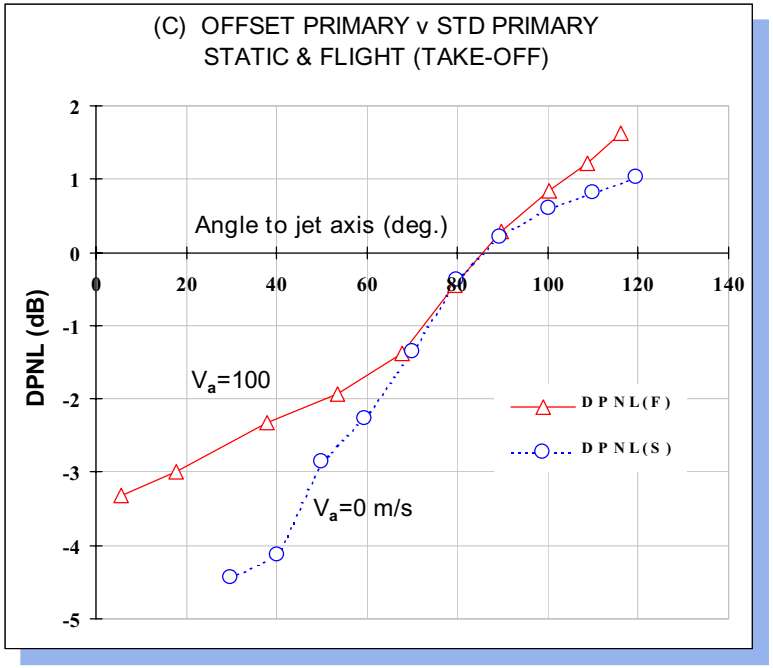
Presented with acknowledgements to DTI CARAD





EXAMPLE 1: OFFSET PRIMARY NOZZLE



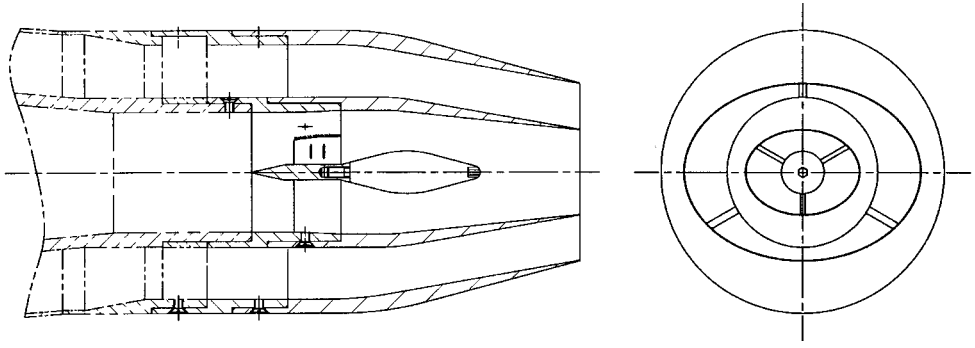


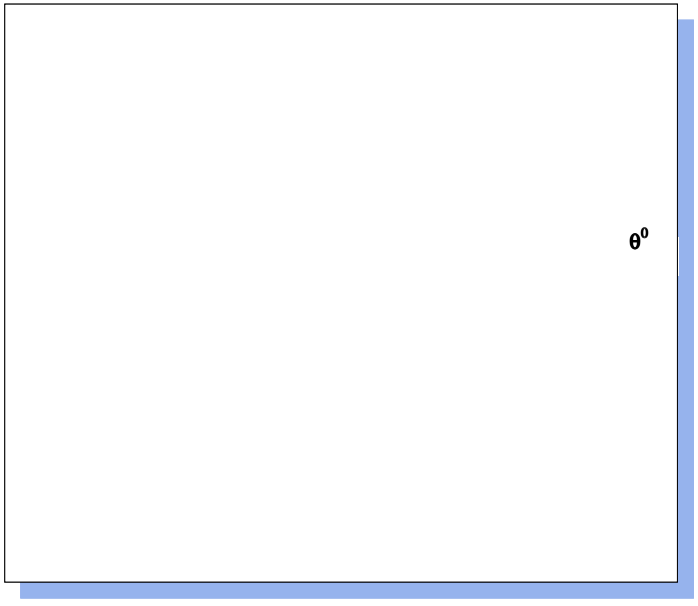
"Physics of Jet Noise Suppression"

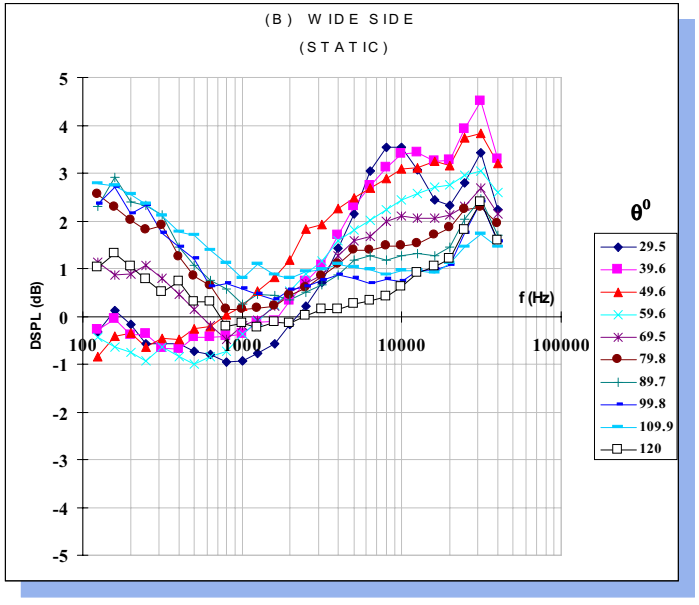
M Harper-Bourne
OAI, 8 Nov 2000

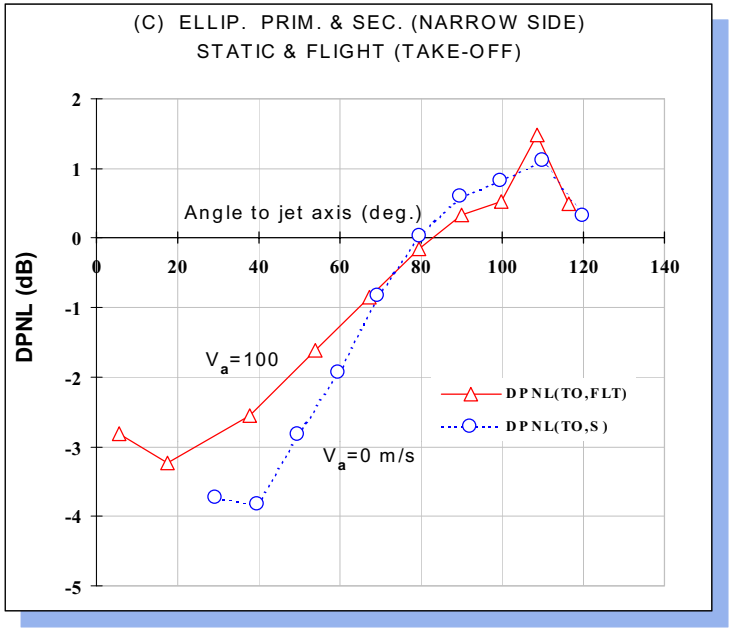
Presented with acknowledgements to DTI CARAD

EXAMPLE 2: COAXIAL ELLIPTIC NOZZLES







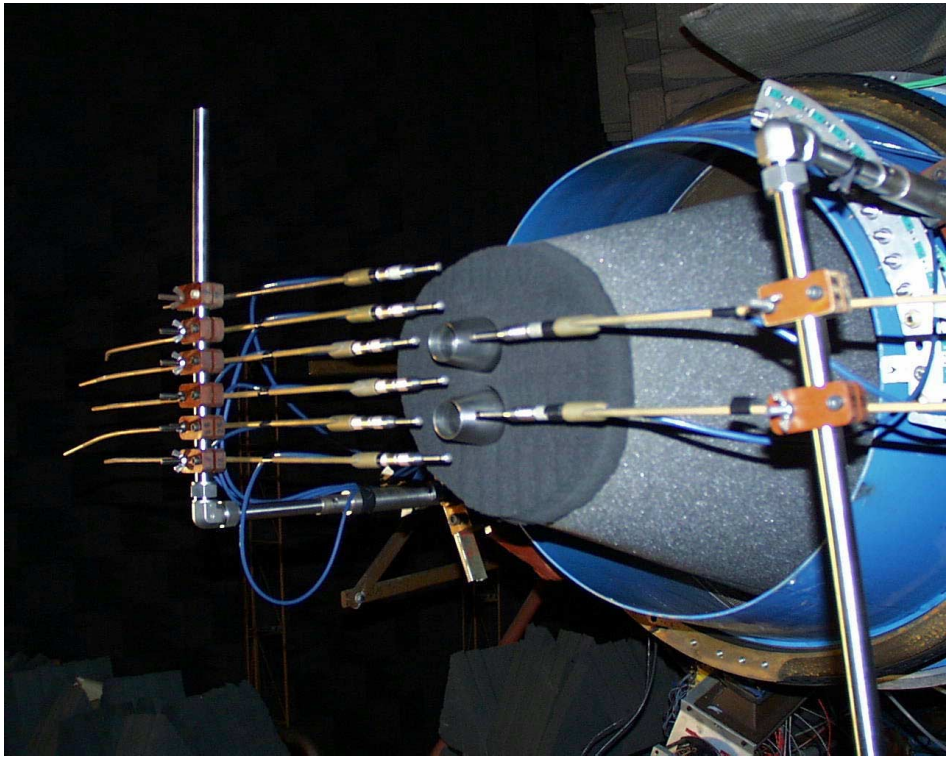


EXAMPLE 3: HARMONIC FORCING OF TWIN JETS

ARP TEST WITH STRAIGHT JET PIPES: ACOUSTIC PIPE RESONANCE AT Mj=0.9 (HEATED AND UNHEATED)



IRC WITH WRIGHT LABS: TWIN-JET INTERACTION TESTS EMPLOYED JOGGLED JET PIPES (NO RESONANCE)



Presented with acknowledgements to UK MOD

DERA

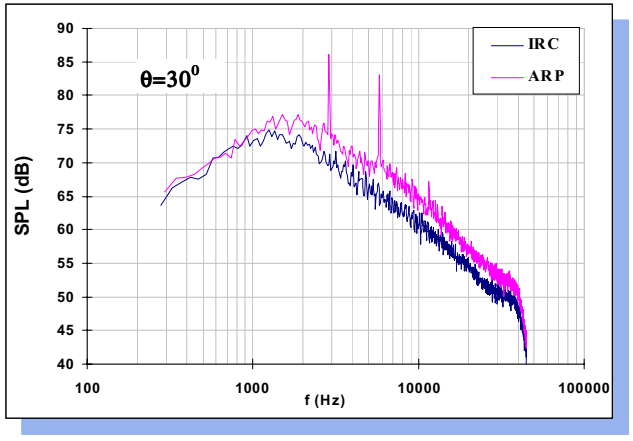
"Physics of Jet Noise Suppression"

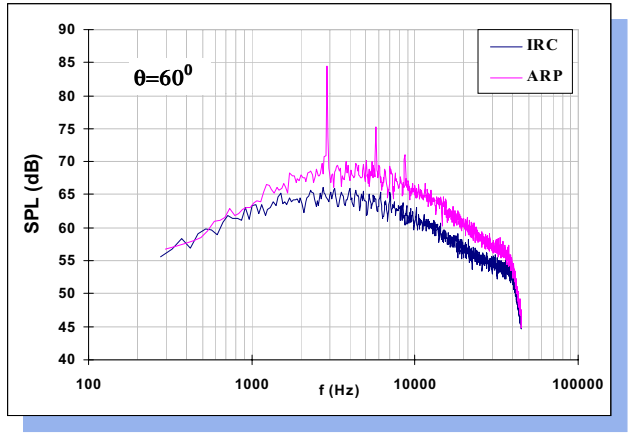
M Harper-Bourne
OAI, 8 Nov 2000

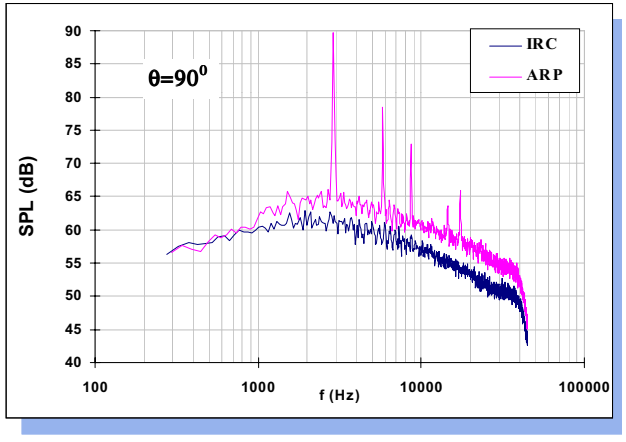
HARMONIC FORCING OF TWIN JETS
FAR-FIELD SPECTRA ON LOUD SIDE SHOWING BROADBAND AMPLIFICATION OF MIXING NOISE CAUSED BY JET-PIPE TONE

UNHEATED: Mj=0.9, Tj=288K, BW=50 Hz

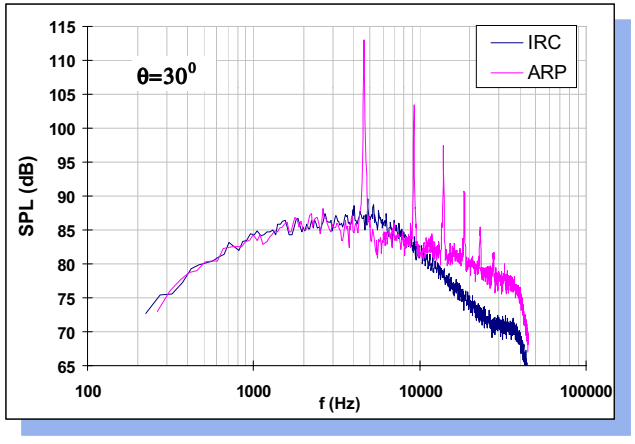
Presented with acknowledgements to UK MOD

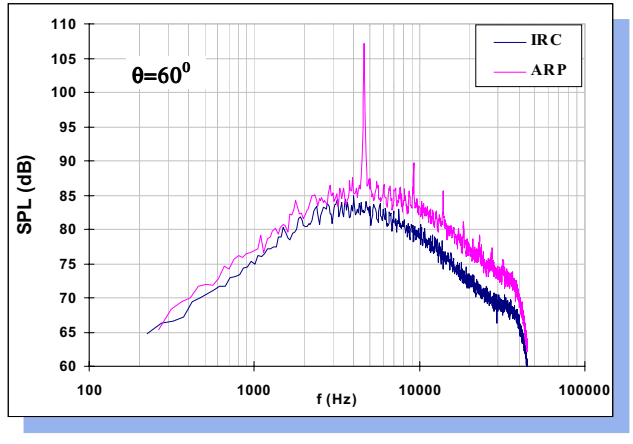


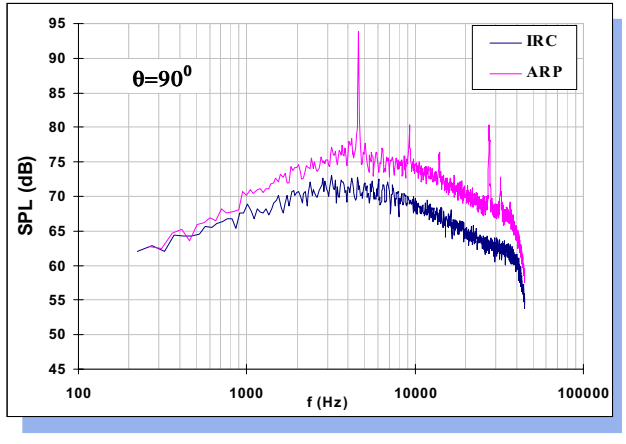




HEATED: Mj=0.9, Tj=850K, BW=50 Hz





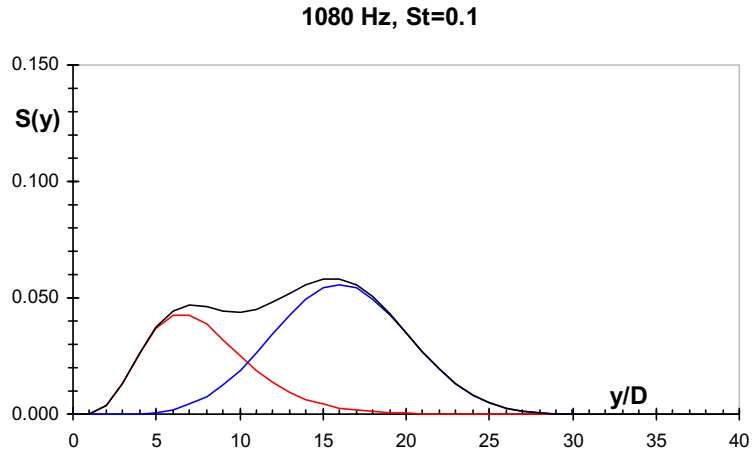


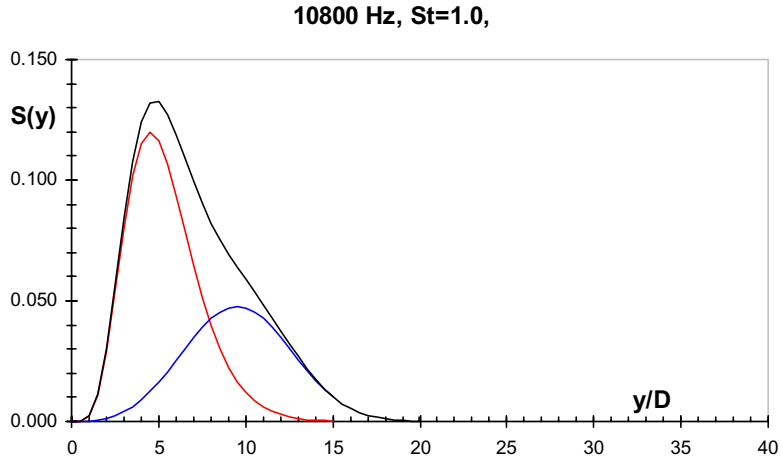
DERA

"Physics of Jet Noise Suppression"

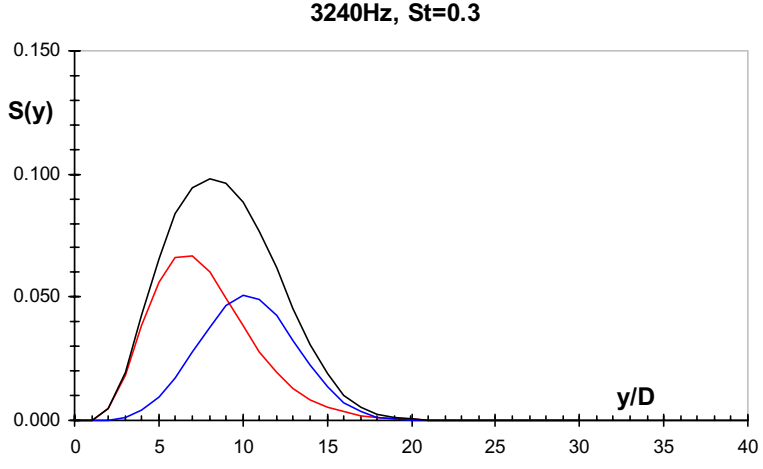
M Harper-Bourne
OAI, 8 Nov 2000

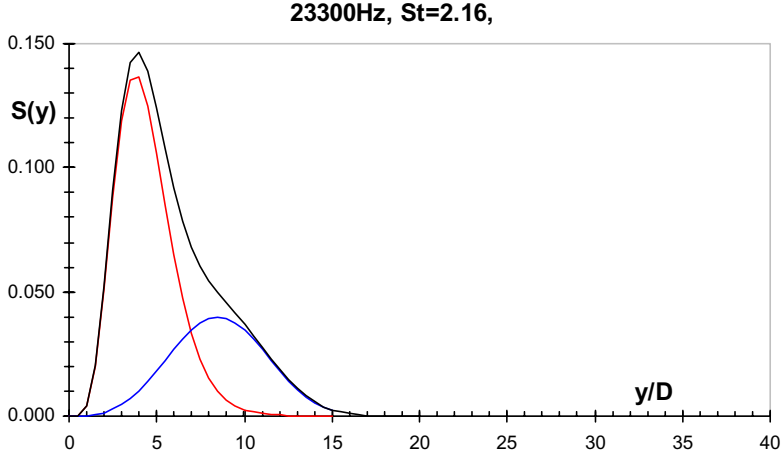
SINGLE JET SOURCE MODEL (POLAR CORRELATION, Uj=0.8a_0, UNHEATED)





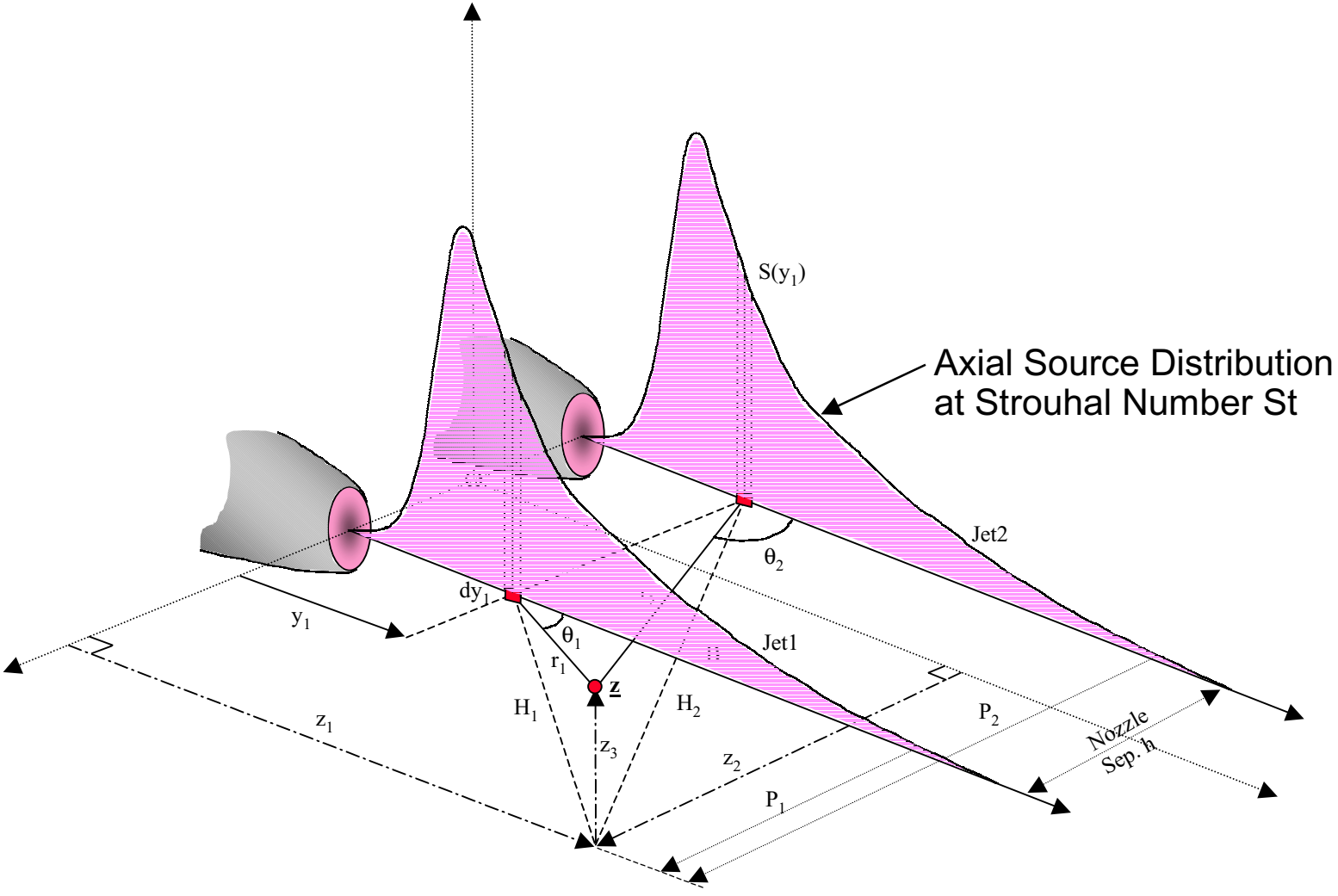
TWO-SOURCE BREAKDOWN OF JET MIXING NOISE





DERA

ILLUSTRATION OF TWIN-JET SOURCE MODEL (AIAA 2000-2084)



"Physics of Jet Noise Suppression"

M Harper-Bourne
OAI, 8 Nov 2000

LINE SOURCE MODEL BASED ON ACOUSTIC ANALOGY

(AIAA 99-1838 & AIAA 2000-2084)

$$S_r(y_1,St) = G_{90}(St).D_p(y_1,\theta,St).C_A(y_1,D_f,S_e).S(y_1,St).D_N{}^2$$

Source strength per unit length

$$\int_0^\infty S(y_1,\omega)dy_1 = 1$$

$$C_A = \frac{I(\theta,\omega)}{I(\pi/2,\omega)} \quad \text{where} \quad I = \frac{1}{\left(1+\left(\frac{\omega L_1}{U_c}\right)^2(1-M_C\cos\theta)^2\right)^{\frac{m}{2}}}$$

Non-compactness factor (fixed frame analysis, Exp/Gaus model yields m=3)

$$G_p(\hat{x},\omega) = \sum_i \frac{S_r(y_i,\omega)}{r_1^2}\Delta y_i$$

Single Jet

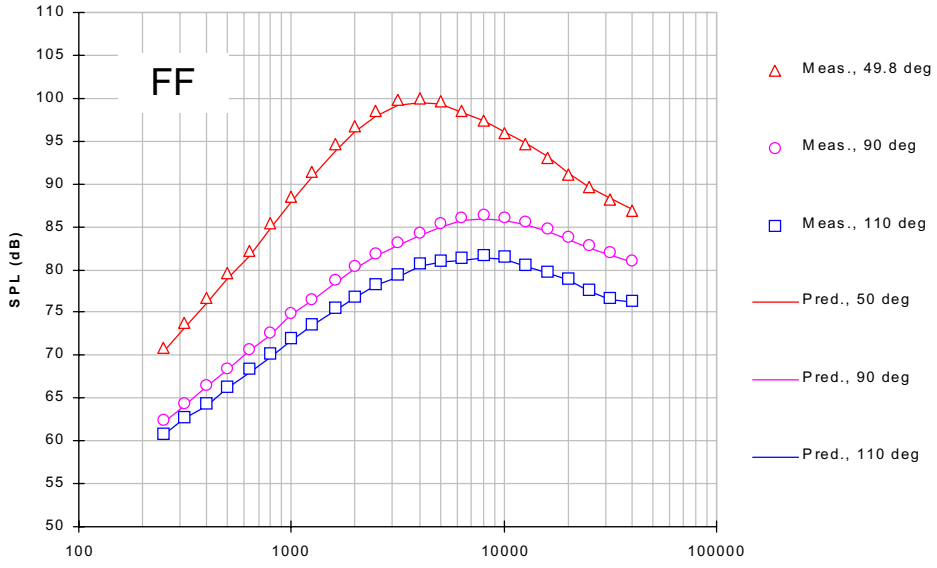
$$G_p(\hat{x},\omega) = \sum_i \frac{S_{r_1}(y_i,\omega)}{r_1^2}\Delta y_i + \sum_i \frac{S_{r_2}(y_i,\omega)}{r_2^2}\Delta y_i$$

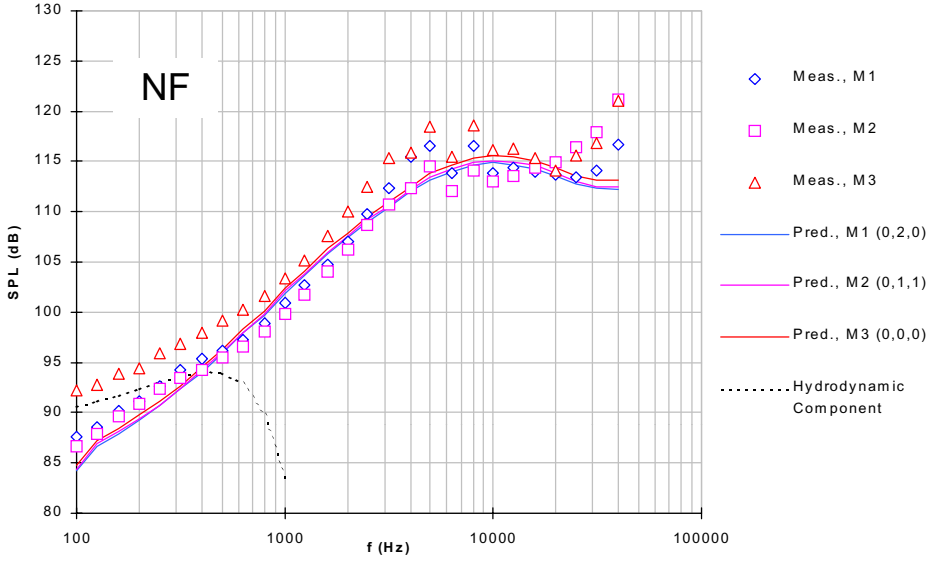
Twin Jet

"Physics of Jet Noise Suppression"

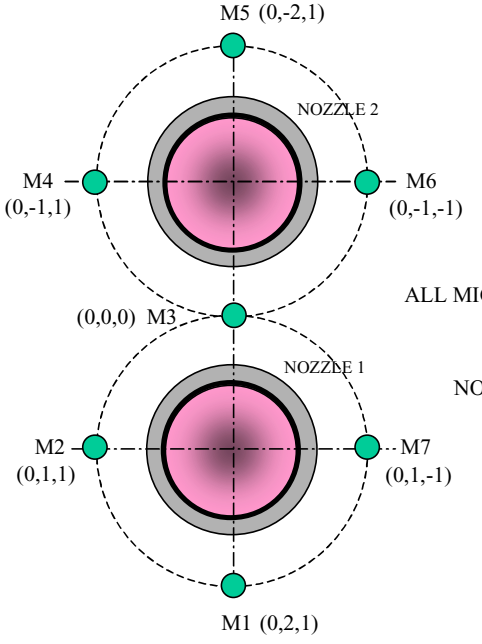
M Harper-Bourne
OAI, 8 Nov 2000

Presented with acknowledgements to UK MOD





COMPARISON OF NEAR-FIELD PREDICTION WITH IRC (HOT) MEASUREMENTS (15% SOURCE COMPRESSION))



ALL MICROPHONES IN NOZZLE EXIT PLANE

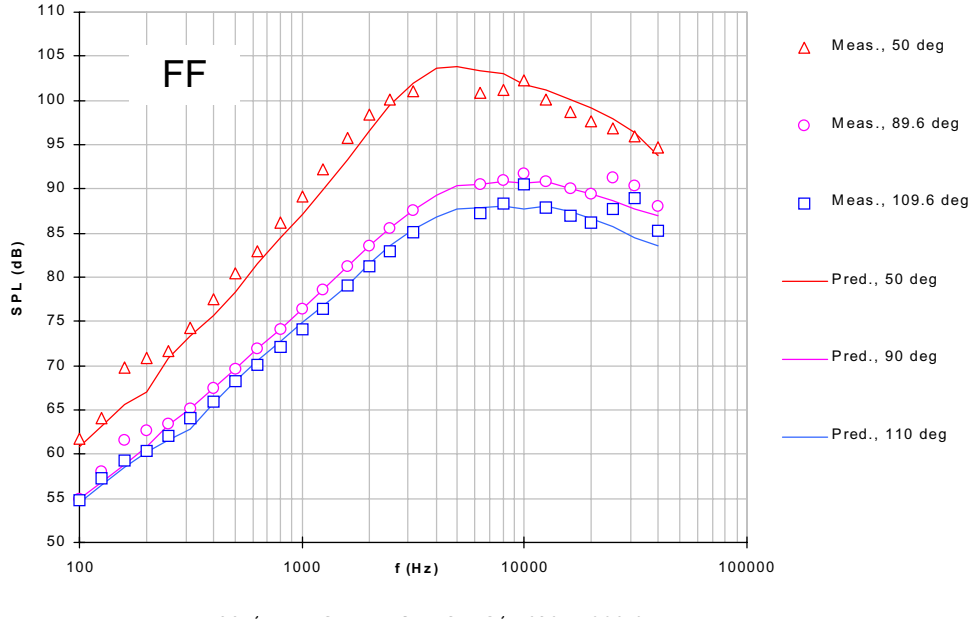
NOZZLE DIA.=32.9 mm

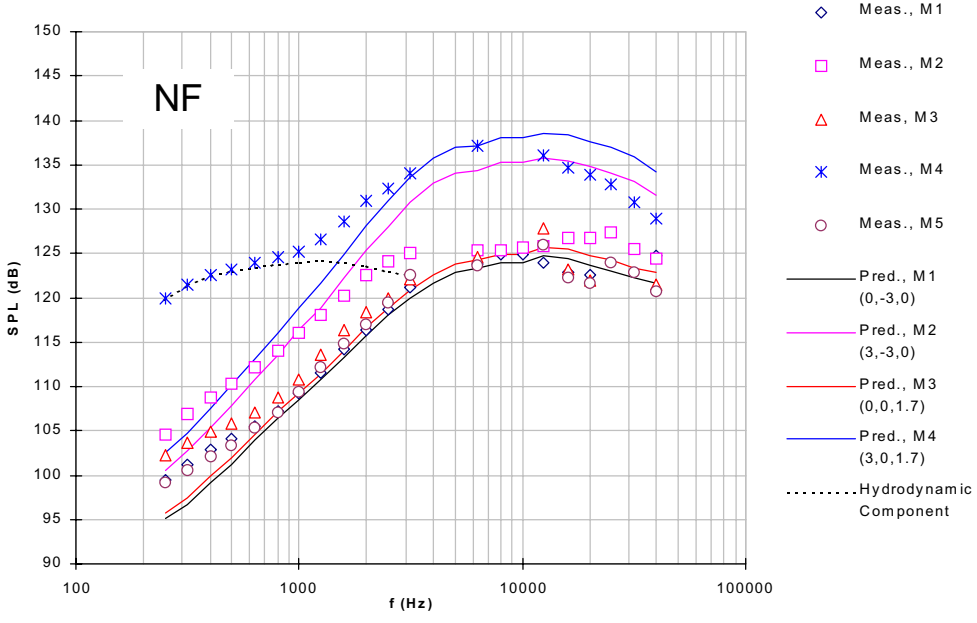
MICROPHONE CO-ORDINATES FOR TWIN-JET SCREECH TESTS

"Physics of Jet Noise Suppression"

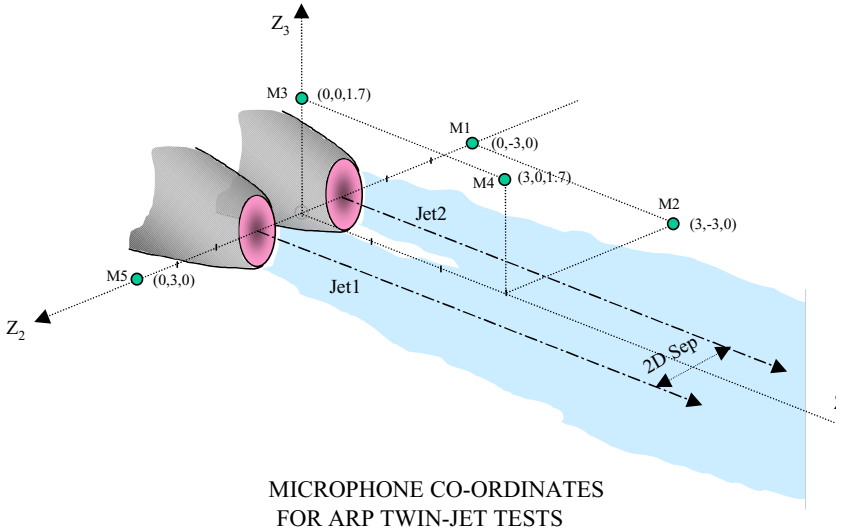
M Harper-Bourne
OAI, 8 Nov 2000

Presented with acknowledgements to UK MOD





COMPARISON OF NEAR-FIELD PREDICTION WITH ARP (HOT) MEASUREMENTS (50% SOURCE COMPRESSION)



MICROPHONE CO-ORDINATES
FOR ARP TWIN-JET TESTS

CONCLUSIONS

- SUPPRESSION OF THE NOISE AT SOURCE ON HIGH-SPEED JETS WITHOUT SIGNIFICANT THRUST LOSS OR WEIGHT/DRAG PENALTY CONTINUES TO BE A CHALLENGE FOR THE AEROACOUSTICIAN.

- HOWEVER, IT IS SHOWN THAT A 'HOLE' IN THE SOUND FIELD CAN BE CREATED BY HARNESSING THE STRONG EFFECT OF REFRACTION SHOWN TO EXIST IN THE PRESENCE OF ENGINEERED ASYMMETRY IN THE JET FLOW FIELD. CLEARLY, SUCH AN EFFECT CAN ONLY BE MODELLED EXTERNAL TO THE ACOUSTIC ANALOGY.

- AN EXAMPLE OF SOURCE MODIFICATION (NEGATIVE SUPPRESSION) THROUGH BROADBAND AMPLIFICATION OF JET MIXING NOISE, CAUSED BY HARMONIC FORCING, HAS BEEN DEMONSTRATED FOR TWIN-JETS.

- ANALYSIS OF THE NEAR-FIELD OF THE AMPLIFIED MIXING NOISE USING A FIXED FRAME ACOUSTIC ANALOGY NOISE SOURCE MODEL INDICATES THAT THE JET MIXING REGION IS SHORTENED (BY ~50%) IN THE PRESENCE OF BROADBAND AMPLIFICATION, WHICH IS IN KEEPING WITH EXPECTATION.

M. Harper-Bourne References

1. M Harper-Bourne, “Radial Distribution of Jet Noise Sources Using Far-Field Microphones”, AIAA Paper 98-237, 4th AIAA/CEAS Aeroacoustics Conference, Toulouse, France, June 1998.

2. M Harper-Bourne, “Jet Near-Field Noise Prediction”, AIAA Paper 99-1838, 5th AIAA/CEAS Aeroacoustics Conference, Seattle, May 1999.

3. M Harper-Bourne, “Twin-Jet Near-Field Noise Prediction”, AIAA Paper 2000-2084, 6th AIAA/CEAS Aeroacoustics Conference, Maui, June 2000.

Dr. Abbas Khavaran of Dynacs Engineering-NASA Glenn presented evidence which indicated MGBK model theory can match the data. The self-noise, shear-noise, and source modeling approaches utilized in the MGBK code were presented and discussed. Khavaran compared the noise predicted by the MGBK code to the experimental data acquired during the Separate Flow Nozzle test. The 3D CFD RANS calculation, that is the input to the MGBK code, was performed by an outside contractor. Khavaran explained that there was an effect on the solution based on the values of the turbulence quantities that were specified. The solutions are very dependent on the ratio of axial to radial RMS velocity fluctuations and the ratio of axial to radial turbulence length scales, which can be quite different from unity, as was pointed out by Prof. Lilley in his invited presentation. The overall conclusion is that the MGBK code is doing a good job of predicting the noise when compared to the data.

Dr. Dimitri Papamoschou of UC Irvine presented his work in the area of Mach wave suppression. Papamoschou presented experimental results of coannular and eccentric nozzle testing. Results showed evidence of significant noise reduction from the eccentric nozzle. Papamoschou discussed the crackle phenomena and its relation to the data.

Dr. Vinod Mengle of Rolls-Royce reviewed another physical mechanism for noise reduction—changing the nozzle length. For a given lobed-mixer nozzle configuration, an experiment was conducted which varied the length of the nozzle by 25% and 50%. The experimental data indicated that a 25% decrease in the length of the nozzle resulted in a noise reduction in the intermediate frequency range. Conversely, the data indicated that a 50% decrease in the length of the nozzle resulted in a noise increase at the higher frequencies. Mengle presented the aerodynamic unshielding “hypothesis” as a possible explanation of the experimental results.

Small-Scale Turbulence Noise

Abbas Khavaran
Dynacs Engineering
NASA Glenn Research Center

NASA/CP—2001-211152

SMALL-SCALE TURBULENCE NOISE

Abbas Khavaran
DYNACS ENGINEERING, INC.
NASA GLENN RESEARCH CENTER
CLEVELAND, OH

Jet Noise Workshop
Nov. 7-9, 2000
Ohio Aerospace Institute

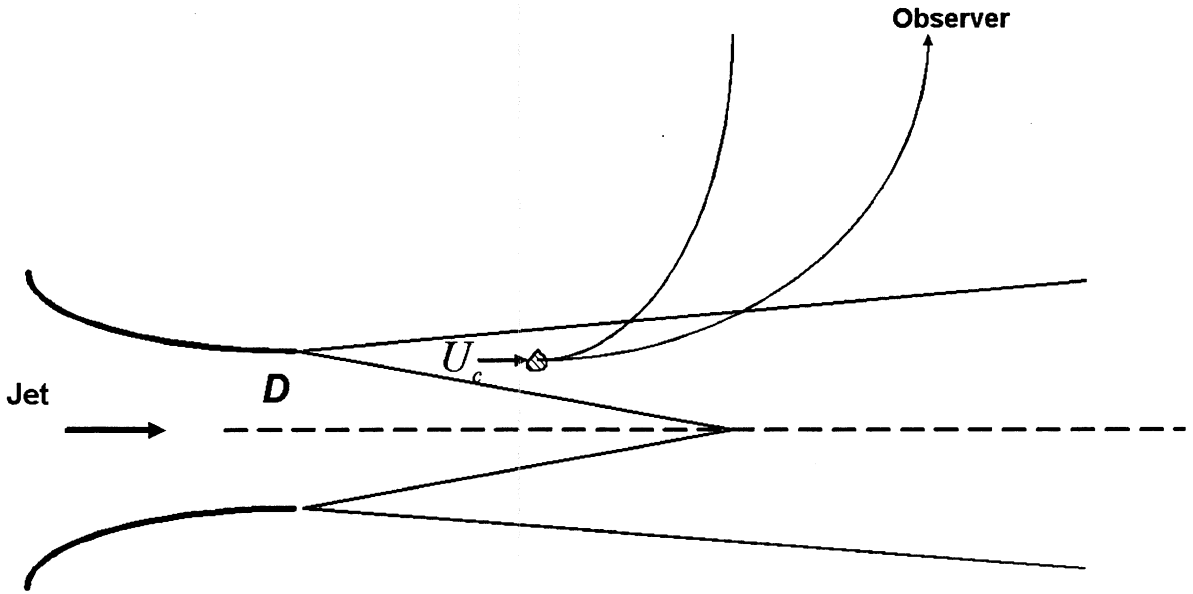
NASA/CP—2001-211152

COMPUTATIONAL BASED METHODOLOGY

- Governing Eq.: (Lilley's Eq)
- Source: Self- and Shear-Noise Terms
- Flow: RANS - ke
- Source Modeling: Two-Point Space-Time Correlation
- Acoustic/Mean-Flow Interaction
  - High Freq., Axisymmetric Jets (Balsa)

724

TURBULENCE MIXING NOISE



- Turbulence length-scale is small relative to acoustic wave length
- High frequency Green's Function

LILLEY'S EQUATION

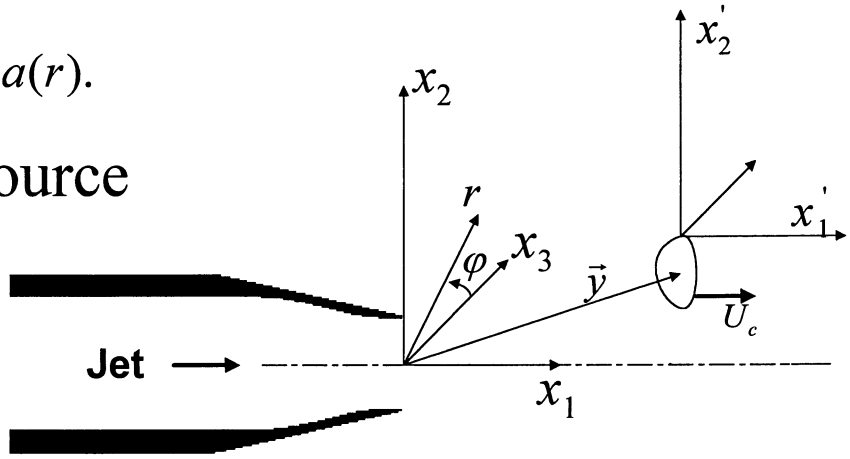
$$L(p;U,x_1) \equiv \frac{1}{a^2} D^3 p - D\nabla^2 p - \frac{d}{dr}(\log a^2) D \frac{\partial p}{\partial r} + 2\frac{dU}{dr}\frac{\partial^2 p}{\partial x_1 \partial r} =$$

$$\underbrace{\rho D \frac{\partial^2 (u_i u_j)}{\partial x_i \partial x_j}}_{Self-Noise} \underbrace{- 2\rho \frac{dU}{dr}\frac{\partial^2 (u_2 u_j)}{\partial x_1 \partial x_j}}_{Shear-Noise} + \cdots,$$

$$D = \partial/\partial t + U\partial/\partial x_1,$$

$$U = U(r), \quad \rho = \rho(r), \quad a = a(r).$$

⇨ Convecting Monopole Source

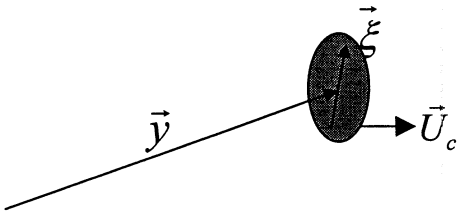


$$\vec{x}' = \vec{x} - \vec{U}_c t,$$

$$V = U - U_c, \quad D = \partial/\partial t + V\partial/\partial x_1',$$

$$L(Ge^{-i\Omega t};V,x_1') = e^{-i\Omega t}\delta(x_1')\delta(\varphi - \varphi_o)\delta(r - r_o)/r.$$

FAR-FIELD ACOUSTICS



$$\vec{\xi}_m = \vec{\xi} - \vec{U}_c \tau$$

$$\overline{p^2}(\vec{x}',\Omega) = \int_{\vec{y}} \int_{\vec{\xi}_m} G^*(\vec{x}', \vec{y} - \vec{\xi}/2, \Omega) G(\vec{x}', \vec{y} + \vec{\xi}/2, \Omega) Q_m(\vec{y}, \vec{\xi}_m, \Omega) d\vec{\xi}_m d\vec{y}$$

⇨ Two-point space-time correlation: $R_m(\vec{y}, \vec{\xi}_m, \tau)$

$$Q_m(\vec{y}, \vec{\xi}_m, \Omega) = \int_{-\infty}^{+\infty} R_m(\vec{y}, \vec{\xi}_m, \tau) e^{i\Omega\tau} d\tau$$

⇨ Doppler Effect: $\Omega = \omega \sqrt{(1 - M_c \cos\theta)^2 + (\alpha_c \kappa^{0.5} / a_\infty)^2}$

SELF NOISE

➪ Source and Green's Function

$$L(p_{self};V,x_1^{'}) = D\left(\rho_o \frac{\partial^2(u_i u_j)}{\partial x_i^{'}\partial x_j^{'}}\right)$$

$$p_{self}(\vec{x},t) = \int_{t_1}\int_{\vec{y}} S(\vec{x}^{'},t;\vec{y},t_1)\rho_o \frac{\partial^2(u_i u_j)}{\partial y_i \partial y_j} dt_1 d\vec{y}$$

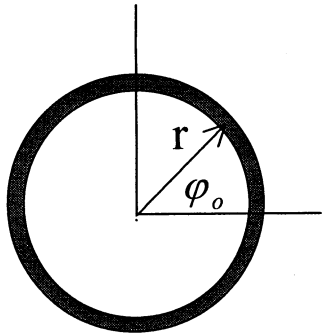
$$S(\vec{x}^{'},\vec{y},\Omega) = -i\Omega \frac{1-M_o\cos\theta}{1-M_c\cos\theta} G(\vec{x}^{'},\vec{y},\Omega)$$

$$p_{self}(\vec{x},t) = \int_{t_1}\int_{\vec{y}} u_i u_j \frac{\partial^2(\hat{S})}{\partial y_i \partial y_j} dt_1 d\vec{y}\,, \quad \hat{S} \equiv \rho_o S$$

$a_o^2 = P\gamma/\rho_o$, P is constant static pressure

SELF NOISE (Cont'd)

⇨ Ring Source Directivity Factor:



$$\overline{p^2_{self}}(\vec{x},\Omega) = \int_{y_1}\int_{r} a_{ijkl} I_{ijkl}(\vec{y},\Omega)\, dr\, dy_1$$

$$I_{ijkl}(\vec{y},\Omega) \equiv \int_{\xi}\int_{-\infty}^{+\infty} \overline{(u_i u_j)(u_k' u_l')}\, e^{i\Omega\tau}\, d\tau\, d\xi\,.$$

$$a_{ijkl} \equiv \frac{1}{4\pi^2}\int_{-\pi}^{+\pi}\int_{-\pi}^{+\pi} \hat{S}_{,ij}\hat{S}^*_{,kl}\, d\varphi\, d\varphi_o$$

⇨ Spectral Density

$$\overline{p^2_{self}}(\vec{x},\Omega;\vec{y}) = a_{1111}I_{1111} + 4a_{1122}I_{1122} + 8a_{1212}I_{1212} + 2a_{2222}I_{2222} + 2a_{2233}I_{2233} + 4a_{2323}I_{2323}.$$

SHEAR NOISE

➪ Source and Green's Function

$$p_{shear}(\vec{x},t) = -2\int_{t_1}\int_{\vec{y}} G(\vec{x}',t;\vec{y},t_1)\rho\frac{dU}{dr}\frac{\partial^2(u_2u_j)}{\partial y_1\partial y_j}dt_1d\vec{y}$$

➪ Parallel Flow $\quad \partial\rho/\partial y_1 = 0, \quad \partial U/\partial y_1 = 0$

$$\overline{p^2_{shear}}(\vec{x},\Omega) = \int_{y_1}\int_{r} b_{ij}I_{2i2j}(\vec{y},\Omega)drdy_1$$

➪ Spectral Density

$$\overline{p^2_{shear}}(\vec{x},\Omega;\vec{y}) = 4(b_{11}I_{2121} + b_{12}I_{2222} + b_{13}I_{2323})$$

SOURCE MODELING

⇨ Reduction in Order (Batchelor)

$$\overline{u_i u_j u_k' u_l'} = (\overline{u_i u_j})(\overline{u_k' u_l'}) + (\overline{u_i u_k'})(\overline{u_j u_l'}) + (\overline{u_i u_l'})(\overline{u_j u_k'})$$

⇨ Axisymmetric Turb. (Khavaran, AIAA Journal, 37(7) , July 1999)

$$\overline{u_2^2} = \overline{u_3^2}, \qquad \overline{u_i' u_j'} = \varepsilon_{jlm} \frac{\partial q_{im}}{\partial \xi_l}$$

⇨ Time & Length Scales

$$L_1 = \alpha_1 (\overline{u_1^2})^{3/2} / \varepsilon, \quad \tau_o = \frac{1}{\Omega_o} = \alpha_2 \frac{\kappa}{\varepsilon}, \qquad \kappa = (\overline{u_1^2} + \overline{u_2^2} + \overline{u_3^2})/2.$$

SOURCE MODELING (Cont'd)

➪ Source Correlation Coefficients

$$I_{1111}(\vec{y},\Omega) = (\overline{u_1^2})^2 \frac{L_1^3 \Delta^2}{2\sqrt{2}} \int_{-\infty}^{+\infty} \mathrm{g}^2(\tau) e^{i\Omega\tau} d\tau \,.$$

$$I_{2222} = I_{3333} = C_1 I_{1111},$$

$$I_{1122} = I_{1133} = C_2 I_{1111},$$

$$I_{2233} = C_3 I_{1111},$$

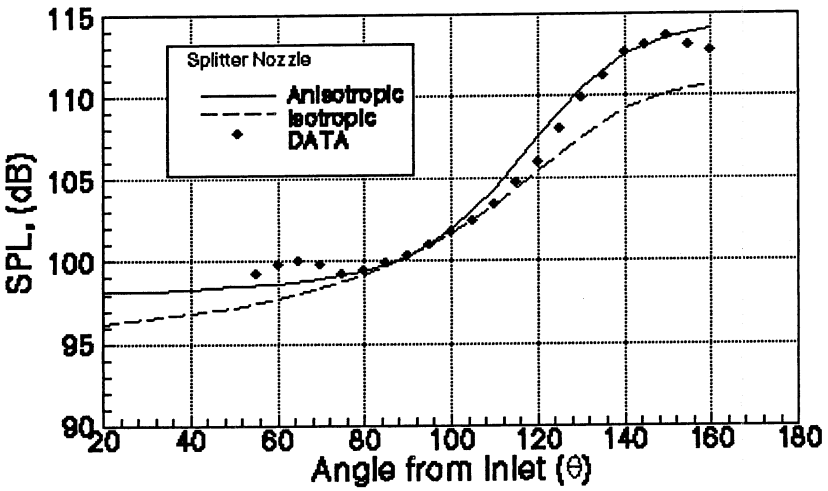
$$I_{1313} = I_{1212} = C_4 I_{1111},$$

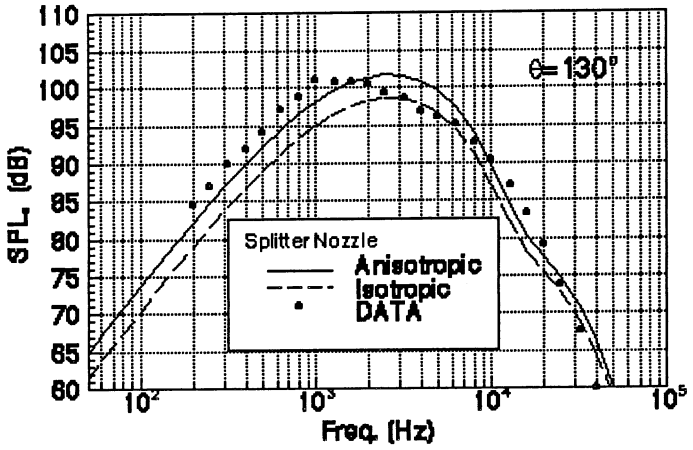
$$I_{2323} = C_5 I_{1111} \qquad C_i = C_i(\Delta,\beta), \qquad i = 1,\ldots,5$$

where: $\Delta = \dfrac{L_2}{L_1}, \qquad \beta = 1 - \dfrac{\overline{u_2^2}}{\overline{u_1^2}},$

➪ Correlation Time Delay: $\mathrm{g}(\tau) = \exp(-\sqrt{(\sigma/2)^2 + (\tau/\tau_o)^2})$

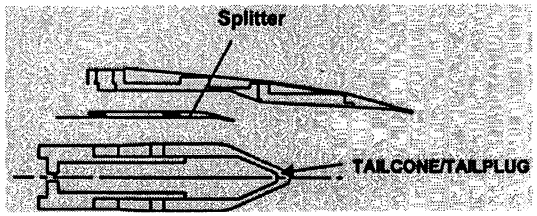
NOISE PREDICTIONS (Splitter Nozzle)



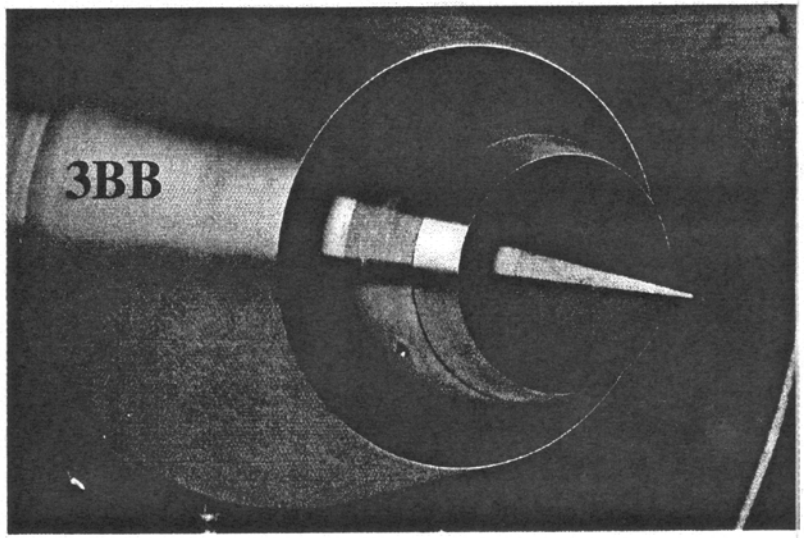


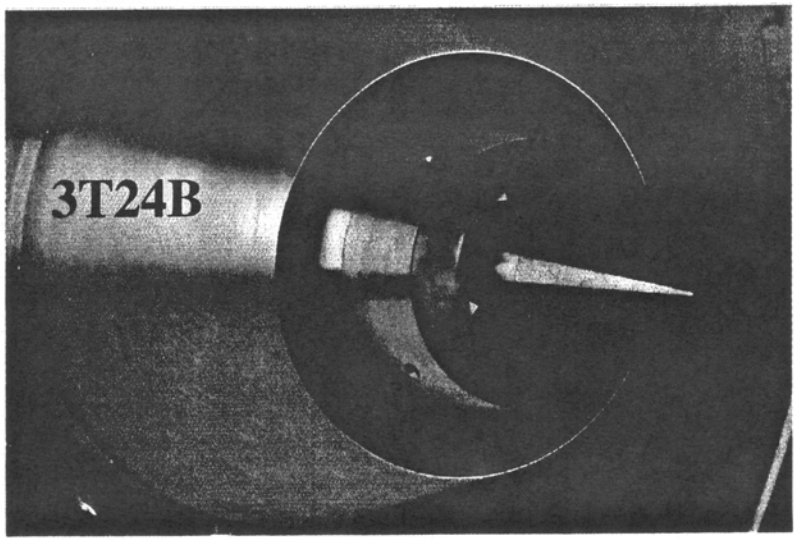
Isotropic: $L_2 / L_1 = 1.0, \quad \overline{u_2^2} / \overline{u_1^2} = 1.0$

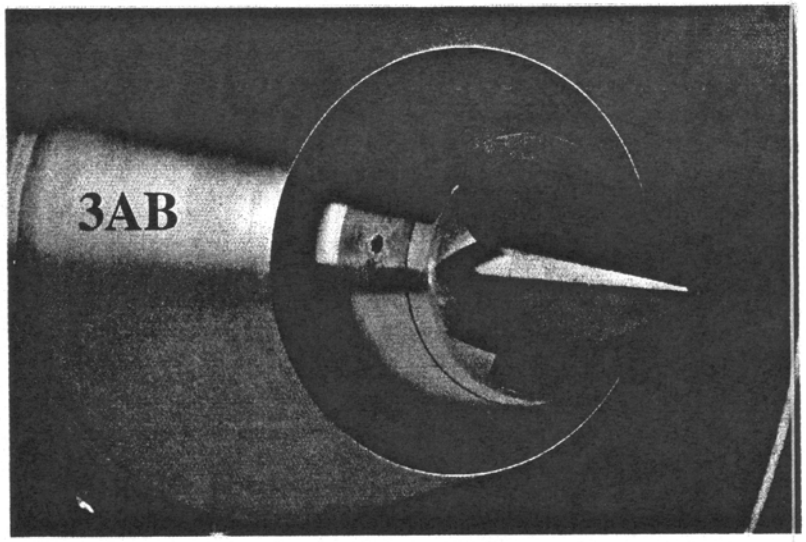
Axisymmetric: $L_2 / L_1 = 0.87, \quad \overline{u_2^2} / \overline{u_1^2} = 0.7$



Separate Flow Nozzles (SFN)

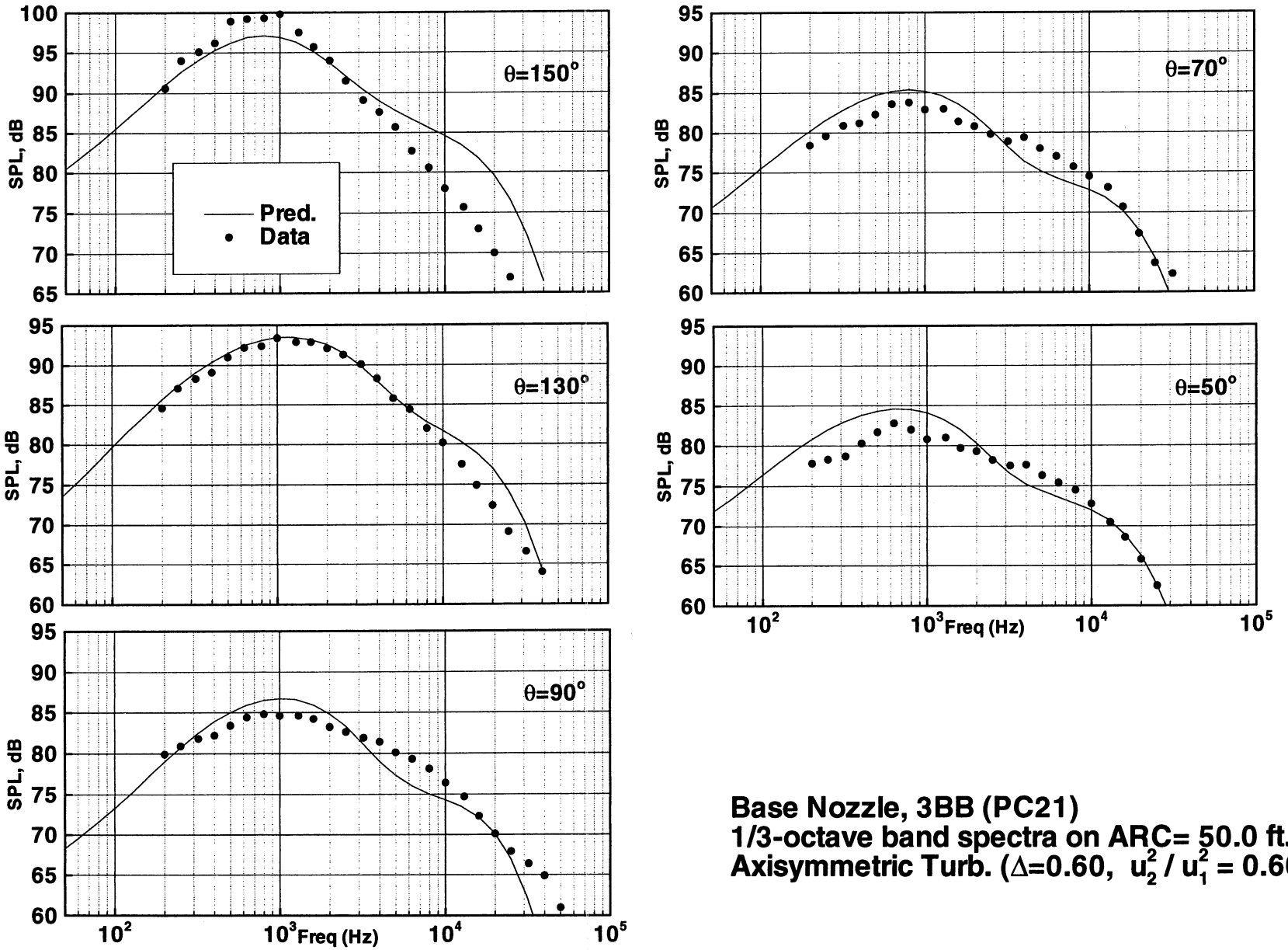






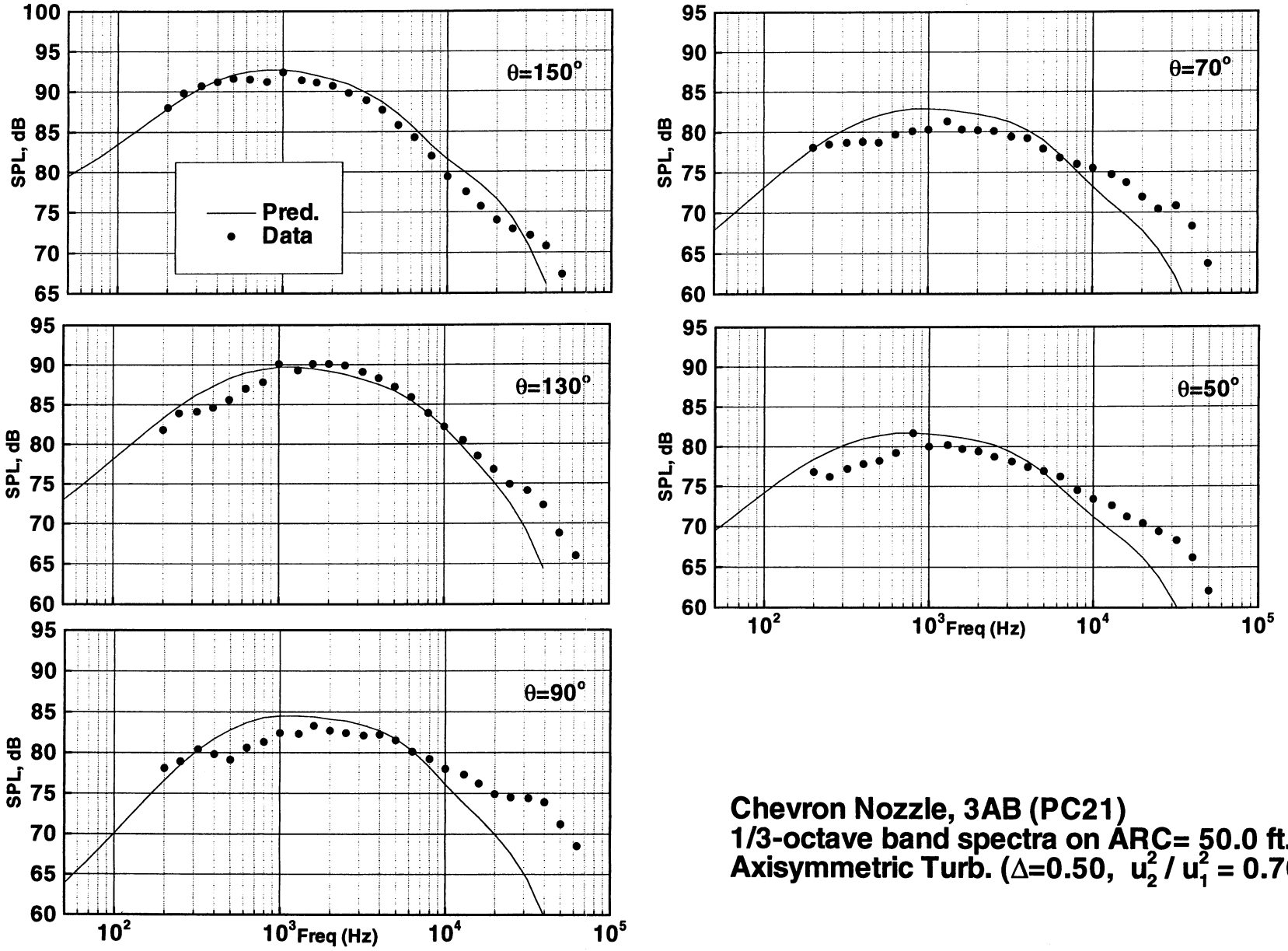
	PC 21		PC 22	
	CORE	FAN	CORE	FAN
Total Pressure (Atm.)	1.65	1.80	1.48	1.70
Total Temperature (K)	794	333	833	333

BASE NOZZLE (3BB), MGBK PREDICTION VS. DATA



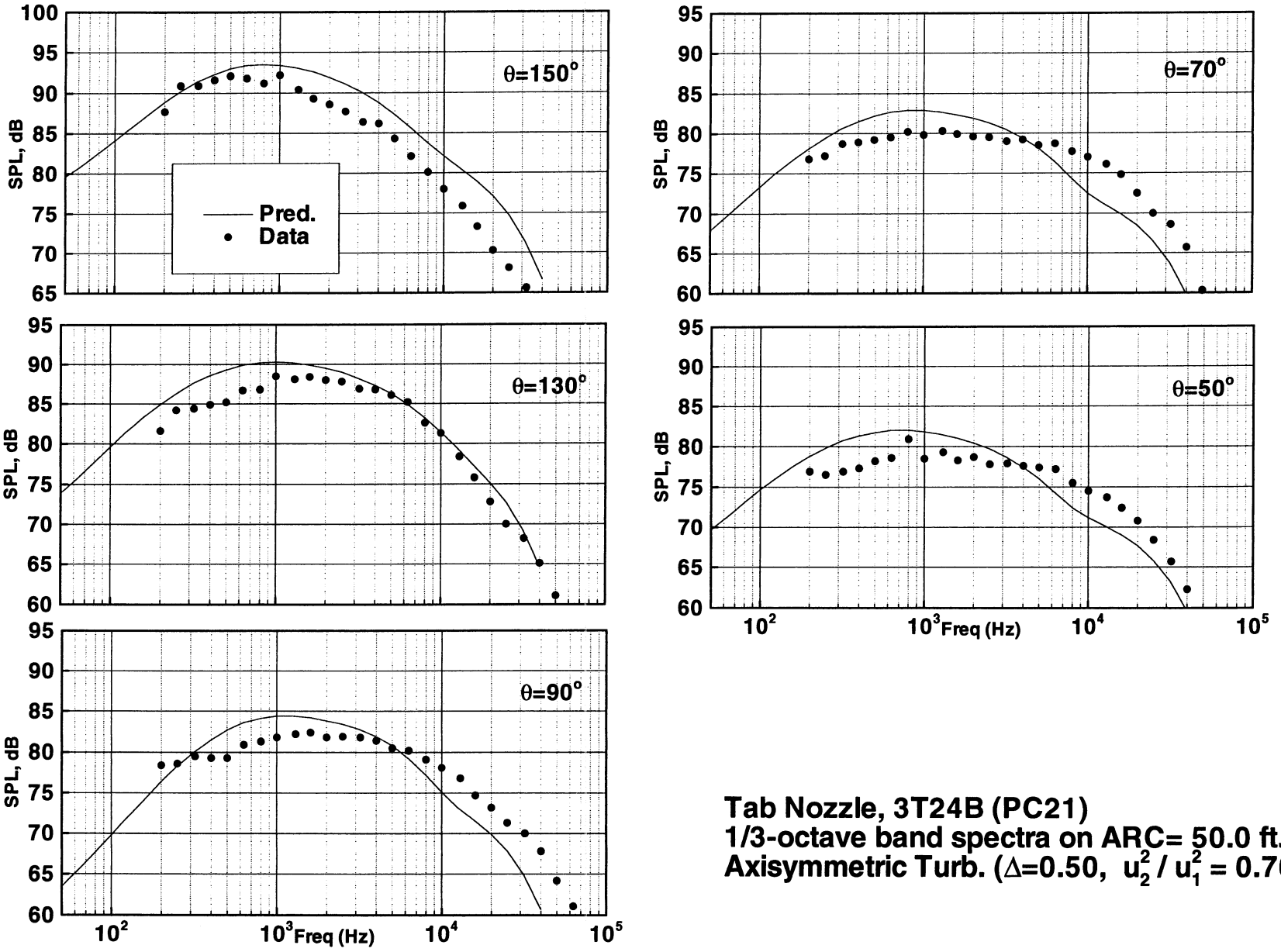
Base Nozzle, 3BB (PC21)
1/3-octave band spectra on ARC= 50.0 ft.
Axisymmetric Turb. (Δ=0.60, u_2^2 / u_1^2 = 0.60)

CHEVRON NOZZLE (3AB), MGBK PREDICTION VS. DATA



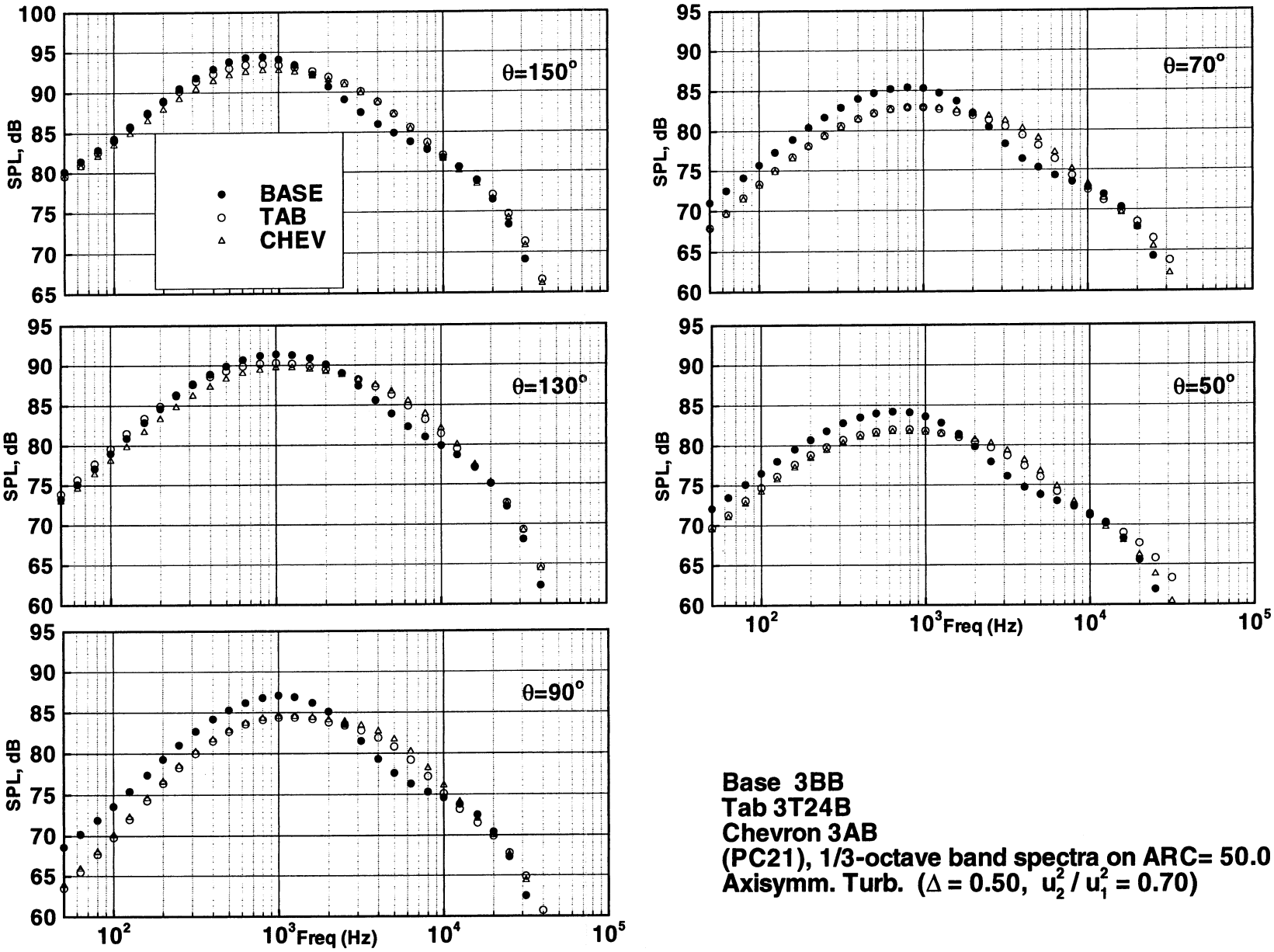
Chevron Nozzle, 3AB (PC21)
1/3-octave band spectra on ARC= 50.0 ft.
Axisymmetric Turb. (Δ=0.50, u_2^2 / u_1^2 = 0.70)

TAB NOZZLE (3T24B), MGBK PREDICTION VS. DATA



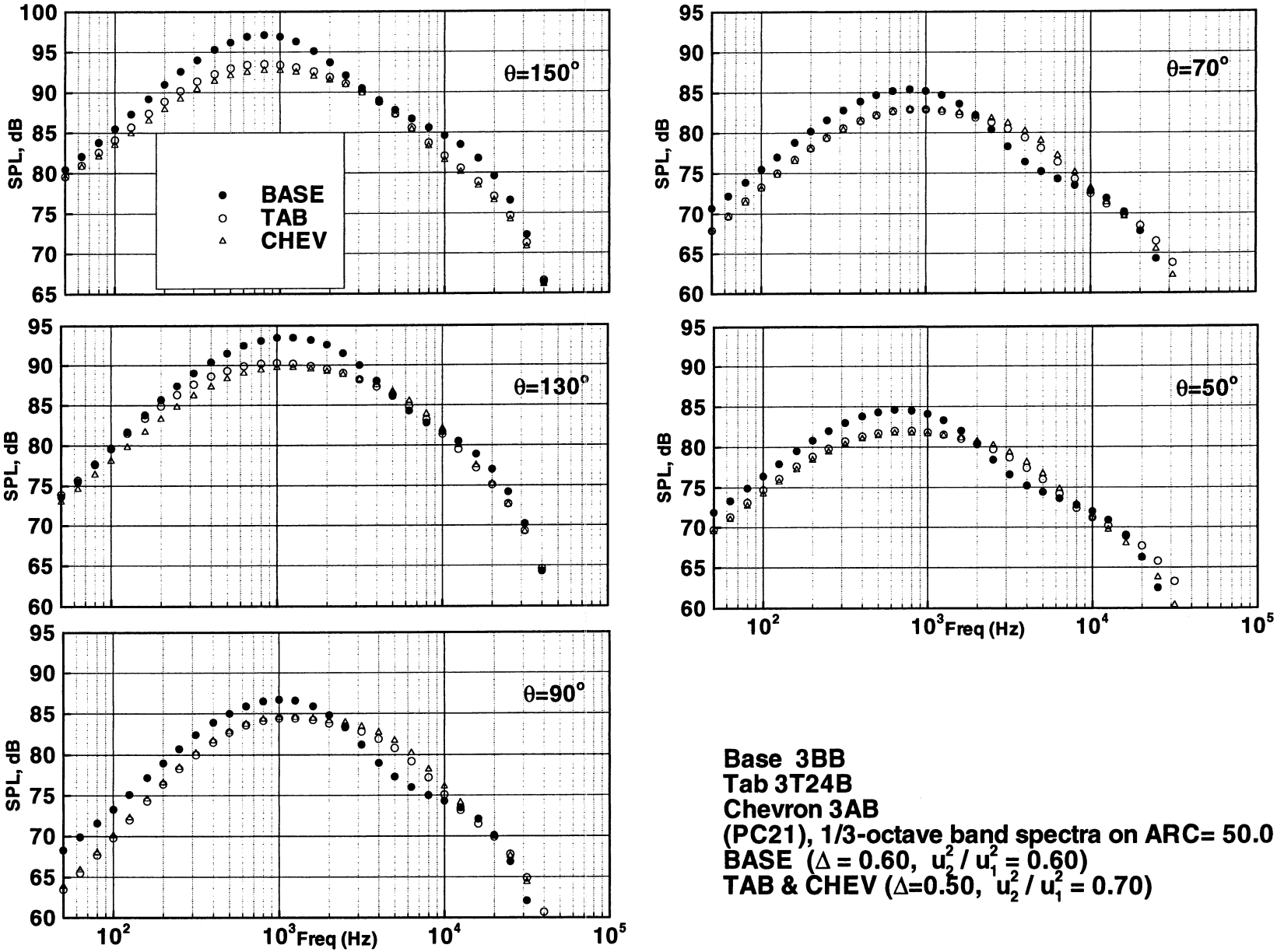
Tab Nozzle, 3T24B (PC21)
1/3-octave band spectra on ARC= 50.0 ft.
Axisymmetric Turb. (Δ=0.50, u_2^2 / u_1^2 = 0.70)

PREDICTED NOISE FOR 3 SFN CONFIGURATIONS



Base 3BB
Tab 3T24B
Chevron 3AB
(PC21), 1/3-octave band spectra on ARC= 50.0 ft.
Axisymm. Turb. ($\Delta = 0.50$, $u_2^2 / u_1^2 = 0.70$)

PREDICTED NOISE FOR 3 SFN CONFIGURATIONS



Base 3BB
Tab 3T24B
Chevron 3AB
(PC21), 1/3-octave band spectra on ARC= 50.0 ft.
BASE ($\Delta = 0.60$, $u_2^2 / u_1^2 = 0.60$)
TAB & CHEV ($\Delta = 0.50$, $u_2^2 / u_1^2 = 0.70$)

A. Khavaran References

1. G. M. Lilley, "Jet Noise Classical Theory and Experiments," Aeroacoustics of Flight Vehicles, (NASA Reference Publication 1258, Vol. 1), pp. 211-289, 1991.

2. M. E. Goldstein, *Aeroacoustics*, McGraw-Hill, 1976.

3. Balsa, T. F., "The Far Field of High Frequency Convected Singularities in Sheared Flows, with an Application to Jet Noise Prediction," Journal of Fluid Mechanics, Vol. 74, March 1976, pp. 193-208.

4. A. Khavaran, "Role of Anisotropy in Turbulent Mixing Noise," AIAA Journal, Vol. 37, No.7, July 1999, pp. 832-841.

5. Podboy, G. G., Bridges, J. E., Saiyed, N. H., and Krupar, M. J., "Laser Doppler Velocimeter System for Subsonic Jet Mixer Nozzle Testing at the NASA Lewis Aeroacoustics Propulsion Lab," AIAA Paper 95-2787, July 1995.

6. Khavaran, A., Krejsa, E. A., and Kim, C. M., "Computation of Supersonic Jet Mixing Noise for an Axisymmetric Convergent-Divergent Nozzle," AIAA Journal of Aircraft, Vol. 31, No. 3, 1994, pp. 603-609.

7. Tam, C. K. W., and Auriault, L., "Mean Flow Refraction Effects on Sound Radiated from Localized Sources in a Jet," Journal of Fluid Mechanics, Vol. 370, Sept. 1998, pp. 149-174.

Mach Wave

Suppression

Dimitri Papamoschou
University of California, Irvine

NASA/CP—2001-211152

743

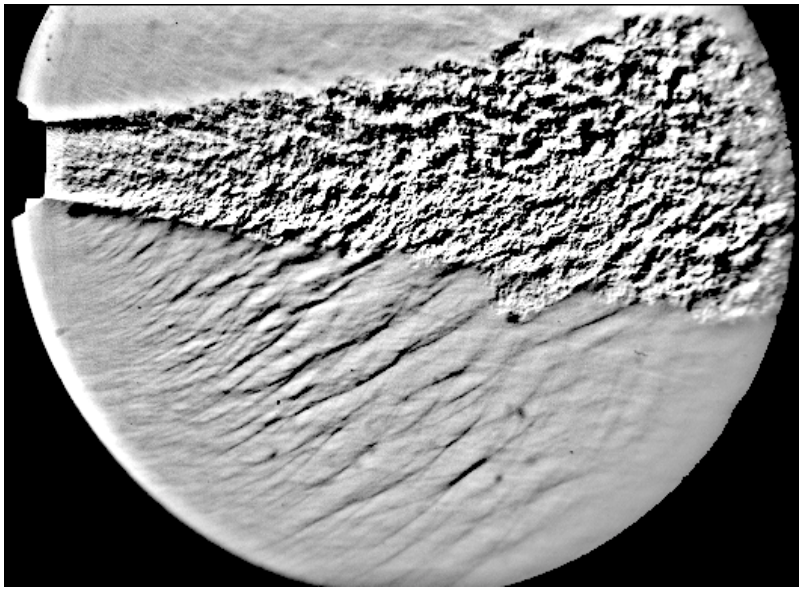
JET NOISE WORKSHOP
Ohio Aerospace Institute
November 7-9, 2000

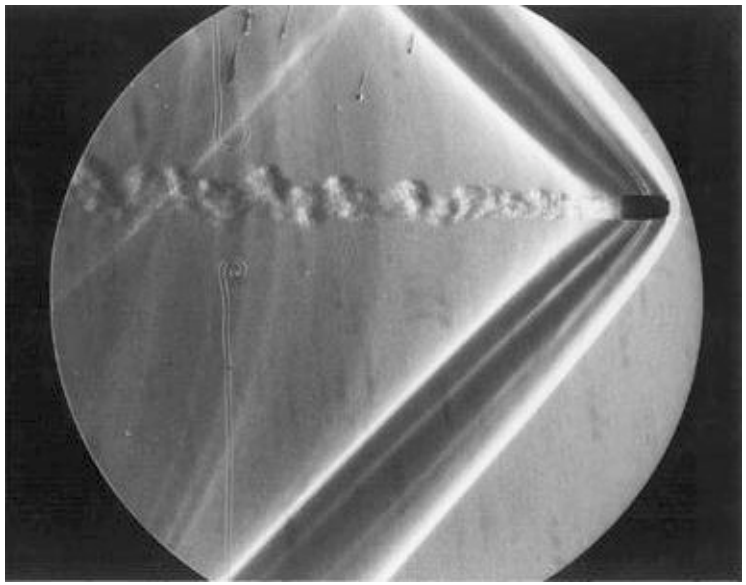
MACH WAVE SUPPRESSION

Dimitri Papamoschou
Department of Mechanical & Aerospace Engineering
University of California at Irvine
Irvine, CA 92697-3975
Email: dpapamos@uci.edu

NASA/CP—2001-211152

MACH WAVE RADIATION
The dominant source of supersonic jet noise

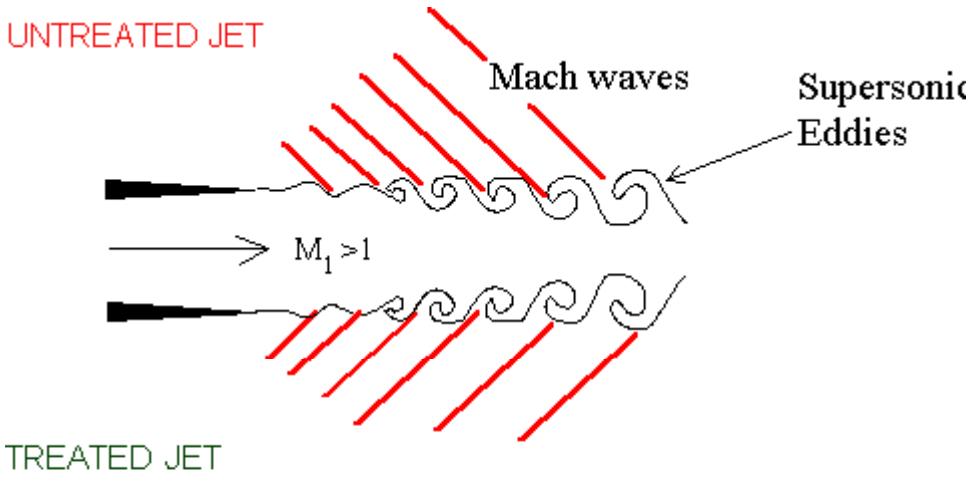




- Caused by the supersonic propagation of turbulent eddies.
- Highly directional acoustic field

•Bishop, Ffowcs Williams, and Smith (1971) JFM 50 (1)
•Tam (1972) JFM 51(1)
•McLaughlin, Morrison, and Trout (1975) JFM 69 (11)
•Trout and McLaughlin (1982) JFM 116
•Tam and Burton (1984) JFM 138
•Seiner, Bhat, and Ponton (1994) AIAA J. 32(12)
•Tam and Chen (1994) AIAA J.32 (9)
•Mitchell, Lele, and Moin (1997) AIAA J. 35(10)
•Dahl and Morris (1997) J. Sound & Vibration 200(5)
•Mankbadi, Hixon, Shih, and Povinelli (1998) AIAA J. 36(2)
•Fenno, Bayliss, and Maestrello (1998) AIAA J. 36(12)

PRINCIPLE OF MACH WAVE ELIMINATION

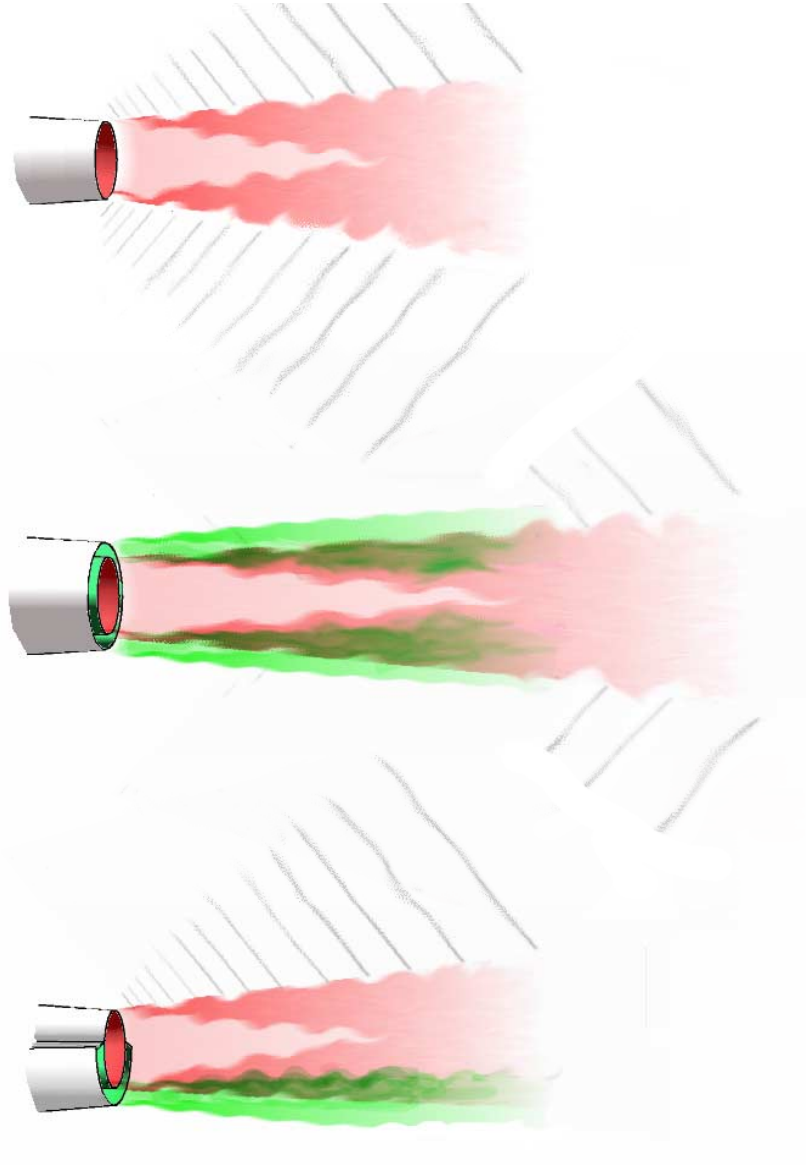


Secondary flow is applied such that:

- Primary eddies become subsonic relative to secondary flow
- Secondary eddies are subsonic relative to the ambient

Papamoschou (1997)
Papamoschou & Debiasi (1999)

TARGETED MACH WAVE ELIMINATION



SINGLE JET

COAXIAL JET.

Jet growth rate is suppressed

Mach wave emitting region is stretched

Far-field Mach waves may escape treatment

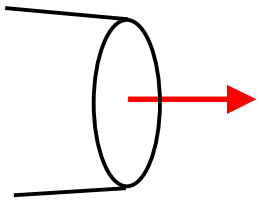
ASYMMETRIC DUAL-STREAM JET.

Allows part of the jet to grow naturally

Noise reduction in downward direction (where it really matters)

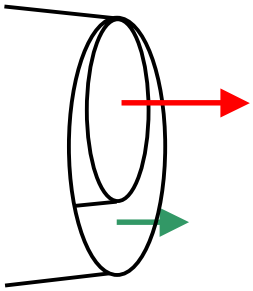
JET CASES

SINGLE



U_1=700 m/s
M_1=1.50

ECC

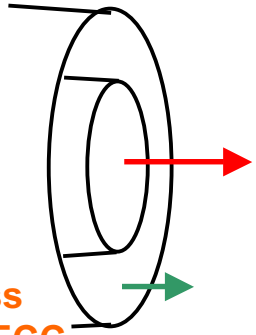


U_1=700 m/s
M_1=1.50

U_2=360 m/s
M_2=1.0
m_2/m_1=0.67

COAX2

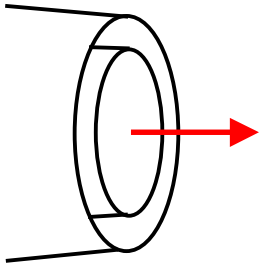
Same coflow thickness
as max. thickness of ECC



U_1=700 m/s
M_1=1.50

U_2=360 m/s
M_2=1.0
m_2/m_1=1.45

COAX1



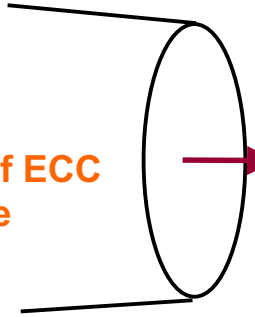
U_1=700 m/s
M_1=1.50

U_2=360 m/s
M_2=1.0
m_2/m_1=0.67

Same m_2/m_1 as ECC

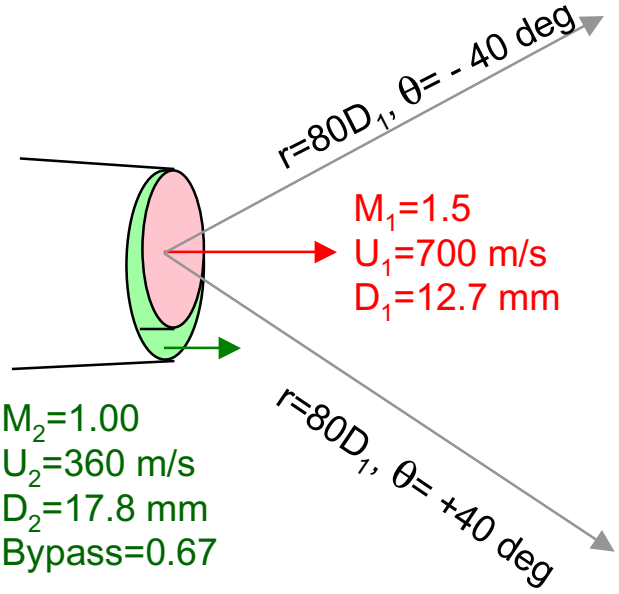
FMEQ

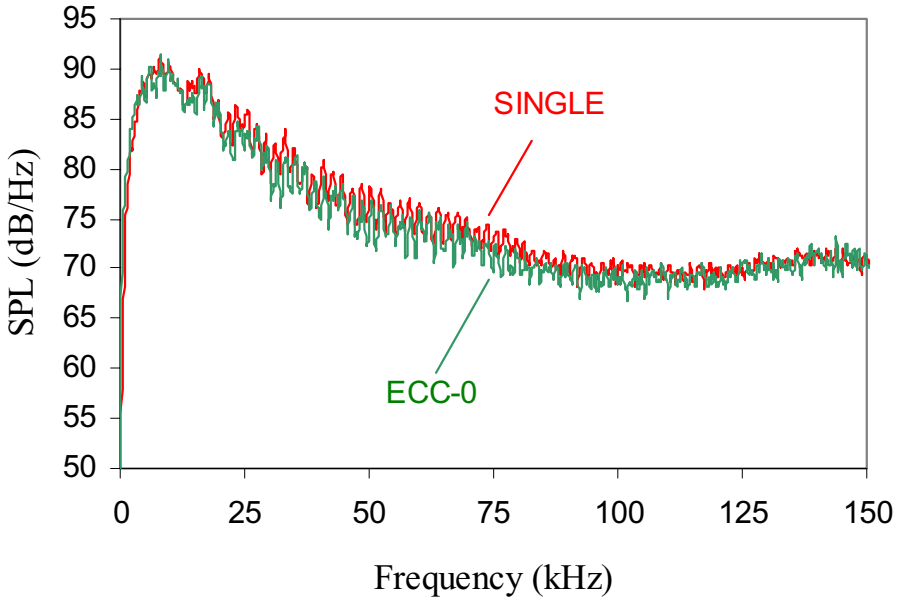
Fully-mixed equiv. of ECC
Same mass flow rate
Same thrust
Same total enthalpy

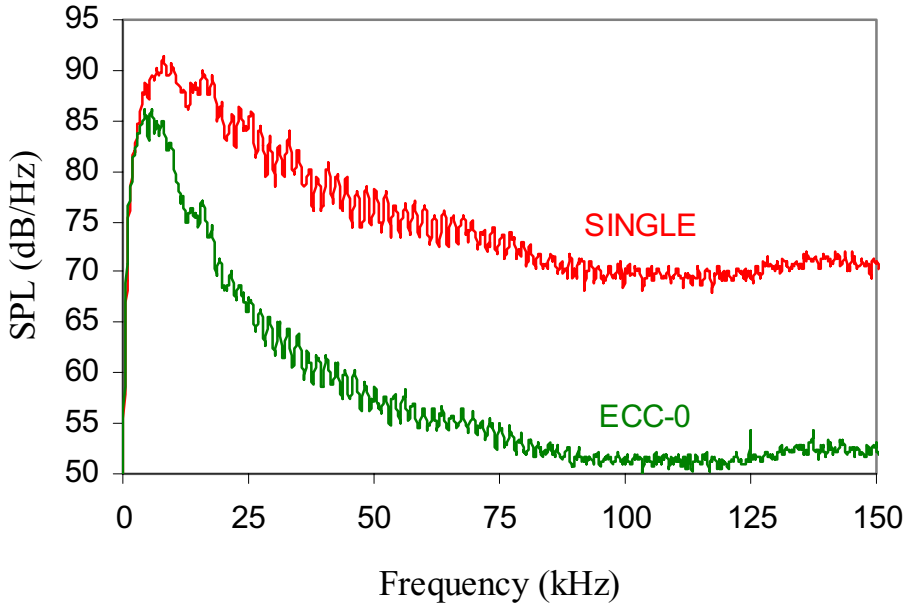


U_1=550 m/s
M_1=1.29

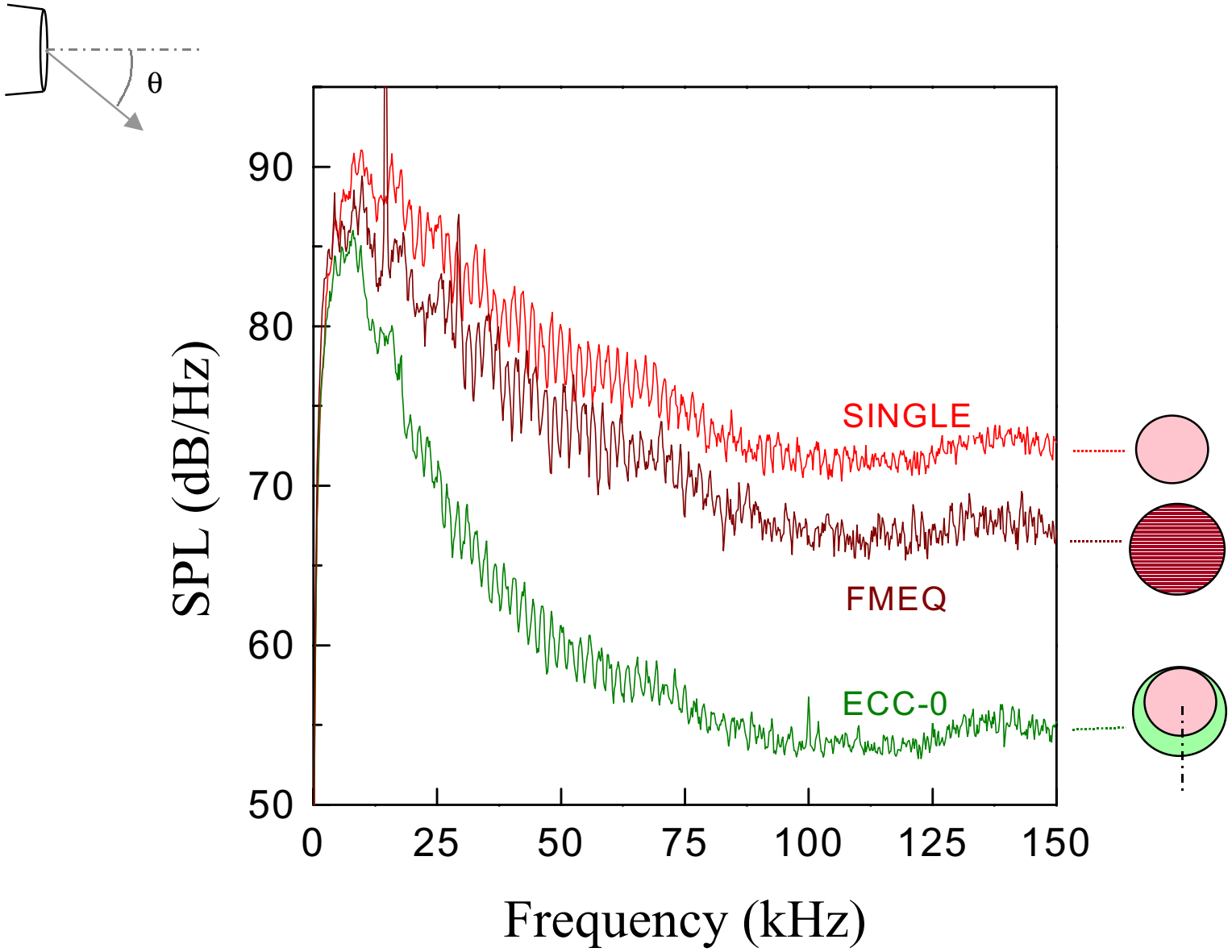
FAR FIELD NOISE SPECTRA



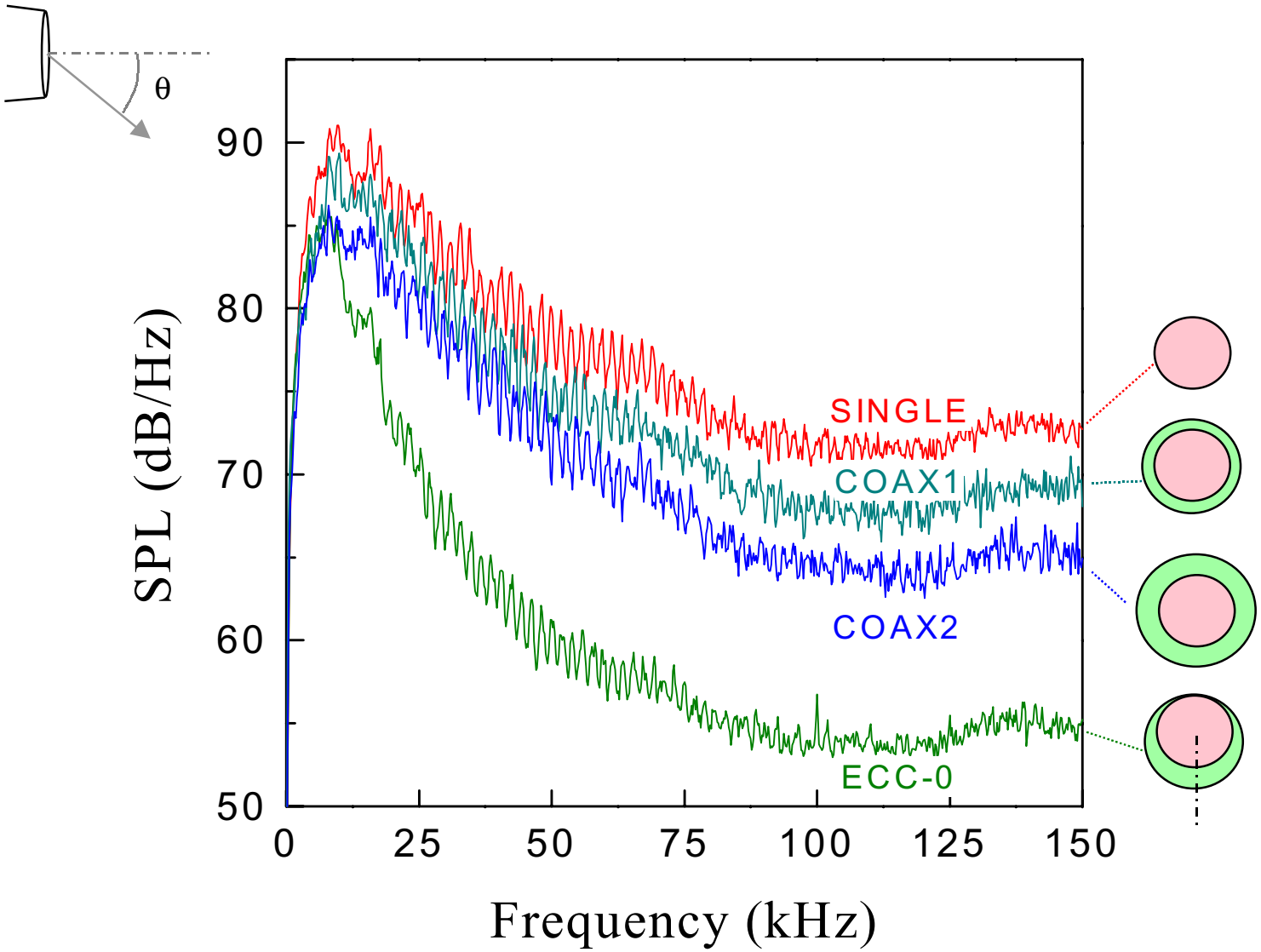




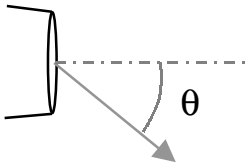
FAR FIELD SPECTRA IN DIRECTION OF PEAK EMISSION (θ =45°)

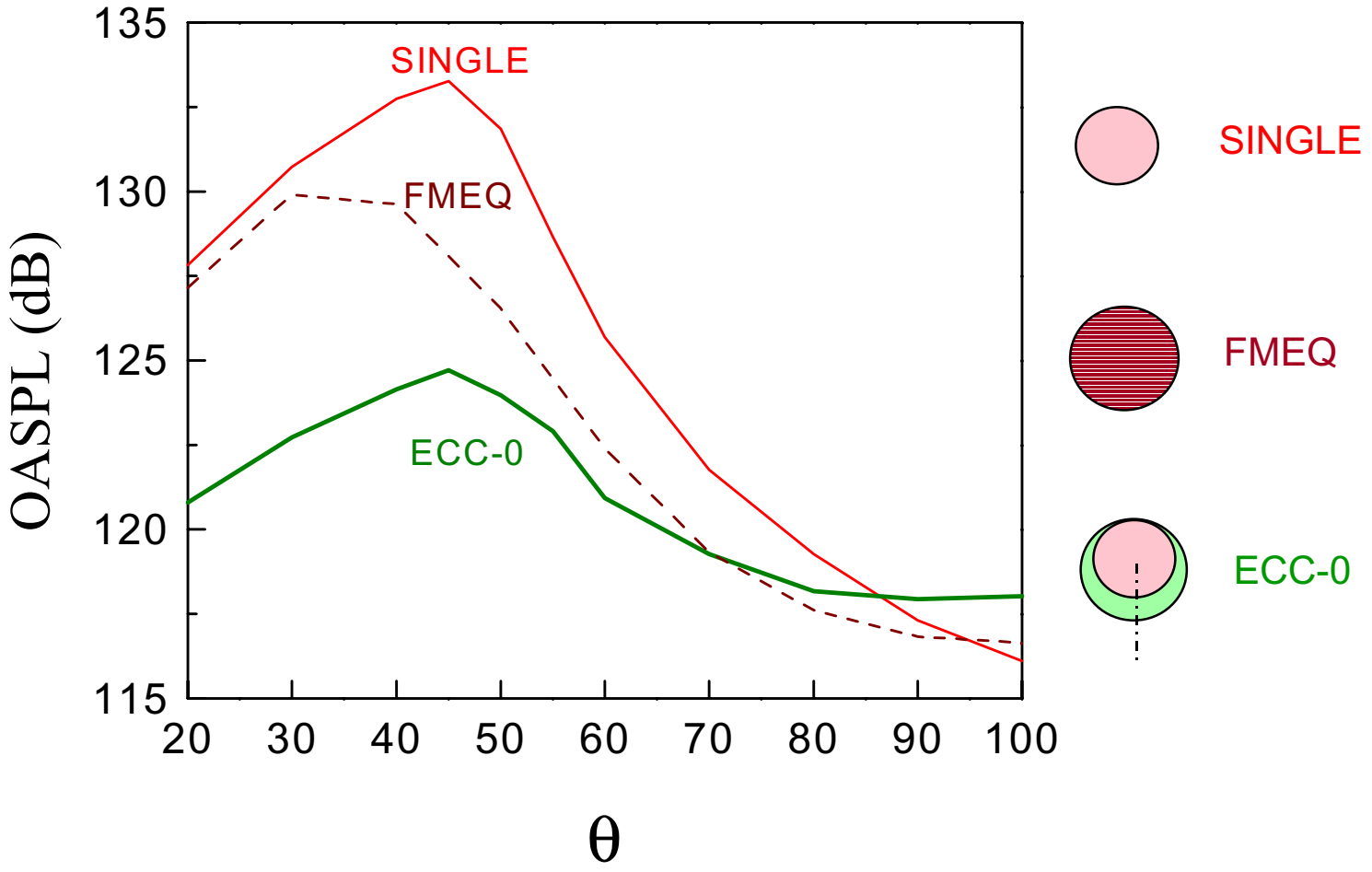


FAR FIELD SPECTRA IN DIRECTION OF PEAK EMISSION (θ =45°)

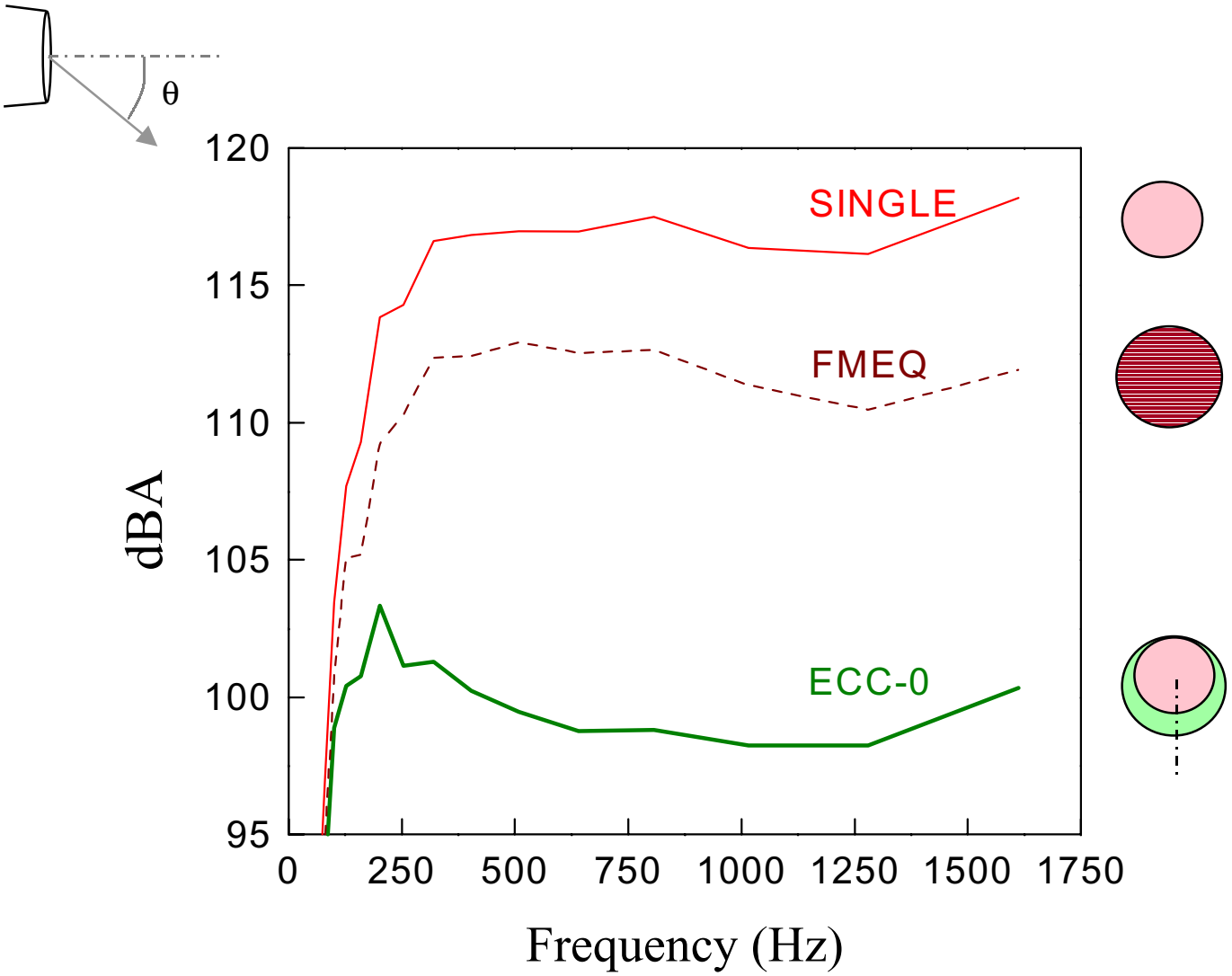


OASPL VERSUS θ

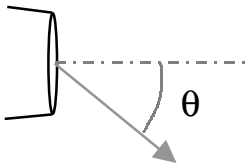


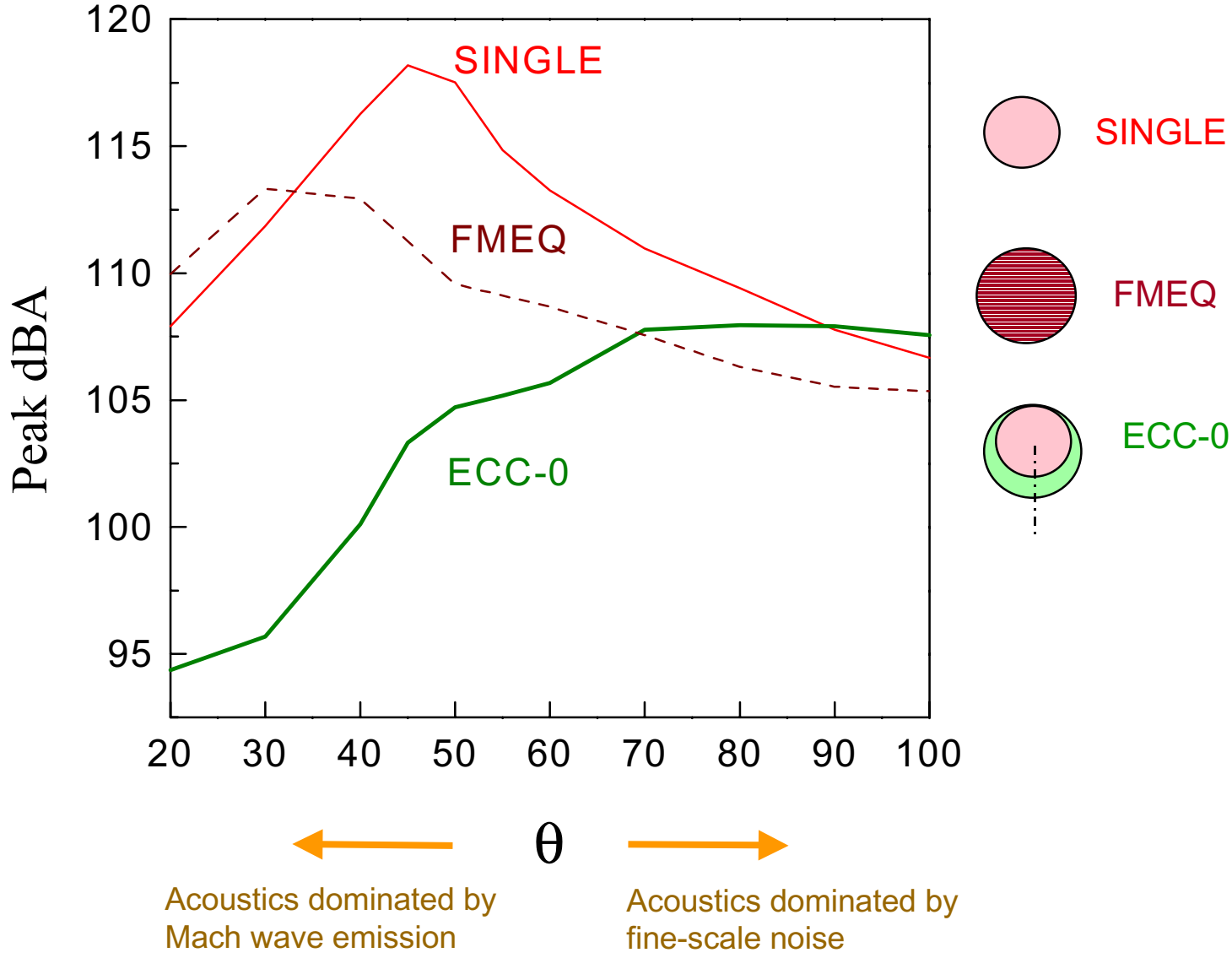


dBA SPECTRA AT θ =45°



dBA SPECTRAL PEAK VERSUS θ

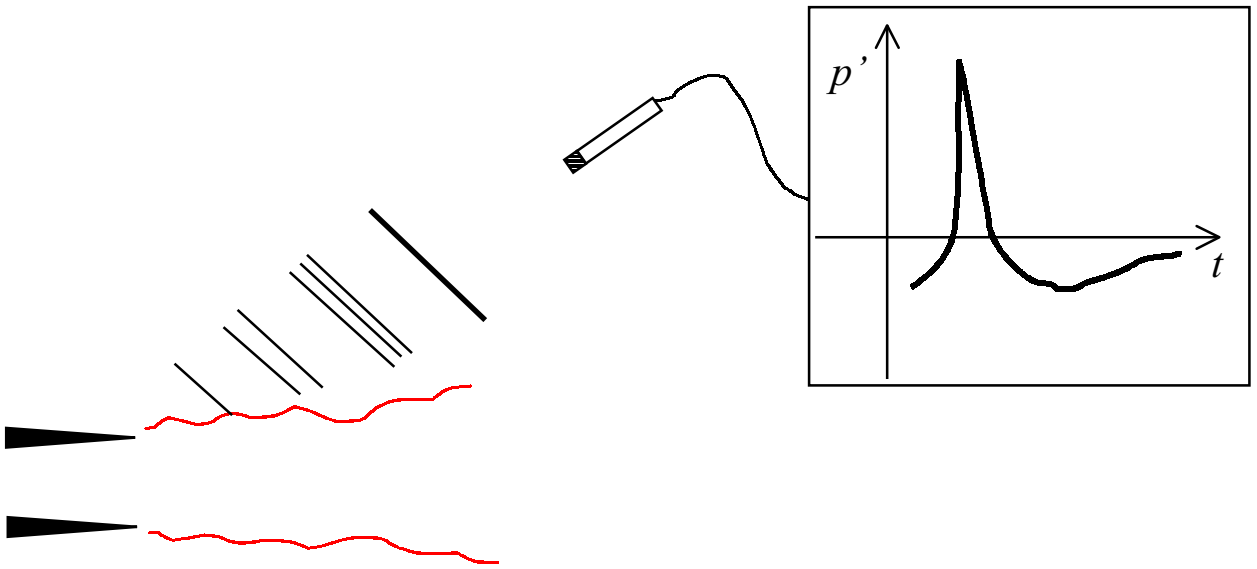




CRACKLE

An annoying component of noise arising from nonlinear wave steepening near the source

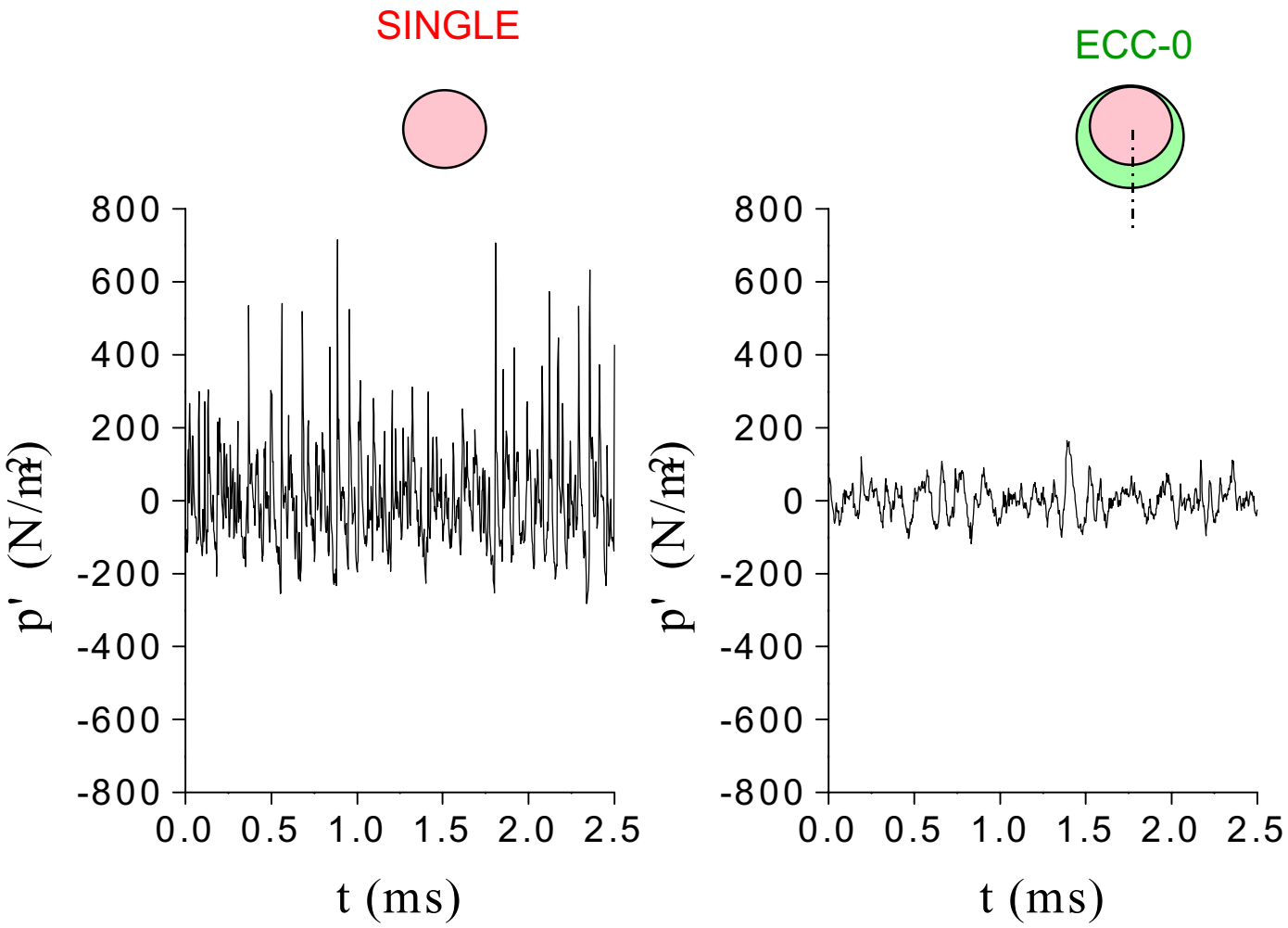
Ffowcs Williams, Simson, and Virchis, JFM 71(2), 1975



Ffowcs Williams et al. quantified crackle in terms of the PDF of the acoustic signal and the skewness of the PDF.

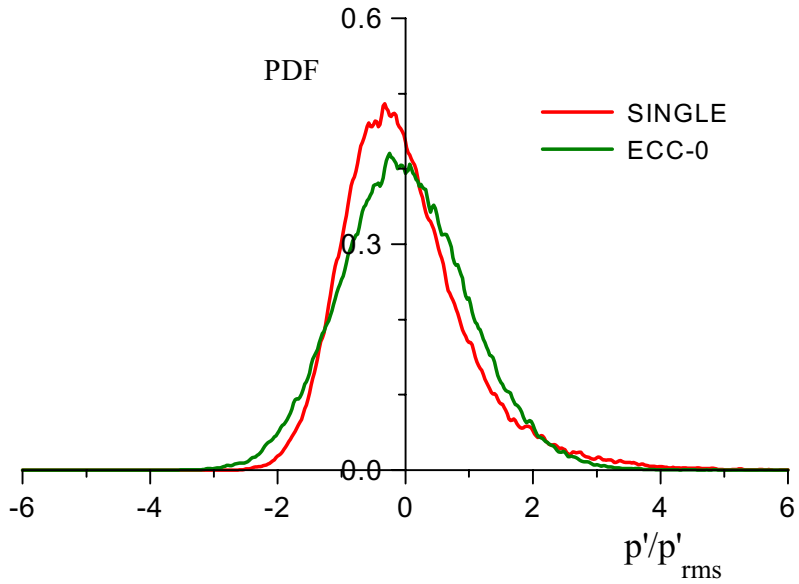
Crackle is not captured by spectra

RAW MICROPHONE TIMETRACES AT θ =45°

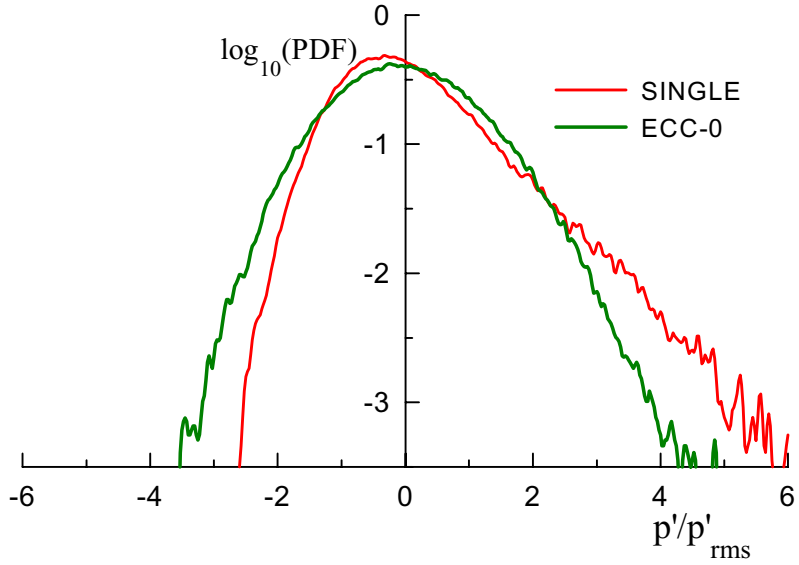


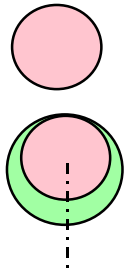
PROBABILITY DENSITY FUNCTION OF NOISE FIELD

Linear



Logarithmic





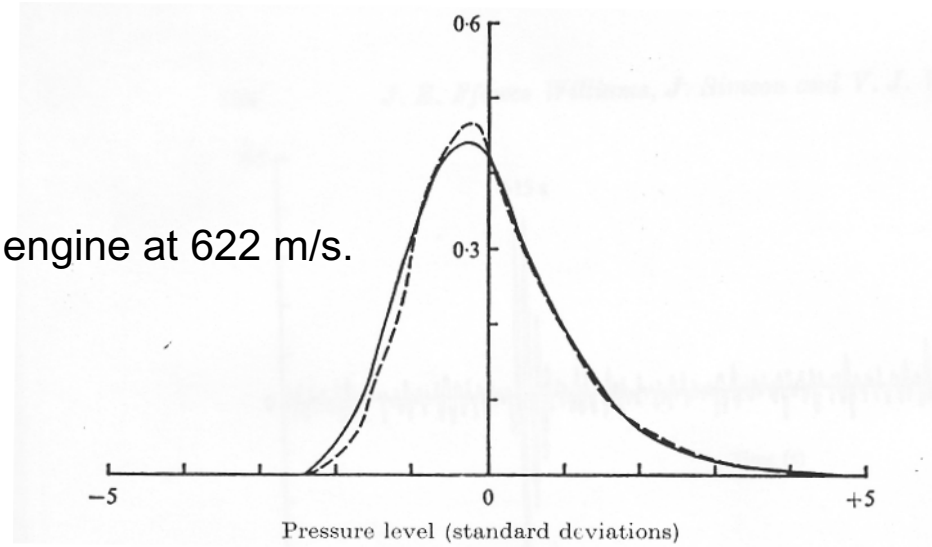
SINGLE

ECC-0

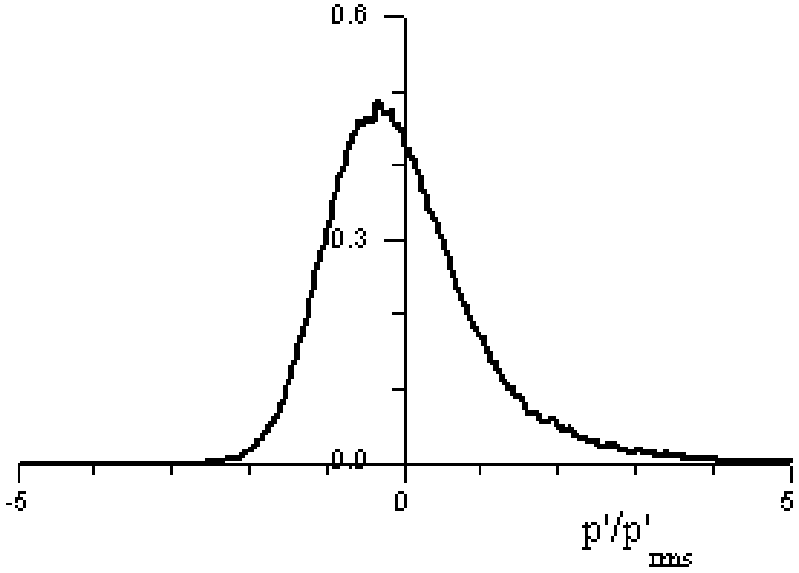
PDF COMPARISON WITH FFOWCS WILLIAMS et al. (1975)

Ffowcs Williams et al.

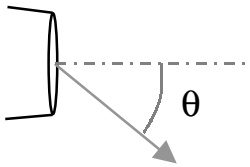
Solid line: Olympus 593 engine at 622 m/s.

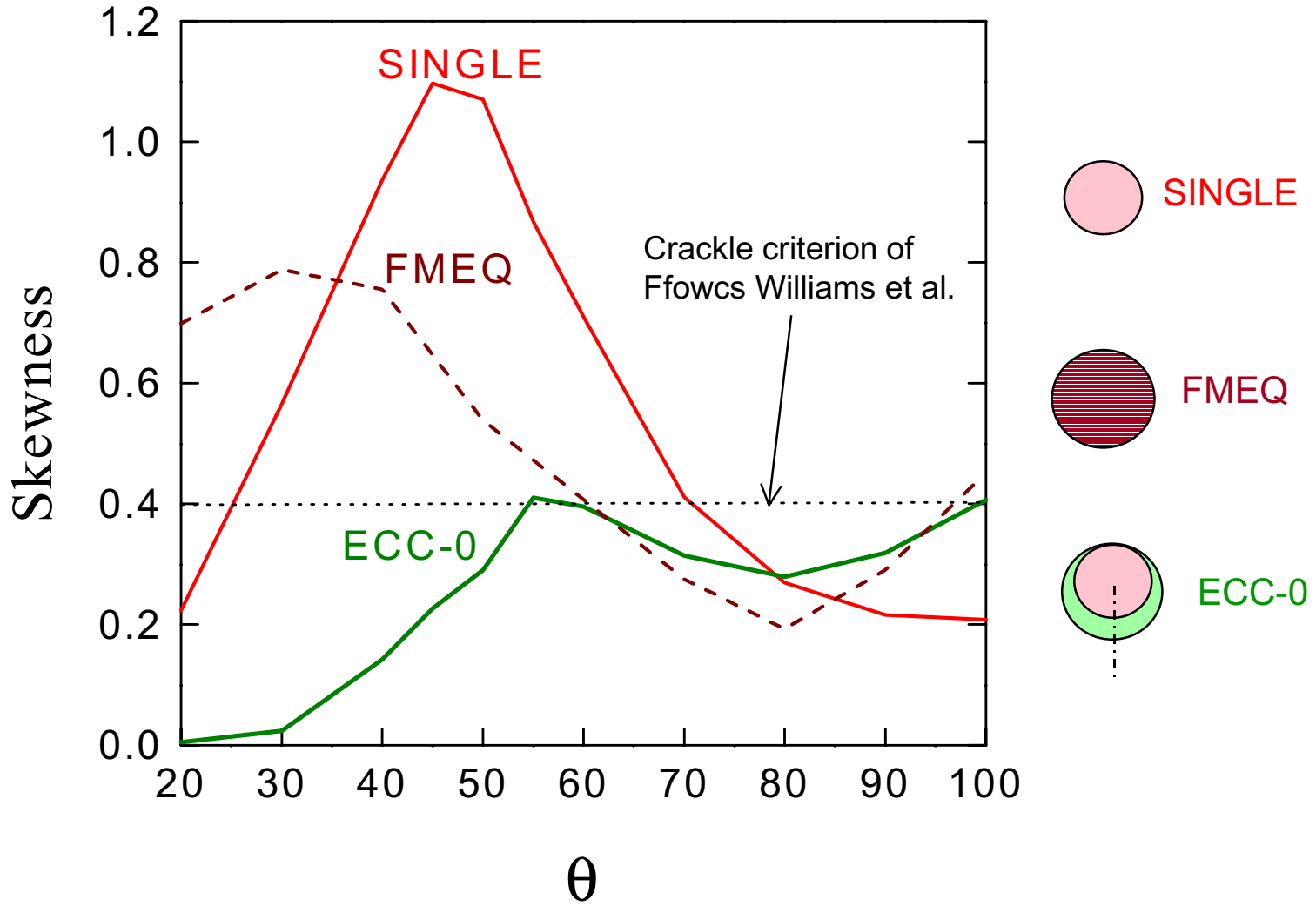


Present study (case SINGLE)



SKEWNESS OF NOISE FIELD VERSUS θ





SUMMARY

- Directional elimination of Mach waves was demonstrated with an eccentric coflow.
- Perceived noise in the aft quadrant was reduced by 15 dBA. As a result, the directivity of perceived noise changed from the aft quadrant to the lateral direction.
- The eccentric coflow suppressed crackle, an annoying component of noise not captured by spectral methods. The suppression of crackle is consistent with elimination of Mach waves.
- The eccentric arrangement was superior to coaxial arrangements and to the fully-mixed equivalent jet.
- The effectiveness of the eccentric arrangement is attributed to the reduced length of the potential core.

D. Papamoschou References

1. Papamoschou, D., "Mach Wave Elimination in Supersonic Jets," AIAA Journal, Vol. 35, No.10, 1997, pp. 1604-1611.

2. Papamoschou, D., and Debiasi, M., "Noise Measurements in Supersonic Jets Treated with the Mach Wave Elimination Method," AIAA Journal, Vol. 37, No.2, 1999, pp. 154-160.

3. Murakami, E., and Papamoschou, D., " Eddy Convection in Supersonic Coaxial Jets," AIAA Journal, Vol. 38, No.4, 2000, pp. 628-635.

4. Papamoschou, D., and Debiasi M., "Directional Suppression of Noise from a High-Speed jet" to appear in AIAA Journal, Vol. 39, No.4, 2001.

Anomalous Effect of Nozzle Length Reduction on Jet Noise of Forced Mixers

Vinod G. Mengle
Rolls-Royce, Indianapolis

NASA/CP—2001-211152

Anomalous Effect of Nozzle Length Reduction on Jet Noise of Forced Mixers

Vinod G. Mengle
Rolls-Royce, Indianapolis

Presented at
NASA/OAI Jet Noise Workshop, Cleveland, OH
Nov. 7-9, 2000

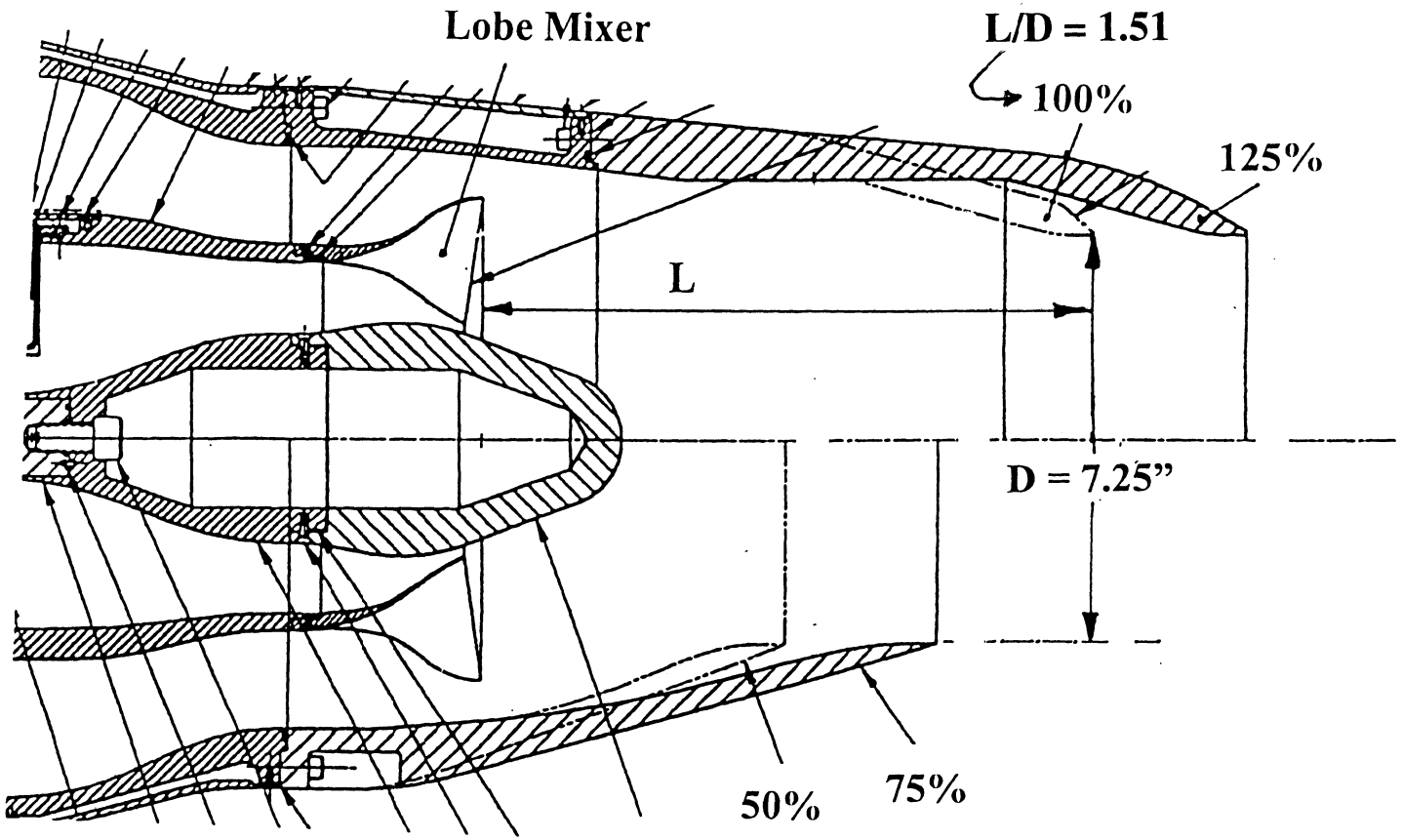
Rolls-Royce

Objectives

- Study the effect of mixing length or nozzle length variation on far-field noise of high BPR forced mixers for a wide range of jet speeds
- Provide physical mechanisms of the phenomena observed in the experimental data

Rolls-Royce

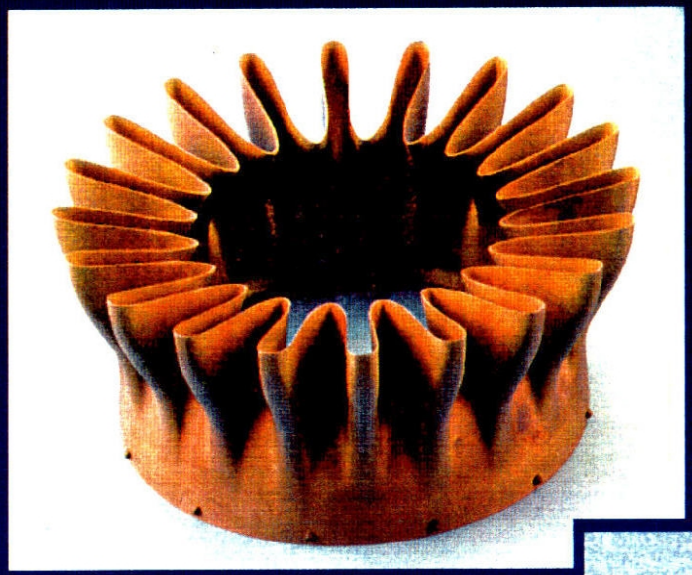
Mixer-Nozzle Model with different nozzle lengths



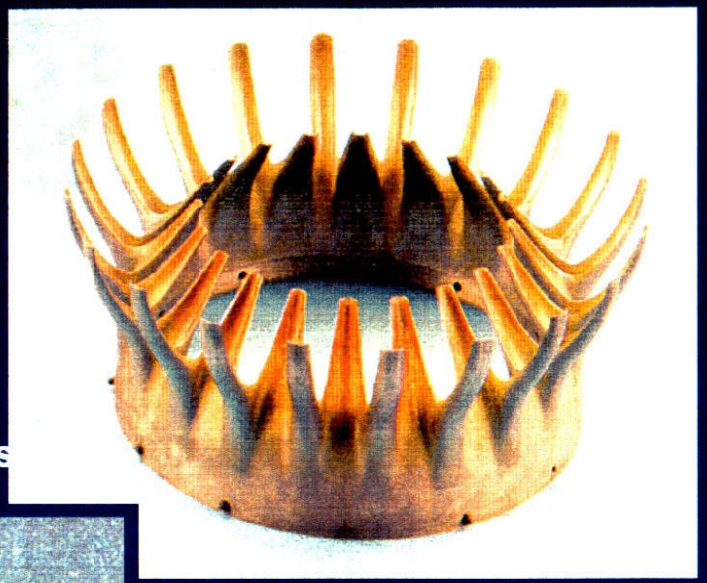
Rolls-Royce

Lobe Mixers Tested

20UH
20-Lobe Unscalloped



20DH
20-Lobe Deeply Scalloped

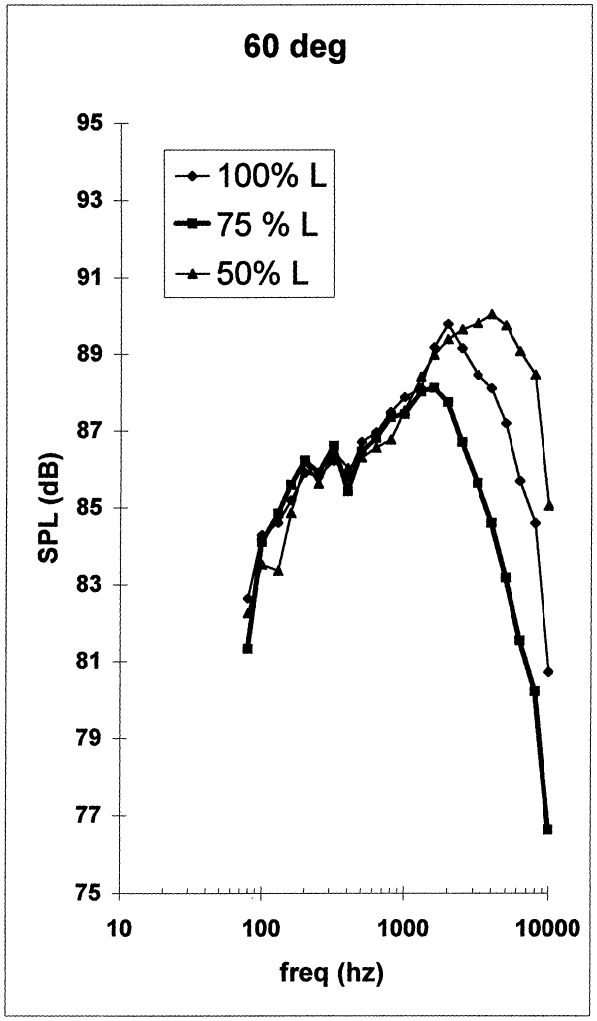


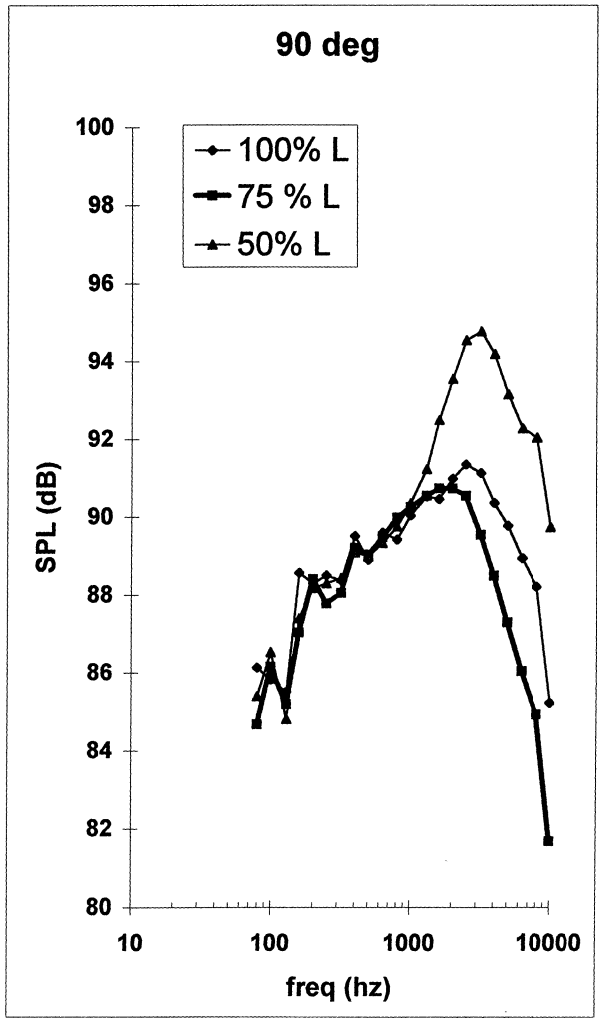
12CL
12-Lobe Mixer W/Cut-outs

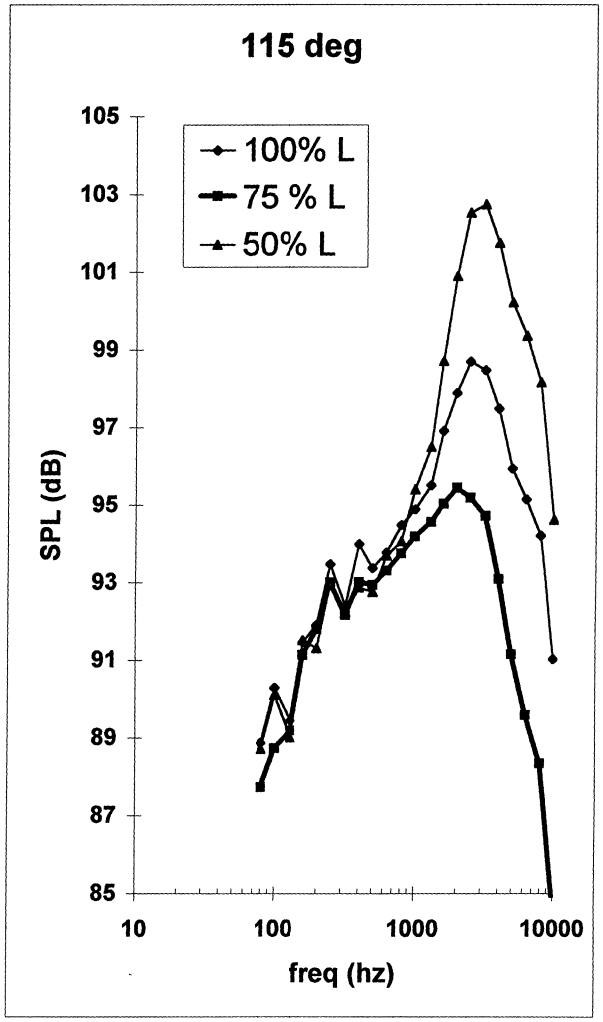


Rolls-Royce

20UH, TO #3, M_{fj} = 0.0



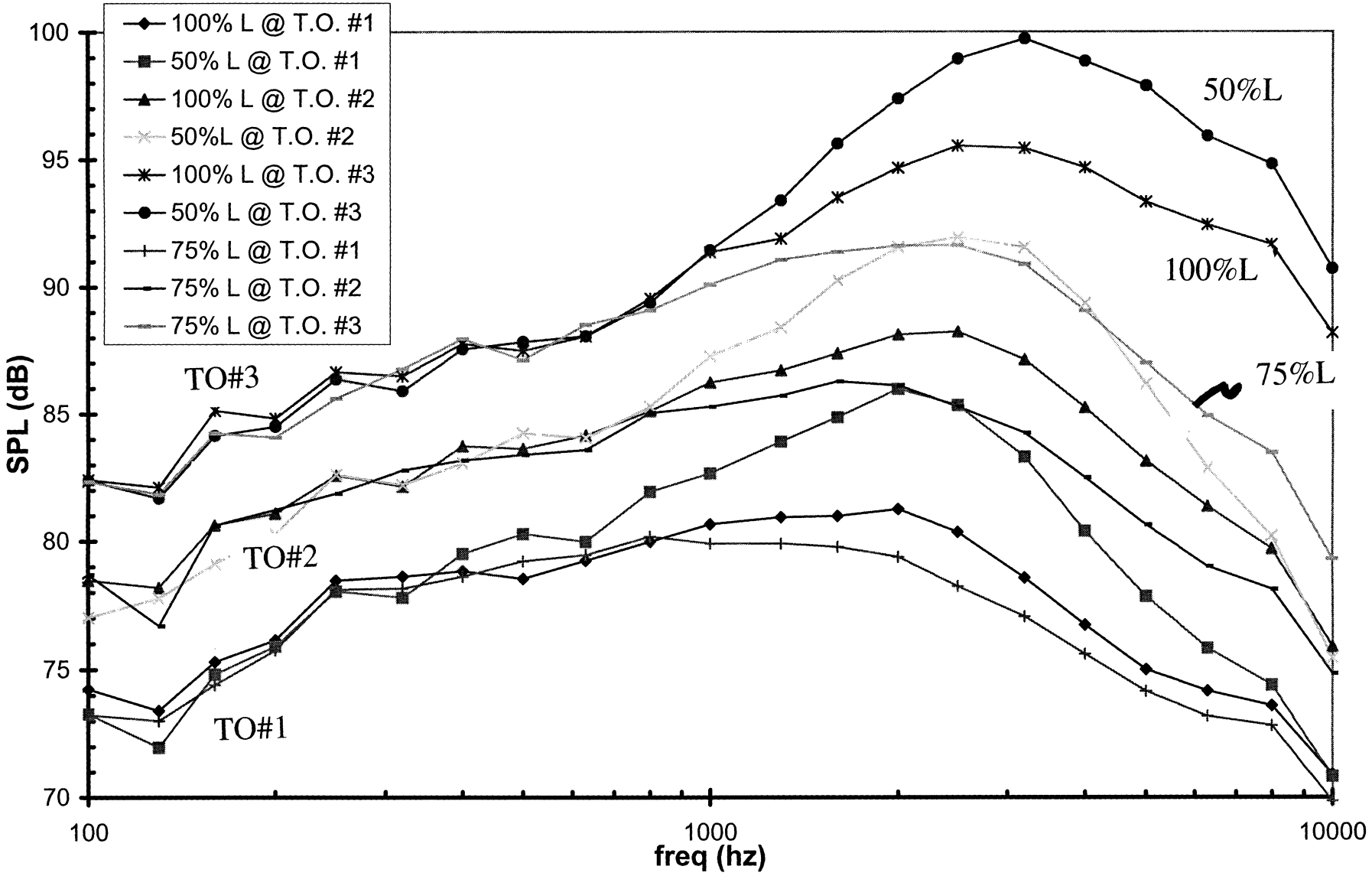




Rolls-Royce

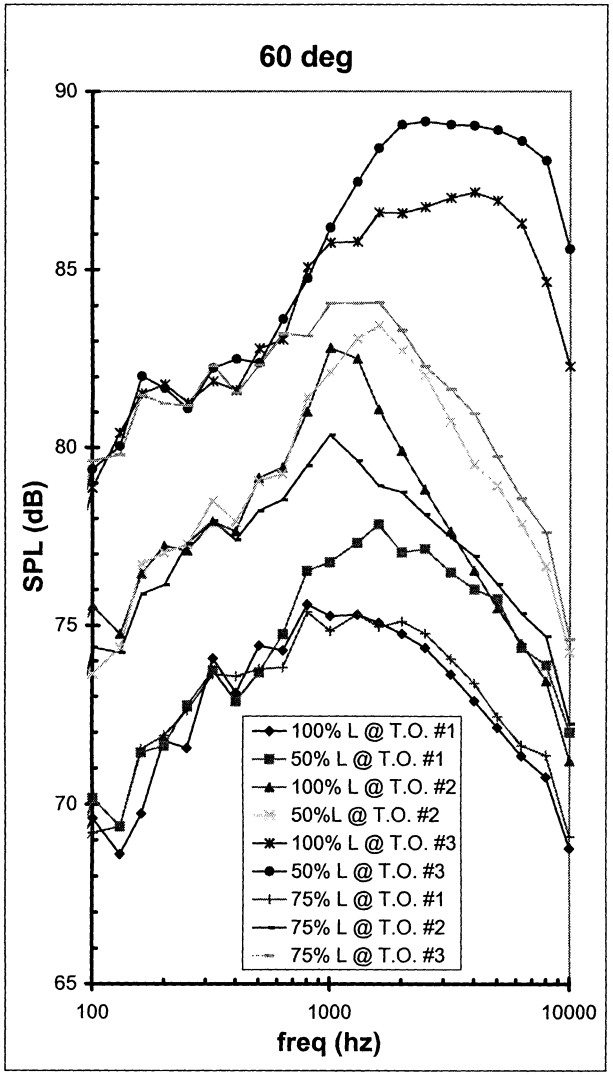
At M_{fj} = 0.0, without any external boundary layer, SPL ***reduces*** at mid-to-high frequencies when 100%L → 75%L

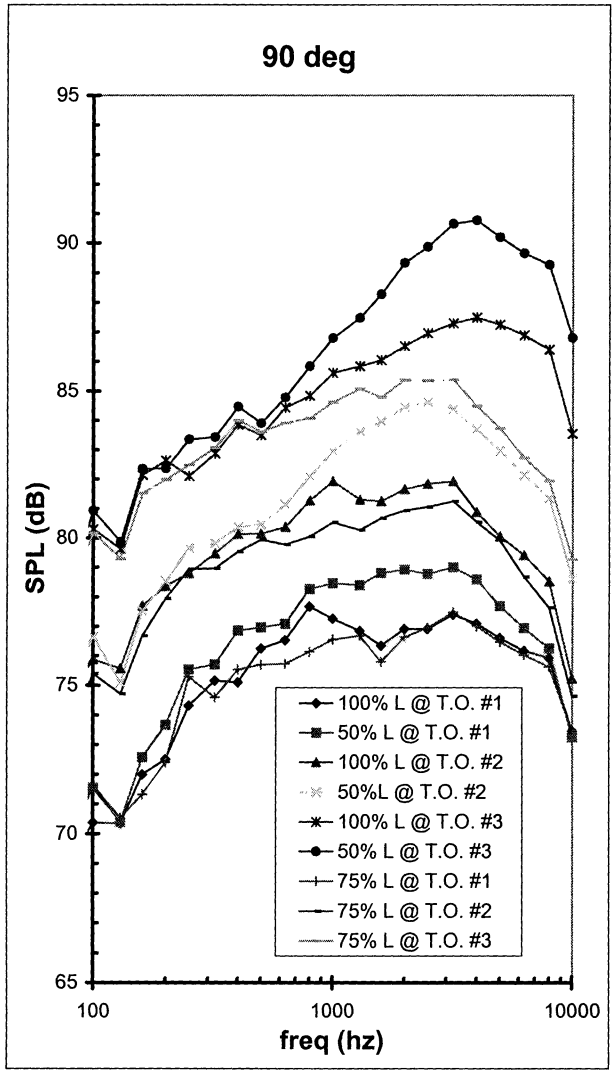
20UH, M_{fj} = 0.2, 115 deg

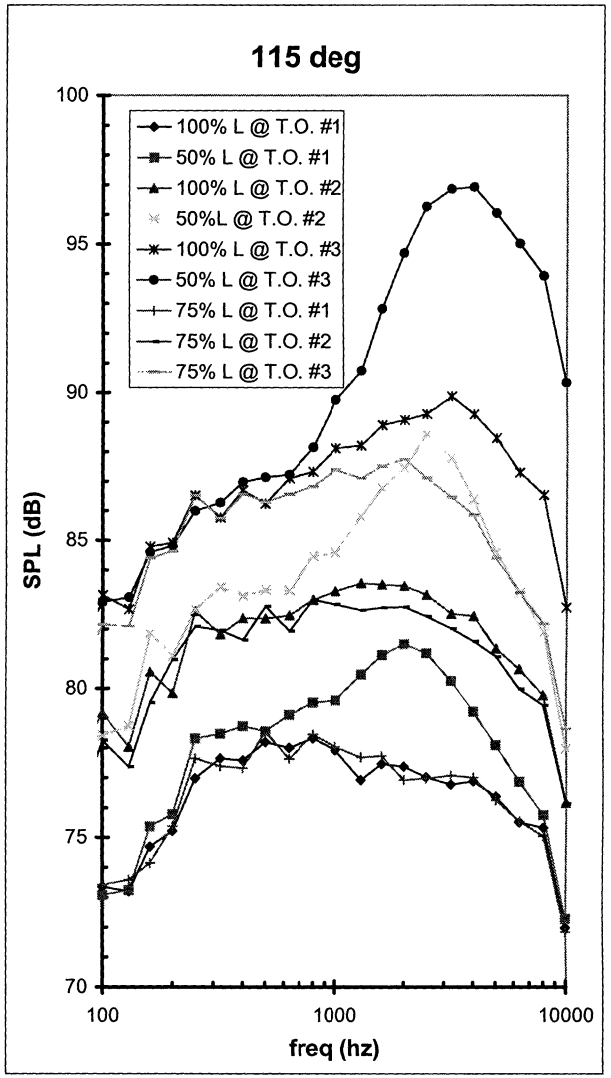


Rolls-Royce

20DH, M_{fj} = 0.2







Rolls-Royce

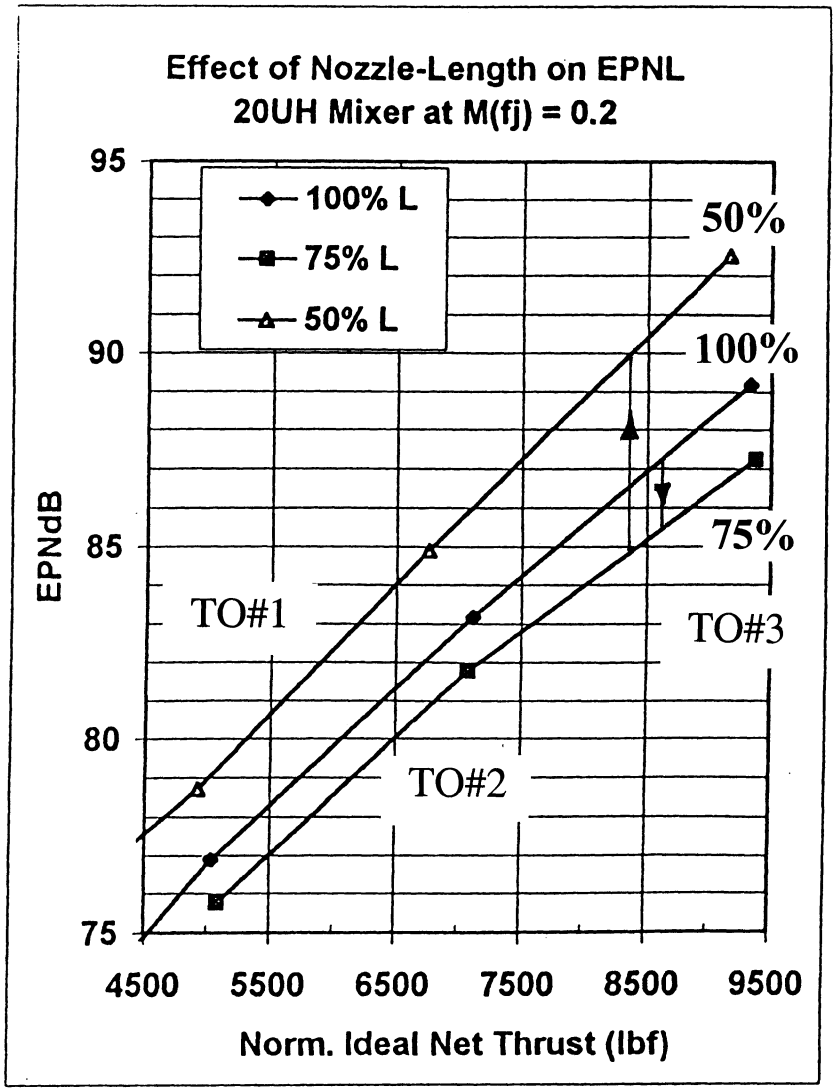
EFFECT OF NOZZLE-LENGTH REDUCTION

20UH, 1500 ft Flyover EPNL, M_{fj} = 0.2
(29 in. diam. nozzle)

Even larger effect for higher free-jet Mach numbers:

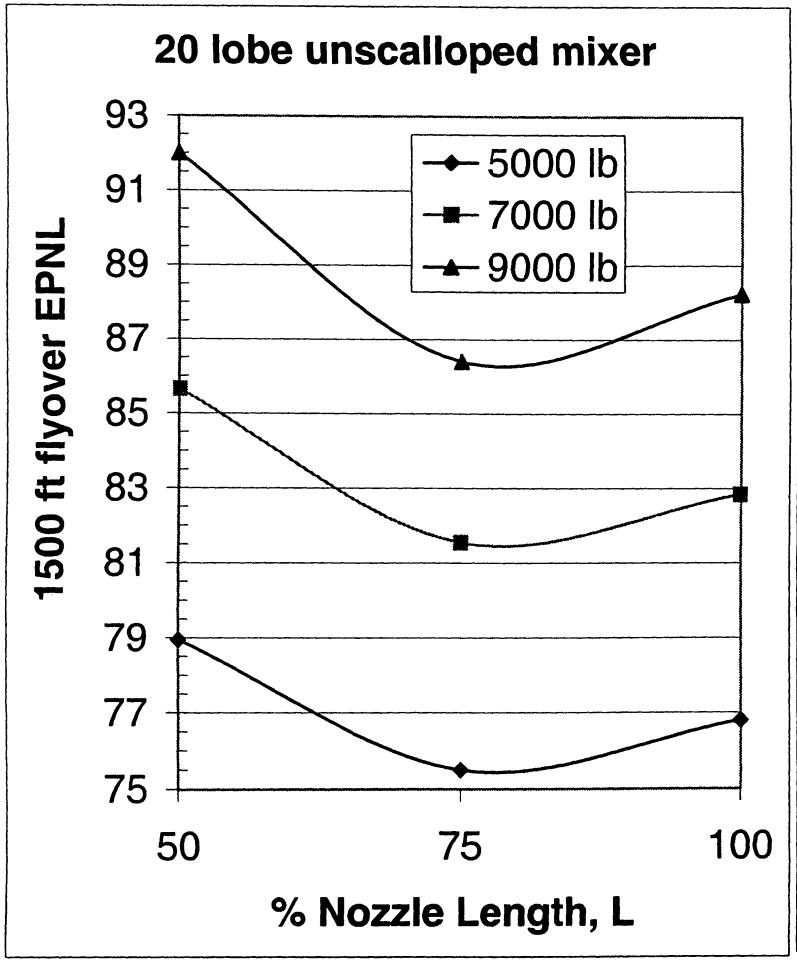
at M_{fj} = 0.3

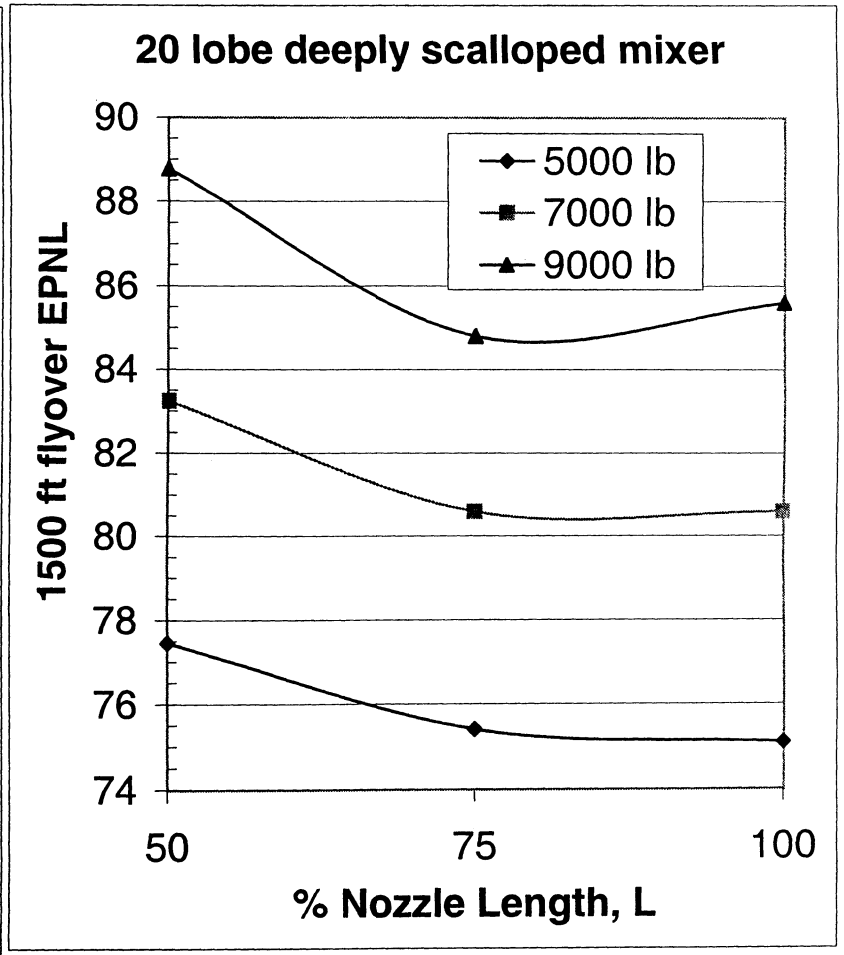
3 EPNdB max. reduction for 100%L → 75%L



Rolls-Royce

Local Minimum In Noise with Change in Nozzle Length





Rolls-Royce

Physical Mechanism

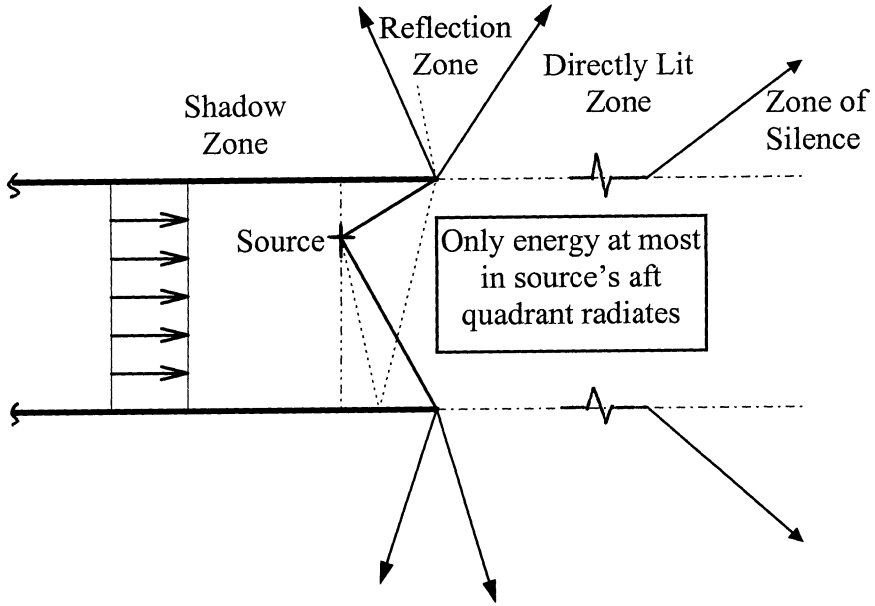
- **Low frequency did not change with ↓ L**
  - Large eddies far downstream responsible
  - Depend primarily on total mass-flow rate & nozzle diameter, which did not change with L
  - Independent of small "initial" perturbations at exit plane
  - (similar observation found for degree of lobe scalloping)

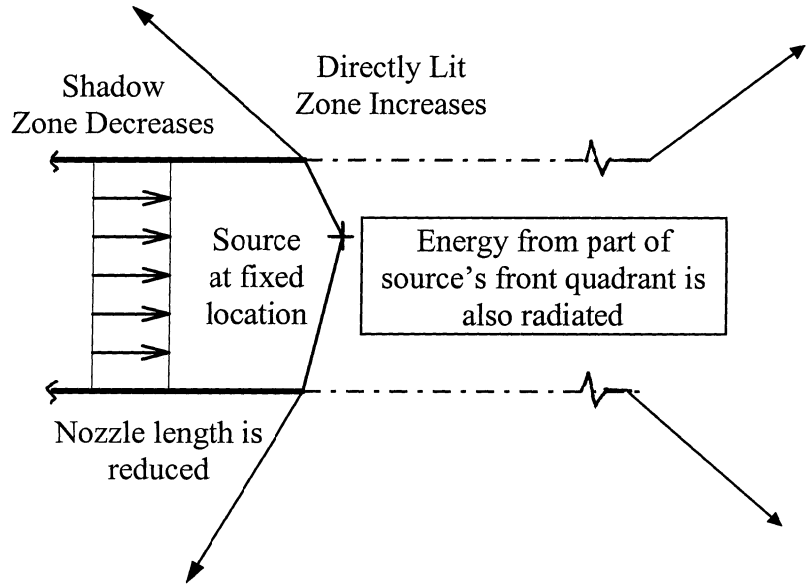
- **Intermediate to high frequency changes**
  - ↓ L ⇨ Local minimum in SPL
  - Competing mechanisms present: ↑ SPL and ↓ SPL

Rolls-Royce

Noise Increasing Mechanism

- Acoustic Unshielding:





- Secondary Mechanisms:
  - Faster flow near source if it is now in convergent portion
  - Convective amplification in downstream quadrant of nozzle

Rolls-Royce

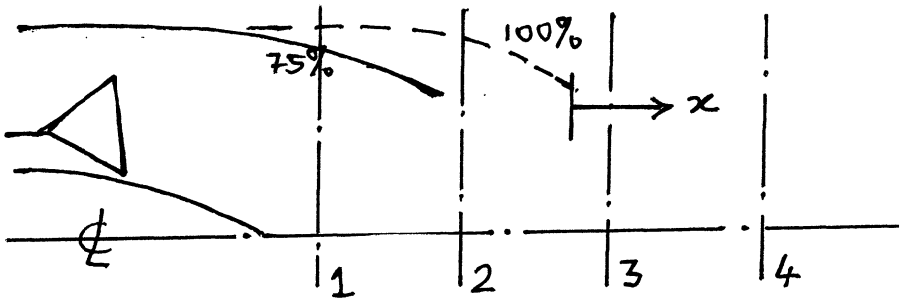
Noise Decreasing Mechanism

Aerodynamic Unshielding "Hypothesis"

- Compare sources at same distance from the mixer exit plane, not nozzle exit plane

- Streamwise vortices released to ambient pressure earlier due to ↓ L
  - ⇨ "Relief" effect, i.e., ↓ radial gradients in mean flow
  - ⇨ ↓ Turbulent velocity amplitudes which depend on those radial gradients
  - ⇨ ↓ Noise source strength
  - ⇨ ↓ Far-field SPL

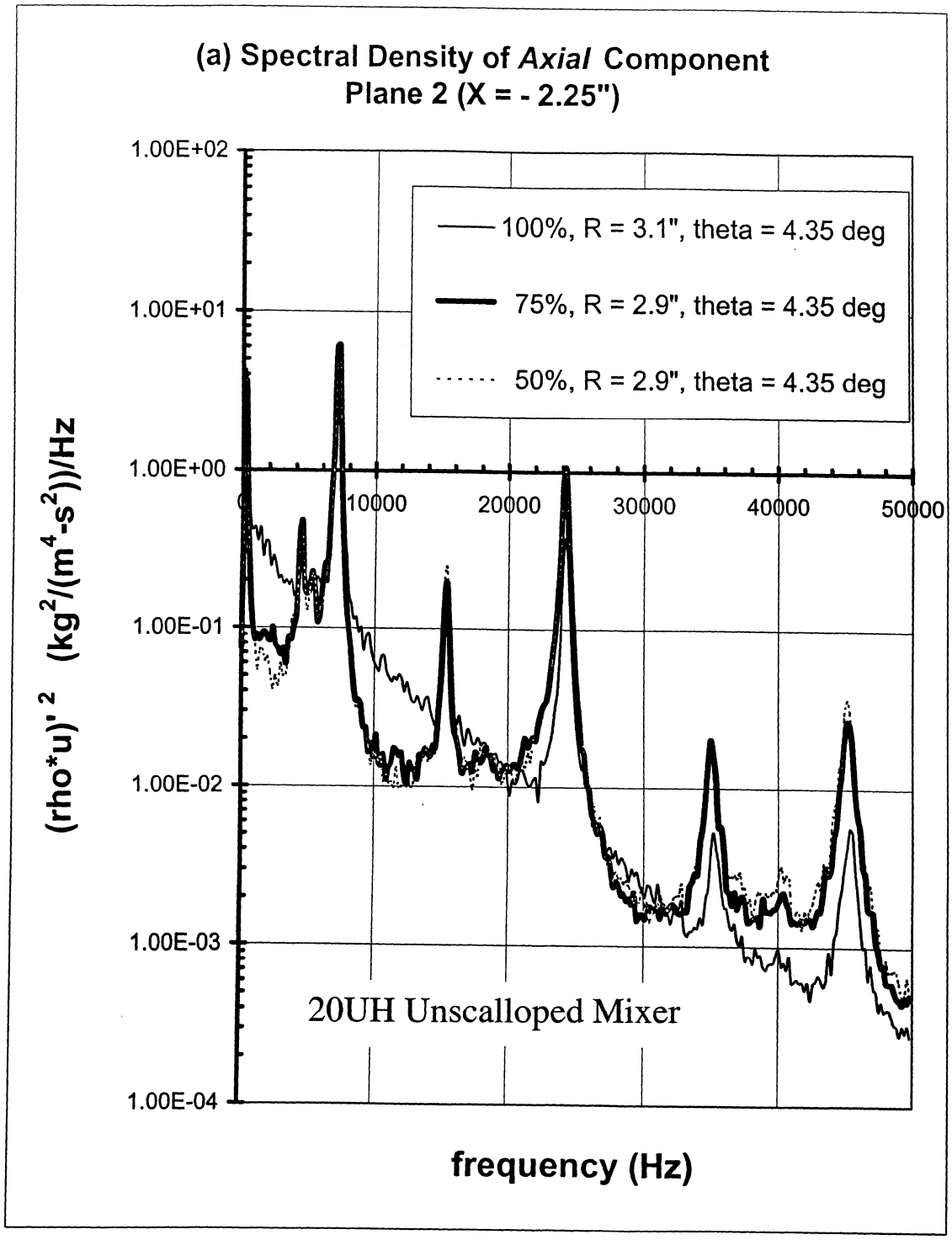
Comparison of Turbulence Spectra
- Experimental Data -



- Compared u' and v' turbulent spectra for different nozzle lengths at same axial distance from the mixer exit plane in the region of maximum turbulent intensity using hot-film at FluiDyne Labs (see next 2 charts)
- For plane 2, for a certain range of broadband frequencies where the turbulent velocities are dominant:

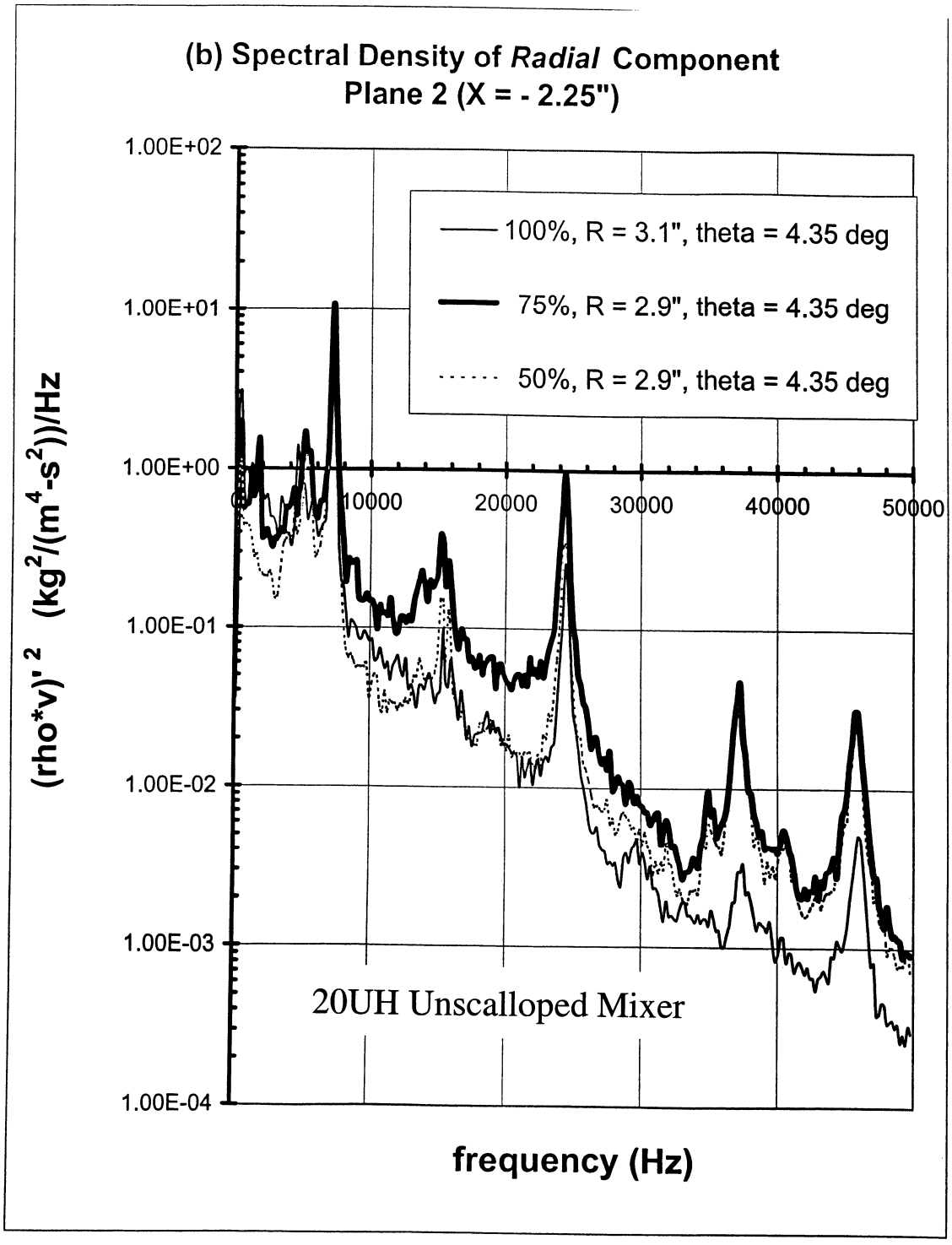
  $(\rho u)'_{75\%L} < (\rho u)'_{100\%L}$ but $(\rho v)'_{75\%L} > (\rho v)'_{100\%L}$
- This is consistent with the axial stretching of vortices at throat for 75%L
- But for plane 3: $(\rho u)'_{75\%L} < (\rho u)'_{100\%L}$ $(\rho v)'_{75\%L} < (\rho v)'_{100\%L}$
- This is a partial verification of the hypothesis in Mengle (1999)

Rolls-Royce



Compare the broadband features.
(The spikes are most likely a spurious phenomenon due to the use of hot-film anemometer rather than hot-wire.)

Rolls-Royce



Compare the broadband features.
(The spikes are most likely a spurious phenomenon due to the use of hot-film anemometer rather than hot-wire.)

Rolls-Royce

References

- Mengle, V. G. (1999): Anomalous effect of nozzle length reduction on jet noise of forced mixers. AIAA Paper 99-1968. (The work presented here is partially based on this paper.)

V. G. Mengle References

1. Mengle, V. G., Shin, H-W., Askew, J., Whitfield, C.E. (1992): *Aero-Performance and Aero-Mixing Tests of 2D-CD Mixer/Ejector Nozzles. Part II. Sample of Aero-Mixing Test Data & Inferences.* Paper No. 1, 1st NASA/Industry High Speed Research Program Nozzle Symposium, NASA CP (to be numbered), pp. 3-23 to 3-35, Nov. 17-19, 1992.

2. Mengle, V. G., Shin, H-W., Whitfield, C. E., Wisler, S., Askew, J. (1992*): Acoustic and Aero-Mixing Tests of Fluid-Shield Nozzles. Part II - 2D Fluid-Shield Nozzle Aero-Mixing Tests.* Paper No. 2, 1st NASA/Industry High Speed Research Program Nozzle Symposium, NASA CP (to be numbered), pp. 4-21 to 4-28, Nov. 17-19, 1992.

3. Salikuddin, M., Brausch, J., Mengle, V. (1992): *Acoustic and Aero-Mixing Tests of Fluid-Shield Nozzles. Part I -Acoustics.* Paper No. 2, 1st NASA/Industry High Speed Research Program Nozzle Symposium, NASA CP (to be numbered), pp. 4-1 to 4-19, Nov. 17-19, 1992.

4. Mengle, V. G. (1995*): Acoustic Duct Waveguide Modes Excited by an Axially Convecting Noise Source in Sheared Flow*. 1st NASA Advanced Subsonic Technology Engine Noise Workshop Proceedings, Session 2: Jet Noise, pp. 269-284, Dec. 12-14, 1995.

5. Mengle, V. G., Dalton, W. N., Bridges, J., Boyd, K. (1997): *Noise Reduction with Lobed Mixers - Nozzle Length and Free-Jet Speed Effects.* AIAA Paper No. 97-1682. 18th AIAA Aeroacoustics Conference, May 10-14, 1997.

6. Mengle, V. G. (1997): *Certain Limitations and Extensions of MGB Jet Noise Computer Code.* NASA Advanced Subsonic Technology "MGB Jet Noise Prediction Workshop" Proceedings, Sept. 9, 1997.

7. Janardan, B.A., Hoff, G.E., Barter, J.W., Martens, Gliebe, P. R., Mengle, V. and Dalton, W.N. (1998*): Separate-Flow Exhaust System Noise Reduction Concept Evaluation.* Final Report, NASA Contract NAS3-27720, GE Report No. R98AEB152, May 1998. NASA CR (to be numbered).

8. Mengle, V. G., Dalton, W. N.(1998): *Lobed Mixer Design for Noise Suppression. Vol. 1 - Acoustic and Aerodynamic Test Data Analysis.* Final Report, NASA Contract NAS3-27394, Task Order No. 6, Rolls-Royce EDR No. 18580, July 1, 1998, NASA CR (to be numbered), 298 p.

9. Mengle, V. G., Baker, V. D., Dalton, W. N. (1998): *Lobed Mixer Design for Noise Suppression. Vol. 2 - Plume, Aerodynamic & Acoustic Data.* Final Report, NASA Contract NAS3-27394, Task Order No. 6, Rolls-Royce EDR No. 18581, July 1, 1998. NASA CR (to be numbered), 629 p.

10. Mengle, V. G. (1999): *Jet Noise Reduction by Lobed Mixers with Boomerang Scallops*. AIAA Paper No. 99-1923, 5th AIAA/CEAS Aeroacoustics Conf., May 10-12, 1999.

11. Mengle, V. G. (1999): *Anomalous Effect of Nozzle Length Reduction on Jet Noise of Forced Mixers*. AIAA Paper No. 99-1968, 5th AIAA/CEAS Aeroacoustics Conf., May 10-12, 1999.

12. Mengle, V. G. (1999): *Finding Excess Noise in Internally-Mixed Jets by Varying Free-Jet Speed*. AIAA Paper No. 99-1967, 5th AIAA/CEAS Aeroacoustics Conf., May 10-12, 1999.

13. Mengle, V. G. (2000): *Optimization of Lobe Mixer Geometry and Nozzle Length for Minimum Jet Noise*. AIAA Paper No. 2000-1963, 6th AIAA/CEAS Aeroacoustics Conf., June 12-14, 2000.

14. Mengle, V. G. (2000): *Finding Internal Excess Jet Noise Source Characteristics by Varying Free-Jet Speed*. NASA/OAI Jet Noise Workshop, November 7-9, 2000, NASA CP (to be numbered).

15. Mengle, V. G. (2000): *Vorticity Dynamics and Its Relation to Jet Noise Reduction in Chevrons*. NASA/OAI Jet Noise Workshop, November 7-9, 2000, NASA CP (to be numbered).

16. Mengle, V. G. (2000): *Anomalous Effect of Nozzle Length Reduction on Jet Noise of Forced Mixers*. NASA/OAI Jet Noise Workshop, November 7-9, 2000, NASA CP (to be numbered).

17. Mengle, V. G. (2001): *Tongue Mixer - A New Concept for Jet Noise Reduction*. (Submitted for presentation at the 7th AIAA/CEAS Aeroacoustics Conf., May 28-30, 2001).

18. Mengle, V. G. (2001): *Duct Waveguide Mode Excitation by Sound Sources Convecting in Sheared Flows*. (Submitted for presentation at the 7th AIAA/CEAS Aeroacoustics Conf., May 28-30, 2001).

SESSION 4: ROLE OF CAA FOR JET NOISE PHYSICS

Summary by Eugene Krejsa, Consultant

This session consisted of three invited presentations and several presentations during the discussion.

INVITED PRESENTATIONS

***CAA for Jet Noise Physics: Issues and Recent Progress* - Sanjiva K. Lele, Stanford University**

Dr. Lele presented an overview of issues and recent progress in CAA for jet noise. He summarized the issues in jet noise physics, including issues on which there is general agreement and those where there are diverse opinions. Also summarized were the variety of physical aspects of jet noise and the variety of possible jet noise mechanisms.

The major computational issues in the use of CAA to compute the noise from jets are the disparity in length scales and amplitudes, the need for accurate treatment of unsteady shocks, and the critical need for "quiet" boundaries (i.e. boundary conditions that are both non-reflecting and that are not sources of noise as disturbances pass through them). Examples of recent progress in jet noise prediction, based on model problems were presented. Results from analyses using DNS, linearized Euler, and LES were also presented. Good agreement with data was achieved.

Other computational issue addressed were those in regard to grid requirements, inflow forcing functions, flow and sound statistics, boundary conditions, high-resolution schemes for complex domains, interaction of shocks with other disturbances, high-resolutions methods for LES, hybrid methods for prediction of radiated noise.

Dr. Lele concluded his presentation with the following summary of where we go from the current status in CAA:

- Develop better understanding of jet noise physics with CAA.
- Benchmark databases for developing hybrid noise prediction method. Subgrid noise models, approximate methods for flow-noise interaction
- Better aerodynamic and aeroacoustic design. Mixing optimization for noise reduction.

CAA for Jet Noise Physics: Issues and Recent Progress

Sanjiva K. Lele
Stanford University

NASA/CP—2001-211152

CAA for Jet Noise Physics: Issues and Recent Progress

Sanjiva K. Lele

lele@stanford.edu
Stanford University

Acknowledge
George Constantinescu, Stanford/CTR
Bendiks Jan Boersma, Delft
Ted A. Manning, Stanford
Jonathan B. Freund, UCLA
Tim Colonius, Caltech
Parviz Moin, Stanford
Brian Mitchell, GE

Jet Noise Workshop, Ohio Aerospace Institute, November 7-9, 2000.

NASA/CP—2001-211152

Outline

- Issues in Jet Noise Physics
- Computational Issues in CAA for Jet Noise
- Some Examples of Recent Progress
  - ⋆ Noise-sources in an unsteady shear layer (Colonius, Lele & Moin)
  - ⋆ DNS of Jet Noise (Freund et. al., Freund)
  - ⋆ Screech Generation (Manning & Lele)
  - ⋆ LES for Jet Noise (Constantinescu & Lele)
- Of things to come
- Closure

Issues in Jet Noise Physics

It is agreed that

- Jet turbulence is the noise source
- Jet turbulence has broadband spatial and temporal distribution
- Jet turbulence has quasi-organized and irregular components
- Jet flow is a 'tuned' amplifier of instability waves
- Jet noise is a small by-product of the flow

Views on Jet Noise Mechanism

Organized large scale

- Dominant noise source: Turbulence dynamics vs. Instability wave dynamics
  Instability wave dynamics → low frequency noise source
  Turbulence dynamics → high frequency noise source

How to decompose the dynamics at different interacting scales ?

Can the flow be separated into turbulent eddies & (instability) waves packets

Issues in Jet Noise Physics (contd.)

- Jet Noise source Mechanisms

  Unsteady momentum exchange between fluid lumps
  → Lighthill quadrupoles,
  and generalization to transversely-sheared flow

  Unsteady heat exchange between fluid lumps
  → dipole and multipoles (Morfey, Lilley)

  Fine-scale turbulence noise due to 'turbulence pressure' (Tam)

  Spatial Modulation of instability wave amplitude (Crighton, Tam, Morris)
  subsonic or supersonic jets

  Supersonic instability waves - Mach wave radiation (Tam)

  Supersonically convected eddies
  with finite spatial scale and finite life-time
  → Eddy Mach-wave emission (Ffowcs Williams)

Issues in Jet Noise Physics (contd.)

- Spatial distribution of source strength (at a given frequency)
- Fixed vs. moving sources (Doppler factors)
- Mean flow refraction/shielding
- Intermittancy of strong noise emission
- Flow/turbulence management for noise reduction

- Jet Noise source Mechanisms (Contd.)

'Crackle' in very high speed jets
(Ffowcs Williams)

Interaction of turbulence with shock-cell structure
(Broadband shock-associated noise)
Harper-Bourne and Fisher; Tam and Tanna; Tam, Jackson and Seine

Interaction of instability waves with shock-cell structure
(Jet Screech)
Powell; Tam; Kerschen & Cain; Manning & Lele

Other jet resonance phenomena
(Edge tones, Impingment tones, etc.)

Computational Issues Particular to Jet Noise

Example: Laboratory Jet (cold) with $D_j = 2.5$ cm. at $M_j = 0.9$
$U_j = 290$ m/s, $Re_D = 600,000$

In mixing region: (Davies, Fisher & Barratt, 1963, JFM)
$L_x/D_j = 0.13x/D_j$ (integral scale), $U_c/U_j \approx 0.65$
$\tau_L \approx 4.5/\frac{\partial U}{\partial r}$ (Lagrangian time scale)
$u'\tau_L/L_x = 0.9$, $u'/U_j = 0.14$ (Bradshaw, et. al. 1964, JFM
$U_c\tau_L/L_x = 4.1$

- At $x/D_j = 2$: $Re_L \equiv u'L_x/\nu \approx$ 22,000!
- At 90°, $St_D = 0.3 \rightarrow f_0 = 3.5$ kHz $\rightarrow \lambda_0/D = 3.7$
- $f_pD/C_\infty = 0.16$ (Lush, Tanna)$\rightarrow f_p = 2$ kHz $\rightarrow \lambda_p/D = 6.25$

- At $x/D = 2$: $\lambda_0/L_x = 14$, $\lambda_p/L_x = 24$ 'compact' eddy

- In mixing region (locally): $\lambda(x) \sim C_\infty\tau_L(x)$
$\lambda(x)/L_x(x) \approx 7$ $\lambda(x)/(C_\infty\tau_L(x)) \approx 1.5$ Not compact

NASA/CP—2001-211152

Key Computational Issues in Computational Aeroacoustics

- Disparity in length scales, disparity in amplitudes
- Amplitude and Phase accuracy
  (low dispersive and dissipative errors)
- Accurate treatment of unsteady shocks, discontinuities
- 'Quiet' Boundary conditions
  (Inflow, Outflow of non-acoustic disturbances,
  non-reflecting for sound, Induced potential flow)
- Prediction of radiated sound
  (non-compact sources, spatially extensive sources,
  scattering from bodies and sharp edges, resonators,
  interaction with non-uniform background flow)

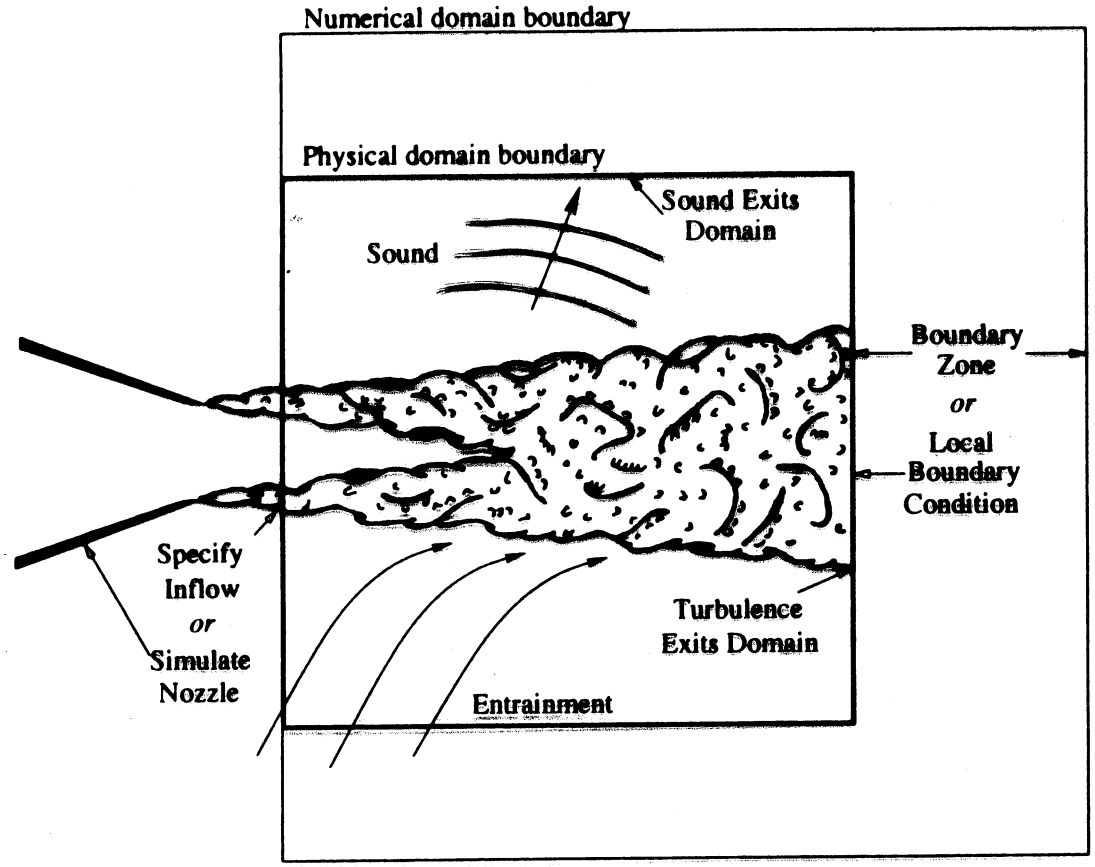


Figure 3: Computational domain schematic illustrating boundary condition issues.

From: Freund & Lele (2000)
in 'High-speed Jet Flows' ed. McLaughlin, Morris, Rama

Recent Progress in CAA for Jet Noise Physics

Sound Generation in a Mixing Layer (Colonius, Lele & Moin)

JFM, v. 330, 1997.

- Laminar mixing layer with multi-frequency forcing
  $M_1 = 0.5, \quad M_2 = 0.25, \quad Re_\delta = (U_1 - U_2)\delta/\nu = 250$
- Direct computation of sound
- Assessment of approximate source terms for Acoustic analogy

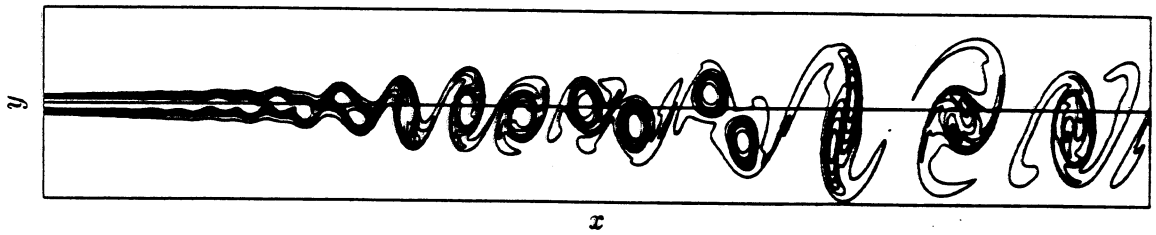


Figure 5.4. Vorticity contours in near field mixing region. The normal axis is expanded by a factor of 2.5. A portion of the computational domain is shown which extends to 285δ in the streamwise direction and $\pm 10\delta$ in the normal direction. Contour levels: Min: -.13, Max: .01, Increment: .02.

Note: expanded scale in y.

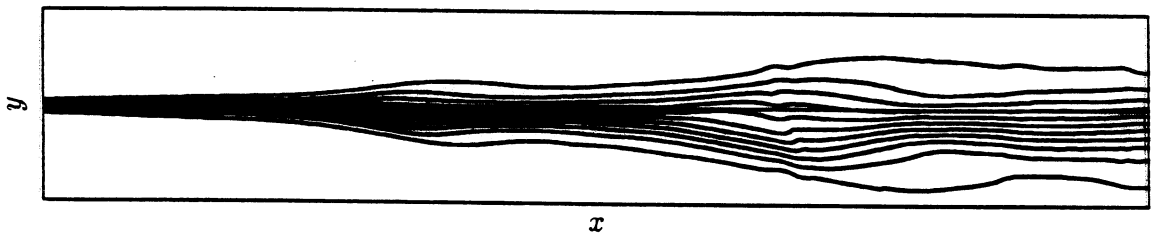


Figure 5.5. Mean streamwise velocity contours in near field mixing region. The portion of the domain is the same as in figure 5 4.

Lilley's Eqn.

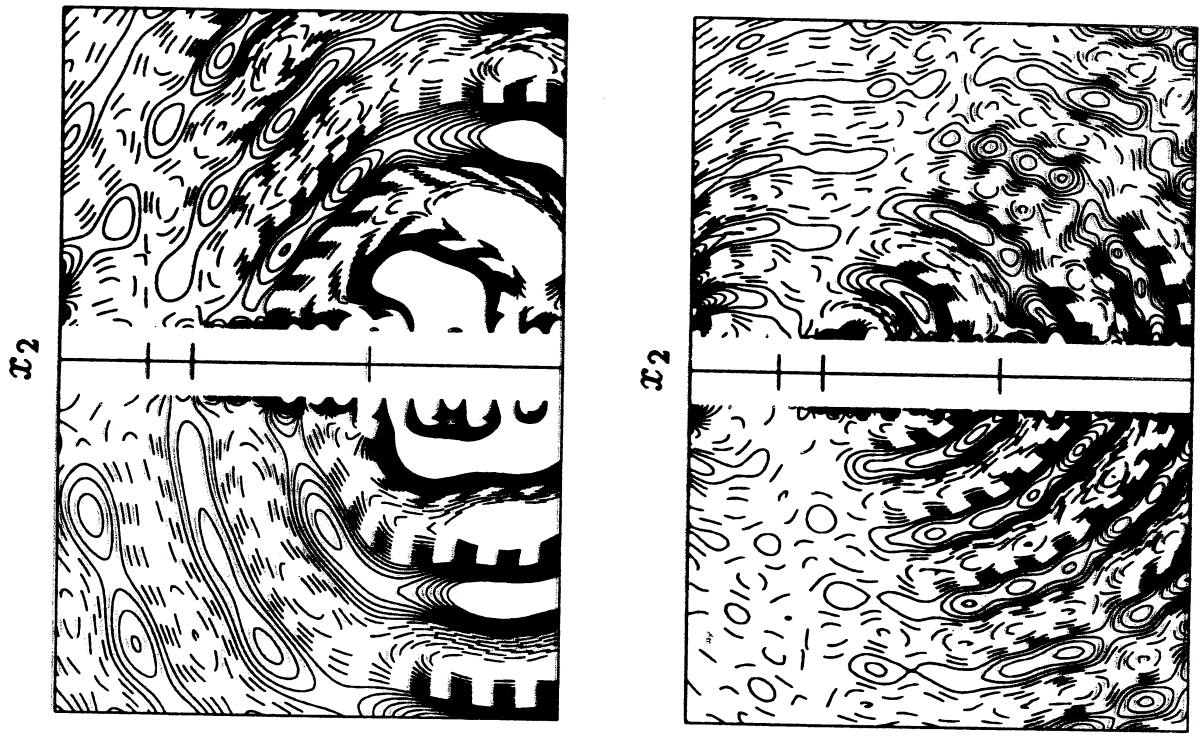
$$\frac{D_o}{Dt}\left(\frac{D_o{}^2\Pi'}{Dt^2} - \frac{\partial}{\partial x_j}\left(\frac{\partial \Pi'}{\partial x_j}\right)\right) + 2\frac{\partial U}{\partial x_2}\frac{\partial^2 \Pi'}{\partial x_1 \partial x_2} = \Gamma,$$

where $\frac{D_o}{Dt} = \frac{\partial}{\partial t} + U(x_2)\frac{\partial}{\partial x_1}$, and Γ, is given by:

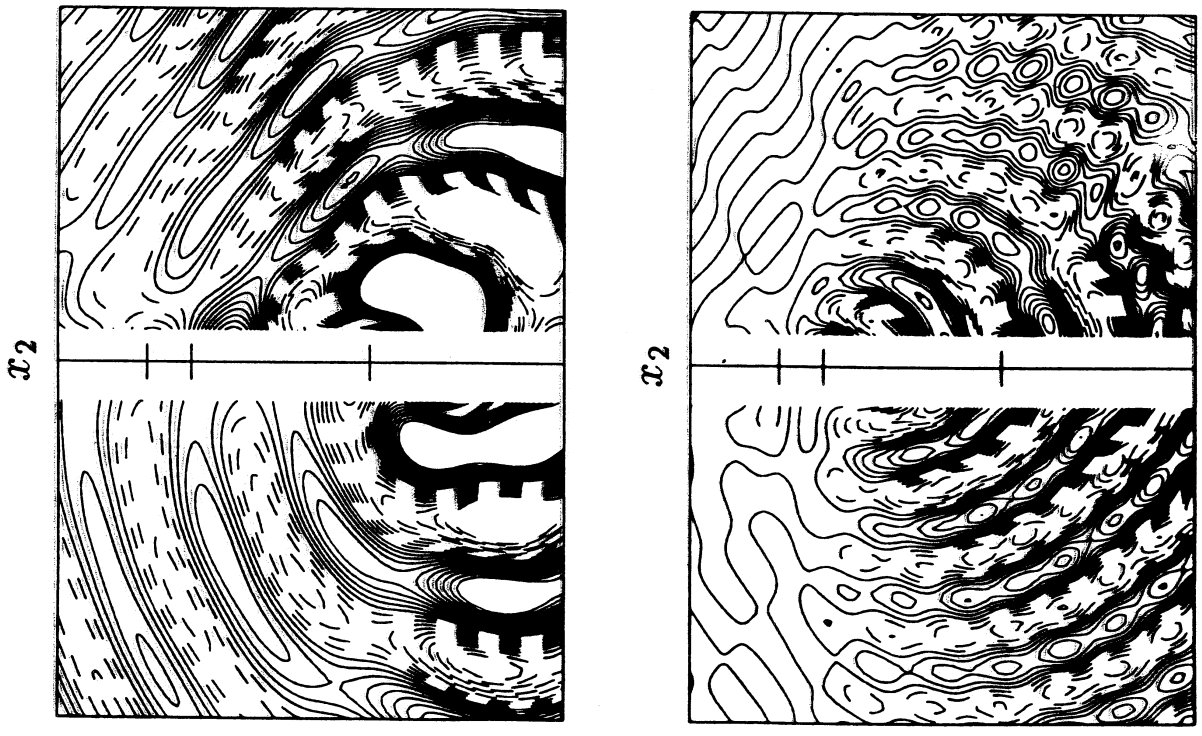
$$\Gamma \approx \frac{D_o}{Dt}\left(\underbrace{\frac{\partial^2 u_i' u_j'}{\partial x_i x_j}}_{\text{Term Ia}}\right) - 2\frac{dU}{dx_2}\underbrace{\frac{\partial^2 u_2' u_j'}{\partial x_1 x_j}}_{\text{Term Ib}}.$$

Goldstein (1976), (1984)

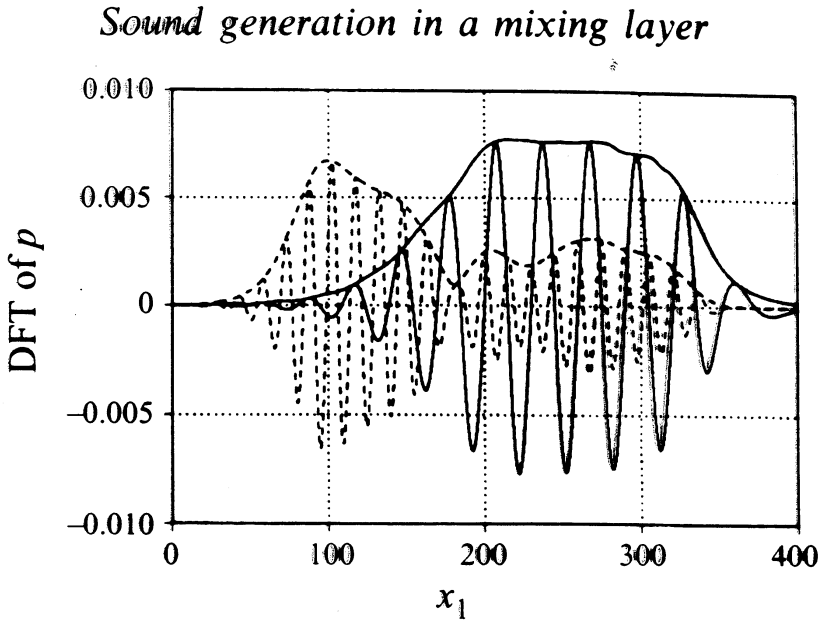
DNS:



Acoustic theory:



(a) $f/4$ (b) $f/2$



URE 15. The DFT of p at $x_2 = 0$ for $f/2$ (- - - -) and $f/4$ (———). The real part and magnitude shown – the imaginary part is similar to the real part in each case but shifted in phase by $\pi/2$.

Colonius et. al. (1997) JFM

- Wave packets
- Nonlinear

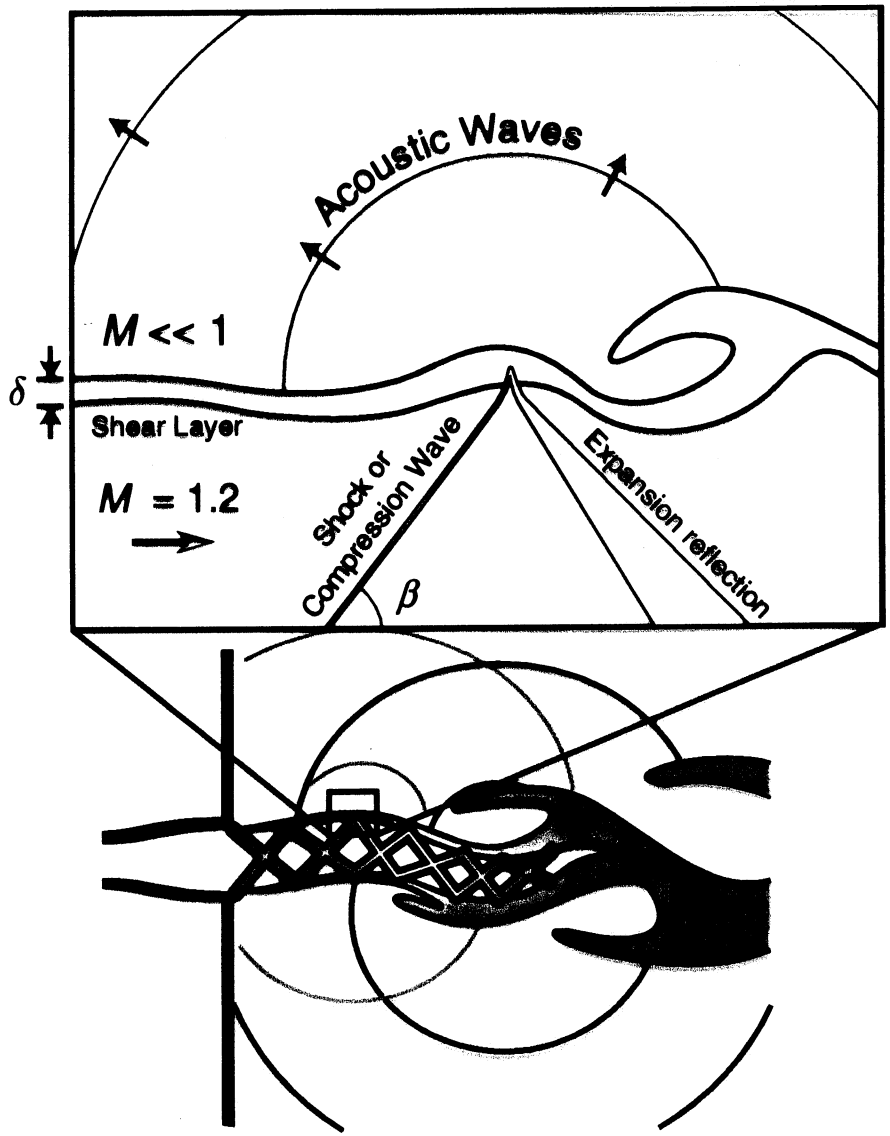
Recent Progress in CAA for Jet Noise Physics

Screech Noise Generation
(Manning & Lele, AIAA/CEAS 2000-2081)

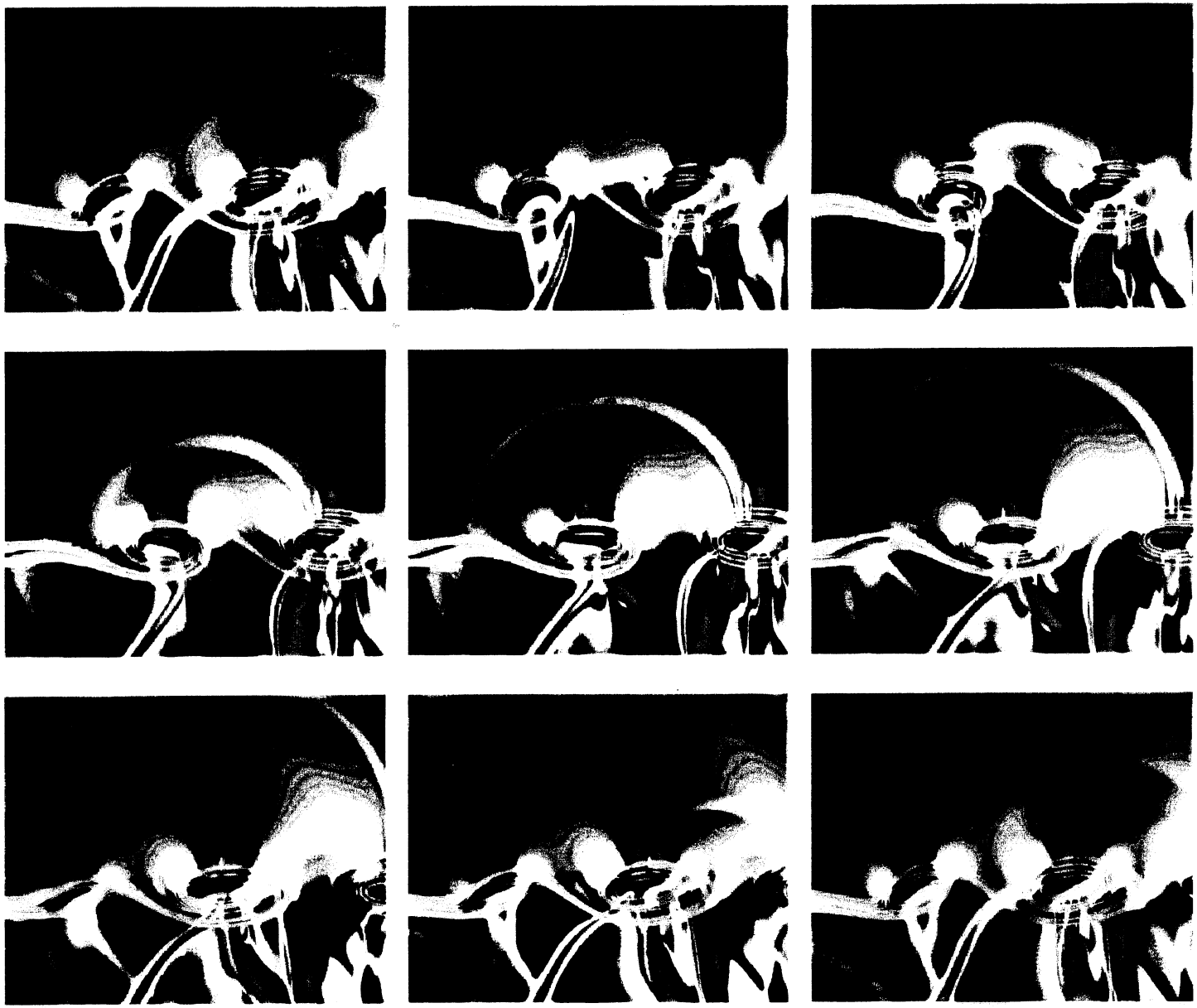
- Model problem of an isolated screech source
- **Focus:** Amplitude prediction
- DNS
- Linearized Euler Solution (with unsteady base flow)
- Geometrical Acoustics

Screech-type Source: Model Problem

- **Single screech-type source**
  - one shear layer
  - part of shock cell
- **Large, organized instability waves at single frequency**
- **Incident oblique shock**
- **No receptivity**



Weak Compression Wave — Vortex Interaction

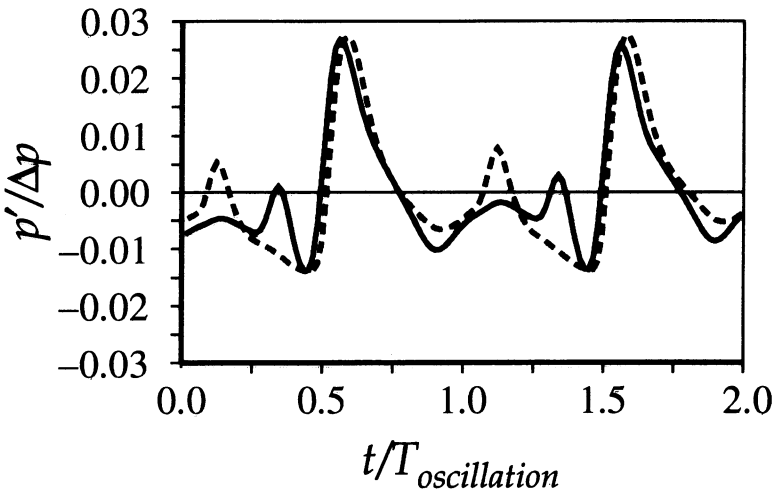


Effect of Compression Wave Amplitude Variation

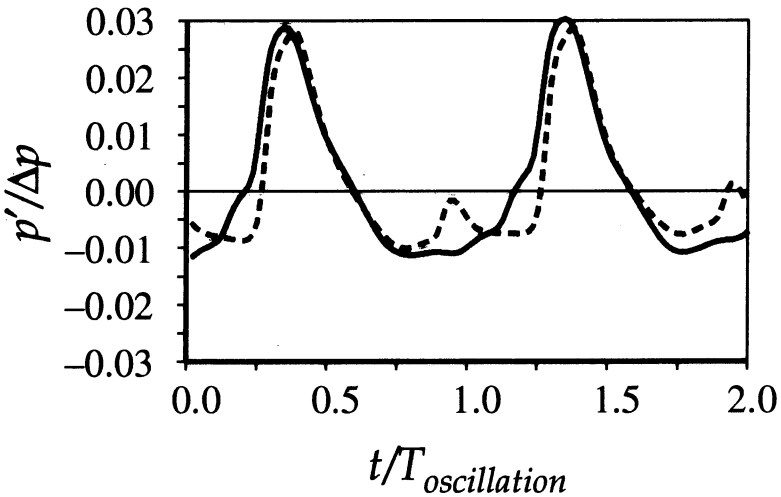
(*normalized to compression wave amplitude* Δp)

——— $\Delta p/p_\infty = 0.05$ (Case B1)

- - - - - - - - $\Delta p/p_\infty = 0.10$ (Case B2)



$(r, \theta) = (1.3\lambda, 135°)$



$(r, \theta) = (1.1\lambda, 160°)$

Linearized Euler Method

- **Decomposition:** *unsteady* base flow and perturbation

$$Q(\mathbf{x},t) = \tilde{Q}(\mathbf{x},t) + q(\mathbf{x},t)$$

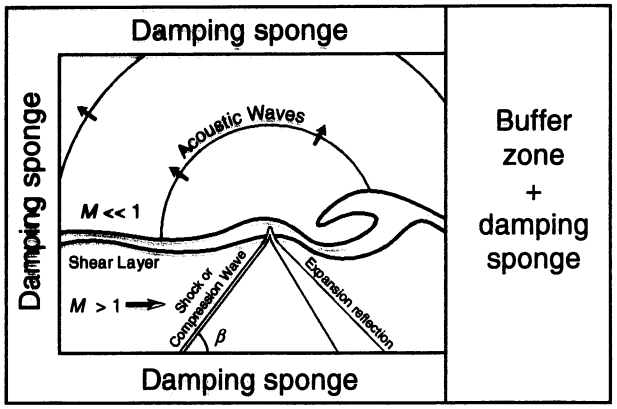
- **Linearized Euler equations**

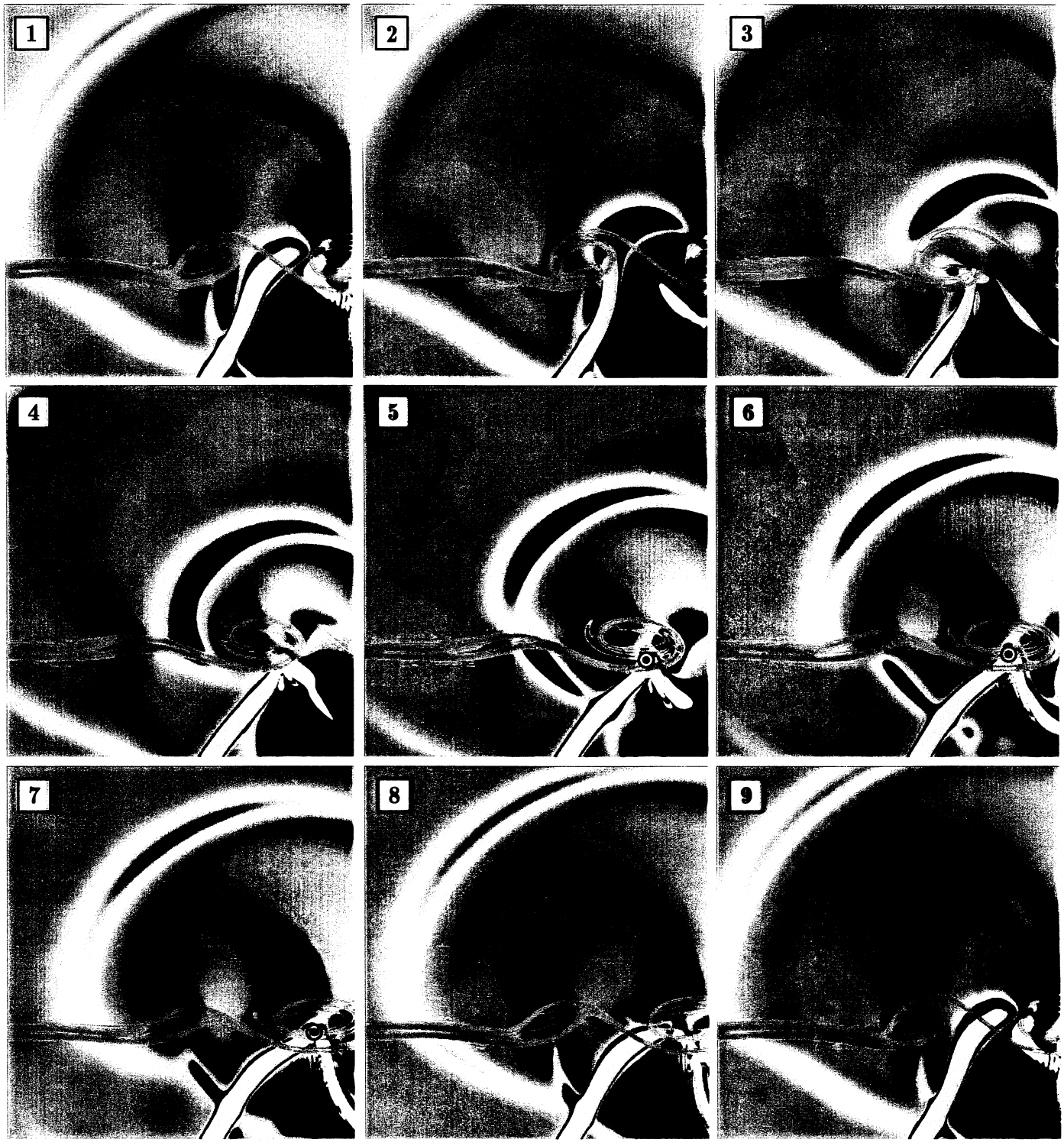
$$\underbrace{L_{NS}(\tilde{Q}+q) - L_{NS}(\tilde{Q})}_{\text{linearize } q \text{ about } \tilde{Q} \text{ and neglect viscous terms}} = 0$$

$$\boxed{L_{LinEuler}(\tilde{Q},q) = 0}$$

- **Numerical method**

Discretization:	*6th-order Padé and RK3*
Boundary Cond.:	*Damping sponge, bufferzone, & Riemann*
Baseflow storage:	*Fourier series in time*





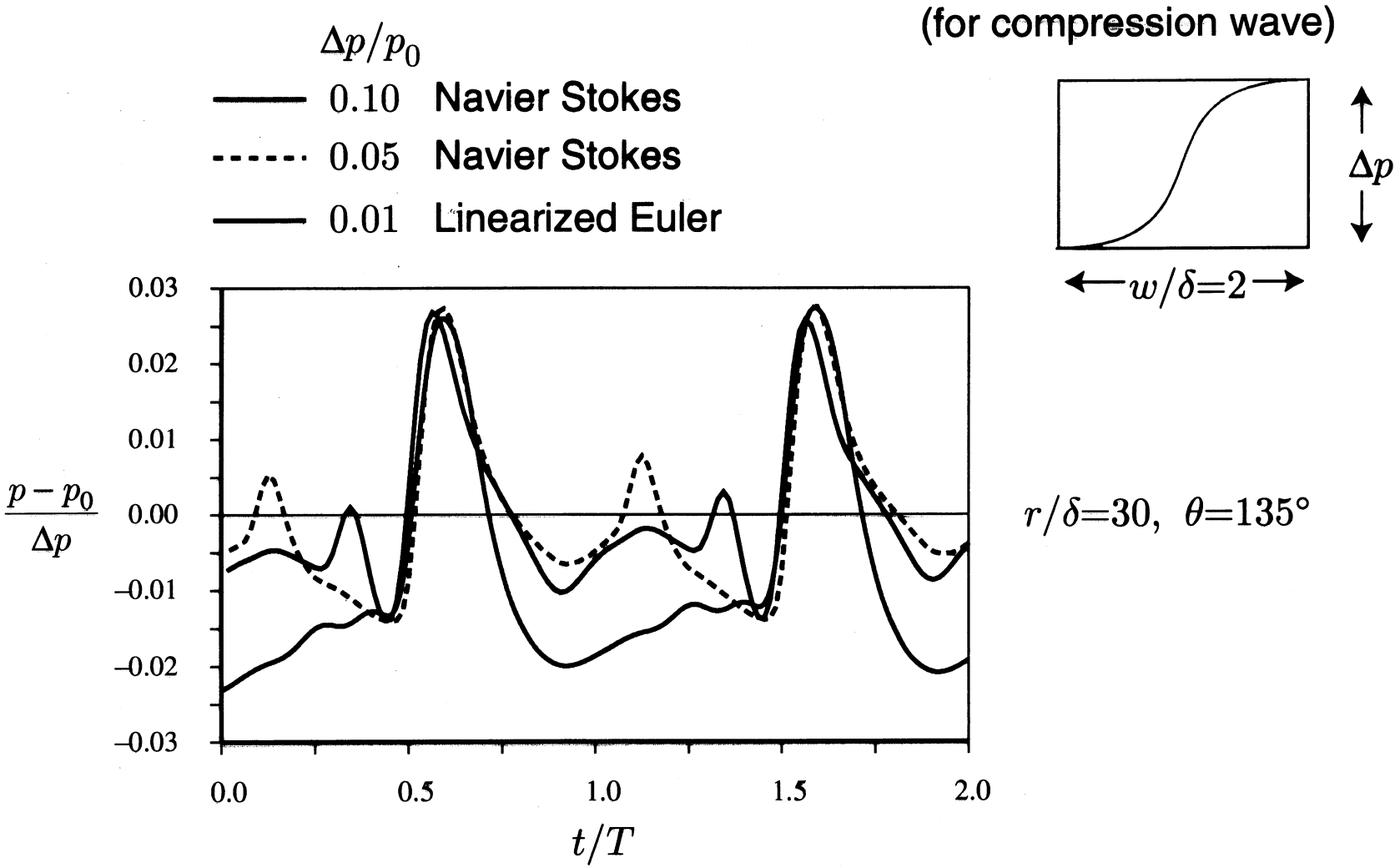


–0.20 –0.16 –0.12 –0.08 –0.04 0.00 0.04 0.08 0.12 0.16 0.20

$p'/\Delta p$

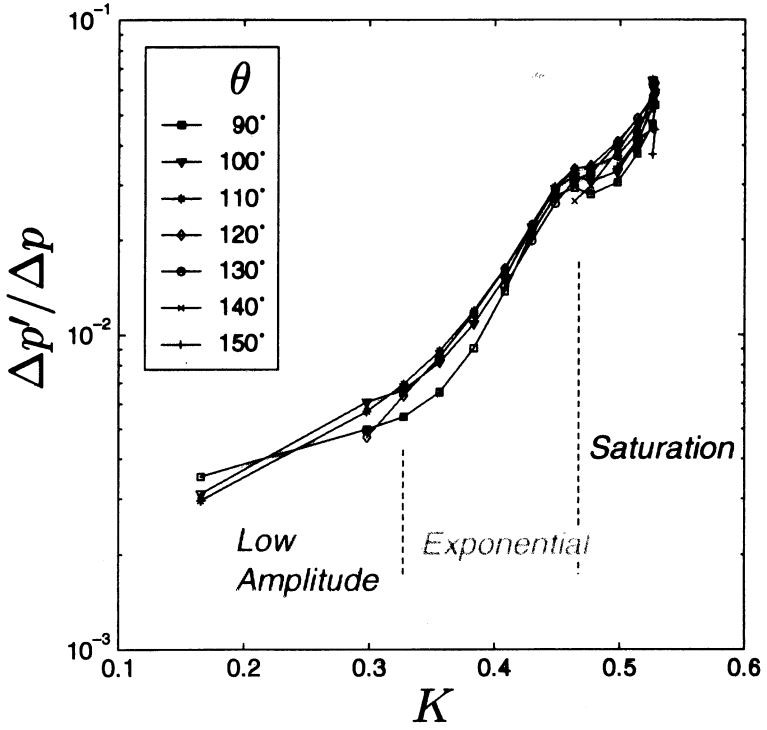
Linearized Euler Results

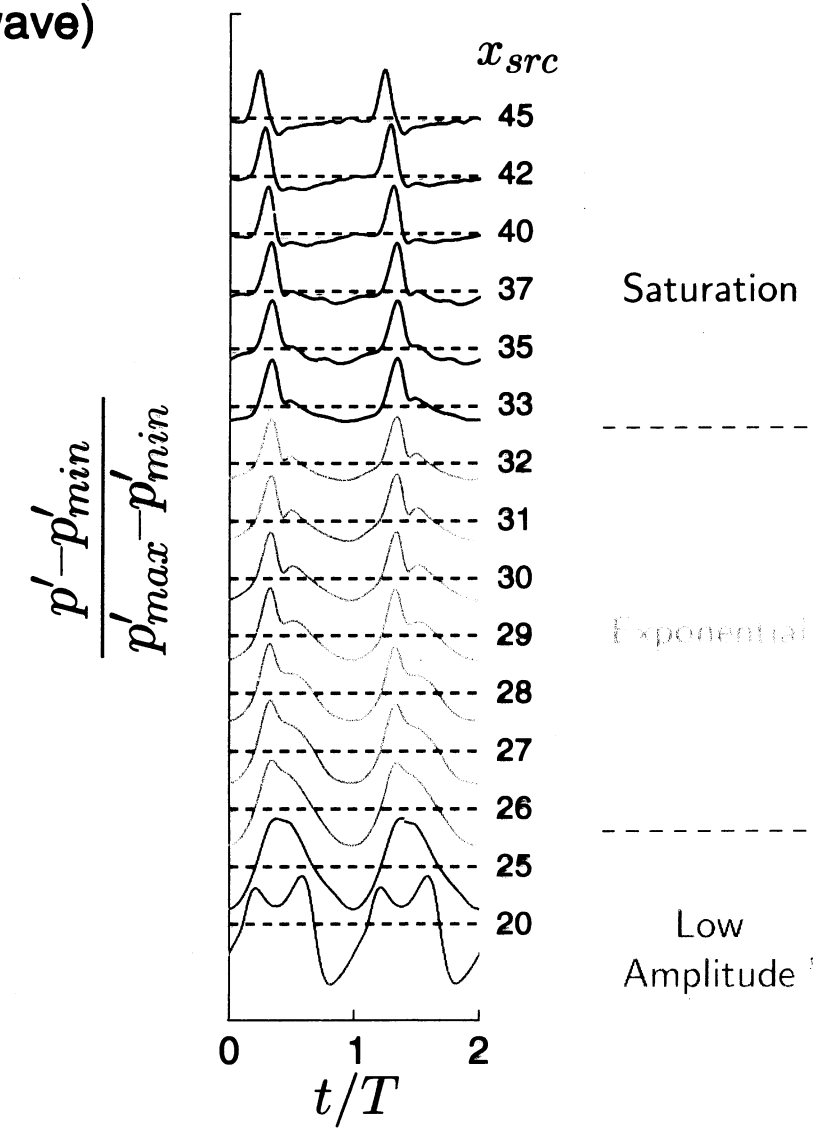
- **Acoustic scaling agrees well with Navier Stokes**



Waveform Dependence on Instability Wave

DNS base flow, Gaussian profile (G-wave)





Stuart Vortex Mixing Layer

- Idealized mixing layer used as base flow (Stuart 1967)
- *Incompressible* solution, velocity field only (p', ρ', $T' = 0$)

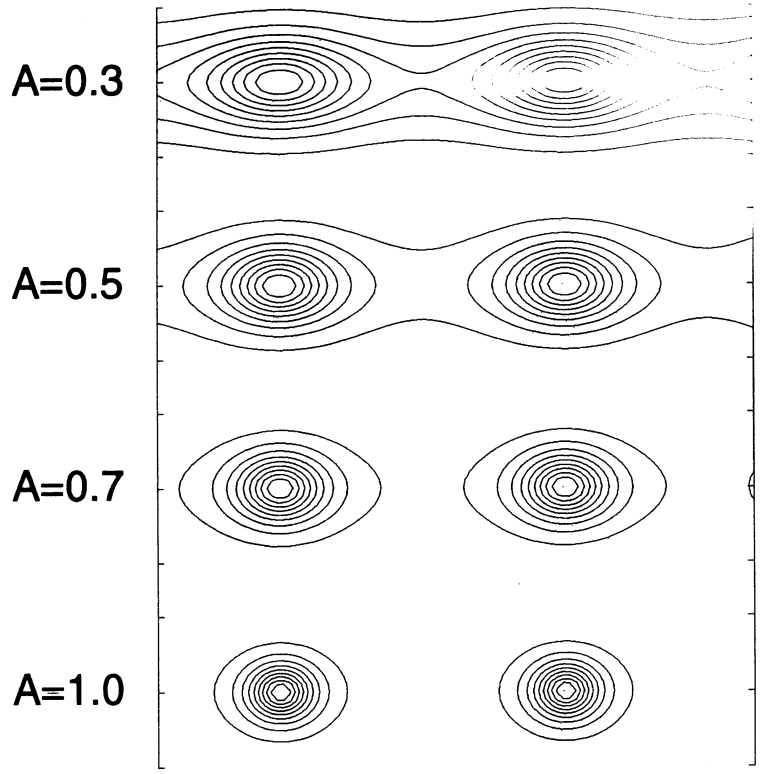
$$u = c + b\frac{C\sinh\eta}{C\cosh\eta + A\cos\xi}$$

$$v = b\frac{A\sin\xi}{C\cosh\eta + A\cos\xi}$$

$$\xi = a(x - U_c t) \qquad \eta = a(y - y_0)$$

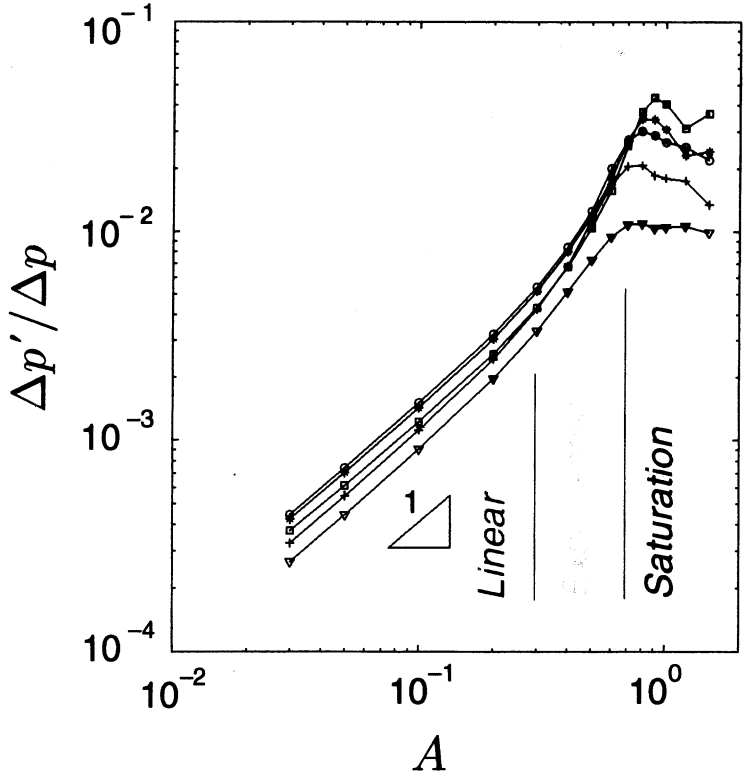
$$C = \sqrt{A^2 + 1} \qquad U_c = U_1/2$$

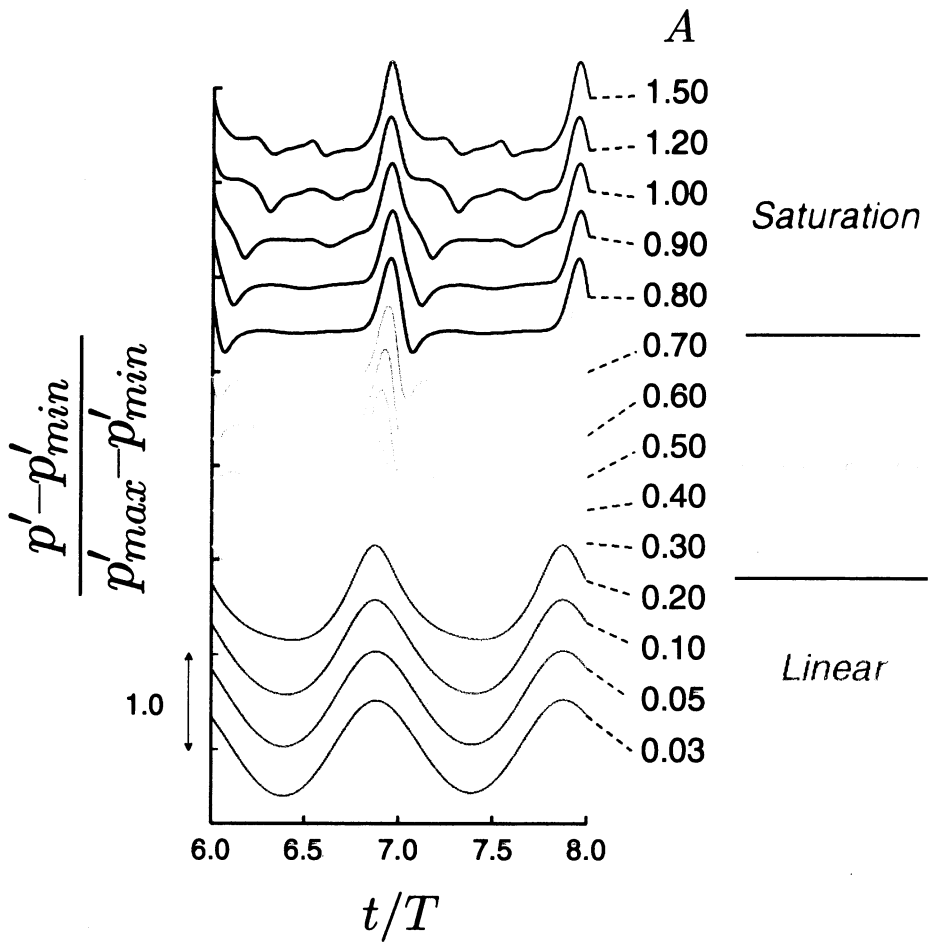
$$a = \omega/U_c \qquad b = -U_1/2$$



Waveform Dependence on Instability Wave

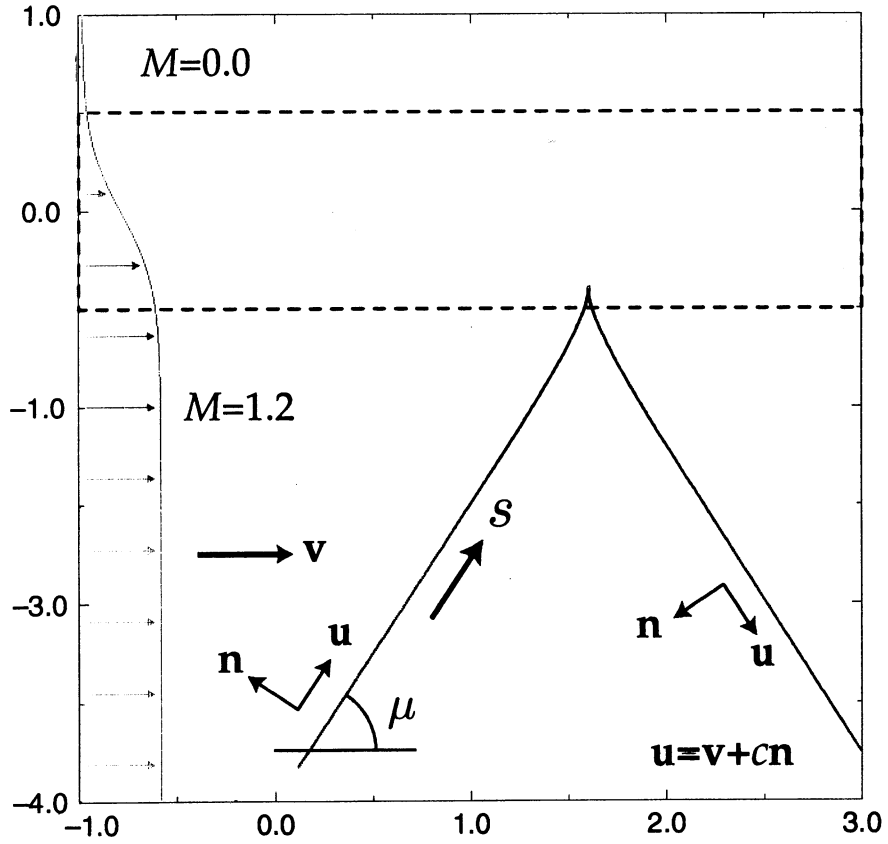
Stuart vortex base flow, Gaussian profile (G-wave)

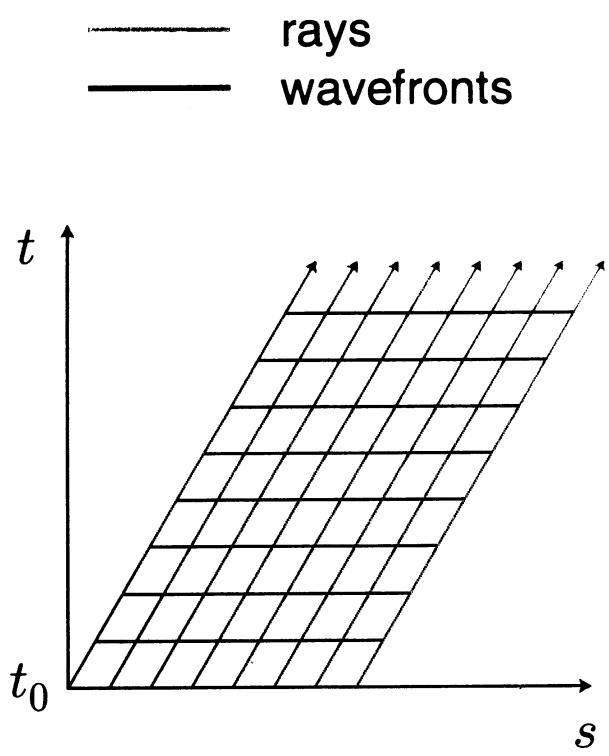




Geometrical Acoustics: Initial Condition

- **Oblique standing wave in supersonic flow** (steady shear layer example)

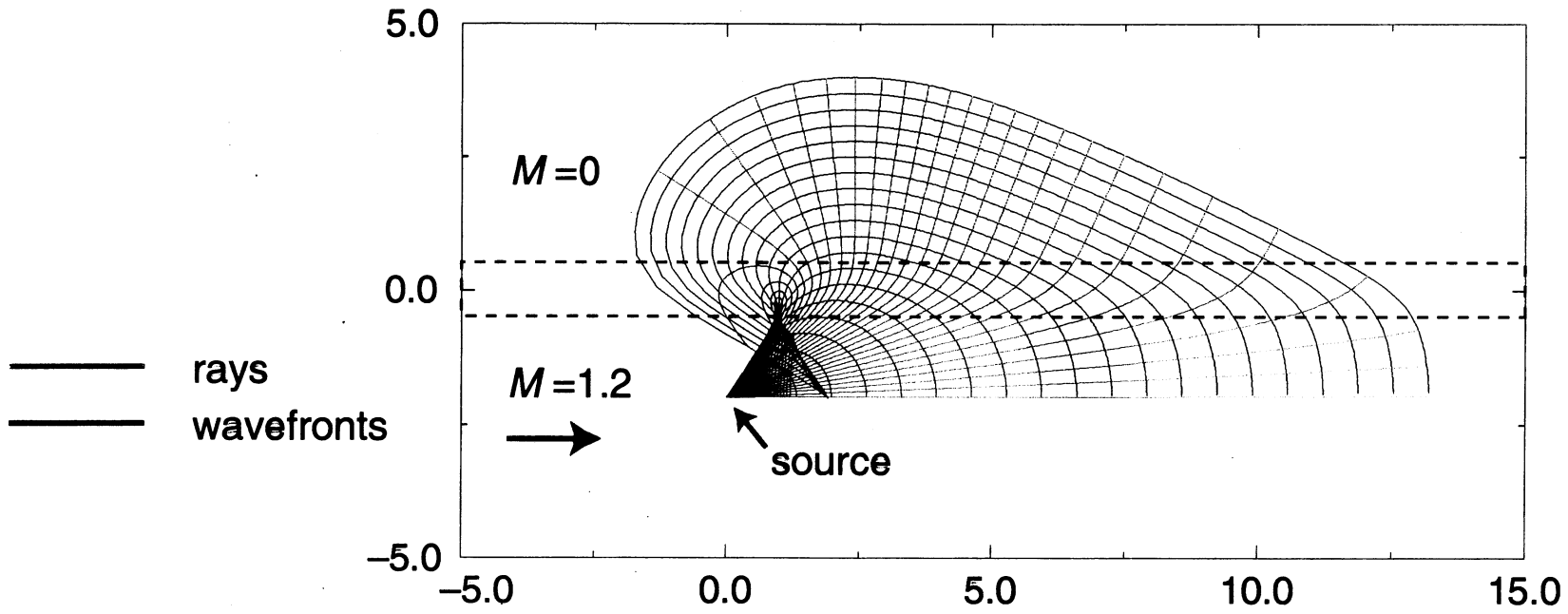




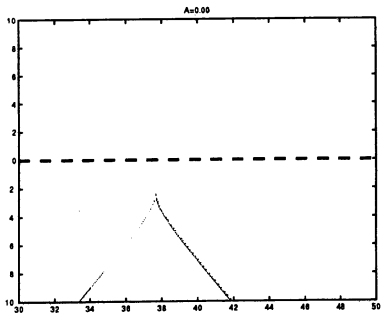
Geometrical Acoustics: Method

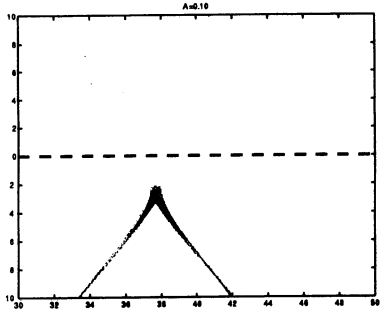
- Analogous to geometric optics
- Integrate acoustic "rays" through refracting medium
- Refraction occurs due to velocity shear and speed of sound variation
- Assumes high wave number limit

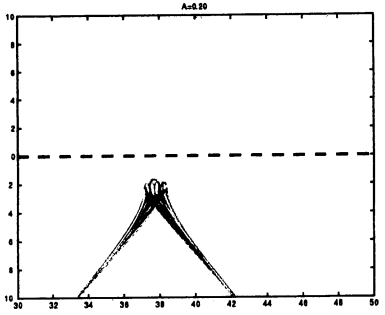
Steady flow example

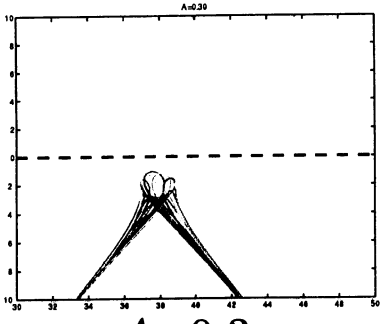


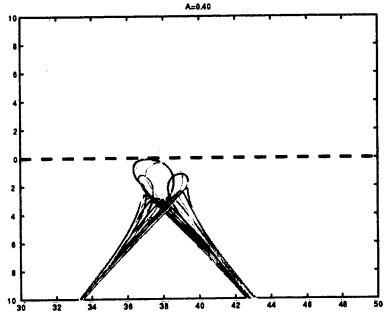
Onset of Transmission: rays

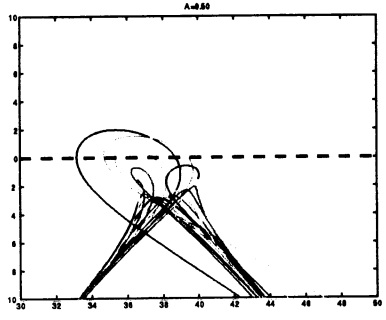

A=0.0

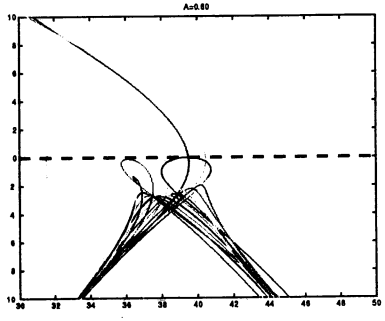

A=0.1

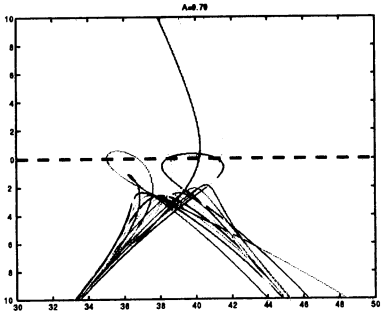

A=0.2

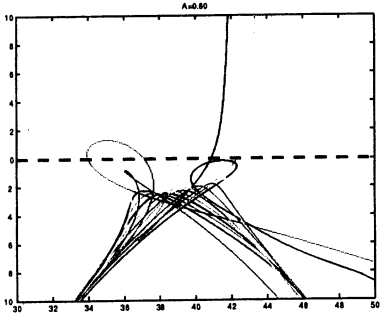

A=0.3

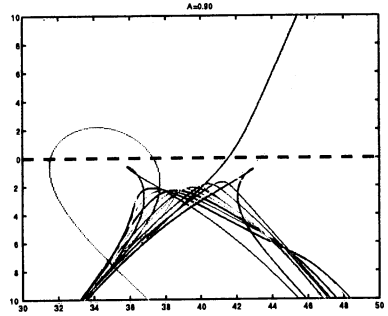

A=0.4

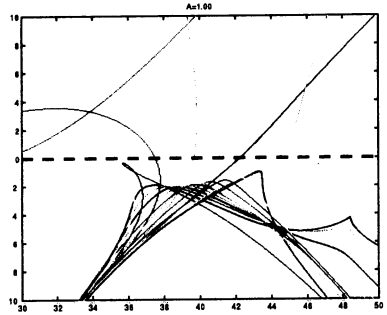

A=0.5


A=0.6


A=0.7

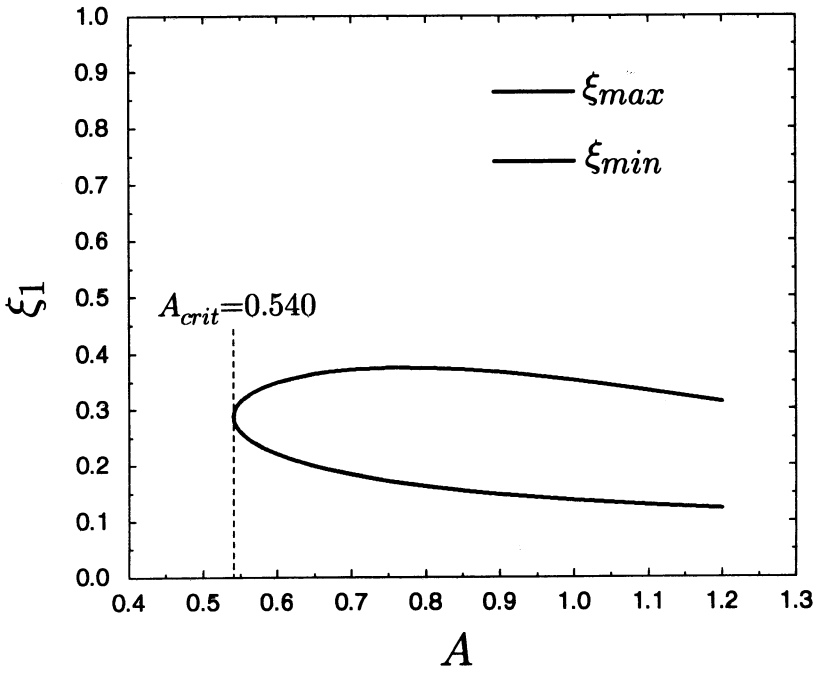

A=0.8


A=0.9

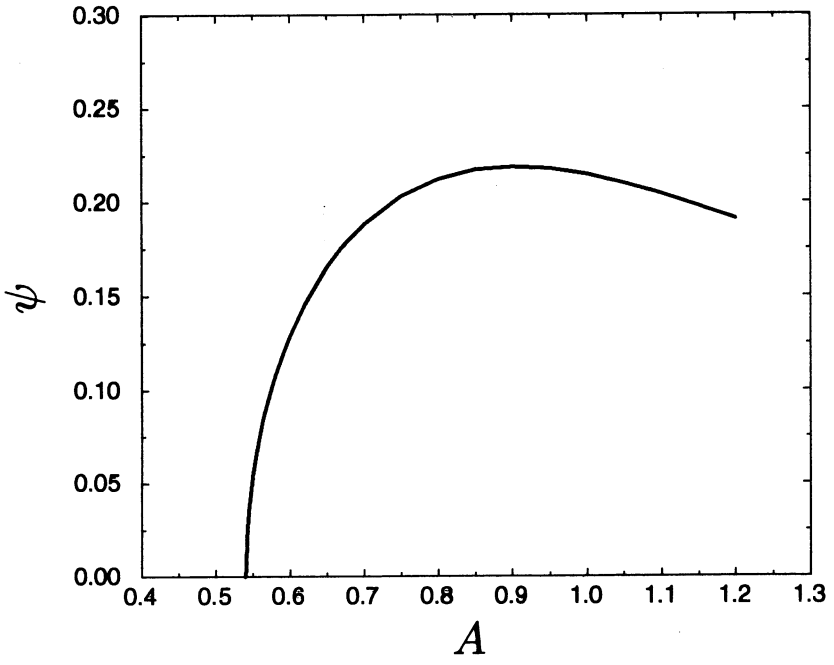

A=1.0

Transmission Fraction

Transmission range



Transmission Fraction



Recent Progress in CAA for Jet Noise Physics

Acoustic Sources in Turbulent Jet: A DNS study

(Freund, J. B., AIAA/CEAS 99-1858)

- DNS of a Mach 0.9 turbulent jet and its sound field
  $Re_D = 3600$

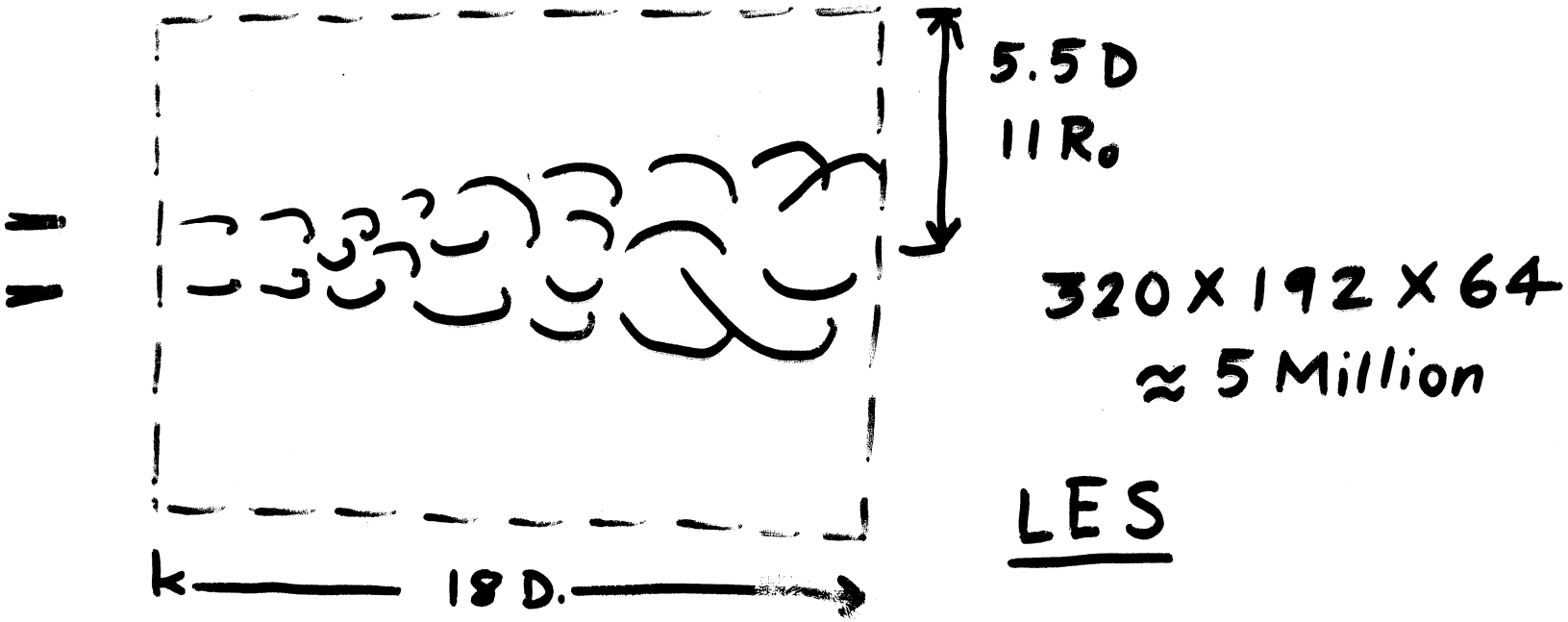
- Excellent agreement with Stromberg et. al. experiment
  Jet flow and turbulence, and near-field noise

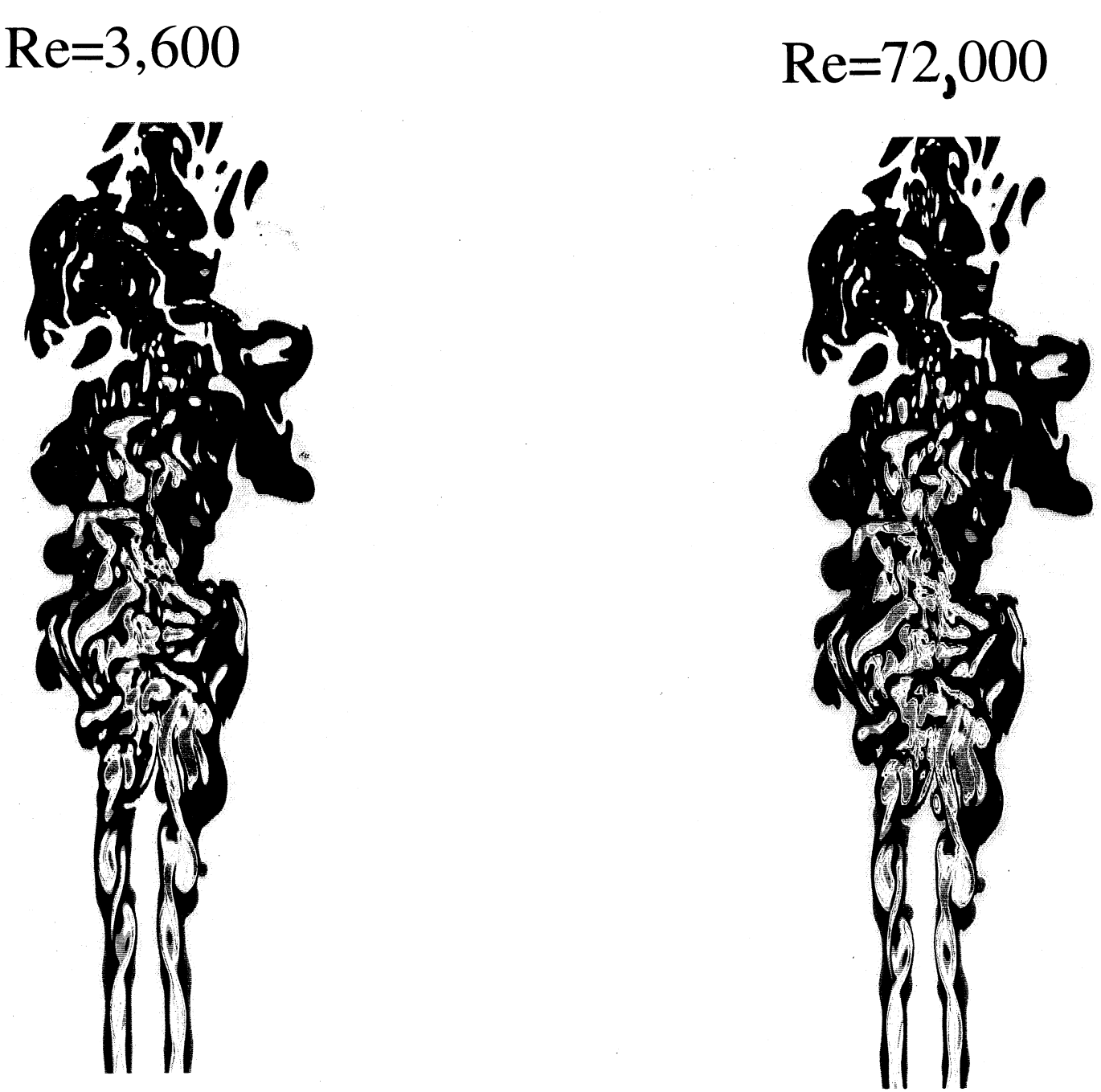
- Sound source distributions: Wave packets

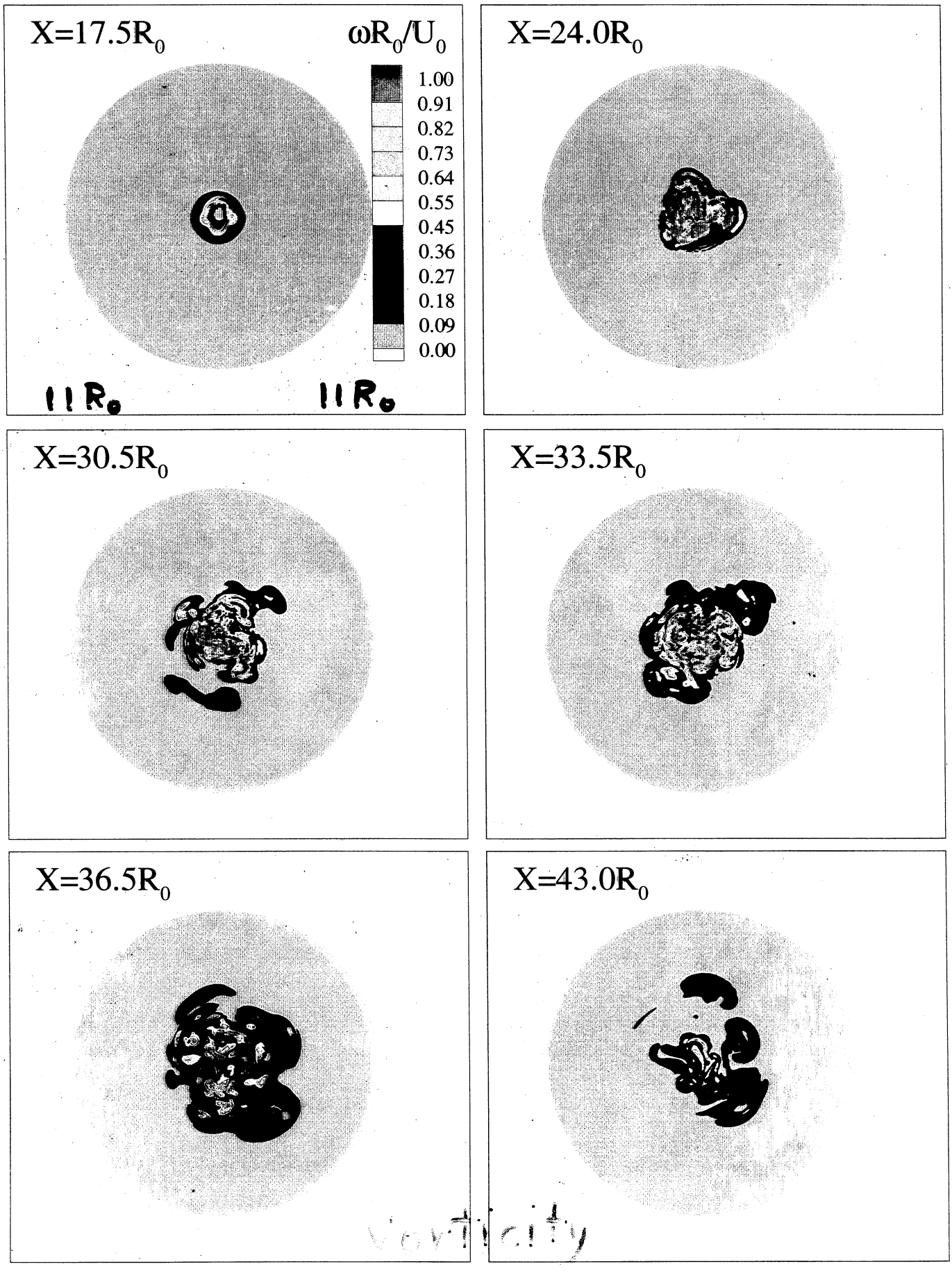
Recent Progress in CAA for Jet Noise Physics

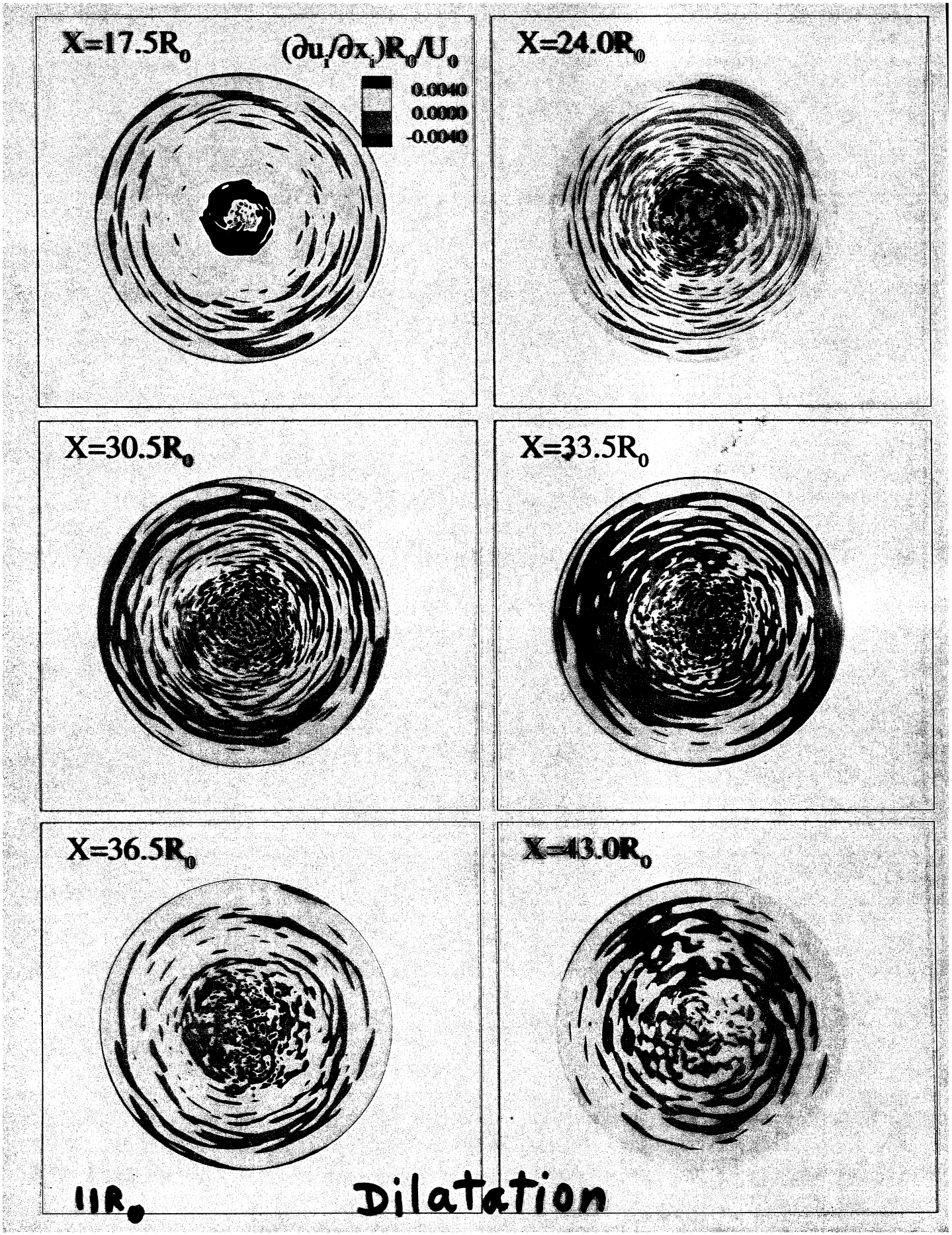
LES of turbulent jets
(Constatinescu & Lele, AIAA Reno 2001 *to appear*)

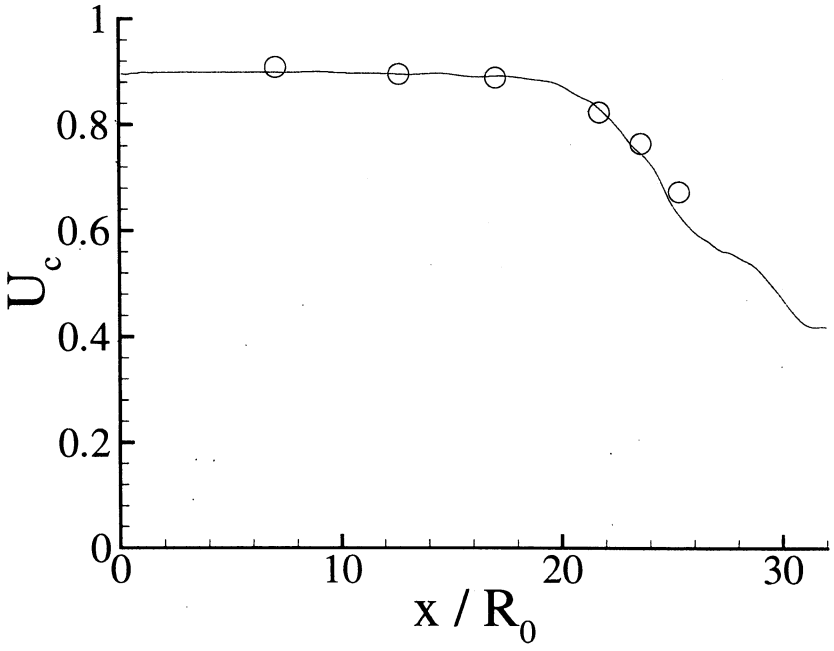
- Improvement on Boersma & Lele (1999) study (AIAA 99-1874)
- Improved numerical treatment of cylindrical co-ordinate singularity
- Simultaneous data on turbulence and noise



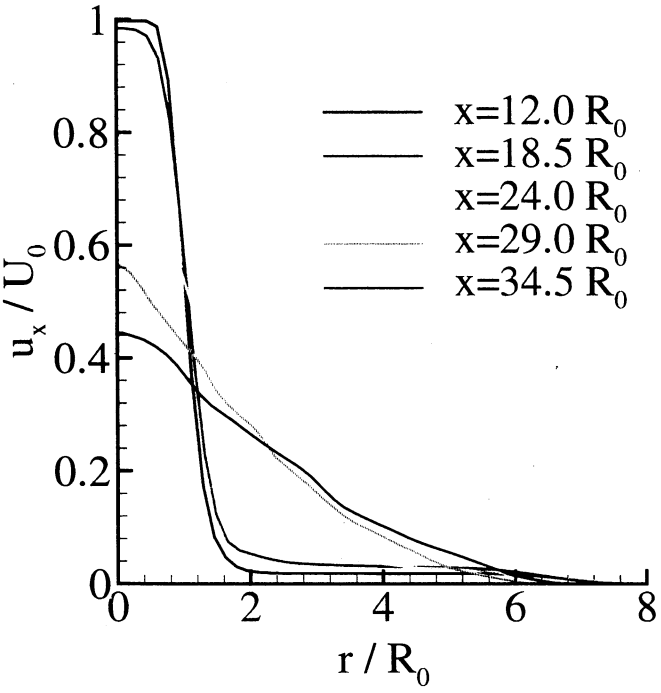

Re=3,600
Re=72,000


X=17.5R0
ωR0/U0
1.00
0.91
0.82
0.73
0.64
0.55
0.45
0.36
0.27
0.18
0.09
0.00
11R0
11R0
X=24.0R0
X=30.5R0
X=33.5R0
X=36.5R0
X=43.0R0
Vorticity

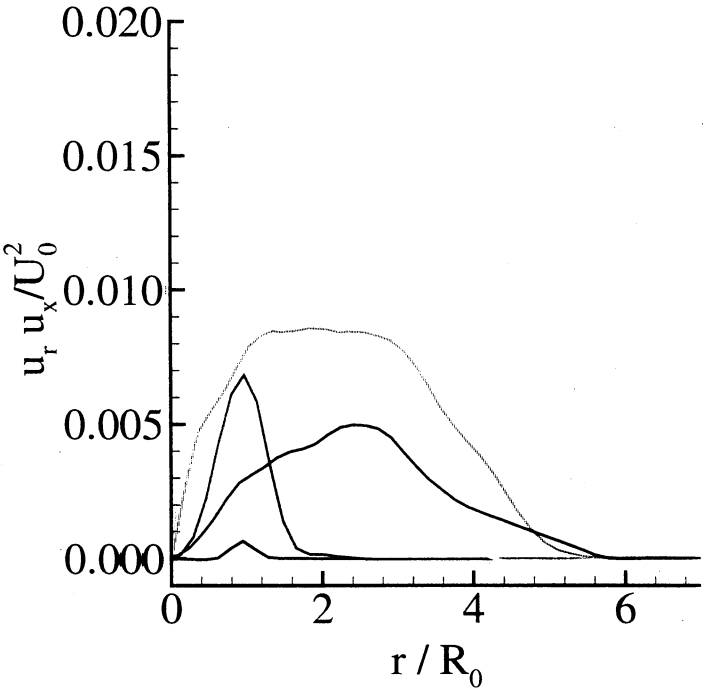

X=17.5R0
(∂ui/∂xi)R0/U0
0.0040
0.0000
-0.0040
X=24.0R0
X=30.5R0
X=33.5R0
X=36.5R0
X=43.0R0
11R0
Dilatation



Mean centerline velocity



Mean streamwise velocity



Reynolds shear-stress

Of things to come ?

Converged stats. on

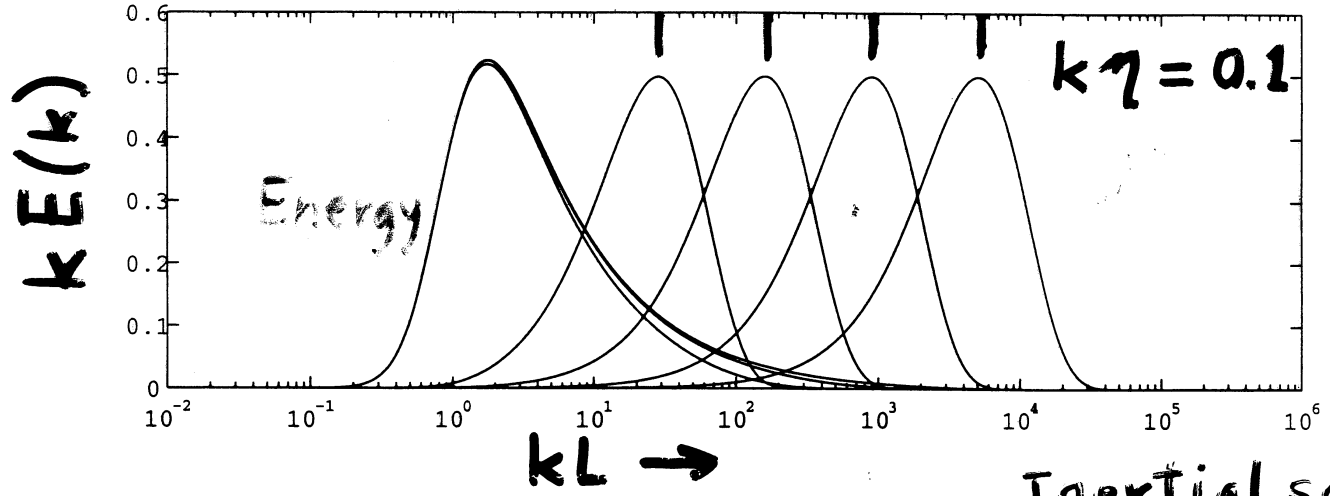
- turbulence
- noise
- 'noise-source' stats. & mechanisms

Higher Re LES

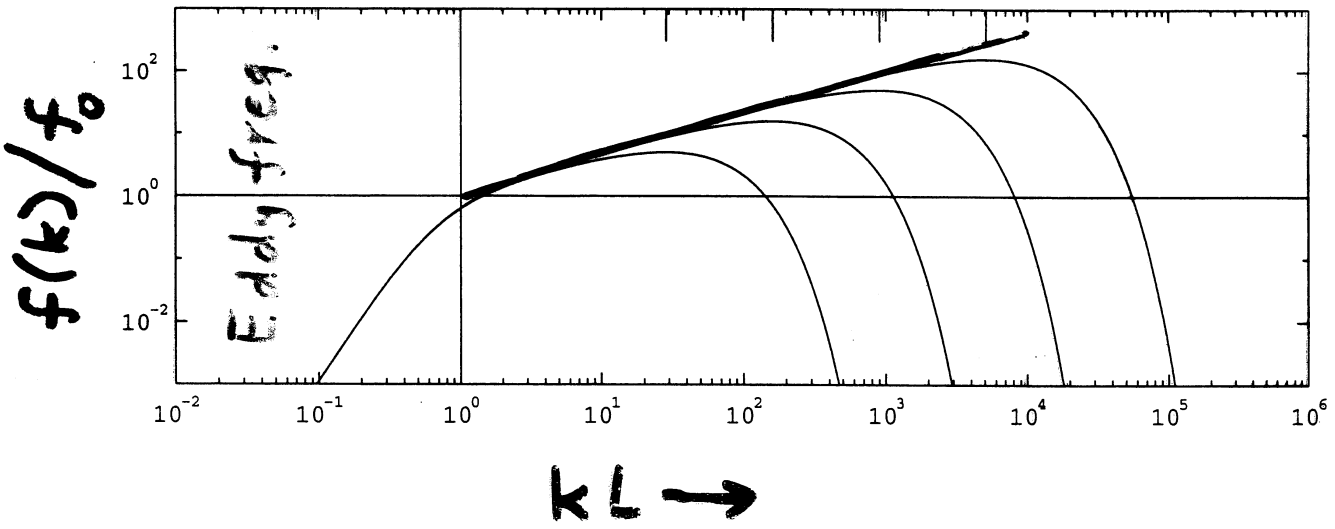
$$Re_L \equiv \frac{u' L}{\nu}$$

$$Re_L = 10^3, 10^4, 10^5, 10^6$$

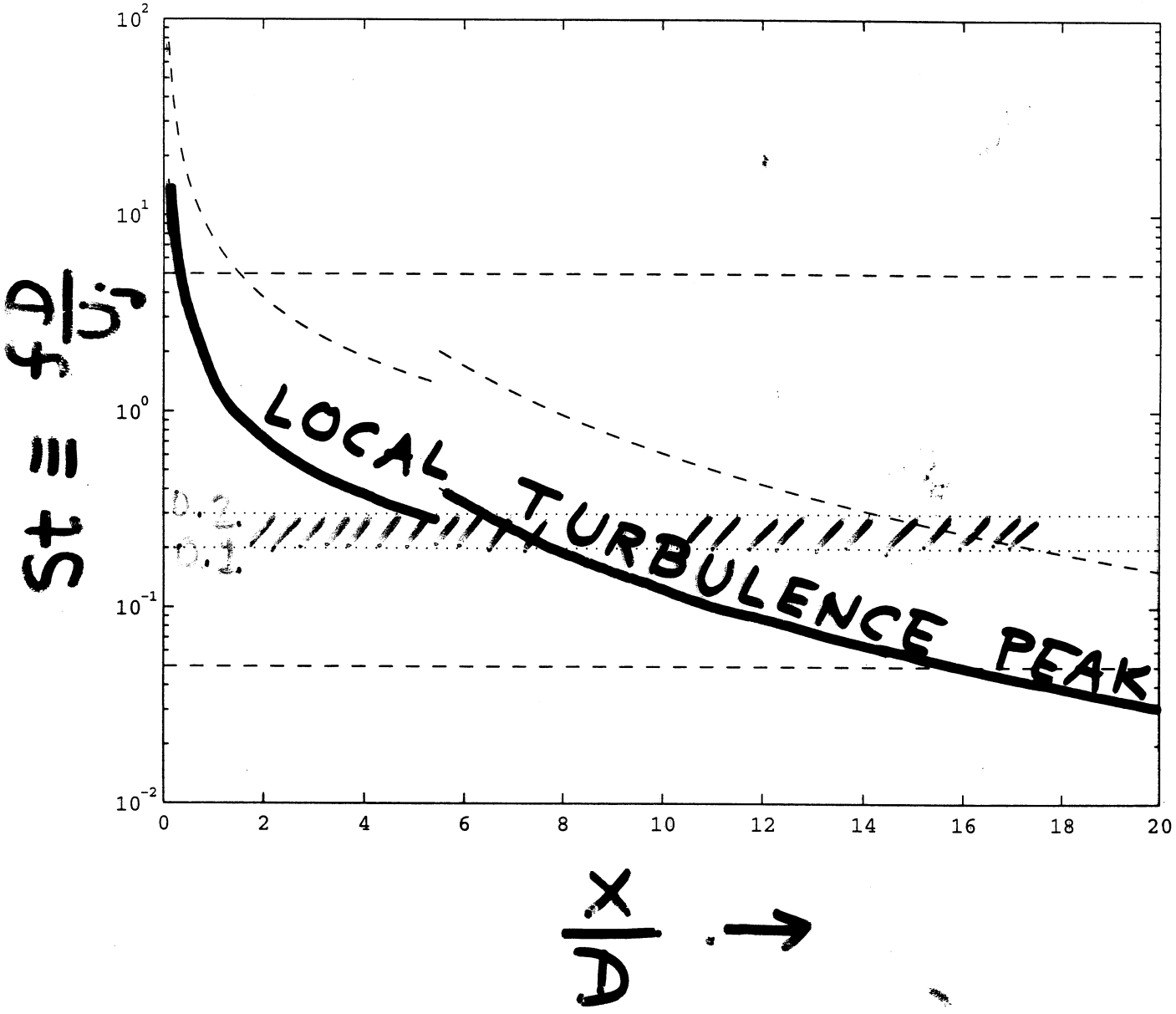
Dissipation Peak



Inertial scaling



$$f(k) \equiv \left(k^3 E(k)\right)^{1/2}$$



Jet Turbulence

Computational Issues Particular to Jet Noise(Contd.)

Grid requirement:

- Driven by frequency range to be resolved, *not* Reynolds number
- Inertial range scaling and overall jet data give grid point estimate
- Ideal numerical method gives $f_{max}/f_0 \approx 5$ with $\Delta/L = \frac{1}{32}$

At $x/D = 0.1$, $\delta_\omega/D \approx 0.02$: With $\Delta/L = \frac{1}{32}$ and $\Delta_x = \Delta_r = \Delta_\theta$
the region $0.1 < x/D < 0.2$ would require approx. 77 million points!!!
Assuming geometric grid-stretching total grid points $\approx 150 - 200$ million
why ?
For a 1" near sonic jet with $Re_D = 600,000$
$Re_L = u'L_x/\nu = 1,100$ at $x/D = 0.1$, and *much* higher for larger scale jets
$\pi D/\Delta \approx 5000!$ azimuthal points

- Need Hybrid Numerical method to:
  - ⋆ represent higher frequencies
  - ⋆ provide statistical results without full coverage at high resolution

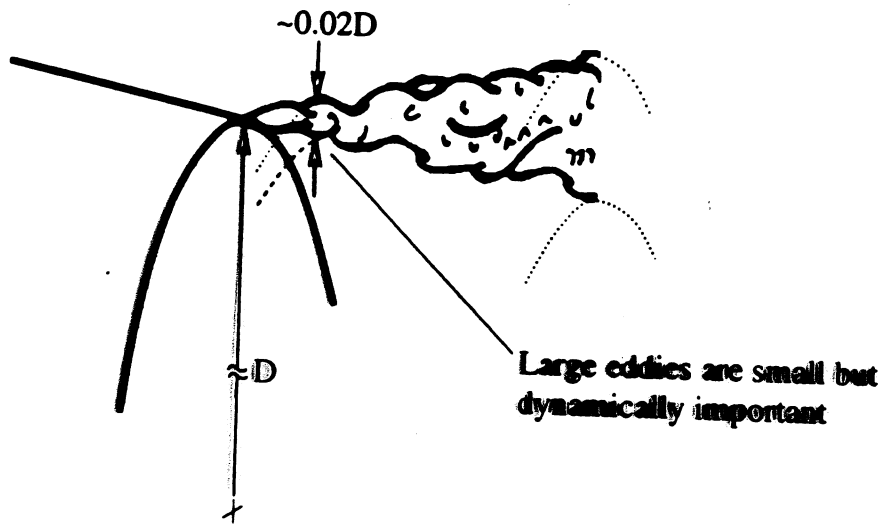


Figure 6: Schematic of near-nozzle jet shear layer.

From:- Freund & Lele (2000)

Computational Issues Particular to Jet Noise(Contd.)

Inflow :

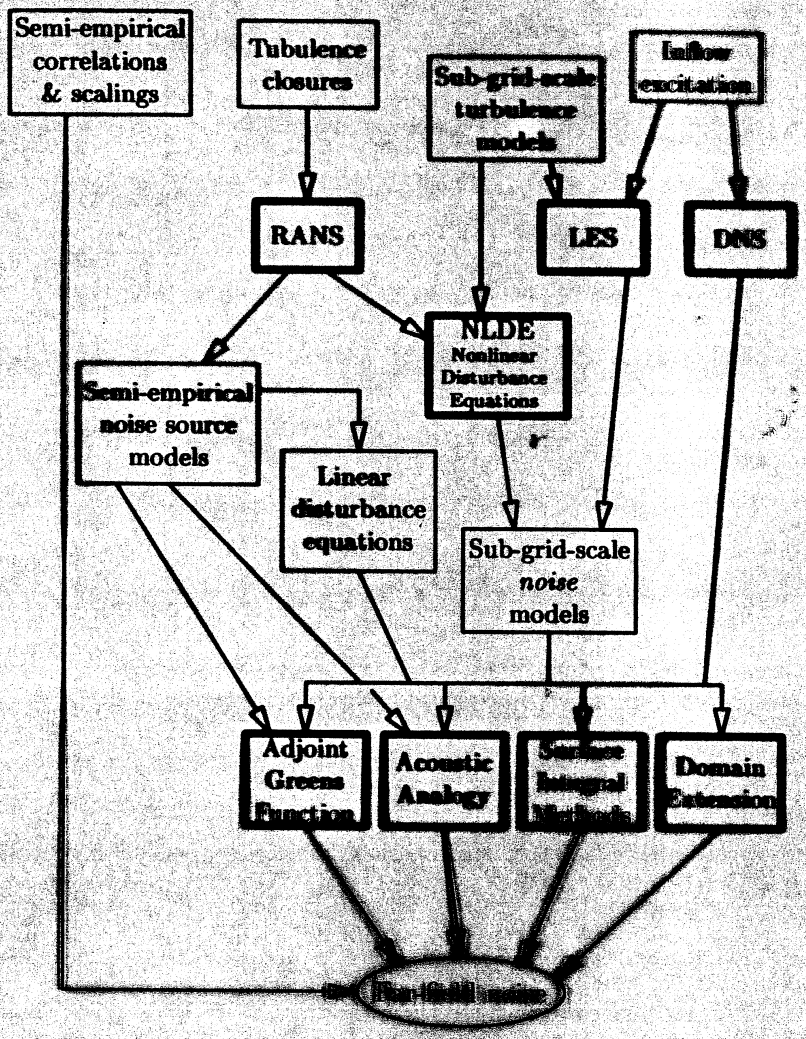
⋆ Efficient method to generate/specify turbulent inflow data
⋆ Minimize spurious 'noise' due to forcing
⋆ Non-reflecting for upstream-directed sound
⋆ 'Represent' noise-suppression concepts

Flow and Sound Statistics :

⋆ Long time record for statistics
⋆ Temporal decorrelation in inflow forcing
⋆ Minimize contamination from un-represented scales (on flow and sound)

Current Issues in Computational Aeroacoustics

- Boundary Conditions
- High-resolution schemes for complex domains
- Interaction of shocks with other disturbances
- High-resolution methods for LES
  (Stable/robust numerical methods for underresolved fields)
- Prediction of radiated noise (hybrid methods)
- Broadband noise – Noise of scales not represented



Approaches to noise-prediction

Closure : Where do we go from here ?

- Develop better understanding of jet noise physics with CAA

  Science of Aerodynamic Sound
  'Second golden age of aeroacoustics ??' (Lighthill)

- Benchmark database for developing hybrid noise prediction methods
  Subgrid noise models, Approx. methods for flow-noise interaction

- Better Aerodynamic and Aeroacoustic design
  Mixing optimization for noise reduction

S. Lele References

1. Colonius, T., S. K. Lele, and P. Moin. ``Sound Generation in a Mixing Layer," J. Fluid Mech. Vol. 330, 1997, pp. 375-409.

2. Mitchell, B. E., S. K. Lele and P. Moin. ``Direct Computation of Mach Wave Radiation in an Axisymmetric Supersonic Jet", AIAA J. Vol. 35, 1997, pp.1574-1580.

3. Mitchell, B. E., S. K. Lele, and P. Moin. ``Direct Computation of the sound generated by vortex pairing in an axisymmetric jet," J. Fluid Mech., Vol. 383, 1999, pp. 113-142.

4. Freund, J. B., S. K. Lele and P. Moin. ``Direct numerical simulation of a low Reynolds number Mach 1.92 turbulent jet and its sound field," to appear in AIAA J., 2000.

5. Lele, S. K. ``Direct Numerical Simulations of Compressible Turbulent Flows: Fundamentals and Applications," Invited lectures at the 2nd ERCOFTAC Summer School on Transition and Turbulence Modeling, Editors: H. Alfredsson, A. Johansson, D. Henningson and A. Hanifi, Kluwer Academic Publishers, 1999, Chapter 7, p. 421-488.

6. Lele, S. K. and Freund, J. B. ``Computer Simulation and Prediction of Jet Noise," 2001. High Speed Jet Flows, Editors: G. Raman, D. McLaughlin, P. Morris, Taylor Francis.

7. Manning, T. and S. K. Lele. ``Numerical Simulation of Shock-Vortex Interaction in Supersonic Jet Screech," AIAA paper, 98-0282, Reno, January 1998.

8. Boersma, B. J. and S. K. Lele. ``Large-Eddy Simulation of a Mach 0.9 Turbulent Jet," AIAA/CEAS Paper, 99-1874, Aeroacoustics Conference, Seattle.

9. Manning, T. A. and S. K. Lele. ``A Numerical investigation of sound Generation in supersonic jet screech," AIAA/CEAS Paper, 2000-2081, Aeroacoustics Conference, Lahaina.

10. Constantinescu, G. S. and S. K. Lele. ``Large Eddy Simulation of a near sonic turbulent jet and its radiated noise," AIAA Paper, 2001-0376, Aerospace Sciences Meeting, Reno, 2001.

11. Freund, J. B. ``Acoustic sources in a turbulent jet: A Direct Numerical Simulation study," AIAA Paper 99-1858, AIAA/CEAS Aeroacoustics Conference, Seattle.

12. Bogey, C., Bailly, C. and D. Juve. ``Computations of sound radiated by a 3-D jet using large-eddy simulations,'' AIAA Paper 2000-2009, AIAA/CEAS Aeroacoustics Conference, Lahaina.

13. Lighthill, J. ``On sound generated aerodynamically. I. General theory,'' Proc. Roy. Soc. A., 1952, Vol. 211, p. 564-587.

14. Lighthill, M. J. ``Sound generated aerodynamically,'' Proc. Roy. Soc. A., 1962, Vol. 267, p. 147-182.

15. Lighthill, M. J. ``Jet noise,'' AIAA J., 1963, Vol. 1, p. 1507-1517.

16. Goldstein, M. ***Aeroacoustics***, 1976, Mc Graw Hill.

17. Goldstein, M. ``Aeroacoustics of turbulent shear flows,'' Annual Review of Fluid Mechanics, 1984, Vol. 16, p. 263-285.

18. Morfey, C. ``Sound radiation due to unsteady dissipation in turbulent flows,'' J. Sound Vib., Vol. 48, 1976, p. 95-111.

19. Lilley, G. M. ``On the noise from jets'', AGARD CP 131, Noise Mechanisms, 1974.

20. Tam, C. K. W. and Auriault, L. ``Jet mixing noise from fine-scale turbulence,'' AIAA J. 1999, Vol. 37, p. 145-153.

21. Crighton, D. G. ``Basic principles of aerodynamic noise generation,'' Progr. Aerospace Sci., Vol. 16, 1975, p. 129-146.

22. Tam, C. K. W. and Morris, P. J. ``The radiation of sound by the instability waves of a compressible plane turbulent shear layer,'' J. Fluid Mech., Vol. 98, 1980, p. 349-381.

23. Tam, C. K. W. "On the noise of a nearly ideally expanded supersonic jet," J. Fluid Mech., Vol. 51, 1972, p. 69-95.

24. Liu, J. T. C. ``Developing large-scale wavelike eddies and the near jet noise field,'' J. Fluid Mech., Vol 62, 1974, p. 437-464.

25. Ffowcs Williams, J. E. ``The noise from turbulence convected at high speed,'' Phil. Trans. Roy. Soc. A., 1963, Vol. 255, 469-503.

26. Ffocws Williams, J. E. and Maidanik, G. ``The Mach wave field radiated by supersonic turbulent shear flows,'' J. Fluid Mech., Vol. 21, 1965, p. 641-657.

27. Ffocws Williams, J. E., Simon, J. and Virchis, V. J. ```Crackle': an annoying component of jet noise,'' J. Fluid Mech., Vol. 71, 1975, p. 251-271.

28. Harper-Bourne, M. and Fisher, M. J. ``The noise from shock waves in supersonic jets,” AGARD CP 131, Noise Mechanisms, 1974.

29. Tam, C. K. W. and Tanna, H. K.. ``Shock-associated noise of supersonic jets from convergent-divergent nozzles,” J. Sound Vib., Vol. 81, 1982, p. 337-358.

30. Tam, C. K. W. ``Stochastic model theory of broadband shock associated noise from supersonic jets,” J. Sound Vib., Vol. 116, 1987, p. 265-302.

31. Powell, A. ``On the mechanism of choked jet noise,” Proceedings Physical Society, London, Vol. 66, 1953, p. 1039-1056.

32. Tam, C. K. W. ``Supersonic jet noise,” Annual Rev. Fluid Mech., Vol. 27, 1995, p. 17-43.

33. Kerschen, E. J. and Cain, A. B. ``Modeling supersonic jet screech, Part 2: Acoustic radiation from shock-vortex interaction,” AIAA Paper 95-0507, AIAA Aerospace Sciences Meeting, Reno.

34. Tam, C. K. W. ``Computational Aeroacoustics: Issues and methods,” AIAA J., Vol. 33, 1995, p. 1788-1796.

35. Davies, P. O. A. L., Fisher, M. J. and Barratt M. J. ``The characteristics of the turbulence in the mixing region of a round jet,” J. Fluid Mech., Vol. 15, 1963, p. 337-367, and Corrigendum J. Fluid Mech., Vol. 15, 1963, p. 559.

36. Bradshaw, P., Ferriss, D. H. and Johnson, R. F. ``Turbulence in the noise-producing region of a circular jet,” J. Fluid Mech., Vol. 19, 1964, p. 591-624.

37. Lush, P. A. ``Measurements of subsonic jet noise and comparison with theory,” J. Fluid Mech., Vol. 46, 1974, p. 477-500.

38. Tanna, H. K. ``An experimental study of jet noise. Part I: Turbulent mixing noise,” J. Sound Vib., Vol. 50, 1977, Vol. 50, p. 405-428.

39. Zaman, K. B. M. Q. and Yu, J. C. ``Power spectral density of subsonic jet noise,” J. Sound Vib.,1985, Vol. 98, p. 519-537.

40. Lighthill, J. ``The final panel discussion,” in Computational Aeroacoustics, Proceedings of ICASE-NASA Langley workshop, Editors Hardin, J. C. and Hussaini, M. Y., Springer-Verlag, 1993.

Jet Noise Computation: Direct and Hybrid Approaches

Christophe Bailly,
Christophe Bogey & Daniel Juvé
Centre Acoustique Laboratoire de Mecanique
des Fluides et d'Acoustique

***Jet Noise Computation: Direct and Hybrid Approaches* - Christophe Bailly, Christophe Bogey and Daniel Juve, Centre Acoustique Laboratoire de Mecanique des Fluides et d'Acoustique as summarized by Eugene Krejsa.**

Dr. Bailly presented an overview of experimental observations of jet noise and direct and hybrid approaches to jet noise prediction. LES combined with CAA numerical methods is able to simulate turbulent flows. Results showed good agreement between calculations and measured jet characteristics. The following difficulties in making direct calculations were given:

- Direct acoustic calculation is restricted to geometric basic flows.
- Use of compressible flow field requires efficient boundary conditions.
- Acoustic far field can be obtained via a Kirchhoff surface or by solving a wave equation or linearized Euler's equation.
- It seems difficult to apply a direct approach for low Mach number flows.

The principles, advantages, and restrictions of hybrid methods were summarized. Features of the hybrid method are:

- Separation of sound generation and propagation
- Three steps to obtain the acoustic field
- Determination of the aerodynamic field
- Calculation of source terms
- Calculation of acoustic field

Advantages of the hybrid method include the ability to use the most appropriate computation method at each step and the use of conventional CFD codes to study complex geometries. Restrictions on the use of hybrid methods include the loss of information about flow-acoustic interactions and ambiguity in the definition of acoustic source terms.

Jet Noise Workshop
Ohio Aerospace Institute
November 7-9, 2000

Jet noise computation:

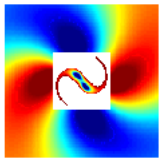
direct and hybrid approaches

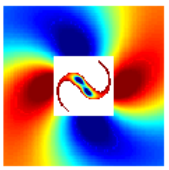
Christophe Bailly

Christophe Bogey & Daniel Juv´e



Centre Acoustique
Laboratoire de **M**écanique des **F**luides et d'**A**coustique
Ecole Centrale de Lyon & UMR CNRS 5509
BP 163, 69131 Ecully c édex, F rance.





Simulations Numériques et Modélisations en Aéroacoustique
équipe du Centre Acoustique, LMFA, ECL & UMR CNRS 5509

Introduction

- Computational AeroAcoustics

- Experimental observations of jet noise

Direct calculation of jet noise

Hybrid approaches

- Lighthill's analogy

- Effets of the mean flow on propagation

- Linearized Euler's Equations as wave operator

References

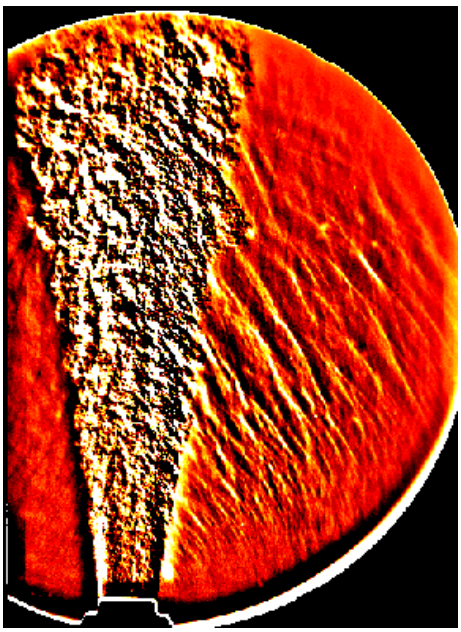
Introduction

Computational AeroAcoustics

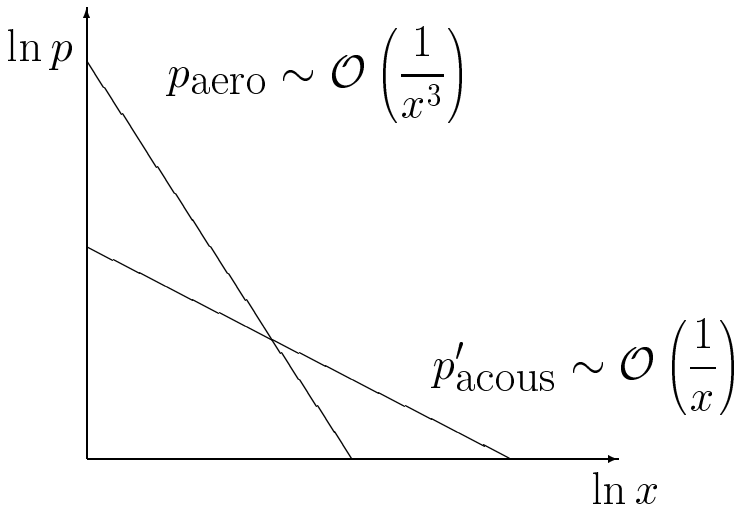
• **Goal of computational aeroacoustics:** determining accurately pressure fluctuations at every point in the field ...

• **Acoustical pressure fluctuations**

Ribner (1964), Crow (1970), Lilley (1972), Howe (1975), Yates (1978), ..., Ristorcelli (1997), ...



P apamoschou, AIAA J. (1997)



$$u = u_{\text{aero}} + u'_{\text{acous}} \qquad \frac{\partial}{\partial t}\nabla.\mathbf{u} = \frac{\partial}{\partial t}\nabla.\mathbf{u}'_{\text{acous}}$$

Dilatation $\Theta = \nabla.\mathbf{u}$

Experimental observations of jet noise

- **Aerodynamic noise sources not very efficient** $M_c \to 0$

$$\eta = \frac{\text{acoustic energy}}{\text{mechanical energy}} \sim M_c^5 \quad \text{with} \quad M_c \leq 1$$

M	OAPWL	St_{pic}	u_j/c_o	u_j	p'_{acous}	u'_{acous}	u'_{acous}/u_j	Re
0.9	147.8 dB	0.174	0.84	285 m.s^{-1}	12 Pa	0.03 m.s^{-1}	1.0×10^{-4}	1.02×10^6
1.5	163.6 dB	0.161	1.24	425 m.s^{-1}	76 Pa	0.18 m.s^{-1}	4.2×10^{-4}	2.49×10^6
2.0	169.1 dB	0.158	1.49	509 m.s^{-1}	142 Pa	0.34 m.s^{-1}	8.1×10^{-4}	5.19×10^6

Acoustic fluctuations measured at $40D$

After: Seiner, Mc Laughlin & Liu, NASA TP-2072
Seiner & Ponton, NASA TM-86296

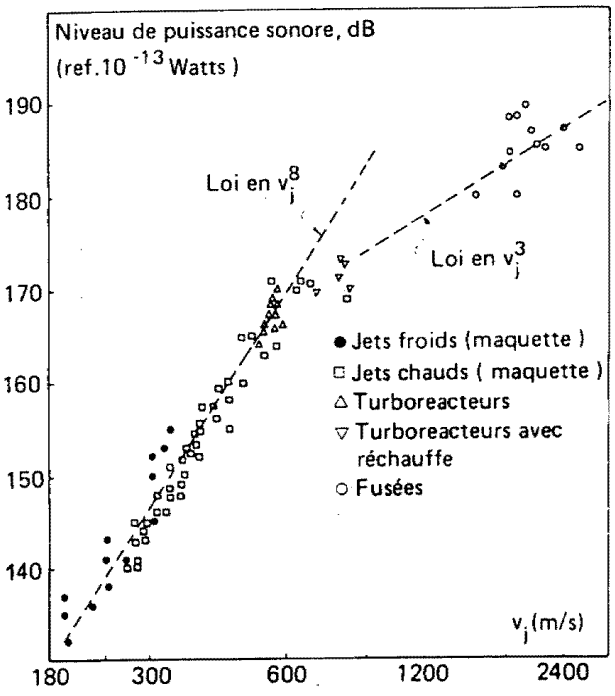
Jet $M = 0.9$

$$M_c \simeq 0.6 \qquad p'_{\text{aero}} \sim \rho u'^2_{\text{aero}} \qquad u'_{\text{aero}} \sim 0.2 U_c$$

$$p'_{\text{aero}} \sim 10^2 \, p'_{\text{acous}} \qquad \text{and} \qquad u'_{\text{aero}} \sim 10^3 \text{ to } 10^4 \, u'_{\text{acous}}$$

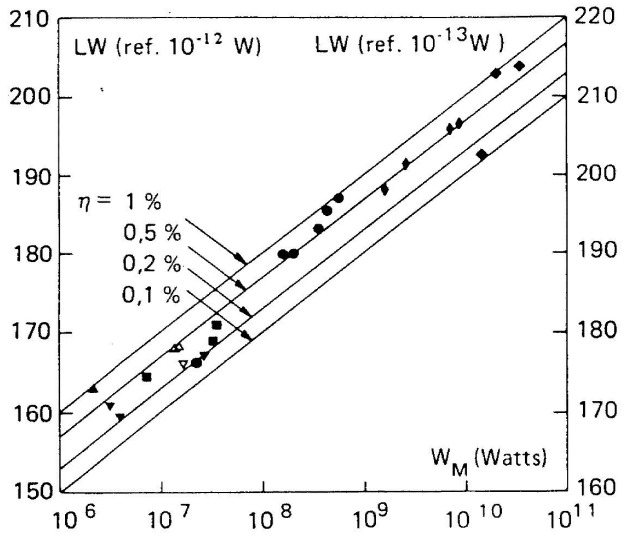
Experimental observations of jet noise

Variation of acoustic power level with jet velocity for subsonic and supersonic jets



Candel, La Recherche Aérospatiale (1983)

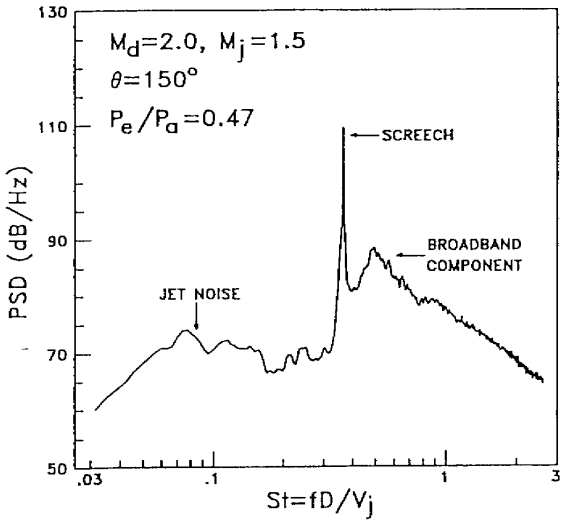
acoustic efficiency for supersonic jets



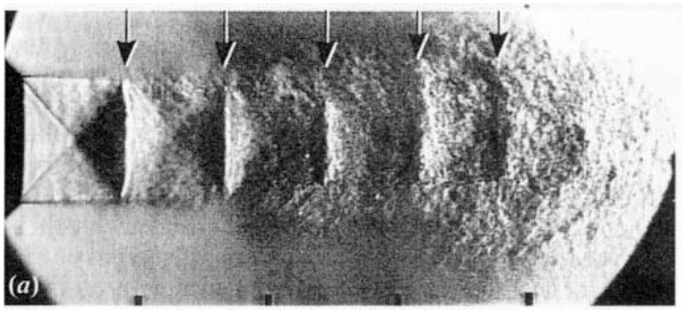
Eldred, NASA SP-8072 (1971) - Candel (1983)

Experimental observations of jet noise

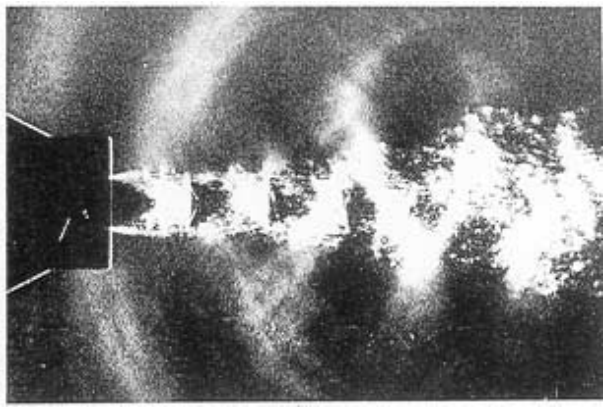
Supersonic jet noise



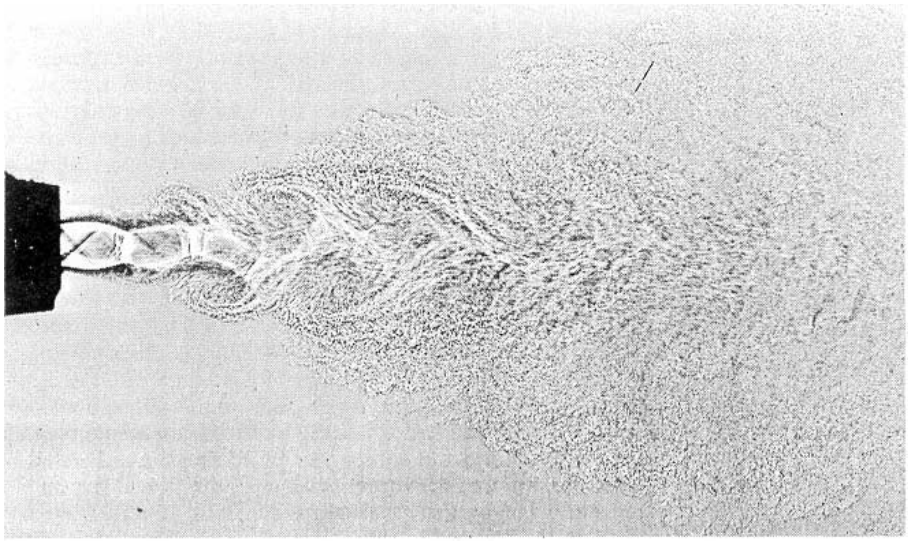
Seiner, AIAA 84-2275



P anda, J. Fluid Mech. (1999)



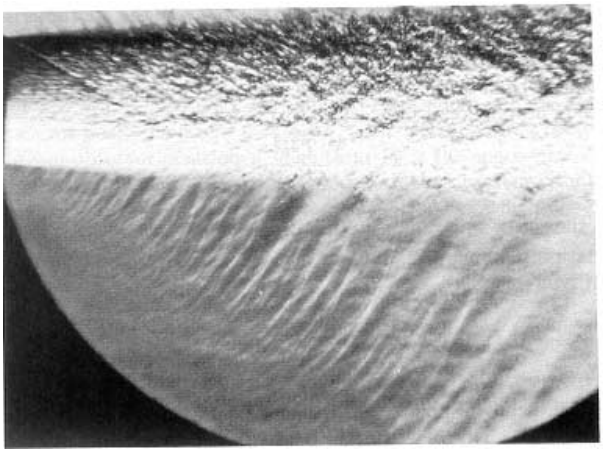
P ow ell, J. Acoust Soc. Am. (1992)



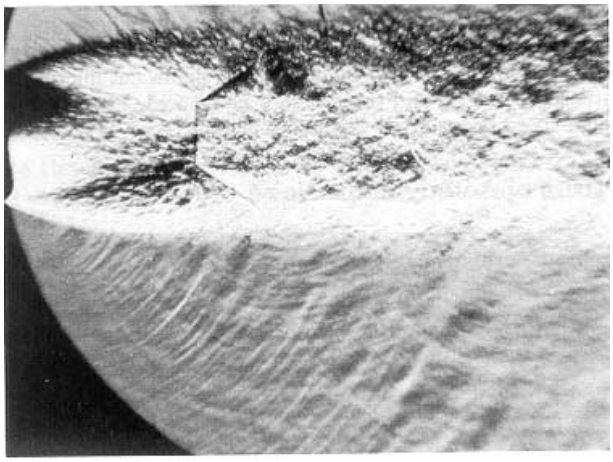
Banerian, AIAA J. (1978)

Experimental observations of jet noise

Supersonic jet noise



Seiner, AIAA 84-2275. M=2, $p_j/p_\infty = 1.00$



Seiner, AIAA 84-2275. M=1.8, $p_j/p_\infty = 3.05$.

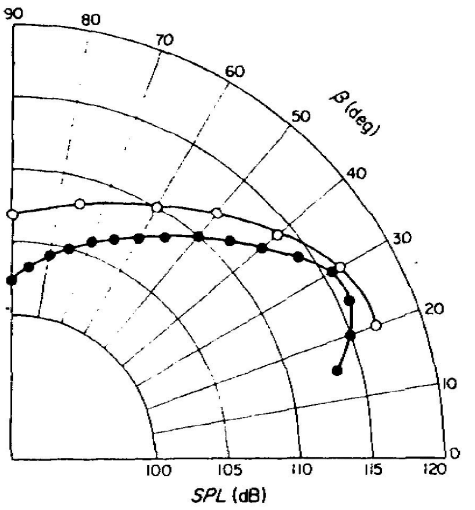
Experimental observations of jet noise

Influence of Reynolds number

Subsonic jet M = 0.9

- Re = 3600
- Re = 5.4×10^5

Mollo-Christensen et al., J.Fluid Mech. (1964)



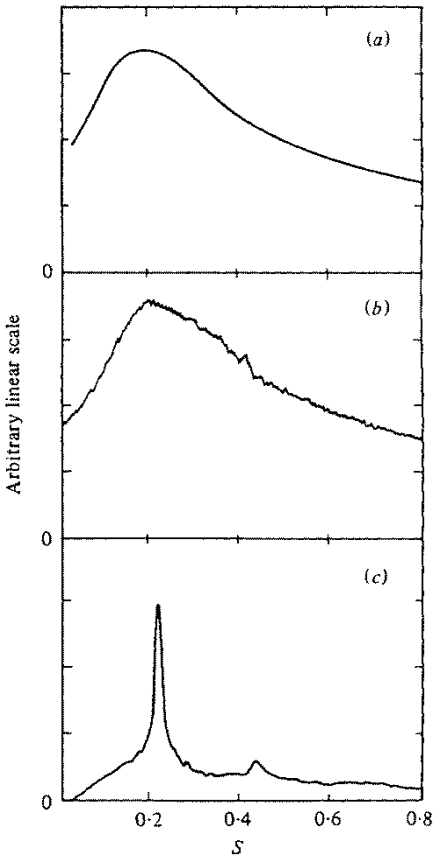
Stromberg, J. Sound Vib. (1980)

Supersonic jet: acoustic spectra in direction of maximum noise radiation

(a) $M = 2.0$ and $\mathrm{Re} = 2.6 \times 10^6$

(b) $M = 2.1$ and $\mathrm{Re} = 7 \times 10^4$

(c) $M = 2.1$ and $\mathrm{Re} = 7900$



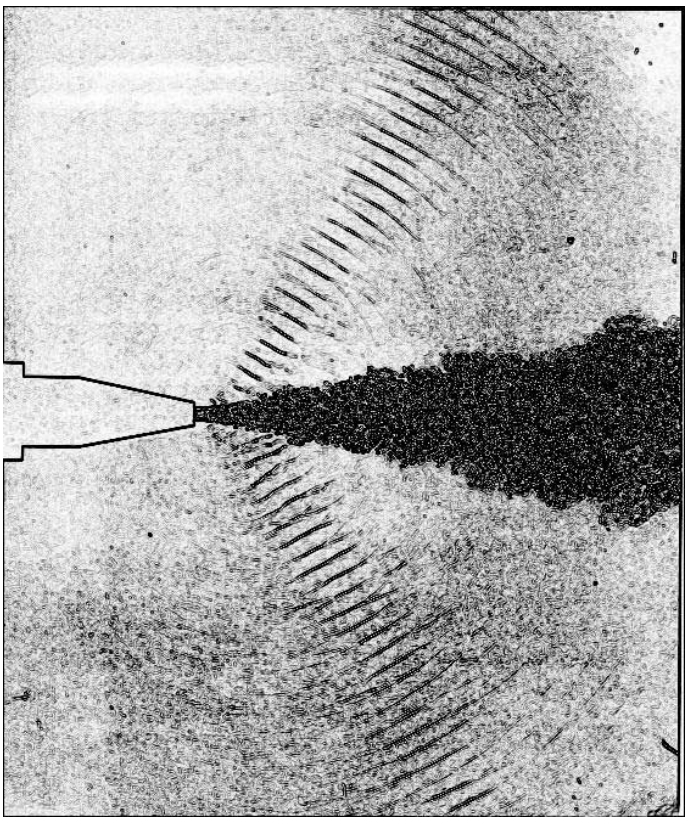
T routt & McLaughlin, J. Sound Vib.(1982)

Experimental observations of jet noise

- **Large wavelength scales of sound field / shear thickness**

Jet velocity profile approximations (Michalke, 1971):

$$\begin{cases} \dfrac{\bar{U}}{u_j} = \dfrac{1}{2}\left\{1 + \tanh\left[\dfrac{R}{2\delta_\theta}\left(1 - \dfrac{r}{R}\right)\right]\right\} & \delta_\theta/R < 0.08 \\ \dfrac{\bar{U}}{u_j} = \dfrac{1}{2}\left\{1 + \tanh\left[\dfrac{R}{4\delta_\theta}\left(\dfrac{R}{r} - \dfrac{r}{R}\right)\right]\right\} & \delta_\theta/R \geq 0.08 \end{cases}$$



Van Dyke - An album of Fluid Motion (1982)

$$\delta_\theta \simeq 0.03x/R + 0.04R$$

Mesh grid

$$\Delta r_{\text{acous}} \simeq 50 \times \Delta r_{\text{aéro}}$$

Direct calculation of the acoustic field

Direct acoustic calculation

- **Solve compressible Navier-Stokes equations** to determine both the aerodynamic field and the sound field directly, via a DNS, a LES or a SDM (Semi-Deterministic Modelling or unsteady RANS) calculation.

direct calculation of sound $\longrightarrow$ reference solution

- **Interest**
  - understand noise generation mechanism
  - v alidatehybrid approaches

- **First achievements**

- Colonius, Lele & Moin (1995,1997): DNS 2-D mixing lay er
- Mitchell, Lele & Moin (1997, 1999): DNS axi. supersonic and sub. jet
- Manning & Lele (1998): DNS 2-D mixing la yer with shock (screech)
- Tam & Shen (1999) : unsteady RANS of axisymmetric jet screech tones
- $\star$ Freund, Lele & Moin (1998, 1999): DNS sub- and supersonic 3-D jet
  M = 0.9 and Re $= u_j D/\nu = 3600$, $M = 1.92$ and Re $= u_j D/\nu = 2000$
- Choi, Barber, Chiappetta & Nishimura (1999): LES 3-D supersonic jet
- Morris, Long & Scheidegger (1999): LES 3-D jet $M = 2.1$ and Re $= 70000$
- Shieh & Morris (1999): DNS 2-D cavity noise
- Colonius, Basu & Rowley (1999): DNS 2-D cavity noise
- $\star$ Bogey, Bailly & Juv´e (2000): LES 3-D jet M = 0.9 and Re = 65000
- Gloerfelt, Bailly & Juv´e (2000): DNS 2-D cavity

Direct calculation: numerical issues

- **Intrinsic to aerodynamic simulations**

$$\mathrm{St} = \frac{fL}{u_j} \sim 1 \quad \longrightarrow \quad \frac{L}{\lambda} \sim \mathrm{M}$$

DNS	**LES**
Number of points in one direction	
$n_x \sim \frac{\lambda}{l_\eta} \sim \frac{1}{\mathrm{M}} \mathrm{Re}_L^{3/4} \quad \mathrm{Re}_L = \frac{u'L}{\nu}$	$n_x \sim \frac{\lambda}{\lambda_g} \sim \frac{1}{\mathrm{M}} \mathrm{Re}_L^{1/2}$
Number of mesh points	
$N \sim n_x^3 \sim \frac{1}{\mathrm{M}^3} \mathrm{Re}_L^{9/4}$	$N \sim n_x^3 \sim \frac{1}{\mathrm{M}^3} \mathrm{Re}_L^{3/2}$
Time step	
$\Delta t \sim \frac{l_\eta}{c}$	$\Delta t \sim \frac{\lambda_g}{c}$
Number of time steps	
$n_t \sim \frac{T}{\Delta t} \sim \frac{L}{u_j}\frac{c}{l_\eta} \sim \mathrm{Re}_L^{3/4} \frac{1}{\mathrm{M}}$	$n_t \sim \frac{T}{\Delta t} \sim \frac{L}{u_j}\frac{c}{\lambda_g} \sim \mathrm{Re}_L^{1/2} \frac{1}{\mathrm{M}}$
$\mathrm{cost} \sim N \times n_t \sim \mathrm{Re}_L^3 \times \frac{1}{\mathrm{M}^4}$	$\mathrm{cost} \sim N \times n_t \sim \mathrm{Re}_L^2 \times \frac{1}{\mathrm{M}^4}$

Direct calculation: numerical constraints

Notations

- L size of large eddies, $L \sim D$ jet diameter
- u_j jet velocity
- λ acoustic wavelength
- M Mach number $\mathrm{M} = u_j/c$
- l_η Kolmogorov length scale
- λ_g Taylor length scale
- n_x number of points in one direction
- N number of mesh points $N \sim n_x^3$
- Δt time step
- c sound speed
- T characteristic time of large eddies $T \sim L/u_j$
- n_t number of time steps $n_t \sim T/\Delta t$

$$\frac{L}{l_\eta} \sim \left(\frac{u'L}{\nu}\right)^{3/4} \sim \mathrm{Re}_L^{3/4} \qquad \frac{L}{\lambda_g} \sim \mathrm{Re}_L^{1/2} \qquad \text{(IHT)}$$

Direct calculation: numerical issues

- **specific to computational aeroacoustics**

  - numerical schemes

    Lele (compact, 1992), Tam & Webb (DRP, 1993)

    Hu, Hussaini & Manthey (1996)

    ...

  - treatment of boundary conditions: key point

    - **Engquist & Majda (1977)**
    - **Hedstrom (1979)**
    - **Rudy & Strikwerda (1980)**
    - **Bayliss & T urkel (1982)**
    - **Thompson (1987, 1990)**
    - **Giles (1990)**
    - **Poinsot & Lele (1992)**
    - **Colonius, Lele & Moin (1993)**
    - **Tam & Webb (1993)**
    - **Collino (1996)**
    - **Tam & Dong (1996)**

    not an exhaustive list

    ...

    No one of these formulations leads to a totally efficient treatment of boundary conditions when vortical perturbations leave out the computational domain (in an acoustic point of view).

ALESIA code

(Appropriate Large Eddy SImulation for Aeroacoustics)

- **2D/3D code solving the Navier-Stokes equations**
  - numerical algorithm

    DRP scheme of Tam & Webb + 4th order Runge-Kutta
  - non-uniform cartesian mesh
  - non-reflecting boundary conditions of Tam & Dong
  - sponge zone into the outflow
  - DNS or LES with Smagorinsky's subgrid scale model
  - vectorization: CPU speed $>$ 4000 Mflops on Nec SX-5

- **Studied configurations**
  - two co-rotative vortices
  - 2-D subsonic mixing layer
  - 3-D subsonic jet

Bogey, Bailly & Juvé AIAA Paper 99-1871 (accepted in AIAA J.)
AIAA Paper 2000-2009 & 2000-2047

- **Use of a sponge zone into the outflow**

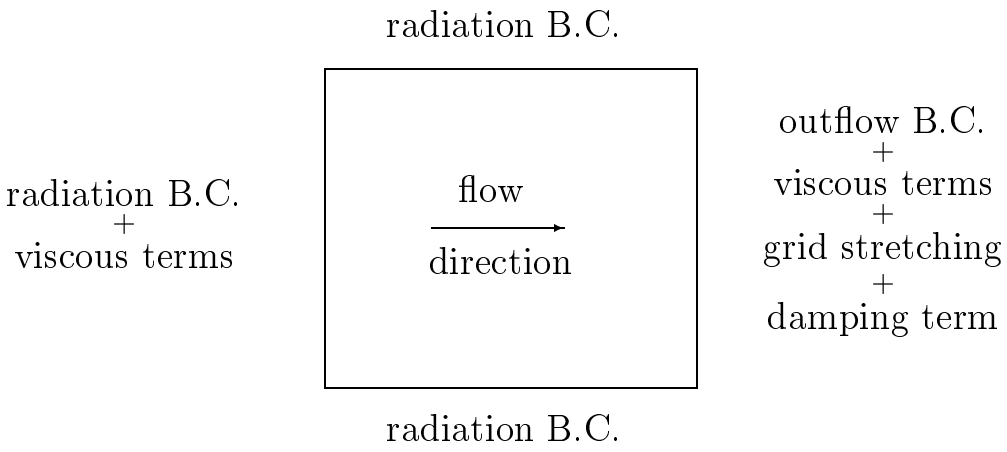
  → grid stretching over about fifty points

  → addition of an artificial damping term

  introduced gradually with an exponential profile

  Ref. Colonius, Lele & Moin (1993)
  Ta'asan & Nark (1995)
  Hu (1996)
  3rd CAA workshop (1999), ...

- **Viscous terms** are taken into the inflow and outflow boundaries



LES of a 3-D subsonic round jet

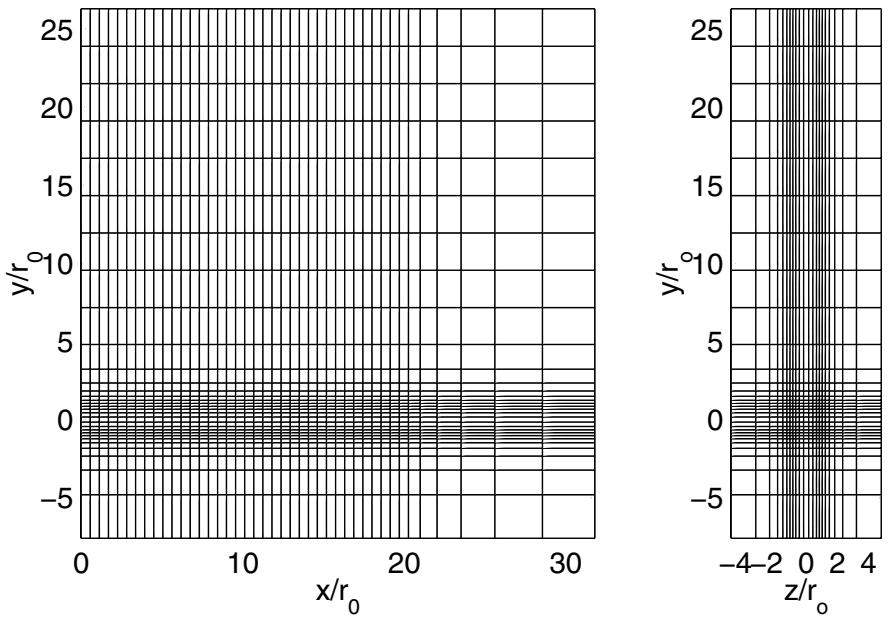
- **Configuration**
  - Mach number : $M_j = 0.9$
  - Reynolds number : $Re_D = D \times U_j/\nu = 65000$

- **Random excitation into the inflow**

  with addition of vortical perturbations in the sheared zone

  $\rightarrow$ natural aerodynamic development

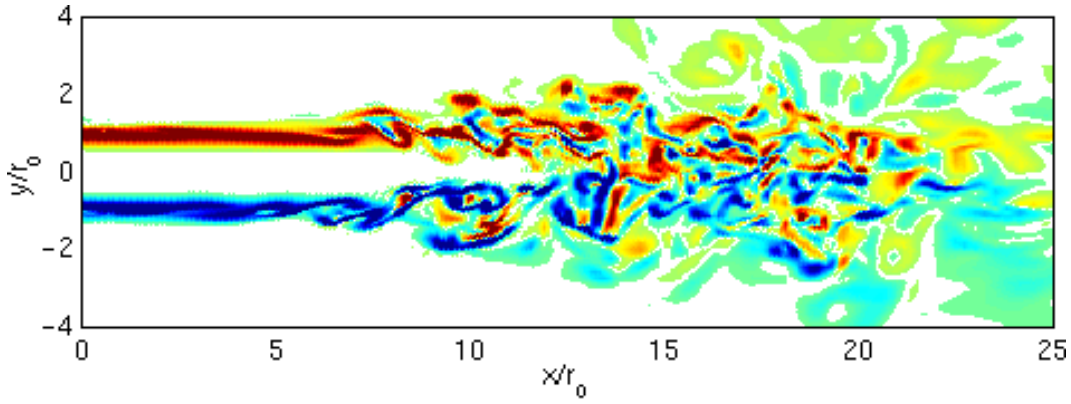
- **Numerical parameters**
  - mesh of $255 \times 187 \times 127$ points (cut-off Strouhal number in the acoustic far-field : $St_c = f_c \times D/U_j \simeq 1.1$)
  - computation time: 15h on a Nec SX-5 for 30000 iterations



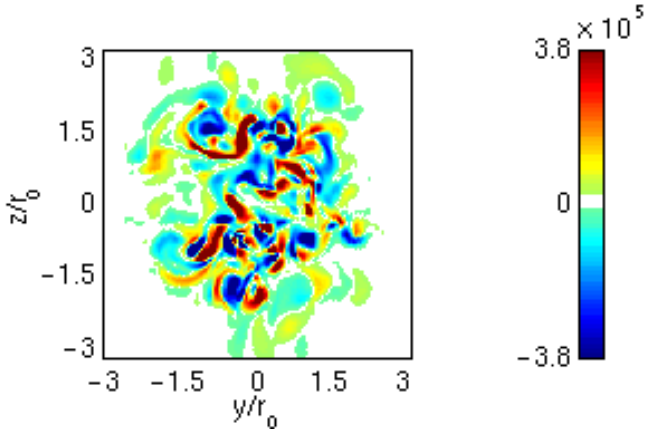
Aerodynamic development

- **Longitudinal and transversal vorticity fields**

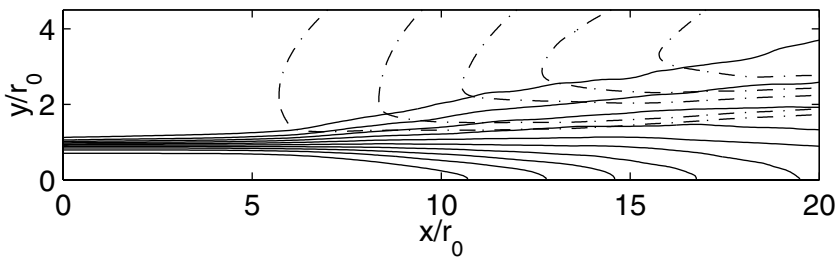
ω_{xy} at $z = 0$



ω_{yz} at $x = 12r_0$



- **Mean flow development**



—— isolines of the mean axial velocity

– · – · streamlines

→ end of the potential core around $x = 10r_0$ (consistent with Lau, Morris & Fisher, 1979)

→ entrainment of the surrounding flow

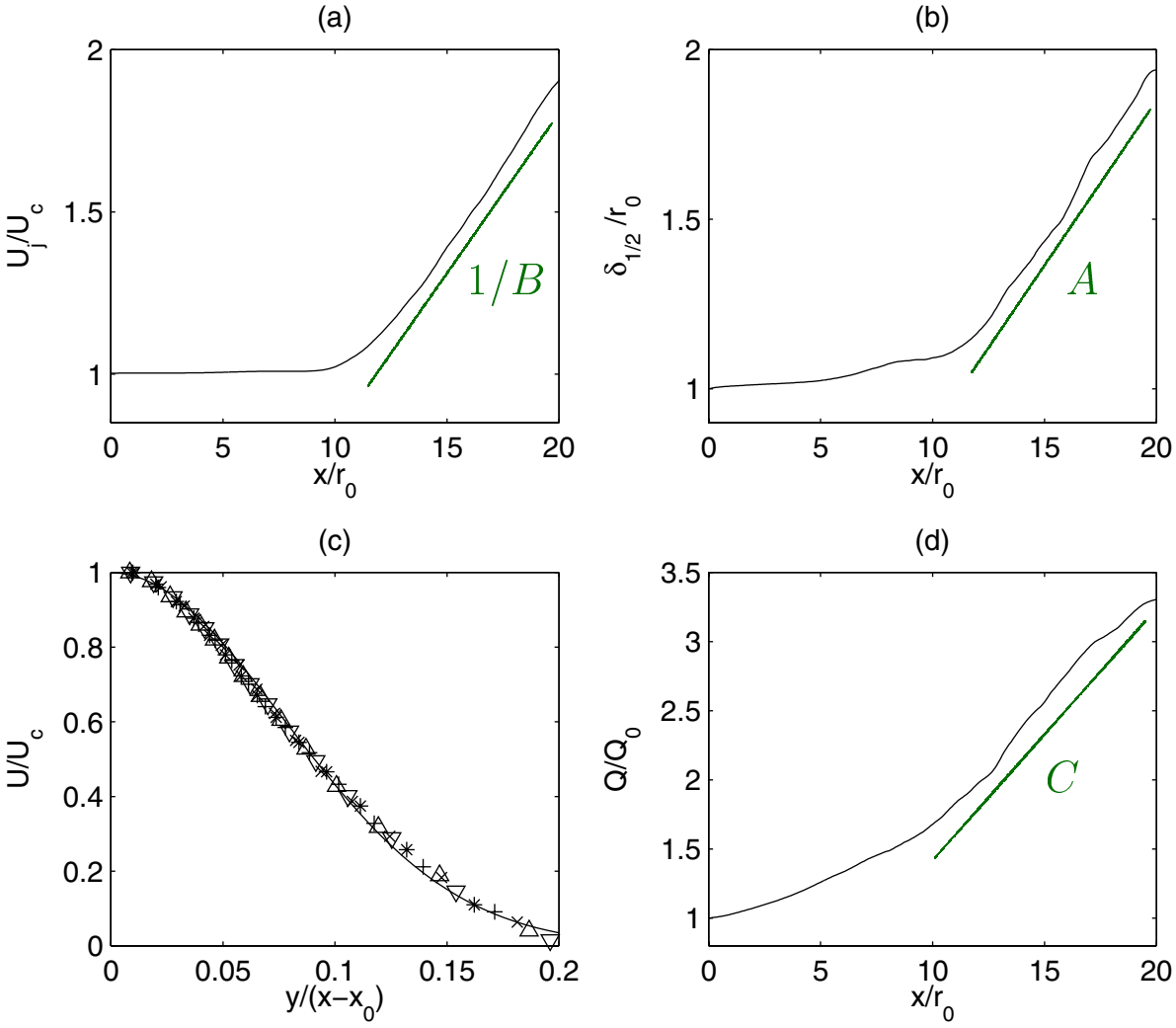
- **Mean flow properties**

  (a) in v erseof the mean centerline longitudinal velocity : U_c/U_j

  (b) half-width of the jet : $\delta_{1/2}/r_0$

  (c) 5 radial profiles of mean longitudinal velocity between $15r_0$ and $20r_0$

  (d) mean flow rate : Q/Q_0



B	A	Reference
5.4	0.086	Wygnanski & Fiedler (1969)
6.1	0.096	P anchapakesan & Lumley (1993)
5.8	0.094	Hussein, Capp & George (1994)
5.5	0.096	Present computation

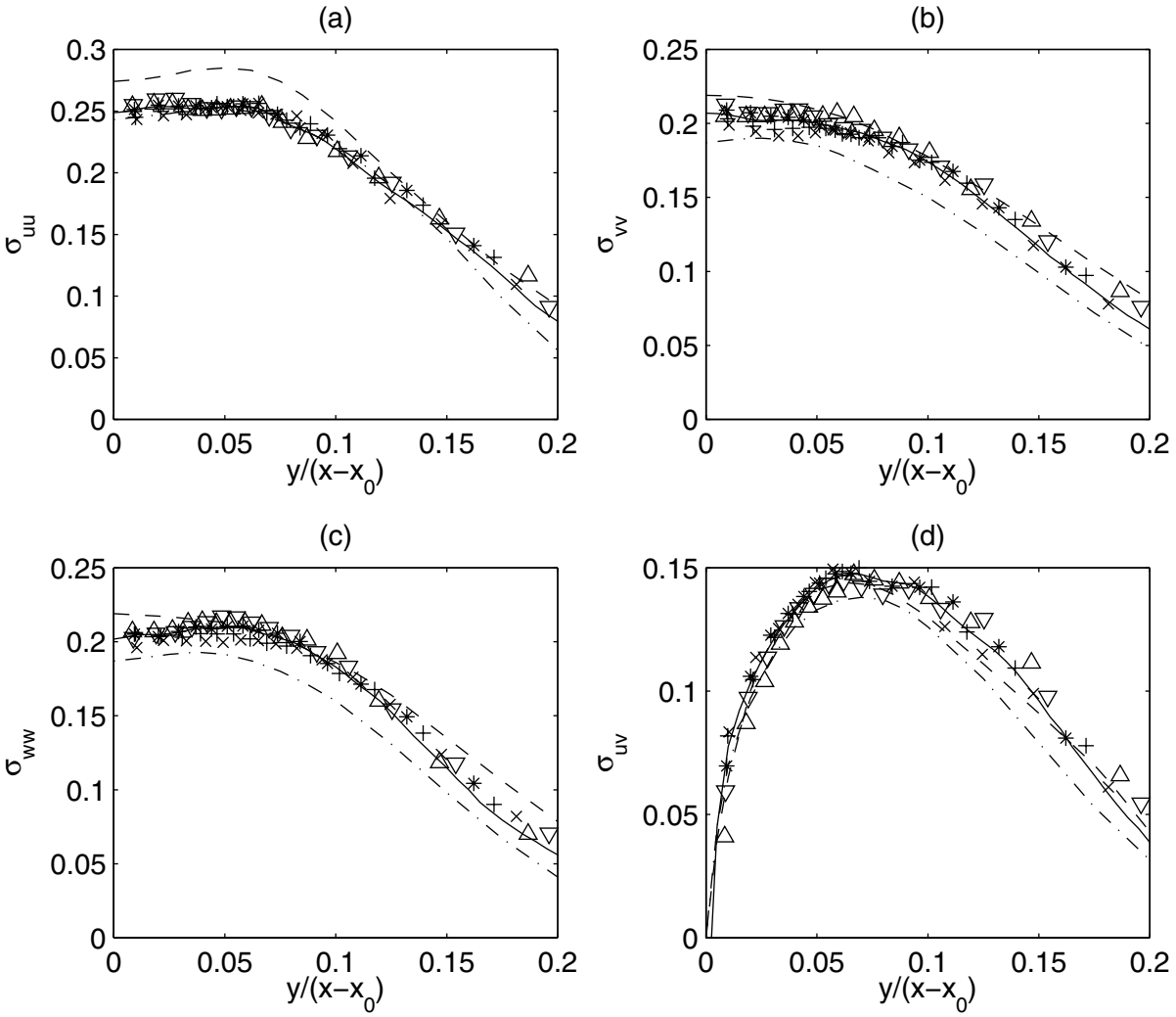
C = 0.32 (similar to Ricou & Spalding, 1961)

→ mean jet development in agreement with experiments

- **Radial profiles of turbulent intensities**

(a) $\sigma_{uu} = u'/U_c$ (b) $\sigma_{vv} = v'/U_c$

(c) $\sigma_{ww} = w'/U_c$ (d) $\sigma_{uv} = \sqrt{u'v'}/U_c$



×, +, ∗, ▽, △, 5 profiles between $x = 15r_0$ and $x = 20r_0$

——— , mean profile

– – – , Hussein, Capp & George (1994)

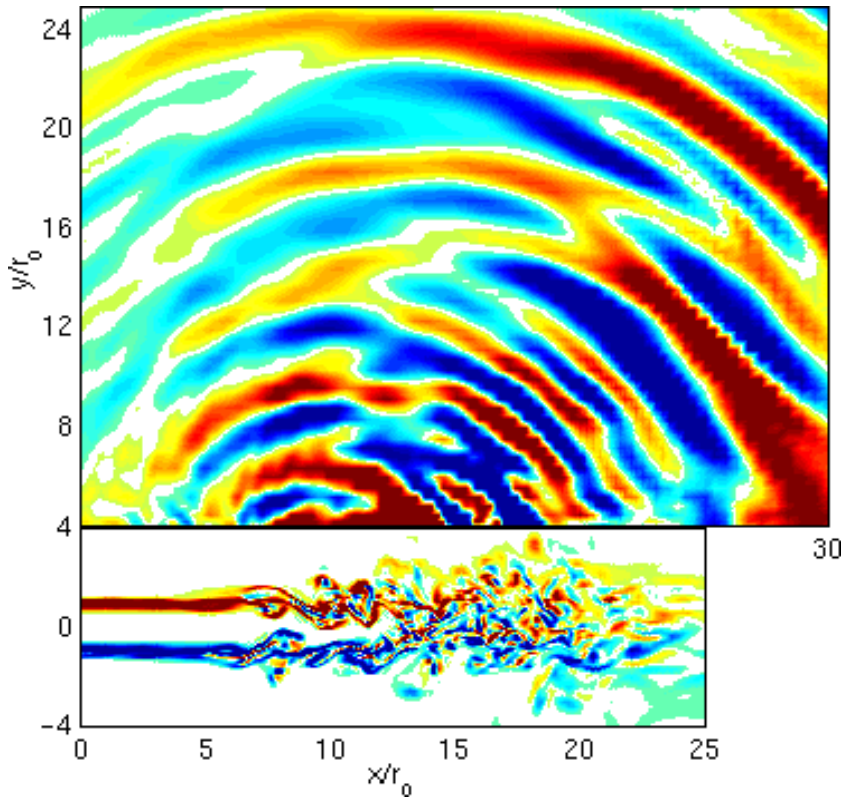
– - – - , Panchapakesan & Lumley (1993)

→ self-similar profiles

→ turbulent intensities in accordance with measurements

Radiated acoustic field

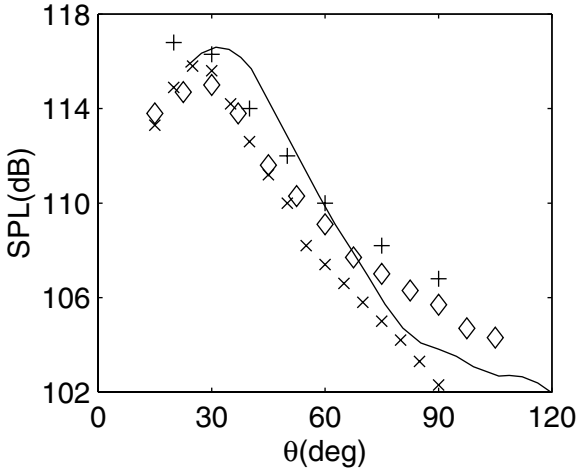
- **Dilatation field $\Theta = \nabla.\mathbf{u}$ provided by LES**



$\rightarrow$ acoustic sources located at the end of the potential core around $x \simeq 11 r_0$ (as shown experimentally)

- **Directivity of the acoustic radiation**

Sound pressure levels at a distance of $60r_0$ from the inflow



	M	Re_D	Reference
+	0.9	5.4×10^5	Mollo-Christensen, Kolpin & Martucelli (1964)
◇	0.88	5×10^5	Lush (1971)
×	0.9	3600	Stromberg, McLaughlin & T routt(1980)
-	0.9	65000	Present computation

→ directivity and levels in good agreement with experimental data

Concluding remarks

- **LES** combined with **CAA** numerical methods is able to simulate turbulent flows

  $\longrightarrow$ flow development in good agreement with experimental data

- Faisability of direct calculation of jet noise using LES

  $\longrightarrow$ SPL and directivity consistent with measurements

- **Numerical investigation of jet noise**

  $\longrightarrow$ need new criteria to identify turbulent events associated with noise generation

Difficulties of direct calculation

- **Direct acoustic calculation** is restricted to geometrically basic flows,
  at low Reynolds numbers for DNS, $\mathrm{Re}_D \sim 10^3$ to 10^4, and
  at moderate Reynolds numbers for LES, $\mathrm{Re}_D \sim 10^4$ to 10^5 (discussions about turbulence models).

- Use of the compressible field requires efficient/outstanding boundary conditions

- Acoustic far field can be obtained via a Kirchhoff surface (with a retarded time problem to solve), or by solving a wave equation or linearized Euler's equations.

- It seems difficult to apply a direct approach for low Mach number flows (car & train studies: acoustic comfort in surface transports, ...).

$\longrightarrow$ **reference solution**

Some hybrid approaches to predict aerodynamic noise

Hybrid methods

- **Principle**

  → separation of sound generation and propagation

  → 3 steps to obtain the acoustic field

  - *determination of the aerodynamic field*
    (computation or modelling)
  - *building of source terms*
  - *resolution via a wave operator*
    Lighthill's equation, Linearized Euler's Equations, ...

- **Advantages**

  → use of the most appropriate method at each step

  → use of conventional CFD codes to study complex geometries

- **Restrictions**

  → loss of informations about flow - acoustic interactions
  (refraction & convection)

  → modelling of source terms

  How define acoustic sources in a turbulent flow ?

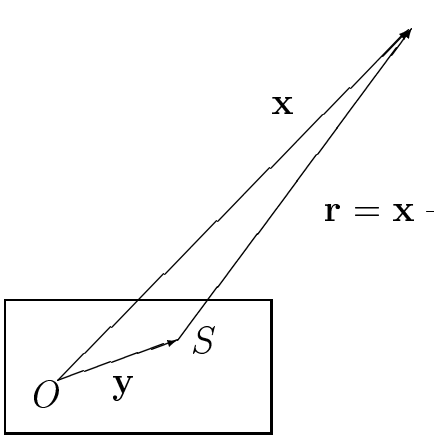
Lighthill's analogy

Lighthill's theory (1952)

Lighthill's wave equation:

$$\frac{\partial^2 \rho'}{\partial t^2} - c_o^2 \nabla^2 \rho' = \frac{\partial^2 T_{ij}}{\partial x_i \partial x_j}$$

$$\text{with} \quad T_{ij} = \rho u_i u_j + \left(p' - c_o^2 \rho'\right) \delta_{ij} - \tau_{ij}$$



$$\rho'(\mathbf{x}, t) \simeq \frac{1}{4\pi c_o^4 x} \frac{x_i x_j}{x^2} \int_V \frac{\partial^2 T_{ij}}{\partial t^2} \left(\mathbf{y}, t - \frac{r}{c_o}\right) d\mathbf{y}$$
$$x \to \infty$$

source volume V of turbulence

- for a perfect gas: $p' = c_o^2 \rho' + (p_o / c_v)\, s'$
- high Reynolds number flow without entropy fluctuations:

$$T_{ij} \simeq \rho u_i u_j$$

- **Some applications**

Sarkar & Hussaini (1993): DNS isotropic turbulence

Mitchell, Lele & Moin (1995): DNS vortex pairing

Wang, Lele & Moin (1996): DNS vortex shedding and boundary layer

Witkowska, Juvé & Brasseur (1997): LES isotropic turbulence

Bastin, Lafon & Candel (1997): unsteady RANS plane jet

Whitmire & Sarkar (2000): DNS homogeneous turbulence

Colonius & Freund (2000): DNS supersonic jet

Sérore, Sagaut, Bailly & Juvé (2000): LES homogeneous turbulence

Bogey, Bailly & Juvé (2000): LES plane mixing layer

- **Main problems**

  - accurate interpolation to solve the retarded time problem,
  - meanflow - acoustic interactions in the source term

→ Phillips' equation (1960)

→ Lilley's equation (1972)

Lighthill's integral solution

Considering a volume V surrounding all the sound sources, all these expressions are equivalent in the acoustic far field:

$$\rho'(\mathbf{x},t) = \frac{1}{4\pi c_o^2}\int_V \frac{\partial^2 T_{ij}}{\partial y_i \partial y_j}\left(\mathbf{y}, t-\frac{r}{c_o}\right)\frac{d\mathbf{y}}{r} \qquad \text{exact formulation (i)}$$

$$\rho'(\mathbf{x},t) \simeq \frac{1}{4\pi c_o^2 x}\int_V \frac{\partial^2 T_{ij}}{\partial y_i \partial y_j}\left(\mathbf{y}, t-\frac{r}{c_o}\right)d\mathbf{y} \qquad \text{far-field approximation}$$

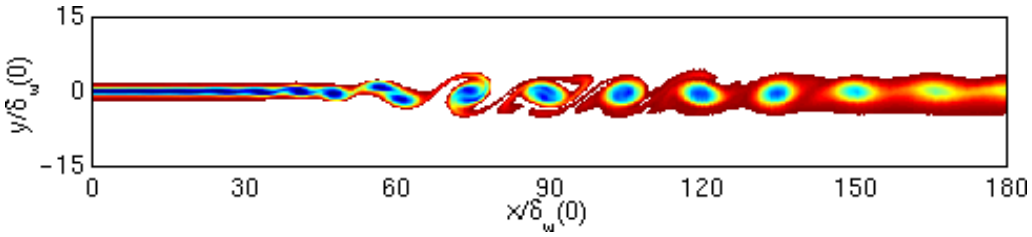
$$\rho'(\mathbf{x},t) = \frac{1}{4\pi c_o^2}\frac{\partial^2}{\partial x_i \partial x_j}\int_V T_{ij}\left(\mathbf{y}, t-\frac{r}{c_o}\right)\frac{d\mathbf{y}}{r} \qquad \text{exact formulation}$$

$$\rho'(\mathbf{x},t) \simeq \frac{1}{4\pi c_o^2 x}\frac{\partial^2}{\partial x_i \partial x_j}\int_V T_{ij}\left(\mathbf{y}, t-\frac{r}{c_o}\right)d\mathbf{y} \qquad \text{far-field approximation}$$

$$\rho'(\mathbf{x},t) \simeq \frac{1}{4\pi c_o^2 x}\frac{x_i x_j}{x^2}\int_V \frac{\partial^2}{\partial t^2} T_{ij}\left(\mathbf{y}, t-\frac{r}{c_o}\right)d\mathbf{y} \qquad \text{far-field approximation (ii)}$$

- Some formulations are more sensitive to retarded time approximation to evaluate the integral (Crighton, 1974).
- Use of space derivatives, in formulation (i), induces numerical errors of the order of $1/M_c^2$ with respect to formulation (ii) with time derivatives. (Sarkar & Hussaini, 1993).

Noise generated by a 2-D mixing layer forced at f_0 and $f_0/2$



- **Application of Lighthill's analogy**

  $\rightarrow$ Use of LES aerodynamic data to construct T_{ij} on a domain extending from 5 to $235\delta_\omega(0)$ in x and from -50 to $50\delta_\omega(0)$ in y, every 10 iterations

  $\rightarrow$ 4th-order time interpolation of source terms

  $\rightarrow$ Weighting of the source volume in the outflow direction to cancel their v alueson the boundary

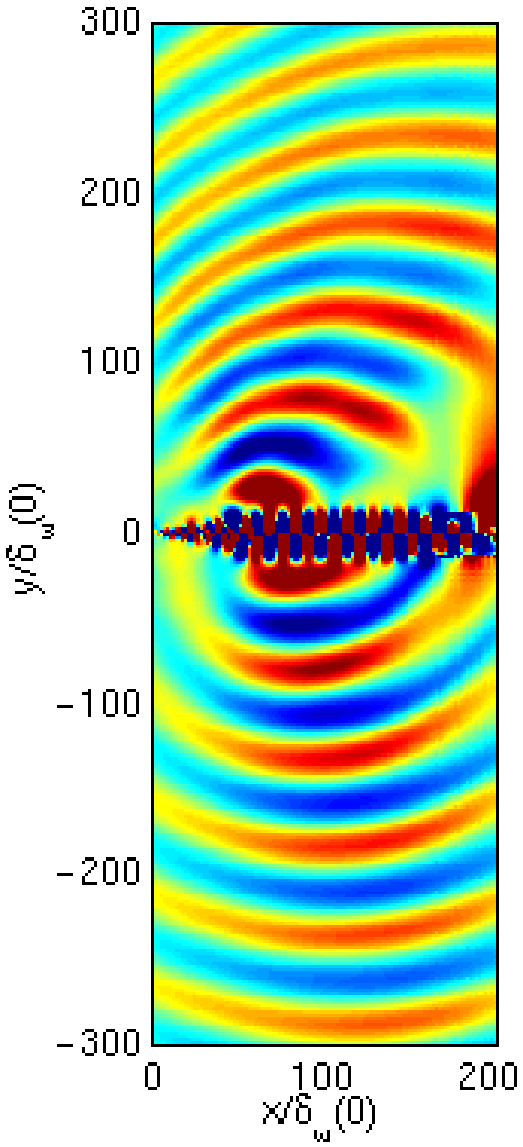
  Radiated acoustic field basically harmonic:

$$\begin{cases} G_{2D}(\mathbf{r}) \simeq \dfrac{1}{4i}\sqrt{\dfrac{2}{\pi k_0 r}}\, e^{ik_0 r - \frac{i\pi}{4}} & k_0 r > 4 \\ \\ G_{3D}(\mathbf{r}) = -\dfrac{1}{4\pi r}\, e^{ik_0 r} \end{cases}$$

  $\rightarrow$ phase delay of $\pi/4$ and decay of the acoustic field as $1/r$ instead of $1/\sqrt{r}$

Noise generated by a mixing layer

– **Dilatation field $\Theta = \nabla.\mathbf{u}$** on the whole physical domain



→ LES result

→ wave fronts coming from the pairing location with a **wavelength corresponding to frequency** $f_p = f_o/2$

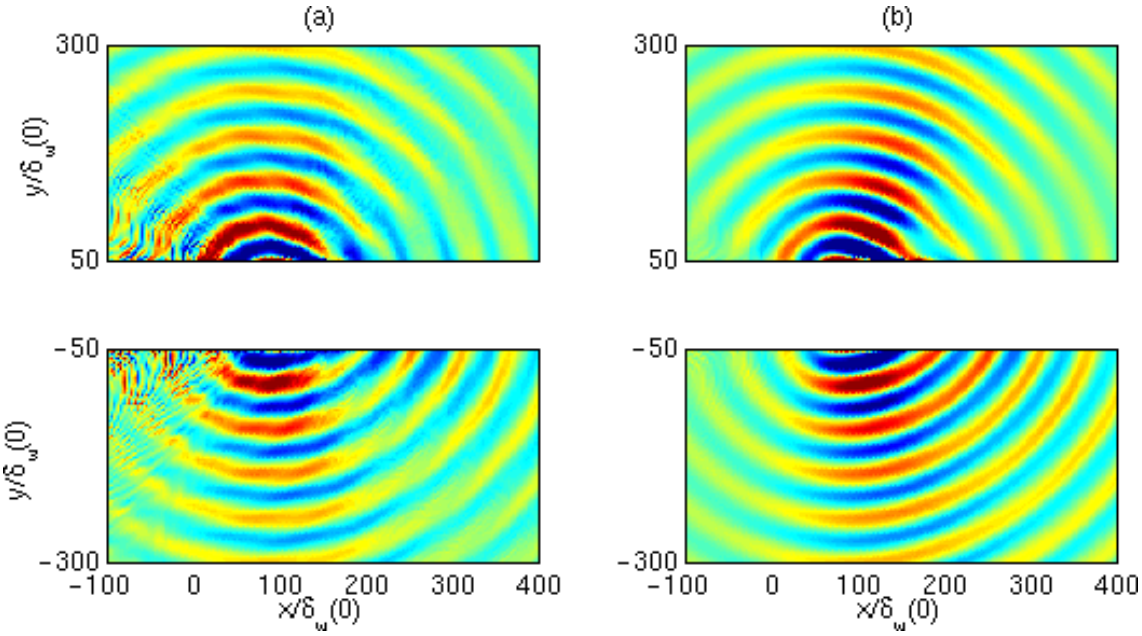
$$\lambda_{f_p} = 51.5\delta_\omega(0)$$

→ **convection effects** (particularly visible in the upper rapid flow)

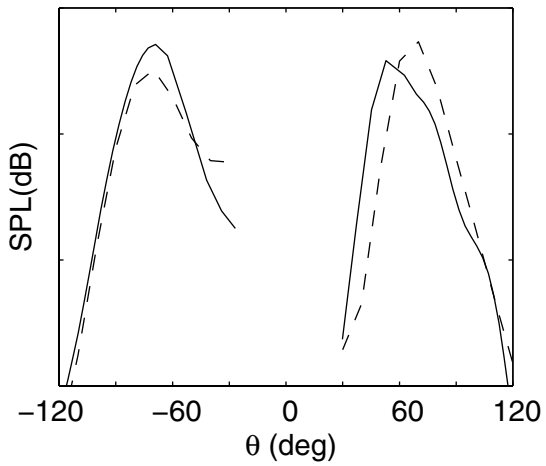
Ref. Colonius, Lele & Moin J. Fluid Mech., **320**, 1997. (DNS)
Bogey, Bailly & Juvé AIAA P aper99-1871 (accepted in AIAA J.)

- **Pressure field provided by Lighthill s analogy**

$\partial^2 T_{ij}/\partial y_i \partial y_j$ $\partial^2 T_{ij}/\partial t^2$



- **Directivity**



——— , LES

- - - , Lighthill's analogy with time derivatives

4 dB between two graduations

→ Lighthill's analogy compares more favorably in the slow flow than in the rapid flow (difference of 20°).

Ambiguity of Lighthill's source term

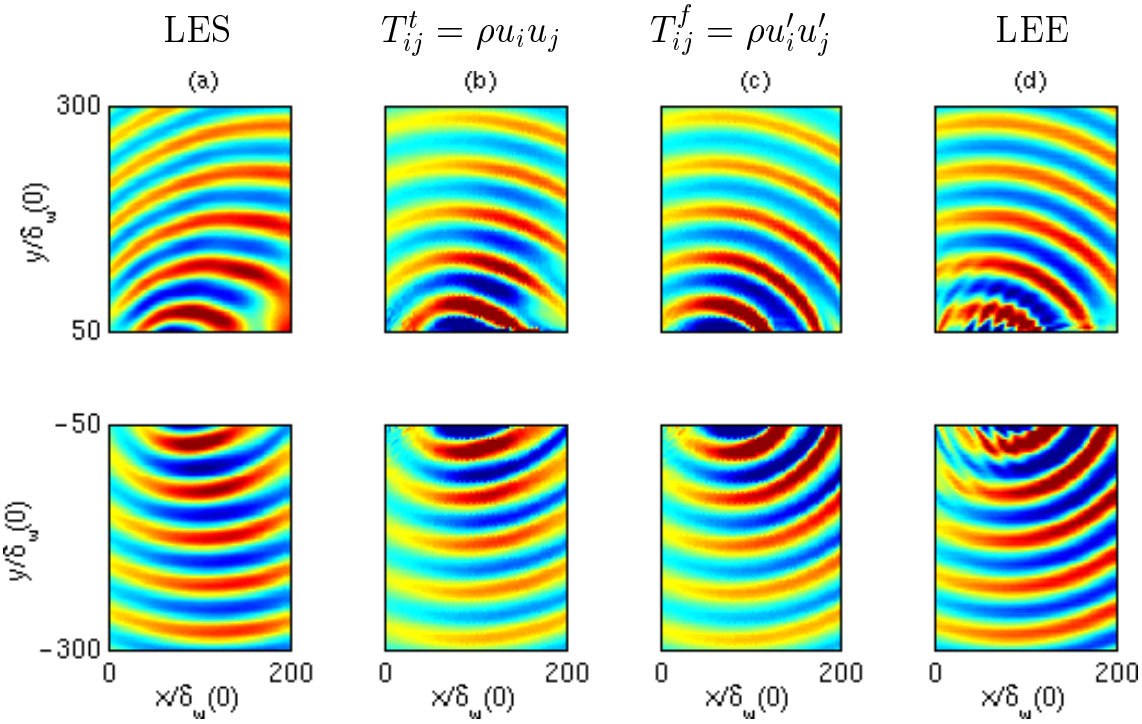
By applying an acoustic analogy, one can expect to separate the radiated field and the aerodynamic field, where $T_{ij} \simeq \bar{\rho} u_i u_j$

$$
\begin{aligned}
T_{ij}^t &= T_{ij} - \bar{T}_{ij} \qquad \text{(centered source term)} \\
&\simeq \bar{\rho} u_i u_j - \bar{\rho}\, \overline{u_i u_j} \\
&\simeq \underbrace{\bar{\rho}\bar{u}_i u'_j + \bar{\rho} u'_i \bar{u}_j}_{\text{shear-noise}} + \underbrace{\bar{\rho} u'_i u'_j - \bar{\rho}\, \overline{u_i u_j}}_{\text{self-noise}} \\
&\simeq T_{ij}^s + T_{ij}^f
\end{aligned}
$$

In practice:

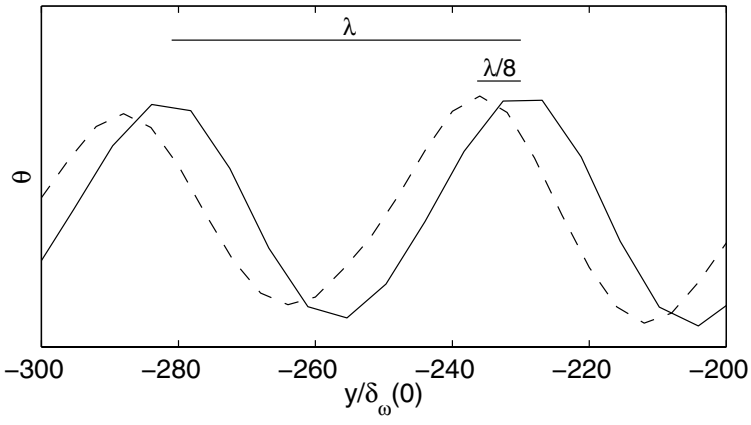
$$
\begin{cases}
\text{if} \quad u_i = \bar{u}_i + u'_{i\text{aero.}} & \Longrightarrow \quad \text{lost interactions} \\
\text{if} \quad u_i = \bar{u}_i + u'_{i\text{aero. + acous}} & \Longrightarrow \quad \text{interactions into } T_{ij}^s
\end{cases}
$$

- **Dilatation field obtained with 4 methods**



$\rightarrow$ Lighthill with $T_{ij}^f \sim$ LEE without mean flow with S_{ij}^f

$\rightarrow$ Lighthill with $T_{ij}^t \sim$ LES



Dilatation profile at $x = 70\delta_\omega(0)$

—— LEE with S_{ij}^f

– – – Lighthill with T_{ij}^f

Lighthill's analogy

- In the framework of an acoustic analogy, only the aerodynamic field is calculated accurately.

  $\longrightarrow$ numerically less difficult

  However mean flow effects on acoustic propagation are lost: these effects have to be included in the source term.

- Storage of source terms, retarded-time problem and truncation of the source volume must be carefully treated.

- But nevertheless, Lighthill's analogy is useful in many engineering problems ...

- **Can we build an acoustic analogy where mean flow interactions are included into the wave operator rather than in the source term ?**

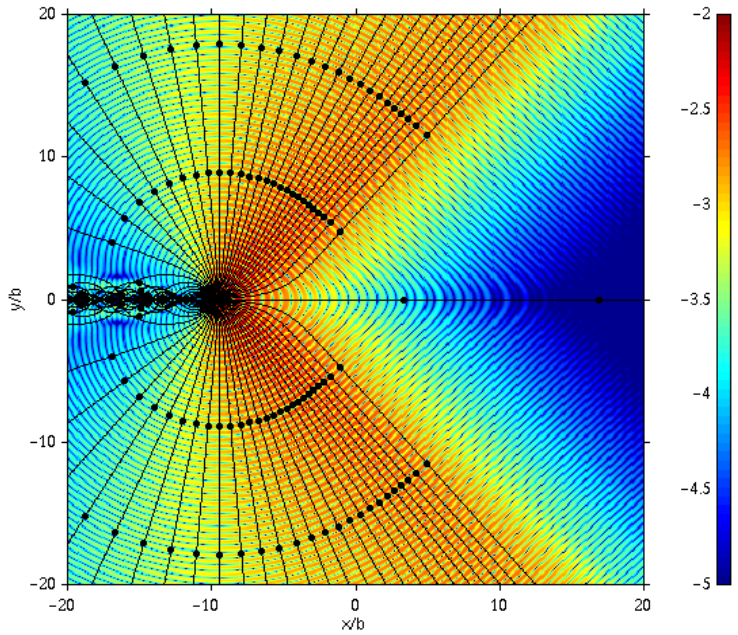
Mean flow effects

Propagation in a sheared mean flow

■ Exact wave operator

$$\text{LEE} \quad \Longrightarrow \quad \frac{\bar{D}}{\bar{D}t}\left(\frac{1}{c_o^2}\frac{\bar{D}^2 p'}{\bar{D}t^2} - \nabla^2 p'\right) + 2\frac{d\bar{U}}{dx_2}\frac{\partial^2 p'}{\partial x_1 \partial x_2} = 0 \qquad (1)$$

- **Pridmore-Brown (1958)**
- **Landahl (1967)**
- **Lilley (1972)**



$$\log_{10}\left(|p'| + \epsilon\right)$$

Bickley jet - M = 0.5 - St $\simeq$ 4.4

Pressure fluctuations in (1) of the form

$$p'(\mathbf{x}, t) = \varphi(x_2)\, e^{i(k_1 x_1 - \omega t)}$$

HF approximation $\Longrightarrow$ cone of silence

$$\cos\theta^\star = \frac{1}{M+1}$$

$\rightarrow$ mean flow effects in the wave operator

■ Lilley's analogy (1972)

$$\frac{\partial u_j}{\partial x_j} = -\frac{1}{\rho}\frac{d\rho}{dt} = -\frac{1}{\gamma p}\frac{dp}{dt} + \frac{1}{c_p}\frac{ds}{dt}$$

$\rightarrow$ **Acoustic v ariable**- Phillips (1960) $\qquad \pi = \frac{1}{\gamma}\ln\frac{p}{p_o}$

$$\frac{d}{dt}\left\{\frac{d^2\pi}{dt^2} - \frac{\partial}{\partial x_i}\left(c^2\frac{\partial \pi}{\partial x_i}\right)\right\} + 2\frac{\partial u_i}{\partial x_j}\frac{\partial}{\partial x_i}\left(c^2\frac{\partial \pi}{\partial x_j}\right) = -2\frac{\partial u_i}{\partial x_j}\frac{\partial u_j}{\partial x_k}\frac{\partial u_k}{\partial x_i}$$

$$+2\frac{\partial u_i}{\partial x_j}\frac{\partial}{\partial x_i}\left(\frac{1}{\rho}\frac{\partial \tau_{ij}}{\partial x_i}\right) + \frac{d^2}{dt^2}\left(\frac{1}{c_p}\frac{ds}{dt}\right) - \frac{d}{dt}\left\{\frac{\partial}{\partial x_i}\left(\frac{1}{\rho}\frac{\partial \tau_{ij}}{\partial x_j}\right)\right\}$$

After linearization $\pi' \simeq (1/\gamma)p'/p_o$ and $u_i = \bar{U}\left(x_2\right)\delta_{1i} + u_i'$

$$\frac{\bar{D}}{\bar{D}t}\left\{\frac{\bar{D}^2 p'}{\bar{D}t^2} - c_o^2\frac{\partial^2 p'}{\partial x_i \partial x_i}\right\} + 2c_o^2\frac{d\bar{U}}{dx_2}\frac{\partial^2 p'}{\partial x_1 \partial x_2} = S$$

with

$$S = -2\gamma p_o\left\{3\frac{d\bar{U}}{dx_2}\frac{\partial u_2'}{\partial x_k}\frac{\partial u_k'}{\partial x_1} + \frac{\partial u_i'}{\partial x_j}\frac{\partial u_j'}{\partial x_k}\frac{\partial u_k'}{\partial x_i}\right\}$$

Some remarks about acoustic analogy

- Other acoustic analogies - more physical source term:

  Powell (1964) - Howe (1975) - Möhring (1978) - Doak (1998) - ...

$$\frac{\partial}{\partial t}\left(\frac{1}{\rho c^2}\frac{dp}{dt}\right) - \nabla^2 h_t = \nabla.\left[\boldsymbol{\omega}\times\mathbf{u} - T\nabla s\right] \qquad h_t = h + \frac{u^2}{2}$$

- **Statistical models**

  Ribner (1964) - Ffowcs Williams (1963) - Goldstein (1973)

  $k-\epsilon$ solutions $\rightarrow$ Béchara, Bailly, Lafon & Candel (1994-1997)

- Three modes of fluctuations - **Chu & Kovasznay (1958)**

  These modes are coupled for a sheared mean flow field, even for small perturbations in using linearized equations.

  Modes are uncoupled in the HF approximation $\longrightarrow$ geometrical acoustic

- Difficult to build an acoustic analogy without ambiguity where propagation effects are eliminated as much as possible from source terms.

  Lilley $\equiv$ generalization of Rayleigh's equation for compressible flows

  Lilley's analogy = self-noise + instability waves + radiation of instability waves

  $\longrightarrow$ **Linearized Euler's equations: same problems !**

Linearized Euler's Equations

Linearized Euler's Equations (LEE)

- **Formulation**

$$\frac{\partial \mathbf{U}}{\partial t} + \frac{\partial \mathbf{E}}{\partial x} + \frac{\partial \mathbf{F}}{\partial y} + \frac{\partial \mathbf{G}}{\partial z} + \mathbf{H} = 0$$

$$\mathbf{U} = \begin{pmatrix} \rho' \\ \rho_o u' \\ \rho_o v' \\ \rho_o w' \\ p' \end{pmatrix} \qquad \mathbf{E} = \begin{pmatrix} \rho' u_o + \rho_o u' \\ u_o \rho_o u' + p' \\ u_o \rho_o v' \\ u_o \rho_o w' \\ u_o p' + \gamma p_o u' \end{pmatrix}$$

$$\mathbf{H} = \begin{pmatrix} 0 \\ (\rho_o u' + \rho' u_o)\dfrac{\partial u_o}{\partial x} + (\rho_o v' + \rho' v_o)\boxed{\dfrac{\partial u_o}{\partial y}} + (\rho_o w' + \rho' w_o)\dfrac{\partial u_o}{\partial z} \\ (\rho_o u' + \rho' u_o)\dfrac{\partial v_o}{\partial x} + (\rho_o v' + \rho' v_o)\dfrac{\partial v_o}{\partial y} + (\rho_o w' + \rho' w_o)\dfrac{\partial v_o}{\partial z} \\ (\rho_o u' + \rho' u_o)\dfrac{\partial w_o}{\partial x} + (\rho_o v' + \rho' w_o)\dfrac{\partial w_o}{\partial y} + (\rho_o w' + \rho' w_o)\dfrac{\partial w_o}{\partial z} \\ (\gamma - 1)\left(p' \nabla . \mathbf{u}_o - u' \dfrac{\partial p_o}{\partial x} - v' \dfrac{\partial p_o}{\partial y} - w' \dfrac{\partial p_o}{\partial z}\right) \end{pmatrix}$$

Hybrid method based on LEE

■ LEE as acoustic wave operator

$$\frac{\partial \mathbf{U}}{\partial t} + \frac{\partial \mathbf{E}}{\partial x} + \frac{\partial \mathbf{F}}{\partial y} + \mathbf{H} = \mathbf{S} \qquad \mathbf{S} = [0,\ S_1\ ,\ S_2\ , 0]^t$$

■ Expression of source terms

For an unidirectional sheared mean flow $\bar{u}_1(x_2)$

$$\text{LEE} \quad \rightarrow \quad \mathcal{L}[p'] = \Lambda \ \equiv \ \text{Lilley equation} \qquad \Lambda?$$

$$\Lambda = -\frac{\bar{D}}{\bar{D}t}\nabla.\mathbf{S} + 2\frac{d\bar{u}_1}{dx_2}\frac{\partial S_2}{\partial x_1} \quad \equiv \ \text{Lilley}$$

$$S_i = S_i^f - \overline{S_i^f} = -\frac{\partial \rho u_i' u_j'}{\partial x_j} + \overline{\frac{\partial \rho u_i' u_j'}{\partial x_j}}$$

Ref. Béchara, Bailly, Lafon & Candel, 1994, AIAA J., 32(3)

Bailly, Lafon & Candel, 1995, AIAA Paper 95-092

Longatte, Lafon & Candel, AIAA Paper 98-2332

Bailly & Juv´e, AIAA Paper 99-1872

Kalitzin & Wilde, Aeroacoustic workshop, Dresden, 1999.

Bogey, Bailly & Juvé, C.R.A.S. 328 IIb, 2000

Bailly, Bogey & Juvé, AIAA Paper 2000-2047.

SPRINT code

(Sound PRopagation IN mean Turbulent flows)

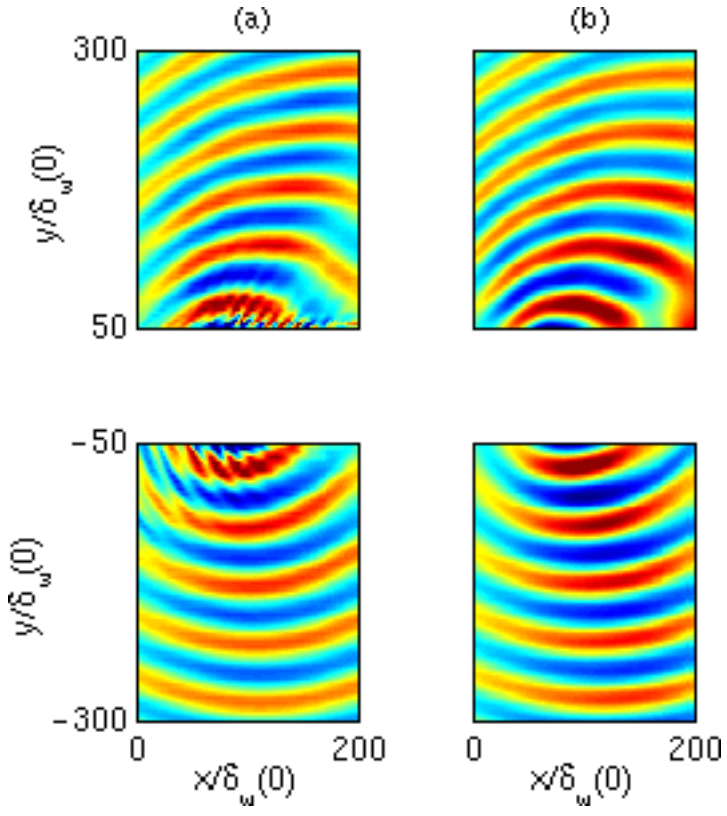
- **2D/3D Linearized Euler's Equations**
  - n umericalalgorithm
    7-point DRP scheme of Tam & Webb + 4th-order Runge-Kutta
  - Artificial selective damping of Tam & Shen (Tam, Webb & Dong)
  - non-uniform cartesian mesh
  - Non-reflecting radiation and outflow boundary condition of Tam & Webb
  - Thompson's c haracteristic inflow boundary condition (incoming plane wa v e)
  - Wall boundary: Tam & Dong, or 3-ghost points (extrapolation)
  - Symmetric boundary condition: 3-ghost points
  - Absorbing boundary conditions
  - Time-domain impedance boundary conditions
  - v ectorization > 4000 Mflops on Nec SX-5

Ref. Gr`everie & Bailly, C.R.A.S., 326 IIb, 1998
Bailly & Juv´e, AIAA J., 38(1), 2000
Bailly, C., 3rd CAA workshop, NASA, 2000
Bailly, Bogey & Juv´e, AIAA Paper 2000-2047.

Sound field generated by a mixing layer

$$\mathbf{S} = \mathbf{S}^f - \overline{\mathbf{S}^f} \qquad \mathbf{H} \equiv 0$$

- **Dilatation field**

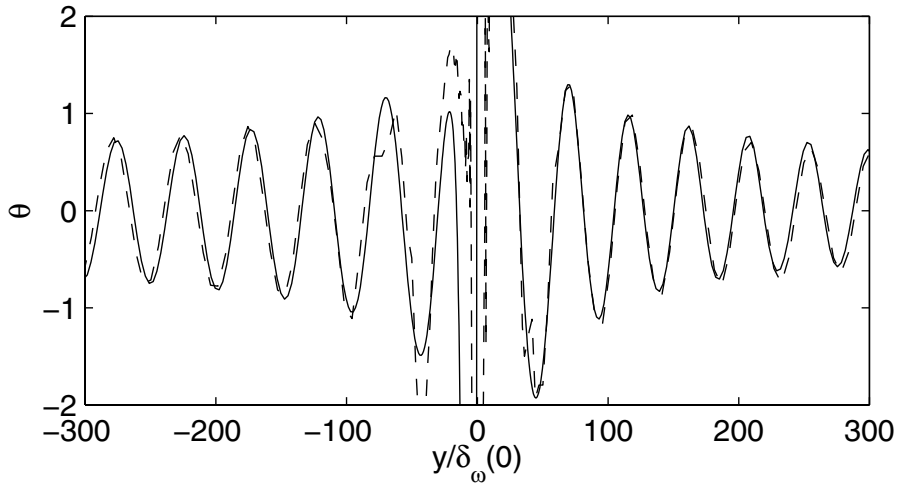


(a) LEE result

(b) LES result (direct calculation)

Bogey, Bailly & Juvé
C.R.A.S., 328, IIb (2000)
AIAA P aper2000-2047

- **Dilatation profiles at** $x = 70\delta_\omega(0)$



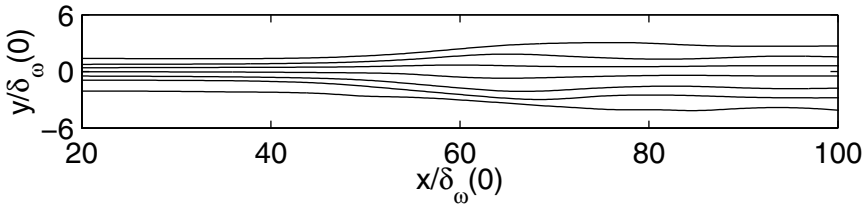
—— LES result

– – – LEE result

Noise generated by a mixing layer

- **Mean axial velocity introduced into LEE**

7 isolines from 44 to 156 m.s^{-1}



- **Simplified formulation of LEE**

$\rightarrow$ $\mathbf{H} = 0$ to prevent the exponential development of instability waves

no significant effect on acoustic propagation, since $\lambda_p = 51.5\delta_\omega(0)$

LEE $\rightarrow$ Rayleigh's stability equation

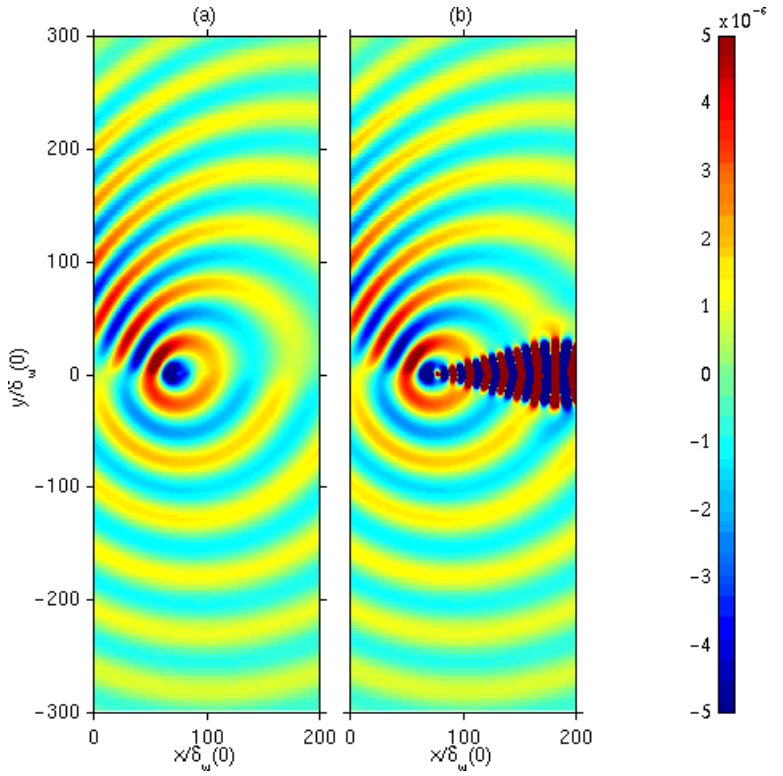
$$\left(\bar{u}_1 - \frac{\omega}{k}\right)\left[\frac{d^2\hat{u}_2}{dx_2^2} - k^2\hat{u}_2\right] - \frac{d^2\bar{u}_1}{dx_2^2}\hat{u}_2 = 0$$

LEE with $\mathbf{H} \equiv 0$

$$\left(\bar{u}_1 - \frac{\omega}{k}\right)\left[\frac{d^2\hat{u}_2}{dx_2^2} - k^2\hat{u}_2\right] + \frac{d\bar{u}_1}{dx_2}\frac{d\hat{u}_2}{dx_2} = 0$$

Noise generated by a mixing layer

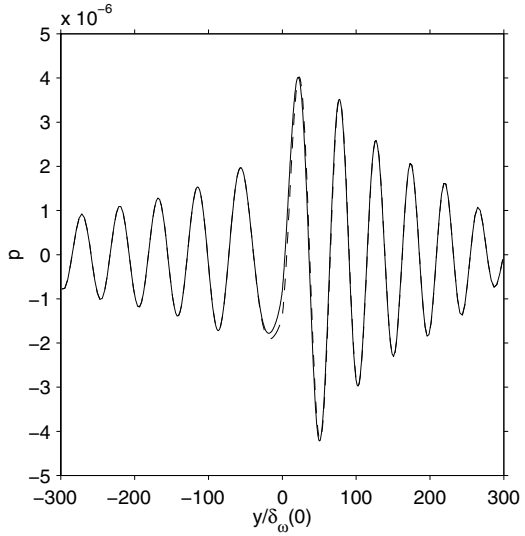
- **Acoustic radiation of a monopolar source**



(a) from LEE with $\mathbf{H} = 0$

(b) from full LEE

- **Radial pressure profiles at** $x = 25\delta_\omega(0)$



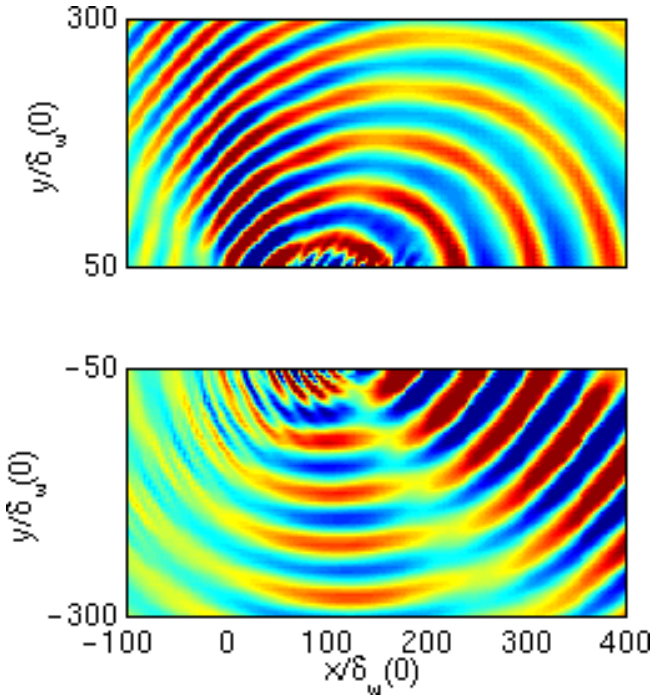
—— from LEE with $\mathbf{H} = 0$

- - - from full LEE

Noise generated by a mixing layer

• **Inappropriate formulation of the source term**

$\mathbf{S}^t$ introduced as source term into LEE



$$S_i^t = \left(\frac{\partial \rho u_i u_j}{\partial x_j} - \overline{\frac{\partial \rho u_i u_j}{\partial x_j}} \right)$$

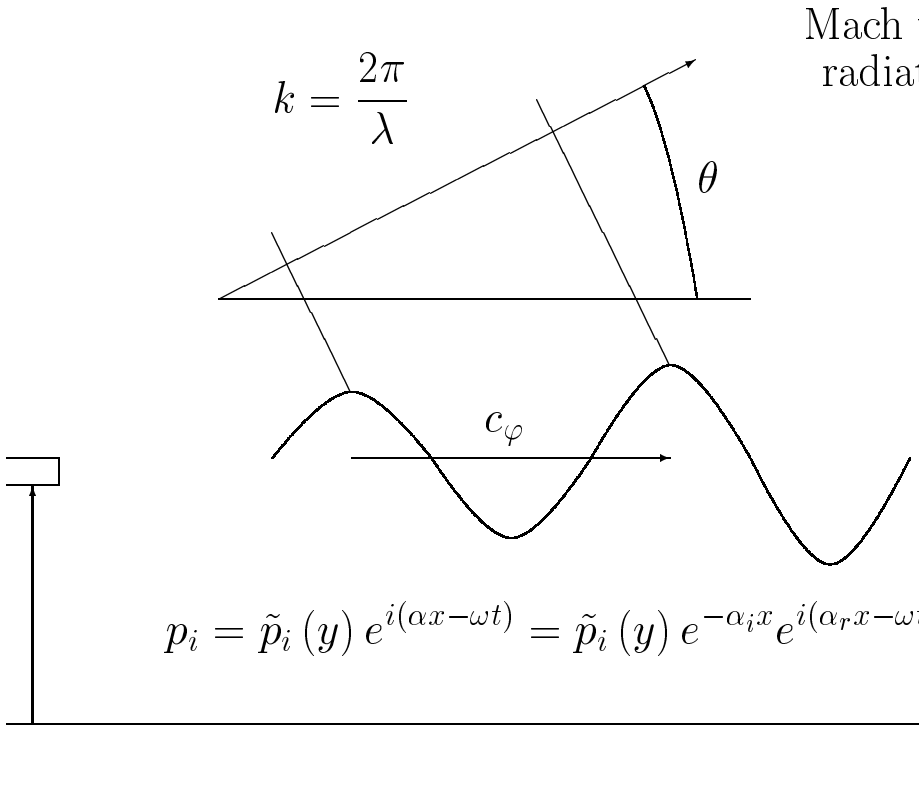
→ overestimation of refraction effects

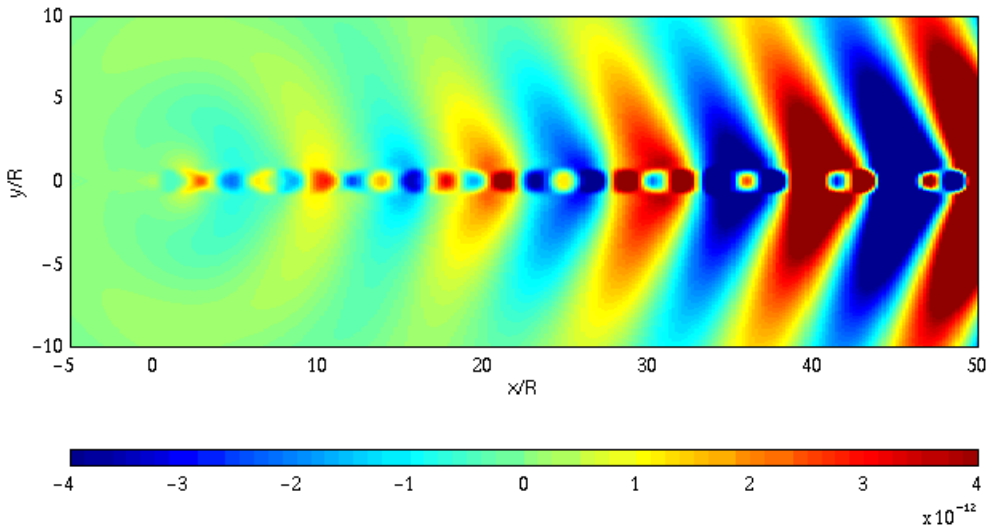
$$\begin{aligned} S_i^t &= \frac{\partial \rho u_i u_j}{\partial x_j} - \overline{\frac{\partial \rho u_i u_j}{\partial x_j}} \\ &= \underbrace{\frac{\partial \rho \bar{u}_i u_j'}{\partial x_j} + \frac{\partial \rho u_i' \bar{u}_j}{\partial x_j}}_{\text{shear-noise}} + \underbrace{\frac{\partial \rho u_i' u_j'}{\partial x_j} - \overline{\frac{\partial \rho u_i' u_j'}{\partial x_j}}}_{\text{self-noise } s_i^f} \end{aligned}$$

Instability wave radiation

Mach waves

$$c_\varphi = \frac{c_\infty}{\cos\theta} \quad \text{or} \quad \cos\theta = \frac{c_\infty}{c_\varphi} = \frac{\alpha_r c_\infty}{\omega}$$





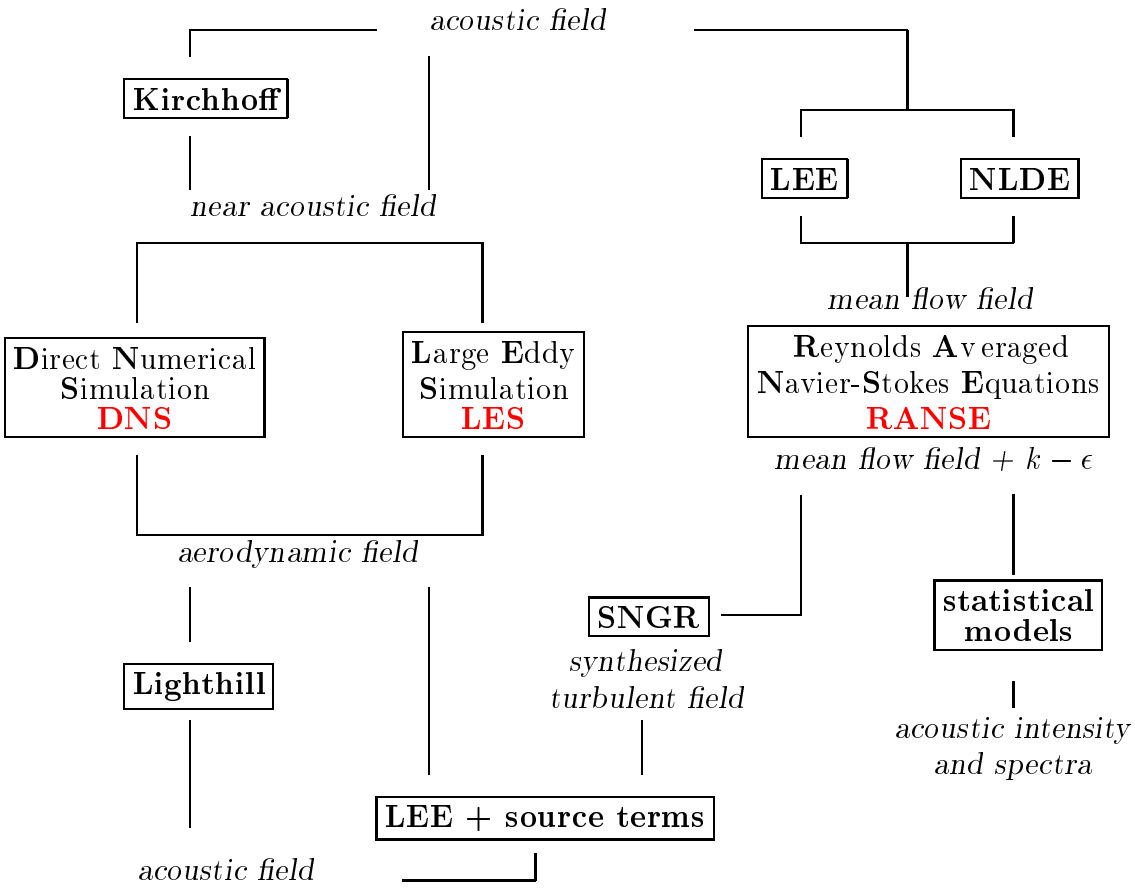
3rd CAA workshop

NASA - CP

Problem 5

From Computational Fluid Dynamics ...

... To Computational AeroAcoustics



Some references

Some references ...

Bailly, C., Bogey, C. & Juvé, D., 2000, Noise computation using source terms in the Linearized Euler equations, *6th AIAA/CEAS AeroAcoustics Conference*, AIAA Paper 2000-2047.

Bailly, C. & Juvé, D., 1999, A stochastic approach to compute subsonic noise using linearized Euler's equations, *5th AIAA/CEAS AeroAcoustics Conference, Seattle*, AIAA Paper 99-1872.

Bailly, C., Lafon, P. & Candel, S., 1997, Subsonic and supersonic jet noise predictions from statistical source models, *American Institute of Aeronautics and Astronautics Journal*, **35**(11), 1688-1696.

Bailly, C., Lafon, P. & Candel, S., 1996, Calculations of eddy Mach wave acoustic radiation using a statistical model and a compressible turbulence closure, *Journal of Sound and Vibration*, **194**(2), 219-242.

Bailly, C., Lafon, P. & Candel, S., 1995, A stochastic approach to compute noise generation and radiation of free turbulent flows, AIAA 95-092.

Bastin, F., Lafon, P. & Candel, S., 1997, Computation of jet mixing noise due to coherent structures: the plane jet case, *J. Fluid Mech.*, **335**, 261-304.

Bogey, C., Bailly, C. & Juvé, D., 2000, Computation of the sound radiated by a 3-D jet using Large Eddy Simulation, *6th AIAA/CEAS AeroAcoustics Conference*, AIAA Paper 2000-2009.

Bogey, C. & Bailly, C., 2000, Modeling and numerical simulation of free shear flows, *von K´arm´an Institute for Fluid Dynamics*, Lectures Series 2000-02, 14-17 February 50 pages.

Bogey, C., Bailly, C. & Juvé, D., 1999, Numerical simulation of sound generated by vortex pairing in a mixing layer, *AIAA Journal*, **38**(12), 2210-2218.

Gamet, L. & Estivalezes, J.L., 1998, Application of large-eddy simulations and Kirchoff method to jet noise prediction, *AIAA Journal*, **36**(12), 2170-2178.

Séror, C., Sagaut, P., Bailly, C. & Juvé, D., 2000, Subgrid-scale contribution to noise production in decaying isotropic turbulence, *AIAA Journal*, **38**(10), 1795-1803.

Witkowska, A., Juvé, D. & Brasseur, J.G., 1997, Numerical study of noise from isotropic turbulence, *J. Comput. Acous.*, **5**(3), 317-336.

C. Bailley References

1. BAILLY, C. & JUVÉ, D., 1999, A stochastic approach to compute subsonic noise using linearized Euler's equations, *5th AIAA/CEAS AeroAcoustics Conference, Seattle,* AIAA Paper 99-1872.

2. BAILLY, C., LAFON, P. & CANDEL, S., 1997, Subsonic and supersonic jet noise predictions from statistical source models, *American Institute of Aeronautics and Astronautics Journal,* **35**(11), 1688-1696.

3. BAILLY, C., LAFON, P. & CANDEL, S., 1996, Calculations of eddy Mach wave acoustic radiation using a statistical model and a compressible turbulence closure, *Journal of Sound and Vibration,* **194**(2), 219-242.

4. BAILLY, C., LAFON, P. & CANDEL, S., 1995, A stochastic approach to compute noise generation and radiation of free turbulent flows, AJAA 95-092.

5. BASTIN, F., LAFON, P. & CANDEL, S., 1997, Computation of jet mixing noise due to coherent structures: the plane jet case, *J. Fluid Mech.*, **335**, 261-304.

6. BOGEY, C., BAILLY, C. & JUVÉ, D., 2000, Computation of the sound radiated by a 3-D jet using Large Eddy Simulation, *6th AIAA/CEAS AeroAcoustics Conference,* AIAA Paper 2000-2009.

7. BOGEY, C. & **BAILLY,** C., 2000, Modeling and numerical simulation of free shear flows, *von Kármán Institute for Fluid Dynamics,* Lectures Series 2000-02, 14-17 February, 50 pages.

8. DAHAN, C., ELIAS, G., MAULARD, J. & PERULLJ, M., 1978, Coherent structures in the mixing zone of a subsonic hot free jet, *J. Sound Vib.*, **59**(3), 3 13-333.

9. GAMET, L. & ESTIVALEZES, J.L., 1998, Application of large-eddy simulations and Kirchoff method to jet noise prediction, *AIAA Journal,* **36**(12), 2170-2178.

10. JUVÉ, D., SUNYACH, M. **&** COMTE-BELLOT, G., 1980, Intermittency of the noise emission in subsonic cold jets, *J. Sound Vib.*, **71**(3), 319-332.

11. JUVÉ, D. & SUNYAcH, M., 1981, Near and far field azimuthal correlations for excited jets, *7th AIAA Aeroacoustics Conference,* AIAA Paper 81-2011.

12. ZOPELLARI, E. & JUVÉ,, D., 1997, Reduction of jet noise by water injection, AIAA Paper 97-1622.

13. ZOPELLARI, E. & JUVÉ, D., 1998, Reduction of hot supersonic jet noise by water injection, AIAA Paper 98-2204.

CAA For

Jet Noise

Physics

Reda Mankbadi
Embry-Riddle
Aeronautical University

***CAA For Jet Noise Physics* - Reda Mankbadi, Embry-Riddle Aeronautical University as summarized by Eugene Krejsa**.

Dr. Mankbadi summarized recent CAA results. Examples of the effect of various boundary condition schemes on the computed acoustic field, for a point source in a uniform flow, were shown. Solutions showing the impact of inflow excitations on the result were also shown. Results from a large eddy simulation, using a fourth-order MacCormack scheme with a Smagorinsky sub-grid turbulence model, were shown for a Mach 2.1 unheated jet. The results showed that the results were free from spurious modes. Results were shown for a Mach 1.4 jet using LES in the near field and the Kirchhoff method for the far field. Predicted flow field characteristics were shown to be in good agreement with data and predicted far field directivities were shown to be in qualitative agree with experimental measurements.

Dr. Mankbadi also presented results using linearized Euler equations. Comparison of predicted directivities agreed well with measurements for supersonic jet. Agreement was not as good for jet with Mach numbers less than 0.9. Results from very large eddy simulation were also presented. Dr. Mankbadi concluded his presentation with observations that CAA can provide:

- Prediction of sound propagation.
- Physics of the very large flow structures.
- Correlation for other approaches, such as MGB.
- Numerical experiments with various ideas for identification and control of the noise sources.

There are still many challenges:

- LES is CPU intensive
- Shock-acoustic wave interaction is difficult
- Coupling to the engine requires curvilinear meshes, grid generations, and a much faster code.

NASA/CP—2001-211152

CAA FOR JET NOISE PHYSICS

Reda Mankbadi
Embry-Riddle Aeronautical University, Daytona Beach, FL
ICOMP, NASA Glenn Research Center, Cleveland, Ohio
Mankbadr@cts.db.erau.edu

OUTLINE

1. Numerical Issues
2. LES/VLES for Jet Noise
3. Physics-based Methods for Jet Noise Predictions

Numerical Issues

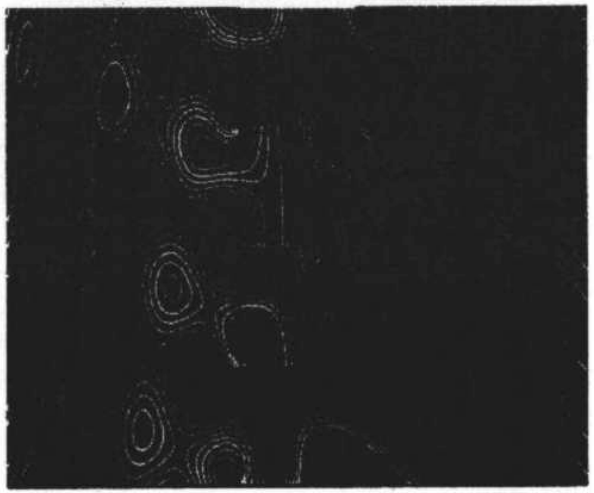
- Large Computational Domain (60 D x 40 D)
- Three-Dimensional Problem
- Large Range of Length Scales
    - Acoustics: Acoustic Wavelength
    - Large Scale Structures: Jet Diameter
    - Shear-Layer Scales: Momentum Thickness
    - Mean Flow
- High-accuracy numerical scheme is needed to resolve these scales in large domain
- Dispersion and dissipation errors must be small for amplitude and phase accuracy
- For linear problems, several schemes are available.
- For mixing noise (nonlinear), few schemes are suitable: DRP, High-accuracy MacCormack, Compact, Prefactored Compact
- Boundary Conditions are still the major difficulty

Technical Highlight:

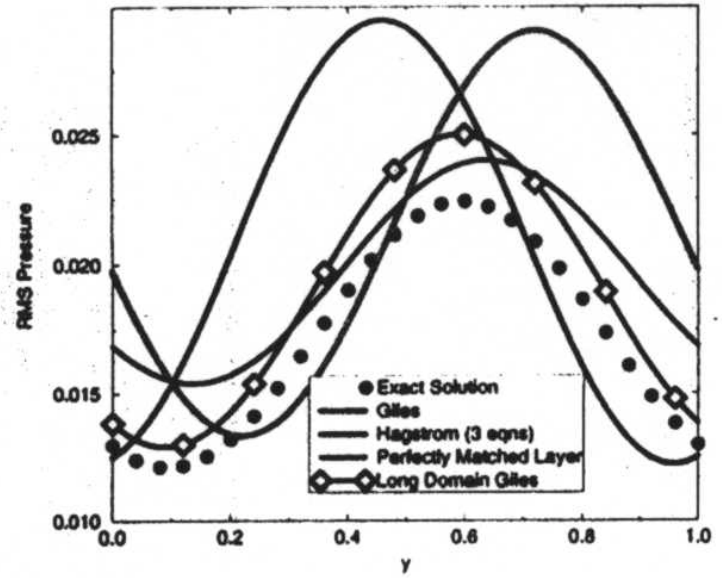
Evaluation of Boundary Conditions on Benchmark Cascade Case

- **In this benchmark problem, a periodic vortical gust impinges on a flat plate cascade. The close proximity of the computational boundaries makes this problem extremely difficult. The results of several boundary conditions are shown.**

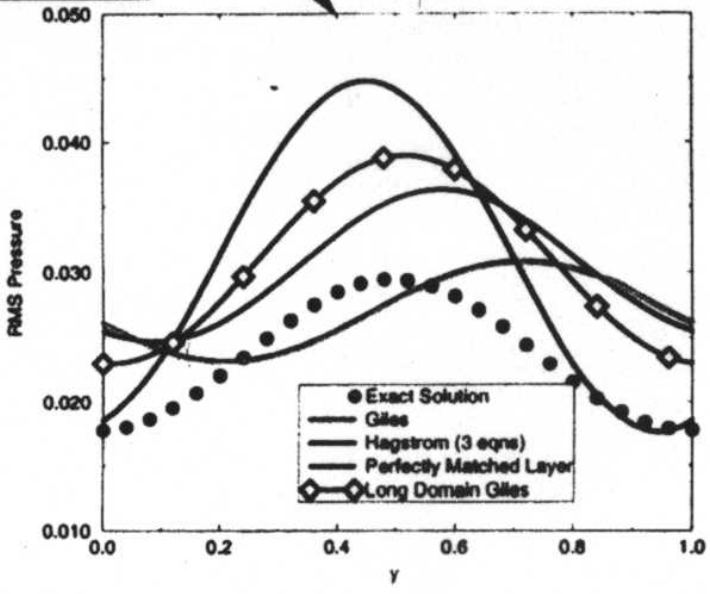
Instantaneous Pressure Distribution



Inflow RMS Pressure



Outflow RMS Pressure



NASA/CP—2001-211152

EFFECT OF BOUNDARY TREATMENT ON ACCOUSTIC RADIATION

POINT SOURCE IN A UNIFORM FLOW

Exact Solution

Tam and Webb Boundary Condition

Giles Boundary Condition

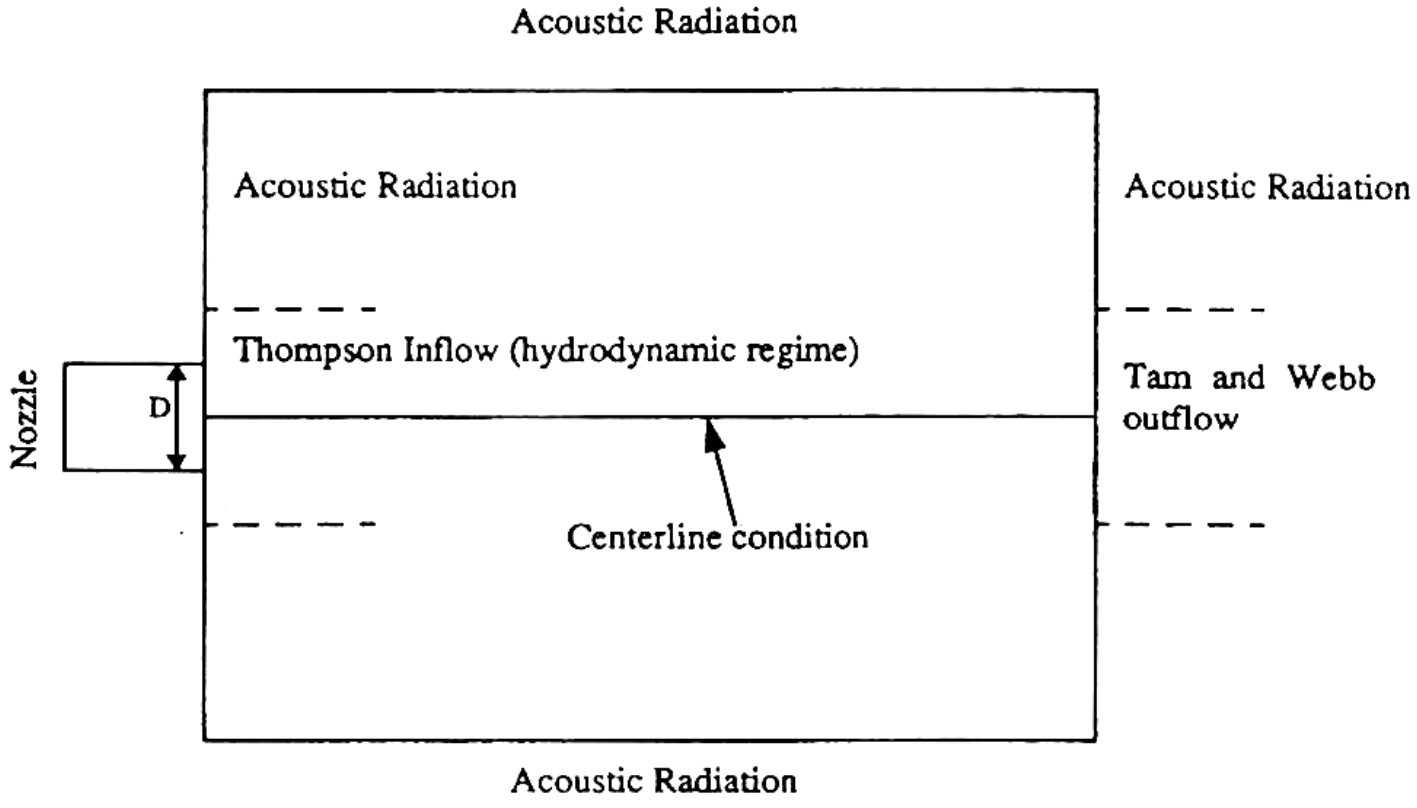
Thompson Boundary Condition

NASA/CP—2001-211152

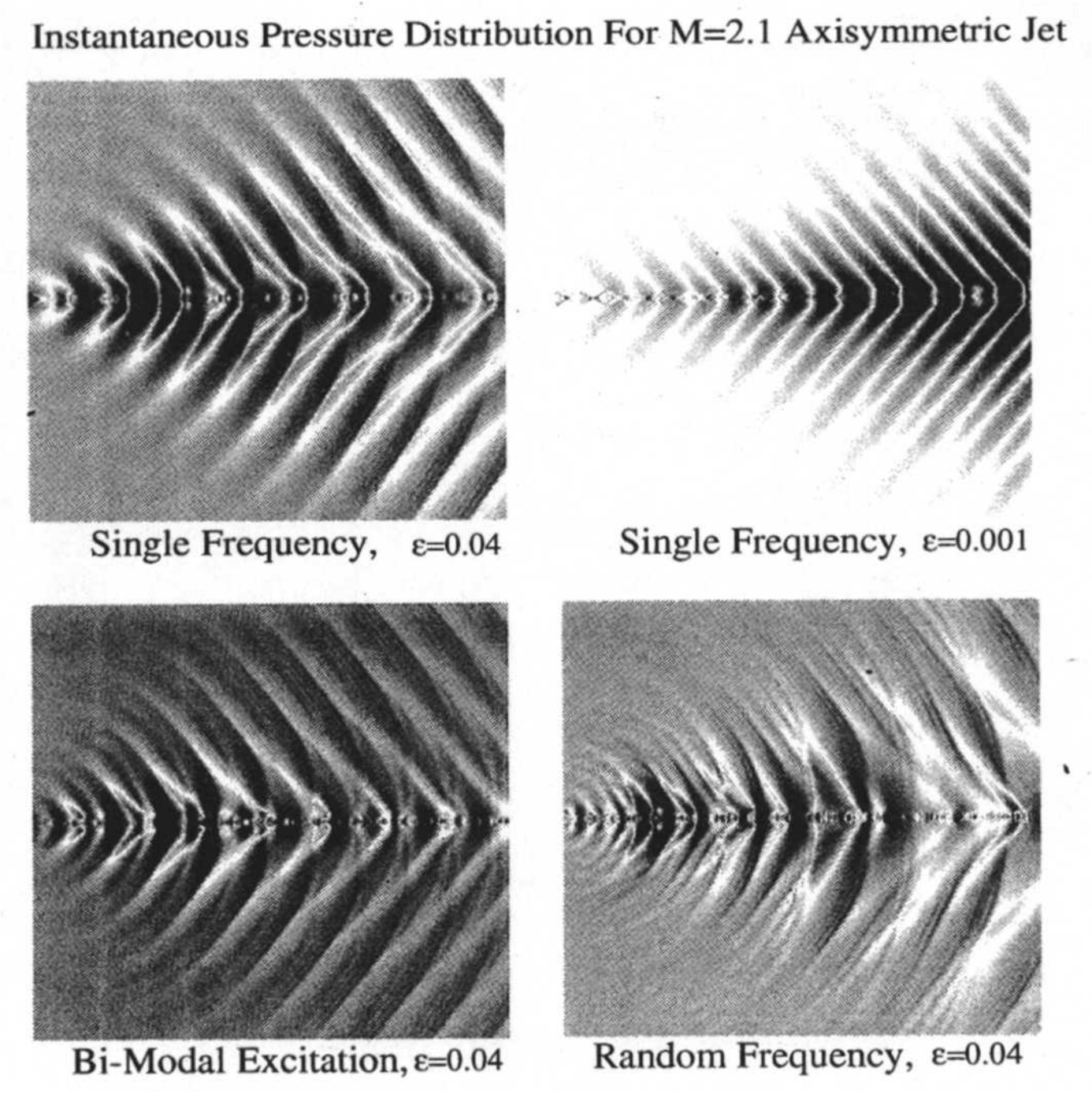
901

AXISYMETRIC COMPUTATION FOR ACOUSTIC RADIATION FROM AXISYMMETRIC LARGE SCALE STRUCTURE

Boundary Conditions



$M_j = 2.1$
$u_o/u_j = 0$
$Re = 70000$
$T_t = 294^{o}k$


Instantaneous Pressure Distribution For M=2.1 Axisymmetric Jet
Single Frequency, ε=0.04
Single Frequency, ε=0.001
Bi-Modal Excitation, ε=0.04
Random Frequency, ε=0.04

INFLOW EXCITAITONS

- Single Frequency:

$$\left[u'\ v'\ p'\ \rho'\right] = \varepsilon \Re \left\{ \Phi(r)\, e^{i(\alpha x - \omega t)} \right\}$$

ε = input excitation level, α = eigenvalue.

$\Phi(r)$ is the corresponding eigenfunctions $\Phi(r) = \left[\hat{u}(r)\ \hat{v}(r)\ \hat{p}(r)\ \hat{\rho}(r)\right]$

- Bi-Modal Excitation:

$$\left[u'\ v'\ p'\ \rho'\right] = \varepsilon \Re \left\{ \Phi(r)\, e^{i(\alpha x - \omega t)} \right\} + \varepsilon \Re \left\{ \Phi_s(r)\, e^{i\left(\alpha_s x - \omega_s t + \beta\right)} \right\}$$

where the subscript s represents subharmonic frequency.
β = initial phase difference between the fundamental and the subharmonic.

- Random Disturbance:

$$\left[u'\ v'\ p'\ \rho'\right] = \varepsilon A(t) \exp\left[-\ln(2) \left(\frac{r - h(0)}{b(0)} \right)^2 \right]$$

A(t) is a random function in time, created by random function generator.
b(0) and h(0) are the half-width and potential core radius of the shear layer at jet inflow.

AXISYMMETRIC SIMULATIONS

- A fourth-order scheme is appropriate
- Clean solution can be achieved via careful attention to boundary treatment
- The solution is dependent on the inflow disturbances
- The wavelike nature of the large-scale structure

NASA/CP—2001-211152

LARGE- EDDDY SIMULATIONS

Fourth-Order MacCormack
Smagronisky Model

AXISYMMETRIC JET, unheated, fully expanded, M=2.1. St=0.2 & 0.4

COMPUTATIONAL DETAILS:

Uniform grid spacing in the axial & Azimuthal directions.

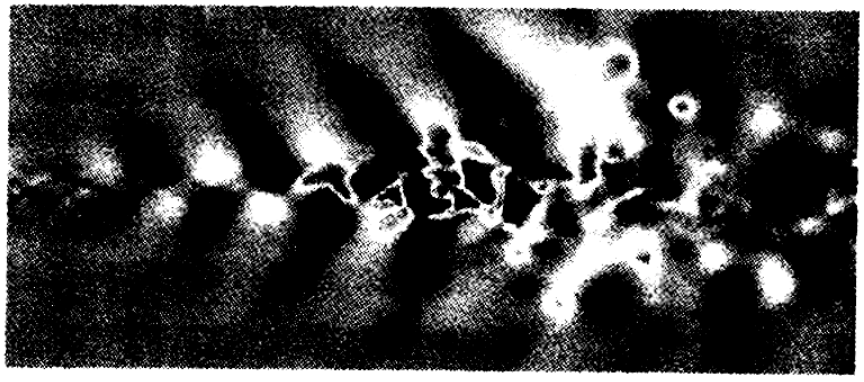
Stretched grid in the radial direction
The domain: 5<x/R<70, 0<r/R< 32
theta 0 to pi
CFL=0.5
25 points per wavelength

675 time steps per cycle, 100 time steps per cycle

AXIAL (196) radial (385), x=391 r=300
x=196, r=385, n=12
RESULTS:

Though viscous and damping effects are damping the solution is free from spurious modes.

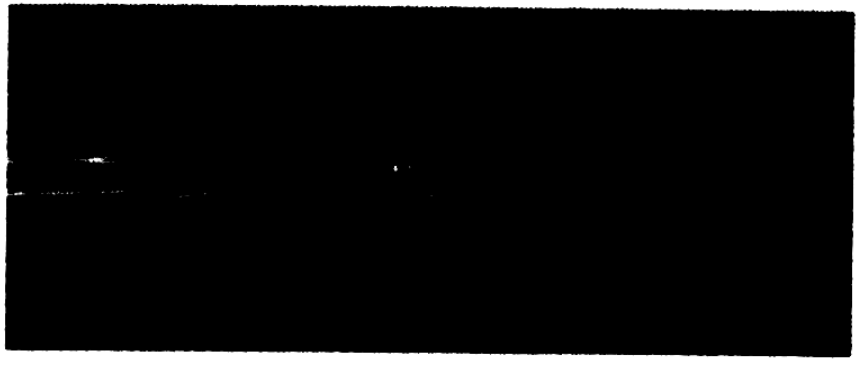
M=2.1 Supersonic Jet Excited by First Helical Mode



Pressure



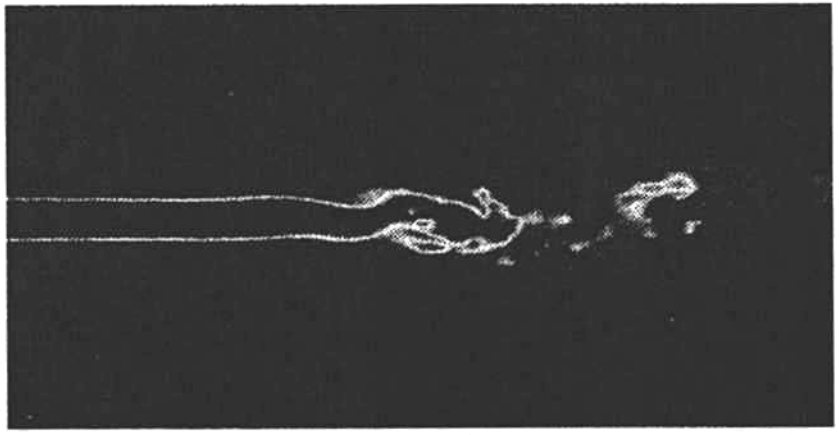
Axial Velocity



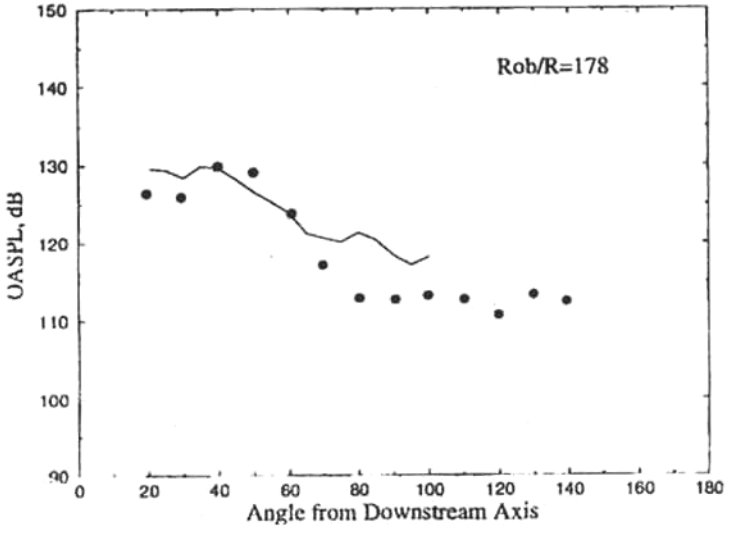
Vorticity

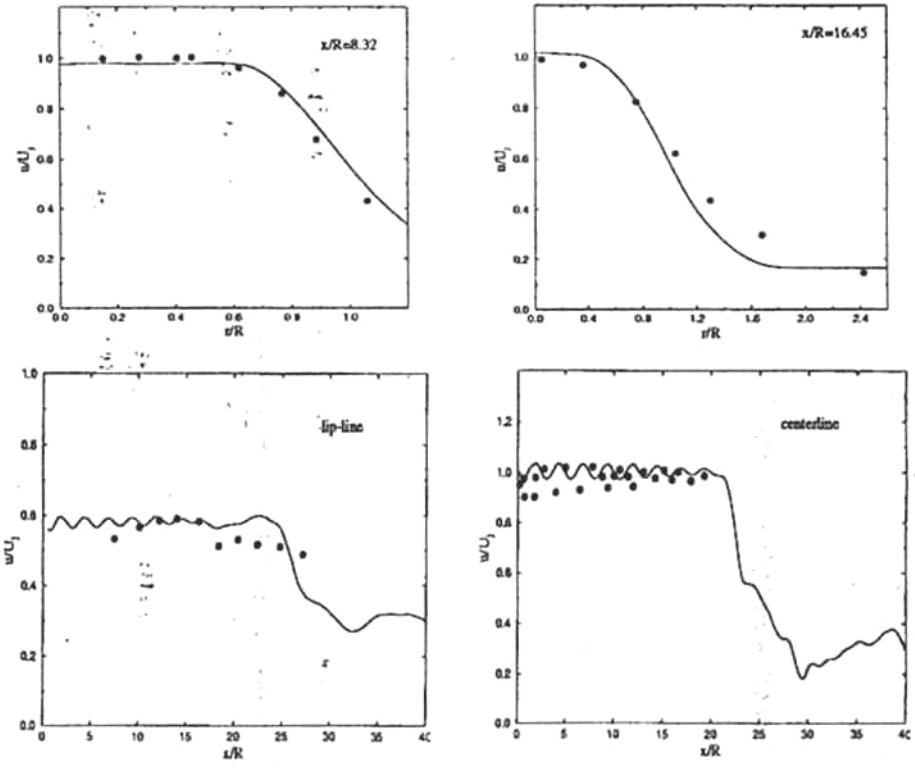
Technical Highlight

M=1.4 supersonic round jet excited by multiple frequencies at nozzle exit: Large–Eddy Simulation in the near field + Kirchhoff Method in the far field.



Mach Number





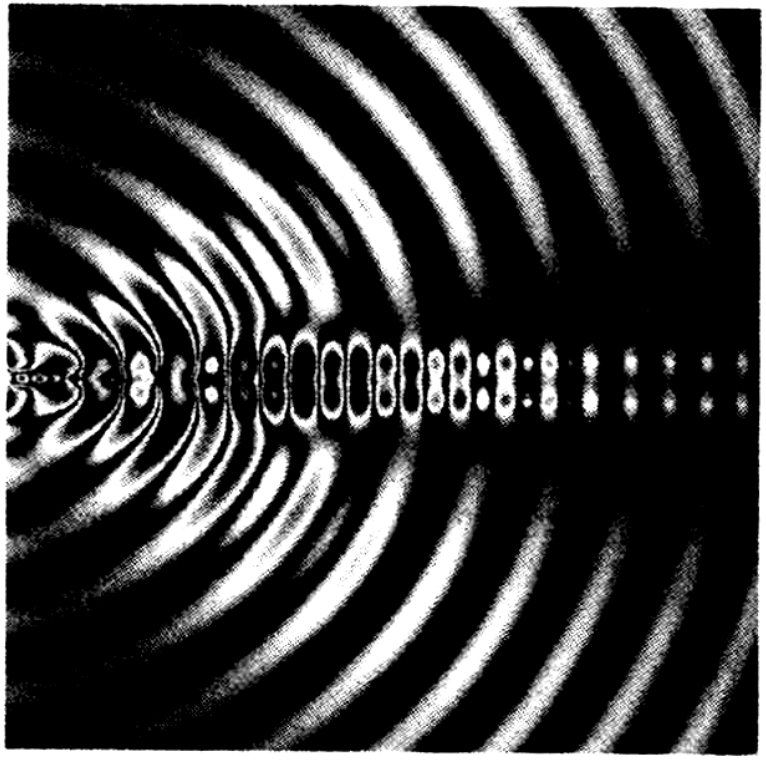
Enhanced mixing and the breakdown of organized structures downstream of jet are observed. The far field noise directivity shows qualitative agreement with the experimental measurement.

3D LES

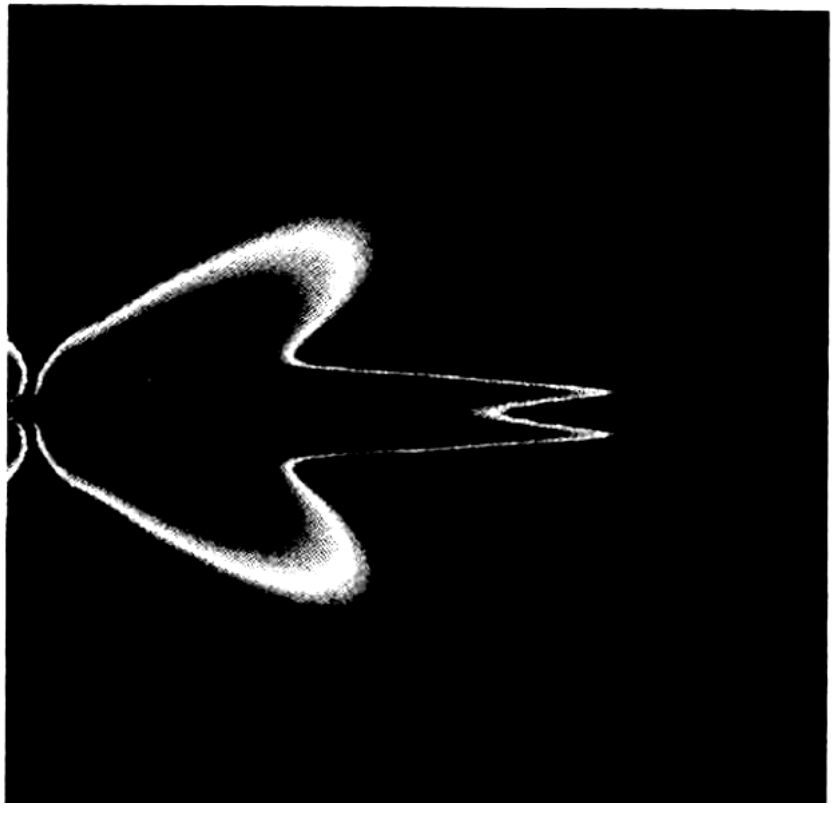
- **Direct, 3D predictions is expensive**
- **Need to split the problem into a source regime in the near field and a propagation regime and use physically based approximation**

CAN LEE APPROXIMATE BOTH THE NEAR AND FAR FIELD ?

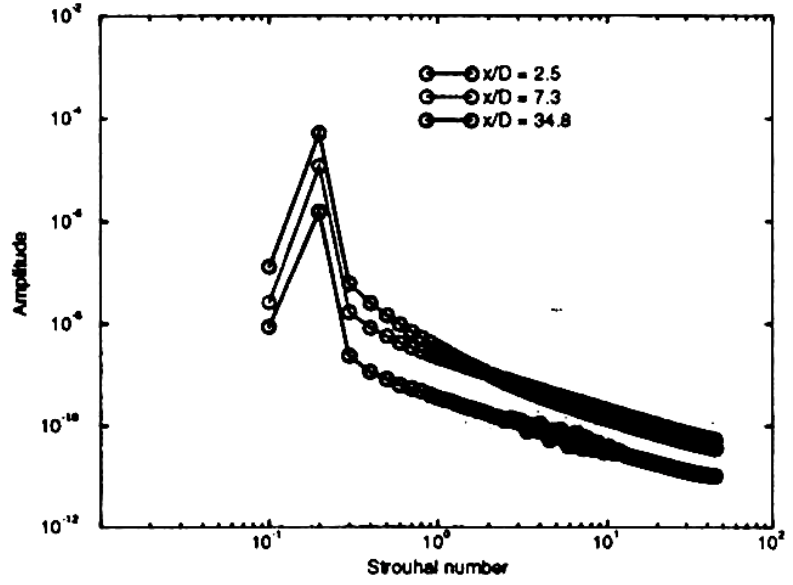
Snapshot of Oscillating Pressure Field



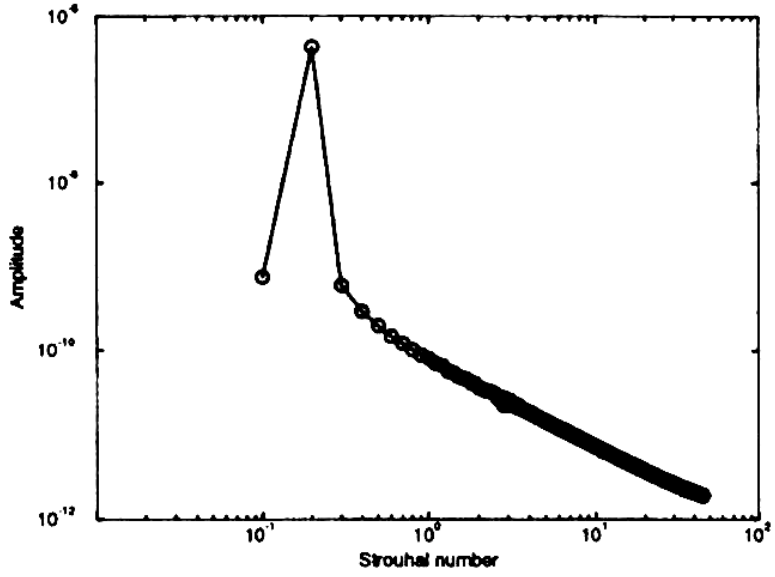
RMS Values of the Pressure Disturbance



Frequency Spectra in the Shear Layer

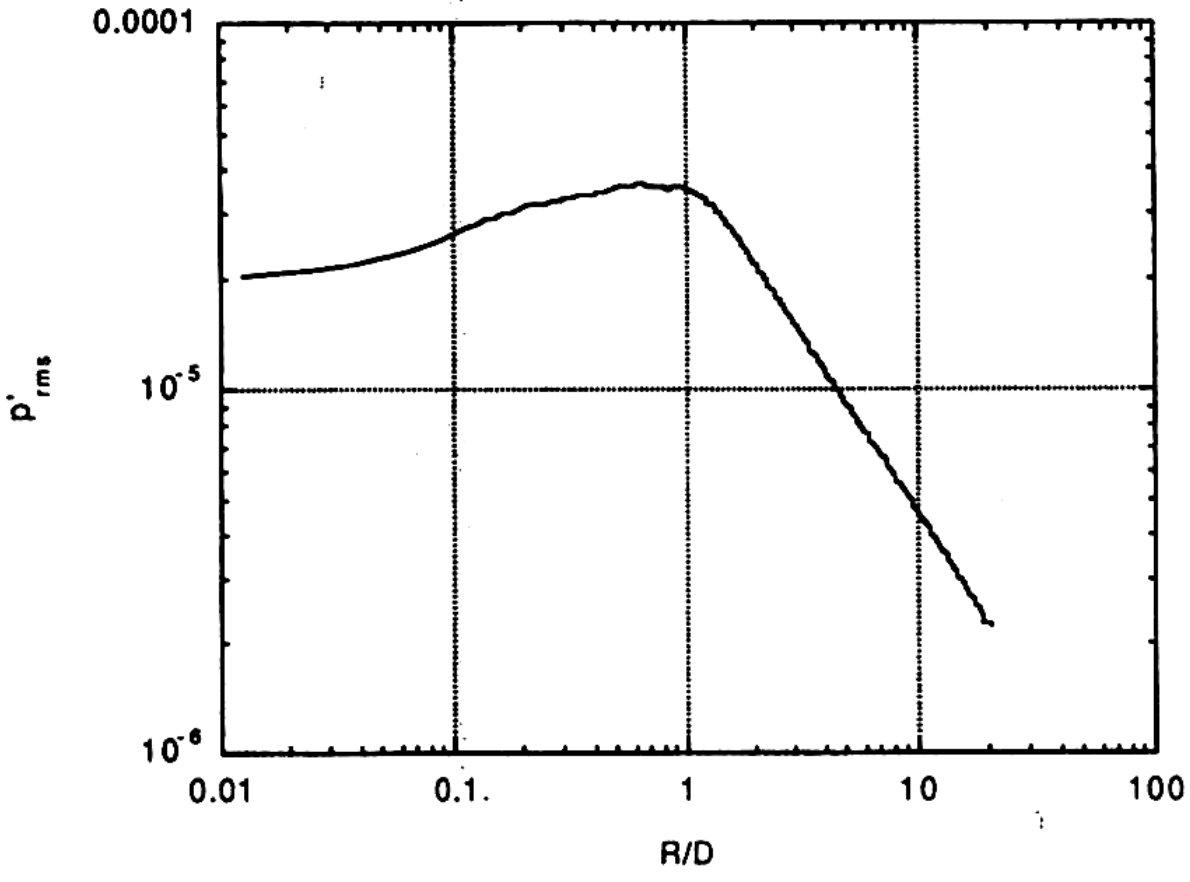


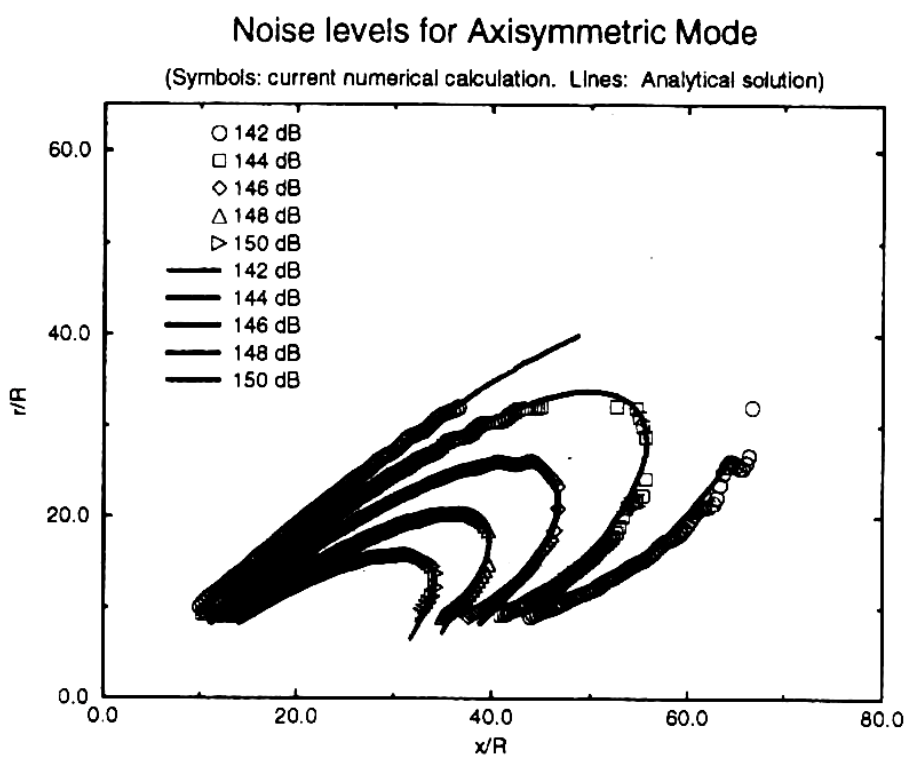
Frequency Spectra in the Far Field

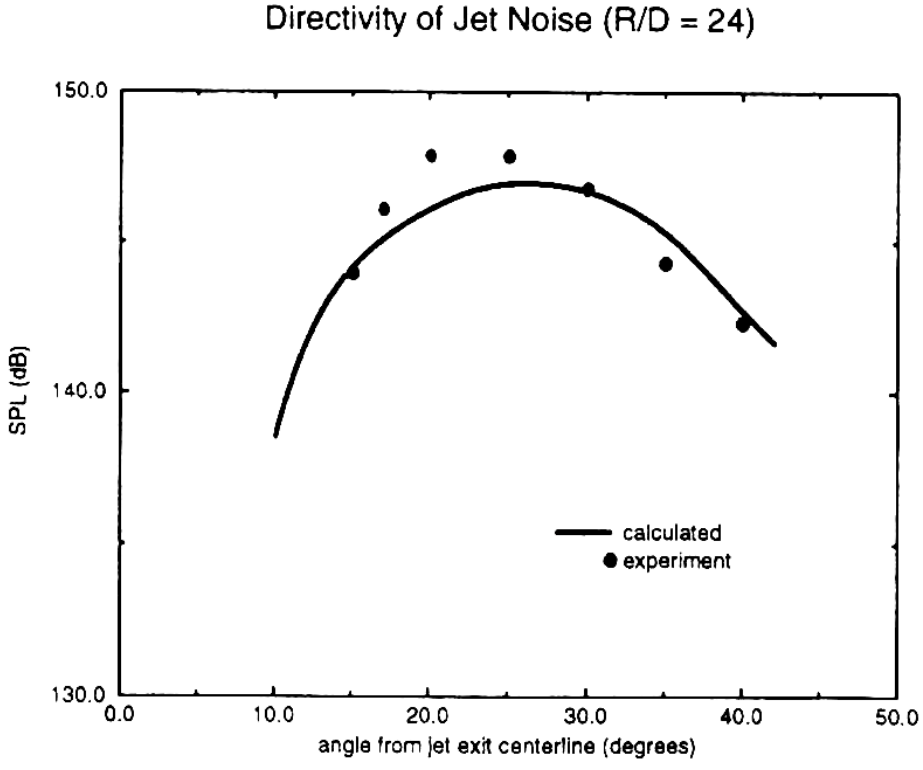


(x/D = 10; r/D = 11.75)

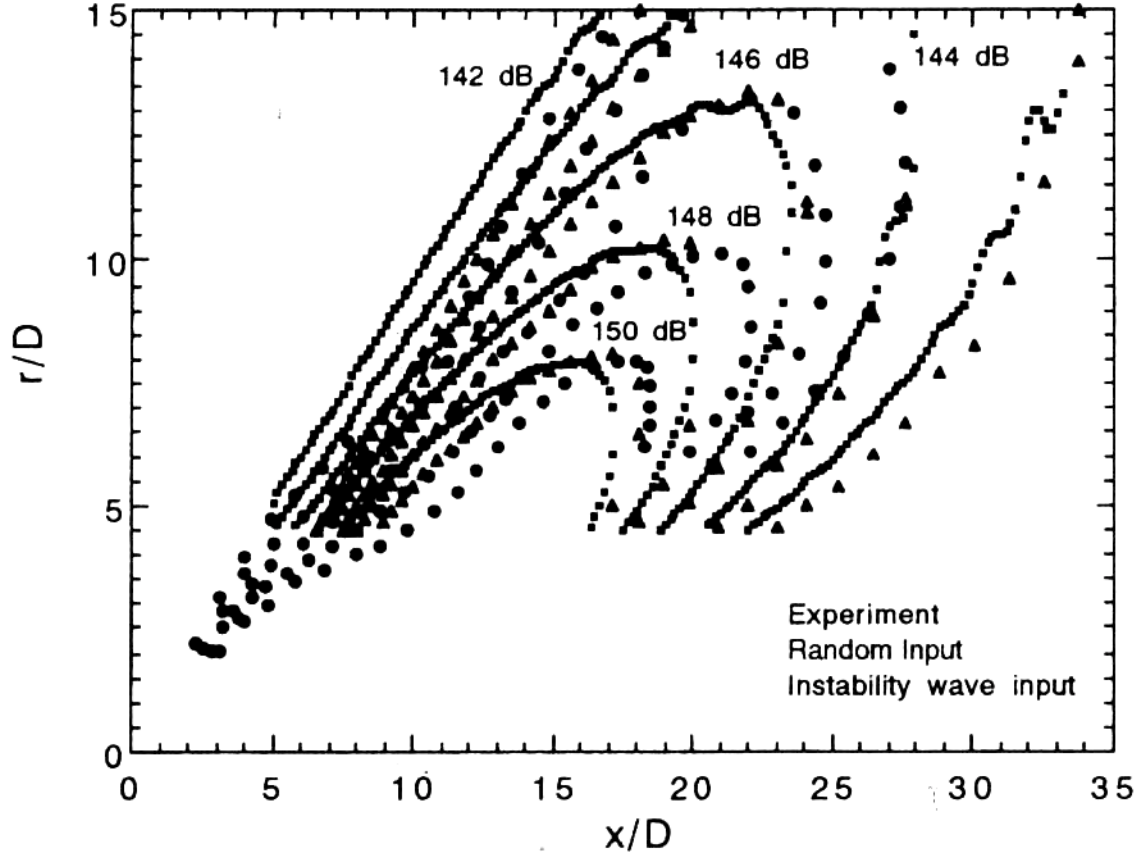
Far Field Radial Decay



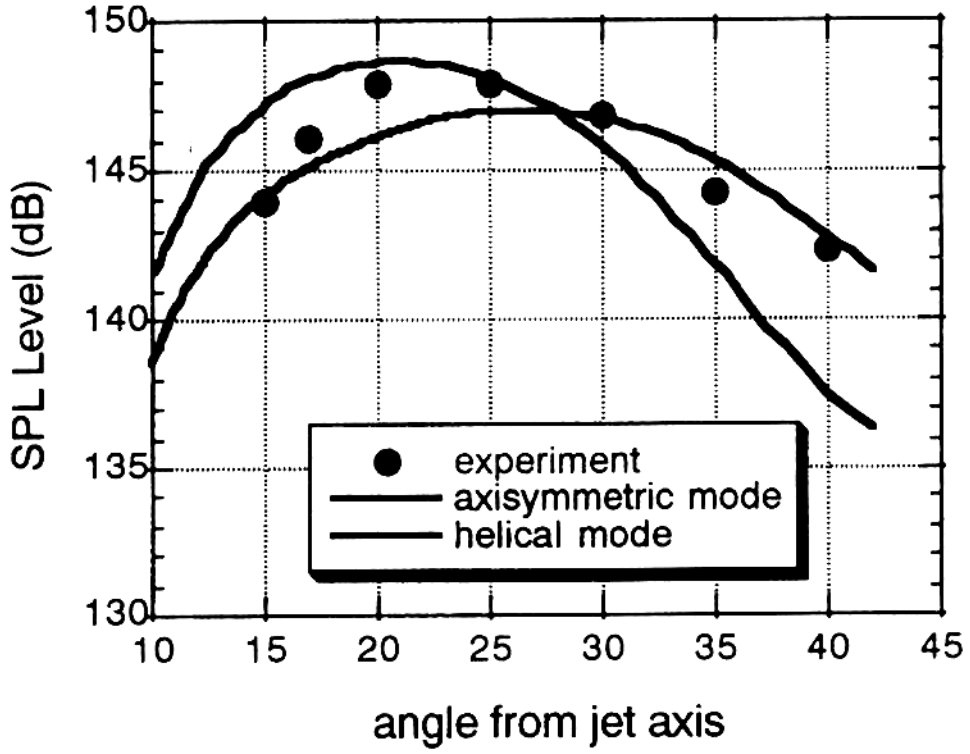

Noise levels for Axisymmetric Mode
(Symbols: current numerical calculation. Lines: Analytical solution)
142 dB
144 dB
146 dB
148 dB
150 dB
142 dB
144 dB
146 dB
148 dB
150 dB
r/R
x/R
0.0
20.0
40.0
60.0
80.0


Directivity of Jet Noise (R/D = 24)
SPL (dB)
angle from jet exit centerline (degrees)
calculated
experiment
130.0
140.0
150.0
0.0
10.0
20.0
30.0
40.0
50.0

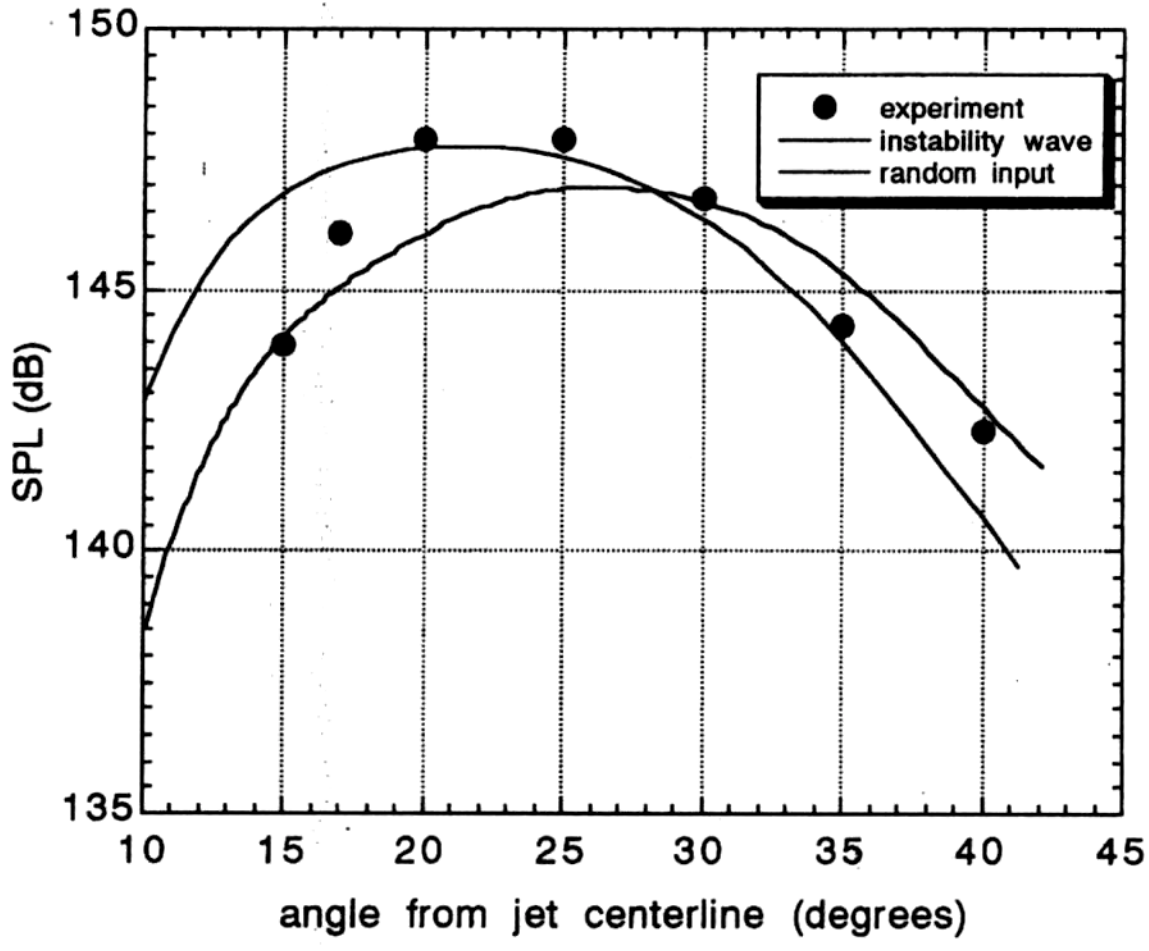
Overall Comparison (St = 0.2)



Directivity of Jet Noise (R = 24)



Directivity of Jet Noise (R = 24)



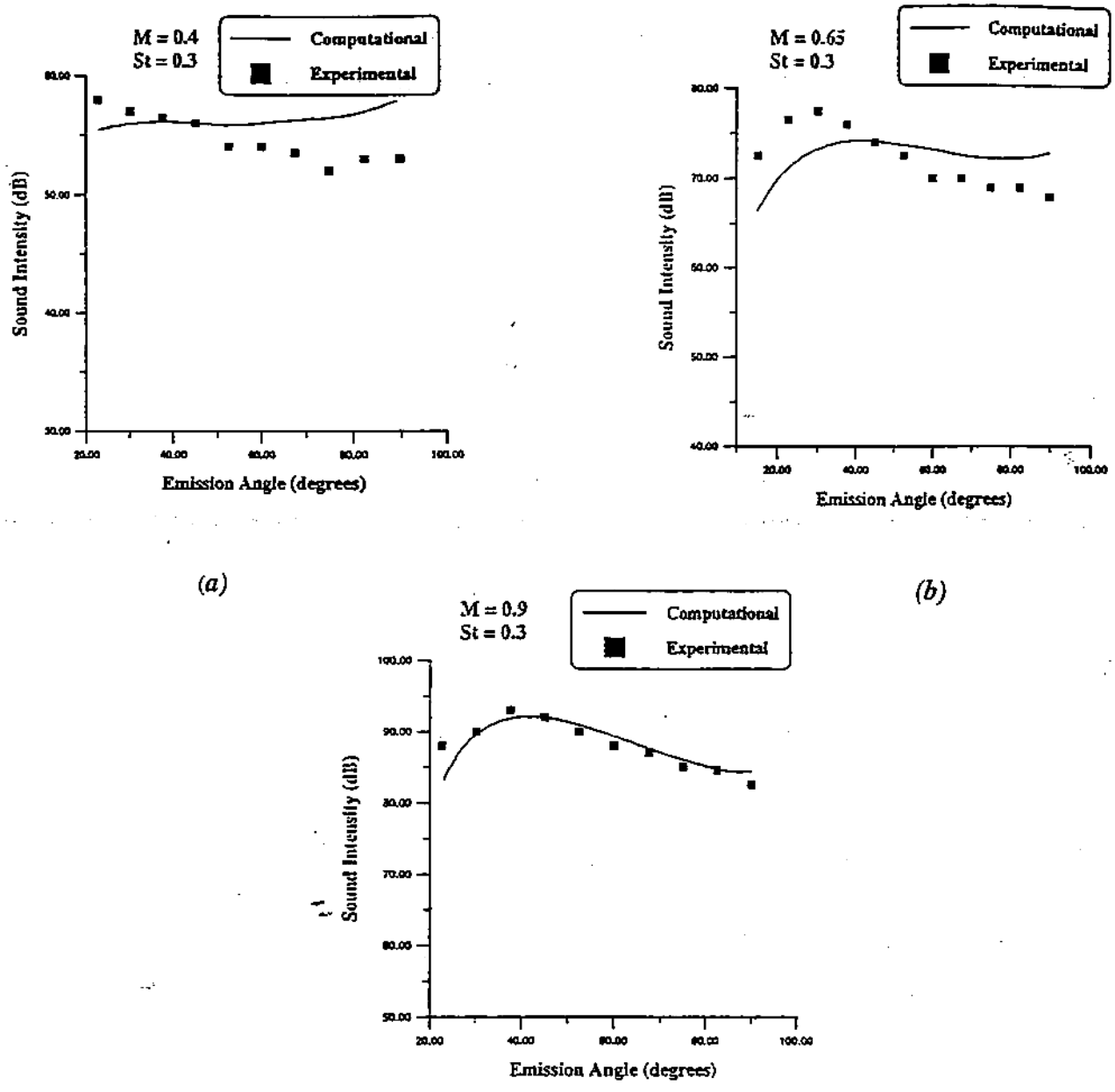


Figure (7) Directivity of Sound Intensity at St=0.3, ((a)M=0.4, (b)M=0.65, (c)M=0.9)

SOUND PROPGATION- LEE

Assuming the mean flow is assumed to be given, Linear Euler Equations (LEE) can be used for prediction of sound propagation and for approximate prediction of the sound source

PHYSICS

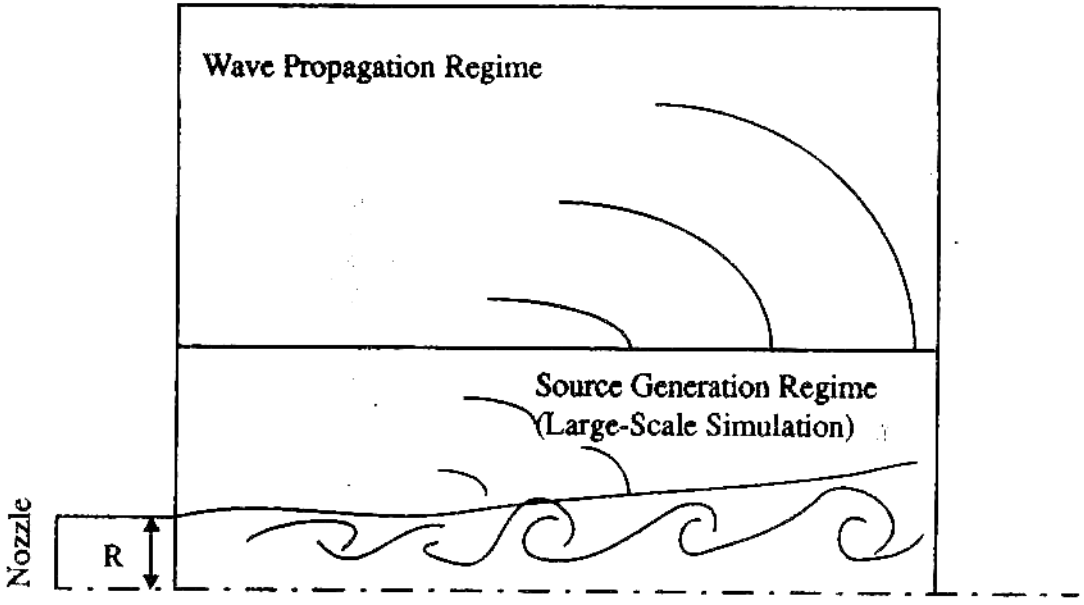
- **Errors may amplify more in the linear simulations!**
- **Need to make sure that no spurious modes are generated**
- **The solution should decay as 1/r in the far field**
- **Excellent agreement with Tam & Burton asymptotic analysis for instability waves**
- **Reasonable agreement with Trout & McLaughlin M=2.1 controlled experiment**
- **LEE can provide reasonable accurate approximate prediction for the large scale structure as low as M=0.9**

OUTLINE

- Computational domain is split into two regimes:

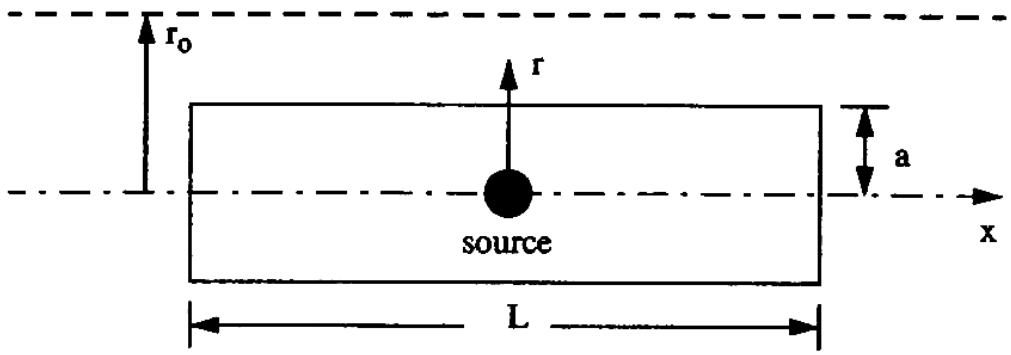
  ❑Non-linear source generation regime---Large-Scale Simulation.

  ❑Linear acoustic wave propagation regime--- Surface-Integral Formulation (SIF).
  Linearized Euler.
  Kirchhoff's Method.
  Lighthill's Theory.



Surface-Integral Formulation (SIF)

Consider a cylinder of radius a, and length L enclosing the jet sound sources.



The mean flow outside this cylinder is stagnant and the disturbances are taken to be purely acoustic in nature, described by the simple wave equation

$$\nabla^2 p - \frac{1}{c^2}\frac{\partial^2 p}{\partial t^2} = 0$$

The Fourier transform with respect to t is defined as

$$p(\omega) = \int_{-\infty}^{\infty} p(t)\, e^{-i\omega t}\, dt$$

Substituting in the wave equation, we obtain

$$\nabla^2 p + k^2 p = 0 \qquad k = \frac{\omega}{c} = 2\pi S M_j \qquad S = \frac{fD}{U_j}$$

The integral solution is given by

$$p\left(X_o, \omega\right) = -\int\left[G\frac{\partial p}{\partial n} - p\frac{\partial G}{\partial n}\right] dS$$

where $p(X_o, \omega)$ is the acoustic pressure at the observation point $X_o=(x_o,r_o,\phi_o)$. G is the Green function, n is the normal to the surface $\bar{S}$ and $p(X, \omega)$ is the pressure distribution on the surface at the point $X=(x,r,\phi)$.

and

$$\frac{\partial G}{\partial r} = \Xi\int_{-\infty}^{\infty} e^{ik_x\left(x_o - x\right)}\frac{H_m\left(qr_o\right)}{H_m(qa)}q\left[J'_m(qr)\,H_m(qa) - J_m(qa)\,H'_m(qr)\right]dk_x$$

For r=a, we can make use of the following relation

$$H'(u)\,J(u) - J'(u)\,H(u) = \frac{2i}{\pi u}$$

where u=qa. Substituting, we obtain

$$\frac{\partial G}{\partial r} = \frac{1}{4\pi^2 a}\sum_{m=0}^{m=\infty}\varepsilon_m\cos\left[m\left(\phi - \phi_o\right)\right]\int_{-\infty}^{\infty} e^{ik_x\left(x_o - x\right)}\frac{H_m\left(qr_o\right)}{H_m(qa)}dk_x$$

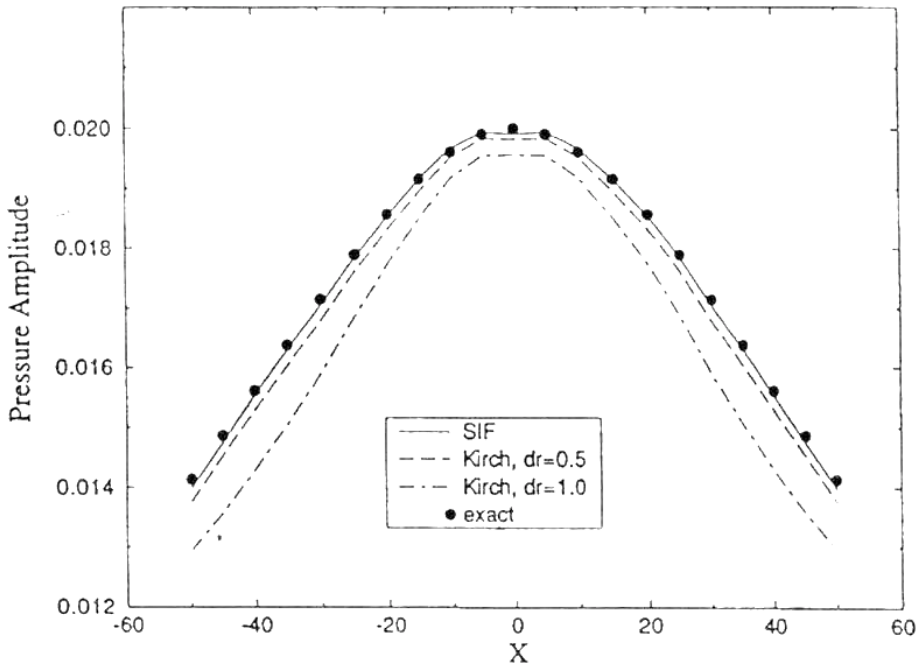
With G = 0 at the surface, the integral solution reduces to

$$p = \int p\frac{\partial G}{\partial r}a\,dx\,d\phi$$

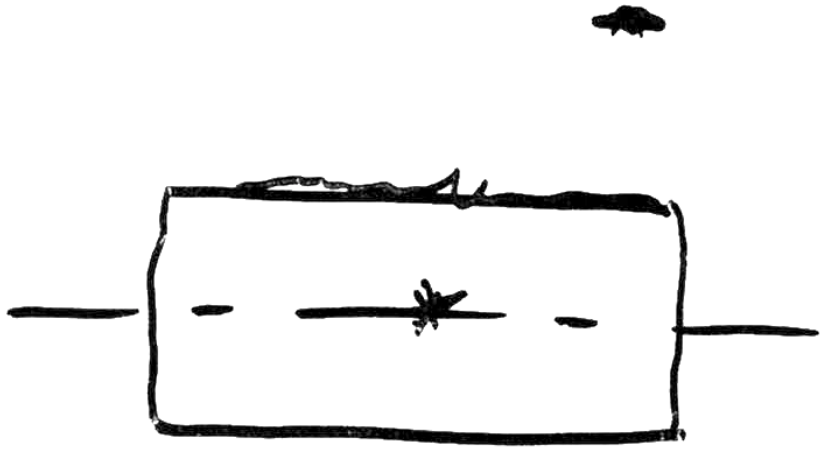
Substituting, we obtain the acoustic field as

$$p\left(x_o, r_o, \phi_o\right) = \frac{1}{4\pi^2}\int\int p(x, a, \phi)\sum_{m=0}^{m=\infty}\varepsilon_m\cos\left[m\left(\phi - \phi_o\right)\right]\bullet$$
$$\int_{-\infty}^{\infty} e^{ik_x\left(x_o - x\right)}\frac{H_m\left(qr_o\right)}{H_m(qa)}dk_x\,dx\,d\phi$$

This is the final formula describing the relation between the acoustic far field and the pressure distribution on a cylindrical surface surrounding the jet noise sources.



Effect of grid spacing dr on pressure amplitude, L/a=30, dx=0.5.



Directivity of jet noise at a circle of radius R=48.

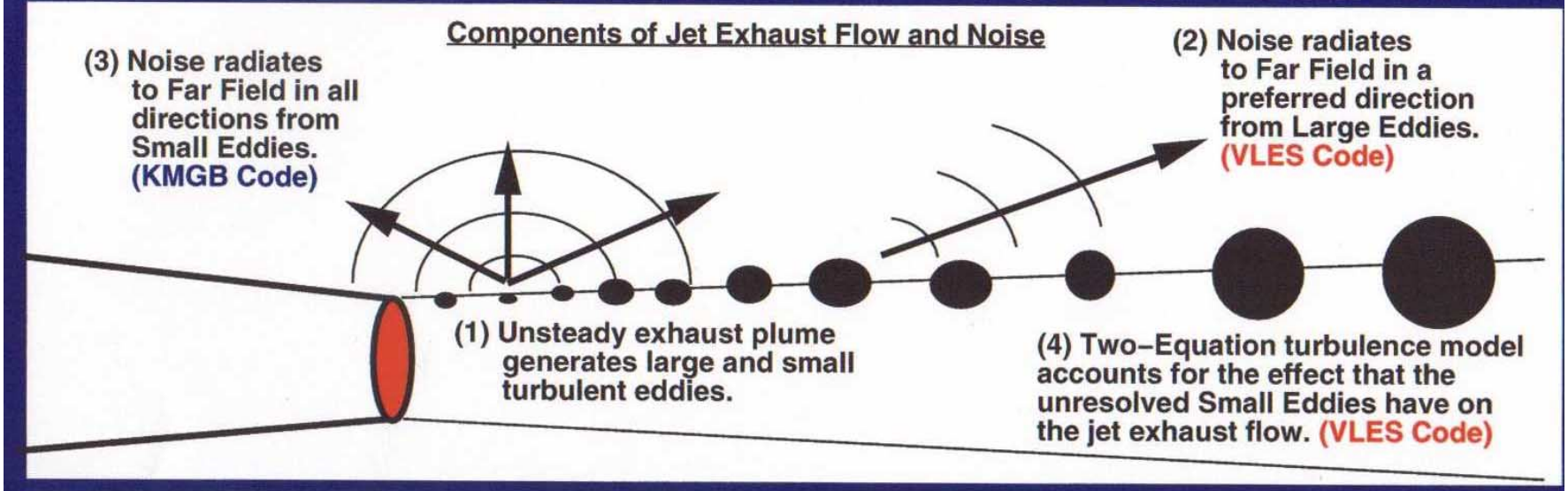
OTHER TECHNIQUES FOR SOUND PROPGATION

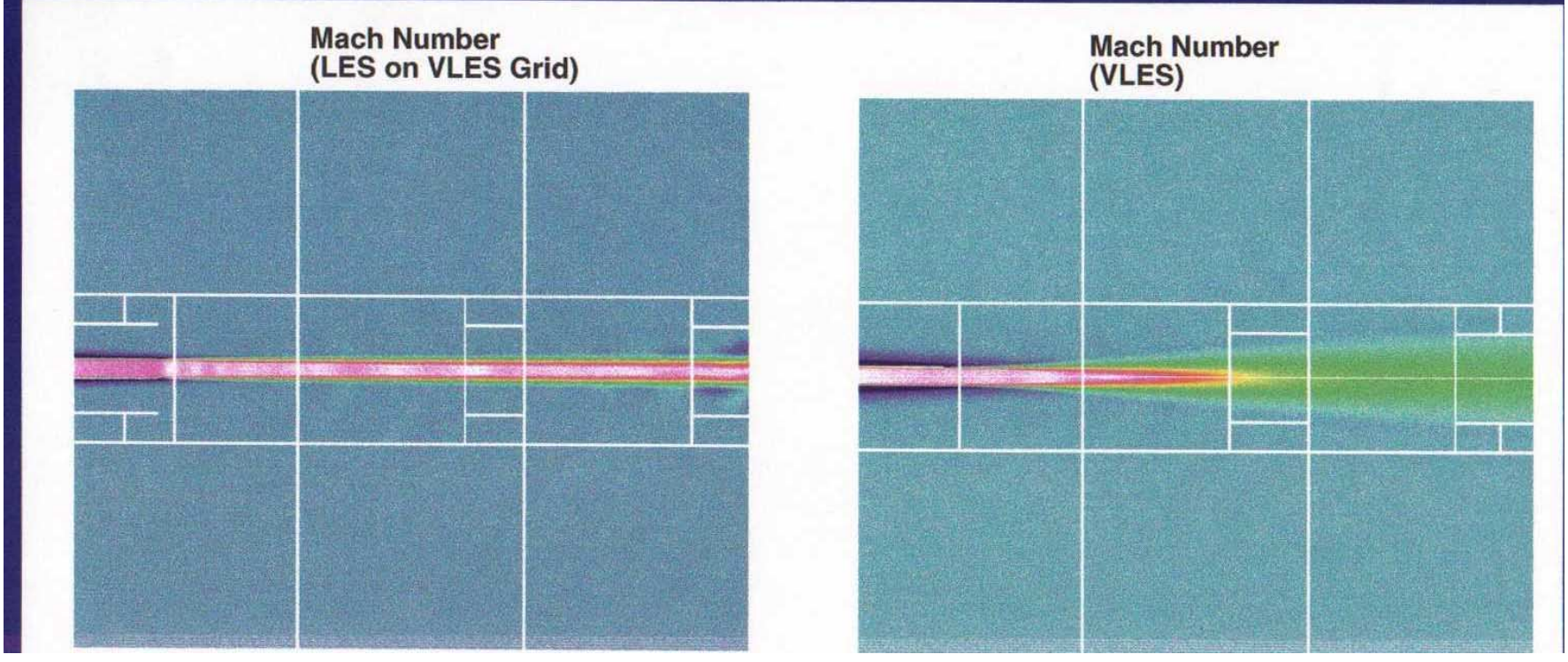
- **Lighthill Sound source may be noncompact**
- **Kirchoof solution can be used to calculate the Fairfield sound given the pressure distribution over a cylindrical surface enclosing the source**
- **An Analytical solution in terms of Hankel function can be used for extending the near field solution to the Fairfield- no pressure derivative term**

THE SOURCE REGIME- VLES

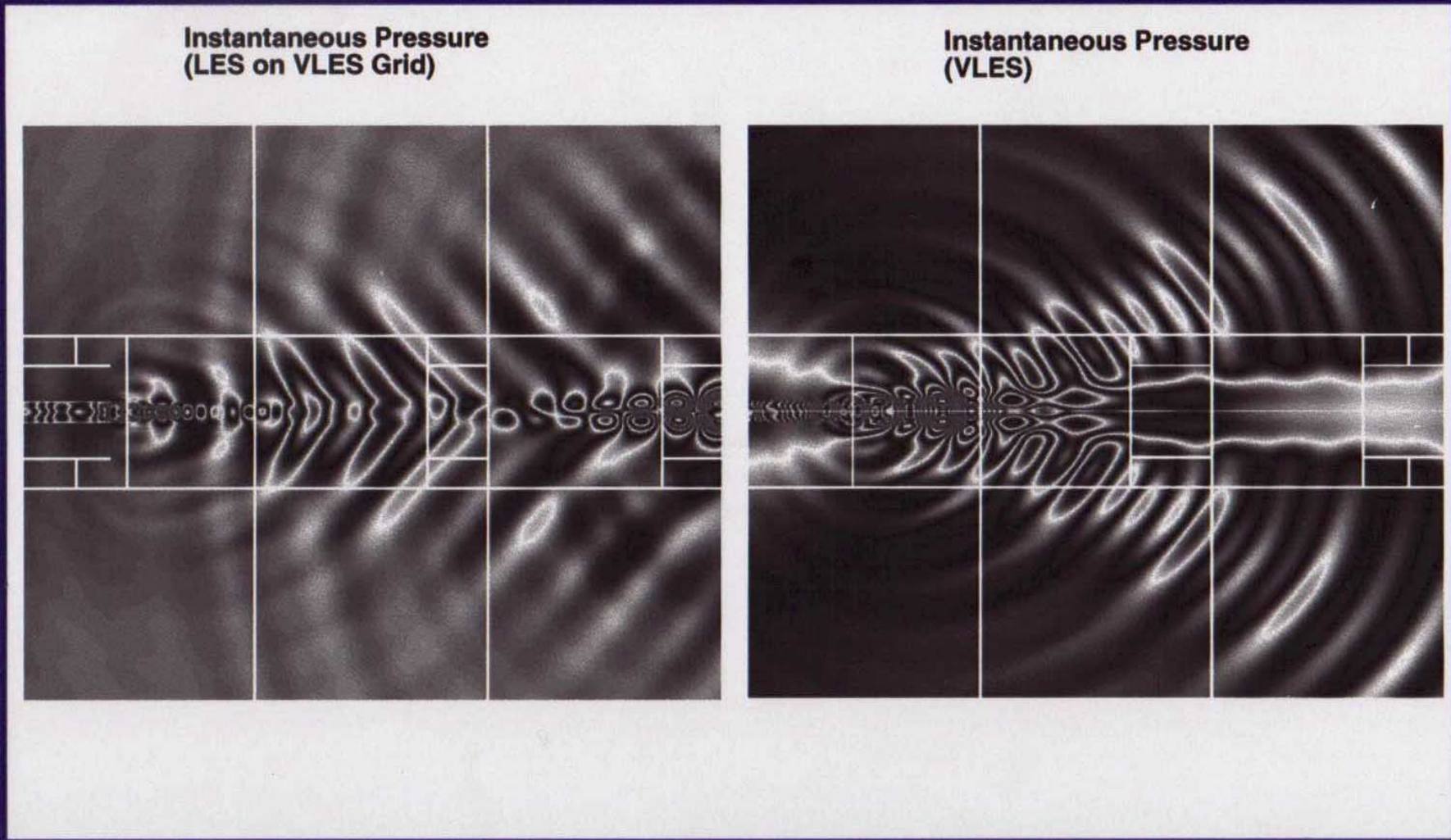
IMPROVED NUMERICAL SCHEME
USE A COURSE MESH TO RESOLVE ONLY THE VLS
MODEL THE UNRESOVED SCALES USING A HIGH-ORDER TURBULRENCE MODEL (K-epsilon)

Initial Comparison of Very Large Eddy Simulation and Large Eddy Simulation

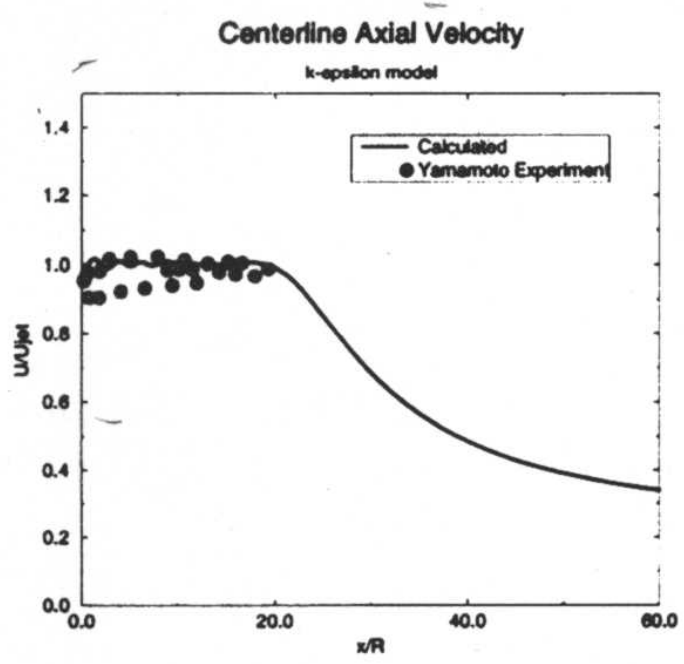


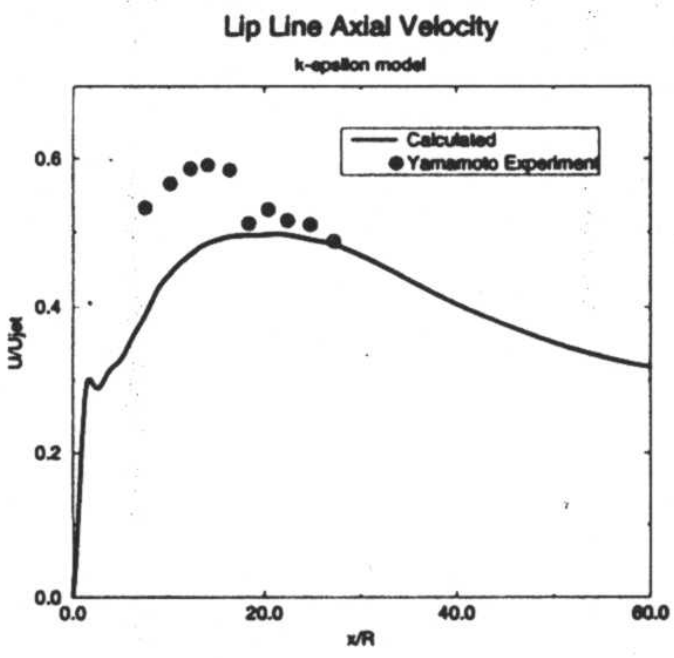


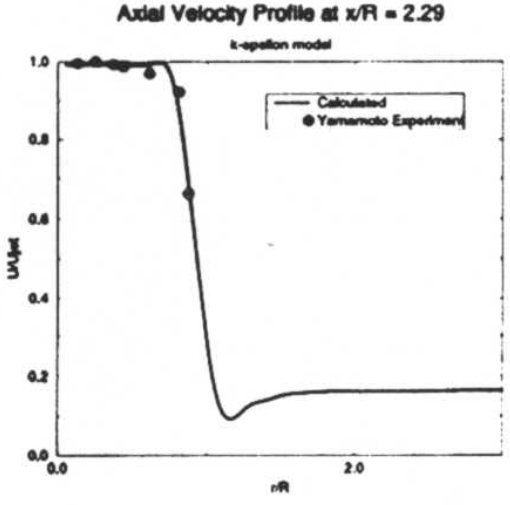
Initial Comparison of Very Large Eddy Simulation and Large Eddy Simulation (2)

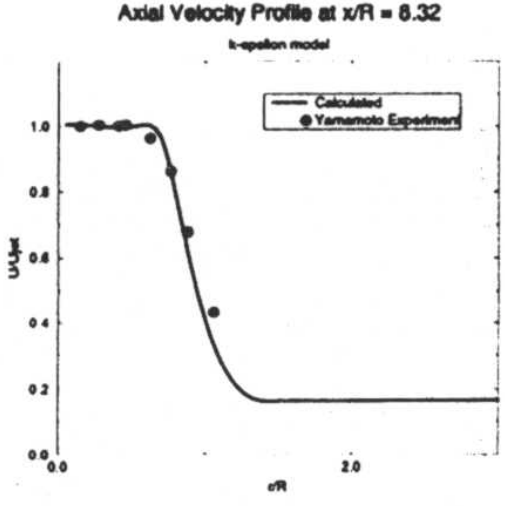


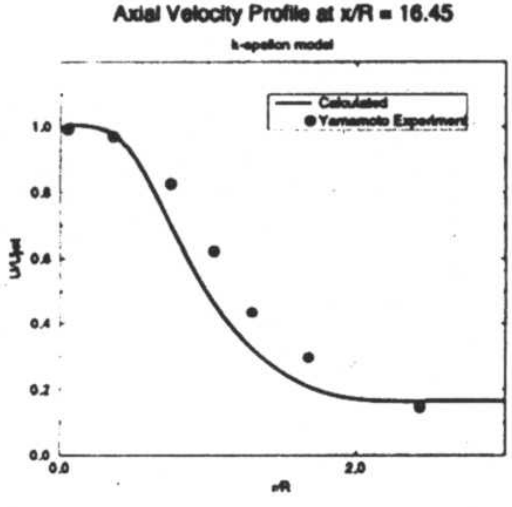
Very Large Eddy Simulation Method for Fast Prediction of Jet Exhaust Noise

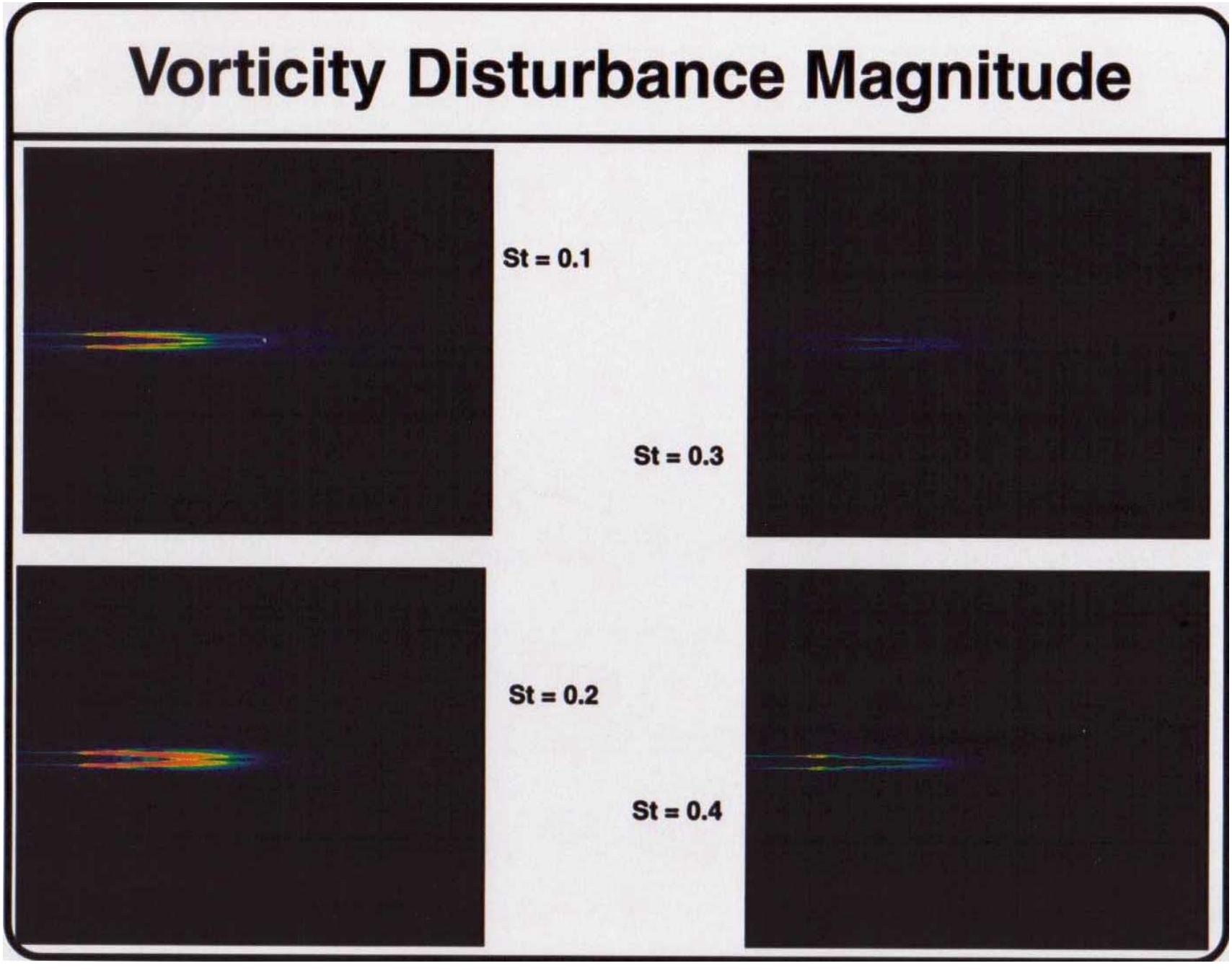




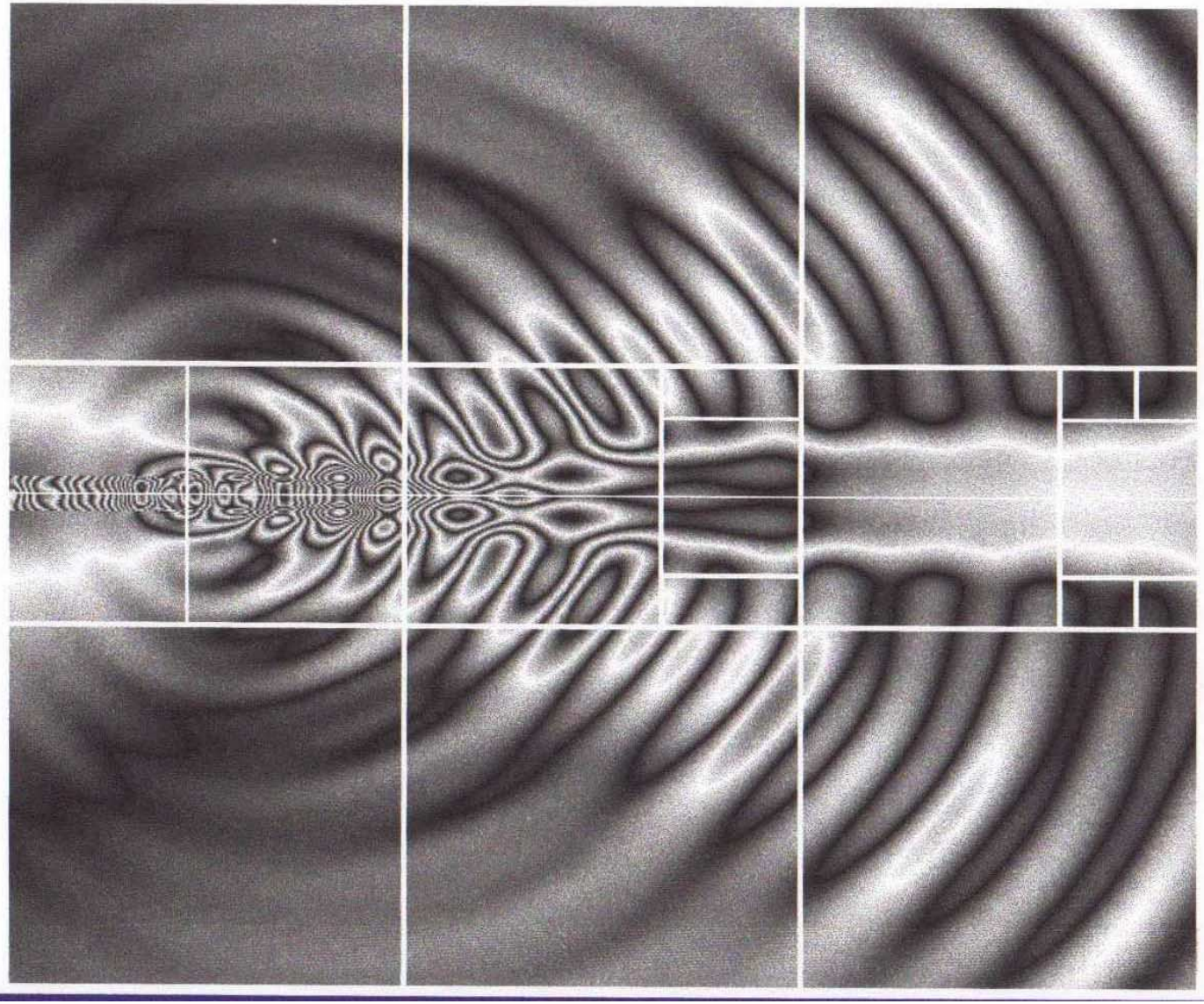


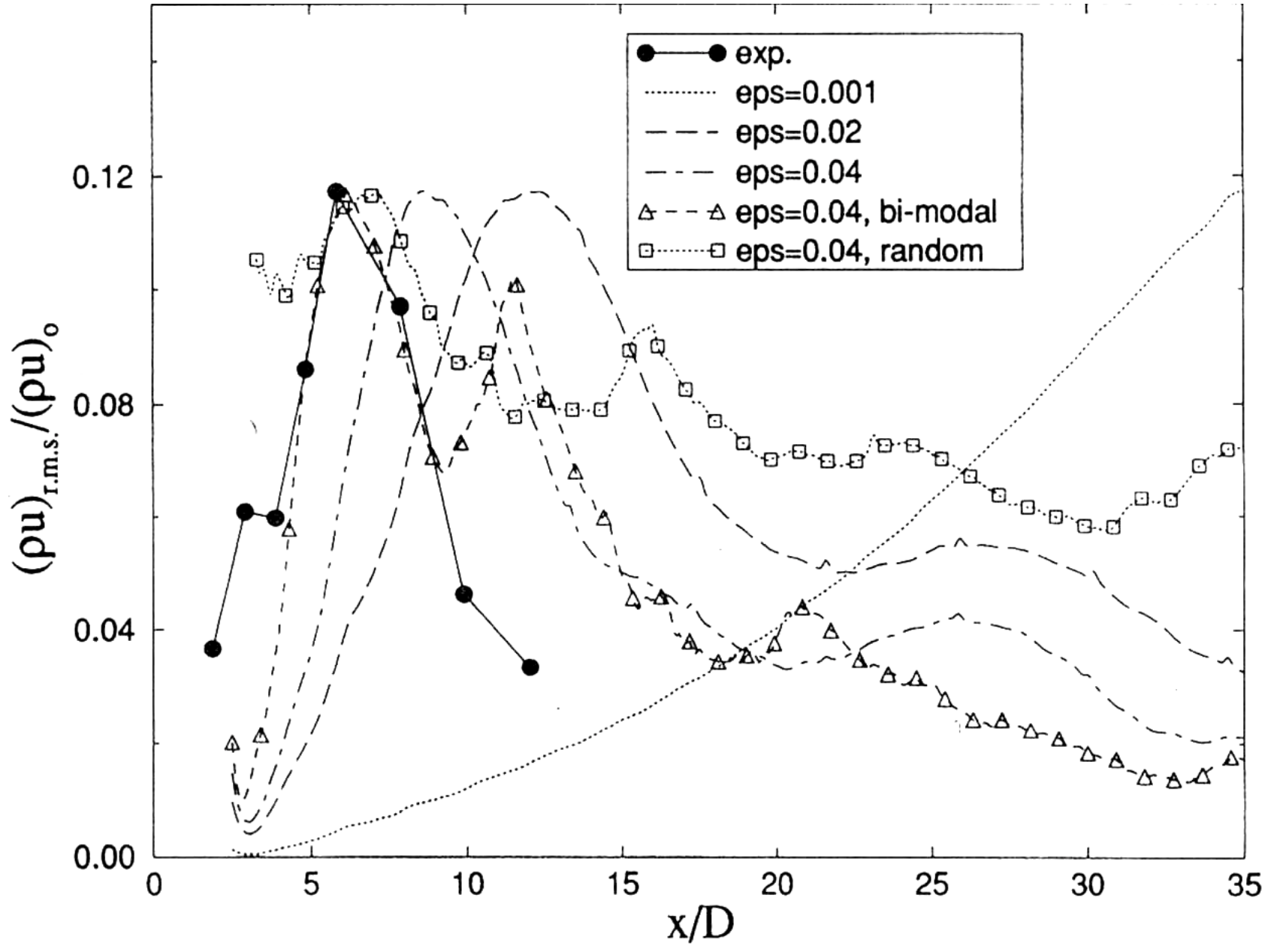





Vorticity Disturbance Magnitude
St = 0.1
St = 0.3
St = 0.2
St = 0.4

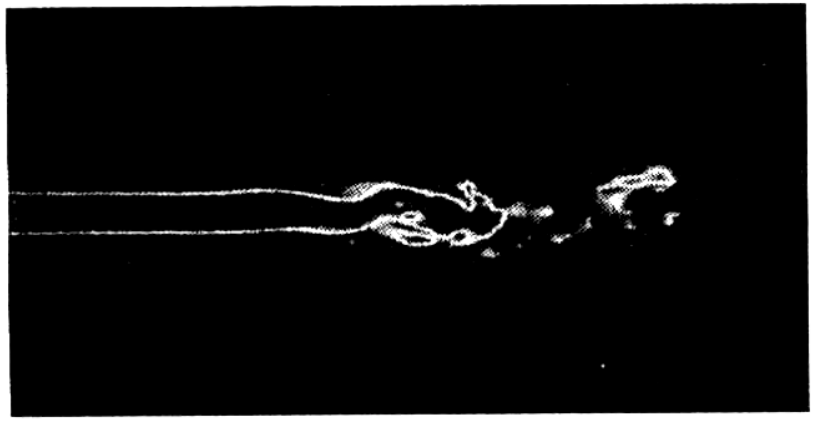
Snapshot of Very Large Eddy Simulation Pressure Field



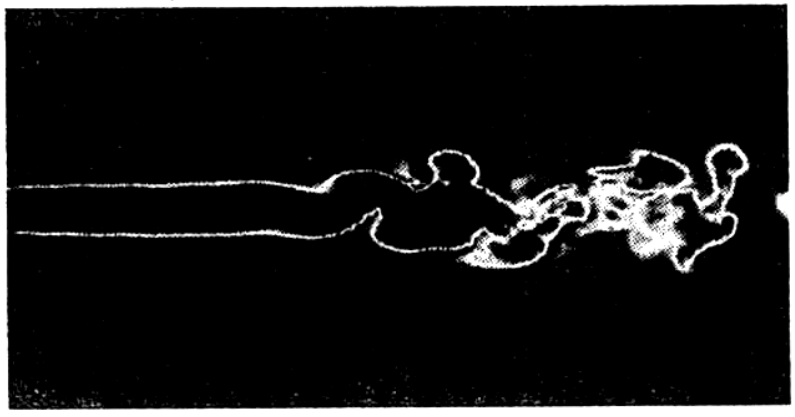

exp.
eps=0.001
eps=0.02
eps=0.04
eps=0.04, bi-modal
eps=0.04, random
0.12
0.08
0.04
0.00
0
5
10
15
20
25
30
35
x/D
(ρu)r.m.s./(ρu)o

Technical Highlight

3–D, Large–Eddy Simulation of a M=1.4 supersonic round jet excited by multiple frequencies at nozzle exit



Mach Number



Density

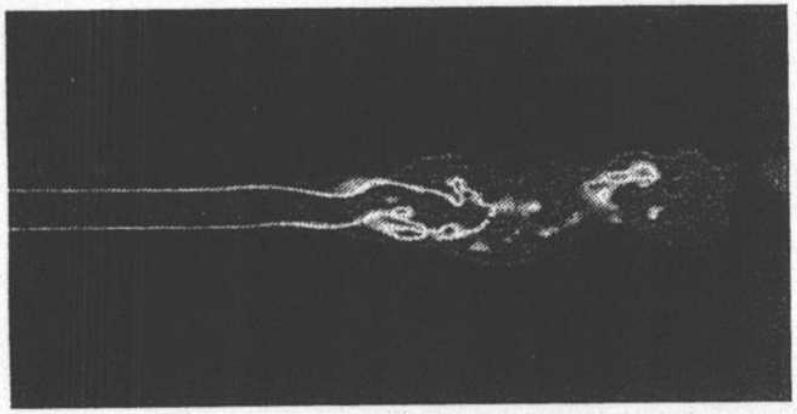


Vorticity

Enhanced mixing and the breakdown of organized structures downstream of jet are observed. This near–field solution will be used to obtain far–field noise through the use of Kirchhoff–type methods.

Technical Highlight

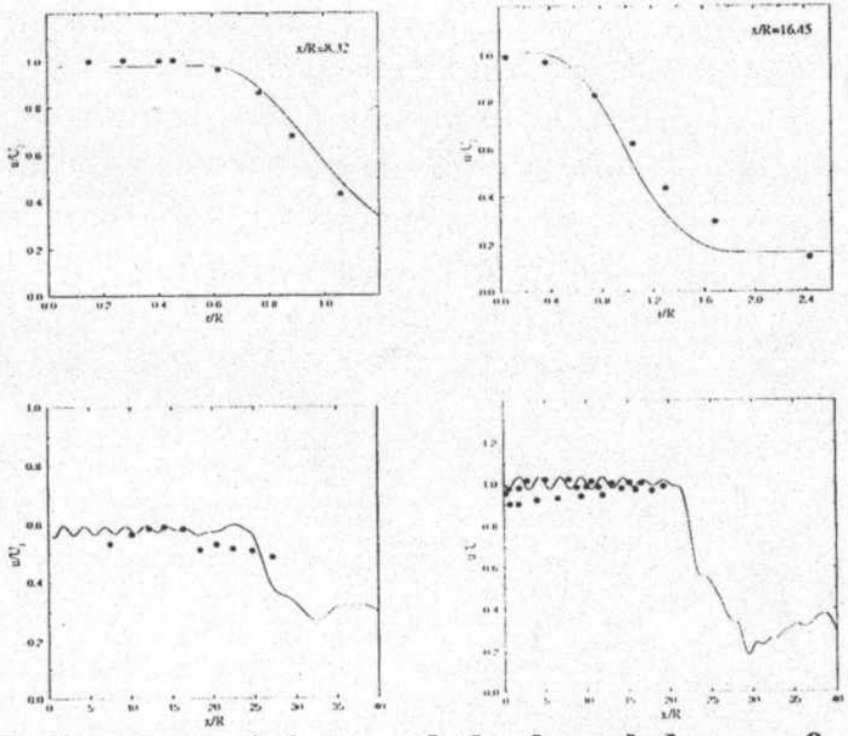
3–D, Large–Eddy Simulation of a M=1.4 supersonic round jet excited by multiple frequencies at nozzle exit



Mach Number



Vorticity



Enhanced mixing and the breakdown of organized structures downstream of jet are observed. This near–field solution will be used to obtain far–field noise through the use of Kirchhoff–type methods.

NUMERICAL ISSUES

- Extensive Computational Domain 60D x 40D
- Helical modes- 3D
- Various length scales:
  - Acoustic: Acoustic Wavelength
  - large-scale: diameter of the jet
  - Shear layer scales: momentum thickness
  - Mean flow
- High-order scheme is needed to cover these scales in this large domain
- Amplitude and phase accuracy (Dispersive and dissipation errors need to be minimized)
- Several Schemes are available for linear problems-Linear sound propagation can be handled.
- Few Schemes are available for mixing noise (nonlinear): DRP, High-Order McCormick. Compact, Split Compact.
- A suitable-scheme for acoustics-shock wave interaction is still being sought
- Boundary Conditions still represent the major difficulty

R. Mankbadi References

1. "Transition, Turbulence, and Noise," *Kluwer* Academic Press, Boston, 1994.

2. "Computational Aeroacoustics," R. R. Mankbadi, in "New Trends in Turbulence, (Ed. M. Leisure), Springer, 2001.

3. Mankbadi, R. R., Hayder, M. E. & Povinelli, L. A., 1994, "Structure of Supersonic Jet Flow and Its Radiated Sound," *AIAA Journal*, Vol. 31, No.5, pp. 897-906.

4. Hixon, D. R., Shih, S. H., and Mankbadi, R. R., 1995, "Evaluation of Boundary Conditions for Computational Aero-Acoustics," *AIAA Journal*, Vol. 33, No. 11, pp. 2006-2012.

5. Lyrintzis, A. and Mankbadi, R. R., 1996, "Prediction of the Far-Field of Noise Using Kirchhoff Method," *AIAA Journal*, Vol. 34, pp. 413-416.

6. Shih, S-H, Hixon, D. R., and Mankbadi, R. R., 1997, "Zonal Approach for Computational Aeroacoustics," *AIAA Journal of Propulsion and Power*, Vol. 13, No.6, pp. 745-758.

7. Mankbadi, R. R., Hixon, D. R., Shih, S-H, and Povinelli, L. A., 1998, "Use of Linearized Euler Equations for Supersonic Jet Noise Prediction," *AIAA Journal*, Vol. 36, No.2, February 1998, pp. 140-147.

8. Bui, T. and Mankbadi, R. R., 1998, "Numerical Simulations of Acoustic Waves Interaction with Shock Wave in a Quasi-1D Convergent-Divergent Nozzle Using an Unstructured Finite Volume Algorithms," Journal *of Computational Fluid Dynamics*, Vol. 10, No. 4, pp. 281-290.

9. Mankbadi, R. R., Shih, S-H., Hixon, D. R., Stuart, J. T. and Povinelli, L. A., 1998, "A Surface-Integral Formulation for Jet Noise Prediction Based on The Pressure Signal Alone," *Journal of Computational Acoustics*, Vol. 6, No. 3, pp. 307-320.

10. Dong, T. Z. and Mankbadi, R. R., 1999, "Simulation of Unsteady Flow in Nozzle-Ejector Mixer," *AIAA Journal of Propulsion and Power*, Vol. 15, Number 4, pp. 539-543.

11. Mankbadi, R. R., 1999, "Review of Computational Aeroacoustics in Propulsion Systems," *AIAA Journal of Propulsion and Power*, Vol. 15, Number 4, pp. 504-512.

12. Hixon, R., Shih, S-H. and Mankbadi, R. R., 1999, "Evaluation of Boundary Conditions for the Gust-Cascade Problem," *AIAA Journal of Propulsion & Power*, 2000, Vol. 16, No. 1, pp. 72-78.

13. Mankbadi, R. R., Shih, S-H, Hixon, D. R., and Povinelli, L. A., "Direct Computation of Jet Noise Produced by Large-Scale Axisymmetric Structures," AIAA Journal of Propulsion and Power, Vol. 15, No.5, September-October, 1999, pp 207-215.

14. Mankbadi, R. R. and Ali, A. A., 1999, "Evaluation of Subsonic Inflow Treatments for Unsteady Jet Flow," *Journal of Computational Acoustic*, Vol. 7, No. 4, 1999, pp.147-160.

15. Shih, S-H., Hixon, D. R., and Mankbadi, R. R., "Three-Dimensional Large-Eddy Simulations: Behavior Near Centerline," *Journal of Computational Fluid Dynamics*.

16. Mankbadi, R. R., Hixon, R., Povinelli, L. A., 2000, Very Large Eddy Simulations of Jet Noise, " AIAA 2000-2008, 6th AIAA/CEAS Aeroacoustics Conference, 12-14 June 2000, Lahaina, Hawaii.

Dr. Jonathan Freund of UCLA presented results from DNS calculations. Flow field properties and far field noise were predicted. Comparisons made with the data of Stromberg for a low Reynolds number flow showed good agreement.

Dr. Ray Hixon of NASA Glenn presented results from the application of a high order CAA code which used body-fitted curvilinear grids to compute nonlinear flows about complex geometries. Results for test cases from the 3rd CAA workshop were presented. Good results were obtained.

Dr. Anastasios Lyrintzis from Purdue University presented an overview on Integral Methods for Jet Aeroacoustics. Methods that can be used for this type of analysis include: Lighthill's acoustic analogy, which requires a volume integral of the source terms; Kirchhoff's method, which requires a surface integral with a good flow solver to get a good solution on that surface; and the porous Ffowcs Williams - Hawkings equation. Dr. Lyrintzis recommended that work continue to improve refraction corrections and high frequency predictions.

Dr. K. Viswanathan of Boeing presented an assessment of existing jet noise prediction methods. In particular, the MGBK method and the method of Tam were evaluated. A total of seven test cases, covering a range of jet Mach numbers and temperatures were used to evaluate these methods. Predicted spectra were compared with measured spectra for selected angles for each of the test cases. The same CFD solution (based on work of Thies and Tam) for the mean flow and turbulent energy was used for both noise prediction procedures. The method of Tam appeared to predict overall levels better than the MGBK method. Also, the MGBK method tended to under-predict the high frequency portion of the spectra while Tam's method predicted the spectral shape very well at angles away from the jet axis. Tam asserts that large scales are responsible for the noise near the axis and thus would not expect his method to predict the spectra shape at those angles. The MGBK method attempts to predict the spectra at all angles. In discussions after the presentation it was suggested that the better agreement of Tam's method with overall levels may be due to the fact that this method has been "calibrated" using aerodynamic input generated using the same method used in this study, whereas the MGBK code was "calibrated" using aerodynamic data from a different code. Though the choice of the CFD solution would play a role, as pointed out by Dr. Morris, there could be more fundamental issues with the acoustic analogy approach that would cause the observed discrepancy.

Dr. Philip Morris of Penn State University presented information comparing the source terms in the Tam and MGBK methods. Dr. Morris' main conclusion was that the difference in predicted spectral shape between the two methods may be due to the frame of reference used to model the source auto-correlation function and the choice of model for the turbulent statistics.

DNS

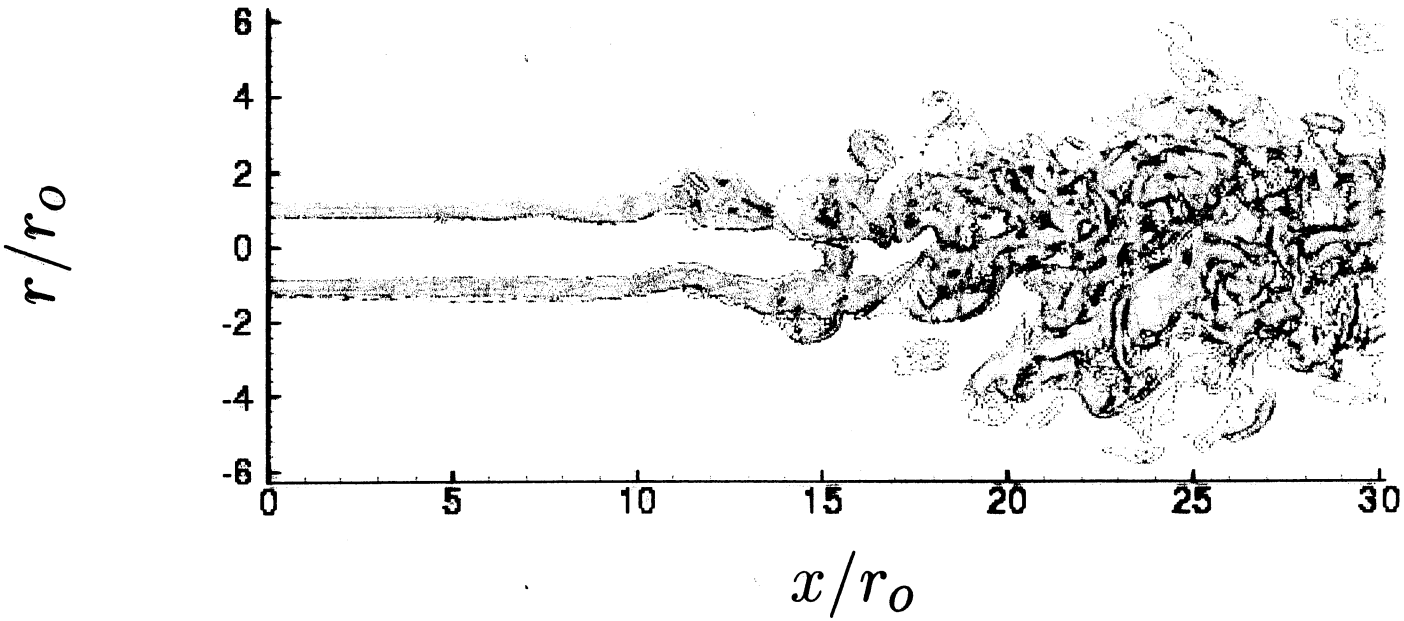
Vorticity

Visualizations

Jonathan Freund
University of California
Los Angeles

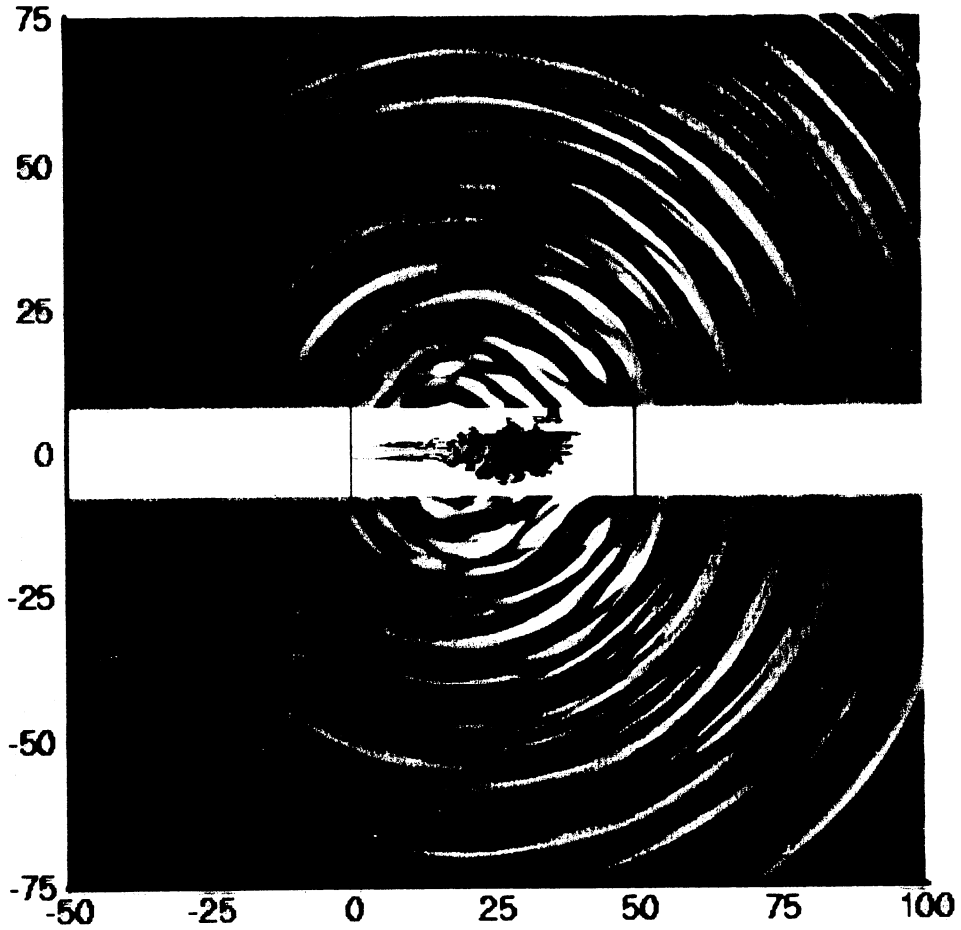
DNS Vorticity Visualization

Freund, AIAA 99-1858

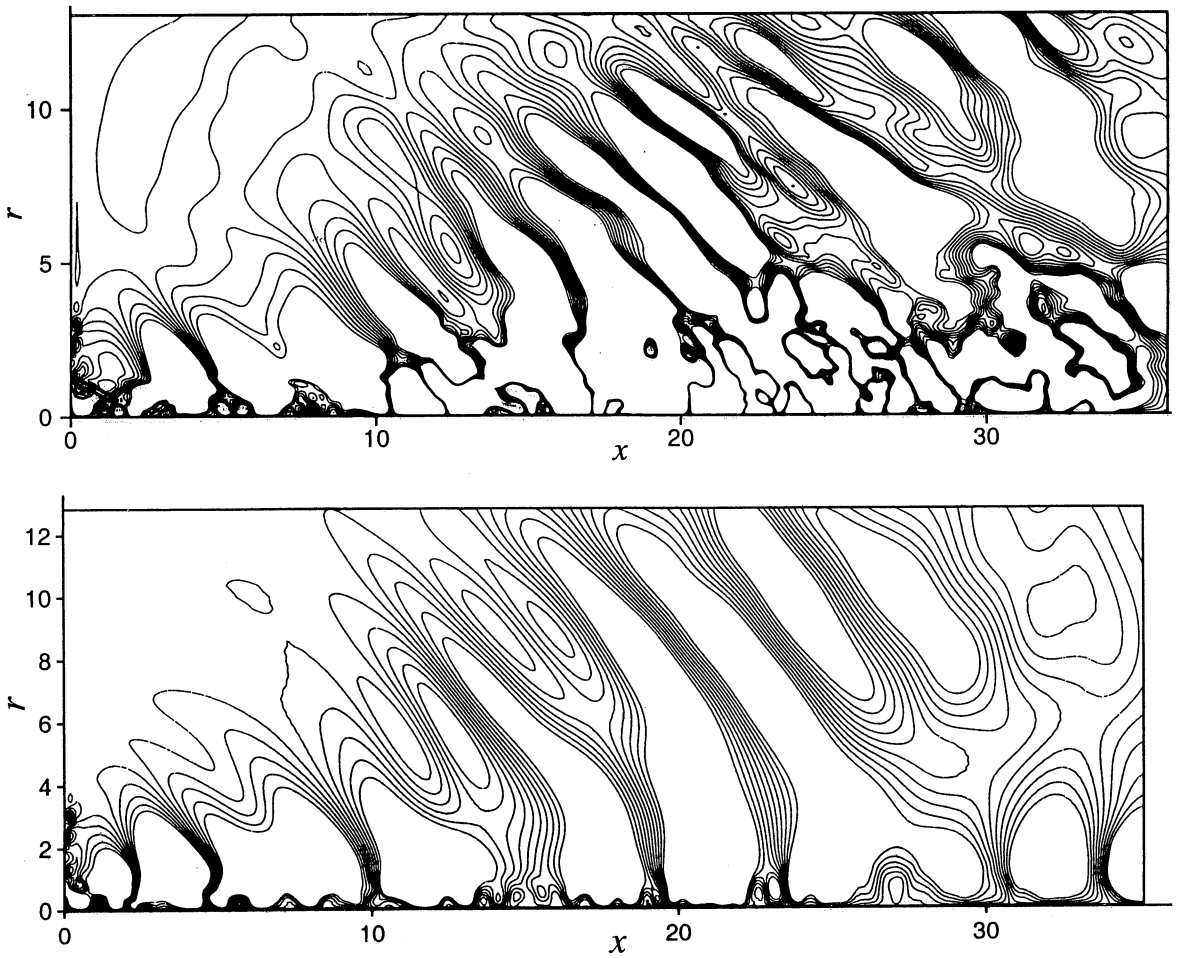


- Matches experimental conditions of Stromberg *et al.* (JSV, 1980)
- Mach number: $M = 0.9$
- Reynolds number: $Re = 3600$
- Numerical mesh: $640 \times 250 \times 160$ in (x, r, θ)

Far-Field Noise



$n = 1$, real



DNS/LNS

Colonius
Moshini
Freund
Reno
2001



Compressible Flow Equations (DNS)

M=1.92
Re=2000

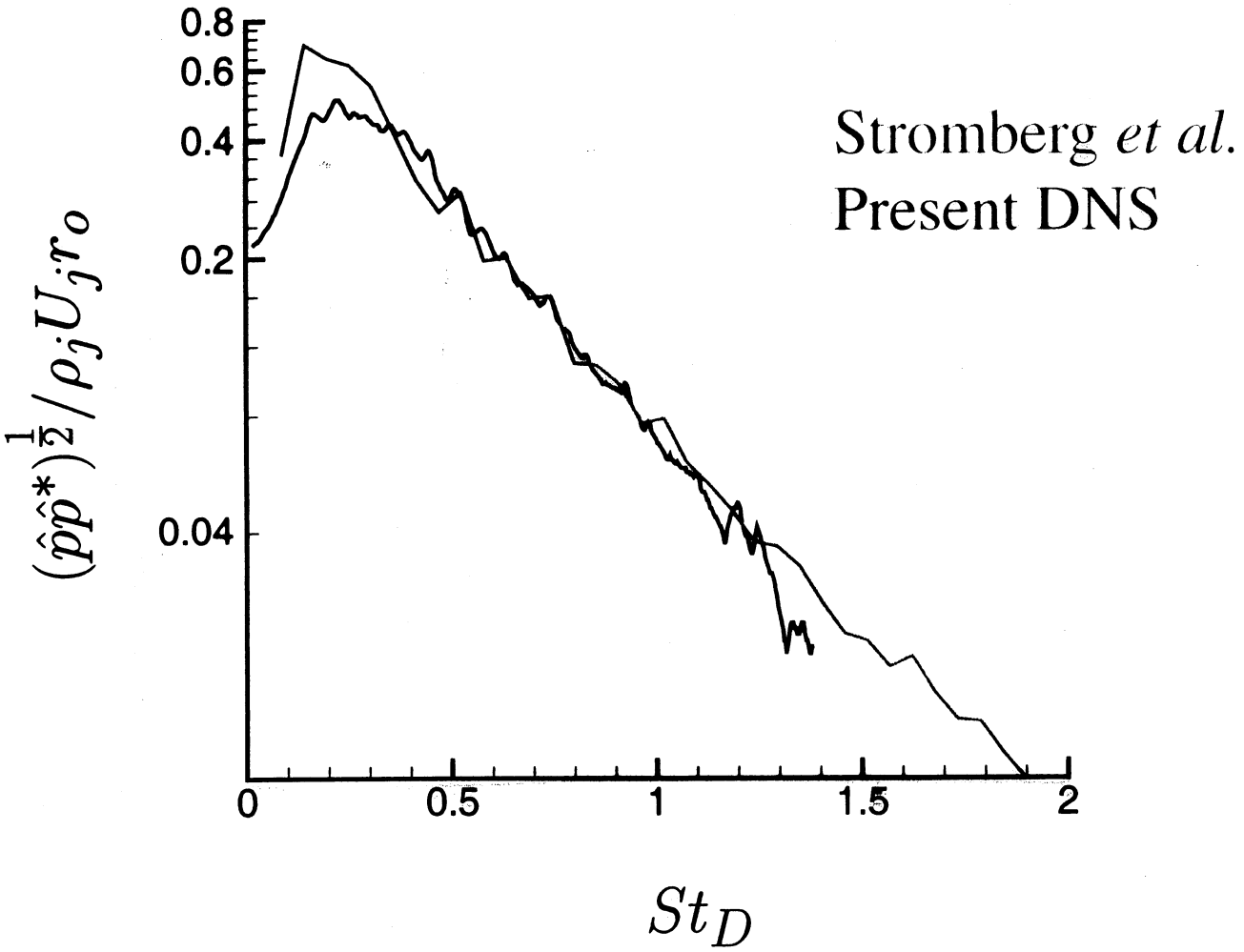
Same DNS Inflow Data



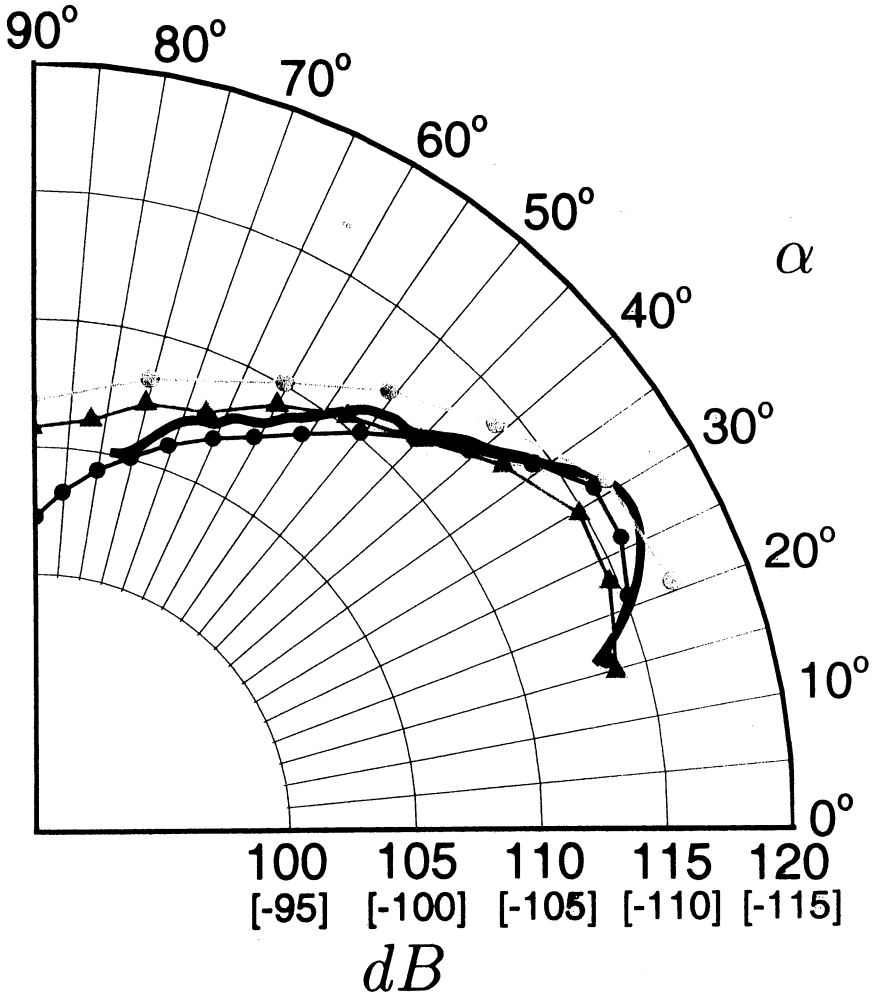
Linearized Compressible Flow Equations (LNS)

Linearized About DNS Mean Flow

Spectrum


0.8
0.6
0.4
0.2
0.04
0
0.5
1
1.5
2
$(\hat{p}\hat{p}^*)^{\frac{1}{2}}/\rho_j U_j r_o$
St_D
Stromberg *et al.*
Present DNS

Far-Field Directivity



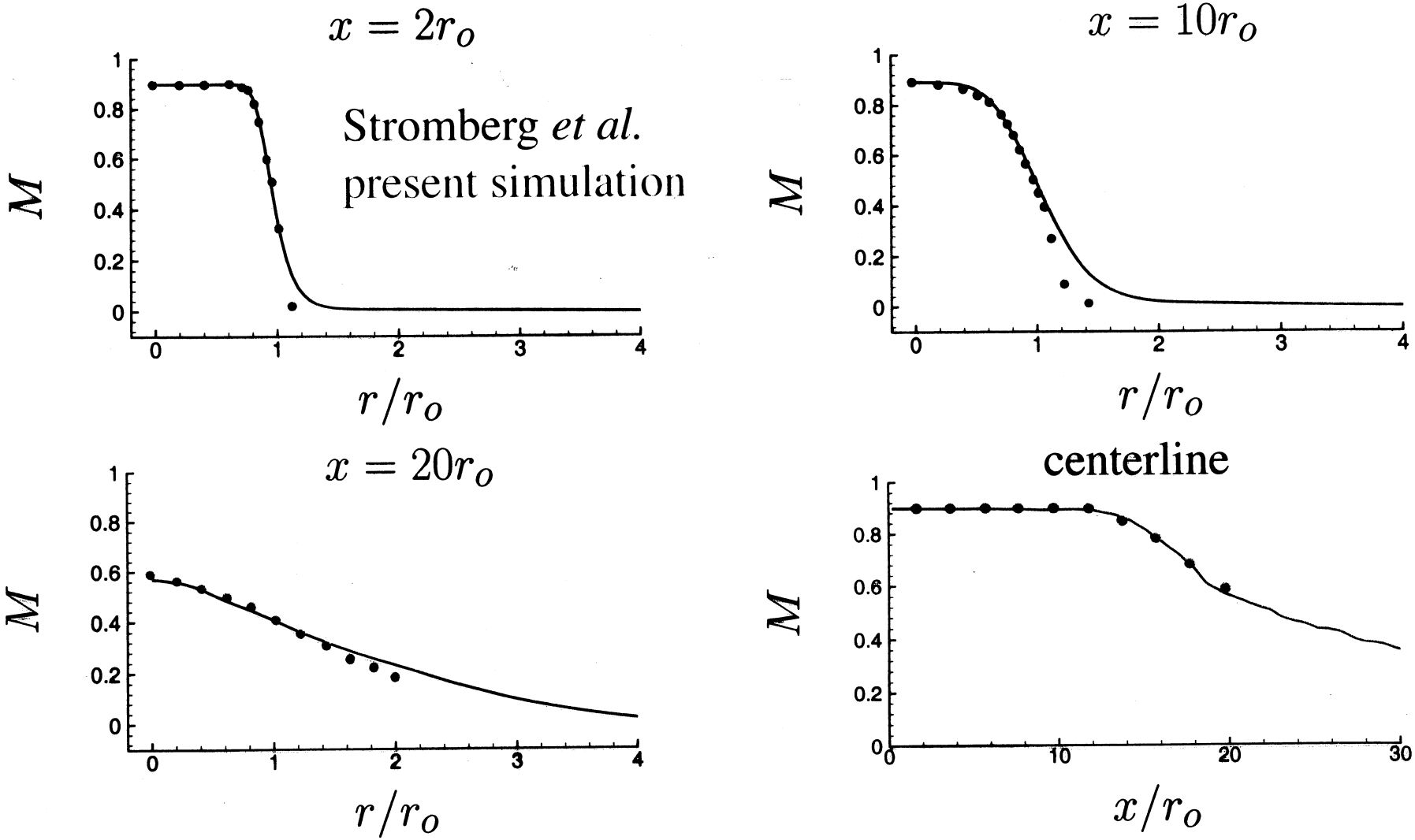
Present simulation

Stromberg *et al.*

Mollo-Christensen *et al.*

Lush

Mean flow


$x = 2r_o$
Stromberg *et al.*
present simulation
M
r/r_o
$x = 10r_o$
M
r/r_o
$x = 20r_o$
M
r/r_o
centerline
M
x/r_o

Validation of a High-Order Compact Code for Nonlinear Flows about Complex Geometric

Ray Hixon
NASA Glenn Research Center

NASA/CP—2001-211152

Validation of a High−Order Compact Code for Nonlinear Flows about Complex Geometries

953

R. Hixon

R. R. Mankbadi

Computational Requirements for Nozzle Exhaust Flow and Noise Calculations

- The code must be capable of accurately calculating nonlinear flowfields.
- Very small amplitude waves must be accurately captured.
- Complex geometries must be accurately represented.
- The code must be written to take advantage of distributed computing environments.
- The code should be robust and capable of being applied to arbitrary geometries.

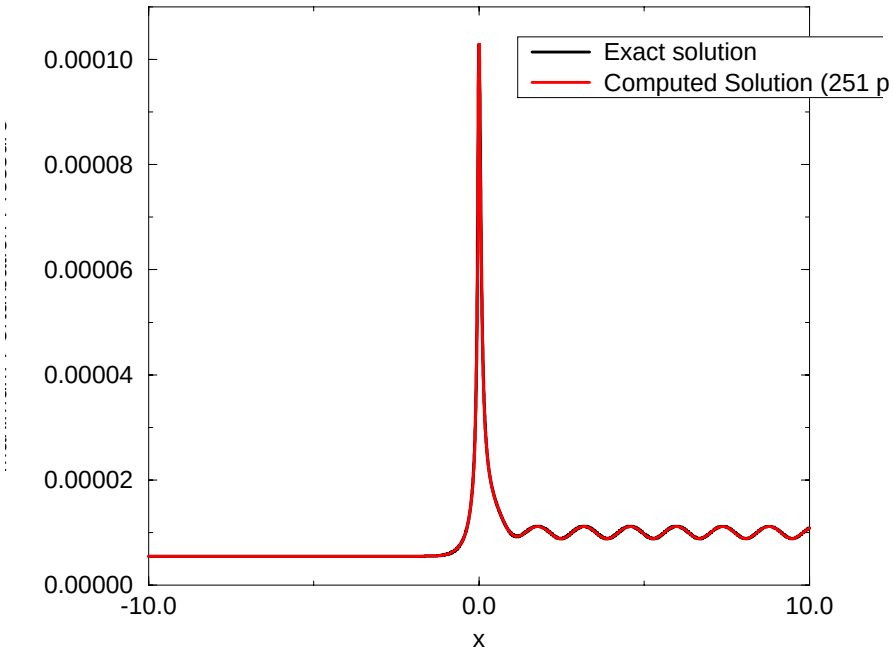
Current Numerical Method

- 4th order low−storage optimized Runge−Kutta time marching (LDDRK 5−6).
- Prefactored small−stencil 6th order compact spatial differencing.
- Explicit 10th order filtering applied at each stage.
- 3−D generalized curvilinear coordinates.
- Structured multi−block grids.
- MPI parallel for distributed computer clusters.
- Allows different equations in each block for more efficient use of resources.
- F90 used for memory management and improved data structures.
- Solves full nonlinear Euler, Navier−Stokes, LES (Smagorinsky), VLES (k−ε).

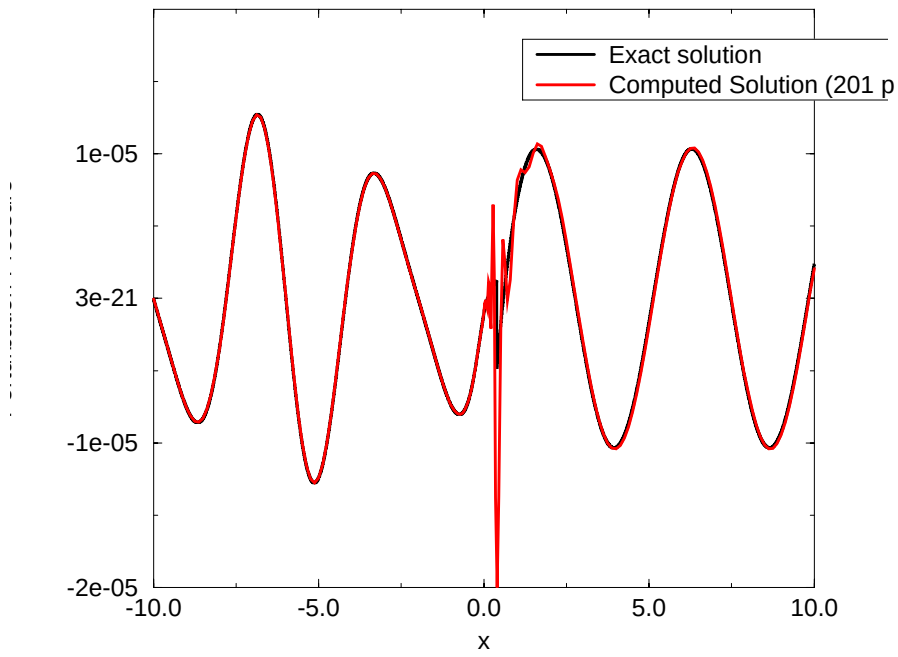
Validation of Prefactored Compact Scheme on CAA Benchmark Problems

These problems showcase the ability of the scheme to accurately calculate the propagation of small disturbances through nonlinear mean flows on highly stretched grids.

Acoustic Wave Through Transonic Nozzle (Category 1, Problem 1, 3rd CAA Workshop)

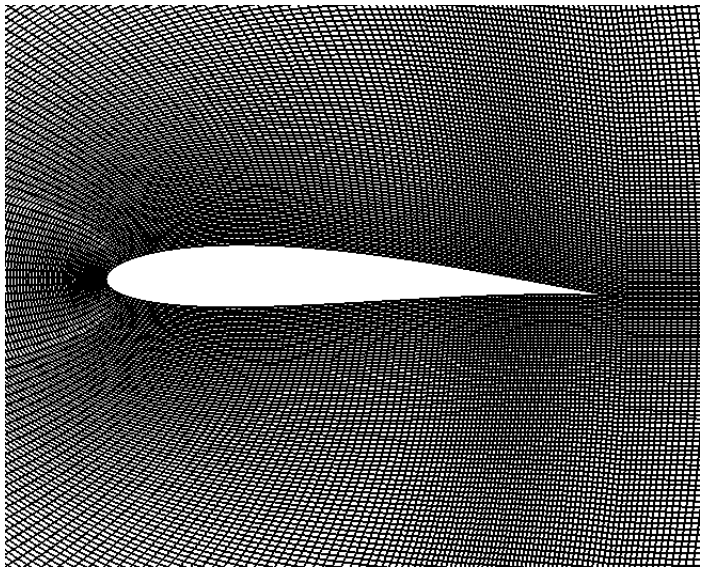


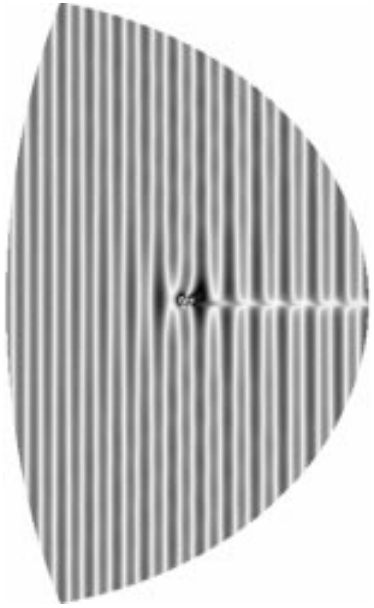
Acoustic Wave Through Shock (Category 1, Problem 2, 3rd CAA Workshop)



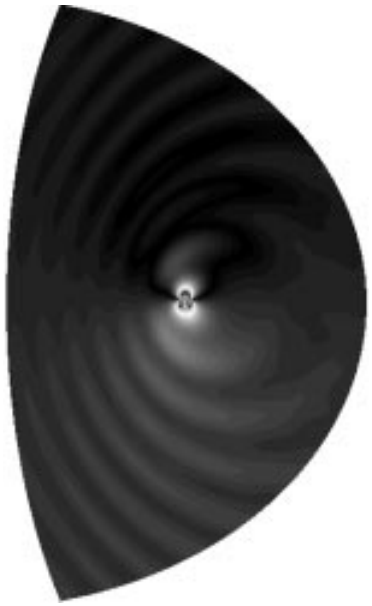
Curvilinear Grid Performance Test: Gust Response of a Joukowski Airfoil

Closeup of Cambered Airfoil Grid





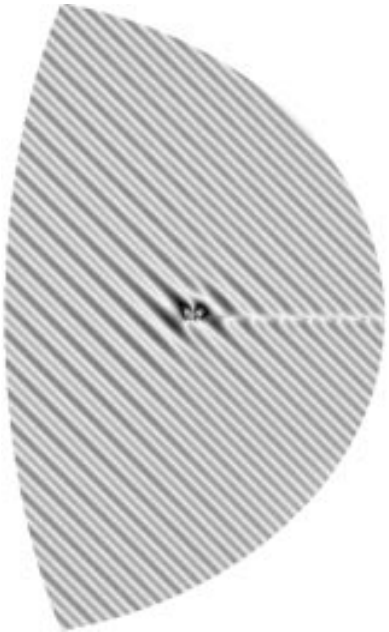
k = 1.0
1D gust



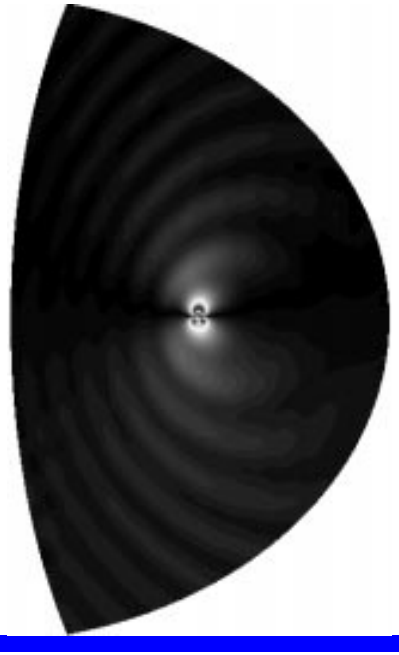
V velocity

Perturbation Pressure

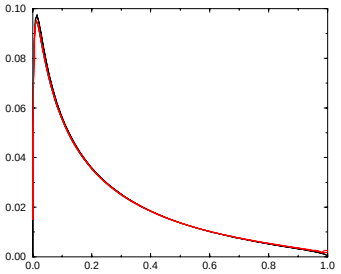
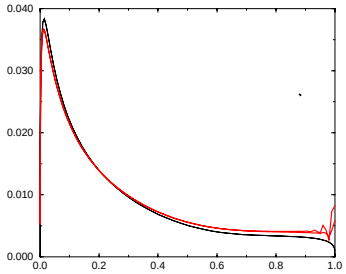
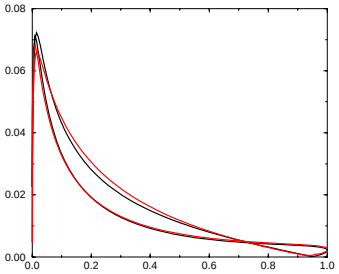
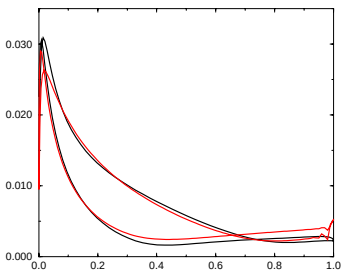
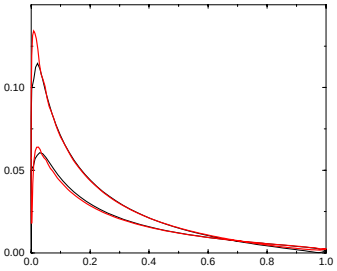
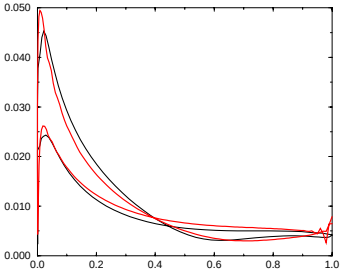
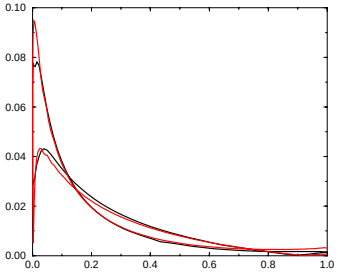
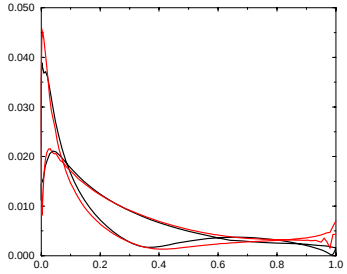
In this benchmark CAA problem, the effects of wall geometry, gust geometry, curvilinear grids, and farfield boundary conditions are tested.



k = 1.0
2D gust



Airfoil Surface RMS Pressure Disturbance for Joukowski Airfoil in a Vortical Gust

	1−D Gust, k = 0.1	1−D Gust, k = 1.0	2−D Gust, k = 0.1	2−D Gust, k = 1.0
Symmetric Airfoil				
Cambered Airfoil				

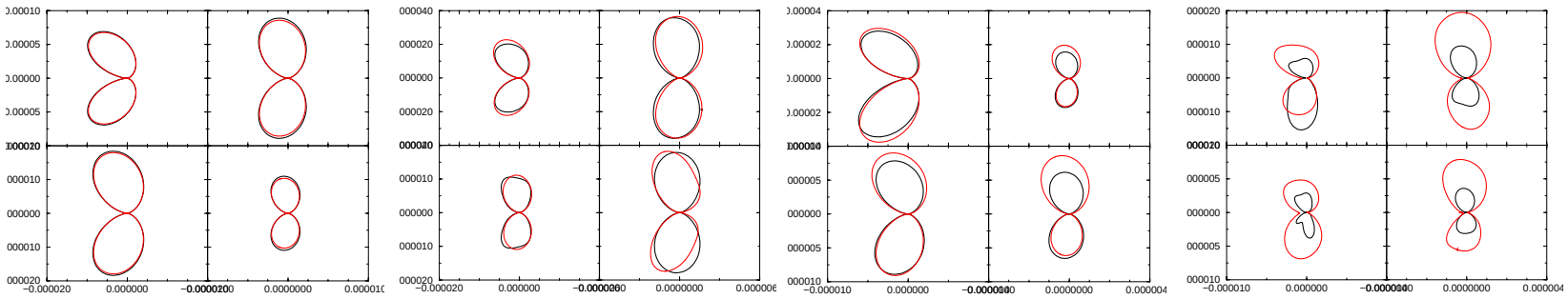
GUST3D Results

Computed Results

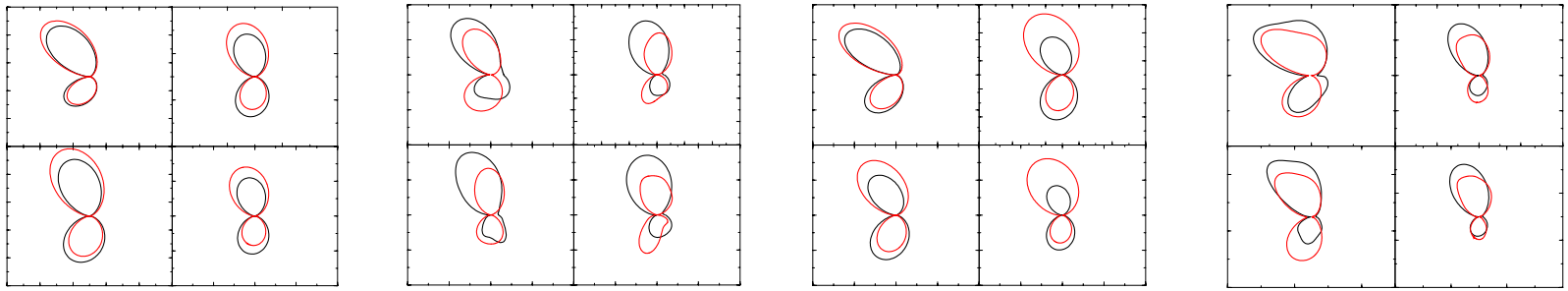
Far Field Noise Radiation Results for Joukowski Airfoil in a Vortical Gust

1−D Gust, k = 0.1 | **1−D Gust, k = 1.0** | **2−D Gust, k = 0.1** | **2−D Gust, k = 1.0**

Symmetric Airfoil



Cambered Airfoil



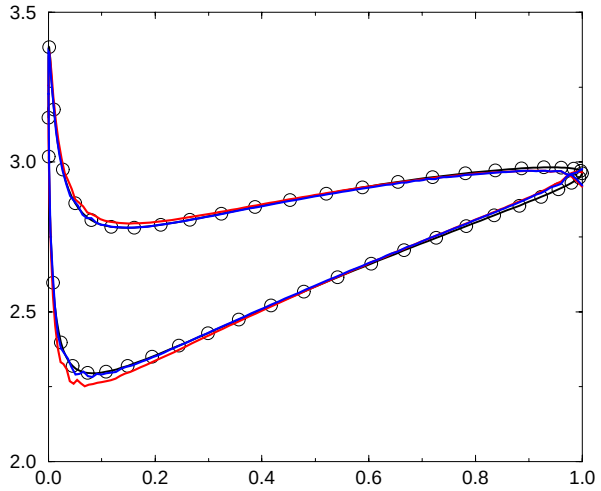
R = 1	**R = 3**
R = 2	**R = 4**

GUST3D Results

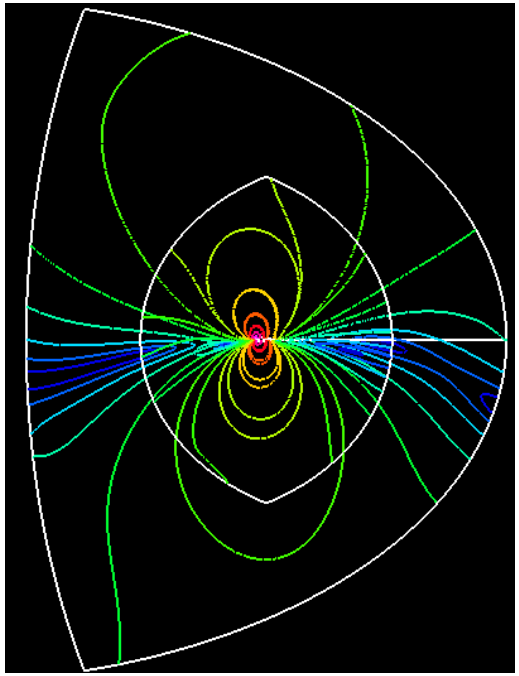
Computed Results

Boundary Distance Study for Joukowski Airfoil Problem (Cambered, k=0.1, 2D gust)

Mean Pressure on Airfoil



Log Pressure Perturbation Contours

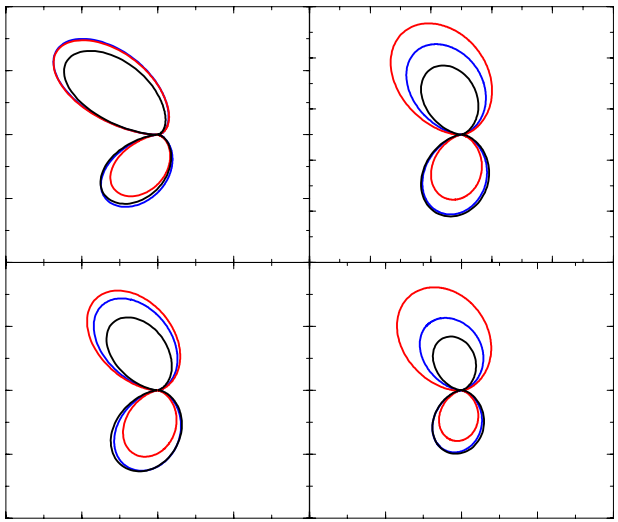


GUST3D Results

Computed Results (Coarse Grid = 433 x 125 = 54,125 points)

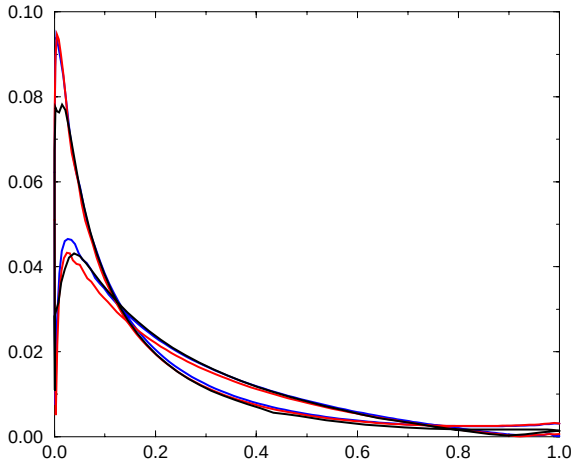
Computed Results (Large Grid = 605 x 240 = 145,200 points)

Pressure Perturbation in Far Field

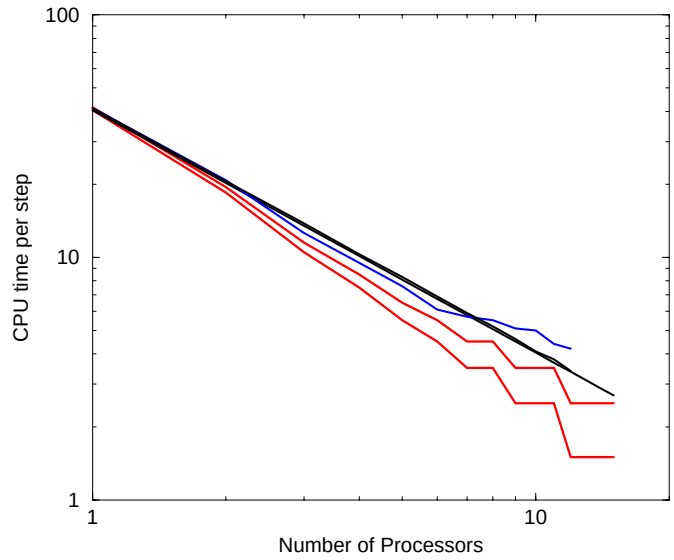


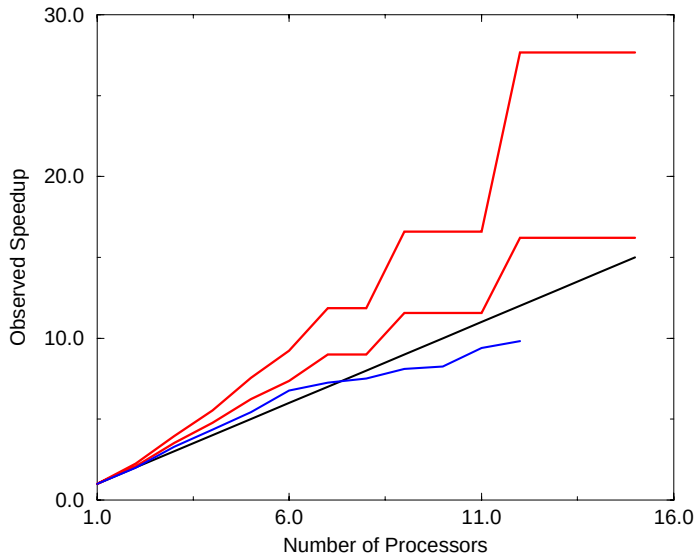
R = 1	R = 3
R = 2	R = 4

RMS Pressure Perturbation on Airfoil



Performance of ICOMP Parallel Macintosh Cluster





Best Expected Performance
ICOMP Mac G4 Cluster (2 G4/400 + 13 G4/450 DP)
ICOMP SGI Octane Cluster (6 R12000 + 6 R10000)

- The two red lines show best and worst performance of Mac cluster on the F90 MPI prefactored compact code.
- With 15 processors, the program is 17 times faster!

R. Hixon References

1. Carpenter, M. H., Gottlieb, D., and Abarbanel, S. (1993) Stable and Accurate Boundary Treatments for Compact, High-Order Finite-Difference Schemes, Applied Numerical Mathematics, 12, 55-87.
2. Casper, J. and Carpenter, M. H. (1995) Computational Considerations for the Simulation of Shock-Induced Sound, NASA Technical Memorandum 110222, Hampton, VA.
3. Constantinescu, G. and Lele, S. (2001) Large Eddy Simulation of a Near Sonic Turbulent Jet and its Radiated Noise, AIAA Paper 2001-0376, Reno, Nevada.
4. Freund, J. B. (1999) Acoustic Sources in a Turbulent Jet – A Direct Numerical Simulation Study, AIAA Paper 99-1858, Bellevue, WA.
5. Freund, J., Fleischman, T, Johnson, D., and Wei, M. (2001) A Numerical Study of Jet Noise Mechanisms, AIAA Paper 2001-0375, Reno, Nevada.
6. Gaitonde, D. V. and Visbal, M. R. (1999) Further Development of a Navier-Stokes Solution Procedure Based on Higher-Order Formulas, AIAA Paper 99-0557, Reno, Nevada.
7. Gottlieb, D. and Turkel, E. (1976) Dissipative Two-Four Method for Time Dependent Problems, Mathematics of Computation, 30, 703-723.
8. Haras, Z. and Ta'asan, S. (1994) Finite-Difference Schemes for Long-Time Integration, J. Comp. Physics, 114, 265-279.
9. Hariharan, S. I., Ping, Y., and Scott, J. R., (1992) Time Domain Numerical Calculations of Unsteady Vortical Flows about a Flat Plate Airfoil, Journal of Computational Physics, 101, 2, pp. 419-430.
10. Harten, A., Enquist, A., Osher, S., and Chakravarthy, S. (1987) Uniformly High Order Accuracy Essentially Non-oscillatory Schemes III', J. Comp. Phys., 71, 231-323.
11. Hindman, R. G., (1982) Generalized Coordinate Forms of Governing Fluid Equations and Associated Geometrically Induced Errors, AIAA Journal, 20, 10, p. 1359-1367.
12. Hixon, R., Shih, S.-H., and Mankbadi, R. R. (1995) Evaluation of Boundary Conditions for Computational Aeroacoustics, AIAA Journal, 33, 11, pp. 2006-2012.
13. Hixon, R. (1998a) Evaluation of a High-Accuracy MacCormack-Type Scheme Using Benchmark Problems, J. Comp. Acoust., 6, 291-305.
14. Hixon, R.(1998b) A New Class of Compact Schemes, AIAA Paper 98-0367, Reno, Nevada. Accepted for publication in Journal of Computational Physics, 2001.

15. Hixon, R., Shih, S.-H., Dong, T., and Mankbadi, R. R. (1998) Evaluation of Generalized Curvilinear Coordinate Transformations Applied to High-Accuracy Finite-Difference Schemes, AIAA Paper 98-0370, Reno, Nevada.

16. Hixon, R., Shih, S.-H., Mankbadi, R. R., and Scott, J. R., (1998) Time Domain Solution of the Airfoil Gust Problem Using a High-Order Compact Scheme, AIAA Paper 98-3241, Cleveland, OH.

17. Hixon, R. and Turkel, E.(1998) High-Accuracy Compact MacCormack-Type Schemes for Computational Aeroacoustics, AIAA Paper 98-0365, Reno, Nevada.

18. Hixon, R., Shih, S.-H., and Mankbadi, R. R. (1999) Numerical Treatment of Cylindrical Coordinate Centerline Singularities, AIAA Paper 99-2391, Los Angeles, CA. Accepted for publication in International Journal of Computational Fluid Dynamics, 2001.

19. Hixon, R. (1999) Curvilinear Wall Boundary Conditions for Computational Aeroacoustics, AIAA Paper 99-2395, Los Angeles, CA.

20. Hixon, R. and Mankbadi, R. R., (2000) Validation of a High-Order Prefactored Compact Scheme on Nonlinear Flows with Complex Geometries, to appear in Proceedings of the Third CAA Workshop on Benchmark Problems.

21. Hixon, R., Shih, S.-H., and Mankbadi, R. R. (2000) Evaluation of Boundary Conditions for the Gust-Cascade Problem, Journal of Propulsion and Power, 16, 1, pp. 72- 78.

22. Hixon, R (2000a) Numerically Consistent Strong Conservation Grid Motion for Finite-Difference Schemes, AIAA Journal, 38, 9, p. 1586-1593.

23. Hixon, R. (2000b) Nonlinear Comparison of High-Order and Optimized Finite-Difference Schemes, International Journal of Computational Fluid Dynamics, 13, 3, p. 259-277.

24. Hixon, R., Mankbadi, R. R., and Scott, J. R. (2001) Validation of a High-Order Prefactored Compact Code on Nonlinear Flows with Complex Geometries, AIAA Paper 2001-1103, Reno, Nevada.

25. Hu, F. Q., Hussaini, M. Y., and Manthey, J. (1996) Low-Dissipation and -Dispersion Runge-Kutta Schemes for Computational Acoustics, J. Comp. Phys., 124, 121-133.

26. Kennedy, C. A. and Carpenter, M. H. (1994) Several New Numerical Methods for Compressible Shear-Layer Simulations, Appl. Num. Math., 14, 397-433.

27. Lele, S. K. (1992) Compact Finite Difference Schemes with Spectral-like Resolution, J. Comp. Phys., 103, 16-42.

28. Lele, S. K. (1997) Computational Aeroacoustics: A Review, AIAA Paper 97-0018, Reno, Nevada.

29. Lockard, D. P. and Morris, P. J. (1996) A Parallel Implementation of a Computational Aeroacoustic Algorithm for Airfoil Noise, AIAA Paper 96-1754, Reno, Nevada.

30. Lockard, D. P. and Morris, P. J. (1997) The Radiated Noise from Airfoils in Realistic Mean Flows, AIAA Paper 97-0286, Reno, Nevada.

31. Mankbadi, R. R., Hixon, R., and Povinelli, L. A., (2000) Very Large Eddy Simulations of Jet Noise, AIAA Paper 2000-2008, Lahaina, Hawaii.

32. Mankbadi, R. R., Shih, S.-H, Hixon, R., and Povinelli, L. A. (1999) Large-Scale Simulations of Nonlinear Effects in Jet Noise, Journal of Propulsion and Power, 14, 5.

33. Mankbadi, R. R., Shih, S.-H., Hixon, R., Stuart, J. T., and Povinelli, L. A., (1998) A Surface-Integral Formulation for Jet Noise Prediction Based on the Pressure Signal Alone, Journal of Computational Acoustics, 6, 3, pp. 307-320.

34. Mankbadi, R. R., Hixon, R., Shih, S.-H., and Povinelli, L. A. (1998) Linearized Euler Equations as a Tool in Jet Noise Prediction', AIAA Journal, 36, 2, pp. 140-147.

35. Meadows, K. R., Casper, J., and Caughey, D. A. (1993) A Numerical Investigation of Sound Amplification by a Shock Wave, FED-Vol. 147, Computational Aero- and Hydro-Acoustics, ASME, 47-52.

36. Mohseni, K., Colonius, T., and Freund, J. (2001) On the Role of Nonlinearity in Mach Wave Radiation in a Mach =1.92 Jet, AIAA Paper 2001-0377, Reno, Nevada.

37. Program Development Corporation (1996) GridPro™/az3000, White Plains, NY.

38. Scott, J. R. and Atassi, H. M. (1990) Numerical Solutions of the Linearized Euler Equations for Unsteady Vortical Flows Around Lifting Airfoils, AIAA Paper 90-0694, Reno, Nevada.

39. Scott, J. R., and Atassi, H. M. (1995) A Finite-Difference, Frequency-Domain Numerical Scheme for the Solution of the Gust-Response Problem, Journal of Computational Physics, 119, p. 75-93.

40. Shen, H. and Tam, C. K. W. (2001) Three-Dimensional Numerical Simulation of the Jet Screech Phenomenon, AIAA Paper 2001-0820, Reno, Nevada.

41. Shih, S.-H., Hixon, R., Povinelli, L. A., and Mankbadi, R. R. (1998) Large-Scale Simulation of Supersonic Jet Noise, AIAA Paper 98-3014, Albuquerque.

42. Stanescu, D. and Habashi, W. G. (1998) 2N-Storage Low Dissipation and Dispersion Runge- Kutta Schemes for Computational Acoustics, J. Comp. Phys., 143, 674-681.

43. Tam, C. K. W. and Shen, H. (1993) Direct Computation of Nonlinear Acoustic Pulses Using High Order Finite Difference Schemes, AIAA Paper 93-4325, 15th AIAA Aeroacoustics Conference, Long Beach, CA.

44. Tam, C. K. W. and Webb, J. C. (1993) Dispersion-Relation-Preserving Finite Difference Schemes for Computational Acoustics, J. Comp. Phys.,. 107, 262-281.

45. Tam, C. K. W., (1995) Computational Aeroacoustics: Issues and Methods, AIAA J., 33, pp. 1788-1796.

46. Thomas, P. D. and Lombard, C. K. (1979) Geometric Conservation Law and Its Application to Flow Computations on Moving Grids, AIAA Journal, 17, 10, p. 1030-1037.

47. Visbal, M. R. and Gaitonde, D. V. (1999) Computation of Aeroacoustic Fields on General Geometries using Compact Differencing and Filtering Schemes, AIAA Paper 99-3706, Norfolk, VA.

48. Whitham, G. B. (1974) Linear and Nonlinear Waves, John Wiley and Sons, New York.

49. Zingg, D. W., Lomax, H., and Jurgens, H. M. (1993) An Optimized Finite-Difference Scheme for Wave Propagation Problems, AIAA Paper 93-0459, Reno, Nevada.

50. Zingg, D. Q., 'A Review of High-Order and Optimized Finite-Difference Methods for Simulating Linear Wave Phenomena', AIAA Paper 97-2088, Snowmass, Colorado.

Integral Methods for Jet AeroAcoustics

Anastasios S. Lyrintzis
Purdue University

NASA/CP—2001-211152

INTEGRAL METHODS FOR JET AEROACOUSTICS

Anastasios S. Lyrintzis
School of Aeronautics and Astronautics
Purdue University
West Lafayette, Indiana 47907



Methods of Acoustic Analysis

1. Lighthill's coustic analogy -need volume integrals

2. Kirchhoff's method -need surface integrals
   near-field: CFD - nonlinear
   far-field: acoustic - linear

3. Porous FW-H equation

School of Aeronautics and Astronautics
Purdue University, IN, U. S. A.



Kirchhoff's Method

Wave equation is valid outside a stationary surface:

$$4\pi\phi(\vec{x},t) = \int_S \frac{1}{r}\left[\frac{1}{a_\circ}\dot{\phi}\cos\theta - \frac{\partial\phi}{\partial n}\right]_{ret} dS + \int_S \frac{[\phi]_{ret}}{r^2}\, dS \qquad (1)$$

ϕ: some acoustic variable, e.g. p'

$a_\circ$: free stream sound speed

r is the distance from source to observer

$[\ ]_{ret}$ implies evaluation at the retarded time t-r/c

θ is the source emission angle $\cos\theta = \hat{r}\cdot\hat{n}$

$\hat{n}$ is the Kirchhoff surface normal vector

A dot indicates a source time derivative

School of Aeronautics and Astronautics
Purdue University, IN, U. S. A.



Porous FW-H equation

Define new variables U_i and

$$U_i = \frac{\rho u_i}{\rho_o} \tag{2}$$

and

$$L_i = P_{ij}\hat{n}_j + \rho u_i u_n \tag{3}$$

where subscript o implies ambient conditions, superscript $'$ implies disturbances.

School of Aeronautics and Astronautics
Purdue University, IN, U. S. A.



Porous FW-H equation (continued)

The integral expression for the porous FW-H equation can be written as

$$p'(\vec{x},\ t) = p'_T(\vec{x},\ t) + p'_L(\vec{x},\ t) + p'_Q(\vec{x},\ t) \qquad (4)$$

where

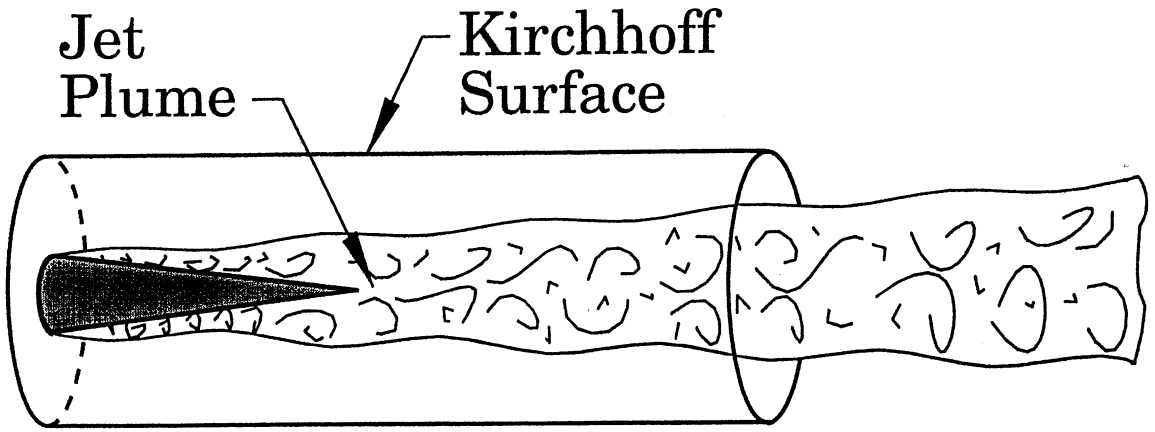
$$4\pi p'_T(\vec{x},\ t) = \int_S \left[\frac{\rho_o \dot{U}_n}{r}\right]_{ret} dS \qquad (5)$$

$$4\pi p'_L(\vec{x},\ t) = \frac{1}{a_o} \int_S \left[\frac{\dot{L}_r}{r}\right]_{ret} dS + \int_S \left[\frac{L_r}{r^2}\right]_{ret} dS \qquad (6)$$

School of Aeronautics and Astronautics
Purdue University, IN, U. S. A.

Jet Noise Predictions

- S Cannot surround entire source region in complex flows
  - Modified Kirchhoff formulation / porous FW-H
  - Mean flow refraction effects





Refraction Corrections

Pilon and Lyrintzis (1997): Simple geometric acoustics (Amiet, 1977) For an axisymmetric parallel shear flow to find a correction for the observer angle.

$$\frac{a_\circ}{\cos\vartheta_\circ} = U_s + \frac{a_\circ}{\cos\vartheta_s} \tag{7}$$

U_s is the velocity at the downstream end of the Kirchhoff surface, ϑ_s is the sound emission angle with respect to the jet axis, $\vartheta_\circ$ the emission angle in the ambient air.

School of Aeronautics and Astronautics
Purdue University, IN, U. S. A.

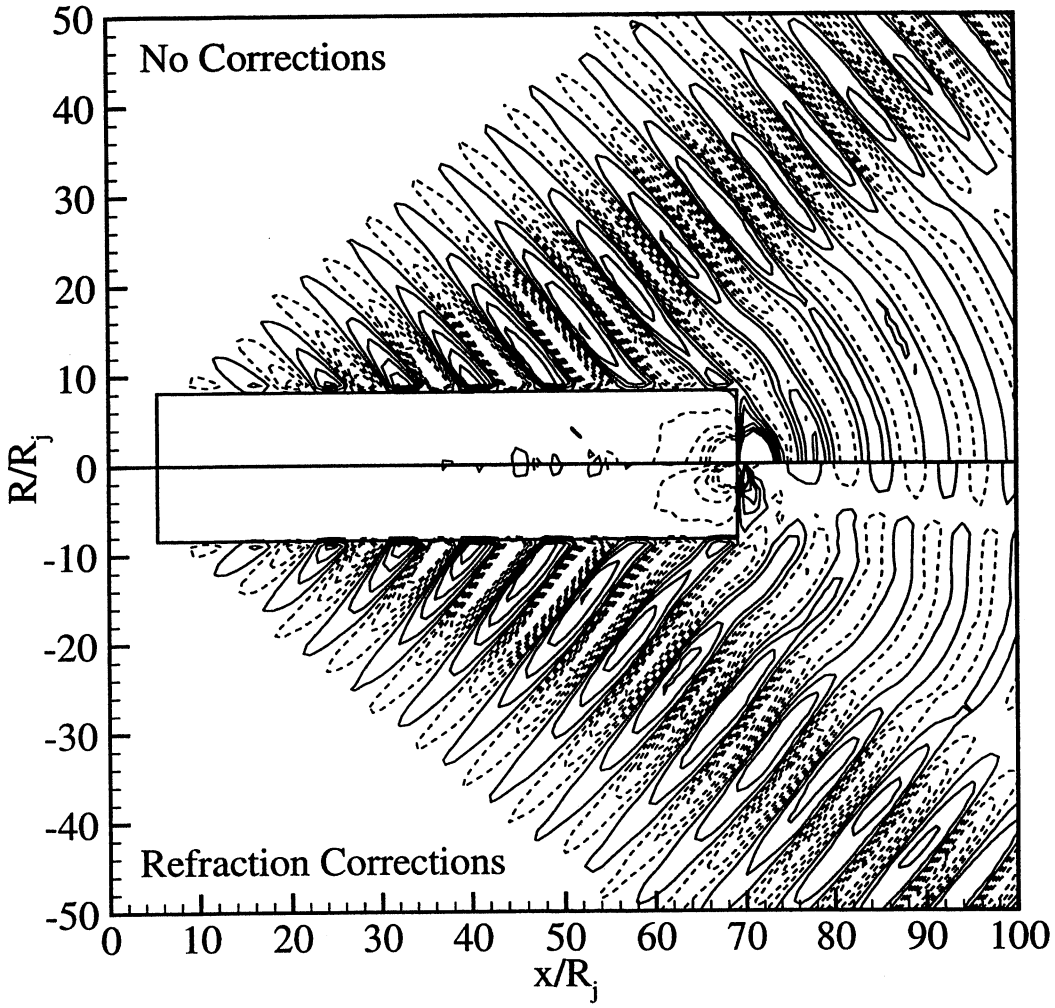


Figure 1. Instantaneous contours of $a_o^2\rho'/p_o$. $R > 0$: No refraction corrections. $R < 0$: Refraction corrections imposed.



Suggestions for Future Work

- Improve refraction corrections
- High frequency noise predictions

School of Aeronautics and Astronautics
Purdue University, IN, U. S. A.

Assessment of Jet Noise Theory/Prediction Methods

K. Viswanathan
Boeing

BOEING

NASA/CP—2001-211152

Assessment of Jet Noise Theory/Prediction Methods

K. Viswanathan

Jet Noise Workshop
Ohio Aerospace Institute, Cleveland
November 7–9, 2000

NASA/CP—2001-211152

BOEING

Background

- **Many variants of the Acoustic Analogy proposed**
- **Assess the various theories/prediction methods against a set of good quality data**
- **Some level of empiricism in *all* methods**
- **Groundrules**
  - ***fixed* set of empirical constants**
  - **same flow field solution**

  (Thies & Tam, AIAAJ, Vol. 34 (2), Feb. 1996)

NASA/CP—2001-211152

Theoretical approaches

- **Abbas Khavaran – MGBK**
  - **Lilley's equation**
  - **anisotropic turbulence (=0.6 for all predictions)**

    (many references, Khavaran, AIAA paper 2000–2059, 2000)

- **Phil Morris & Tony Pilon – JNOISE**
  - **Tester, Morfey & Szewczyk approach**
  - **separate source terms for quadrupole & dipole**

    (Pilon & Morris, AIAA paper 99–0076, 1999)

- **Chris Tam – only fine scale turbulence noise**
  - **predictions confined to lower inlet angles**

    (Tam & Auriault, AIAAJ, Vol. 37 (2), Feb. 1999)

NASA/CP—2001-211152

Test cases

- Mach number effect: M=0.5, 0.9, 1.5, Tr/Ta=1.0
- Hot subsonic jet: M=0.87, Tr/Ta=2.78
- Temperature effect: M=2, Tr/Ta=1.12, 2.72, 4.89
- Total of 7 test cases
- Data & predictions on a polar arc of 100 jet diameters

NASA/CP—2001-211152

Choice of x–axis

- 1/3–octave band frequencies in terms of band #;
  1/3–octave band SPL

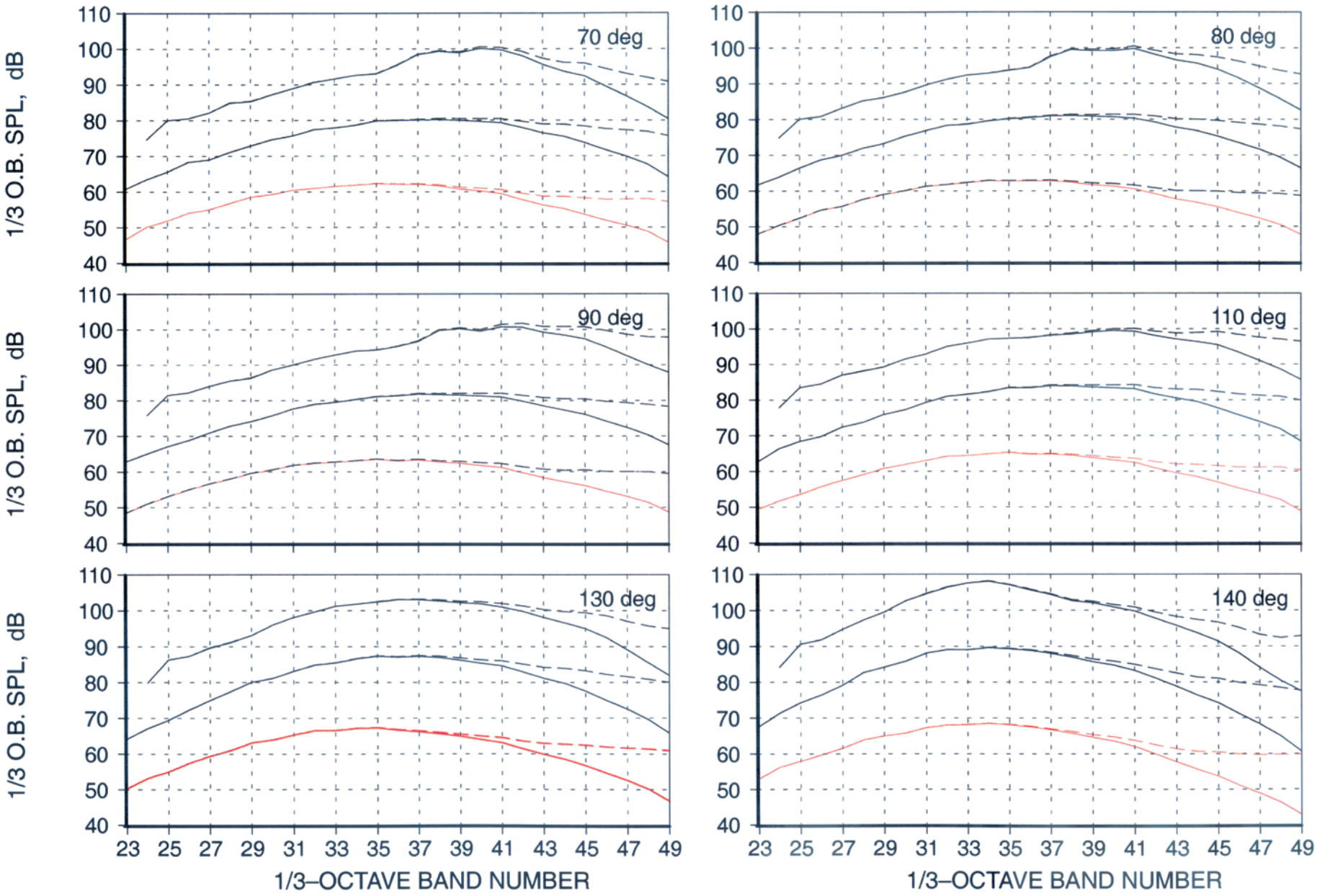
$$\text{band \#} = 10.0 * \log_{10}(f), \quad f \text{ in Hz.}$$

f (Hz.)	band #
100	20
1000	30
25000	44, etc.

- Strouhal # = f D/U; narrowband SPL

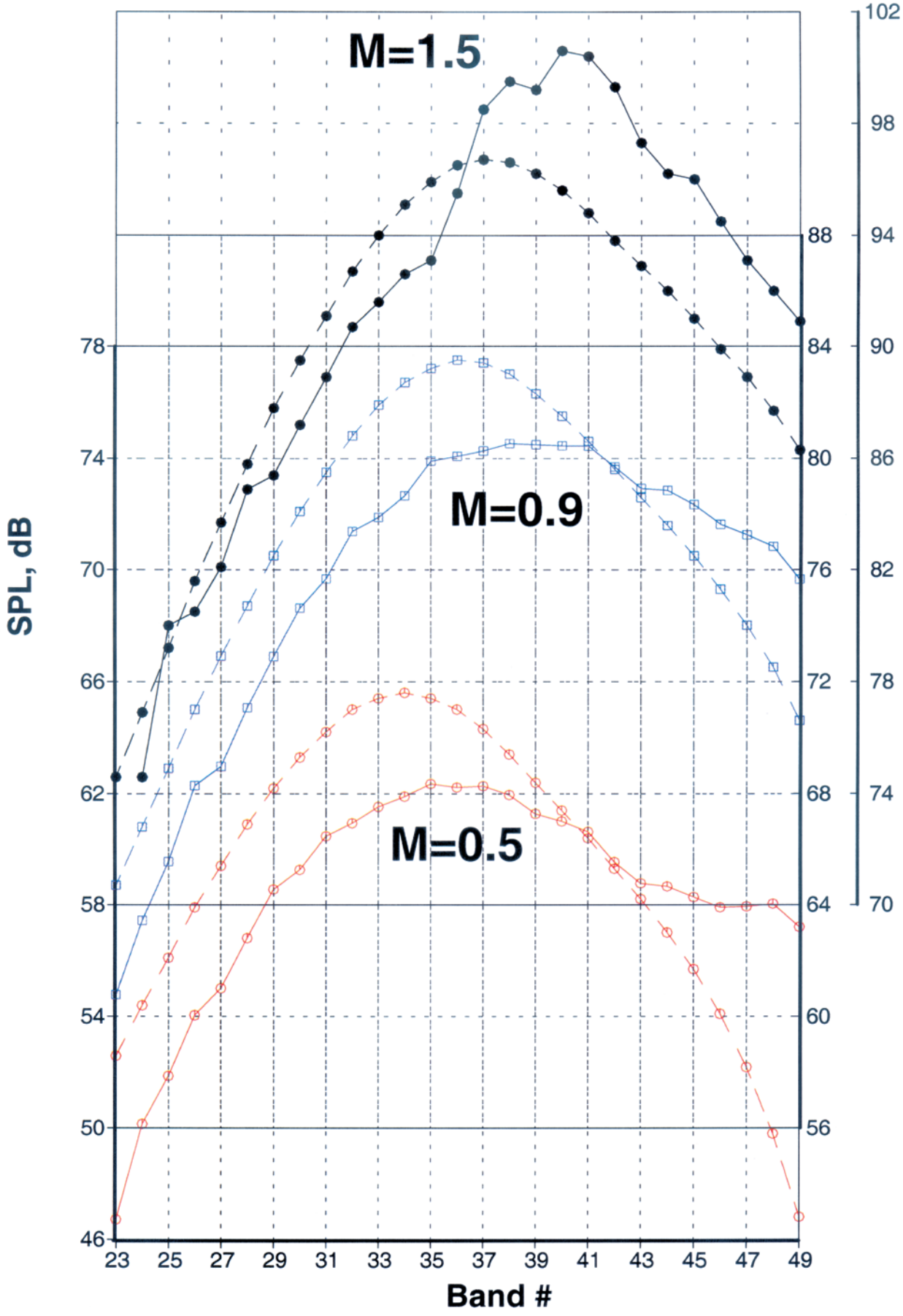
BOEING

Cold jet data: M=0.5, 0.9, 1.5

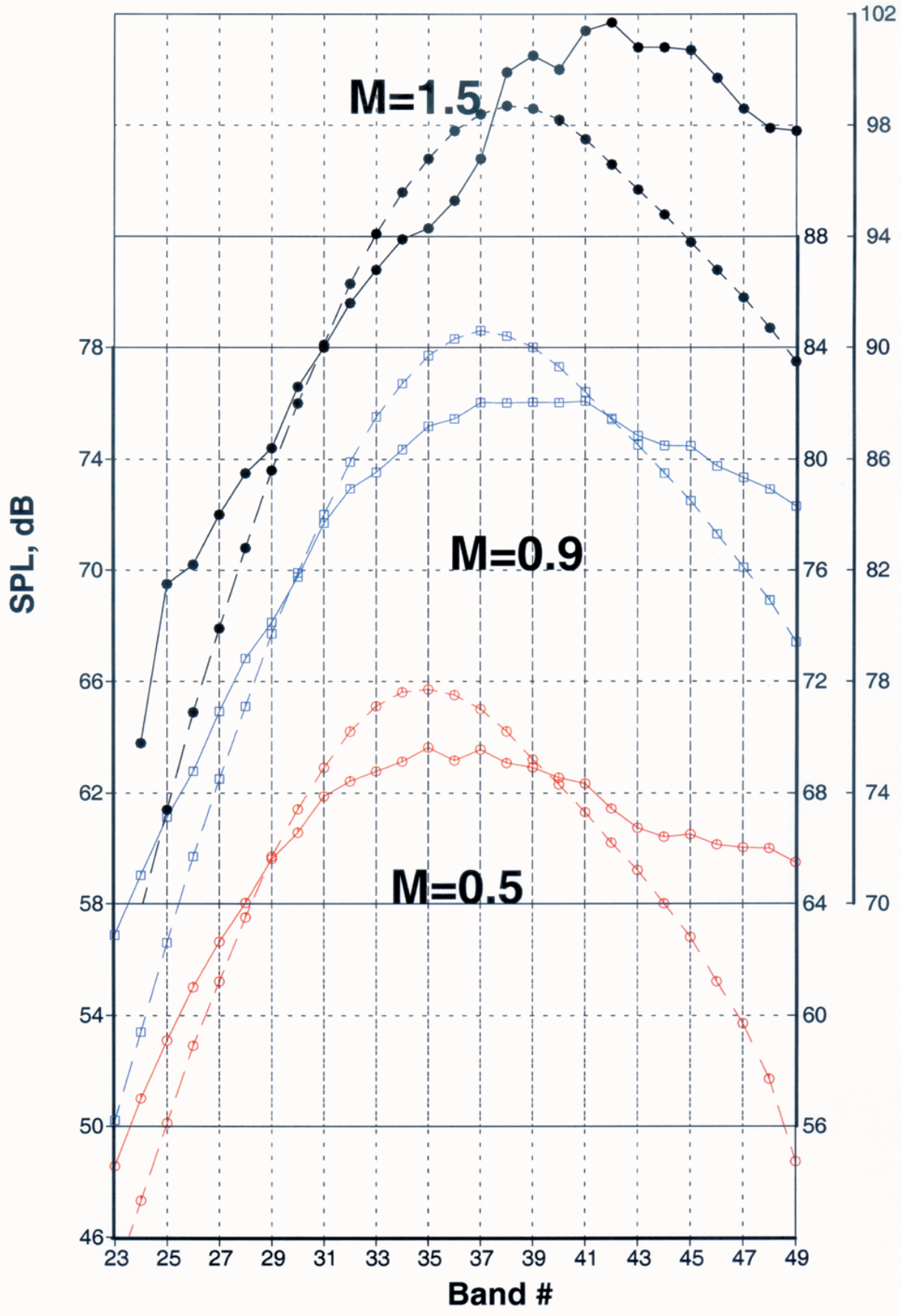


NASA/CP—2001-211152

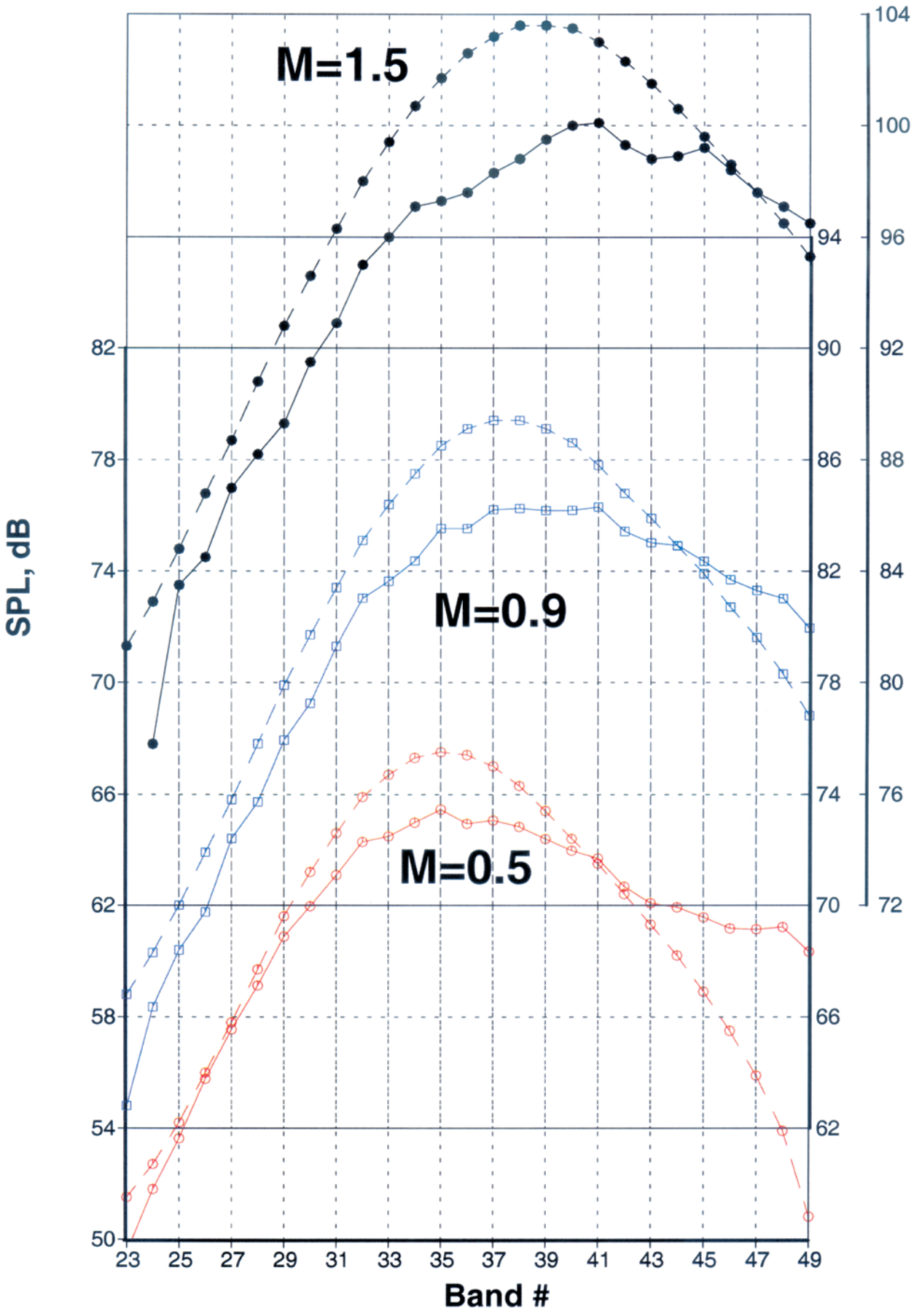
Cold jets: inlet angle = 70 degrees



Cold jets: inlet angle = 90 degrees

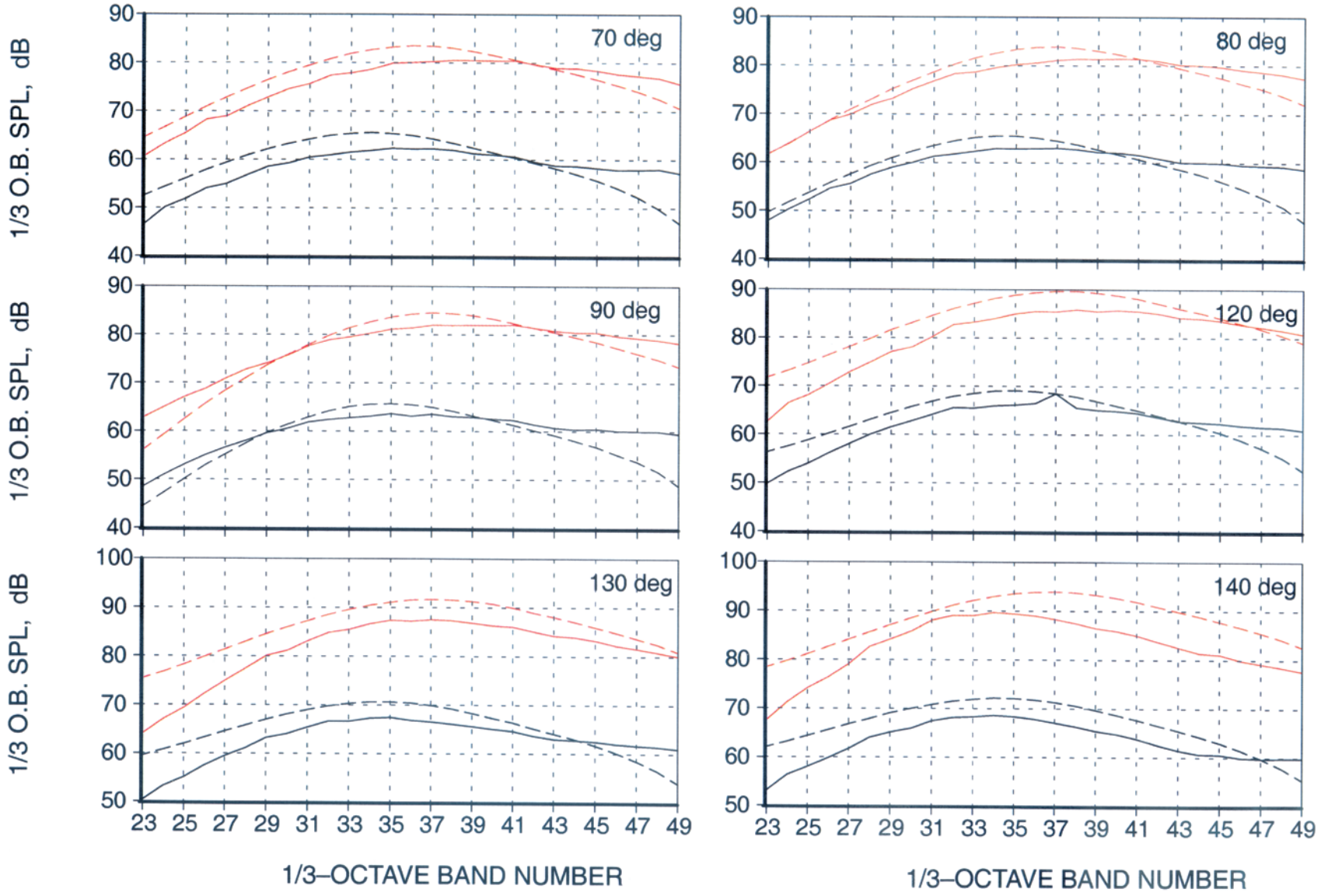


Cold jets: inlet angle = 110 degrees

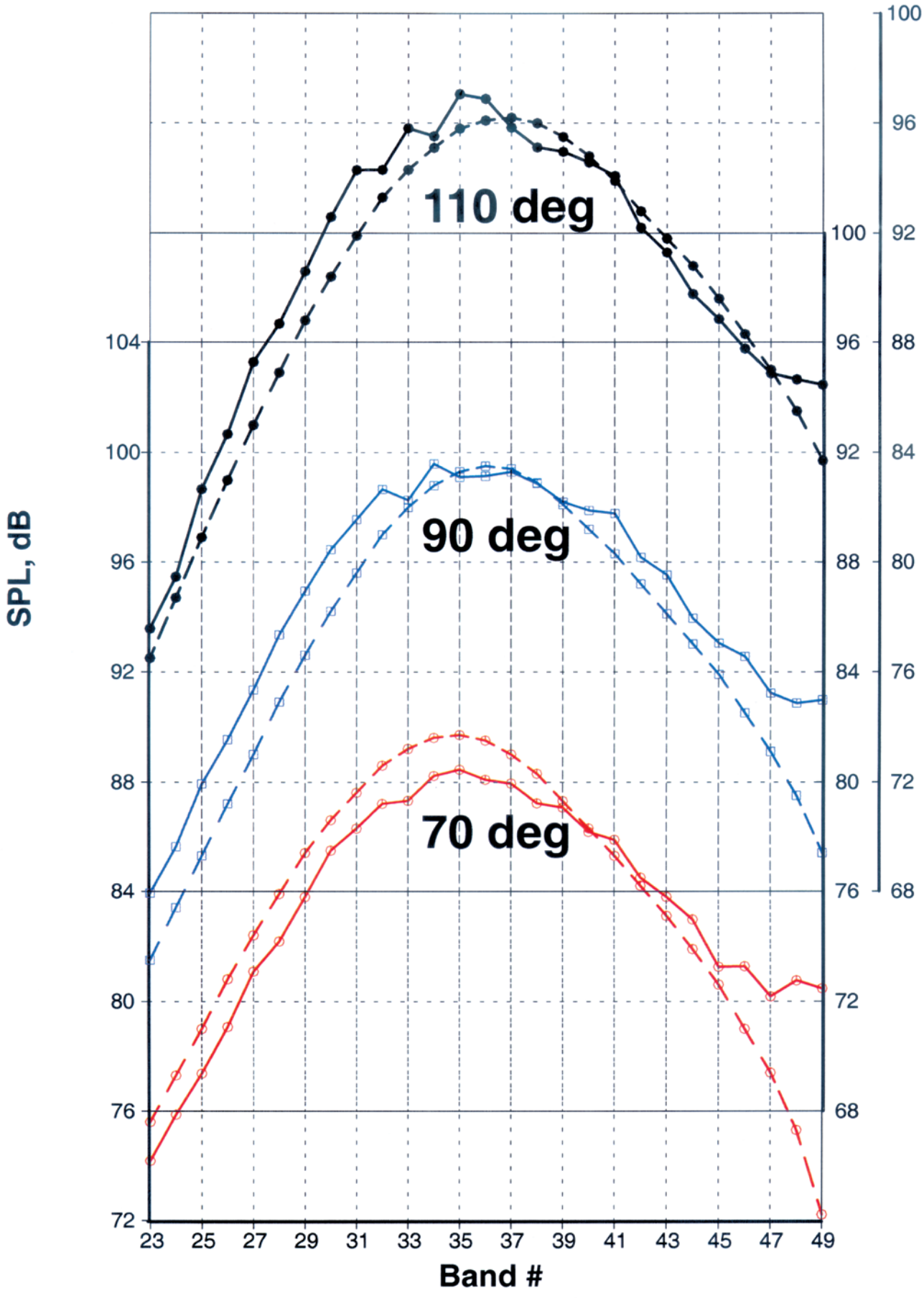


BOEING

Cold jets: data & prediction. M=0.5 & .9

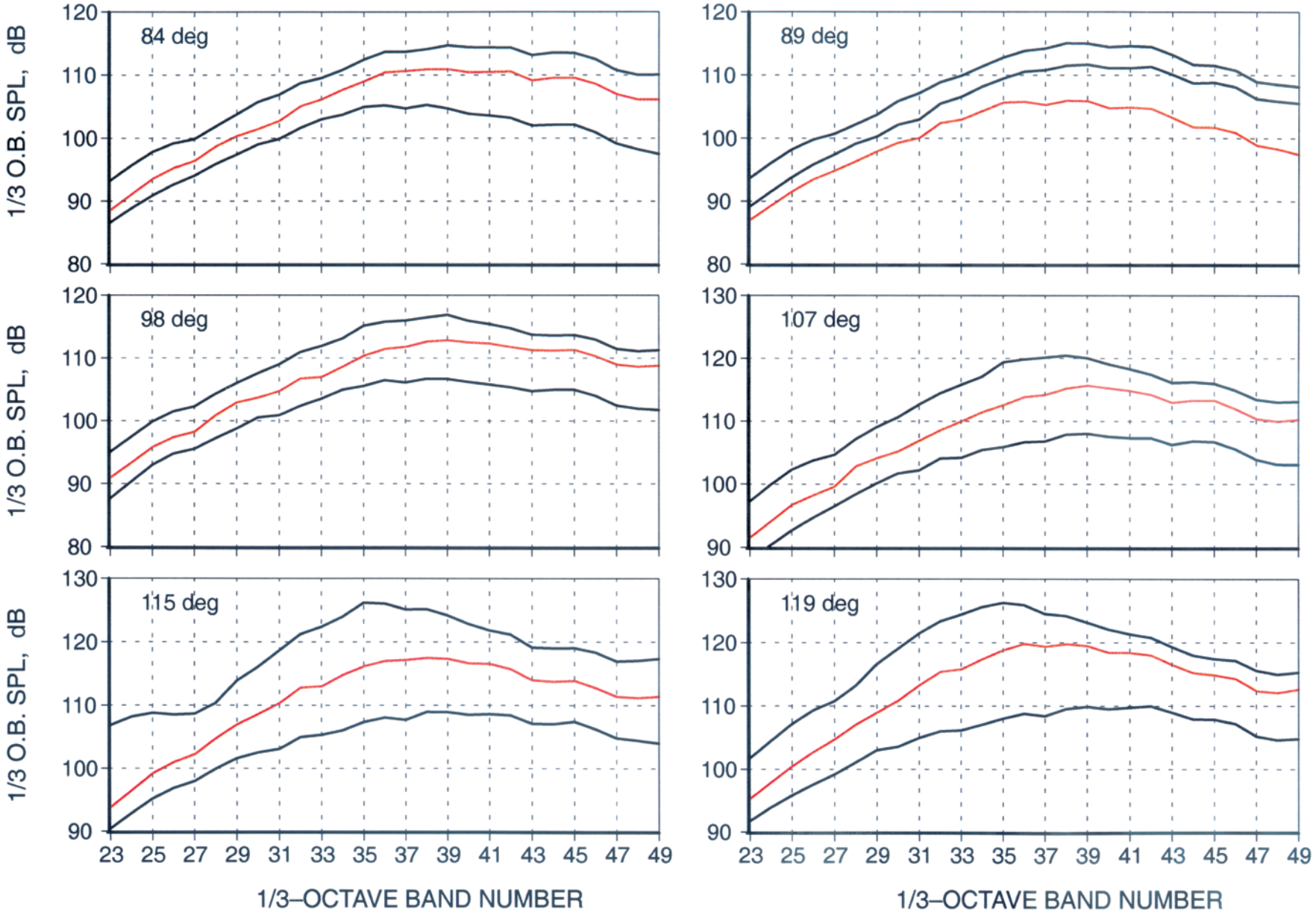


NASA/CP—2001-211152

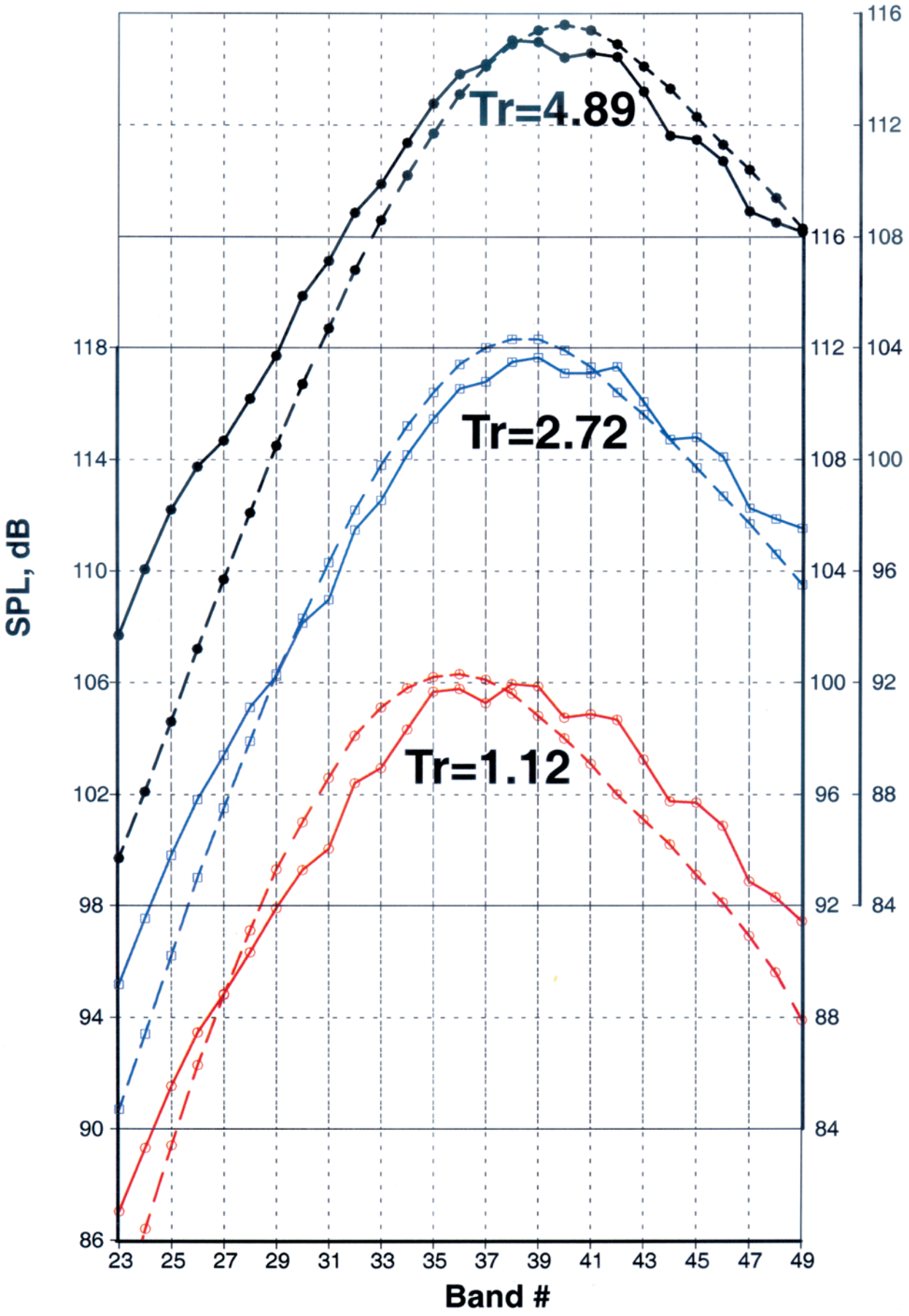

Hot jet: M=0.87, Tr=2.78
110 deg
90 deg
70 deg
SPL, dB
Band #
104
100
96
92
88
84
80
76
72
100
96
92
88
84
80
76
72
68
23
25
27
29
31
33
35
37
39
41
43
45
47
49

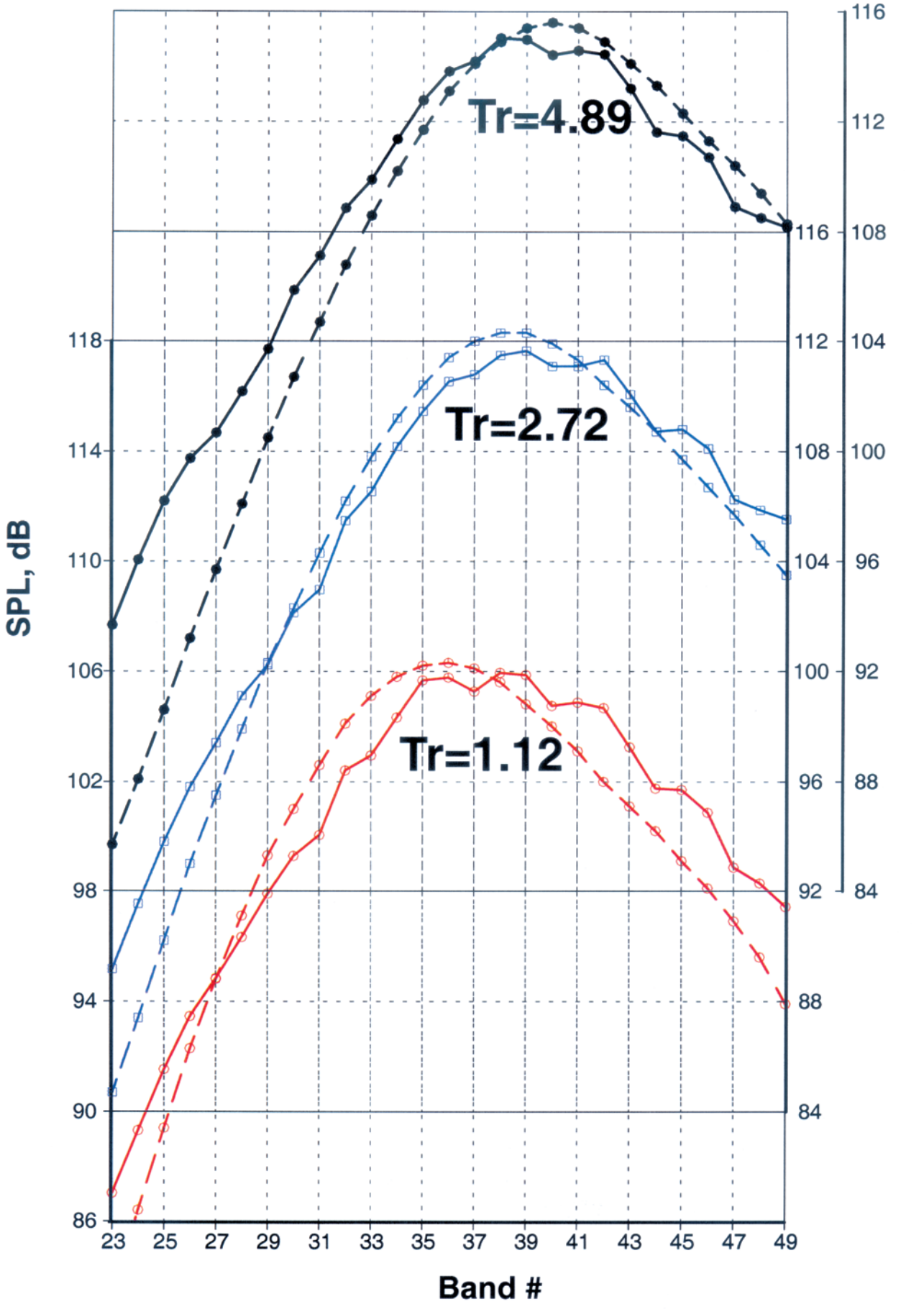
BOEING

Temperature effect, M=2: Tr=1.12, 2.72, 4.89

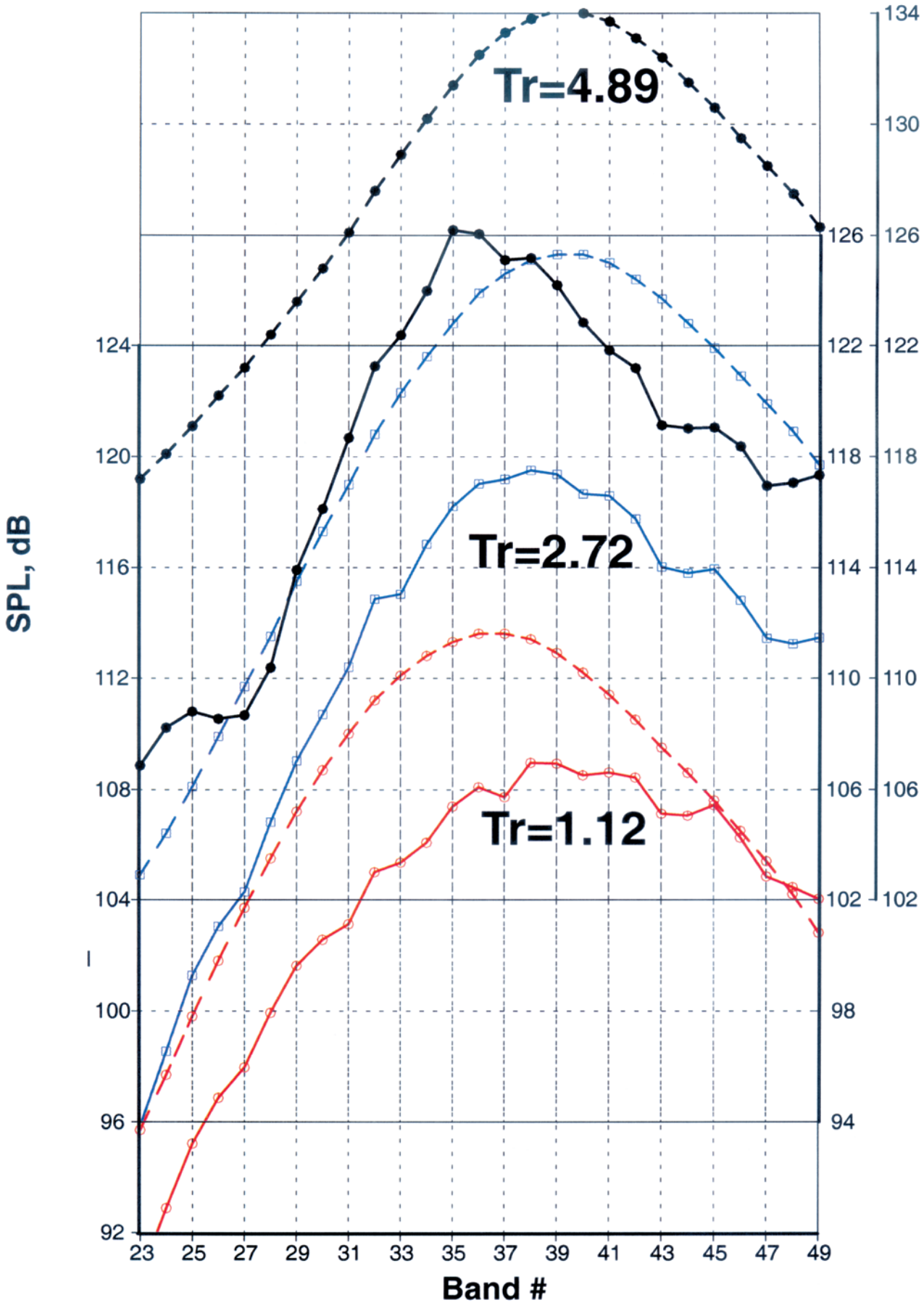


Temperature effect, M=2 jet: 89 degrees



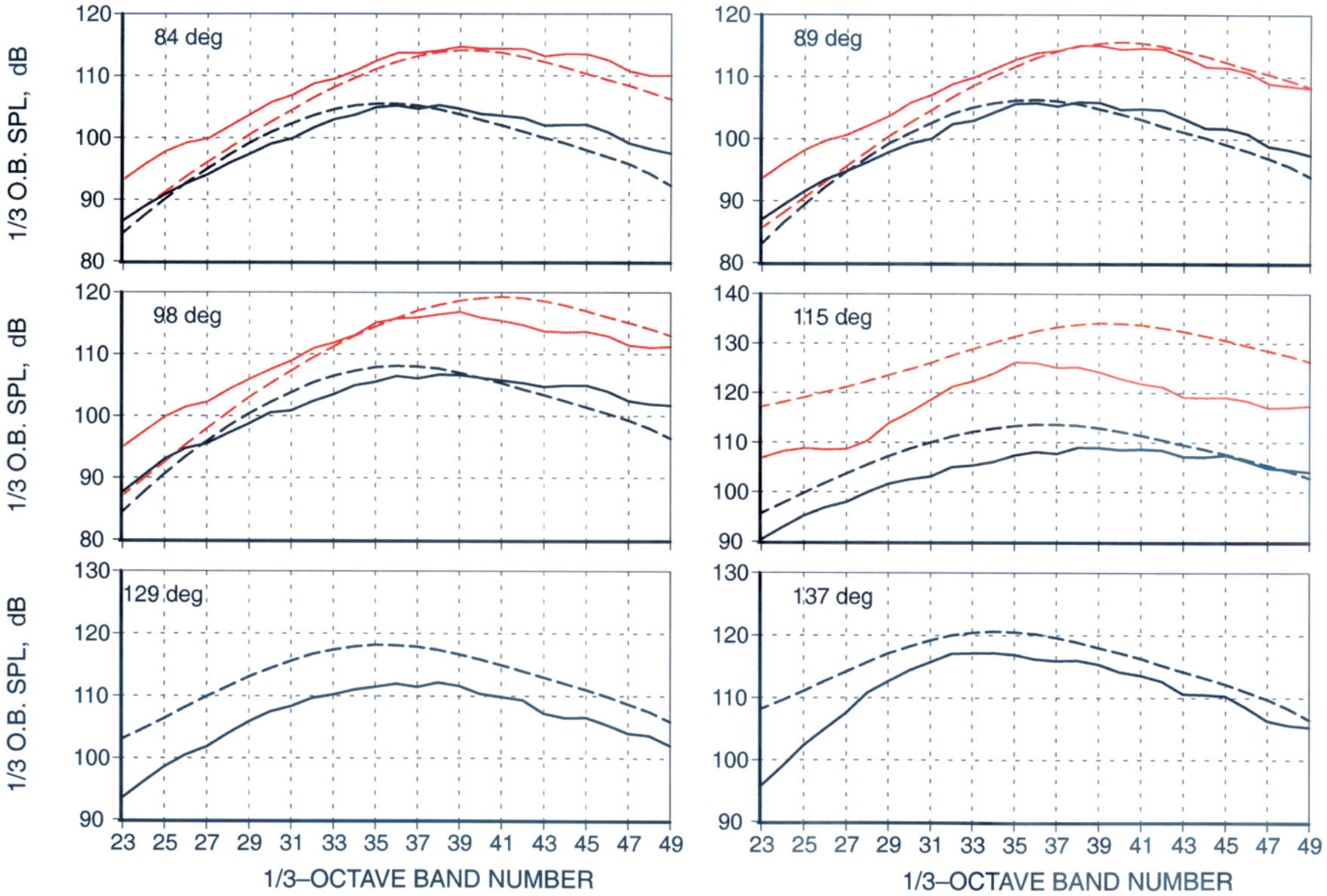

Temperature effect, M=2 jet: 98 degrees
Tr=4.89
Tr=2.72
Tr=1.12
SPL, dB
Band #
116
112
108
104
100
96
92
88
84
86
90
94
98
102
106
110
114
118
23
25
27
29
31
33
35
37
39
41
43
45
47
49

Temperature effect, M=2 jet: 115 degrees



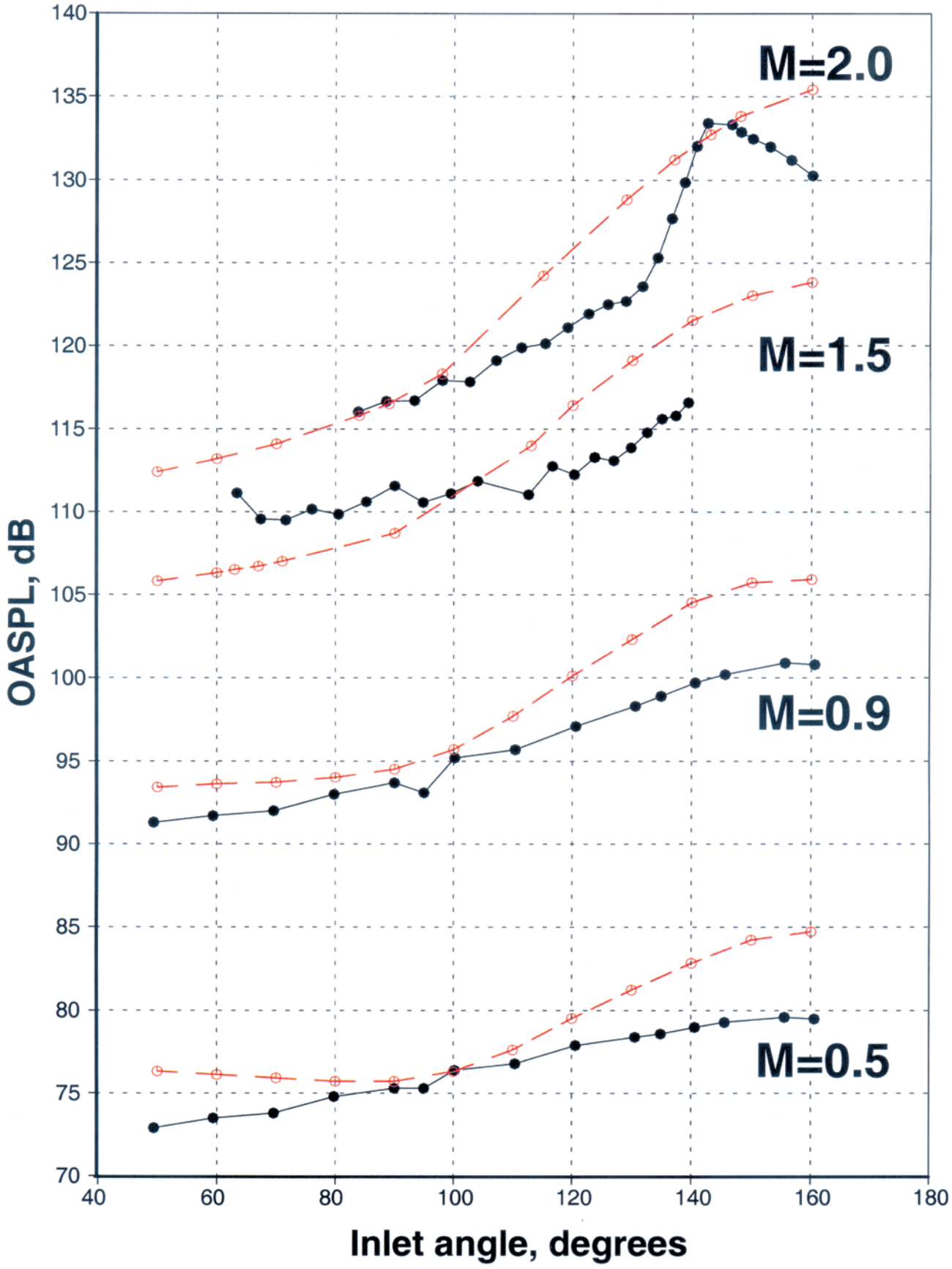
BOEING

M=2 jet: data & prediction. Tr=1.12, 4.89

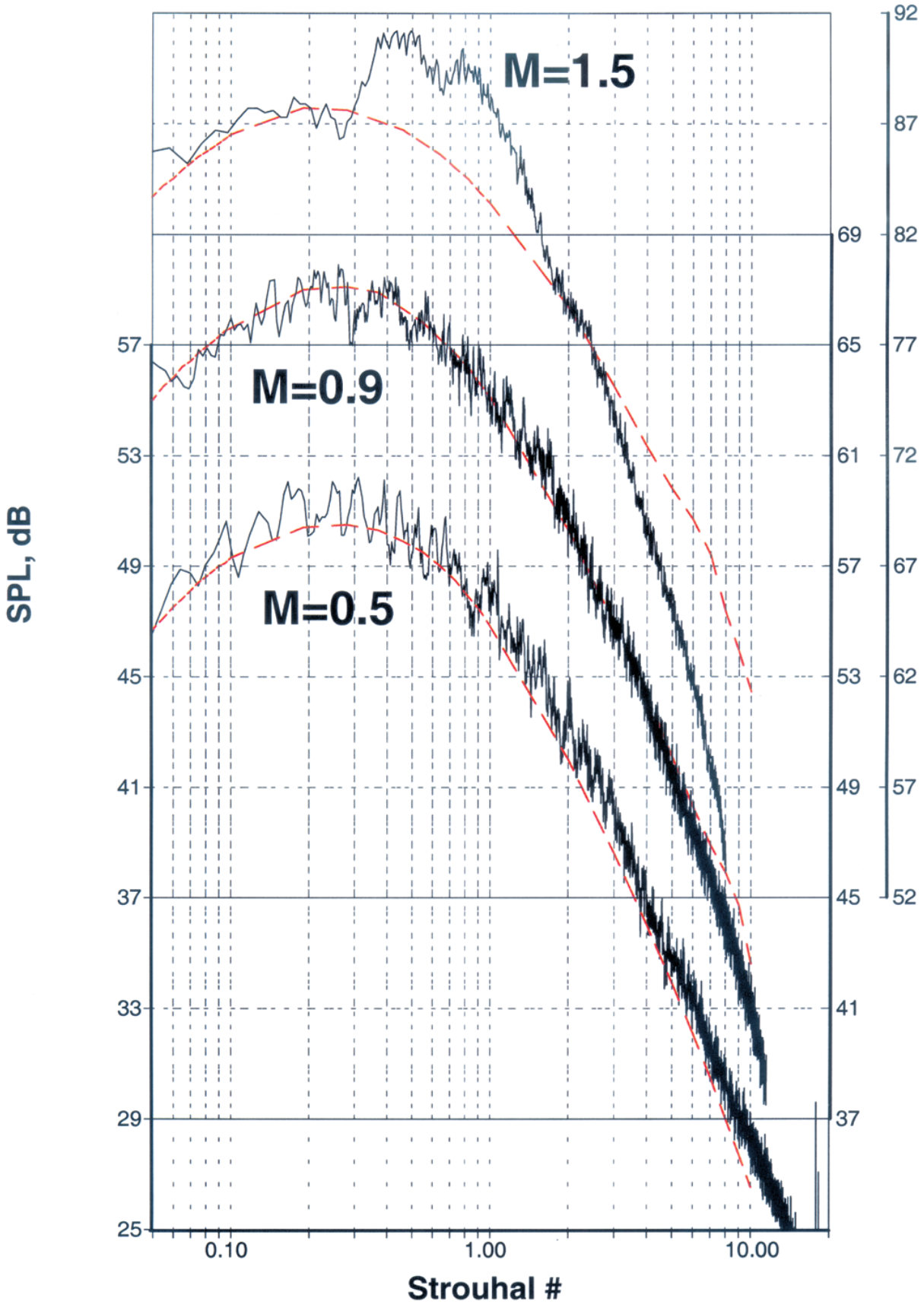


OASPL directivity: cold jets

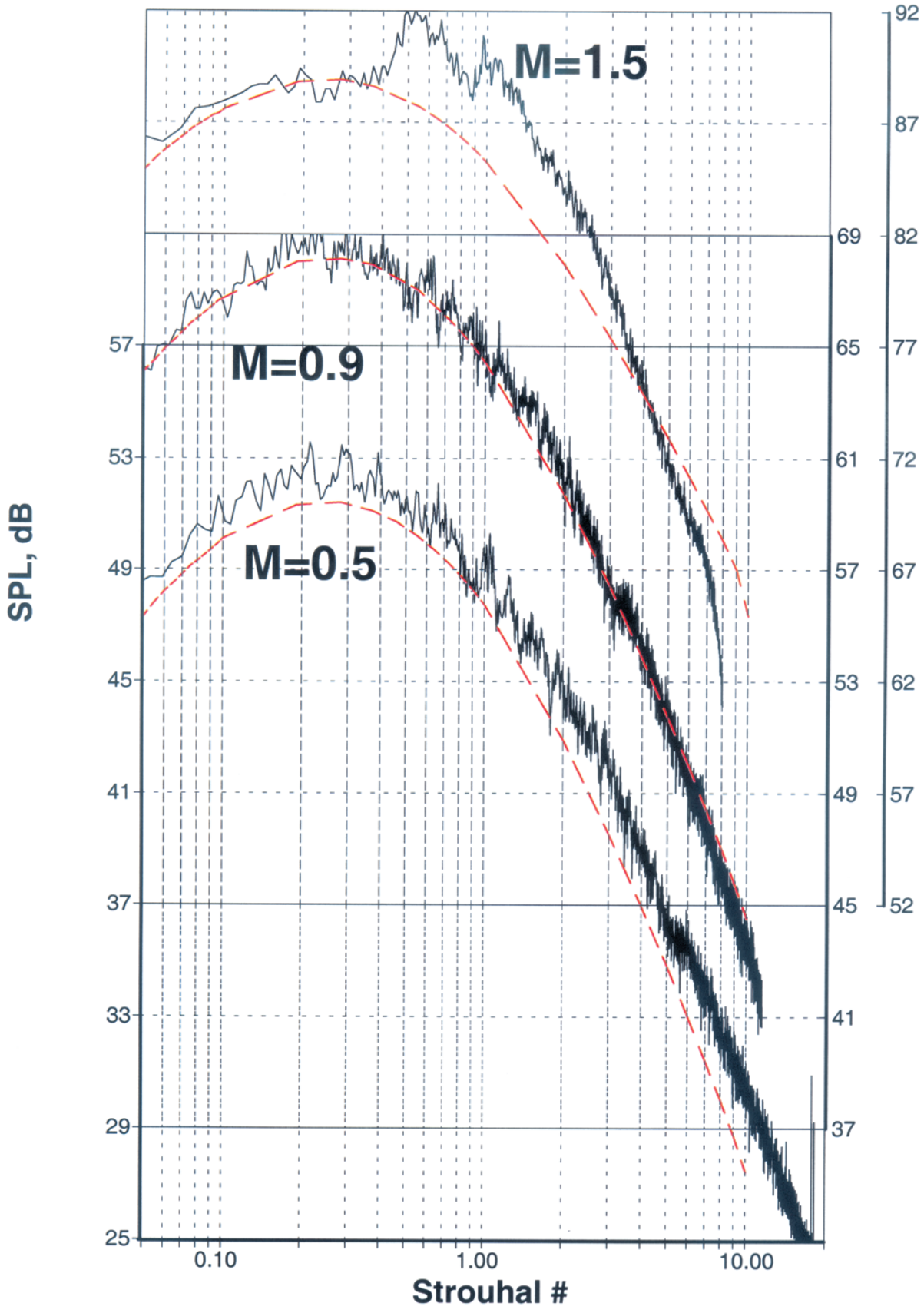
black: data; red: predictions

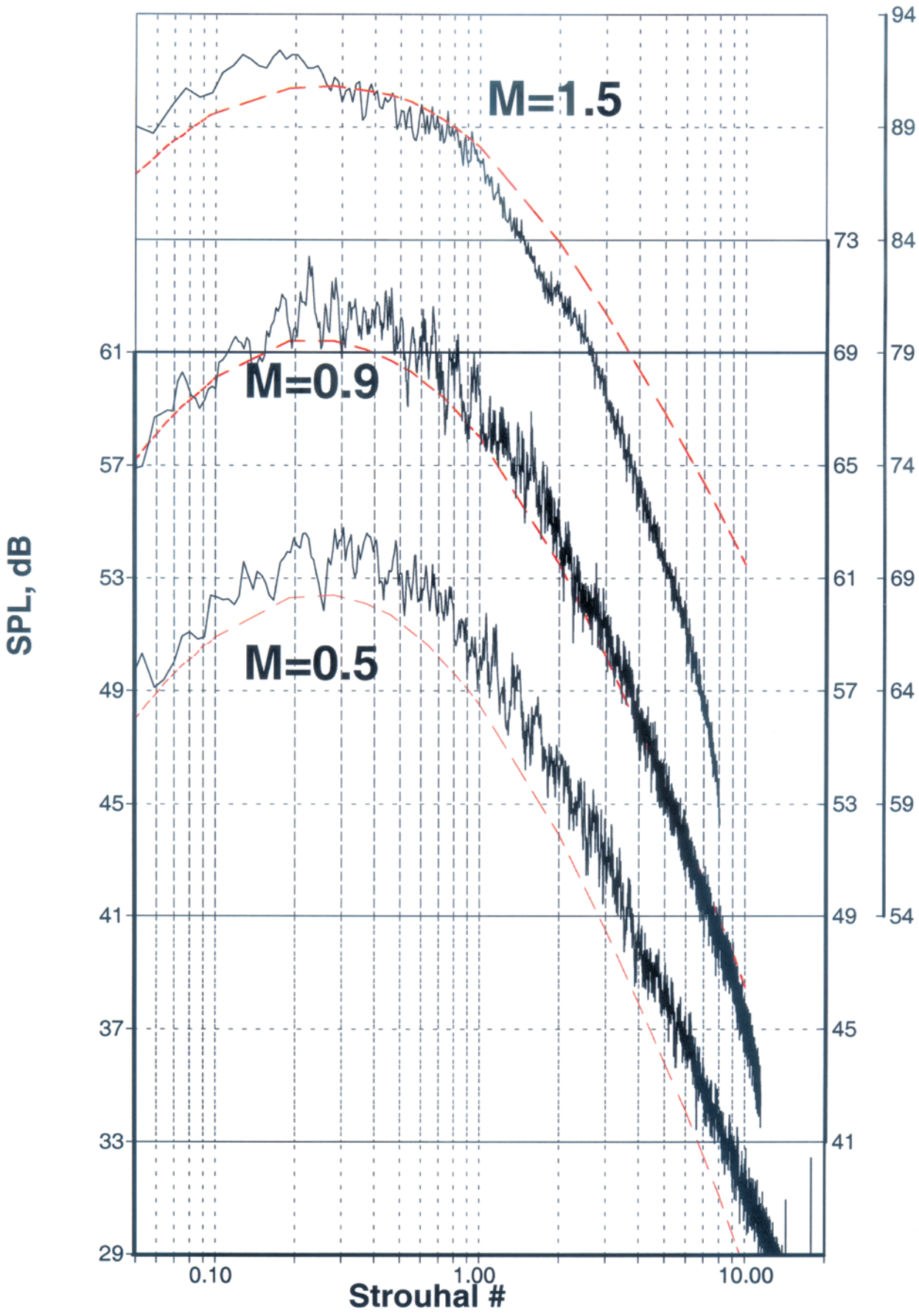


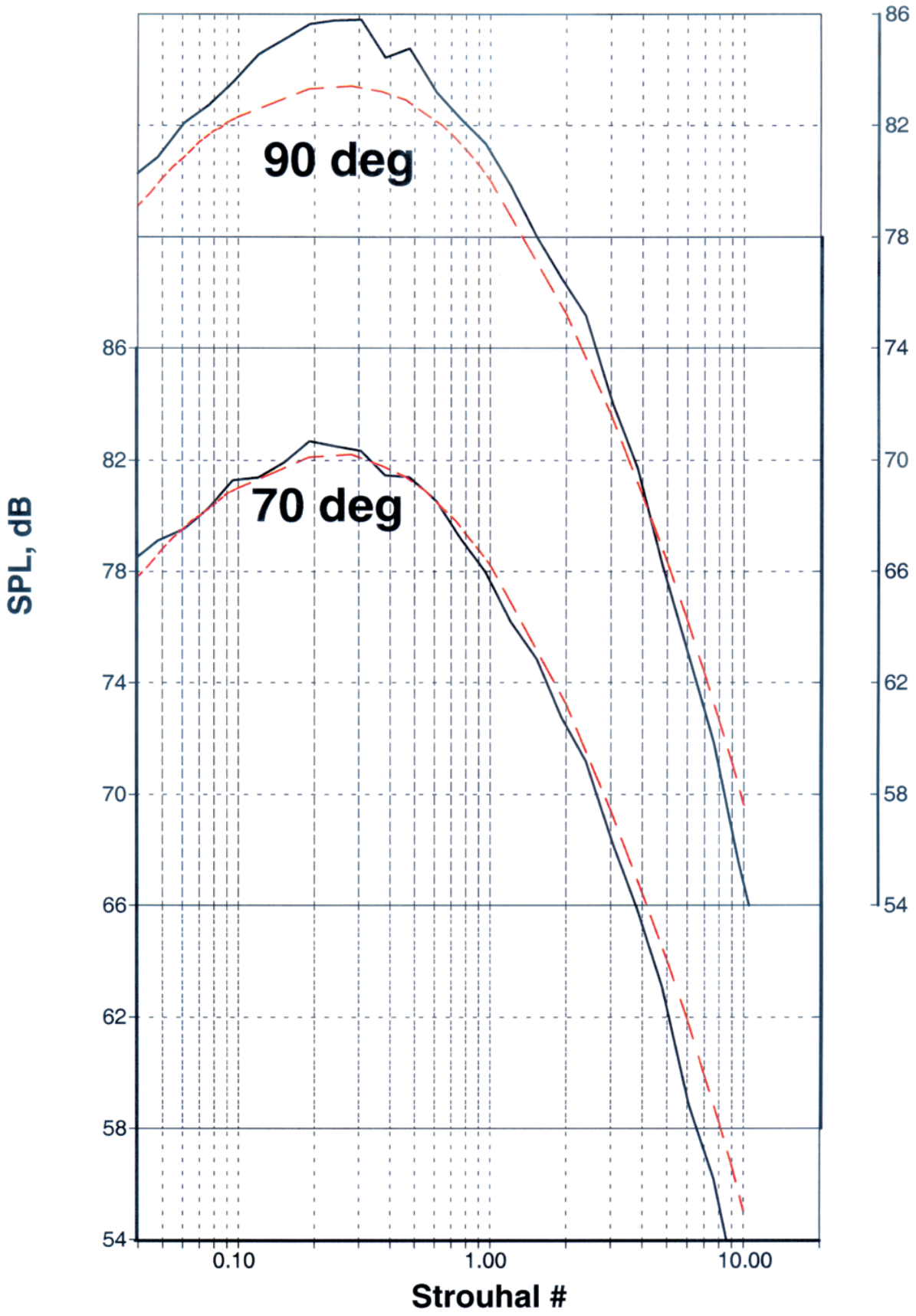
Cold jets: inlet angle = 70 degrees



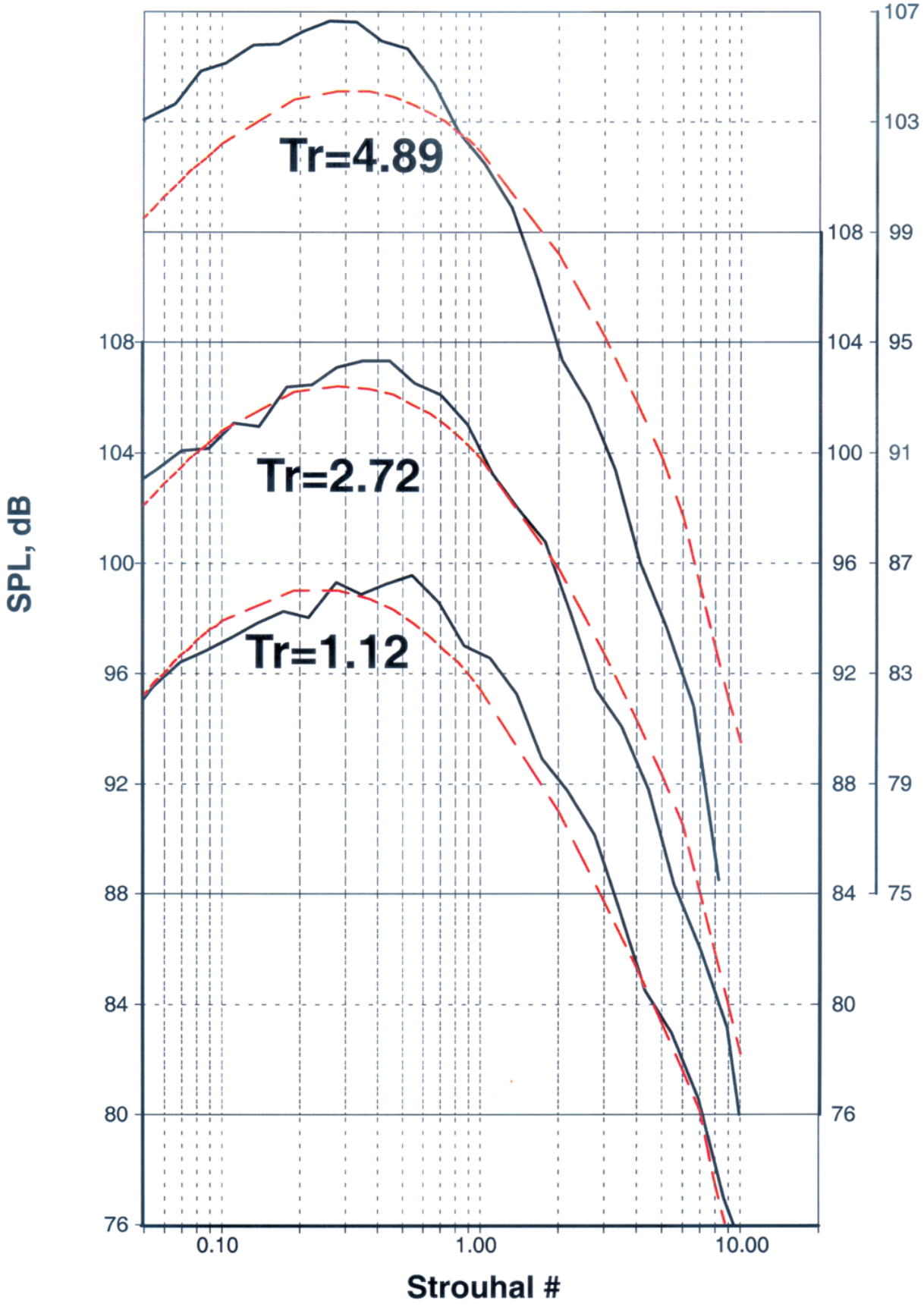
Cold jets: inlet angle = 90 degrees



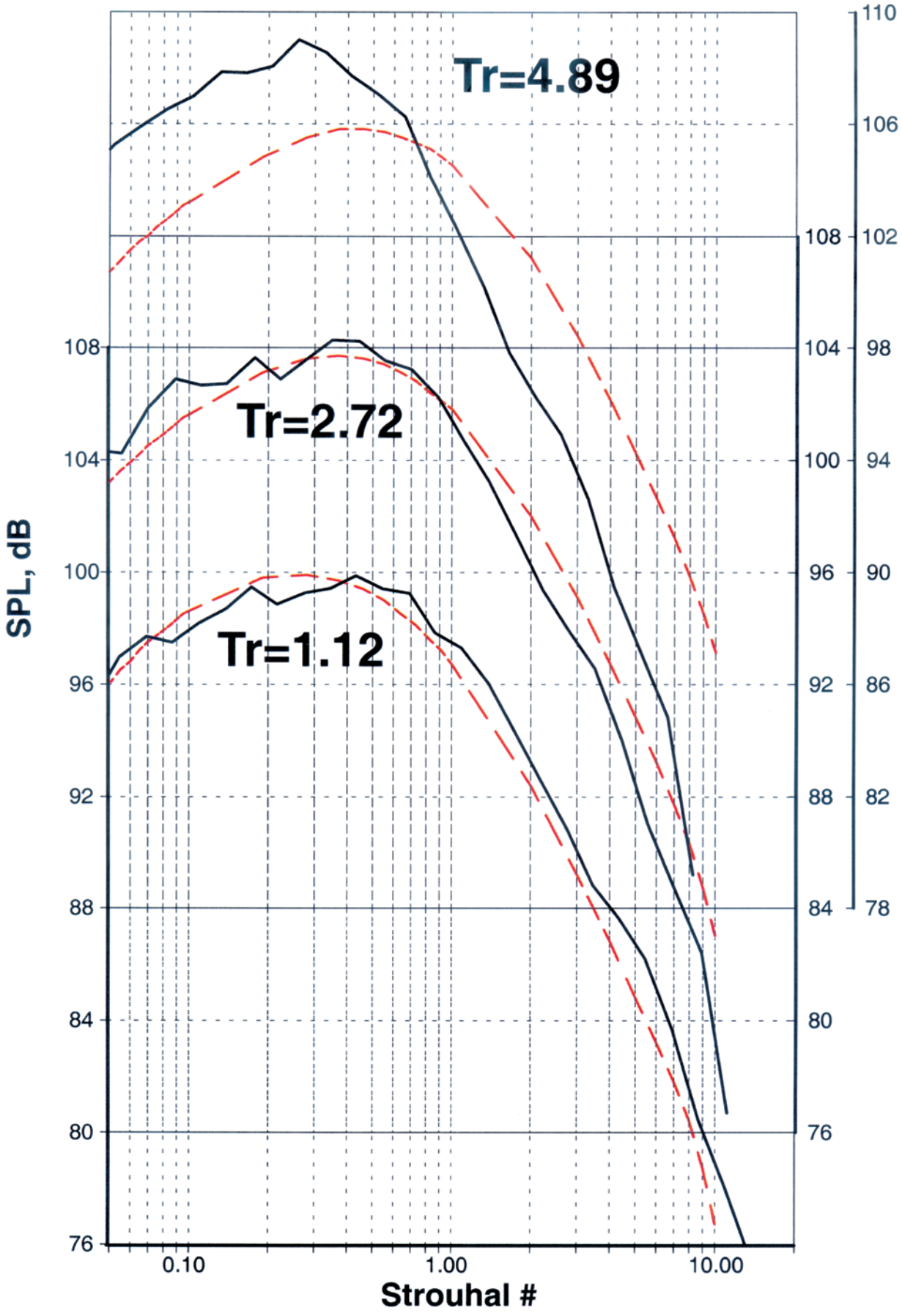

Cold jets: inlet angle = 110 degrees
M=1.5
M=0.9
M=0.5
SPL, dB
Strouhal #
0.10
1.00
10.00
29
33
37
41
45
49
53
57
61
73
69
65
61
57
53
49
45
41
94
89
84
79
74
69
64
59
54


Hot jet: M=0.87, Tr=2.78
90 deg
70 deg
SPL, dB
Strouhal #
0.10
1.00
10.00
86
82
78
74
70
66
62
58
54

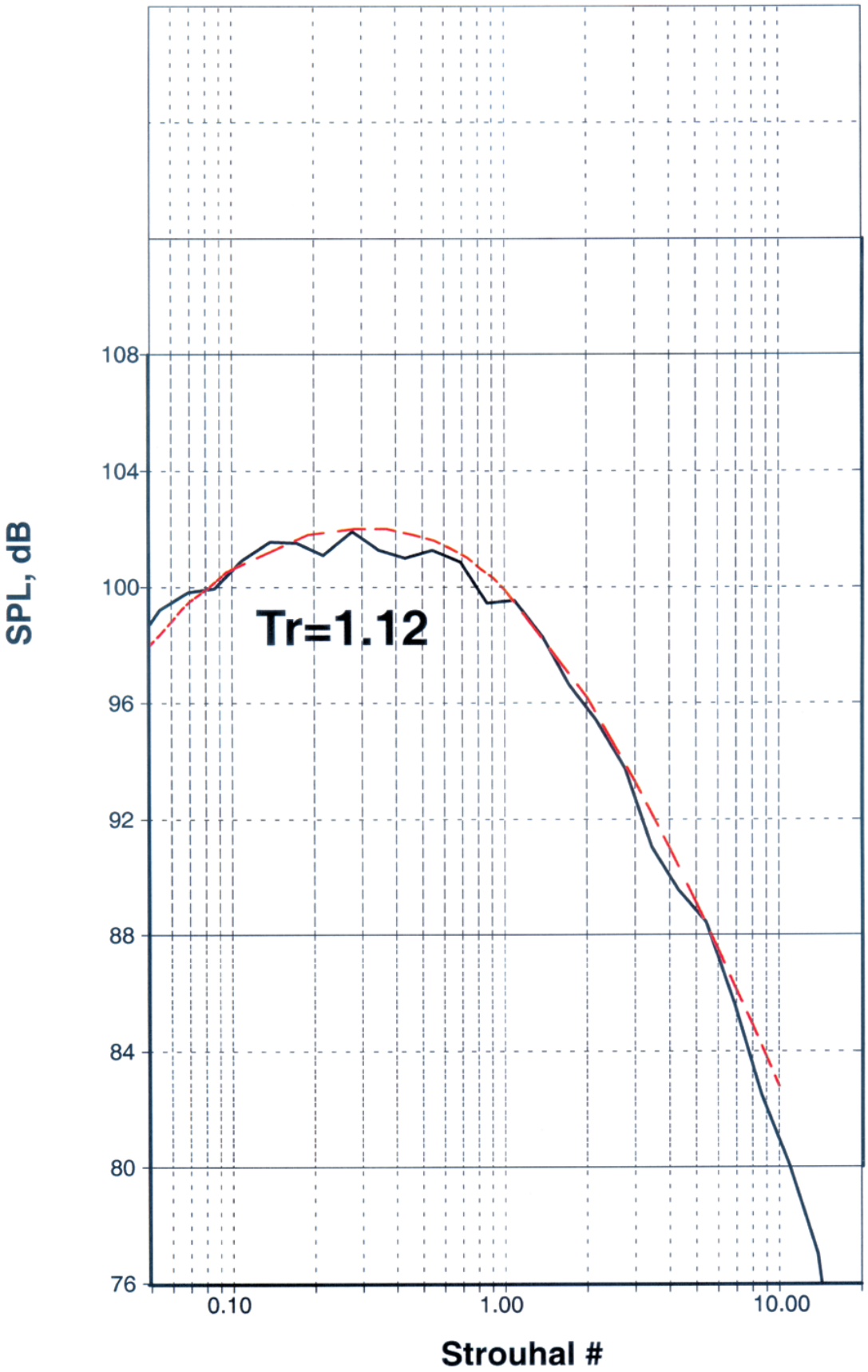
Temperature effect, M=2 jet: 89 degrees



Temperature effect, M=2 jet: 98 degrees



Temperature effect, M=2 jet: 115 degrees



NASA/CP—2001-211152

Summary

- Carried out a critical assessment of theories/methods
- Started with same CFD solution (provided by Tam)
- Evaluated two different approaches
- MGBK
  - general trends of OASPL directivity predicted
  - spectral predictions (shapes & levels) are significantly different
- Fine–scale turbulence approach – very good spectral agreement except for the very high temperature jet

NASA/CP—2001-211152

Remarks

- Spectral characteristics are important for aircraft noise predictions

- Implications for development of noise reduction concepts
  - nozzle T.E. mods. (tabs, chevrons) being studied
  - mostly cut & try approach and engineering judgment

- For optimizing concepts
  - must be able to quantify changes in flowfield first
  - must be able to resolve changes in radiated spectra due to changes in flowfield

Synopsis

This work attempts to evaluate the different jet noise theories and the prediction methods that implement the above theories with suitable empirical adjustments to fit data. This is not meant as a competition; rather, this effort is a rigorous attempt at understanding the different viewpoints and obtaining a status report.

One of the fundamental difficulties that bedevil any evaluation of different jet noise theories is the computation of the mean flow and the turbulence information, which are then used for noise prediction. Different CFD codes and turbulence models produce different flow fields. To eliminate this variable, a single set of CFD solutions was provided to all the researchers making jet noise predictions. Specifically, mean flow solutions for all the test cases were generated using the modified κ-ε turbulence model of Thies and Tam [1]. This turbulence model, incorporated in a Parabolized Navier-Stokes (PNS) solver, has been shown to provide excellent agreement with the measured jet mean flow data for a wide range of jet Mach numbers and temperature ratios. Thus, a consistent set of good mean flow data served as the starting point for all noise predictions. The computational domain extended to 35 jet diameters in the downstream direction, thereby ensuring that the important noise source region was included.

Seven test cases, that would establish different observed effects, were chosen. These cases sought to:

1. predict the effect on the radiated noise when increasing the jet Mach number at constant reservoir temperature (cold jets with M=0.5, 0.9, 1.5)
2. predict the noise from a subsonic heated jet (M=0.87, temperature ratio=2.78)
3. predict the effect of increasing temperature while holding the Mach number constant (M=2.0, temperature ratio = 1.12, 2.72, 4.89).

For all cases, comparisons are shown at a radial distance of 100 jet diameters from the nozzle exit. All angles are measured from the jet inlet axis, with 180° corresponding to the jet exhaust axis.

Three researchers who have developed jet noise prediction methodologies using computed flow fields were invited to participate in this evaluation process. Brief descriptions of the three approaches are given below.

1. Abbas Khavaran: MGBK approach

   In this approach, Lilley's equation is solved, with modeled self-noise and shear-noise terms. The far-field noise is obtained through a volume integral of the noise source region, with the source convection and mean-flow refraction effects properly accounted. Description of the methodology may be found in Khavaran [2] and the references therein.

2. C. K. W. Tam: fine-scale turbulence approach

   Tam and Auriault [3] recently developed a semi-empirical theory for the prediction of fine-scale turbulence noise, based on an analogy of the kinetic theory of gases. The noise source is thought to be associated with the fluctuating kinetic energy of the fine-scale turbulence. The requisite length scale, time scale and source strength are obtained using the κ-ε turbulence model. Mean flow/acoustic interaction effects are computed using an Adjoint Green's function. It is well established that the large-scale structures/instability waves are dominant noise generators in the aft quadrant, at large angles from the jet inlet. Tam's model computes noise only from the fine-scale turbulence and hence the predictions from this methodology are restricted to lower angles, where the fine-scale turbulence noise is dominant. In this approach, the far-field noise is formulated in terms of power spectral density per Strouhal number, which is more suited for making predictions of narrowband data. Hence, narrowband predictions in terms of Strouhal number are shown here.

3. P. J. Morris: approach based on master spectra for quadrupole and dipole contributions

   This approach, described in Pilon and Morris [4], is an extension of an empirical noise prediction scheme developed by Morfey and Szewczyk [5, 6]. Whereas Morfey's method relied on empirical models for the description of the noise sources, the extension by Morris utilized the computed flow field solution for the characterization of the length and time scales, compactness factor, convection velocity, source strength, etc.

Significant findings

Only two sets of results are presented since Morris was unable to complete the predictions before the workshop. Furthermore, Morris carried out a detailed evaluation of the jet noise theories and identified some fundamental issues that set the different approaches apart (see below). Comparisons of predictions and data are shown in the accompanying charts. The results of the MGBK predictions are shown first – these may be identified by the use of the band number for the x-axis. Note that Tam's results have the Strouhal number on the x-axis.

The results indicate that,

1. The MGBK methodology fails to predict the measured spectral shape. The levels are also significantly off.
2. Tam's approach provides very good predictions of amplitudes and spectra for the various cases considered, except for the extremely heated jet case.

For aircraft applications and for the development of noise suppression devices, spectral shapes are important. There is a clear need for the development of models that would address this vital issue.

In a companion presentation, Morris explained that the choice of the reference frame plays a crucial role in the shape of the predicted spectra. Whereas Tam formulated the two-point cross correlation in a nozzle-fixed frame of reference, the analogy theories employ the moving frame of reference. For more details, see the charts presented by Morris.

K. Viswanathan References

1. Thies, A. T., and Tam, C. K. W., "Computation of Turbulent Axisymmetric and Nonaxisymmetric Jet Flows Using the κ-ε Model, AIAA Journal, Vol. 34, No. 2, February 1996.
2. Khavaran, A., "Influence of Mean-Density Gradient on Small-Scale Turbulence Noise", AIAA/CEAS Paper 2000-2059.
3. Tam, C. K. W., and Auriault, L., "Jet Mixing Noise from Fine-Scale Turbulence", AIAA Journal, Vol. 37, No. 2, February 1999.
4. Pilon, A. R., and Morris, P. J., "A Semi-Analytical Method for Jet Noise Prediction", AIAA Paper 99-0076.
5. Morfey, C. L., and Szewczyk, V. M., "Jet Noise Modeling by Geometric Acoustics, Par 1. Theory and Prediction Outside the Cone of Silence", ISVR Technical Report No. 91, Sept. 1977.
6. Morfey, C. L., and Szewczyk, V. M., "Jet Noise Modeling by Geometric Acoustics, Par 2. Theory and Prediction Inside the Cone of Silence", ISVR Technical Report No. 92, Sept. 1977.

Comparison of Lilley's Equation/Acoustic Analogy and Tam & Auriault's Model

Philip Morris
Penn State University

Comparison of Lilley's Equation/Acoustic Analogy and Tam & Auriault's Model

Tam and Auriault's Model

$$\bar{\rho}\left[\frac{\partial u_i}{\partial t}+\bar{u}_j\frac{\partial u_i}{\partial x_j}+u_j\frac{\partial \bar{u}_i}{\partial x_j}\right]+\frac{\partial p}{\partial x_j}=-\frac{\partial q_s}{\partial x_i}$$

$$\frac{\partial p}{\partial t}+\bar{u}_j\frac{\partial p}{\partial x_j}+\gamma\bar{p}\frac{\partial u_i}{\partial x_i}=0$$

$$\text{with } q_s \sim \rho k_s$$

This can be rearranged to give,

$$\frac{1}{c^2}\frac{\bar{D}^3 p}{Dt^3}+2\frac{d\bar{u}}{dr}\frac{\partial^2 p}{\partial r\partial x}-\frac{\bar{D}}{Dt}\nabla^2 p=\left\{\frac{\bar{D}}{Dt}\nabla^2+2\frac{d\bar{u}}{dr}\frac{\partial^2}{\partial r\partial x}\right\}q_s$$

This is nearly identical to Lilley's equation

$$\frac{1}{c^2}\frac{\bar{D}^3 p}{Dt^3}+2\frac{d\bar{u}}{dr}\frac{\partial^2 p}{\partial r\partial x}-\frac{\bar{D}}{Dt}\nabla^2 p=-2\rho_o\frac{d\bar{u}}{dr}\frac{\partial v}{\partial x_j}\frac{\partial u_j}{\partial z}+\text{third order terms}$$

PENNSTATE

Comparison of Lilley's Equation/Acoustic Analogy and Tam & Auriault's Model

- Tam and Auriault:
  - Linearized Euler equations
  - Two-point cross correlation in fixed reference frame
  - Adjoint solution for mean flow/acoustic interaction effects
- Lilley's Equation/Acoustic Analogy
  - Convected wave equation
  - Two-point cross correlation in moving reference frame
  - High and low frequency solutions of Lilley's equation for mean flow/acoustic interaction effects

Comparison of Lilley's Equation/Acoustic Analogy and Tam & Auriault's Model

- For the same level of empiricism solutions using models based on the acoustic analogy fail to yield the correct spectral shape at 90° to jet axis.
- Solutions to models based on the acoustic analogy using a cross correlation in a fixed reference frame and an adjoint solution of the wave equation yield improved results. (But not as good as Tam and Auriault's model.)
- However, if consistent models are used to describe the turbulent statistics, both Tam and Auriault's model and models based on the acoustic analogy yield ***identical results!*** (to be published).

P. Morris References

1. Khavaran, A., Krejsa, E. A. and Kim, C. M., "Computation of Supersonic jet Mixing Noise for an Axisymmetric Convergent Divergent Nozzle," Journal of Aircraft, Vol. 31, No. 3, 1994, pp. 603-609.

2. Khavaran, A., "Role of Anisotropy in Turbulent Mixing Noise," AIAA Journal, Vol. 37, No. 7, 1999, pp. 832-841.

3. Tam, C. K. W. and Auriault, L., "Jet Mixing Noise From Fine-Scale Turbulence," AIAA Journal, Vol. 37, No. 2, 1999, pp. 145-153.

4. Morris, P. J. and Farassat, F., "The Acoustic Analogy and Alternative Theories for Jet Noise Prediction," submitted to AIAA Journal, Feb. 2001.

5. Chung, C. and Morris, P. J., "Acoustic Scattering From Two- and Three-Dimensional Bodies," J. Computational Acoustics, Vol. 6, Part 3, 1998, pp. 357-375.

6. Laik, O. A. and Morris, P. J., "Simulation of Acoustic Scattering by Two and Three-Dimensional Bodies," Journal of Aircraft, Vol. 37, No. 1, 2000, pp. 68-75.

7. Agarwal, A. and Morris, P. J., "Generation and Radiation of Acoustic Waves From a 2-D Shear Layer," rd Benchmarks Problems in Computational Aeroacoustics Workshop, Cleveland, OH. Nov. 8-9, 1999.

8. Agarwal, A. and Morris, P. J., "Direct Simulation of Acoustic Scattering by a Rotorcraft Surface and Flow," AIAA Paper 2000-2030. th AIAA/CEAS Aeroacoustics Conference, Lahaina, Hawaii, June 12-14, 2000.

9. Tam, C. K. W. and Auriault, L., "Mean Flow Refraction Effects on Sound Radiated From Localized Sources in a Jet," Journal of Fluid Mechanics, Vol. 370, 1998, pp. 149-174.

APPENDIX A

A HISTORICAL PERSPECTIVE ON JET NOISE RESEARCH

Geoffrey Lilley, University of South Hampton
Marvin Goldstein, NASA Glenn Research Center

In Prof. Lilley's opening remarks, he gave a short historical account of the origins of the Lighthill acoustic analogy. From 1949 to 1951 Lilley and Westley were engaged in the first extensive experimental program on jet noise research. In 1950 they were visited by Mr. Henry Irving, the Principal Scientist of the UK Ministry of Supply. After reviewing the progress of their research, which had not been funded by the Government, Mr. Irving asked what theory would be used against which the experimental data could be compared. It was explained no theory existed for the noise generated by and radiated from turbulence for this was one of the few topics not considered by Lord Rayleigh in his 'Theory of Sound'. It had been noted there were similarities with electromagnetic radiation. It was their intention to carefully interrogate their new experimental database, and were confident this would lead to the theory of noise generated by turbulence and so establish the properties of the source function, or forcing term, in the resulting inhomogeneous wave equation. Mr. Irving later decided to consult Professor Sydney Goldstein, Head of the Mathematics Department at Manchester University, regarding the possibility that a complete theory could be derived for the noise generated by turbulence. Professor Goldstein suggested this was just the challenge to put to their brilliant mathematician, Michael Lighthill, who we know as the late Sir James Lighthill. Lighthill's theory of AERODYNAMIC NOISE was first announced in 1951 and published in 1952. Thus Mr. Irving's vision in getting a complete theory of jet noise established was of immense importance and allowed the experimental data of Westley and Lilley to quickly gain wide acceptance and application to jet aircraft noise prediction and reduction.

In 1951 Westley and Lilley showed Lighthill's theory was in good agreement with their experimental data. However their experiments on jet noise reduction had been completed from the knowledge they had gained of the jet noise source locations deduced from their jet flow and experimental noise data, and which had been completed before Lighthill's theory was disclosed to them. In the Westley-Lilley experiments the flow was very uniform at the nozzle exit through having a 16:1 contraction ratio upstream. The thickness of the boundary layer at the nozzle exit was very small and was pseudo laminar. The mixing region just downstream of the nozzle exit was also pseudo-laminar although transition to a fully developed mixing region occurred beyond about one jet diameter from the nozzle exit, and therefore changed the effective origin of the linearly growing fully developed turbulent mixing region. When later they investigated numerous noise reduction devices based on the principle of the vortex generator, the flow was then always fully turbulent from the nozzle exit.

Lilley confirmed from their subsonic jet observations, that the dominant high frequency noise generation was from the region close to the nozzle exit. However most of the dominant low frequency noise was generated downstream of the end of the potential core, which in their experiment had a length of about 5 diameters from the nozzle exit. Most of the noise was generated in less than 20 diameters from the nozzle exit, but the first 5 diameters of the initial mixing region was responsible for the bulk of the high frequency noise and contributed to about half the amplitude of the peak noise. The dominant low frequency and the remainder of noise near the peak frequency was generated from around the end of the potential core and in the 'transition' region between the potential core and the fully developed jet flow downstream. It appeared the major noise source at any cross-section came from the center of the mixing region around the dividing stream surface, or streamline, which divides the mixing region into that part derived from the core jet flow, and that derived from the entrainment. The convection speed of the turbulence was connected with the mean speed on the dividing streamline, and was a function of the velocity and temperature ratios between the jet exit conditions and the external flow.

Collaboration with Rolls Royce soon followed and led to the design and installation of the corrugated nozzle and its derivatives on all commercial jet aircraft in the period 1955 –1970. The initial idea of the corrugated nozzle had been developed by Westley, Young and Lilley, but its success depended on an enormous effort by Rolls Royce in perfecting the design for a large noise reduction in flight with a small or zero thrust penalty.

However by the mid–1950's it was realized by virtue of Lighthill's 8th velocity power law that the only course open to the achievement of large aircraft noise reductions was to use aircraft engines designed to have low mixed jet velocities. This change in thermodynamic cycle also had the benefit of reducing the specific fuel consumption and increasing the engine thermal efficiency. Some early work was done on the use of aircraft engines with small bypass ratio but in the late 1950's Lilley joined a small research consulting panel at Rolls Royce to consider what further noise reduction could be expected from the introduction of the large front fan turbojet engine. These studies suggested the noise would decrease with increase in bypass ratio and the outcome was the introduction of the RB211 for installation on the 'Tristar'.

While much of the fundamental theory of jet noise was initiated in the U.K., much of the subsequent development occurred in the United States. Prof. Lilley first introduced the idea of using an inhomogeneous version of the convected wave equation for a transversely sheared mean flow to replace Lighthill's equation while he was in residence at Lockheed (Georgia) Company and supported by a grant from the FAA. This equation was eventually found to produce somewhat better predictions of the sound field than those that could be obtained from Lighthill's equation and considerable effort was ultimately invested in its further development. As Prof. Lilley noted in his invited remarks, one of the most frequently voiced objection to Lighthill's theory is that the density appears in the source as well as in

the propagation term (even when entropy fluctuations are neglected), which means that it leads to an integral equation for the sound field rather than an explicit formula for that entity. Goldstein (1984,1976) used a systematic expansion procedure to show that this does not occur in the Lilley approach when appropriate logarithmic variables are used for the sound field. This also led to a simplified expression for the source term which produced results that Colonius, Liley and Moin (1997,Sound Generation in a Mixing Layer. J. of Fl. Mech., 330 pp 375-409) showed to be in excellent agreement with the DNS computations.

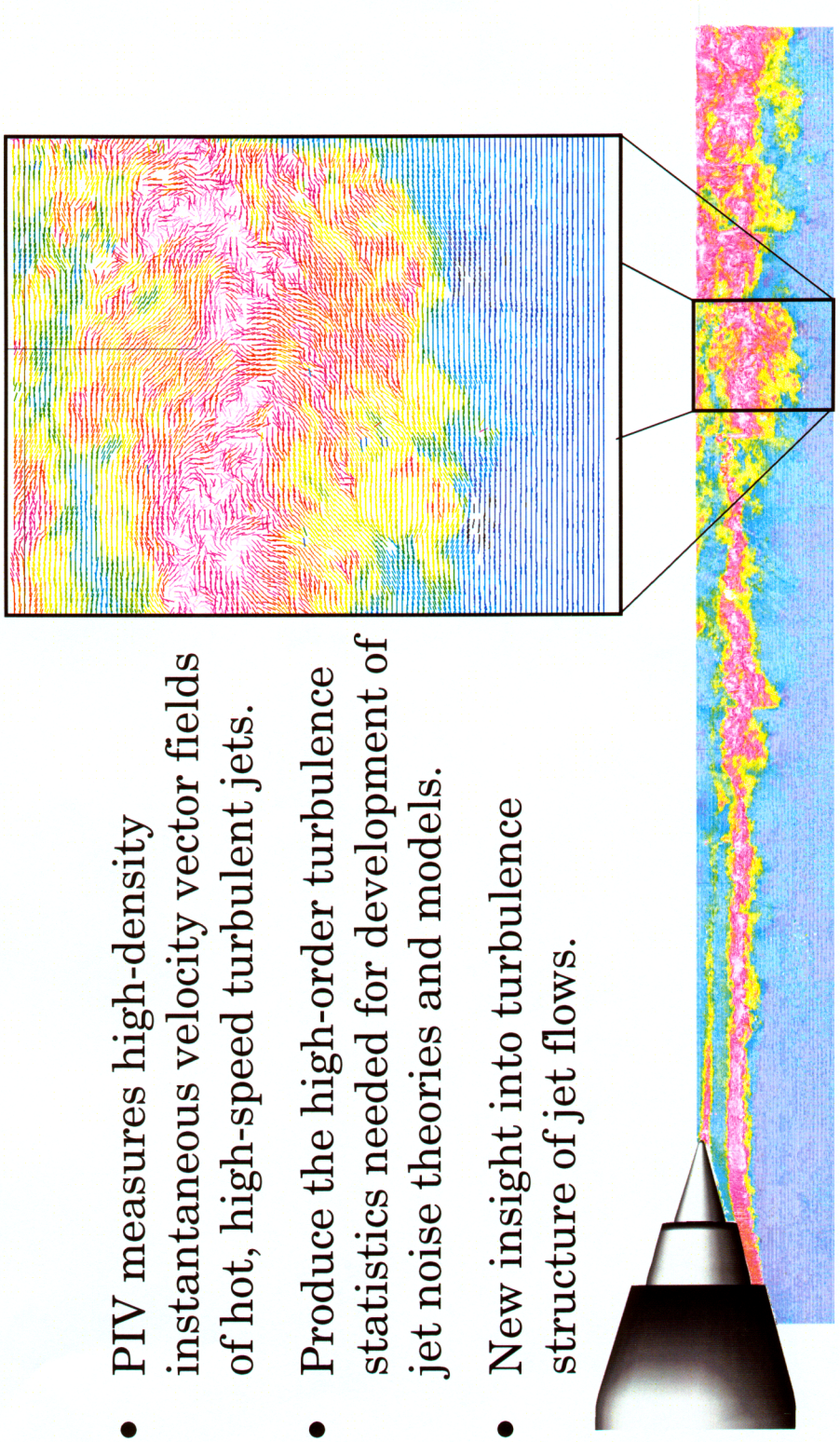
A major disadvantage of Lilley's equation is that it is much more difficult to solve than Lighthill's equation. However a number of investigators (1976 Balsa, 1974 Lilley, 1982 Goldstein, 1974 Berman, 1974 Tester and Burren) worked out approximate high frequency solutions that were found to be in excellent agreement with the exact solutions down to Strouhal numbers as low as one. These results were eventually incorporated into noise prediction codes (such as the MGB code, discussed extensively in this workshop).

Another approach to jet noise theory is the linear instability wave modeling of the large-scale structure noise that was discussed in considerable detail by Prof. Morris in his invited remarks. Crow and Champaign initiated this approach when they were employed by the Boeing Company and it has now been extensively developed by Tam, Morris and many others.

RECENT PARTICLE VELOCIMETRY MEASUREMENTS FROM GLENN RESEARCH CENTER

Particle Image Velocimetry (PIV) in Jet Noise Research

- PIV measures high-density instantaneous velocity vector fields of hot, high-speed turbulent jets.
- Produce the high-order turbulence statistics needed for development of jet noise theories and models.
- New insight into turbulence structure of jet flows.



Velocity vectors in axisymmetric separate flow nozzle at typical takeoff conditions.
Structure convection speed subtracted from vectors to enhance structures.
1080 by 120 vectors, 2.25mm/vector density.
Bridges & Wernet, NASA Glenn, 2000.

APPENDIX C

MODEL PROBLEM PROPOSED BY CHRISTOPHER TAM

To provide an example to show clearly that the Lighthill's Acoustic Analogy, when implemented, fails to identify the correct noise sources, let us consider the following initial value problem governed by the Euler equations. With respect to length scale L, velocity scale a_0 (ambient speed of sound), time scale L/a_0, density scale ρ_0 (ambient gas density) and pressure scale $\rho_0 a_0^2$, the dimensionless Euler equations and initial conditions are,

$$\begin{aligned}
&\frac{\partial \rho}{\partial t}+\frac{\partial \rho u}{\partial x}+\frac{\partial \rho v}{\partial y}=0\\
&\frac{\partial u}{\partial t}+u\frac{\partial u}{\partial x}+v\frac{\partial u}{\partial y}+\frac{1}{\rho}\frac{\partial p}{\partial x}=0\\
&\frac{\partial v}{\partial t}+u\frac{\partial v}{\partial x}+v\frac{\partial v}{\partial y}+\frac{1}{\rho}\frac{\partial p}{\partial y}=0\\
&\frac{\partial p}{\partial t}+u\frac{\partial p}{\partial x}+v\frac{\partial p}{\partial y}+\gamma p\left(\frac{\partial u}{\partial x}+\frac{\partial v}{\partial y}\right)=0
\end{aligned} \tag{1}$$

At t=0

$$u=v=0 \tag{2}$$

$$p=\frac{1}{\gamma}+A\exp\left[-(\ln 2)\left(\frac{x^2+y^2}{36}\right)\right] \tag{3}$$

$$\rho=1 \tag{4}$$

where γ is the ratio of specific heats and A is the strength of the initial pressure pulse. This initial value problem is a slightly modified nonlinearized version of the Category 3 problem of the First CAA Workshop on Benchmark Problems.

Equation (1) and initial conditions (2) to (4) can be solved computationally by the Dispersion-Relation-Preserving (DRP) scheme. By using a 7-point stencil and $L=\Delta x=\Delta y$, it is easy to show that the time accurate DRP marching scheme would give a "numerically exact" solution. Figure 1 shows the density contours in the x–y plane at t=25, 50 and 75 with initial pulse amplitude A=0.4. Figure 2 shows the

corresponding density waveform along the *x*-axis. The wave amplitude is quite high so that there is nonlinear wave steepening of the waveform at the wave front.

Lighthill derived his famous equation by using the continuity and momentum equations of a compressible fluid,

$$\frac{\partial \rho}{\partial t} + \frac{\partial \rho u_j}{\partial x_j} = 0 \tag{5}$$

$$\frac{\partial \rho u_i}{\partial t} + \frac{\partial \rho u_i u_j}{\partial x_j} + \frac{\partial p}{\partial x_i} = \frac{\partial \tau_{ij}}{\partial x_j} \tag{6}$$

where τ_{ij} are the viscous stresses.

By differentiating (5) with respect to *t* and using (6) to replace the time derivative of ρu_j in the second term, it is straightforward to derive the Lighthill equation,

$$\left(\frac{\partial^2}{\partial t^2} - a_0^2 \frac{\partial^2}{\partial x_j^2} \right) \rho = \frac{\partial^2 T_{ij}}{\partial x_i \partial x_j} \tag{7}$$

where,

$$T_{ij} = \rho u_i u_j + \left(p - \rho a_0^2 \right) \delta - \tau_{ij} \tag{8}$$

In the literature, T_{ij} is called the Lighthill stress tensor. The right side of equation (7) is usually referred to as the quadrupole source terms.

By means of the "numerically exact" solution, the Lighthill quadrupole source terms are computed. Contours of these source terms at *t*=25, 50 and 75 are plotted in figure 3. Figure 4 shows the cross-sectional profiles of the Lighthill noise sources at these same instants in time.

Now an important point can be made using the numerical solution. First, one can substitute the Lighthill quadrupole sources (see figures 3 and 4) into the right side

of the Lighthill's equation (equation (7)) and solve the nonhomogeneous wave equation using (4) and $\partial\rho/\partial t=0$ (derived by setting $t=0$ in the first equation of (1) and using (2) and (4)) as the initial conditions. It would surprise no one that the computed solution is nearly identical to the original solution of the Euler equations (equation (1)). In the past, exercises like this have been claimed as proofs of the correctness of Lighthill's Acoustic Analogy and that it could be used to identify the noise sources of aeroacoustic problems. On judging by the present example, the exercise proves nothing. The only thing one can say is that the wave equation has been solved correctly. It is worthwhile to note that part of the quadrupole source terms are actually nonlinear wave propagation terms of the Euler equations. They are not responsible for generating the acoustic pulse of the present problem. The noise source is the initial condition.

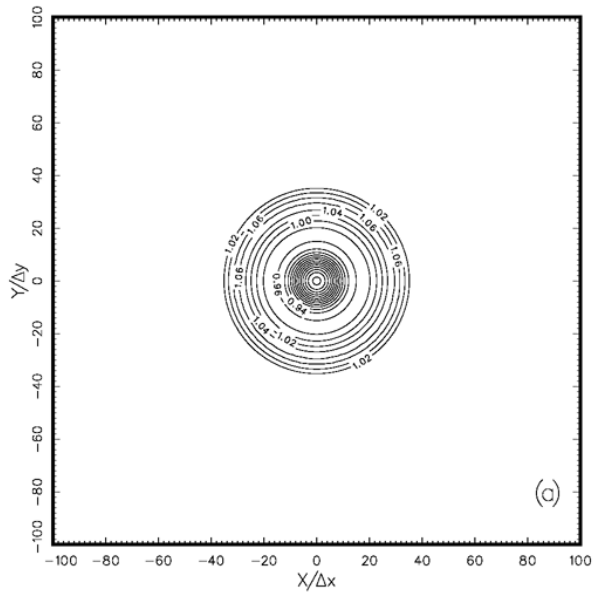


Figure 1a.
Contours of constant density, ρ/ρ_0.
(a) t=25.0, (b) t=50.0, (c) t=75.0

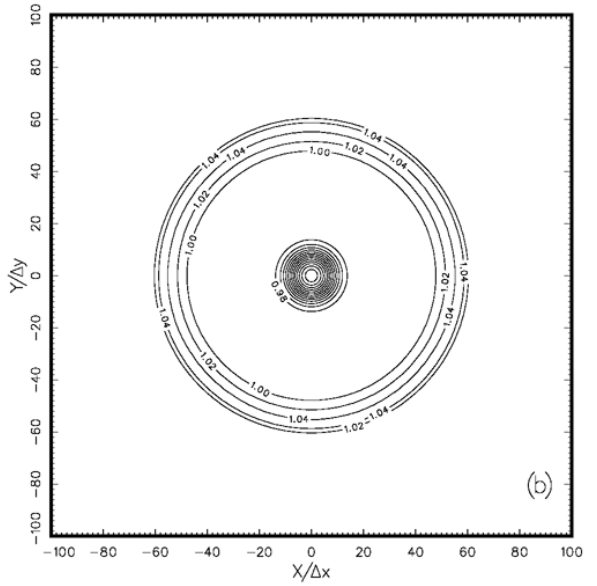


Figure 1b.

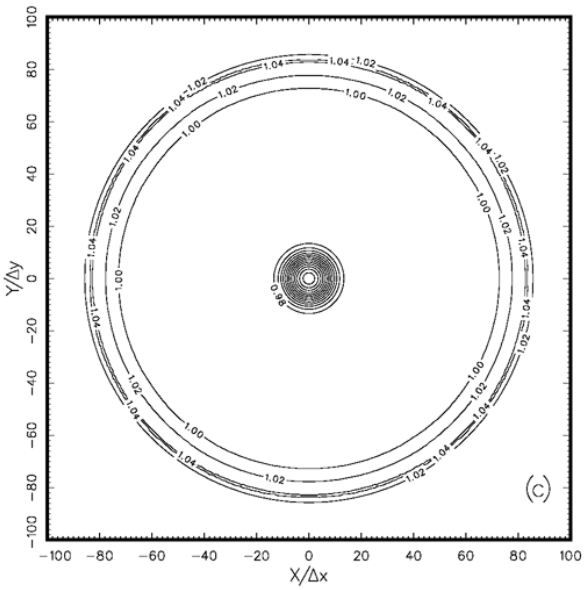


Figure 1c.

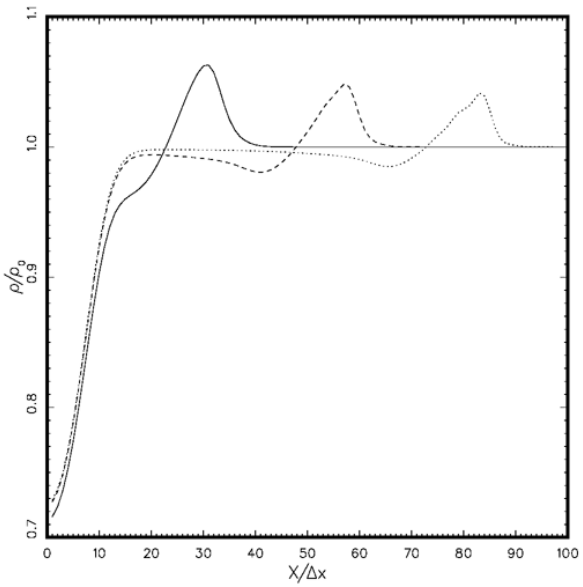


Figure 2. Distribution of density, ρ/ρ_0, along the positive X axis.
t=25.0, - - - t=50.0, ····· t=75.0.

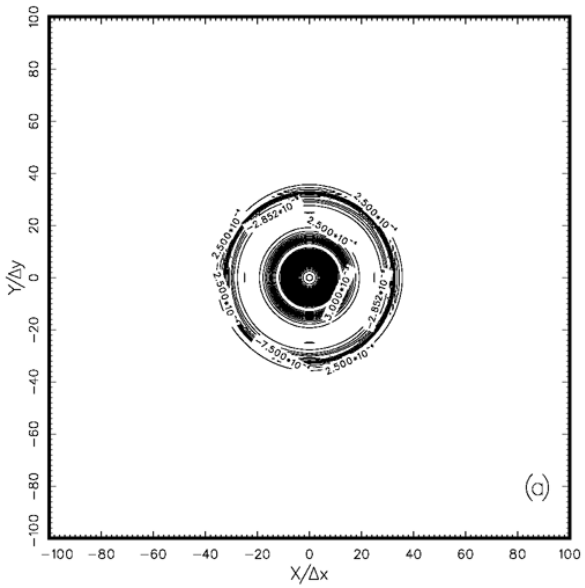


Figure 3a.

Contours of nondimensional Lighthill quadrupole sources, $\partial_2 T_{ij}/x_i \partial x_j$.
(a) t=25.0, (b) t=50.0, (c) t=75.0

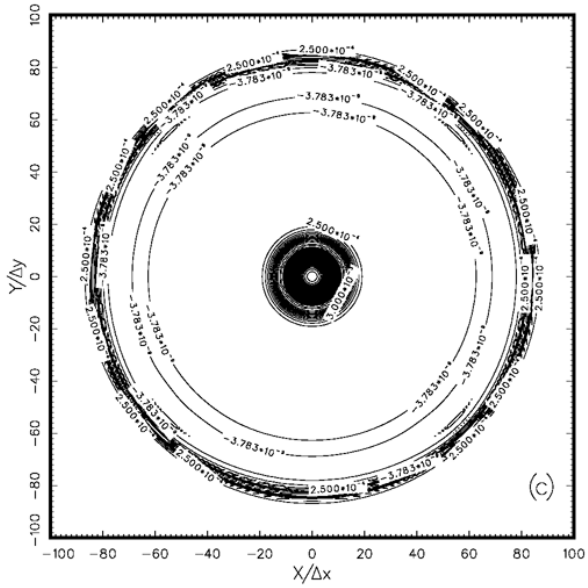


Figure 3c.

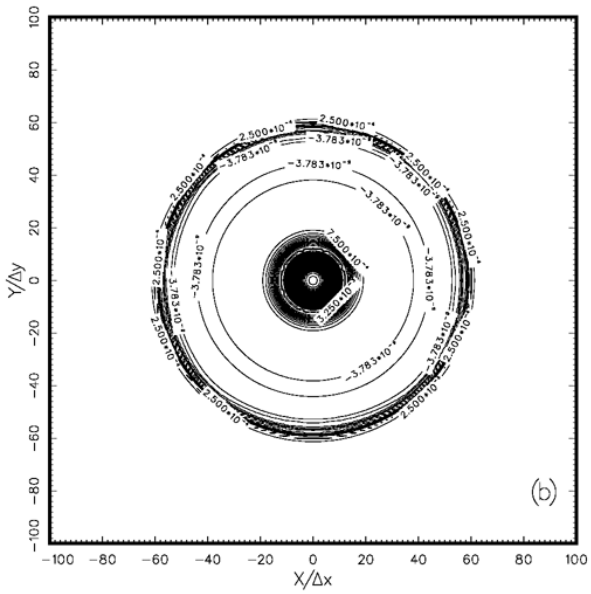


Figure 3b.

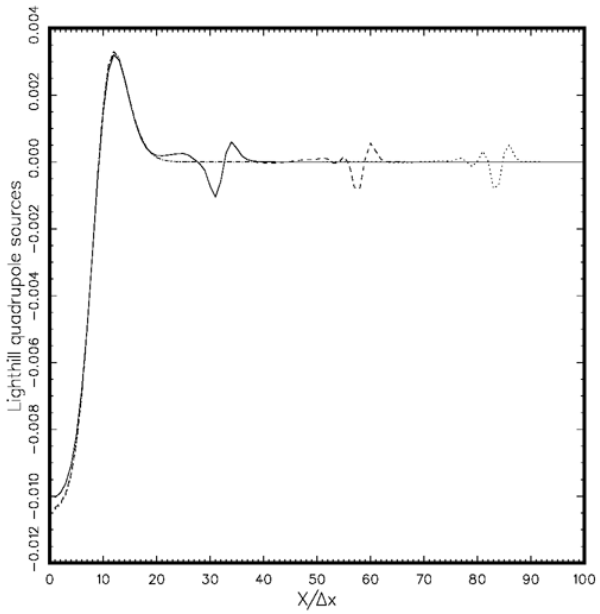


Figure 4.

Distribution of nondimensional Lighthill quadrupole sources along the positive X axis. ——— t=25.0, - - - - - t=50.0, t=75.0.

APPENDIX D

JET NOISE REFERENCES SUGGESTED BY WORKSHOP PARTICIPANTS

1. "Preliminary Experiments on the Noise Generated by Target-Type Thrust Reverser Models," with O.A. Gutierrez (1st author), NASA TM X-2553, May 1972.

2. "Target-Type Thrust Reverser Noise," with O.A. Gutierrez, J. Aircraft, Vol. 10, No. 5, May 1973, pp. 283-288. (Originally presented as "Noise of STOL Core-Jet Thrust Reversers," AIAA Paper 72-791 (NASA TM-68082), August 1972).

3. "Aircraft Noise Reduction Technology," (one of 37 co-authors) Lewis Research Center, NASA TM X-68241, March 1973.

4. "Thrust Reverser Noise," with O.A. Gutierrez, Working Paper for International Commercial Aircraft Organization (ICAO) Committee on Aircraft Noise Meeting, Montreal, Canada, March 1973.

5. "Small-Scale Noise Tests of a Slot Nozzle with V-Gutter Target Thrust Reverser," with O.A. Gutierrez, NASA TM X-2758, April 1973.

6. "Noise Tests of High-Aspect-Ratio Slot Nozzle with Various V-Gutter Target Thrust Reversers," with O.A. Gutierrez, NASA TM X-71470, 86th Meeting of the Acoustical Society of America, Los Angeles, CA, October 30 - November 2, 1973.

7. "Results from Cascade Thrust Reverser Noise and Suppression Experiments," with O.A. Gutierrez (1st author) and R. Friedman (3rd author), J. Aircraft, Vol. 12, No. 3, May 1975, pp. 479-486. (Originally presented as AIAA Paper 74-46 (NASA TM-71500), May 1974).

8. "Noise of Model Target Type Thrust Reversers for Engine-Over-the-Wing Applications," with O.A. Gutierrez, NASA TM X-71621, 88th Meeting of the Acoustical Society of America, St. Louis, MO, November 5-8, 1974.

9. "Interim Prediction Method for Jet Noise," NASA TM X-71618, November 1974.

10. "On the Effects of Flight on Jet Engine Exhaust Noise," NASA TM X-71819, 90th Meeting of the Acoustical Society of America, San Francisco, CA, November 4-7, 1974.

11. "Developments in Aircraft Jet Noise Technology," with O.A. Gutierrez (1st author), Aircraft Safety and Operating Problems, NSA SP-416, October 1976, pp. 497-512.

12. "Effects of Forward Velocity on Noise for a J85 Turbojet Suppressor as Determined from Wind Tunnel and Flight Tests," with J.H. Miles and N.B. Sargent, NASA TM-73542, 92nd Meeting of the Acoustical Society of America, San Diego, CA, November 16-29, 1976.

13. "An Empirical Model for Inverted-Velocity-Profile Jet Noise Prediction," NASA TM-73838, 94th Meeting of the Acoustical Society of America, Miami, FL, December 13-16, 1977.

14. "Prediction of In-Flight Jet Noise for Turbojet and Turbofan Engines," Noise Control Engineering, Vol. 10, No. 1, January-February 1978, pp. 40-46. (Originally presented at 92nd Meeting of the Acoustical Society of America, San Diego, CA, November 16-29, 1976 as "Flight Effects on Exhaust Noise for Turbojet and Turbofan Engines - Comparison of Experimental Data with Prediction," NASA TM-73552).

15. "On the Use of Relative Velocity Exponents for Jet Engine Exhaust Noise," NASA TM-78873, 95th Meeting of the Acoustical Society of America, Providence, RI, May 16-19, 1978.

16. "Experimental Study of Coaxial Nozzle Exhaust Noise," with J.H. Goodykoontz (1st author), AIAA Paper 79-0631, March 1979.

17. "Effects of Geometric and Flow-Field Variables on Inverted-Velocity-Profile Coaxial Jet Noise and Source Distributions," with J.H. Goodykoontz and O.A. Gutierrez, AIAA Paper 79-0635, March 1979.

18. "An Improved Method for Predicting the Effects of Flight on Jet Mixing Noise," NASA TM-79155, 97th Meeting of the Acoustical Society of America, Cambridge, MA, June 11-15, 1979.

19. "Noise Reduction," with C.E. Feiler (1st author), J.F. Groeneweg, F.J. Montegani, J.P. Raney, and E.J. Rice, Aeropropulsion 1979, NASA CP-2092, October 1979, pp. 85-128.

19. "Status of Noise Technology for Advanced Supersonic Cruise Aircraft," with O.A. Gutierrez, NASA Langley Supersonic Cruise Research '79 Conference, NASA CP-2108, November 1979, Part 1, pp. 493-518.

20. "An Improved Prediction Method for the Noise Generated in Flight by Circular Jets," with F.J. Montegani, NASA TM-81537, 99th Meeting of the Acoustical Society of America, Atlanta, GA, April 21-25, 1980.

22. "Prediction of Unsuppressed Jet Engine Exhaust Noise in Flight from Static Data," AIAA Paper 80-1008, June 1980.

21. "Recent Developments in Aircraft Engine Noise Technology," with C.E. Feiler, NASA Langley 1980 Aircraft Safety and Operating Problems Conference, NASA CP-2170, March 1981, Part 2, pp. 671-698.

23. "NASA Research in Supersonic Propulsion - A Decade of Progress," with L.H. Fishbach (1st author), L.E. Stitt (2nd author), and J.B. Whitlow (4th author), AIAA Paper 82-1048, June 1982.

24. "Conventional Profile Coaxial Jet Noise Prediction," with D.E. Groesbeck and C.L. Zola, AIAA J., Vol. 21, No. 3, March 1983, pp.336-344.

25. “Comparison of Measured and Predicted Flight Effects on High-Bypass Coaxial Jet Exhaust Noise,” AIAA Paper 83-0749, April 1983.

26. “Acoustic Excitation – A Promising New Means of Controlling Shear Layers,” with D.J. McKinzie, NASA TM-83772, Invited Paper, American Society of Mechanical Engineers (ASME) Summer Meeting, San Antonio, TX, June 15-17, 1984.

27. “Supersonic Jet Noise Shock Noise Reduction,” AIAA Paper 84-2278, October 1984.

28. “An Improved Model for Conventional and Inverted-Velocity-Profile Coannular Jet Noise,” with C.L. Zola and B.J. Clark, AIAA-99-0078, January 1999.

29. “Noise Suppression Nozzles for a Supersonic Business Jet,” with E.A. Krejsa, I. Halliwell, and B.J. Clark, AIAA-2000-3194, July 2000.

K. Ahuja References

Theses

M. Phil. - “An Experimental Study of Subsonic Jet Noise with Particular Reference to the Effects of Upstream Disturbances,” September 1972, Advisor: Prof. A. D. Young, University of London, U.K.

Ph.D. - “Noise Studies of Cold and Heated Model Jets at Supersonic and Subsonic Speeds with particular Reference to Noise Reduction,” July 1976, Advisor: Prof. D. S. Dosanjh, Syracuse University, N.Y.

Published Books and Parts of Books

Dosanjh, D. S., Ahuja, K. K., Bassiouni, M. R. and Bhutiani, P. K., “Some Recent Developments in Supersonic Jet Noise Reduction,” in Aeroacoustics: Jet Noise, Combustion, and Core Engine Noise, pp. 353-377. (Ira R. Schwartz, Ed.), Vol. 43, Progress in Astronautics and Aeronautics, AIAA, New York and MIT Press, Cambridge (1976).

Published Papers (non-refereed)

1. Ahuja, K. K., Hsu, J., Cataldi, Paul and Elsbernd, T. M.., "Investigation of the Propagation of Internal Noise to the Farfield," Final Report Prepared for NASA Lewis Research Center. in support of Grant NAG3-1682, March 1, 1998.

2. Ahuja, K. K., Stoker, R., and Massey, K. C., "In-Flow and Nearfield Out-of-Flow Noise in Open-Jet Wind Tunnels," Final Report, Prepared for National Wind Tunnel Complex Office, September 1995.

3. Ahuja, K. K., "Aeroacoustic Performance of Open-Jet Wind Tunnels with Particular Reference to Jet/Collector Interactions," Final Report AEDC-SBIR-94-02, June 1995.

4. K. K. Ahuja, K. C. Massey, C. K. W. Tam, and R. R. Jones, III "Temperature Effects on Acoustic Interactions between Altitude Test Facilities and Jet Engine Plumes," AEDC-TR-94-10, October 1994.

5. Brown, W. H. and Ahuja, K. K., “Jet and Wing/Flap Interaction Noise,” Final Report on Lockheed Project 84R465, Lockheed Georgia Report No. LG84ER0146, October 1984.

6. Salikuddin, M., Brown, W. H., and Ahuja, K. K., “Noise From circulation Control Wing with Upper Surface Blowing; Vol. I - Detailed Results, Final Report on Lockheed Project 84R465, Lockheed Georgia Report No. LG84ER0129, October 1984.

7. Salikuddin, M., Brown, W. H., and Ahuja, K. K., “Noise From circulation Control Wing with Upper Surface Blowing; Vol. II - Summary, Final Report on Lockheed Project 84R465, Lockheed Georgia Report No. LG84ER0130, October 1984.

8. Salikuddin, M., Brown, W. H., and Ahuja, K. K., “Noise From circulation Control Wing with Upper Surface Blowing; Vol. III - Tabulated Data, Final Report on Lockheed Project 84R465, Lockheed Georgia Report No. LG84ER0164, October 1984.

9. Lepicovsky, J., Bell, W. A., and Ahuja, K. K., “Conditional Sampling with a Laser Velocimeter and its Application for Large-Scale Turbulent Structure Measurement,” Final Report on Lockheed Project 82R465, Lockheed Georgia Report No. LGER0007, January 1983.

10. Ahuja, K. K., Manes, J., and Massey, K., “Supersonic Jet Noise Reduction from Single and Coaxial Rectangular Jets,” Final Report A8422, Prepared for NASA under Grant Number NAG3-1066, February 1992.

11. Ahuja, K. K., Jones, R. R. III, Tam, C. K., Massey, K. C. and Fleming, A. J., “Acoustic Interactions Between an Altitude Test Facility and Jet Engine Plumes: Theory and Experiments,” Final Report, AEDC-TR-91-20, Jan. 1992.

12. Ahuja, K. K., “Tiltrotor Aircraft Noise - A Summary of the Presentations and Discussions At the 1991 FAA / Georgia Tech Workshop,” Final Report DOT/FAA/RD-91/23, Prepared for FAA under Subcontract from Systems Control Technology, Inc., January 1992.

13. Ahuja, K. K., Tam, C. K. W., Salikuddin, M., Burrin, R. H., Roads, R. “Aeroacoustic Environment of Single and Twin Impinging Model Plumes in Relation to STOVL Aircraft. I – Experimental and Analytical Results,” NASA CR-4291, Vol. I, 1990.

14. Ahuja, K. K., Tam, C. K. W., Salikuddin, M., Burrin, R. H., Roads, R. “Aeroacoustic Environment of Single and Twin Impinging Model Plumes in Relation to STOVL Aircraft. II – Near-Field Noise Spectra and Contour Plots,” NASA CR-4291, Vol. II, 1990

15. Lepicovsky, J., Ahuja, K. K., Brown, W. H., Salikuddin, M. and Morris, P. J., “Acoustically Excited Heated Jets - Internal Excitation,” NASA Final Report, NASA CR-4129, 1988.

16. Lepicovsky, J., Ahuja, K. K., Brown, W. H., Salikuddin, M. and Morris, P. J., “Acoustically Excited Heated Jets - In Search of a Better Understanding,” NASA Final Report, NASA CR-4129, 1988.

17. Lepicovsky, J., Ahuja, K. K., Brown, W. H., Salikuddin, M. and Morris, P. J., “Acoustically Excited Heated Jets - Mean Flow Data,” NASA Final Report, NASA CR-4129, 1988.

18. Burrin, R. H., Ahuja, K. K., and Salikuddin, M. S., “High Speed Flight Effects on Noise Propagation,” AFWAL-TR-86-3086, December 1986.

19. Lepicovsky, J., Ahuja, K. K., Brown, W. H., and Burrin, R. H., “Coherent Large-Scale Structures in High Reynolds Number Supersonic Jets,” Final Report, NASA CR-3952, 1985.

20. Ahuja, K. K., “Basic Experimental Study of the Coupling Between Flow Instabilities and Incident Sound,” Final Report, NASA CR-3789, 1984.

21. Ahuja, K. K., Lepicovsky, J., Tam, C. K. W., Morris, P. J., and Burrin, R. H., “Tone-Excited Jet: Theory and Experiments, Final Report, NASA CR-3538, 1982.

22. Ahuja, K. K., Salikuddin, M., Burrin, R. H., and Plumbee, H. E., Jr. “A Study of the Transmission Characteristics of Suppressor Nozzles,” Final Report, NASA CR-165138, 1980.

23. Ahuja, K. K., Tester, B. J., and Tanna, H. K., “The Free Jet as a Simulator of Forward Velocity Effects on Jet Noise,” Final Report, NASA CR-3056, 1978. Dosanjh, D. S., Bhutiani, P. K., and Ahuja, K. K., “Supersonic Jet-Noise Reduction of Coaxial Cold / Heated Jet Flows,” Final Report Submitted to Office of Noise Abatement, Department of Transportation, Washington, D. C. under Grant No. DOT-OS-20094, March 1977.

Conference Presentations (with Proceedings, non-refereed)

1. Hsu, J. S., and Ahuja, K. K., “A Coherence-Based Technique to Separate Ejector Internal Mixing Noise From Farfield Measurements,” AIAA 98-2296, 4th AIAA/CEAS Aeroacoustic Conference, Toulouse, France, June 2-4, 1998.

2. Ahuja, K. K., Massey, K. C., and D’Agostino, M. S., “A simple Technique of Locating Noise Sources of a Jet Under Simulated Forward Motion, “AIAA 98-2359, 4th AIAA/CEAS Aeroacoustic Conference, Toulouse, France, June 2-4, 1998.

3. Ahuja, K. K., Massey, K. C., and D’Agostino, M. S., "Flow/Acoustic Interactions in Open-Jet Wind Tunnels," AIAA 97-1691, 3rd AIAA/CEAS Aeroacoustics Conference, Atlanta, GA, May 12-14, 1997.

4. Stoker, R., Ahuja, K. K., and Hsu, J., "Separation of Wind-Tunnel Background Noise and Wind Noise from Interior Measurements," AIAA paper 96-1763, presented at AIAA/CEAS Aeroacoustics Conference, State College, Pennsylvania, May 6-8, 1996.

5. Ahuja, K. K., Massey, K. C., and Entrekin, A. C., “Contribution of Mixing Within an Ejector to the Farfield Noise Measurements,” AIAA Paper 96-0639, 34th AIAA Aerospace Sciences Meeting, Reno, Nevada, January 15-18, 1996.

6. Ahuja, K. K., Manes, J. and Massey, K. C., "Control of Jet Mixing and Supersonic Jet Noise by Resonance Effects in wake Shedding from Parallel Plates," CEAS/AIAA paper 95-018, presented at The First Joint CEAS/AIAA Aeroacoustics Conference (16th AIAA Aeroacoustics Conference), Munich, Germany, June 12 - 15. 1995.

7. Massey, K. C., Ahuja, K. K., Jones, R. R. III, and Tam, C. K. W., “Screech Tones of Supersonic Heated Free Jets,” AIAA 94-0141, 32nd AIAA Aerospace Sciences Meeting, Reno, Nevada, January 10-13, 1994.

8. Ahuja, K. K., “Mixing Enhancement and Jet Noise Reduction Through Tabs Plus Ejectors,” AIAA Paper 93-4347, 15th Aeroacoustics Conference, Long Beach, CA., October 25-27, 1993.

9. Tam, C. K. W., Ahuja, K. K., and Jones, R. R. III, “Screech Tones From Free and Ducted Supersonic Jets,” AIAA 93-0732, 31st AIAA Aerospace Sciences Meeting and Exhibit, Reno, January 1993.

10. Jones, R. R. III, Ahuja, K. K., Tam, C. K. W., and Abdelwahab, M., “Measured Acoustic Characteristics of Ducted Supersonic Jets at Different Model Scales,” AIAA 93-0731, 31st AIAA Aerospace Sciences Meeting and Exhibit, Reno, January 1993.

11. Ahuja, K.K., "Laboratory Simulation of Point Monopole and Point Dipole Sound Sources," 2nd International Congress on Recent Developments in Air- and Structure-Borne Sound and Vibration, Auburn University, AL. March 4-6, 1992.

12. Ahuja, K. K., Manes, J. P., and Massey, K. C., “Supersonic Jet Noise Reduction by Coaxial Rectangular Nozzle,” AIAA 92-02127, 14th DGLR/AIAA Aeroacoustics Conference, Aachen, Germany, May 1992.

13. Ahuja, K. K., “Controlling Plume Deflection by Acoustic Excitation - An Experimental Demonstration,” AIAA 90-4006, 13th AIAA Aeroacoustics Conference, Tallahassee, FL, October 1990.

14. Brown, W. H. and Ahuja, K. K., “Jet Mixing Enhancement by Hydrodynamic Excitation,” AIAA 90-4005, 13th AIAA Aeroacoustics Conference, Tallahassee, FL, October 1990.

15. Ahuja, K. K., Manes, J. P. and Massey, K. C., “An Evaluation of Various Concepts of Reducing Supersonic Jet Noise,” AIAA 90-3982, 13th AIAA Aeroacoustics Conference, Tallahassee, FL, October 1990.

16. Ahuja, K. K., McCaulley, J. A. and Tam, C. K. W., “Noise and Instability Waves in Supersonic Jets in the Proximity of Flat and Cylindrical Walls,” AIAA 89-1136, 12th AIAA Aeroacoustics Conference, San Antonio, TX, April 1989.

17. Ahuja, K. K. and Brown, W. H., “Shear Flow Control by Mechanical Tabs,” AIAA 89-0994, 2nd AIAA Shear Flow Conference, Tempe, AZ, March 1989.

18. Burrin, R. H., Ahuja, K. K., and Salikuddin, M., “High Speed Flight Effects on Noise Propagation,” AIAA 87-0013, 25th AIAA Aerospace Sciences Meeting, Reno, NV, January 1987.

19. Lepicovsky, J., Ahuja, K. K. and Salikuddin, M., “An Experimental Study of Tone-Excited Heated Jets,” AIAA 84-2362, 9th AIAA Aeroacoustics Conference, Williamsburg, VA, October 1984.

20. Salikuddin, M., Brown, W. H., and Ahuja, K. K., “Noise from a Circulation Control Wing with Upper Surface Blowing,” AIAA 85-3083, AIAA Aircraft Design Systems and Operations Meeting, Colorado Springs, CO, October 1985.

21. Lepicovsky, J., Ahuja, K. K. Brown, W. H., and Morris, P. J., “Acoustic Control of Free Jet Mixing,” AIAA 85-0569, AIAA Shear Flow Control Conference, Boulder, CO, March 1985.

22. Ahuja, K. K., “Some Unique Experiments on Receptivity,” AIAA 85-0533, AIAA Shear Flow Control Conference, Boulder, CO, March 1985.

23. Dosanjh, D., Ahuja, K. K., Bassiouni, M., and Bhutiani, P., “Supersonic Jet Noise Suppression by Coaxial Cold/Heated Jet Flows,” AIAA 76-507, 3rd AIAA Aeroacoustics Conference, Palo Alto, CA, July 1976.

24. Brown, W. H., and Ahuja, K. K., “Jet and Wing/Flap Interaction Noise,” AIAA 84-2362, 9th AIAA Aeroacoustics Conference, Williamsburg, VA, October 1984.

25. Lepicovsky, J., Ahuja, K. K., and Salikuddin, M., “An Experimental Study of Tone Excited Heated Jets,” AIAA 84-2341, 9th AIAA Aeroacoustics Conference, Williamsburg, VA, October 1984.

26. Ahuja, K. K., and Burrin, R. H., “Control of Flow Separation by Sound,” AIAA 84-2298, 9th AIAA Aeroacoustics Conference, Williamsburg, VA, October 1984.

27. Lepicovsky, J., and Ahuja, K. K., “Some New Results on Edge-Tone Oscillations in High-Speed Subsonic Jets,” AIAA 83-0665, 8th AIAA Aeroacoustics conference, Atlanta, GA, April 1983.

28. Ahuja, K. K., Lepicovsky, J. and Burrin, R. H., “Noise and Flow Structure of a Tone-Excited Jet,” 7th AIAA Aeroacoustics Conference, Palo Alto, CA, October 1981.

29. Ahuja, K. K., Lepicovsky, J., and Burrin, R. H., “Acoustic and Turbulence Measurements of a Tone-Excited Jet With and Without Flight Simulation,” AIAA 81-2007, 7th AIAA Aeroacoustics Conference, Palo Alto, CA, October 1981.

30. Ahuja, K. K., Salikuddin, M., and Plumblee, H. E., Jr., “Characteristics of Internal- and Jet-Noise Radiation from a Multi-tube Suppressor Nozzle Tested Statically and Under Flight Simulation,” AIAA 80-1027, 6th AIAA Aeroacoustics Conference, Hartford, CT, June 1980.

31. Ahuja, K. K., Tanna, H. K., and Tester, B. J., “Effects of Simulated Forward Flight on Jet Noise, Shock Noise and Internal Noise,” AIAA 79-0615, 5th AIAA Aeroacoustics Conference, Seattle, WA, March 1979.

32. Ahuja, K. K., Tester, B. J., and Tanna, H. K., “Calculation of Far-Field Jet Noise Spectra From Near-Field Measurements Using True Source Location,” AIAA 78-1153, 11th AIAA Fluid and Plasma Dynamics Conference, Seattle, WA, July 1978.

33. Ahuja, K. K. and Dosanjh, D. S., “Heated Fluid Shroud as an Acoustic Shield for Noise Reduction - An Experimental Study,” AIAA 77-1286, 4th AIAA Aeroacoustics Conference, Atlanta, GA, October 1977.

34. Ahuja, K. K., Tester, B. J., Tanna, H. K., and Searle, N., “An Experimental Study of Transmission, Reflection and Scattering in a Free-Jet Flight simulation Facility and Comparison with Theory,” AIAA 77-1266, 4th AIAA Aeroacoustics Conference, Atlanta, GA, October 1977.

35. Dosanjh, D. S., Ahuja, K. K., Bassiouni, M. R., and Bhutiani, P. K., “ Some Recent Developments in Supersonic Jet Noise Reduction,” AIAA 75-502, 2nd AIAA Aeroacoustics Conference, Hampton, VA, March 1975.

36. Lush, P. A., Fisher, M. J., and Ahuja, K. K., “Noise of Hot Jets” Proceedings of British Acoustical Society, Spring Meeting, 1973.

Conference Presentations without Proceedings

1. Ahuja, K., Massey, K. C., and Dreyer, E., "Mixing Enhancement and Noise Control through the Use of Splitter Plates Upstream of Nozzle Exits," 47th Annual Meeting of the division of Fluid Dynamics of the American Physical Society. (Abstract appeared in the Bulletin of the American Physical Society, Vol. 39, No. 9, November 1994).

2. Massey, K. C., and Ahuja, K. K., "Screech at Elevated Temperatures," 47th Annual Meeting of the division of Fluid Dynamics of the American Physical Society. (Abstract appeared in the Bulletin of the American Physical Society, Vol. 39, No. 9, November 1994).

3. Ahuja, K. K., Massey, K. C., and Saliga, D. C., “Mechanical Tabs, Mixing Enhancement, Ejectors, and Supersonic Jet Noise Reduction,” 43rd Annual Meeting of the Division of Fluid Dynamics of the American Physical Society, Ithaca, New York, Nov. 18-20, 1990. (Abstract appeared in the Bulletin of the American Physical Society, Vol. 35, No. 10, November 1990).

4. Ahuja, K. K., “Acoustic Control of a Canada Jets,” 41st Annual Meeting of the division of Fluid Dynamics of the American Physical Society. (Abstract appeared in the Bulletin of the American Physical Society, Vol. 33, No. 10, November 1988).

5. Ahuja, K. K., “Similarities Between Acoustically Excited Jets and Separated Flows,” 39th Annual Meeting of the Division of Fluid Dynamics of the American Physical Society, Columbus, Ohio, November 23-25, 1986. (Abstract appeared in the Bulletin of the American Physical Society, Vol. 31, No. 10, November 1986).

6. Ahuja, K. K., “Do We Need a Trailing Edge for Efficient Flow Sound Coupling,” 37th Annual Meeting of the Division of Fluid Dynamics, Providence, Rhode Island, Nov. 18-20, 1984. (Abstract appeared in the Bulletin of the American Physical Society, Vol. 29, No. 9, November 1984).

S. Glegg Additional References

1. Tang and Kop, N.W.M., “A study on the noise generation mechanism in a circular jet”, Jnl. Of Fluids Engineering, Vol 115, pp 425-435 (1993).

2. Seiner, J.M. “A new rationale approach to jet noise reduction” Theoretical Comp. Fluid Dynamics, vol. 10, 1998, p.373.

3. Side, C. JASA 96(2) August 1994, p. 848-849.

4. H. Fuchs, Journal of Sound and Vibration.

5. G.L. Morrison and D.K. McLaughlin, " Noise generation by instabilities in low Reynolds number supersonic jets" J. Sound and Vibration, Vol 65, 1979, pp 177-191.

6. J.L. Stromberg, D.K. McLaughlin T.R. Troutt, "Flow field and acoustic properties of a mach number 0.9 jet at a low Reynolds number ", J. Sound and Vibration, Vol 72, 1980, pp 159-176.

7. J.C. Yu and D.S. Dosanjh, "Noise field of a supersonic mach 1.5 cold model jet" JASA Vol 51(5), Pt 1, 1972, pp 1400-1410.

8. M. Schaffer, " Direct measurements of the correlation between axial in-jet velocity fluctuations and far field noise near the axis of a cold jet", J. Sound and Vibration, Vol 64, 1979, pp 73-83.

9. J. Lepicovsky, K.K. Ahuja, W.H. Brown and R.H. Burrin, "Coherent large scale structures in high Reynolds number supersonic jets", AIAA Jnl. Vol. 25, No 11, 1987, pp 1419-1425.

10. J.M. Seiner, "Fluid Dynamics and Noise Emission associated with supersonic jets" Studies in turbulence, edited by T.B. Gatski, S. Sarkar and G. Speziale, Springer Verlag, New York, 1992, pp 297-323.

11. L. Maestrello and E. McDaid, "Acoustic characteristics of a high subsonic jet" AIAA Jnl. Vol 9. No. 6. June 1971, pp 1058-1066.

12. Bridges, J. and Podboy, G. G. "Measurements of two point correlations in a round jet with applications to jet noise" AIAA 99-1966, AIAA/CEAS Aeroacoustics conference, Seattle, May 1999.

13. Bridges, J. "Measurements of jet acoustic source density" AIAA 99-3787, 30th AIAA Fluid Dynamics conference, Norfolk, VA, July 1999.

14. B. Thurow, W. Lempert and W. Samimy, "MHz rate imaging of large scale structures within a high speed axisymmetric jet" AIAA paper no 2000-0659, Reno, NV January 2000.

V. G. Mengle References

1. Mengle, V. G., Shin, H-W., Askew, J., Whitfield, C.E. (1992): *Aero-Performance and Aero-Mixing Tests of 2D-CD Mixer/Ejector Nozzles. Part II. Sample of Aero-Mixing Test Data & Inferences.* Paper No. 1, 1st NASA/Industry High Speed Research Program Nozzle Symposium, NASA CP (to be numbered), pp. 3-23 to 3-35, Nov. 17-19, 1992.

2. Mengle, V. G., Shin, H-W., Whitfield, C. E., Wisler, S., Askew, J. (1992*): Acoustic and Aero-Mixing Tests of Fluid-Shield Nozzles. Part II - 2D Fluid-Shield Nozzle Aero-Mixing Tests.* Paper No. 2, 1st NASA/Industry High Speed Research Program Nozzle Symposium, NASA CP (to be numbered), pp. 4-21 to 4-28, Nov. 17-19, 1992.

3. Salikuddin, M., Brausch, J., Mengle, V. (1992): *Acoustic and Aero-Mixing Tests of Fluid-Shield Nozzles. Part I -Acoustics.* Paper No. 2, 1st NASA/Industry High Speed Research Program Nozzle Symposium, NASA CP (to be numbered), pp. 4-1 to 4-19, Nov. 17-19, 1992.

4. Mengle, V. G. (1995*): Acoustic Duct Waveguide Modes Excited by an Axially Convecting Noise Source in Sheared Flow.* 1st NASA Advanced Subsonic Technology Engine Noise Workshop Proceedings, Session 2: Jet Noise, pp. 269-284, Dec. 12-14, 1995.

5. Mengle, V. G., Dalton, W. N., Bridges, J., Boyd, K. (1997): *Noise Reduction with Lobed Mixers - Nozzle Length and Free-Jet Speed Effects.* AIAA Paper No. 97-1682. 18th AIAA Aeroacoustics Conference, May 10-14, 1997.

6. Mengle, V. G. (1997): *Certain Limitations and Extensions of MGB Jet Noise Computer Code.* NASA Advanced Subsonic Technology "MGB Jet Noise Prediction Workshop" Proceedings, Sept. 9, 1997.

7. Janardan, B.A., Hoff, G.E., Barter, J.W., Martens, Gliebe, P. R., Mengle, V. and Dalton, W.N. (1998): *Separate-Flow Exhaust System Noise Reduction Concept Evaluation.* Final Report, NASA Contract NAS3-27720, GE Report No. R98AEB152, May 1998. NASA CR (to be numbered).

8. Mengle, V. G., Dalton, W. N.(1998): *Lobed Mixer Design for Noise Suppression. Vol. 1 - Acoustic and Aerodynamic Test Data Analysis.* Final Report, NASA Contract NAS3-27394, Task Order No. 6, Rolls-Royce EDR No. 18580, July 1, 1998, NASA CR (to be numbered), 298 p.

9. Mengle, V. G., Baker, V. D., Dalton, W. N. (1998): *Lobed Mixer Design for Noise Suppression. Vol. 2 - Plume, Aerodynamic & Acoustic Data.* Final Report, NASA Contract NAS3-27394, Task Order No. 6, Rolls-Royce EDR No. 18581, July 1, 1998. NASA CR (to be numbered), 629 p.

10. Mengle, V. G. (1999): *Jet Noise Reduction by Lobed Mixers with Boomerang Scallops*. AIAA Paper No. 99-1923, 5th AIAA/CEAS Aeroacoustics Conf., May 10-12, 1999.

11. Mengle, V. G. (1999): *Anomalous Effect of Nozzle Length Reduction on Jet Noise of Forced Mixers*. AIAA Paper No. 99-1968, 5th AIAA/CEAS Aeroacoustics Conf., May 10-12, 1999.

12. Mengle, V. G. (1999): *Finding Excess Noise in Internally-Mixed Jets by Varying Free-Jet Speed*. AIAA Paper No. 99-1967, 5th AIAA/CEAS Aeroacoustics Conf., May 10-12, 1999.

13. Mengle, V. G. (2000): *Optimization of Lobe Mixer Geometry and Nozzle Length for Minimum Jet Noise.* AIAA Paper No. 2000-1963, 6th AIAA/CEAS Aeroacoustics Conf., June 12-14, 2000.

14. Mengle, V. G. (2000): *Finding Internal Excess Jet Noise Source Characteristics by Varying Free-Jet Speed.* NASA/OAI Jet Noise Workshop, November 7-9, 2000, NASA CP (to be numbered).

15. Mengle, V. G. (2000): *Vorticity Dynamics and Its Relation to Jet Noise Reduction in Chevrons.* NASA/OAI Jet Noise Workshop, November 7-9, 2000, NASA CP (to be numbered).

16. Mengle, V. G. (2000): *Anomalous Effect of Nozzle Length Reduction on Jet Noise of Forced Mixers.* NASA/OAI Jet Noise Workshop, November 7-9, 2000, NASA CP (to be numbered).

17. Mengle, V. G. (2001): *Tongue Mixer - A New Concept for Jet Noise Reduction*. (Submitted for presentation at the 7th AIAA/CEAS Aeroacoustics Conf., May 28-30, 2001).

18. Mengle, V. G. (2001): *Duct Waveguide Mode Excitation by Sound Sources Convecting in Sheared Flows*. (Submitted for presentation at the 7th AIAA/CEAS Aeroacoustics Conf., May 28-30, 2001).

APPENDIX E

Jet Noise Workshop Speakers

Contact Information

Ahuja, Krish
Professor
Georgia Tech Research Institute
GTRI/ATASL
Atlanta, GA 30332-0844
770-528-7054
770-528-7077
krishan.ahuja@gtri.gatech.edu

Bailly, Christophe
Assistant Professor
Ecole Centrale de Lyon
Centre Acoustique
BP 163
Ecully cedex, FRANCE 69131
04 72 18 60 12
04 72 18 91 43
Christophe.Bailly@ec-lyon.fr

Barna, Gerald
Acting Deputy Director
NASA Glenn Research Center
21000 Brookpark Rd.
Mail Stop 3-2
Cleveland, OH 44135
216-433-2929
216-433-8000
Gerald.J.Barna@grc.nasa.gov

Bhat, Thonse (Srini)
Dr./Principal Engineer
Boeing
P.O.Box 3707
MS 67-ML
Seattle, WA 98124-2207
425-234-9550
425-237-5247
srini.bhat@boeing.com

Glegg, Stewart
Dr.
Florida Atlantic University
Dept. of Ocean Engineering
Boca Raton, FL 33431
561 297 2633
561 297 3885
glegg@oe.fau.edu

Gliebe, Philip
Principal Engineer
GE Aircraft Engines
Acoustics Technology
1 Neumann Way; M/D A411
Cincinnati, OH 45215-1988
513-243-2865
513-243-3261
philip.gliebe@ae.ge.com

Goldstein, Marvin
Chief Scientist
NASA Glenn Research Center
21000 Brookpark Rd.
Mail Stop 3-2
Cleveland, OH 44135
216.433.5825
216.433.5531
marvin.goldstein@grc.nasa.gov

Harper-Bourne, Marcus
DERA Pyestock
RM 25G, Bldg. 401
Farnborough
Hants, GU14 0LS, UK,
01252 37 4330
01252 37 42020
MHBOURNE@DERA.GOV.UK

Kempton, Andrew
Dr.
Rolls-Royce
PO Box 31
Derby, DE24 8BJ U 4
44 1332 249350
44 1332 24951
andrew.j.kempton@rolls-royce.com

Krejsa, Eugene
Aeroacoustic Consultant
9382 Greenbriar Dr.
Parma Heights, OH 44130
440-888-7515
eakrejsa@juno.com

Lele, Sanjiva
Associate Professor, Department of
Aeronautics and Astronautics
Stanford University
Stanford University
Durand Bldg.
Stanford, CA 94305-4035
650-723-7721
650-725-3377
lele@stanford.edu

Lilley, Geoffrey
Professor
University of Southampton
Highfield
Southampton
SO17 1BJ, United Kingdom
44 (0)23 8059 4893
44 (0)23 8059 3058
G.M.Lilley@soton.ac.uk

Lord, Wesley
Acoustics Discipline Leader
Pratt & Whitney
400 Main Street
MS 165-29
East Hartford, CT 06108
860-565-0362
860-656-7373
lordwk@pweh.com

Mankbadi, Reda
Embry-Riddle Aeronautical University
600 S. Clyde
Morris Blvd.
Daytona Beach, FL 32114
904-226-6258
904-226-6747
mankbadr@cts.db.erau.edu

Michel, Ulf
Dr.
DLR
Turbulence Research Section
Mueller-Breslau-Str. 8
Berlin, GERMANY 10623
49 30 310006-26
49 30 310006-39
ulf.michel@dlr.de

Morfey, Christophe
Professor
University of Southampton
Institute of Sound and Vibration
Highfield
SO17 1BJ, United Kingdom
CLM@isvr.soton.ac.uk

Morris, Philip
Boeing/A.D. Welliver Professor
Penn State University
233 J Hammond Building
University Park, PA 16802
814-863-0157
708-810-5329
pjm.psu@edu

Salkind, Michael
President
OAI
22800 Cedar Point Rd.
Cleveland, OH 44142
40-962-3001
440-962-3120
michealsalkind@oai.org

Seiner, John
Associate Director
National Center for Physical Acoustics
1 Coliseum Drive
University, MS 38677
662-915-5630
662-915-1235
jseiner@olemiss.edu

Tam, Christopher
Dr.
Florida State University
Department of Mathematics
Tallahassee, FL 32306-4510
850-644-2455
850-644-4053
tam@math.fsu.edu

Weir, Don
Senior Principal Engineer
Honeywell Engines and Systems
P.O.Box 52181
Mail Stop 554-15
Phoenix, AZ 85072-2181
602-231-1214
602-231-2918
don.weir@honeywell.com

APPENDIX F

Jet Noise Workshop Attendees and Contact Information

Barber, Thomas
University of Connecticut
23 Ravenwood Road
West Hartford, CT 06107
860-521-9001
860-521-3036
barbertj1@earthlink.net

Bertolotti, Fabio
United Technologies Research Center
411 Silver Lane; MS 129-17
East Hartford, CT 6108
860-610-7242
860-670-7134

Birch, Stanley F.
Boeing Commercial Airplane
P.O. Box 3707, MS 67-ML
Seattle, WA 98059
425-237-4906
425-237-5247
stanley.f.birch@boeing.com

Bodony, Daniel
Stanford University
Dept. of Aero/Astro, Durand Bldg.
RM 250
Stanford, CA 94305-4035
650-725-3318
650-725-3377
bodony@Stanford.edu

Bogey, Christophe
ECOLE CENTRALE DE LYON
CENTRE ACOUSTIQUE
ECL, BP 163
Ecully n.a. 69131--FRANCE
33 4 72 18 60 18
33 4 72 18 91 43
christophe.bogey@ec-lyon.fr

Bridges, James
NASA Glenn Research Center
21000 Brookpark Rd; MS 54-3
Cleveland, OH 44135
216-433 2693
216-433 3918
james.bridges@grc.nasa.gov

Butler, Bill
Acoustics and Fluid Mechanics
Boeing 10-16, Bldg.535/Garden Ave N.
Renton, WA 98055
425- 234-4153
425-237-5247
bill.butler@boeing.com

Cain, Alan
Innovative Technology
PO Box 6971
Chesterfield, MO 63006-6971
314-576-1639
314-576-5620
itacabc@aol.com

Chien, Eugene
BFGoodrich
13225 Larkfield Ct
San Diego, CA 92130
619-691-6547
619-691-3550
echien@rohr.com

Choi, Dochul
United Technologies Research Center
411 Silver Lane
East Hartford, CT 06108
860-610-7242
860-670-7134

Dahl, Milo
NASA Glenn Research Center
21000 Brookpark Rd.; MS 54-3
Cleveland, OH 44135
216-433-3578
216-433-3918
Milo.Dahl@grc.nasa.gov

Debonis, Jim
NASA Glenn Research Center
21000 Brookpark Rd., MS 86-7
Cleveland, Ohio 44135
216-433-6581
216-977-7500
Jim.DeBonis@grc.nasa.gov

Djaffar, Ait-Ali
Pratt & Whitney Canada
1000 Marie-Victorin (01SR4)
Longueuil, Quebec J4G 1A1
Canada
450-677-9411 X. 2
450-647-7280
Djaffar.Ait-Ali-Yahia@pwc.ca

Elias, Georges
ONERA
29, av.de la Div. Leclerc
BP 72
CHATILLON CEDEX F-92322
FRANCE
+33 - 1 46 73 4818
+33 - 1 46 73 4166
elias@onera.fr

Envia, Ed
NASA Glenn Research Center
21000 Brookpark Rd.; M.S. 54-3
Cleveland, OH 44135
216-433-8956
216-433-3918
envia@grc.nasa.gov

Farassat, Fereidoun
NASA Langley Research Center
Mail Stop 461
Hampton, VA 23681-2199
757 864-3626
757 864-8290
F. Farassat@larc.nasa.gov

Feng, J. Z.
Pratt & Whitney
400 Main St.; M.S. 163-17
East Hartford, CT 6108
860-565-7914
860-565-2668
fengji@pweh.com

Freund, Jonathan
UCLA
38-137 Engineering IV
Los Angeles, CA 90095-1597
310-206-8587
310-206-2302
jfreund@ucla.edu

Georgiadis, Nicholas
NASA Glenn Research Center
21000 Brookpark Rd., MS 86-7
Cleveland, OH 44135
216-433-3958
216-433-2182
Nicholas.J.Georgiadis@grc.nasa.gov

Goodrich, John
NASA Glenn Research Center
21000 Brookpark Rd.; MS 54-3
Cleveland, OH 44135
216-433-5922
216-433-8000
fsgdrch@jgoodrich.grc.nasa.gov

Grady, Joe
NASA Glenn Research Cent
21000 Brookpark Rd.; MS 60-5
Cleveland, Ohio 44135
216-433-6728
216-433-5100
Joseph.E.Grady@grc.nasa.gov

Guo, Yueping
The Boeing Company
2401 E. Wardlow Rd
Mail Code C078-0420
Long Beach, CA 90807
562-593-9027
yueping@guo@boeing.com

Hagstrom, Thomas
University of New Mexico
Dept. of Math. And Stat.
Albuquerque, NM 87131
505-277-8920
505-277-5505
hagstram@math.unm.edu

Hamed, Awatef
University of Cincinnati
Department of Aerospace Engineering
ML70
Cincinnati, OH 45221-0070
513-556-3553
513-556-5038
Awatef.Hamed@UC.Edu

Henderson, Brenda
Kettering University
Mechanical Engineer Dept.
1700 W. Third Ave.
Flint, MI 48504-4898
810-762-7856
810-762-7860
bhenders@kettering.edu

Heyward, Ann O.
OAI
Workforce Enhancement
22800 Cedar Point Rd.
Cleveland, OH 44142
440-962-3030
440-962-3200
annheyward@oai.org

Hileman, James
Ohio State University
2300 West Case Rd
Columbus, OH 43235
614-292-5515
614-292-5552
hileman.3@osu.edu

Himansu, Ananda
Taitech at NASA Glenn
Research Center
21000 Brookpark Rd., MS 5-11
Cleveland, OH 44135
216-433 5876
216-433 5802
Ananda.Himansu@grc.nasa.gov

Hixon, Duane
University of Toledo
NASA Glenn Research Center
21000 Brookpark Rd., MS 54-3
Cleveland OH 44135
(440) 979-1783
fshixon@apu.grc.nasa.gov

Huff, Dennis
NASA Glenn Research Center
21000 Brookpark Road, M.S.
54-3
Clevelend Ohio 44135
216-433-3913
216-433-3918
Dennis.L.Huff@grc.nasa.gov

Hunter, Craig
NASA Langley Research Center
16 Victory St.; Mail Stop 499
Hampton, VA 23681
757-864-3020
757-864-8469
c.a.hunter@larc.nasa.gov

Kao, Hsiao
NASA Glenn Research Center
21000 Brookpark Rd., MS 86-7
Cleveland, OH 44135
216-433-5866
216-433-8000
Hsiao.C.Kao@grc.nasa.gov

Khavaran, Abbas
NASA Glenn Research Center
Mail Stop: Dynacs
Cleveland, OH 44135
216-977-1120
216-898-6290
khavaran@grc.nasa.gov

Kinzie, Kevin
NASA Langley Research Center
MS 166
Hampton, VA 23681
757-864-5375
757-864-8316
k.w.kinzie@larc.nasa.gov

Koch, Danielle
NASA Glenn Research Center
21000 Brookpark Rd., Mail Stop 54-3
Cleveland, OH 44135
216-433-5656
216-433-3918
L.D.Koch@grc.nasa.gov

Lee, Sang Soo
NASA Glenn Research Center
Dynacs Inc.
21000 Brookpark Road
Cleveland, OH 44135
216-977-1378
216-898-6290
Sang.S.Lee@grc.nasa.gov

Lee, Jaesoo
Boeing Commercial Airplanes
P.O. Box 3707, MC 67-ML
Seattle, Washington 98124-2207
425-234-9209
425-237-5247
jaesoo.lee@boeing.com

Leib, Stewart
OAI
NASA Glenn Research Center
21000 Brookpark Rd.; MS 5-9
Cleveland, Ohio 44135
216-433 - 8639
216-433 -8864
leib@grc.nasa.gov

Lieser, Jan
Rolls-Royce Deutschland
Eschenweg 11
Dahlewitz, Germany 15827
++49 3370861978
++49 3370863611
jan.lieser@rolls-royce.com

Liou, Meng-Sing
NASA Glenn Research Center
21000 Brookpark Rd.; MS 5-11
Cleveland, OH 44135
216-433-5855
216-433-5802
meng-sing.liou@grc.nasa.gov

Loh, Ching
Taitech Inc
NASA Glenn Research Center
21000 Brookpark Rd.; M.S. 5-11
Cleveland, Ohio 44135
216-433-3981
216-433-5802
fsloh@turbot.grc.nasa.gov

Long-Davis, Mary Jo
NASA Glenn Research Center
21000 Brookpark Rd; MS 60-2
Cleveland, OH 44135
216-433-8708
216-977-7133
Mary.J.Long-Davis@grc.nasa.gov

Lyrintzis, Anastasios
Purdue University
Aeronautics & Astro
Grissom Hall
West Lafayette, IN 47907-1282
765-494-5142
765-494-0307
lyrintzi@ecn.purdue.edu

Maeder, Thierry
United Technologies Research Center
411 Silver Lane; MS 129-17
East Hartford, CT 6108
860 610 7615
860 610 7134
maedert@utrc.utc.com

Martens, Steve
General Electric Aircraft Engines
One Neumann Way; M/D A411
Cincinnati, OH 45215
513-243-9149
513-243-3261
steve.martens@ae.ge.com

Mclaughlin, Dennis
Dept. of Aerospace Engineering
Penn State University
229 Hammond Building
University Park, PA 16802
814-865-2560
814-865-7092
dkmaer@engr.psu.edu

Mengle, Vinod
The Boeing Company
Acoustics & Fluid Mechanics
M/S 67-ML
P. O. Box 3707
Seattle, WA 98124-2207
425-237-6414
425-237-5247
vinod.g.mengle@boeing.com

Miles, Jeffrey
NASA Glenn Research Center
21000 Brookpark Rd; MS 54-3
Cleveland, OH 44135
216-433-5909
216-433-3918
Jeffrey.H.Miles@grc.nasa.gov

Miller, Christopher
NASA Glenn Research Center
21000 Brookpark Rd; MS 54-3
Cleveland, OH 44135
216-433-6179
216-433-3918
Christopher.J.Miller@grc.nasa.gov

Nallasamy, Rajagounder
Dynacs Engineering, Co.
21000 Brookpark Rd.; MS DYNACS
Cleveland, OH 44135
216 977-1287
216-898-6290
nallasamy@grc.nasa.gov

Narayanan, Satish
United Technologies Research Center
411 Silver Lane; MS 129-17
East Hartford, CT 6108
860-610-7242
860-670-7134

Nedungadi, Ashish
United Technologies Research Center
411 Silver Lane; MS 129-17
East Hartford, CT 6084
860-610-7561
860-610-7134

Norum, Thomas
NASA Langley Research Center
MS 166
Hampton, VA 23681-2199
757-864-7902
757-864-8316
t.d.norum@larc.nasa.gov

Panda, Jay
OAI
22800 Cedar Point R
Cleveland, OH 44142
216-433-8891
216-977-7500
jayanta.panda@grc.nasa.gov

Papamoschou, Dimitri
University of California, Irvine
Mechanical & Aerospace Engineering
Irvine, CA 92697
949-824-6590
949-824-8585
dpapamos@uci.edu

Posey, Joe
NASA Langley Research Center
MS 461
Hampton, Virginia 23681
757-864-7686
757-864-8290
j.w.posey@larc.nasa.gov

Reba, Ramons
United Technologies Research Center
411 Silver Lane; MS 129-17
East Hartford, CT 6108
860-610-7242
860-610-7134

Reed, David
The Boeing Company
PO Box 3707; MS 67-ML
Seattle, WA 98034
425-237-6448
425-237-5247
david.h.reed@boeing.com

Salikuddin, Mohammed
GE Aircraft Engines
1 Neumann Way; MD A411
Cincinnati, OH 45215-6301
513-243-7151
513-243-3261
mohammed.salikuddin@ae.ge.com

Samimy, Mo
The Ohio State University
Department of Mechanical
Engineering
206 West 18th Avenue
Columbus, OH 43210
614-292-6988
614-292-5552
samimy.1@osu.edu

Schlinker, Robert
United Technologies Research Center
411 Silver Lane; MS 129-17
East Hartford, CT 6108
860-610-7242
860-670-7134

Scott, James N.
The Ohio State University
332-B Bolz Hall
2036 Neil Ave
Columbus, OH 43210
614-292-3828
614-292-8290
jscott@mps.ohio-state.edu

Shivashanka ra, Belur
The Boeing Company
P. O. Box 3707 MS: 67-ML
Seattle, WA 98124-2207
425-234-9551
425-237-5247
belur.n.shivashankar@boeing.com

Simonich, John
United Technologies Research Center
411 Silver Lane; MS 129-17
East Hartford, CT 6108
860-610-7242
860-670-7134

Soteriou, Marios
United Technologies Research Center
411 Silver Lane
East Hartford, CT 6084
860-610-7561
860-610-7134

Stone, James
Modern Technologies Corporation
8530 Lucerne Drive; Suite 206
Middleburg Heights, Ohio 44130
440-243-8488
440-243-8490
jstone_mtc@stratos.net

Thomas, Russell
NASA Langley Research Center
MS 166
Hampton, VA 23681
757 864 9550
757 864 8316
R.H.Thomas@larc.nasa.gov

Ukeiley, Lawrence S.
University of Mississippi
NCPA/Coliseum Drive
University, Mississippi 38677
662 915-7194
662 915-1235
lukeiley@olemiss.edu

Uzun, Ali
Purdue University
School of Aeronautics and Astronautics
1282 Grissom Hall, Room 309
West Lafayette, Indiana 47907
765-494-5144
765-494-0307
uzun@ecn.purdue.edu

Viswanathan, Krishnamurthy
The Boeing Company
M/S 67-ML, PO Box 3707
Seattle, WA 98006
425-965-1186
425-237-5247
k.viswanathan@boeing.com

Wang, Frank
NASA Glenn Research Center
21000 Brookpark Road; Mail Stop 86-7
Cleveland Ohio 44135
216-433-3591
216-977-7500
frank.y.wang@grc.nasa.gov

Wat, Joseph
The Boeing Company
2401 E. Wardlow Rd.
MC C078-0420
Long Beach CA 90807-5309
562-593-8642
562-593-7593
joseph.k.wat@boeing.com

Whitmire, Julia
BFGoodrich Aerospace
850 Lagoon Drive
Mail Zone 107X
Chula Vista, CA 91910-2098
619-691-2082
619-691-3050
jwhitmire@aerostructures.bfg.com

REPORT DOCUMENTATION PAGE

Form Approved
OMB No. 0704-0188

Public reporting burden for this collection of information is estimated to average 1 hour per response, including the time for reviewing instructions, searching existing data sources, gathering and maintaining the data needed, and completing and reviewing the collection of information. Send comments regarding this burden estimate or any other aspect of this collection of information, including suggestions for reducing this burden, to Washington Headquarters Services, Directorate for Information Operations and Reports, 1215 Jefferson Davis Highway, Suite 1204, Arlington, VA 22202-4302, and to the Office of Management and Budget, Paperwork Reduction Project (0704-0188), Washington, DC 20503.

1. AGENCY USE ONLY (*Leave blank*)	2. REPORT DATE	3. REPORT TYPE AND DATES COVERED
	November 2001	Conference Publication

4. TITLE AND SUBTITLE

Proceedings of the Jet Noise Workshop

5. FUNDING NUMBERS

WU–910–30–11–00

6. AUTHOR(S)

Dennis Huff, compiler

7. PERFORMING ORGANIZATION NAME(S) AND ADDRESS(ES)

National Aeronautics and Space Administration
John H. Glenn Research Center at Lewis Field
Cleveland, Ohio 44135–3191

8. PERFORMING ORGANIZATION REPORT NUMBER

E–13008

9. SPONSORING/MONITORING AGENCY NAME(S) AND ADDRESS(ES)

National Aeronautics and Space Administration
Washington, DC 20546–0001

10. SPONSORING/MONITORING AGENCY REPORT NUMBER

NASA CP—2001-211152

11. SUPPLEMENTARY NOTES

Contents were reproduced from the best available copy as provided by the authors. Responsible person, Dennis Huff, organization code 5940, 216–433–3913.

12a. DISTRIBUTION/AVAILABILITY STATEMENT

Unclassified - Unlimited
Subject Category: 71 Distribution: Nonstandard

Available electronically at http://gltrs.grc.nasa.gov/GLTRS

This publication is available from the NASA Center for AeroSpace Information, 301–621–0390.

12b. DISTRIBUTION CODE

13. ABSTRACT ***(Maximum 200 words)***

Jet noise has been a major problem for aircraft for nearly 50 years. There has been considerable research performed around the world aimed at identifying ways to reduce jet noise. This work was first intended for turbojet aircraft and later extended to low bypass ratio turbofans. Many of the people who performed this pioneering research have retired or are no longer active in aeroacoustics. After so many years of work in jet noise, it is a challenge to piece together the history of its development through existing publications due to the large volume of documents. It is possible to forget important developments from the past as new researchers tackle similar problems. Therefore, a jet noise workshop was organized by the AeroAcoustics Research Consortium (AARC) with the intent of reviewing research that has been done by experts throughout the world. The forum provided a unique opportunity for current researchers to hear the diverse views from world experts on issues related to jet noise modeling and interpretation of experimental data.

14. SUBJECT TERMS	15. NUMBER OF PAGES
Aeroacoustics; Jet noise; Computational aeroacoustics; Noise prediction	00
	16. PRICE CODE

17. SECURITY CLASSIFICATION OF REPORT	18. SECURITY CLASSIFICATION OF THIS PAGE	19. SECURITY CLASSIFICATION OF ABSTRACT	20. LIMITATION OF ABSTRACT
Unclassified	Unclassified	Unclassified	